

RH-TRU 72-B

Safety Analysis Report



Revision 7
October 2015

This page intentionally left blank to facilitate duplex printing.

TABLE OF CONTENTS

1.0 GENERAL INFORMATION 1.1-1
1.1 Introduction 1.1-1
1.2 Package Description 1.2-1
1.2.1 Packaging 1.2-1
1.2.2 Operational Features 1.2-5
1.2.3 Contents of Packaging 1.2-6
1.2.4 Package Evaluation 1.2-6
1.3 Appendices 1.3-1
1.3.1 Packaging General Arrangement Drawings 1.3.1-1
1.3.2 Glossary of Terms and Acronyms 1.3.2-1

2.0 STRUCTURAL EVALUATION 2.1-1
2.1 Structural Design 2.1-1
2.1.1 Discussion 2.1-2
2.1.2 Design Criteria 2.1-3
2.2 Weights and Centers of Gravity 2.2-1
2.3 Mechanical Properties of Materials 2.3-1
2.4 General Standards for All Packages 2.4-1
2.4.1 Minimum Package Size 2.4-1
2.4.2 Tamper Indicating Feature 2.4-1
2.4.3 Positive Closure 2.4-1
2.4.4 Chemical and Galvanic Reactions 2.4-1
2.5 Lifting and Tie-down Standards for All Packages 2.5-1
2.5.1 Lifting Devices 2.5-1
2.5.2 Tie-down Devices 2.5-5
2.6 Normal Conditions of Transport 2.6-1
2.6.1 Heat 2.6-1
2.6.2 Cold 2.6-7
2.6.3 Reduced External Pressure 2.6-7
2.6.4 Increased External Pressure 2.6-7
2.6.5 Vibration 2.6-7
2.6.6 Water Spray 2.6-8
2.6.7 Free Drop 2.6-8
2.6.8 Corner Drop 2.6-39
2.6.9 Compression 2.6-39

2.6.10 Penetration 2.6-39
2.7 Hypothetical Accident Conditions 2.6-82
2.7.1 Free Drop 2.7-1
2.7.2 Crush 2.7-22
2.7.3 Puncture 2.7-23
2.7.4 Thermal 2.7-32
2.7.5 Immersion ï Fissile Material 2.7-35
2.7.6 Immersion ï All Packages 2.7-35
2.7.7 Deep Water Immersion Test 2.7-35
2.7.8 Summary of Damage 2.7-36
2.8 Special Form 2.7-78
2.9 Fuel Rods 2.9-1
2.10 Appendices 2.10-1
2.10.1 Finite Element Analysis (FEA) Models 2.10.1-1
2.10.2 Drop Analysis Codes Description 2.10.2-1
2.10.3 Drop Impact Evaluation Results 2.10.3-1
2.10.4 Slapdown Assessment 2.10.4-1
2.10.5 Buckling Design Criteria and Detailed Evaluation 2.10.5-9
2.10.6 Closure Bolt Stress Evaluations 2.10.6-1
2.10.7 Static and Dynamic Testing 2.10.7-1
2.10.8 Fabrication Stresses Due to Lead Pour 2.10.8-1

3.0 THERMAL EVALUATION 3.1-1
3.1 Discussion 3.1-1
3.1.1 Packaging Configuration 3.1-1
3.1.2 Payload Configurations 3.1-1
3.1.3 Boundary Conditions 3.1-2
3.1.4 Analysis Summary 3.1-3
3.2 Summary of Thermal Properties of Materials 3.2-1
3.3 Technical Specifications of Components 3.3-1
3.3.1 Packaging Components 3.3-1
3.3.2 Payload Canister Components 3.3-1
3.3.3 Payload Material 3.3-2
3.4 Thermal Evaluation for Normal Conditions of Transport 3.4-1
3.4.1 Thermal Model 3.4-1
3.4.2 Package Conditions and Environment 3.4-6
3.4.3 Maximum Temperatures 3.4-7

3.4.4 Minimum Temperatures 3.4-8
3.4.5 Maximum Internal Pressure 3.4-8
3.4.6 Maximum Thermal Stresses 3.4-14
3.4.7 Evaluation of Package Performance for Normal Conditions of Transport 3.4-14
3.5 Thermal Evaluation for Hypothetical Accident Conditions 3.5-1
3.5.1 Thermal Model 3.5-1
3.5.2 Package Conditions and Environment 3.5-2
3.5.3 Package Temperatures 3.5-4
3.5.4 Maximum Internal Pressure 3.5-4
3.5.5 Maximum Thermal Stresses 3.5-6
3.5.6 Evaluation of Package Performance for the Hypothetical Accident Thermal Conditions 3.5-6
3.6 Appendices 3.6-1
3.6.1 Thermal Model Details 3.6.1-1
3.6.2 Sensitivity Studies 3.6.2-1
3.6.3 Polyurethane Foam Performance Tests 3.6.3-1
3.6.4 Containment O-ring Seal Material Tests 3.6.4-1

4.0 CONTAINMENT 4.1-1
4.1 Containment Boundary 4.1-1
4.1.1 Containment Vessel 4.1-1
4.1.2 Containment Penetrations 4.1-3
4.1.3 Seals and Welds 4.1-3
4.1.4 Closure 4.1-4
4.2 Requirements for Normal Conditions of Transport 4.2-1
4.2.1 Containment of Radioactive Material 4.2-1
4.2.2 Pressurization of Containment Vessel 4.2-1
4.2.3 Containment Criterion 4.2-1
4.3 Containment Requirements for the Hypothetical Accident Conditions 4.3-1
4.3.1 Fission Gas Products 4.3-1
4.3.2 Containment of Radioactive Material 4.3-1
4.3.3 Containment Criterion 4.3-2

5.0 SHIELDING EVALUATION 5.1-1
5.1 Description of Shielding Design 5.1-1
5.1.1 Design Features 5.1-1
5.1.2 Summary Table of Maximum Radiation Levels 5.1-7
5.2 Source Specification 5.2-1

5.2.1 Gamma Source 5.2-1
5.2.2 Neutron Source 5.2-2
5.3 Shielding Model 5.3-1
5.3.1 Configuration of Source and Shielding 5.3-1
5.3.2 Material Properties 5.3-15
5.4 Shielding Evaluation 5.4-1
5.4.1 Methods 5.4-1
5.4.2 Input and Output Data 5.4-1
5.4.3 Flux-to-Dose Conversion 5.4-2
5.4.4 External Radiation Levels 5.4-3
5.5 Activity Limits 5.5-1
5.5.1 RH-TRU Waste Canister 5.5-3
5.5.2 NS15 Neutron Shielded Canister 5.5-7
5.5.3 NS30 Neutron Shielded Canister 5.5-11
5.5.4 Determination of Acceptable Activity 5.5-15
5.6 Conclusions 5.5-22
5.7 Appendices 5.7-1
5.7.1 Sample MCNP Input Files 5.7.1-1
5.7.2 Sample MCNP Output Files 5.7.2-1

6.0 CRITICALITY EVALUATION 6.1-1
6.1 Discussion of Results 6.1-2
6.2 Package Contents 6.2-1
6.2.1 Applicability of Case A Limits ï General Payload 6.2-1
6.2.2 Applicability of Case B Limits ï Special Reflector Payload 6.2-3
6.2.3 Applicability of Case C Limits ï Machine-Compacted Payload 6.2-3
6.2.4 Applicability of Case D Limits ï LEU Homogeneous Payload 6.2-4
6.2.5 Applicability of Case E Limits ï LEU Heterogeneous Payload 6.2-5
6.3 Model Specifications 6.3-1
6.3.1 Contents Models 6.3-1
6.3.2 Package Model 6.3-4
6.3.3 Single Package Models 6.3-6
6.3.4 Array Models 6.3-6
6.3.5 Package Regional Densities 6.3-6
6.4 Criticality Calculations 6.4-1
6.4.1 Calculational or Experimental Method 6.4-1
6.4.2 Fuel Loading or Other Contents Loading Assumptions 6.4-2

6.4.3 Criticality Results 6.4-2
6.5 Critical Benchmark Experiments 6.5-1
6.5.1 Benchmark Experiments and Applicability 6.5-1
6.5.2 Details of Benchmark Calculations 6.5-3
6.5.3 Results of Benchmark Calculations 6.5-4
6.6 Appendices 6.6-1
6.6.1 KENO-V.a Input Files for the Criticality Analyses 6.6.1-1

7.0 OPERATING PROCEDURES 7.1-1
7.1 Procedures for Loading the Package 7.1-1
7.1.1 Loading the Payload Canister 7.1-1
7.1.2 Loading the RH-TRU 72-B Package 7.1-1
7.2 Procedures for Unloading the Package 7.2-1
7.3 Preparation of an Empty Package for Transport 7.3-1
7.3.1 Shipment of the Package as LSA Material 7.3-1
7.4 Appendices 7.4-1
7.4.1 Preshipment Leakage Rate Test 7.4.1-1

8.0 ACCEPTANCE TESTS AND MAINTENANCE PROGRAM 8.1-1
8.1 Acceptance Tests 8.1-1
8.1.1 Visual Inspection 8.1-1
8.1.2 Structural and Pressure Tests 8.1-1
8.1.3 Fabrication Leakage Rate Tests 8.1-2
8.1.4 Component Tests 8.1-9
8.1.5 Tests for Shielding Integrity 8.1-17
8.1.6 Thermal Acceptance Tests 8.1-18
8.1.7 Lead Installation Tests 8.1-18
8.2 Maintenance Program 8.2-1
8.2.1 Structural and Pressure Tests 8.2-1
8.2.2 Maintenance/Periodic Leakage Rate Tests 8.2-2
8.2.3 Subsystems Maintenance 8.2-7
8.2.4 Valves, Rupture Discs, and Gaskets 8.2-8
8.2.5 Shielding 8.2-8
8.2.6 Thermal 8.2-9
8.2.7 Criticality Control Materials 8.2-9
8.3 Appendices 8.3-1
8.3.1 Lead Installation Procedure 8.3.1-1

9.0 QUALITY ASSURANCE 9.1-1
9.1 Introduction 9.1-1
9.2 Quality Assurance Requirements 9.2-1
9.2.1 U.S. Nuclear Regulatory Commission 9.2-1
9.2.2 U.S. Department of Energy 9.2-1
9.2.3 Transportation to/from WIPP 9.2-1
9.3 Quality Assurance Program 9.3-1
9.3.1 NRC Regulatory Guide 7.10 ..... 9.3-1
9.3.2 Design 9.3-1
9.3.3 Procurement, Fabrication, Assembly, Testing, and Modificaton 9.3-1
9.3.4 Use 9.3-1
9.3.5 Maintenance and Repair 9.3-2

LIST OF TABLES

Table 1.2-1 ï Overall Component Weights 1.2-8
Table 2.1-1 ï Containment Components Allowable Stress Limits 2.1-8
Table 2.1-2 ï Non-Containment Components Allowable Stress Limits 2.1-9
Table 2.1-3 ï Shell Buckling Geometries 2.1-9
Table 2.2-1 ï RH-TRU 72-B Package Component Weights, Centers of Gravity, and Mass Moments of Inertia 2.2-2
Table 2.3-1 ï Mechanical Properties of Steel Used in the RH-TRU 72-B Package 2.3-3
Table 2.3-2 ï Mechanical Properties of Lead Used in the RH-TRU 72-B Package 2.3-4
Table 2.3-3 ï Crush Stress vs. Strain for 11Ï lb/ftę Nominal Density Polyurethane Foam 2.3-4
Table 2.5-1 ï Material Properties for Type 304 Stainless Steel at 153 ÜF 2.5-13
Table 2.5-2 ï Data Used in Tie-down Trunnion Lifting Stress Analysis 2.5-14
Table 2.5-3 ï Trunnion Stress Analysis for a Vertical Lift 2.5-15
Table 2.5-4 ï Trunnion Stress Analysis for a Horizontal Lift 2.5-16
Table 2.6-1 ï Summary of NCT Material Properties for Analysis 2.6-40
Table 2.6-2 ï Maximum NCT Temperatures 2.6-41
Table 2.6-3 ï Package Parameters for Pressure Stress Calculations 2.6-41
Table 2.6-4 ï Unit Pressure Stress Results for P1 ï P6 ..... 2.6-42
Table 2.6-5 ï Unit Pressure Stress Results for P7 ï P10 ..... 2.6-42
Table 2.6-6 ï Maximum Pressure Stress Results for P1 ï P10 ..... 2.6-42
Table 2.6-7 ï Package Stresses Due to Side Drop 2.6-43

Table 2.6-8 – NCT End Drop, OC Lid Bending 2.6-43
Table 2.6-9 – NCT Top-End Drop, IV Shell with 42.5*g* Acceleration 2.6-44
Table 2.6-10 – NCT Bottom-End Drop, IV Shell with 42.5*g* Acceleration 2.6-44
Table 2.6-11 – Fabrication Induced OC Inner Shell Hoop Stress, Interface Pressure, and Axial Load That Can Be Supported 2.6-45
Table 2.6-12 – OC Shell Stresses with Maximum End Drop Fab Condition 2.6-45
Table 2.6-13 – NCT Fab & End Drop, OC Inner Shell with 42.5*g* at -20 °F 2.6-45
Table 2.6-14 – NCT Fab & End Drop, OC Inner Shell with 42.5*g* at 70 °F 2.6-46
Table 2.6-15 – NCT Fab & End Drop, OC Inner Shell with 42.5*g* at 160 °F 2.6-46
Table 2.6-16 – NCT End Drop, Lead Pressure and Hoop Stress Summary 2.6-47
Table 2.6-17 – NCT End Drop, OC Shell Stresses with Zero Fabrication Condition with 42.5*g* Acceleration 2.6-47
Table 2.6-18 – NCT End Drop, OC Inner Shell with 42.5*g* at -20 °F 2.6-47
Table 2.6-19 – NCT End Drop, OC Inner Shell with 42.5*g* at 70 °F 2.6-48
Table 2.6-20 – NCT End Drop, OC Inner Shell with 42.5*g* at 160 °F 2.6-48
Table 2.6-21 – NCT Temperature-Corrected Margin of Safety Against Lead Slump 2.6-49
Table 2.6-22 – OC Shell Stresses with Max Oblique Drop Fab Condition 2.6-49
Table 2.6-23 – NCT Fab & Oblique Drop, OC Inner Shell with 17.9*g* at -20 °F 2.6-49
Table 2.6-24 – NCT Fab & Oblique Drop, OC Inner Shell with 17.9*g* at 70 °F 2.6-50
Table 2.6-25 – NCT Fab & Oblique Drop, OC Inner Shell with 17.9*g* at 160 °F 2.6-50
Table 2.6-26 – NCT Oblique Drop, IV Shell with 17.9*g* at 70 °F 2.6-51
Table 2.6-27 – NCT Oblique Drop, Canister Shell with 17.9*g* at 210 °F 2.6-51
Table 2.6-28 – OC Shell Stresses with Max Side Drop Fab Condition 2.6-52
Table 2.6-29 – NCT Fab & Side Drop, OC Inner Shell with 19.3*g* at -20 °F 2.6-52
Table 2.6-30 – NCT Fab & Side Drop, OC Inner Shell with 19.3*g* at 70 °F 2.6-53
Table 2.6-31 – NCT Fab & Side Drop, OC Inner Shell with 19.3*g* at 160 °F 2.6-53
Table 2.6-32 – NCT Side Drop, IV Shell with 19.3*g* at 160 °F 2.6-54
Table 2.6-33 – NCT Side Drop, Canister Shell with 19.3*g* at 210 °F 2.6-54
Table 2.6-34 – NCT Fab & Side Drop, OC Shells’ Welds with 19.3*g* at -20 °F 2.6-55
Table 2.7-1 – Summary of HAC Material Properties for Analysis 2.7-37
Table 2.7-2 – Fabrication Induced OC Inner Shell Hoop Stress, Interface Pressure, and Axial Load That Can Be Supported 2.7-38
Table 2.7-3 – OC Shell Stresses with Maximum End Drop Fab Condition 2.7-38

Table 2.7-4 – HAC Fab & End Drop, OC Inner Shell with 89.7*g* at -20 °F 2.7-38
Table 2.7-5 – HAC Fab & End Drop, OC Inner Shell with 89.7*g* at 70 °F 2.7-39
Table 2.7-6 – HAC Fab & End Drop, OC Inner Shell with 89.7*g* at 160 °F 2.7-39
Table 2.7-7 – HAC End Drop, Lead Pressure and Hoop Stress Summary 2.7-40
Table 2.7-8 – HAC End Drop, OC Shell Stresses with Zero Fabrication Condition with 89.7*g* Acceleration 2.7-40
Table 2.7-9 – HAC End Drop, OC Inner Shell with 89.7*g* at -20 °F 2.7-40
Table 2.7-10 – HAC End Drop, OC Inner Shell with 89.7*g* at 70 °F 2.7-41
Table 2.7-11 – HAC End Drop, OC Inner Shell with 89.7*g* at 160 °F 2.7-41
Table 2.7-12 – HAC Temperature-Corrected Margin of Safety Against Lead Slump 2.7-42
Table 2.7-13 – OC Shell Stresses with Max Oblique Drop Fab Condition 2.7-42
Table 2.7-14 – HAC Fab & Oblique Drop, OC Inner Shell with 48.1*g* at -20 °F 2.7-42
Table 2.7-15 – HAC Fab & Oblique Drop, OC Inner Shell with 48.1*g* at 70 °F 2.7-43
Table 2.7-16 – HAC Fab & Oblique Drop, OC Inner Shell with 48.1*g* at 160 °F 2.7-43
Table 2.7-17 – HAC Oblique Drop, IV Shell with 48.1*g* at 70 °F 2.7-44
Table 2.7-18 – HAC Oblique Drop, Canister Shell with 48.1*g* at 210 °F 2.7-44
Table 2.7-19 – OC Shell Stresses with Max Side Drop Fab Condition 2.7-45
Table 2.7-20 – HAC Fab & Side Drop, OC Inner Shell with 81.2*g* at -20 °F 2.7-45
Table 2.7-21 – HAC Fab & Side Drop, OC Inner Shell with 81.2*g* at 70 °F 2.7-46
Table 2.7-22 – HAC Fab & Side Drop, OC Inner Shell with 81.2*g* at 160 °F 2.7-46
Table 2.7-23 – HAC Side Drop, IV Shell with 81.2*g* at 160 °F 2.7-47
Table 2.7-24 – HAC Side Drop, Canister Shell with 81.2*g* at 210 °F 2.7-47
Table 2.7-25 – HAC Fab & Side Drop, OC Shells‐Welds with 81.2*g* at -20 °F 2.7-48
Table 2.7-26 – Stress-Strain Values for Type 304 Stainless Steel at 212 °F 2.7-48
Table 2.7-27 – Stresses Due to 300 psig Pressure 2.7-49
Table 2.7-28 – Thermal Stress Summary 2.7-49
Table 2.7-29 – Buckling Geometry Parameters per Code Case N-284 ..... 2.7-50
Table 2.7-30 – Stresses for 290 psig External Pressure + Fabrication 2.7-50
Table 2.7-31 – Buckling Summary for 290 psig External Pressure + Fab 2.7-51
Table 2.10.1-1 – Input Listing for Trunnion Loading the OC Outer Shell 2.10.1-3
Table 2.10.1-2 – Input Listing for IV Radius Transition Zone Stresses Due to Pressure 2.10.1-11

Table 2.10.1-3 – Input Listing for IV Radius Transition Zone Stresses Due to 1*g* Acceleration 2.10.1-15
Table 2.10.1-4 – Containment Assembly Node and Element Numbering 2.10.1-20
Table 2.10.1-5 – Input Listing for OC Bottom Stresses Due to Puncture 2.10.1-22
Table 2.10.2-1 – CASKDROP Sample Problem Output Files 2.10.2-7
Table 2.10.2-2 – Sample Inputs to the SLAPDOWN Program 2.10.2-13
Table 2.10.2-3 – Sample Force-Deflection to the SLAPDOWN Program 2.10.2-13
Table 2.10.2-4 – Sample of SLAPDOWN General Output 2.10.2-14
Table 2.10.2-5 – Sample of SLAPDOWN Time History Output 2.10.2-15
Table 2.10.2-6 – Comparison of SLAPDOWN and SCANS Results 2.10.2-16
Table 2.10.3-1 – Polyurethane Foam Data used in CASKDROP 2.10.3-3
Table 2.10.3-2 – CASKDROP Output File for NCT End Drop, Cold (-20 °F) 2.10.3-4
Table 2.10.3-3 – CASKDROP Output File for NCT End Drop, Warm (140 °F) 2.10.3-5
Table 2.10.3-4 – CASKDROP Output File for NCT Side Drop, Cold (-20 °F) 2.10.3-6
Table 2.10.3-5 – CASKDROP Output File for NCT Side Drop, Warm (140 °F) 2.10.3-7
Table 2.10.3-6 – CASKDROP Output File for HAC End Drop, Cold (-20 °F) 2.10.3-8
Table 2.10.3-7 – CASKDROP Output File for HAC End Drop, Warm (140 °F) 2.10.3-9
Table 2.10.3-8 – CASKDROP Output File for HAC Side Drop, Cold (-20 °F) 2.10.3-10
Table 2.10.3-9 – CASKDROP Output File for HAC Side Drop, Warm (140 °F) 2.10.3-11
Table 2.10.3-10 – Summary of End and Side Drop Impact Accelerations and Impact Limiter Deflections 2.10.3-12
Table 2.10.3-11 – Maximum Package Responses as a Function of Initial Impact Angle (-20 °F Cases) 2.10.3-13
Table 2.10.3-12 – Maximum Package Responses as a Function of Initial Impact Angle (140 °F Cases) 2.10.3-14
Table 2.10.3-13 – Summary of Impact Limiter Separation Moments 2.10.3-15
Table 2.10.3-14 – Time-History Details from the Maximum Impact Force Condition SLAPDOWN Analyses (NCT, -20 °F, 1-foot Drop) 2.10.3-15
Table 2.10.3-15 – Time-History Details from the Maximum Impact Force Condition SLAPDOWN Analyses (HAC, -20 °F, 30-foot Drop) 2.10.3-16
Table 2.10.4-1 – Impact Force and Maximum Deflections for Cold (-20 °F) HAC Slapdown Cases 2.10.4-3
Table 2.10.4-2 – Impact Force and Maximum Deflections for Warm (140 °F) HAC Slapdown Cases 2.10.4-3

Table 2.10.4-3 ï Force-Deflection Data for Cold (-20 ÜF) and Warm (140 ÜF) HAC 0Ü Slapdowns 2.10.4-4
Table 2.10.4-4 ï Shear and Moment During Slapdown 2.10.4-5
Table 2.10.4-5 ï Thrust and Moment Due to HAC Cold (-20 ÜF) Slapdown Cases 2.10.4-5
Table 2.10.4-6 ï Thrust and Moment Due to HAC Warm (140 ÜF) Slapdown Cases 2.10.4-5
Table 2.10.4-7 ï Stresses and Margins of Safety Due to HAC Cold (-20 ÜF) Slapdown 2.10.4-6
Table 2.10.4-8 ï Stresses and Margins of Safety Due to HAC Warm (140 ÜF) Slapdown . 2.10.4-6
Table 2.10.4-9 ï Comparison of Allowable and Predicted Deformations for Warm (140 ÜF) Slapdown 2.10.4-6
Table 2.10.5-1 ï Geometry, Geometric Parameters, and Material Data Used in Buckling Evaluations 2.10.5-18
Table 2.10.5-2 ï Temperature Dependent Material Properties for Type 304 Stainless Steel 2.10.5-18
Table 2.10.5-3 ï Theoretical Elastic Buckling Stress Values (General Temperature Independent Form) 2.10.5-19
Table 2.10.5-4 ï Temperature Dependent Theoretical Elastic Buckling Stresses for Each RH-TRU 72-B Package Shell 2.10.5-19
Table 2.10.5-5 ï Temperature Dependent Capacity Reduction Factors 2.10.5-20
Table 2.10.5-6 ï Upper Bounds for Compressive Stresses and In-Plane Shear Stresses .. 2.10.5-20
Table 2.10.5-7 ï Compressive Membrane and In-Plane Shear Stress Summary for the Outer Cask Inner Shell 2.10.5-20
Table 2.10.5-8 ï Compressive Membrane and In-Plane Shear Stress Summary for the Outer Cask Outer Shell 2.10.5-21
Table 2.10.5-9 ï Compressive Membrane and In-Plane Shear Stress Summary for the Inner Vessel 2.10.5-22
Table 2.10.5-10 ï Worst-Case Load Combinations for the Outer Cask Inner Shell 2.10.5-23
Table 2.10.5-11 ï Worst-Case Load Combinations for the Outer Cask Outer Shell 2.10.5-23
Table 2.10.5-12 ï Worst-Case Load Combinations for the Inner Vessel 2.10.5-24
Table 2.10.5-13 ï Interaction Equation Checks 2.10.5-25
Table 2.10.6-1 ï Outer Cask NCT Bolt Stresses, Torque Coefficient = 0.13 ..... 2.10.6-9
Table 2.10.6-2 ï Outer Cask NCT Bolt Stresses, Torque Coefficient = 0.20 ..... 2.10.6-10
Table 2.10.6-3 ï Inner Vessel NCT Bolt Stresses, Torque Coefficient = 0.13 ..... 2.10.6-11
Table 2.10.6-4 ï Inner Vessel NCT Bolt Stresses, Torque Coefficient = 0.20 ..... 2.10.6-12
Table 2.10.6-5 ï Outer Cask HAC Bolt Stresses, Torque Coefficient = 0.13 ..... 2.10.6-13
Table 2.10.6-6 ï Outer Cask HAC Bolt Stresses, Torque Coefficient = 0.20 ..... 2.10.6-14

Table 2.10.6-7 – Inner Vessel HAC Bolt Stresses, Torque Coefficient = 0.13 ..... 2.10.6-15
Table 2.10.6-8 – Inner Vessel HAC Bolt Stresses, Torque Coefficient = 0.20 ..... 2.10.6-16
Table 2.10.7-1 – Static Crush Test Summary 2.10.7-13
Table 2.10.7-2 – Static Test Article Stress-Strain Properties 2.10.7-13
Table 2.10.7-3 – End Crush CASKDROP Output 2.10.7-14
Table 2.10.7-4 – Side Crush CASKDROP Output 2.10.7-15
Table 2.10.7-5 – Oblique Crush CASKDROP Output 2.10.7-16
Table 2.10.7-6 – Dynamic Drop Test Summary 2.10.7-17
Table 2.10.7-7 – Dynamic Test Article Stress-Strain Properties 2.10.7-17
Table 2.10.7-8 – End Drop CASKDROP Output 2.10.7-18
Table 2.10.7-9 – Side Drop CASKDROP Output 2.10.7-19
Table 2.10.7-10 – Oblique Drop CASKDROP Output 2.10.7-20
Table 2.10.7-11 – Oblique Drop SLAPDOWN Output 2.10.7-21
Table 2.10.7-12 – Free Drop Test Result Summary 2.10.7-22
Table 2.10.8-1 – Mechanical Properties of Stainless Steel (Type 304) 2.10.8-11
Table 2.10.8-2 – Mechanical Properties of Lead (Copperized) 2.10.8-11
Table 2.10.8-3 – Steel Shell Geometry at 70 °F 2.10.8-11
Table 2.10.8-4 – Initial Shell Conditions Before Lead Solidification 2.10.8-11
Table 2.10.8-5 – Stress-Free OC Inner Shell Dimensions 2.10.8-12
Table 3.1-1 – Maximum NCT Temperatures with Insolation (°F) 3.1-4
Table 3.1-2 – Maximum HAC Fire Transient Temperatures (°F) 3.1-5
Table 3.2-1 – Thermophysical Properties of Air at One Atmosphere 3.2-3
Table 3.2-2 – Thermophysical Properties of Type 304 Stainless Steel 3.2-4
Table 3.2-3 – Thermophysical Properties of Carbon Steel 3.2-5
Table 3.2-4 – Thermophysical Properties of ASTM B29 Lead 3.2-6
Table 3.2-5 – Thermophysical Properties of the Thermal Shield Gap 3.2-7
Table 3.2-6 – Thermophysical Properties of High-Density Polyethylene (HDPE) 3.2-8
Table 3.2-7 – Thermophysical Properties of 11 lb/ft³ Polyurethane Foam 3.2-8
Table 3.2-8 – Thermophysical Properties of the Payload Material 3.2-9
Table 3.2-9 – Optical Properties of Package Materials 3.2-10
Table 3.4-1 – Total Insolation for a 12-Hour Period 3.4-6
Table 3.4-2 – Maximum NCT Temperatures without Insolation (°F) 3.4-15
Table 3.4-3 – Maximum NCT Temperatures with Insolation (°F) 3.4-16

Table 3.4-4 ï Equation Coefficients for NCT Temperatures (ÜF) Based on Decay Heat Load (W) 3.4-17

Table 3.5-1 ï HAC Pre-Fire Steady State Temperatures with Insolation (ÜF) 3.5-8

Table 3.5-2 ï HAC Fire Temperatures (T) and Time (t) After End-of-Fire 3.5-9

Table 3.5-3 ï HAC Post-Fire Steady State Temperatures with Insolation (ÜF) 3.5-10

Table 3.5-4 ï Temperature-Dependent Physical Properties of Type 304 Stainless Steel 3.5-11

Table 3.6.1-1 ï Calculated and Adjusted Maximum Decay Heat vs. Payload Density 3.6.1-7

Table 3.6.1-2 ï Maximum HAC Temperatures (ÜF) with Insolation for Various Payload Configurations with a Constant Payload Mass of 600 Pounds and Proportional Density, and Decay Heat Adjusted to the Maximum Calculated Limit 3.6.1-8

Table 3.6.2-1 ï Maximum NCT Temperatures (ÜF) for the Baseline vs. High-Resolution RLC Models with 12 lb/ftį Payload Density and 90 Watts of Decay Heat 3.6.2-5

Table 3.6.2-2 ï Maximum NCT Temperatures (ÜF) for Centered vs. Axially-Shifted RLC Models with 12 lb/ftį Payload Density and 90 Watts of Decay Heat 3.6.2-6

Table 3.6.2-3 ï Maximum HAC Temperatures (ÜF) for Centered vs. Radially-Shifted RLC Models with 12 lb/ftį Payload Density and 90 Watts of Decay Heat 3.6.2-7

Table 3.6.2-4 ï HAC Pre-Fire and HAC Fire/Post-Fire Internal Convection Coefficient Calculations 3.6.2-8

Table 3.6.2-5 ï HAC Pre-Fire Steady State Temperatures with Insolation (ÜF) for an RLC with 30-Gallon Drums Containing a 100 lb/ftį Payload with 270 Watts Decay Heat; without and with Internal Convection 3.6.2-9

Table 3.6.2-6 ï HAC Fire Transient Temperatures (T) and Time (t) after End-of-Fire for an RLC with 30-Gallon Drums Containing a 100 lb/ftį Payload with 270 Watts Decay Heat; without and with Internal Convection 3.6.2-10

Table 3.6.4-1 ï Formulation Qualification Test O-ring Seal Compression and Temperature Parameters 3.6.4-4

Table 3.6.4-2 ï Rainier Rubber R0405-70 Formulation Qualification O-ring Seal Test Results 3.6.4-9

Table 5.1-1 ï RH-TRU 72-B with RH-TRU Waste Canister Summary of Maximum Dose Rates (mrem/hr) 5.1-7

Table 5.1-2 ï RH-TRU 72-B with NS15 Neutron Shielded Canister Summary of Maximum Dose Rates (mrem/hr) 5.1-7

Table 5.1-3 ï RH-TRU 72-B with NS30 Neutron Shielded Canister Summary of Maximum Dose Rates (mrem/hr) 5.1-8

Table 5.3-1 ï Summary of Shield Regional Densities 5.3-15

Table 5.4-1 ï Case Naming Conventions 5.4-2

Table 5.4-2 ï Neutron Flux-to-Dose Rate Conversion Factors from ANSI/ANS-6.1.1-1977 ..... 5.4-2

Table 5.4-3 ï Gamma Flux-to-Dose Rate Conversion Factors from ANSI/ANS-6.1.1-1977 .... 5.4-3
Table 5.4-4 ï RH-TRU 72-B ï RH-TRU Waste Canister Dose Rates for 1 par/s Source 5.4-4
Table 5.4-5 ï RH-TRU 72-B ï NS15 Neutron Shielded Canister Dose Rates for 1 par/s Source 5.4-5
Table 5.4-6 ï RH-TRU 72-B ï NS30 Neutron Shielded Canister Dose Rates for 1 par/s Source 5.4-5
Table 5.5-1 ï Discrete Gamma and Neutron Energies 5.5-2
Table 5.5-2 ï RH-TRU 72-B ï RH-TRU Waste Canister Gamma Activity Limits 5.5-4
Table 5.5-3 ï RH-TRU 72-B ï RH-TRU Waste Canister Neutron Activity Limits 5.5-5
Table 5.5-4 ï RH-TRU 72-B ï NS15 Neutron Shielded Canister Gamma Activity Limits 5.5-8
Table 5.5-5 ï RH-TRU 72-B ï NS15 Neutron Shielded Canister Neutron Activity Limits 5.5-9
Table 5.5-6 ï RH-TRU 72-B ï NS30 Neutron Shielded Canister Gamma Activity Limits .. 5.5-12
Table 5.5-7 ï RH-TRU 72-B ï NS30 Neutron Shielded Canister Neutron Activity Limits .. 5.5-13
Table 5.5-8 ï Acceptable Activity Example #1 ..... 5.5-17
Table 5.5-9 ï Acceptable Activity Example #2 ..... 5.5-19
Table 5.5-10 ï Acceptable Activity Example #3 ..... 5.5-21
Table 6.1-1 ï Fissile Material Limit per RH-TRU 72-B Package 6.1-4
Table 6.1-2 ï Summary of Criticality Analysis Results 6.1-5
Table 6.2-1 ï Special Reflector Material Parameters that Achieve the Reactivity of a 25%/75% Polyethylene/Water Mixture Reflector 6.2-6
Table 6.3-1 ï Fissile Contents Model Properties for 315 g Pu Spheres (Case A)Φ 6.3-9
Table 6.3-2 ï Fissile Contents Model Properties for Various Pu Spheres with Pu-240 Added as Indicated (Case A)Φ 6.3-10
Table 6.3-3 ï Fissile Contents Model Properties for 100 g Pu Spheres (Case B) 6.3-11
Table 6.3-4 ï Fissile Contents Model Properties for 245 g Pu Spheres (Case C) 6.3-13
Table 6.3-5 ï Fissile Contents Model Properties for 0.96 wt% U-235 FEM (Case D) 6.3-13
Table 6.3-6 ï Fissile Contents Model Properties for 0.96 wt% U-235 FEM (Case D with Variable Beryllium Moderator and H/U-235=500) 6.3-14
Table 6.3-7 ï Fissile Contents Model Properties Cylindrical Arrays of Cylinders (Rods) for 0.84 wt% U-235 FEM (Case E) 6.3-15
Table 6.3-8 ï Fissile Contents Model Properties Cylindrical Arrays of Spheres for 0.84 wt% U-235 FEM (Case E) 6.3-16
Table 6.3-9 ï Fissile Contents Model Properties Special Reflector Studies Yielding Adjusted Height at 0.84 wt% U-235 FEM (Case E) 6.3-17
Table 6.3-10 ï Structural Model Properties for the RH-TRU 72-B Package (All Cases) 6.3-19

Table 6.3-11 ï Reflector Model Properties for the RH-TRU 72-B Package by Case 6.3-20

Table 6.4-1 ï Single-Unit, NCT and HAC, Case A, Sphere Centered, 315 FGE, k_s vs. H/Pu Ratio with Different Moderator/Reflector Combinations 6.4-14

Table 6.4-2 ï Single-Unit, NCT and HAC, Case A, Sphere Top and Radially Displaced, 315 FGE, H/Pu at 900, k_s vs. Variable Interspersed Moderation Volume Fraction in the IV 6.4-15

Table 6.4-3 ï Infinite-Unit, NCT and HAC, Case A, Sphere Top and Radially Displaced, 315 FGE, k_s vs. H/Pu Ratio with Different Moderator/Interspersed Moderator Combinations 6.4-16

Table 6.4-4 ï Infinite-Unit, NCT and HAC, Case A, Sphere Top and Radially Displaced, 315 FGE, k_s vs. Variable Interspersed Moderator at H/Pu Ratios of Interest 6.4-17

Table 6.4-5 ï Infinite-Unit, NCT and HAC, Case A, Sphere Top and Radially Displaced, k_s vs. H/Pu Ratio for Limiting Pu-240/Pu-239 Combinations with Optimum Moderator/Reflector 6.4-18

Table 6.4-6 ï Infinite-Unit, NCT and HAC, Case B, Sphere Centered, 100 FGE, k_s vs. H/Pu Ratio with Different Reflector Conditions 6.4-19

Table 6.4-7 ï Infinite-Unit, NCT and HAC, Case B, Sphere Centered, 100 FGE, k_s vs. H/Pu Ratio with Different Moderator Conditions in 100% Be Reflector 6.4-20

Table 6.4-8 ï Infinite-Unit, NCT and HAC, Case B, Sphere Centered, 305 FGE, k_s vs. H/Pu Ratio with the Indicated Moderator Conditions 6.4-22

Table 6.4-9 ï Infinite Unit, NCT and HAC, Case C, Sphere Top Side, 245 FGE, k_s vs. H/Pu Ratio with Different Moderator/Reflector Combinations 6.4-24

Table 6.4-10 ï Single-Unit, NCT and HAC, Case D, Cylindrical Fissile Region, 0.96 wt% U-235 FEM, k_s vs. H/U-235 Ratio 6.4-24

Table 6.4-11 ï Infinite-Unit, NCT and HAC, Case D, Cylindrical Fissile Region, 0.96 wt% U-235, k_s vs. H/U-235 Ratio and Variable Density Interspersed Moderation Conditions 6.4-25

Table 6.4-12 ï Single-Unit, NCT and HAC, Case D, Be Reflected, Cylindrical Fissile Region, 0.96 wt% U-235 FEM, k_s vs. H/U-235 Ratio 6.4-26

Table 6.4-13 ï Infinite-Unit, NCT and HAC, Case D, Be Reflected, Short, Squat, Cylindrical Fissile Region, 0.96 wt% U-235 FEM, k_s vs. H/U-235 Ratio and Variable Interspersed Moderation Between Packages 6.4-27

Table 6.4-14 ï Infinite-Unit, NCT and HAC, Case D, Be Reflected, Short, Squat, Cylindrical Fissile Region, 0.96 wt% U-235 FEM, Moderated to H/U-235=500, k_s vs. Be in Moderator 6.4-28

Table 6.4-15 ï Single-Unit, NCT and HAC, Case E, Cylindrical Array Fissile Region, 0.84 wt% ^{235}U FEM, k_s vs. H/^{235}U Ratio (and Array Pitch) for Arrays of Cylinders and Spheres (most reactive element diameter of 1.25 cm) 6.4-29

Table 6.4-16 ï Infinite-Unit, NCT and HAC, Case E, Cylindrical Fissile Region, 0.84 wt% ^{235}U, k_s vs. H/^{235}U Ratio and Variable Density Interspersed Moderation Conditions 6.4-30

Table 6.4-17 ï Single-Unit, NCT and HAC, Case E, Cylindrical Array Fissile Region, 0.84 wt% ^{235}U FEM with Unlimited Special Reflector at 1, 2, 4, 8, 16, and 32 30 cm, k_s vs. Array Pitch for Arrays of Cylinders (most reactive element diameter of 1.25 cm)..... 6.4-32

Table 6.4-18 ï Infinite-Unit, NCT and HAC, Case E, Cylindrical Fissile Region, 0.84 wt% ^{235}U, k_s vs. H/^{235}U Ratio with Unlimited Special Reflector at 30 cm for Arrays of Spheres (most reactive element diameter of 1.25 cm)..... 6.4-34

Table 6.4-19 ï Single-Unit, NCT and HAC, Case E, Cylindrical Array Fissile Region, 0.84 wt% ^{235}U FEM with Unlimited Special Reflector Interspersed in the Moderator/Reflector Regions, k_s vs. Be Concentration at Various Array Pitches for Arrays of Spheres (most reactive element diameter of 1.25 cm)..... 6.4-35

Table 6.4-20 ï Infinite-Unit, NCT and HAC, Case E, Cylindrical Fissile Region, 0.84 wt% ^{235}U, k_s vs. H/^{235}U Ratio with Unlimited Special Reflector Interspersed in the Moderator/Reflector Regions, k_s vs. Be Volume % at 1.25 cm Array Pitch for Arrays of Cylinders (most reactive element diameter of 1.25 cm)..... 6.4-38

Table 6.4-21 ï Fissile Payload Limits 6.4-39

Table 6.5-1 ï ^{239}Pu Benchmark Experiment Description 6.5-7

Table 6.5-2 ï ^{239}Pu Benchmark Case Parameters and Computed Results..... 6.5-8

Table 6.5-3 ï Calculation of Pu-239 USL with Be..... 6.5-16

Table 6.5-4 ï Low Enriched U-235 Benchmark Experiment Description 6.5-16

Table 6.5-5 ï Low Enriched U-235 Benchmark Case Parameters, Computed Results and Reported Experimental Benchmark Uncertainty 6.5-17

Table 6.5-6 ï SCALE 5.1 LEU and Be Benchmark Case Parameters, Computed Results and Reported Experimental Benchmark Uncertainty 6.5-20

Table 6.5-7 ï Calculation of Low Enriched U-235 USL..... 6.5-24

Table 8.1-1 ï Compressive Stress Ranges at Room Temperature (psi) 8.1-18

LIST OF FIGURES

Figure 1.1-1 ï RH-TRU 72-B Package..... 1.1-3

Figure 1.1-2 ï RH-TRU 72-B Package Components 1.1-4

Figure 1.1-3 ï View of the RH-TRU 72-B Closure Regions 1.1-5

Figure 1.2-1 ï Inner Vessel Containment Components..... 1.2-9

Figure 1.2-2 ï Outer Cask Containment Components..... 1.2-10

Figure 2.2-1 ï RH-TRU 72-B Package Component Weight Breakdown..... 2.2-3

Figure 2.3-1 ï True Stress/Strain for Type 304 Stainless at 212 ŰF 2.3-5

Figure 2.3-2 ï Crush Stress vs. Strain for 11Ï lb/ftį Nominal Density Polyurethane Foam ... 2.3-6

Figure 2.3-3 ï Tensile Curves at a Strain Rate of 0.05 in/in/min 2.3-7

Figure 2.3-4 ï Strain Rate Effects on Tensile Curves at 100 ÜF and 250 ÜF 2.3-7
Figure 2.3-5 ï Tensile Curves at a Strain Rate of 0.005 in/in/min 2.3-8
Figure 2.3-6 ï Compression Curves at a Strain Rate of 0.005 in/in/min 2.3-8
Figure 2.3-7 ï Total Strain vs. Creep Time 2.3-9
Figure 2.3-8 ï Stress vs. Creep Time Curves 2.3-10
Figure 2.5-1 ï Lifting Trunnion Geometry 2.5-17
Figure 2.5-2 ï Horizontal Lift Loading Configuration 2.5-17
Figure 2.5-3 ï Attachment Loads for WRC Bulletin 107 ..... 2.5-18
Figure 2.5-4 ï Figure 1A from WRC Bulletin 107 ..... 2.5-19
Figure 2.5-5 ï Figure 2A from WRC Bulletin 107 ..... 2.5-20
Figure 2.5-6 ï Figure 3A from WRC Bulletin 107 ..... 2.5-21
Figure 2.5-7 ï Figure 4A from WRC Bulletin 107 ..... 2.5-22
Figure 2.5-8 ï Figure 1B from WRC Bulletin 107 ..... 2.5-23
Figure 2.5-9 ï Figure 1B-1 from WRC Bulletin 107 ..... 2.5-24
Figure 2.5-10 ï Figure 2B from WRC Bulletin 107 ..... 2.5-25
Figure 2.5-11 ï Figure 2B-1 from WRC Bulletin 107 ..... 2.5-26
Figure 2.5-12 ï Figure 3B from WRC Bulletin 107 ..... 2.5-27
Figure 2.5-13 ï Figure 4B from WRC Bulletin 107 ..... 2.5-28
Figure 2.5-14 ï Lifting Trunnion Weld Evaluation 2.5-29
Figure 2.5-15 ï Center-Pivot Trailer Configuration 2.5-29
Figure 2.5-16 ï Lift-Off Trailer Configuration 2.5-30
Figure 2.5-17 ï Center-Pivot Trunnion Loading Configuration 2.5-30
Figure 2.5-18 ï Tie-down Loading Configuration 2.5-31
Figure 2.5-19 ï Center-Pivot Trailer Free-Body Diagram for Tie-down 2.5-31
Figure 2.5-20 ï Lift-Off Trailer Free-Body Diagram for Tie-down 2.5-32
Figure 2.6-1 ï Package Locations for Pressure Stress Calculations 2.6-56
Figure 2.6-2 ï Figure I-9.2.2 from Appendix I of the ASME Code 2.6-57
Figure 2.6-3 ï Free-Body Diagrams of Axial Forces in OC Components 2.6-58
Figure 2.6-4 ï OC Bottom-End Plate Configuration 2.6-59
Figure 2.6-5 ï Axial Pressure Distribution Due to Lead 2.6-60
Figure 2.6-6 ï NCT Cold (-20 ÜF) Outer Cask Stresses 2.6-61
Figure 2.6-7 ï NCT Cold (-20 ÜF) Inner Vessel Stresses 2.6-62
Figure 2.6-8 ï NCT Cold (-20 ÜF) Canister Stresses 2.6-63

Figure 2.6-9 – NCT Cold (-20 °F) Thrust 2.6-64
Figure 2.6-10 – NCT Cold (-20 °F) Shear 2.6-65
Figure 2.6-11 – NCT Cold (-20 °F) Bending Moment 2.6-66
Figure 2.6-12 – Comparison of *g*-Loads Used for Calculating Cold (-20 °F) NCT Stresses . 2.6-67
Figure 2.6-13 – NCT Hot (140 °F) Outer Cask Stresses 2.6-68
Figure 2.6-14 – NCT Hot (140 °F) Inner Vessel Stresses 2.6-69
Figure 2.6-15 – NCT Hot (140 °F) Canister Stresses 2.6-70
Figure 2.6-16 – NCT Hot (140 °F) Thrust 2.6-71
Figure 2.6-17 – NCT Hot (140 °F) Shear 2.6-72
Figure 2.6-18 – NCT Hot (140 °F) Bending Moment 2.6-73
Figure 2.6-19 – NCT Cold (-20 °F) Shear Due to a Distributed Payload 2.6-74
Figure 2.6-20 – NCT Cold (-20 °F) Moment Due to a Distributed Payload 2.6-75
Figure 2.6-21 – NCT Cold (-20 °F) Shear Due to a Concentrated Payload 2.6-76
Figure 2.6-22 – NCT Cold (-20 °F) Moment Due to a Concentrated Payload 2.6-77
Figure 2.6-23 – NCT Hot (140 °F) Shear Due to a Distributed Payload 2.6-78
Figure 2.6-24 – NCT Hot (140 °F) Moment Due to a Distributed Payload 2.6-79
Figure 2.6-25 – NCT Hot (140 °F) Shear Due to a Concentrated Payload 2.6-80
Figure 2.6-26 – NCT Hot (140 °F) Moment Due to a Concentrated Payload 2.6-81
Figure 2.7-1 – HAC Cold (-20 °F) Outer Cask Stresses 2.7-52
Figure 2.7-2 – HAC Cold (-20 °F) Inner Vessel Stresses 2.7-53
Figure 2.7-3 – HAC Cold (-20 °F) Canister Stresses 2.7-54
Figure 2.7-4 – HAC Cold (-20 °F) Thrust 2.7-55
Figure 2.7-5 – HAC Cold (-20 °F) Shear 2.7-56
Figure 2.7-6 – HAC Cold (-20 °F) Bending Moment 2.7-57
Figure 2.7-7 – Comparison of *g*-Loads Used for Calculating Cold (-20 °F) HAC Stresses ... 2.7-58
Figure 2.7-8 – HAC Hot (140 °F) Outer Cask Stresses 2.7-59
Figure 2.7-9 – HAC Hot (140 °F) Inner Vessel Stresses 2.7-60
Figure 2.7-10 – HAC Hot (140 °F) Canister Stresses 2.7-61
Figure 2.7-11 – HAC Hot (140 °F) Thrust 2.7-62
Figure 2.7-12 – HAC Hot (140 °F) Shear 2.7-63
Figure 2.7-13 – HAC Hot (140 °F) Bending Moment 2.7-64
Figure 2.7-14 – HAC Cold (-20 °F) Shear Due to a Distributed Payload 2.7-65
Figure 2.7-15 – HAC Cold (-20 °F) Moment Due to a Distributed Payload 2.7-66

Figure 2.7-16 ï HAC Cold (-20 ÜF) Shear Due to a Concentrated Payload 2.7-67
Figure 2.7-17 ï HAC Cold (-20 ÜF) Moment Due to a Concentrated Payload..... 2.7-68
Figure 2.7-18 ï HAC Hot (140 ÜF) Shear Due to a Distributed Payload..... 2.7-69
Figure 2.7-19 ï HAC Hot (140 ÜF) Moment Due to a Distributed Payload 2.7-70
Figure 2.7-20 ï HAC Hot (140 ÜF) Shear Due to a Concentrated Payload 2.7-71
Figure 2.7-21 ï HAC Hot (140 ÜF) Moment Due to a Concentrated Payload..... 2.7-72
Figure 2.7-22 ï Finite Element Model for Puncture on the OC Lid..... 2.7-73
Figure 2.7-23 ï Stress and Deformation for Puncture on the OC Lid 2.7-73
Figure 2.7-24 ï OC Gas Samping Port Region..... 2.7-74
Figure 2.7-25 ï Package Orientation for the Puncture Drop 2.7-75
Figure 2.7-26 ï Geometry of the Puncture Bar at the Gas Sampling Port..... 2.7-76
Figure 2.7-27 ï Figure I-9.2.1 from Appendix I of the ASME Code 2.7-77
Figure 2.10.1-1 ï Finite Element Analysis Model of the Center-Pivot Trunnion Interface 2.10.1-7
Figure 2.10.1-2 ï Center-Pivot Trunnion Longitudinal and Vertical Cosine-Distributed Loads..... 2.10.1-8
Figure 2.10.1-3 ï OC Outer Shell Stress Intensities..... 2.10.1-9
Figure 2.10.1-4 ï Stress Intensity Linearization at the Bottom-Right Corner of the Trunnion Base..... 2.10.1-10
Figure 2.10.1-5 ï Finite Element Analysis Model of the IV Bottom Transition Due to Pressure..... 2.10.1-13
Figure 2.10.1-6 ï IV Bottom Transition Stress Intensities Due to Pressure..... 2.10.1-14
Figure 2.10.1-7 ï Finite Element Analysis Model of the IV Bottom Transition Due to 1*g* Acceleration..... 2.10.1-17
Figure 2.10.1-8 ï IV Bottom Transition Stress Intensities Due to 1*g* Acceleration..... 2.10.1-18
Figure 2.10.1-9 ï Containment Assembly Oblique Analysis Model..... 2.10.1-21
Figure 2.10.1-10 ï Finite Element Analysis Model of the OC Bottom Due to Puncture.. 2.10.1-25
Figure 2.10.1-11 ï Finite Element Analysis Model of the OC Bottom Due to Puncture (Close-up) 2.10.1-26
Figure 2.10.1-12 ï OC Bottom Stress Intensities Due to Puncture 2.10.1-27
Figure 2.10.1-13 ï Linearized Stress Intensities at the OC Bottom Centerline..... 2.10.1-28
Figure 2.10.2-1 ï Impact Limiter Force and Centroid Development 2.10.2-17
Figure 2.10.2-2 ï Strain Determination 2.10.2-18
Figure 2.10.2-3 ï Determination of Impact Limiter Separation Moments 2.10.2-19

Figure 2.10.2-4 ï Example Problem 2.10.2-20
Figure 2.10.2-5 ï CASKDROP Program Input Windows 2.10.2-21
Figure 2.10.2-6 ï SLAPDOWN Analytical Model 2.10.2-22
Figure 2.10.3-1 ï Impact Limiter Deflection and Residual Clearance for the NCT Oblique Drop, Cold (-20 ÜF) 2.10.3-17
Figure 2.10.3-2 ï Impact Limiter Separation Moments for the NCT Oblique Drop, Cold (-20 ÜF) 2.10.3-17
Figure 2.10.3-3 ï Impact Limiter Deflection and Residual Clearance for the NCT Oblique Drop, Warm (140 ÜF) 2.10.3-18
Figure 2.10.3-4 ï Impact Limiter Separation Moments for the NCT Oblique Drop, Warm (140 ÜF) 2.10.3-18
Figure 2.10.3-5 ï Impact Limiter Deflection and Residual Clearance for the HAC Oblique Drop, Cold (-20 ÜF) 2.10.3-19
Figure 2.10.3-6 ï Impact Limiter Separation Moments for the HAC Oblique Drop, Cold (-20 ÜF) 2.10.3-19
Figure 2.10.3-7 ï Impact Limiter Deflection and Residual Clearance for the HAC Oblique Drop, Warm (140 ÜF) 2.10.3-20
Figure 2.10.3-8 ï Impact Limiter Separation Moments for the HAC Oblique Drop, Warm (140 ÜF) 2.10.3-20
Figure 2.10.4-1 ï Free-Body Diagram for Slapdown Loads 2.10.4-7
Figure 2.10.4-2 ï Shear Diagram for Package During Slapdown 2.10.4-8
Figure 2.10.4-3 ï Moment Diagram for Package During Slapdown 2.10.4-8
Figure 2.10.7-1 ï End Orientation Test 2.10.7-23
Figure 2.10.7-2 ï End Orientation, Post-Test Configuration 2.10.7-23
Figure 2.10.7-3 ï End Orientation, View of Open End 2.10.7-24
Figure 2.10.7-4 ï End Crush Data Versus Prediction 2.10.7-24
Figure 2.10.7-5 ï Side Orientation Test 2.10.7-25
Figure 2.10.7-6 ï Side Orientation, Post-Test Configuration 2.10.7-26
Figure 2.10.7-7 ï Side Crush Data Versus Prediction 2.10.7-27
Figure 2.10.7-8 ï Oblique Orientation Test 2.10.7-28
Figure 2.10.7-9 ï Oblique Orientation, Post-Test Configuration 2.10.7-29
Figure 2.10.7-10 ï Oblique Orientation, Post-Test Side View 2.10.7-29
Figure 2.10.7-11 ï Oblique Crush Data Versus Prediction 2.10.7-30
Figure 2.10.7-12 ï End Drop Configuration 2.10.7-31
Figure 2.10.7-13 ï End Drop, Post-Test Configuration 2.10.7-32

Figure 2.10.7-14 ï Side Drop Configuration 2.10.7-33
Figure 2.10.7-15 ï Side Drop, Crush Gage Detail (Before Test) 2.10.7-34
Figure 2.10.7-16 ï Side Drop, Post-Test Configuration 2.10.7-34
Figure 2.10.7-17 ï Oblique Drop Configuration 2.10.7-35
Figure 2.10.7-18 ï Oblique Drop, Post-Test Configuration 2.10.7-36
Figure 2.10.7-19 ï Oblique Drop, Post-Test Configuration (Detail) 2.10.7-36
Figure 2.10.7-20 ï Oblique Free Drop, Measurement of Deflection 2.10.7-37
Figure 2.10.7-21 ï Drawing 9715-015, *RH-72B Dummy Package*, Sheet 1 ..... 2.10.7-39
Figure 2.10.7-22 ï Drawing 9715-015, *RH-72B Dummy Package*, Sheet 2 ..... 2.10.7-40
Figure 2.10.7-23 ï Drawing 9715-010, *Impact Limiter Test Article RH-72B*, Sheet 1 ..... 2.10.7-41
Figure 2.10.7-24 ï Drawing 9715-010, *Impact Limiter Test Article RH-72B*, Sheet 2 ..... 2.10.7-42
Figure 2.10.7-25 ï Drawing 9715-010, *Impact Limiter Test Article RH-72B*, Sheet 3 ..... 2.10.7-43
Figure 2.10.7-26 ï Drawing 9715-010, *Impact Limiter Test Article RH-72B*, Sheet 4 ..... 2.10.7-44
Figure 2.10.8-1 ï Free-Body Diagram of Molten Lead in the Lead Column 2.10.8-12
Figure 3.1-1 ï RLC with Three, 30-Gallon Drums 3.1-6
Figure 3.1-2 ï NS15 NSC with Three, Approximately 15-Gallon Drums 3.1-7
Figure 3.1-3 ï NS30 NSC with Three, Approximately 30-Gallon Drums 3.1-8
Figure 3.4-1 ï NCT Package Thermal Model with an RLC 3.4-19
Figure 3.4-2 ï OC Thermal Model 3.4-20
Figure 3.4-3 ï IV Thermal Model 3.4-21
Figure 3.4-4 ï NCT Impact Limiter Thermal Model (Polyurethane Foam Hidden) 3.4-22
Figure 3.4-5 ï NCT Impact Limiter Thermal Model (Steel Contactor Region Shown in Red) 3.4-23
Figure 3.4-6 ï RLC Thermal Model with a 30-Gallon Drum Payload 3.4-24
Figure 3.4-7 ï NS15 Thermal Model with an Approximately 15-Gallon Drum Payload 3.4-25
Figure 3.4-8 ï NS30 Thermal Model with an Approximately 30-Gallon Drum Payload 3.4-26
Figure 3.4-9 ï NCT Case 1 Maximum Temperature for the Drum Contents Center Nodes; 12 lb/ftį Waste with 90 Watts Decay Heat 3.4-27
Figure 3.4-10 ï NCT Case 1 Transient Temperatures for the Major Package Components; 12 lb/ftį Waste with 90 Watts Decay Heat 3.4-28
Figure 3.4-11 ï NCT Case 1 ï Package with RLC; 12 lb/ftį Waste with 90 Watts Decay Heat and Insolation 3.4-29
Figure 3.4-12 ï NCT Case 1 ï Package with RLC; 12 lb/ftį Waste with 90 Watts Decay Heat and Insolation (Drums Hidden) 3.4-30

Figure 3.4-13 ï NCT Case 1 ï Package with RLC; 12 lb/ftį Waste with 90 Watts Decay Heat and No Insolation 3.4-31

Figure 3.4-14 ï NCT Case 1 ï Package with RLC; 12 lb/ftį Waste with 90 Watts Decay Heat and No Insolation (Drums Hidden) 3.4-32

Figure 3.4-15 ï NCT Case 1 ï Package with RLC; 100 lb/ftį Waste with 270 Watts Decay Heat nd Insolation 3.4-33

Figure 3.4-16 ï NCT Case 1 ï Package with RLC; 100 lb/ftį Waste with 270 Watts Decay Heat and Insolation (Drums Hidden) 3.4-34

Figure 3.4-17 ï NCT Case 1 ï Package with RLC; 100 lb/ftį Waste with 270 Watts Decay Heat and No Insolation 3.4-35

Figure 3.4-18 ï NCT Case 1 ï Package with RLC; 100 lb/ftį Waste with 270 Watts Decay Heat and No Insolation (Drums Hidden) 3.4-36

Figure 3.4-19 ï NCT Case 2 ï Package with NS15; 12 lb/ftį Waste with 50 Watts Decay Heat and Insolation 3.4-37

Figure 3.4-20 ï NCT Case 2 ï Package with NS15; 12 lb/ftį Waste with 50 Watts Decay Heat and Insolation (Drums Hidden) 3.4-38

Figure 3.4-21 ï NCT Case 2 ï Package with NS15; 12 lb/ftį Waste with 50 Watts Decay Heat and No Insolation 3.4-39

Figure 3.4-22 ï NCT Case 2 ï Package with NS15; 12 lb/ftį Waste with 50 Watts Decay Heat and No Insolation (Drums Hidden) 3.4-40

Figure 3.4-23 ï NCT Case 3 ï Package with NS30; 12 lb/ftį Waste with 50 Watts Decay Heat and Insolation 3.4-41

Figure 3.4-24 ï NCT Case 3 ï Package with NS30; 12 lb/ftį Waste with 50 Watts Decay Heat and Insolation (Drums Hidden) 3.4-42

Figure 3.4-25 ï NCT Case 3 ï Package with NS30; 12 lb/ftį Waste with 50 Watts Decay Heat and No Insolation 3.4-43

Figure 3.4-26 ï NCT Case 3 ï Package with NS30; 12 lb/ftį Waste with 50 Watts Decay Heat and No Insolation (Drums Hidden) 3.4-44

Figure 3.5-1 ï HAC Package Thermal Model with an RLC 3.5-13

Figure 3.5-2 ï HAC Package Thermal Model with an RLC (Upper Impact Limiter Close-Up) 3.5-14

Figure 3.5-3 ï HAC Case 1 Temperatures of External Package Surfaces; 12 lb/ftį Waste with 90 Watts Decay Heat ï Fire *Before* Insolation 3.5-15

Figure 3.5-4 ï HAC Case 1 Temperatures of Internal Package Surfaces; 12 lb/ftį Waste with 90 Watts Decay Heat ï Fire *Before* Insolation 3.5-16

Figure 3.5-5 ï HAC Case 1 Temperatures of the OC and IV O-ring Seals; 12 lb/ftį Waste with 90 Watts Decay Heat ï Fire *Before* Insolation 3.5-17

Figure 3.5-6 ï HAC Case 1 Temperatures of the Drum Contents Center Nodes; 12 lb/ftį Waste with 90 Watts Decay Heat ï Fire *Before* Insolation 3.5-18

Figure 3.5-7 ï HAC Case 1 Temperatures of External Package Surfaces; 12 lb/ftį Waste with 90 Watts Decay Heat ï Fire *After* Insolation 3.5-19

Figure 3.5-8 ï HAC Case 1 Temperatures of Internal Package Surfaces; 12 lb/ftį Waste with 90 Watts Decay Heat ï Fire *After* Insolation 3.5-20

Figure 3.5-9 ï HAC Case 1 Temperatures of the OC and IV O-ring Seals; 12 lb/ftį Waste with 90 Watts Decay Heat ï Fire *After* Insolation 3.5-21

Figure 3.5-10 ï HAC Case 1 Temperatures of the Drum Contents Center Nodes; 12 lb/ftį Waste with 90 Watts Decay Heat ï Fire *After* Insolation 3.5-22

Figure 3.5-11 ï HAC Case 1 ï Package with RLC; 12 lb/ftį Waste with 90 Watts Decay Heat and Insolation ï Pre-Fire Temperatures 3.5-23

Figure 3.5-12 ï HAC Case 1 ï Package with RLC; 12 lb/ftį Waste with 90 Watts Decay Heat and Insolation ï Pre-Fire Temperatures (Drums Hidden) 3.5-24

Figure 3.5-13 ï HAC Case 1 ï Package with RLC; 12 lb/ftį Waste with 90 Watts Decay Heat ï Package Fire Temperatures 3.5-25

Figure 3.5-14 ï HAC Case 1 ï Package with RLC; 12 lb/ftį Waste with 90 Watts Decay Heat ï OC Outer Shell Fire Temperatures 3.5-26

Figure 3.5-15 ï HAC Case 1 ï Package with RLC; 12 lb/ftį Waste with 90 Watts Decay Heat ï OC Lead Fire Temperatures 3.5-27

Figure 3.5-16 ï HAC Case 1 ï Package with RLC; 12 lb/ftį Waste with 90 Watts Decay Heat ï OC Inner Shell Fire Temperatures 3.5-28

Figure 3.5-17 ï HAC Case 1 ï Package with RLC; 12 lb/ftį Waste with 90 Watts Decay Heat ï IV Fire Temperatures 3.5-29

Figure 3.5-18 ï HAC Case 1 ï Package with RLC; 12 lb/ftį Waste with 90 Watts Decay Heat ï RLC Fire Temperatures 3.5-30

Figure 3.5-19 ï HAC Case 1 ï Package with RLC; 12 lb/ftį Waste with 90 Watts Decay Heat ï Drum and Waste Fire Temperatures 3.5-31

Figure 3.5-20 ï HAC Case 1 ï Package with RLC; 12 lb/ftį Waste with 90 Watts Decay Heat and Insolation ï Post-Fire Temperatures 3.5-32

Figure 3.5-21 ï HAC Case 1 ï Package with RLC; 12 lb/ftį Waste with 90 Watts Decay Heat and Insolation ï Post-Fire Temperatures (Drums Hidden) 3.5-33

Figure 3.5-22 ï HAC Case 1 ï Package with RLC; 100 lb/ftį Waste with 270 Watts Decay Heat and Insolation ï Pre-Fire Temperatures 3.5-34

Figure 3.5-23 ï HAC Case 1 ï Package with RLC; 100 lb/ftį Waste with 270 Watts Decay Heat and Insolation ï Pre-Fire Temperatures (Drums Hidden) 3.5-35

Figure 3.5-24 ï HAC Case 1 ï Package with RLC; 100 lb/ftį Waste with 270 Watts Decay Heat ï Package Fire Temperatures 3.5-36

Figure 3.5-25 ï HAC Case 1 ï Package with RLC; 100 lb/ftį Waste with 270 Watts Decay Heat ï OC Outer Shell Fire Temperatures 3.5-37

Figure 3.5-26 ï HAC Case 1 ï Package with RLC; 100 lb/ftį Waste with 270 Watts Decay Heat ï OC Lead Fire Temperatures 3.5-38

Figure 3.5-27 ï HAC Case 1 ï Package with RLC; 100 lb/ftį Waste with 270 Watts Decay Heat ï OC Inner Shell Fire Temperatures 3.5-39

Figure 3.5-28 ï HAC Case 1 ï Package with RLC; 100 lb/ftį Waste with 270 Watts Decay Heat ï IV Fire Temperatures 3.5-40

Figure 3.5-29 ï HAC Case 1 ï Package with RLC; 100 lb/ftį Waste with 270 Watts Decay Heat ï RLC Fire Temperatures 3.5-41

Figure 3.5-30 ï HAC Case 1 ï Package with RLC; 100 lb/ftį Waste with 270 Watts Decay Heat ï Drum and Waste Fire Temperatures 3.5-42

Figure 3.5-31 ï HAC Case 1 ï Package with RLC; 100 lb/ftį Waste with 270 Watts Decay Heat and Insolation ï Post-Fire Temperatures 3.5-43

Figure 3.5-32 ï HAC Case 1 ï Package with RLC; 100 lb/ftį Waste with 270 Watts Decay Heat and Insolation ï Post-Fire Temperatures (Drums Hidden) 3.5-44

Figure 3.5-33 ï HAC Case 2 ï Package with NS15; 12 lb/ftį Waste with 50 Watts Decay Heat ï RLC (NSC) Fire Temperatures 3.5-45

Figure 3.5-34 ï HAC Case 2 ï Package with NS15; 12 lb/ftį Waste with 50 Watts Decay Heat ï HDPE Shield Insert Fire Temperatures 3.5-46

Figure 3.5-35 ï HAC Case 2 ï Package with NS15; 12 lb/ftį Waste with 50 Watts Decay Heat ï Drum and Waste Fire Temperatures 3.5-47

Figure 3.5-36 ï HAC Case 3 ï Package with NS30; 12 lb/ftį Waste with 50 Watts Decay Heat ï RLC (NSC) Fire Temperatures 3.5-48

Figure 3.5-37 ï HAC Case 3 ï Package with NS30; 12 lb/ftį Waste with 50 Watts Decay Heat ï HDPE Shield Insert Fire Temperatures 3.5-49

Figure 3.5-38 ï HAC Case 3 ï Package with NS30; 12 lb/ftį Waste with 50 Watts Decay Heat ï Drum and Waste Fire Temperatures 3.5-50

Figure 3.5-39 ï Maximum OC Thermal Stress Intensity vs. Time Relative to Start-of-Fire 3.5-51

Figure 3.5-40 ï ANSYS HAC Thermal Stress Model 3.5-52

Figure 3.5-41 ï HAC Case 1 ï OC Temperatures @ 15m after Start-of-Fire; 100 lb/ftį Waste with 270 Watts Decay Heat 3.5-53

Figure 3.5-42 ï ANSYS HAC Thermal Stress Model ï OC Temperatures @ 15m after Start-of-Fire for Comparison 3.5-54

Figure 3.5-43 ï ANSYS HAC Thermal Stress Model ï Maximum Thermal Stress Intensity @ 15m after Start-of-Fire 3.5-55

Figure 3.5-44 ï ANSYS HAC Thermal Stress Model ï Maximum Thermal Stress Intensity @ 15m after Start-of-Fire (Rotated) 3.5-56

Figure 3.5-45 ï ANSYS HAC Thermal Stress Model ï Maximum Thermal Stress Intensity @ 15m after Start-of-Fire (Rotated without Trunnions) 3.5-57

Figure 3.6.1-1 ï Thermal Shield Gap Configuration 3.6.1-1

Figure 3.6.1-2 ï Impact Limiter Compressed Foam Geometry 3.6.1-2

Figure 3.6.1-3 ï Calculated and Adjusted Maximum Decay Heat vs. Payload Density 3.6.1-9

Figure 3.6.1-4 ï HAC Case 1 ï Package with RLC; 50 lb/ftį Waste with 216 Watts Decay Heat and Insolation ï 30-Gallon Drum Payload 3.6.1-11

Figure 3.6.1-5 ï HAC Case 1 ï Package with RLC; 27 lb/ftį Waste with 159 Watts Decay Heat and Insolation ï 55-Gallon Drum Payload 3.6.1-12

Figure 3.6.1-6 ï HAC Case 1 ï Package with RLC; 18 lb/ftį Waste with 126 Watts Decay Heat and Insolation ï Direct-Filled RLC 3.6.1-13

Figure 3.6.2-1 ï NCT Case 1 ï Package with RLC; 12 lb/ftį Waste with 90 Watts Decay Heat and Insolation ï High-Resolution Model 3.6.2-11

Figure 3.6.2-2 ï NCT Case 1 ï Package with RLC; 12 lb/ftį Waste with 90 Watts Decay Heat and Insolation ï High-Resolution Model (Drums Hidden) 3.6.2-12

Figure 3.6.2-3 ï NCT Case 1 ï Package with RLC; 12 lb/ftį Waste with 90 Watts Decay Heat and No Insolation ï High-Resolution Model 3.6.2-13

Figure 3.6.2-4 ï NCT Case 1 ï Package with RLC; 12 lb/ftį Waste with 90 Watts Decay Heat and No Insolation ï High-Resolution Model (Drums Hidden) 3.6.2-14

Figure 3.6.2-5 ï NCT Case 1 ï Package with RLC; 12 lb/ftį Waste with 90 Watts Decay Heat and Insolation ï Downward Axial Bias 3.6.2-15

Figure 3.6.2-6 ï NCT Case 1 ï Package with RLC; 12 lb/ftį Waste with 90 Watts Decay Heat and Insolation ï Downward Axial Bias (Drums Hidden) 3.6.2-16

Figure 3.6.2-7 ï NCT Case 1 ï Package with RLC; 12 lb/ftį Waste with 90 Watts Decay Heat and No Insolation ï Downward Axial Bias 3.6.2-17

Figure 3.6.2-8 ï NCT Case 1 ï Package with RLC; 12 lb/ftį Waste with 90 Watts Decay Heat and No Insolation ï Downward Axial Bias (Drums Hidden) 3.6.2-18

Figure 3.6.2-9 ï NCT Case 1 ï Package with RLC; 12 lb/ftį Waste with 90 Watts Decay Heat and Insolation ï Upward Axial Bias 3.6.2-19

Figure 3.6.2-10 ï NCT Case 1 ï Package with RLC; 12 lb/ftį Waste with 90 Watts Decay Heat and Insolation ï Upward Axial Bias (Drums Hidden) 3.6.2-20

Figure 3.6.2-11 ï NCT Case 1 ï Package with RLC; 12 lb/ftį Waste with 90 Watts Decay Heat and No Insolation ï Upward Axial Bias 3.6.2-21

Figure 3.6.2-12 ï NCT Case 1 ï Package with RLC; 12 lb/ftį Waste with 90 Watts Decay Heat and No Insolation ï Upward Axial Bias (Drums Hidden) 3.6.2-22

Figure 3.6.2-13 ï HAC Case 1 ï Package with RLC; 12 lb/ftį Waste with 90 Watts Decay Heat ï Radial Bias ï Package Temperatures 3.6.2-23

Figure 3.6.2-14 ï HAC Case 1 ï Package with RLC; 12 lb/ftį Waste with 90 Watts Decay Heat ï Radial Bias ï OC Outer Shell Temperatures 3.6.2-24

Figure 3.6.2-15 ï HAC Case 1 ï Package with RLC; 12 lb/ftį Waste with 90 Watts Decay Heat ï Radial Bias ï OC Lead Temperatures 3.6.2-25

Figure 3.6.2-16 ï HAC Case 1 ï Package with RLC; 12 lb/ftį Waste with 90 Watts Decay Heat ï Radial Bias ï OC Inner Shell Temperatures 3.6.2-26

Figure 3.6.2-17 ï HAC Case 1 ï Package with RLC; 12 lb/ftį Waste with 90 Watts Decay Heat ï Radial Bias ï IV Temperatures 3.6.2-27

Figure 3.6.2-18 ï HAC Case 1 ï Package with RLC; 12 lb/ftį Waste with 90 Watts Decay Heat ï Radial Bias ï RLC Temperatures 3.6.2-28

Figure 3.6.2-19 ï HAC Case 1 ï Package with RLC; 12 lb/ftį Waste with 90 Watts Decay Heat ï Radial Bias ï Drum Temperatures 3.6.2-29

Figure 3.6.2-20 ï HAC Case 1 ï Package with RLC; 12 lb/ftį Waste with 90 Watts Decay Heat ï Radial Bias ï RLC Shell Depicting Radial Bias 3.6.2-30

Figure 3.6.4-1 ï Test Fixture for O-ring Seal Performance Testing 3.6.4-11

Figure 4.1-1 ï Inner Vessel Containment Components 4.1-5

Figure 4.1-2 ï Outer Cask Containment Components 4.1-6

Figure 5.1-1 ï RH-TRU Waste Canister 5.1-4

Figure 5.1-2 ï NS15 Neutron Shielded Canister 5.1-5

Figure 5.1-3 ï NS30 Neutron Shielded Canister 5.1-6

Figure 5.3-1 ï Analytic Model Distance Squared Relationships Satisfying A_2 = 10 mrem/hr at 2 meters from the Package Surface 5.3-5

Figure 5.3-2 ï RH-TRU 72-B RLC Payload MCNP Model for NCT 5.3-6

Figure 5.3-3 ï RH-TRU 72-B RLC Payload MCNP Model for HAC 5.3-7

Figure 5.3-4 ï RH-TRU 72-B RLC Payload MCNP Model for HAC (close-up) 5.3-8

Figure 5.3-5 ï RH-TRU 72-B NS15 Payload MCNP Model for NCT 5.3-9

Figure 5.3-6 ï RH-TRU 72-B NS15 Payload MCNP Model for HAC 5.3-10

Figure 5.3-7 ï RH-TRU 72-B NS15 Payload MCNP Model for HAC (close-up) 5.3-11

Figure 5.3-8 ï RH-TRU 72-B NS30 Payload MCNP Model for NCT 5.3-12

Figure 5.3-9 ï RH-TRU 72-B NS30 Payload MCNP Model for HAC 5.3-13

Figure 5.3-10 ï RH-TRU 72-B NS30 Payload MCNP Model for HAC (close-up) 5.3-14

Figure 5.4-1 ï Allowable Activity Comparison for Concentrated Sources 5.4-7

Figure 5.5-1 ï RH-TRU 72-B ï RH-TRU Waste Canister MCNP Model for Distributed Source at Unit Density 5.5-6

Figure 5.5-2 ï RH-TRU 72-B ï RH-TRU Waste Canister DCF 5.5-6

Figure 5.5-3 ï RH-TRU 72-B ï NS15 Neutron Shielded Canister MCNP Model for Distributed Source at Unit Density 5.5-10

Figure 5.5-4 ï RH-TRU 72-B ï NS15 Neutron Shielded Canister DCF 5.5-10

Figure 5.5-5 ï RH-TRU 72-B ï NS30 Neutron Shielded Canister MCNP Model for Distributed Source at Unit Density 5.5-14

Figure 5.5-6 ï RH-TRU 72-B ï NS30 Neutron Shielded Canister DCF 5.5-14

Figure 6.3-1 ï Simplified Drawing of RH-TRU 72-B Package 6.3-21

Figure 6.3-2 ï KENO-V.a NCT and HAC Single Unit, Case A through C, Sphere Centered Model Representation (Top and Side Views) 6.3-22

Figure 6.3-3 - KENO-V.a NCT and HAC Single Unit, Case A through C, Sphere Centered Top Model Representation (Top and Side Views) 6.3-23

Figure 6.3-4 ï KENO-V.a NCT and HAC Single Unit, Case A through C, Sphere Centered Top and Displaced Radially, Model Representation (Top and Side Views) ... 6.3-24

Figure 6.3-5 ï KENO-V.a NCT and HAC Infinite Unit, Case D, Cylindrical Fissile Region Model Representation (Top and Side Views) 6.3-25

Figure 6.3-6 ï KENO-V.a NCT and HAC Single-Unit, Case D, Cylindrical Fissile Region Models with Various Be Reflector Regions (Long, Skinny; Short, Squat; and Encapsulated Location Models both Top and Side Views) 6.3-26

Figure 6.3-7 ï KENO-V.A (SCALE 5.1) NCT and HAC Single-Unit, Case E, Cylindrical Array of Cylinders at the Top of the IV 6.3-27

Figure 6.3-8 ï KENO-V.A (SCALE 5.1) NCT and HAC Single-Unit, Case E, Cylindrical Array of Spheres at the Top of the IV 6.3-28

Figure 6.3-9 ï KENO-V.A (SCALE 5.1) NCT and HAC Single-Unit, Case E, Cylindrical Array of Cylinders at the Center of the IV with Be Reflector (Cylindrical Array of Spheres is similar) 6.3-29

Figure 6.4-1 ï Plot of Peak Reactivities of Cylindrical Arrays of Spheres at Optimum Pitch and at 0.96 wt% ^{235}U Vs. Sphere Diameter 6.4-40

Figure 7.4-1 ï Pressure Rise Leakage Rate Test Schematic 7.4.1-3

Figure 8.1-1 ï Testing the IV Lid Seal Integrity 8.1-19

Figure 8.1-2 ï Testing the OC Lid Seal Integrity 8.1-19

1.0 GENERAL INFORMATION

This chapter of the Safety Analysis Report (SAR) for the Remote-Handled Transuranic (RH-TRU) 72-B waste shipping package presents a general introduction and description of the RH-TRU 72-B package. The RH-TRU 72-B package is presented in Figure 1.1-1, and schematics of the key components are presented as Figure 1.1-2 and Figure 1.1-3. Figure 1.1-2 presents an exploded view of all packaging components. Figure 1.1-3 presents a detailed view of the closure/seal areas. Drawing X-106-500-SNP, presenting all design details associated with the RH-TRU 72-B packaging, and Drawings X-106-501-SNP, X-106-502-SNP, and X-106-503-SNP, presenting design details associated with the RH-TRU payload canister and optional neutron shielding components, are included in Appendix 1.3.1, *Packaging General Arrangement Drawings*. Terminology and notation used throughout the report is presented in Appendix 1.3.2, *Glossary of Terms and Acronyms*. All details relating to payloads and payload preparation for shipment in a RH-TRU 72-B package are presented in the *Remote-Handled Transuranic Waste Authorized Methods for Payload Control* (RH-TRAMPAC)[1]. A description of the RH-TRU payload canister with the addition of neutron shielding components, or neutron shielded canister (NSC), is provided in Appendix 5.1 of the *RH-TRU Payload Appendices*[2].

1.1 Introduction

The Remote-Handled Transuranic Waste Shipping Package (Model No. RH-TRU 72-B) has been developed as a safe means of transporting, via ground transportation, remote-handled transuranic (RH-TRU) wastes from various sites around the United States. The RH-TRU 72-B package is a Category I packaging. RH-TRU waste is transported within the RH-TRU 72-B package by highway and rail. Limits for allowable external temperature and radiation levels have been established to ensure compliance with 10 CFR Ä71.43[3] and Ä71.47. The design is optimized for minimum weight and maximum safety during loading, transport, and unloading operations.

The RH-TRU 72-B package provides up to two levels of leakage rate tested containment for the payload during both normal conditions of transport (NCT) and hypothetical accident conditions (HAC). An outer cask (OC), which has been designed, manufactured, and maintained to provide a containment function, establishes the primary containment boundary. An inner vessel (IV), which has also been designed, manufactured and maintained to provide a containment function, is configured at the time of loading in a manner intended and expected to provide a secondary containment boundary. Prior to shipment of a loaded RH-TRU 72-B package, the OC boundary is subjected to a preshipment leakage rate test in accordance with Section 7.6.1 of ANSI N14.5[4],

[1] U.S. Department of Energy (DOE), *Remote-Handled Transuranic Waste Authorized Methods for Payload Control* (RH-TRAMPAC), U.S. Department of Energy, Carlsbad Field Office, Carlsbad, New Mexico.

[2] U.S. Department of Energy (DOE), *RH-TRU Payload Appendices*, U.S. Department of Energy, Carlsbad Field Office, Carlsbad, New Mexico.

[3] Title 10, Code of Federal Regulations, Part 71 (10 CFR 71), *Packaging and Transportation of Radioactive Material*, 01-01-14 Edition.

[4] ANSI N14.5-2014, *American National Standard for Radioactive Materials ï Leakage Tests on Packages for Shipment*, American National Standards Institute, Inc. (ANSI).

the purpose of which is to demonstrate proper assembly of the OC, thus ensuring a leaktight containment boundary during transport. However, from an As-Low-As-Reasonably-Achievable (ALARA), or operator dose perspective, and in the interest of minimizing overall loading times, a corresponding IV preshipment leakage rate test is optional. If the optional test is successfully performed, a second level of containment is also ensured during transport. Importantly, even if the IV preshipment leakage rate test is not performed, the secondary level of containment will still likely exist since the IV is loaded and configured in the same manner, with containment O-ring seals in place, independent of whether or not the leakage rate test is ultimately performed. Although credit for the secondary level of containment is not taken in the absence of the IV preshipment leakage rate test, IV components designed, manufactured, and maintained in a manner intended to provide leaktight containment are still identified as containment boundary components within this SAR. Top level identification of the OC and IV containment boundary components are provided in the following paragraph, with additional detail provided in Section 1.2.1.1.1, *Inner Vessel,* and Section 1.2.1.1.2, *Outer Cask.*

The packaging is composed of an IV that optionally provides an inner containment boundary, an OC that provides an outer containment boundary and acts as an environmental barrier, and energy-absorbing impact limiters at each end of the OC. The containment boundary components provided by the IV include a 1İ -inch thick bottom plate, a 3/8-inch thick, 32-inch outside diameter shell, a lid-end forging, and a 6İ inch thick lid. IV lid closure is accomplished using eight (8), 7/8-inch diameter bolts. The actual containment boundary provided by the OC consists of a 5-inch thick bottom plate, a 1-inch thick, 32⅜-inch inside diameter inner shell, a lid-end forging, and a 6-inch thick lid. OC lid closure is accomplished using eighteen (18), 1ı -inch diameter bolts. Polyurethane foam filled energy absorbers (impact limiters) are attached to each end of the OC using six (6), 1ı -inch diameter bolts, to limit the consequences of NCT and HAC.

The RH-TRU 72-B package is designed for truck and rail transport. The maximum allowable total weight of the loaded RH-TRU 72-B package is 45,000 pounds. The empty package weighs approximately 37,000 pounds. The maximum allowable total weight of the loaded payload canister is 8,000 pounds. The payload of the RH-TRU 72-B package consists of one payload canister of waste. The payload canister is part of the packaging contents and, as such, is not required to meet the containment requirements of 10 CFR Ä71.51[3]. The authorized contents are defined by the RH-TRAMPAC[1].

The RH-TRU 72-B package is designed for shipment by ground transportation as a Type B(M)F-96 package per the definitions delineated in 10 CFR 71.4[3].

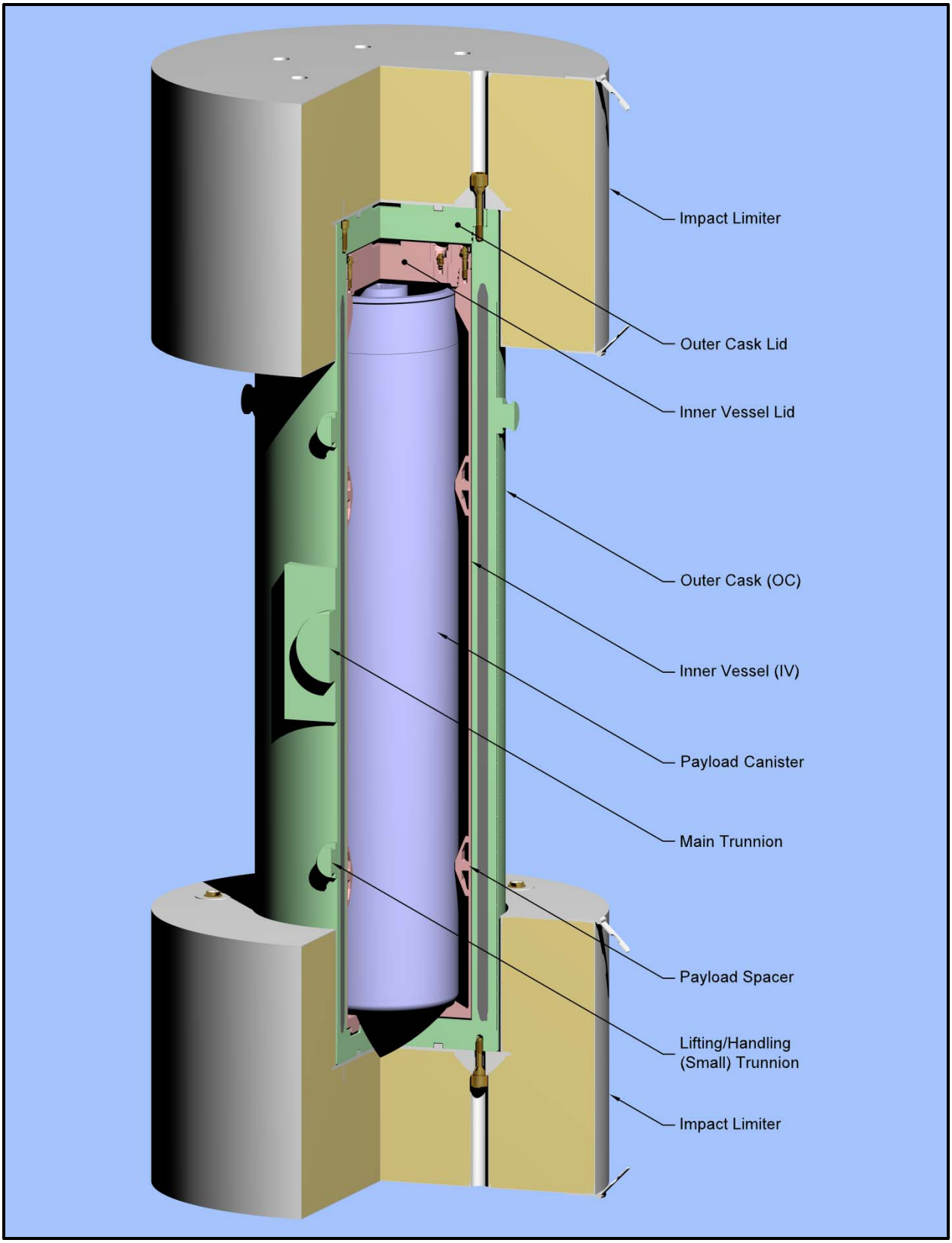

Figure 1.1-1 ï RH-TRU 72-B Package

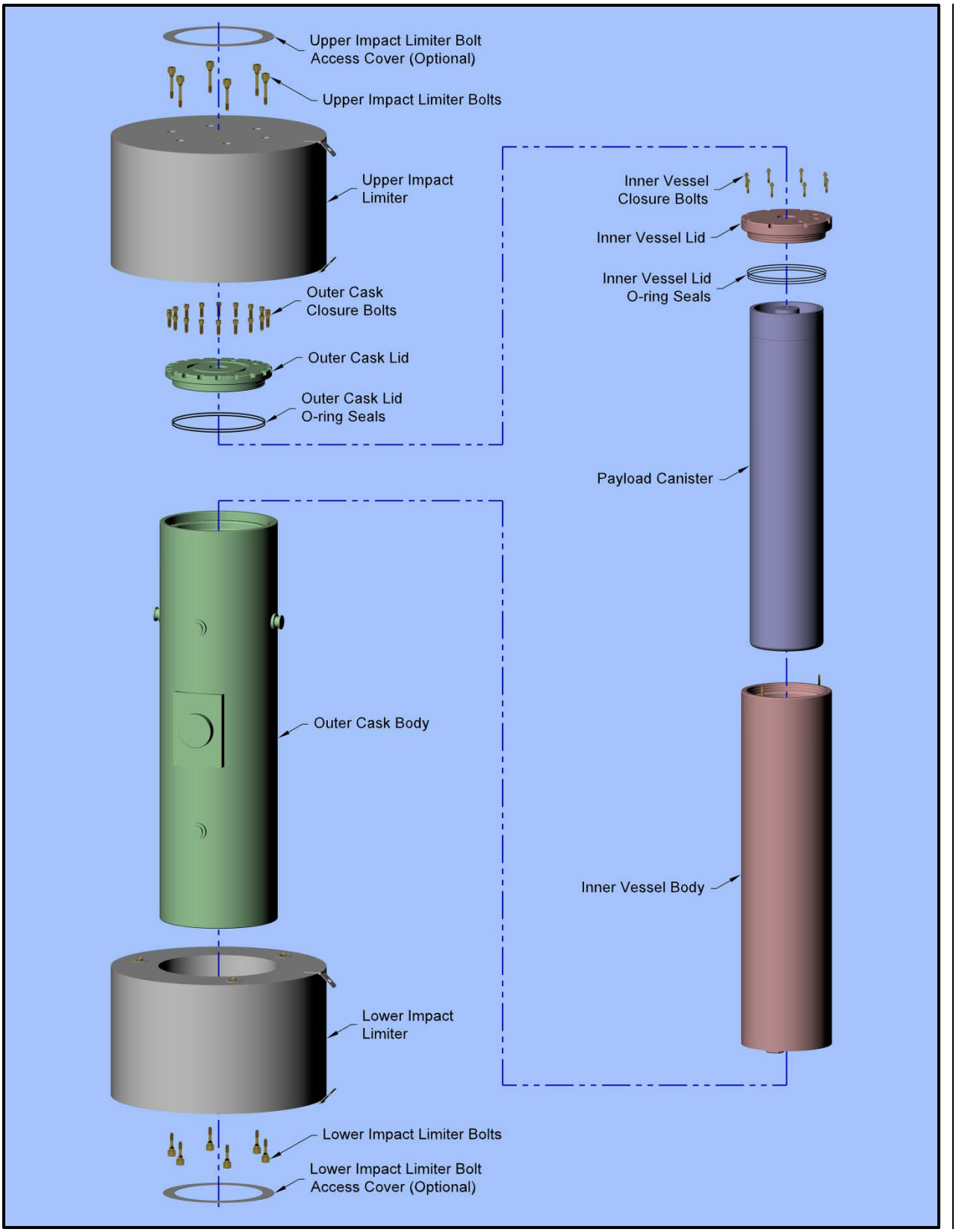

Figure 1.1-2 ï RH-TRU 72-B Package Components

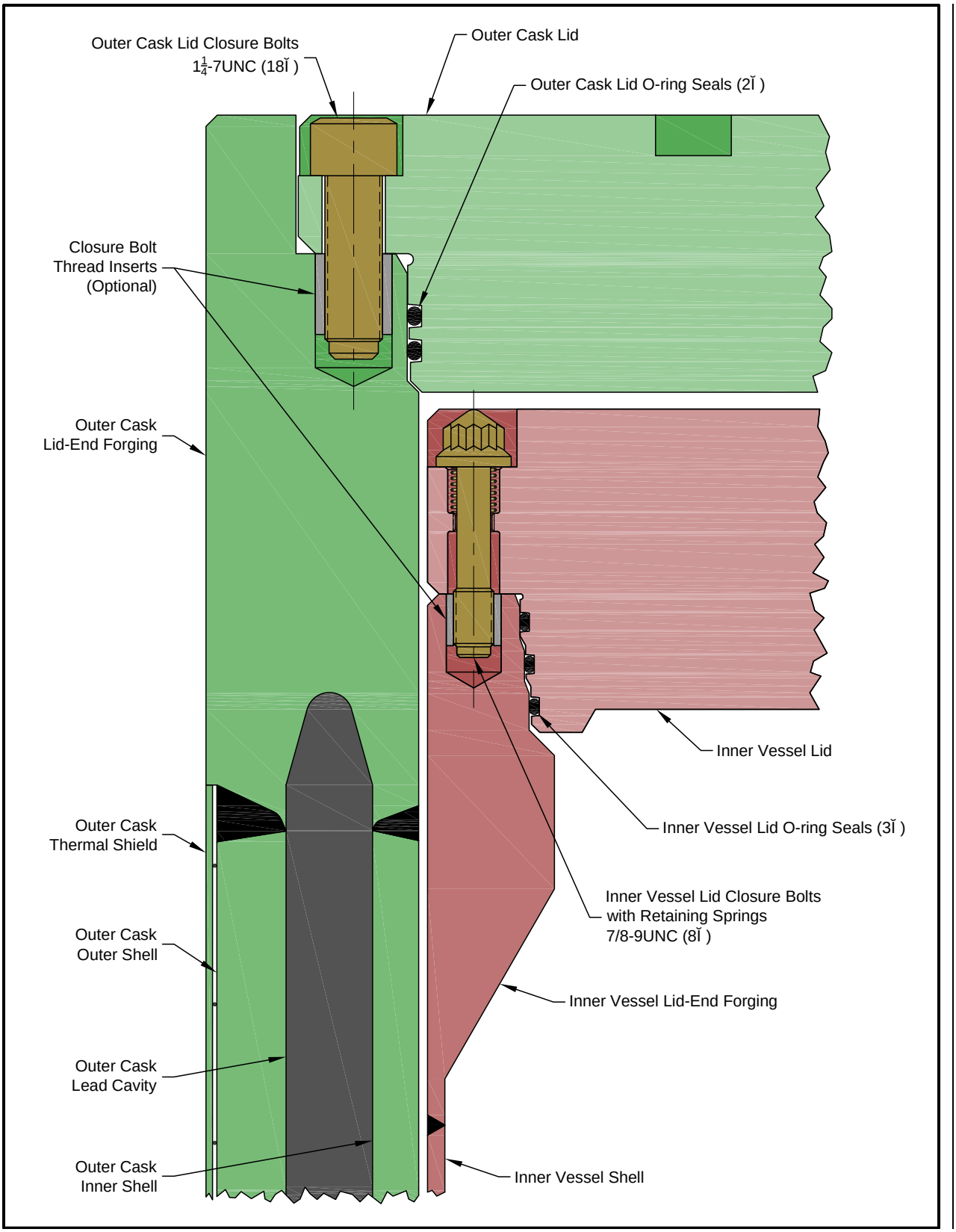

Figure 1.1-3 ï View of the RH-TRU 72-B Closure Regions

This page intentionally left blank.

1.2 Package Description

This section presents a basic description of the RH-TRU 72-B package and the contents that may be transported. The *Packaging General Arrangement Drawing* for the RH-TRU 72-B package is presented in Appendix 1.3.1, *Packaging General Arrangement Drawings*.

1.2.1 Packaging

1.2.1.1 General Design Description, Containment Boundary and Closure Identification, Overall Dimensions and Materials of Construction

The RH-TRU 72-B package provides up to two levels of containment for the radioactive contents. When demonstrated to pass an optional preshipment leakage rate test, the inner vessel (IV) is credited with providing an inner containment boundary for the package payload (loaded payload canister). The outer cask (OC) is always subjected to a preshipment leakage rate test and provides an outer containment boundary for the payload and also acts as an environmental barrier. The lead-shielded OC is protected at each end by energy absorbing impact limiters that consist of stainless steel skins filled with medium density, closed-cell polyurethane foam. These impact limiters also provide thermal insulation that protects seal areas during the hypothetical accident condition (HAC) thermal event. The OC is passively cooled due to the relatively low, maximum decay heat loading of 270 thermal watts per payload canister. The maximum design pressure of the RH-TRU 72-B package is 150 psig. The maximum temperatures for the major components of the RH-TRU 72-B package under normal conditions of transport (NCT) and HAC are presented in Chapter 3.0, *Thermal Evaluation*. The overall arrangement of the RH-TRU 72-B package and design details of the IV and OC are presented in Appendix 1.3.1, *Packaging General Arrangement Drawings*. The IV, OC, and impact limiters are more fully described in the following sections.

1.2.1.1.1 Inner Vessel

The IV structure is fabricated primarily of ASTM A240, Type 304, stainless steel for the shells, and ASTM A240, Type 304, or ASTM A182, Type F304, austenitic stainless steel for the lid and end closure. Non-Type 304 stainless members include butyl rubber O-ring seals, and Nitronic 60 port closure bolts. The O-ring seal material is Rainier Rubber butyl rubber compound R0405-70[1], or equivalent, per Appendix 3.6.4, *Containment O-ring Seal Material Tests*. Certification of compliance with this specification is provided by the supplier for Rainier Rubber Compound R0405-70, or equivalent. Eight (8), 7/8-9UNC, ASTM A320, Grade L43, carbon steel closure bolts secure the IV lid to the IV body.

With reference to Appendix 1.3.1, *Packaging General Arrangement Drawings*, the IV includes the following containment boundary components:

1. A 1İ -inch thick, Type 304 or Type F304 stainless steel bottom closure;

2. A 3/8-inch thick, 32-inch outside diameter, Type 304 stainless steel shell, with a full-length, full penetration seam weld;

[1] Rainier Rubber Company, Seattle, WA.

3. A full-penetration girth weld joining the shell to the bottom forging;

4. An upper-end (lid-end), Type F304 stainless steel ring forging;

5. A full-penetration girth weld joining the upper-end ring forging to the shell;

6. A 6İ -inch thick, Type 304 or Type F304 stainless steel lid;

7. A butyl rubber containment O-ring seal that forms the seal between the upper end forging and the lid (the containment O-ring seal is the middle of the three IV closure seals);

8. A Type 304 or Type 316 stainless steel gas sampling port insert, containing a Nitronic 60 closure bolt with butyl O-ring seal (the upper O-ring seal is the containment seal);

9. A 1/4-inch bevel weld which seals the gas sampling port insert to the lid;

10. A Type 304 or Type 316 stainless steel backfill port insert, containing a Nitronic 60 closure bolt with butyl O-ring seal;

11. A 1/4-inch bevel weld which seals the backfill port insert to the lid;

12. A Type 304 or Type 316 stainless steel test port insert; and

13. A 1/4-inch bevel weld that seals the test port insert to the lid.

The inside diameter of the IV is 31ı inches. Two (2) intermediate support rings and a pair of optional guide rails are located inside the IV for payload canister support. Including the support rings, guide rails, and upper forging, a 26İ -inch diameter by 121İ -inch long cavity is provided within the IV for the packaging payload.

The specific IV containment components are illustrated in Figure 1.2-1.

The weight of the IV is approximately 4,023 pounds, the overall length is 130 inches, and the outside diameter is 32 inches.

1.2.1.1.2 Outer Cask

The OC is fabricated primarily of ASTM A240, Type 304, stainless steel for the shells, and ASTM A240, Type 304, or ASTM A182, Type F304, austenitic stainless steel for the lid and end closure. Non-Type 304 stainless members include the cast lead shell, butyl rubber O-ring seals (identical material as described for the IV per Section 1.2.1.1.1, *Inner Vessel*), and Nitronic 60 port closure bolts. Eighteen (18), 1ı -7UNC, ASTM A320, Grade L43, carbon steel closure bolts secure the OC lid to the OC body. The body of the OC is constructed of two concentric stainless steel shells that sandwich the cast lead shell.

With reference to Appendix 1.3.1, *Packaging General Arrangement Drawings,* the OC containment boundary consists of the following components:

1. A 5-inch thick, Type 304 or Type F304 stainless steel bottom closure;

2. A 1-inch thick, 34⅜-inch outside diameter, Type 304 stainless steel inner shell, with a full length, full penetration seam weld;

3. A full-penetration girth weld joining the inner shell to the bottom forging;

4. An upper end (lid-end), Type F304 stainless steel ring forging;

5. A full-penetration girth weld joining the upper end ring forging to the inner shell;

6. A 6-inch thick, Type 304 or Type F304 stainless steel lid;

7. A butyl rubber containment O-ring seal that forms the seal between the upper-end forging and the lid (the containment O-ring seal is the innermost of the two OC closure seals);

8. A Type 304 or Type 316 stainless steel gas sampling port insert, containing a Nitronic 60 closure bolt with butyl O-ring seal;

9. A 1/4-inch bevel weld which seals the gas sampling port insert to the lid;

10. A Type 304 or Type 316 stainless steel test port insert; and

11. A 1/4-inch bevel weld which seals the test port insert to the lid.

12. A 32⅜-inch diameter by 130IJ-inch long cavity is provided within the OC for the IV.

The specific OC containment components are illustrated in Figure 1.2-2.

The 1İ -inch thick, 41⅛-inch outside diameter outer shell and the 1⅞-inch thickness of cast lead filling the annular space between the inner and outer shells are non-containment. A thermal shield of ten (10) gauge stainless steel sheet surrounds the outside of the outer shell. The thermal shield is spaced outward from the outer shell by a twelve (12) gauge wire wrap on a 3-inch pitch spacing.

The overall external dimensions of the OC are an outside diameter of 41⅝ inches and a length of 141IJ inches. The total weight of the OC is computed to be approximately 27,883 pounds, with 10,739 pounds comprising the 1⅞-inch thick cast lead shell.

Several protrusions from the OC external cylindrical surface extend through the thermal shield. The protrusions include two (2) trunnions (180Ü apart) near the base end of the OC, that can be used as pivot points during loading and unloading the package onto or from the trailer, to secure the OC in an upright position during payload canister loading and unloading, and for stabilizing the package during transport, and four (4) trunnions (90Ü apart) near the lid end of the OC, that can be used for lifting the entire package as well as stabilizing the package during transport. At approximately mid length of the package are two (2) larger trunnions (180Ü apart) used for package tie-down to the trailer during transport, and used for pivoting the package during some loading and unloading operations.

As discussed in Appendix 8.3.1, *Lead Installation Procedure*, installation of the cast lead into the OC is done in a carefully controlled manner. Temperatures of the inner and outer shells are continuously monitored and controlled during the lead fill and cooldown processes. In addition, the weld connecting the outer shell to the bottom end plate is made after the cooldown process is complete and the entire OC has reached a uniform temperature. The lead pour process is described in Appendix 8.3.1, *Lead Installation Procedure*, subsequent shielding integrity testing is described in Section 8.1.5, *Tests for Shielding Integrity*, and fabrication verification testing is described in Section 8.1.3, *Fabrication Leakage Rate Tests*.

1.2.1.1.3 Impact Limiters

The impact limiter skins are fabricated from 300 series stainless steel. Non-stainless members include the closed-cell polyurethane foam and the ASTM A320, Grade L43, impact limiter attachment bolts. The polyurethane foam has a nominal density of 11İ pounds per cubic foot. Six (6), 1ı -7UNC bolts necked down to a 1-inch diameter secure each impact limiter to the OC.

The outside diameter of each impact limiter is 76 inches and the length is 46 inches. The approximate weight of each impact limiter is 2,547 pounds.

1.2.1.1.4 Payload Canister

All RH-TRU waste will be loaded directly into the payload canister or into inner containers within the payload canister. The RH-TRU payload canister design must meet the requirements of Appendix 1.3.1, *Packaging General Arrangement Drawings.* The payload canister uses a 26-inch outside diameter 1/4-inch thin-wall cylinder fabricated of carbon or stainless steel as the outer shell. Including a lift pintle at the top of the payload canister, the overall length is 120İ inches.

The payload canister is basically a one- or two-piece construction unit (fixed or removable lid versions, respectively, either of which may be configured with a through-pintle fill port and plug) capable of transporting RH-TRU waste.

The removable lid canister may be utilized as a neutron shielded canister in two configurations, NS15 and NS30, which incorporate neutron shielding components that provide neutron shielding for approximately 15- and 30-gallon inner containers, respectively.

1.2.1.2 Gross Weight

Gross shipping weight of the RH-TRU 72-B package is 45,000 pounds, maximum. A summary of overall component weights is detailed in Table 1.2-1.

1.2.1.3 Neutron Moderation and Absorption

The RH-TRU 72-B package contains no specific neutron moderators or absorbers.

1.2.1.4 Receptacles, Valves, Testing and Sampling Ports

The OC lid has a seal test port and a gas sampling port. The seal test port accesses the volume between the two O-ring seals on the OC lid, thereby verifying assembly prior to shipping the loaded package. The IV lid has a seal test port, a gas sampling port, and a helium backfill port. The seal test port accesses the volume between the upper and middle (containment) O-ring seals on the IV lid, thereby verifying assembly prior to shipping the loaded package. The helium backfill port accesses the volume between the lower and middle (containment) O-ring seals on the IV lid, thereby allowing a helium atmosphere to be introduced below the containment O-ring seal for the purpose of conducting helium leakage rate tests (note that preshipment leakage rate tests use pressure rise testing without helium, as delineated in Appendix 7.4.1, *Preshipment Leakage Rate Test*). For both the IV and OC lids, the gas sampling port is opened at the loading end of shipment for ease of lid installation, and is used as a sampling port at the receiving end of shipment to determine contamination levels and to equalize pressure. Air or helium fills all void spaces within the packaging for NCT. There are no receptacles or valves utilized on this package. A more detailed discussion of the package test, gas sampling, and helium backfill port features is provided in Chapter 4.0, *Containment.*

1.2.1.5 Heat Dissipation

The package design heat capacity is 270 thermal watts maximum. The RH-TRU 72-B package dissipates this relatively low internal heat load entirely by passive heat transfer. No special devices or features are needed or utilized to enhance the normal dissipation of heat. A more detailed discussion of the package thermal characteristics is provided in Chapter 3.0, *Thermal Evaluation*.

1.2.1.6 Coolants

There are no coolants utilized within the RH-TRU 72-B package.

1.2.1.7 Protrusions

There are no outer or inner protrusions on the package other than the eight (8) external lifting, handling and tie-down trunnions discussed in Section 2.5, *Lifting and Tie-down Standards for All Packages*, all of which are located well within the envelope protected by the impact limiters. Refer to Appendix 1.3.1, *Packaging General Arrangement Drawings*, for more detail.

1.2.1.8 Lifting and Tie-down Devices

Of the eight trunnions located on the exterior of the package, four are intended for lifting (four trunnions near the lid-end) and six for tie-down (two pivot trunnions, two trunnions near the lid, and the two trunnions near the base). The two trunnions nearest the base of the package and two of the four near the lid of the package are also used to stabilize the package during loading and unloading. A more detailed discussion of the package lifting and tie-down features is provided in Section 2.5, *Lifting and Tie-down Standards for All Packages*.

1.2.1.9 Pressure Relief System

No pressure relief systems are utilized for the IV or OC. Plastic pipe plugs are included on the impact limitersô skins to preclude excessive pressurization of the impact limiters in a HAC fire transient event.

1.2.1.10 Shielding

Radiation attenuation is achieved through the 1⅞ inches of lead and 2⅞ inches of steel maintained between the outside diameter of the payload canister and the exterior surface of the package. The bottom of the package is shielded by 6İ inches of steel. A minimum of 12İ inches shields the top end. Further details are provided in Chapter 5.0, *Shielding Evaluation*.

1.2.2 Operational Features

The RH-TRU 72-B package is not considered to be operationally complex. All operational features are readily apparent from an inspection of the drawing provided in Appendix 1.3.1, *Packaging General Arrangement Drawings*, and the previous discussions presented in Section 1.2.1, *Packaging*.

Generally, the package is designed so that it may be rotated, after removing the impact limiters, to a vertical orientation (about the center-pivot trunnions) and secured in place for loading

and unloading operations, while still on the trailer. In order to rotate the package, the impact limiters must first be removed. Alternatively, the package may be upended and removed from the trailer using a crane and lifting yoke attached to two of the trunnions near the package lid.

Both the OC and IV are fitted with four-point handling fixture holes and a pintle receptacle where a pintle can be installed. The lids can be lifted with standard eyebolts and four-point rigging and/or a handling fixture. The lid can also be lifted using the pintle grapple that is used for handling the payload canister.

The IV lid also incorporates use of captured, spring-loaded closure bolts and stepped O-ring sealing surfaces to improve installation efficiency in remote environments. Captured closure bolts aid installation and removal in remote environments. Stepped sealing surfaces help minimize potential for lid binding and help reduce lid installation forces required.

Detailed operational procedures are listed in Chapter 7.0, *Operating Procedures*.

To improve remote and non-remote lid installation operations, tapered lid alignment guide pins on the OC and IV may be used to assist in lid rotational alignment for bolt installation. The guide pins may optionally be removed prior to transport.

1.2.3 Contents of Packaging

The RH-TRU 72-B package is designed to transport remote-handled transuranic (RH-TRU) materials for the U.S. Department of Energy (DOE). RH-TRU payload materials transported in the RH-TRU 72-B package must meet the restrictions set forth in the *Remote-Handled Transuranic Waste Authorized Methods for Payload Control* (RH-TRAMPAC)[2].

1.2.4 Package Evaluation

1.2.4.1 Structural

Chapter 2.0, *Structural Evaluation*, summarizes the effects on the RH-TRU 72-B package of tests specified by 10 CFR 71[3] for NCT and HAC. Maximum stresses were found to be below allowables for various types of stress combinations, given in Table 2.1-1 and Table 2.1-2 of Section 2.1.2, *Design Criteria*. The corresponding margins of safety are presented in Chapter 2.0, *Structural Evaluation*, where margins of safety are calculated for both NCT and HAC allowables for all structural components.

1.2.4.2 Thermal

Chapter 3.0, *Thermal Evaluation*, summarizes a thermal evaluation of the packaging to assure that containment integrity would not be compromised due to changes from thermal loadings. Maximum temperatures were found for major package components under both NCT and HAC.

[2] U.S. Department of Energy (DOE), *Remote-Handled Transuranic Waste Authorized Methods for Payload Control* (RH-TRAMPAC), U.S. Department of Energy, Carlsbad Field Office, Carlsbad, New Mexico.

[3] Title 10, Code of Federal Regulations, Part 71 (10 CFR 71), *Packaging and Transportation of Radioactive Material*, 01-01-14 Edition.

These values are summarized in Section 3.1, *Discussion*, and are found to be within the operating limits of the materials of the corresponding components.

1.2.4.3 Containment

Chapter 4.0, *Containment,* summarizes that containment of the payload is verified by evaluating the containment boundary, including the containment vessel, containment penetrations, seals and welds, and positive closure. Requirements for NCT are addressed, including containment of radioactive material, pressurization of the containment vessel, and NCT containment criteria. Similarly, requirements for HAC, including fission gas products, containment of radioactive material, and HAC containment criteria, are addressed. These containment verification requirements are discussed in Chapter 4.0, *Containment*.

1.2.4.4 Shielding

Chapter 5.0, *Shielding Evaluation*, summarizes the shielding evaluation and describes the process by which compliance with radiation dose rate limits, as specified in 10 CFR Ä71.47(b)[3] for NCT, and 10 CFR Ä71.51(a)(2) for HAC, is determined. Measurement of the radiation dose rates will be performed as specified in 10 CFR Ä71.47(b) for an exclusive use shipment in compliance with Section 3.2 of the RH-TRAMPAC: 200 mrem/hr on the external surface of the package, 10 mrem/hr at any point 2 meters from the vertical planes projected by the outer edges of the vehicle, and 2 mrem/hr in any normally occupied space (if required).

1.2.4.5 Criticality

The presence and location of the stainless steel in the package walls and a half-thickness of the impact limiters are shown in Chapter 6.0, *Criticality Evaluation*, to be all that is required for maintaining criticality safety for infinite arrays of undamaged or damaged packages, as dictated by 10 CFR 71[3] for NCT or HAC. KENO calculations are performed to verify that the authorized quantity of fissile material in a single RH-TRU 72-B package meets the requirements of 10 CFR Ä71.55. Additional KENO calculations are then done to show that an infinite array of undamaged or damaged RH-TRU 72-B packages meet the requirements of 10 CFR Ä71.59. Details of the models used and the results obtained are included in Chapter 6.0, *Criticality Evaluation*. Based on an unlimited number of damaged or undamaged RH-TRU 72-B packages, the criticality safety index (CSI), per 10 CFR Ä71.59, is 0.0.

1.2.4.6 Acceptance Tests

Acceptance tests were devised to ensure that the RH-TRU 72-B package performs as required before its first use, and a maintenance program was created to ensure its continued performance. These procedures are described in Section 8.1, *Acceptance Tests,* and Section 8.2, *Maintenance Program,* and comply with Subpart G of 10 CFR 71[3].

Table 1.2-1 ï Overall Component Weights

Component	Weight	
	(lbs)	(kg)
Outer Cask	27,883	12,647
Inner Vessel	4,023	1,825
Impact Limiters	5,094	2,311
Loaded Canister	8,000	3,629
TOTAL	***45,000***	***20,412***

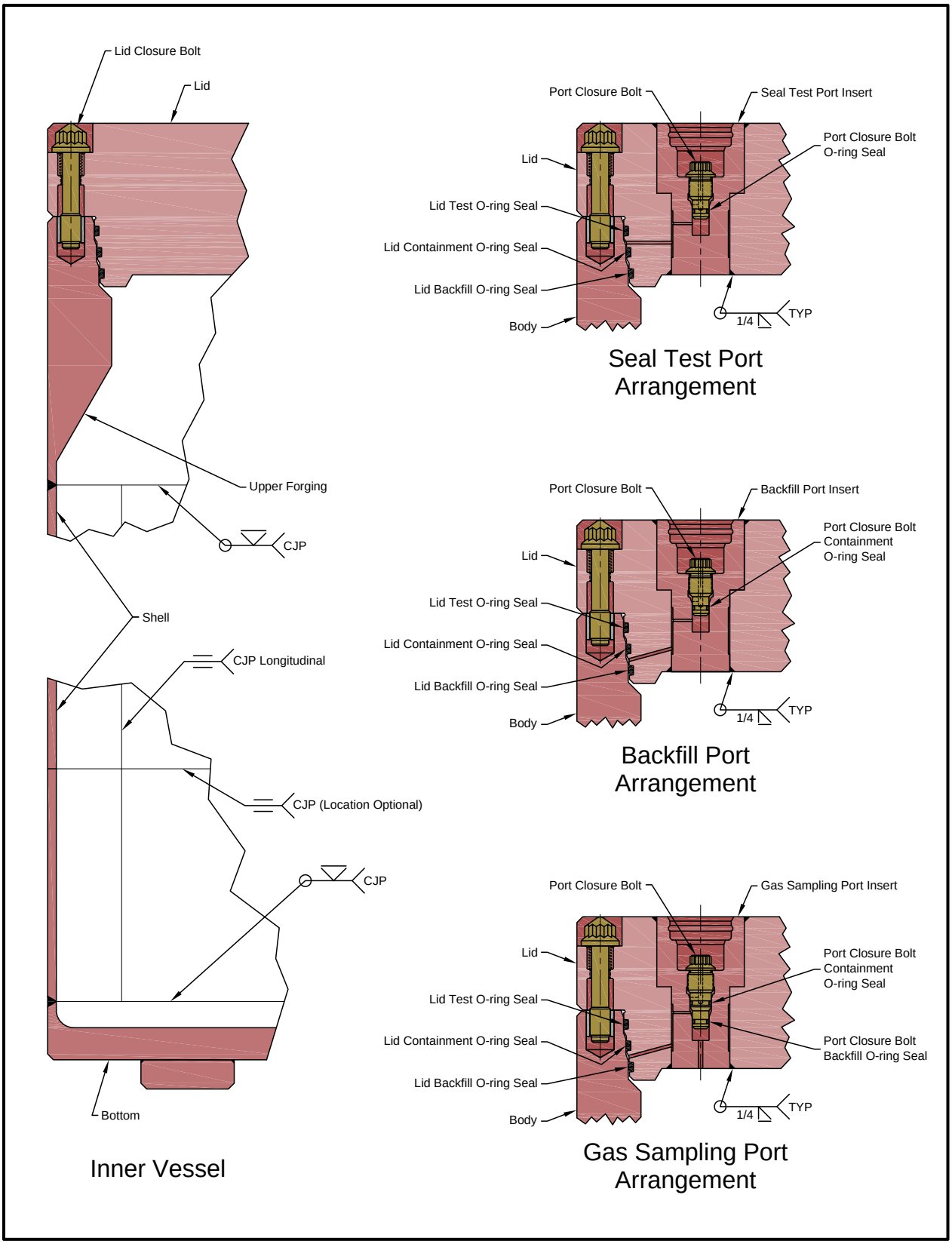

Figure 1.2-1 ï Inner Vessel Containment Components

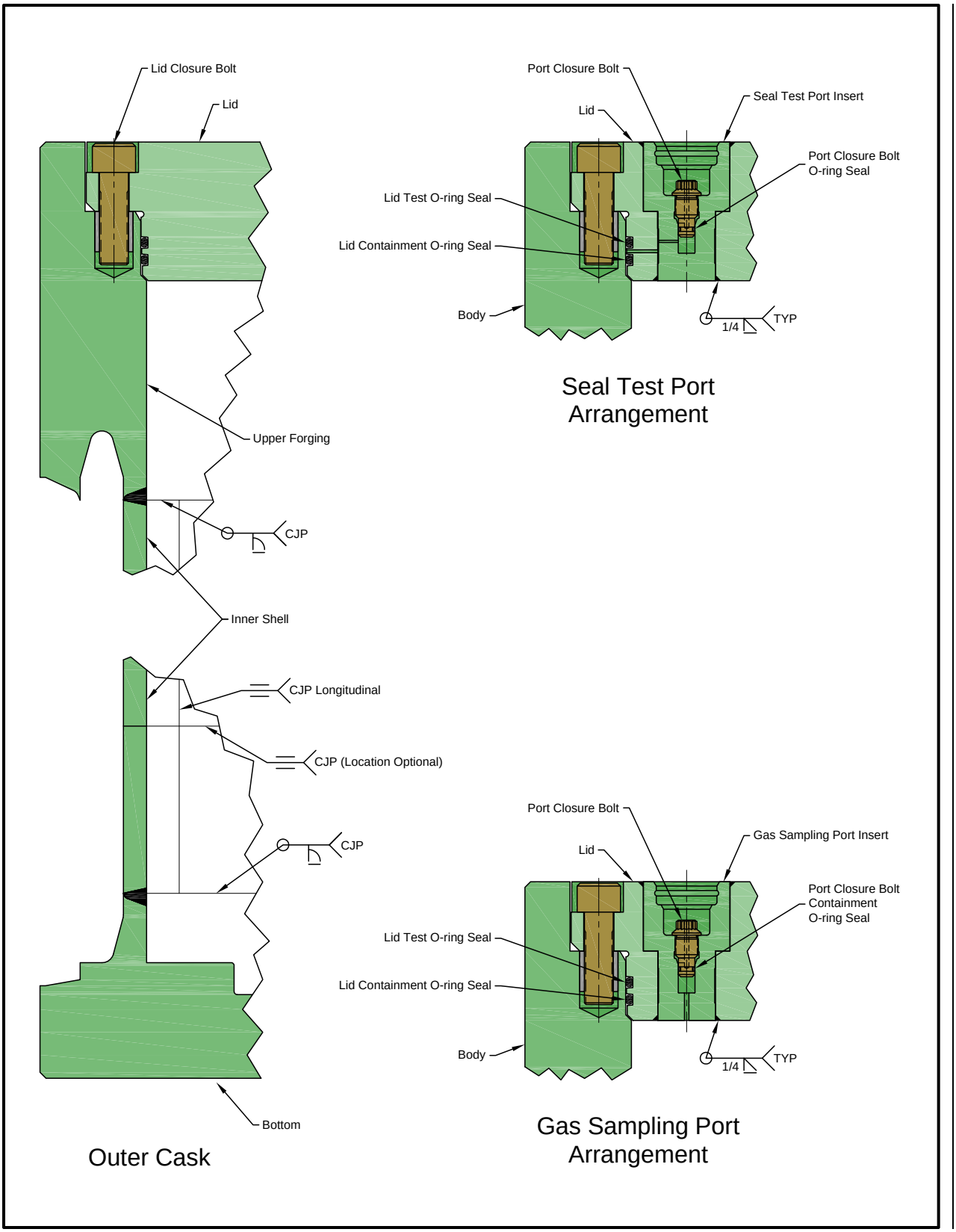

Figure 1.2-2 ï Outer Cask Containment Components

1.3 Appendices

1.3.1 *Packaging General Arrangement Drawings*

1.3.2 *Glossary of Terms and Acronyms*

This page intentionally left blank.

1.3.1 Packaging General Arrangement Drawings

This page intentionally left blank.

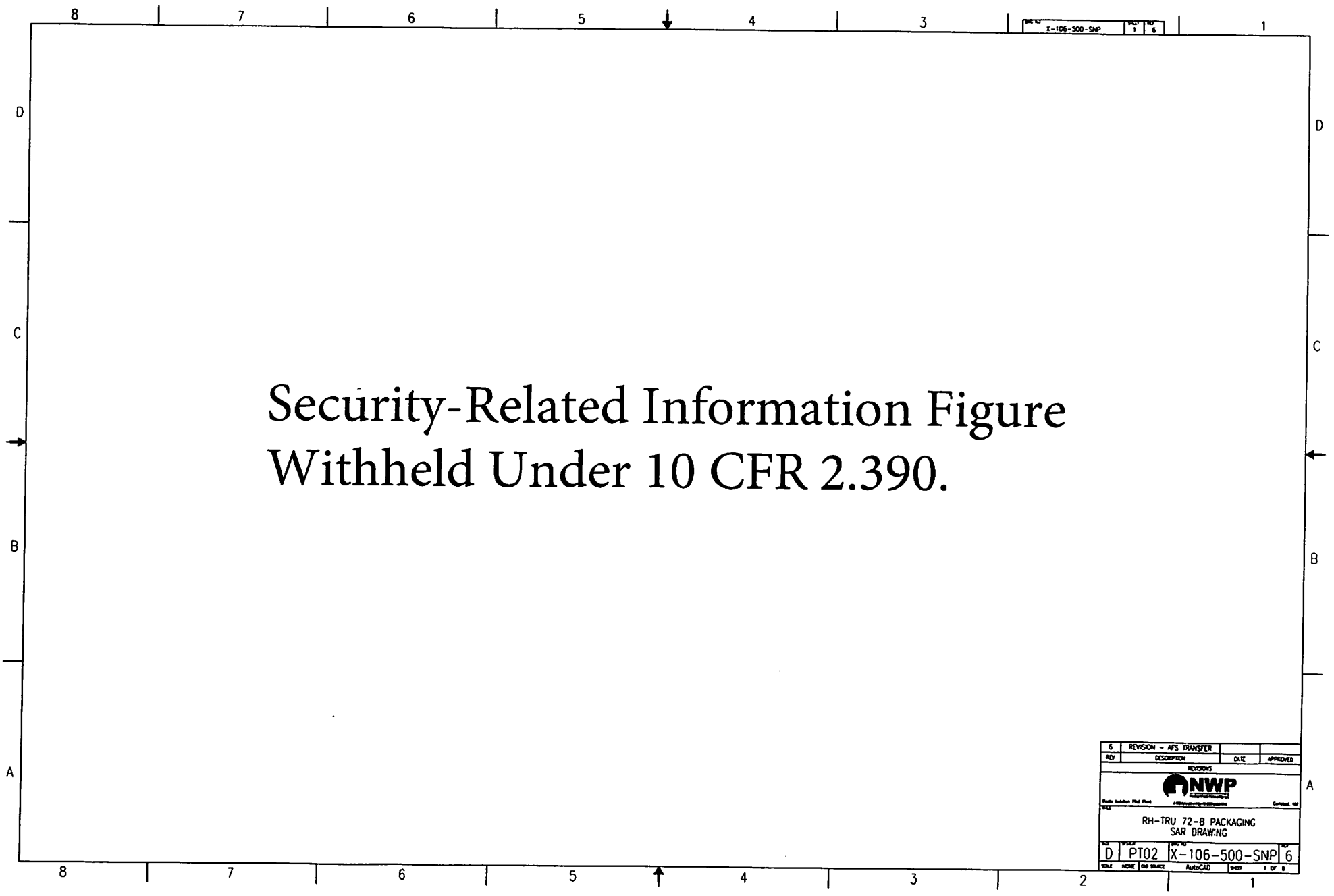
Security-Related Information Figure
Withheld Under 10 CFR 2.390.
6 REVISION - AFS TRANSFER
REV DESCRIPTION DATE APPROVED
REVISIONS
NWP
RH-TRU 72-B PACKAGING
SAR DRAWING
D PT02 X-106-500-SNP 6
AutoCAD

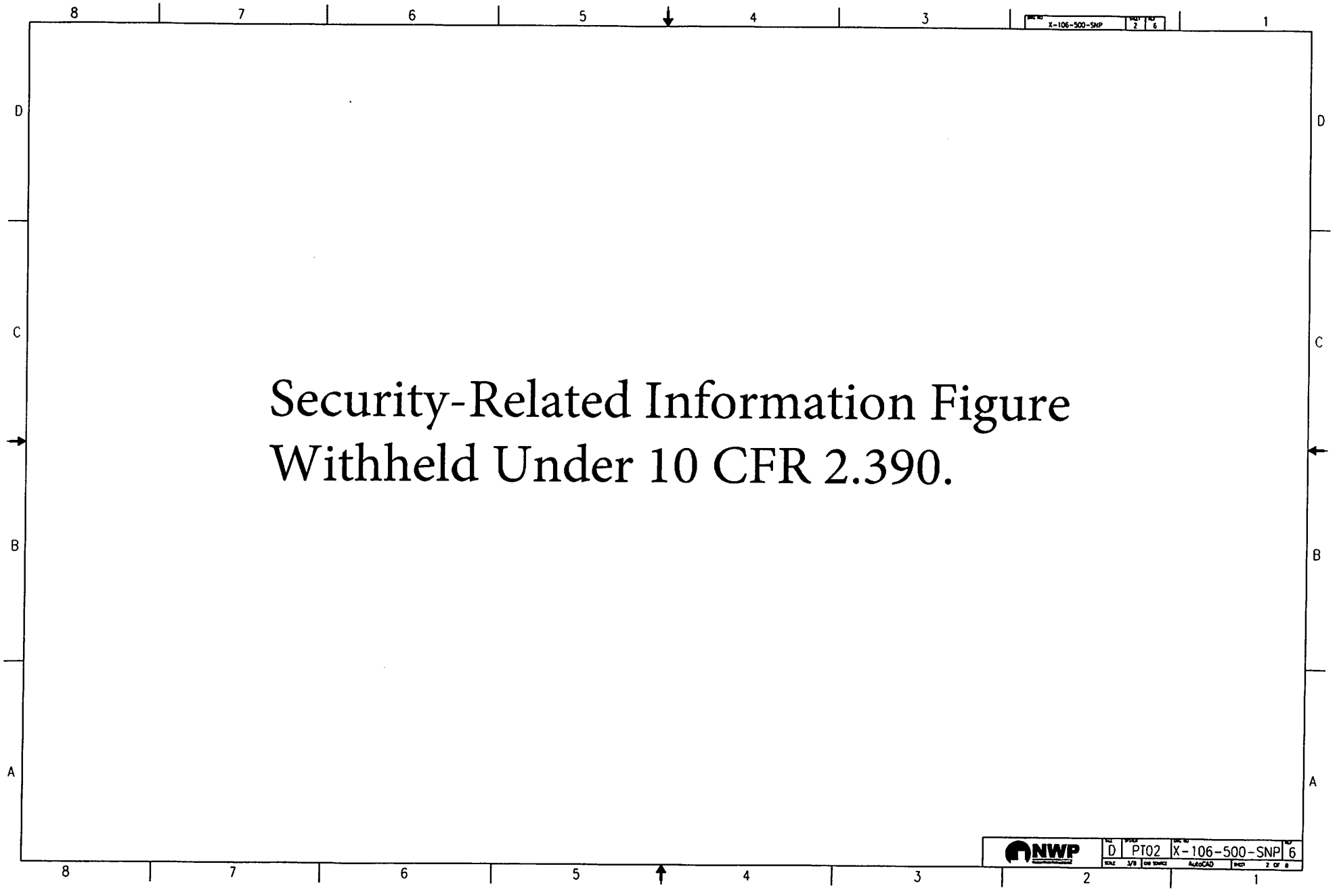
Security-Related Information Figure
Withheld Under 10 CFR 2.390.

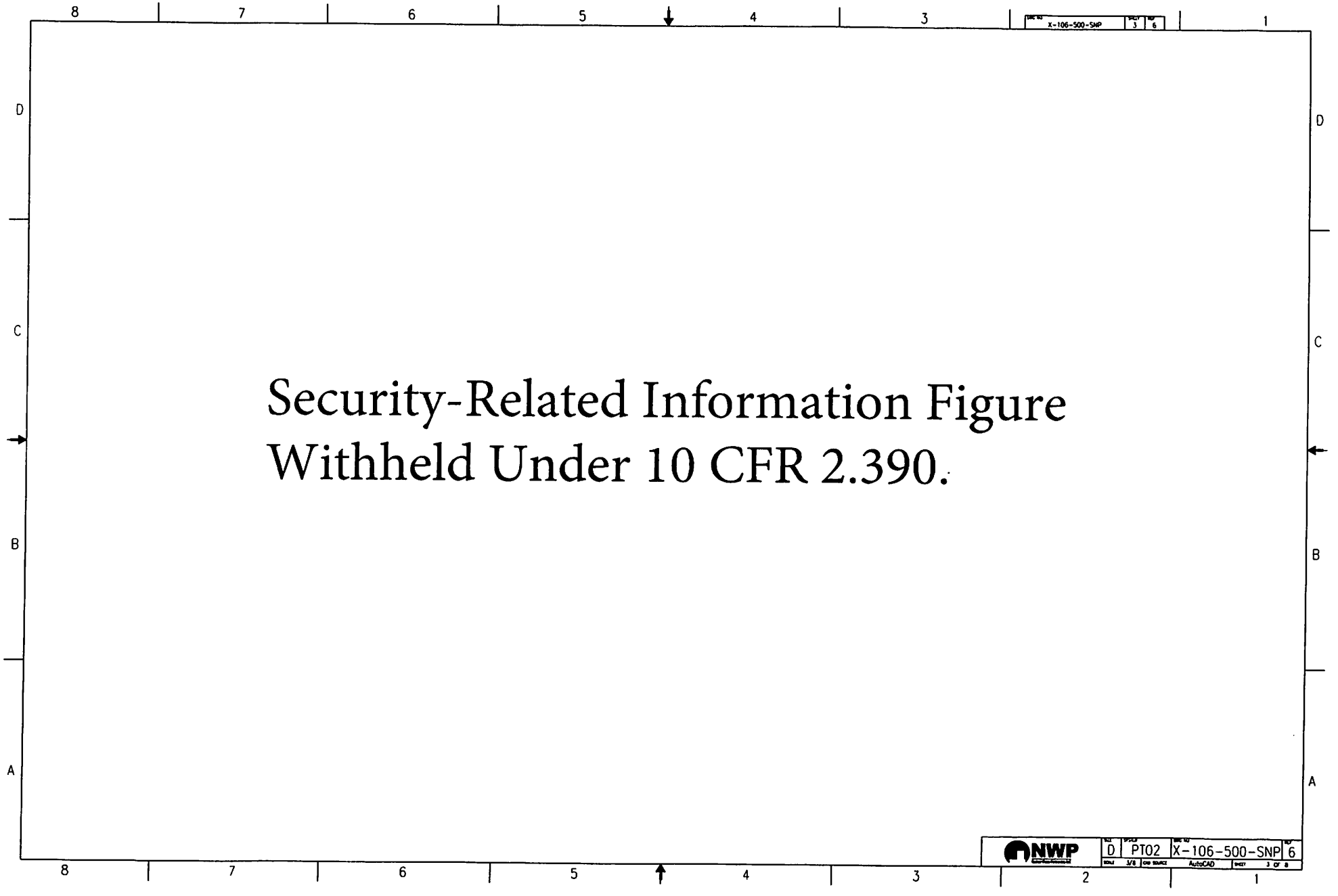
Security-Related Information Figure
Withheld Under 10 CFR 2.390.

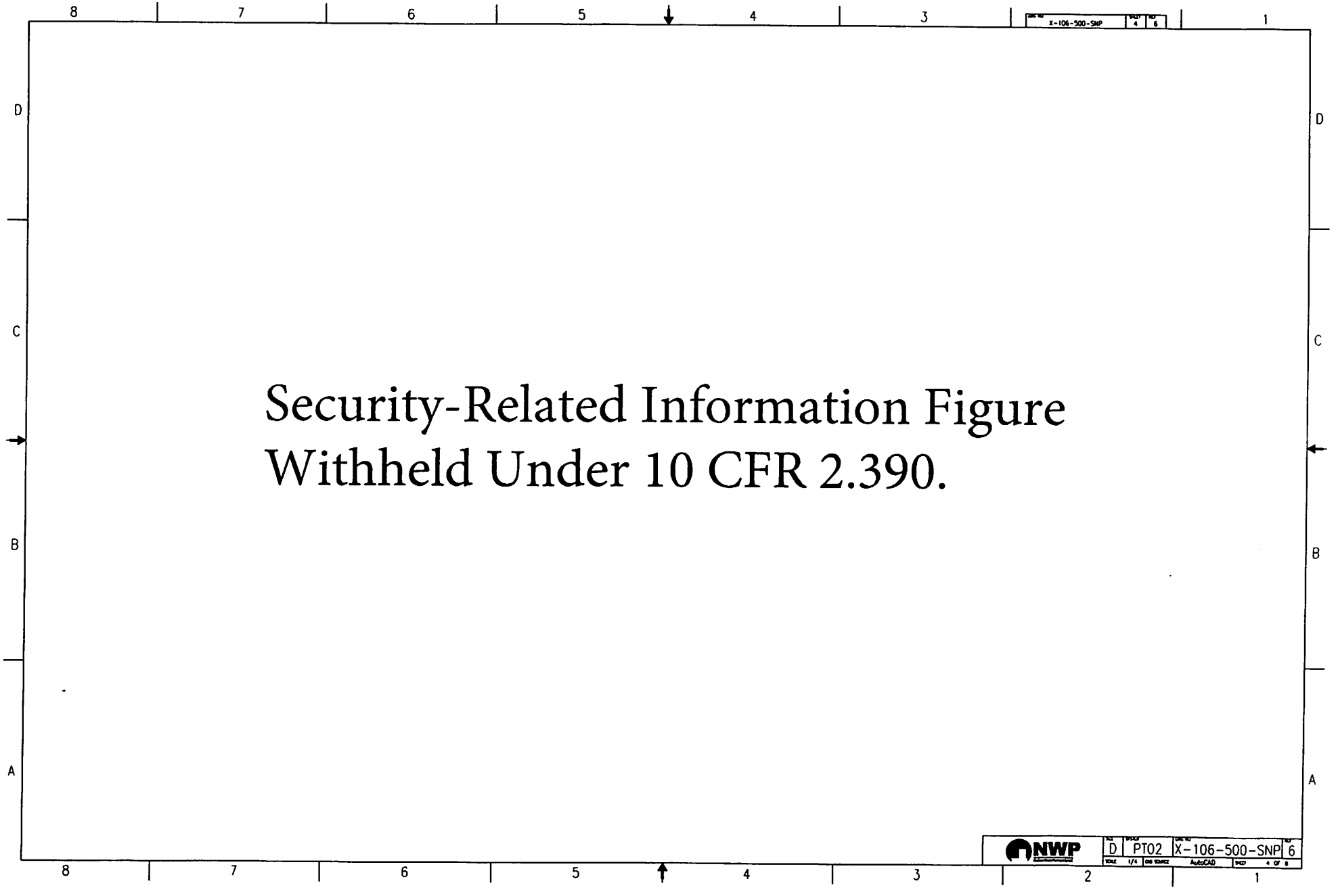
Security-Related Information Figure
Withheld Under 10 CFR 2.390.

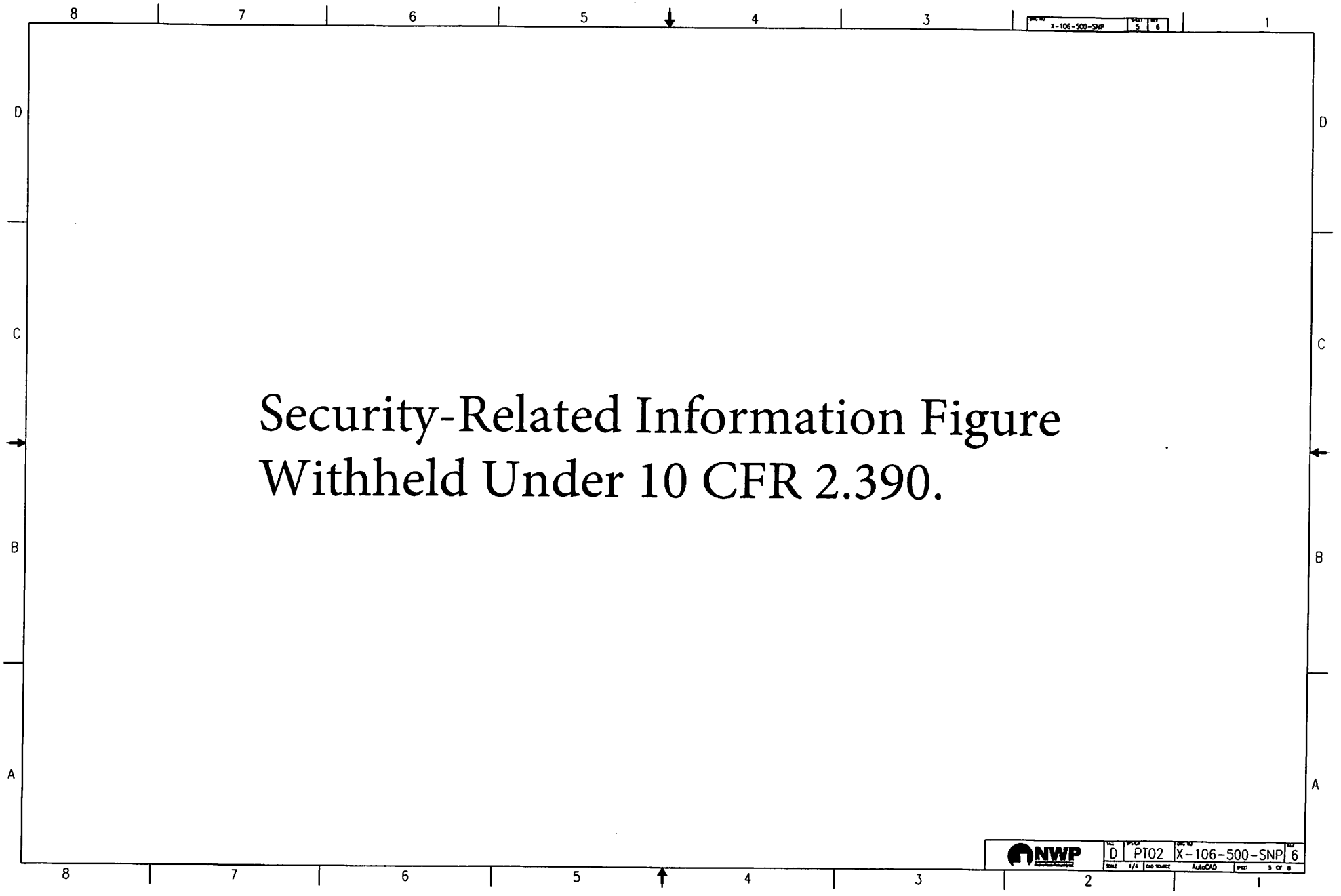
Security-Related Information Figure
Withheld Under 10 CFR 2.390.

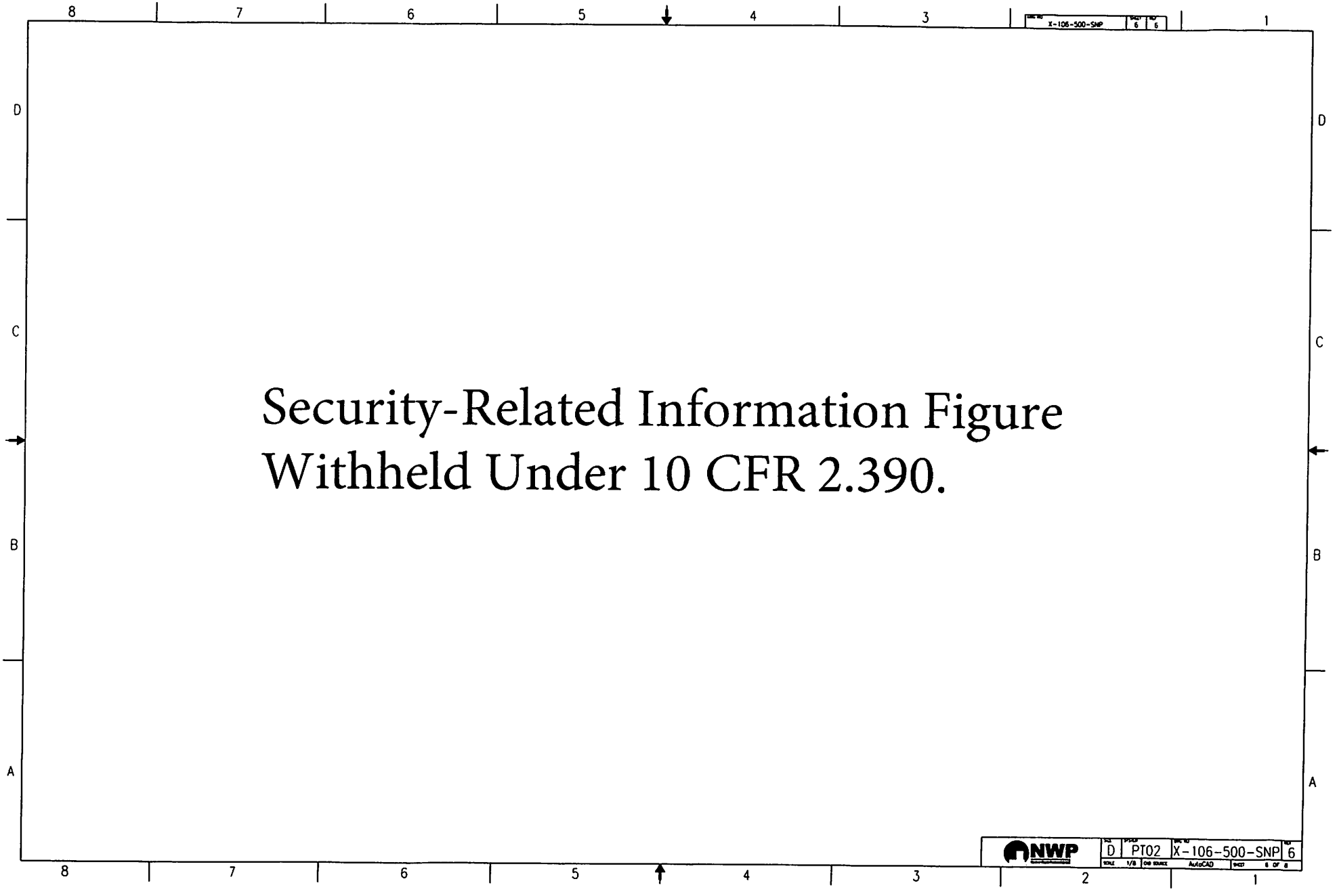
Security-Related Information Figure
Withheld Under 10 CFR 2.390.

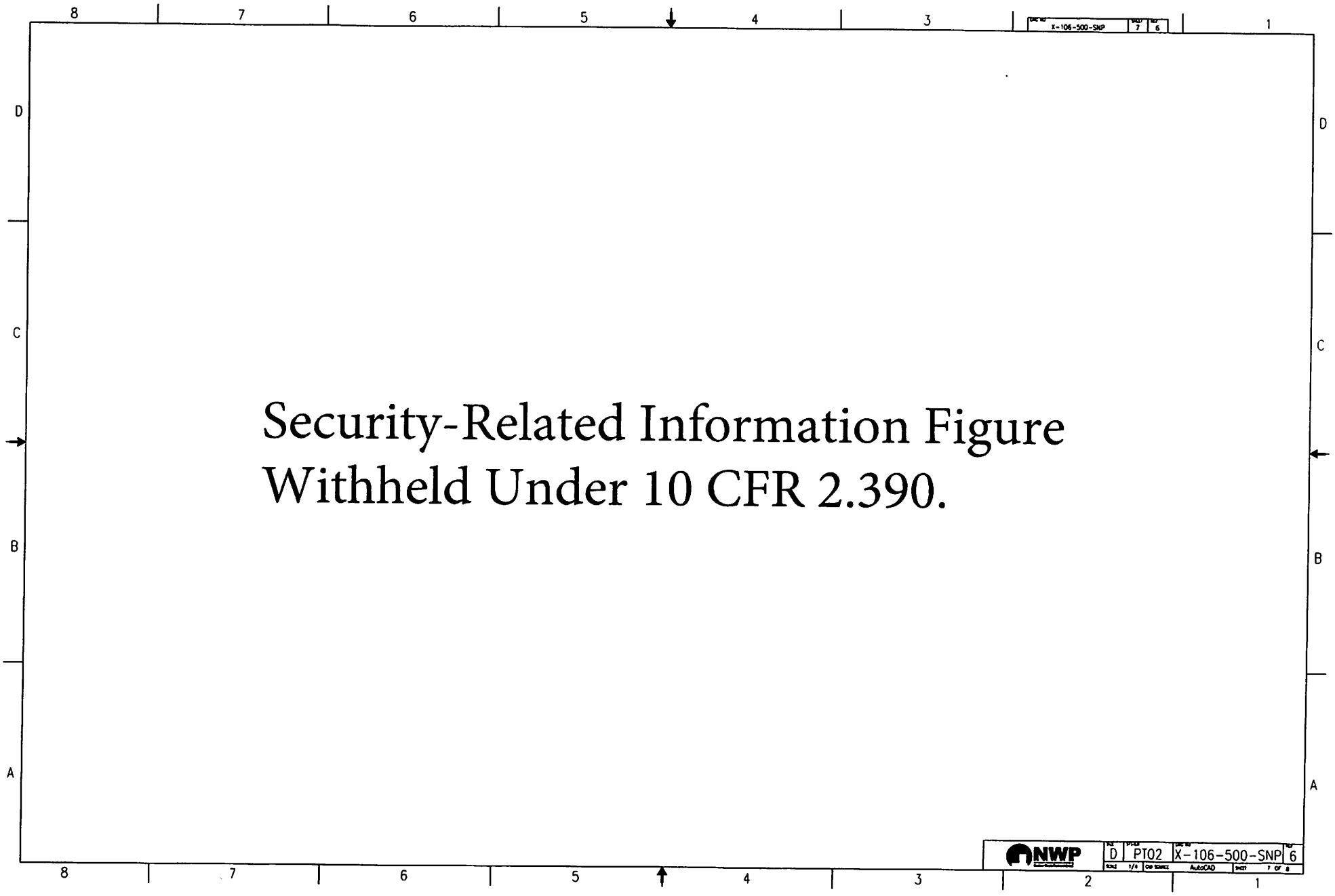
Security-Related Information Figure
Withheld Under 10 CFR 2.390.
X-106-500-SNP
NWP
D
PT02
X-106-500-SNP
6
AutoCAD

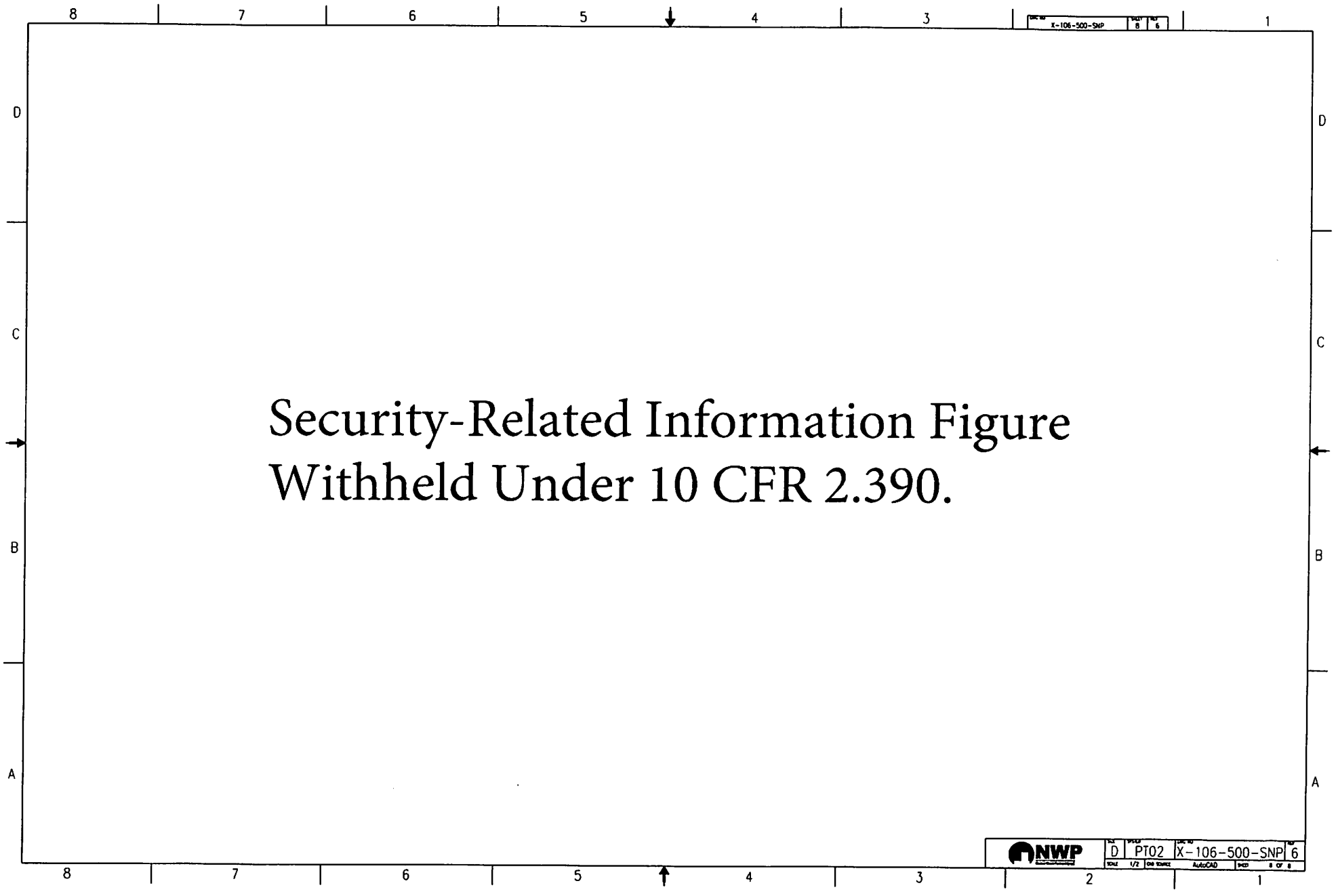
Security-Related Information Figure
Withheld Under 10 CFR 2.390.
NWP
D
PT02
X-106-500-SNP
6

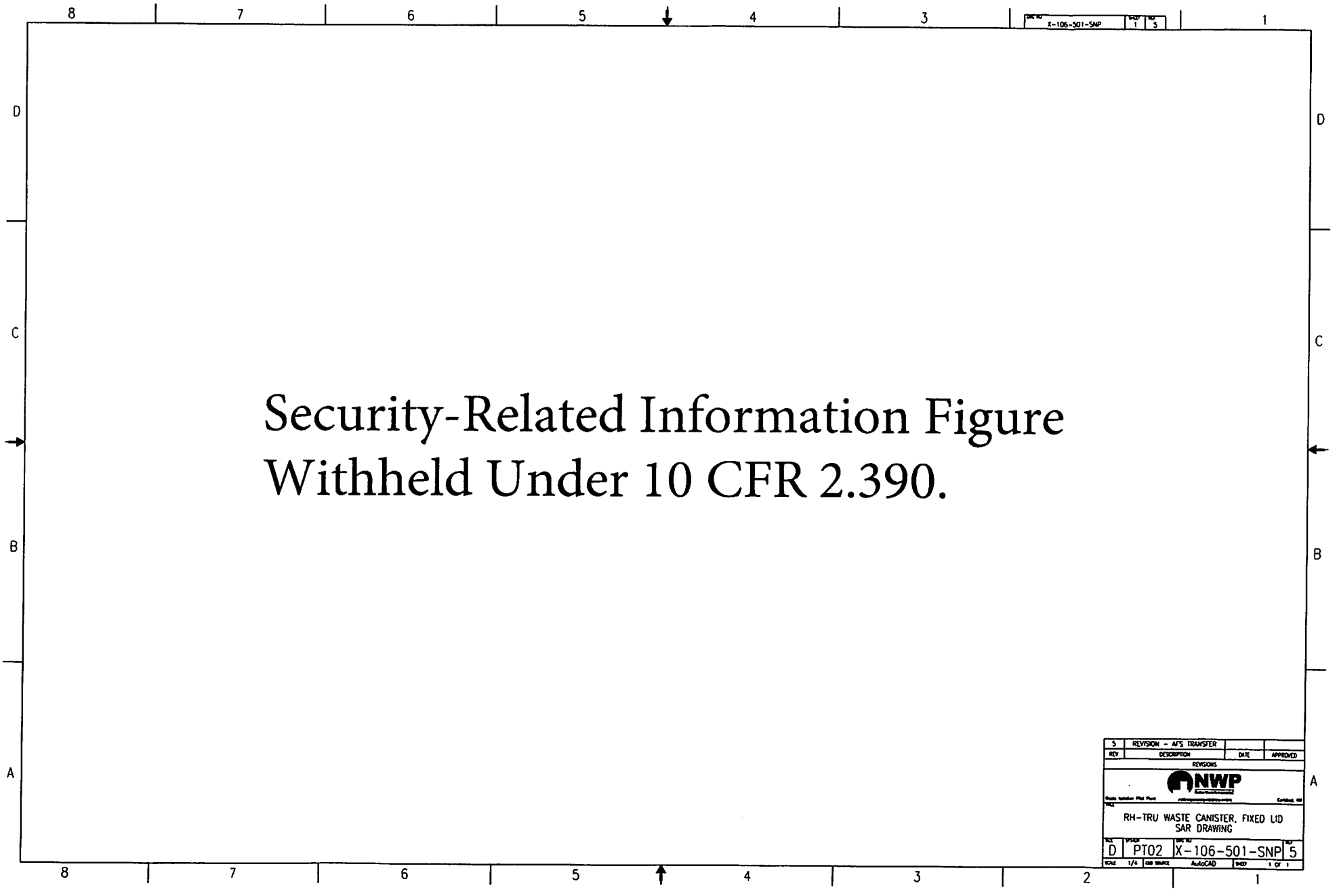
Security-Related Information Figure
Withheld Under 10 CFR 2.390.
5 REVISION - AFS TRANSFER
REVISIONS
NWP
RH-TRU WASTE CANISTER, FIXED LID
SAR DRAWING
D PT02 X-106-501-SNP 5

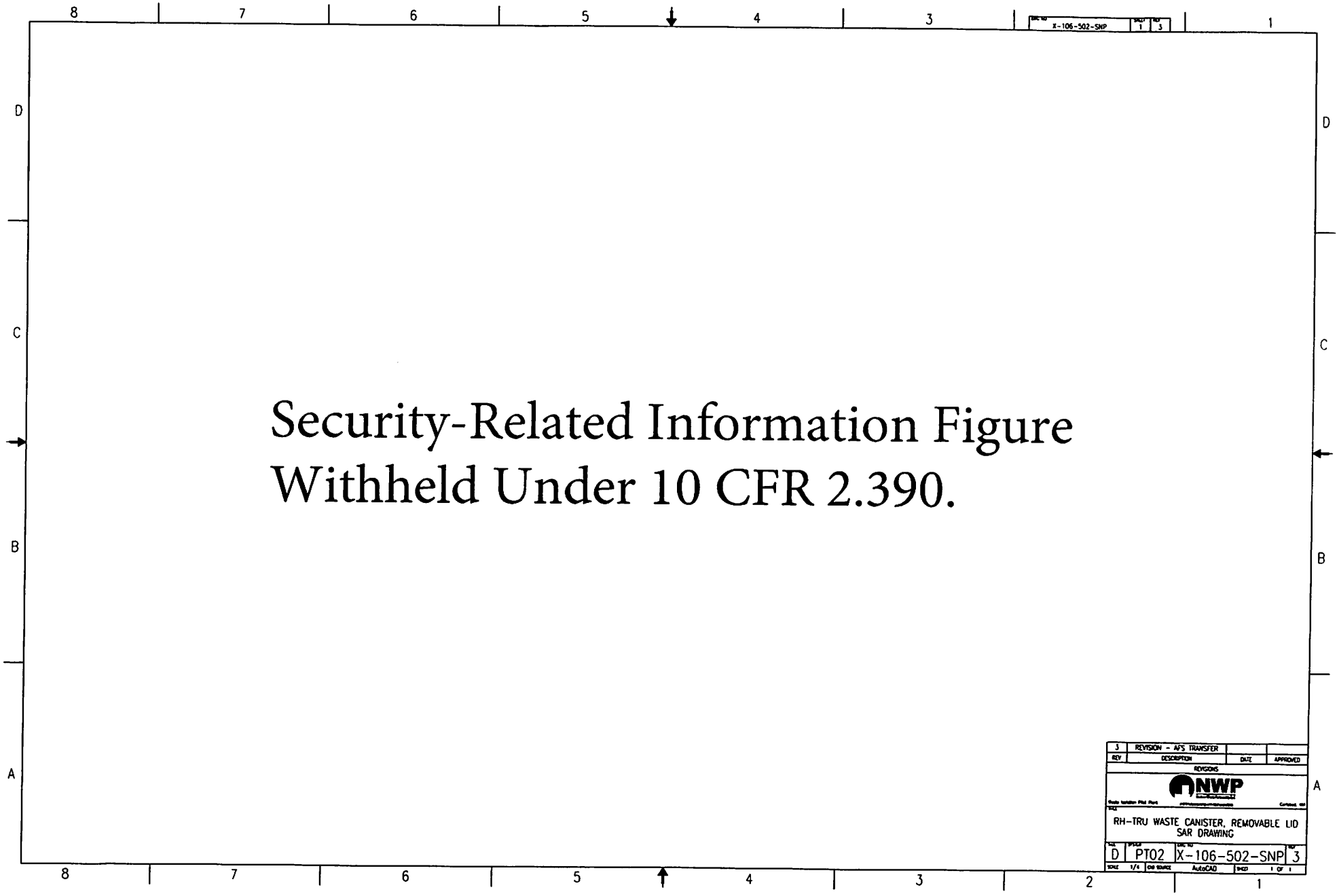
Security-Related Information Figure
Withheld Under 10 CFR 2.390.
3 REVISION - AFS TRANSFER
REVISIONS
RH-TRU WASTE CANISTER, REMOVABLE LID
SAR DRAWING
D PT02 X-106-502-SNP 3
AutoCAD

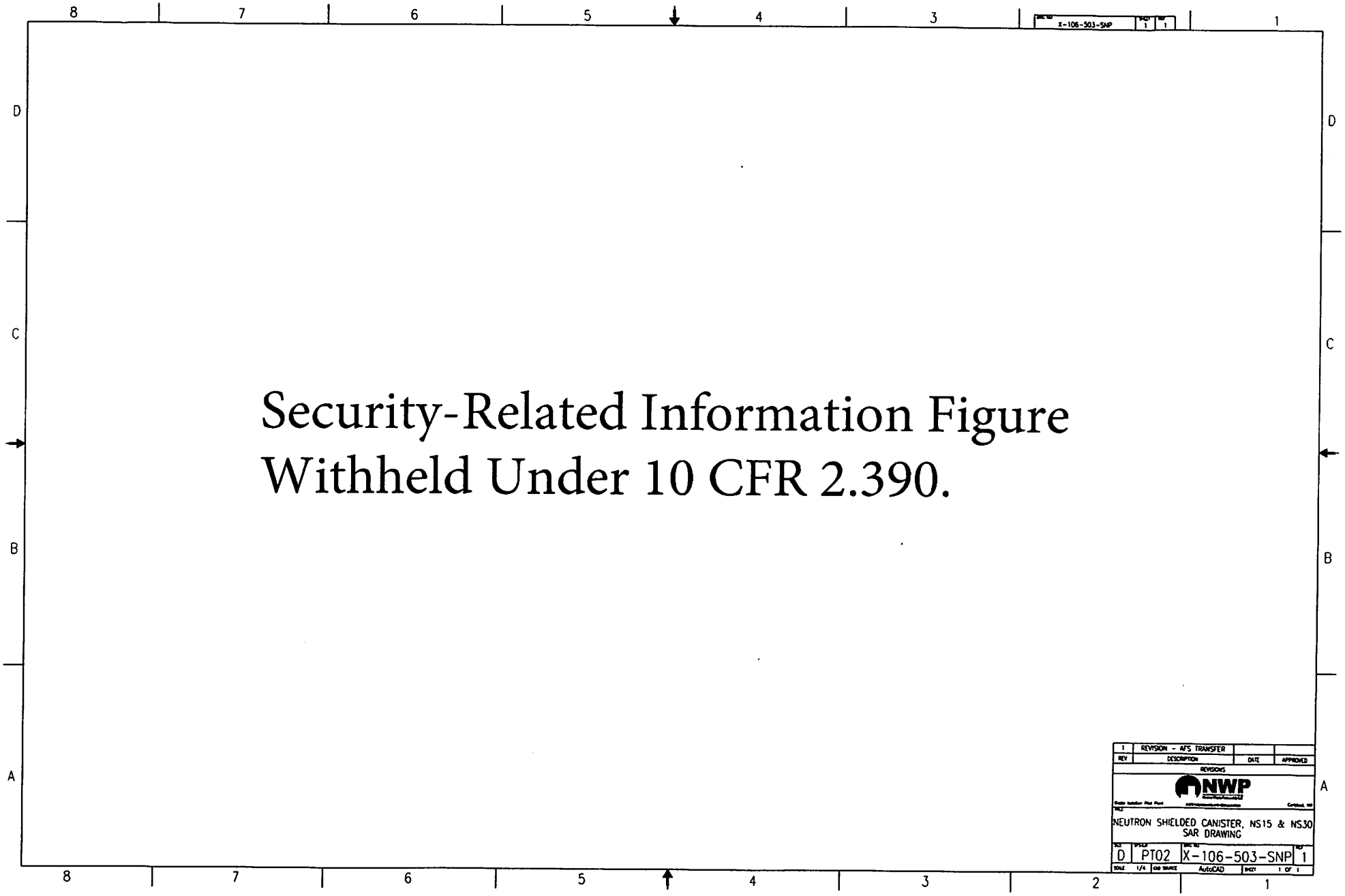
Security-Related Information Figure
Withheld Under 10 CFR 2.390.
NEUTRON SHIELDED CANISTER, NS15 & NS30
SAR DRAWING
X-106-503-SNP
PT02
AutoCAD

This page intentionally left blank to facilitate duplex printing.

1.3.2 Glossary of Terms and Acronyms

ALARA – As Low As Reasonably Achievable; the radiation safety principle for minimizing radiation doses and releases of radioactive materials by employing all reasonable methods.

ASME – American Society of Mechanical Engineers.

ASME B&PVC – ASME Boiler and Pressure Vessel Code.

Bolt Hole Access Debris Ring – An optional ring covering the six impact limiter attachment bolt access tubes on each impact limiter.

Cask – The assembly of components comprising the RH-TRU 72-B packaging (see ***Packaging***).

Center-Pivot Trunnions – The two circular trunnions located at the OC's center of length that serve as the package's main tie-down points, and allow uprighting of the package while situated on a transport trailer.

Impact Limiters – Polyurethane foam-filled impact energy absorbers and thermal insulators that are located at each end of the OC.

Impact Limiter Attachment Bolts – The six 1¼-7UNC socket head cap screws used to secure each impact limiter to the OC body.

Inner Vessel – The assembly (comprised of an IV lid and IV body) providing an optional secondary level of containment for the payload. Credit for this secondary level of containment is only taken if an optional preshipment leakage rate test is successfully performed.

IV – Inner Vessel (secondary containment vessel).

IV Alignment Lug – The flat external protuberance located at the bottom of the IV body for aligning the IV with the mating socket in the OC body bottom.

IV Backfill Port – The penetration into IV lid that allows tracer gas backfill between the lower (backfill) O-ring seal and the middle (containment) O-ring seal.

IV Backfill Port Closure Bolt – The IV backfill port closure assembly consisting of a cross-drilled bolt and an O-ring seal.

IV Backfill Port Insert – The replaceable IV backfill port component that provides the interface for the IV backfill port closure bolt.

IV Body – The assembly consisting of the IV seal flange, cylindrical shell, and bottom closure.

IV Closure Bolts – The eight 7/8-9UNC socket head cap screws used to secure the IV lid to the IV body; each assembly consists of a necked-down bolt, a spring, and an optional stainless steel washer to enhance remote operations.

IV Closure Bolt Thread Insert – The optional thread insert to allow thread replacement, if necessary.

IV Gas Sampling Port – The penetration through the IV lid that allows venting and gas sampling of the IV cavity.

IV Gas Sampling Port Closure Bolt – The IV gas sampling port closure assembly consisting of a cross-drilled bolt and an O-ring seal.

IV Gas Sampling Port Insert – The replaceable IV gas sampling port component that provides the interface for the IV gas sampling port closure bolt.

IV Lid – The monolithic mating closure for the IV body.

IV Lid Pintle Socket – The bayonet-type recess at the lid's centerline for handling the IV lid.

IV Lower O-ring Seal – The lower elastomeric O-ring seal in the IV seal flange that forms the tracer gas boundary for leakage rate testing.

IV Middle O-ring Seal – The middle elastomeric O-ring seal in the IV seal flange that forms the containment boundary.

IV Seal Test Port – The penetration into the IV lid that allows testing between the middle (containment) O-ring seal and upper (test) O-ring seal.

IV Seal Test Port Closure Bolt – The IV upper seal test port closure assembly consisting of a cross-drilled bolt and an O-ring seal.

IV Seal Test Port Insert – The replaceable IV upper seal test port component that provides the interface for the IV upper seal test port closure bolt.

IV Upper O-ring Seal – The upper elastomeric O-ring seal in the IV seal flange that forms the test boundary for leakage rate testing.

FEM – Fissile Equivalent Mass of ^{235}U.

FGE – Fissile Gram Equivalent of ^{239}Pu.

HAC – Hypothetical Accident Conditions.

LEU – Low-Enriched Uranium.

Lift/Tie-down Trunnions – The four circular trunnions located near the OC's closure end; two lift/tie-down trunnions serve as the package's lift points, and two serve as secondary tie-down points.

NCT – Normal Conditions of Transport.

NSC – Neutron Shielded Canister.

OC – Outer Cask (primary containment vessel).

OC Body – The assembly consisting of the OC seal flange, inner and outer cylindrical shells, lead biological shielding, thermal shield, and bottom closure.

OC Closure Bolts – The eighteen 1¼-7UNC socket head cap screws used to secure the OC lid to the OC body.

OC Closure Bolt Thread Insert – The optional thread insert to allow thread replacement, if necessary.

OC Gas Sampling Port – The penetration through the OC lid that allows venting and gas sampling of the OC cavity.

OC Gas Sampling Port Closure Bolt – The OC gas sampling port closure assembly consisting of a cross-drilled bolt and an O-ring seal.

OC Gas Sampling Port Insert – The replaceable OC gas sampling port component that provides the interface for the OC gas sampling port closure bolt.

OC Lid – The monolithic mating closure for the OC body.

OC Lid Pintle Socket – The bayonet-type recess at the lid's centerline for handling the OC lid.

OC Lower O-ring Seal – The lower elastomeric O-ring seal in the OC seal flange that forms the containment boundary.

OC Seal Test Port – The penetration into the OC lid that allows testing between the lower (containment) O-ring seal and upper (test) O-ring seal.

OC Seal Test Port Closure Bolt – The OC seal test port closure assembly consisting of a cross-drilled bolt and an O-ring seal.

OC Seal Test Port Insert – The replaceable OC seal test port component that provides the interface for the OC seal test port closure bolt.

OC Thermal Shield – The thin shell outside the heavy OC outer shell that prevents hot gasses and flames from directly impinging on the OC surface in the event of a HAC fire.

OC Upper O-ring Seal – The upper elastomeric O-ring seal in the OC seal flange that forms the test boundary for leakage rate testing.

Outer Cask – The assembly (comprised of an OC lid and OC body) providing a primary level of containment for the payload.

Package – The packaging with its radioactive contents, or payload, as presented for transportation as defined in 10 CFR §71.4. Within this SAR, the package is denoted as the RH-TRU 72-B package.

Packaging – The assembly of components necessary to ensure compliance with packaging requirements as defined in 10 CFR §71.4. Within this SAR, the packaging is denoted as the RH-TRU 72-B packaging.

Payload – Remote-handled transuranic (RH-TRU) waste or other authorized contents contained within the approved payload container. In this SAR, the payload includes a payload canister. Payload requirements are defined by the RH-TRAMPAC.

Payload Canister – The receptacle containing the RH-TRU waste. Multiple design variants include the RH-TRU Waste Canister (fixed and removable lid; FLC and RLC) and Neutron Shielded Canister (NS15 and NS30).

RH-TRAMPAC – Remote-Handled Transuranic Waste Authorized Methods for Payload Control defines the authorized contents for the RH-TRU 72-B packaging.

RH-TRU 72-B Package – The package consisting of a RH-TRU 72-B packaging and the payload.

RH-TRU 72-B Packaging – The packaging consisting of an outer cask (OC), an inner vessel (IV), and two impact limiters.

RH-TRU Waste – Remote-Handled Transuranic Waste.

RTV – Room Temperature Vulcanizing.

SAR – Safety Analysis Report (this document).

Tamper Indicating Device – A lock-wire or equivalent device that is installed between the closure-end impact limiter and the OC body prior to each shipment.

Tie-down Trunnions – The two circular trunnions located near the OC's bottom end, serving as secondary tie-down points.

2.0 STRUCTURAL EVALUATION

This chapter presents structural evaluations demonstrating that the RH-TRU 72-B package design meets all applicable structural criteria. The energy absorbing external impact limiters, outer cask (OC), and inner vessel (IV) are evaluated and shown to provide adequate protection for the package payload (loaded payload canister). Normal conditions of transport (NCT) and hypothetical accident condition (HAC) evaluations, using analytical and experimental techniques, are performed in accordance with 10 CFR 71[1] requirements. Analytical demonstration techniques comply with the methodology presented in NRC Regulatory Guide 7.6[2].

A description of the neutron shielded canister structural evaluation is provided in Appendix 5.1 of the *RH-TRU Payload Appendices*[3]. The following evaluations are presented for payload canisters without supplemental neutron shielding components.

2.1 Structural Design

Component tests have been performed to verify mechanical properties and physical performance. These tests are described within subsequent sections where appropriate. For example, component testing of package external impact limiters has been carried out to refine the design and to characterize the behavior and performance of the impact limiters. Burn tests, on the polyurethane foam used in the impact limiters, have been performed to establish foam characteristics during exposure to the hypothetical fire event. These tests were performed in conjunction with the NuPac 125-B cask[4] development program. Since that package utilizes the same type and density of foam as used in the RH-TRU 72-B package, the test results are directly applicable. These results are presented in Appendix 3.6.3, *Polyurethane Foam Performance Tests*. As indicated by the preceding discussions, detailed test results are typically relegated to the appendices herein.

The RH-TRU 72-B package bears a strong resemblance to the NuPac 125-B cask[4]. Analytical techniques, successfully utilized for the licensing of the NuPac 125-B cask, are generally repeated for the RH-TRU 72-B package. Additionally, parallels between the two packages are frequently taken advantage of herein to simplify and clarify the analysis methodologies.

The following table summarizes NuPac 125-B cask[4] test results that are specifically considered when evaluating the RH-TRU 72-B package design:

[1] Title 10, Code of Federal Regulations, Part 71 (10 CFR 71), *Packaging and Transportation of Radioactive Material*, 01-01-14 Edition.

[2] U. S. Nuclear Regulatory Commission, Regulatory Guide 7.6, *Design Criteria for the Structural Analysis of Shipping Package Containment Vessels*, Revision 1, March 1978.

[3] U.S. Department of Energy (DOE), *RH-TRU Payload Appendices*, U.S. Department of Energy, Carlsbad Field Office, Carlsbad, New Mexico.

[4] Nuclear Packaging, Inc., *Safety Analysis Report for the NuPac 125-B Fuel Shipping Package*, USNRC Certificate of Compliance 71-9200, U.S. Department of Energy, Washington, D.C.

Section	72-B Evaluation	Utilization of Previous 125-B Data
2.7.1	Free Drop	Accelerometer traces from 125-B testing indicate the 125-B and 72-B packages can be reasonably treated as rigid bodies, thus helping to justify static application of impact accelerations.
2.7.1.1(9)	End Drop Lead Slump	The 72-B evaluation approach used to demonstrate that lead slump will not occur is further validated by reference to the fact that no lead slump was observed in end drop testing of a prototypic 125-B package body.
2.7.8	Side Punch Lead Deformation	72-B lead deformation is established by comparing to 125-B testing which employed a prototypic package body. 72-B testing only used an all steel, dummy package mass simulation and could not be used for this assessment.
3.6.3	Polyurethane Foam Burn Performance	Burn tests of 125-B foam, which is essentially identical to 72-B foam, are directly referenced.

2.1.1 Discussion

The RH-TRU 72-B, Type B(M)F-96, package consists of three basic components: (1) the energy-absorbing external impact limiters that protect the ends of the OC, (2) the OC (primary containment), and (3) the IV (secondary containment). The polyurethane foam-filled impact limiters serve the dual purposes of limiting *g*-loads acting on the package under drop conditions and providing thermal insulation for the hypothetical accident fire event. By selecting a proper density foam, *g*-loads acting upon the package are limited to acceptable levels.

The basic structure of the OC consists entirely of stainless steel (Type 304 or 304L) materials and is comprised of a 5-inch thick bottom closure plate, which welds directly to an outer shell (1½-inch thick, 41⅛-inch OD) and an inner shell (1-inch thick, 34⅜-inch OD). The annular region between these shells (1⅞-inch thick) is filled with lead shielding. The top closure consists of a thick-walled forging (ring) which welds directly to the inner and outer shells and a 6-inch thick closure plate (lid) which bolts to the body forging via eighteen (18), ASTM A320, Grade L43, 1¼-7UNC bolts. The bottom closure plate, inner shell, top forging and top closure plate form the outer containment boundary. Lifting and handling trunnions are attached to the outer, 1½-inch thick shell.

The basic structure of the IV is fabricated of stainless steel (Type 304 or 304L) materials and consists of a 1½-inch thick bottom closure plate which welds directly to a 3/8-inch thick shell (32-inch OD). At the top end, the shell is welded to a thick upper forging and final closure is provided by a 6½-inch thick closure plate (lid). The closure lid plate attaches to the upper forging via eight (8), ASTM A320, Grade L43, 7/8-9UNC bolts. The inner containment boundary, therefore, consists of the bottom closure plate, shell, upper forging, and the top closure plate. The IV is designed so that, with the package vertical, the IV top or bottom closure plate will rest on the corresponding OC closure plate.

2.1.2 Design Criteria

2.1.2.1 Basic Design Criteria (Allowable Stresses)

This section defines the stress allowables for primary-membrane, primary-bending, secondary, peak, bearing, shear, and buckling stresses for containment structures and fasteners, and non-containment structures and fasteners.

NRC Regulatory Guide 7.6[2] is used in conjunction with NRC Regulatory Guide 7.8[5] to evaluate the integrity of the RH-TRU 72 B-package. Where the loads specified by NRC Regulatory Guide 7.6[2] conflict with those given in the current version of 10 CFR 71, the latter is used. Material properties and design stress intensity values, S_m, used in the analyses can be found in Table 2.3-1 and Table 2.3-2.

2.1.2.1.1 Containment Structures

NRC Regulatory Guide 7.6[2] was used for all package containment boundaries for both NCT and the HAC. Material data used in the evaluation correspond to the design stress values, S_m, yield strengths, S_y, and ultimate strengths, S_u, given in the ASME Code, Section III, Class I[6]. The primary containment is considered to be the 32⅜-inch inside diameter, 1-inch thick inner OC shell, the OC upper forging, the 6-inch thick bolted OC closure lid, and the 5-inch thick OC bottom plate. The secondary containment is considered to be the 1½-inch thick IV bottom plate, the 31¼-inch inside diameter, 3/8-inch thick IV shell, the IV upper forging, and the 6½-inch thick bolted IV closure lid. A summary of allowable stresses used for containment structures and fasteners is presented in Table 2.1-1. These data are consistent with Regulatory Guide 7.6[2] and Section NB-3000 and Appendix F of the ASME Code, Section III[6].

2.1.2.1.2 Non-Containment Structures

Structural evaluations of non-containment boundaries, such as the OC outer shell, and tie-down and center-pivot trunnions, use allowable stresses for NCT and HAC as presented in Table 2.1-2. The impact limiters are allowed to exceed yield for all conditions. The acceptance criterion for all impact related loads within the impact limiters is that no package "hard points" directly come into contact with the impact surface. Adherence to this criterion is assured by designing the impact limiters so that no impact limiter deformation for any regulatory drop event ever exceeds the maximum strain level achieved in polyurethane foam crush tests. Foam samples have been tested to strains of up to 87%. Static testing of prototypic, half-scale RH-TRU 72-B package impact limiters imposed strains of up to 97% (for 35º from vertical orientation, see Appendix 2.10.7, *Static and Dynamic Testing*). For purposes of this Safety Analysis Report, a strain limit of 85% is imposed for the polyurethane foam. Requirements for foam mechanical properties are presented in Section 2.3, *Mechanical Properties of Materials*. For lifting and handling loads, the "non-containment" NCT allowables of Table 2.1-2 are utilized in conjunction with a load factor of three (3), per 10 CFR §71.45.

---

[5] U. S. Nuclear Regulatory Commission, Regulatory Guide 7.8, *Load Combinations for the Structural Analysis of Shipping Packages for Radioactive Material*, Revision 1, March 1989.

[6] American Society of Mechanical Engineers (ASME) Boiler and Pressure Vessel Code, Section III, *Rules for Construction of Nuclear Power Plant Components*, Division 1, Subsection NB and Appendices, 1986 Edition.

2.1.2.2 Miscellaneous Structural Failure Modes

2.1.2.2.1 Brittle Fracture

With the exception of the closure bolts and the canister (if ASTM A516, Grade 55, 60, or 70 carbon steel is used for payload canister construction), all containment, and nearly all non-containment structural components, are fabricated of Type 304, Type F304, or Type 304L austenitic stainless steel. Since this material does not undergo a ductile-to-brittle transition in the temperature range of interest (to -40 ºF), it is safe from brittle fracture.

The closure bolts are fabricated from ASTM A320, Grade L43, alloy steel, an ASME Section III, Class I, material. As such, it is in compliance with the applicable brittle fracture requirements of ASME Section III, Subsection NB. As part of the manufacturing process, bolts with a diameter greater than 1-inch must be examined in accordance with ASME Section III, Subsection NB, Paragraph NB-2580, and tested in accordance with ASME Section III, Subsection NB, Paragraph NB-2333. Per Section 5 of NUREG/CR-1815[7], bolts are generally not considered as fracture critical components because multiple load paths exist and because bolted systems are designed to be redundant. However, for purposes of comparison, the nil ductility transition (NDT) temperature of the closure bolts will be calculated and compared with the requirements of NUREG/CR-1815[7].

According to Section 6.2.1.1 of the ASTM A320, Grade L43, specification, the minimum impact energy absorption is 20 ft-lbs at -150 ºF. The Charpy impact measurement may be transformed into a fracture toughness value by using the empirical relation developed in Section 4.2 of NUREG/CR-1815[7], as follows:

$$K_{ID} = \sqrt{5E(C_V)} = 53{,}665 \text{ psi-in}^{1/2}$$

where K_{ID} = dynamic fracture toughness, psi $\text{in}^{1/2}$ and the elastic modulus, $E = 28.8(10)^6$ psi at -150 ºF (from Table I-6.0 in Appendix I of the ASME Code[6]), and the Charpy impact measurement, C_v = 20 ft-lbs.

The dynamic fracture toughness is translated to an equivalent nil-ductility transition (NDT) temperature by using the Design Reference K_{ID} curve given as Figure 2 of NUREG/CR-1815[7]. By interpolation, the temperature relative to the NDT temperature is found as:

$$T - NDT = 30 \text{ ºF}$$

Accordingly, the NDT temperature is:

$$NDT = -150 - (+30) = -180 \text{ ºF}$$

For Category I fracture critical components, and for section thicknesses of 1.25 inches (i.e., bolt diameter), Figure 3 of NUREG/CR-1815[7] gives the minimum offset, "A", as approximately 40 ºF. Thus, the maximum NDT temperature value is:

$$T_{NDT} = LST - A = -20 - 40 = -60 \text{ ºF}$$

[7] U.S. Nuclear Regulatory Commission, *Recommendations for Protecting Against Failure By Brittle Fracture in Ferritic Steel Shipping Containers Up to Four Inches Thick*, NUREG/CR-1815, June 1981.

where the maximum NDT temperature is T_{NDT} per NUREG/CR-1815[7], the lowest service temperature, LST = -20 ºF per NRC Regulatory Guide 7.6[2], and A = 40 ºF per Figure 3 of NUREG/CR-1815[7].

The ASTM A320, Grade L43, closure bolts experience a ductile-to-brittle transition temperature at -180 ºF, whereas the criterion of NUREG/CR-1815[7] prescribes a maximum NDT temperature of -60 ºF. The 120 ºF margin between criteria requirements and material capability provides conservative assurance that brittle fracture failures will not occur in these ferritic closure-bolt materials.

The RH-TRU payload canisters are fabricated from Type 304 (or Type 304L) austenitic stainless steel, or ASTM A516, Grade 55, 60, or 70 carbon steel. This carbon steel conforms to the fine austenitic grain size requirement of ASTM A20/A20M. Because of the fine grain structure, coupled with the less than 0.40-inch thickness, the potential for brittle fracture of the payload canister steel is minimized.

2.1.2.2.2 Fatigue

2.1.2.2.2.1 Normal Operating Cycles

Normal operating cycles do not present a fatigue concern for the RH-TRU 72-B package components which have no stress concentrations. This is because the allowable stress for NCT ($3.0S_m$) will not exceed the allowable fatigue stress limit for the expected number of operating cycles. From Table I-1.2 in Appendix I of the ASME Code[6], the maximum value of the stress intensity (S_m) at the maximum normal operating temperature established herein, 210 ºF, is 20,000 psi for the Type 304 stainless steel used in the RH-TRU 72-B package. The expected number of operating cycles (defined as the process of going from an empty package, to one with maximum heat load, at the maximum normal operating temperature, and back again) for the RH-TRU 72-B package is below 10,000. From Figure I-9.2.1 in Appendix I of the ASME Code[6], the fatigue allowable stress intensity amplitude, S_a, of the alternating stress component (one-half of the alternating stress range) for 10,000 cycles is 64,000 psi. This value, when multiplied by the ratio of elastic modulus, $27.5(10)^6/28.3(10)^6$, gives a fatigue allowable alternating stress intensity amplitude of 62,200 psi. The non-fatigue allowable stress intensity range, from Section NB 3222.2 of the ASME Code[6], however, is 60,000 psi ($3.0S_m$). Since one-half of this range (30,000 psi) is less than the fatigue allowable alternating stress intensity (62,200 psi), the non-fatigue allowable stress criterion will govern.

Areas of stress concentration for the package occur at the threads of the IV and OC closure bolts and the impact limiter attachment bolts, but the cyclic stresses for these bolts are dominated by preload and the minimum margin of safety for any bolt under NCT is 0.19 (for the OC per Table 2.10.6-1 of Appendix 2.10.6, *Closure Bolt Stress Evaluations*). Due to the redundant nature of these fasteners, a calculated fatigue life and associated tracking of individual bolt or component (lid or impact limiter) installation and removal cycles for each RH-TRU 72-B packaging is not required. In the event of an unexpected failure of a bolt during installation, all bolts of the same type currently in use on that packaging shall be replaced prior to continued use of the packaging.

2.1.2.2.2.2 Normal Vibration Over the Road

The criterion applied to analyze over-the-road vibration will be limited to the *g*-loading requirements established by 10 CFR 71. The vertical loading, 2*g*, will be used to evaluate the fatigue life of the RH-TRU 72-B package. Refer to Section 2.6.5, *Vibration*, for further discussion.

2.1.2.2.2.3 Extreme Total Stress Intensity Range

Per Paragraph C.7 of NRC Regulatory Guide 7.6[2], "The extreme total stress intensity range (including stress concentrations) between the initial state, the fabrication state, the normal operating conditions, and the accident conditions should be less than twice the adjusted value (adjusted to account for modulus of elasticity at the highest temperature) of S_a at 10 cycles given by the appropriate design fatigue curves." Evaluation of stresses per this criterion is addressed in Section 2.7.4.4, *Comparison with Allowable Stresses*.

2.1.2.2.3 Buckling

Buckling, per Paragraph C.5 of NRC Regulatory Guide 7.6[2], is an unacceptable failure mode for the containment vessels. The intent of this provision is to preclude large deformations that would compromise the validity of linear analysis assumptions and quasi-linear stress allowables, as given in Paragraph C.6 of NRC Regulatory Guide 7.6[2].

There are two shells within the RH-TRU 72-B package where buckling prevention criteria are applicable: the inner shell of the OC and the IV shell. For additional conservatism, the OC outer shell will also be evaluated. For reference purposes, the principal geometric features of these shells are listed in Table 2.1-3.

To demonstrate that buckling will not occur for these three shell geometries, the methodology of ASME Code Case N 284[8] is directly applied. The basic steps involved are summarized below. Details of the buckling assessments are presented in Appendix 2.10.5, *Buckling Design Criteria and Detailed Evaluation*.

1. Theoretical elastic buckling stresses are determined for hoop and axial compression and in-plane shear loadings using classical theory.
2. Capacity reduction factors are applied which account for the difference between classical theory and predicted instability stresses for fabricated shells.
3. Plasticity reduction factors are applied for those cases where elastically determined buckling stresses are above the proportional limit.
4. Elastic and inelastic buckling checks that employ appropriate factors of safety and appropriate interaction equations are made using worst-case applied compressive and in-plane shear stresses.

Consistent with the NRC Regulatory Guide 7.6[2] philosophy, factors of safety corresponding to ASME Code Level A and D Service conditions are employed respectively for NCT and HAC

[8] American Society of Mechanical Engineers (ASME) Boiler and Pressure Vessel Code, Section III, *Rules for Construction of Nuclear Power Plant Components*, Division 1, Class MC, Code Case N-284, *Metal Containment Shell Buckling Design Methods*, August 25, 1980 approval date.

loadings, with applicable factors of safety of 2.0 for NCT and 1.34 for HAC, as specified in ASME Code Case N 284[8].

Although the payload canister is not a containment boundary structure, as shown by the following calculations, a buckling mode of failure is not credible for the canister shell under NCT or HAC because the critical stresses due to uniform axial compression or bending of the canister are well above yield. As shown in step (6) of Section 2.7.1.2, *Corner and Oblique Drops*, canister shell membrane stresses (maximum of 23,703 psi, for HAC oblique drops) are always shown to be below yield (24,750 psi minimum for stainless steel at 210 °F), thus the buckling mode of failure is precluded.

From Table 35, Cases 15 and 16, of Roark[9], the following critical unit compressive stresses, σ', are established. After accounting for observed differences between test and theory, the minimum critical unit compressive stress of 129,272 psi is well above the canister minimum yield strength of 24,750 psi.

Case 15, uniform longitudinal compression, σ':

$$\sigma' = \frac{1}{\sqrt{3}} \frac{E}{\sqrt{1-\mu^2}} \frac{t}{r} = 323{,}180 \text{ psi}$$

where, $E = 27.5\times10^6$ psi at 210 °F, t = 0.25 in, r = 12.875 in, and μ = Poisson's ratio = 0.3.

As noted with the formula, tests indicate an actual buckling strength that is 40 to 60 percent of the theoretical value. Conservatively using 40%, the critical unit compressive stress becomes 129,272 psi.

Case 16, transverse bending moment, M′:

$$M' = K \frac{E}{1-\mu^2} rt^2 = 17.509\times10^6 \text{ in-lb}$$

where K is taken at its stated minimum value of 0.72 to account for differences between test and theory.

Converting to a critical unit compressive stress,

$$\sigma' = \frac{M'c}{I} = 134{,}472 \text{ psi}$$

where, c = r = 12.875 in and $I = (\pi/64)(26.0^4 - 25.5^4) = 1{,}676.4$ in^4.

[9] R. J. Roark, W. C. Young, *Formulas for Stress and Strain*, 5th Edition, McGraw-Hill, Inc., New York, NY, 1975.

Table 2.1-1 – Containment Components Allowable Stress Limits

Stress Category	NCT	HAC
Containment Structure Allowable Stress Limits		
Primary Membrane Stress Intensity	S_m	Lesser of: $2.4S_m$, $0.7S_u$
Primary Membrane + Bending Stress Intensity	$1.5S_m$	Lesser of: $3.6S_m$, S_u
Range of Primary + Secondary Stress Intensity	$3.0S_m$	N/A
Bearing Stress	S_y	Sealing Surfaces: S_y Elsewhere: S_u
Pure Shear Stress	$0.6S_m$	$0.42S_u$
Peak	Per Section 2.1.2.2.2, *Fatigue*	
Buckling	Per Section 2.1.2.2.3, *Buckling*	
Containment Fastener Allowable Stress Limits		
Membrane Stress Intensity①	Lesser of: $2.0S_m$, S_y	S_y
Membrane + Bending Stress Intensity①	Lesser of: $3.0S_m$, S_y	S_y

Notes:

① Not considering stress concentrations; stress concentration is considered in Section 2.1.2.2.2, *Fatigue*.

Table 2.1-2 – Non-Containment Components Allowable Stress Limits

Stress Category	NCT	HAC
Non-Containment Structure Allowable Stress Limits		
Primary Membrane Stress Intensity	Greater of: S_m, S_y	$0.7S_u$
Primary Membrane + Bending Stress Intensity	Greater of: $1.5S_m$, S_y	S_u
Range of Primary + Secondary Stress Intensity	Greater of: $3.0S_m$, S_y	N/A
Bearing Stress	S_y	Sealing Surfaces: S_y Elsewhere: S_u
Pure Shear Stress	Greater of: $0.6S_m$, $0.6S_y$	$0.42S_u$
Peak	Per Section 2.1.2.2.2, *Fatigue*	
Buckling	Per Section 2.1.2.2.3, *Buckling*	
Non-Containment Fastener Allowable Stress Limits		
Membrane Stress Intensity①	Greater of: $2.0S_m$, S_y	Greater of: S_y, $0.7S_u$
Membrane + Bending Stress Intensity①	Greater of: $3.0S_m$, S_y	S_u

Notes:

① Not considering stress concentrations; stress concentration is considered in Section 2.1.2.2.2, *Fatigue*.

Table 2.1-3 – Shell Buckling Geometries

Shell	Dimensions (inches)		
	Mean Radius (R)	**Thickness (t)**	**Length (L)**
OC Inner Shell	16.690	1.000	121.25
OC Outer Shell	19.815	1.500	121.62
IV Shell	15.813	0.375	111.75

This page intentionally left blank.

2.2 Weights and Centers of Gravity

The maximum total weight of the RH-TRU 72-B package, including a maximum payload of 8,000 pounds, is 45,000 pounds. The package is nearly symmetrical and, therefore, the center of gravity (CG) is very near the geometric center of the package. Though no significant deviation from this assumption is anticipated when the package is in service, a worst-case CG offset of 6.46 inches from the geometric center of the package is calculated in Section 2.5.2.1, *Center-Pivot and Tie-down Trunnion Loads*. This small offset is derived from a highly conservative assumption that payload is comprised of a 44.2-inch long, 26.5 inch diameter solid metal slug, weighing 6,900 pounds and located at the extreme end of the payload cavity. Using this assumption, the mass moment of inertia of the packaging can be recalculated. From Table 2.2-1, the mass moment of inertia of the package, less the payload canister, is 278,601 – 26,691 = 251,910 lb-in-s^2. (Figure 2.2-1 provides the component-numbering schematic for components identified in Table 2.2-1).

The mass moment of inertia of the assumed offset payload slug, I_m, can be calculated as:

$$I_m = \frac{m}{48}\left(3d^2 + 4l^2\right) = 3{,}691 \text{ lb-in-s}^2$$

where the mass of the payload, m = 6,900/386.4 = 17.857 lb-s^2/in, the diameter, d = 26.50 inches, and the length, l = 44.2 inches.

As calculated in Section 2.5.2.1, *Center-Pivot and Tie-down Trunnion Loads*, the distance of the offset payload CG from the package geometric center is approximately 26½ inches. The mass moment of inertia for the package with the extreme offset payload is thus 251,910 + 3,691 + $[(26.5)^2 \times 17.857]$ = 268,141 lb-in-s^2. This represents a difference of only [(278,601 – 268,141)/278,601] × 100 = 4% from the nominal value calculated in Table 2.2-1. Such a small difference in inertial characteristics will have a negligible effect on the dynamic response of the package to oblique impacts.

As a bounding case for side impacts, a worst-case assumption for payload distribution is made in Paragraph (3) of Section 2.6.7.3, *Flat Side Drop*, for normal conditions of transport (NCT) and Paragraph (3) of Section 2.7.1.3, *Flat Side Drop*, for hypothetical accident conditions (HAC). This assumption conservatively assumes the entire payload weight is lumped at one end of the inner vessel (IV). The analysis results are discussed in Appendix 2.10.1.5, *Containment Assembly Analysis for Side Drops*. Loading of the analysis model was accomplished by imposing the maximum linear acceleration derived from the impact analysis for a symmetrically loaded package.

Table 2.2-1 – RH-TRU 72-B Package Component Weights, Centers of Gravity, and Mass Moments of Inertia

Component	Approximate Weight (lb)	Distance to Center of Gravity① (in)	Approximate Mass Moment of Inertia② (lb-in-s^2)
1.0 Bottom Impact Limiter	2,547	-1.05	40,224
2.0 Outer Cask (OC)	27,883	71.11	145,287
2.1 Bottom Base Plate	1,967	2.57	24,773
2.2 Lead Shielding	10,739	67.07	38,592
2.3 Inner Shell	3,688	65.63	13,435
2.4 Outer Shell	6,587	65.43	25,147
2.5 Upper Forging	2,000	133.60	20,462
2.6 Lid	1,667	138.93	19,544
2.7 Trunnions	624	72.94	783
2.8 Thermal Shield/Wire	611	65.57	2,551
3.0 Inner Vessel (IV)	4,023	92.19	28,744
3.1 Bottom End Plate	354	5.77	4,149
3.2 Shell	1,216	63.38	3,907
3.3 Upper Forging	604	126.74	5,328
3.4 Lid	1,382	132.93	13,566
3.5 Spacers	467	67.50	1,794
4.0 Payload Canister	8,000	67.00	26,691
5.0 Upper Impact Limiter	2,547	142.80	37,655
TOTAL	**45,000**	**72.24**	**278,601**

Notes:

① The reference datum is the base of the outer cask (OC)

② The transverse-axis mass moment of inertia is about the transverse neutral axis of the package.

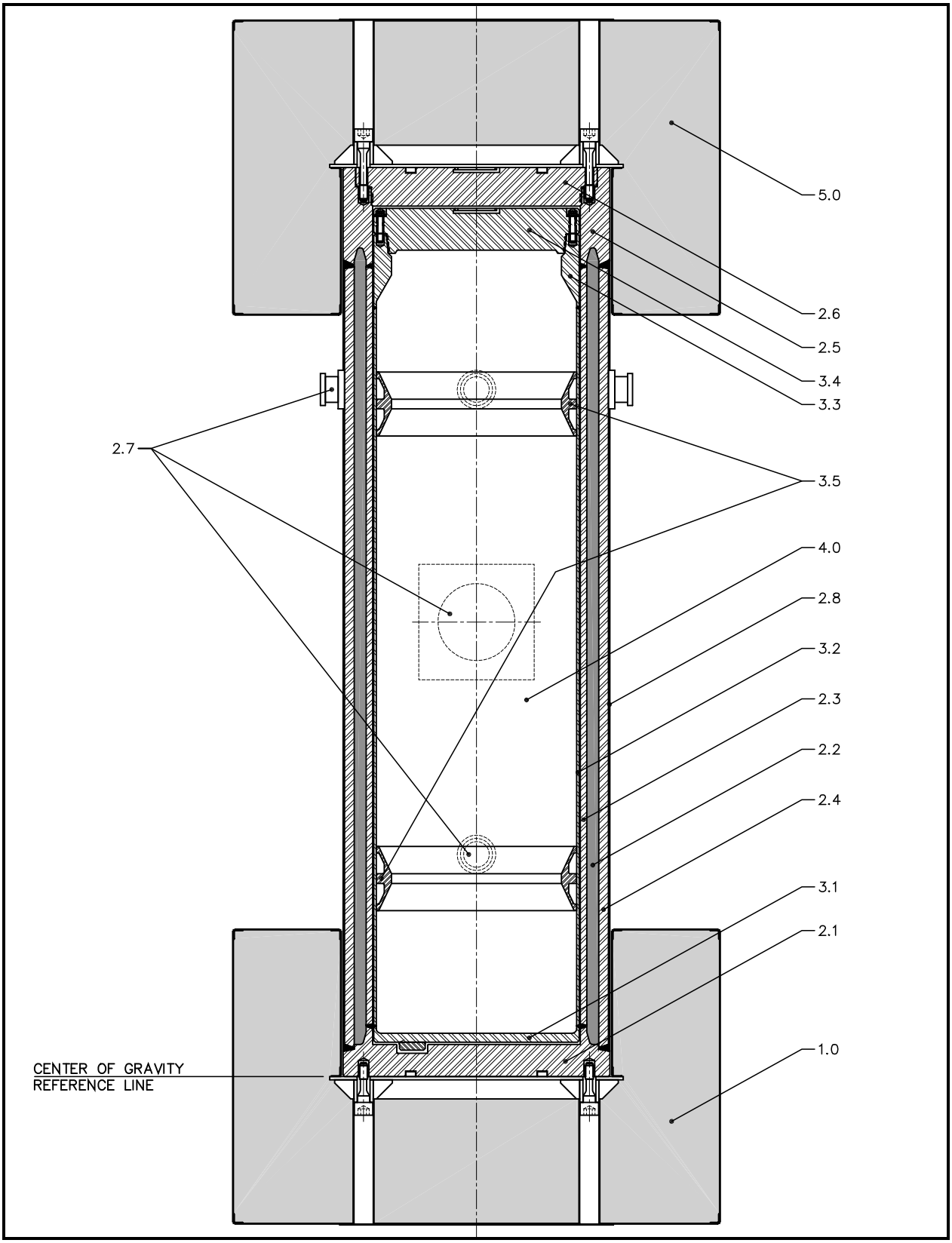

Figure 2.2-1 – RH-TRU 72-B Package Component Weight Breakdown

This page intentionally left blank.

2.3 Mechanical Properties of Materials

The RH-TRU 72-B package is fabricated primarily from Type 304, austenitic stainless steel, structural polyurethane foam, high strength alloy steel bolts, and lead. Appendix 1.3.1, *Packaging General Arrangement Drawings*, defines the specific material used for each item of the RH-TRU 72-B package. Table 2.3-1 presents material properties for the Type 304 stainless steel, the ASTM A320 fasteners, and ASTM A516 carbon steel, and Table 2.3-2 presents material properties for the lead used in the RH-TRU 72-B package. Material properties are linearly interpolated between or, if necessary, linearly extrapolated beyond the temperature values shown. For instance, when temperatures outside the tabulated ranges are of interest (e.g., low temperature properties to -40 ºF), the data are extrapolated. When a particular analysis requires data extrapolation, it is addressed within the applicable section of the SAR.

The stress-strain curve for Type 304 stainless steel at 212 ºF is presented as Figure 2.3-1. This is the same curve employed in the T-3[1] and 125-B[2] SARs. It is further noted that this curve is reasonably consistent with the ASME Code[3] minimum material property data. The ASME Code specifies a modulus of elasticity of $27.53(10)^6$ at 212 ºF versus the $27.7(10)^6$ psi value shown in Figure 2.3-1. In addition, the yield stress at 0.2% offset strain in Figure 2.3-1 (setting $0.002 = a[\sigma - \sigma_p]^b$) is found to be 25,000 psi, as compared with the ASME Code specified 24,700 psi minimum yield stress. Therefore, it is concluded that the Figure 2.3-1 stress-strain curve corresponds very closely to ASME minimum material property data and is justified for use herein.

The applicable stress-strain curves (at room temperature (approximately 70 – 75 ºF), at -20 ºF, and at 140 ºF) for polyurethane foam with density of about 11½ lb/ft^3 used in the RH-TRU 72-B package impact limiters are presented as Figure 2.3-2 and tabulated in Table 2.3-3. Extensive testing of numerous foam samples at various densities (including densities of approximately 11½ lb/ft^3) resulted in the nominal (room temperature) curve shown in Figure 2.3-2.

A ±10% bound on the nominal room temperature curves indicates the acceptance criteria (per Section 8.1.4.1, *Polyurethane Foam*) associated with the foam actually installed within the impact limiters. To be acceptable, when averaged for all pours into a given limiter, parallel- and perpendicular-to-rise stress-strain curves taken at room temperature (70 – 75 ºF) for a production unit impact limiter must fall within ±10% of the corresponding nominal room temperature curves. Stress-strain curves for individual pours must fall within ±15% of nominal. Also shown in Figure 2.3-2 are curves corresponding to foam at -20 ºF and at 140 ºF. The -20 ºF (minimum foam temperature) curve is an upper-bound curve and corresponds to -20 ºF nominal foam, increased by 10%. The 140 ºF (maximum foam temperature) curve is a lower-bound curve and corresponds to 140 ºF nominal foam decreased by 10%. Drop analyses herein typically consider the -20 ºF and the 140 ºF foam curves in order to bound, respectively, package acceleration (*g*) loads and impact-limiter deformations.

---

[1] U.S. Department of Energy, *Safety Analysis Report for the T-3 Spent Fuel Shipping Package*, NRC Certificate of Compliance No. 71-9132, U.S. Department of Energy, Washington, D.C.

[2] U.S. Department of Energy, *Safety Analysis Report for the NuPac 125-B Fuel Shipping Package*, NRC Certificate of Compliance No. 71-9200 U.S. Department of Energy, Washington, D.C.

[3] American Society of Mechanical Engineers (ASME) Boiler and Pressure Vessel Code, Section III, *Rules for Construction of Nuclear Power Plant Components*, Division 1, Subsection NB and Appendices, 1986 Edition.

Appendix 2.10.7, *Static and Dynamic Testing*, presents the results from static crush and dynamic, 30-foot free drop testing of prototypic half-scale impact limiters. As discussed in Appendix 2.10.7, *Static and Dynamic Testing*, when properly correlated with the observed test results, analytic evaluation techniques (described and implemented in Appendix 2.10.2, *Drop Analysis Codes Description*, and Appendix 2.10.3, *Drop Impact Evaluation Results*, respectively) are shown to accurately predict impact limiter behavior.

To adequately address fabrication stresses due to lead shrinkage on the inner shell of the outer cask (OC), stress-strain and creep data are required for lead. The lead used in the package is per Federal Specification QQ-L-171e, or per ASTM B29-79 (for copper-bearing material). The composition of the lead is primarily lead (99.9% minimum) and copper (0.04 to 0.08%). Stress-strain and creep data are therefore extracted from WADC Technical Report 57-695[4] for a copperized lead with a composition of 99.94% lead and 0.0577% copper. Stress-strain curves and creep data from the reference are presented in Figure 2.3-3 through Figure 2.3-8.

ASTM A276 and ASTM A269 stainless steels are used for various portions of the impact limiters. These materials are not ASME Code materials, but are acceptable for use as these components are non-structural in nature. Other materials used in the package that are non-structural in nature are the butyl rubber used for the O-ring seals and the 300-series stainless steel used for the thermal shield wire wrap. Some additional minor non-structural items for the impact limiters are manufactured from plastic, stainless steel, or an alloy steel.

The optional thread inserts used for the inner vessel (IV) and OC lid closure bolts are manufactured from ASTM A434 steel, which is not an ASME code material. However, the room temperature tensile strength of the inserts is rated at a minimum value of 140,000 psi. The inserts have been used in high-temperature aerospace applications with very little weakening at temperatures up to 500 ºF. The inserts will be certified to meet material strength requirements equivalent to the minimum properties of the base material before being installed in the RH-TRU 72-B package.

[4] Thomas Tietz, *Determination of the Mechanical Properties of a High Purity Lead and a 0.058% Copper-Lead Alloy*, WADC Technical Report 57-695, ASTIA Document No. 151165, Stanford Research Institute, April 1958.

Table 2.3-1 – Mechanical Properties of Steel Used in the RH-TRU 72-B Package

Material Specification	Type or Grade	T (ºF)	Strength (ksi)			Elastic Modulus④ (10^6 psi)	Coefficient of Thermal Expansion⑤ (10^{-6} in/in/ºF)
			Yield① S_y	Ultimate② S_u	Allowable③ S_m		
ASTM A240	304	70	—	—	—	28.3	8.46
ASTM A276		100	30.0	75.0	20.0	—	8.55
		200	25.0	71.0	20.0	27.6	8.79
		300	22.5	66.0	20.0	27.0	9.00
		400	20.7	64.4	18.7	26.5	9.19
		500	19.4	63.5	17.5	25.8	9.37
		600	18.2	63.5	16.4	25.3	9.53
		700	17.7	63.5	16.0	24.8	9.69
ASTM A240	304L	70	—	—	—	28.3	8.46
ASTM A276		100	25.0	70.0	16.7	—	8.55
		200	21.3	66.2	16.7	27.6	8.79
		300	19.1	60.9	16.7	27.0	9.00
		400	17.5	58.5	15.8	26.5	9.19
		500	16.3	57.8	14.8	25.8	9.37
		600	15.5	57.0	14.0	25.3	9.53
		700	14.9	56.2	13.5	24.8	9.69
ASTM A182	F304	70	—	—	—	28.3	8.46
ASME SA182		100	30.0	70.0	20.0	—	8.55
(forgings)		200	25.0	66.2	20.0	27.6	8.79
		300	22.5	61.5	20.0	27.0	9.00
		400	20.7	60.0	18.7	26.5	9.19
		500	19.4	59.3	17.5	25.8	9.37
ASTM A320	L43	70	—	—	—	27.8	6.20
(fasteners)		100	105.0	125.0	35.0	—	6.27
		200	99.0	—	33.0	27.1	6.54
		300	95.7	—	31.9	26.7	6.78
		400	91.8	—	30.6	26.1	6.98
		500	88.5	—	29.5	25.7	7.16
ASTM A516	55	70	—	—	—	29.5	5.42
		100	30.0	55.0	18.3	—	5.53
		200	27.3	55.0	18.3	28.8	5.89
		300	26.6	55.0	17.7	28.3	6.26
		400	25.7	55.0	17.2	27.7	6.61
		500	24.5	55.0	16.2	27.3	6.91

Notes:

① ASME Code[3], Table I-2.1, Table I-2.2, Table I-13.3.

② ASME Code[3], Table I-1.3, Table I-3.1, Table I-3.2.

③ ASME Code[3], Table I-1.1, Table I-1.2, Table I-1.3.

④ ASME Code[3], Table I-6.0.

⑤ ASME Code[3], Table I-5.0; mean from 70 ºF.

⑥ Steel density is 0.283 lb/in^3, and Poisson's ratio is 0.3.

Table 2.3-2 – Mechanical Properties of Lead Used in the RH-TRU 72-B Package

Material Specification	Type or Grade	T (ºF)	Strength (psi)					Elastic Modulus④ (10^6 psi)	Coefficient of Thermal Expansion⑤ (10^{-6} in/in/ºF)
			Proportional① S_p		Yield② S_y		Ultimate③ S_u		
			Tens	Comp	Tens	Comp	Tens		
QQ-L-171e	A or C	-99	—	—	—	—	—	2.50	15.28
ASTM B29-79		70	—	—	—	—	—	2.34	16.07
(copper bearing)		100	276	215	584	490	1,570	2.30	16.21
		175	293	107	509	428	1,162	2.20	16.58
		250	277	107	498	391	844	2.09	16.95
		325	189	93	311	320	642	1.96	17.54
		440	—	—	—	—	—	1.74	18.50
		620	—	—	—	—	—	1.36	20.39

Notes:

① WADC Technical Report 57-695[4], Page 21, 26.

② WADC Technical Report 57-695[4], Page 21, 26.

③ WADC Technical Report 57-695[4], Page 14.

④ NUREG/CR-0481[5], Page 66.

⑤ NUREG/CR-0481[5], Page 56; mean from 70 ºF.

⑥ Lead density is 0.41 lb/in^3, Poisson's ratio is 0.45, and the melting point is 620 ºF.

Table 2.3-3 – Crush Stress vs. Strain for 11½ lb/ft³ Nominal Density Polyurethane Foam

Strain	Parallel-to-Rise (psi)			Perpendicular-to-Rise (psi)		
	Upper Bound, Cold (-20 ºF)	Nominal, Room Temp (75 ºF)	Lower Bound, Hot (140 ºF)	Upper Bound, Cold (-20 ºF)	Nominal, Room Temp (75 ºF)	Lower Bound, Hot (140 ºF)
0%	0	0	0	0	0	0
5%	574	372	282	499	324	245
10%	579	376	285	536	348	264
20%	581	377	286	559	363	275
30%	622	404	306	599	389	294
40%	692	449	340	672	436	331
50%	835	543	411	823	534	405
60%	1,163	755	572	1,170	760	575
65%	1,485	964	731	1,529	993	752
70%	2,051	1,332	1,009	2,146	1,394	1,056
75%	3,083	2,002	1,516	3,200	2,078	1,574
80%	5,511	3,578	2,711	5,527	3,589	2,719

[5] H. J. Rack, and G. A. Knorovsky, *An Assessment of Stress-Strain Data Suitable for Finite Element Elastic-Plastic Analysis of Shipping Containers*, NUREG/CR-0481, SAND77-1872, Sandia National Laboratories, Albuquerque, New Mexico, September 1978.

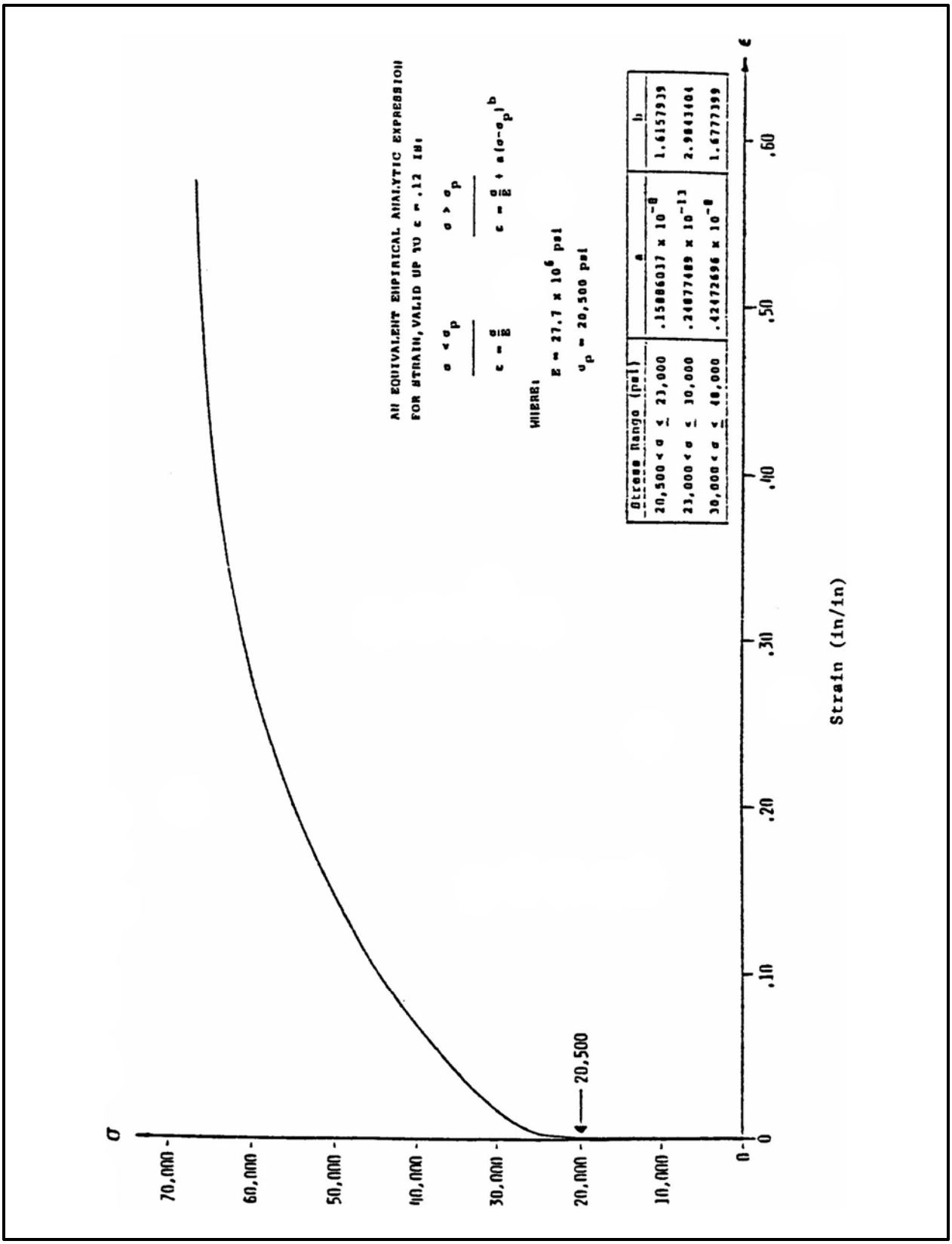

Figure 2.3-1 – True Stress/Strain for Type 304 Stainless at 212 ºF

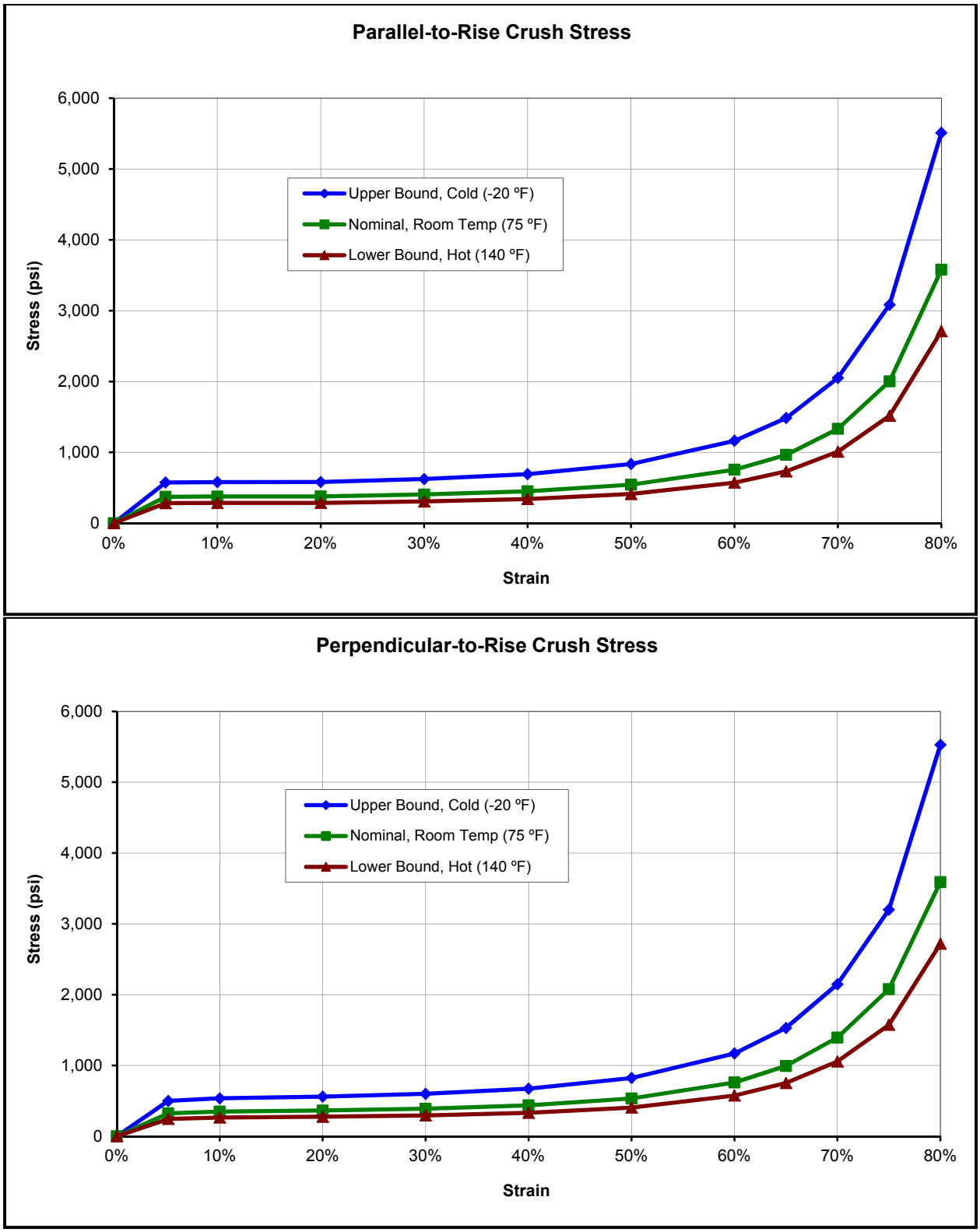

Figure 2.3-2 – Crush Stress vs. Strain for 11½ lb/ft³ Nominal Density Polyurethane Foam

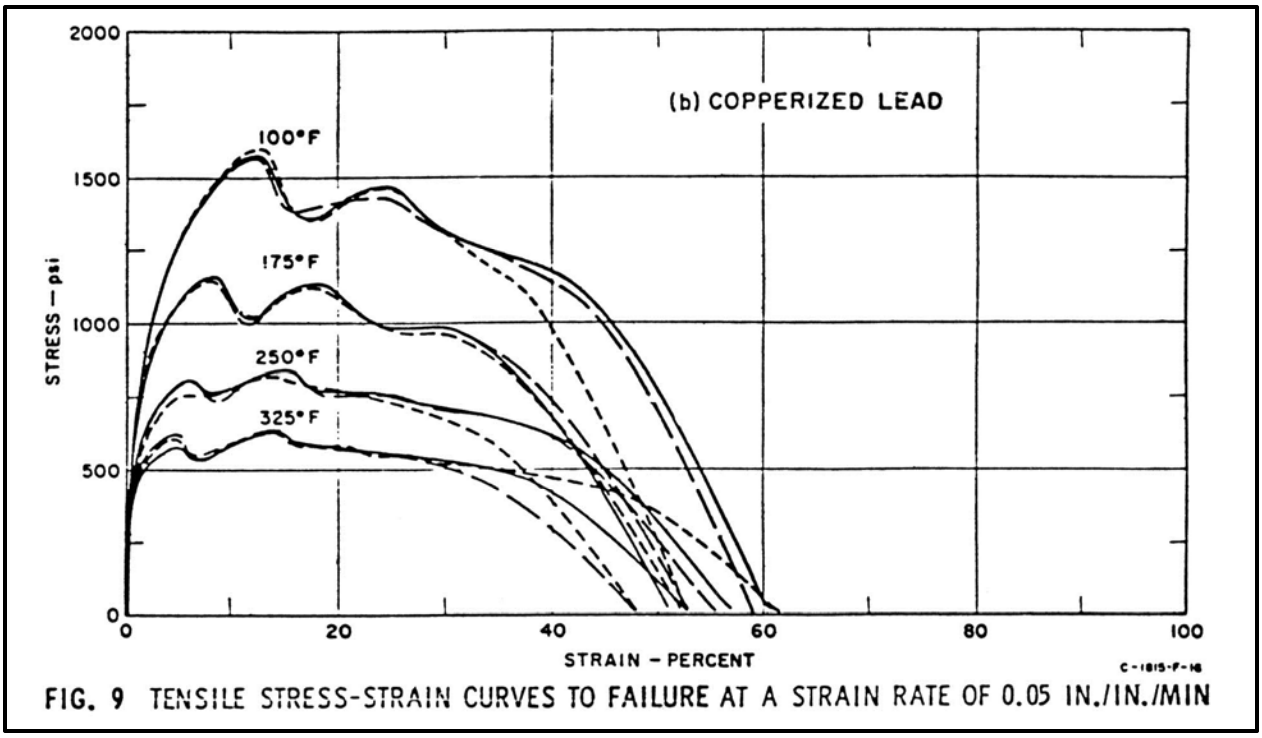

FIG. 9 TENSILE STRESS-STRAIN CURVES TO FAILURE AT A STRAIN RATE OF 0.05 IN./IN./MIN

Figure 2.3-3 – Tensile Curves at a Strain Rate of 0.05 in/in/min

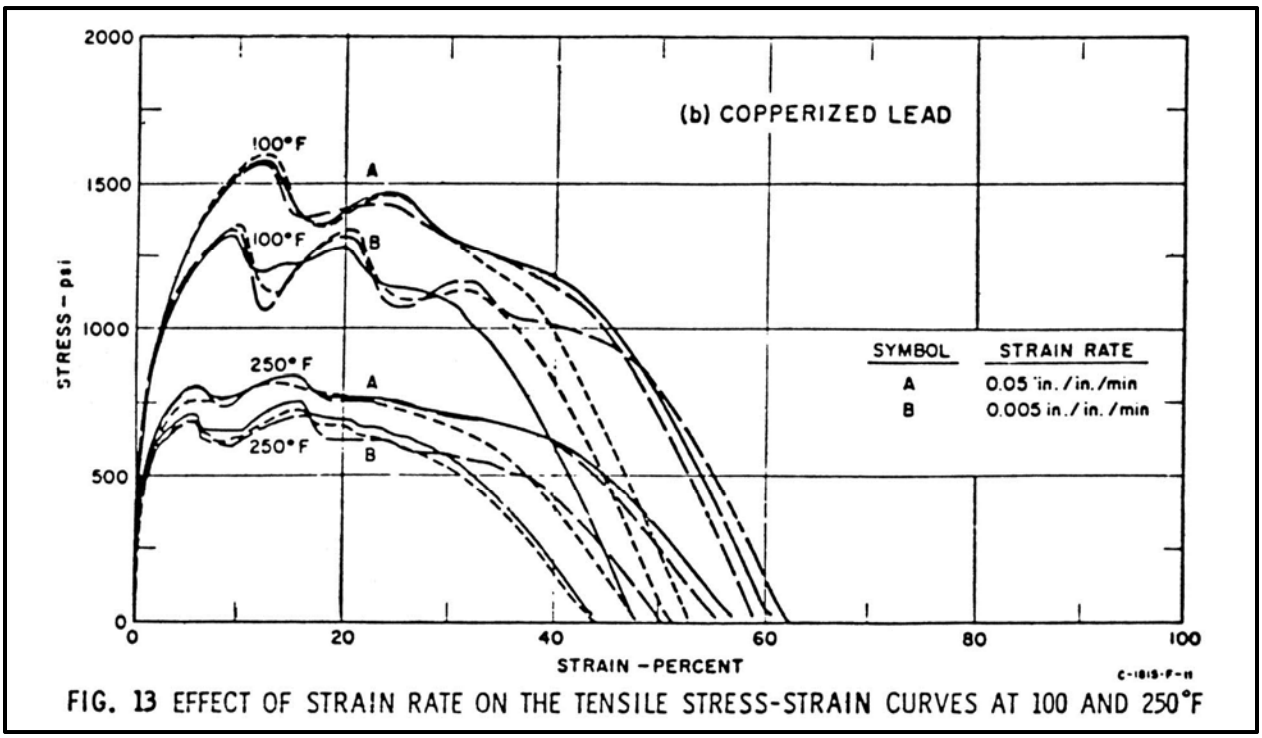

FIG. 13 EFFECT OF STRAIN RATE ON THE TENSILE STRESS-STRAIN CURVES AT 100 AND 250°F

Figure 2.3-4 – Strain Rate Effects on Tensile Curves at 100 ºF and 250 ºF

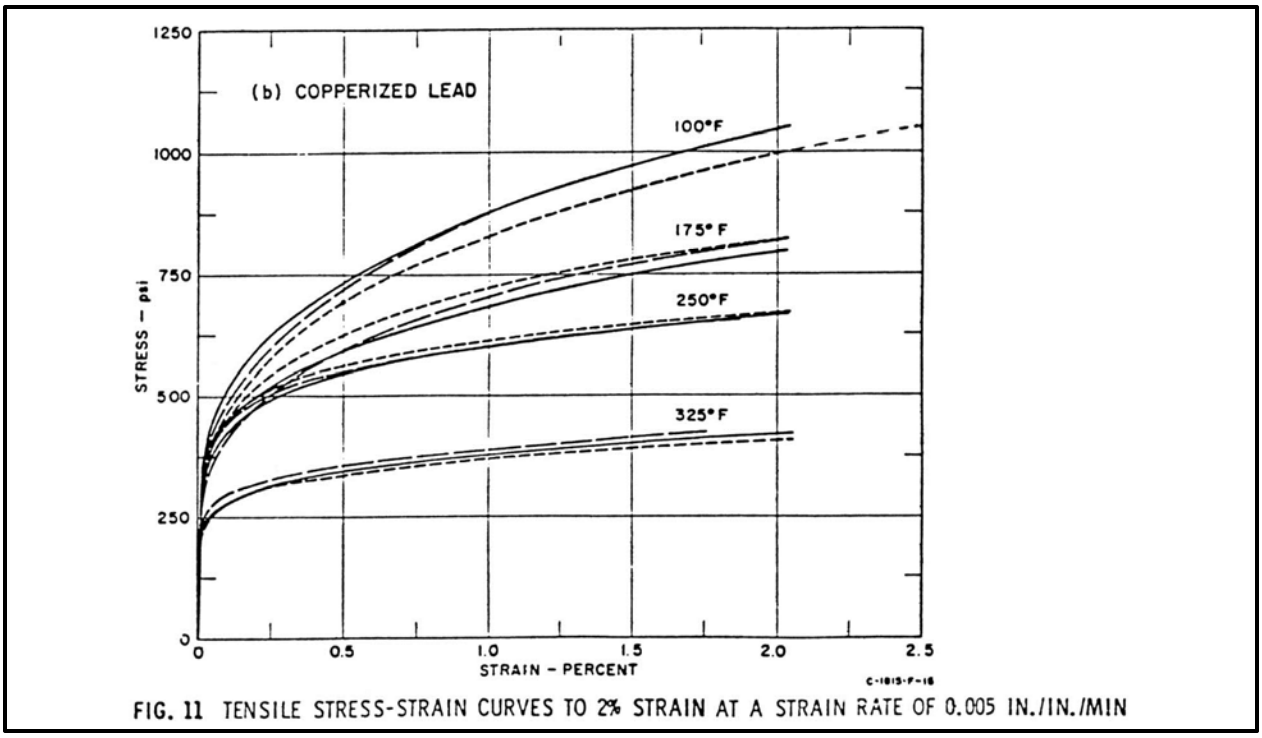

FIG. 11 TENSILE STRESS-STRAIN CURVES TO 2% STRAIN AT A STRAIN RATE OF 0.005 IN./IN./MIN

Figure 2.3-5 – Tensile Curves at a Strain Rate of 0.005 in/in/min

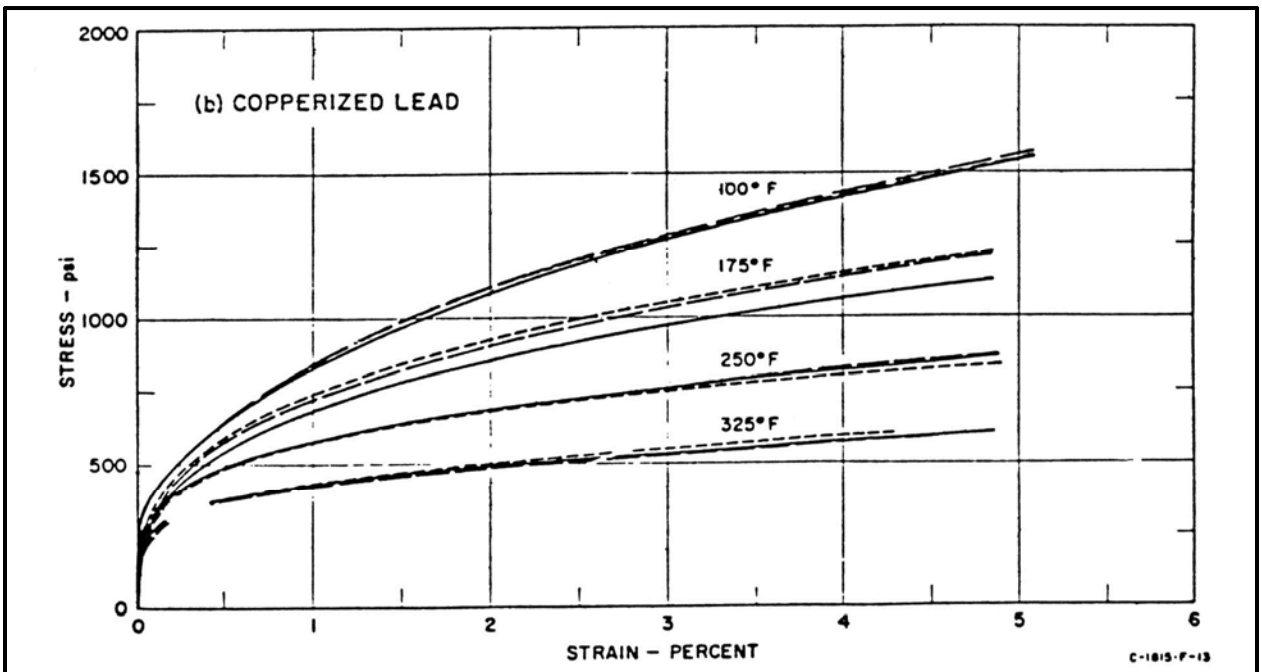

FIG. 14 COMPRESSION STRESS-STRAIN CURVES TO 5% STRAIN AT A STRAIN RATE OF 0.005 IN./IN./MIN

Figure 2.3-6 – Compression Curves at a Strain Rate of 0.005 in/in/min

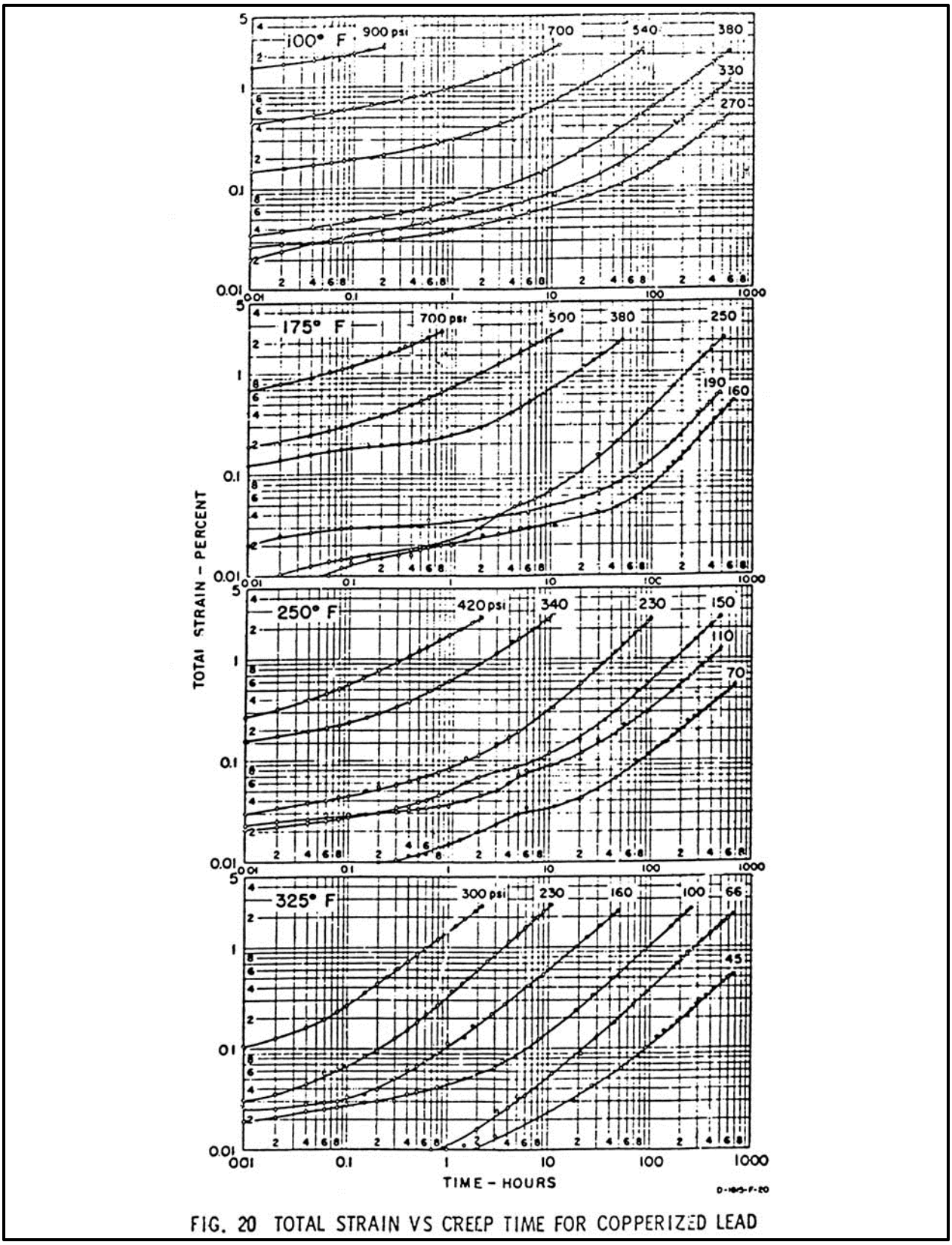

Figure 2.3-7 – Total Strain vs. Creep Time

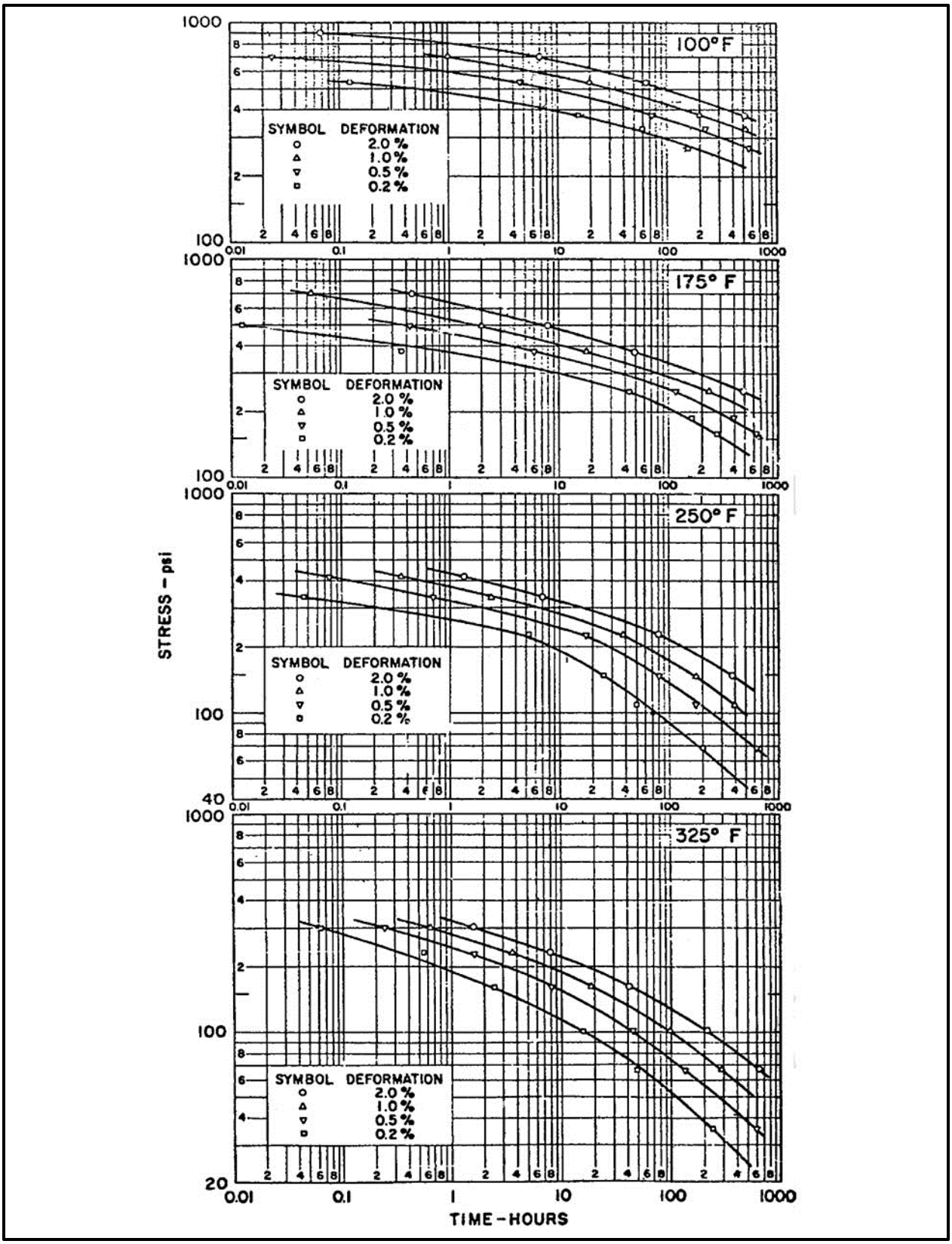

Figure 2.3-8 – Stress vs. Creep Time Curves

2.4 General Standards for All Packages

This section demonstrates that the general standards for all packages are met.

2.4.1 Minimum Package Size

The minimum transverse dimension of the package (not including the outer cask (OC) thermal shield and without the impact limiters) is 41⅛ inches, and the minimum longitudinal dimension is 141¾ inches.

2.4.2 Tamper Indicating Feature

A "lock-wire", or equivalent, is utilized between two tie points on the closure end of the package during a loaded shipment. Specifically, one tie point is affixed to the OC thermal shield, and one tie point is affixed to the closure end impact limiter. Failure of said device will indicate purposeful tampering in accordance with 10 CFR §71.43(b)[1].

2.4.3 Positive Closure

Inadvertent opening of the package closures cannot occur for the RH-TRU 72-B package. Following installation of the package payload, the inner vessel (IV) lid is secured via eight (8), 7/8-9UNC bolts. The OC closure lid is then secured via eighteen (18), 1¼-7UNC bolts, thus eliminating access to the IV closure. The closure-end impact limiter is attached using six (6), 1¼-7UNC bolts. When installed, the impact limiter eliminates access to the OC closure. With this double containment closure and the presence of the impact limiter, inadvertent opening of the package cannot occur.

2.4.4 Chemical and Galvanic Reactions

The materials from which this package is fabricated (i.e., stainless steel, carbon steel, lead, and polyurethane foam) will not cause significant chemical, galvanic, or other reactions in air or water environments. These materials have been previously used in radioactive material (RAM) packages for transport of similar chemical material without incident. This RAM packaging history, combined with successful use of these materials in similar industrial environments, ensures that the integrity of the package will not be compromised by any chemical, galvanic or other reactions. The materials of construction and the payload are evaluated below for potential reactions.

2.4.4.1 RH-TRU 72-B Package Materials of Construction

The RH-TRU 72-B package is primarily constructed of Type 304 stainless steel. This material is highly corrosion-resistant to most environments. The actual metallic structure of the RH-TRU 72-B package is composed entirely of this and appropriate weld material. The weld material and

[1] Title 10, Code of Federal Regulations, Part 71 (10 CFR 71), *Packaging and Transportation of Radioactive Material*, 01-01-14 Edition.

processes have been selected in accordance with the ASME Boiler and Pressure Vessel Code[2] to provide as good or better material properties than the base material, including corrosion resistance. Both the base and weld materials are 300-series stainless steel, which is highly resistant to corrosion. These materials also have approximately the same electrochemical potential, minimizing any galvanic corrosion that could occur.

The polyurethane foam used in the impact limiter of the RH-TRU 72-B package is the same as that which has been successfully used in a number of transportation packages, such as the NuPac 125-B (Docket 71-9200), the CNSI 1-13C II (Docket 71-9152), the NuPac 10-142 (Docket 71-9208), and the NuPac PAS-1 (Docket 71-9184). All of these packages have had a long and successful record of performance demonstrating that the foam does not impose any adverse conditions on the packaging. The polyurethane foam in the impact limiters is a closed-cell foam that is very low in free halogens. The foam material is sealed inside a dry cavity in each impact limiter, to prevent exposure to the elements. Even if moisture were available, for leaching trace chlorides from the foam, very little chloride would be available, since the material is a closed-cell foam and water does not penetrate the material to allow significant leaching.

The butyl rubber and other elastomers used in the O-ring seals contain no corrosives that would adversely affect the packaging. These materials are organic in nature and non-corrosive to the stainless steel body of the RH-TRU 72-B package.

2.4.4.2 RH-TRU 72-B Package Materials of Construction and Payload Compatibility

The materials of construction of the RH-TRU 72-B package have been evaluated for compatibility with the authorized contents as described in the *Remote-Handled Transuranic Waste Authorized Methods for Payload Control* (RH-TRAMPAC)[3].

Corrosive materials are prohibited from the payloads. All payloads are contained in the payload canister. Typically, the payload may be further confined within drums and liners. This configuration ensures that the chemistry of the payloads has very little interaction with the IV. However, the evaluation of compatibility is based on complete interaction of payload materials with the packaging.

Since corrosives are prohibited from the payload, the only potential material that could be, in theory, of concern for the IV is the release of free chlorides. Gaseous free chlorides could potentially be available only from the radiolysis of polyvinyl chloride and/or halogenated organic compounds within the payload. In both cases, the total quantity of gaseous free chlorides that would be available for diffusion into the IV is very small. The distribution of volatile organic compounds is discussed in Appendix 4.4 of the *RH-TRU Payload Appendices*[4]. The source term for gaseous-free chlorides in the payload and the potential for stress corrosion cracking are discussed in Appendix 4.2 of the *RH-TRU Payload Appendices*[4].

---

[2] American Society of Mechanical Engineers (ASME) Boiler and Pressure Vessel Code, Section III, *Rules for Construction of Nuclear Power Plant Components*, Division 1, Subsection NB and Appendices, 1986 Edition.

[3] U.S. Department of Energy (DOE), *Remote-Handled Transuranic Waste Authorized Methods for Payload Control* (RH-TRAMPAC), U.S. Department of Energy, Carlsbad Field Office, Carlsbad, New Mexico.

[4] U.S. Department of Energy (DOE), *RH-TRU Payload Appendices*, U.S. Department of Energy, Carlsbad Field Office, Carlsbad, New Mexico.

Any small quantities of free-gaseous chlorides that could potentially be generated in the waste would be retarded from diffusing out of a payload container due to the high solubility in absorbed water and/or moisture. The potential for free-gaseous chloride generation and interactions within payload containers is discussed in detail in Appendix 4.2 of the *RH-TRU Payload Appendices*[4].

2.4.4.3 Seal Material and Payload

The butyl rubber O-ring seal material was evaluated for chemical compatibility with identified payload chemicals by review of the published literature on the performance of the seal material in the presence of the chemical. This evaluation determined that only a few payload constituents were potentially incompatible with butyl rubber under expected operating conditions. Those chemicals determined to potentially pose a problem were a few volatile organic compounds (VOC's). Specifically, they were Freon-113, carbon tetrachloride, methylene chloride, and 1,1,1-trichloroethane. All of these compounds are highly-volatile and, in general, volatilize or permeate through the waste-confinement materials prior to the closure of payload containers. A discussion of the occurrence of VOCs in the waste and headspace (void volumes) of confinement layers is presented in Appendix 4.4 of the *RH-TRU Payload Appendices*[4]. Estimates of VOC concentrations in the IV headspace is also provided in Appendix 4.4 of the *RH-TRU Payload Appendices*[4].

The very small quantities of these compounds could have a small effect on the O-ring seal material. All of these compounds interact with butyl rubber by permeating and straining the polymer structure, causing the O-ring seal to swell. The O-ring seal will not readily lose its shape due to the crosslinking that occurs during manufacturing. Butyl rubber is a co-polymer of polyisobutylene with a small amount of polyisoprene. The polyisoprene allows cross-linking of the polymer chains that make up the O-ring seal material. This cross-linking limits the amount of swelling that can occur, as does the amount of compression the material experiences. If a sufficient quantity of solvent is present, the O-ring seal material can swell to the point where some softening of the material occurs, reducing its sealing force. This reduction of sealing force is offset by the osmotic pressure generated by the swelling. The force due to swelling may well be greater than the sealing force lost due to softening of the material.

The combined effect of the very small quantities of incompatible solvents found in the payload, combined with the mechanism of attack on the butyl, indicate that the payload will not significantly degrade the performance of the seals. Additionally, exposure to gamma radiation in the doses expected will not adversely effect the performance of the O-ring seals. IV O-ring seals will be inspected before each shipment to determine if damage is present. A more detailed discussion is provided in Appendix 4.4 of the *RH-TRU Payload Appendices*[4].

2.4.4.4 Chemical Compatibility Determination for RH-TRU Waste

The design of the RH-TRU 72-B package is for transport of waste that is limited to solid or solidified material. Corrosives, pressurized containers, explosives, radioactive and non-radioactive pyrophorics greater than 1%, and liquid volumes greater than 1% are prohibited. These restrictions ensure that the waste in the payload is in a non-reactive form for safe transport in the RH-TRU 72-B package.

In addition to the above restrictions, the chemical components in the payload are restricted to those that have been evaluated as described in the RH-TRAMPAC[3] and Appendix 4.1 of the *RH-TRU Payload Appendices*[4].

2.5 Lifting and Tie-down Standards for All Packages

This section addresses the lifting and tie-down design requirements. The RH-TRU 72-B package incorporates eight (8) trunnions for all package lifting and tie-down loads. The design criteria of ANSI N14.6[1] and 10 CFR §71.45[2] are used for the lifting and tie-down analyses. Lifting devices for the lids (non-structural member) are described in Section 1.2.2, *Operational Features*, and are identified in Appendix 1.3.1, *Packaging General Arrangement Drawings*.

Material properties used in this section are based on an enveloping normal condition temperature of 153 ºF for the outer cask (OC) trunnions and outer shell, and are summarized in Table 2.5-1 for ASTM A240 and ASTM A182, Type 304, stainless steels, based on non-containment allowable stresses from Table 2.1-2 in Section 2.1.2.1.2, *Non-Containment Structures*. The remaining material for the OC is ASTM A276, Type 304, stainless steel. This is not an ASME Code material, but it has a chemical composition and mechanical properties that are virtually identical to those of the ASTM A240 material. Therefore, the properties listed in Table 2.5-1 for ASTM A240 stainless steel are also valid for ASTM A276 stainless steel. Although margins of safety reported in this section correspond to material properties at 153 ºF, with a minimum margin of safety of 0.25 for the OC outer shell as demonstrated in Section 2.5.2.2, *OC Outer Shell Stresses*, and a decrease in allowable yield stress from 27,350 psi at 153 ºF to 27,000 psi at 160 ºF, use of a 160 ºF maximum temperature limit in Chapter 3.0, *Thermal Evaluation*, for the OC shell is justified.

2.5.1 Lifting Devices

2.5.1.1 Lifting Trunnion Loads

The RH-TRU 72-B package has four trunnions provided for lifting which are located 90º apart on a cross-sectional plane near the lid-end of the package. Two trunnions are intended for primary use while two additional trunnions provide redundancy as desired for lifting and handling safety.

10 CFR §71.45[2] criteria are applicable to the lifting trunnions. These criteria require the device to lift three times the combined package weight while maintaining stresses less than yield.

The following analysis uses WRC Bulletin 107[3]. Loads are applied first in the longitudinal direction to simulate vertical lift, and then in the circumferential direction to represent horizontal lift. Figure 2.5-1 illustrates the load components on the lifting trunnion.

$$d_o = ½(1.5) + 1.03 + (0.75)(1.6) = 2.98 \text{ in}$$

Analyzing the two trunnions carrying the lifting load, the critical load for each trunnion is:

---

[1] ANSI N14.6-1993, *Special Lifting Devices for Shipping Containers Weighing 10,000 Pounds (4,500 Kg) or More,* American National Standards Institute, Inc. (ANSI).

[2] Title 10, Code of Federal Regulations, Part 71 (10 CFR 71), *Packaging and Transportation of Radioactive Material*, 01-01-14 Edition.

[3] K. R. Wickman, A. G. Hopper, and J. L. Mershon, *Local Stresses in Spherical and Cylindrical Shells Due to External Loadings*, Welding Research Council Bulletin 107, Welding Research Council, New York, June 1977.

$$V_L = \frac{3(\text{Package Weight})}{2} = \frac{3(45{,}000)}{2} = 67{,}500 \text{ lb}$$

The trunnion bending moment then becomes:

$$M_L = V_L d_o = (67{,}500)(2.98) = 201{,}150 \text{ in-lb}$$

The critical lifting load for the horizontally oriented package is determined by assuming that the package is lifted from the horizontal orientation at the tie-down trunnion location nearest the lid-end, and that the package rotates about the opposite tie-down trunnions (see Figure 2.5-2). The center of gravity of the package is assumed to be 8 inches from the center-pivot trunnion toward the lid-end (this offset distance of 8 inches is derived in Section 2.5.2.1, *Center-Pivot and Tie-down Trunnion Loads*).

Summing moments about the assumed pivot point results in the following:

$$(36.25 + 36.25)(2V_C) - (36.25 + 8.0)(135{,}000) = 0$$

Solving for V_C:

$$V_C = \frac{(44.25)(135{,}000)}{2(72.50)} = 41{,}200 \text{ lb}$$

Using the same moment arm for the tie-down trunnions as before:

$$M_C = V_C d_o = (41{,}200)(2.98) = 122{,}770 \text{ in-lb}$$

The above moment arm, d_o, assumes load V_C is applied at the most conservative location.

There are no torsional forces, M_T, or forces acting on the trunnions normal to the OC outer shell, P, during lifting. The OC outer shell is not considered a pressure boundary, so there is no internal pressure acting on the outer shell. Therefore, loads V_L and M_L are the only loads applied in the trunnion analysis.

2.5.1.2 OC Outer Shell Stresses

The analysis method used to determine these stresses is from WRC Bulletin 107[3]. Required parameters and input data used in the tie-down trunnion lifting stress analysis are presented in Table 2.5-2.

Analysis results are given in Table 2.5-3 (vertical lift) and Table 2.5-4 (horizontal lift). The maximum combined stress intensity (membrane plus bending) in the OC outer shell is 18,390 psi. The resulting margin of safety (MS) against the allowable yield strength, σ_y, is:

$$MS = \frac{\sigma_y}{S} - 1 = \frac{27{,}350}{18{,}390} - 1 = +0.49$$

The corresponding maximum membrane stress intensity is equal to twice the maximum shear stress, or 9,550 psi. For this case, the resulting margin of safety against the allowable yield strength, σ_y, is:

$$MS = \frac{\sigma_y}{S} - 1 = \frac{27{,}350}{9{,}550} - 1 = +1.86$$

2.5.1.3 Trunnion Stresses

Bearing stress in the trunnion is found by applying the lifting load, V, over the projected area (length = 1.6 inches) of the 4-inch diameter trunnion (see Figure 2.5-1):

$$S_b = \frac{V}{A_b} = \frac{67{,}500}{(4.0)(1.6)} = 10{,}547 \text{ psi}$$

The margin of safety for bearing is then:

$$MS = \frac{\sigma_y}{S_b} - 1 = \frac{27{,}350}{10{,}547} - 1 = +1.59$$

2.5.1.4 Lifting Trunnion Attachment Weld

The maximum lateral force acting on the trunnion base plate weld through the lifting trunnion is V = 67,500 pounds, as derived in Section 2.5.1.1, *Lifting Trunnion Loads*. To conservatively evaluate base plate weld requirements due to this force and due to the accompanying bending moment, an additional offset of the force from the weld due to the curvature of the OC outer shell will be accounted for as follows (see Figure 2.5-14 for a pictorial representation of θ and e):

$$\theta = \frac{6.0}{20.56} = 0.292 \text{ rad} = 16.7^\circ$$

and

$$e = 20.56\left[1 - \cos\left(\frac{\theta}{2}\right)\right] = 0.22 \text{ in}$$

The total offset of load, V, is thus 0.22 + 2.23 = 2.45 inches. The bending moment acting on the weld is then M = (2.45)(V) = (2.45)(67,500) = 165,375 in-lb. To determine minimum weld throat size, relationships from *Design of Weldments*[4] may be employed in the following calculation to calculate the unit shear load, f_s, and unit bending load, f_b:

$$f_s = \frac{V}{L_w} = 3{,}581 \text{ lb/in}$$

and

$$f_b = \frac{M}{S_w} = 5{,}850 \text{ lb/in}$$

[4] Omer W. Blodgett, *Design of Welded Structures*, The James F. Lincoln Arc Welding Foundation, Cleveland, Ohio, June 1966.

where the trunnion load, V = 67,500 pounds, the unit thickness weld length, $L_w = \pi D = \pi(6.0) =$ 18.85 in/in, the trunnion bending moment, M = 165,375 in-lb, and the unit thickness weld section modulus, $S_w = (\pi/4)D^2 = (\pi/4)(6.0)^2 = 28.27$ in^3/in.

The total unit weld load, f_{total}, is the vector sum of these two components:

$$f_{total} = \sqrt{f_s^2 + f_b^2} = \sqrt{(3{,}581)^2 + (5{,}850)^2} = 6{,}859 \text{ lb/in}$$

Using a shear stress allowable of $0.6S_y = 0.6(27{,}350) = 16{,}410$ psi, and assuming a bevel weld, the minimum acceptable weld size, w, is:

$$w = \frac{6{,}859}{16{,}410} = 0.418 \text{ in}$$

The attachment weld for the trunnion is a 5/8-inch bevel weld, resulting in a weld margin of safety of:

$$MS = \frac{0.625}{0.418} - 1 = +0.50$$

2.5.1.5 Excessive Lifting Trunnion Loads

To preclude damage to the package due to inadvertent overloading of the lifting trunnions, the trunnion weld should fail before the OC outer shell stress reaches ultimate strength. The specified allowable tensile stress for the outer shell material is 72,880 psi at an outer shell temperature of 153 ºF. The outer shell will reach ultimate strength when the membrane stress of the shell reaches ultimate stress. During excessive loading, plastic hinges will occur at areas of peak bending stress. The ultimate strength of the OC outer shell is therefore based on the shell membrane stress reaching ultimate stress.

The maximum outer shell membrane stress intensity induced by the 67,500 pound lifting load is 2,847 + 751 = 3,598 psi for the vertical lift case (see Table 2.5-3). Therefore, the smallest possible load required to induce failure in the OC outer shell is:

$$V_{shell} = (67{,}500)\left(\frac{72{,}880}{3{,}598}\right) = 1{,}367{,}200 \text{ lb}$$

The weld failure load for the 5/8-inch trunnion outer shell bevel weld can be derived as:

$$f_{fail} = (0.6)(72{,}880)(0.625) = 27{,}330 \text{ lb/in}$$

This weld load would result from a failure load, V_{weld}, applied to the trunnion as derived from the following equation:

$$f_{fail} = \sqrt{\left(\frac{V_{weld}}{L_{weld}}\right)^2 + \left(\frac{M_{weld}}{S_{weld}}\right)^2} = 27{,}330 \text{ lb/in}$$

where V_{weld} is the load needed to induce failure of weld, the length of the weld, $L_{weld} = 18.85$ in/in, the moment in the weld due to V_{weld}, $M_{weld} = (2.45)V_{weld}$, and the elastic section modulus, $S_{weld} = 28.27$ in^3/in. Substituting:

$$\sqrt{\left(\frac{V_{weld}}{18.85}\right)^2+\left(\frac{(2.45)V_{weld}}{28.27}\right)^2}=27{,}330\ \text{lb/in}$$

Solving results in a maximum weld failure load, V_{weld} = 268,964 pounds. Therefore, the trunnion weld will fail under excessive loading before the OC outer shell fails. The margin of safety against OC outer shell failure is then

$$MS=\frac{1{,}367{,}260}{268{,}964}-1=+4.08$$

2.5.2 Tie-down Devices

2.5.2.1 Center-Pivot and Tie-down Trunnion Loads

The RH-TRU 72-B package can be transported on either of two types of trailers. Each trailer design incorporates a specially engineered tie-down system to secure the package. The first, the Center-Pivot Trailer (CPT), utilizes an onboard uprighting system which allows the package to be unloaded while still attached to the trailer (see Figure 2.5-15). The second, the Lift-Off Trailer (LOT), requires an external crane to upright the package, lift it off the trailer, and place it in an unloading area away from the trailer (see Figure 2.5-16). The CPT uses two of the upper lifting trunnions as well as the center-pivot and lower trunnions for tie-down attachments. Thus, only the two remaining upper trunnions, both vertically oriented, one on the top surface of the package and the other on the lower surface of the package, need to be evaluated for inadvertent tie-down use. Inspection of the trailer design shows that the top trunnion is not in a useable position while the bottom trunnion is inaccessible because of trailer structure.

Because the LOT requires access to the upper lifting trunnions for the crane attachment, only the center-pivot and lower trunnions are used for tie-down attachments. The vertically oriented trunnions near the lid are unusable or inaccessible as discussed above. The horizontally oriented trunnions near the lid end are accessible for inadvertent use, but any attachment to them with chains or cable would be much less rigid than the engineered tie-down system components and thus would not experience significant loads.

The analysis of the two tie-down systems is given below. Worst-case tie-down loads on the lifting and tie-down trunnions and the center-pivot trunnions are determined for both trailer designs described above. The lifting and tie-down trunnion loads are shown to be smaller than those experienced during the lifting procedure analyzed in Section 2.5.1, *Lifting Devices*. The center-pivot trunnion loads are shown to be nearly the same for either trailer configuration.

Transport loads applied to the center-pivot trunnions are assumed to act at the center of a 2½-inch wide bearing area that interfaces with the transporter support system, as shown in Figure 2.5-17.

Due to the center-pivot arrangement as primary support for the package in transit, the response of the system to transportation induced loads will depend strongly on the location of the center of gravity (CG) of the loaded package. Nominally, for an empty package, the package CG will be approximately 3 inches from the pivot point of the trunnions, toward the lid-end of the package. A uniformly loaded canister placed inside the package will result in the CG being shifted back to a location about 1⅞ inches from the pivot point, toward the lid-end (refer to Table 2.2-1). For this

case, where the package CG is very near the support point, trunnion loading in response to the regulatory requirements of 10*g* longitudinal, 5*g* transverse and 2*g* vertical is fairly straightforward.

However, if the package CG is offset significantly from the support point, additional loading will be induced into the center-pivot trunnions in the form of reacting couples. To conservatively bound the worst-case CG offset, and thus the worst-case trunnion loading situation, the payload canister CG will be calculated for a worst-case load imbalance. It will be assumed that an entire payload will consist of a solid steel slug with a density of 0.283 lb/in^3 and weighing 6,900 pounds (the maximum useful canister payload weight), and that this slug is located at the extreme top end of the canister.

The inside diameter of the canister spacer is 26½ inches, so it will be assumed that the steel slug has a 26½-inch outside diameter. The length of the slug will thus be:

$$L = \frac{6{,}900/0.283}{(\pi/4)(26.5)^2} = 44.2 \text{ in}$$

The payload canister is 121 inches long. Therefore, the CG of the steel slug, which is approximately 31 inches from the top of the canister (the worst-case load imbalance occurs when the steel slug is shifted to the top of the canister instead of the bottom), will be approximately 26½ inches from the center-pivot trunnions (towards the lid-end). The CG of the 1,100 pound canister is less than 3½ inches from the pivot point (geometric center) of the package, toward the bottom of the package. The weight of the empty package is 37,000 pounds (45,000 – 8,000).

The offset distance of the CG of the package from the pivot point (toward the lid-end of the package) with the unbalanced load is:

$$L_{offset} = \frac{(37{,}000)(-3.02) + (1{,}100)(3.50) + (6{,}900)(-26.5)}{45{,}000} = 6.46 \text{ in}$$

To allow for uncertainties in the location of the canister CG (the lead pig at the bottom-end of the payload canister is optional), a total package CG offset distance of 8 inches (in either direction) will be conservatively used to calculate the tie-down loads.

The 10*g* longitudinal load (in the direction of travel) will not be affected by the offset of the package CG in the longitudinal direction. Therefore, the longitudinal load on each of the two primary center-pivot trunnions is:

$$F_L = \frac{10(45{,}000)}{2} = 225{,}000 \text{ lb/trunnion}$$

The 5*g* transverse load will result in reaction loading on the center-pivot trunnions, as shown in Figure 2.5-18. To derive reaction loads R_1, R_2, and R_3, equations of force and moment balance for static equilibrium are used:

$$\sum F_{trans} = F_T - R_1 = 0$$

$$\sum F_{long} = R_2 - R_3 = 0$$

$$\sum M_o = 2(23.05)R_3 - (8.0)F_T = 0$$

Solving the equations simultaneously for the unknown reactions yields $F_T = R_1 = 225{,}000$ pounds, and $R_2 = R_3 = 39{,}050$ pounds.

Shown, in Figure 2.5-19 and Figure 2.5-20, the two trailer designs support the package differently. The CPT design uses the upper trunnions and the center-pivot trunnions for the tie-down system. The LOT design uses the lower trunnions and the center-pivot trunnions for the tie-down system. As such, the CPT and LOT analyses are identical, although on different sets of trunnions.

For either design, the 2*g* vertical load will result in the following worst-case loading on the center-pivot and upper/lower trunnions:

$$R_4 = F_v\left(\frac{a}{L}\right) = 19{,}862 \text{ lb} = 9{,}931 \text{ lb/trunnion}$$

$$R_5 = F_v + R_4 = 109{,}862 \text{ lb} = 54{,}931 \text{ lb/trunnion}$$

where the vertical force, $F_v = 2W = 2(45{,}000) = 90{,}000$ pounds based on a package weight, $W = 45{,}000$ pounds, $a = 8.0$ inches, and $L = 36.25$ inches.

The 2*g* vertical upload will result in the same loading case as above since there are trunnion caps for the center-pivot trunnions.

The worst-case forces from either trailer design on the center-pivot trunnions are required to be imposed simultaneously on the package tie-down system (force components for each direction must be summed and applied to the trunnions), as listed below:

Longitudinal Forces: $F_L = 225{,}000 + 39{,}050 = 264{,}050$ pounds (transversely loaded trunnion)
$F_L = 225{,}000 - 39{,}050 = 185{,}950$ pounds (non-transversely loaded trunnion)

Transverse Forces: $F_T = 225{,}000$ pounds (transversely loaded trunnion only)

Vertical Forces: $F_V = 54{,}931$ pounds (each trunnion)

A calculation was also performed to determine the forces associated with yawing. Yawing can occur during rapid negotiations of curves in highways, as the result of tracking due to grooves in highway lanes, or as the result of rapid lane changes.

The yawing calculation assumed a rotation of the package about a vertically oriented axis through the package's centroid. For conservatism, the center-pivot trunnions' resistance to yawing was neglected.

The package's mass moment of inertia about its vertical axis has been previously determined to be 278,601 lb-sec^2-in (see Table 2.2-1). The package's average angular acceleration during a rapid turning event was estimated utilizing the following assumptions:

1. The turning angle for the front wheels of the tractor can vary between –35º to +35º.
2. The corresponding steering wheel movement varies between –1.5 and +1.5 revolutions.
3. The driver can turn the steering wheel a quarter revolution per second.
4. The angular acceleration at the package location on the trailer is the same as the angular acceleration of the tractor.

5. The tractor-trailer is initially traveling in a straight line and therefore, has no initial angular velocity.

Using the above listed assumptions, the average angular acceleration for the turning event was estimated as shown below:

- Average steering wheel angular velocity $\omega_s = (\pi/2)$ rad/sec
- Average tractor wheel angular velocity ω_{avg}
  $= \omega_s$ (rad/sec) × (35º tractor wheel rotation/1.5 steering wheel rotation)
  $= (\pi/2)(35/540) = 0.102$ rad/sec
- Average angular acceleration (α) over a 1 second interval
  $= \omega_{avg}/\Delta t = (0.102 \text{ rad/sec})/(1 \text{ sec}) = 0.102 \text{ rad/sec}^2$

Using the values for mass moment of inertia and angular acceleration determined above, the torque developed during the turning event is estimated as:

$$\text{Torque} = I_{package}\alpha = (278{,}601(0.102) = 28{,}417 \text{ in-lb}$$

If this torque is entirely reacted at the center-pivot trunnions, the reacting forces are very low, since the moment arm for the reacting forces is approximately 36 inches. Using this approximate moment arm, each reacting force is approximately 790 pounds (28,417/36). These reacting loads are insignificant when compared with the previously determined horizontal reaction of 264,050 pounds for the center-pivot trunnions.

If the torque is entirely reacted at the center-pivot trunnion and at an adjustable side post located at a lid-end tie-down trunnion, as previously illustrated, the reacting force is 1,907/3.0, or approximately 636 pounds, since the moment arm between the center-pivot trunnions and the lid-end tie-down trunnions is approximately 3 feet. Since the reacting load is very small, the required brace cross-sectional area for the side post is also very small.

A tracking type of yaw can lead to a cyclic stress being applied to the center-pivot trunnions. This corresponding cyclic stress would be very low, since simultaneous application of all of the worst-case center-pivot trunnion loads (F_L = 264,050 lbs, F_T = 225,000 lbs, and F_V = 54,931 lbs) results in a maximum stress intensity of 21,892 psi per Section 2.5.2.2, *OC Outer Shell Stresses*. By ratioing, the cyclic stress due to yawing would be under 50 psi, and therefore, would be insignificant with regard to fatigue failure.

2.5.2.2 OC Outer Shell Stresses

The maximum transportation-induced load acting on the two tie-down trunnions at the bottom-end of the package is the load R_4 arising from the 2*g* vertical force. This load, tangent to the OC outer shell, is 9,931 pounds per trunnion. This circumferential load is significantly less than the circumferential lifting load V_C = 67,500 pounds. Since the margin of safety against outer shell yielding for that load case was +0.49 (see Section 2.5.1.2, *OC Outer Shell Stresses*), it may be concluded that an even greater margin exists for transportation induced trunnion loading.

The center-pivot trunnions and the OC outer shell are analyzed for the combined imposition of the worst-case loads calculated above. For conservatism, the strengthening of the OC outer shell by the OC inner shell and lead shielding is neglected in the ANSYS® finite element analysis.

The stresses in the OC outer shell due to the tie-down loads imposed on the center-pivot trunnion are determined using the finite element analysis described in Appendix 2.10.1.1, *Tie-down Trunnion Analysis*. The maximum membrane-plus-bending stress intensity resulting from the combined transport loads is 21,892 psi. This stress intensity occurs midway between the two center-pivot trunnions, near the end of the OC outer shell. Since the maximum OC outer shell temperature under NCT is 153 ºF, the maximum allowable (or yield) stress, obtained from Table 2.5-1, is 27,350 psi. The corresponding margin of safety, for combined worst-case transportation induced loading, is:

$$MS = \frac{27{,}350}{21{,}892} - 1 = +0.25$$

The OC outer shell is therefore adequate under worst-case inertial loads.

2.5.2.3 Center-Pivot Trunnion Stresses

Center-pivot trunnion bearing stress is derived by applying the vector sum of the transport loads which act in a direction perpendicular to the trunnion (F_V and F_L) to the projected area of the 12.0-inch diameter center-pivot trunnion. The width of the bearing surface on the trunnion is assumed to be 2.5 inches. Therefore, the bearing stress is:

$$S_B = \frac{\sqrt{F_V^2 + F_L^2}}{DW} = \frac{\sqrt{(54{,}932)^2 + (264{,}050)^2}}{(12.0)(2.5)} = 8{,}990 \text{ psi}$$

The bearing stress margin of safety (using a yield stress of 27,350 psi) is then:

$$MS = \frac{27{,}350}{8{,}990} - 1 = +2.04$$

2.5.2.4 Center-Pivot Trunnion Attachment Welds

The welds attaching the 12-inch diameter center-pivot trunnion to the 18.0-inch wide, 28.0-inch long center-pivot trunnion base, and the weld attaching the base to OC outer shell, are both analyzed in this section.

The trunnion weld is evaluated using the same method found in Section 2.5.1.4, *Lifting Trunnion Attachment Weld*. The transportation load is offset from the trunnion weld by a distance of 0.4 + ½(2.5) = 1.65 inches. The equivalent transportation load acting perpendicular to the trunnion will be the vector sum of forces F_V and F_L, as used in Section 2.5.2.3, *Center-Pivot Trunnion Stresses*:

$$F_{eq} = \sqrt{F_V^2 + F_L^2} = \sqrt{(54{,}931)^2 + (264{,}050)^2} = 269{,}703 \text{ lb}$$

The bending moment acting on the center-pivot trunnion weld is then:

$$M_{eq} = (269{,}703)(1.65) = 445{,}010 \text{ in-lb}$$

Trunnion weld force components are thus:

$$f_s = \frac{F_{eq}}{L_w} = \frac{269{,}703}{37.7} = 7{,}154 \text{ lb/in}$$

$$f_b = \frac{M_{eq}}{S_w} = \frac{445{,}010}{113.1} = 3{,}935 \text{ lb/in}$$

where the unit thickness weld length, $L_w = \pi(12.0 \text{ in}) = 37.7$ inches, and the unit thickness weld section modulus, $S_w = (\pi/4)(12.0)^2 = 113.1 \text{ in}^2$. The total weld force is:

$$f_{total} = \sqrt{f_s^2 + f_b^2} = \sqrt{(7{,}154)^2 + (3{,}935)^2} = 8{,}165 \text{ lb/in}$$

Using a shear stress allowable of $0.6S_y = 0.6(27{,}350) = 16{,}410$ psi, and assuming a bevel weld, the minimum acceptable weld size, w, is:

$$w = \frac{8{,}165}{16{,}410} = 0.498 \text{ in}$$

Since the trunnion is attached to the base plate with a 3/4-inch bevel weld, the minimum weld margin of safety is:

$$MS = \frac{0.75}{0.498} - 1 = +0.51$$

For the center-pivot trunnion base weld, the maximum load offset from the weld will include offset "e" due to curvature of the OC outer shell (refer to Section 2.5.1.4, *Lifting Trunnion Attachment Weld*, for the analysis methodology):

$$\theta = 2\left[\sin^{-1}\left(\frac{9.0}{20.56}\right)\right] = 51.9^{\circ}$$

and

$$e = 20.56\left[1 - \cos\left(\frac{\theta}{2}\right)\right] = 2.07 \text{ in}$$

The maximum offset is thus 2.07 + 1.03 + 1.65 = 4.75 inches. This rectangular weld pattern will be analyzed by simultaneously applying the relevant separate load components, and conservatively assuming the above maximum offset applies to each. For the vertical load, F_V:

$$f_{sV} = \frac{F_V}{L_w} = \frac{54{,}931}{92} = 597 \text{ lb/in}$$

$$f_{bV} = \frac{M_V}{S_{wV}} = \frac{(54{,}931)(4.75)}{612} = 426 \text{ lb/in}$$

and, for the longitudinal force, F_L:

$$f_{sL} = \frac{F_L}{L_w} = \frac{264{,}050}{92} = 2{,}870 \text{ lb/in}$$

$$f_{bL} = \frac{M_L}{S_{wL}} = \frac{(264{,}050)(4.75)}{765} = 1{,}640 \text{ lb/in}$$

where, the unit thickness weld length, $L_w = 2(b + d) = 2(18.0 + 28.0) = 92.0$ inches, the unit thickness weld section modulus in the vertical direction is, $S_{wV} = bd + d^2/3 = (28.0)(18.0) + (18)^2/3 = 612$ in^2, and the unit thickness weld section modulus in the longitudinal direction is, $S_{wL} = bd + d^2/3 = (18.0)(28.0) + (28)^2/3 = 765$ in^2. The equivalent weld force components are:

$$f_{s,eq} = \sqrt{f_{sV}^2 + f_{sL}^2} = \sqrt{(597)^2 + (2{,}870)^2} = 2{,}931 \text{ lb/in}$$

$$f_{b,eq} = \sqrt{f_{bV}^2 + f_{bL}^2} = \sqrt{(426)^2 + (1{,}640)^2} = 1{,}694 \text{ lb/in}$$

Finally, the total equivalent weld load is:

$$f_{total} = \sqrt{f_{s,eq}^2 + f_{b,eq}^2} = \sqrt{(2{,}931)^2 + (1{,}694)^2} = 3{,}385 \text{ lb/in}$$

Using a shear stress allowable of $0.6S_y = 0.6(27{,}350) = 16{,}410$ psi, and assuming a full penetration bevel weld, the minimum acceptable weld size, w, is:

$$w = \frac{3{,}385}{16{,}410} = 0.206 \text{ in}$$

Since the trunnion is attached to the base plate with a full penetration, 1½-inch bevel weld, the minimum weld margin of safety is:

$$MS = \frac{1.5}{0.206} - 1 = +6.28$$

2.5.2.5 Excessive Center-Pivot Trunnion Loading

To preclude damage to the package due to inadvertent overloading of the center-pivot trunnions, the trunnion welds should fail before the OC outer shell stress reaches the ultimate tensile strength of the material. The specified ultimate tensile strength for the outer shell material, obtained from Table 2.5-1, is 72,880 psi. The outer shell will reach ultimate strength when the membrane stress of the shell reaches ultimate stress. During excessive loading, plastic hinges will occur at areas of peak bending stress. The ultimate strength of the OC outer shell is therefore based on the shell membrane stress reaching ultimate stress.

The stresses in the OC outer shell due to the tie-down loads imposed on the center-pivot trunnion are determined using the finite element analysis described in Appendix 2.10.1.1, *Tie-down Trunnion Analysis*. The maximum outer shell membrane stress intensity from the combined tie-down loads is 12,040 psi at the bottom-right corner of the center-pivot trunnion block. Therefore, the smallest possible load required to induce failure in the OC outer shell for loads acting perpendicular to the trunnion is:

$$V_{shell} = \left(\frac{72{,}880}{12{,}040}\right)\sqrt{(264{,}050)^2 + (54{,}931)^2} = 1{,}632{,}556 \text{ lb}$$

Note that this value is conservatively small, since the shell stress intensity level of 12,040 psi includes effects of the load component which acts to compress the center-pivot trunnion. This load component does not affect the trunnion welds.

Using a shear stress allowable of $0.6S_u = 0.6(72,880) = 43,728$ psi, the weld failure load for the trunnion attachment weld (3/4-inch bevel weld) can be derived as:

$$f_{fail} = (43,728)(0.75) = 32,796 \text{ lb/in}$$

This weld load would result from a failure load V_{weld} applied to the trunnion which can be derived from the following equation:

$$f_{fail} = \sqrt{\left(\frac{V_{weld}}{L_{weld}}\right)^2 + \left(\frac{M_{weld}}{S_{weld}}\right)^2}$$

where the weld failure load, $f_{fail} = 32,796$ lb/in, the load needed to induce failure of weld is V_{weld}, the length of the weld, $L_{weld} = \pi D = \pi(12.0) = 37.7$ inches, the moment in weld due to V_{weld}, $M_{weld} = (1.65)V_{weld}$, and the section modulus, $S_+ = (\pi/4)D^2 = (\pi/4)(12.0)^2 = 113.1$ in^2. Therefore:

$$f_{fail} = \sqrt{\left(\frac{V_{weld}}{37.7}\right)^2 + \left(\frac{(1.65)V_{weld}}{113.1}\right)^2} = 32,796$$

Solving for V_{weld} yields a maximum weld failure load of 1,083,400 pounds. Therefore, the trunnion weld will fail under excessive loading before the OC outer shell fails. The margin of safety against package outer shell failure is then:

$$MS = \frac{1,632,556}{1,083,400} - 1 = +0.51$$

It is thus demonstrated that the package center-pivot trunnions meet regulatory requirements.

Table 2.5-1 – Material Properties for Type 304 Stainless Steel at 153 ºF

Material Property	Value (psi)
Elastic Modulus, E	$27.9(10)^6$
Yield Strength, S_y	27,350
Ultimate Strength, S_u	72,880
Design Stress, S_m	20,000
Allowable Normal Primary Membrane Stress Intensity	27,350
Allowable Normal Primary Membrane + Bending Stress Intensity	30,000
Normal Pure Shear Stress	16,410
Normal Bearing Stress	27,350

Table 2.5-2 – Data Used in Tie-down Trunnion Lifting Stress Analysis

Applied Loads (see Figure 2.5-3)	**Vertical Lift**	**Horizontal Lift**
Circumferential Moment, M_C (in-lb)	0	122,770
Longitudinal Moment, M_L (in-lb)	201,150	0
Circumferential Shear, V_C (lb)	0	41,200
Longitudinal Shear, V_L (lb)	67,500	0
Geometry and Geometric Parameters	**Formula**	**Value**
Outer Shell Thickness, T (in)	T	1.50
Outer Shell Mean Radius (in)	R_m	19.813
Trunnion Base Radius (in)	r_o	3.00
Outer Shell Parameter	$\lambda = R_m/T$	13.209
Trunnion Attachment Parameter	$\beta = 0.875(r_o/R_m)$	0.132

Figure No.	**Parameter**	**Value**	**Stress Formula①**	**Vertical Lift Result (psi)**	**Horizontal Lift Result (psi)**
Figure 2.5-6	$\frac{N_\phi}{M_C/R_m^2\beta} =$	0.30	$K_n\left(\frac{N_\phi}{M_C/R_m^2\beta}\right)\left(\frac{M_C}{R_m^2\beta T}\right) =$	0	474
Figure 2.5-4	$\frac{M_\phi}{M_C/R_m\beta} =$	0.10	$K_b\left(\frac{M_\phi}{M_C/R_m\beta}\right)\left(\frac{6M_C}{R_m\beta T^2}\right) =$	0	12,518
Figure 2.5-12	$\frac{N_\phi}{M_L/R_m^2\beta} =$	1.1	$K_n\left(\frac{N_\phi}{M_L/R_m^2\beta}\right)\left(\frac{M_L}{R_m^2\beta T}\right) =$	2,847	0
Figure 2.5-8 Figure 2.5-9	$\frac{M_\phi}{M_L/R_m\beta} =$	0.054	$K_b\left(\frac{M_\phi}{M_L/R_m\beta}\right)\left(\frac{6M_L}{R_m\beta T^2}\right) =$	11,075	0
Figure 2.5-7	$\frac{N_x}{M_C/R_m^2\beta} =$	0.41	$K_n\left(\frac{N_x}{M_C/R_m^2\beta}\right)\left(\frac{M_C}{R_m^2\beta T}\right) =$	0	648
Figure 2.5-5	$\frac{M_x}{M_C/R_m\beta} =$	0.059	$K_b\left(\frac{M_x}{M_C/R_m\beta}\right)\left(\frac{6M_C}{R_m\beta T^2}\right) =$	0	7,386
Figure 2.5-13	$\frac{N_x}{M_L/R_m^2\beta} =$	0.29	$K_n\left(\frac{N_x}{M_L/R_m^2\beta}\right)\left(\frac{M_L}{R_m^2\beta T}\right) =$	751	0
Figure 2.5-10 Figure 2.5-11	$\frac{M_x}{M_L/R_m\beta} =$	0.086	$K_b\left(\frac{M_x}{M_L/R_m\beta}\right)\left(\frac{6M_L}{R_m\beta T^2}\right) =$	17,639	0
n/a	n/a	n/a	$\frac{V_C}{\pi r_o T} =$	0	2,914
n/a	n/a	n/a	$\frac{V_L}{\pi r_o T} =$	4,775	0

Note:

① The stress concentration factors, K_n (membrane) and K_b (bending), are assumed to be 1.0.

Table 2.5-3 – Trunnion Stress Analysis for a Vertical Lift

Stress Formula	A_U	A_L	B_U	B_L	C_U	C_L	D_U	D_L
$K_n\left(\frac{N_\phi}{M_C/R_m^2\beta}\right)\left(\frac{M_C}{R_m^2\beta T}\right) =$					– 0	– 0	+ 0	+ 0
$K_b\left(\frac{M_\phi}{M_C/R_m\beta}\right)\left(\frac{6M_C}{R_m\beta T^2}\right) =$					– 0	+ 0	+ 0	– 0
$K_n\left(\frac{N_\phi}{M_L/R_m^2\beta}\right)\left(\frac{M_L}{R_m^2\beta T}\right) =$	– 2,847	– 2,847	+ 2,847	+ 2,847				
$K_b\left(\frac{M_\phi}{M_L/R_m\beta}\right)\left(\frac{6M_L}{R_m\beta T^2}\right) =$	– 11,075	+ 11,075	+ 11,075	– 11,075				
Summation of Circumferential Stresses, σ_ϕ	– 13,922	+ 8,228	+ 13,922	– 8,228	– 0	+ 0	+ 0	– 0
$K_n\left(\frac{N_x}{M_C/R_m^2\beta}\right)\left(\frac{M_C}{R_m^2\beta T}\right) =$					– 0	– 0	+ 0	+ 0
$K_b\left(\frac{M_x}{M_C/R_m\beta}\right)\left(\frac{6M_C}{R_m\beta T^2}\right) =$					– 0	+ 0	+ 0	– 0
$K_n\left(\frac{N_x}{M_L/R_m^2\beta}\right)\left(\frac{M_L}{R_m^2\beta T}\right) =$	– 751	– 751	+ 751	+ 751				
$K_b\left(\frac{M_x}{M_L/R_m\beta}\right)\left(\frac{6M_L}{R_m\beta T^2}\right) =$	– 17,639	+ 17,639	+ 17,639	– 17,639				
Summation of Longitudinal Stresses, σ_x	– 18,390	+ 16,888	+ 18,390	– 16,888	– 0	+ 0	+ 0	– 0
$\frac{V_C}{\pi r_o T} =$	+ 0	+ 0	– 0	– 0				
$\frac{V_L}{\pi r_o T} =$					– 4,775	– 4,775	+ 4,775	+ 4,775
Summation of Shear Stresses, τ	+ 0	+ 0	– 0	– 0	– 4,775	– 4,775	+ 4,775	+ 4,775
Stress Intensity, S	18,390	16,888	18,390	16,888	9,550	9,550	9,550	9,550

Table 2.5-4 – Trunnion Stress Analysis for a Horizontal Lift

Stress Formula	A_U	A_L	B_U	B_L	C_U	C_L	D_U	D_L
$K_n\left(\frac{N_\phi}{M_C/R_m^2\beta}\right)\left(\frac{M_C}{R_m^2\beta T}\right) =$					– 474	– 474	+ 474	+ 474
$K_b\left(\frac{M_\phi}{M_C/R_m\beta}\right)\left(\frac{6M_C}{R_m\beta T^2}\right) =$					– 12,518	+ 12,518	+ 12,518	– 12,518
$K_n\left(\frac{N_\phi}{M_L/R_m^2\beta}\right)\left(\frac{M_L}{R_m^2\beta T}\right) =$	– 0	– 0	+ 0	+ 0				
$K_b\left(\frac{M_\phi}{M_L/R_m\beta}\right)\left(\frac{6M_L}{R_m\beta T^2}\right) =$	– 0	+ 0	+ 0	– 0				
Summation of Circumferential Stresses, σ_ϕ	– 0	+ 0	+ 0	– 0	– 12,992	+ 12,044	+ 12,992	– 12,044
$K_n\left(\frac{N_x}{M_C/R_m^2\beta}\right)\left(\frac{M_C}{R_m^2\beta T}\right) =$					– 648	– 648	+ 648	+ 648
$K_b\left(\frac{M_x}{M_C/R_m\beta}\right)\left(\frac{6M_C}{R_m\beta T^2}\right) =$					– 7,386	+ 7,386	+ 7,386	– 7,386
$K_n\left(\frac{N_x}{M_L/R_m^2\beta}\right)\left(\frac{M_L}{R_m^2\beta T}\right) =$	– 0	– 0	+ 0	+ 0				
$K_b\left(\frac{M_x}{M_L/R_m\beta}\right)\left(\frac{6M_L}{R_m\beta T^2}\right) =$	– 0	+ 0	+ 0	– 0				
Summation of Longitudinal Stresses, σ_x	– 0	+ 0	+ 0	– 0	– 8,034	+ 6,738	+ 8,034	– 6,738
$\frac{V_C}{\pi r_o T} =$	+ 2,914	+ 2,914	– 2,914	– 2,914				
$\frac{V_L}{\pi r_o T} =$					– 0	– 0	+ 0	+ 0
Summation of Shear Stresses, τ	+ 2,914	+ 2,914	– 2,914	– 2,914	– 0	– 0	+ 0	+ 0
Stress Intensity, S	5,828	5,828	5,828	5,828	12,992	12,044	12,992	12,044

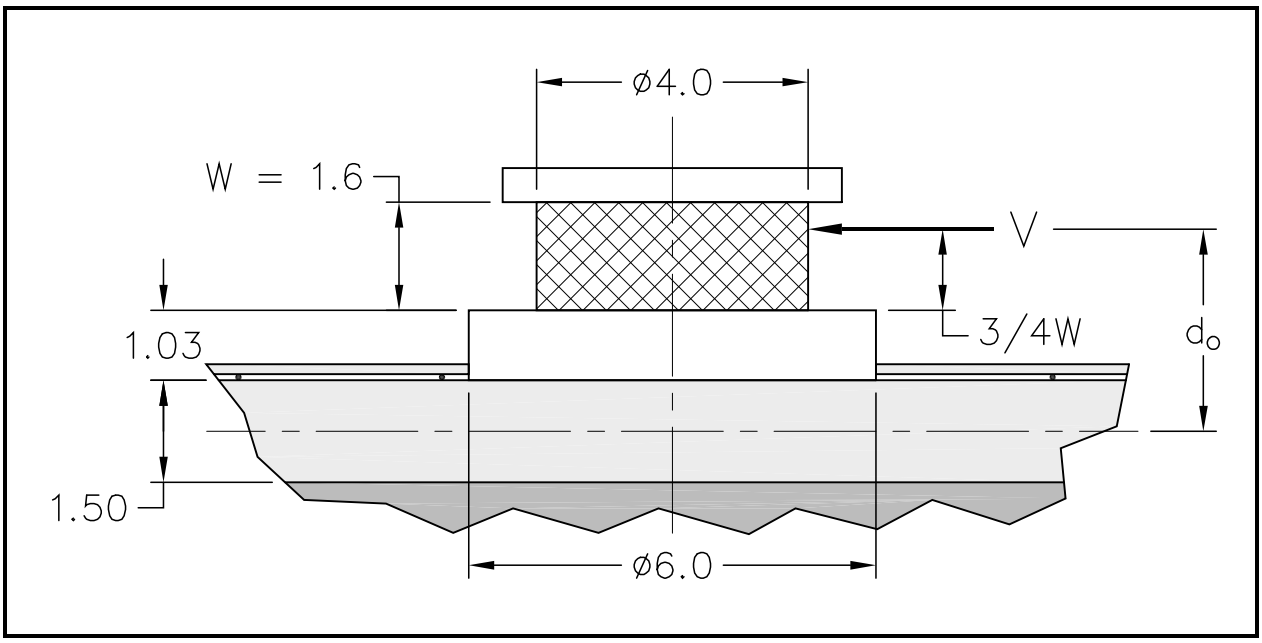

Figure 2.5-1 – Lifting Trunnion Geometry

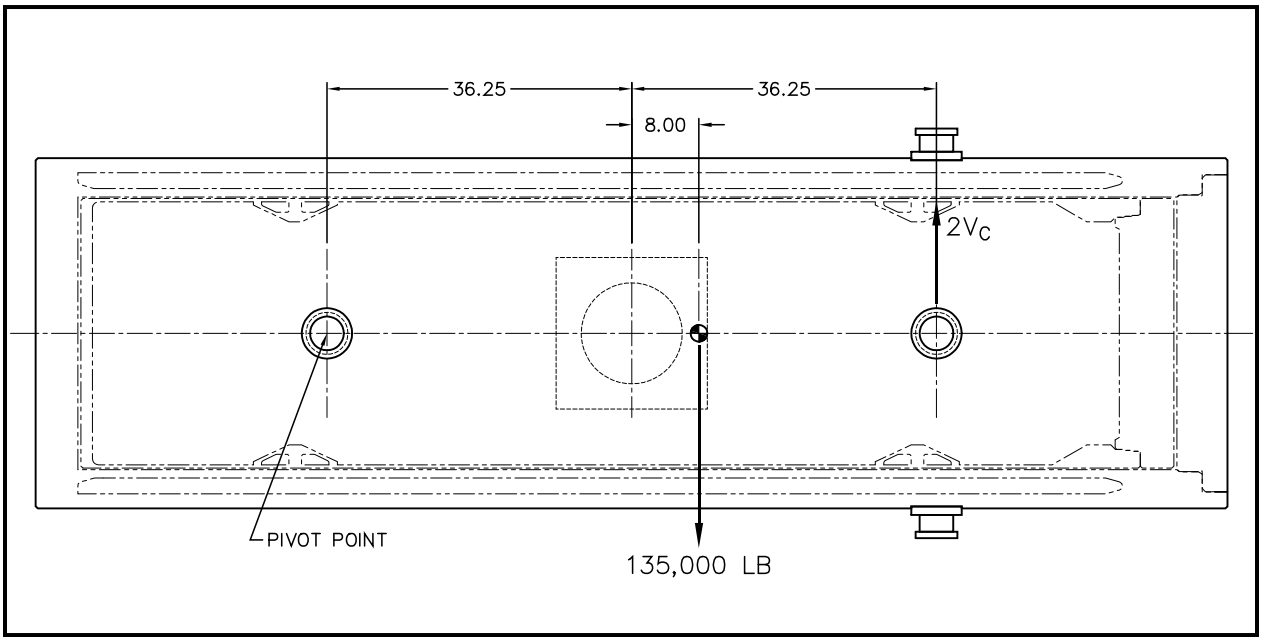

Figure 2.5-2 – Horizontal Lift Loading Configuration

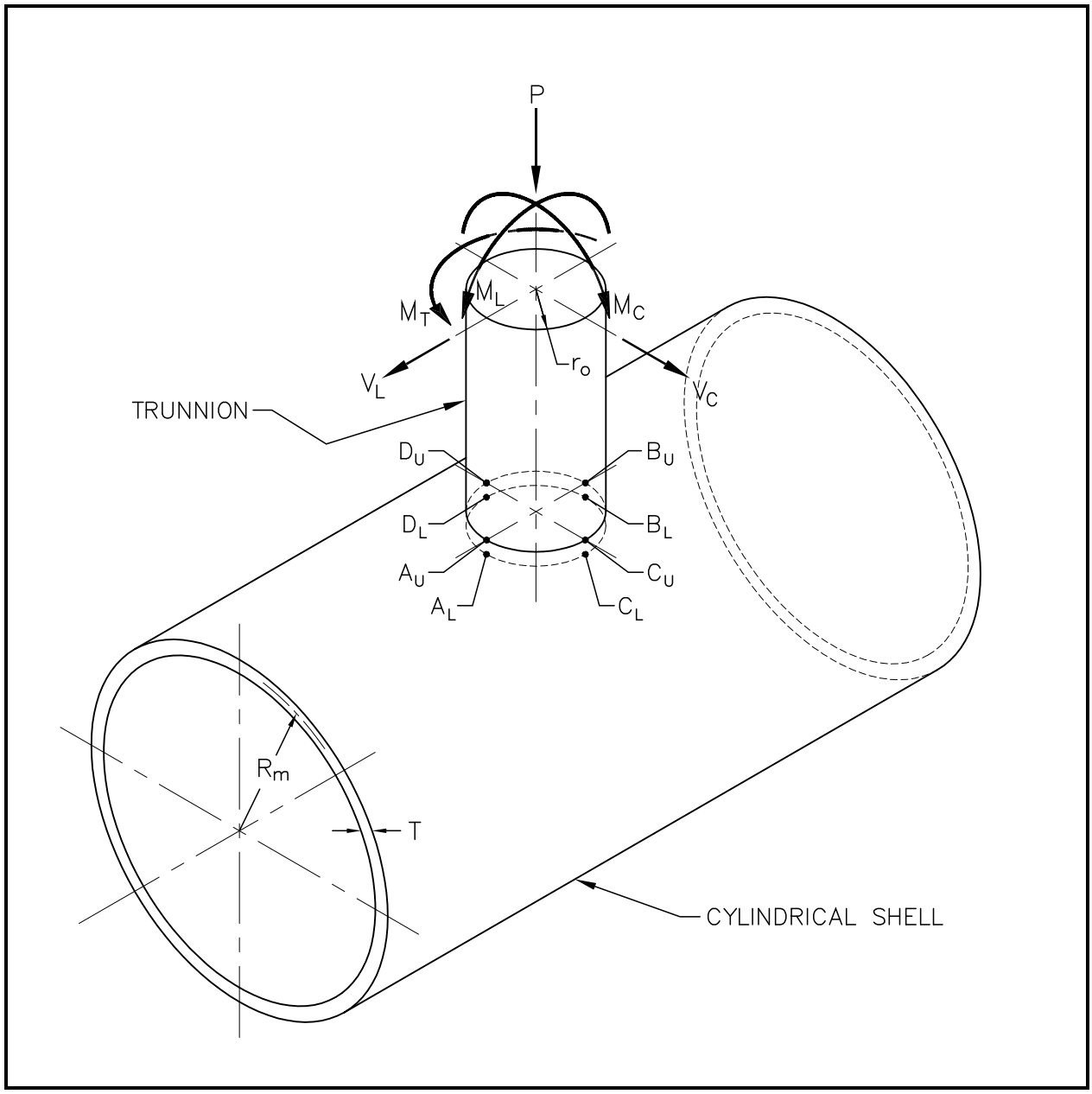

Figure 2.5-3 – Attachment Loads for WRC Bulletin 107

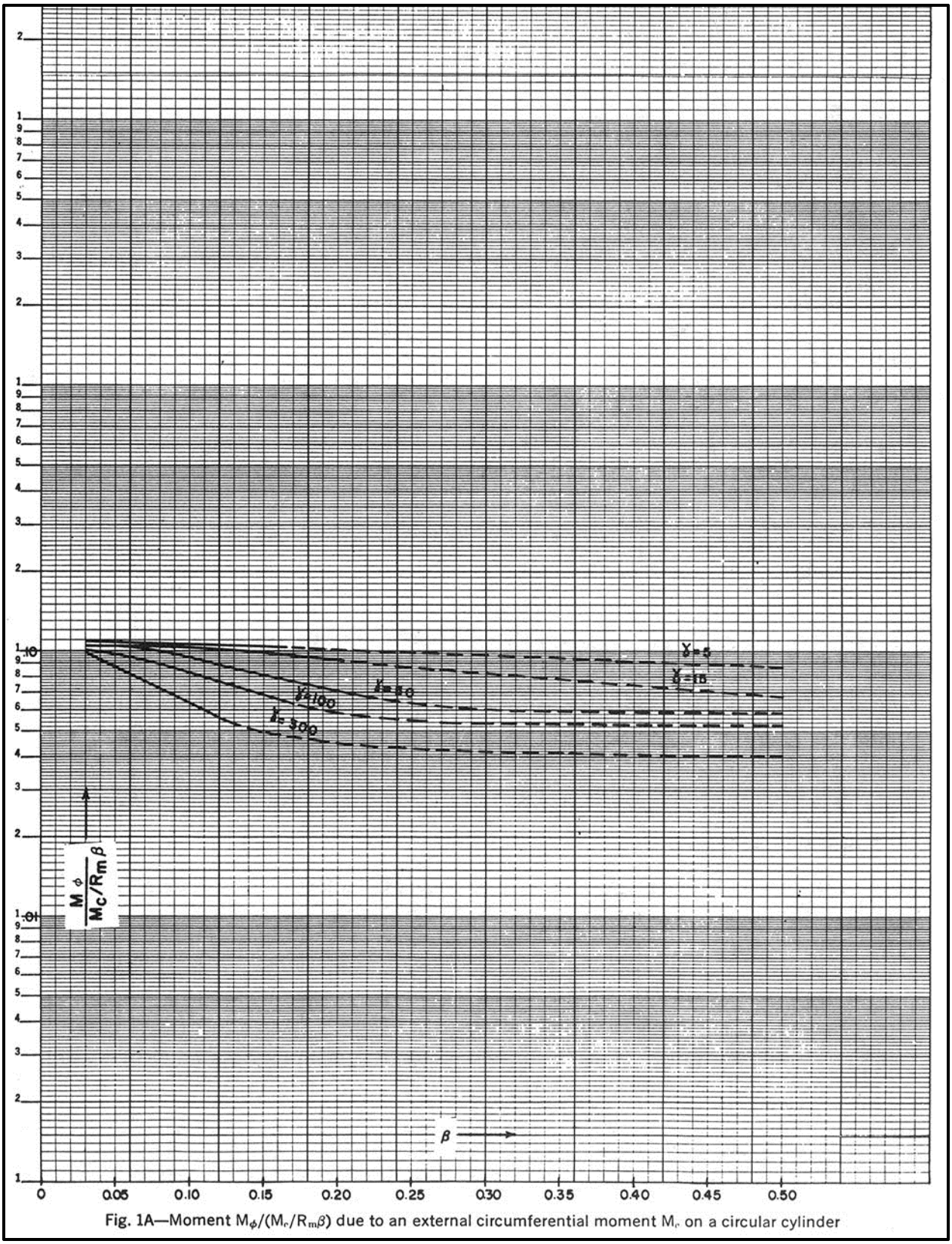

Fig. 1A—Moment $M_\phi/(M_c/R_m\beta)$ due to an external circumferential moment M_c on a circular cylinder

Figure 2.5-4 – Figure 1A from WRC Bulletin 107

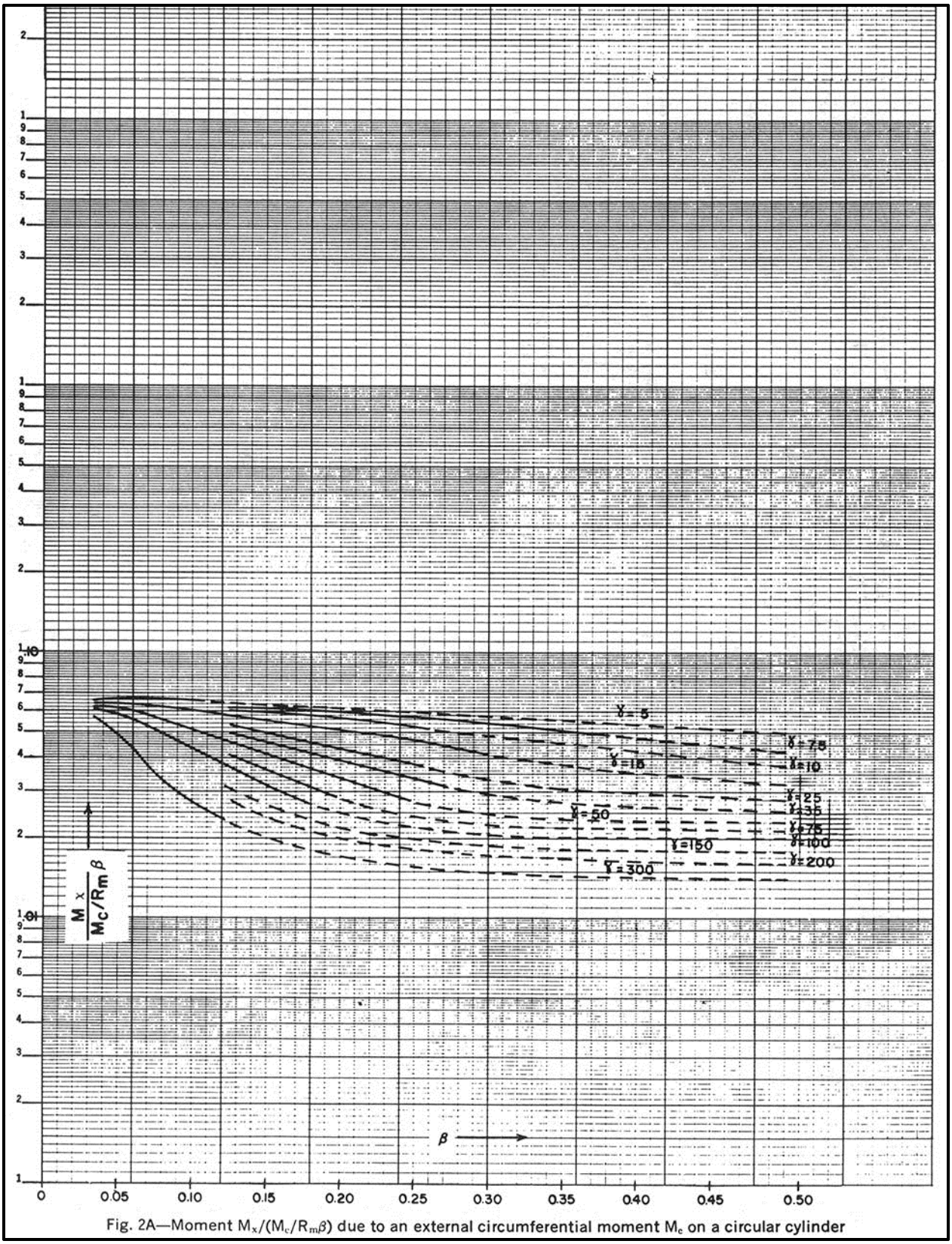

Fig. 2A—Moment $M_x/(M_c/R_m\beta)$ due to an external circumferential moment M_c on a circular cylinder

Figure 2.5-5 – Figure 2A from WRC Bulletin 107

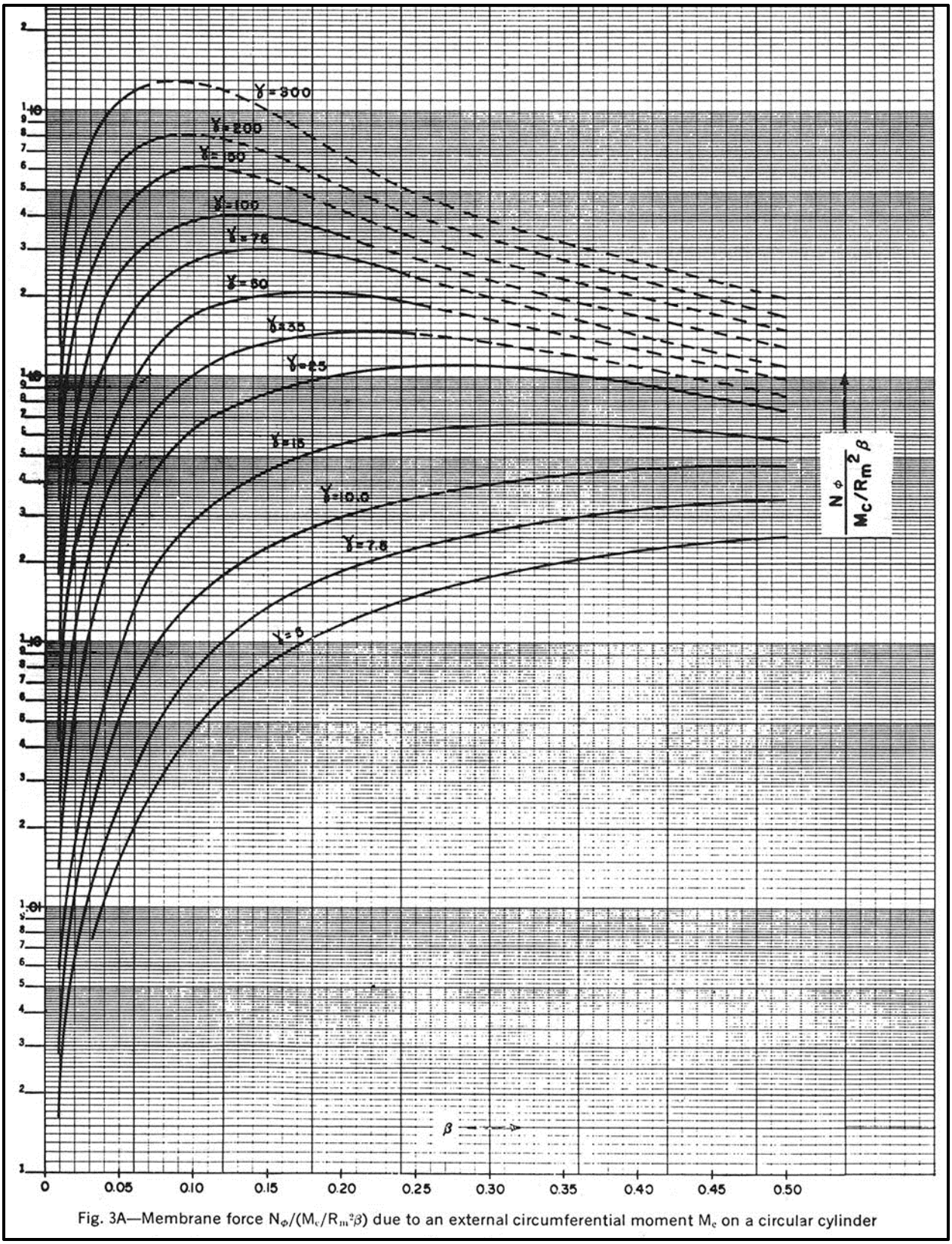

Fig. 3A—Membrane force $N_\phi/(M_c/R_m^2\beta)$ due to an external circumferential moment M_c on a circular cylinder

Figure 2.5-6 – Figure 3A from WRC Bulletin 107

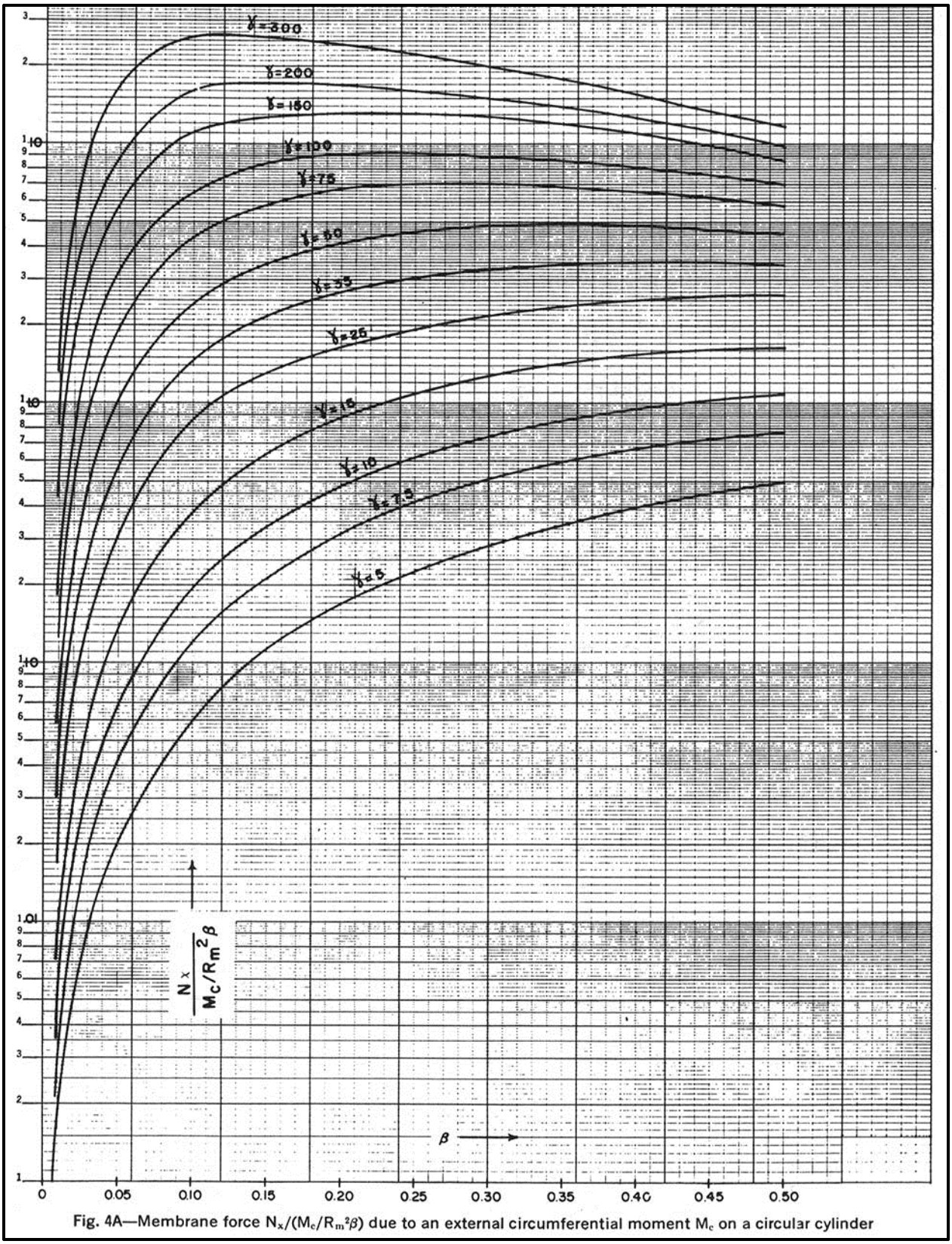

Figure 2.5-7 – Figure 4A from WRC Bulletin 107

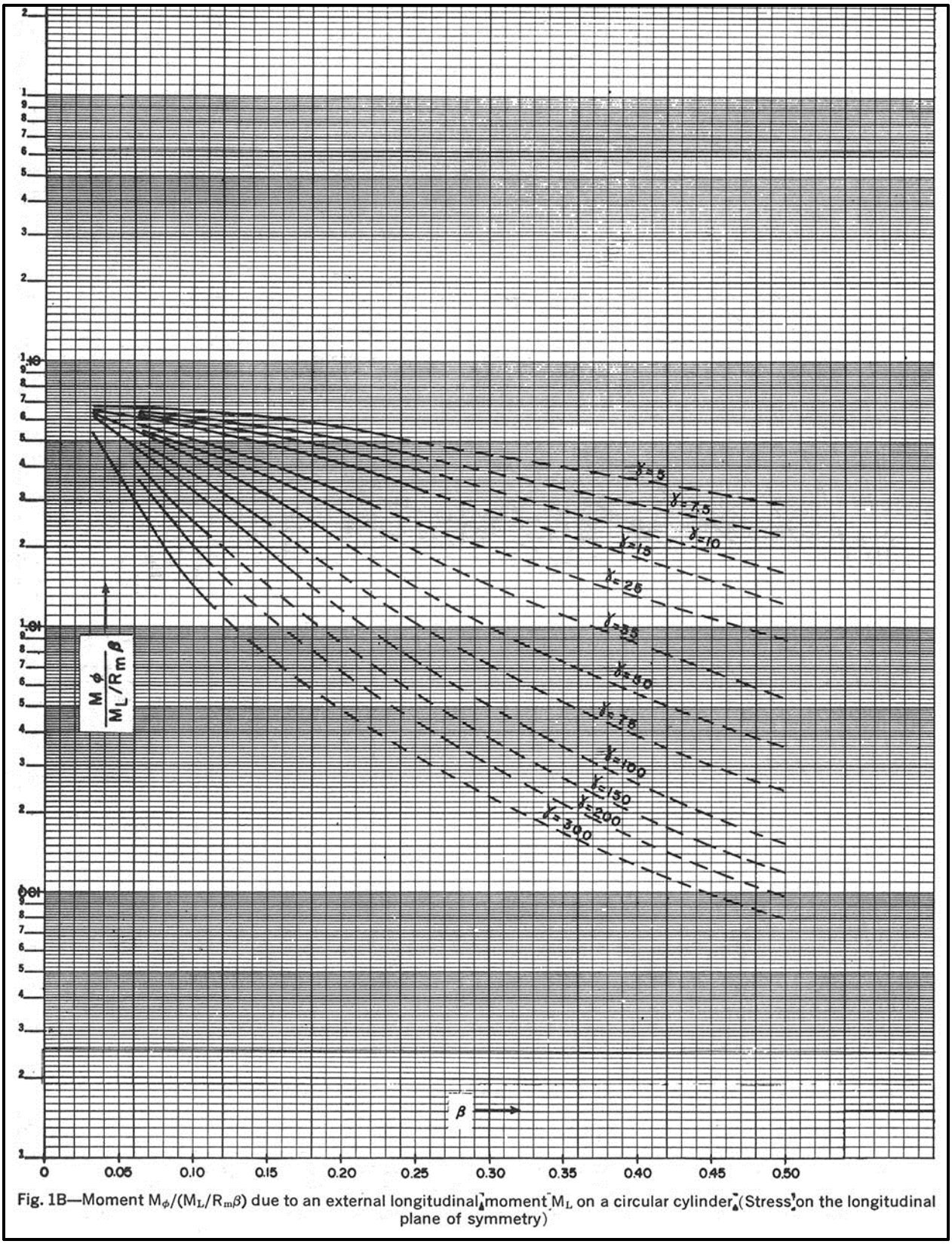

Fig. 1B—Moment $M_\phi/(M_L/R_m\beta)$ due to an external longitudinal moment M_L on a circular cylinder (Stress on the longitudinal plane of symmetry)

Figure 2.5-8 – Figure 1B from WRC Bulletin 107

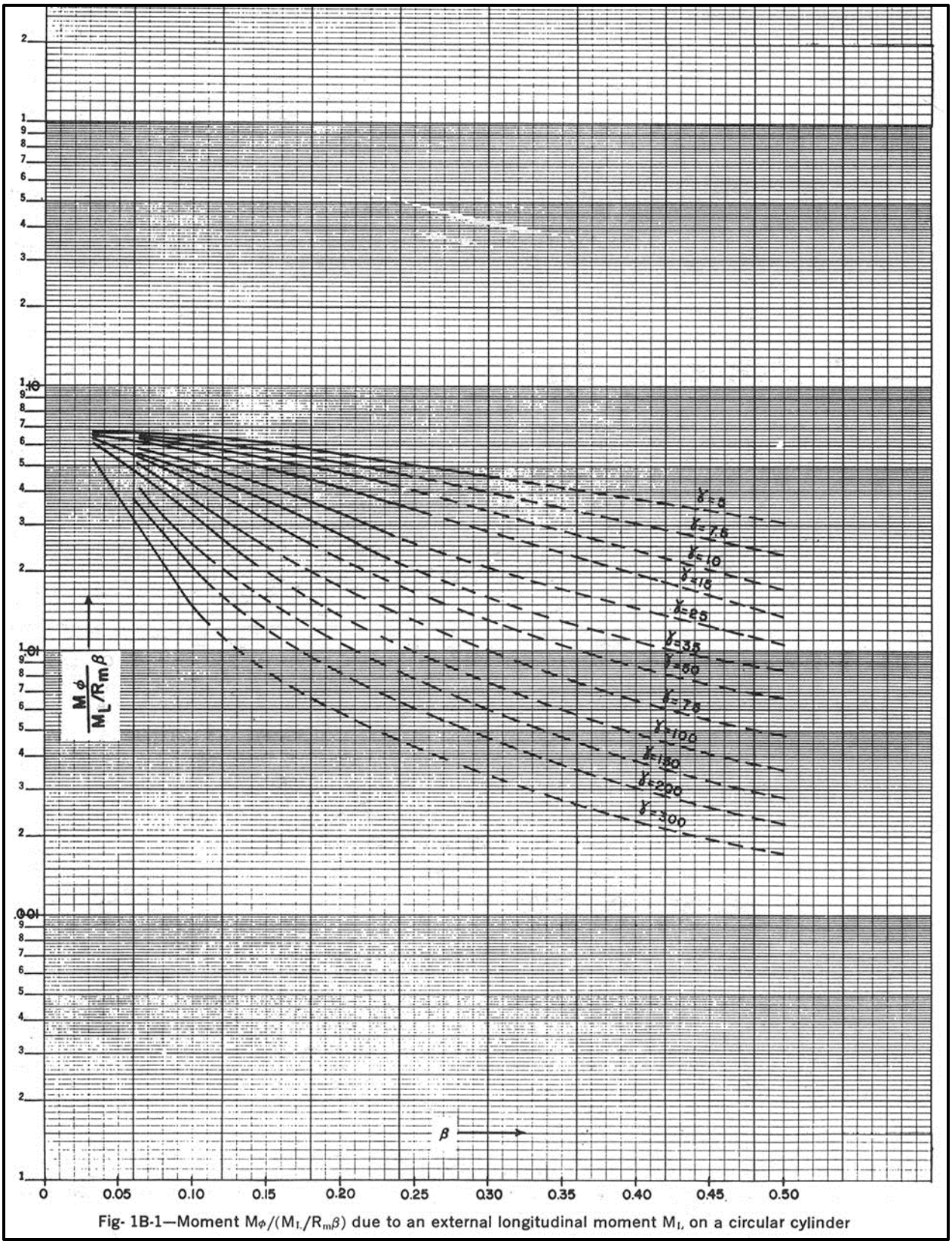

Fig- 1B-1—Moment $M_\phi/(M_L/R_m\beta)$ due to an external longitudinal moment M_L on a circular cylinder

Figure 2.5-9 – Figure 1B-1 from WRC Bulletin 107

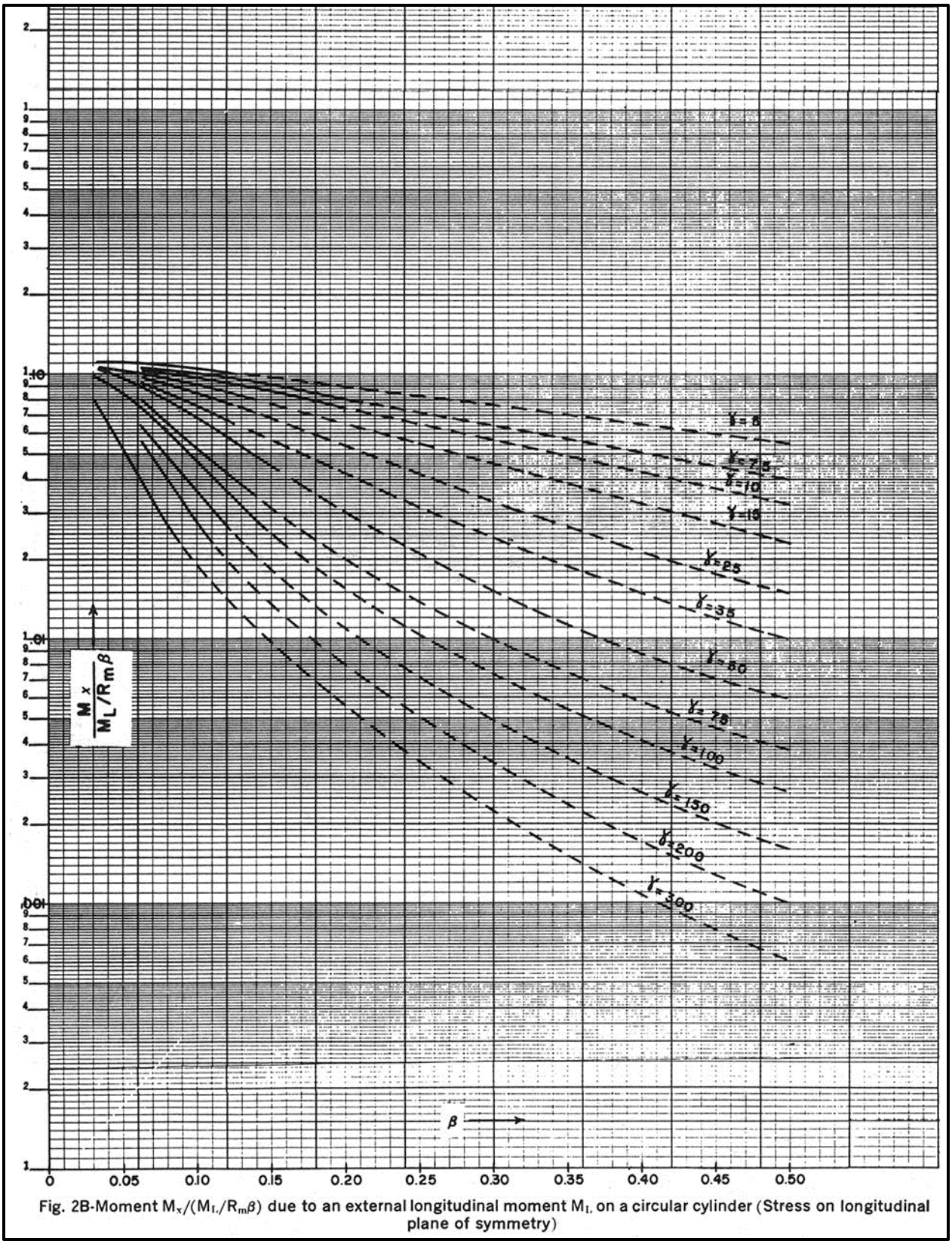

Fig. 2B-Moment $M_x/(M_L/R_m\beta)$ due to an external longitudinal moment M_L on a circular cylinder (Stress on longitudinal plane of symmetry)

Figure 2.5-10 – Figure 2B from WRC Bulletin 107

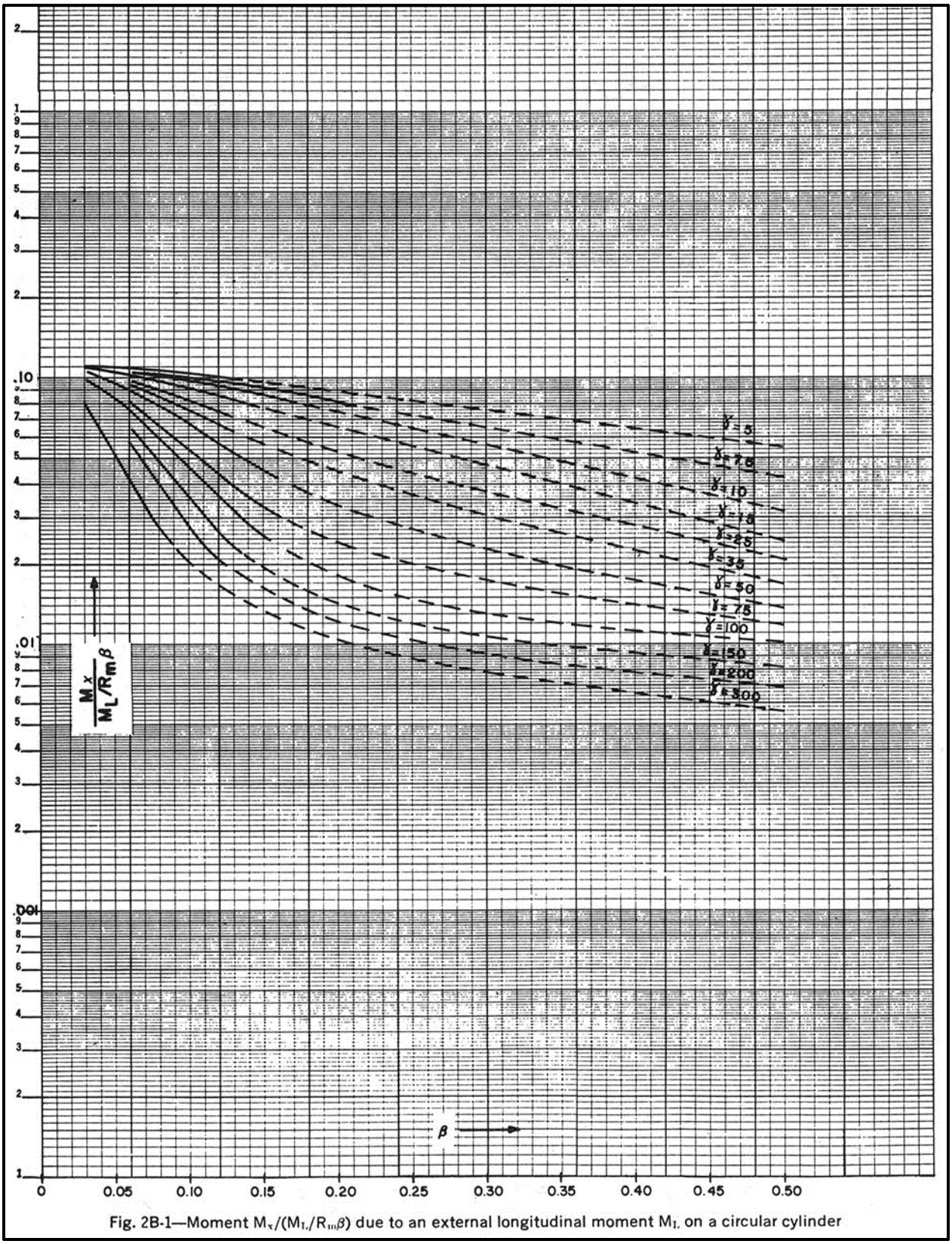

Fig. 2B-1—Moment $M_x/(M_L/R_m\beta)$ due to an external longitudinal moment M_L on a circular cylinder

Figure 2.5-11 – Figure 2B-1 from WRC Bulletin 107

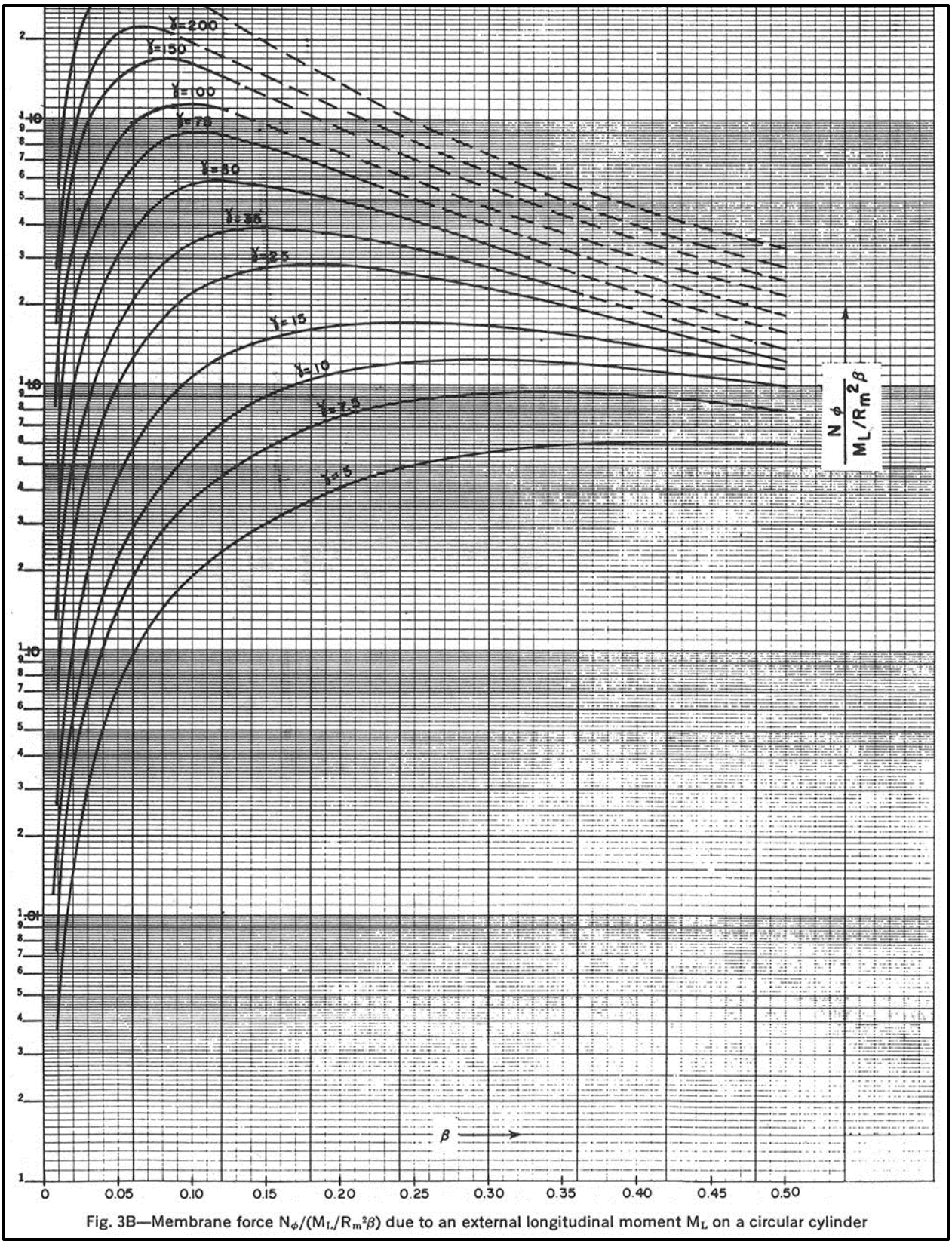

Fig. 3B—Membrane force $N_\phi/(M_L/R_m^2\beta)$ due to an external longitudinal moment M_L on a circular cylinder

Figure 2.5-12 – Figure 3B from WRC Bulletin 107

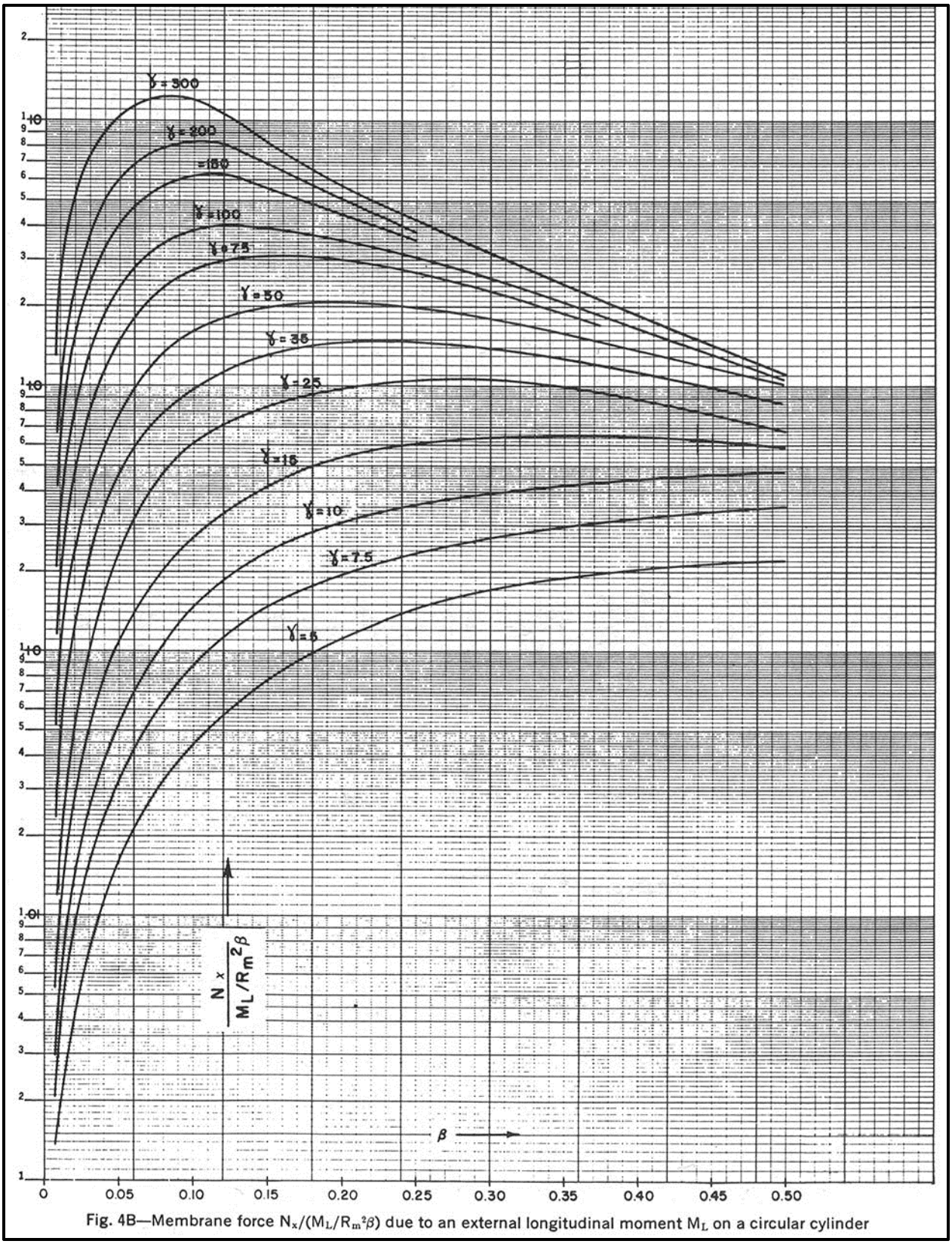

Fig. 4B—Membrane force $N_x/(M_L/R_m^2\beta)$ due to an external longitudinal moment M_L on a circular cylinder

Figure 2.5-13 – Figure 4B from WRC Bulletin 107

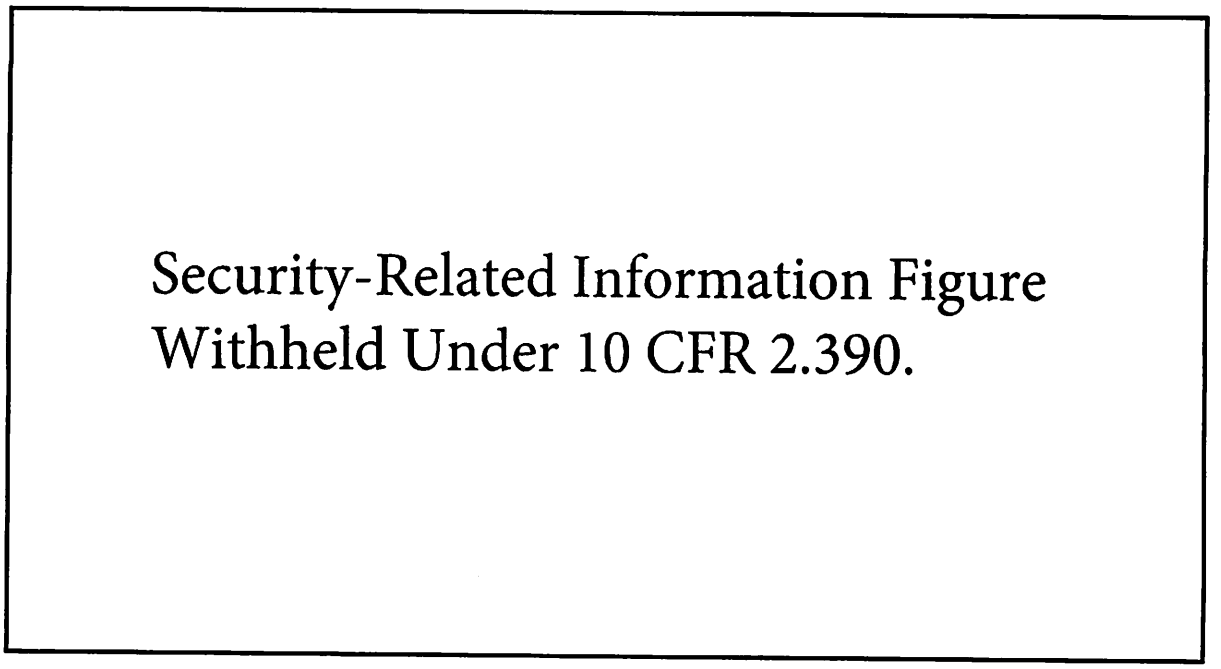

Figure 2.5-14 – Lifting Trunnion Weld Evaluation

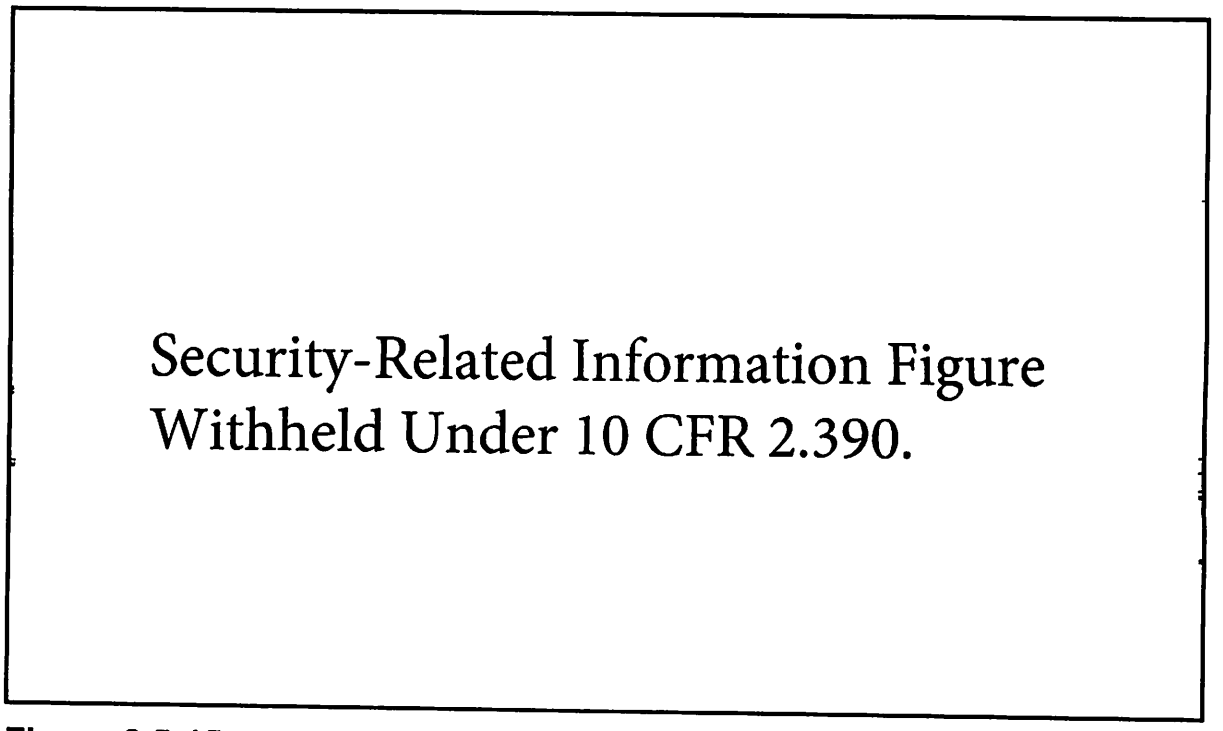

Figure 2.5-15 – Center-Pivot Trailer Configuration

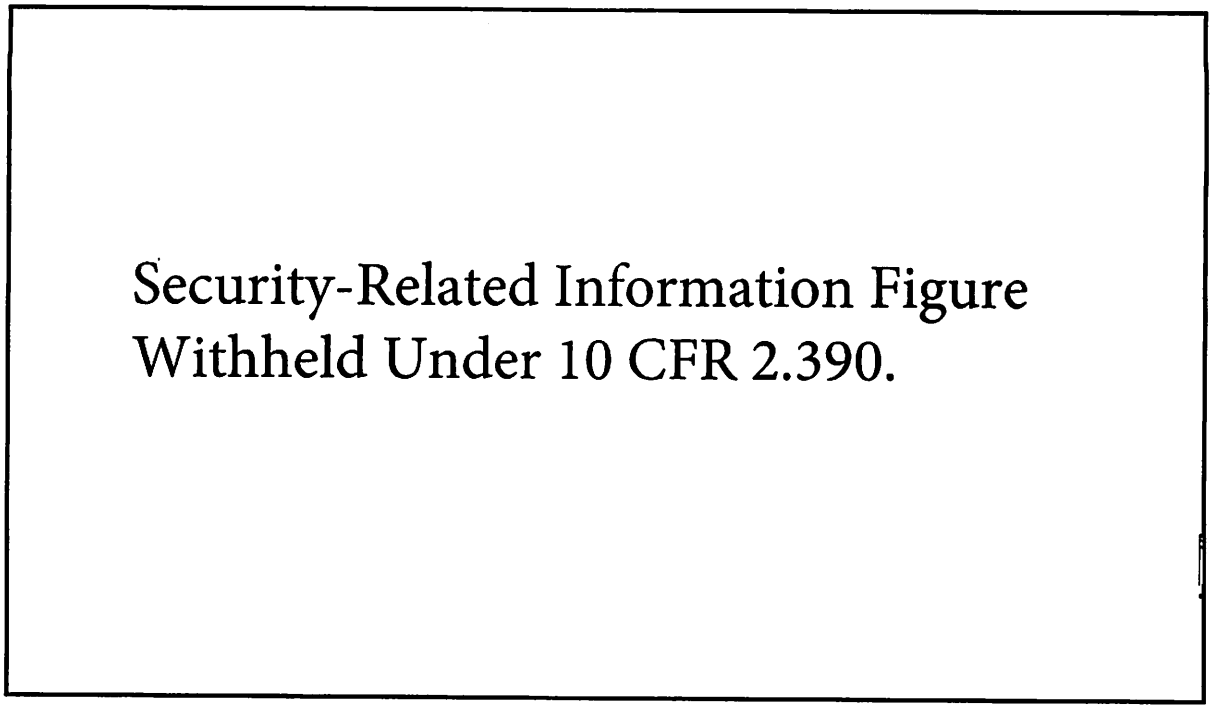

Figure 2.5-16 – Lift-Off Trailer Configuration

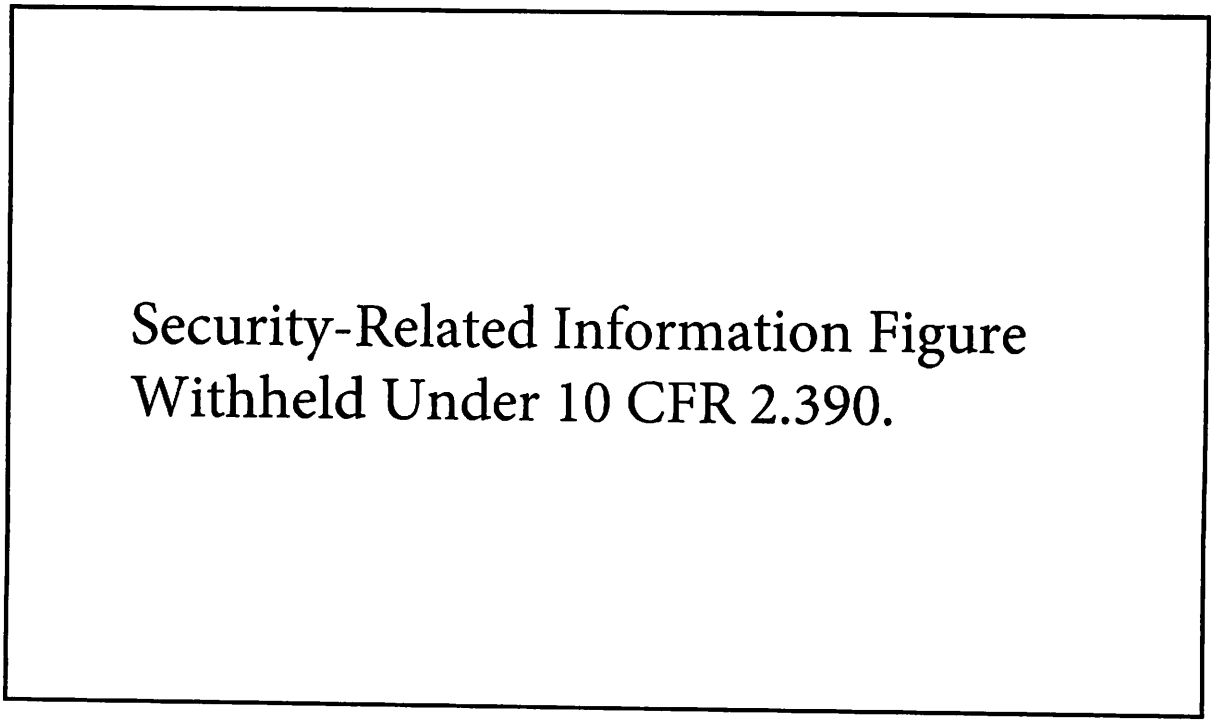

Figure 2.5-17 – Center-Pivot Trunnion Loading Configuration

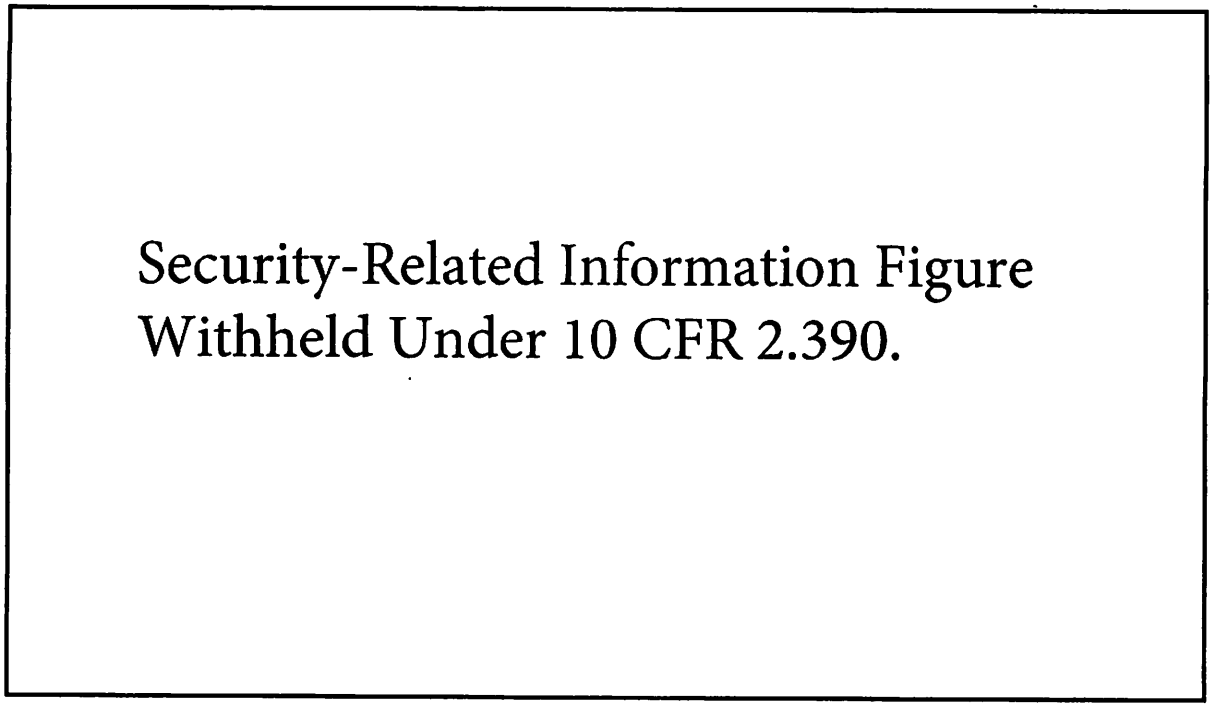

Figure 2.5-18 – Tie-down Loading Configuration

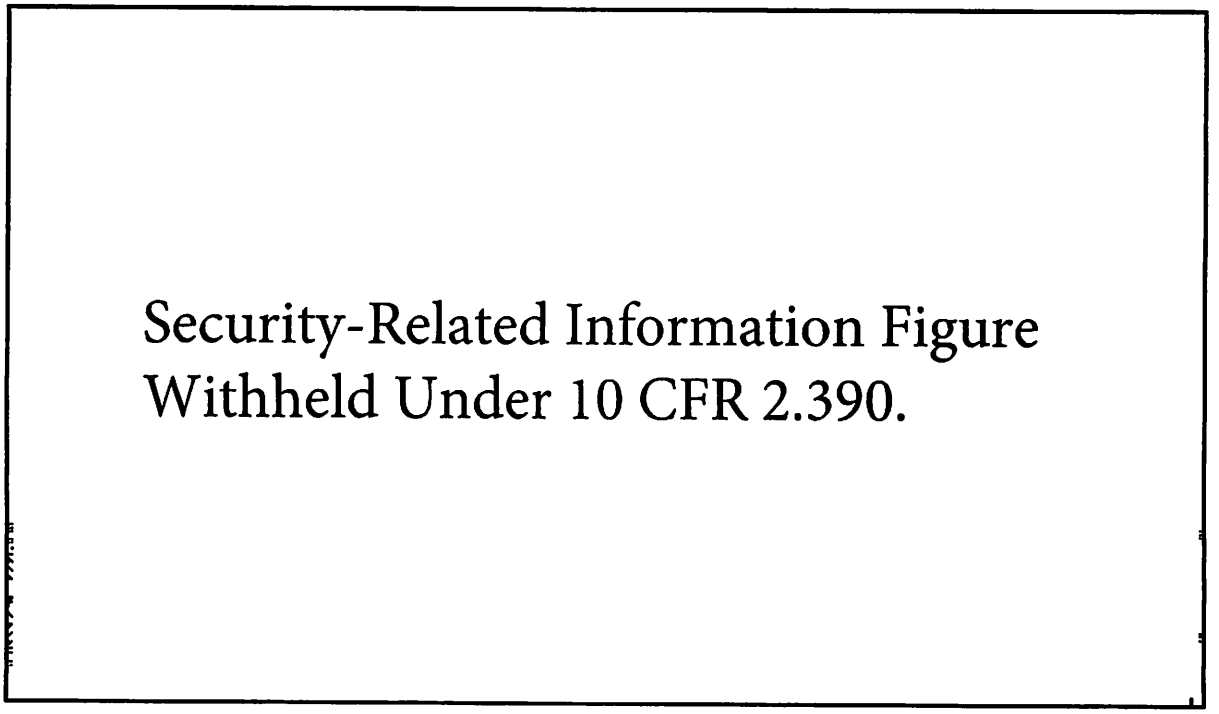

Figure 2.5-19 – Center-Pivot Trailer Free-Body Diagram for Tie-down

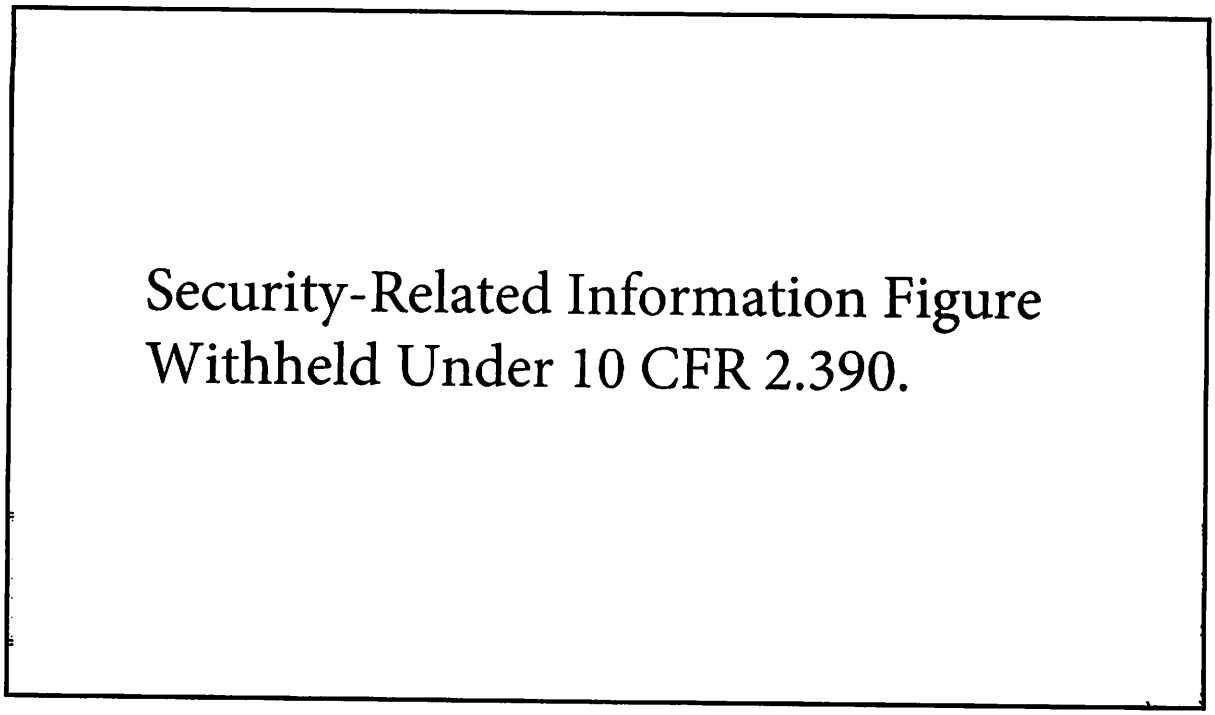

Figure 2.5-20 – Lift-Off Trailer Free-Body Diagram for Tie-down

2.6 Normal Conditions of Transport

The RH-TRU 72-B package, when subjected to normal conditions of transport (NCT) as specified in 10 CFR §71.71[1], meets the performance requirements specified in Subpart E of 10 CFR 71. This conclusion is demonstrated in the following subsections, where each normal condition is addressed and shown to meet the applicable design criteria (except buckling) previously discussed in Section 2.1.2, *Design Criteria*. Buckling evaluations for all buckling sensitive package components are presented in Appendix 2.10.5, *Buckling Design Criteria and Detailed Evaluation*.

Properties of Type 304 stainless steel and lead used in subsequent analyses are summarized in Table 2.6-1.

2.6.1 Heat

The thermal evaluation for the NCT heat condition is presented in Section 3.4, *Thermal Evaluation for Normal Conditions of Transport*. The NCT heat condition consists of exposing the package to direct sunlight and 100 ºF still air per the requirements of 10 CFR §71.71(c)(1)[1], with insolation per NRC Regulatory Guide 7.8[2]. A maximum internal heat load of 270 watts is used for the evaluation.

2.6.1.1 Summary of Pressures and Temperatures

The conditions of normal heat result in rather modest temperatures throughout the package. Maximum temperatures for the various package components are presented in Table 2.6-2. As indicated, all packaging structural component temperatures remain below 160 ºF. For many of the analyses herein, a 160 ºF maximum temperature for both the inner vessel (IV) and outer cask (OC) is conservatively employed. The payload canister temperature reaches a maximum of 202 ºF. Therefore a 210 ºF maximum temperature for analysis of the canister is conservatively employed.

The only differential expansions of significance are the radial expansions of the RH-TRU 72-B package cylindrical shells relative to their respective end plates or end attachment hardware. Worst-case temperature differences between shells and their end hardware are available from Section 3.4.6, *Maximum Thermal Stresses*. The difference in temperature between inner and outer shells of the OC (<0.5 ºF) is negligible. It is noted from the thermal analysis results (see Section 3.1, *Discussion*) that the temperatures of the OC shells and lead are greater than the stress free temperature of 89.9 ºF, determined in Appendix 2.10.8, *Fabrication Stresses Due to Lead Pour*, where fabrication stresses are discussed. Therefore, fabrication induced stresses due to lead shrinkage on the inner shell of the OC are relieved under the normal heat condition.

Initial pressure in both the IV and the OC is one (1) atmosphere (14.7 psia). Per Section 3.4.5, *Maximum Internal Pressure*, the design pressure is 150 psig for any package component.

[1] Title 10, Code of Federal Regulations, Part 71 (10 CFR 71), *Packaging and Transportation of Radioactive Material*, 01-01-14 Edition.

[2] U. S. Nuclear Regulatory Commission, Regulatory Guide 7.8, *Load Combinations for the Structural Analysis of Shipping Packages for Radioactive Material*, Revision 1, March 1989.

2.6.1.2 Differential Thermal Expansion – Radial Expansions of Shells Relative to Their End Hardware

A 7 ºF maximum bulk average temperature difference can exist between the OC end-closure plate or upper forging and the OC inner and outer shells per the thermal analysis presented in Section 3.4, *Thermal Evaluation for Normal Conditions of Transport*. Although this temperature difference is not overtly included in the Section 3.4 temperature summary tables, it is extracted from the thermal results in the same manner as the other data summarized there. Treating the end plate and upper forging as rigid, maximum stresses in the inner and outer shells of the OC are determined as follows (very conservatively assuming a step change in temperature between the shells and their end hardware of 7 ºF):

For the OC inner shell, with a mean shell radius, R_i =16.69 inches, and the coefficient of thermal expansion, $\alpha = 8.69(10)^{-6}$ in/in/ºF, taken at a maximum assumed shell temperature of 160 ºF, the imposed radial deflection is:

$$\delta_i = R_i\alpha(\Delta T) = (16.69)(8.69\times10^{-6})(7) = 0.001015 \text{ in}$$

For the OC outer shell, with a mean shell radius, R_o =19.813 inches, the imposed radial deflection is:

$$\delta_o = R_o\alpha(\Delta T) = (19.813)(8.69\times10^{-6})(7) = 0.001205 \text{ in}$$

Rotations, θ, at the shell ends are set equal to zero. From Table 30, Cases 8 and 10, of Roark[3]:

$$\delta = \frac{V_o}{2D\lambda^3} - \frac{M_o}{2D\lambda^2}$$

$$\theta = -\frac{V_o}{2D\lambda^2} + \frac{M_o}{D\lambda}$$

Shell parameters D and λ for the OC inner shell are:

$$D = \frac{Et^3}{12(1-\mu^2)} = \frac{(27.8\times10^6)(1.0)^3}{12(1-(0.3)^2)} = 2.546\times10^6 \text{ in-lb}$$

$$\lambda = \sqrt[4]{\frac{3(1-\mu^2)}{R^2t^2}} = \sqrt[4]{\frac{3(1-(0.3)^2)}{(16.69)^2(1.0)^2}} = 0.3146 \text{ in}^{-1}$$

where the mean inner shell radius, R = 16.69 inches, the shell thickness, t = 1.00 inch, the elastic modulus, $E = 27.8(10)^6$ psi at 160 ºF, and Poisson's ratio, μ = 0.3.

With the displacement of the inner shell, δ_i = 0.001015 inches and the slope, θ = 0 radians, solving for V_o and M_o from the above equations yields V_o = 321.9 lb/in, and M_o = 511.5 in-lb/in.

The stress components, from Table 30, Cases 8 and 10, of Roark[3] are:

σ_1 = 0.0 psi (axial membrane stress)

[3] R. J. Roark, W. C. Young, *Formulas for Stress and Strain*, 5th Edition, McGraw-Hill, Inc., New York, NY, 1975.

$$\sigma_2 = \frac{2V_o\lambda R}{t} - \frac{2M_o\lambda^2 R}{t} = 1{,}691 \text{ psi (hoop membrane stress)}$$

$$\sigma_1' = \frac{6M_o}{t^2} = 3{,}069 \text{ psi (axial bending stress)}$$

$$\sigma_2' = \mu\sigma_1' = 921 \text{ psi (hoop bending stress)}$$

Repeating the above analysis for the OC outer shell yields the following:

$$D = \frac{Et^3}{12(1-\mu^2)} = \frac{(27.8\times10^6)(1.5)^3}{12(1-(0.3)^2)} = 8.592\times10^6 \text{ in-lb}$$

$$\lambda = \sqrt[4]{\frac{3(1-\mu^2)}{R^2t^2}} = \sqrt[4]{\frac{3(1-(0.3)^2)}{(19.813)^2(1.5)^2}} = 0.2358 \text{ in}^{-1}$$

where the mean inner shell radius, R = 19.813 inches, the shell thickness, t = 1.50 inches, the elastic modulus, E = 27.8(10)^6 psi at 160 ºF, and Poisson's ratio, μ = 0.3.

With the displacement of the outer shell, δ_o = 0.001205 inches and the slope, θ = 0 radians, solving for V_o and M_o from the above equations yields V_o = 543 lb/in, and M_o = 1,151 in-lb/in.

The stress components, from Table 30, Cases 8 and 10, of Roark[3] are:

σ_1 = 0.0 psi (axial membrane stress)

$$\sigma_2 = \frac{2V_o\lambda R}{t} - \frac{2M_o\lambda^2 R}{t} = 1{,}692 \text{ psi (hoop membrane stress)}$$

$$\sigma_1' = \frac{6M_o}{t^2} = 3{,}069 \text{ psi (axial bending stress)}$$

$$\sigma_2' = \mu\sigma_1' = 921 \text{ psi (hoop bending stress)}$$

The above analyses are now repeated for the IV. From the thermal analyses of Section 3.4, *Thermal Evaluation for Normal Conditions of Transport*, the thermal gradient applicable for the IV shell is 9 ºF. This represents a bounding difference in bulk average temperatures between the IV end-closure plate or upper end forging and the IV shell. Maximum temperature for the IV is taken as 160 ºF for these calculations. For the IV shell, with a mean shell radius, R_i =15.81 inches, and the coefficient of thermal expansion, α = 8.69(10)$^{-6}$ in/in/ºF, the imposed radial deflection is:

$$\delta = R\alpha(\Delta T) = (15.81)(8.69\times10^{-6})(9) = 0.001237 \text{ in}$$

Shell parameters D and λ for the IV shell are:

$$D = \frac{Et^3}{12(1-\mu^2)} = \frac{(27.8\times10^6)(0.375)^3}{12(1-(0.3)^2)} = 1.343\times10^5 \text{ in-lb}$$

$$\lambda = \sqrt[4]{\frac{3(1-\mu^2)}{R^2t^2}} = \sqrt[4]{\frac{3(1-(0.3)^2)}{(15.81)^2(0.375)^2}} = 0.5279 \text{ in}^{-1}$$

where the mean inner shell radius, R = 15.81 inches, the shell thickness, t = 0.375 inches, the elastic modulus, E = $27.8(10)^6$ psi at 160 ºF, and Poisson's ratio, $\mu = 0.3$.

With the displacement of the inner shell, $\delta = 0.001237$ inches and the slope, $\theta = 0$ radians, solving for V_o and M_o from the above equations yields $V_o = 97.8$ lb/in, and $M_o = 92.6$ in-lb/in.

The stress components, from Table 30, Cases 8 and 10, of Roark[3] are:

$$\sigma_1 = 0.0 \text{ psi (axial membrane stress)}$$

$$\sigma_2 = \frac{2V_o\lambda R}{t} - \frac{2M_o\lambda^2 R}{t} = 2{,}177 \text{ psi (hoop membrane stress)}$$

$$\sigma_1' = \frac{6M_o}{t^2} = 3{,}951 \text{ psi (axial bending stress)}$$

$$\sigma_2' = \mu\sigma_1' = 1{,}185 \text{ psi (hoop bending stress)}$$

Since these thermal stresses are deformation limited, they can be classified as secondary stresses. The NCT allowable for range of primary-plus-secondary stress intensity is $3.0S_m$, or 60,000 psi for the Type 304 stainless steel used within the RH-TRU 72-B package. Conservatively combining the highest NCT secondary stress intensity determined above (3,951 psi) with the highest NCT primary membrane-plus-bending stress intensity anywhere in the package, excluding bolts (11,153 psi at the center of the OC lid for pressure-plus-end drop loading, per Table 2.6-8 of Section 2.6.7.1, *Flat End Drop*) results in a primary-plus-secondary stress intensity of 11,153 + 3,951 = 15,104 psi. By conservatively assuming fully reversing stress states, the range of primary-plus-secondary stress intensity becomes:

$$SI_{range} = 2(15{,}104) = 30{,}208 \text{ psi}$$

and the corresponding margin of safety is:

$$MS = \frac{60{,}000}{30{,}208} - 1 = +0.99$$

Per the above discussion, the remainder of this section does not specifically address thermal stresses when load combinations are made. In other words, the design is governed by primary, load-controlled stresses and the corresponding limits specified in Section C.2 of NRC Regulatory Guide 7.6[4] rather than by primary-plus-secondary stresses and the $3.0S_m$ limit specified in Section C.4. However, buckling evaluations presented in Appendix 2.10.5, *Buckling Design Criteria and Detailed Evaluation*, do consider secondary thermal stresses.

2.6.1.3 Stress Calculations

This section presents calculations of pressure induced stresses on the various package components. Unit pressure is first considered and appropriate factors are then applied to arrive at stresses for particular loading cases of interest. Locations of interest for the RH-TRU 72-B package are shown in Figure 2.6-1.

[4] U. S. Nuclear Regulatory Commission, Regulatory Guide 7.6, *Design Criteria for the Structural Analysis of Shipping Package Containment Vessels*, Revision 1, March 1978.

The only significant mechanical loading on the RH-TRU 72-B package is dead weight. As free drop cases impose higher mechanical loadings on the package than does dead weight alone, combinations of pressure loads and mechanical loadings due to free drop govern the design and are presented in Section 2.6.7, *Free Drop*. Fatigue is not a concern as discussed in Section 2.1.2.2.2, *Fatigue*.

2.6.1.3.1 Stresses Due To Unit Pressures

Referring to Figure 2.6-1, geometries and temperatures for the various locations (P1 through P10) are summarized in Table 2.6-3.

For locations P1, P2, and P3 (away from the cylinder ends),

$$\sigma_1 = \frac{pr}{2t} \text{ (axial membrane stress)}$$

$$\sigma_2 = \frac{pr}{t} \text{ (hoop membrane stress)}$$

$$\sigma_1' = 0 \text{ (axial bending stress)}$$

$$\sigma_2' = 0 \text{ (hoop bending stress)}$$

For locations P4 and P5 (at the OC cylinder ends), stresses are determined from Table 29, Case 1c, and Table 30, Cases 8 and 10, of Roark[3]:

$$\sigma_1 = \frac{pr}{2t} \text{ (axial membrane stress)}$$

$$\sigma_2 = \frac{pr}{t} - \frac{2V_o\lambda r}{t} + \frac{2M_o\lambda^2 r}{t} \text{ (hoop membrane stress)}$$

$$\sigma_1' = -\frac{6M_o}{t^2} \text{ (axial bending stress)}$$

$$\sigma_2' = -\frac{\mu 6M_o}{t^2} \text{ (hoop bending stress)}$$

where shell parameters D and λ are:

$$D = \frac{Et^3}{12(1-\mu^2)}$$

$$\lambda = \sqrt[4]{\frac{3(1-\mu^2)}{r^2t^2}}$$

In addition, the radial displacement, δ, and axial slope, θ, are as follows:

$$\delta = \frac{pr^2}{Et}\left(1-\frac{\mu}{2}\right) - \frac{V_o}{2D\lambda^3} + \frac{M_o}{2D\lambda^2} = 0$$

$$\theta = \frac{V_o}{2D\lambda^2} - \frac{M_o}{D\lambda} = 0$$

where the elastic modulus, $E = 27.8(10)^6$ psi at 160 ºF, Poisson's ratio, $\mu = 0.3$, and the unit pressure, $p = 1.0$ psi.

For locations P4 and P5 it is necessary to solve the two equations ($\delta = 0 = ...$) and ($\theta = 0 = ...$) simultaneously for V_o and M_o in each case. This yields the following results:

$V_o = 3.604$ lb/in (for P4)

$M_o = 7.644$ in-lb/in (for P4)

$V_o = 2.701$ lb/in (for P5)

$M_o = 4.292$ in-lb/in (for P5)

For location P6, a radius transition is provided between the shell and the end plate. The complicated geometry of this transition precludes the use of classical stress analysis techniques. Therefore, a finite element analysis has been performed for this structure to obtain the stresses associated with P6. For more details of this finite element model see Appendix 2.10.1.2, *Inner Vessel Radius Transition Zone Stresses Due to Pressure*.

Table 2.6-4 summarizes the results for locations P1 through P6.

Locations P7 through P10 are considered utilizing Table 24, Case 10a, of Roark[3]. Assuming a simply-supported plate with a uniform loading, the bending moment, M_o, and stress, σ, are:

$$M_o = \frac{pa^2(3+\mu)}{16}$$

$$\sigma = \frac{6M_o}{t^2} = \frac{3pa^2(3+\mu)}{8t^2}$$

where a is the plate radius, t is the plate thickness, Poisson's ratio, $\mu = 0.3$, and the unit pressure, $p = 1.0$ psi.

Table 2.6-5 summarizes the results for locations P7 through P10.

2.6.1.3.2 Stresses Due to Maximum Pressures

The maximum internal pressure acting on any component in the RH-TRU 72-B Package is 150 psig. Utilizing the unit stresses developed in Section 2.6.1.3.1, *Stresses Due To Unit Pressures*, maximum pressure stress results are shown in Table 2.6-6 for P1 – P10.

2.6.1.4 Comparison with Allowable Stresses

As discussed in Section 2.6.1.3, *Stress Calculations*, load combinations and comparisons with allowable stress limits are presented in Section 2.6.7, *Free Drop*, where worst-case combined load cases are addressed.

2.6.2 Cold

For the cold condition, a -40 ºF steady state ambient temperature and no internal heat generation are assumed. This results in a uniform temperature throughout the package of -40 ºF. The materials of construction for the package are not adversely affected by the -40 ºF condition. In particular, brittle fracture is not a concern, as discussed in Section 2.1.2.2.1, *Brittle Fracture*.

The only concern identified with the cold condition is with shrinkage of the lead onto the inner shell of the OC. As shown in Appendix 2.10.8, *Fabrication Stresses Due to Lead Pour*, a hoop stress of -1,837 psi and an axial stress of -1,979 psi can develop in the inner shell when cooled to -40 ºF. This case is independent of other load cases and will not, therefore, limit the package design. However, a -20 ºF case must be considered as a possible initial condition for other load cases, per 10 CFR §71.71(b)[1]. The hoop stress is -1,821 psi, and the axial stress is -1,963 psi at -20 ºF, per Appendix 2.10.8, *Fabrication Stresses Due to Lead Pour*. These stresses are determined by conservatively neglecting the beneficial effects of lead creep.

An additional discussion of fabrication induced stresses due to lead shrinkage onto the OC inner shell is contained in Section 2.6.7.1, *Flat End Drop*. The analysis therein assesses the consequences of a flat end drop of the package. In order to arrive at appropriate initial conditions for the drop, a special process of molten lead cooldown is followed, to properly control solidification.

2.6.3 Reduced External Pressure

The effect of reduced external pressure of 3.5 psia (11.2 psig internal pressure), per 10 CFR §71.71(c)(3)[1], is considered negligible to the RH-TRU 72-B package. This conclusion is based upon the calculations presented in Section 2.6.1.3.2, *Stresses Due to Maximum Pressures*, which assesses package survivability at a NCT internal pressure of 150 psig.

2.6.4 Increased External Pressure

The effect of increased external pressure of 20 psia (5.3 psig external pressure), per 10 CFR §71.71(c)(4)[1], is considered negligible to the RH-TRU 72-B package due to the thick OC outer shell and end closures. Additionally, Section 2.6.7, *Free Drop*, addresses a multiplicity of different loading cases in excess of the prescribed requirements.

2.6.5 Vibration

The effect of vibrations normally incident to transport are considered to be negligible. This conclusion is drawn based on the small stresses obtained throughout the OC and IV for the side drop event discussed in Section 2.6.7.3, *Flat Side Drop*. Per that section, the NCT side drop results in a 19.3*g* lateral acceleration on the package that translates to stresses in the package, as given in Table 2.6-7.

As a conservative worst-case, normal vibration *g*-loads are assumed equal to the normal vertical loading imposed on tie-downs. Utilizing the specification in 10 CFR §71.45(b)(1)[1] of 2*g* in the vertical direction, the maximum combined stress, S, is found by ratioing to be 489 psi in the IV. This stress is well below the endurance limit for Type 304 stainless steel at 160 ºF. From Figure

2.6-2 (Figure I-9.2.2 from Appendix I of the ASME Code[5]), for 10^9 cycles, and correcting for the ratio of elastic moduli at room temperature and 160 ºF, the minimum allowable alternating stress intensity, S_a, becomes

$$S_a = (14{,}000)\left(\frac{27.8(10)^6}{28.3(10)^6}\right) = 13{,}753 \text{ psi}$$

The IV shell vibratory stress margin of safety is:

$$MS = \frac{S_a}{S} - 1 = \frac{13{,}753}{489} - 1 = +27.1$$

The tie-down trunnions must also resist the 2*g* vibration loading. The maximum center-pivot trunnion load, P, with an inertia load of 2*g* is:

$$P = \frac{(2g)(45{,}000)}{2 \text{ trunnions}} = 45{,}000 \text{ lb}$$

The center-pivot trunnion was evaluated with a vertical load (i.e., no longitudinal or transverse loads included), P_v = 54,931 pounds, as discussed in Appendix 2.10.1.1, *Tie-down Trunnion Analysis*, with a resulting maximum OC outer shell stress intensity, S_{max} =1,972 psi.

With a maximum temperature for the trunnions taken at 160 ºF, and assuming 10^9 cycles of stress, the allowable alternating stress intensity, S_a, has previously been calculated to be 13,753 psi. The center-pivot trunnion vibratory stress minimum margin of safety is therefore:

$$MS = \frac{S_a}{S} - 1 = \frac{13{,}753}{1{,}972} - 1 = +5.97$$

Therefore, the requirements of 10 CFR §71.71(c)(5)1 have been met.

2.6.6 Water Spray

Due to the materials of construction utilized for the RH-TRU 72-B package, the water spray test requirement, per 10 CFR §71.71(c)(6)[1], will have a negligible effect on this package.

2.6.7 Free Drop

The RH-TRU 72-B shipping package weighs 45,000 pounds. Subpart F of 10 CFR 71[1] requires that a package in excess of 33,000 pounds weight be dropped one (1) foot onto a flat, essentially unyielding, horizontal surface, striking the surface in a position for which maximum damage is expected. The following subsections address free drops at all angles with respect to horizontal. It is shown that all conditions of 10 CFR §71.71[1] have been met.

The analyses in this section extract accelerations from impact analysis results summarized in Appendix 2.10.3, *Drop Impact Evaluation Results*, and statically apply them to the package. The durations of impact loadings are relatively long as the result of using soft (relative to the steel

[5] American Society of Mechanical Engineers (ASME) Boiler and Pressure Vessel Code, Section III, *Rules for Construction of Nuclear Power Plant Components*, Division 1, Subsection NB and Appendices, 1986 Edition.

structures) energy absorbing impact limiters to protect the package during free drop events. The package frequencies are high as the result of using relatively thick, stiff shells for the OC. To verify these assertions, the impact duration and natural frequency of the package will be approximated using simple, conservative calculations. For illustration purposes, end impact will be analyzed, since flat end drop immediately mobilizes the largest area of the impact limiter, the flat end surface. Consequently, the impact duration for end drop can be expected to be the least of all drop orientations, and will thus conservatively bound impact durations for the other free drop orientations.

For the purpose of approximating impact duration, the package is considered to be a rigid mass on a constant force damper, which is the impact limiter. The assumption of a constant force response from the impact limiter is based on the conservative presumption that all of the foam is mobilized in pure compression throughout the duration of the event. This type of response is referred to as "fully effective" in the drop analysis results presented in Appendix 2.10.3, *Drop Impact Evaluation Results*. Such a response will result in greater energy absorption in less time, thus minimizing impact duration.

This system can be represented by the following single degree of freedom equation:

$$M\frac{\partial^2 y}{\partial t^2} = F_y - Mg$$

where the package mass, $M = W/g = 45{,}000/386.4 = 116.5$ lb-sec^2/in, the package weight, $W = 45{,}000$ lb, the gravitational constant, $g = 386.4$ in/sec^2, the direction of the drop, assumed positive upward, is y, the time is t, and the impact limiter crush force for flat end drop is F_y.

For the assumed constant force response, the impact limiter reaction force is:

$$F_y = \sigma_c A$$

where the polyurethane foam "plateau" stress, $\sigma_c \approx 700$ lb/in^2 at 40% strain per Table 2.3-3 for the parallel-to-rise orientation cold condition, the impact limiter cross-sectional area, $A = (\pi/4)D^2 = 4{,}536.5$ in^2, and the impact limiter diameter, $D = 76.0$ inches.

Since the impact limiter reaction force is independent of time, the governing equation may be integrated once to yield:

$$M\frac{dy}{dt} = (F_y - Mg)t + c$$

where the vertical velocity, $dy/dt = v_y$, and the constant of integration is c. To evaluate the constant of integration, consider that, at time t = 0 seconds (instant of initial impact):

$$v_y = v_o = \sqrt{2gh} = -527.5 \text{ in/sec}$$

where the drop height, h = 30 ft = 360 inches, and the gravitational constant, $g = 386.4$ in/sec^2. Inserting t = 0 seconds and $v_y = v_o$ into the previous equation and solving for c results in:

$$c = Mv_o$$

With this constant now defined, and recognizing that $W = Mg$, the governing equation can be solved for time t:

$$t = -\frac{W(v_y - v_o)}{g(\sigma_c A - W)}$$

The duration of the impact, t, can be determined by realizing that, at the end of the impact event, $v_y = 0$ in/sec. Substituting in the appropriate quantities, the minimum free drop impact duration may thus be approximated as:

$$t = -\frac{(45{,}000)(0 - 527.5)}{(386.4)[(700)(4{,}536.5) - 45{,}000]} = 0.02 \text{ sec}$$

The corresponding fundamental natural period of the package will now be determined. The response of the OC is assumed to dominate the package system for end impact, and the mass and damping effect of the IV and payload are ignored. The OC is modeled as a massless spring with a rigid mass (closure components plus impact limiter) at each end. From the tables on Page 1-12 of *Shock and Vibration Handbook*[6], the governing equation for the assumed vibratory system is:

$$\omega_n = \sqrt{\frac{k(m_1 + m_2)}{m_1 m_2}}$$

where the fundamental angular natural frequency of the spring-mass system is ω_n, the spring constant of the massless spring, k = AE/L, the cross-section area of the OC is A, the modulus of elasticity of the OC material is E, the length of the OC shells is L, the mass of bottom impact limiter and base plate, $m_1 = W_1/g$, the weight of bottom impact limiter and base plate is W_1, the mass of the top impact limiter, upper forging, and lid, $m_2 = W_2/g$, the weight of the top impact limiter, upper forging, and lid is W_2, and the gravitational constant, $g = 386.4$ in/sec^2.

The fundamental natural frequency of the spring-mass system, f_n, is:

$$f_n = \frac{\omega_n}{2\pi}$$

and the fundamental natural period of the spring-mass system, τ_n, is:

$$\tau_n = \frac{1}{f_n} = \frac{2\pi}{\omega_n} = 2\pi\sqrt{\frac{m_1 m_2}{k(m_1 + m_2)}} = 2\pi\sqrt{\frac{W_1 W_2}{kg(W_1 + W_2)}}$$

The composite equivalent axial stiffness, EA, of the OC can be determined from the method described in Section 2.1.3 of NUREG/CR-3966[7]:

$$EA = E_1A_1 + E_2A_2 + E_3A_3$$

where the modulus of elasticity of the OC inner shell is E_1, the cross-sectional area of OC inner shell, $A_1 = \pi(r_2^2 - r_1^2)$, the modulus of elasticity of the lead column is E_2, the cross-sectional area of lead column, $A_2 = \pi(r_3^2 - r_2^2)$, the modulus of elasticity of the OC outer shell is E_3, the cross-sectional area of OC outer shell, $A_3 = \pi(r_4^2 - r_3^2)$, the OC inner shell inner radius is r_1, the OC

[6] Cyril M. Harris, *Shock and Vibration Handbook*, 3rd edition, McGraw-Hill, Inc., New York, NY, 1988.

[7] T. A. Nelson, R. C. Chun, *Methods for Impact Analysis of Shipping Containers*, NUREG/CR-3966, Lawrence Livermore National Laboratory, Livermore, CA, November 1987.

inner shell outer radius and lead column inner radius is r_2, the OC outer shell inner radius and lead column outer radius is r_3, and the OC outer shell outer radius is r_4.

From Table 2.2-1 in Section 2.2, *Weights and Centers of Gravity*, W_1 = 2,547 lb (bottom impact limiter) + 1,967 lb (base plate) = 4,514 lb, and W_2 = 2,547 lb (top impact limiter) + 2,000 lb (upper forging) + 1,667 lb (lid) = 6,214 lb. From the drawings in Appendix 1.3.1, *Packaging General Arrangement Drawings*, r_1 = 16.19 inches, r_2 = 17.19 inches, r_3 = 19.07 inches, r_4 = 20.57 inches, and L = 124.25 inches.

From Table 2.6-1, $E_1 = E_3 = 28.3(10)^6$ lb/in^2 for Type 304 stainless steel, and $E_2 = 2.34(10)^6$ lb/in^2 for lead.

Substituting the above quantities into the appropriate equations results in:

$$EA = [28.3(10)^6](104.9) + [2.34(10)^6](214.2) + [28.3(10)^6](186.8) = 8.75(10)^9 \text{ lb}$$

$$k = \frac{EA}{L} = \frac{8.75(10)^9}{124.25} = 70.43(10)^6 \text{ lb/in}$$

$$\tau_n = 2\pi\sqrt{\frac{(4{,}514)(6{,}214)}{[70.43(10)^6](386.4)(4{,}514+6{,}214)}} = 0.002 \text{ sec}$$

Since the fundamental natural period of the package is an order of magnitude less than the minimum impact duration, it may be concluded that dynamic effects of the package arising from the impact will be negligible.

In addition, inspection of accelerometer data available from NuPac 125-B quarter-scale drop tests (NRC Certificate of Compliance No. 9200[8]) indicates that this type of package responds essentially as a rigid body (e.g., for end and oblique drops, all axial accelerometer traces are very nearly the same and, for side drop, the accelerations for all accelerometers oriented in the direction of the drop are nearly identical). This observation further justifies static application of *g*-loads.

2.6.7.1 Flat End Drop

Analysis of RH-TRU 72-B package behavior for the end drop event is performed in the following steps:

(1) Analyze the impact force using the CASKDROP computer program.

(2) Analyze the OC lid for bending assuming the IV and payload canister act as a uniform load on a simply supported plate (no impact limiter support).

(3) Analyze the OC lid for bending, as performed in (2), but with the impact limiter foam pressure acting in the opposite direction (impact limiter support).

(4) Analyze the stresses in the OC lid bolts.

(5) Analyze the IV stresses.

(6) Analyze the axial and hoop stresses in the OC shells and lead (maximum fabrication stress condition assumed).

[8] Nuclear Packaging, Inc., *Safety Analysis Report for the NuPac 125-B Fuel Shipping Package*, USNRC Certificate of Compliance 71-9200, U.S. Department of Energy, Washington, D.C.

(7) Analyze the axial and hoop stresses in the OC shells and lead (zero fabrication stress condition assumed).

(8) Analyze the payload canister stresses.

(9) Determine the amount of lead slump.

Material properties and allowable stresses corresponding to maximum enveloping temperature of 160 ºF for the Type 304 stainless steel OC and IV and lead are given in Table 2.6-1. Buckling is addressed in Appendix 2.10.5, *Buckling Design Criteria and Detailed Evaluation*.

Where possible, the analyses in this section are performed on the basis of a unit (1*g*) axial acceleration, with actual acceleration numbers being substituted at the final point of calculating stresses. From Table 2.10.3-10 in Appendix 2.10.3, *Drop Impact Evaluation Results*, the maximum *g*-load for the NCT flat end drop case is 42.5*g* (i.e., at -20 ºF and fully effective foam).

(1) End Drop Computer Analysis Using CASKDROP

The end drop analysis was performed utilizing the energy balance computer program, CASKDROP, documented in Appendix 2.10.2.1, *Description of the CASKDROP Computer Code*. Two cases were run assuming fully effective impact limiters, and considering the variations in foam strength due to temperature effects and the possible variations in foam strength from nominal values (see Section 2.3, *Mechanical Properties of Materials*). Fully effective impact limiter cases consider the entire impact limiter impact area available for crush. Based on the half-scale test results documented in Appendix 2.10.7, *Static and Dynamic Testing*, the fully effective impact limiter assumption is realistic. Output for each of the end drop cases is presented in Appendix 2.10.3, *Drop Impact Evaluation Results*. The worst-case deflections and accelerations are utilized for all analyses. From Appendix 2.10.3, *Drop Impact Evaluation Results*, the maximum NCT acceleration and maximum impact limiter deflection for a one-foot end drop is 42.5*g* at -20 ºF (Table 2.10.3-2) and 0.86 inches at 140 ºF (Table 2.10.3-3), respectively.

(2) OC Lid Bending Analysis Assuming No Impact Limiter Support

The OC lid is 6.00 inches thick and the welded end closure plate is 5.00 inches thick. The welded end closure plate is reasonably treated as a fixed-edge plate. Treating the bolted lid as a simply supported plate is conservative.

Therefore, to conservatively bound the problem, a 5-inch thick plate is analyzed as simply supported. The unit stress in the OC lid, σ, may be calculated by utilizing Table 24, Case 10a, of Roark[3], assuming a uniform load across the entire area:

$$\sigma = \frac{6M}{t^2} = \frac{3qa^2(3+\mu)}{8t^2} = 216\,\text{psi}/g$$

where the unit pressure, q = W/A = 13,690/1,110 = 12.33 lb/in^2, the IV weight + canister weight + OC lid weight, W = 13,690 pounds, the exterior OC lid area, A = $\pi(18.80)^2$ = 1,110 in^2, the exterior OC lid radius, a = 18.80 inches, Poisson's ratio, μ = 0.3, and the OC lid thickness, t = 5.00 inches.

Applying 42.5*g* acceleration from the NCT end drop analysis (Table 2.10.3-10 in Appendix 2.10.3, *Drop Impact Evaluation Results*) the bending stress, σ, becomes:

$$\sigma = (216)(42.5) = 9{,}180 \text{ psi}$$

Table 2.6-8 combines this stress with that due to a 150 psig normal pressure loading. As shown, the resultant margin of safety is +1.69. This margin is somewhat conservative as accelerations applied to the lid are those corresponding to a drop at -20 ºF, whereas allowables are taken at a temperature of 160 ºF.

(3) OC Lid Bending Analysis Assuming Full Impact Limiter Support

As analyzed above, assume the OC lid is supported across the impact plane by the foam. As before, the unit stress in the OC lid, σ, may be calculated by utilizing Table 24, Case 10a, of Roark[3], assuming a uniform load across the entire area:

$$\sigma' = \frac{6M'}{t^2} = \frac{3q'a^2(3+\mu)}{8t^2} = 494\ \text{psi}/g$$

where the unit pressure, $q' = W/A = 45{,}000/1{,}110 = 40.54\ \text{lb/in}^2$, the total package weight, W = 45,000 pounds, the exterior OC lid area, $A = \pi(18.80)^2 = 1{,}110\ \text{in}^2$, the exterior OC lid radius, a = 18.80 inches, Poisson's ratio, $\mu = 0.3$, and the OC lid thickness, t = 5.00 inches.

Once again applying 42.5*g* acceleration from the NCT end drop analysis (Table 2.10.3-10 in Appendix 2.10.3, *Drop Impact Evaluation Results*) the bending stress, σ', becomes:

$$\sigma' = (494)(42.5) = 20{,}995\ \text{psi}$$

Internal pressure would reduce this bending stress, but is conservatively ignored. From Table 2.6-1, the NCT allowable primary membrane-plus-bending stress intensity, $S_a = 30{,}000$ psi at 160 ºF for Type F304 stainless steel. Therefore, the minimum OC lid bending stress margin of safety, MS, is:

$$MS = \frac{S_a}{\sigma'} - 1 = \frac{30{,}000}{20{,}995} - 1 = +0.43$$

(4) OC Lid Bolt Stresses

OC bolt stresses under end impact conditions are computed and summarized within Table 2.10.6-1 and Table 2.10.6-2 from Appendix 2.10.6, *Closure Bolt Stress Evaluations*. Assuming an impact acceleration of 42.5*g* acting on the full weight of the lid (1,667 pounds), IV (4,023 pounds), and canister (8,000 pounds), the maximum bolt stress intensity is 56,702 psi, including pressure stress effects. This value exceeds the maximum bolt preload stress of 53,346 psi (51,692 lb/0.969 in^2). This stress conservatively neglects impact limiter reaction forces that would reduce estimated bolt impact stresses to near zero, if considered. From Table 2.6-1, the NCT allowable containment fastener primary membrane-plus-bending stress intensity, $S_a = 67{,}600$ psi at 160 ºF for ASTM A320, Grade L43, bolting material. With a total tensile stress of 56,702 psi, the resultant minimum margin of safety is computed as +0.19, in Table 2.10.6-5 of Appendix 2.10.6, *Closure Bolt Stress Evaluations*.

An assessment of OC bolt and thread insert engagement is provided in Appendix 2.10.6, *Closure Bolt Stress Evaluations*, and shown to have a minimum margin of safety of +0.13.

A detailed analysis of the OC lid bolts for various drop angles and torque coefficients is presented in Appendix 2.10.6, *Closure Bolt Stress Evaluations*.

(5) IV Stresses

The IV is designed so that, on end impact, the end closures (lid and bottom plate) will be flush against the end closures of the OC. This will tend to minimize bending stresses in IV end plates. IV analyses are performed for both top-end down and bottom-end down flat end drop.

Top-End Down: The IV bottom plate is loaded only by self-weight for the top-end down drop. Conservatively assuming a simply supported plate, the unit stress in the IV bottom plate, σ, may be calculated by using Table 24, Case 10a, of Roark[3]:

$$\sigma = \frac{6M}{t^2} = \frac{3qa^2(3+\mu)}{8t^2} = 62.0\,\text{psi}/g$$

where the unit pressure, q = W/A = 354/804.2 = 0.44 lb/in^2, the IV bottom plate weight, W = 354 pounds, the IV bottom plate area, A = $\pi(16.00)^2$ = 804.2 in^2, the IV bottom plate radius, a = 16.00 inches, Poisson's ratio, μ = 0.3, and the IV bottom plate thickness, t = 1.50 inches.

Applying 42.5*g* acceleration from the NCT end drop analysis (Table 2.10.3-10 in Appendix 2.10.3, *Drop Impact Evaluation Results*) the bending stress, σ, becomes:

$$\sigma = (62.0)(42.5) = 2{,}635 \text{ psi}$$

Internal pressure would reduce this bending stress, but is conservatively ignored. From Table 2.6-1, the NCT allowable primary membrane-plus-bending stress intensity, S_a = 30,000 psi at 160 ºF for Type F304 stainless steel. Therefore, the minimum IV bottom plate bending stress margin of safety, MS, is:

$$MS = \frac{S_a}{\sigma} - 1 = \frac{30{,}000}{2{,}635} - 1 = +10.4$$

The stresses resulting in the radius transition between the bottom plate and the IV shell are analyzed by the ANSYS® model shown in Appendix 2.10.1.3, *Inner Vessel Radius Transition Zone Stresses Due to 1g Acceleration*. A unit acceleration (1*g*) is applied to the model and scaled for final drop loading results. The maximum stress intensity, SI, in the radius transition is 110 psi for a 1*g* acceleration.

For the NCT end drop loading of 42.5*g*, the maximum radius transition stress intensity, SI, is:

$$SI = (110)(42.5) = 4{,}675 \text{ psi}$$

The stress in the radius transition is opposite in nature to the stresses resulting from internal pressure; hence, stresses from internal pressure are conservatively ignored in this calculation. From Table 2.6-1, the NCT allowable primary membrane-plus-bending stress intensity, S_a = 30,000 psi at 160 ºF for Type F304 stainless steel. Therefore, the minimum IV radius transition bending stress margin of safety, MS, is:

$$MS = \frac{S_a}{SI} - 1 = \frac{30{,}000}{4{,}675} - 1 = +5.42$$

The maximum stress acting on the shell away from the transition region will be a compressive membrane stress due to self-weight:

$$\sigma = -\frac{P}{A} = -54.67 \text{ psi}/g$$

where the weight of IV bottom plate (354 pounds), spacers (467 pounds), and shell (1,216 pounds), P = 2,037 pounds, and the shell cross-sectional area, $A = \pi[(16.00)^2 - (15.625)^2] = 37.26$ in^2.

Applying 42.5*g* acceleration from the NCT end drop analysis (Table 2.10.3-10 in Appendix 2.10.3, *Drop Impact Evaluation Results*), the axial stress, σ, becomes:

$$\sigma = (-54.67)(42.5) = -2{,}323 \text{ psi}$$

Table 2.6-9 combines this stress with that due to a 150 psig normal pressure loading. As shown, the resultant margin of safety is +2.09. This margin is somewhat conservative, as accelerations applied to the IV shell are those corresponding to a drop at -20 ºF, whereas allowables are taken at a temperature of 160 ºF. A detailed buckling analysis for this load combination is presented in Appendix 2.10.5, *Buckling Design Criteria and Detailed Evaluation*.

The IV lid is supported during top-end down end drop by the OC lid, which is of comparable thickness and diameter. Because the OC lid will tend to limit deflections of the IV lid, it may be assumed that the large margins of safety derived for the OC lid in both backed and unbacked bending will be applicable to the IV lid.

Bottom-End Down: For bottom-end impact, the IV bottom plate will be supported by the OC bottom plate. The IV bottom plate is of approximately the same diameter, yet of significantly smaller thickness than the OC lid. Therefore, the IV bottom plate will see lower stresses than the OC bottom plate when forced into the OC bottom plate. This is because the OC closure will limit deflections of the IV closure, thereby assuring margins of safety in excess of the already conservative values presented for the OC closures.

The maximum stress acting on the IV shell away from the transitions with the upper flange forging and lower bottom plate will be a compressive membrane stress due to self-weight:

$$\sigma = -\frac{P}{A} = -98.47 \text{ psi}/g$$

where the weight of IV lid (1,382 pounds), flange (604 pounds), shell (1,216 pounds), and spacers (467 pounds), P = 3,669 pounds, and the shell cross-sectional area, $A = \pi[(16.00)^2 - (15.625)^2] = 37.26$ in^2.

Applying 42.5*g* acceleration from the NCT end drop analysis (Table 2.10.3-10 in Appendix 2.10.3, *Drop Impact Evaluation Results*) the axial stress, σ, becomes:

$$\sigma = (-98.47)(42.5) = -4{,}185 \text{ psi}$$

Table 2.6-10 combines this stress with that due to a 150 psig NCT pressure loading. As shown, the resultant margin of safety is +1.72. This margin is somewhat conservative, as accelerations applied to the shell are those corresponding to a drop at -20 ºF, whereas allowables are taken at a temperature of 160 ºF. A detailed buckling analysis for this load combination is presented in Appendix 2.10.5, *Buckling Design Criteria and Detailed Evaluation*.

The IV lid is loaded only by self-weight for a bottom-down end drop. Conservatively assuming a simply supported circular plate, the unit bending stress may be calculated by using Table 24, Case 10a, of Roark[3]:

$$\sigma = \frac{6M}{t^2} = \frac{3qa^2(3+\mu)}{8t^2} = 12.9 \text{ psi}/g$$

where the unit pressure, q = W/A = 1,382/804.2 = 1.72 lb/in^2, the IV lid weight, W = 1,382 pounds, the IV lid area, A = $\pi(16.00)^2$ = 804.2 in^2, the IV lid radius, a = 16.00 inches, Poisson's ratio, μ = 0.3, and the IV lid thickness, t = 6.50 inches.

Applying 42.5*g* acceleration from the NCT end drop analysis (Table 2.10.3-10 in Appendix 2.10.3, *Drop Impact Evaluation Results*), the bending stress, σ, becomes:

$$\sigma = (12.9)(42.5) = 548 \text{ psi}$$

Internal pressure would reduce this bending stress, but is conservatively ignored. From Table 2.6-1, the NCT allowable primary membrane-plus-bending stress intensity, S_a = 30,000 psi at 160 ºF for Type F304 stainless steel. Therefore, the minimum IV lid bending stress margin of safety, MS, is:

$$MS = \frac{S_a}{\sigma} - 1 = \frac{30{,}000}{548} - 1 = +54.7$$

IV bolt stresses under end impact conditions are computed and summarized within Table 2.10.6-3 and Table 2.10.6-4 from Appendix 2.10.6, *Closure Bolt Stress Evaluations*. Assuming an impact acceleration of 42.5*g* acting on the full weight of the lid (1,382 pounds) and canister (8,000 pounds), the maximum bolt stress intensity is 56,179 psi, including pressure stress effects. This value exceeds the maximum bolt preload stress of 51,840 psi (21,099 lbs/0.407 in²). These stresses neglect impact limiter reaction forces, which would reduce estimated bolt impact stresses to near zero, if considered. However, for added conservatism, all impact limiter forces have been neglected. From Table 2.6-1, the NCT allowable containment fastener primary membrane-plus-bending stress intensity, S_a = 67,600 psi at 160 ºF for ASTM A320, Grade L43, bolting material. With a total tensile stress of 56,179 psi, the resultant minimum margin of safety is computed as +0.20, in Table 2.10.6-3 of Appendix 2.10.6, *Closure Bolt Stress Evaluations*.

An assessment of IV bolt and thread insert engagement is provided in Appendix 2.10.6, *Closure Bolt Stress Evaluations*, and shown to have a minimum margin of safety of +0.18.

A detailed analysis of the IV lid bolts for various drop angles and torque coefficients is presented in Appendix 2.10.6, *Closure Bolt Stress Evaluations*.

(6) Stresses in the OC Shells and Lead (Maximum Fabrication Stress Condition Assumed)

The principal concern for the OC under NCT end drop is with buckling of the inner shell. As shown by the following stress calculations and the detailed buckling evaluations presented in Appendix 2.10.5, *Buckling Design Criteria and Detailed Evaluation*, buckling will not occur as the result of the hoop and axial compressive stresses which develop in the OC inner shell under the NCT end drop event.

Various initial conditions can be assumed for the NCT end drop event. In particular, a temperature must be assumed in order to establish an initial fabrication stress for the inner shell. A lower

assumed temperature will result in a higher initial hoop stress on the inner shell (see Appendix 2.10.8, *Fabrication Stresses Due to Lead Pour*), but higher allowable stresses. For purposes of this analysis, drops at 160 ºF (conservatively bounding the maximum OC lead and inner and outer shell NCT temperatures per Section 3.4.2, *Package Conditions and Environment*), 70 ºF, and -20 ºF are considered. Regardless of temperature, the maximum inertia load of 42.5*g* (for -20 ºF drop case) is conservatively employed.

To adequately bound the consequences of the drop event at a given temperature, two initial lead conditions are also considered. The first assumes that the lead has shrunk onto the inner shell and away from the outer shell. In addition, due to the combined effects of friction between the lead and inner shell, and axial shrinkage of the lead relative to the stainless shells, axial gaps will develop between the lead and the steel structures at the top and bottom end of the lead column. These axial gaps are important in that, until friction is overcome, under increased axial loading, the lead will impose a direct axial load on the inner shell. Once friction is overcome, the lead will become supported at its base (the bottom of the lead column) and will grow radially outward due to the "Poisson effect" under increased axial loading. This radial growth will tend to relieve the initial fabrication hoop stress as the lead separates from the inner shell. If sufficient axial load develops, the lead would grow out to the outer shell creating tensile hoop stresses therein, and under further loading would eventually flow back inward into the inner shell, thereby developing compressive hoop stresses in the inner shell.

From Appendix 2.10.8, *Fabrication Stresses Due to Lead Pour*, the hoop stress in the inner shell due to fabrication is -1,413 psi at 70 ºF, and -1,821 psi at -20 ºF. Extrapolating, the hoop stress in the inner shell is -1,038 psi at 160 ºF. (Note that the outer shell hoop stress is considered to be negligible since the lead separates from the outer shell upon cooling.)

The equivalent pressure at the lead/inner shell interface, p, is:

$$p = \frac{\sigma t}{r}$$

where the shell thickness, t = 1.00 inch, and the shell radius, r = 16.69 inches. Therefore, the interface pressure is 62.2 psi at 160 ºF, 84.7 psi at 70 ºF, and 109.1 psi at -20 ºF.

With a coefficient of friction, *f*, for lead on stainless steel assumed to fall in the 0.5 to 1.0 range[9], the load, P, which can be supported by friction at the lead/inner shell interface, may be determined as follows:

$$P = \pi D L p f$$

where inner shell outside diameter, D = 34.38 inches, the lead column height, L = 123.5 inches, the interface pressure is p, and the coefficient of friction, $f = 0.5 – 1.0$.

Applying the above interface pressures, the total axial load that may be supported for each case is provided in Table 2.6-11.

With the total lead weight equal to 10,739 pounds, per Table 2.2-1 in Section 2.2, *Weights and Centers of Gravity*, the minimum *g*-load that can be supported by friction is 414,842/10,739 = 38.6*g*. This minimum *g*-load is based on the total lead weight that can be supported with the

[9] Theodore Baumeister, *Mark's Standard Handbook for Mechanical Engineers*, Ninth Edition, McGraw-Hill Book Company, New York, NY, 1987, Table 3.2.1.

package at an assumed (conservatively high) maximum NCT temperature of 160 ºF. At -20 ºF, the minimum *g*-load is 727,641/10,739 = 67.8*g*. Since this *g*-load exceeds the maximum NCT end drop of 42.5*g* at -20 ºF, the lead will not slip under the cold end drop condition. Axial stress in the inner shell is, therefore, governed by the cold case and is determined, with reference to Table 2.2-1 and Figure 2.6-3(a), as follows:

$$w_1 = \eta W_1 = 264{,}095 \text{ lb}$$

$$w_2 = \eta W_2 = 305{,}915 \text{ lb}$$

$$w_3 = \eta W_3 = 156{,}740 \text{ lb}$$

$$w_L = \eta W_L = 456{,}408 \text{ lb}$$

$$w_4 = \eta W_4 = 510{,}978 \text{ lb}$$

$$q_2 = \frac{w_4}{A_4} = 620.5 \text{ lb/in}^2$$

$$q_1 = \frac{w_1 + w_2 + w_3 + w_L + w_4}{A_5} = 1{,}246.4 \text{ lb/in}^2$$

where the impact acceleration, $\eta = 42.5g$, the weight of the top impact limiter, OC lid, and OC flange, W_1 = 6,214 pounds, the weight of the OC outer shell and thermal shield, W_2 = 7,198 pounds, the weight of the package inner shell, W_3 = 3,688 pounds, the weight of the lead, W_L = 10,739 pounds, the weight of the loaded payload canister and IV, W_4 = 12,023 pounds, the area of the OC bottom, $A_4 = \pi R_i^2 = 823.5$ in^2, the radius of the OC bottom (inside), R_i = 16.19 inches, the weight of the loaded payload canister and IV, $A_5 = \pi R_o^2 = 1{,}359.2$ in^2, and the radius of the OC bottom (outside), R_o = 20.8 inches.

Free-body diagrams of the OC shells and end plate are illustrated in Figure 2.6-3(b).

The reaction forces R_1 and R_2 can be calculated by distributing W_1 to the inner and outer shells based on their relative stiffnesses. The stiffnesses of the shells are directly dependant on their cross-sectional areas. Therefore, R_1 and R_2 are calculated as follows:

$$R_1 = W_1\left(\frac{A_3}{A_2 + A_3}\right) = 94{,}972 \text{ lb}$$

$$R_2 = W_1\left(\frac{A_2}{A_2 + A_3}\right) = 169{,}123 \text{ lb}$$

where the cross-sectional area of the inner shell, $A_3 = \pi(R_{io}^2 - R_{ii}^2) = 104.87$ in^2, the inner shell outer radius, R_{io} = 17.19 inches, the inner shell inner radius, R_{ii} = 16.19 inches, the cross-sectional area of the outer shell, $A_2 = \pi(R_{oo}^2 - R_{oi}^2) = 186.75$ in^2, the outer shell outer radius, R_{oo} = 20.565 inches, and the outer shell inner radius, R_{oi} = 19.065 inches.

Assuming reaction R_3 does not affect the deflection of the bottom-end plate (conservative for the maximum R_3), the differential deflection may be calculated. As shown in Figure 2.6-4, utilizing Table 24, Case 10a, of Roark[3], assuming a simply supported circular plate with a uniform load, the differential deflection, $\delta_1 - \delta_2$, may be determined as follows:

$$\delta_1 - \delta_2 = y_c + \frac{M_c r^2}{2D(1+\mu)} - \frac{qr^4 G_{11}}{D} = \frac{128{,}863}{E} \text{ in}$$

given:

$$y_c = \frac{qa^4(5+\mu)}{64D(1+\mu)} = \frac{536{,}965}{E} \text{ in}$$

$$M_c = \frac{qa^2(3+\mu)}{16} = 50{,}686 \text{ in-lb/in}$$

$$D = \frac{Et^3}{12(1-\mu^2)} = (11.4469)E \text{ in-lb}$$

$$G_{11} = \frac{1}{64}\left\{1 + 4\left(\frac{r_o}{r}\right)^2 - 5\left(\frac{r_o}{r}\right)^4 - 4\left(\frac{r_o}{r}\right)^2\left[2 + \left(\frac{r_o}{r}\right)^2\right]\ln\left(\frac{r}{r_o}\right)\right\}\langle r - r_o\rangle^0 = \frac{1}{64}$$

where the net pressure, $q = -(q_1 - q_2) = -(1{,}264.4 - 620.5) = 625.9$ lb/in^2, the outside plate/pressure radius, $a = 19.815$ inches, the mean inner shell radius, $r = 16.69$ inches, the inner pressure radius, $r_o = 0.0$ inches, the bottom-end plate thickness, $t = 5.0$ inches, and Poisson's ratio, $\mu = 0.3$.

Also, from the free-body diagrams of the OC inner and outer shells (see in Figure 2.6-3(b)), and axial stiffness relations for the shells ($\delta = PL/AE$ for an end load, and $\delta = PL/2AE$ for self-weight, i.e., a uniformly distributed load), the deflections, δ_1 and δ_2, and reactions, R_3 and R_4, may be found:

$$\delta_1 = \frac{(R_3 - R_1)L}{A_3 E} - \frac{(w_3 - w_L)L}{2A_3 E}$$

$$\delta_2 = \frac{(R_4 - R_2)L}{A_2 E} - \frac{w_2 L}{2A_2 E}$$

where the shell length, $L = 124.65$ inches and, as before, the cross-sectional area of the inner shell, $A_3 = 104.87$ in^2, and the cross-sectional area of the outer shell, $A_2 = 186.75$ in^2. Substituting values:

$$\delta_1 = R_3\left(\frac{1.1886}{E}\right) - \frac{477{,}278}{E}$$

$$\delta_2 = R_4\left(\frac{0.6675}{E}\right) - \frac{214{,}989}{E}$$

Summing vertical forces:

$$R_3 + R_4 = w_1 + w_2 + w_3 + w_L = 1{,}183{,}158 \text{ lb}$$

Solving the above equations simultaneously yields the following:

$$R_3 = \frac{\frac{128{,}863}{E} + \frac{477{,}278}{E} - \frac{214{,}989}{E} + (1{,}183{,}158)\left(\frac{0.6675}{E}\right)}{\frac{1.1886}{E} + \frac{0.6675}{E}} = 636{,}232 \text{ lb}$$

$$R_4 = 1{,}183{,}158 - 636{,}232 = 546{,}926 \text{ lb}$$

Therefore, the axial compressive stress in the OC inner shell, σ_3, and outer shell, σ_2, is:

$$\sigma_3 = -\frac{R_3}{A_3} = -6{,}067 \text{ psi}$$

$$\sigma_2 = -\frac{R_4}{A_2} = -2{,}929 \text{ psi}$$

where, as before, the cross-sectional area of the inner shell, $A_3 = 104.87$ in^2, and the cross-sectional area of the outer shell, $A_2 = 186.75$ in^2.

It has been shown above, based upon the stated assumptions, that the elastic modulus, E, is independent of the axial stresses calculated. Therefore, the shell stresses are summarized, with reference to Appendix 2.10.8, *Fabrication Stresses Due to Lead Pour*, for hoop stresses, as given in Table 2.6-12.

Table 2.6-13, Table 2.6-14, and Table 2.6-15 present the corresponding margins of safety for the more critical inner shell. Zero internal pressure is used in order to maximize compressive stresses in the inner shell. Note that axial stresses will actually decrease with increasing drop temperature since *g*-loads are lower at higher temperatures (due to decreased foam strength with increased temperature); this effect is conservatively ignored in Table 2.6-13, Table 2.6-14, and Table 2.6-15.

Buckling is addressed in Appendix 2.10.5, *Buckling Design Criteria and Detailed Evaluation*.

(7) Stresses in the OC Shells and Lead (Zero Fabrication Stress Condition Assumed)

The second initial lead condition assumes the fabrication stress has fully crept away, resulting in a stress-free column of lead just in contact with the inner and outer shells. This is potential worst-case since any axial load imposed on the lead will directly load in the radial direction both the inner and outer shells (i.e., the lead need not flow away from the inner shell, into the outer shell, and back into the inner shell to develop a compressive hoop stress in the inner shell).

For this condition, initial stresses in the lead and the steel shells are taken as zero. As an axial load is applied to the lead and the shells, the lead will attempt to move downward and outward, and develop pressures on both the inner and outer shells, as shown in Figure 2.6-5.

For the purpose of this analysis, let $p_i = p_o = p$. This assumption is considered reasonable once lead starts to flow.

Conservatively assuming that the lead receives no axial support at its base, but rather is supported solely by friction at the inner and outer shells, the maximum value of the pressure, p_{max}, is determined based on a lead weight, $W_L = 10{,}739$ pounds, being acted on by an end drop acceleration, $\eta = 42.5g$, resulting in a total lead force, w_L, of:

$$w_L = \eta W_L = 456{,}408 \text{ lb}$$

For the maximum pressure, p_{max}, use the minimum expected coefficient of friction, $f = 0.5$, resulting in a force, w, of:

$$w = p_{max}(2\pi r_L)(L - d)\,f$$

where the mean lead shell radius, $r_L = \frac{1}{2}(r_o^2 + r_i^2) = 18.1275$ inches, the lead shell outer radius, $r_o = 19.065$ inches, the lead shell inner radius, $r_i = 17.19$ inches, and the shell length, L = 123.5 inches. Letting $w = w_L = 456{,}408$ pounds, the maximum pressure, p_{max}, is:

$$p_{max} = \frac{8{,}014}{(123.5 - d)} \text{ psi}$$

Assuming lead flow initiates at the yield strength of the lead, σ_y, the height of the lead column, d, required to yield the lead cross-section due to the 42.5*g* NCT acceleration is:

$$\sigma_y = \rho d(42.5g)$$

where σ_y is lead's yield strength at temperature, and the lead density, $\rho = 0.41$ lb/in^3. Therefore:

$$d = (0.05739)\sigma_y$$

For lead temperatures of 160 ºF, 70 ºF, and -20 ºF, and conservatively estimating an upper bound on the lead properties delineated in Figure 2.3-3 through Figure 2.3-6 of Section 2.3, *Mechanical Properties of Materials*, the pressures and hoop stresses may be summarized as shown in Table 2.6-16.

The maximum axial stress in the shells is determined using the same approach as developed in the preceding calculations in Paragraph (6) of Section 2.6.7.1, *Flat End Drop*, except that one-half of the lead weight is considered to act on each shell rather than all lead weight being carried on the inner shell. Again, no support is considered at the base of the lead.

Repeating the previous calculational approach:

$$\delta_1 - \delta_2 = \frac{128{,}863}{E} \text{ in}$$

$$\delta_1 = \frac{(R_3 - R_1)L}{A_3 E} - \frac{\left(w_3 + \frac{w_L}{2}\right)L}{2A_3 E} = R_3\left(\frac{1.1886}{E}\right) - \frac{228{,}775}{E}$$

$$\delta_2 = \frac{(R_4 - R_2)L}{A_2 E} - \frac{\left(w_2 + \frac{w_L}{2}\right)L}{2A_2 E} = R_4\left(\frac{0.6675}{E}\right) - \frac{178{,}254}{E}$$

where the shell length, L = 124.65 inches and, as before, the cross-sectional area of the inner shell, $A_3 = 104.87$ in^2, and the cross-sectional area of the outer shell, $A_2 = 186.75$ in^2.

Summing vertical forces as before:

$$R_3 + R_4 = w_1 + w_2 + w_3 + w_L = 1{,}183{,}158 \text{ lb}$$

Solving the above equations simultaneously yields the following:

$$R_3 = \frac{\frac{128{,}863}{E} + \frac{228{,}775}{E} - \frac{178{,}254}{E} + (1{,}183{,}158)\left(\frac{0.6675}{E}\right)}{\frac{1.1886}{E} + \frac{0.6675}{E}} = 523{,}218 \text{ lb}$$

$$R_4 = 1{,}183{,}158 - 523{,}218 = 662{,}940 \text{ lb}$$

Therefore, the axial compressive stress in the OC inner shell, σ_3, and outer shell, σ_2, is:

$$\sigma_3 = -\frac{R_3}{A_3} = -4{,}989 \text{ psi}$$

$$\sigma_2 = -\frac{R_4}{A_2} = -3{,}550 \text{ psi}$$

It has been shown above, based upon the stated assumptions, that the elastic modulus, E, is independent of the axial stresses calculated. Therefore, the shell stresses are summarized at temperatures of 160 ºF, 70 ºF, and -20 ºF for a NCT drop load of 42.5*g* in Table 2.6-17.

Table 2.6-18, Table 2.6-19, and Table 2.6-20 present the corresponding margins of safety for the more critical inner shell. Zero internal pressure is used in order to maximize compressive stresses in the inner shell. Again, it is noted that the margins presented for the 70 ºF and 160 ºF cases are conservative in that at these temperatures, *g*-loads will actually be less than the 42.5*g* considered herein.

Buckling is addressed in Appendix 2.10.5, *Buckling Design Criteria and Detailed Evaluation*.

(8) Discussion of Payload Canister Behavior in End Drop

Hoop and axial stresses in the canister are addressed for the one-foot NCT end drop condition. Hoop stress in the canister is maximized by assuming a water-filled canister. The maximum axial stress, σ_a, in the canister shell for a 1*g* load is defined as:

$$\sigma_a = \frac{P}{A} = 87.14 \text{ psi}$$

where the worst-case weight of an empty canister, the fixed-lid version, P = 1,762 pounds, the canister cross-sectional shell area, $A = \pi(r_o^2 - r_i^2) = 20.22$ in^2, and the canister shell's outer and inner radii, $r_o = 13.00$ inches and $r_i = 12.75$ inches, respectively.

For the 42.5*g* end drop load, the axial shell stress, σ_a, is:

$$\sigma_a = (87.14)(42.5) = 3{,}703 \text{ psi (compression)}$$

The canister shell hoop stress, σ_h, is defined as:

$$\sigma_h = \frac{pr}{t} = 225.1 \text{ psi}$$

where the hydrostatic pressure, $p = \gamma h = (0.0361)(121) = 4.37$ psi, the density of water, $\gamma = 0.0361$ lb/in^3, the canister height, h = 121 inches, the mean canister radius, r = 12.875 inches, and the canister shell thickness, t = 0.25 inches.

For the 42.5*g* end drop load, the hoop shell stress, σ_h, is:

$$\sigma_h = (225.1)(42.5) = 9{,}567 \text{ psi (tension)}$$

The maximum canister shell stress intensity (SI) is therefore, 3,703 + 9,567 = 13,270 psi. From Table 2.6-1, the NCT allowable primary membrane stress intensity, S_a = 21,100 psi at 210 ºF for worst-case Type 304L stainless steel as the material of construction. The margin of safety (MS) for the canister shell is then:

$$MS = \frac{S_a}{SI} - 1 = \frac{21{,}100}{13{,}270} - 1 = +0.59$$

(9) Lead Slump

Lead slump for the RH-TRU 72-B package is negligible. The lack of slump is directly attributable to the presence of relatively "soft" impact limiters at the ends of the RH-TRU 72-B package. Because of these "soft" limiters, it can be shown that the resultant accelerations associated with free end drops of the package are insufficient for the stress in the lead to reach its minimum flow stress magnitude as established in the *Cask Designers Guide*.[10] As such, direct use of the *Cask Designers Guide* formula for lead slump would be overly conservative for the case of the RH-TRU 72-B package because the formula is specifically based on the drop of a bare, unprotected package. However, as shown below, the concept of a lead flow stress, as used in the lead slump formula, can be utilized to establish that no lead slump will occur for the RH-TRU 72-B package.

Unless and until the minimum flow stress for lead is reached at the bottom of the lead column, no significant lead flow or slumping can occur. The *Cask Designers Guide* identifies lead flow stress as generally falling between 5,000 and 10,000 psi. Thus, if 5,000 psi is not reached at the bottom of the lead column, no lead slump would be expected.

For example, using the maximum Normal Condition of Transport (NCT) end drop impact acceleration, g = 42.5, applicable to the RH-TRU 72-B as available from Table 2.10.3-10, maximum stress at the bottom end of the lead column, σ, can be readily determined from the following formula where ρ = density of lead = 0.41 lb/in^3 (Table 2.3-2 note 6) and h = lead column height = 124.25 inches per the SAR drawings.

$$\sigma = \rho(g)(h) = 0.41(42.5)(124.25) = 2{,}165 \text{ psi}$$

Missing from the above calculation is a consideration of the potential affect of temperature on lead slump. Although it is not overtly stated in the *Cask Designers Guide*, it is reasonably assumed that the 5,000 psi minimum lead flow stress value corresponds to room temperature, or 70 ºF. It is further assumed that flow stress magnitude will vary with temperature in a manner similar to how lead compressive strength varies with temperature. With reference to Figure 2.3-6, by linearly extrapolating and interpolating the 100 ºF and 175 ºF curves at 4% strain, it can be shown that at -20 ºF, lead strength is approximately 27% greater than at 70 ºF and, at 160 ºF (upper bound NCT temperature for lead per Section 2.6.1.1), lead strength is approximately 27% less than at 70 ºF. Applying these adjustments to the room temperature lead flow stress of 5,000 psi results in flow stresses of 6,350 psi at -20 ºF and 3,650 psi at 160 ºF. Table 2.6-21

[10] L. B. Shappert, *Cask Designers Guide, A Guide for the Design, Fabrication, and Operation of Shipping Casks for Nuclear Applications*, ORNL-NSIC-68, Oak Ridge National Laboratory, Oak Ridge, Tennessee, February 1970.

establishes NCT end drop lead stresses at these minimum and maximum temperature extremes. As shown, at both extremes, lead stresses remain well below the temperature-adjusted flow stress magnitudes. Table 2.6-21 establishes the primary basis for why lead slump will not occur for the RH-TRU 72-B package.

As additional validation of the conclusion that lead slump will not occur for the RH-TRU 72-B package, reference is made to the NuPac 125-B cask[8] (NRC Certificate of Compliance 71-9200). By comparison, the RH-TRU 72-B package provides a more restrictive structure to lead slump. Comparatively, the RH-TRU 72-B package has thicker containment shells and thinner lead than the scaled NuPac 125-B cask. Similar methods of fabrication are also used for both packages. It can therefore be assumed that lead slump for the RH-TRU 72-B package will be bounded by the magnitude of lead slump for the NuPac 125-B cask. The quarter-scale end drop test of the NuPac 125-B cask resulted in no measurable lead slump due to a 30-foot drop. It can then be concluded that no lead slump will occur during the much less critical one-foot end drop for the RH-TRU 72-B package.

2.6.7.2 Corner and Oblique Drops

Analysis of RH-TRU 72-B package behavior during the corner drop event, including oblique drop orientations, is performed in the following steps:

(1) Determine the force-deflection relations for a range of initial impact angles, using the CASKDROP computer program. Utilize the force-deflection data from CASKDROP as input to the computer program SLAPDOWN to determine the package response for various initial impact angles.

(2) Based on the accelerations and rotations predicted in (1), determine the equivalent "static" forces on the OC and IV, considered as a rigid body with distributed and lumped masses.

(3) Based on the loads from (2), analyze the OC shells and IV as simple beams, finding the internal forces: shear, moment, and thrust. Compute stresses for the maximum value of each of these forces, and by inspection of the relative magnitudes of these maximum component stresses, select load cases for further analysis which will have the maximum combined stresses.

(4) Analyze the OC shells for stress, assuming the two shells act as parallel beams, under the loads determined in (3).

(5) Analyze the IV for stress under the loads determined in (3).

(6) Analyze the payload canister for stress under the loads determined in (3).

(7) Analyze impact limiter attachment forces.

(8) Based on the forces from (7), calculate the impact limiter attachment stresses.

(9) Analyze the stresses in the OC and IV lid bolts.

(10) Calculate the maximum impact limiter deformations and residual clearances for package hard spots.

Material properties and allowable stresses corresponding to the maximum enveloping temperature of 160 ºF for the Type 304 stainless steel OC and IV and lead are given in Table 2.6-1. Buckling is addressed in Appendix 2.10.5, *Buckling Design Criteria and Detailed Evaluation*.

(1) Corner Drop Computer Analysis (CASKDROP and SLAPDOWN)

Analytic predictions of package performance for drop orientations impacting upon the corner of the package employ two computer programs: CASKDROP and SLAPDOWN, documented in Appendix 2.10.2, *Drop Analysis Codes Description*. CASKDROP uses an energy-balance technique to determine loads and deformations of the impact limiter. Since CASKDROP assumes all drop energy is absorbed in deformation of the impact limiter, it provides valid results when the impact orientation places the center-of-gravity (CG) directly over the impacted corner, approximately 68º from the horizontal for the RH-TRU 72-B package. At other impact orientations, the force-deflection values generated by CASKDROP are used in SLAPDOWN, a dynamic analysis program that considers rotational motion effects. For initial impact angles between the CG-over-corner and vertical, dynamic effects (such as a secondary slapdown) are negligible, and results at the upper, or secondary impact limiter are unimportant. For such cases, CASKDROP is used to conservatively calculate the primary impact results.

Two (2) cases were run which accounted for variations in foam strength due to temperature effects and the possible variations in foam strength from nominal values (see Section 2.3, *Mechanical Properties of Materials*). Detailed output for each of the two analysis cases is presented in Appendix 2.10.3, *Drop Impact Evaluation Results*. Note that the load and stress evaluations presented in this section are typically based on the results from the -20 ºF foam stress case. Impact limiter responses (i.e., attachment forces, deformations, and residual clearances) presented herein directly consider both analytic cases.

(2) Equivalent "Static" Loads:

The OC and IV are treated as rigid bodies under longitudinal, transverse and angular accelerations, along with an angular velocity. The two bodies are assumed to move together, and the forces between them, needed to make them do so, are found. The centers of gravity of the two bodies are assumed to be coincident.

Slapdown impacts are not governing, as shown in Appendix 2.10.4, *Slapdown Assessment*. The only potentially serious slapdown loading problem will affect package impact limiter attachment fastener and OC lid fastener integrity. These load cases are addressed in Paragraphs (7) and (9), below.

(3) Internal Forces

The OC shells are analyzed as if they are two beams acting in parallel. The payload canister is analyzed as one beam attached to the IV at the two spacer disk locations, and the IV connects to the OC via a series of interface (gap) elements. A schematic representation of the finite element analysis model used is presented as Figure 2.10.1-9 in Appendix 2.10.1.4, *Containment Assembly Analysis for Oblique Drops*.

Maximum stresses are given as functions of impact angle for the cold foam (-20 ºF) conditions in Figure 2.6-6, Figure 2.6-7, and Figure 2.6-8 for the OC, IV, and payload canister, respectively, based on maximum thrust, shear, and bending moment given in Figure 2.6-9, Figure 2.6-10, and Figure 2.6-11, respectively. The stresses shown in Figure 2.6-6, Figure 2.6-7, and Figure 2.6-8 were calculated using slightly different *g*-loadings than those found in Appendix 2.10.3, *Drop Impact Evaluation Results*. A comparison of the *g*-loading from Appendix 2.10.3, *Drop Impact Evaluation Results* for the NCT cold free drop and those data used in calculating the peak stresses is presented in Figure 2.6-12. Since the *g*-loads match closely for all the orientations

considered here, scaling of the previously calculated stresses is an appropriate method for evaluating package components.

In a similar manner, the values from Figure 2.6-13, Figure 2.6-14, and Figure 2.6-15, showing the maximum stresses for the OC, IV, and payload canister, respectively, for hot foam (140 ºF) conditions are also scaled accordingly, based on maximum thrust, shear, and bending moment given in Figure 2.6-16, Figure 2.6-17, and Figure 2.6-18.

The stresses are computed as follows:

$$S_t = \frac{P}{A} \times \frac{g_{new}}{g_{old}} = \text{stress due to thrust, psi}$$

$$S_v = \frac{V}{A} \times \frac{g_{new}}{g_{old}} = \text{stress due to shear, psi}$$

$$S_m = \frac{Mc}{I} \times \frac{g_{new}}{g_{old}} = \text{stress due to bending moment, psi}$$

where P is the thrust force (lb), V is the shear force (lb), and M is the bending moment (in-lb). The distance to the neutral axis, c = 20.565 inches for the OC outer shell, c = 17.19 inches for the OC inner shell, c = 16.00 inches for the IV shell, and c = 13.00 inches for the payload canister. The moment of intertia, I = 51,334 in^4 for the OC, I = 4,718 in^4 for the IV, and I = 1,676 in^4 for the payload canister. Finally, the area, A = 292 in^2 for the OC, A = 38 in^2 for the IV, and A = 20 in^2 for the payload canister.

From Figure 2.6-6, it can be deduced that an 85º impact angle with cold foam (-20 ºF), yields the worst stresses for the OC. Similarly, from Figure 2.6-7 and Figure 2.6-8, it can be deduced that an 85º impact angle with cold foam also yields the worst stresses for the IV and payload canister.

Although the maximum thrust, shear, and bending moment do not occur at the same location for each component, the true maximums are used to provide a conservative analysis. The figures are based on a *g*-load of 15.7*g*, whereas the impact of an 85º angle is 17.9*g*. The scale factor is therefore 17.9/15.7 = 1.14.

For the OC, these maximums are P_{max} = 444,680 × 1.14 = 506,935 pounds, V_{max} = 155,730 × 1.14 = 177,532 pounds, and M_{max} = 12,754,000 × 1.14 = 14,539,560 in-lb. For the IV, the maximums are P_{max} = 57,278 × 1.14 = 65,297 pounds, V_{max} = 69,976 × 1.14 = 79,773 pounds, and M_{max} = 923,570 × 1.14 = 1,052,870 in-lb. Finally, for the payload canister, the maximums are P_{max} = 125,100 × 1.14 = 142,614 pounds, V_{max} = 7,956 × 1.14 = 9,070 pounds, and M_{max} = 106,350 × 1.14 = 121,239 in-lb.

(4) OC Stresses

The maximum membrane stress in the OC inner shell, for the load case selected in Paragraph (3), is:

$$S_m = \frac{Mc}{I} + \frac{P}{A} = \frac{(14{,}539{,}560)[17.19 - (½)(1.0)]}{51{,}334} + \frac{506{,}935}{292} = 6{,}463\,\text{psi}$$

The maximum membrane-plus-bending stress in the OC inner shell is:

$$S_{mb} = \frac{Mc}{I} + \frac{P}{A} = \frac{(14{,}539{,}560)(17.19)}{51{,}334} + \frac{506{,}935}{292} = 6{,}605\,\text{psi}$$

Similarly, the maximum stresses in the OC outer shell are:

$$S_m = \frac{Mc}{I} + \frac{P}{A} = \frac{(14{,}539{,}560)\left[20.565 - (½)(1.5)\right]}{51{,}334} + \frac{506{,}935}{292} = 7{,}348\,\text{psi}$$

$$S_{mb} = \frac{Mc}{I} + \frac{P}{A} = \frac{(14{,}539{,}560)(20.565)}{51{,}334} + \frac{506{,}935}{292} = 7{,}561\,\text{psi}$$

In addition, shear stress must be added in the calculation of the membrane stress intensities for the OC inner and outer shells. The shear stress is:

$$S_v = \frac{V}{A} = \frac{177{,}532}{292} = 608\ \text{psi}$$

Axial fabrication stresses used in the oblique drop analyses are scaled from those used in the end drop analysis (see Table 2.6-12 from Section 2.6.7.1, *Flat End Drop*) using the respective *g*-loadings of the package (17.9/42.5). Fabrication stresses for the oblique drop analyses are given in Table 2.6-22.

Table 2.6-23, Table 2.6-24, and Table 2.6-25 present the corresponding margins of safety for the more critical OC inner shell. Zero internal pressure is used in order to maximize compressive stresses in the OC inner shell. Again, note that the margins presented for the 70 ºF and 160 ºF cases are conservative in that at these temperatures, *g*-loads will actually be less than the 17.9*g* conservatively considered herein.

(5) IV Stresses

The maximum membrane stress in the IV shell, for the load case selected in Paragraph (3), is:

$$S_m = \frac{Mc}{I} + \frac{P}{A} = \frac{(1{,}052{,}870)\left[16.00 - (½)(0.38)\right]}{4{,}718} + \frac{65{,}297}{38} = 5{,}247\ \text{psi}$$

The maximum membrane-plus-bending stress in the IV shell is:

$$S_{mb} = \frac{Mc}{I} + \frac{P}{A} = \frac{(1{,}052{,}870)(16.00)}{4{,}718} + \frac{65{,}297}{38} = 5{,}289\ \text{psi}$$

In addition, shear stress must be added in the calculation of the membrane stress intensity for the IV shell. The shear stress is:

$$S_v = \frac{V}{A} = \frac{79{,}773}{38} = 2{,}099\ \text{psi}$$

Table 2.6-26 presents stress and margin of safety results for the IV for the worst-case load combination.

(6) Discussion of Payload Canister Behavior in Oblique Drops

The maximum membrane stress in the payload canister shell, for the load case selected in Paragraph (3), is:

$$S_m = \frac{Mc}{I} + \frac{P}{A} = \frac{(121{,}239)[13.00 - (½)(0.25)]}{1{,}676} + \frac{142{,}614}{20} = 8{,}062 \text{ psi}$$

The maximum membrane-plus-bending stress in the payload canister shell is:

$$S_{mb} = \frac{Mc}{I} + \frac{P}{A} = \frac{(121{,}239)(13.00)}{1{,}676} + \frac{142{,}614}{20} = 8{,}071 \text{ psi}$$

In addition, shear stress must be added in the calculation of the membrane stress intensity for the payload canister shell. The shear stress is:

$$S_v = \frac{V}{A} = \frac{9{,}070}{20} = 454 \text{ psi}$$

Table 2.6-27 presents stress and margin of safety results for the payload canister shell for the worst load combination. The NCT allowable stress, S_a, from Table 2.1-2 in Section 2.1.2.1.2, *Non-Containment Structures*, is the greater of S_m or S_y for primary membrane stress intensity. From Table 2.3-1 in Section 2.3, *Mechanical Properties of Materials*, the allowable stress, S_a = 21,100 psi at 210 ºF is based on S_y using worst-case Type 304L stainless steel as the material of construction (conservative maximum payload canister temperature; see Table 2.6-2). Buckling is addressed in Section 2.1.2.2.3, *Buckling*.

(7) Impact Limiter Attachment Forces

The maximum NCT impact limiter attachment moment, $2.16(10)^6$ in-lb, is given in Table 2.10.3-13 of Appendix 2.10.3, *Drop Impact Evaluation Results*. Six, ASTM A320, Grade L43, 1¼-7UNC bolts (necked down to a 1.0-inch diameter) secure each impact limiter to the package structure. Assuming that tension varies linearly from one side of the package to the other, the moment is resisted by the six bolts as follows:

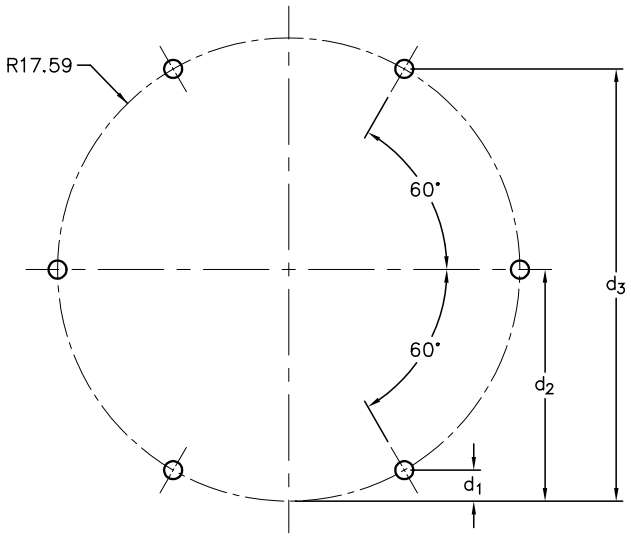

$$M = 2P_{max}\left(\frac{d_1^2 + d_2^2 + d_3^2}{d_3}\right) = (84.8)P_{max}$$

where $d_1 = (17.59)(1 - \sin 60^o) = 2.36$ inches, $d_2 = 17.59$ inches, and $d_3 = (17.59)(1 + \sin 60^o) = 32.82$ inches.

Thus, for a maximum separation moment of $2.16(10)^6$ in-lb, the maximum force in the bolts, P_{max}, is:

$$P_{max} = \frac{M}{84.8} = \frac{2.16(10)^6}{84.8} = 25{,}472 \text{ lb}$$

(8) Impact Limiter Attachment Stresses

The tensile stress area of a 1¼-7UNC bolt of 0.969 in^2 exceeds the cross-sectional area of the 1.0-inch diameter shaft (A = 0.785 in^2). Therefore, maximum impact limiter attachment bolt stress is:

$$S_B = \frac{P_{max}}{A} = \frac{25{,}472}{0.785} = 32{,}448 \text{ psi}$$

From Table 2.6-1, the NCT allowable non-containment fastener primary membrane stress intensity, S_a = 101,400 psi at 160 ºF for ASTM A320, Grade L43, bolting material. Therefore, the impact limiter attachment bolt margin of safety is:

$$MS = \frac{S_a}{S_B} - 1 = \frac{101{,}400}{32{,}448} - 1 = +2.13$$

Bolt engagement is checked by using, from the preceding calculations, the maximum bolt force, P = 25,472 pounds. Per Appendix 1.3.1, *Packaging General Arrangement Drawings*, the minimum engagement length for these fasteners, L = 1.75 inches. The shear area per inch of

engagement for a 1¼-7UNC-2B internal thread, A = 2.9441 in^2/in[11]. The resultant shear stress is therefore:

$$\tau = \frac{P}{LA} = \frac{25{,}472}{(1.75)(2.9441)} = 4{,}944 \text{ psi}$$

From Table 2.6-1, the NCT allowable pure shear stress intensity, S_a = 12,000 psi at 160 ºF, conservatively assuming the threads are Type F304 stainless steel. Therefore, the thread shear margin of safety is:

$$MS = \frac{S_a}{\tau} - 1 = \frac{12{,}000}{4{,}944} - 1 = +1.43$$

Thread insert engagement is checked by using the same maximum force from above, P = 25,472 pounds, to determine the maximum thread insert force. The engagement length for the thread inserts is 1.75 inches. The shear area per inch of engagement for a 1¾-12UN-2B internal thread is 3.9804 in^2/in[11]. The resultant shear stress is therefore:

$$\tau = \frac{P}{LA} = \frac{25{,}472}{(1.75)(3.9804)} = 3{,}657 \text{ psi}$$

From Table 2.6-1, the NCT allowable pure shear stress intensity, S_a = 12,000 psi at 160 ºF, for Type F304 stainless steel. Therefore, the thread shear margin of safety is:

$$MS = \frac{S_a}{\tau} - 1 = \frac{12{,}000}{3{,}657} - 1 = +2.28$$

(9) Stresses in the OC and IV Lid Bolts

Four basic loading mechanisms exist for the OC and IV closure bolts:

- Longitudinal impact forces inducing tensile bolt stresses which attempt to separate the lid from the body (OC or IV),
- Lateral impact forces inducing bolt shear,
- Pressure forces inducing tensile bolt stresses, and
- Bolt preload effects.

Maximum longitudinal impact forces are experienced during vertical or near-vertical impact. These forces are conservatively assessed in Section 2.6.7.1, *Flat End Drop*. In this early analysis, conservatism is assured by neglecting the external energy absorber forces imposed upon the lid that directly react impact associated with bolt tensile stresses. Thus, in this earlier end drop analysis, all impact forces are conservatively reacted by direct uniform bolt tension.

Similarly, maximum lateral impact forces are experienced during side impacts and have been assessed in Section 2.6.7.3, *Flat Side Drop*. In this section, lateral impact forces are assumed to be carried by one or more of three bounding mechanisms. The first and most probable mechanism assumes frictional forces between the lid and body carry all lateral forces. Bolt preloads are shown to be sufficient to assure a positive margin of safety.

[11] *Table Speeds Calculation of Strength of Threads*, Product Engineering, November 27, 1961, pp41-49.

The second lateral force reacting mechanism demonstrates that in the absence of bolt preload forces, all loads are carried in bearing between the stepped lid and the body. Under this mechanism, clearances are such that no lateral loads are imposed via bearing stresses upon the bolts themselves. Specifically, the maximum radial clearance between the OC lid and body is 0.017 inches, and the minimum bolt radial clearance is 0.034 inches. Similarly, the IV lid-to-body gap is 0.011 inches, and the minimum bolt radial clearance is 0.015 inches, precluding the possibility of shear loading the bolts.

In the third and least likely lateral force reacting mechanism, friction force resistance capability is assumed degraded (to zero) by internal pressure effects and all lateral forces are shown to be resisted by bolt shear.

Although the consequences of both maximum lateral and longitudinal impact forces are addressed in the analysis of end and side drops, corner and oblique drops pose a somewhat different set of circumstances. Specifically, friction forces between lid and body, associated with bolt preloads, may not exist (or be sufficient) to carry lateral loads where longitudinal impact forces are sufficiently large as to relieve the normal forces between lid and body. In these circumstances, associated only with corner and oblique loads, lateral forces may be imposed on the bolts. Such circumstances are addressed in analyses discussed below.

(a) Stresses in the OC Lid Bolts

Comprehensive analysis of all oblique orientations is summarized in Table 2.10.6-1 and Table 2.10.6-2 of Appendix 2.10.6, *Closure Bolt Stress Evaluations*. The minimum margin of safety is found at a near-vertical orientation of 85º with respect to horizontal. At this orientation angle, direct tensile stress due to impact, pressure effects, and preload effects is estimated at 55,504 psi. The associated shear stress is 149 psi. From Table 2.6-1, the NCT allowable containment fastener primary membrane stress intensity, S_a = 67,600 psi at 160 ºF for ASTM A320, Grade L43, bolting material. The resultant margin of safety is computed at +0.22.

As described in Appendix 2.10.6, *Closure Bolt Stress Evaluations*, bolt impact stresses are calculated assuming a triangular distribution of bolt forces and external impact forces arbitrarily (and conservatively) applied at the corner of the package. Thus, external energy absorber forces are not employed to reduce bolt tensile forces. For near vertical impacts, this assumption is most conservative.

The margin of safety for bolt engagement need not be calculated since it is greater than for the end drop case possessing a margin of safety of +0.19. An assessment of OC bolt and thread insert engagement is provided in Appendix 2.10.6, *Closure Bolt Stress Evaluations*, and shown to have a minimum margin of safety of +0.13.

(b) Stresses in the IV Lid Bolts

The bolts must resist only preloads, pressure stresses, and lateral forces. No impact forces exist since all axial loads are transmitted directly to the OC lid; both surfaces are flat and parallel.

Comprehensive analysis of all impact orientations is summarized in Table 2.10.6-3 and Table 2.10.6-4 of Appendix 2.10.6, *Closure Bolt Stress Evaluations*. The minimum margin of safety is found at a near-horizontal orientation of 5º with respect to horizontal. This differs from the OC conditions because impact loads are directly transferred to the OC lid (in direct bearing) and do not contribute to bolt stresses. At an angle of 5º, total direct tension, due to pressure and preload

effects, is estimated at 53,737 psi, with an associated shear stress of 2,199 psi. From Table 2.6-1, the NCT allowable containment fastener primary membrane stress intensity, S_a = 67,600 psi at 160 ºF for ASTM A320, Grade L43, bolting material. The resultant margin of safety is computed as +0.25.

Bolt engagement stresses are nearly identical to end impact values since the dominant tensile stress component is due to pressure, which is identical in both analyses. An assessment of IV bolt and thread insert engagement is provided in Appendix 2.10.6, *Closure Bolt Stress Evaluations*, and shown to have a minimum margin of safety of +0.18.

(10) Impact Limiter Deformations and Residual Clearances

Maximum impact limiter deformations and residual clearances due to normal corner/oblique drops are directly available from Figure 2.10.3-3 in Appendix 2.10.3, *Drop Impact Evaluation Results*. Per that section, maximum crush of an impact limiter corner is 9.68 inches for the 140 ºF foam stress case, and occurs for a drop angle of 45º with respect to horizontal. Minimum residual clearance for the main package body is 14.4 inches for the 140 ºF foam stress case, and occurs for a drop angle of 5º with respect to horizontal. These deformations and residual clearances are of little consequence for the RH-TRU 72-B package.

2.6.7.3 Flat Side Drop

Analysis of RH-TRU 72-B package behavior for the side drop event is performed in the following steps:

(1) Analyze the impact force using the CASKDROP computer program.

(2) Based on the accelerations predicted in (1), determine the equivalent "static" forces on the OC and IV, considered as a rigid body with distributed and lumped masses.

(3) Based on the loads from (2), analyze the OC shells and IV as simple beams, finding the internal forces: thrust, shear, and moment. Compute stresses for the maximum value of each of these forces.

(4) Analyze the OC shells for stress, assuming the two shells act as parallel beams, under the loads determined in (3).

(5) Analyze the IV for stress under the loads determined in (3).

(6) Analyze the payload canister for stress under the loads determined in (3).

(7) Analyze the OC lid for bearing against the top OC ring forging, analyze the OC closure bolts, and analyze the top OC ring forging for shear.

(8) Analyze the OC end plate welds for shear.

(9) Analyze the IV lid for bearing against the IV ring forging, analyze the IV closure bolts, and analyze the IV ring forging.

(10) Calculate the maximum impact limiter deformations and residual clearances for package hard spots.

Material properties and allowable stresses corresponding to maximum enveloping temperature of 160 ºF for the Type 304 stainless steel OC and IV are given in Table 2.6-1. Buckling is addressed in Appendix 2.10.5, *Buckling Design Criteria and Detailed Evaluation*.

Where possible, the analyses in this section are performed on the basis of a unit (1*g*) axial acceleration, with actual acceleration numbers being substituted at the final point of calculating stresses.

(1) Side Drop Computer Analysis Using CASKDROP

The side drop analysis was performed utilizing the energy-balance computer program, CASKDROP, documented in Appendix 2.10.2.1, *Description of the CASKDROP Computer Code*. Two cases were run which accounted for variations in foam strength due to temperature effects and the possible variations in foam strength from nominal values (see Section 2.3, *Mechanical Properties of Materials*). Each of these two cases consists of two different loading studies for a total of four different cases. The two different loading cases are as follows: (1) distributed payload within the canister, and (2) concentrated payload and canister weight at either of the IV spacer disk supports.

The drop cases consider the impact limiter as fully effective, as defined in Appendix 2.10.3, *Drop Impact Evaluation Results*. Worst-case deflections and accelerations obtained from the bounding cases are utilized for all analyses. The maximum resultant acceleration for the NCT side drop is 19.3*g* for cold (-20 ºF) foam per Table 2.10.3-10, and the maximum impact limiter deflection is 2.12 inches for warm (140 ºF) foam per Table 2.10.3-5 of Appendix 2.10.3, *Drop Impact Evaluation Results*.

(2) Equivalent "Static" Loads

The OC and IV are treated as rigid bodies under transverse acceleration. The two bodies are assumed to move together, and the forces between them needed to make them do so, is found. The centers of gravity of the two bodies are assumed to be coincident.

(3) Internal Forces

The OC shells are analyzed as if they are two beams acting in parallel. The payload canister is analyzed as one beam attached to the IV at the two spacer disk locations, and the IV connects to the OC via a series of interface (gap) elements. A schematic representation of the finite element analysis model used is presented as Figure 2.10.1-9 in Appendix 2.10.1.4, *Containment Assembly Analysis for Oblique Drops*.

Worst-case loading conditions on the OC and IV are found to occur under the following combinations of temperature and payload distribution: cold (-20 ºF) foam with a distributed payload for the OC, and cold (-20 ºF) foam with a concentrated payload for the IV.

Shear and moment diagrams for cold (-20 ºF) foam with a distributed payload are shown in Figure 2.6-19 and Figure 2.6-20, and with a concentrated payload in Figure 2.6-21 and Figure 2.6-22 with each component on the same figure. As discussed in Section 2.6.7.2, *Corner and Oblique Drops*, the figures were created using slightly different impact *g*-loadings than given in Appendix 2.10.3, *Drop Impact Evaluation Results*. The difference, however, is small. The figures were created using a side drop g load of 20.3*g*, which is comparable to the actual side drop *g*-load of 19.3*g*. Therefore, scaling of the shear and moments is appropriate. Similarly, the

shear and moment diagrams for hot (140 ºF) foam with a distributed payload, shown in Figure 2.6-23 and Figure 2.6-24, and with a concentrated payload in Figure 2.6-25 and Figure 2.6-26, are scaled accordingly.

As previously discussed, the cold foam yields the worst stresses. The OC experiences worst-case stresses under a distributed payload, while the IV experiences its worst stresses due to a concentrated payload/canister force. The canister stresses are calculated for the distributed payload case and included only for the sake of consistency with other sections herein. Although the maximum shear and moment do not occur at the same location for each component, the maximums will be used to determine combined stresses, since this approach provides a conservative analysis. The figures are based on a *g*-load of 20.3*g*, whereas the actual side drop impact is 19.3*g*. The scale factor is therefore 19.3/20.3 = 0.951.

The maximum shear, V_{max}, and moment, M_{max}, for the OC are:

$$V_{max} = (385{,}325)(0.951) = 366{,}444 \text{ lb}$$

$$M_{max} = (12{,}551{,}000)(0.951) = 11{,}936{,}000 \text{ in-lb}$$

The maximum shear, V_{max}, and moment, M_{max}, for the IV are:

$$V_{max} = (88{,}456)(0.951) = 84{,}122 \text{ lb}$$

$$M_{max} = (1{,}462{,}600)(0.951) = 1{,}390{,}930 \text{ in-lb}$$

The maximum shear, V_{max}, and moment, M_{max}, for the payload canister, with only the distributed payload considered, are:

$$V_{max} = (50{,}084)(0.951) = 47{,}630 \text{ lb}$$

$$M_{max} = (547{,}920)(0.951) = 521{,}072 \text{ in-lb}$$

Maximum stresses can be calculated from the maximum shear and moments (given above) as follows:

$$S_v = \frac{V}{A} = \text{stress due to shear, psi}$$

$$S_m = \frac{Mc}{I} = \text{stress due to bending moment, psi}$$

where V is the shear force (lb) and M is the bending moment (in-lb). The distance to the neutral axis, c = 20.565 inches for the OC outer shell, c = 17.19 inches for the OC inner shell, c = 16.00 inches for the IV shell, and c = 13.00 inches for the payload canister. The moment of intertia, I = 51,334 in^4 for the OC, I = 4,718 in^4 for the IV, and I = 1,676 in^4 for the payload canister. Finally, the area, A = 292 in^2 for the OC, A = 38 in^2 for the IV, and A = 20 in^2 for the payload canister.

(4) OC Stresses

The maximum membrane stress in the OC inner shell, for the load case selected in Paragraph (3), is:

$$S_m = \frac{Mc}{I} = \frac{(11{,}936{,}000)\left[17.19 - (½)(1.0)\right]}{51{,}334} = 3{,}881 \text{ psi}$$

The maximum membrane-plus-bending stress in the OC inner shell is:

$$S_{mb} = \frac{Mc}{I} = \frac{(11{,}936{,}000)(17.19)}{51{,}334} = 3{,}997 \text{ psi}$$

Similarly, the maximum stresses in the OC outer shell are:

$$S_m = \frac{Mc}{I} = \frac{(11{,}936{,}000)[20.565 - (½)(1.5)]}{51{,}334} = 4{,}607 \text{ psi}$$

$$S_{mb} = \frac{Mc}{I} = \frac{(11{,}936{,}000)(20.565)}{51{,}334} = 4{,}782 \text{ psi}$$

In addition, shear stress must be added in the calculation of the membrane stress intensities for the OC inner and outer shells. The shear stress is:

$$S_v = \frac{V}{A} = \frac{366{,}444}{292} = 1{,}255 \text{ psi}$$

Hoop fabrication stresses used in the NCT side drop analyses are identical to those used in the end drop analysis (refer to Table 2.6-12 in Section 2.6.7.1, *Flat End Drop*), and axial fabrication stresses are -1,963 psi per Appendix 2.10.8.5, *Axial Stress Evaluation after Cooldown from 620 ºF to -20 ºF*. Fabrication stresses for the side drop analyses are given in Table 2.6-28.

Table 2.6-29, Table 2.6-30, and Table 2.6-31 present the corresponding margins of safety for the more critical OC inner shell. Zero internal pressure is used in order to maximize compressive stresses in the inner shell. Again, it is noted that the margins presented for the 70 ºF and 160 ºF cases are conservative since at these temperatures, *g*-loads will actually be less than the 19.3*g* considered herein.

(5) IV Stresses

The maximum membrane stress in the IV shell, for the load case selected in Paragraph (3), is:

$$S_m = \frac{Mc}{I} = \frac{(1{,}390{,}930)[16.00 - (½)(0.38)]}{4{,}718} = 4{,}661 \text{ psi}$$

The maximum membrane-plus-bending stress in the IV shell is:

$$S_{mb} = \frac{Mc}{I} = \frac{(1{,}390{,}930)(16.00)}{4{,}718} = 4{,}717 \text{ psi}$$

In addition, shear stress must be added in the calculation of the membrane stress intensity for the IV shell. The shear stress is:

$$S_v = \frac{V}{A} = \frac{84{,}122}{38} = 2{,}214 \text{ psi}$$

Table 2.6-32 presents stress and margin of safety results for the IV for the worst-case load combination selected in Paragraph (3).

(6) Discussion of Payload Canister Behavior in Side Drops

The maximum membrane stress in the payload canister shell, for the load case selected in Paragraph (3), is:

$$S_m = \frac{Mc}{I} = \frac{(521{,}072)[13.00 - (½)(0.25)]}{1{,}676} = 4{,}003 \text{ psi}$$

The maximum membrane-plus-bending stress in the payload canister shell is:

$$S_{mb} = \frac{Mc}{I} = \frac{(521{,}072)(13.00)}{1{,}676} = 4{,}042 \text{ psi}$$

In addition, shear stress must be added in the calculation of the membrane stress intensity for the payload canister shell. The shear stress is:

$$S_v = \frac{V}{A} = \frac{47{,}630}{20} = 2{,}382 \text{ psi}$$

Table 2.6-33 presents stress and margin of safety results for the canister shell for the load combination selected in Paragraph (3). Allowable stresses were conservatively determined for 210 ºF material temperature. Buckling is addressed in Section 2.1.2.2.3, *Buckling*.

(7) OC Lid Analysis

Since the clearance between the OC lid and sealing surface is less than the clearance between the bolt and bolt hole, the lid will displace laterally to bear against the sealing surface in the forging before lateral loading of the lid bolts occurs. Therefore, the following analysis addresses the stress resulting from lateral loading of the body ring forging by the lid.

In the most unlikely event that the lid displaces laterally to bear upon the body ring forging, lateral loads will be transferred by bearing. The following calculations demonstrate the adequacy of this load transfer mechanism.

The weight of the OC lid may be carried in bearing against the lid-end OC ring forging if sliding occurs at the lid-to-forging interface. The side drop acceleration of 19.3*g* is utilized in a Hertzian analysis to determine the bearing stress between the two cylinders. Because this analysis is sensitive to very small variations in the diametric gap between the cylinders, the worst-case tolerance stackup has been factored into the following calculation using Table 33, Case 2c, from Roark and Young[12], assuming the elastic modulus, E, and Poisson's ratio, μ, are equal for the mating materials:

$$S_b = 0.591\sqrt{\frac{PE}{LK_D}} = 3{,}903 \text{ psi}$$

where the OC lid weight with 19.3*g*, P = (1,667)(19.3) = 32,173 pounds, the elastic modulus, $E = 27.8(10)^6$ psi at 160 ºF from Table 2.3-1 in Section 2.3, *Mechanical Properties of Materials*, the contact length, L = 0.664 inches (approximately), and the diametral stiffness, K_D, is:

[12] R. J. Roark, W. C. Young, *Formulas for Stress and Strain*, 5th Edition, McGraw-Hill, Inc., New York, NY, 1975.

$$K_D = \frac{D_1 D_2}{D_1 - D_2} = 30{,}886 \text{ in}$$

where the outer cylinder diameter, D_1 = 32.896 inches, and the inner cylinder diameter, D_2 = 32.861 inches.

From Table 2.6-1, the NCT allowable sealing surface bearing stress intensity, S_a = 27,000 psi at 160 ºF for Type F304 stainless steel. Therefore, the bearing stress margin of safety is:

$$MS = \frac{S_a}{S_b} - 1 = \frac{27{,}000}{3{,}903} - 1 = +5.92$$

The lip of the forging that supports the OC lid is loaded in shear by the lid. Conservatively assuming only one-half of the lip is effective in resisting the 19.3*g* load, the shear stress is:

$$S_v = \frac{V}{½\pi(R_o^2 - R_i^2)} = 269 \text{ psi}$$

where the weight of the lid is the shear load with 19.3*g*, V = (1,667)(19.3) = 32,173 pounds, the outside radius of the lip, R_o = 20.81 inches, and the inside radius of the lip, R_i = 18.89 inches.

From Table 2.6-1, the NCT allowable shear stress intensity, S_a = 12,000 psi at 160 ºF for Type F304 stainless steel. Therefore, the shear stress margin of safety is:

$$MS = \frac{S_a}{S_v} - 1 = \frac{12{,}000}{269} - 1 = +43.6$$

(8) Welds Joining the OC Shells to the End Closure Plate

The worst-case shear load at the joints of the OC shells to the end closure plate is taken as the maximum shear load determined from Figure 2.6-19 at the package locations corresponding to the welded joints (0 inches and 120 inches). Therefore, the maximum shear load at the welded joints, V = 353,152 pounds.

Since the welds are full penetration bevel welds, the effective shear area for shells may be found by the following equation (i.e., conservatively use half the total weld area):

$$A_w = \frac{2\pi(R_i t_i + R_o t_o)}{2} = 145.8 \text{ in}^2$$

where the mean OC inner shell radius, R_i = 16.69 inches, the OC inner shell thickness, t_i = 1.00 inches, the mean OC outer shell radius, R_o = 19.81 inches, and the OC outer shell thickness, t_o = 1.50 inches.

The direct shear stress in the OC shells' welds is:

$$\tau_w = \frac{V}{A_w} = 2{,}422 \text{ psi}$$

Table 2.6-34 presents stress and margin of safety results for the OC shells' welds under worst-case load combinations.

(9) IV Lid Analysis

Since the clearance between the lid and sealing surface is less than the clearance between the bolt and bolt hole, the IV lid will displace laterally to bear against the sealing surface in the forging before lateral loading of the bolts. Therefore, the following analysis addresses the stress resulting from lateral loading of the IV body ring forging by the IV lid.

In the most unlikely event that the lid displaces laterally to bear upon the body ring forging, lateral loads will be transferred by bearing. The following calculation demonstrates the adequacy of this load transfer mechanism.

The weight of the IV lid may be carried in bearing against the IV body ring forging if sliding occurs at the lid-to-forging interface.

This analysis accounts for only the uppermost race surface being in contact with the forging for bearing. As with Paragraph (7), the side drop acceleration of 19.3*g* is utilized in a Hertzian analysis to determine the bearing stress between two cylinders for the worst-case tolerance stackup using the following calculation using Table 33, Case 2c, from Roark and Young[12], assuming the elastic modulus, E, and Poisson's ratio, μ, are equal for the mating materials:

$$S_b = 0.591\sqrt{\frac{PE}{LK_D}} = 4{,}657 \text{ psi}$$

where the IV lid weight with 19.3*g*, P = (1,382)(19.3) = 26,673 pounds, the elastic modulus, $E = 27.8(10)^6$ psi at 160 ºF from Table 2.3-1 in Section 2.3, *Mechanical Properties of Materials*, the contact length, L = 0.32 inches (approximately), and the diametral stiffness, K_D, is:

$$K_D = \frac{D_1 D_2}{D_1 - D_2} = 37{,}321 \text{ in}$$

where the outer cylinder diameter, D_1 = 28.006 inches, and the inner cylinder diameter, D_2 = 27.985 inches.

From Table 2.6-1, the NCT allowable sealing surface bearing stress intensity, S_a = 27,000 psi at 160 ºF for Type F304 stainless steel. Therefore, the bearing stress margin of safety is:

$$MS = \frac{S_a}{S_b} - 1 = \frac{27{,}000}{4{,}657} - 1 = +4.80$$

The lip of the forging that supports the IV lid is loaded in shear by the lid. Conservatively assuming only one-half of the lip is effective in resisting the 19.3*g* load, the shear stress is:

$$S_v = \frac{V}{½\pi(R_o^2 - R_i^2)} = 283 \text{ psi}$$

where the weight of the lid is the shear load with 19.3*g*, V = (1,382)(19.3) = 26,673 pounds, the outside radius of the lip, R_o = 16.00 inches, and the inside radius of the lip, R_i = 14.00 inches.

From Table 2.6-1, the NCT allowable shear stress intensity, S_a = 12,000 psi at 160 ºF for Type F304 stainless steel. Therefore, the shear stress margin of safety is:

$$MS = \frac{S_a}{S_v} - 1 = \frac{12{,}000}{283} - 1 = +41.4$$

(10) Impact Limiter Deformations and Residual Clearances

Maximum impact limiter deformations and residual clearances due to NCT side drop are directly available from Appendix 2.10.3, *Drop Impact Evaluation Results*. Per Table 2.10.3-10 in Appendix 2.10.3, *Drop Impact Evaluation Results*, maximum crush of an impact limiter side is 2.12 inches for the 140 ºF foam stress case resulting in a minimum residual clearance for the main package body of 14.88 inches (based on a 16.00 inch nominal radial thickness). These deformations and residual clearances are of little consequence for the RH-TRU 72-B package.

2.6.8 Corner Drop

This test does not apply to the RH-TRU 72-B package since the package weight is in excess of 100 kg (220 pounds) and the materials of construction do not include wood or fiberboard.

2.6.9 Compression

This test does not apply to the RH-TRU 72-B package since the package weight is in excess of 5,000 kg (11,000 pounds).

2.6.10 Penetration

Due to the lack of sensitive external protuberances, the one meter (40-inch) drop of a 13-pound hemispherical headed, 1¼-inch diameter, steel cylinder is of negligible consequence to the RH-TRU 72-B package.

Table 2.6-1 – Summary of NCT Material Properties for Analysis

Material Property	Material Property Value (psi)						Reference
	-40 °F	-20 °F	70 °F	160 °F	200 °F	210 °F	
ASTM A240/A276, Type 304 Stainless Steel							
Elastic Modulus, E ($\times 10^6$)	28.9	28.8	28.3	27.8	27.6	27.5	Table 2.3-1
Design Stress Intensity, S_m	20,000	20,000	20,000	20,000	20,000	20,000	
Yield Strength, S_y	30,000	30,000	30,000	27,000	25,000	24,750	
Ultimate Strength, S_u	75,000	75,000	75,000	72,600	71,000	70,500	
Stress Intensity Allowable for Containment Structures (Table 2.1-1)							
Primary Membrane	20,000	20,000	20,000	20,000	20,000	20,000	
Primary Membrane-Plus-Bending	30,000	30,000	30,000	30,000	30,000	30,000	
ASTM A182/SA182, Type F304, Stainless Steel							
Elastic Modulus, E ($\times 10^6$)	28.9	28.8	28.3	27.8	27.6	27.5	Table 2.3-1
Design Stress Intensity, S_m	20,000	20,000	20,000	20,000	20,000	20,000	
Yield Strength, S_y	30,000	30,000	30,000	27,000	25,000	24,750	
Ultimate Strength, S_u	70,000	70,000	70,000	67,700	66,200	65,700	
Stress Intensity Allowable for Containment Structures (Table 2.1-1)							
Primary Membrane	20,000	20,000	20,000	20,000	20,000	20,000	
Primary Membrane-Plus-Bending	30,000	30,000	30,000	30,000	30,000	30,000	
Pure Shear	12,000	12,000	12,000	12,000	12,000	12,000	
Bearing (Sealing Surfaces)	30,000	30,000	30,000	27,000	25,000	24,750	
Stress Intensity Allowable for Non-Containment Structures (Table 2.1-2)							
Primary Membrane	30,000	30,000	30,000	27,000	25,000	24,750	
Primary Membrane-Plus-Bending	30,000	30,000	30,000	30,000	30,000	30,000	
ASTM A240/A276, Type 304L Stainless Steel							
Elastic Modulus, E ($\times 10^6$)	28.9	28.8	28.3	27.8	27.6	27.5	Table 2.3-1
Design Stress Intensity, S_m	16,700	16,700	16,700	16,700	16,700	16,700	
Yield Strength, S_y	25,000	25,000	25,000	22,800	21,300	21,100	
Ultimate Strength, S_u	70,000	70,000	70,000	67,700	66,200	65,700	
Stress Intensity Allowable for Non-Containment Structures (Table 2.1-2)							
Primary Membrane	25,000	25,000	25,000	22,800	21,300	21,100	
Primary Membrane-Plus-Bending	25,050	25,050	25,050	25,050	25,050	25,050	
ASTM A320, Grade L43, Alloy Steel							
Elastic Modulus, E ($\times 10^6$)	27.8	27.8	27.8	27.3	27.1	27.1	Table 2.3-1
Design Stress Intensity, S_m	35,000	35,000	35,000	33,800	33,000	32,900	
Yield Strength, S_y	105,000	105,000	105,000	101,400	99,000	98,700	
Ultimate Strength, S_u	125,000	125,000	125,000	125,000	125,000	125,000	
Stress Intensity Allowable for Containment Fasteners (Table 2.1-1)							
Primary Membrane	70,000	70,000	70,000	67,600	66,000	65,800	
Primary Membrane-Plus-Bending	105,000	105,000	105,000	101,400	99,000	98,700	
Stress Intensity Allowable for Non-Containment Fasteners (Table 2.1-2)							
Primary Membrane	105,000	105,000	105,000	101,400	99,000	98,700	
Primary Membrane-Plus-Bending	105,000	105,000	105,000	101,400	99,000	98,700	
Lead							
Elastic Modulus, E ($\times 10^6$)	2.44	2.43	2.34	2.22	2.16	2.15	Table 2.3-2

Table 2.6-2 – Maximum NCT Temperatures

Location	Temperature, ºF
	270 Watt Payload
Canister Shell	202
Inner Vessel Shell	158
Outer Cask Inner Shell	150
Outer Cask Lead Shell	150
Outer Cask Outer Shell	150
Thermal Shield	152
Outer Cask Upper Ring Forging	143
Inner Vessel Lid	146
Outer Cask Lid	141
Inner Vessel O ring Seals	146
Outer Cask O ring Seals	141
Impact Limiter Shell	158
Trunnions	150

Table 2.6-3 – Package Parameters for Pressure Stress Calculations

Location	Temperature (ºF)	Radius (in)	Thickness (in)	Diameter (in)	Thickness (in)
P1	160	19.813	1.50	—	—
P2	160	16.69	1.00	—	—
P3	160	15.81	0.375	—	—
P4	160	19.813	1.50	—	—
P5	160	16.69	1.00	—	—
P6	160	15.81	0.375	—	—
P7	160	—	—	41.60	5.00
P8	160	—	—	37.60	6.00
P9	160	—	—	32.00	6.50
P10	160	—	—	32.00	1.50

Table 2.6-4 – Unit Pressure Stress Results for P1 – P6

Location	Temperature (ºF)	λ (in^{-1})	D (lb-in)	V_o (lb-in)	M_o (in-lb/in)	σ_1 (psi)	σ_2 (psi)	σ_1' (psi)	σ_2' (psi)
P1	160	—	—	—	—	6.60	13.21	0.0	0.0
P2	160	—	—	—	—	8.35	16.69	0.0	0.0
P3	160	—	—	—	—	21.08	42.16	0.0	0.0
P4	160	0.2357	$8.592(10)^6$	3.604	7.644	6.60	1.94	-20.43	-6.13
P5	160	0.3146	$2.546(10)^6$	2.701	4.292	8.35	2.44	-25.83	-7.75
P6	160	—	—	—	—	21.67	-37.74	-220.2	-68.66

Table 2.6-5 – Unit Pressure Stress Results for P7 – P10

Location	Temperature (ºF)	M_o (in-lb/in)	σ (psi)
P7	160	89.23	21.42
P8	160	72.90	12.15
P9	160	52.80	7.50
P10	160	52.80	140.80

Table 2.6-6 – Maximum Pressure Stress Results for P1 – P10

Shell / End Plate Location	Axial Membrane σ_1 (psi)	Hoop Membrane σ_2 (psi)	Axial Bending① σ_1' (psi)	Hoop Bending① σ_2' (psi)	Radial Bending σ (psi)
P1	990	1,982	0	0	—
P2	1,252	2,504	0	0	—
P3	3,162	6,324	0	0	—
P4	990	291	-3,064	-920	—
P5	1,252	366	-3,874	-1,162	—
P6	3,251	-5,661	-33,030	-10,299	—
P7	—	—	—	—	3,213
P8	—	—	—	—	1,823
P9	—	—	—	—	1,125
P10	—	—	—	—	21,120

Notes:

① σ_1' and σ_2' are positive when tensile on the shell outside diameter.

Table 2.6-7 – Package Stresses Due to Side Drop

Component	Membrane-Plus-Bending Stress Intensity (psi)
OC Outer Shell	4,782
OC Inner Shell	3,997
IV Shell	4,717

Table 2.6-8 – NCT End Drop, OC Lid Bending

Evaluation Parameters	
Loading Condition:	NCT Flat End Drop, -20 ºF Foam
Structural Material:	ASTM A240, Type F304, Stainless Steel
Stress Condition:	Primary Membrane-Plus-Bending
Structural Criterion:	Containment Boundary
Stress Allowable (from Table 2.1-1):	$1.5S_m$
Material Temperature:	160 ºF
Allowable Stress, S_a:	30,000 psi

Load Condition	Stress Components (psi)				Reference Section
	Radial σ_r	Hoop σ_t	Axial σ_z	Shear τ_{rz}	
Internal Pressure	1,823	0	-150	0	2.6.1.3.2
End Drop	9,180	9,180	0	0	2.6.7.1(2)
Direct Stress Summation	11,003	9,180	-150	0	—
Principal Stresses	11,003	9,180	-150	—	—
Stress Differences	11,153	9,330	1,823	—	—
Maximum Stress Intensity (SI)	11,153	—	—	—	—
Allowable Stress Intensity (S_a)	30,000	—	—	—	—
Margin of Safety ($MS = S_a/SI - 1$)	+1.69	—	—	—	—

Table 2.6-9 – NCT Top-End Drop, IV Shell with 42.5*g* Acceleration

Evaluation Parameters	
Loading Condition:	NCT Flat End Drop, -20 ºF Foam
Structural Material:	ASTM A240, Type 304, Stainless Steel
Stress Condition:	Primary Membrane
Structural Criterion:	Containment Boundary
Stress Allowable (from Table 2.1-1):	S_m
Material Temperature:	160 ºF
Allowable Stress, S_a:	20,000 psi

Load Condition	Stress Components (psi)				Reference Section
	Radial σ_r	Hoop σ_t	Axial σ_z	Shear τ_{rz}	
Internal Pressure	-150	6,324	3,162	0	2.6.1.3.2
End Drop	0	0	-2,323	0	2.6.7.1(5)
Direct Stress Summation	-150	6,324	839	0	—
Principal Stresses	6,324	-150	839	—	—
Stress Differences	5,485	-989	6,474	—	—
Maximum Stress Intensity (SI)	6,474	—	—	—	—
Allowable Stress Intensity (S_a)	20,000	—	—	—	—
Margin of Safety (MS = S_a/SI – 1)	+2.09	—	—	—	—

Table 2.6-10 – NCT Bottom-End Drop, IV Shell with 42.5*g* Acceleration

Evaluation Parameters	
Loading Condition:	NCT Flat End Drop, -20 ºF Foam
Structural Material:	ASTM A240, Type 304, Stainless Steel
Stress Condition:	Primary Membrane
Structural Criterion:	Containment Boundary
Stress Allowable (from Table 2.1-1):	S_m
Material Temperature:	160 ºF
Allowable Stress, S_a:	20,000 psi

Load Condition	Stress Components (psi)				Reference Section
	Radial σ_r	Hoop σ_t	Axial σ_z	Shear τ_{rz}	
Internal Pressure	-150	6,324	3,162	0	2.6.1.3.2
End Drop	0	0	-4,185	0	2.6.7.1(5)
Direct Stress Summation	-150	6,324	-1,023	0	—
Principal Stresses	6,324	-150	-1,023	—	—
Stress Differences	7,347	873	6,474	—	—
Maximum Stress Intensity (SI)	7,347	—	—	—	—
Allowable Stress Intensity (S_a)	20,000	—	—	—	—
Margin of Safety (MS = S_a/SI – 1)	+1.72	—	—	—	—

Table 2.6-11 – Fabrication Induced OC Inner Shell Hoop Stress, Interface Pressure, and Axial Load That Can Be Supported

Temperature (ºF)	Hoop Stress (psi)	Interface Pressure (psi)	Coefficient of Friction	Axial Load (lb)
160	-1,038	62.2	0.5	414,842
			1.0	829,685
70	-1,413	84.7	0.5	564,906
			1.0	1,129,812
-20	-1,821	109.1	0.5	727,641
			1.0	1,455,283

Table 2.6-12 – OC Shell Stresses with Maximum End Drop Fab Condition

Temperature (ºF)	Inner Shell Stresses (psi)		Outer Shell Stresses (psi)	
	Hoop σ_t	Axial σ_z	Hoop σ_t	Axial σ_z
160	-1,038	-6,067	0	-2,929
70	-1,413	-6,067	0	-2,929
-20	-1,821	-6,067	0	-2,929

Table 2.6-13 – NCT Fab & End Drop, OC Inner Shell with 42.5*g* at -20 ºF

Evaluation Parameters	
Loading Condition:	NCT Flat End Drop, -20 ºF Foam
Structural Material:	ASTM A240, Type 304, Stainless Steel
Stress Condition:	Primary Membrane
Structural Criterion:	Containment Boundary
Stress Allowable (from Table 2.1-1):	S_m
Material Temperature:	-20 ºF
Allowable Stress, S_a:	20,000 psi

Load Condition	Stress Components (psi)				Reference Section
	Radial σ_r	Hoop σ_t	Axial σ_z	Shear τ_{rz}	
Fabrication and End Drop	0	-1,821	-6,067	0	2.6.7.1(6)
Direct Stress Summation	0	-1,821	-6,067	0	—
Principal Stresses	0	-1,821	-6,067	—	—
Stress Differences	6,067	4,246	1,821	—	—
Maximum Stress Intensity (SI)	6,067	—	—	—	—
Allowable Stress Intensity (S_a)	20,000	—	—	—	—
Margin of Safety ($MS = S_a/SI - 1$)	+2.30	—	—	—	—

Table 2.6-14 – NCT Fab & End Drop, OC Inner Shell with 42.5*g* at 70 ºF

Evaluation Parameters	
Loading Condition:	NCT Flat End Drop, -20 ºF Foam
Structural Material:	ASTM A240, Type 304, Stainless Steel
Stress Condition:	Primary Membrane
Structural Criterion:	Containment Boundary
Stress Allowable (from Table 2.1-1):	S_m
Material Temperature:	70 ºF
Allowable Stress, S_a:	20,000 psi

Load Condition	Stress Components (psi)				Reference Section
	Radial σ_r	Hoop σ_t	Axial σ_z	Shear τ_{rz}	
Fabrication and End Drop	0	-1,413	-6,067	0	2.6.7.1(6)
Direct Stress Summation	0	-1,413	-6,067	0	—
Principal Stresses	0	-1,413	-6,067	—	—
Stress Differences	6,067	4,654	1,413	—	—
Maximum Stress Intensity (SI)	6,067	—	—	—	—
Allowable Stress Intensity (S_a)	20,000	—	—	—	—
Margin of Safety (MS = S_a/SI – 1)	+2.30	—	—	—	—

Table 2.6-15 – NCT Fab & End Drop, OC Inner Shell with 42.5*g* at 160 ºF

Evaluation Parameters	
Loading Condition:	NCT Flat End Drop, -20 ºF Foam
Structural Material:	ASTM A240, Type 304, Stainless Steel
Stress Condition:	Primary Membrane
Structural Criterion:	Containment Boundary
Stress Allowable (from Table 2.1-1):	S_m
Material Temperature:	160 ºF
Allowable Stress, S_a:	20,000 psi

Load Condition	Stress Components (psi)				Reference Section
	Radial σ_r	Hoop σ_t	Axial σ_z	Shear τ_{rz}	
Fabrication and End Drop	0	-1,038	-6,067	0	2.6.7.1(6)
Direct Stress Summation	0	-1,038	-6,067	0	—
Principal Stresses	0	-1,038	-6,067	—	—
Stress Differences	6,067	5,029	1,038	—	—
Maximum Stress Intensity (SI)	6,067	—	—	—	—
Allowable Stress Intensity (S_a)	20,000	—	—	—	—
Margin of Safety (MS = S_a/SI – 1)	+2.30	—	—	—	—

Table 2.6-16 – NCT End Drop, Lead Pressure and Hoop Stress Summary

Temperature (ºF)	σ_y (psi)	d (in)	p_{max} (psi)	$\sigma_t = p_{max}R/t$ (psi)	
				Inner Shell	Outer Shell
160	~600	34.4	89.9	-1,500	1,188
70	~800	45.9	103.3	-1,724	1,365
-20	~1,000	57.4	121.2	-2,023	1,601

Table 2.6-17 – NCT End Drop, OC Shell Stresses with Zero Fabrication Condition with 42.5*g* Acceleration

Temperature (ºF)	Inner Shell Stresses (psi)		Outer Shell Stresses (psi)	
	Hoop σ_t	Axial σ_z	Hoop σ_t	Axial σ_z
160	-1,500	-4,989	1,188	-3,550
70	-1,724	-4,989	1,365	-3,550
-20	-2,023	-4,989	1,601	-3,550

Table 2.6-18 – NCT End Drop, OC Inner Shell with 42.5*g* at -20 ºF

Evaluation Parameters	
Loading Condition:	NCT Flat End Drop, -20 ºF Foam
Structural Material:	ASTM A240, Type 304, Stainless Steel
Stress Condition:	Primary Membrane
Structural Criterion:	Containment Boundary
Stress Allowable (from Table 2.1-1):	S_m
Material Temperature:	-20 ºF
Allowable Stress, S_a:	20,000 psi

Load Condition	Stress Components (psi)				Reference Section
	Radial σ_r	Hoop σ_t	Axial σ_z	Shear τ_{rz}	
Fabrication and End Drop	0	-2,023	-4,989	0	2.6.7.1(7)
Direct Stress Summation	0	-2,023	-4,989	0	—
Principal Stresses	0	-2,023	-4,989	—	—
Stress Differences	4,989	2,966	2,023	—	—
Maximum Stress Intensity (SI)	4,989	—	—	—	—
Allowable Stress Intensity (S_a)	20,000	—	—	—	—
Margin of Safety ($MS = S_a/SI - 1$)	+3.01	—	—	—	—

Table 2.6-19 – NCT End Drop, OC Inner Shell with 42.5*g* at 70 ºF

Evaluation Parameters					
Loading Condition:	NCT Flat End Drop, -20 ºF Foam				
Structural Material:	ASTM A240, Type 304, Stainless Steel				
Stress Condition:	Primary Membrane				
Structural Criterion:	Containment Boundary				
Stress Allowable (from Table 2.1-1):	S_m				
Material Temperature:	70 ºF				
Allowable Stress, S_a:	20,000 psi				
	Stress Components (psi)				
Load Condition	**Radial σ_r**	**Hoop σ_t**	**Axial σ_z**	**Shear τ_{rz}**	**Reference Section**
Fabrication and End Drop	0	-1,724	-4,989	0	2.6.7.1(7)
Direct Stress Summation	0	-1,724	-4,989	0	—
Principal Stresses	0	-1,724	-4,989	—	—
Stress Differences	4,989	3,265	1,724	—	—
Maximum Stress Intensity (SI)	4,989	—	—	—	—
Allowable Stress Intensity (S_a)	20,000	—	—	—	—
Margin of Safety (MS = S_a/SI – 1)	+3.01	—	—	—	—

Table 2.6-20 – NCT End Drop, OC Inner Shell with 42.5*g* at 160 ºF

Evaluation Parameters					
Loading Condition:	NCT Flat End Drop, -20 ºF Foam				
Structural Material:	ASTM A240, Type 304, Stainless Steel				
Stress Condition:	Primary Membrane				
Structural Criterion:	Containment Boundary				
Stress Allowable (from Table 2.1-1):	S_m				
Material Temperature:	160 ºF				
Allowable Stress, S_a:	20,000 psi				
	Stress Components (psi)				
Load Condition	**Radial σ_r**	**Hoop σ_t**	**Axial σ_z**	**Shear τ_{rz}**	**Reference Section**
Fabrication and End Drop	0	-1,500	-4,989	0	2.6.7.1(7)
Direct Stress Summation	0	-1,500	-4,989	0	—
Principal Stresses	0	-1,500	-4,989	—	—
Stress Differences	4,989	3,489	1,500	—	—
Maximum Stress Intensity (SI)	4,989	—	—	—	—
Allowable Stress Intensity (S_a)	20,000	—	—	—	—
Margin of Safety (MS = S_a/SI – 1)	+3.01	—	—	—	—

Table 2.6-21 – NCT Temperature-Corrected Margin of Safety Against Lead Slump

Lead Temperature (ºF)	Impact Acceleration, g (per Table 2.10.3-10)	Lead Stress, $\sigma = \rho gh$ (psi)	Minimum Flow Stress (psi)	Margin of Safety
-20	42.5	2,165	6,350	+1.93
160	28.6	1,457	3,650	+1.51

Table 2.6-22 – OC Shell Stresses with Max Oblique Drop Fab Condition

Temperature (ºF)	Inner Shell Stresses (psi)		Outer Shell Stresses (psi)	
	Hoop σ_t	Axial σ_z	Hoop σ_t	Axial σ_z
160	-1,038	-2,555	0	-1,234
70	-1,413	-2,555	0	-1,234
-20	-1,821	-2,555	0	-1,234

Table 2.6-23 – NCT Fab & Oblique Drop, OC Inner Shell with 17.9*g* at -20 ºF

Evaluation Parameters	
Loading Condition:	NCT 85º Oblique Drop, -20 ºF Foam
Structural Material:	ASTM A240, Type 304, Stainless Steel
Stress Condition:	Primary Membrane
Structural Criterion:	Containment Boundary
Stress Allowable (from Table 2.1-1):	S_m
Material Temperature:	-20 ºF
Allowable Stress, S_a:	20,000 psi

Load Condition	Stress Components (psi)				Reference Section
	Radial σ_r	Hoop σ_t	Axial σ_z	Shear τ_{rz}	
Fabrication	0	-1,821	-2,555	0	2.6.7.2(4)
Oblique Drop	0	0	-6,463	608	2.6.7.2(4)
Direct Stress Summation	0	-1,821	-9,018	608	—
Principal Stresses	41	-1,821	-9,059	—	—
Stress Differences	9,100	7,238	1,862	—	—
Maximum Stress Intensity (SI)	9,100	—	—	—	—
Allowable Stress Intensity (S_a)	20,000	—	—	—	—
Margin of Safety ($MS = S_a/SI - 1$)	+1.20	—	—	—	—

Table 2.6-24 – NCT Fab & Oblique Drop, OC Inner Shell with 17.9*g* at 70 ºF

Evaluation Parameters	
Loading Condition:	NCT 85º Oblique Drop, -20 ºF Foam
Structural Material:	ASTM A240, Type 304, Stainless Steel
Stress Condition:	Primary Membrane
Structural Criterion:	Containment Boundary
Stress Allowable (from Table 2.1-1):	S_m
Material Temperature:	70 ºF
Allowable Stress, S_a:	20,000 psi

Load Condition	Stress Components (psi)				Reference Section
	Radial σ_r	Hoop σ_t	Axial σ_z	Shear τ_{rz}	
Fabrication	0	-1,413	-2,555	0	2.6.7.2(4)
Oblique Drop	0	0	-6,463	608	2.6.7.2(4)
Direct Stress Summation	0	-1,413	-9,018	608	—
Principal Stresses	41	-1,413	-9,059	—	—
Stress Differences	9,100	7,646	1,454	—	—
Maximum Stress Intensity (SI)	9,100	—	—	—	—
Allowable Stress Intensity (S_a)	20,000	—	—	—	—
Margin of Safety (MS = S_a/SI – 1)	+1.20	—	—	—	—

Table 2.6-25 – NCT Fab & Oblique Drop, OC Inner Shell with 17.9*g* at 160 ºF

Evaluation Parameters	
Loading Condition:	NCT 85º Oblique Drop, -20 ºF Foam
Structural Material:	ASTM A240, Type 304, Stainless Steel
Stress Condition:	Primary Membrane
Structural Criterion:	Containment Boundary
Stress Allowable (from Table 2.1-1):	S_m
Material Temperature:	160 ºF
Allowable Stress, S_a:	20,000 psi

Load Condition	Stress Components (psi)				Reference Section
	Radial σ_r	Hoop σ_t	Axial σ_z	Shear τ_{rz}	
Fabrication	0	-1,038	-2,555	0	2.6.7.2(4)
Oblique Drop	0	0	-6,463	608	2.6.7.2(4)
Direct Stress Summation	0	-1,038	-9,018	608	—
Principal Stresses	41	-1,038	-9,059	—	—
Stress Differences	9,100	8,021	1,079	—	—
Maximum Stress Intensity (SI)	9,100	—	—	—	—
Allowable Stress Intensity (S_a)	20,000	—	—	—	—
Margin of Safety (MS = S_a/SI – 1)	+1.20	—	—	—	—

Table 2.6-26 – NCT Oblique Drop, IV Shell with 17.9*g* at 70 ºF

Evaluation Parameters	
Loading Condition:	NCT 85º Oblique Drop, -20 ºF Foam
Structural Material:	ASTM A240, Type 304, Stainless Steel
Stress Condition:	Primary Membrane
Structural Criterion:	Containment Boundary
Stress Allowable (from Table 2.1-1):	S_m
Material Temperature:	70 ºF
Allowable Stress, S_a:	20,000 psi

Load Condition	Stress Components (psi)				Reference Section
	Radial σ_r	Hoop σ_t	Axial σ_z	Shear τ_{rz}	
Oblique Drop	0	0	-5,247	2,099	2.6.7.2(5)
Direct Stress Summation	0	0	-5,247	2,099	—
Principal Stresses	736	0	-5,983	—	—
Stress Differences	6,719	5,983	736	—	—
Maximum Stress Intensity (SI)	6,719	—	—	—	—
Allowable Stress Intensity (S_a)	20,000	—	—	—	—
Margin of Safety (MS = S_a/SI – 1)	+1.98	—	—	—	—

Table 2.6-27 – NCT Oblique Drop, Canister Shell with 17.9*g* at 210 ºF

Evaluation Parameters	
Loading Condition:	NCT 85º Oblique Drop, -20 ºF Foam
Structural Material:	ASTM A240, Type 304L, Stainless Steel
Stress Condition:	Primary Membrane
Structural Criterion:	Non-containment Boundary
Stress Allowable (from Table 2.1-2):	S_y
Material Temperature:	210 ºF
Allowable Stress, S_a:	21,100 psi

Load Condition	Stress Components (psi)				Reference Section
	Radial σ_r	Hoop σ_t	Axial σ_z	Shear τ_{rz}	
Oblique Drop	0	0	-8,062	454	2.6.7.2(6)
Direct Stress Summation	0	0	-8,062	454	—
Principal Stresses	25	0	-8,087	—	—
Stress Differences	8,112	8,087	25	—	—
Maximum Stress Intensity (SI)	8,112	—	—	—	—
Allowable Stress Intensity (S_a)	21,100	—	—	—	—
Margin of Safety (MS = S_a/SI – 1)	+1.60	—	—	—	—

Table 2.6-28 – OC Shell Stresses with Max Side Drop Fab Condition

Temperature (ºF)	Inner Shell Stresses (psi)		Outer Shell Stresses (psi)	
	Hoop σ_t	Axial① σ_z	Hoop σ_t	Axial σ_z
160	-1,038	-1,963	0	0
70	-1,413	-1,963	0	0
-20	-1,821	-1,963	0	0

Note:

① Axial compressive stress in the inner shell per Appendix 2.10.8.5, *Axial Stress Evaluation after Cooldown from 620 ºF to -20 ºF*.

Table 2.6-29 – NCT Fab & Side Drop, OC Inner Shell with 19.3*g* at -20 ºF

Evaluation Parameters	
Loading Condition:	NCT Flat Side Drop, -20 ºF Foam
Structural Material:	ASTM A240, Type 304, Stainless Steel
Stress Condition:	Primary Membrane
Structural Criterion:	Containment Boundary
Stress Allowable (from Table 2.1-1):	S_m
Material Temperature:	-20 ºF
Allowable Stress, S_a:	20,000 psi

Load Condition	Stress Components (psi)				Reference Section
	Radial σ_r	Hoop σ_t	Axial σ_z	Shear τ_{rz}	
Fabrication	0	-1,821	-1,963	0	2.6.7.3(4)
Side Drop	0	0	-3,881	1,255	2.6.7.3(4)
Direct Stress Summation	0	-1,821	-5,844	1,255	—
Principal Stresses	258	-1,821	-6,102	—	—
Stress Differences	6,360	4,281	2,079	—	—
Maximum Stress Intensity (SI)	6,360	—	—	—	—
Allowable Stress Intensity (S_a)	20,000	—	—	—	—
Margin of Safety (MS = S_a/SI – 1)	+2.14	—	—	—	—

Table 2.6-30 – NCT Fab & Side Drop, OC Inner Shell with 19.3*g* at 70 ºF

Evaluation Parameters	
Loading Condition:	NCT Flat Side Drop, -20 ºF Foam
Structural Material:	ASTM A240, Type 304, Stainless Steel
Stress Condition:	Primary Membrane
Structural Criterion:	Containment Boundary
Stress Allowable (from Table 2.1-1):	S_m
Material Temperature:	70 ºF
Allowable Stress, S_a:	20,000 psi

Load Condition	Stress Components (psi)				Reference Section
	Radial σ_r	Hoop σ_t	Axial σ_z	Shear τ_{rz}	
Fabrication	0	-1,413	-1,963	0	2.6.7.3(4)
Side Drop	0	0	-3,881	1,255	2.6.7.3(4)
Direct Stress Summation	0	-1,413	-5,844	1,255	—
Principal Stresses	258	-1,413	-6,102	—	—
Stress Differences	6,360	4,689	1,671	—	—
Maximum Stress Intensity (SI)	6,360	—	—	—	—
Allowable Stress Intensity (S_a)	20,000	—	—	—	—
Margin of Safety (MS = S_a/SI – 1)	+2.14	—	—	—	—

Table 2.6-31 – NCT Fab & Side Drop, OC Inner Shell with 19.3*g* at 160 ºF

Evaluation Parameters	
Loading Condition:	NCT Flat Side Drop, -20 ºF Foam
Structural Material:	ASTM A240, Type 304, Stainless Steel
Stress Condition:	Primary Membrane
Structural Criterion:	Containment Boundary
Stress Allowable (from Table 2.1-1):	S_m
Material Temperature:	160 ºF
Allowable Stress, S_a:	20,000 psi

Load Condition	Stress Components (psi)				Reference Section
	Radial σ_r	Hoop σ_t	Axial σ_z	Shear τ_{rz}	
Fabrication	0	-1,038	-1,963	0	2.6.7.3(4)
Side Drop	0	0	-3,881	1,255	2.6.7.3(4)
Direct Stress Summation	0	-1,038	-5,844	1,255	—
Principal Stresses	258	-1,038	-6,102	—	—
Stress Differences	6,360	5,064	1,296	—	—
Maximum Stress Intensity (SI)	6,360	—	—	—	—
Allowable Stress Intensity (S_a)	20,000	—	—	—	—
Margin of Safety (MS = S_a/SI – 1)	+2.14	—	—	—	—

Table 2.6-32 – NCT Side Drop, IV Shell with 19.3*g* at 160 ºF

Evaluation Parameters					
Loading Condition:	NCT Flat Side Drop, -20 ºF Foam				
Structural Material:	ASTM A240, Type 304, Stainless Steel				
Stress Condition:	Primary Membrane				
Structural Criterion:	Containment Boundary				
Stress Allowable (from Table 2.1-1):	S_m				
Material Temperature:	160 ºF				
Allowable Stress, S_a:	20,000 psi				
	Stress Components (psi)				
Load Condition	**Radial σ_r**	**Hoop σ_t**	**Axial σ_z**	**Shear τ_{rz}**	**Reference Section**
Side Drop	0	0	-4,661	2,214	2.6.7.3(5)
Direct Stress Summation	0	0	-4,661	2,214	—
Principal Stresses	884	0	-5,545	—	—
Stress Differences	6,429	5,545	884	—	—
Maximum Stress Intensity (SI)	6,429	—	—	—	—
Allowable Stress Intensity (S_a)	20,000	—	—	—	—
Margin of Safety (MS = S_a/SI – 1)	+2.11	—	—	—	—

Table 2.6-33 – NCT Side Drop, Canister Shell with 19.3*g* at 210 ºF

Evaluation Parameters					
Loading Condition:	NCT Flat Side Drop, -20 ºF Foam				
Structural Material:	ASTM A240, Type 304L, Stainless Steel				
Stress Condition:	Primary Membrane				
Structural Criterion:	Non-containment Boundary				
Stress Allowable (from Table 2.1-2):	S_y				
Material Temperature:	210 ºF				
Allowable Stress, S_a:	21,100 psi				
	Stress Components (psi)				
Load Condition	**Radial σ_r**	**Hoop σ_t**	**Axial σ_z**	**Shear τ_{rz}**	**Reference Section**
Side Drop	0	0	-4,003	2,382	2.6.7.3(6)
Direct Stress Summation	0	0	-4,003	2,382	—
Principal Stresses	1,110	0	-5,113	—	—
Stress Differences	6,223	5,113	1,110	—	—
Maximum Stress Intensity (SI)	6,223	—	—	—	—
Allowable Stress Intensity (S_a)	21,100	—	—	—	—
Margin of Safety (MS = S_a/SI – 1)	+2.39	—	—	—	—

Table 2.6-34 – NCT Fab & Side Drop, OC Shells' Welds with 19.3*g* at -20 ºF

Evaluation Parameters	
Loading Condition:	NCT Flat Side Drop, -20 ºF Foam
Structural Material:	ASTM A240, Type 304, Stainless Steel
Stress Condition:	Primary Membrane
Structural Criterion:	Containment Boundary
Stress Allowable (from Table 2.1-1):	S_m
Material Temperature:	-20 ºF
Allowable Stress, S_a:	20,000 psi

Load Condition	Stress Components (psi)				Reference Section
	Radial σ_r	Hoop σ_t	Axial σ_z	Shear τ_{rz}	
Fabrication	0	-1,821	-1,963	0	2.6.7.3(4)
Side Drop	0	0	-3,881	2,422	2.6.7.3(4)(8)
Direct Stress Summation	0	-1,821	-5,844	2,422	—
Principal Stresses	873	-1,821	-6,717	—	—
Stress Differences	7,590	4,896	2,694	—	—
Maximum Stress Intensity (SI)	7,590	—	—	—	—
Allowable Stress Intensity (S_a)	20,000	—	—	—	—
Margin of Safety ($MS = S_a/SI - 1$)	+1.64	—	—	—	—

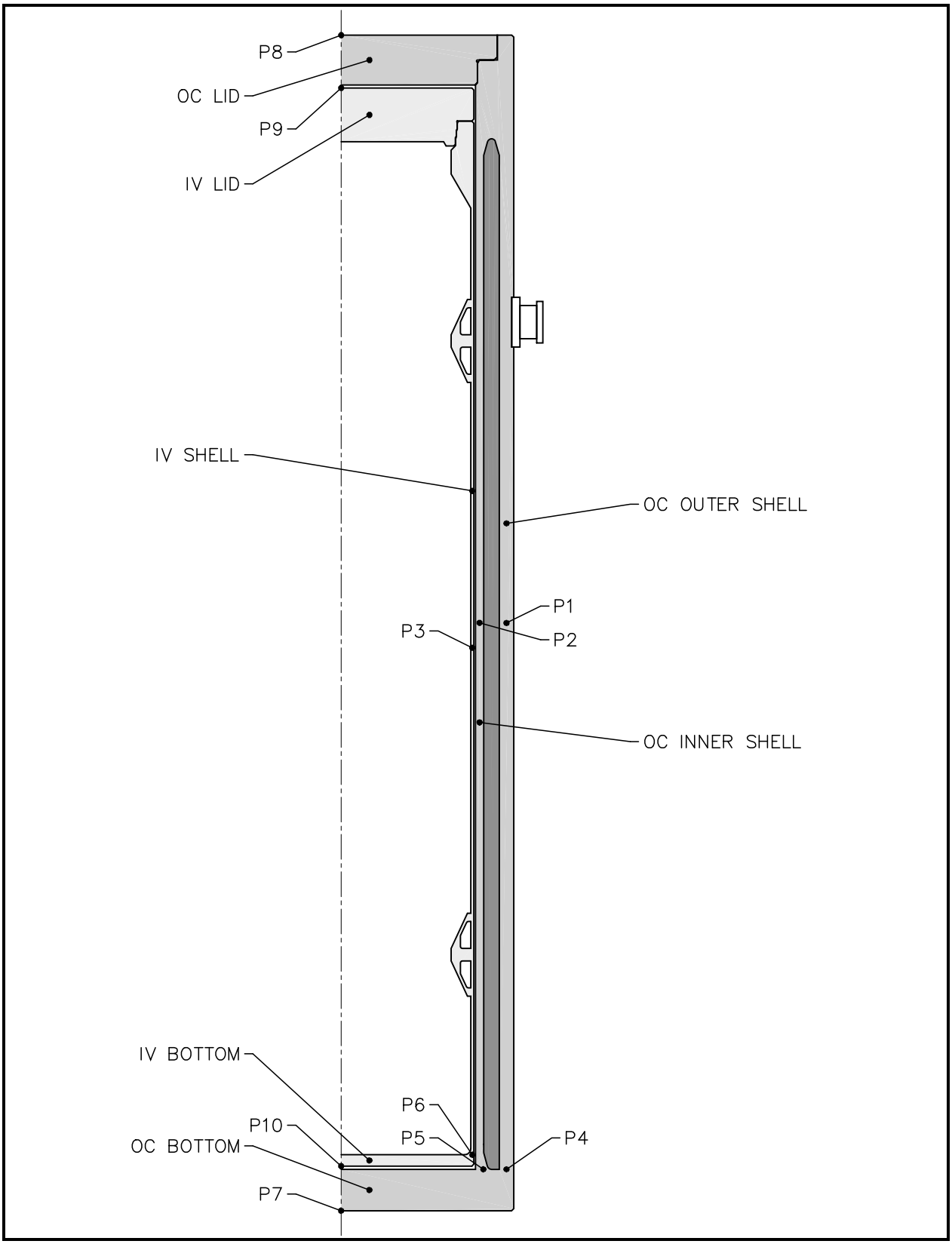

Figure 2.6-1 – Package Locations for Pressure Stress Calculations

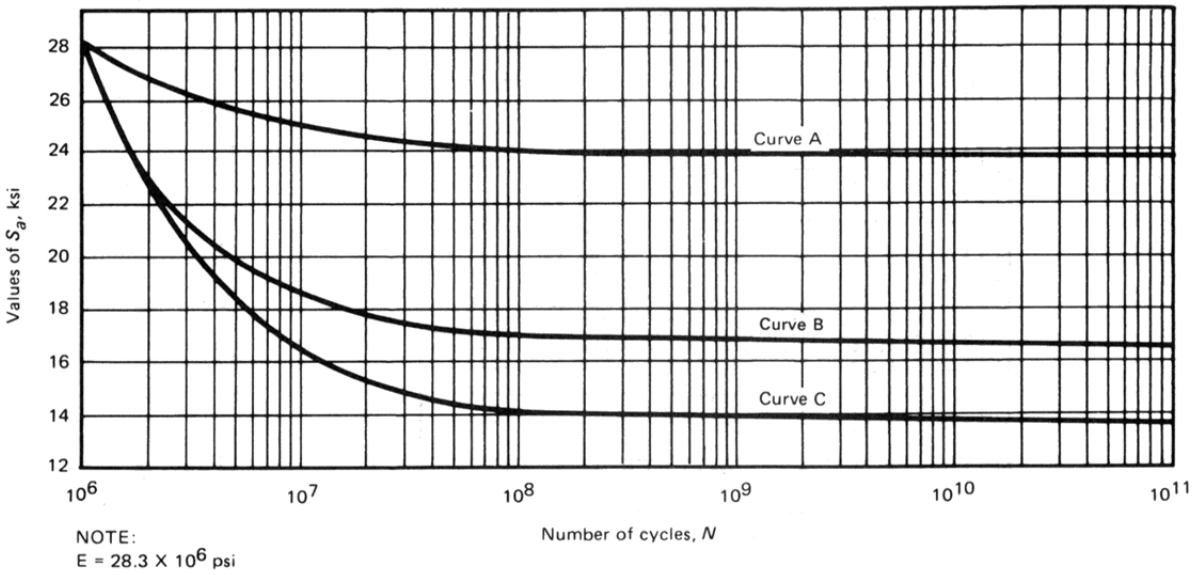

Criteria for the Use of the Curves in This Figure
[Notes (1)–(5)]

Curve	Elastic Analysis of Material Other Than Welds and Adjacent Base Metal	Elastic Analysis of Welds and Adjacent Base Metal
A	$(P_L + P_b + Q)_{Range} \leq 27.2$ ksi	. . .
B	$(P_L + P_b + Q)_{Range} > 27.2$ ksi and S_a is corrected for applied mean stress	$(P_L + P_b + Q)_{Range} \leq 27.2$ ksi
C	$(P_L + P_b + Q)_{Range} > 27.2$ ksi	$(P_L + P_b + Q)_{Range} > 27.2$ ksi

NOTES:
(1) Range applies to the individual quantities P_L, P_b, and Q and applies to the set of cycles under consideration.
(2) Thermal bending stresses resulting from axial and radial gradients are excluded from Q.
(3) Curve A is also to be used with inelastic analysis with $S_a = \frac{1}{2} \Delta \epsilon_t E$, where $\Delta \epsilon_t$ is the total effective strain range.
(4) The maximum effect of retained mean stress is included in Curve C.
(5) The adjacent base metal is defined as three wall thicknesses from the center line of the weld.

FIG. I-9.2.2 DESIGN FATIGUE CURVES FOR AUSTENITIC STEELS, NICKEL–CHROMIUM–IRON ALLOY, NICKEL–IRON–CHROMIUM ALLOY, AND NICKEL–COPPER ALLOY FOR $S_a \leq 28.2$ ksi, FOR TEMPERATURES NOT EXCEEDING 800°F

Figure 2.6-2 – Figure I-9.2.2 from Appendix I of the ASME Code

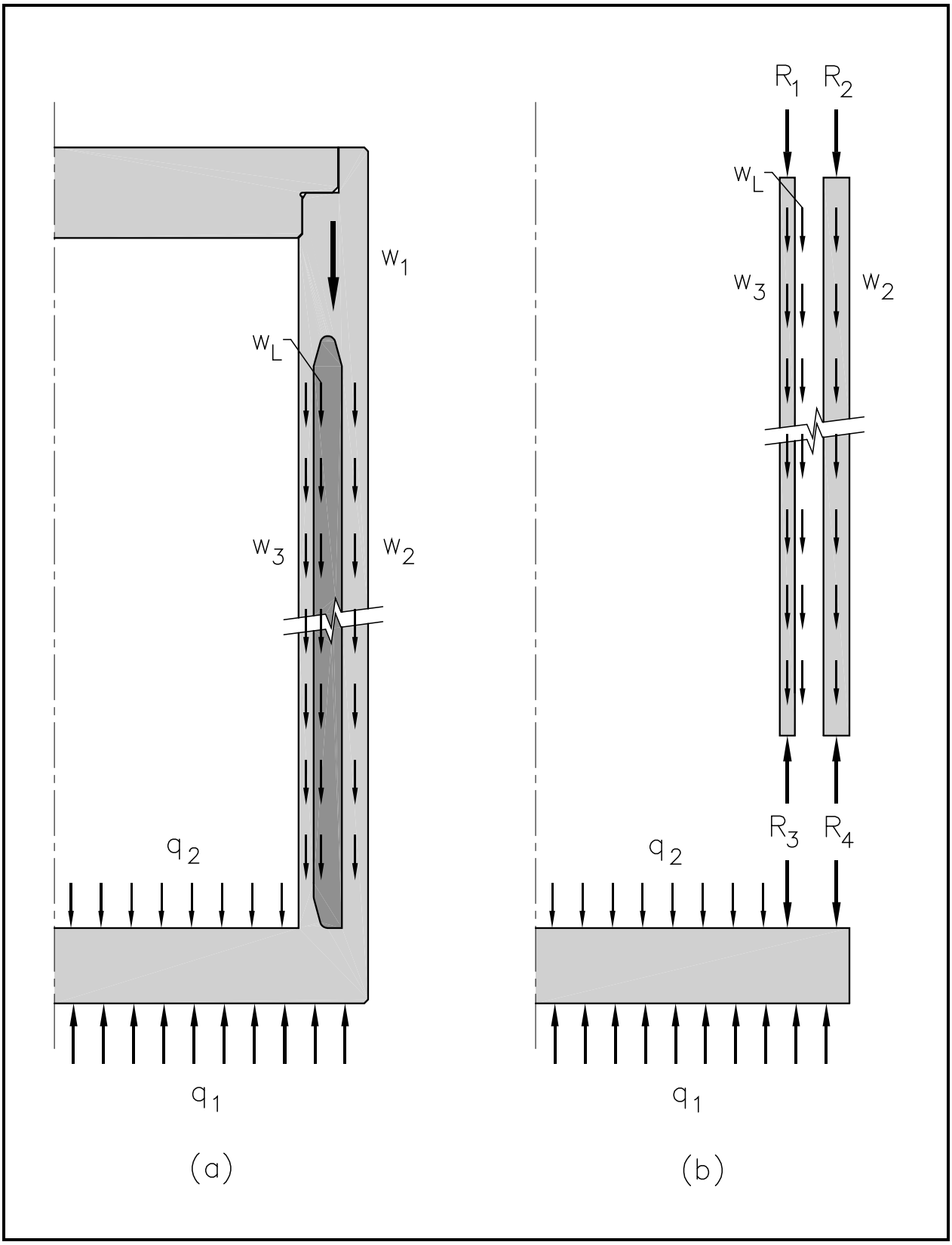

Figure 2.6-3 – Free-Body Diagrams of Axial Forces in OC Components

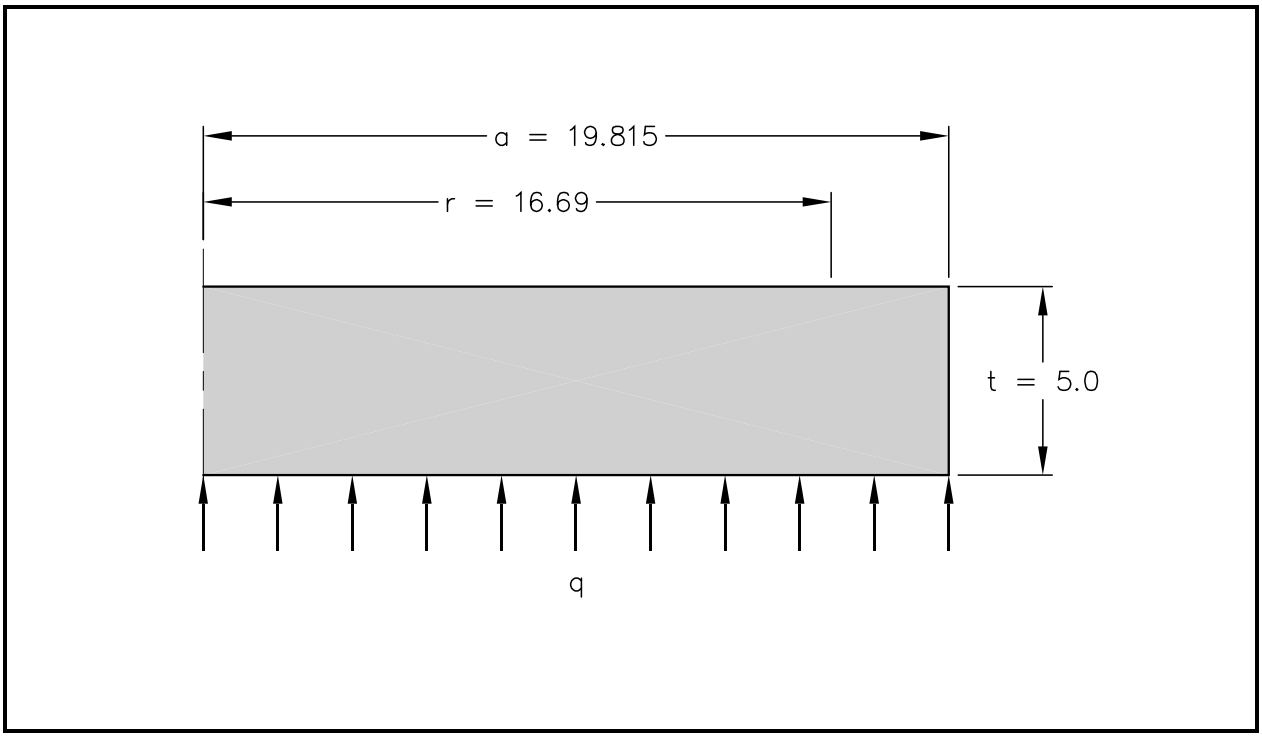

Figure 2.6-4 – OC Bottom-End Plate Configuration

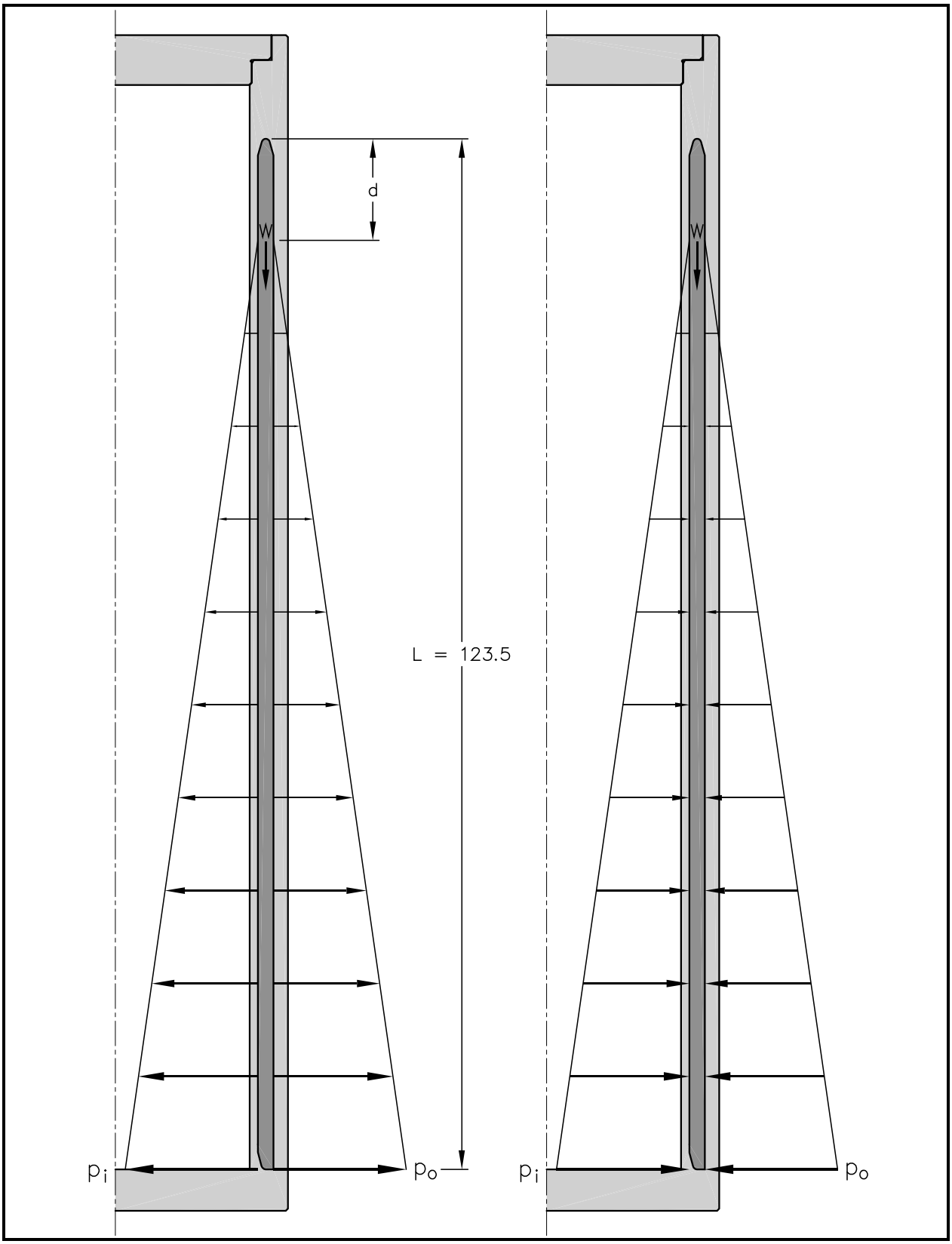

Figure 2.6-5 – Axial Pressure Distribution Due to Lead

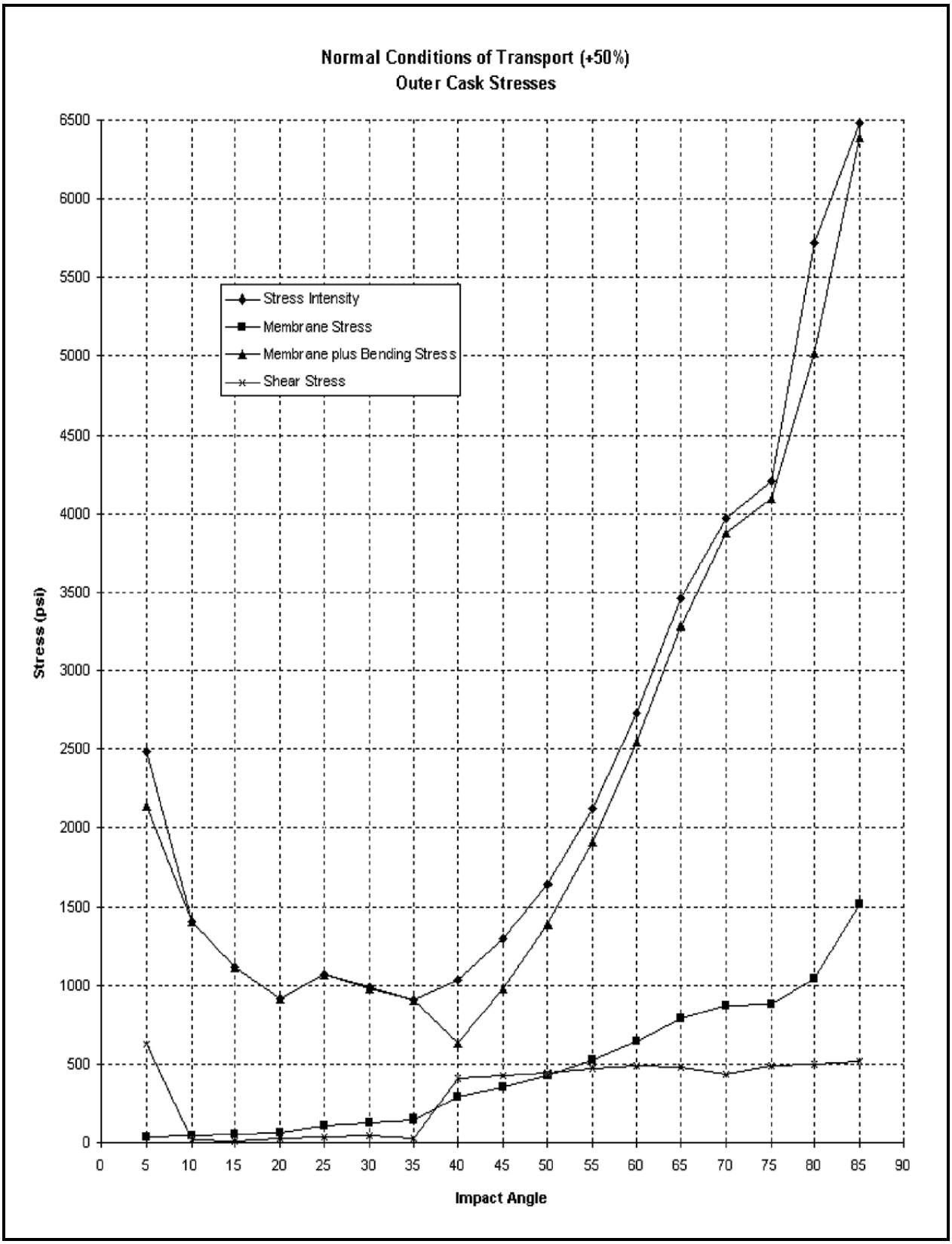

Figure 2.6-6 – NCT Cold (-20 ºF) Outer Cask Stresses

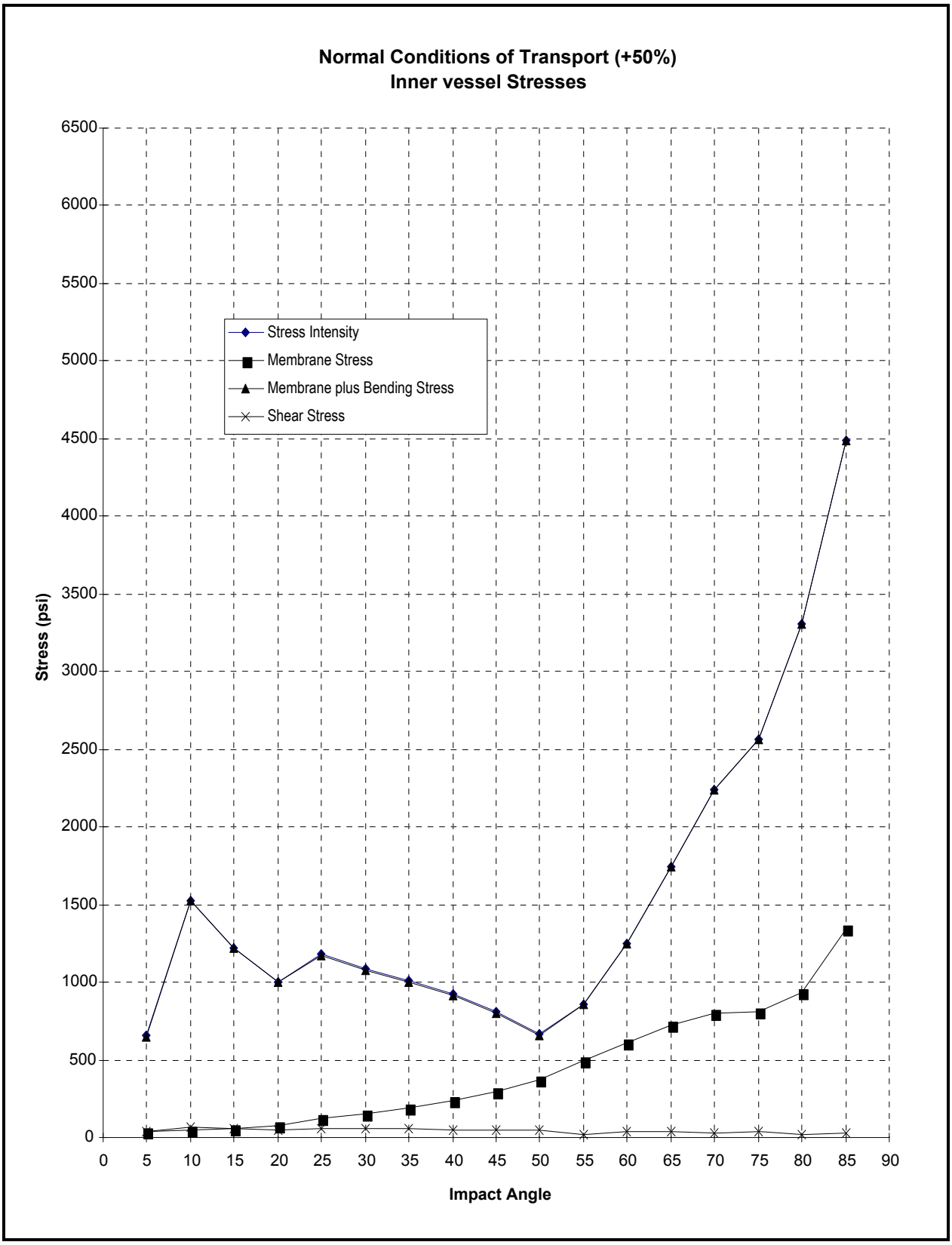

Figure 2.6-7 – NCT Cold (-20 ºF) Inner Vessel Stresses

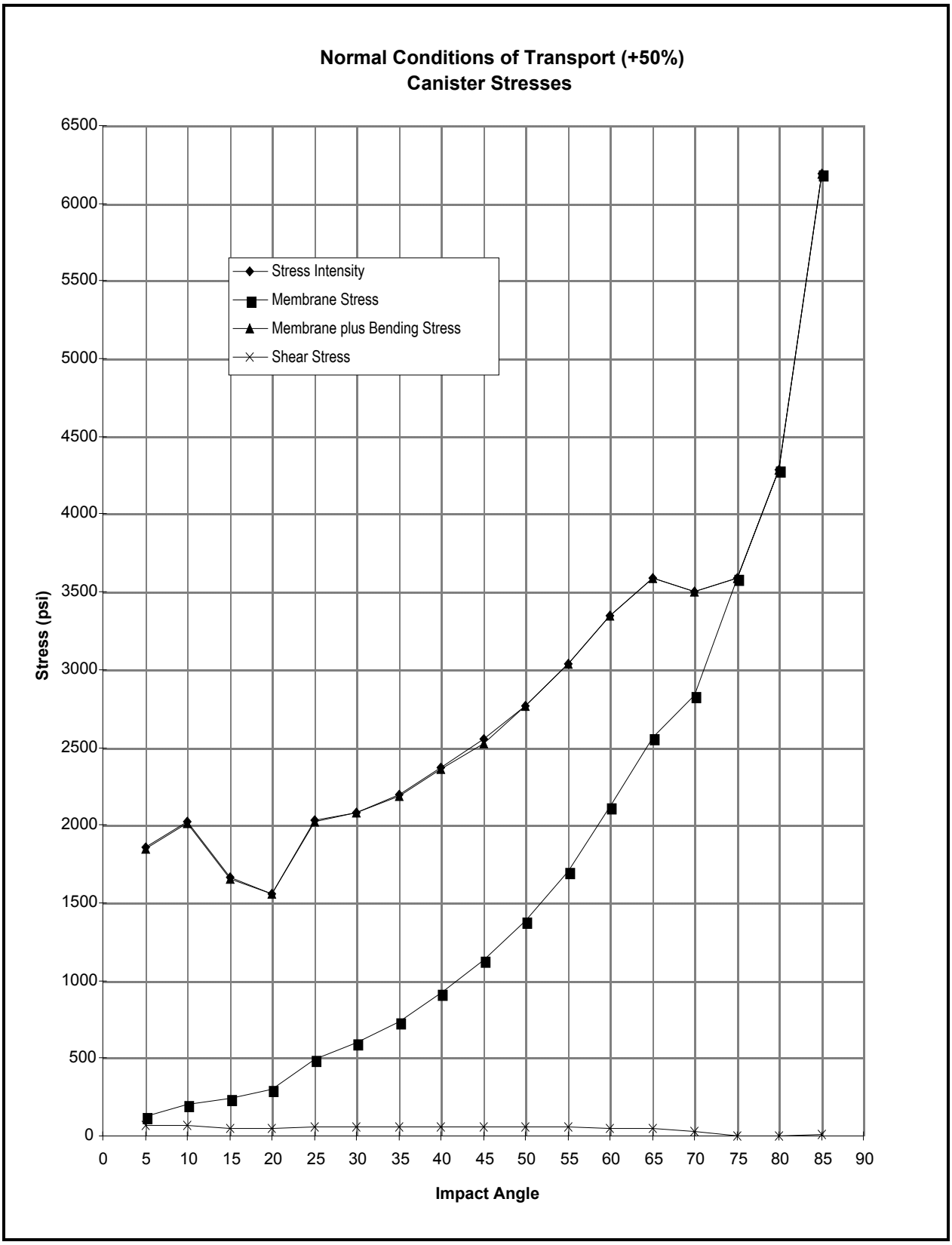

Figure 2.6-8 – NCT Cold (-20 ºF) Canister Stresses

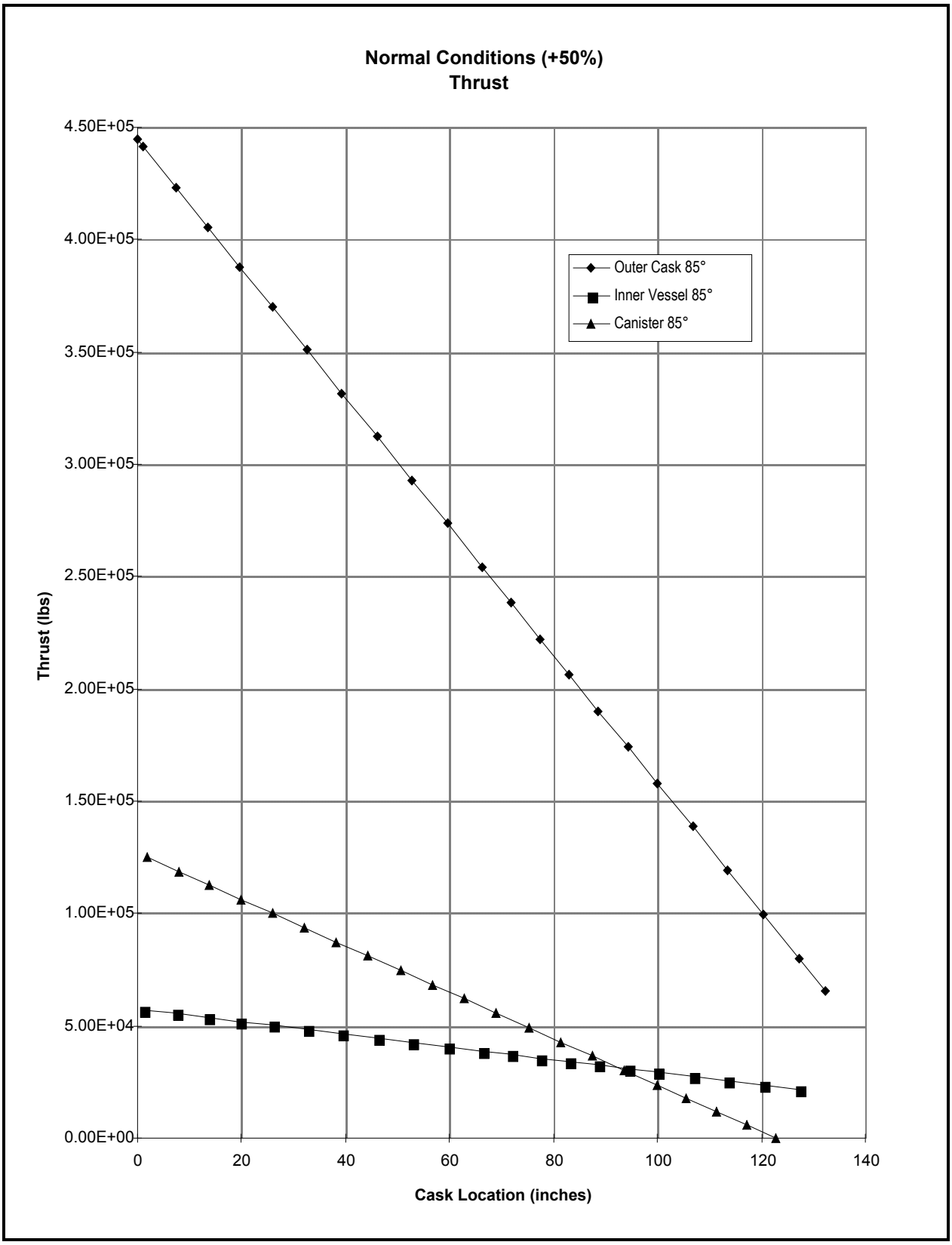

Figure 2.6-9 – NCT Cold (-20 ºF) Thrust

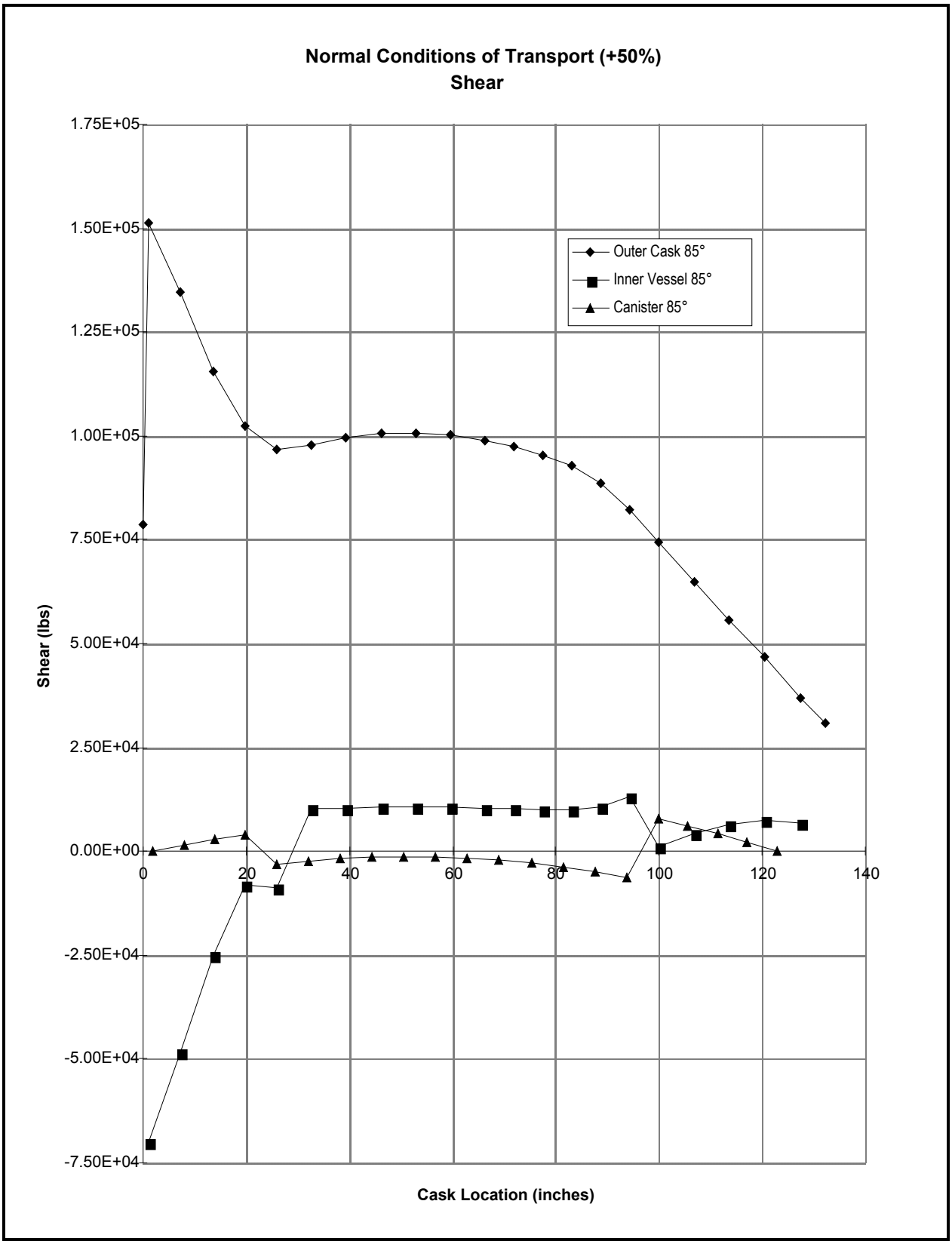

Figure 2.6-10 – NCT Cold (-20 ºF) Shear

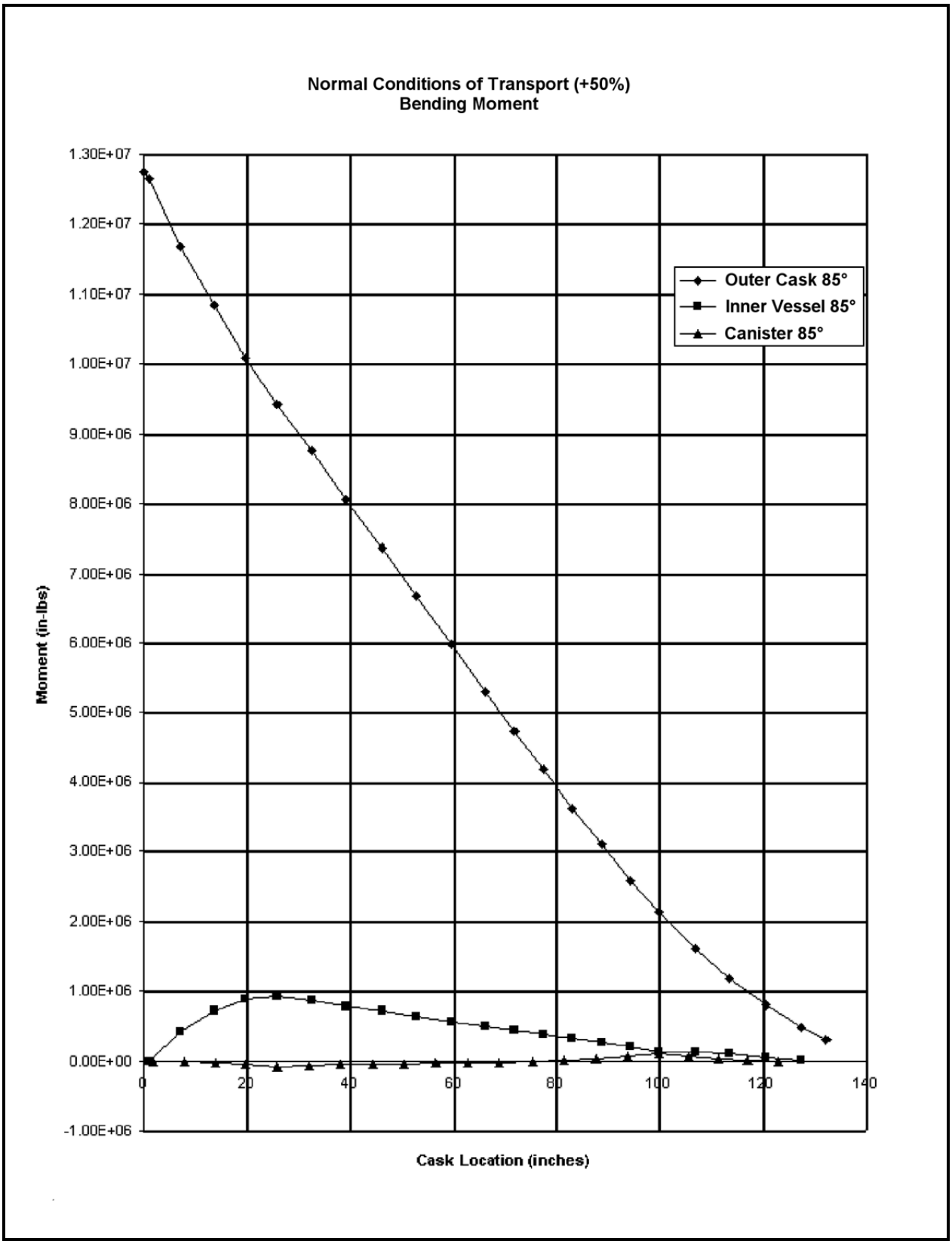

Figure 2.6-11 – NCT Cold (-20 ºF) Bending Moment

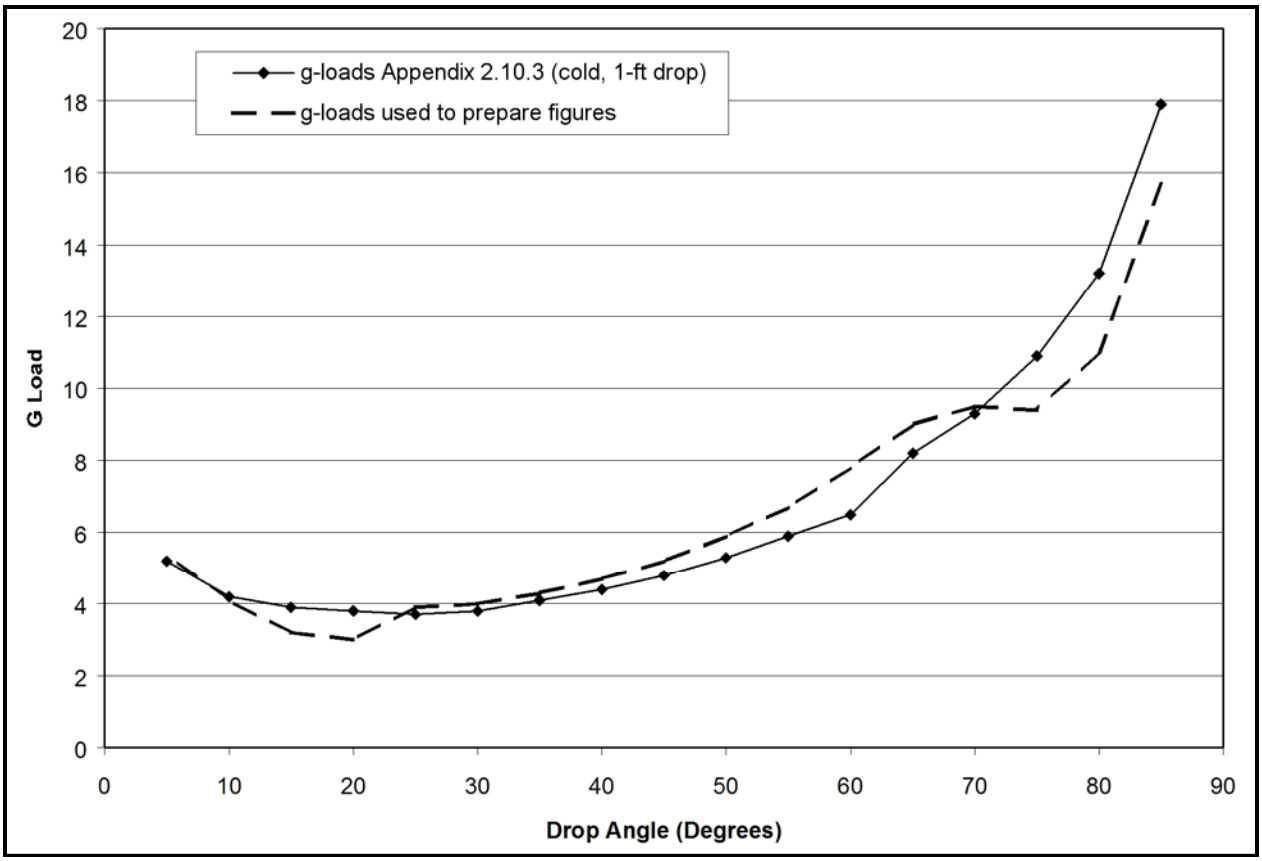

Figure 2.6-12 – Comparison of *g*-Loads Used for Calculating Cold (-20 ºF) NCT Stresses

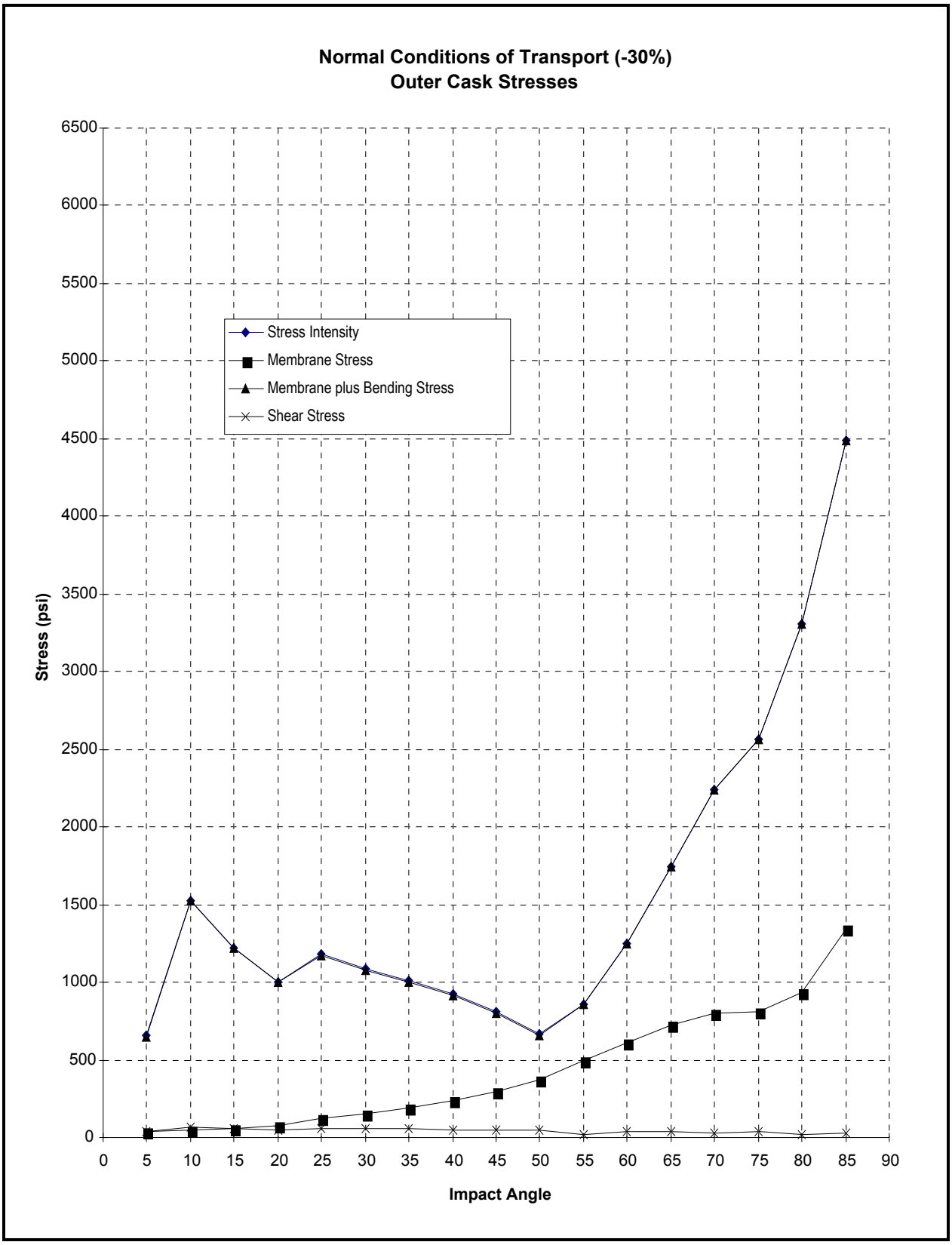

Figure 2.6-13 – NCT Hot (140 ºF) Outer Cask Stresses

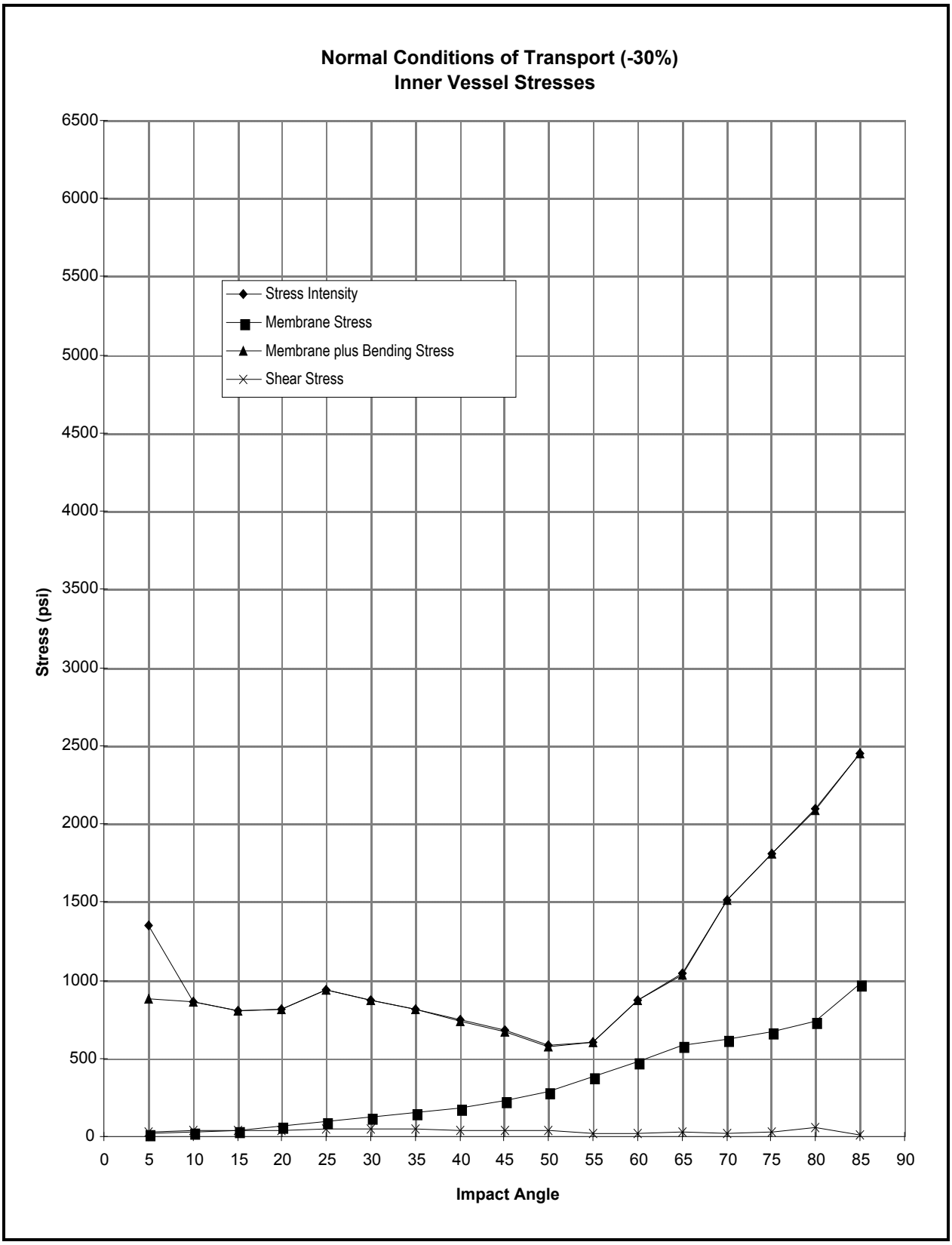

Figure 2.6-14 – NCT Hot (140 ºF) Inner Vessel Stresses

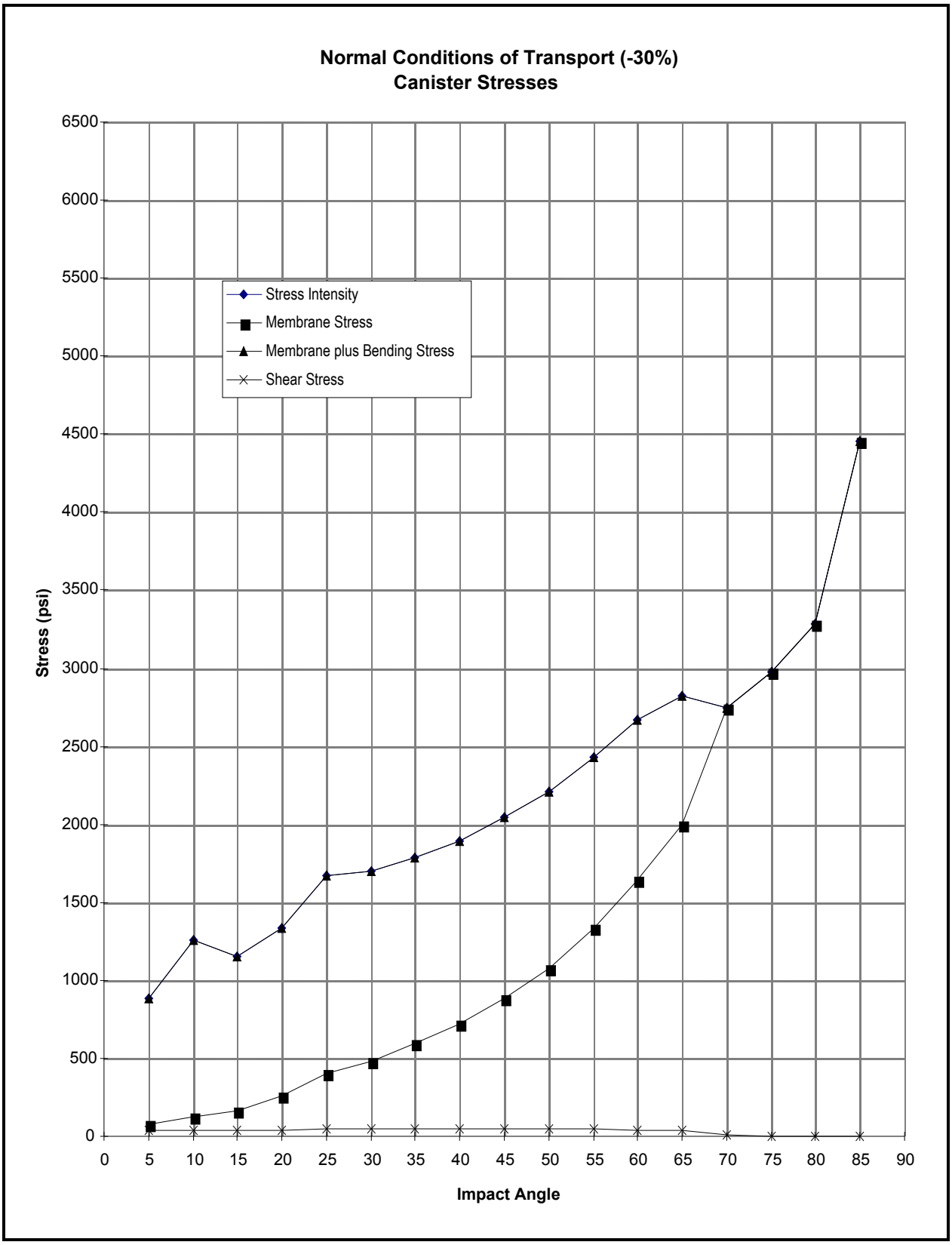

Figure 2.6-15 – NCT Hot (140 ºF) Canister Stresses

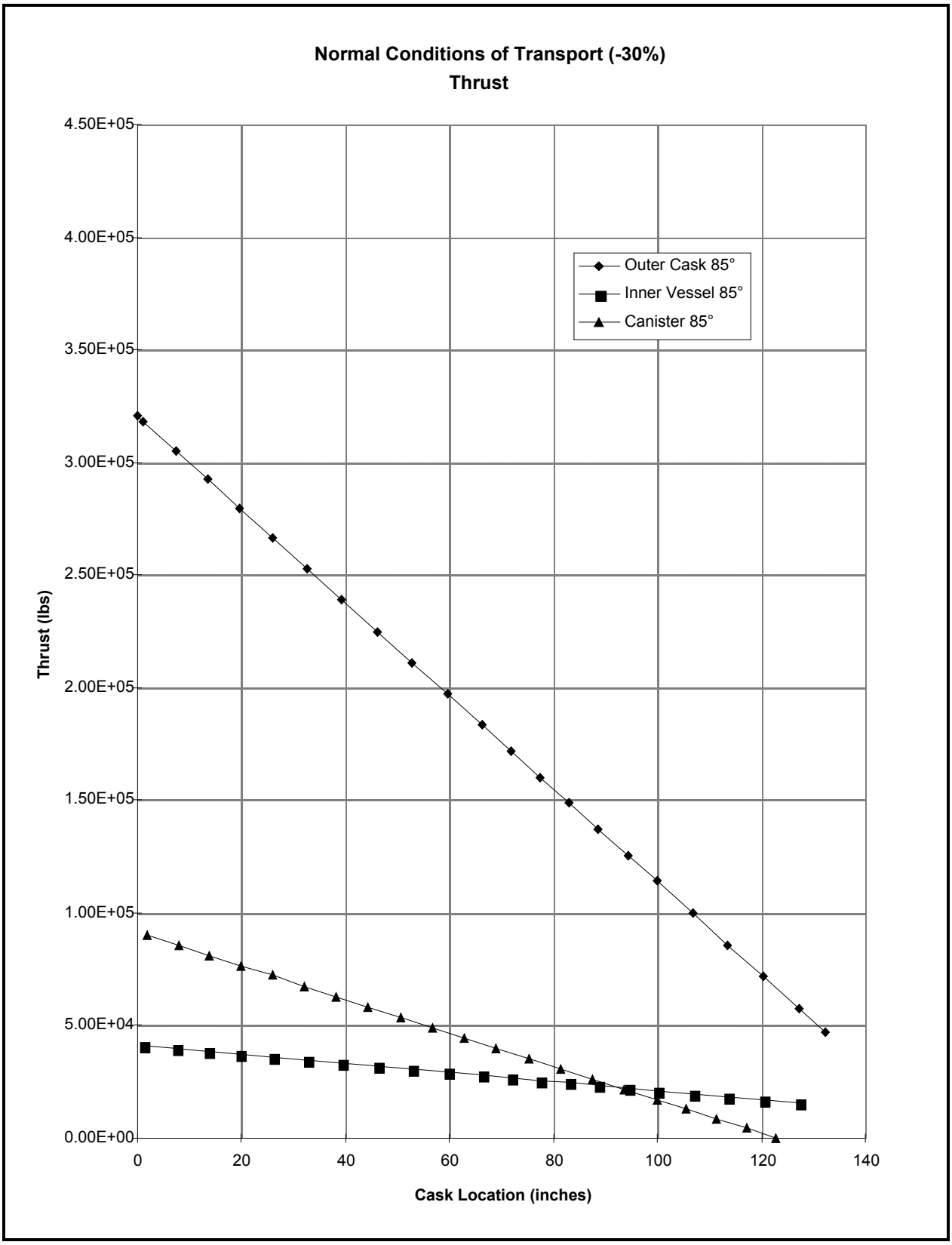

Figure 2.6-16 – NCT Hot (140 ºF) Thrust

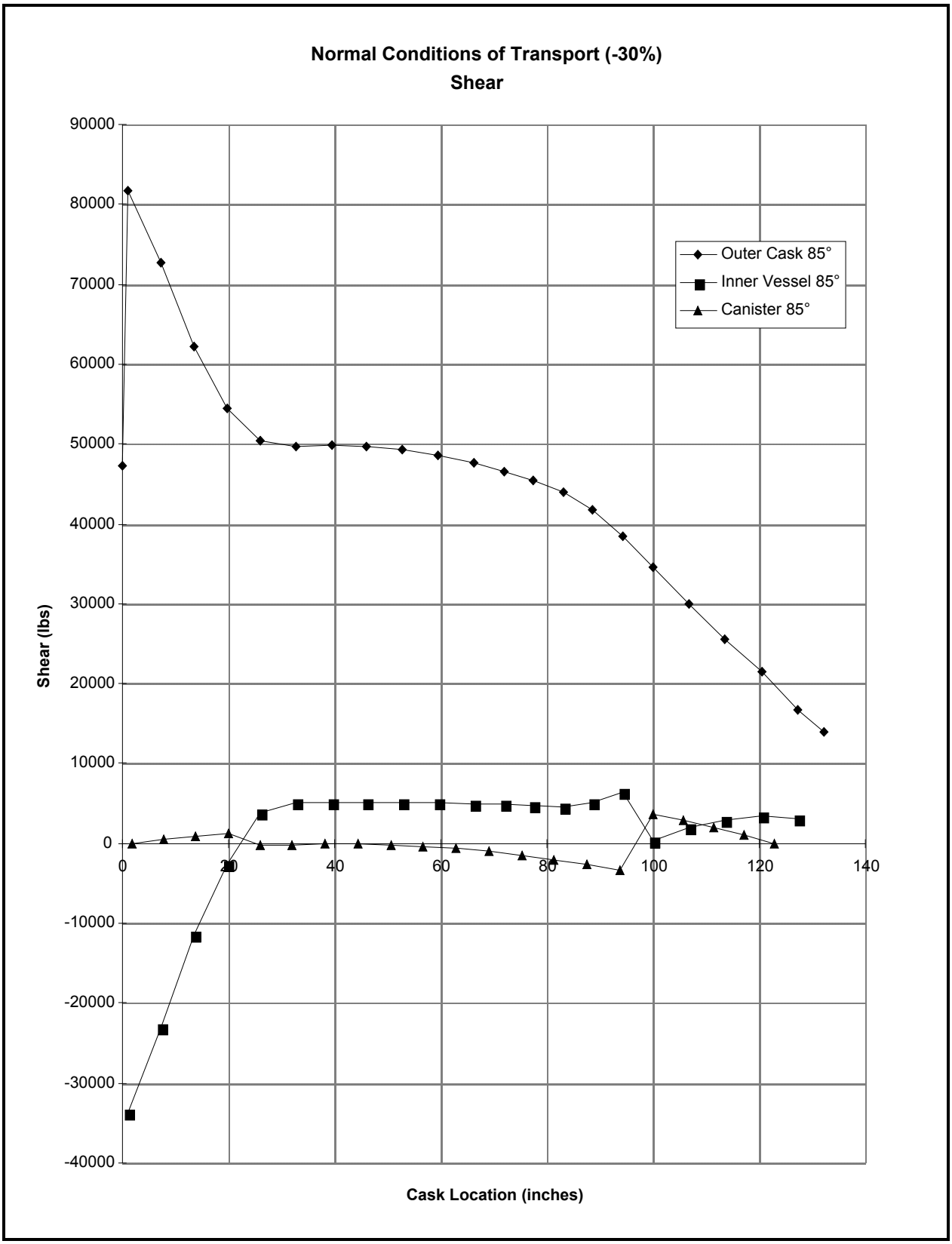

Figure 2.6-17 – NCT Hot (140 ºF) Shear

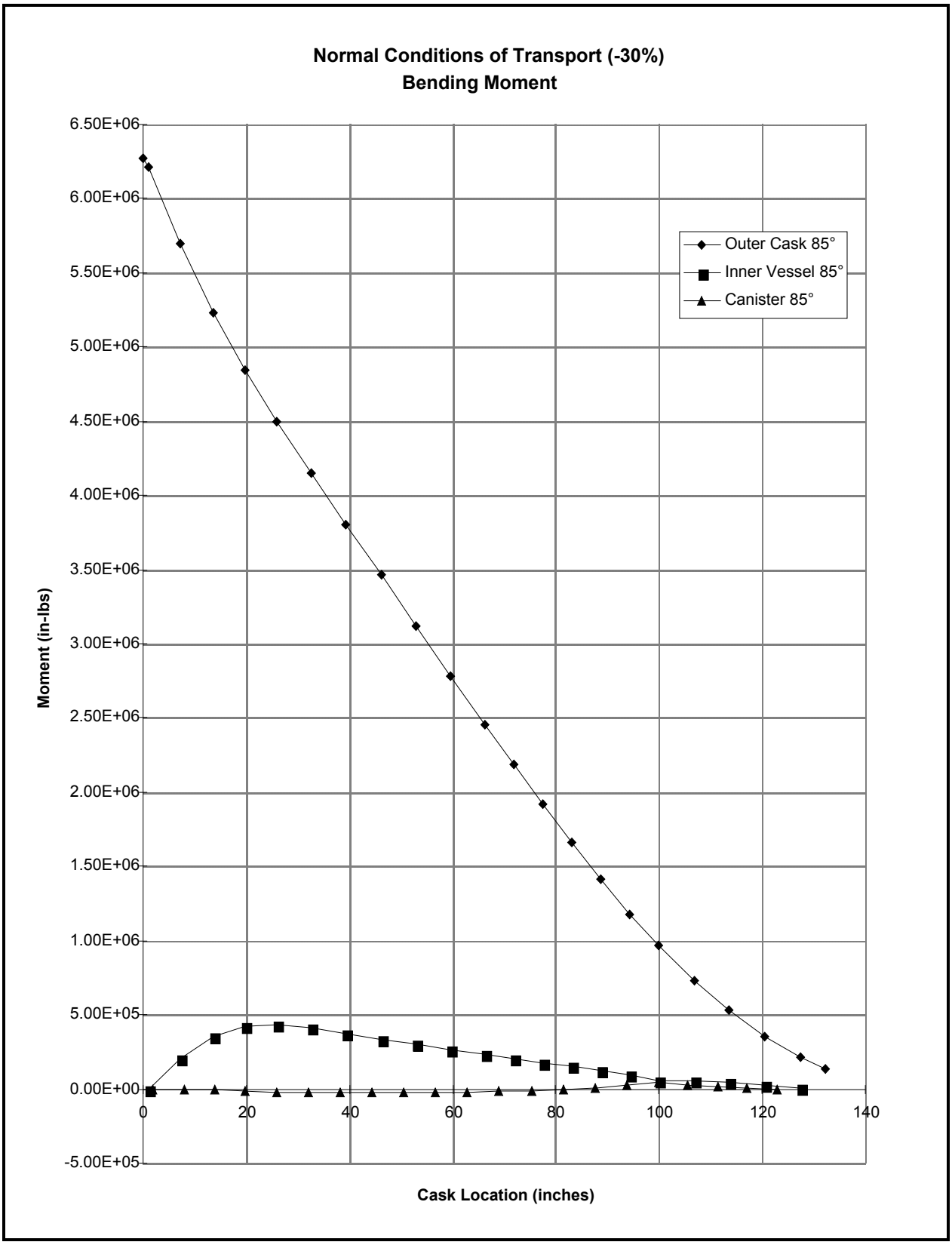

Figure 2.6-18 – NCT Hot (140 ºF) Bending Moment

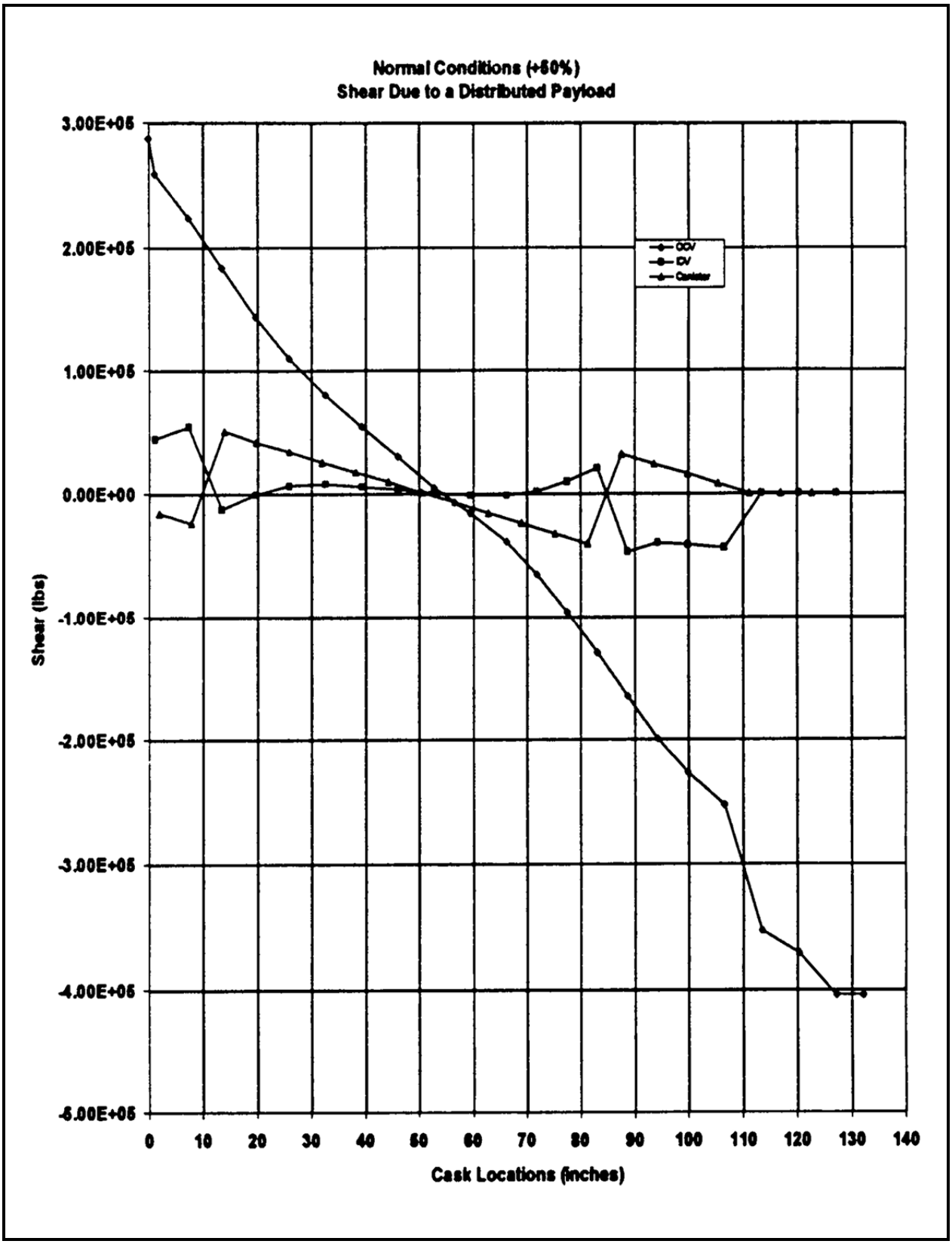

Figure 2.6-19 – NCT Cold (-20 ºF) Shear Due to a Distributed Payload

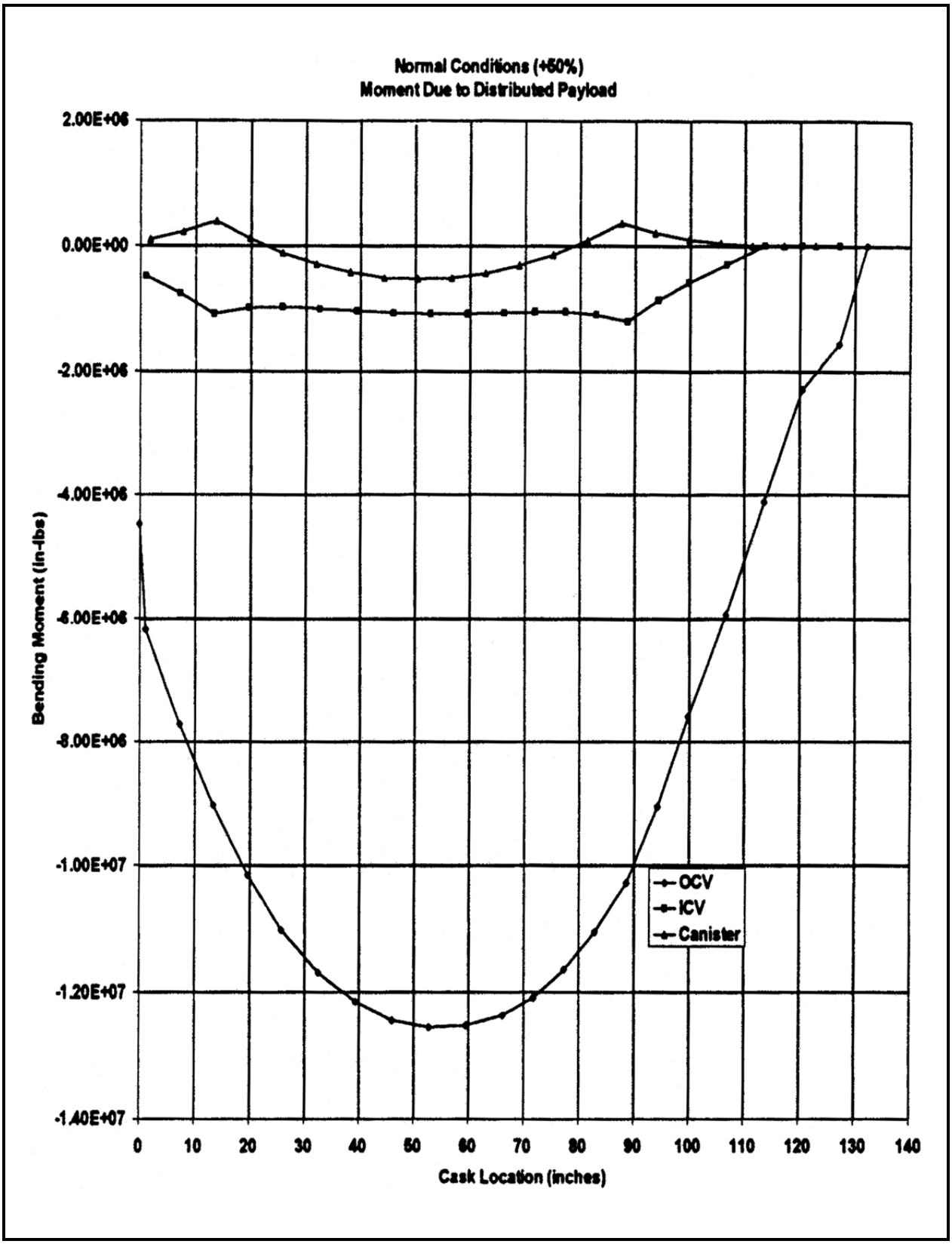

Figure 2.6-20 – NCT Cold (-20 ºF) Moment Due to a Distributed Payload

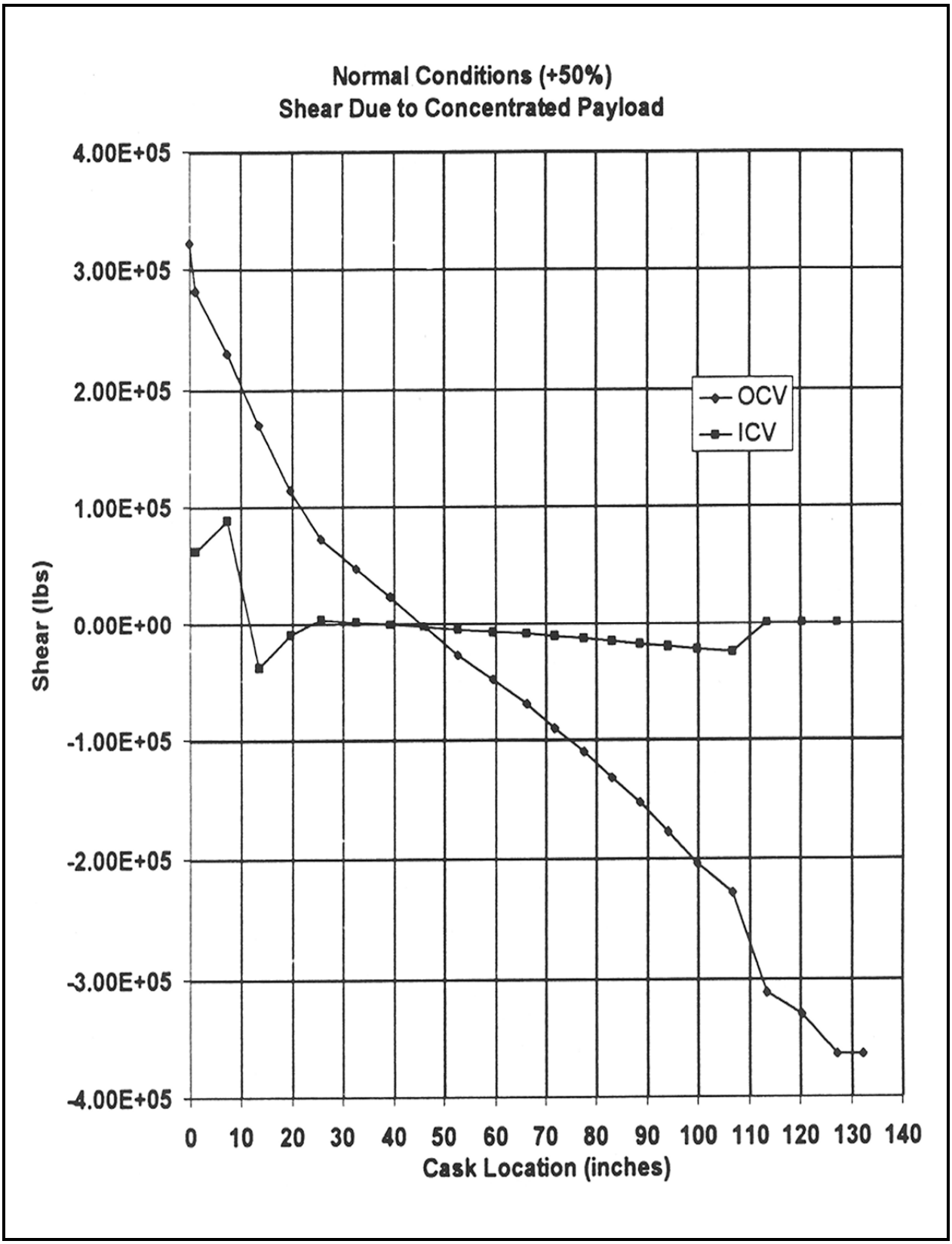

Figure 2.6-21 – NCT Cold (-20 ºF) Shear Due to a Concentrated Payload

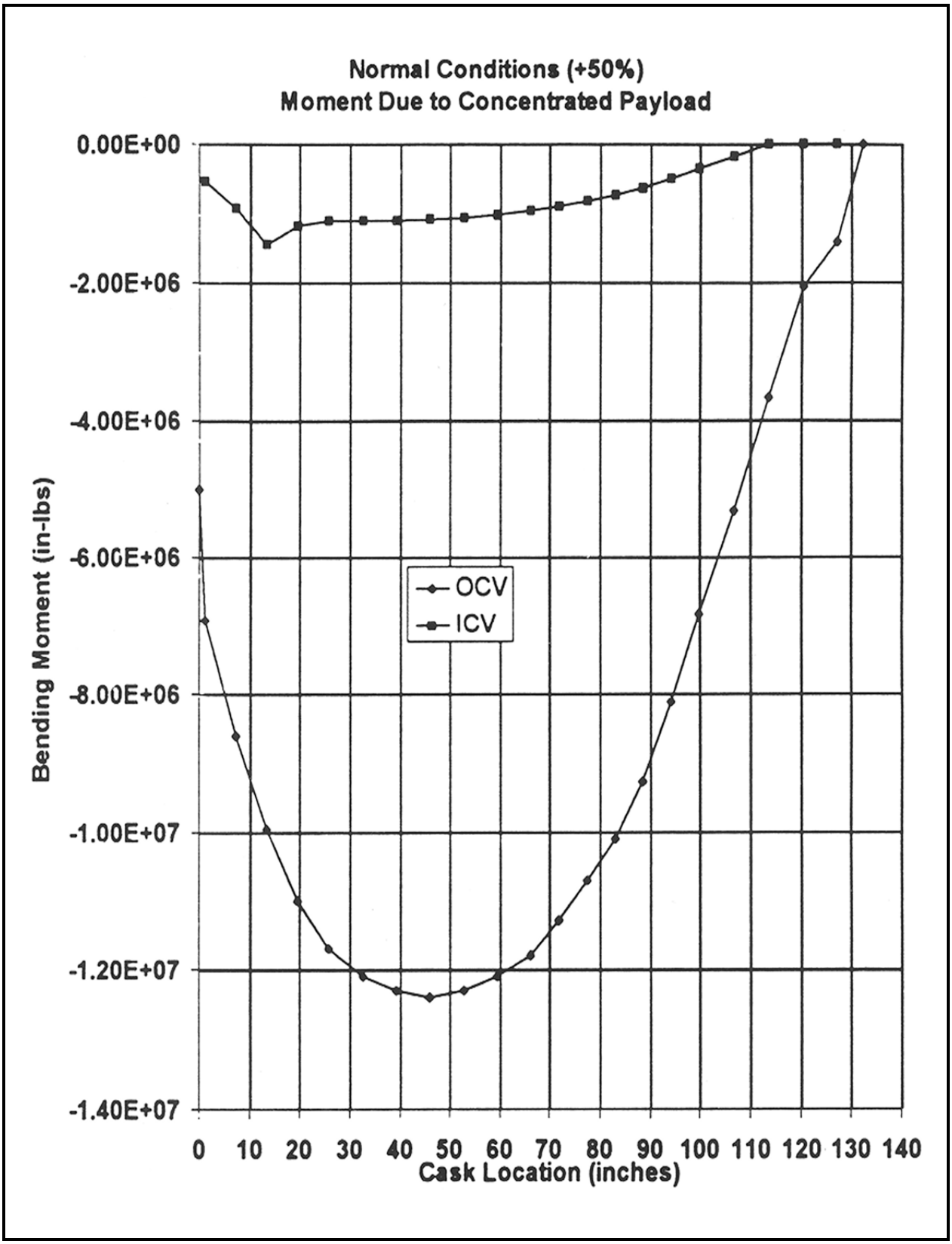

Figure 2.6-22 – NCT Cold (-20 ºF) Moment Due to a Concentrated Payload

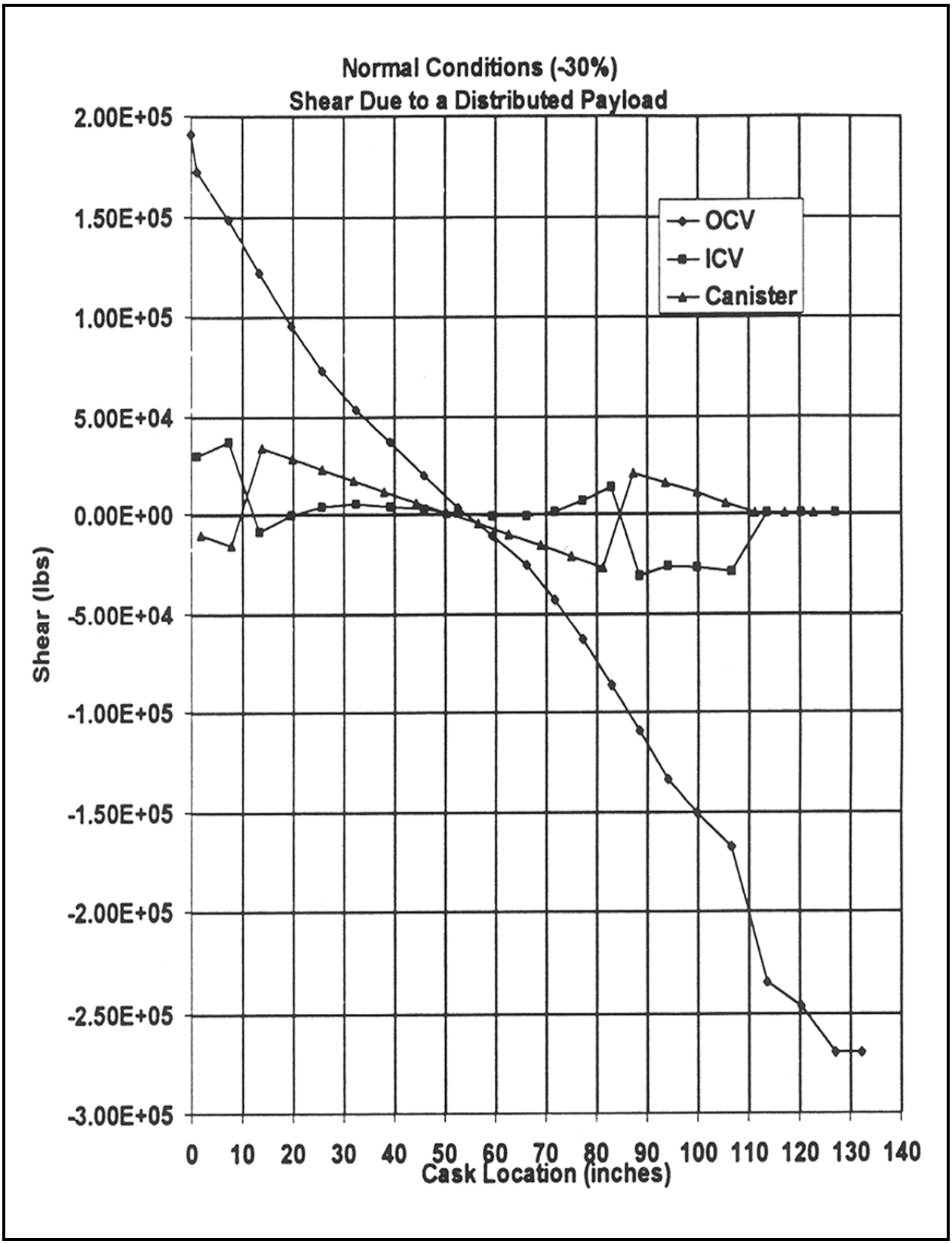

Figure 2.6-23 – NCT Hot (140 ºF) Shear Due to a Distributed Payload

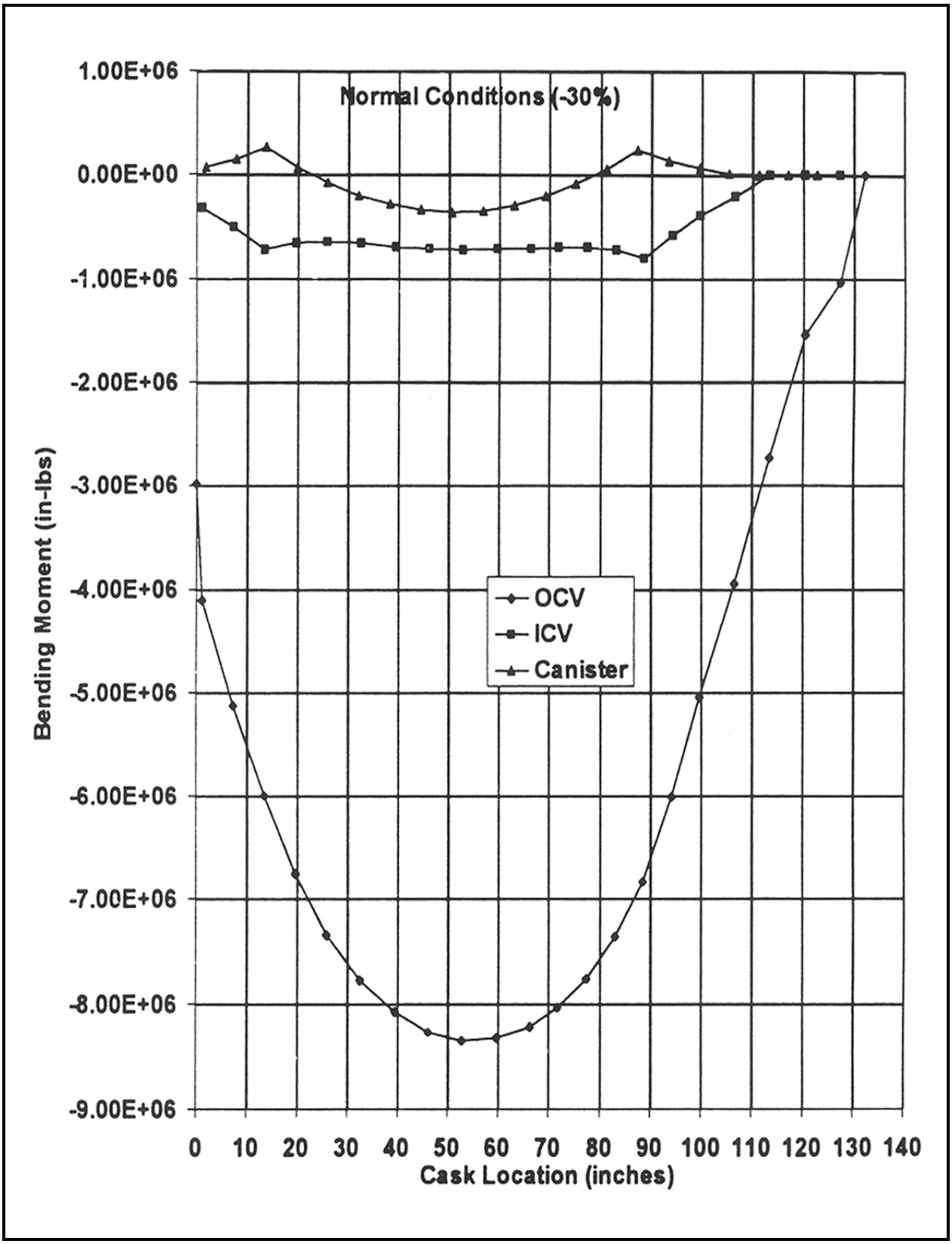

Figure 2.6-24 – NCT Hot (140 ºF) Moment Due to a Distributed Payload

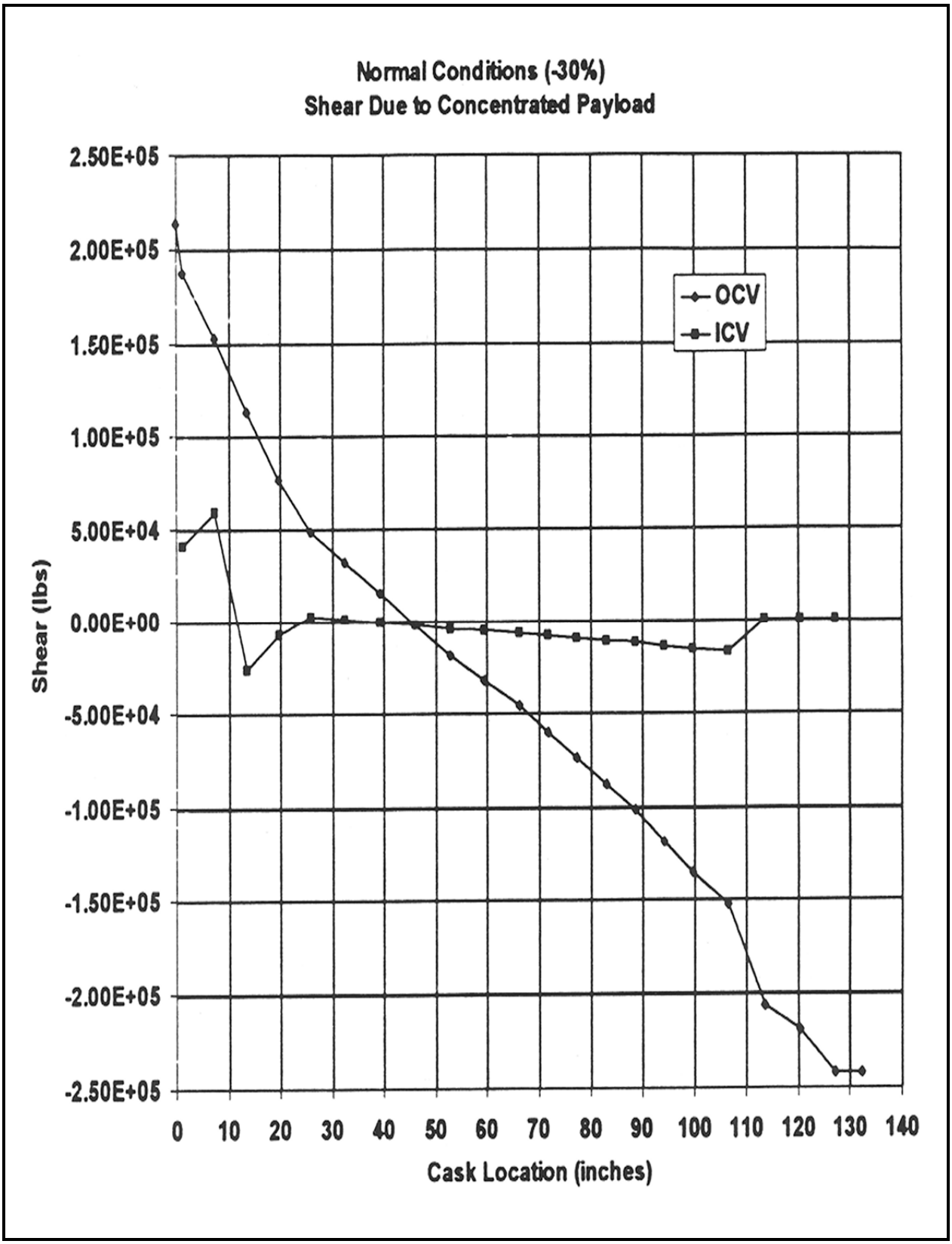

Figure 2.6-25 – NCT Hot (140 ºF) Shear Due to a Concentrated Payload

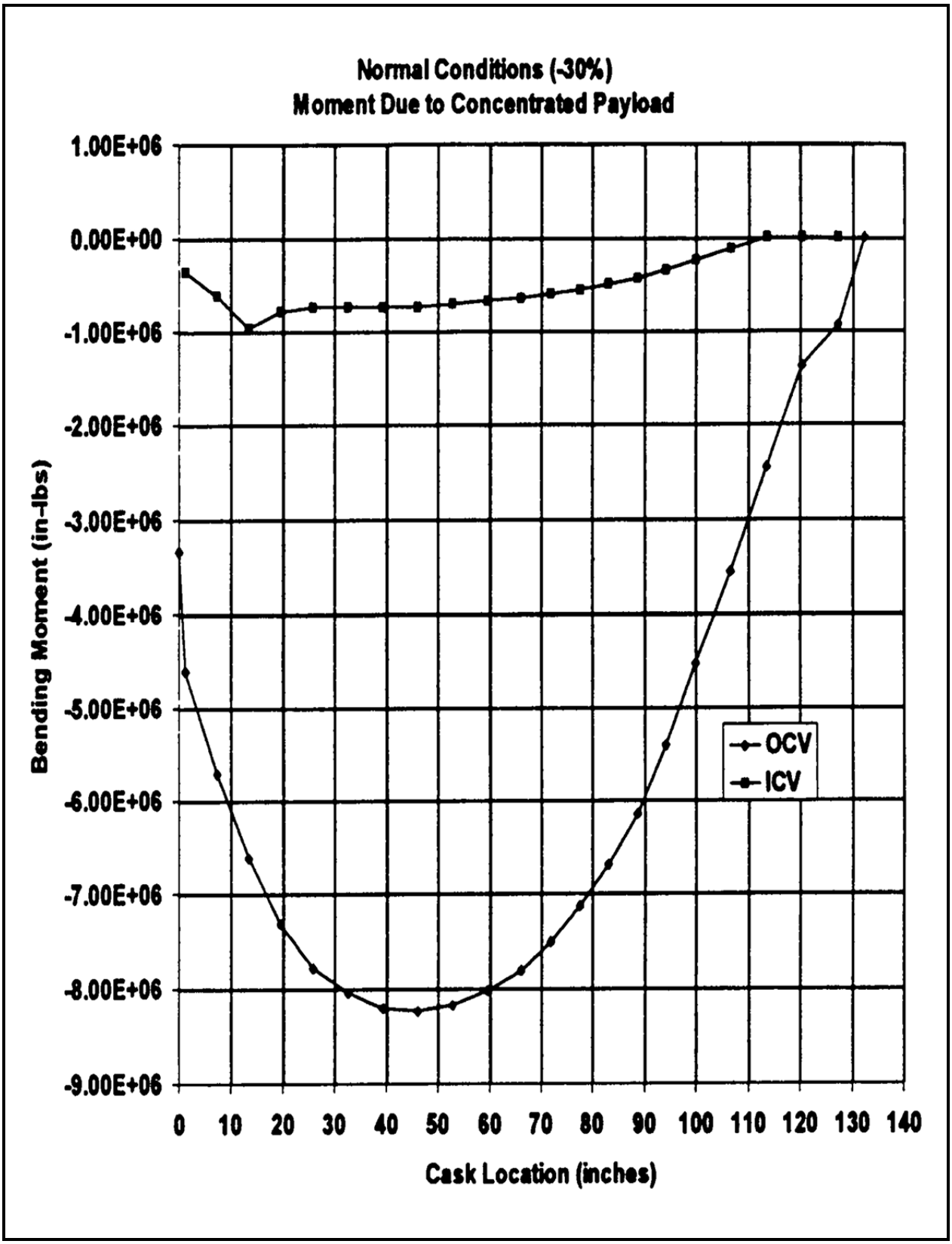

Figure 2.6-26 – NCT Hot (140 ºF) Moment Due to a Concentrated Payload

This page intentionally left blank.

2.7 Hypothetical Accident Conditions

The RH-TRU 72-B package, when subjected to the sequence of hypothetical accident conditions (HAC) as specified in 10 CFR §71.73[1], meets the performance requirements specified in Subpart E of 10 CFR 71. With the exception of buckling, this is demonstrated in the following subsections where each HAC is addressed and shown to meet the applicable design criteria previously discussed in Section 2.1.2, *Design Criteria*. Buckling evaluations for all buckling-sensitive package components are presented in Appendix 2.10.5, *Buckling Design Criteria and Detailed Evaluation*. The structural response of the payload canister is briefly summarized in this section.

2.7.1 Free Drop

Subpart F of 10 CFR 71[1] requires that a 30-foot free drop be considered for the RH-TRU 72-B package. The drop is to be onto a flat, essentially unyielding, horizontal surface, and the package is to strike the surface in a position for which maximum damage is expected. Per 10 CFR §71.73(b)[1], the initial temperature for the free drop is to be the worst-case constant ambient air temperature between -20 ºF and 100 ºF. Internal heat generation from the payload and insolation are also considered when it is conservative to do so. Regarding initial internal pressure, the design pressure of 150 psig must be considered unless a lower internal pressure consistent with the ambient temperature assumed to precede and follow the drop is more unfavorable.

The analyses in this section extract accelerations from impact analysis results summarized in Appendix 2.10.3, *Drop Impact Evaluation Results*, and statically apply them to the package. Static application is justified since the natural frequencies of the package are relatively high and the duration of the impact loadings relatively long. The package frequencies are high as the result of using relatively thick, stiff shells for the outer cask (OC).

The durations of impact loadings are relatively long as the result of using soft (relative to the steel structures) energy absorbing impact limiters to protect the package during free drop events. In addition, inspection of accelerometer data available from the NuPac 125-B quarter-scale drop tests[2] indicates that the package responds essentially as a rigid body (e.g., for end and oblique drops, all accelerometer traces are very nearly the same, and for side drop, the accelerations for all accelerometers oriented in the direction of the drop are nearly identical). This observation further justifies static application of *g*-loads.

2.7.1.1 Flat End Drop

Analysis of RH-TRU 72-B package behavior during the end impact is performed in the following steps:

(1) Analyze the impact force using the CASKDROP computer program.

[1] Title 10, Code of Federal Regulations, Part 71 (10 CFR 71), *Packaging and Transportation of Radioactive Material*, 01-01-14 Edition.

[2] Nuclear Packaging, Inc., *Safety Analysis Report for the NuPac 125-B Fuel Shipping Package*, USNRC Certificate of Compliance 71-9200, U.S. Department of Energy, Washington, D.C.

(2) Analyze the OC lid for bending assuming the inner vessel (IV) and payload canister act as a uniform load on a simply supported plate (no impact limiter support).

(3) Analyze the OC lid for bending, as performed in (2), but with the impact limiter foam pressure acting in the opposite direction (impact limiter support).

(4) Analyze the stresses in the OC lid bolts.

(5) Analyze the IV stresses.

(6) Analyze the axial and hoop stresses in the OC shells and lead (maximum fabrication stress condition assumed).

(7) Analyze the axial and hoop stresses in the OC shells and lead (zero fabrication stress condition assumed).

(8) Analyze the payload canister stresses.

(9) Determine the amount of lead slump.

Material properties and allowable stresses corresponding to maximum enveloping temperatures of 160 ºF for the stainless steel OC and IV, and lead, and 210 ºF for the carbon steel payload canister are given in Table 2.7-1. Buckling is addressed in Appendix 2.10.5, *Buckling Design Criteria and Detailed Evaluation*.

The nine steps of this HAC end drop analysis are carried out in the same fashion as was done for the normal conditions of transport (NCT) end drop analysis presented in Section 2.6.7.1, *Flat End Drop*. In most cases, HAC results can be obtained directly from NCT results by applying the ratio of the maximum HAC *g*-load to the maximum NCT *g*-load. This ratio is 89.7/42.5 = 2.11.

(1) End Drop Computer Analysis Using CASKDROP

The end drop analysis was performed utilizing the energy-balance computer program, CASKDROP, documented in Appendix 2.10.2.1, *Description of the CASKDROP Computer Code*. Two cases were considered assuming fully effective impact limiters and considering the variations in foam strength due to temperature effects and the possible variations in foam strength from nominal values (see Section 2.3, *Mechanical Properties of Materials*). Fully effective impact limiter cases consider the entire impact limiter impact area available for crush. Based on NuPac 125-B quarter-scale test results[2] (i.e., observed impact limiter displacements and package acceleration), the fully effective impact limiter assumption is realistic. Output for each of the two end drop cases is presented in Appendix 2.10.3, *Drop Impact Evaluation Results*. Worst-case deflections and accelerations are utilized for all analyses. From Table 2.10.3-10 of Appendix 2.10.3, *Drop Impact Evaluation Results*, the maximum HAC acceleration and impact limiter deflection for a 30-foot end drop are 89.7*g* (cold foam) and 8.67 inches (hot foam), respectively.

(2) OC Lid Bending Analysis Assuming No Impact Limiter Support

From Paragraph (2) in Section 2.6.7.1, *Flat End Drop*, the maximum OC lid bending stress, σ, for a unit (1*g*) acceleration is 216 psi/*g*. Applying 89.7*g* acceleration, the bending stress is:

$$\sigma = (216)(89.7) = 19{,}375 \text{ psi}$$

Combining this bending stress with the stresses due to a 150-psig internal pressure (1,823 psi bending stress, –150 psi radial stress) results in a stress intensity (SI) of 19,375 + 1,823 + 150 = 21,348 psi.

From Table 2.7-1, the HAC allowable primary membrane-plus-bending stress intensity, S_a = 67,700 psi at 160 ºF for Type F304 stainless steel. Therefore, the OC lid bending stress margin of safety is:

$$MS = \frac{S_a}{SI} - 1 = \frac{67,700}{19,375} - 1 = +2.17$$

(3) OC Lid Bending Analysis Assuming Full Impact Limiter Support

From Paragraph (3) in Section 2.6.7.1, *Flat End Drop*, the maximum OC lid bending stress, σ, for a unit (1*g*) acceleration is 494 psi/*g*. Applying 89.7*g* acceleration, the bending stress is:

$$\sigma = (494)(89.7) = 44,312 \text{ psi}$$

Note that internal pressure would reduce this bending stress; therefore, the stress intensity (SI) is 44,312 psi. From Table 2.7-1, the HAC allowable primary membrane-plus-bending stress intensity, S_a = 67,700 psi at 160 ºF for Type F304 stainless steel. Therefore, the OC lid bending stress margin of safety is:

$$MS = \frac{S_a}{SI} - 1 = \frac{67,700}{44,312} - 1 = +0.53$$

(4) OC Lid Bolt Stresses

OC bolt stresses under end impact conditions are computed and summarized in Table 2.10.6-5 and Table 2.10.6-6 of Appendix 2.10.6, *Closure Bolt Stress Evaluations*. The minimum margin of safety occurs at an impact angle of 85º. For this angle, the maximum deceleration is 90.7*g*. Assuming this deceleration acts on the full weight of the OC lid (1,667 pounds), IV (4,023 pounds), and payload canister (8,000 pounds), the maximum bolt stress intensity is 78,233 psi, assuming uniform loading of the 18 lid bolts. These values include pressure stress effects. This stress conservatively neglects impact limiter reaction forces that would reduce estimated bolt impact stresses to near zero, if considered. From Table 2.7-1, the HAC allowable containment fastener primary membrane-plus-bending stress intensity, S_a = 101,400 psi at 160 ºF for ASTM A320, Grade L43, bolting material. With a total tensile stress of 78,233 psi, the resultant minimum margin of safety is computed as +0.30, in Table 2.10.6-5 of Appendix 2.10.6, *Closure Bolt Stress Evaluations*.

An assessment of OC bolt and thread insert engagement is provided in Appendix 2.10.6, *Closure Bolt Stress Evaluations*, and shown to have a minimum margin of safety of +0.93.

A detailed analysis of the OC lid bolts for various drop angles and torque coefficients is presented in Appendix 2.10.6, *Closure Bolt Stress Evaluations*.

(5) IV Stresses

The IV is designed so that, on end impact, the end closures (lid and bottom plate) will be flush against the end closures of the OC. This will tend to minimize bending stresses in IV end plates. IV analyses are performed for both top-end down and bottom-end down flat end drop.

Top-End Down: From Paragraph (5) in Section 2.6.7.1, *Flat End Drop*, the maximum bottom plate bending stress for a unit (1*g*) acceleration is 62.0 psi/*g*. Applying 89.7*g* maximum acceleration, the bending stress becomes:

$$\sigma = (62.0)(89.7) = 5{,}561 \text{ psi}$$

Note that internal pressure would reduce this bending stress, but is conservatively ignored; therefore, the stress intensity (SI) is 5,561 psi. From Table 2.7-1, the HAC allowable primary membrane-plus-bending stress intensity, S_a = 67,700 psi at 160 ºF for Type F304 stainless steel. Therefore, the IV bottom plate bending stress margin of safety is:

$$MS = \frac{S_a}{SI} - 1 = \frac{67{,}700}{5{,}561} - 1 = +11.2$$

From Paragraph (5) in Section 2.6.7.1, *Flat End Drop*, the maximum IV shell stress for a unit (1*g*) acceleration resulting from the top-end down drop is -54.67 psi/*g*. Applying 89.7*g* maximum acceleration, the membrane stress becomes:

$$\sigma = (-54.67)(89.7) = -4{,}904 \text{ psi}$$

Combining this stress with stresses due to a 150-psig internal pressure (3,162 psi axial membrane, 6,324 psi hoop membrane, and -150 psi radial) results in a stress intensity (SI) of 6,324 – (–4,904 + 3,162) = 8,066 psi.

From Table 2.7-1, the HAC allowable primary membrane stress intensity, S_a = 48,000 psi at 160 ºF for Type 304 stainless steel. Therefore, the IV shell stress margin of safety is:

$$MS = \frac{S_a}{SI} - 1 = \frac{48{,}000}{8{,}066} - 1 = +4.95$$

A detailed buckling analysis for this load combination is presented in Appendix 2.10.5, *Buckling Design Criteria and Detailed Evaluation*.

The IV lid is supported during top-end down end drop by the OC lid, which is of comparable thickness and diameter. Because the OC lid will tend to limit deflections of the IV lid, it may be assumed that the large margins of safety derived for the OC lid in both backed and unbacked bending will be applicable to the IV lid.

Bottom-End Down: For the bottom-end impact, the IV bottom plate will be supported by the OC bottom plate. The IV bottom-end closure is of approximately the same diameter, yet of significantly smaller thickness than the OC end closure. The IV bottom plate will therefore see lower stresses than the OC bottom plate when forced into the OC bottom plate. This is because the OC closure will limit deflections of the IV closure, thereby assuring margins of safety in excess of the already conservative values presented for the OC closures.

From Paragraph (5) in Section 2.6.7.1, *Flat End Drop*, the maximum IV shell stress for a unit (1*g*) acceleration resulting from the bottom-end down drop is -98.47 psi/*g*. Applying 89.7*g* maximum acceleration, the membrane stress becomes:

$$\sigma = (-98.47)(89.7) = -8{,}833 \text{ psi}$$

Combining this stress component with those due to a 150-psig internal pressure (3,162 psi axial membrane, 6,324 psi hoop membrane, and -150 psi radial) results in a stress intensity (SI) of 6,324 – (-8,833 + 3,162) = 11,995 psi.

From Table 2.7-1, the HAC allowable primary membrane stress intensity, S_a = 48,000 psi at 160 ºF for Type 304 stainless steel. Therefore, the IV shell stress margin of safety is:

$$MS = \frac{S_a}{SI} - 1 = \frac{48{,}000}{11{,}995} - 1 = +3.00$$

A detailed buckling analysis for this load combination is presented in Appendix 2.10.5, *Buckling Design Criteria and Detailed Evaluation*.

From Paragraph (5) in Section 2.6.7.1, *Flat End Drop*, the maximum IV lid bending stress for a unit (1*g*) acceleration resulting from the bottom-end down drop is 12.9 psi/*g*. Applying the 89.7 g's acceleration results in:

$$\sigma = (12.9)(89.7) = 1{,}157 \text{ psi}$$

Internal pressure would reduce this bending stress, but is conservatively ignored. From Table 2.7-1, the HAC allowable primary membrane-plus-bending stress intensity, S_a = 67,700 psi at 160 ºF for Type F304 stainless steel. Therefore, the minimum IV lid bending stress margin of safety, MS, is:

$$MS = \frac{S_a}{\sigma} - 1 + \frac{67{,}700}{1{,}157} - 1 = +61.2$$

Per Table 2.10.6-7 and Table 2.10.6-8 of Appendix 2.10.6, *Closure Bolt Stress Evaluations*, the maximum total IV bolt tensile stress is estimated at 53,737 psi, including pressure and preload effects. It should be observed that no impact loads are applied to IV bolts since loads are directly transferred to the OC lid in direct compression. This stress of 53,737 psi results in a margin of safety of +0.89 based on an allowable, S_a = 101,400 psi. It should be noted that the estimated stress includes a preload stress of 51,840 psi (21,099 lbs/0.407 in^2). In conventional bolting analyses, per established codes (e.g., American Institute of Steel Construction and Appendix F, Section III, of the ASME Boiler and Pressure Vessel Code), preload effects are neglected when assessing the capacity of a bolted connection. This conclusion is because preloads have little effect upon the ultimate capacity of a bolted connection[3]. Thus, the reported margin of safety is extraordinarily conservative, when compared with the methodology of conventional codes.

An assessment of IV bolt and thread insert engagement is provided in Appendix 2.10.6, *Closure Bolt Stress Evaluations*, and shown to have a minimum margin of safety of +1.79.

A detailed analysis of the IV lid bolts for various drop angles and torque coefficients is presented in Appendix 2.10.6, *Closure Bolt Stress Evaluations*.

(6) Stresses in the OC Shells and Lead (Maximum Fabrication Stress Condition Assumed)

The principal concern for the OC under HAC end drop conditions is with buckling of the inner shell. As shown by the following stress calculations and the detailed buckling evaluation presented in Appendix 2.10.5, *Buckling Design Criteria and Detailed Evaluation*, buckling will

[3] Joseph E. Shigley and Larry D. Mitchell, *Mechanical Engineering Design*, 4th Edition, McGraw-Hill, 1983.

not occur as the result of the hoop and axial compressive stresses that develop in the OC inner shell under HAC end drop conditions.

Various initial conditions can be assumed for the HAC end drop event. In particular, a temperature must be assumed in order to establish an initial fabrication stress for the inner shell. A lower assumed temperature will result in a higher initial hoop stress on the inner shell (see Section 2.6.2, *Cold*), but higher allowable stresses. For purposes of this analysis, drops at 160 ºF (conservatively bounding the maximum lead and OC shells normal temperatures per Section 3.4.2, *Package Conditions and Environment*), 70 ºF, and -20 ºF are considered. Regardless of temperature, the maximum *g*-load of 89.7*g* for the -20 ºF drop case is conservatively employed.

To adequately bound the consequences of the drop event at a given temperature, two initial lead conditions are also considered. The first assumes that the lead has shrunk onto the inner shell and away from the outer shell. In addition, due to the combined effects of friction between the lead and inner shell, and axial shrinkage of the lead relative to the stainless shells, axial gaps will develop between the lead and the steel structures at the top and bottom end of the lead column. These axial gaps are important in that, until friction is overcome, under increased axial loading, the lead will impose a direct axial load on the inner shell. Once friction is overcome, the lead will become supported at its base (the bottom of the lead column) and will grow radially outward due to the "Poisson effect" under increased axial loading. This radial growth will tend to relieve the initial fabrication hoop stress as the lead separates from the inner shell. If sufficient axial load develops, the lead would grow out to the outer shell creating tensile hoop stresses therein, and under further loading would eventually flow back inward into the inner shell, thereby developing compressive hoop stresses in the inner shell.

From Appendix 2.10.8, *Fabrication Stresses Due to Lead Pour*, the hoop stress in the inner shell due to fabrication is -1,413 psi at 70 ºF, and -1,821 psi at -20 ºF. Extrapolating, the hoop stress in the inner shell is -1,038 psi at 160 ºF. (Note that the outer shell hoop stress is considered to be negligible since the lead separates from the outer shell upon cooling.)

The equivalent pressure at the lead/inner shell interface, p, is:

$$p = \frac{\sigma t}{r}$$

where the shell thickness, t = 1.00 inch, and the shell radius, r = 16.69 inches. Therefore, the interface pressure is 62.2 psi at 160 ºF, 84.7 psi at 70 ºF, and 109.1 psi at -20 ºF.

With a coefficient of friction, *f*, for lead on stainless steel assumed to fall in the 0.5 to 1.0 range[4], the load, P, that can be supported by friction at the lead/inner shell interface, may be determined as follows:

$$P = \pi DLpf$$

where inner shell outside diameter, D = 34.38 inches, the lead column height, L = 123.5 inches, the interface pressure is p, and the coefficient of friction, $f = 0.5 – 1.0$.

Applying the above interface pressures, the total axial load that may be supported for each case is provided in Table 2.7-2.

[4] Theodore Baumeister, *Mark's Standard Handbook for Mechanical Engineers*, Ninth Edition, McGraw-Hill Book Company, New York, NY, 1987, Table 3.2.1.

With the total lead weight equal to 10,739 pounds, per Table 2.2-1 in Section 2.2, *Weights and Centers of Gravity*, the minimum *g*-load that can be supported by friction is 414,842/10,739 = 38.6*g*. The maximum *g*-load that can be supported by friction is 1,455,283/10,739 = 135.5*g* (-20 ºF with friction coefficient of 1.0). Since end drop *g*-loads range from 51.1*g* at the maximum foam temperature of 140 ºF to 89.7*g* at the minimum foam temperature of -20 ºF, lead slippage may or may not occur. The following analysis assumes no slippage for the HAC 89.7*g* load. This assumption conservatively maximizes loading on the inner shell. Axial stress in the OC inner and outer shells are therefore determined by ratioing the NCT end drop results available in Paragraph (6) of Section 2.6.7.1, *Flat End Drop*, by a factor of 89.7/42.5 = 2.11. Table 2.7-3 summarizes the axial and hoop stress results.

Table 2.7-4, Table 2.7-5, and Table 2.7-6 present the corresponding margins of safety for the more critical inner shell at temperatures of -20 ºF, 70 ºF, and 160 ºF, respectively. Zero internal pressure is used in order to maximize compressive stresses in the inner shell. Note that axial stresses will actually decrease with increasing drop temperature since *g*-loads are lower at higher temperatures (due to decreased foam strength with increased temperature). This effect is conservatively ignored in Table 2.7-4, Table 2.7-5, and Table 2.7-6.

Buckling is addressed in Appendix 2.10.5, *Buckling Design Criteria and Detailed Evaluation*.

(7) Stresses in the OC Shells and Lead (Zero Fabrication Stress Condition Assumed)

The second initial lead condition assumes that the fabrication stress has fully crept away resulting in a stress free column of lead just in contact with the OC inner and outer shells. This is a potential worst case since any axial load imposed on the lead will directly load, radially, both the inner and outer shells (i.e., the lead need not flow away from the inner shell, into the outer shell and back into the inner shell to develop a compressive hoop stress in the inner shell).

For this condition, initial stresses in the lead and the steel shells are taken as zero. As axial load is applied to the lead and shells, the lead will attempt to move downward and outward and develop pressures on both the inner and outer shells, as shown in Figure 2.6-5 in Paragraph (7) of Section 2.6.7.1, *Flat End Drop*.

For the purpose of this analysis, let $p_i = p_o = p$. This assumption is considered reasonable once lead starts to flow.

Conservatively assuming that the lead receives no axial support at its base, but rather is supported solely by friction at the inner and outer shells, the maximum value of the pressure, p_{max}, is determined based on a lead weight, W_L = 10,739 pounds, being acted on by an end drop acceleration, $\eta = 89.7g$, resulting in a total lead force, w_L, of:

$$w_L = \eta W_L = 963{,}288 \text{ lb}$$

For the maximum pressure, p_{max}, use the minimum expected coefficient of friction, $f = 0.5$, resulting in a force, w, of:

$$w = p_{max}(2\pi r_L)(L - d)\, f$$

where the mean lead shell radius, $r_L = \frac{1}{2}(r_o^2 + r_i^2) = 18.1275$ inches, the lead shell outer radius, $r_o = 19.065$ inches, the lead shell inner radius, $r_i = 17.19$ inches, and the shell length, L = 123.5 inches. Letting $w = w_L = 963{,}288$ pounds, the maximum pressure, p_{max}, is:

$$p_{max} = \frac{16{,}915}{(123.5 - d)} \text{ psi}$$

Assuming lead flow initiates at the yield strength of the lead, σ_y, the height of the lead column, d, required to yield the lead cross-section due to the 89.7*g* HAC acceleration is:

$$\sigma_y = \rho d(89.7g)$$

where σ_y is lead's yield strength at temperature, and the lead density, $\rho = 0.41$ lb/in^3. Therefore:

$$d = (0.02719)\sigma_y$$

For lead temperatures of 160 ºF, 70 ºF, and -20 ºF, and conservatively estimating an upper bound on the lead properties delineated in Figure 2.3-3 through Figure 2.3-6 of Section 2.3, *Mechanical Properties of Materials*, the pressures and hoop stresses may be summarized as shown in Table 2.7-7.

The maximum axial stress in the shells is determined by multiplying the results available from Paragraph (7) of Section 2.6.7.1, *Flat End Drop*, by the ratio of HAC-to-NCT end drop *g*-loads. The resultant stresses in the OC inner and outer shells for the HAC end drop load of 89.7*g* are summarized in Table 2.7-8.

Table 2.7-9, Table 2.7-10, and Table 2.7-11 present the corresponding margins of safety for the more critical inner shell. Zero internal pressure is used in order to maximize compressive stresses in the inner shell. Again, it is noted that the margins presented for the 70 ºF and 160 ºF cases are conservative since at these temperatures, *g*-loads will actually be less than the 89.7*g* conservatively considered. Buckling is addressed in Appendix 2.10.5, *Buckling Design Criteria and Detailed Evaluation*.

(8) Discussion of Payload Canister Behavior in End Drop

Hoop and axial stresses in the canister are addressed for the thirty-foot HAC end drop condition. Stresses resulting due to a 1*g* load, from Paragraph (8) of Section 2.6.7.1, *Flat End Drop*, are scaled by the 89.7*g* HAC drop loading. The payload canister shell hoop stress due to a 1*g* load is 225.1 psi, and the axial stress due to a 1*g* load is 87.14 psi.

The HAC end drop hoop (σ_h) and axial (σ_a) stresses are:

$$\sigma_h = (225.1)(89.7) = 20{,}191 \text{ psi (tension)}$$
$$\sigma_a = (87.14)(89.7) = 7{,}816 \text{ psi (compression)}$$

The maximum canister shell stress intensity (SI) is therefore, 20,191 + 7,816 = 28,007 psi. From Table 2.7-1, the HAC allowable primary membrane stress intensity, S_a = 38,500 psi at 210 ºF using worst-case ASTM A516, Grade 55, carbon steel as the material of construction (conservative maximum canister temperature; see Table 2.6-2 in Section 2.6, *Normal Conditions of Transport*). Therefore, the margin of safety (MS) for the payload canister shell is:

$$MS = \frac{S_a}{SI} - 1 = \frac{38{,}500}{28{,}007} - 1 = +0.37$$

(9) Lead Slump

Lead slump for the RH-TRU 72-B package is negligible. The lack of slump is directly attributable to the presence of relatively "soft" impact limiters at the ends of the RH-TRU 72-B package. Because of these "soft" limiters, it can be shown that the resultant accelerations associated with free end drops of the package are insufficient for the stress in the lead to reach its minimum flow stress magnitude as established in the *Cask Designers Guide*[5]. As such, direct use of the *Cask Designers Guide* formula for lead slump would be overly conservative for the case of the RH-TRU 72-B package because the formula is specifically based on the drop of a bare, unprotected package. However, as shown below, the concept of a lead flow stress, as used in the lead slump formula, can be utilized to establish that no lead slump will occur for the RH-TRU 72-B package.

For example, using the maximum Hypothetical Accident Condition (HAC) end drop impact acceleration, g = 89.7, applicable to the RH-TRU 72-B as available from Table 2.10.3-10, maximum stress at the bottom end of the lead column, σ, can be readily determined from the following formula where ρ = density of lead = 0.41 lb/in^3 (Table 2.3-2 note 6) and h = lead column height = 124.25 inches per the SAR drawings.

$$\sigma = \rho(g)(h) = 0.41(89.7)(124.25) = 4{,}570 \text{ psi}$$

Missing from the above calculation is a consideration of the potential affect of temperature on lead slump. Although it is not overtly stated in the *Cask Designers Guide*, it is reasonably assumed that the 5,000 psi minimum lead flow stress value corresponds to room temperature, or 70 ºF. It is further assumed that flow stress magnitude will vary with temperature in a manner similar to how lead compressive strength varies with temperature. With reference to Figure 2.3-6, by linearly extrapolating and interpolating the 100 ºF and 175 ºF curves at 4% strain, it can be shown that at -20 ºF, lead strength is approximately 27% greater than at 70 ºF and, at 160 ºF (upper bound temperature for lead per Section 2.6.1.1), lead strength is approximately 27% less than at 70 ºF. Applying these adjustments to the room temperature lead flow stress of 5,000 psi results in flow stresses of 6,350 psi at -20 ºF and 3,650 psi at 160 ºF. Table 2.7-12 establishes HAC end drop lead stresses at these minimum and maximum temperature extremes. As shown, at both extremes, lead stresses remain well below the temperature-adjusted flow stress magnitudes with the smallest margin of safety being for the -20 ºF condition. Table 2.7-12 establishes the primary basis for why lead slump will not occur for the RH-TRU 72-B package.

As previously noted in Paragraph (9) of Section 2.6.7.1, *Flat End Drop*, lead slump of the NuPac 125-B cask[2] (NRC Certificate of Compliance 71-9200) is expected to bound lead slump of the RH-TRU 72-B package. Quarter-scale testing of the NuPac 125-B cask showed no measurable lead slump due to the 30-foot end drop at -20 °F. This provides additional validation of the conclusion that lead slump will not occur for the RH-TRU 72-B package as a result of the HAC, 30-foot end drop.

[5] L. B. Shappert, *Cask Designers Guide, A Guide for the Design, Fabrication, and Operation of Shipping Casks for Nuclear Applications*, ORNL-NSIC-68, Oak Ridge National Laboratory, Oak Ridge, Tennessee, February 1970.

2.7.1.2 Corner and Oblique Drops

Analysis of the RH-TRU 72-B package behavior during the HAC corner drop, including oblique drop orientations, uses the same methods as those used for the NCT corner drop. HAC corner and oblique drops lead to the possibility of a secondary impact, or slapdown, of the package on the end opposite the initially impacted end. This possibility is addressed in Appendix 2.10.4, *Slapdown Assessment*. In that section, the consequences of slapdown are shown to be less severe for the RH-TRU 72-B package than those associated with a flat side drop from a height of 30 feet. For this reason, slapdown is not a limiting case for the package and is not further addressed in this section.

Analysis of RH-TRU 72-B package behavior during the corner drop event, including oblique drop orientations, is performed in the following steps:

(1) Determine the force-deflection relations for a range of initial impact angles, using the CASKDROP computer program. Utilize the force-deflection data from CASKDROP as input to the computer program SLAPDOWN to determine the package response for various initial impact angles.

(2) Based on the accelerations and rotations predicted in (1), determine the equivalent "static" forces on the OC and IV, considered as a rigid body with distributed and lumped masses.

(3) Based on the loads from (2), analyze the OC shells and IV as simple beams, finding the internal forces: shear, moment, and thrust. Compute stresses for the maximum value of each of these forces, and by inspection of the relative magnitudes of these maximum component stresses, select load cases for further analysis which will have the maximum combined stresses.

(4) Analyze the OC shells for stress, assuming the two shells act as parallel beams, under the loads determined in (3).

(5) Analyze the IV for stress under the loads determined in (3).

(6) Analyze the payload canister for stress under the loads determined in (3).

(7) Analyze impact limiter attachment forces.

(8) Based on the forces from (7), calculate the impact limiter attachment stresses.

(9) Analyze the stresses in the OC and IV lid bolts.

(10) Calculate the maximum impact limiter deformations and residual clearances for package hard spots.

Material properties and allowable stresses corresponding to the maximum enveloping temperature of 160 ºF for the Type 304 stainless steel OC and IV and lead are given in Table 2.7-1. Buckling is addressed in Appendix 2.10.5, *Buckling Design Criteria and Detailed Evaluation*.

(1) Corner Drop Computer Analysis (CASKDROP and SLAPDOWN)

Analytic predictions of package performance for drop orientations impacting upon the corner of the package employ two computer programs: CASKDROP and SLAPDOWN, documented in Appendix 2.10.2, *Drop Analysis Codes Description*. CASKDROP uses an energy-balance technique to determine loads and deformations of the impact limiter. Since CASKDROP assumes all drop energy is absorbed in deformation of the impact limiter, it provides valid results when the impact orientation places the center-of-gravity (CG) directly over the impacted corner,

approximately 68º from the horizontal for the RH-TRU 72-B package. At other impact orientations, the force-deflection values generated by CASKDROP are used in SLAPDOWN, a dynamic analysis program that considers rotational motion effects. For initial impact angles between the CG-over-corner and vertical, dynamic effects (such as a secondary slapdown) are negligible, and results at the upper, or secondary impact limiter are unimportant. For such cases, CASKDROP is used to conservatively calculate the primary impact results.

Two (2) cases were run which accounted for variations in foam strength due to temperature effects and the possible variations in foam strength from nominal values (see Section 2.3, *Mechanical Properties of Materials*). Detailed output for each of the two analysis cases is presented in Appendix 2.10.3, *Drop Impact Evaluation Results*. Note that the load and stress evaluations presented in this section are typically based on the results from the -20 ºF foam stress case. Impact limiter responses (i.e., attachment forces, deformations, and residual clearances) presented herein directly consider both analytic cases.

(2) Equivalent "Static" Loads:

Equivalent static loads acting on the RH-TRU 72-B package as the result of a HAC corner/oblique drop are determined in exactly the same manner as for the NCT corner/oblique drop (see Paragraph (2) in Section 2.6.7.2, *Corner and Oblique Drops*).

Slapdown impacts are not governing, as shown in Appendix 2.10.4, *Slapdown Assessment*. The only potentially serious slapdown loading problem will affect package impact limiter attachment fastener and OC lid fastener integrity. These load cases are addressed in Paragraphs (7) and (9) , below.

(3) Internal Forces

The OC shells are analyzed as if they are two beams acting in parallel. The payload canister is analyzed as one beam attached to the IV at the two spacer disk locations, and the IV connects to the OC via a series of interface (gap) elements. A schematic representation of the finite element analysis model used is presented as Figure 2.10.1-9 in Appendix 2.10.1.4, *Containment Assembly Analysis for Oblique Drops*.

Maximum stresses are given as functions of impact angle for the cold foam (-20 ºF) conditions in Figure 2.7-1, Figure 2.7-2, and Figure 2.7-3 for the OC, IV, and payload canister, respectively, based on maximum thrust, shear, and bending moment given in Figure 2.7-4, Figure 2.7-5, and Figure 2.7-6, respectively. The stresses shown in Figure 2.7-1, Figure 2.7-2, and Figure 2.7-3 were calculated using slightly different *g*-loadings than those found in Appendix 2.10.3, *Drop Impact Evaluation Results*. A comparison of the *g*-loading from Appendix 2.10.3, *Drop Impact Evaluation Results* for the HAC cold free drop and those data used in calculating the peak stresses is presented in Figure 2.7-7. Since the *g*-loads match closely for all the orientations considered here, scaling of the previously calculated stresses is an appropriate method for evaluating package components.

In a similar manner, the values from Figure 2.7-8, Figure 2.7-9, and Figure 2.7-10, showing the maximum stresses for the OC, IV, and payload canister, respectively, for hot foam (140 ºF) conditions are also scaled accordingly, based on maximum thrust, shear, and bending moment given in Figure 2.7-11, Figure 2.7-12, and Figure 2.7-13.

The stresses are computed as follows:

$$S_t = \frac{P}{A} \times \frac{g_{new}}{g_{old}} = \text{stress due to thrust, psi}$$

$$S_v = \frac{V}{A} \times \frac{g_{new}}{g_{old}} = \text{stress due to shear, psi}$$

$$S_m = \frac{Mc}{I} \times \frac{g_{new}}{g_{old}} = \text{stress due to bending moment, psi}$$

where P is the thrust force (lb), V is the shear force (lb), and M is the bending moment (in-lb). The distance to the neutral axis, c = 20.565 inches for the OC outer shell, c = 17.19 inches for the OC inner shell, c = 16.00 inches for the IV shell, and c = 13.00 inches for the payload canister. The moment of intertia, I = 51,334 in^4 for the OC, I = 4,718 in^4 for the IV, and I = 1,676 in^4 for the payload canister. Finally, the area, A = 292 in^2 for the OC, A = 38 in^2 for the IV, and A = 20 in^2 for the payload canister.

From Figure 2.7-1, it can be deduced that a 5º impact angle with cold foam (-20 ºF), yields the worst stresses for the OC. Similarly, from Figure 2.7-2 and Figure 2.7-3, it can be deduced that a 5º impact angle with cold foam also yields the worst stresses for the IV and payload canister. Although the maximum thrust, shear, and bending moment do not occur at the same location for each component, the true maximums are used to provide a conservative analysis. The figures are based on a *g*-load of 32.2*g*, whereas the impact of a 5º angle is 48.1*g*. The scale factor is therefore 48.1/32.2 = 1.49.

For the OC, these maximums are P_{max} = 30,366 × 1.49 = 45,245 pounds, V_{max} = 939,900 × 1.49 = 1,400,451 pounds, and M_{max} = 34,873,000 × 1.49 = 51,960,770 in-lb. For the IV, the maximums are P_{max} = 2,596 × 1.49 = 3,868 pounds, V_{max} = 191,350 × 1.49 = 285,112 pounds, and M_{max} = 4,260,000 × 1.49 = 6,347,400 in-lb. Finally, for the payload canister, the maximums are P_{max} = 12,107 × 1.49 = 18,039 pounds, V_{max} = 163,610 × 1.49 = 243,779 pounds, and M_{max} = 1,992,000 × 1.49 = 2,968,080 in-lb.

(4) OC Stresses

The maximum membrane stress in the OC inner shell, for the load case selected in Paragraph (3), is:

$$S_m = \frac{Mc}{I} + \frac{P}{A} = \frac{(51{,}960{,}770)[17.19 - (½)(1.0)]}{51{,}334} + \frac{45{,}245}{292} = 17{,}049 \text{ psi}$$

The maximum membrane-plus-bending stress in the OC inner shell is:

$$S_{mb} = \frac{Mc}{I} + \frac{P}{A} = \frac{(51{,}960{,}770)(17.19)}{51{,}334} + \frac{45{,}245}{292} = 17{,}555 \text{ psi}$$

Similarly, the maximum stresses in the OC outer shell are:

$$S_m = \frac{Mc}{I} + \frac{P}{A} = \frac{(51{,}960{,}770)[20.565 - (½)(1.5)]}{51{,}334} + \frac{45{,}245}{292} = 20{,}212 \text{ psi}$$

$$S_{mb} = \frac{Mc}{I} + \frac{P}{A} = \frac{(51{,}960{,}770)(20.565)}{51{,}334} + \frac{45{,}245}{292} = 20{,}971 \text{ psi}$$

In addition, shear stress must be added in the calculation of the membrane stress intensities for the OC inner and outer shells. The shear stress is:

$$S_v = \frac{V}{A} = \frac{1{,}400{,}451}{292} = 4{,}796 \text{ psi}$$

Axial fabrication stresses used in the oblique drop analyses are scaled from those used in the end drop analysis (see Table 2.6-12 from Section 2.6.7.1, *Flat End Drop*) using the respective *g*-loadings of the package (48.1/42.5). Fabrication stresses for the oblique drop analyses are given in Table 2.7-13.

Table 2.7-14, Table 2.7-15, and Table 2.7-16 present the corresponding margins of safety for the more critical OC inner shell. Zero internal pressure is used in order to maximize compressive stresses in the OC inner shell. Again, note that the margins presented for the 70 ºF and 160 ºF cases are conservative in that at these temperatures, *g*-loads will actually be less than the 48.1*g* conservatively considered herein.

(5) IV Stresses

The maximum membrane stress in the IV shell, for the load case selected in Paragraph (3), is:

$$S_m = \frac{Mc}{I} + \frac{P}{A} = \frac{(6{,}347{,}400)\left[16.00 - (½)(0.38)\right]}{4{,}718} + \frac{3{,}868}{38} = 21{,}372 \text{ psi}$$

The maximum membrane-plus-bending stress in the IV shell is:

$$S_{mb} = \frac{Mc}{I} + \frac{P}{A} = \frac{(6{,}347{,}400)(16.00)}{4{,}718} + \frac{3{,}868}{38} = 21{,}628 \text{ psi}$$

In addition, shear stress must be added in the calculation of the membrane stress intensity for the IV shell. The shear stress is:

$$S_v = \frac{V}{A} = \frac{285{,}112}{38} = 7{,}503 \text{ psi}$$

Table 2.7-17 presents stress and margin of safety results for the IV for the worst-case load combination.

(6) Discussion of Payload Canister Behavior in Oblique Drops

The maximum membrane stress in the payload canister shell, for the load case selected in Paragraph (3), is:

$$S_m = \frac{Mc}{I} + \frac{P}{A} = \frac{(2{,}968{,}080)\left[13.00 - (½)(0.25)\right]}{1{,}676} + \frac{18{,}039}{20} = 23{,}703 \text{ psi}$$

The maximum membrane-plus-bending stress in the payload canister shell is:

$$S_{mb} = \frac{Mc}{I} + \frac{P}{A} = \frac{(2{,}968{,}080)(13.00)}{1{,}676} + \frac{18{,}039}{20} = 23{,}924 \text{ psi}$$

In addition, shear stress must be added in the calculation of the membrane stress intensity for the payload canister shell. The shear stress is:

$$S_v = \frac{V}{A} = \frac{243{,}779}{20} = 12{,}189 \text{ psi}$$

Table 2.7-18 presents stress and margin of safety results for the canister shell for the worst load combination. Buckling is addressed in Section 2.1.2.2.3, *Buckling*.

(7) Impact Limiter Attachment Forces

The maximum HAC impact limiter attachment moment, $2.76(10)^6$ in-lb, is given in Table 2.10.3-13 of Appendix 2.10.3, *Drop Impact Evaluation Results*. The NCT analysis given in Paragraph (7) of Section 2.6.7.2, *Corner and Oblique Drops*, addressed a $2.16(10)^6$ in-lb moment, resulting in a 25,472-pound maximum attachment force. By ratio, the maximum HAC attachment force is 32,548 pounds.

(8) Impact Limiter Attachment Stresses

The tensile stress area of a 1¼-7UNC bolt of 0.969 in^2 exceeds the cross-sectional area of the 1.0-inch diameter shaft (A = 0.785 in^2). Therefore, maximum impact limiter attachment bolt stress is:

$$S_B = \frac{P_{max}}{A} = \frac{32{,}548}{0.785} = 41{,}462 \text{ psi}$$

From Table 2.7-1, the HAC allowable non-containment fastener primary membrane stress intensity, S_a = 101,400 psi at 160 ºF for ASTM A320, Grade L43, bolting material. Therefore, the impact limiter attachment bolt margin of safety is:

$$MS = \frac{S_a}{S_B} - 1 = \frac{101{,}400}{41{,}462} - 1 = +1.45$$

From Paragraph (8) of Section 2.6.7.2, *Corner and Oblique Drops*, a 32,448 psi bolt stress corresponds to a shear stress in the internal threads of the thread insert equal to 4,944 psi. For the 41,462 psi HAC bolt stress, the corresponding shear stress, τ = 6,317 psi.

From Table 2.7-1, the HAC allowable shear stress for the internal threads, S_a = 28,400 psi at 160 ºF, conservatively using Type F304 stainless steel. Therefore, the margin of safety is:

$$MS = \frac{S_a}{\tau} - 1 = \frac{28{,}400}{6{,}317} - 1 = +3.50$$

From Paragraph (8) of Section 2.6.7.2, *Corner and Oblique Drops*, a 32,448 psi bolt stress corresponds to a shear stress in the external threads of the insert equal to 3,657 psi. For the 41,462 psi accident condition bolt stress, the corresponding shear stress, τ = 4,673 psi.

From Table 2.7-1, the HAC allowable shear stress for the external threads, S_a = 28,400 psi at 160 ºF for Type F304 stainless steel. Therefore, the margin of safety is:

$$MS = \frac{S_a}{\tau} - 1 = \frac{28{,}400}{4{,}673} - 1 = +5.08$$

(9) Stresses in the OC and IV Lid Bolts

This evaluation directly parallels the analysis and rationale of that used for NCT, as discussed in Paragraph (9) of Section 2.6.7.2, *Corner and Oblique Drops*.

(a) Stresses in the OC Lid Bolts

Comprehensive analysis of all oblique orientations is summarized in Table 2.10.6-5 and Table 2.10.6-6 of Appendix 2.10.6, *Closure Bolt Stress Evaluations*. The minimum margin of safety is found at a near-vertical orientation of 85º with respect to horizontal. At this orientation angle, direct tensile stress due to impact, pressure effects, and preload effects is estimated at 78,219 psi. The associated shear stress is 756 psi. From Table 2.7-1, the HAC allowable containment fastener primary membrane stress intensity, S_a = 101,400 psi at 160 ºF for ASTM A320, Grade L43, bolting material. The resultant margin of safety is +0.30.

As described in Appendix 2.10.6, *Closure Bolt Stress Evaluations*, bolt impact stresses are calculated assuming a triangular distribution of bolt forces and external impact forces arbitrarily (and conservatively) applied at the corner of the package. Thus, external energy absorber forces are not employed to reduce bolt tensile forces. For near vertical impacts (≥80º), a uniform force distribution is employed.

Note that a yield criterion for closure bolts is very conservative for bore-sealed packages such as the RH-TRU 72-B package, since sealing is dependent on radial, not axial, geometry. This fact was graphically demonstrated by a successful leak test of the quarter-scale NuPac 125-B cask[2] with "loose" (i.e., untightened) bolts. For face-sealed packages, a yield criterion may be quite appropriate since sealing in this instance depends upon unchanging geometry in the axial direction.

An assessment of OC bolt and thread insert engagement is provided in Appendix 2.10.6, *Closure Bolt Stress Evaluations*, and shown to have a minimum margin of safety of +0.93.

(b) Stresses in the IV Lid Bolts

Comprehensive analysis of the IV bolts for all impact orientations is summarized in Table 2.10.6-7 and Table 2.10.6-8 of Appendix 2.10.6, *Closure Bolt Stress Evaluations*. The minimum margin of safety is found at a near-horizontal orientation of 5º with respect to horizontal. This differs from OC conditions because impact loads are directly transferred to the OC lid (in direct bearing) and do not contribute to bolt stresses. At an angle of 5º, total direct tension, due to pressure and preload effects, is estimated at 53,737 psi. The associated shear stress is 20,338 psi. From Table 2.7-1, the HAC allowable containment fastener primary membrane stress intensity, S_a = 101,400 psi at 160 ºF for ASTM A320, Grade L43, bolting material. The resultant margin of safety is +0.50.

An assessment of IV bolt and thread insert engagement is provided in Appendix 2.10.6, *Closure Bolt Stress Evaluations*, and shown to have a minimum margin of safety of +1.79.

(10) Impact Limiter Deformations and Residual Clearances

Maximum impact limiter deformations and residual clearances due to HAC corner/oblique drops are directly available from Figure 2.10.3-7 in Appendix 2.10.3, *Drop Impact Evaluation Results*. Per that appendix, maximum crush of an impact limiter corner is 23.7 inches for the 140 ºF foam stress case and occurs for a drop angle of 55º with respect to horizontal.

Minimum residual clearance for the main package body is 4.69 inches for the 140 ºF foam stress case and occurs for a drop angle of 40º with respect to horizontal. These deformations and residual clearances are of little consequence for the RH-TRU 72-B package.

2.7.1.3 Flat Side Drop

Analysis of RH-TRU 72-B package behavior for the side drop event is performed in the following steps:

(1) Analyze the impact force using the CASKDROP computer program.

(2) Based on the accelerations predicted in (1), determine the equivalent "static" forces on the OC and IV, considered as a rigid body with distributed and lumped masses.

(3) Based on the loads from (2), analyze the OC shells and IV as simple beams, finding the internal forces: thrust, shear, and moment. Compute stresses for the maximum value of each of these forces.

(4) Analyze the OC shells for stress, assuming the two shells act as parallel beams, under the loads determined in (3).

(5) Analyze the IV for stress under the loads determined in (3).

(6) Analyze the payload canister for stress under the loads determined in (3).

(7) Analyze the OC lid for bearing against the top OC ring forging, analyze the OC closure bolts, and analyze the top OC ring forging for shear.

(8) Analyze the OC end plate welds for shear.

(9) Analyze the IV lid for bearing against the IV ring forging, analyze the IV closure bolts, and analyze the IV ring forging.

(10) Calculate the maximum impact limiter deformations and residual clearances for package hard spots.

Material properties and allowable stresses corresponding to the maximum enveloping temperature of 160 ºF for the Type 304 stainless steel OC and IV are given in Table 2.7-1. Buckling is addressed in Appendix 2.10.5, *Buckling Design Criteria and Detailed Evaluation*.

Where possible, the analyses in this section are performed on the basis of a unit (1*g*) axial acceleration, with actual acceleration numbers being substituted at the final point of calculating stresses.

(1) Side Drop Computer Analysis Using CASKDROP

The side drop analysis was performed utilizing the energy-balance computer program, CASKDROP, documented in Appendix 2.10.2.1, *Description of the CASKDROP Computer Code*. Two cases were run which accounted for variations in foam strength due to temperature effects and the possible variations in foam strength from nominal values (see Section 2.3, *Mechanical Properties of Materials*). Each of these two cases consists of two different loading studies for a total of four different cases. The two different loading cases are as follows: (1) distributed payload within the canister, and (2) concentrated payload and canister weight at either of the IV spacer disk supports.

The drop cases consider the impact limiter as fully effective, as defined in Appendix 2.10.3, *Drop Impact Evaluation Results*. The worst-case deflections and accelerations obtained from the bounding cases are utilized for all analyses. The maximum resultant acceleration for the HAC side drop is 81.2*g* (-20 ºF foam), and the maximum impact limiter deflection is 11.5 inches (140 ºF foam) per Table 2.10.3-10 of Appendix 2.10.3, *Drop Impact Evaluation Results*.

(2) Equivalent "Static" Loads

The OC and IV are treated as rigid bodies under transverse acceleration. The two bodies are assumed to move together, and the forces between them needed to make them do so, is found. The centers of gravity of the two bodies are assumed to be coincident.

(3) Internal Forces

The OC shells are analyzed as if they are two beams acting in parallel. The payload canister is analyzed as one beam attached to the IV at the two spacer disk locations, and the IV connects to the OC via a series of interface (gap) elements. A schematic representation of the finite element analysis model used is presented as Figure 2.10.1-9 in Appendix 2.10.1.4, *Containment Assembly Analysis for Oblique Drops*.

To avoid plastic deformation of the payload canister shell, the payload must very nearly be restricted to a uniformly distributed load over the entire length of the canister. Since, this uniformly distributed payload weight does not necessarily impose the worst loading conditions on the OC and IV, the concentrated payload weight is considered at either of the spacer disk supports. Maximum loading conditions are found to occur under the following conditions:

- OC – cold foam (-20 ºF), distributed payload
- IV – cold foam (-20 ºF), concentrated payload

Shear and moment diagrams for -20 ºF foam with a distributed payload are shown in Figure 2.7-14 and Figure 2.7-15, respectively, and with a concentrated payload in Figure 2.7-16 and Figure 2.7-17, respectively, with each component on the same figure. As discussed in Section 2.7.1.2, *Corner and Oblique Drops*, the figures were created using slightly different impact *g*-loadings than given in Appendix 2.10.3, *Drop Impact Evaluation Results*. The difference, however, is small because the figures were created using a side drop *g*-loading of 81.4*g*, which is comparable to the actual side drop *g*-load of 81.2*g*. Therefore, scaling of the shear and moments is appropriate. Similarly, the shear and moment diagrams for hot foam (140 ºF) with a distributed payload, shown in Figure 2.7-18 and Figure 2.7-19, and with a concentrated payload, shown in Figure 2.7-20 and Figure 2.7-21, are scaled accordingly.

As previously discussed, the cold foam yields the worst stresses. The OC experiences worst-case stresses under a distributed payload, while the IV experiences its worst stresses due to a concentrated payload/canister force. The payload canister stresses for the distributed load case are included only for the sake of consistency with other sections herein. Although the maximum shear and moment do not occur at the same location for each component, the maximums will be used to determine combined stresses as this provides a conservative analysis. The figures are based on a side drop *g*-loading of 81.4*g*, whereas the actual side drop impact is 81.2*g*. Therefore, the scale factor is 81.2/81.4 = 0.998.

The maximum shear, V_{max}, and moment, M_{max}, for the OC are:

$$V_{max} = (1{,}625{,}100)(0.998) = 1{,}621{,}850 \text{ lb}$$
$$M_{max} = (50{,}329{,}000)(0.998) = 50{,}228{,}342 \text{ in-lb}$$

The maximum shear, V_{max}, and moment, M_{max}, for the IV are:

$$V_{max} = (354{,}760)(0.998) = 354{,}050 \text{ lb}$$
$$M_{max} = (5{,}864{,}000)(0.998) = 5{,}852{,}272 \text{ in-lb}$$

The maximum shear, V_{max}, and moment, M_{max}, for the payload canister, with only the distributed payload considered, are:

$$V_{max} = (200{,}830)(0.998) = 200{,}428 \text{ lb}$$
$$M_{max} = (2{,}197{,}100)(0.998) = 2{,}192{,}706 \text{ in-lb}$$

Maximum stresses can be calculated from the maximum shear and moments (given above) as follows:

$$S_v = \frac{V}{A} = \text{stress due to shear, psi}$$

$$S_m = \frac{Mc}{I} = \text{stress due to bending moment, psi}$$

where V is the shear force (lb) and M is the bending moment (in-lb). The distance to the neutral axis, c = 20.565 inches for the OC outer shell, c = 17.19 inches for the OC inner shell, c = 16.00 inches for the IV shell, and c = 13.00 inches for the payload canister. The moment of intertia, I = 51,334 in^4 for the OC, I = 4,718 in^4 for the IV, and I = 1,676 in^4 for the payload canister. Finally, the area, A = 292 in^2 for the OC, A = 38 in^2 for the IV, and A = 20 in^2 for the payload canister.

(4) OC Stresses

The maximum membrane stress in the OC inner shell, for the load case selected in Paragraph (3), is:

$$S_m = \frac{Mc}{I} = \frac{(50{,}228{,}342)[17.19 - (½)(1.0)]}{51{,}334} = 16{,}331 \text{ psi}$$

The maximum membrane-plus-bending stress in the OC inner shell is:

$$S_{mb} = \frac{Mc}{I} = \frac{(50{,}228{,}342)(17.19)}{51{,}334} = 16{,}820 \text{ psi}$$

Similarly, the maximum stresses in the OC outer shell are:

$$S_m = \frac{Mc}{I} = \frac{(50{,}228{,}342)[20.565 - (½)(1.5)]}{51{,}334} = 19{,}388 \text{ psi}$$

$$S_{mb} = \frac{Mc}{I} = \frac{(50{,}205{,}300)(20.565)}{51{,}334} = 20{,}122 \text{ psi}$$

In addition, shear stress must be added in the calculation of the membrane stress intensities for the OC inner and outer shells. The shear stress is:

$$S_v = \frac{V}{A} = \frac{1{,}621{,}850}{292} = 5{,}554 \text{ psi}$$

Fabrication stresses applicable to HAC side drop analyses are identical to those used in the NCT side drop analyses (refer to Table 2.6-28 in Section 2.6.7.1, *Flat End Drop*). Fabrication stresses for the side drop analyses are given in Table 2.7-19.

Table 2.7-20, Table 2.7-21, and Table 2.7-22 present the corresponding margins of safety for the more critical OC inner shell. Zero internal pressure is used in order to maximize compressive stresses in the inner shell. Again, it is noted that the margins presented for the 70 ºF and 160 ºF cases are conservative since at these temperatures, *g*-loads will actually be less than the 81.2*g* considered herein.

(5) IV Stresses

The maximum membrane stress in the IV shell, for the load case selected in Paragraph (3), is:

$$S_m = \frac{Mc}{I} = \frac{(5{,}852{,}272)[16.00 - (½)(0.38)]}{4{,}718} = 19{,}611 \text{ psi}$$

The maximum membrane-plus-bending stress in the IV shell is:

$$S_{mb} = \frac{Mc}{I} = \frac{(5{,}852{,}272)(16.00)}{4{,}718} = 19{,}847 \text{ psi}$$

In addition, shear stress must be added in the calculation of the membrane stress intensity for the IV shell. The shear stress is:

$$S_v = \frac{V}{A} = \frac{354{,}050}{38} = 9{,}317 \text{ psi}$$

Table 2.7-23 presents stress and margin of safety results for the IV for the worst-case load combination selected in Paragraph (3).

(6) Discussion of Payload Canister Behavior in Side Drops

The maximum membrane stress in the payload canister shell, for the load case selected in Paragraph (3), is:

$$S_m = \frac{Mc}{I} = \frac{(2{,}192{,}706)[13.00 - (½)(0.25)]}{1{,}676} = 16{,}844 \text{ psi}$$

The maximum membrane-plus-bending stress in the payload canister shell is:

$$S_{mb} = \frac{Mc}{I} = \frac{(2{,}192{,}706)(13.00)}{1{,}676} = 17{,}008 \text{ psi}$$

In addition, shear stress must be added in the calculation of the membrane stress intensity for the payload canister shell. The shear stress is:

$$S_v = \frac{V}{A} = \frac{200{,}428}{20} = 10{,}021 \text{ psi}$$

Table 2.7-24 presents stress and margin of safety results for the canister shell for the load combination selected in Paragraph (3). Allowable stresses were conservatively determined for 210 ºF material temperature. Buckling is addressed in Section 2.1.2.2.3, *Buckling*.

(7) OC Lid Analysis

Since the clearance between the OC lid and sealing surface is less than the clearance between the bolt and bolt hole, the lid will displace laterally to bear against the sealing surface in the forging before lateral loading of the lid bolts occurs. Therefore, the following analysis addresses the stress resulting from lateral loading of the body ring forging by the lid.

In the most unlikely event that the lid displaces laterally to bear upon the body ring forging, lateral loads will be transferred by bearing. The following calculations demonstrate the adequacy of this load transfer mechanism.

The weight of the OC lid may be carried in bearing against the lid-end OC ring forging if sliding occurs at the lid-to-forging interface. The side drop acceleration of 81.2*g* is utilized in a Hertzian analysis to determine the bearing stress between the two cylinders. Because this analysis is sensitive to very small variations in the diametric gap between the cylinders, the worst-case tolerance stackup has been factored into the following calculation using Table 33, Case 2c, from Roark and Young[6], assuming the elastic modulus, E, and Poisson's ratio, μ, are equal for the mating materials:

$$S_b = 0.591\sqrt{\frac{PE}{LK_D}} = 8{,}006 \text{ psi}$$

where the OC lid weight with 81.2*g*, P = (1,667)(81.2) =135,360 pounds, the elastic modulus, E = 27.8(10)^6 psi at 160 ºF from Table 2.3-1 in Section 2.3, *Mechanical Properties of Materials*, the contact length, L = 0.664 inches (approximately), and the diametral stiffness, K_D, is:

$$K_D = \frac{D_1 D_2}{D_1 - D_2} = 30{,}886 \text{ in}$$

where the outer cylinder diameter, D_1 = 32.896 inches, and the inner cylinder diameter, D_2 = 32.861 inches.

From Table 2.7-1, the HAC allowable sealing surface bearing stress, S_a = 27,000 psi at 160 ºF for Type F304 stainless steel. Therefore, the margin of safety is:

$$MS = \frac{S_a}{S_b} - 1 = \frac{27{,}000}{8{,}006} - 1 = +2.37$$

The lip of the forging that supports the OC lid is loaded in shear by the lid. Conservatively assuming only one-half of the lip is effective in resisting the 81.2*g* load, the shear stress is:

$$S_v = \frac{V}{½\pi(R_o^2 - R_i^2)} = 1{,}131 \text{ psi}$$

where the weight of the lid is the shear load with 81.2*g*, V = (1,667)(81.2) = 135,360 pounds, the outside radius of the lip, R_o = 20.81 inches, and the inside radius of the lip, R_i = 18.89 inches.

From Table 2.7-1, the HAC allowable shear stress, S_a = 28,400 psi at 160 ºF for Type F304 stainlesss steel. Therefore, the margin of safety is:

[6] R. J. Roark, W. C. Young, *Formulas for Stress and Strain*, 5th Edition, McGraw-Hill, Inc., New York, NY, 1975.

$$MS = \frac{S_a}{S_v} - 1 = \frac{28{,}400}{1{,}131} - 1 = +24.1$$

(8) Welds Joining the OC Shells to the End Closure Plate

The worst-case shear load at the joints of the OC shells to the end closure plate is taken as the maximum shear load determined from Figure 2.7-14 at the package locations corresponding to the welded joints (0 inches and 120 inches). Therefore, the maximum shear load at the welded joints, V = 1,485,800 pounds.

Since the welds are full penetration bevel welds, the effective shear area for shells may be found by the following equation (i.e., conservatively use half the total weld area):

$$A_w = \frac{2\pi(R_i t_i + R_o t_o)}{2} = 145.8 \text{ in}^2$$

where the mean OC inner shell radius, R_i = 16.69 inches, the OC inner shell thickness, t_i = 1.00 inches, the mean OC outer shell radius, R_o = 19.81 inches, and the OC outer shell thickness, t_o = 1.50 inches.

The direct shear stress in the OC shells' welds is:

$$\tau_w = \frac{V}{A_w} = 10{,}191 \text{ psi}$$

Table 2.7-25 presents stress and margin of safety results for the OC shells' welds under worst-case load combinations.

(9) IV Lid Analysis

Since the clearance between the lid and sealing surface is less than the clearance between the bolt and bolt hole, the IV lid will displace laterally to bear against the sealing surface in the forging before lateral loading of the bolts. Therefore, the following analysis addresses the stress resulting from lateral loading of the IV body ring forging by the IV lid.

In the most unlikely event that the lid displaces laterally to bear upon the body ring forging, lateral loads will be transferred by bearing. The following calculation demonstrates the adequacy of this load transfer mechanism.

The weight of the IV lid may be carried in bearing against the IV body ring forging if sliding occurs at the lid-to-forging interface.

This analysis accounts for only the uppermost race surface being in contact with the forging for bearing. As with Paragraph (7), the side drop acceleration of 81.2*g* is utilized in a Hertzian analysis to determine the bearing stress between two cylinders for the worst-case tolerance stackup using the following calculation using Table 33, Case 2c, from Roark and Young[6], assuming the elastic modulus, E, and Poisson's ratio, μ, are equal for the mating materials:

$$S_b = 0.591\sqrt{\frac{PE}{LK_D}} = 9{,}552 \text{ psi}$$

where the IV lid weight with 81.2*g*, P = (1,382)(81.2) = 112,218 pounds, the elastic modulus, E = 27.8(10)^6 psi at 160 ºF from Table 2.3-1 in Section 2.3, *Mechanical Properties of Materials*, the contact length, L = 0.32 inches (approximately), and the diametral stiffness, K_D, is:

$$K_D = \frac{D_1 D_2}{D_1 - D_2} = 37{,}321 \text{ in}$$

where the outer cylinder diameter, D_1 = 28.006 inches, and the inner cylinder diameter, D_2 = 27.985 inches.

From Table 2.7-1, the HAC allowable sealing surface bearing stress, S_a = 27,000 psi at 160 ºF for Type F304 stainless steel. Therefore, the bearing stress margin of safety is:

$$MS = \frac{S_a}{S_b} - 1 = \frac{27{,}000}{9{,}552} - 1 = +1.83$$

The lip of the forging that supports the IV lid is loaded in shear by the lid. Conservatively assuming only one-half of the lip is effective in resisting the 81.2*g* load, the shear stress is:

$$S_v = \frac{V}{½\pi(R_o^2 - R_i^2)} = 1{,}191 \text{ psi}$$

where the weight of the lid is the shear load with 81.2*g*, V = (1,382)(81.2) = 112,218 pounds, the outside radius of the lip, R_o = 16.00 inches, and the inside radius of the lip, R_i = 14.00 inches.

From Table 2.7-1, the HAC allowable shear stress, S_a = 28,400 psi at 160 ºF for Type F304 stainlesss steel. Therefore, the shear stress margin of safety is:

$$MS = \frac{S_a}{S_v} - 1 = \frac{28{,}400}{1{,}191} - 1 = +22.8$$

(10) Impact Limiter Deformations and Residual Clearances

Maximum impact limiter deformations and residual clearances due to NCT side drop are directly available from Appendix 2.10.3, *Drop Impact Evaluation Results*. Per Table 2.10.3-10 in Appendix 2.10.3, *Drop Impact Evaluation Results*, maximum crush of an impact limiter side is 11.52 inches for the 140 ºF foam stress case resulting in a minimum residual clearance for the main package body of 5.48 inches (based on a 16.00 inch nominal radial thickness). These deformations and residual clearances are of little consequence for the RH-TRU 72-B package.

2.7.2 Crush

Subpart F of 10 CFR 71[1] requires performing a dynamic crush test in accordance with the requirements of 10 CFR §71.73(c)(2)[1]. Since the RH-TRU 72-B package weight exceeds 1,100 pounds, the dynamic crush test is not required.

2.7.3 Puncture

Subpart F of 10 CFR 71[1] requires that a 40-inch free drop of the RH-TRU 72-B package onto the upper end of a solid, vertical, cylindrical, mild steel bar mounted on an essentially unyielding, horizontal surface be considered. The bar must have a 6-inch diameter, with the top horizontal and its edge rounded to a radius of not more than 0.25 inches. The package is to be oriented in a position for which maximum damage is expected and the length of the pin is to be such that maximum damage will occur.

2.7.3.1 Side Puncture

For impact occurring on the side of the RH-TRU 72-B package, the required OC outer shell thickness, t, for puncture integrity is determined using three independent equations as follows:

(1) Nelms' Equation[7]

$$t = \left(\frac{W}{S_u}\right)^{0.71} = 0.712 \text{ in}$$

where the weight of the package, W = 45,000 pounds, and the ultimate strength of Type 304 stainless steel, S_u = 72,600 psi at 160 ºF (Table 2.7-1). Therefore, given an OC outer shell thickness, t_o = 1.50 inches, the thickness-basis margin of safety resisting puncture is:

$$MS = \frac{t_o}{t} - 1 = \frac{1.50}{0.712} - 1 = +1.11$$

For purposes of comparison, utilize Nelms' equation to calculate the package weight, W_p, necessary to puncture a 1½-inch thick stainless steel shell:

$$W_p = S_u t^{\left(\frac{1}{0.71}\right)} = 128{,}515 \text{ pounds}$$

Therefore, the OC outer shell energy-basis margin of safety resisting puncture is:

$$MS = \frac{W_p}{W} - 1 = \frac{128{,}515}{45{,}000} - 1 = +1.86$$

(2) Sakamoto's Equation[8]

$$\frac{E}{S_u} = \left[0.0030 + (0.047)\left(\frac{t}{D}\right) + (0.002)\left(\frac{d}{D}\right) + (0.006)\left(\frac{r}{d}\right)\right]\left\{t^{[1.585-(0.11)r]}\right\}\left\{d^{[1.465+(0.077)r]}\right\}$$

[7] L. B. Shappert, *Package Designers Guide – A Guide for the Design, Fabrication, and Operation of Shipping Packages for Nuclear Applications*, ORNL-NSIC-68, Oak Ridge National Laboratory, Oak Ridge, Tennessee, February 1970.

[8] I. Sakamoto, K. Hinkino, A. Onodera, Y. Sakai, S. Maezawa, *An Experimental Study on Puncture Resistance of Spent Fuel Shipping Packages by Drop Impact Test*, 4th International Symposium on Packaging and Transportation of Radioactive Materials, Miami Beach, Florida, September 1984, pp. 262-276.

where the puncture drop energy, E = W × h, the weight of the package, W = 45,000 pounds (20,412 kg = 20.412 metric tons), the drop height, h = 40 inches (1,016 mm), the ultimate strength of Type 304 stainless steel, S_u = 72,600 psi at 160 ºF per Table 2.7-1 (51.04 kg/mm), the OC outer shell outside diameter, D = 41.13 inches (1,044.7 mm), the puncture bar diameter, d = 6.0 inches (152.4 mm), and the puncture bar edge radius, r = 0.25 inches (6.35 mm). Substituting the known quantities results in the following equation:

$$\frac{(20.412)(1{,}016)}{51.04} = \left[0.003542 + (0.000045)t\right]\left\{t^{0.8865}\right\}\left\{18{,}426.5\right\}$$

Solving, the required OC outer shell thickness, t = 7.135 mm = 0.281 inches. Therefore, given an outer shell thickness, t_o = 1.50 inches, the thickness-basis OC outer shell margin of safety is:

$$MS = \frac{t_o}{t} - 1 = \frac{1.50}{0.281} - 1 = +4.34$$

For purposes of comparison, utilize Sakamoto's equation to calculate the package weight to puncture a 1½-inch (38.1 mm) thick shell:

$$W_p = \left(\frac{S_u}{h}\right)\left[0.0030 + (0.047)\left(\frac{t}{D}\right) + (0.002)\left(\frac{d}{D}\right) + (0.006)\left(\frac{r}{d}\right)\right]\left\{t^{[1.585-(0.11)r]}\right\}\left\{d^{[1.465+(0.077)r]}\right\}$$

Substituting the known quantities results in the following equation and solving, the package weight, W_p = 122.63 metric tons. Therefore, the OC outer shell energy-basis margin of safety is:

$$MS = \frac{W_p}{W} - 1 = \frac{122.63}{20.412} - 1 = +5.01$$

Because 10 CFR §71.73(c)(2)[1] specifies a puncture bar radius, r, of not more than 0.25 inches, a 0.0-inch radius is also considered. This assumption results in t = 0.552 inches and the OC outer shell thickness-basis margin of safety is:

$$MS = \frac{t_o}{t} - 1 = \frac{1.50}{0.552} - 1 = +1.72$$

On an energy-basis, the OC outer shell margin of safety is +1.84.

(3) Shieh's Equation[9]

$$\frac{W}{S_u} = \frac{0.37\left[1 + \frac{6}{D} + \left(\frac{41}{D}\right)^2\right]e^{\left(\frac{t}{3}\right)}t^{1.68}}{1 + (0.1)t^{0.87}}$$

where the parameters (in inches) apply:

$$0.5 < t < D/30;\ \ 45 < D < 90;\ \ 2D < L < 3D$$

[9] R. C. Shieh, *Empirical Equations for Puncture Analysis of Lead-Shielded Spent Fuel Shipping Packages*, Transporation Branch, U.S. Nuclear Regulatory Commission, Washington, D.C.

These conditions are not met for the RH-TRU 72-B package geometry under consideration, but are sufficiently close to warrant solving for required OC outer shell thickness, t. Substituting and solving for the OC outer shell thickness, t = 0.776 inches. Therefore, the OC outer shell thickness-basis margin of safety resisting puncture is:

$$MS = \frac{t_o}{t} - 1 = \frac{1.50}{0.776} - 1 = +0.93$$

For purposes of comparison, utilize Shieh's equation to calculate the package weight to puncture a 1½-inch thick OC outer shell:

$$W_p = \frac{(0.37)S_u\left[1 + \frac{6}{D} + \left(\frac{41}{D}\right)^2\right]e^{\left(\frac{t}{3}\right)}t^{1.68}}{1 + (0.1)t^{0.87}} = 163{,}933 \text{ pounds}$$

Therefore, the OC outer shell energy-basis margin of safety is:

$$MS = \frac{W_p}{W} - 1 = \frac{163{,}933}{45{,}000} - 1 = +2.64$$

(4) Conclusion

The lowest thickness-basis margin of safety using any of the three documented empirical equations is +0.93. On an energy-basis, the margin of safety is much larger.

2.7.3.2 Package Bending Due to Side Puncture

To determine the overall effect on the package, consider the puncture impact occurring at the center of length of the package. Applying a unit acceleration and conservatively ignoring the strength of the lead, the membrane stress induced in the OC inner shell by the bending moment is:

$$S_{mi} = \frac{Mc}{I} = \frac{\left(\frac{w_C L^2}{8} + \frac{W_{IL} L}{2}\right)c_i}{I} = 289 \text{ psi}$$

where the package weight per unit length, less impact limiters, $w_C = W_C/L = 281.52$ lb/in, the package weight, less impact limiters, $W_C = 39{,}906$ pounds, the package length, L = 141.75 inches, the impact limiter weight, $W_{IL} = 2{,}547$ pounds, the mid-plane OC inner shell radius, $c_i = ½(R_{io} + R_{ii}) = 16.69$ inches, the OC inner shell outer radius, $R_{io} = 17.19$ inches, the OC inner shell inner radius, $R_{ii} = 16.19$ inches, and the OC inner and outer shell moment of inertia, I, is:

$$I = \left(\frac{\pi}{4}\right)\left[\left(R_{oo}^4 - R_{oi}^4\right) + \left(R_{io}^4 - R_{ii}^4\right)\right] = 51{,}334 \text{ in}^4$$

where the the OC outer shell outer radius, $R_{oo} = 20.565$ inches, the OC outer shell inner radius, $R_{oi} = 19.065$ inches, the OC inner shell outer radius, $R_{io} = 17.19$ inches, and the OC inner shell inner radius, $R_{ii} = 16.19$ inches.

Correspondingy, the membrane stress induced in the OC outer shell by the bending moment is:

$$S_{mo} = \frac{Mc}{I} = \frac{\left(\frac{w_C L^2}{8} + \frac{W_{IL} L}{2}\right) c_o}{I} = 343 \text{ psi}$$

where the mid-plane OC outer shell radius, $c_o = ½(R_{oo} + R_{oi}) = 19.815$ inches.

The impact acceleration can be estimated from the puncture bar cross-section area, A_P, and dynamic flow stress, σ_f, of the 6-inch diameter, mild steel puncture bar. Assuming a dynamic flow stress for the mild steel puncture bar is the mean of the yield and ultimate strengths for ASTM A36 carbon steel, $\sigma_f = ½(36{,}000 + 58{,}000) = 47{,}000$ psi, the acceleration, η, is:

$$\eta = \frac{P_f}{W} = 29.5g$$

where the puncture bar force, $P_f = \sigma_f \times A_P = 1{,}328{,}878$ pounds, the puncture bar cross cross-sectional area, $A_P = \pi(3.0)^2 = 28.274$ in^2, and the package weight, W = 45,000 pounds.

Thus, the OC inner shell membrane stress, $S_{mi} = (29.5)(289) = 8{,}526$ psi, and OC outer shell membrane stress, $S_{mo} = (29.5)(343) = 10{,}119$ psi.

Shear stress, τ, for the OC shells is determined by using an effective shear area equal to half the cross-sectional area, A, of the OC inner and outer shells, as follows:

$$\tau = \frac{V}{½A} = 4{,}546 \text{ psi}$$

where the maximum shear force, $V = ½W\eta = 663{,}750$ pounds, the package weight, W = 45,000 pounds, the acceleraton, $\eta = 29.5g$, the cross-sectional area, A, of the OC inner and outer shells is:

$$A = \pi\left[\left(R_{oo}^2 - R_{oi}^2\right) + \left(R_{io}^2 - R_{ii}^2\right)\right] = 292 \text{ in}^2$$

The two principal stresses in the OC inner shell on the side of the package opposite the point of puncture bar impact, σ_1 and σ_2, are:

$$\sigma_{1,2} = \frac{S_{mi}}{2} \pm \sqrt{\left(\frac{S_{mi}}{2}\right)^2 + \tau^2} = 10{,}495 \text{ psi}, -1{,}969 \text{ psi}$$

The corresponding OC inner shell stress intensity, SI, is:

$$SI = |\sigma_1 - \sigma_2| = 12{,}464 \text{ psi}$$

From Table 2.7-1, the HAC allowable primary membrane stress intensity, $S_a = 48{,}000$ psi at 160 ºF for Type 304 stainless steel. Therefore, the OC inner shell margin of safety is:

$$MS = \frac{S_a}{SI} - 1 = \frac{48{,}000}{12{,}464} - 1 = +2.85$$

The two principal stresses in the OC outer shell on the side of the package opposite the point of puncture bar impact, σ_1 and σ_2, are:

$$\sigma_{1,2} = \frac{S_{mi}}{2} \pm \sqrt{\left(\frac{S_{mi}}{2}\right)^2 + \tau^2} = 11{,}861 \text{ psi}, -1{,}742 \text{ psi}$$

The corresponding OC outer shell stress intensity, SI, is:

$$SI = |\sigma_1 - \sigma_2| = 13{,}604 \text{ psi}$$

From Table 2.7-1, the HAC allowable primary membrane stress intensity, S_a = 48,000 psi at 160 ºF for Type 304 stainless steel. Therefore, the OC outer shell margin of safety is:

$$MS = \frac{S_a}{SI} - 1 = \frac{48{,}000}{13{,}604} - 1 = +2.53$$

These are the maximum global stresses that arise from puncture bar impact on the package side. For impacts at locations other than the center of the package's side, a portion of the drop kinetic energy will be converted into rotational energy of the package, and the package stress levels will be correspondingly lower.

2.7.3.3 End Puncture

To evaluate the effects of puncture bar impact on the OC end closures, both closures will be analyzed. The top closure is a 6-inch thick bolted lid. For conservatism, it is analyzed as a simply supported circular plate using Table 24, Case 16, from Roark and Young[6]:

$$M_{max} = \left(\frac{W}{4\pi}\right)\left[(1+\mu)\ln\frac{a}{r_o'} + 1\right] = 369{,}998 \text{ in-lb/in}$$

where the center load, $W = W_P\eta$ = 1,327,500 pounds, the package weight, W_P = 45,000 pounds, the puncture bar acceleration, $\eta = 29.5g$, Poisson's ratio, $\mu = 0.3$, the lid radius, a = 20.565 inches, and the effective load radius, r_o' = 3.0 inches.

For a lid thickness, t = 6.0 inches, the maximum lid bending stress is:

$$\sigma = \frac{6M_{max}}{t^2} = 61{,}666 \text{ psi}$$

Internal pressure acts in the opposite direction to relieve this bending stress, so zero internal pressure is assumed. From Table 2.7-1, the HAC allowable primary membrane-plus-bending stress intensity, S_a = 67,700 psi at 160 ºF for Type F304 stainless steel. Therefore, the OC lid bending stress margin of safety is:

$$MS = \frac{S_a}{\sigma} - 1 = \frac{67{,}700}{61{,}666} - 1 = +0.10$$

Since it is continuously welded at its outer edge by two relatively thick cylindrical shells, the 5-inch thick bottom closure plate is initially analyzed as a fixed-edge circular plate using Table 24, Case 17, from Roark and Young[6]:

$$M_{max} = \left(\frac{W}{4\pi}\right)\left[(1+\mu)\ln\frac{a}{r_o'}\right] = 264{,}359 \text{ in/lb-in}$$

For a bottom closure thickness, t = 5.0 inches, the maximum bottom closure bending stress is:

$$\sigma = \frac{6M_{max}}{t^2} = 63{,}446 \text{ psi}$$

Since this stress level approaches the allowable limit for membrane-plus-bending stress intensity and the fixed-edge assumption is potentially non-conservative, a more detailed finite element analysis was also performed, as documented in Appendix 2.10.1.6, *Outer Cask Bottom Stresses Due to Puncture*. Per that Appendix, the maximum linearized membrane-plus-bending stress intensity occurs at the inside center of the closure plate, and has a magnitude of 66,760 psi.

From Table 2.7-1, the HAC allowable primary membrane-plus-bending stress intensity, S_a = 67,700 psi at 160 ºF for Type F304 stainless steel. Therefore, the OC bottom closure bending stress margin of safety is:

$$MS = \frac{S_a}{\sigma} - 1 = \frac{67{,}700}{66{,}760} - 1 = +0.01$$

Note that the above stress values are conservative, since backing of the plates by the IV and payload caniser is neglected. For impacts other than at the center of the plates, part of the drop kinetic energy will be converted to rotational energy, and stress levels will be lower than shown. Therefore, the end closures are adequate for the puncture event.

2.7.3.4 Puncture on the Lifting Trunnions

A puncture bar impacting a lifting trunnion from the side will, at worst, fail the attachment weld, without compromising the integrity of the OV outer shell. Justification for this assumption can be found in Section 2.5.1.5, *Excessive Lifting Trunnion Loads*.

The effects of a puncture bar axially impacting a lifting trunnion will be no worse than a direct strike of the puncture bar onto the OC outer shell because the trunnion is mounted on a 6-inch diameter base that is welded to the outer shell. The puncture force acting through this base will have an equivalent effect on the outer shell as the 6-inch diameter puncture bar itself. Since it has been shown that a puncture bar impact on the outer shell will not compromise the integrity of the outer shell (see Section 2.7.3.1, *Package Bending Due to Side Puncture*), puncture bar impact directly onto a lifting trunnion will likewise not detrimentally affect the package integrity. In fact, the effect will be less than that of a puncture bar impact on the outer shell since the lifting trunnions are removed from the center of gravity of the package and some of the drop's kinetic energy will be converted to rotational energy without imposing the full puncture load.

2.7.3.5 Puncture on the Center-Pivot Trunnions

To evaluate the effects of a puncture bar impact on the side of a center-pivot trunnion, reference is made to Section 2.5.2.4, *Center-Pivot Trunnion Attachment Welds*, where it is demonstrated that the weld attaching the trunnion to the trunnion base will always fail before the weld attaching the trunnion base to the OC outer shell. It may be assumed, therefore, that a puncture bar impact on the

side of the center-pivot trunnion will have no worse effect than that of separating the trunnion from the trunnion mount, and the integrity of the OC outer shell will not be compromised. As with the lifting trunnions, the puncture bar load will be offset from the package center-of-gravity in this impact orientation; therefore, the full punch force is not developed on the trunnion.

A direct puncture bar impact onto the face of one of the center-pivot trunnions will impose a maximum load, $P = \sigma_f \times A_P = 1{,}328{,}878$ pounds, as determined in see Section 2.7.3.1, *Package Bending Due to Side Puncture*. The shear area of the trunnion mount weld, $A_w = 2(L_w + H_w) \times T_w = 138$ in^2, where the trunnion mount length, $L_w = 28$ inches, the trunnion mount height, $H_w = 18$ inches, and the weld thickness, $T_w = 1.5$ inches for a full penetration weld. The resulting shear stress, $\tau = P/A_w = 9{,}630$ psi.

From Table 2.7-1, the HAC allowable shear stress intensity, $S_a = 28{,}400$ psi at 160 ºF for Type F304 stainless steel. Therefore, the minimum weld margin of safety is:

$$MS = \frac{S_a}{\tau} - 1 = \frac{28{,}400}{9{,}630} - 1 = +1.95$$

2.7.3.6 Puncture Bar Impact on Containment Penetrations

The OC has two containment penetrations: the closure lid and the gas sampling port. The effects of a puncture impact on these structures are addressed in the following sections.

2.7.3.6.1 Puncture Bar Impact on the OC Closure Lid

As shown in Section 2.7.3.3, *End Puncture*, the stress in the OC closure lid due to a puncture impact in the center of the lid exceeds the yield point of the lid material at temperature. The stress, 61,666 psi, is determined by a conservative analysis technique, but since it is above the material's yield point, some plastic deformation can be expected. However, the following analysis shows that the ability of the lid's O-ring seals to remain leaktight is not affected by the resulting plastic deformation.

Since the containment seal is located on the inside of the lid, i.e., the side that goes into tension due to the inward deformation of the lid, compression of the seal is shown to increase slightly, thus improving its performance. The amount and direction of permanent deformation is determined with a nonlinear finite element analysis using ANSYS® Revision 5.4[10]. The closure lid, including the flange and two O-ring seal grooves, is modeled axisymmetrically, as shown in Figure 2.7-22. The closure lid thickness is 6 inches, and the outer diameter is 37.59 inches. PLANE42, two-dimensional structural solid elements are used. The model is loaded over a 3-inch radius, with a pressure based on the maximum load that can be sustained by the puncture bar. For ASTM A36 mild steel, the maximum load that can be applied, assuming no buckling of the puncture bar, is bounded by the flow stress in the material. The flow stress taken as the average of the yield and ultimate strengths of ASTM A36. Thus, the average stress is ½(36,000 + 58,000) = 47,000 psi, which for purposes of this analysis, is conservatively rounded up to 50,000 psi. The lid is supported beneath the flange at the OC inner radius. All of the load spreading effect of the impact limiter foam and 1/2-inch thick plate adjacent to the lid is conservatively ignored.

[10] ANSYS®, Inc., Revision Release 5.4, Houston, PA.

Nonlinear stress-strain material properties are taken from the closure lid analysis of the NuPac 125-B cask[2], and summarized in Table 2.7-26 from Figure 2.3-1 in Section 2.3, *Mechanical Properties of Materials*. Although the temperature of the lid is bounded by 160 ºF, the material properties from the reference are for a conservatively higher temperature of 212 ºF. The modulus of elasticity is $27.7(10)^6$ psi, and the proportional limit is 20,500 psi.

Results are shown in Figure 2.7-23. One point on the containment O-ring seal groove, node 280, moves 0.0104 inches radially outward, consistent with the expected deformation under the applied loading. This movement equates to a small increase in containment O-ring seal compression. Therefore, containment is not affected by the puncture event.

2.7.3.6.2 Puncture at the OC Gas Sampling Port

The consequence of a puncture bar impact on the OC gas sampling port is not significant, as demonstrated below. For contact between the puncture bar and the head of the port closure bolt, the worst-case is for impact at an oblique angle. As shown in the following analysis, the puncture bar cannot penetrate deeply enough to contact the gas sampling port closure bolt head. Figure 2.7-24 shows a detail of the gas sampling port region with the impact limiter installed.

The following conservative assumptions are made in the analysis:

- The package is assumed to contact the puncture bar at an angle of 45º to the horizontal. This angle ensures the maximum initial penetration of the puncture bar into the sampling port opening. The sampling port is assumed to be oriented with respect to the package so it will fall a maximum distance before contacting the puncture bar (see Figure 2.7-25).
- The analysis conservatively ignores any energy absorbtion contributed by the crushed foam in the impact limiter.
- The analysis conservatively ignores any resistance to impact contributed by the 1/2-inch thick stainless steel plate on the inner surface of the impact limiter (adjacent to the OC lid) or the perpendicular stiffening ring (see Figure 2.7-24).
- Although the package center of gravity is not over the impact point, the analysis conservatively assumes that no energy is transformed into rotational energy.

The impact between the puncture bar and the package closure lid can be modeled as a steel plate being perforated by a missile. This analysis is described by Equation 2-7 in Section 2.2 of *Design of Structures for Missile Impact*[11]. The thickness of the perforation is calculated by:

$$T = \frac{\left(\tfrac{1}{2}MV_s^2\right)^{2/3}}{672D} = 1.36 \text{ in}$$

where the mass of the package, M = 45,000 pounds = 1,397.5 slugs, the velocity of the puncture bar relative to the package, $V = (2gh)^{1/2} = 22.27$ ft/s, the acceleration due to gravity, $g = 32.2$ ft/s^2, the total drop height, h = 92.4 inches = 7.7 feet (see Figure 2.7-25), and D is the effective diameter of the missile's projected area, calculated as follows. Because the puncture bar is making contact with an annular area, the effective diameter is the diameter of a circle that has an

[11] Bechtel Power Corporation, *Design of Structures for Missile Impact*, BC-TOP-9-A, Rev. 2, September 1974.

area, A, equal to the difference between the areas of the 6-inch diameter puncture bar and the 2.625-inch diameter opening as follows:

$$A = \left(\frac{\pi}{4}\right)\left[(6)^2 - (2.625)^2\right] = 22.86 \text{ in}^2$$

Therefore, the effective puncture bar diameter is:

$$D = \sqrt{\left(\frac{4}{\pi}\right)A} = 5.40 \text{ in}$$

The geometric interface between the obliquely oriented puncture bar and the cylindrical test port opening must also be considered. Figure 2.7-26 shows that at the time of initial contact between the puncture bar and the lid, the puncture bar has already slightly penetrated the upper plane of the lid. The distance of penetration can be solved geometrically by considering the view shown in Figure 2.7-26. The end of the bar has an elliptical profile (in the 45º oblique plane) equal to

$$\frac{x^2}{a^2} + \frac{y^2}{b^2} = 1$$

where the ellipse's major axis, a = 3 inches, and the ellipse's minor axis, b = 3(sin 45º) = 2.12 inches for an oblique bar angle of 45º. Given that the puncture bar contacts the opening at the value of x = ½(2.625) inches, y = 1.91 inches.

$$y = b\sqrt{1 - \frac{x^2}{a^2}} = 1.91 \text{ in}$$

The depth of penetration, d, at incipient contact, is:

$$d = b - y = 2.12 - 1.91 = 0.21 \text{ in}$$

Therefore, the maximum penetration is the sum of T and d:

$$p_{max} = T + d = 1.36 + 0.21 = 1.57 \text{ in}$$

As shown in Figure 2.7-26, the distance from the top of the port closure bolt to the top of the closure lid, e = 1.64 inches. Therefore, the margin of safety is:

$$MS = \frac{e}{p_{max}} - 1 = \frac{1.64}{1.57} - 1 = +0.04$$

The positive margin demonstrates that the puncture bar cannot contact the gas sampling port closure bolt despite the very conservative assumptions incorporated in the analysis.

The most conservative assumption is the neglect of the substantial steel structures in the adjacent impact limiter, i.e., the 1/2-inch thick inner plate and vertical stiffening ring. These structures also make extrusion of compressed foam into the port opening impossible. Finally, note that even if contact with the closure port bolt is made, the bolt seal is a bore-type O-ring seal. Since any impact-related motion of the bolt would be along the bolt axis, the ability of the O-ring seal to seal would not be affected.

2.7.4 Thermal

The HAC fire transient, presented in Section 3.5, *Thermal Evaluation for Hypothetical Accident Conditions*, provides maximum temperatures and pressures.

2.7.4.1 Summary of Pressures and Temperatures

The maximum HAC fire temperatures for the various package components are presented in Table 2.7-28. Maximum internal pressure resulting from the fire transient is 16.54 psig for any package component, from Section 3.5.4, *Maximum Internal Pressure*. The stresses resulting from the HAC thermal pressure are addressed in Section 2.7.4.3, *Pressure Stress Calculations*.

2.7.4.2 Differential Thermal Expansion

Differential thermal expansions due to the HAC fire are of little consequence for the RH-TRU 72-B package. All stresses resulting from differential expansions can be classified as secondary, displacement limited stresses. As limits on secondary stresses do not apply for HAC, per Table 2.1-1 in Section 2.1.2.1.1, *Containment Structures*, differential thermal expansions in themselves do not compromise the integrity of the package.

Through-wall (and through-thickness) thermal gradients also result in secondary stresses and again are of little consequence for the package. To address the requirement specified in Paragraph C.7 of NRC Regulatory Guide 7.6[12], and discussed in Section 2.1.2.2.2.3, *Extreme Total Stress Intensity Range*, a finite element analysis was performed to determine maximum stresses associated with the HAC fire transient event. Details of this analysis are presented in Section 3.5.5, *Maximum Thermal Stresses*. The resultant maximum stress intensity in the OC outer shell is 76,600 psi and the maximum stress intensity anywhere in the model is 118,570 psi, occurring in the main trunnion block.

2.7.4.3 Pressure Stress Calculations

Stresses from a unit internal pressure are calculated at 10 points on the containment vessels, as discussed in Section 2.6.1.3.1, *Stresses Due To Unit Pressures*, and shown in Figure 2.6-1. Table 2.7-27 summarizes the stresses at these points under a very conservative 300 psig internal pressure, as calculated from the unit pressure stresses in Table 2.6-4 and Table 2.6-5 in Section 2.6.1.3.2, *Stresses Due to Maximum Pressures*.

The radius transition at location P6 is analyzed using an ANSYS® finite element model. Stresses resulting in the radius transition due to a 1.0-psi internal pressure are reported in Section 2.6.1.3.1, *Stresses Due To Unit Pressures*. The bending stress at location P6, between the flat head and the cylindrical shell, is a secondary stress per NRC Regulatory Guide 7.6[12], and need not be considered for this Level D Accident Pressure Condition. The maximum local axial and hoop membrane stresses at location P6 are 6,501 psi and -11,322 psi, respectively, for 300 psig internal pressure. The maximum local membrane stress intensity at 300 psig is 6,501 – (-11,322) = 17,823 psi.

[12] U. S. Nuclear Regulatory Commission, Regulatory Guide 7.6, *Design Criteria for the Structural Analysis of Shipping Package Containment Vessels*, Revision 1, March 1978.

The stress in the OC lid bolts, S_B, due to a 300 psig internal pressure, P, is:

$$S_B = \frac{PA_P}{NA_t} = 14{,}619 \text{ psi}$$

where the area the internal pressure acts upon, $A_P = (\pi/4)D^2 = 849.92$ in^2, the sealing diameter, D = 32.896 inches, the number of bolts, N = 18, and the tensile stress area of a 1¼-7UNC bolt, $A_t = 0.969$ in^2.

The stress in the IV lid bolts, S_B, due to a 300 psig internal pressure, P, is:

$$S_B = \frac{PA_P}{NA_t} = 56{,}759 \text{ psi}$$

where the area the internal pressure acts upon, $A_P = (\pi/4)D^2 = 616.02$ in^2, the sealing diameter, D = 28.006 inches, the number of bolts, N = 8, and the tensile stress area is the shank area for the modified 7/8-9UNC bolt, $A_t = 0.407$ in^2.

Stress calculations for differential thermal expansion are presented in Section 2.7.4.2, *Differential Thermal Expansion*.

2.7.4.4 Comparison with Allowable Stresses

The margins of safety for stresses due to HAC thermal pressure, using NRC Regulatory Guide 7.6[12] HAC allowables, are presented in Table 2.7-28. Allowable stress intensities are conservatively based on a HAC temperature of 300 ºF for the IV and 500 ºF for the OC, except where noted. Furthermore, the allowable stress intensities for locations P1 – P6 (i.e., shell regions) are based on Type 304 stainless steel, and the allowable stress intensities for locations P7 – P10 (i.e., end closures) are conservatively based on Type F304 stainless steel. Calculated stress intensities are presented in Section 2.7.4.3, *Pressure Stress Calculations*.

The maximum stress in the OC lid bolts is 14,619 psi. The HAC allowable stress for ASTM A320, Grade L43, bolts, S_a = 88,500 psi at 500 ºF ($S_a = S_y$ per Table 2.1-1 in Section 2.1.2.1.1, *Containment Structures*, where S_y is taken from Table 2.3-1 in Section 2.3, *Mechanical Properties of Materials*). Therefore, the OC lid bolt margin of safety is:

$$MS = \frac{S_a}{S_B} - 1 = \frac{88{,}500}{14{,}619} - 1 = +5.05$$

The maximum stress in the IV lid bolts is 56,759 psi. The HAC allowable stress for ASTM A320, Grade L43, bolts, S_a = 95,700 psi at 300 ºF ($S_a = S_y$ per Table 2.1-1 in Section 2.1.2.1.1, *Containment Structures*, where S_y is taken from Table 2.3-1 in Section 2.3, *Mechanical Properties of Materials*). Therefore, the IV lid bolt margin of safety is:

$$MS = \frac{S_a}{S_B} - 1 = \frac{95{,}700}{56{,}759} - 1 = +0.69$$

From Section 2.7.4.2, *Differential Thermal Expansion*, the maximum stress intensity is 118,570 psi. To conservatively evaluate the stress state in relation to the requirements from Paragraph C.7 of NRC Regulatory Guide 7.6[12], the worst-case thermal/secondary stress intensity is used.

Note that the stress intensity, SI = 118,570 psi, occurs in the OC main trunnion block, not the containment structure. It has also been demonstrated elsewhere herein that the maximum combined primary membrane-plus-bending stress intensity (due to fabrication stress, dead weight, internal pressure, and HAC drop loading) is in conformance with NRC Regulatory Guide 7.6[12]. Therefore, it is permissible and conservative to assume that the maximum allowable value for the primary stresses, S_u, actually develops within the structure.

Assuming an average through-wall temperature of 700 ºF, the ultimate strength of Type 304 stainless steel plate used for the OC shells, S_u = 63,500 psi per Table 2.3-1 in Section 2.3, *Mechanical Properties of Materials*. Adding this stress to the worst-case thermal stress intensity, the total primary-plus-secondary stress intensity becomes 63,500 + 118,570 = 182,070 psi. The maximum possible stress range will be twice this value, or 2 × 182,070 = 364,140 psi. This value is very conservative because it addresses the peak thermal stresses at the trunnions and combines it with the assumed maximum stress of S_u, and because it assumes the maximum non-thermal stress will exist at the same location as the HAC thermal stress. It could be shown that the actual stress range is significantly lower than this value, including structural discontinuity effects. However, for this calculation, the maximum stress range of 364,140 psi is used. The appropriate alternating stress will be one-half this value, S_{alt} = ½(364,140) = 182,070 psi. As required by NRC Regulatory Guide 7.6[12], the maximum alternating stress intensity (S_{alt}) should be modified by the ratio of the elastic modulus for which the design fatigue curves are based, $E_{70} = 28.3(10)^6$ psi, and the elastic modulus used in the analysis, $E_{700} = 24.8(10)^6$ psi, per Table 2.3-1 in Section 2.3, *Mechanical Properties of Materials* Therefore, the adjusted alternating stress is:

$$S_{alt} \text{ at } 700\,^{\circ}\text{F} = S_{alt}\left(\frac{E_{70}}{E_{700}}\right) = (182{,}070)\left(\frac{28.3(10)^6}{24.8(10)^6}\right) = 207{,}765 \text{ psi}$$

NRC Regulatory Guide 7.6[12] requires that the maximum stress intensity range be less than twice the adjusted value of the allowable alternating stress intensity, S_a, at 10 cycles from the appropriate design fatigue curve. For Type 304 stainless steel, S_a = 708,000 psi per Figure 2.7-27 (Figure I-9.2.1 from Appendix I of the ASME Code[13]). The maximum adjusted stress intensity range is twice the adjusted alternating stress, S_{max} = 2 × 207,765 = 415,530 psi. Therefore, the margin of safety is:

$$MS = \frac{S_a}{S_{max}} - 1 = \frac{708{,}000}{415{,}530} - 1 = +0.70$$

Recognizing the grossly conservative assumptions that are utilized in the preceding evaluation (e.g., use of allowable primary stresses rather than actual stresses, assuming fully reversing primary and secondary stress states to determine ranges, assuming worst-case primary stresses occur simultaneously with the worst-case HAC fire transient stresses, etc.), it is apparent that the actual margin of safety will be significantly larger than +0.70. Regardless, the requirement of Paragraph C.7 of NRC Regulatory Guide 7.6[12] is met.

[13] American Society of Mechanical Engineers (ASME) Boiler and Pressure Vessel Code, Section III, *Rules for Construction of Nuclear Power Plant Components*, Division 1, Subsection NB and Appendices, 1986 Edition.

2.7.5 Immersion – Fissile Material

The criticality evaluation presented in Chapter 6.0, *Criticality Evaluation*, considers the effect of water in-leakage. Thus, the requirement of 10 CFR §71.73(c)(5)[1] is met.

2.7.6 Immersion – All Packages

The effect of a 21 psig external pressure due to immersion in 50 feet of water, as required by 10 CFR §71.73(c)(6)[1], is of negligible consequence for the RH-TRU 72-B package.

2.7.7 Deep Water Immersion Test

A 290 psig external water pressure, for Type B packages containing more than 10^5 A_2, as required by 10 CFR §71.61[1], results in shell and end closure stresses less than those evaluated in Section 2.7.4, *Thermal*, for 300 psig internal pressure. Therefore, reported margins of safety will be greater.

As shown in the following sections, buckling of the OC inner (containment) shell is not of consequence due to the effect of a 290 psig external pressure. The cylindrical portion of the OC is evaluated using ASME Boiler and Pressure Vessel Code Case N-284[14]. Consistent with Regulatory Guide 7.6[12] philosophy, a factor of safety of 1.34 is applied for HAC buckling evaluations per ASME Code Case N-284[14], corresponding to ASME Code, Service Level D conditions.

Buckling analysis geometry parameters are summarized in Table 2.7-29, and loading parameters are summarized in Table 2.7-30. The cylindrical shell buckling analysis utilizes an OC temperature of 70 ºF. The stresses are determined using an external pressure of 290 psig. The hoop stress, σ_θ, and axial stress, σ_ϕ, are found from:

$$\sigma_\theta = \frac{Pr}{t} \qquad \sigma_\phi = \frac{Pr}{2t}$$

where P is the applied external pressure of 290 psi, r is the mean radius, and t is the cylindrical shell thickness. Conservatively included also with the pressure stresses for the OC inner shell are the hoop and axial fabrication stresses, σ_h = 1,413 psi (at 70 ºF), and σ_a = 1,963 psi, respectively, identified in Appendix 2.10.8, *Fabrication Stresses Due to Lead Pour*.

Buckling analysis methodology is addressed in Appendix 2.10.5, *Buckling Design Criteria and Detailed Evaluation*. As shown in Table 2.7-31, since all interaction check parameters are less than 1.0, as required, the design criteria are satisfied.

Thus, the effect of a 290 psig external water pressure, for Type B packages containing more than 10^5 A_2, as required by 10 CFR §71.61[1], is of negligible consequence for the RH-TRU 72-B package.

[14] American Society of Mechanical Engineers (ASME) Boiler and Pressure Vessel Code, Section III, *Rules for Construction of Nuclear Power Plant Components*, Division 1, Class MC, Code Case N-284, *Metal Containment Shell Buckling Design Methods*, August 25, 1980.

2.7.8 Summary of Damage

The analyses presented in the preceding sections demonstrate that the HAC test sequence will not result in any significant structural damage to the RH-TRU 72-B package. Nearly all permanent damage occurs in the external impact limiters, as desired. Minor damage can occur to packaging components, as summarized in the remainder of this section.

For the 30-foot free drop event, no lead slump will occur as detailed in Paragraph (9) of Section 2.7.1.1, *Flat End Drop*. For the 40-inch drop onto a 6-inch diameter puncture bar, occurring on the side of the package at midlength, localized package damage can occur at the impact point. However, overall bending response of the package remains elastic. Additionally, the OC outer shell will not be perforated, and no melting of the lead shielding occurs in the ensuing HAC fire event.

Localized puncture damage occurs in the form of a reduction in lead thickness adjacent to the point of impact of the puncture bar. Puncture drop results from the NuPac 125-B quarter-scale testing program[2] are analyzed to provide a conservative estimate of similar damage that could be expected for the RH-TRU 72-B package. The 40-inch side drop on the puncture bar caused, at most, a 35% localized reduction in the thickness of the lead shielding on the NuPac 125-B cask[2]. This estimate is conservative for the RH-TRU 72-B package because it is significantly lower in weight than the NuPac 125-B cask[2], and puncture-induced deformations are expected to be less.

These permanent deformations are of little consequence for the RH-TRU 72-B package, as they represent only minor changes in package geometry. In particular, damage is not sufficient to compromise "leaktightness" of the IV or OC containment boundaries. Lead deformation is only of concern relative to shielding. The worst-case puncture damage is therefore addressed in the shielding evaluation in Chapter 5.0, *Shielding Evaluation*. For these reasons, the integrity of the package is not considered to be compromised by the HAC test sequence set forth in 10 CFR 71[1].

Table 2.7-1 – Summary of HAC Material Properties for Analysis

Material Property	Material Property Value (psi)						Reference
	-40 °F	-20 °F	70 °F	160 °F	200 °F	210 °F	
ASTM A240/A276, Type 304 Stainless Steel							
Elastic Modulus, E ($\times 10^6$)	28.9	28.8	28.3	27.8	27.6	27.5	Table 2.3-1
Design Stress Intensity, S_m	20,000	20,000	20,000	20,000	20,000	20,000	
Yield Strength, S_y	30,000	30,000	30,000	27,000	25,000	24,750	
Ultimate Strength, S_u	75,000	75,000	75,000	72,600	71,000	70,500	
Stress Intensity Allowable for Containment Structures (Table 2.1-1)							
Primary Membrane	48,000	48,000	48,000	48,000	48,000	48,000	
Primary Membrane-Plus-Bending	72,000	72,000	72,000	72,000	71,000	70,500	
Pure Shear	31,500	31,500	31,500	30,500	29,800	29,600	
Bearing (Sealing Surfaces)	30,000	30,000	30,000	27,000	25,000	24,750	
ASTM A182/SA182, Type F304, Stainless Steel							
Elastic Modulus, E ($\times 10^6$)	28.9	28.8	28.3	27.8	27.6	27.5	Table 2.3-1
Design Stress Intensity, S_m	20,000	20,000	20,000	20,000	20,000	20,000	
Yield Strength, S_y	30,000	30,000	30,000	27,000	25,000	24,750	
Ultimate Strength, S_u	70,000	70,000	70,000	67,700	66,200	65,700	
Stress Intensity Allowable for Containment Structures (Table 2.1-1)							
Primary Membrane	48,000	48,000	48,000	47,400	46,300	46,000	
Primary Membrane-Plus-Bending	70,000	70,000	70,000	67,700	66,200	65,700	
Pure Shear	29,400	29,400	29,400	28,400	27,800	27,600	
Bearing (Sealing Surfaces)	30,000	30,000	30,000	27,000	25,000	24,750	
ASTM A516, Grade 55, Carbon Steel							
Elastic Modulus, E ($\times 10^6$)	29.5	29.5	29.5	29.3	28.8	28.8	Table 2.3-1
Design Stress Intensity, S_m	18,300	18,300	18,300	18,300	18,300	18,200	
Yield Strength, S_y	30,000	30,000	30,000	28,400	27,300	27,200	
Ultimate Strength, S_u	55,000	55,000	55,000	55,000	55,000	55,000	
Stress Intensity Allowable for Non-Containment Structures (Table 2.1-2)							
Primary Membrane	38,500	38,500	38,500	38,500	38,500	38,500	
Primary Membrane-Plus-Bending	55,000	55,000	55,000	55,000	55,000	55,000	
Pure Shear	23,100	23,100	23,100	23,100	23,100	23,100	
ASTM A320, Grade L43, Alloy Steel							
Elastic Modulus, E ($\times 10^6$)	27.8	27.8	27.8	27.3	27.1	27.1	Table 2.3-1
Design Stress Intensity, S_m	35,000	35,000	35,000	33,800	33,000	32,900	
Yield Strength, S_y	105,000	105,000	105,000	101,400	99,000	98,700	
Ultimate Strength, S_u	125,000	125,000	125,000	125,000	125,000	125,000	
Stress Intensity Allowable for Containment Fasteners (Table 2.1-1)							
Primary Membrane	105,000	105,000	105,000	101,400	99,000	98,700	
Primary Membrane-Plus-Bending	105,000	105,000	105,000	101,400	99,000	98,700	
Stress Intensity Allowable for Non-Containment Fasteners (Table 2.1-2)							
Primary Membrane	105,000	105,000	105,000	101,400	99,000	98,700	
Primary Membrane-Plus-Bending	125,000	125,000	125,000	125,000	125,000	125,000	

Table 2.7-2 – Fabrication Induced OC Inner Shell Hoop Stress, Interface Pressure, and Axial Load That Can Be Supported

Temperature (ºF)	Hoop Stress (psi)	Interface Pressure (psi)	Coefficient of Friction	Axial Load (lb)
160	-1,038	62.2	0.5	414,842
			1.0	829,685
70	-1,413	84.7	0.5	564,906
			1.0	1,129,812
-20	-1,821	109.1	0.5	727,641
			1.0	1,455,283

Table 2.7-3 – OC Shell Stresses with Maximum End Drop Fab Condition

Temperature (ºF)	Inner Shell Stresses (psi)		Outer Shell Stresses (psi)	
	Hoop σ_t	Axial σ_z	Hoop σ_t	Axial σ_z
160	-1,038	-12,801	0	-6,180
70	-1,413	-12,801	0	-6,180
-20	-1,821	-12,801	0	-6,180

Table 2.7-4 – HAC Fab & End Drop, OC Inner Shell with 89.7*g* at -20 ºF

Evaluation Parameters	
Loading Condition:	HAC Flat End Drop, -20 ºF Foam
Structural Material:	ASTM A240, Type 304, Stainless Steel
Stress Condition:	Primary Membrane
Structural Criterion:	Containment Boundary
Stress Allowable (from Table 2.1-1):	$2.4S_m$
Material Temperature:	-20 ºF
Allowable Stress, S_a:	48,000 psi

Load Condition	Stress Components (psi)				Reference Section
	Radial σ_r	Hoop σ_t	Axial σ_z	Shear τ_{rz}	
Fabrication and End Drop	0	-1,821	-12,801	0	2.7.1.1(6)
Direct Stress Summation	0	-1,821	-12,801	0	—
Principal Stresses	0	-1,821	-12,801	—	—
Stress Differences	12,801	10,980	1,821	—	—
Maximum Stress Intensity (SI)	12,801	—	—	—	—
Allowable Stress Intensity (S_a)	48,000	—	—	—	—
Margin of Safety ($MS = S_a/SI - 1$)	+2.75	—	—	—	—

Table 2.7-5 – HAC Fab & End Drop, OC Inner Shell with 89.7*g* at 70 ºF

Evaluation Parameters					
Loading Condition:	HAC Flat End Drop, -20 ºF Foam				
Structural Material:	ASTM A240, Type 304, Stainless Steel				
Stress Condition:	Primary Membrane				
Structural Criterion:	Containment Boundary				
Stress Allowable (from Table 2.1-1):	$2.4S_m$				
Material Temperature:	70 ºF				
Allowable Stress, S_a:	48,000 psi				
	Stress Components (psi)				
Load Condition	**Radial σ_r**	**Hoop σ_t**	**Axial σ_z**	**Shear τ_{rz}**	**Reference Section**
Fabrication and End Drop	0	-1,413	-12,801	0	2.7.1.1(6)
Direct Stress Summation	0	-1,413	-12,801	0	—
Principal Stresses	0	-1,413	-12,801	—	—
Stress Differences	12,801	11,388	1,413	—	—
Maximum Stress Intensity (SI)	12,801	—	—	—	—
Allowable Stress Intensity (S_a)	48,000	—	—	—	—
Margin of Safety ($MS = S_a/SI - 1$)	+2.75	—	—	—	—

Table 2.7-6 – HAC Fab & End Drop, OC Inner Shell with 89.7*g* at 160 ºF

Evaluation Parameters					
Loading Condition:	HAC Flat End Drop, -20 ºF Foam				
Structural Material:	ASTM A240, Type 304, Stainless Steel				
Stress Condition:	Primary Membrane				
Structural Criterion:	Containment Boundary				
Stress Allowable (from Table 2.1-1):	$2.4S_m$				
Material Temperature:	160 ºF				
Allowable Stress, S_a:	48,000 psi				
	Stress Components (psi)				
Load Condition	**Radial σ_r**	**Hoop σ_t**	**Axial σ_z**	**Shear τ_{rz}**	**Reference Section**
Fabrication and End Drop	0	-1,038	-12,801	0	2.7.1.1(6)
Direct Stress Summation	0	-1,038	-12,801	0	—
Principal Stresses	0	-1,038	-12,801	—	—
Stress Differences	12,801	11,763	1,038	—	—
Maximum Stress Intensity (SI)	12,801	—	—	—	—
Allowable Stress Intensity (S_a)	48,000	—	—	—	—
Margin of Safety ($MS = S_a/SI - 1$)	+2.75	—	—	—	—

Table 2.7-7 – HAC End Drop, Lead Pressure and Hoop Stress Summary

Temperature (ºF)	σ_y (psi)	d (in)	p_{max} (psi)	$\sigma_t = p_{max}R/t$ (psi)	
				Inner Shell	Outer Shell
160	~600	16.31	157.8	-2,633	2,085
70	~800	21.75	166.2	-2,774	2,197
-20	~1,000	27.19	175.6	-2,931	2,321

Table 2.7-8 – HAC End Drop, OC Shell Stresses with Zero Fabrication Condition with 89.7*g* Acceleration

Temperature (ºF)	Inner Shell Stresses (psi)		Outer Shell Stresses (psi)	
	Hoop σ_t	Axial σ_z	Hoop σ_t	Axial σ_z
160	-2,633	-10,530	2,085	-7,493
70	-2,774	-10,530	2,197	-7,493
-20	-2,931	-10,530	2,321	-7,493

Table 2.7-9 – HAC End Drop, OC Inner Shell with 89.7*g* at -20 ºF

Evaluation Parameters	
Loading Condition:	HAC Flat End Drop, -20 ºF Foam
Structural Material:	ASTM A240, Type 304, Stainless Steel
Stress Condition:	Primary Membrane
Structural Criterion:	Containment Boundary
Stress Allowable (from Table 2.1-1):	$2.4S_m$
Material Temperature:	-20 ºF
Allowable Stress, S_a:	48,000 psi

Load Condition	Stress Components (psi)				Reference Section
	Radial σ_r	Hoop σ_t	Axial σ_z	Shear τ_{rz}	
Fabrication and End Drop	0	-2,931	-10,530	0	2.7.1.1(7)
Direct Stress Summation	0	-2,931	-10,530	0	—
Principal Stresses	0	-2,931	-10,530	—	—
Stress Differences	10,530	7,599	2,931	—	—
Maximum Stress Intensity (SI)	10,530	—	—	—	—
Allowable Stress Intensity (S_a)	48,000	—	—	—	—
Margin of Safety ($MS = S_a/SI - 1$)	+3.56	—	—	—	—

Table 2.7-10 – HAC End Drop, OC Inner Shell with 89.7*g* at 70 ºF

Evaluation Parameters					
Loading Condition:	HAC Flat End Drop, -20 ºF Foam				
Structural Material:	ASTM A240, Type 304, Stainless Steel				
Stress Condition:	Primary Membrane				
Structural Criterion:	Containment Boundary				
Stress Allowable (from Table 2.1-1):	$2.4S_m$				
Material Temperature:	70 ºF				
Allowable Stress, S_a:	48,000 psi				
	Stress Components (psi)				
Load Condition	**Radial σ_r**	**Hoop σ_t**	**Axial σ_z**	**Shear τ_{rz}**	**Reference Section**
End Drop	0	-2,774	-10,530	0	2.7.1.1(7)
Direct Stress Summation	0	-2,774	-10,530	0	—
Principal Stresses	0	-2,774	-10,530	—	—
Stress Differences	10,530	7,756	2,774	—	—
Maximum Stress Intensity (SI)	10,530	—	—	—	—
Allowable Stress Intensity (S_a)	48,000	—	—	—	—
Margin of Safety ($MS = S_a/SI - 1$)	+3.56	—	—	—	—

Table 2.7-11 – HAC End Drop, OC Inner Shell with 89.7*g* at 160 ºF

Evaluation Parameters					
Loading Condition:	HAC Flat End Drop, -20 ºF Foam				
Structural Material:	ASTM A240, Type 304, Stainless Steel				
Stress Condition:	Primary Membrane				
Structural Criterion:	Containment Boundary				
Stress Allowable (from Table 2.1-1):	$2.4S_m$				
Material Temperature:	160 ºF				
Allowable Stress, S_a:	48,000 psi				
	Stress Components (psi)				
Load Condition	**Radial σ_r**	**Hoop σ_t**	**Axial σ_z**	**Shear τ_{rz}**	**Reference Section**
End Drop	0	-2,633	-10,530	0	2.7.1.1(7)
Direct Stress Summation	0	-2,633	-10,530	0	—
Principal Stresses	0	-2,633	-10,530	—	—
Stress Differences	10,530	7,897	2,633	—	—
Maximum Stress Intensity (SI)	10,530	—	—	—	—
Allowable Stress Intensity (S_a)	48,000	—	—	—	—
Margin of Safety ($MS = S_a/SI - 1$)	+3.56	—	—	—	—

Table 2.7-12 – HAC Temperature-Corrected Margin of Safety Against Lead Slump

Lead Temperature (ºF)	Impact Acceleration, g (per Table 2.10.3-10)	Lead Stress, $\sigma = \rho gh$ (psi)	Minimum Flow Stress (psi)	Margin of Safety
-20	89.7	4,570	6,350	+0.39
160	51.1	2,603	3,650	+0.40

Table 2.7-13 – OC Shell Stresses with Max Oblique Drop Fab Condition

Temperature (ºF)	Inner Shell Stresses (psi)		Outer Shell Stresses (psi)	
	Hoop σ_t	Axial σ_z	Hoop σ_t	Axial σ_z
160	-1,038	-6,866	0	-3,315
70	-1,413	-6,866	0	-3,315
-20	-1,821	-6,866	0	-3,315

Table 2.7-14 – HAC Fab & Oblique Drop, OC Inner Shell with 48.1*g* at -20 ºF

Evaluation Parameters	
Loading Condition:	HAC 5º Oblique Drop, -20 ºF Foam
Structural Material:	ASTM A240, Type 304, Stainless Steel
Stress Condition:	Primary Membrane
Structural Criterion:	Containment Boundary
Stress Allowable (from Table 2.1-1):	$2.4S_m$
Material Temperature:	-20 ºF
Allowable Stress, S_a:	48,000 psi

Load Condition	Stress Components (psi)				Reference Section
	Radial σ_r	Hoop σ_t	Axial σ_z	Shear τ_{rz}	
Fabrication	0	-1,821	-6,866	0	2.7.1.2(4)
Oblique Drop	0	0	-17,049	4,796	2.7.1.2(4)
Direct Stress Summation	0	-1,821	-23,915	4,796	—
Principal Stresses	926	-1,821	-24,841	—	—
Stress Differences	25,767	23,020	2,747	—	—
Maximum Stress Intensity (SI)	25,767	—	—	—	—
Allowable Stress Intensity (S_a)	48,000	—	—	—	—
Margin of Safety ($MS = S_a/SI - 1$)	+0.86	—	—	—	—

Table 2.7-15 – HAC Fab & Oblique Drop, OC Inner Shell with 48.1*g* at 70 ºF

Evaluation Parameters	
Loading Condition:	HAC 5º Oblique Drop, -20 ºF Foam
Structural Material:	ASTM A240, Type 304, Stainless Steel
Stress Condition:	Primary Membrane
Structural Criterion:	Containment Boundary
Stress Allowable (from Table 2.1-1):	$2.4S_m$
Material Temperature:	70 ºF
Allowable Stress, S_a:	48,000 psi

Load Condition	Stress Components (psi)				Reference Section
	Radial σ_r	Hoop σ_t	Axial σ_z	Shear τ_{rz}	
Fabrication	0	-1,413	-6,866	0	2.7.1.2(4)
Oblique Drop	0	0	-17,049	4,796	2.7.1.2(4)
Direct Stress Summation	0	-1,413	-23,915	4,796	—
Principal Stresses	926	-1,413	-24,841	—	—
Stress Differences	25,767	23,428	2,339	—	—
Maximum Stress Intensity (SI)	25,767	—	—	—	—
Allowable Stress Intensity (S_a)	48,000	—	—	—	—
Margin of Safety ($MS = S_a/SI - 1$)	+0.86	—	—	—	—

Table 2.7-16 – HAC Fab & Oblique Drop, OC Inner Shell with 48.1*g* at 160 ºF

Evaluation Parameters	
Loading Condition:	HAC 5º Oblique Drop, -20 ºF Foam
Structural Material:	ASTM A240, Type 304, Stainless Steel
Stress Condition:	Primary Membrane
Structural Criterion:	Containment Boundary
Stress Allowable (from Table 2.1-1):	$2.4S_m$
Material Temperature:	160 ºF
Allowable Stress, S_a:	48,000 psi

Load Condition	Stress Components (psi)				Reference Section
	Radial σ_r	Hoop σ_t	Axial σ_z	Shear τ_{rz}	
Fabrication	0	-1,038	-6,866	0	2.7.1.2(4)
Oblique Drop	0	0	-17,049	4,796	2.7.1.2(4)
Direct Stress Summation	0	-1,038	-23,915	4,796	—
Principal Stresses	926	-1,038	-24,841	—	—
Stress Differences	25,767	23,803	1,964	—	—
Maximum Stress Intensity (SI)	25,767	—	—	—	—
Allowable Stress Intensity (S_a)	48,000	—	—	—	—
Margin of Safety ($MS = S_a/SI - 1$)	+0.86	—	—	—	—

Table 2.7-17 – HAC Oblique Drop, IV Shell with 48.1*g* at 70 ºF

Evaluation Parameters	
Loading Condition:	HAC 5º Oblique Drop, -20 ºF Foam
Structural Material:	ASTM A240, Type 304, Stainless Steel
Stress Condition:	Primary Membrane
Structural Criterion:	Containment Boundary
Stress Allowable (from Table 2.1-1):	$2.4S_m$
Material Temperature:	70 ºF
Allowable Stress, S_a:	48,000 psi

Load Condition	Stress Components (psi)				Reference Section
	Radial σ_r	Hoop σ_t	Axial σ_z	Shear τ_{rz}	
Oblique Drop	0	0	-21,372	7,503	2.7.1.2(5)
Direct Stress Summation	0	0	-21,372	7,503	—
Principal Stresses	2,371	0	-23,743	—	—
Stress Differences	26,114	23,743	2,371	—	—
Maximum Stress Intensity (SI)	26,114	—	—	—	—
Allowable Stress Intensity (S_a)	48,000	—	—	—	—
Margin of Safety ($MS = S_a/SI - 1$)	+0.84	—	—	—	—

Table 2.7-18 – HAC Oblique Drop, Canister Shell with 48.1*g* at 210 ºF

Evaluation Parameters	
Loading Condition:	HAC 5º Oblique Drop, -20 ºF Foam
Structural Material:	ASTM A516, Grade 55, Carbon Steel
Stress Condition:	Primary Membrane
Structural Criterion:	Non-containment Boundary
Stress Allowable (from Table 2.1-2):	$0.7S_u$
Material Temperature:	210 ºF
Allowable Stress, S_a:	38,500 psi

Load Condition	Stress Components (psi)				Reference Section
	Radial σ_r	Hoop σ_t	Axial σ_z	Shear τ_{rz}	
Oblique Drop	0	0	-23,703	12,189	2.7.1.2(6)
Direct Stress Summation	0	0	-23,703	12,189	—
Principal Stresses	5,149	0	-28,852	—	—
Stress Differences	34,001	28,852	5,149	—	—
Maximum Stress Intensity (SI)	34,001	—	—	—	—
Allowable Stress Intensity (S_a)	38,500	—	—	—	—
Margin of Safety ($MS = S_a/SI - 1$)	+0.13	—	—	—	—

Table 2.7-19 – OC Shell Stresses with Max Side Drop Fab Condition

Temperature (ºF)	Inner Shell Stresses (psi)		Outer Shell Stresses (psi)	
	Hoop σ_t	Axial σ_z	Hoop σ_t	Axial σ_z
160	-1,038	-1,963	0	0
70	-1,413	-1,963	0	0
-20	-1,821	-1,963	0	0

Note:

① Axial compressive stress in the inner shell per Appendix 2.10.8.5, *Axial Stress Evaluation after Cooldown from 620 ºF to -20 ºF*.

Table 2.7-20 – HAC Fab & Side Drop, OC Inner Shell with 81.2*g* at -20 ºF

Evaluation Parameters	
Loading Condition:	HAC Flat Side Drop, -20 ºF Foam
Structural Material:	ASTM A240, Type 304, Stainless Steel
Stress Condition:	Primary Membrane
Structural Criterion:	Containment Boundary
Stress Allowable (from Table 2.1-1):	$2.4S_m$
Material Temperature:	-20 ºF
Allowable Stress, S_a:	48,000 psi

Load Condition	Stress Components (psi)				Reference Section
	Radial σ_r	Hoop σ_t	Axial σ_z	Shear τ_{rz}	
Fabrication	0	-1,821	-1,963	0	2.7.1.3(4)
Side Drop	0	0	-16,331	5,554	2.7.1.3(4)
Direct Stress Summation	0	-1,821	-18,294	5,554	—
Principal Stresses	1,554	-1,821	-19,848	—	—
Stress Differences	21,402	18,027	3,375	—	—
Maximum Stress Intensity (SI)	21,402	—	—	—	—
Allowable Stress Intensity (S_a)	48,000	—	—	—	—
Margin of Safety ($MS = S_a/SI - 1$)	+1.24	—	—	—	—

Table 2.7-21 – HAC Fab & Side Drop, OC Inner Shell with 81.2*g* at 70 ºF

Evaluation Parameters	
Loading Condition:	HAC Flat Side Drop, -20 ºF Foam
Structural Material:	ASTM A240, Type 304, Stainless Steel
Stress Condition:	Primary Membrane
Structural Criterion:	Containment Boundary
Stress Allowable (from Table 2.1-1):	$2.4S_m$
Material Temperature:	70 ºF
Allowable Stress, S_a:	48,000 psi

Load Condition	Stress Components (psi)				Reference Section
	Radial σ_r	Hoop σ_t	Axial σ_z	Shear τ_{rz}	
Fabrication	0	-1,413	-1,963	0	2.7.1.3(4)
Side Drop	0	0	-16,331	5,554	2.7.1.3(4)
Direct Stress Summation	0	-1,413	-18,294	5,554	—
Principal Stresses	1,554	-1,413	-19,848	—	—
Stress Differences	21,402	18,435	2,967	—	—
Maximum Stress Intensity (SI)	21,402	—	—	—	—
Allowable Stress Intensity (S_a)	48,000	—	—	—	—
Margin of Safety ($MS = S_a/SI - 1$)	+1.24	—	—	—	—

Table 2.7-22 – HAC Fab & Side Drop, OC Inner Shell with 81.2*g* at 160 ºF

Evaluation Parameters	
Loading Condition:	HAC Flat Side Drop, -20 ºF Foam
Structural Material:	ASTM A240, Type 304, Stainless Steel
Stress Condition:	Primary Membrane
Structural Criterion:	Containment Boundary
Stress Allowable (from Table 2.1-1):	$2.4S_m$
Material Temperature:	160 ºF
Allowable Stress, S_a:	48,000 psi

Load Condition	Stress Components (psi)				Reference Section
	Radial σ_r	Hoop σ_t	Axial σ_z	Shear τ_{rz}	
Fabrication	0	-1,038	-1,963	0	2.7.1.3(4)
Side Drop	0	0	-16,331	5,554	2.7.1.3(4)
Direct Stress Summation	0	-1,038	-18,294	5,554	—
Principal Stresses	1,554	-1,038	-19,848	—	—
Stress Differences	21,402	18,810	2,592	—	—
Maximum Stress Intensity (SI)	21,402	—	—	—	—
Allowable Stress Intensity (S_a)	48,000	—	—	—	—
Margin of Safety ($MS = S_a/SI - 1$)	+1.24	—	—	—	—

Table 2.7-23 – HAC Side Drop, IV Shell with 81.2*g* at 160 ºF

Evaluation Parameters	
Loading Condition:	HAC Flat Side Drop, -20 ºF Foam
Structural Material:	ASTM A240, Type 304, Stainless Steel
Stress Condition:	Primary Membrane
Structural Criterion:	Containment Boundary
Stress Allowable (from Table 2.1-1):	$2.4S_m$
Material Temperature:	160 ºF
Allowable Stress, S_a:	48,000 psi

Load Condition	Stress Components (psi)				Reference Section
	Radial σ_r	Hoop σ_t	Axial σ_z	Shear τ_{rz}	
Side Drop	0	0	-19,611	9,317	2.7.1.3(5)
Direct Stress Summation	0	0	-19,611	9,317	—
Principal Stresses	3,721	0	-23,332	—	—
Stress Differences	27,053	23,332	3,721	—	—
Maximum Stress Intensity (SI)	27,053	—	—	—	—
Allowable Stress Intensity (S_a)	48,000	—	—	—	—
Margin of Safety ($MS = S_a/SI - 1$)	+0.77	—	—	—	—

Table 2.7-24 – HAC Side Drop, Canister Shell with 81.2*g* at 210 ºF

Evaluation Parameters	
Loading Condition:	HAC Flat Side Drop, -20 ºF Foam
Structural Material:	ASTM A516, Grade 55, Carbon Steel
Stress Condition:	Primary Membrane
Structural Criterion:	Non-containment Boundary
Stress Allowable (from Table 2.1-2):	$0.7S_u$
Material Temperature:	210 ºF
Allowable Stress, S_a:	38,500 psi

Load Condition	Stress Components (psi)				Reference Section
	Radial σ_r	Hoop σ_t	Axial σ_z	Shear τ_{rz}	
Side Drop	0	0	-16,844	10,021	2.7.1.3(6)
Direct Stress Summation	0	0	-16,844	10,021	—
Principal Stresses	4,668	0	-21,512	—	—
Stress Differences	26,180	21,512	4,668	—	—
Maximum Stress Intensity (SI)	26,180	—	—	—	—
Allowable Stress Intensity (S_a)	38,500	—	—	—	—
Margin of Safety ($MS = S_a/SI - 1$)	+0.47	—	—	—	—

Table 2.7-25 – HAC Fab & Side Drop, OC Shells' Welds with 81.2*g* at -20 ºF

Evaluation Parameters	
Loading Condition:	HAC Flat Side Drop, -20 ºF Foam
Structural Material:	ASTM A240, Type 304, Stainless Steel
Stress Condition:	Primary Membrane
Structural Criterion:	Containment Boundary
Stress Allowable (from Table 2.1-1):	$2.4S_m$
Material Temperature:	-20 ºF
Allowable Stress, S_a:	48,000 psi

Load Condition	Stress Components (psi)				Reference Section
	Radial σ_r	Hoop σ_t	Axial σ_z	Shear τ_{rz}	
Fabrication	0	-1,821	-1,963	0	2.7.1.3(4)
Side Drop	0	0	-16,323	10,191	2.7.1.3(4)(8)
Direct Stress Summation	0	-1,821	-18,286	10,191	—
Principal Stresses	4,548	-1,821	-22,834	—	—
Stress Differences	27,382	21,013	6,369	—	—
Maximum Stress Intensity (SI)	27,382	—	—	—	—
Allowable Stress Intensity (S_a)	48,000	—	—	—	—
Margin of Safety ($MS = S_a/SI - 1$)	+0.75	—	—	—	—

Table 2.7-26 – Stress-Strain Values for Type 304 Stainless Steel at 212 ºF

True Stress, σ (psi)	True Strain, ε (in/in)
20,500	$7.401(10)^{-4}$
24,000	$1.805(10)^{-3}$
26,000	$4.555(10)^{-3}$
36,000	$4.684(10)^{-2}$
48,000	$1.209(10)^{-1}$

Table 2.7-27 – Stresses Due to 300 psig Pressure

Shell / End Plate Location①	Axial Membrane σ_1 (psi)	Hoop Membrane σ_2 (psi)	Axial Bending② σ_1' (psi)	Hoop Bending② σ_2' (psi)	Radial Bending σ (psi)
P1	1,980	3,963	0	0	—
P2	2,505	5,004	0	0	—
P3	6,324	12,648	0	0	—
P4	1,980	582	-6,129	-1,839	—
P5	2,505	753	-7,725	-2,319	—
P6	6,501	-11,322	-66,060	-20,598	—
P7	—	—	—	—	6,426
P8	—	—	—	—	3,645
P9	—	—	—	—	2,250
P10	—	—	—	—	42,240

Notes:

① Locations are shown in Figure 2.6-1 from Section 2.6.1.3, *Stress Calculations*.

② σ_1' and σ_2' are positive when tensile on the shell outside diameter.

Table 2.7-28 – Thermal Stress Summary

Stress Location	Stress Category	HAC Temperature (ºF)	Allowable Stress Intensity (psi)	Actual Stress Intensity (psi)	Margin of Safety
P1	Membrane	705	38,350	3,963	+8.68
P2	Membrane	550	40,700	5,004	+7.13
P3	Membrane	390	45,200	12,648	+2.57
P4	Membrane	500	42,000	1,980	+20.21
	Membrane + Bending	500	63,000	6,129	+9.28
P5	Membrane	500	42,000	2,505	+15.77
	Membrane + Bending	500	63,000	7,725	+7.16
P6	Membrane	300	46,200	17,823	+1.59
P7	Membrane + Bending	500	59,300	6,426	+8.23
P8	Membrane + Bending	500	59,300	3,645	+15.27
P9	Membrane + Bending	300	61,500	2,250	+26.33
P10	Membrane + Bending	300	61,500	42,240	+0.46

Table 2.7-29 – Buckling Geometry Parameters per Code Case N-284

Geometry and Material Input	
	OC
Mean Radius, inch	16.69
Shell Thickness, inch	1.000
Length, inch	121.25
Geometry Output (nomenclature consistent with ASME Code Case N-284)	
R =	16.69
T =	1.000
$(Rt)^{½}$ =	4.085
L_ϕ =	121.25
L_θ =	104.87
M_ϕ =	29.68
M_θ =	25.67
M =	25.67

Table 2.7-30 – Stresses for 290 psig External Pressure + Fabrication

Component	**OC**	
	Axial Stress, σ_ϕ	**Hoop Stress, σ_θ**
Pressure	2,420	4,840
Fabrication	1,963	1,413
Total	4,383	6,253

Table 2.7-31 – Buckling Summary for 290 psig External Pressure + Fab

Condition	Outer Cask	Remarks
Capacity Reduction Factors (-1511)		
$\alpha_{\phi L}$ =	0.2670	
$\alpha_{\theta L}$ =	0.8000	
$\alpha_{\phi\theta L}$ =	0.8000	
Plasticity Reduction Factors (-1610)		
η_{ϕ} =	1.0000	
η_{θ} =	1.0000	
$\eta_{\phi\theta}$ =	1.0000	
Theoretical Buckling Values (-1712.1.1)		
C_{ϕ} =	0.6050	
$\sigma_{\phi eL}$ =	1,025,854 psi	
$C_{\theta r}$ =	0.0291	
$\sigma_{\theta eL} = \sigma_{reL}$ =	49,274 psi	
$C_{\theta h}$ =	0.0291	
$\sigma_{\theta eL} = \sigma_{heL}$ =	49,274 psi	
$C_{\theta h}$ =	0.1369	
$\sigma_{\phi\theta eL}$ =	232,189 psi	
Elastic Interaction Equations (-1713.1.1)		
$\sigma_{\phi s}$ =	21,997 psi	
$\sigma_{\theta s}$ =	10,474 psi	
$\sigma_{\phi\theta s}$ =	0 psi	
Axial + Hoop ⇨ Check (a):	*N/A*	<1 ∴ OK
Axial + Hoop ⇨ Check (b):	*N/A*	<1 ∴ OK
Axial + Shear ⇨ Check (c):	0.0214	<1 ∴ OK
Hoop + Shear ⇨ Check (d):	0.2126	<1 ∴ OK
Axial + Hoop + Shear ⇨ Check (e):	*N/A*	<1 ∴ OK
Inelastic Interaction Equations (-1713.2.1)		
$\sigma_{\phi s}$ =	21,997 psi	
$\sigma_{\theta s}$ =	10,474 psi	
$\sigma_{\phi\theta s}$ =	0 psi	
Axial + Shear ⇨ Check (a):	0.0005	<1 ∴ OK
Hoop + Shear ⇨ Check (b):	0.0452	<1 ∴ OK

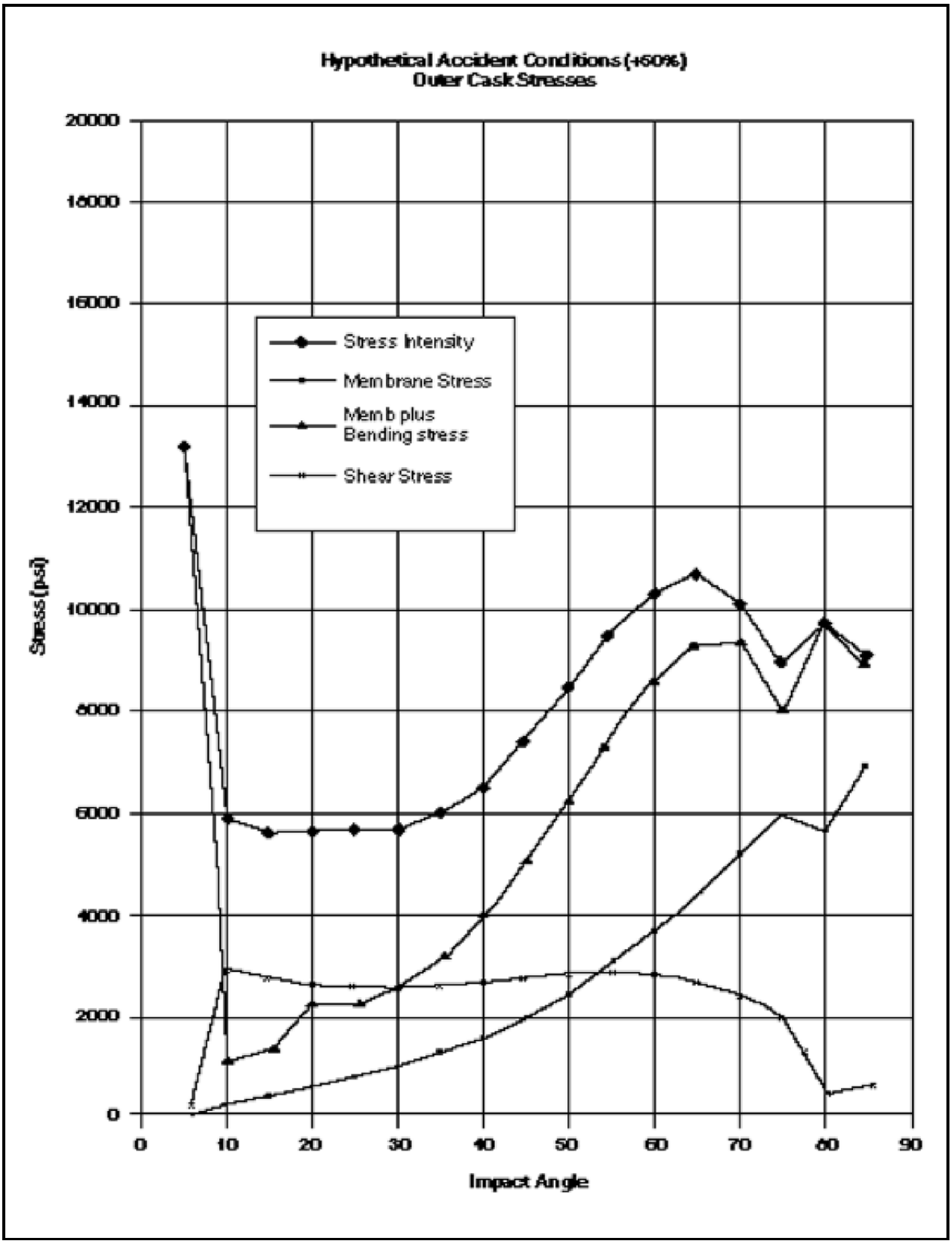

Figure 2.7-1 – HAC Cold (-20 ºF) Outer Cask Stresses

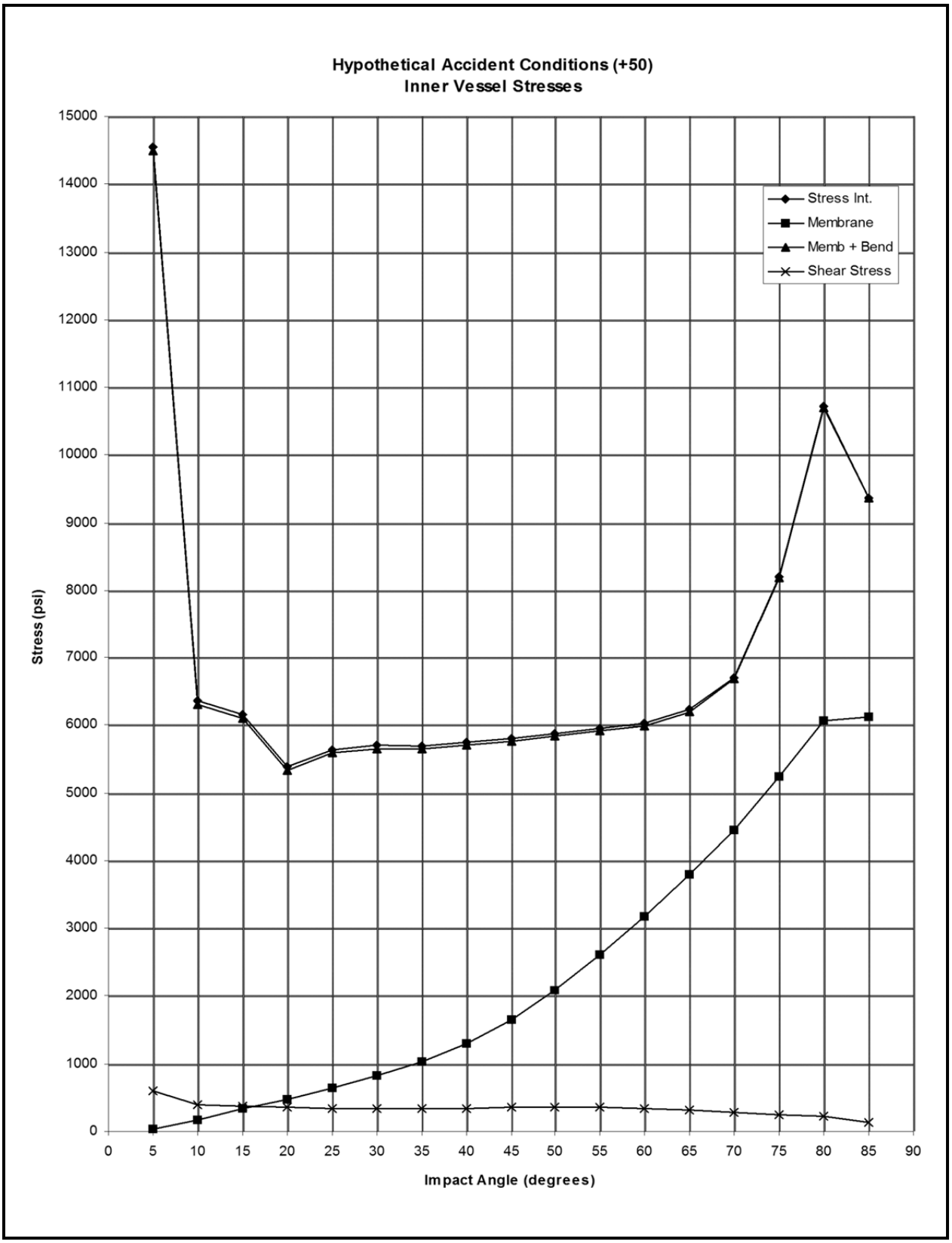

Figure 2.7-2 – HAC Cold (-20 ºF) Inner Vessel Stresses

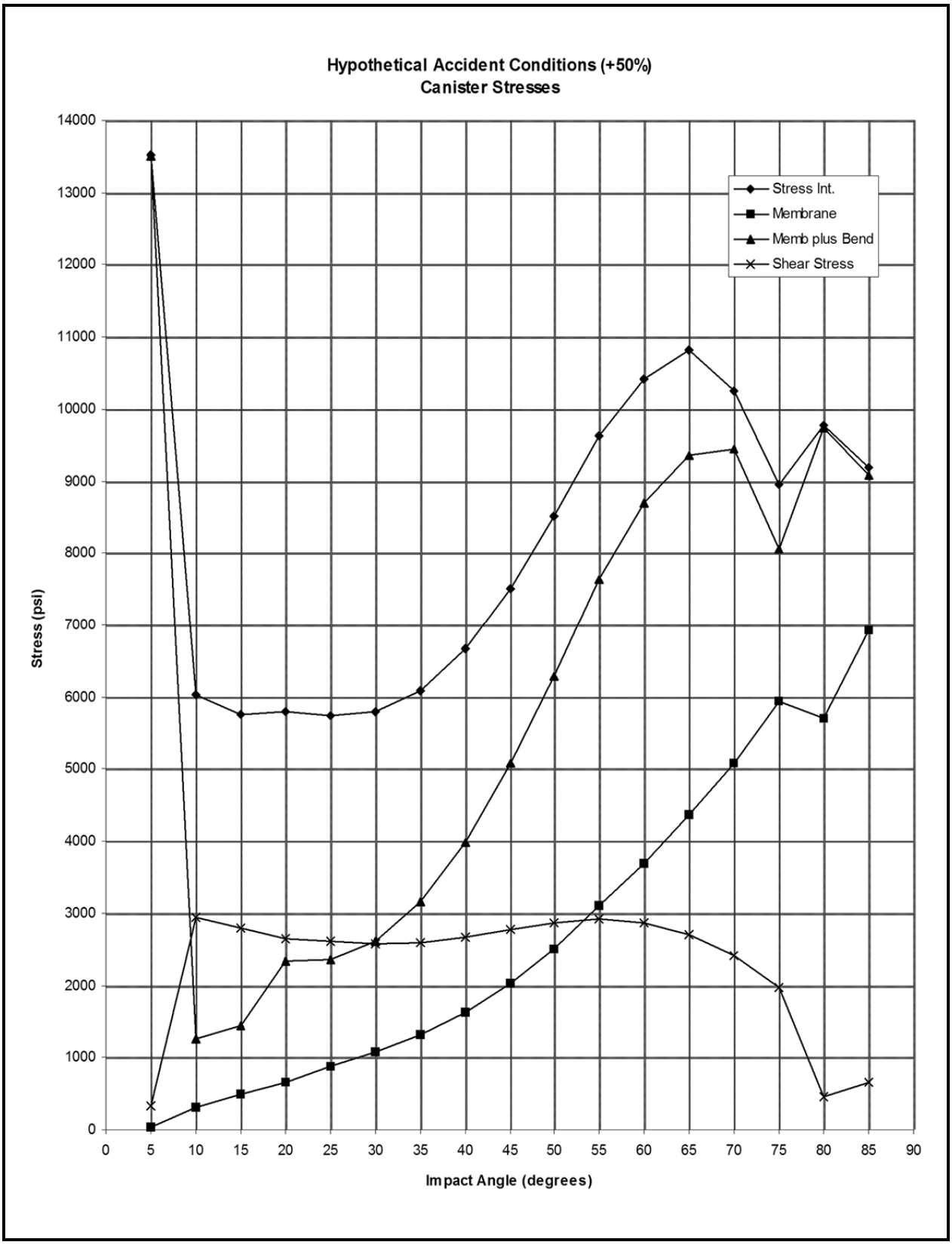

Figure 2.7-3 – HAC Cold (-20 ºF) Canister Stresses

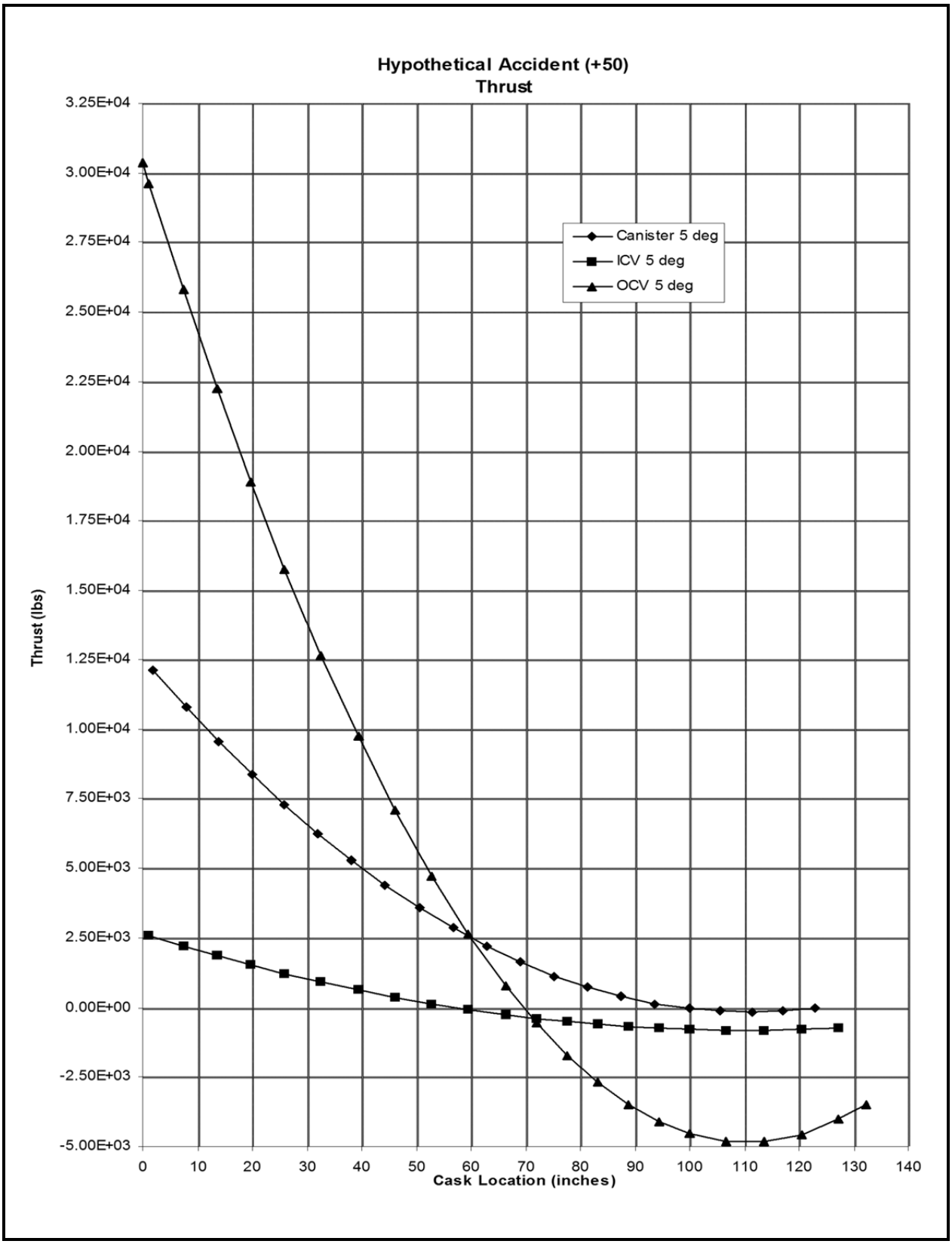

Figure 2.7-4 – HAC Cold (-20 ºF) Thrust

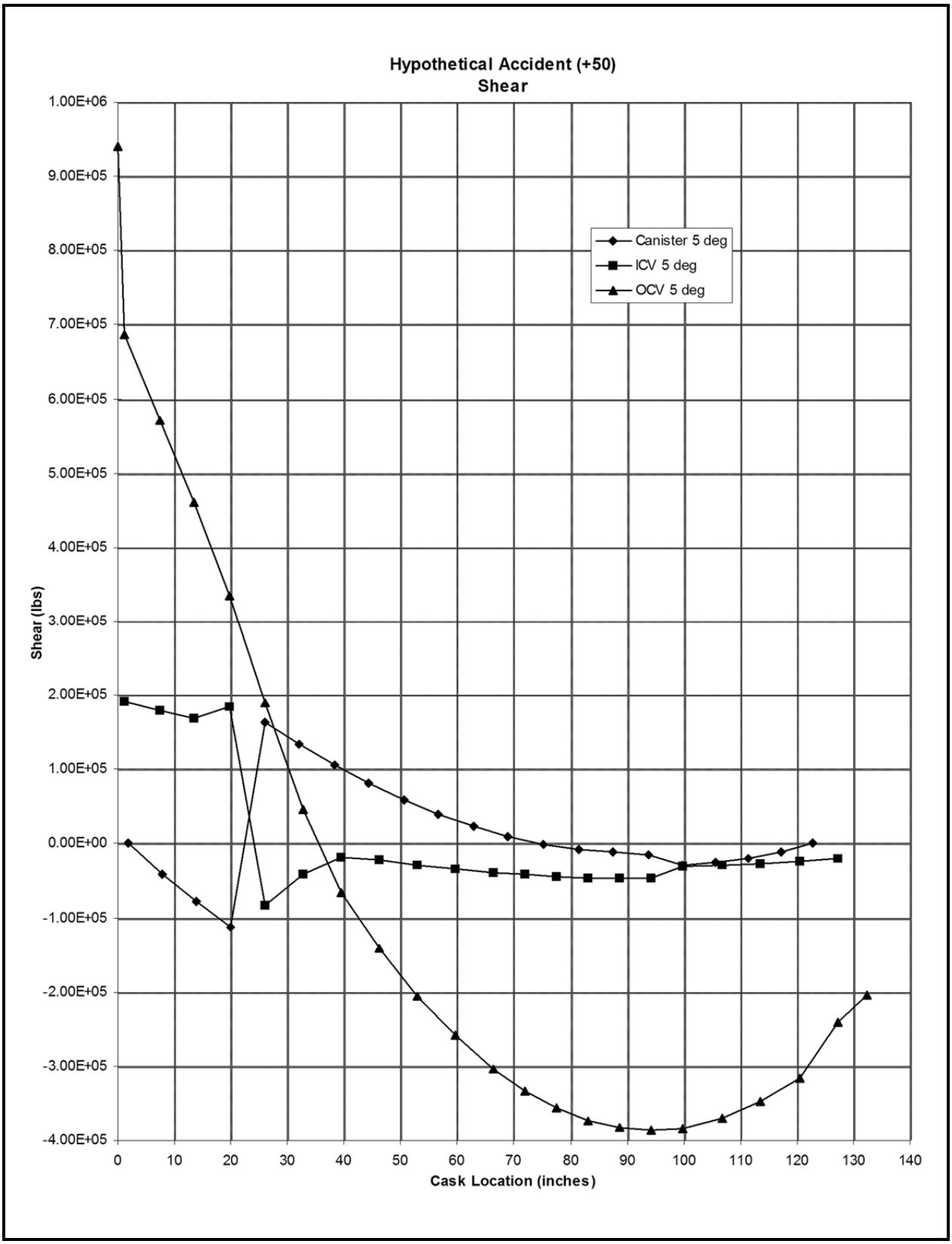

Figure 2.7-5 – HAC Cold (-20 ºF) Shear

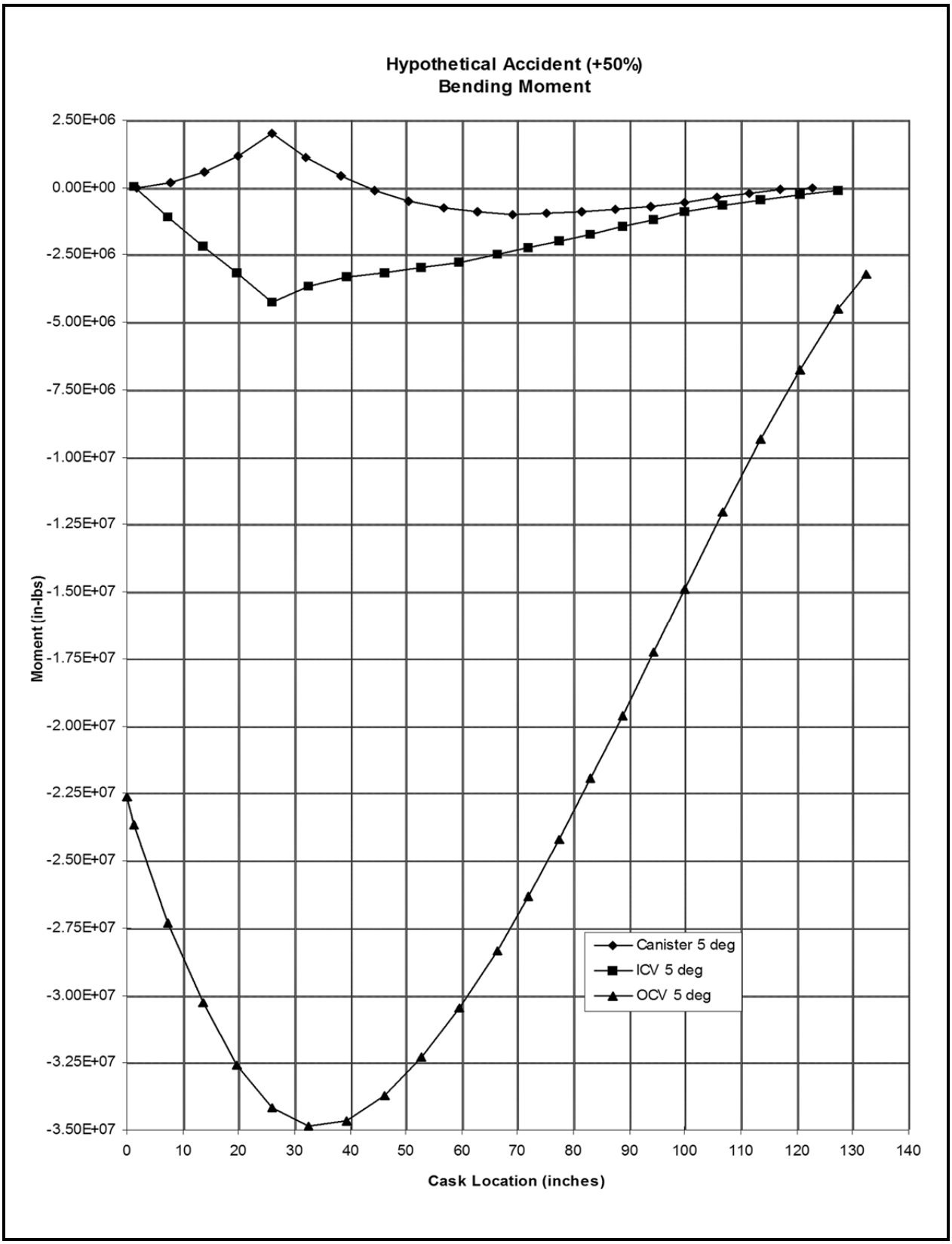

Figure 2.7-6 – HAC Cold (-20 ºF) Bending Moment

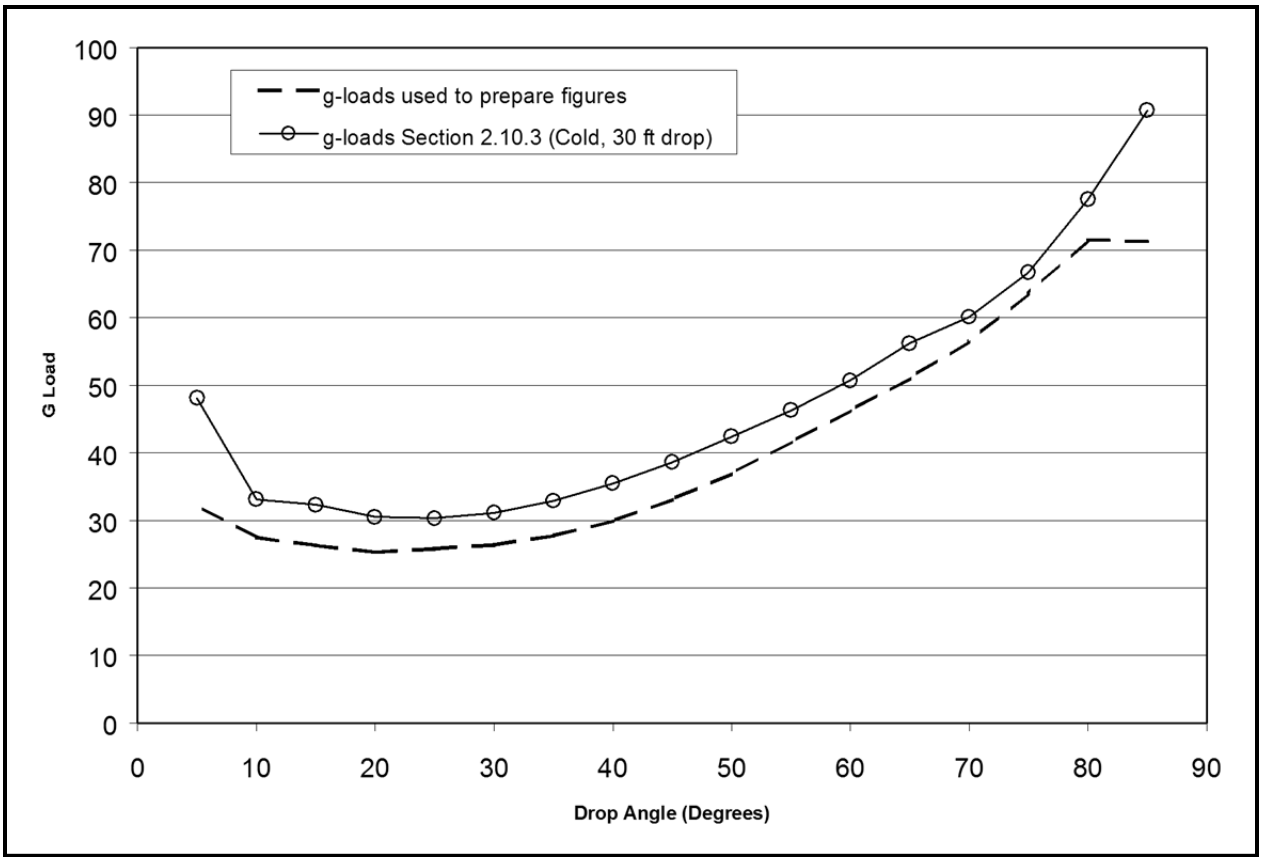

Figure 2.7-7 – Comparison of *g*-Loads Used for Calculating Cold (-20 ºF) HAC Stresses

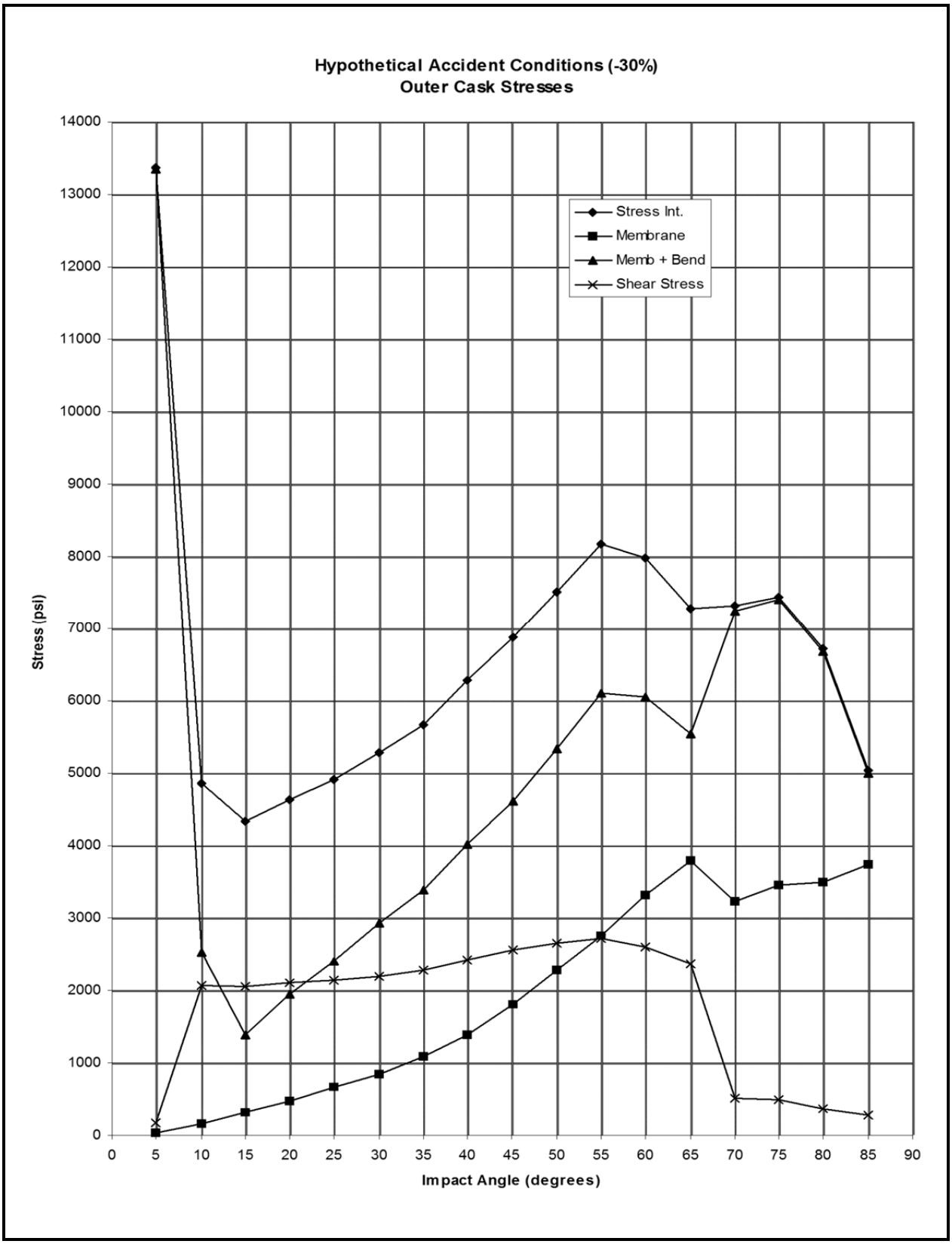

Figure 2.7-8 – HAC Hot (140 ºF) Outer Cask Stresses

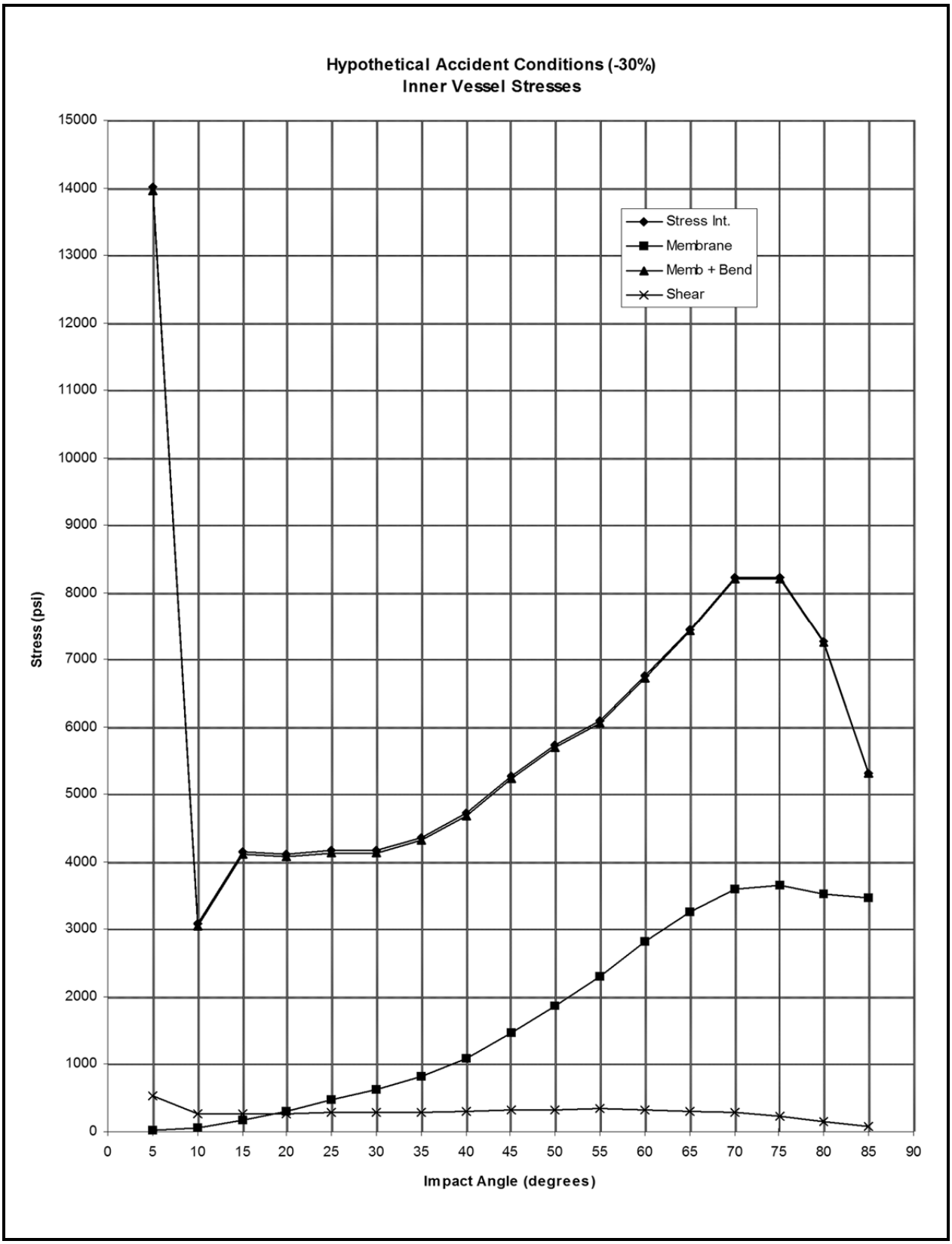

Figure 2.7-9 – HAC Hot (140 ºF) Inner Vessel Stresses

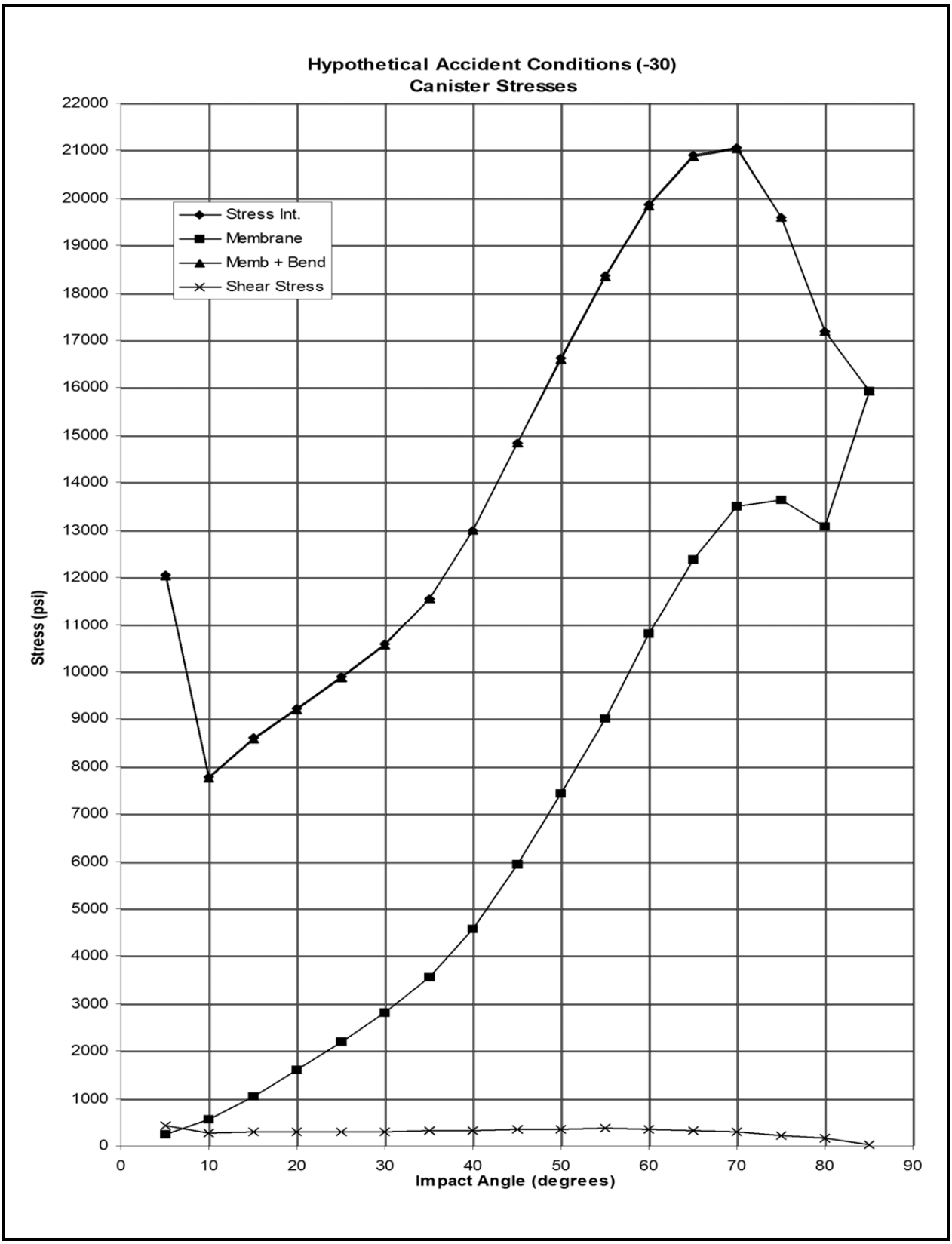

Figure 2.7-10 – HAC Hot (140 ºF) Canister Stresses

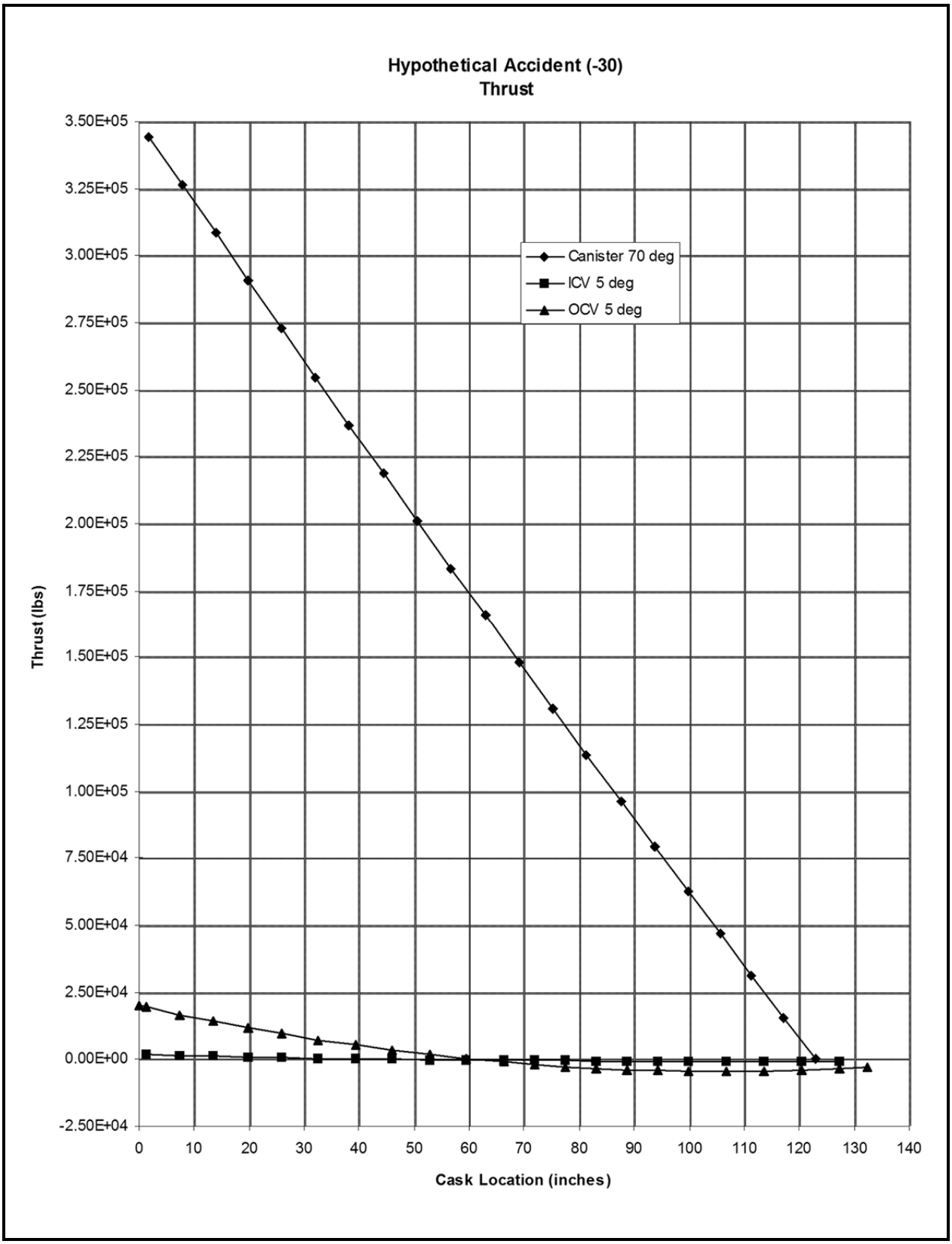

Figure 2.7-11 – HAC Hot (140 ºF) Thrust

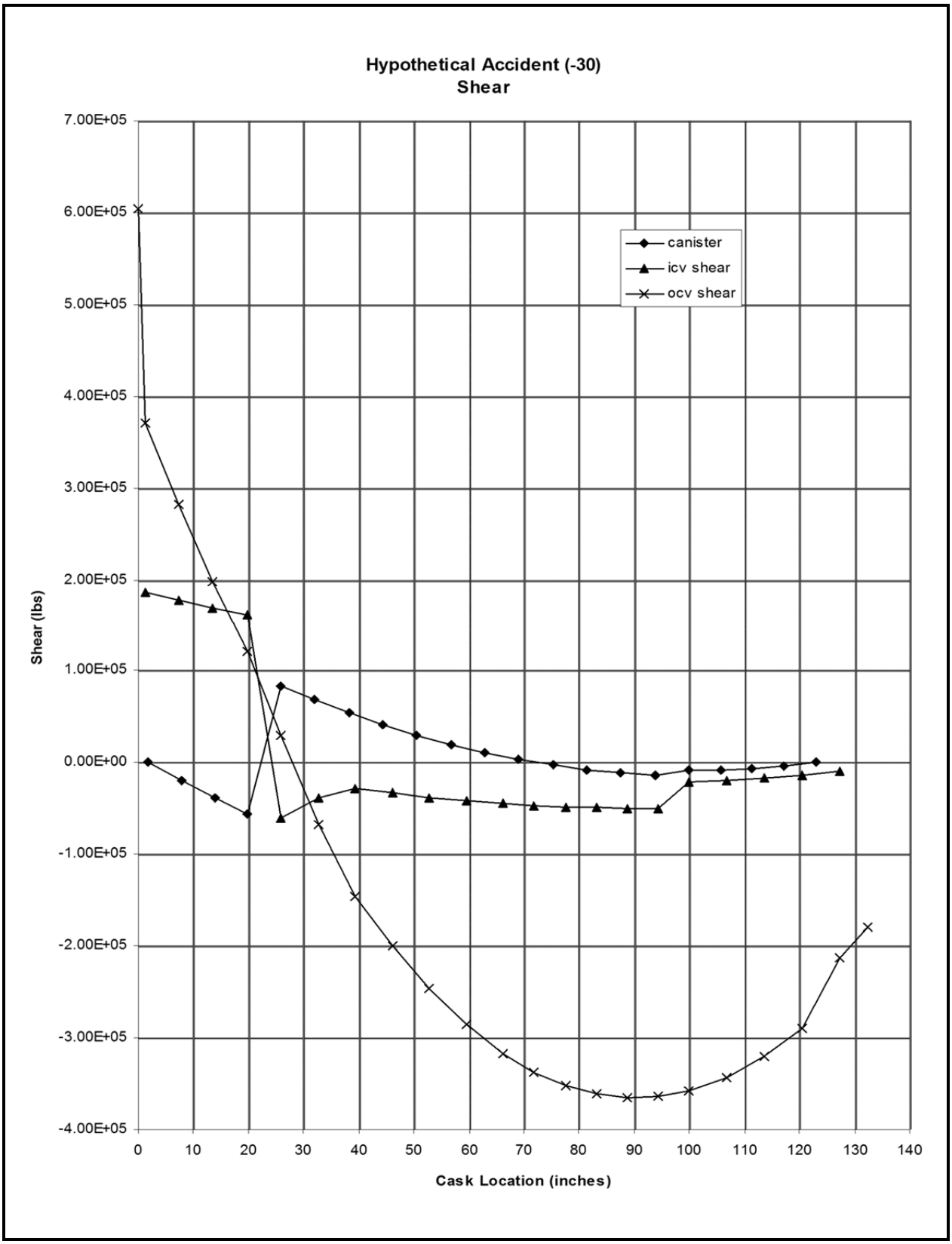

Figure 2.7-12 – HAC Hot (140 ºF) Shear

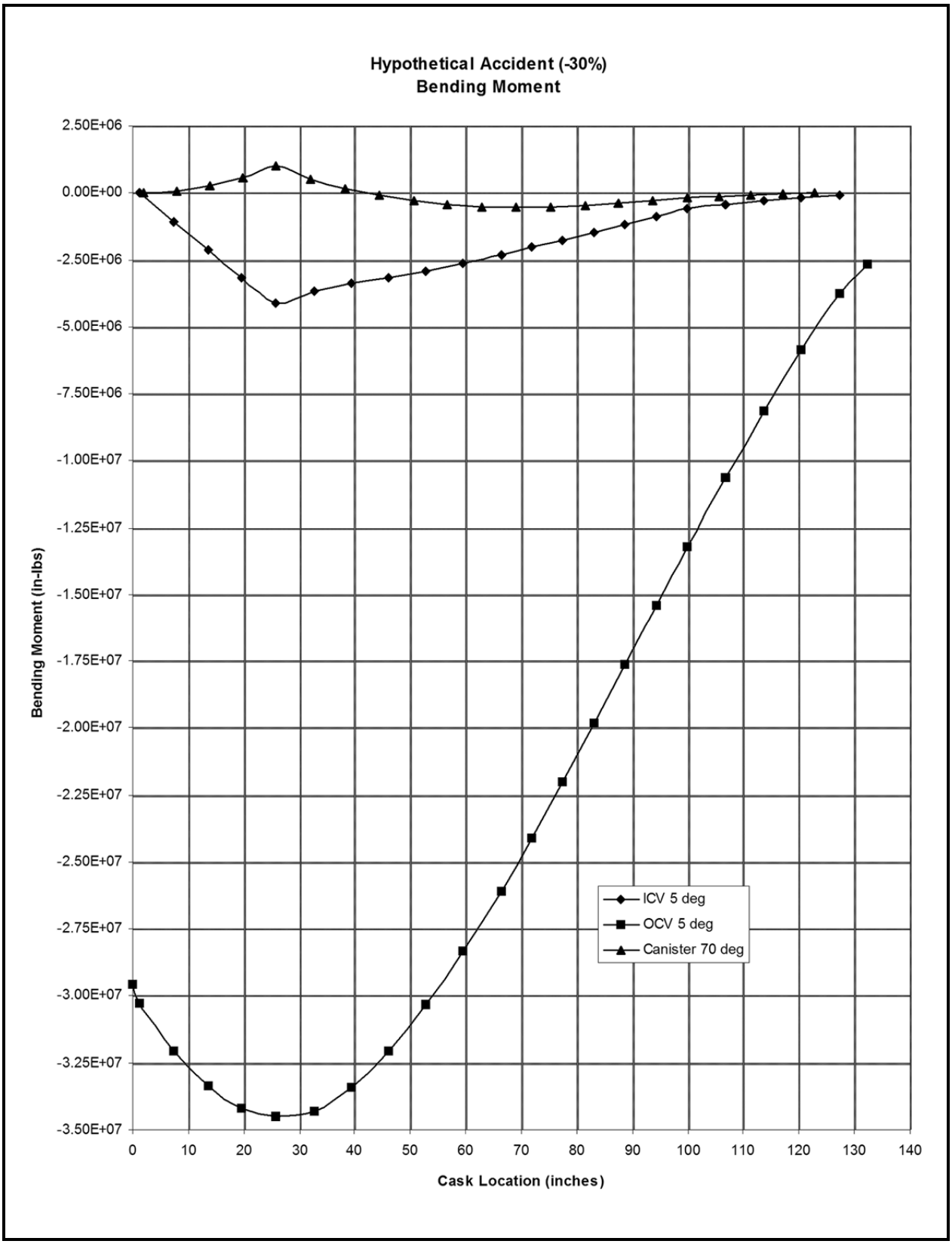

Figure 2.7-13 – HAC Hot (140 ºF) Bending Moment

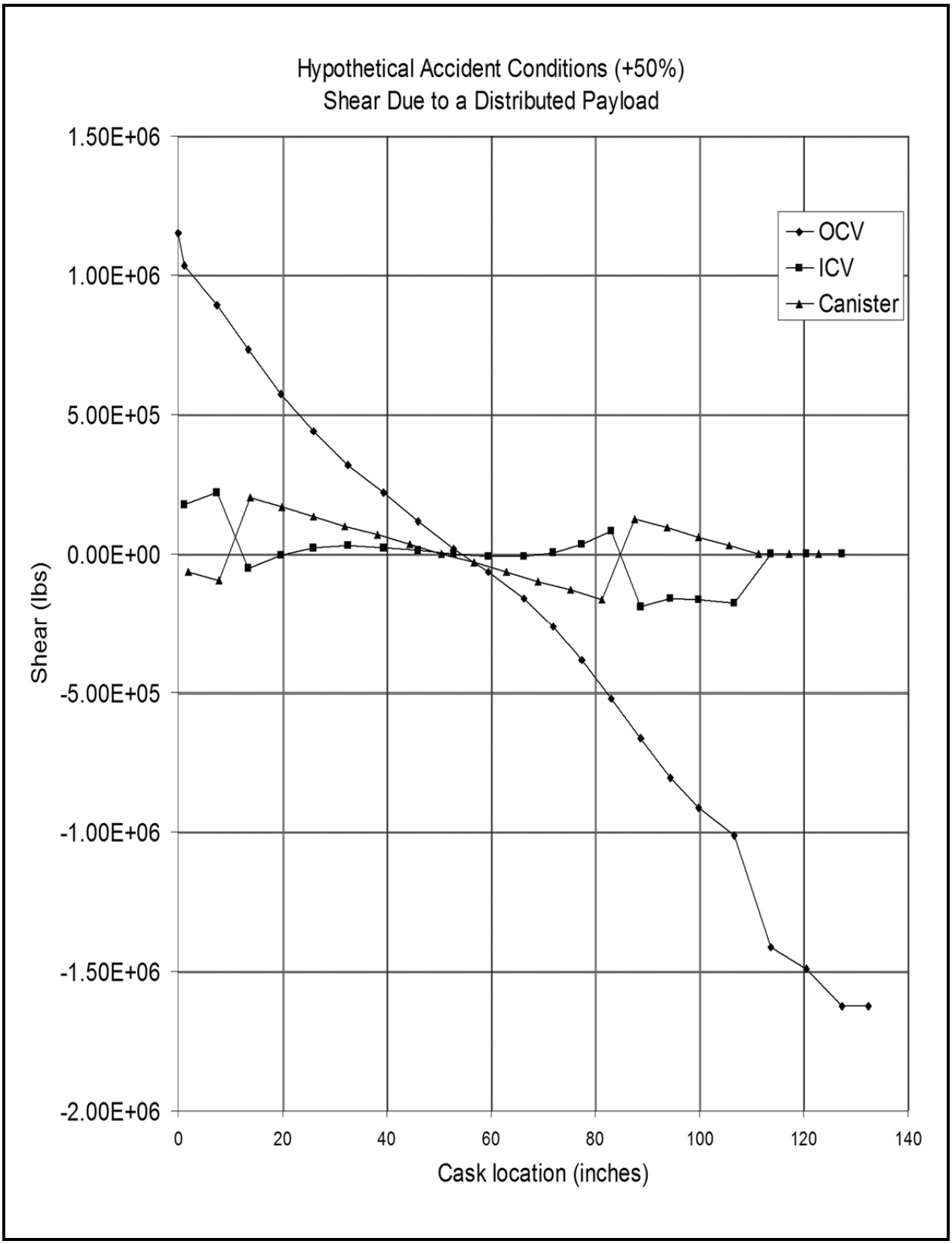

Figure 2.7-14 – HAC Cold (-20 ºF) Shear Due to a Distributed Payload

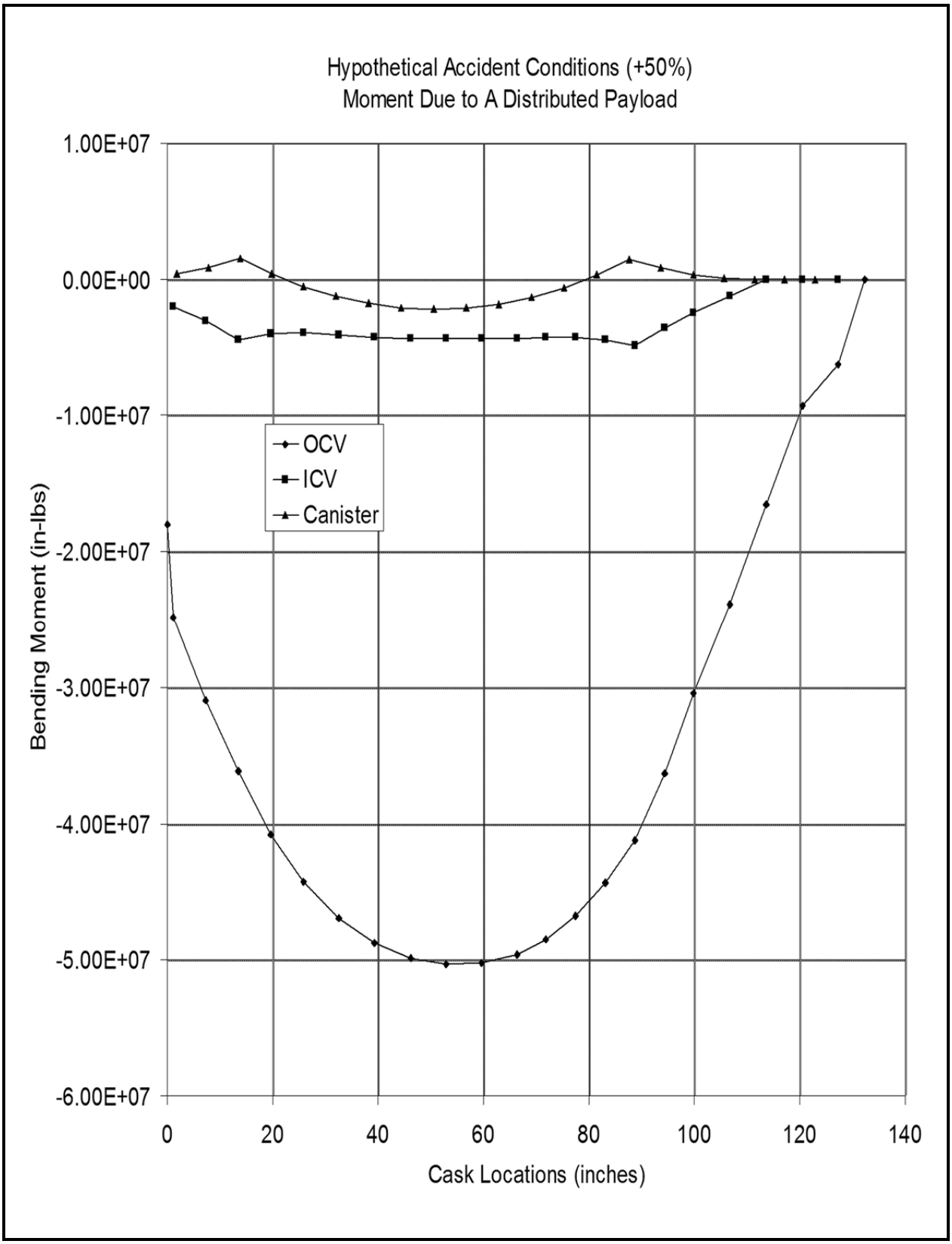

Figure 2.7-15 – HAC Cold (-20 ºF) Moment Due to a Distributed Payload

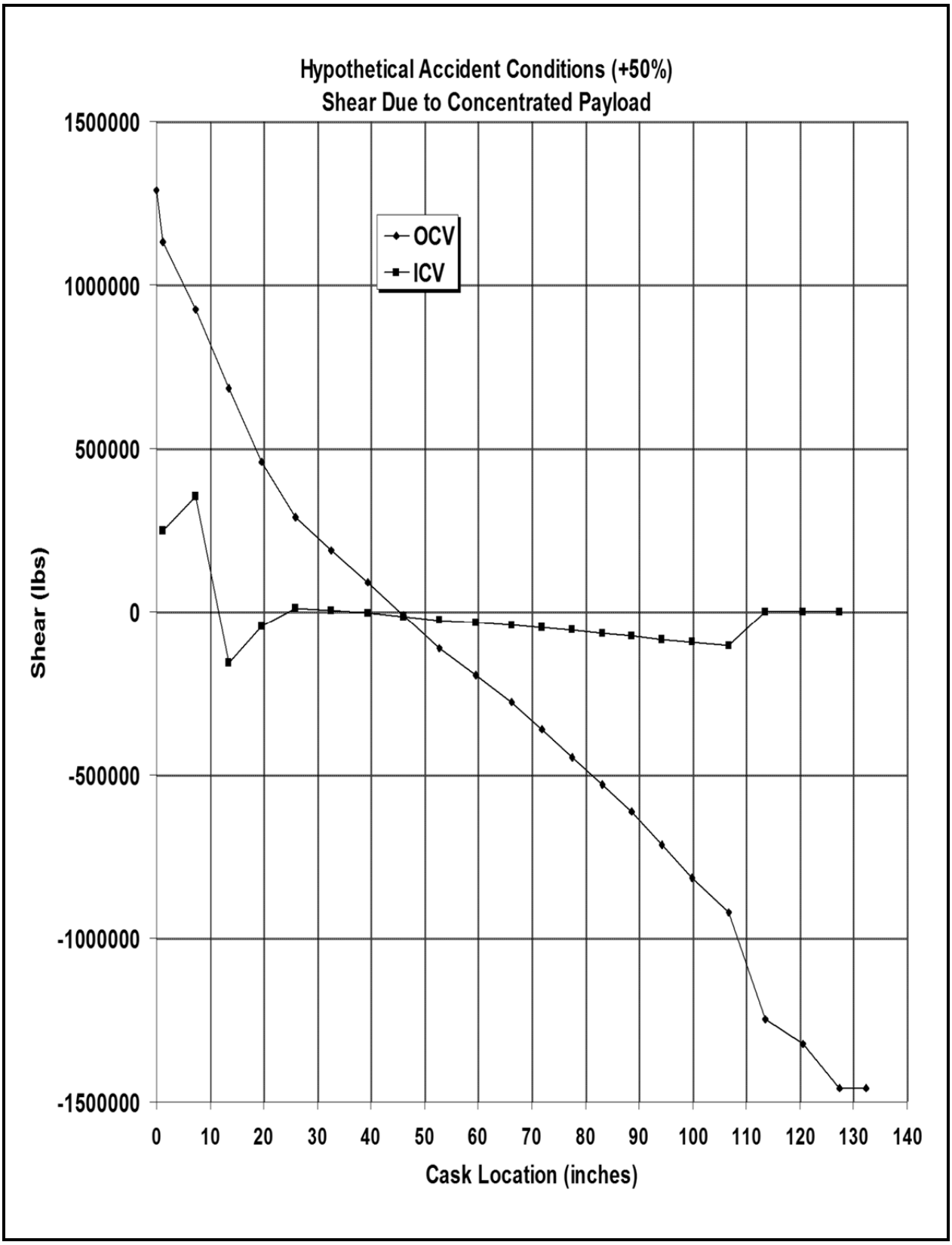

Figure 2.7-16 – HAC Cold (-20 ºF) Shear Due to a Concentrated Payload

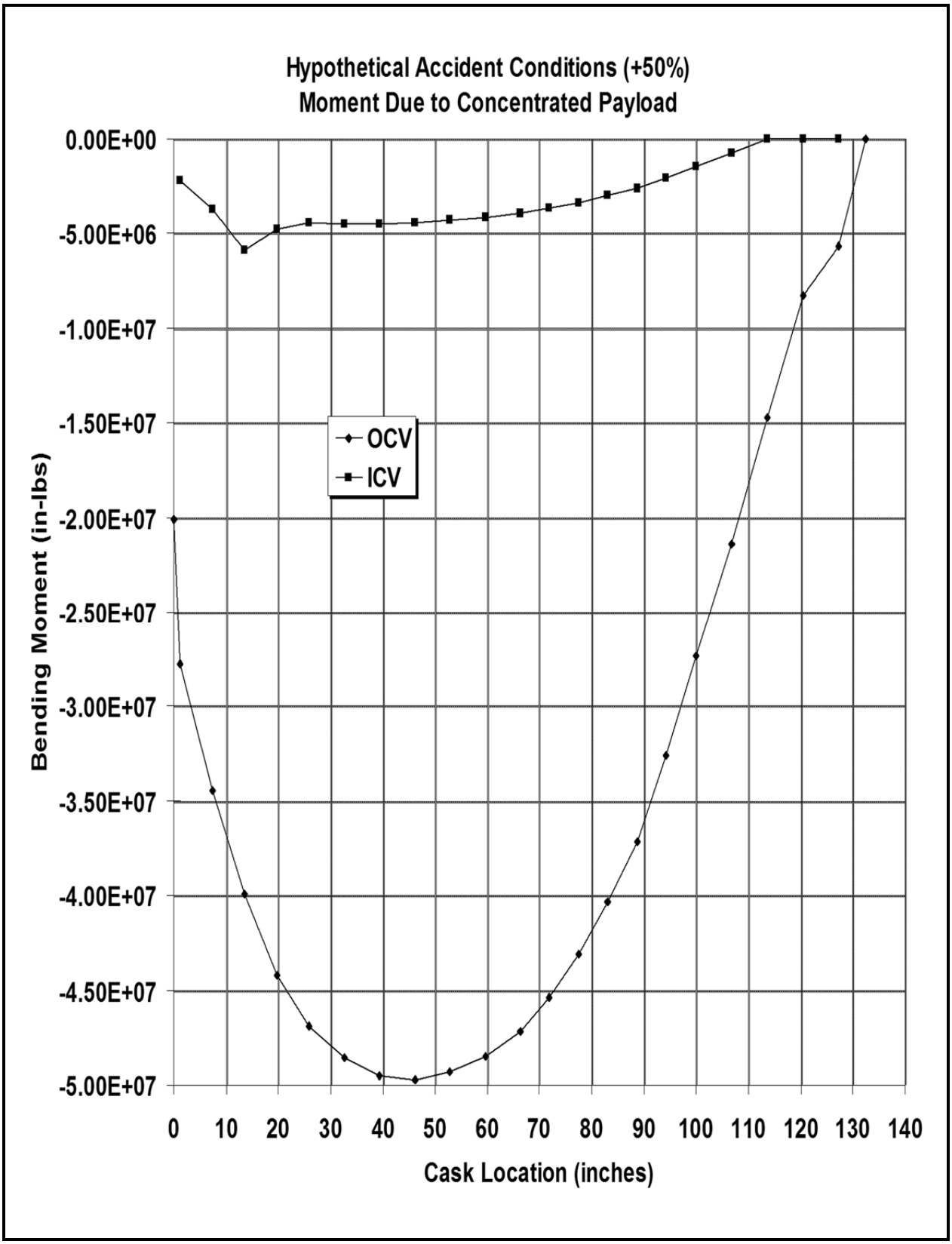

Figure 2.7-17 – HAC Cold (-20 ºF) Moment Due to a Concentrated Payload

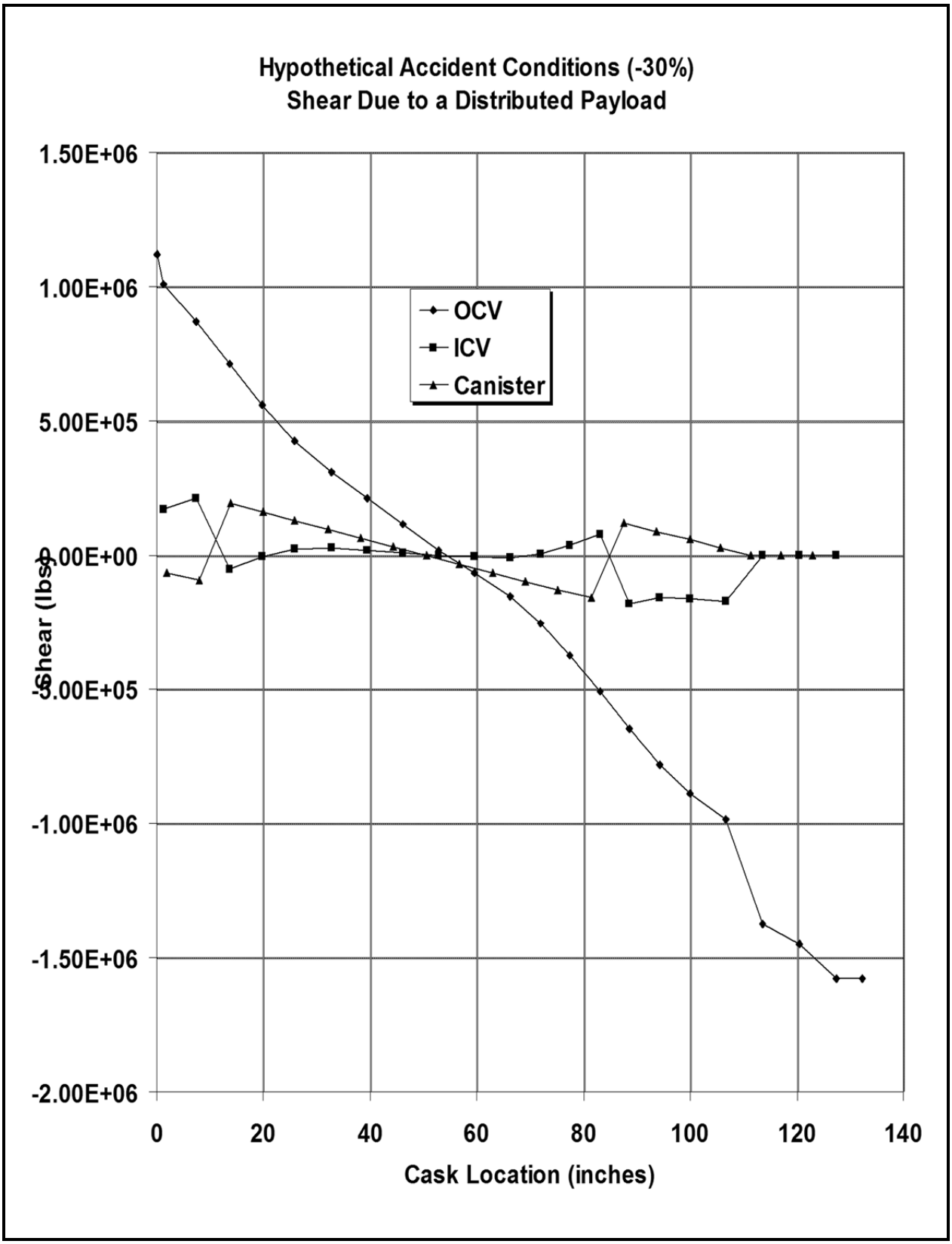

Figure 2.7-18 – HAC Hot (140 ºF) Shear Due to a Distributed Payload

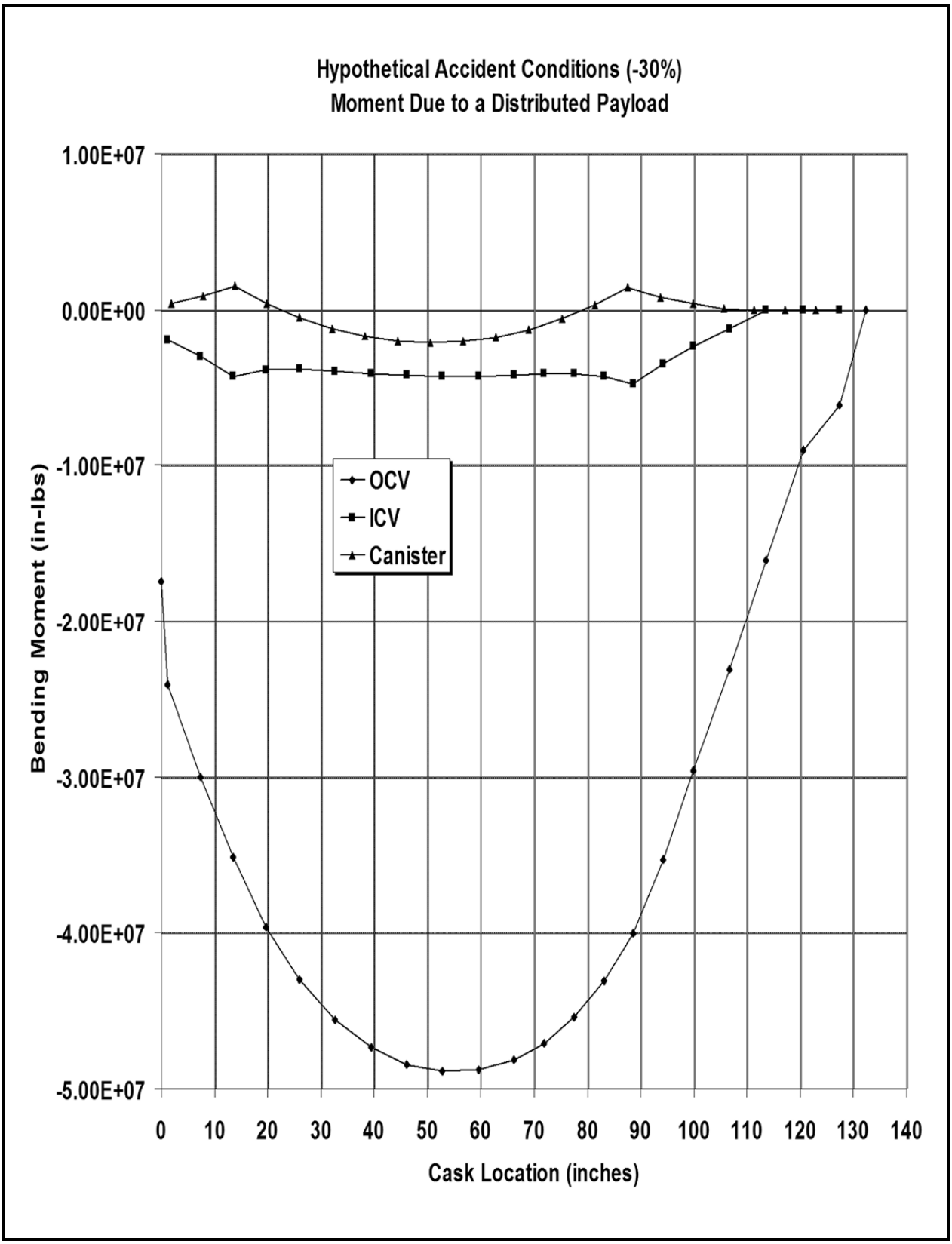

Figure 2.7-19 – HAC Hot (140 ºF) Moment Due to a Distributed Payload

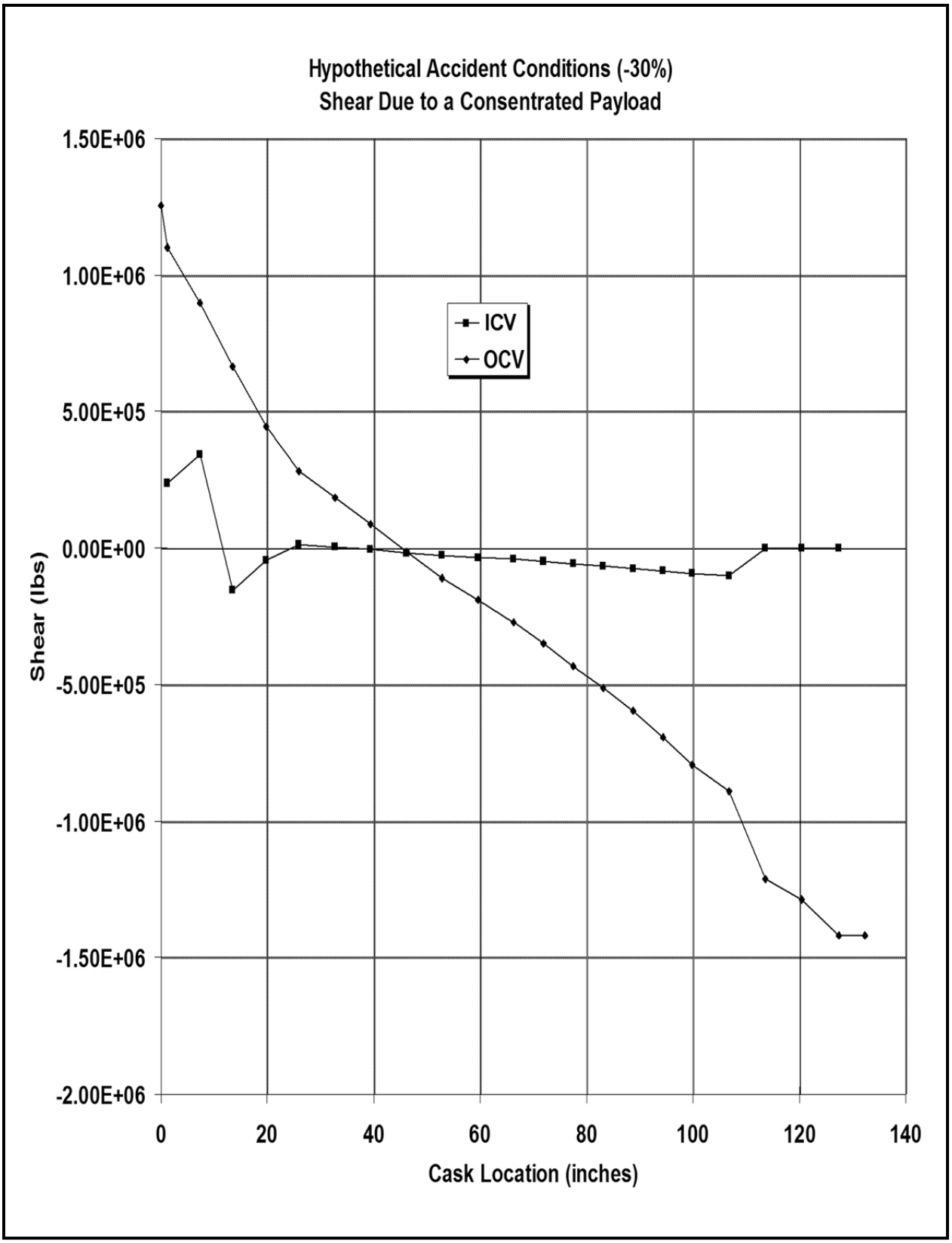

Figure 2.7-20 – HAC Hot (140 ºF) Shear Due to a Concentrated Payload

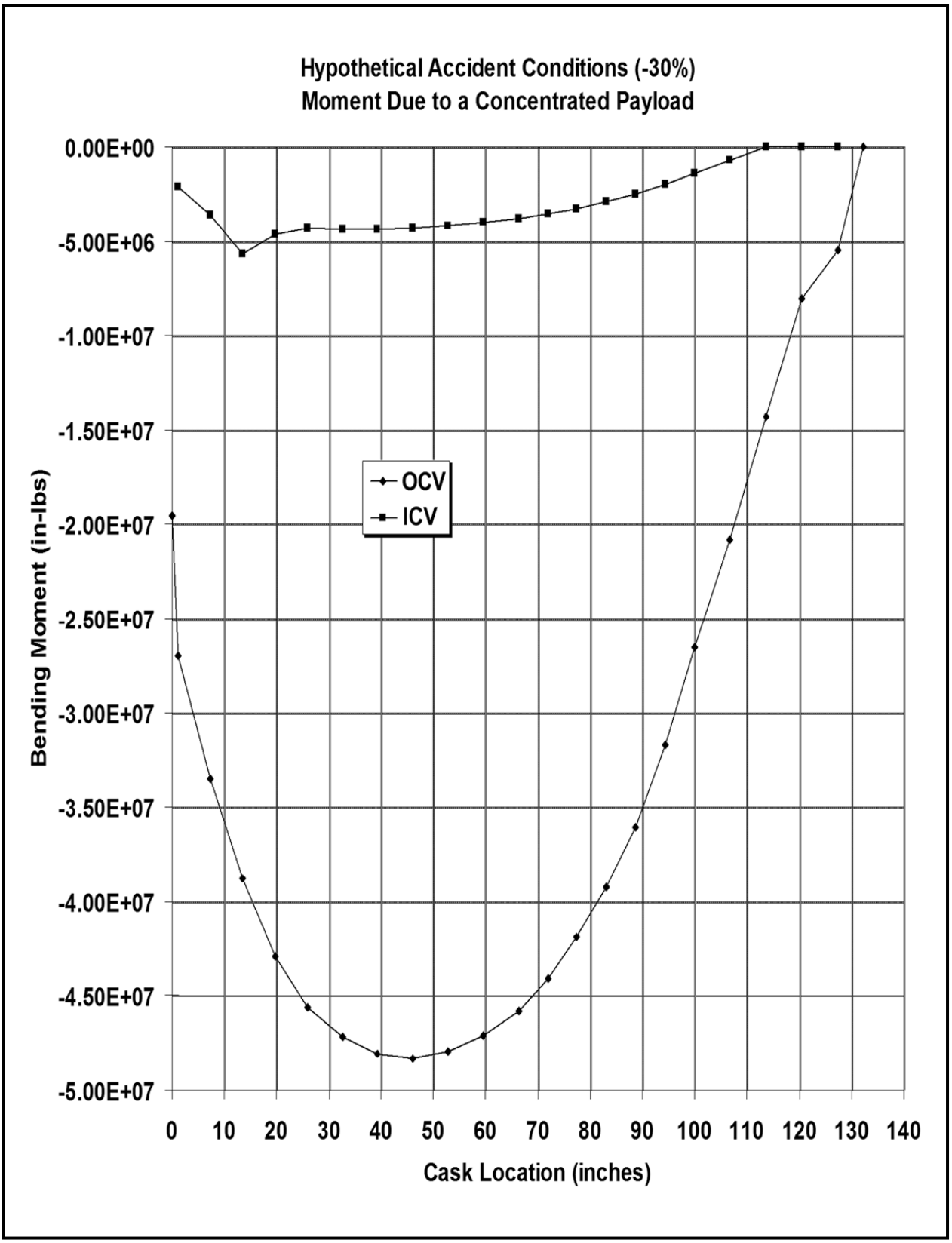

Figure 2.7-21 – HAC Hot (140 ºF) Moment Due to a Concentrated Payload

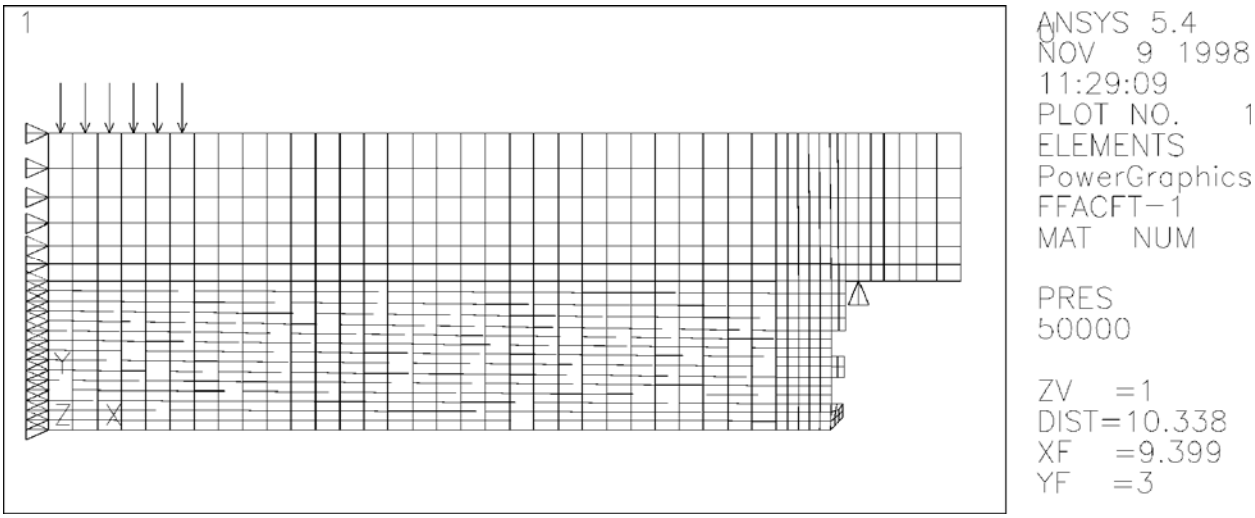

Figure 2.7-22 – Finite Element Model for Puncture on the OC Lid

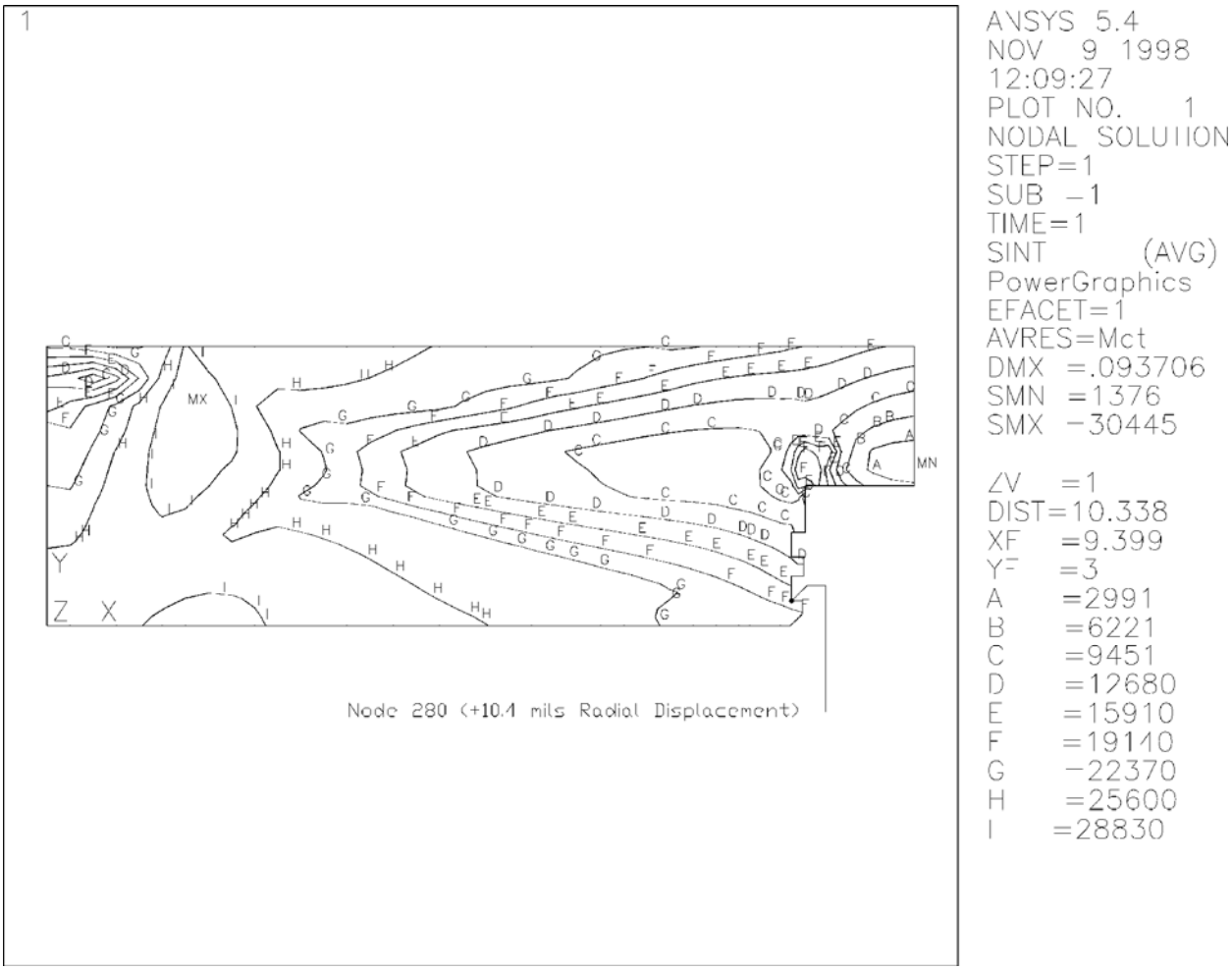

Figure 2.7-23 – Stress and Deformation for Puncture on the OC Lid

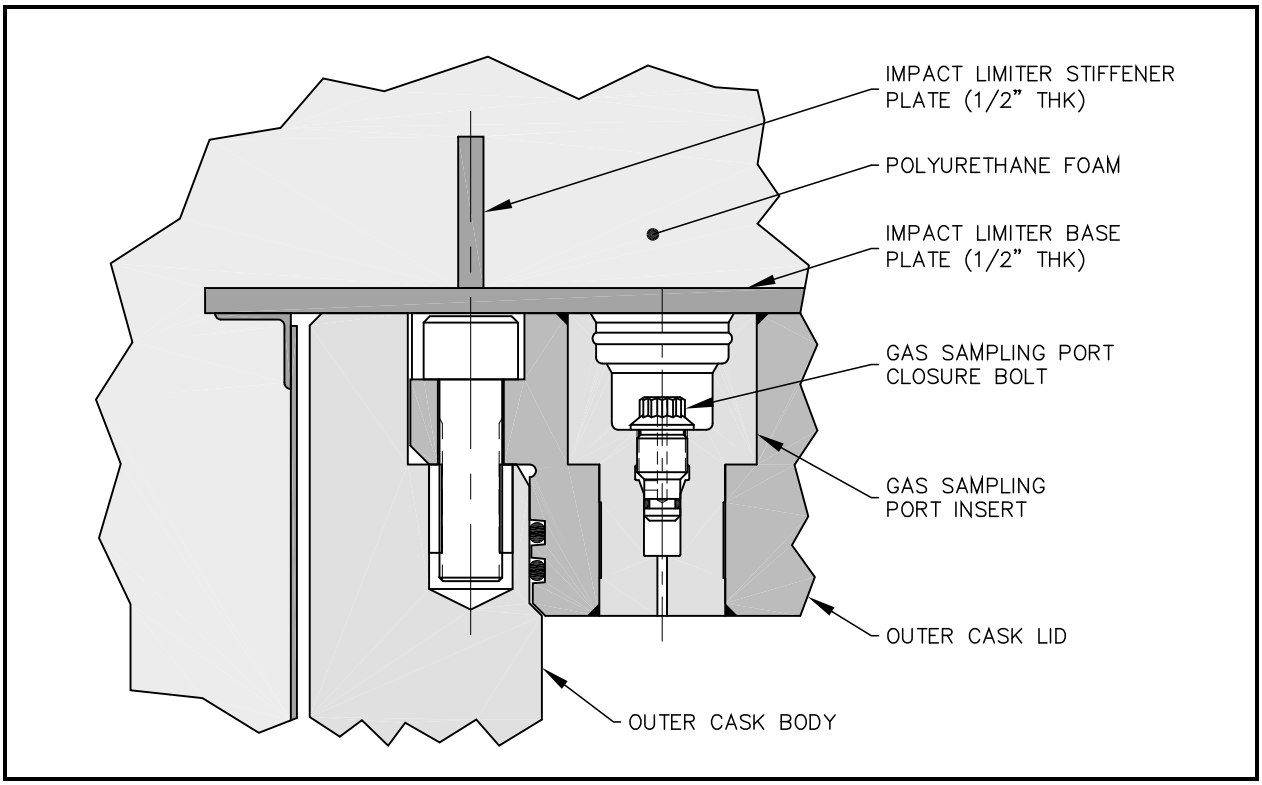

Figure 2.7-24 – OC Gas Samping Port Region

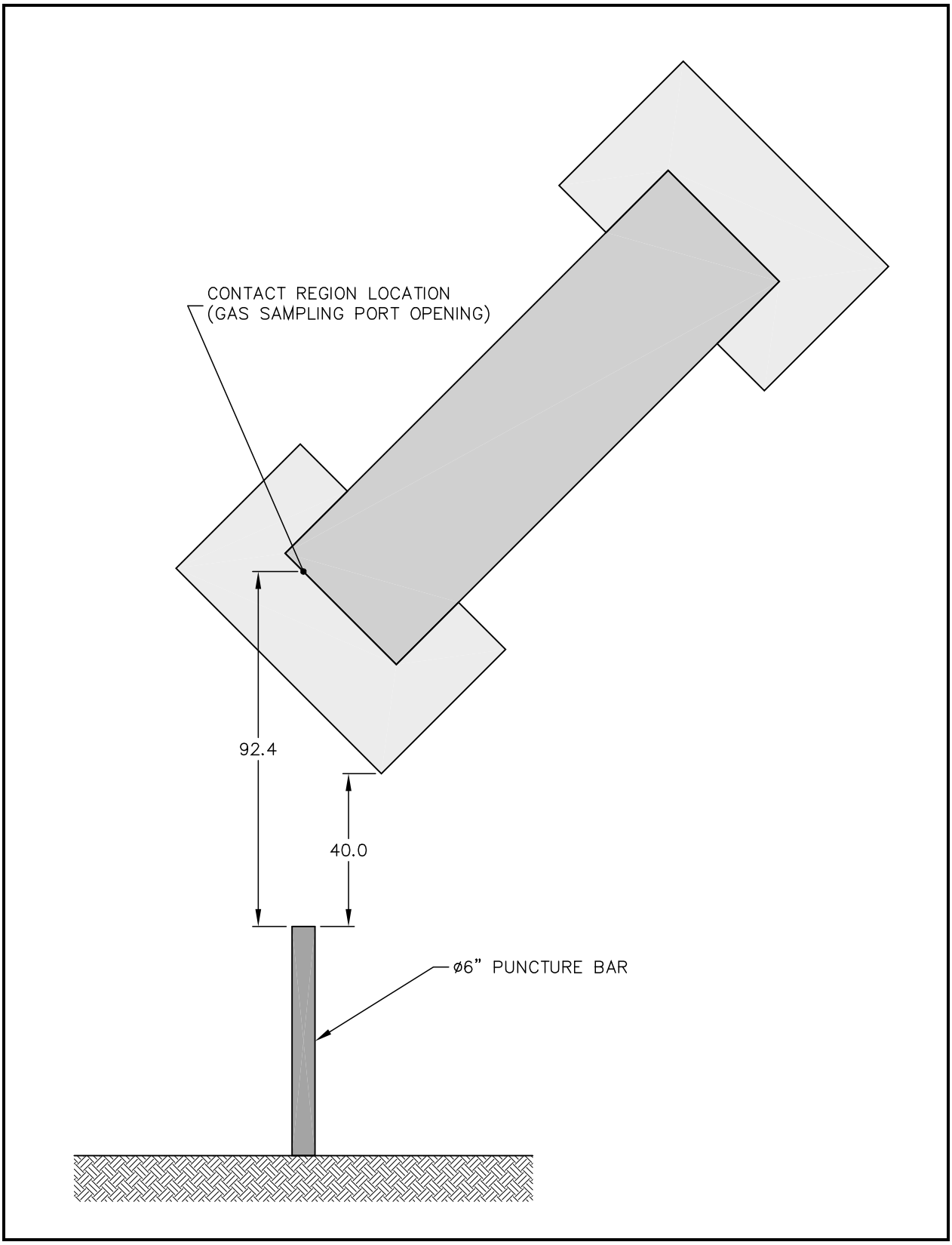

Figure 2.7-25 – Package Orientation for the Puncture Drop

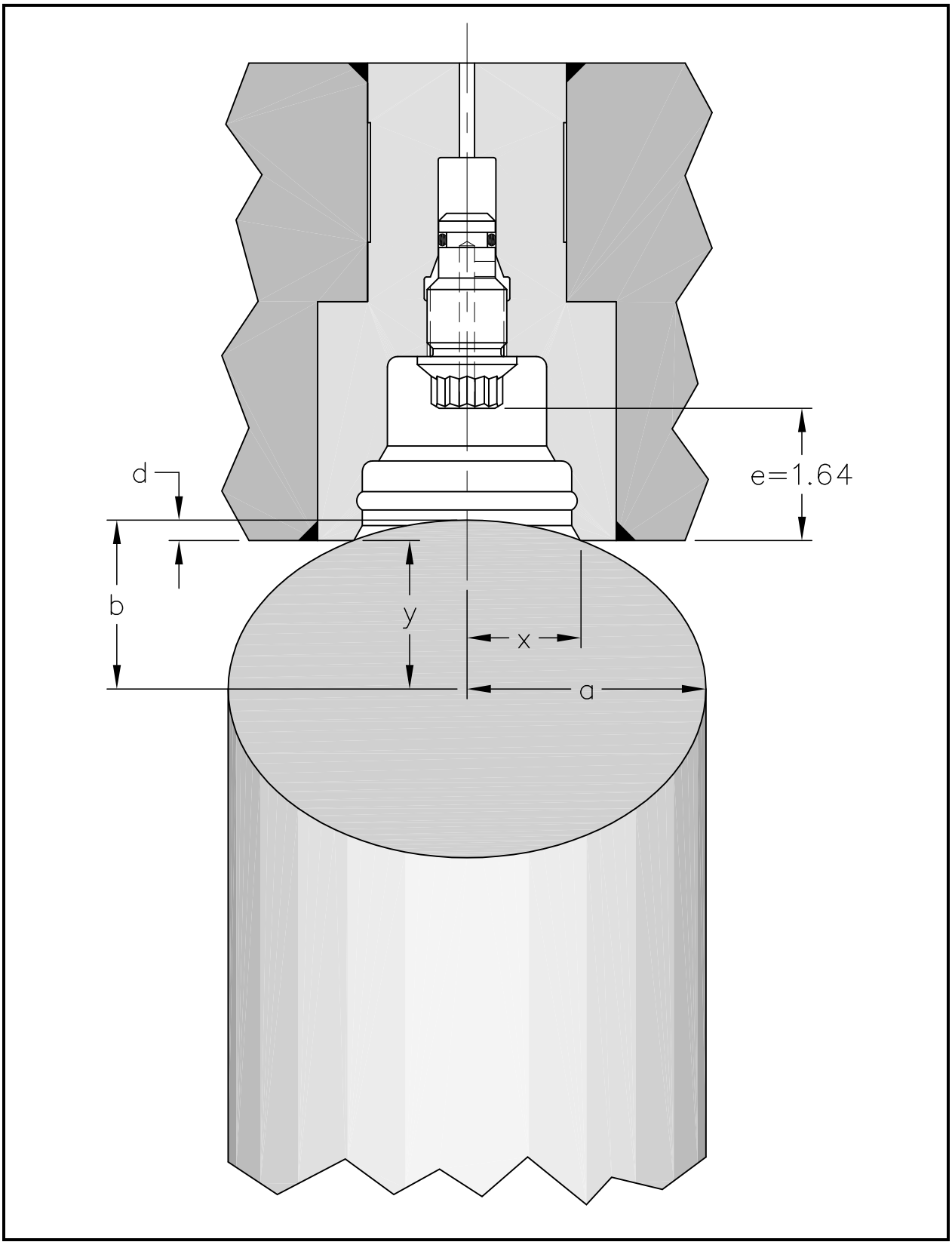

Figure 2.7-26 – Geometry of the Puncture Bar at the Gas Sampling Port

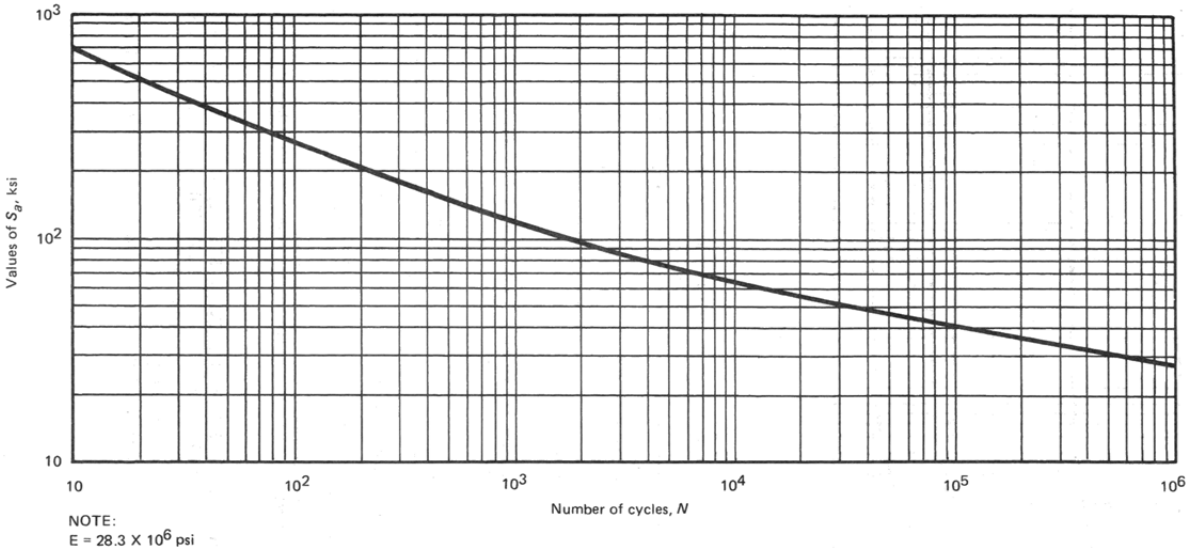

FIG. I-9.2.1 DESIGN FATIGUE CURVE FOR AUSTENITIC STEELS, NICKEL-CHROMIUM-IRON ALLOY, NICKEL–IRON–CHROMIUM ALLOY, AND NICKEL–COPPER ALLOY FOR S_a > 28.2 ksi, FOR TEMPERATURES NOT EXCEEDING 800°F
(For $S_a \leq$ 28.2 ksi, use Fig. I-9.2.2.)
Table I-9.1 Contains Tabulated Values and a Formula for Accurate Interpolation of This Curve

TABLE I-9.1
TABULATED VALUES OF S_a, ksi, FROM FIGS. I-9.0[1,2]

		Number of Cycles [Note (3)]																	
Figure	Curve	1E1	2E1	5E1	1E2	2E2	5E2	8.5E2 [Note (4)]	1E3	2E3	5E3	1E4	1.2E4 [Note (4)]	2E4	5E4	1E5	2E5	5E5	1E6
I-9.1	UTS 115–130 ksi	420	320	230	175	135	100	. . .	78	62	49	44	43	36	29	26	24	22	20
I-9.1	UTS ≤80 ksi	580	410	275	205	155	105	. . .	83	64	48	38	. . .	31	23	20	16.5	13.5	12.5
I-9.2.1	. . .	708	512	345	261	201	148	. . .	119	97	76	64	. . .	55.5	46.3	40.8	35.9	31	28.3
I-9.2.2 (see Table I-9.2.2)																			
I-9.3	S_y = 18.0 ksi	260	190	125	95	73	52	. . .	44	36	28.5	24.5	. . .	21	17	15	13.5	12.5	12.0
I-9.3	S_y = 30.0 ksi	260	190	125	95	73	52	. . .	44	36	28.5	24.5	. . .	19.5	15	13	11.5	9.5	9.0
I-9.3	S_y = 45.0 ksi	260	190	125	95	73	52	46	39	24.5	15.5	12	. . .	9.6	7.7	6.7	6.0	5.2	5.0
I-9.4	MNS ≤2.7S_m [Note (5)]	1150	760	450	320	225	143	. . .	100	71	45	34	. . .	27	22	19	17	15	13.5
I-9.4	MNS = 3S_m [Note (5)]	1150	760	450	300	205	122	. . .	81	55	33	22.5	. . .	15	10.5	8.4	7.1	6	5.3

NOTES:
(1) All notes on the referenced figures apply to these data.
(2) Interpolation between tabular values is permissible based upon data representation by straight lines on a log-log plot. Accordingly, for $S_i > S > S_j$

$$\frac{N}{N_j} = \left(\frac{N_i}{N_j}\right)^{[\log(S_j/S)]/\log(S_j/S_j)}$$

where S, S_i, and S_j are values of S_a; N, N_i, and N_j are corresponding numbers of cycles from design fatigue data.
Example: From the data given in the Table above, use the interpolation formula above to find the number of cycles N for S_a = 53.5 ksi when UTS ≤ 80 ksi in Fig. I-9.1:

$$\frac{N}{2000} = \left(\frac{5000}{2000}\right)^{\log(64/53.5)/\log(64/48)}$$

$$N = 3540 \text{ cycles}$$

(3) The number of cycles indicated shall be read as follows: IEJ = I × 10^J, e.g., 5E2 = 5 × 10^2 or 500.
(4) These data points are included to provide accurate representation of curves at branches or cusps.
(5) MNS is the Maximum Nominal Stress.

Figure 2.7-27 – Figure I-9.2.1 from Appendix I of the ASME Code

This page intentionally left blank.

2.8 Special Form

Since the package is demonstrated to be leaktight and fully capable of meeting the requirements for a Type B package, no credit is taken for any special form characteristics the contents may possess.

This page intentionally left blank.

2.9 Fuel Rods

Since fuel rods are not transported within the RH-TRU 72-B package, this section does not apply.

This page intentionally left blank.

2.10 Appendices

2.10.1 *Finite Element Analysis (FEA) Models*

2.10.2 *Drop Analysis Codes Description*

2.10.3 *Drop Impact Evaluation Results*

2.10.4 *Slapdown Assessment*

2.10.5 *Buckling Design Criteria and Detailed Evaluation*

2.10.6 *Closure Bolt Stress Evaluations*

2.10.7 *Static and Dynamic Testing*

2.10.8 *Fabrication Stresses Due to Lead Pour*

This page intentionally left blank.

2.10.1 Finite Element Analysis (FEA) Models

The finite element analyses presented in the following subsections are performed using the ANSYS® finite element analysis program[1], with the exception of Appendix 2.10.1.4, *Containment Assembly Analysis for Oblique Drops*, and Appendix 2.10.1.5, *Containment Assembly Analysis for Side Drops*, where an earlier version of the ANSYS® finite element analysis program[2] is used. *Data Package for the RH-TRU 72-B Waste Shipping Package*[3] contains additional information regarding the finite element analyses and results for Appendix 2.10.1.4, *Containment Assembly Analysis for Oblique Drops*. Modeling details, including input file listings, are provided for case verification.

2.10.1.1 *Tie-down Trunnion Analysis*

2.10.1.2 *Inner Vessel Radius Transition Zone Stresses Due to Pressure*

2.10.1.3 *Inner Vessel Radius Transition Zone Stresses Due to 1g Acceleration*

2.10.1.4 *Containment Assembly Analysis for Oblique Drops*

2.10.1.5 *Containment Assembly Analysis for Side Drops*

2.10.1.6 *Outer Cask Bottom Stresses Due to Puncture*

2.10.1.1 Tie-down Trunnion Analysis

As shown in Figure 2.10.1-1, the model is comprised of half the outer cask (OC) outer shell and one center-pivot trunnion utilizing approximately 11,000 SOLID92, three-dimensional, 10-node tetrahedral solid elements. SOLID92 elements have a quadratic displacement behavior and are well suited to model irregular meshes and curved surfaces, providing exceptional accuracy for this application. Each element is defined by 10 nodes having three degrees of freedom at each node: translations in the nodal x-, y-, and z-directions.

Circumferential displacement constraints are applied at the symmetry boundary, and each end of the OC shell is constrained from displacing in all directions to simulate rigid ends.

As discussed in Section 2.5.2.1, *Center-Pivot and Tie-down Trunnion Loads*, a longitudinal force of 264,050 pounds, a transverse force of 225,000 pounds, and a vertical force of 54,931 pounds are applied simultaneously to the center-pivot trunnion. As shown in Figure 2.10.1-2, both the longitudinal and vertical forces are applied as cosine-distributed loads to simulate interaction with the corresponding center-pivot trunnion trailer interface, at the center of a 2½-inch wide bearing area that interfaces with the transporter support system, as shown in Figure 2.5-17 of Section 2.5.2.2, *OC Outer Shell Stresses*. Although transverse loads are reacted by the trunnion base, the transverse force is conservatively applied as a pressure load to the 12-inch diameter center-pivot trunnion face.

[1] ANSYS®, Inc., Revision Release 8.0A01, UP20031124, Houston, PA.

[2] ANSYS®, Inc., *ANSYS Engineering Analysis System User's Manual*, Report 1082, June 1, 1997, Version 940.

[3] U.S. Department of Energy, *Data Package for the RH-TRU 72-B Waste Shipping Package*, Current Revision, U.S. Department of Energy, Carlsbad Field Office, Carlsbad, New Mexico.

As shown in Figure 2.10.1-3, the maximum membrane-plus-bending stress intensity in the OC outer shell is 21,892 psi. For the case of a 2*g* only vertical force of 54,931 pounds, the maximum stress intensity in the outer shell is 1,972 psi.

In addition, stresses are linearized at the three locations exhibiting the highest stress intensity peaks: 1) at the top-right corner of the center-pivot trunnion base, 2) at the bottom-right corner of the center-pivot trunnion base, and 3) at the top-right end of the cylinder (i.e., location of highest stress). Stress linearization is performed to extract the maximum membrane stress intensity for the excessive tie-down load evaluation. As shown in Figure 2.10.1-4, the maximum membrane stress intensity is 12,040 psi.

The ANSYS® input file is provided in Table 2.10.1-1.

Table 2.10.1-1 – Input Listing for Trunnion Loading the OC Outer Shell

```
/PREP7                                                          ! Enter the pre-processing module
/UNITS,      BIN                                                ! Specify British (inches) for units

/TITLE,OC Outer Shell Stresses with Center-Pivot Trunnion Tie-down Loads

ET,       1,    SOLID92                                         ! Cylindrical outer shell
ET,       2,    SOLID92                                         ! Trunnion base
ET,       3,    SOLID92                                         ! Trunnion

MP,      EX,    1,         27900000                             ! Properties for stainless steel
MP,    NUXY,    1,           0.3000

K,      100,     0.0000,     0.0000,     0.0000                 ! Define the cylindrical shell keypoints
K,      101,     0.0000,   -20.5625,     0.0000
K,      102,    20.5625,     0.0000,     0.0000
K,      103,     0.0000,    20.5625,     0.0000
K,      104,     0.0000,   -19.0625,     0.0000
K,      105,    19.0625,     0.0000,     0.0000
K,      106,     0.0000,    19.0625,     0.0000

LARC,         101,  102,  100,    20.5625                       ! Define the shell lines
LARC,         102,  103,  100,    20.5625
LARC,         104,  105,  100,    19.0625
LARC,         105,  106,  100,    19.0625
L,            101,  104
L,            103,  106

AL,             1,    2,    3,    4,    5,    6                 ! Define the end-of-cylinder area

VOFFST,         1,  -120.0000,    6                             ! Extrude the area to form a volume

K,      113,    21.5938,     9.0000,   -46.0000                 ! Define the trunnion base keypoints
K,      114,    21.5938,    -9.0000,   -46.0000
K,      115,    21.5938,     9.0000,   -74.0000
K,      116,    21.5938,    -9.0000,   -74.0000

L,            113,  114                                         ! Define the trunnion base lines
L,            115,  116
L,            113,  115
L,            114,  116

AL,            19,   20,   21,   22                             ! Define the trunnion base area

VOFFST,         9,    -6.0000,    4                             ! Extrude the area to form a volume

VSBV,           1,    2, SEPO, KEEP, KEEP                       ! Cut the trunnion base at the shell outer surface
VSBV,           1,    3, SEPO, KEEP, KEEP
ASEL,           S, AREA,      ,   27,   28,    1
VSBA,           2,  ALL, SEPO, DELE, KEEP
VDELE,          1,    6,    5
ASEL,         ALL
VGLUE,          3,    4,    5

NUMCMP,      LINE                                               ! Compress line, area, and volume numbering for convenience
NUMCMP,      AREA
NUMCMP,      VOLU

LOCAL,         11,    1,    24.5000,     0.0000,   -60.0000,     ,     ,   90 ! Define the trunnion keypoints
K,      200,     0.0000,     0.0000,     0.0000
K,      201,     6.0000,     0.0000,     0.0000
KGEN,          24,  201,  201,    0,     0.0000,    15.0000,     0.0000,    1
KGEN,           2,  200,  224,    1,     0.0000,     0.0000,    -1.2500,  100
KGEN,           2,  300,  324,    1,     0.0000,     0.0000,    -3.0000,  100

LARC,         201,  202,  200,     6.0000                       ! Define the trunnion lines
*REPEAT,       23,    1,    1,    0,    0
LARC,         224,  201,  200,     6.0000
LARC,         301,  302,  300,     6.0000
*REPEAT,       23,    1,    1,    0
LARC,         324,  301,  300,     6.0000
LARC,         401,  402,  400,     6.0000
*REPEAT,       23,    1,    1,    0
LARC,         424,  401,  400,     6.0000
L,            201,  301
*REPEAT,       24,    1,    1
L,            301,  401
*REPEAT,       24,    1,    1
L,            200,  201
L,            200,  207
L,            200,  213
L,            200,  219
L,            300,  301
L,            300,  307
L,            300,  313
L,            300,  319
L,            400,  401
L,            400,  407
L,            400,  413
L,            400,  419
L,            200,  300
L,            300,  400

AL,            80,  152,  104,  153                             ! Define the trunnion areas
*REPEAT,       23,    1,    1,    1,    1
```

```
AL,          103,  175,  127,  152
AL,          104,  176,  128,  177
*REPEAT,      23,    1,    1,    1,    1
AL,          127,  199,  151,  176
AL,          200,   80,   81,   82,   83,   84,   85,  201
AL,          201,   86,   87,   88,   89,   90,   91,  202
AL,          202,   92,   93,   94,   95,   96,   97,  203
AL,          203,   98,   99,  100,  101,  102,  103,  200
AL,          204,  104,  105,  106,  107,  108,  109,  205
AL,          205,  110,  111,  112,  113,  114,  115,  206
AL,          206,  116,  117,  118,  119,  120,  121,  207
AL,          207,  122,  123,  124,  125,  126,  127,  204
AL,          208,  128,  129,  130,  131,  132,  133,  209
AL,          209,  134,  135,  136,  137,  138,  139,  210
AL,          210,  140,  141,  142,  143,  144,  145,  211
AL,          211,  146,  147,  148,  149,  150,  151,  208
AL,          152,  204,  212,  200
*REPEAT,       4,    6,    1,    0,    1
AL,          176,  208,  213,  204
*REPEAT,       4,    6,    1,    0,    1

VA,           85,   37,   38,   39,   40,   41,   42,   89,   97,   98       ! Define the trunnion volumes
*REPEAT,       3,    1,    6,    6,    6,    6,    6,    6,    1,    1,    1
VA,           88,   55,   56,   57,   58,   59,   60,   92,  100,   97
VA,           89,   61,   62,   63,   64,   65,   66,   93,  101,  102
*REPEAT,       3,    1,    6,    6,    6,    6,    6,    6,    1,    1,    1
VA,           92,   79,   80,   81,   82,   83,   84,   96,  104,  101

VSEL,          S, VOLU,     ,    8,   11,    1                        ! Cut the trunnion at the trunnion base
VSBA,        ALL,   27, SEPO, DELE, KEEP
VDELE,        16,   19,    1
VSEL,        ALL
VGLUE,       ALL

SMRTSIZE,      3                                                      ! Mesh the volumes into elements
VATT,          1,    1,    3
VMESH,         4,    7,    1
VMESH,        12,   15,    1
VATT,          1,    1,    2
VMESH,         8
VATT,          1,    1,    1
VMESH,         2,    3,    1

*AFUN,       DEG                                                      ! Use degrees for angular calculations
LT = 0                                                               ! Begin calculating the cosine distribution of lengths
*DO,           I,  308,  318,    1                                    ! Total the cosine lengths
   LT = LT + ABS(COS(KY(I)))
*ENDDO

TFX = 264050                                                         ! Define the total longitudinal force
*DO,           I,  308,  318,    1                                    ! Assign forces to the associated keypoints
   FKX = TFX*ABS(COS(KY(I)))/LT
   FK,         I,   FZ, -FKX
*ENDDO

TFZ = 54931                                                          ! Define the total vertical force
*DO,           I,  314,  324,    1                                    ! Assign forces to the associated keypoints
   FKZ = TFZ*ABS(SIN(KY(I)))/LT
   FK,         I,   FY,  FKZ
*ENDDO

TFY = 225000                                                         ! Define the total transverse force
TAY = 113.0973                                                       ! Define the total transverse area
TPY = TFY/TAY                                                        ! Define the total transverse pressure
ASEL,          S, AREA,     ,   85,   88,    1                      ! Select the trunnion surface for the transverse pressure
SFA,         ALL,     , PRES,  TPY

CSYS,          0                                                     ! Transfer back to the global cartesian coordinate system

NSEL,     S,  LOC,    Z,  -120.0000                                  ! Restrain axial nodes at the cylinder's free ends
NSEL,     A,  LOC,    Z,     0.0000
D,      ALL,   UZ,     0.0000,     ,     ,     ,   UX,   UY
NSEL,   ALL

NSEL,     S,  LOC,    X,     0.0000                                  ! Restrain hoop nodes at the cylinder's free ends
D,      ALL,   UX,     0.0000
NSEL,   ALL

SBCTRAN                                                              ! Transfer all loads from keypoints to nodes

WSORT,       ALL                                                     ! Reduce the solution wavefront

/RGB,       INDEX,  100,  100,  100,    0                            ! Invert colors (white background for output plot files)
/RGB,       INDEX,   80,   80,   80,   13
/RGB,       INDEX,   60,   60,   60,   14
/RGB,       INDEX,    0,    0,    0,   15

/DEV,        FONT,    1,Courier*New,  400,    0,  -16,    0,    0       Set the font sizes
/DEV,        FONT,    2,      Arial,  400,    0,  -13,    0,    0
/DEV,        FONT,    3,      Arial,  400,    0,  -13,    0,    0

TIFF,        COMP,    1                                              ! Set the graphics file parameters
TIFF,       ORIEN,HORIZ
TIFF,       COLOR,    2
TIFF,        TMOD,    1
/GFILE,      1800

/WINDOW,       1,    -1.0000,     1.6700,    -0.9260,     0.9260      ! Set the graphics window size to 9.00 x 6.25 ratio
```

```
/FOCUS,         1,    16.2700,     1.4100,   -53.5300                ! Set the graphics window parameters
/DIST,          1,    34.0000
/VIEW,          1,     0.6500,     0.2400,     0.7200
/ANGLE,         1,     0.0000

/PNUM,       TYPE,    1                                              ! Show the elements types as different colors
/NUMBER,        1                                                   ! Turn on element colors only

EPLOT                                                               ! Plot elements to the screen
/SHOW,        PNG
EPLOT                                                               ! Plot elements to a file
/SHOW,      CLOSE

/FOCUS,         1,    15.4400,     0.0000,   -60.0000                ! Set the graphics window parameters
/DIST,          1,    10.7700
/VIEW,          1,     1.0000,     0.0000,     0.0000
/ANGLE,         1,     0.0000

/PBC,           F,    1                                             ! Display applied forces
/NUMBER,       -1                                                   ! Turn off element numbers and colors

EPLOT                                                               ! Plot elements to the screen
/SHOW,        PNG
EPLOT                                                               ! Plot elements to a file
/SHOW,      CLOSE

FINISH

/SOLUTION                                                           ! Enter the solution module

ANTYPE, STATIC                                                      ! Specify a static problem
SOLCONTROL,    ON,   ON                                             ! Set solution controls

SOLVE                                                               ! Solve the problem

FINISH

/POST1                                                              ! Enter the post-processing module

SET,   LAST                                                         ! Retrieve the final load step's data

/GROPT,      AXDV,   ON                                             ! Define linerized stress graph parameters
/GROPT,      AXNM,   ON
/GROPT,     AXNSC,    1
/GROPT,     ASCAL,   ON
/GROPT,      LOGX,  OFF
/GROPT,      LOGY,  OFF
/GROPT,      FILL,  OFF
/GROPT,     CGRID,   ON
/GROPT,      DIG1,    6
/GROPT,      DIG2,    0
/GROPT,      REVX,  OFF
/GROPT,      REVY,  OFF
/GROPT,      DIVX
/GROPT,      DIVY,   11
/GROPT,      LTYP,    0
/AXLAB,         X
/AXLAB,         Y
/GTHK,       AXIS,    2
/GTHK,       GRID,    1
/GTHK,      CURVE,    3
/GRTYP,             0
/GRID,              3
/XRANGE,        DEFAULT
/YRANGE,            0,22000,    0

/NUMBER,        0                                                   ! Turn on element numbers and colors

PATH,          P1,    2,   30,   20                                  ! Linerized stress intensity along Path 1
PPATH,          1, 1386                                            !  (top-right corner of trunnion base)
PPATH,          2, 2475
PMAP,          ACCURATE
/OUTPUT,       TRUNNION,  OUT                                       ! Write output to a file
PRSECT                                                              ! Print path stresses at this location
/OUTPUT
PLSECT,         S,  INT                                             ! Plot linearized stress intensity to the display
/SHOW,        PNG
PLSECT,         S,  INT                                             ! Plot linearized stress intensity to a file
/SHOW,      CLOSE

PATH,          P2,    2,   30,   20                                  ! Linerized stress intensity along Path 2
PPATH,          1, 1390                                            !  (bottom-right corner of trunnion base)
PPATH,          2, 2477
PMAP,          ACCURATE
/OUTPUT,       TRUNNION,  OUT,     ,     APPEND                     ! Write output to a file
PRSECT                                                              ! Print path stresses at this location
/OUTPUT
PLSECT,         S,  INT                                             ! Plot linearized stress intensity to the display
/SHOW,        PNG
PLSECT,         S,  INT                                             ! Plot linearized stress intensity to a file
/SHOW,      CLOSE

PATH,          P3,    2,   30,   20                                  ! Linerized stress intensity along Path 3
PPATH,          1, 9528                                            !  (top-right of cylindrical shell)
PPATH,          2, 9683
PMAP,          ACCURATE
/OUTPUT,       TRUNNION,  OUT,     ,     APPEND                     ! Write output to a file
PRSECT                                                              ! Print path stresses at this location
/OUTPUT
```

```
PLSECT,         S,  INT                                         ! Plot linearized stress intensity to the display
/SHOW,        PNG
PLSECT,         S,  INT                                         ! Plot linearized stress intensity to a file
/SHOW,      CLOSE

/GRAPHICS,   FULL                                               ! Disable PowerGraphics

/FOCUS,         1,    16.2700,     1.4100,   -53.5300           ! Set the graphics window parameters
/DIST,          1,    34.0000
/VIEW,          1,     0.6500,     0.2400,     0.7200
/ANGLE,         1,     0.0000
/DSCALE,        1,     1.0000                                   ! Set displacment scaling to 1

ESEL,           S, TYPE,     ,    1                             ! Select the outer shell elements

PLNSOL,        SI                                               ! Plot stress intensity to the screen
/SHOW,        PNG
PLNSOL,        SI                                               ! Plot stress intensity to a file
/SHOW,      CLOSE
```

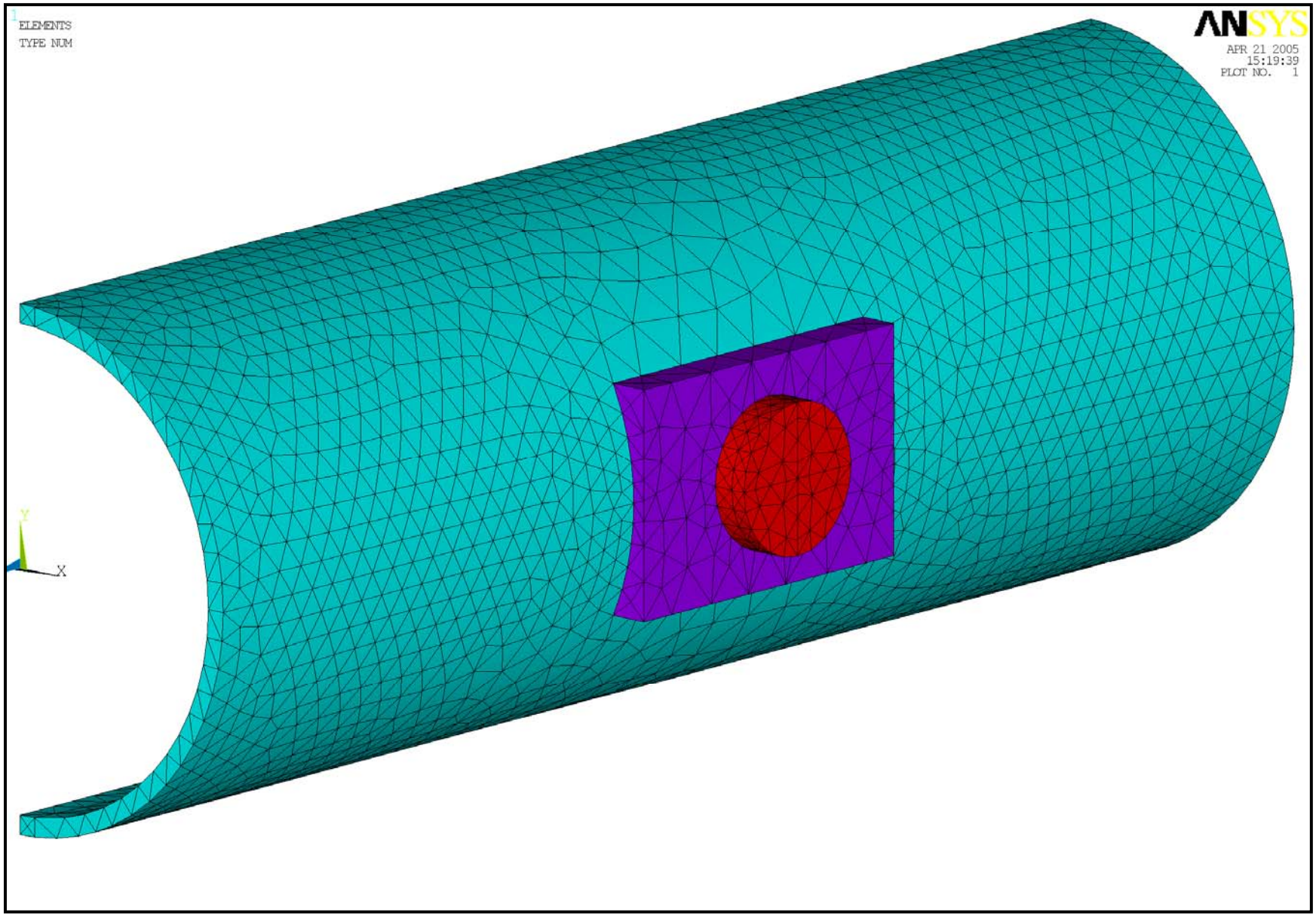

Figure 2.10.1-1 – Finite Element Analysis Model of the Center-Pivot Trunnion Interface

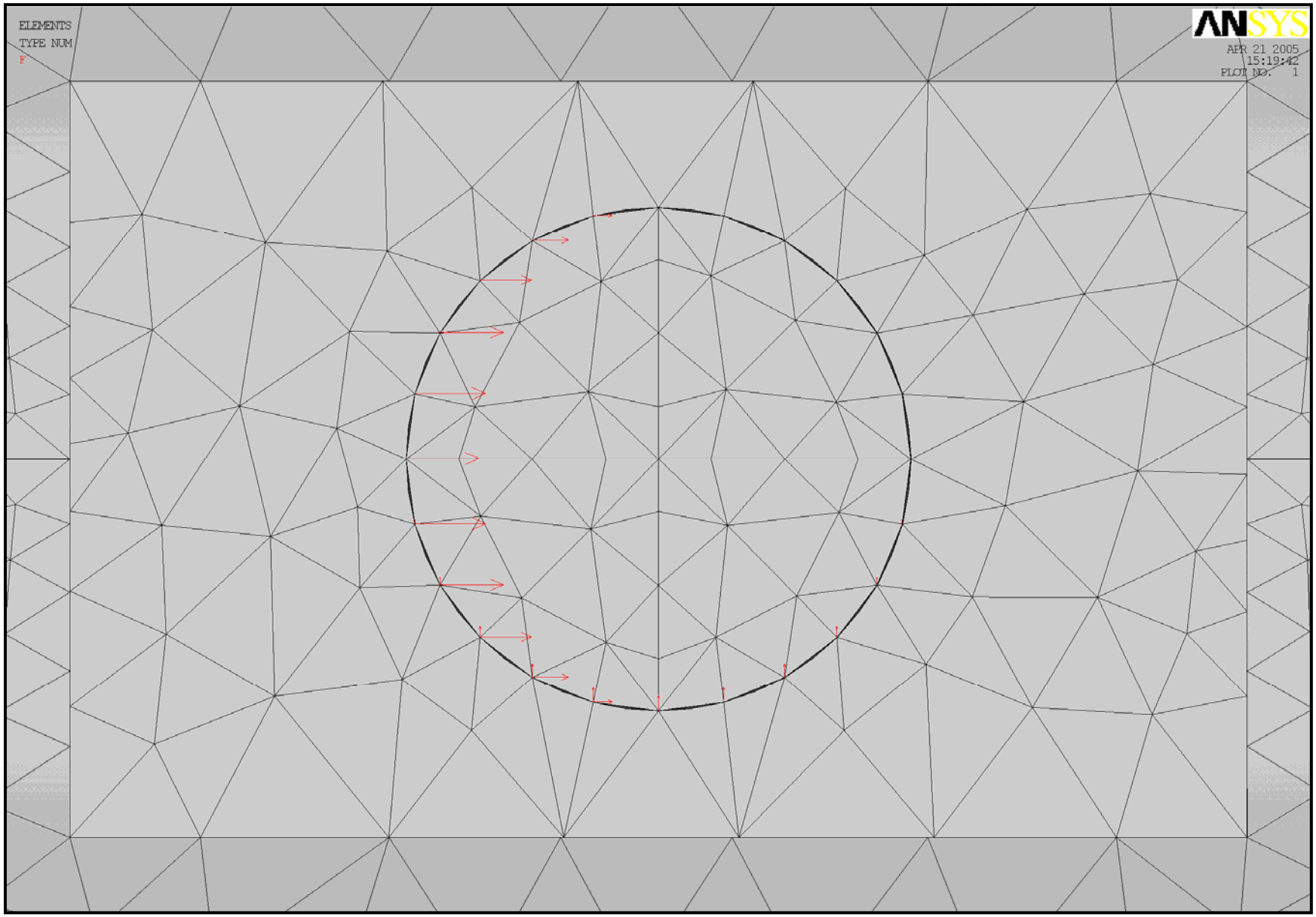

Figure 2.10.1-2 – Center-Pivot Trunnion Longitudinal and Vertical Cosine-Distributed Loads

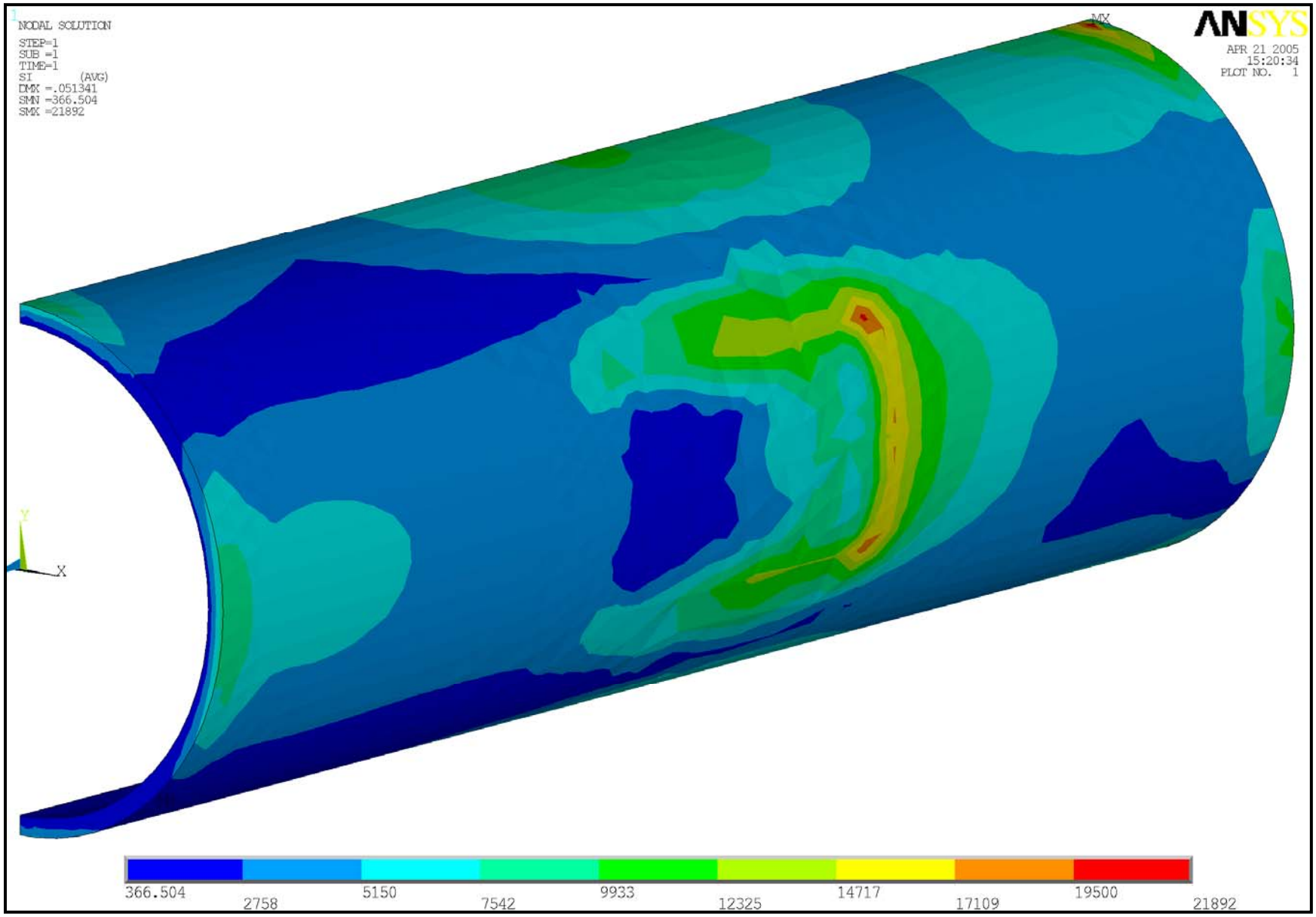

Figure 2.10.1-3 – OC Outer Shell Stress Intensities

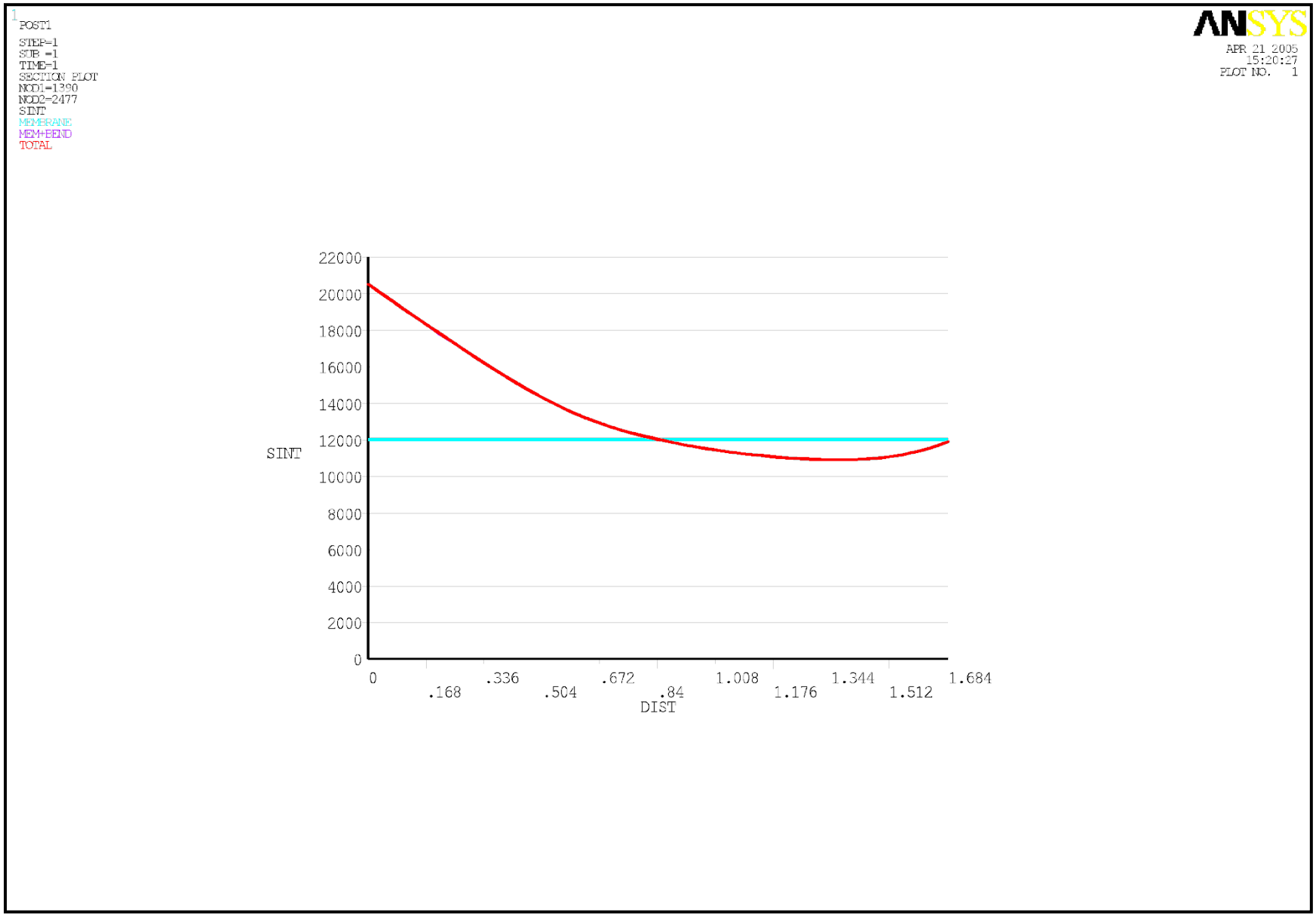

Figure 2.10.1-4 – Stress Intensity Linearization at the Bottom-Right Corner of the Trunnion Base

2.10.1.2 Inner Vessel Radius Transition Zone Stresses Due to Pressure

As shown in Figure 2.10.1-5, the model is comprised of the bottom transition in the inner vessel (IV) shell utilizing approximately 1,700 PLANE82, 8-node axisymmetric solid elements. PLANE82 elements have a quadratic displacement behavior and are well suited to model irregular meshes and curved surfaces, providing exceptional accuracy for this application. Each element is defined by 8 nodes having two degrees of freedom at each node: translations in the nodal x- and y-directions.

Radial displacement constraints are applied at the symmetry boundary, and the end of the IV shell is constrained from displacing in the axial direction.

An internal unit pressure of 1.0 psig is applied to the entire inside surface of the model.

As shown in Figure 2.10.1-6, the maximum stress intensity in the IV shell is 287 psi, occurring at the transition to the cylindrical shell. Stresses are linearized at this location to extract the maximum membrane and bending stress components in both the axial and hoop directions:

$\sigma_1 = 21.67$ psi (axial membrane stress)

$\sigma_2 = -37.74$ psi (hoop membrane stress)

$\sigma_1' = -220.2$ psi (axial bending stress)

$\sigma_2' = -68.66$ psi (hoop bending stress)

The ANSYS® input file is provided in Table 2.10.1-2.

Table 2.10.1-2 – Input Listing for IV Radius Transition Zone Stresses Due to Pressure

```
/PREP7                                                          ! Enter the pre-processing module
/UNITS,       BIN                                               ! Specify British (inches) for units
/TITLE,IV Shell Stresses at Bottom Corner Transition with 1-psig Internal Pressure
ET,       1,    PLANE82,     ,     ,    1                      ! Shell and Bottom
MP,      EX,    1,         27800000                            ! Properties for stainless steel
MP,    NUXY,    1,           0.3000
K,        1,     0.0000,     0.0000                            ! Define the keypoints
K,        2,    15.1250,     0.0000
K,        3,    16.0000,     0.0000
K,        4,    16.0000,     2.0000
K,        5,    16.0000,    13.5000
K,        6,     0.0000,     1.5000
K,        7,    15.1250,     1.5000
K,        8,    15.6250,     2.0000
K,        9,    15.6250,    13.5000
K,       10,    15.1250,     2.0000
L,              1,    2                                         ! Define the lines
*REPEAT,        4,    1,    1
L,              6,    7
LARC,           7,    8,   10,     0.5000
L,              8,    9
L,              1,    6
L,              2,    7
L,              4,    8
L,              5,    9
AL,             1,    9,    5,    8                            ! Define the bottom plate area
AL,             4,   11,    7,   10                            ! Define the cylinder area
AL,             2,    3,   10,    6,    9                     ! Define the transition area
SMRTSIZE,       2                                             ! Mesh the volumes into elements
LESIZE,         2,     ,     ,    9
LESIZE,         3,     ,     ,   21
LESIZE,         8,     ,     ,   16
LESIZE,         9,     ,     ,   16
LESIZE,        10,     ,     ,    4
LESIZE,        11,     ,     ,    4
```

```
AATT,          1,    1,    1
AMESH,         1
AMESH,         2
AMESH,         3

SFL,           5, PRES,     1.0000                          ! Apply a unit pressure load to the inside surface
SFL,           6, PRES,     1.0000
SFL,           7, PRES,     1.0000

NSEL,     S,  LOC,    X,     0.0000                         ! Restrain radial and axial nodes at the free ends
D,      ALL,   UX,     0.0000
NSEL,     S,  LOC,    Y,    13.5000
D,      ALL,   UY,     0.0000
NSEL,   ALL

SBCTRAN                                                    ! Transfer all loads from keypoints to nodes

WSORT,        ALL                                          ! Reduce the solution wavefront

/RGB,       INDEX,  100,  100,  100,    0                  ! Invert colors (white background for output plot files)
/RGB,       INDEX,   80,   80,   80,   13
/RGB,       INDEX,   60,   60,   60,   14
/RGB,       INDEX,    0,    0,    0,   15

/DEV,        FONT,    1,Courier*New,  400,    0,  -16,    0,    0        Set the font sizes
/DEV,        FONT,    2,      Arial,  400,    0,  -13,    0,    0
/DEV,        FONT,    3,      Arial,  400,    0,  -13,    0,    0

PNGR,        COMP,    1                                    ! Set the graphics file parameters
PNGR,       ORIEN,HORIZ
PNGR,       COLOR,    2
PNGR,        TMOD,    1
/GFILE,      1800

/WINDOW,        1,    -1.0000,     1.6700,    -0.9260,     0.9260       ! Set the graphics window size to 9.00 x 6.25 ratio

/FOCUS,         1,     8.6120,     6.6770,     0.0000                  ! Set the graphics window parameters
/DIST,          1,     7.5000
/VIEW,          1,     0.0000,     0.0000,     1.0000
/ANGLE,         1,     0.0000

EPLOT                                                      ! Plot elements to the screen
/SHOW,        PNG
EPLOT                                                      ! Plot elements to a file
/SHOW,      CLOSE

FINISH

/SOLUTION                                                  ! Enter the solution module

ANTYPE, STATIC                                             ! Specify a static problem
SOLCONTROL,    ON,   ON                                    ! Set solution controls

SOLVE                                                      ! Solve the problem

FINISH

/POST1                                                     ! Enter the post-processing module

SET,   LAST                                                ! Retrieve the final load step's data

PATH,          P1,    2,   30,   20                       ! Linerized stress intensity along Path 1
PPATH,          1,    1                                   !  (center of IV bottom)
PPATH,          2,    3
PMAP,          ACCURATE
/OUTPUT,         IVPRES,  OUT                              ! Write output to a file
PRSECT                                                     ! Print path stresses at this location
/OUTPUT

PATH,          P2,    2,   30,   20                       ! Linerized stress intensity along Path 2
PPATH,          1, 5029                                   !  (top of radius transition in cylindrical shell)
PPATH,          2, 5087
PMAP,          ACCURATE
/OUTPUT,         IVPRES,  OUT,     ,     APPEND           ! Write output to a file
PRSECT                                                     ! Print path stresses at this location
/OUTPUT

/GRAPHICS,   FULL                                          ! Disable PowerGraphics

/FOCUS,         1,    14.0800,     1.2470,     0.0000      ! Set the graphics window parameters
/DIST,          1,     1.8000
/VIEW,          1,     0.0000,     0.0000,     1.0000
/ANGLE,         1,     0.0000

PLNSOL,        SI                                          ! Plot stress intensity to the screen
/SHOW,        PNG
PLNSOL,        SI                                          ! Plot stress intensity to a file
/SHOW,      CLOSE
```

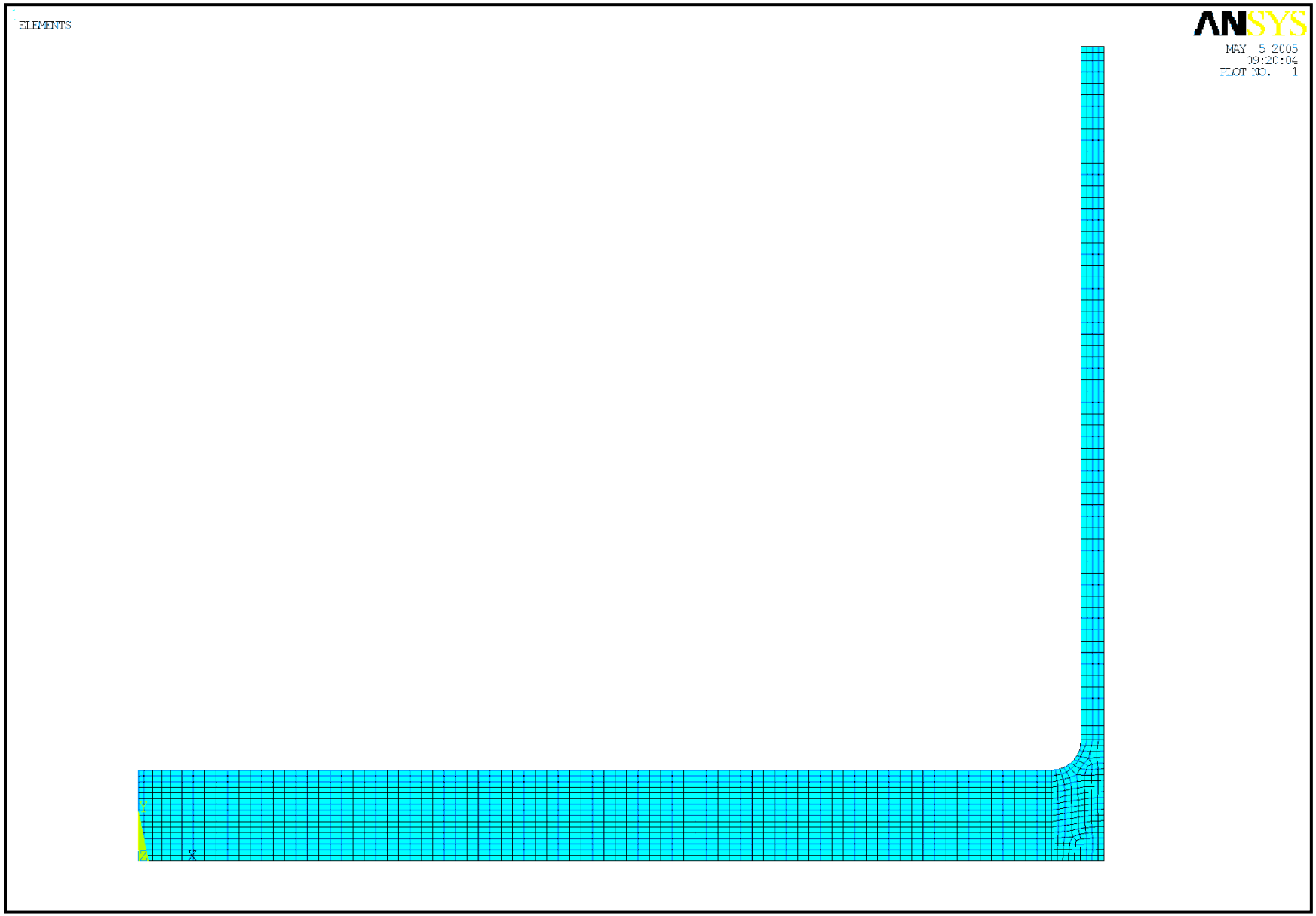

Figure 2.10.1-5 – Finite Element Analysis Model of the IV Bottom Transition Due to Pressure

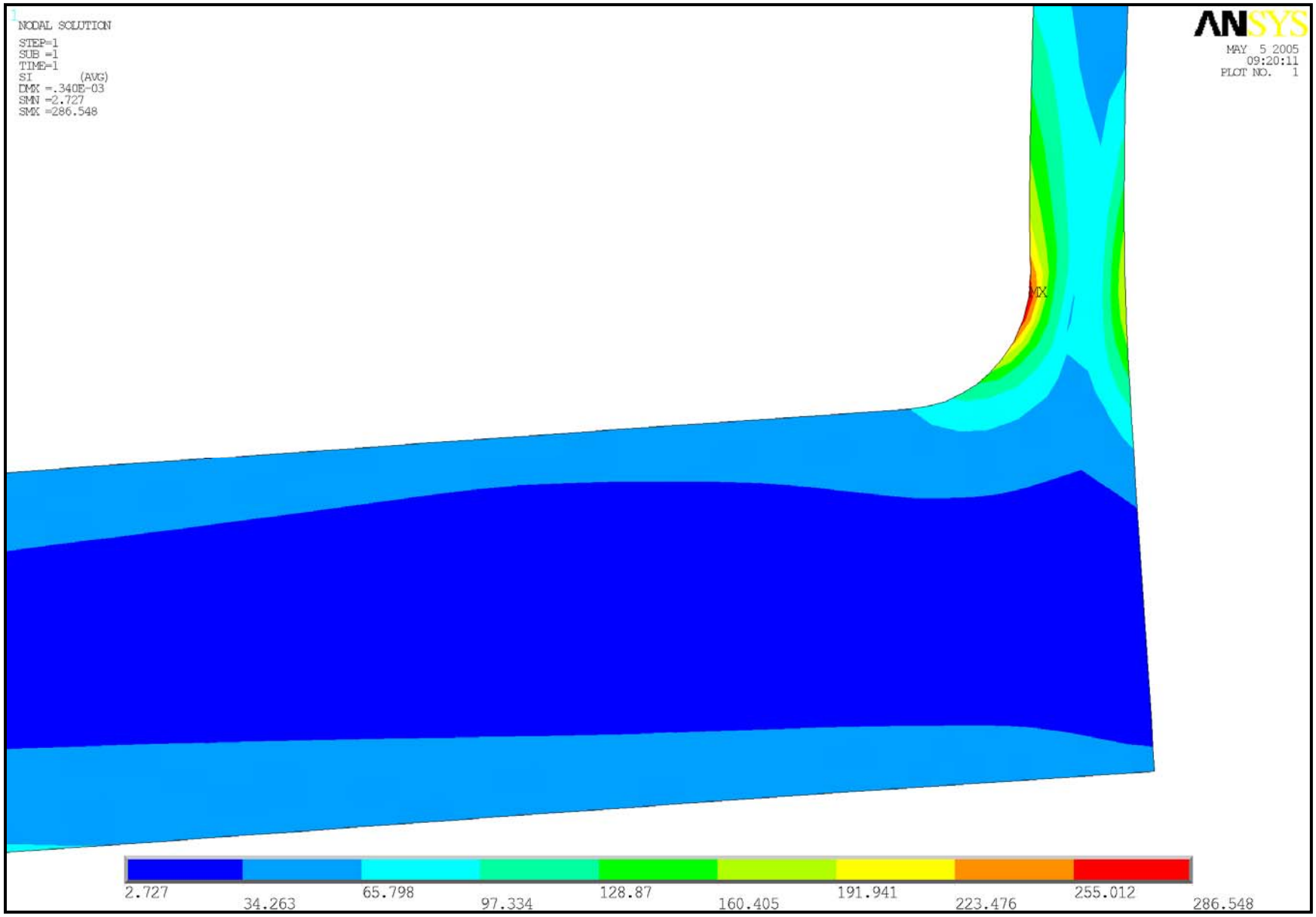

Figure 2.10.1-6 – IV Bottom Transition Stress Intensities Due to Pressure

2.10.1.3 Inner Vessel Radius Transition Zone Stresses Due to 1*g* Acceleration

As shown in Figure 2.10.1-7, the model is comprised of the bottom transition in the inner vessel (IV) shell utilizing approximately 1,700 PLANE82, 8-node axisymmetric solid elements. PLANE82 elements have a quadratic displacement behavior and are well suited to model irregular meshes and curved surfaces, providing exceptional accuracy for this application. Each element is defined by 8 nodes having two degrees of freedom at each node: translations in the nodal x- and y-directions.

Radial displacement constraints are applied at the symmetry boundary, and the end of the IV shell is constrained from displacing in the axial direction to simulate the entire structure.

A unit acceleration load of -386.0 in/s^2 is applied to the model in the axial direction.

As shown in Figure 2.10.1-8, the maximum stress intensity in the IV shell is 110 psi, occurring at the transition to the cylindrical shell.

The ANSYS® input file is provided in Table 2.10.1-3.

Table 2.10.1-3 – Input Listing for IV Radius Transition Zone Stresses Due to 1*g* Acceleration

```
/PREP7                                                          ! Enter the pre-processing module

/UNITS,       BIN                                               ! Specify British (inches) for units

/TITLE,IV Shell Stresses at Bottom Corner Transition with 1g Axial Acceleration

ET,       1,    PLANE82,     ,     ,    1                       ! Shell and Bottom

MP,      EX,    1,         27800000                            ! Properties for stainless steel
MP,    DENS,    1,        7.513E-04
MP,    NUXY,    1,           0.3000

K,        1,     0.0000,     0.0000                            ! Define the keypoints
K,        2,    15.1250,     0.0000
K,        3,    16.0000,     0.0000
K,        4,    16.0000,     2.0000
K,        5,    16.0000,    13.5000
K,        6,     0.0000,     1.5000
K,        7,    15.1250,     1.5000
K,        8,    15.6250,     2.0000
K,        9,    15.6250,    13.5000
K,       10,    15.1250,     2.0000

L,              1,    2                                         ! Define the lines
*REPEAT,        4,    1,    1
L,              6,    7
LARC,           7,    8,   10,     0.5000
L,              8,    9
L,              1,    6
L,              2,    7
L,              4,    8
L,              5,    9

AL,             1,    9,    5,    8                             ! Define the bottom plate area
AL,             4,   11,    7,   10                             ! Define the cylinder area
AL,             2,    3,   10,    6,    9                      ! Define the transition area

SMRTSIZE,       2                                               ! Mesh the volumes into elements
LESIZE,         2,     ,     ,    9
LESIZE,         3,     ,     ,   21
LESIZE,         8,     ,     ,   16
LESIZE,         9,     ,     ,   16
LESIZE,        10,     ,     ,    4
LESIZE,        11,     ,     ,    4
AATT,           1,    1,    1
AMESH,          1
AMESH,          2
AMESH,          3

ACEL,            0.0000,  -386.0000,     0.0000                 ! Apply a unit acceleration load to the model

NSEL,     S,  LOC,    X,     0.0000                             ! Restrain radial and axial nodes at the free ends
D,      ALL,   UX,     0.0000
NSEL,     S,  LOC,    Y,    13.5000
D,      ALL,   UY,     0.0000
NSEL,   ALL

SBCTRAN                                                         ! Transfer all loads from keypoints to nodes
```

```
WSORT,       ALL                                                    ! Reduce the solution wavefront

/RGB,       INDEX,  100,  100,  100,    0                           ! Invert colors (white background for output plot files)
/RGB,       INDEX,   80,   80,   80,   13
/RGB,       INDEX,   60,   60,   60,   14
/RGB,       INDEX,    0,    0,    0,   15

/DEV,        FONT,    1,Courier*New,  400,    0,  -16,    0,    0       Set the font sizes
/DEV,        FONT,    2,      Arial,  400,    0,  -13,    0,    0
/DEV,        FONT,    3,      Arial,  400,    0,  -13,    0,    0

PNGR,        COMP,    1                                             ! Set the graphics file parameters
PNGR,       ORIEN,HORIZ
PNGR,       COLOR,    2
PNGR,        TMOD,    1
/GFILE,      1800

/WINDOW,        1,    -1.0000,     1.6700,    -0.9260,     0.9260    ! Set the graphics window size to 9.00 x 6.25 ratio

/FOCUS,         1,     8.6120,     6.6770,     0.0000                ! Set the graphics window parameters
/DIST,          1,     7.5000
/VIEW,          1,     0.0000,     0.0000,     1.0000
/ANGLE,         1,     0.0000

EPLOT                                                              ! Plot elements to the screen
/SHOW,        PNG
EPLOT                                                              ! Plot elements to a file
/SHOW,      CLOSE

FINISH

/SOLUTION                                                          ! Enter the solution module

ANTYPE, STATIC                                                     ! Specify a static problem
SOLCONTROL,    ON,   ON                                            ! Set solution controls

SOLVE                                                              ! Solve the problem

FINISH

/POST1                                                             ! Enter the post-processing module

SET,   LAST                                                        ! Retrieve the final load step's data

PATH,          P1,    2,   30,   20                                ! Linerized stress intensity along Path 1
PPATH,          1,    1                                           !  (center of IV bottom)
PPATH,          2,    3
PMAP,          ACCURATE
/OUTPUT,         IVPRES,  OUT                                      ! Write output to a file
PRSECT                                                             ! Print path stresses at this location
/OUTPUT

PATH,          P2,    2,   30,   20                                ! Linerized stress intensity along Path 2
PPATH,          1, 5029                                          !  (top of radius transition in cylindrical shell)
PPATH,          2, 5087
PMAP,          ACCURATE
/OUTPUT,         IVPRES,  OUT,     ,     APPEND                    ! Write output to a file
PRSECT                                                             ! Print path stresses at this location
/OUTPUT

/GRAPHICS,   FULL                                                  ! Disable PowerGraphics

/FOCUS,         1,    14.0800,     1.2470,     0.0000                ! Set the graphics window parameters
/DIST,          1,     1.8000
/VIEW,          1,     0.0000,     0.0000,     1.0000
/ANGLE,         1,     0.0000

PLNSOL,         SI                                                 ! Plot stress intensity to the screen
/SHOW,        PNG
PLNSOL,         SI                                                 ! Plot stress intensity to a file
/SHOW,      CLOSE
```

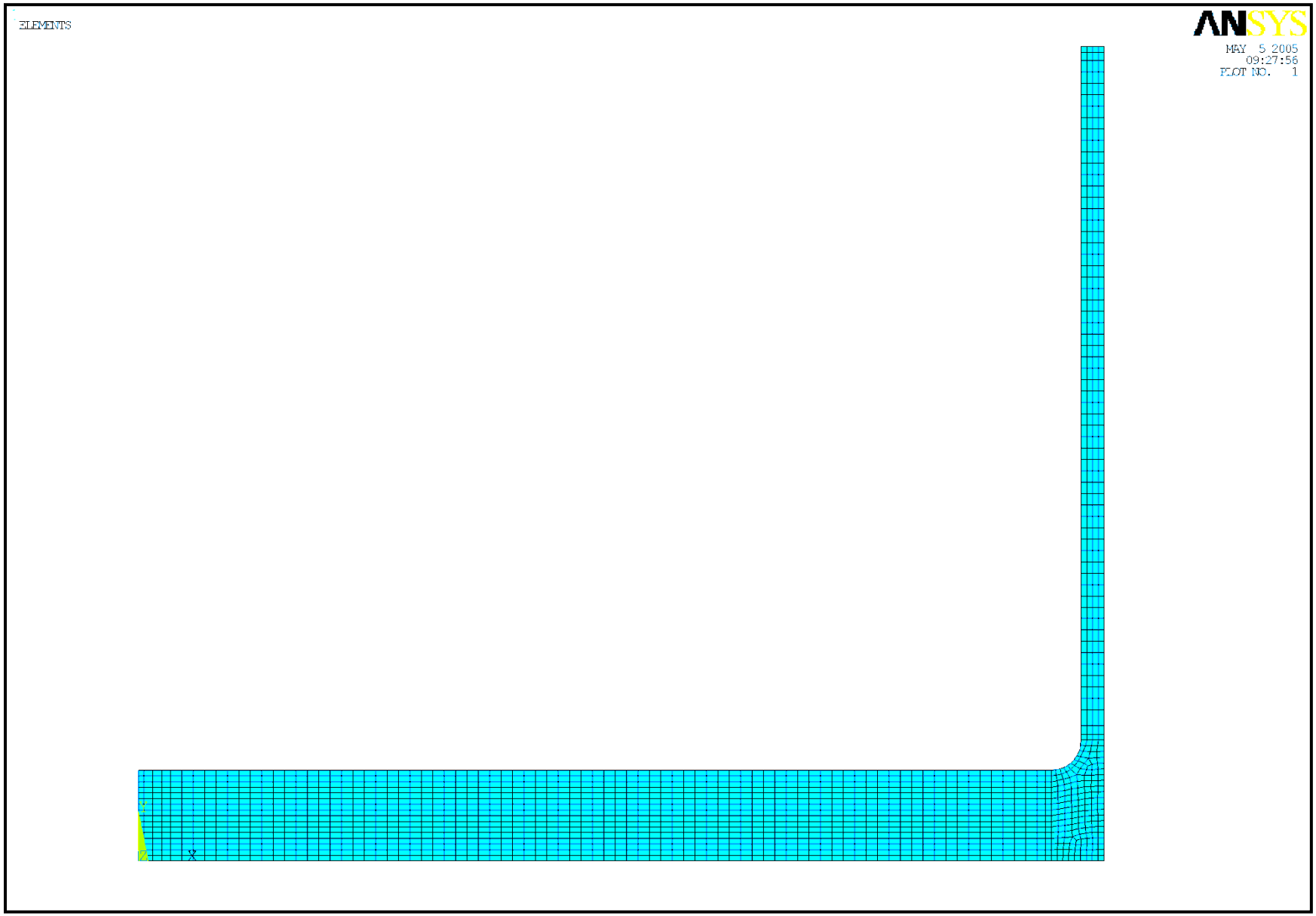

Figure 2.10.1-7 – Finite Element Analysis Model of the IV Bottom Transition Due to 1*g* Acceleration

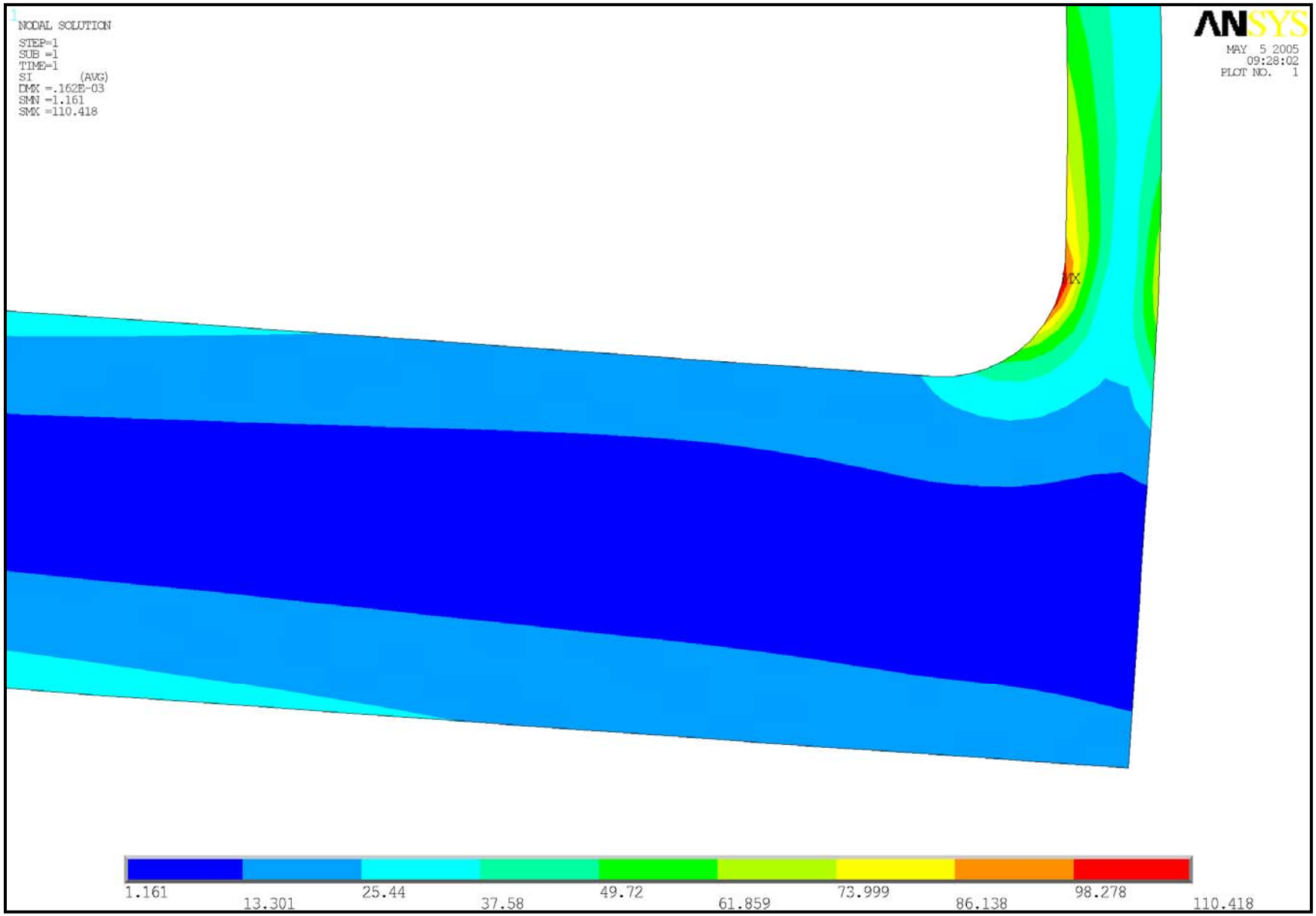

Figure 2.10.1-8 – IV Bottom Transition Stress Intensities Due to 1*g* Acceleration

2.10.1.4 Containment Assembly Analysis for Oblique Drops

The oblique drop finite element model represents all components of the RH-TRU 72-B package: the impact limiters, the outer cask (OC) and inner vessel (IV) base plates, shells, and lids, and the payload canister. Table 2.10.1-4 summarizes node and element numbering for each of the structural components. The model was built so that varying drop angles, accelerations, rotational velocities, rotational accelerations, and distances between impact and the center of gravity could be accommodated. These parameters are available from the SLAPDOWN program results and used as input to the finite element model (see Appendix 2.10.4, *Slapdown Assessment*).

The OC, IV, and payload canister are all modeled with two-dimensional, elastic beam elements (STIF3). The element is defined by two nodal points having three degrees of freedom at each node: translations in the nodal x- and y-directions, and rotation about the nodal z-axis. The elastic beam element is a uniaxial element with tension, compression, torsion, and bending capabilities. The OC is modeled only with the structural properties of the stainless steel inner and outer shells, assuming the lead provides no structural support. The material density of the OC beam is adjusted to include the mass of the lead. Similarly, the material densities of the IV and canister are adjusted to account for the mass of the contents and other components not included in the ANSYS® model.

The impact limiters, lids, and bases are modeled as generalized two-dimensional mass elements with rotary inertia (STIF21). These elements are defined by one node which has three degrees of freedom: translations in the nodal x- and y-directions, and rotation about the nodal z-axis. This element contributes only to the structural mass and has no displacement function.

The lower impact limiter also has five elements (1-5) associated with it that are two-dimensional, elastic beams (STIF3) being used as rigid connectors. These rigid connectors are needed so that the loads from the drop impact will be transmitted to the package properly.

Combination elements (STIF40) are used to interface between the OC and IV. The element is defined by two nodal points having one degree of freedom: either a translation in a nodal coordinate direction or a rotation about a nodal coordinate axis. The combination element is representative of a spring coupled to a gap in series. The combination elements are used to interface between the OC and IV so that the load of the IV on the OC is distributed properly for the various drop orientations considered. To properly model this aspect, a stiff spring (spring stiffness, $k = (10)^8$ lb/in) having no mass is used. The interface elements are modeled with an initial gap of $1(10)^{-6}$ inches, assuming that the IV and OC are initially in contact along the entire length of the IV. For this model, the combination elements are restricted to displacement in the nodal y-direction (or in the package's radial direction).

The origin of the nodal coordinate system is located at the center of gravity of the package (node 117) as shown in Figure 2.10.1-9. The nodal x-axis corresponds to the horizontal direction with respect to the ground, and the nodal y-axis corresponds to the vertical direction with respect to the ground.

Nodes 105 (OC base), 207 (IV base), and 307 (canister base) are coupled to move in the x-direction together since the bases of all the vessels rest directly on each other and would move together vertically. Nodes 107 (OC shell adjacent to the IV base) and 207 (IV base) are coupled to move in the y-direction since the IV base is laterally restricted in movement by the OC shell. Nodes 127 (OC shell adjacent to the IV lid) and 227 (IV lid) are coupled to move in the y

direction since the IV lid is laterally restricted in movement by the OC shell. Nodes 211 and 311 are coupled in the y-direction to simulate the spacer belt that is at that location to support the payload canister in the IV. Nodes 223 and 323 are coupled in the y-direction to simulate the spacer belt at the other location.

The model is restrained from translating and rotating in all directions at node 1, which represents the corner of impact.

As discussed previously the model is loaded with appropriate accelerations and velocities from SLAPDOWN program results.

In addition, a temperature of 160 ºF is utilized to determine the temperature dependent material property values of the OC and IV. The only material property affected by a temperature of 160 ºF is Young's modulus which, consistent with Table 2.3-1 in Section 2.3, *Mechanical Properties of Materials*, is set to $27.8(10)^6$ psi for Type 304 stainless steel. A temperature of 175 ºF is utilized to determine the temperature dependent material property values of the canister. Again, the only material property affected by a temperature of 175 ºF is Young's modulus which, consistent with Table 2.3-1 in Section 2.3, *Mechanical Properties of Materials*, is set to $28.9(10)^6$ psi for ASTM A516, Grade 55, carbon steel.

2.10.1.5 Containment Assembly Analysis for Side Drops

The side drop finite element model has the identical geometry as that for the oblique drops. Therefore, refer to Appendix 2.10.1.4, *Containment Assembly Analysis for Oblique Drops*, for geometry details. The side drop model, like the oblique model, requires the acceleration from the CASKDROP program results as input for the finite element model (see Appendix 2.10.2.1, *Description of the CASKDROP Computer Code*). However, the angle of impact, rotational velocity, rotational acceleration, and distance between impact and the center of gravity, parameters that are needed for the oblique finite element model, are not necessary for the side drop and therefore have been deleted.

Table 2.10.1-4 – Containment Assembly Node and Element Numbering

Component	Node Numbers	Element Numbers
Lower Impact Limiter	101 – 104	1 - 5, 30
Outer Cask Base Plate	105	31
Outer Cask Shells	106 – 128	6 - 27
Outer Cask Lid	129	32
Inner Vessel Base Plate	207	54
Inner Vessel Shell	207 – 227	34 - 53
Inner Vessel Lid	227	55
Payload Canister	307 – 327	56 - 75
Upper Impact Limiter	128 – 130	28, 29, 33

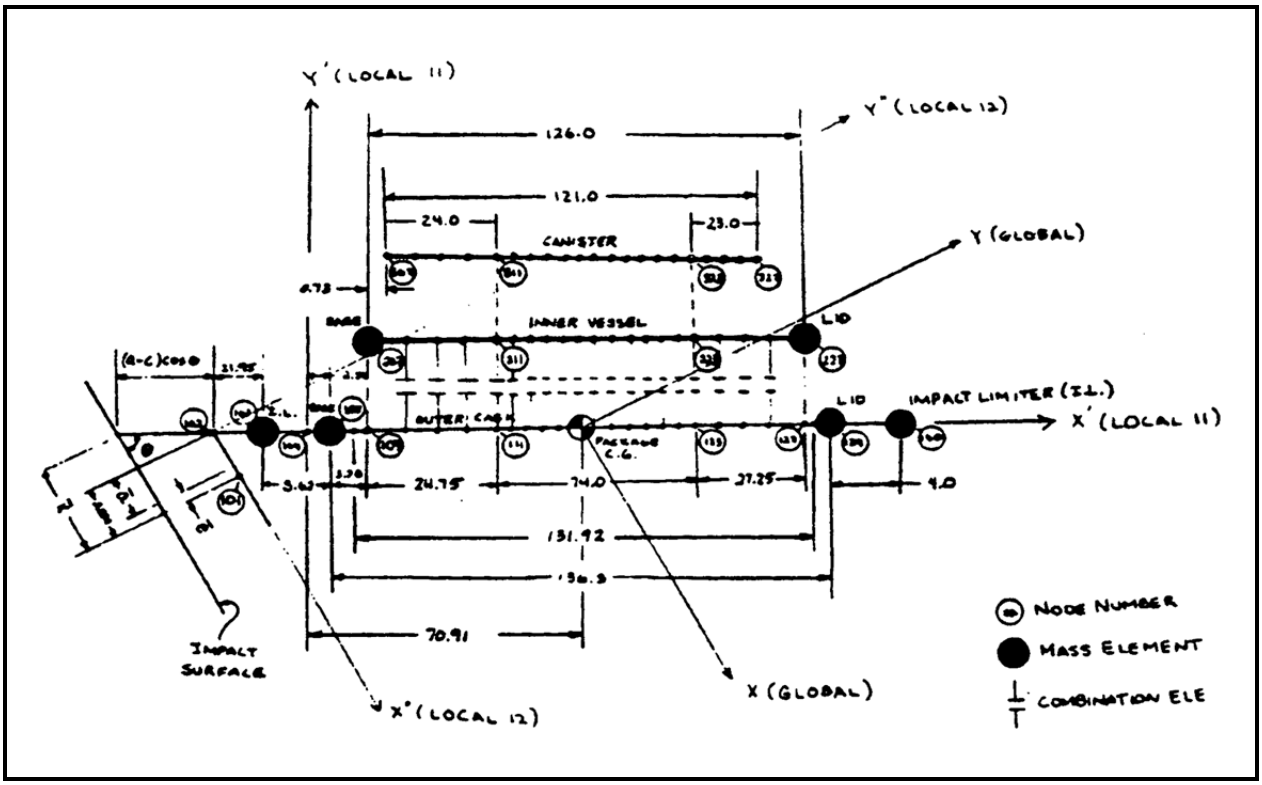

Figure 2.10.1-9 – Containment Assembly Oblique Analysis Model

2.10.1.6 Outer Cask Bottom Stresses Due to Puncture

As shown in Figure 2.10.1-10 and Figure 2.10.1-11, the model is comprised of the outer cask (OC) bottom and shells utilizing approximately 26,000 PLANE42, 4-node axisymmetric solid elements. Each element is defined by 4 nodes having two degrees of freedom at each node: translations in the nodal x- and y-directions.

Radial displacement constraints are applied at the symmetry boundary, and the end of the OC shells are constrained from displacing in the radial and axial directions. Any structural stiffening contribution by the lead between the OC shells was conservatively ignored.

A pressure of 47,000 psi was applied to a 3.0-inch radius at the centerline of the OC bottom surface. In addition, the following three downward acting axisymmetric point (ring) loads were applied to the OC bottom:

- 236,000 pounds applied at a radius of 12.875 inches at the top surface of the OC bottom, representing the 8,000-pound payload canister with a 29.5*g* inertia load,
- 118,679 pounds applied at a radius of 15.8125 inches at the top surface of the OC bottom, representing the 4,023-pound inner vessel (IV) with a 29.5*g* inertia load, and
- 75,137 pounds applied at a radius of 17.59375 inches at the bottom surface of the OC bottom, representing the 2,547-pound impact limiter with a 29.5*g* inertia load.

Also, a positive vertical inertia load of $386.0 \times 29.5g = 11{,}387$ in/s^2 was applied to the model. The stainless steel density was assumed to be 7.51295E-04 lb-s^2/in^4 (0.29 lb/in^3).

As shown in Figure 2.10.1-12, the peak stress intensity in the OC bottom is 75,071 psi, occurring at the radial centerline. As shown in Figure 2.10.1-13, linearized stress intensities at this location result in a maximum membrane-plus-bending stress intensity at the top surface of 66,760 psi.

The ANSYS® input file is provided in Table 2.10.1-5.

Table 2.10.1-5 – Input Listing for OC Bottom Stresses Due to Puncture

```
/PREP7                                                                  ! Enter the pre-processing module

/UNITS,       BIN                                                       ! Specify British (inches) for units

/TITLE,OC Outer Cask Bottom Stresses with 29.5g (47,000 psi) Puncture Bar Pressure Load

ET,       1,    PLANE42,     ,     ,    1                              ! Bottom forging
ET,       2,    PLANE42,     ,     ,    1                              ! Inner Shell
ET,       3,    PLANE42,     ,     ,    1                              ! Outer Shell

MP,      EX,    1,         27820000                                    ! Properties for stainless steel at 160 °F
MP,    NUXY,    1,           0.3000
MP,    DENS,    1,      7.51295E-04

K,      101,   0.000000,   0.000000                                    ! Define the keypoints
K,      102,   3.000000,   0.000000
K,      103,   9.437500,   0.000000
K,      104,   9.437500,   0.875000
K,      105,  11.062500,   0.875000
K,      106,  11.062500,   0.000000
K,      107,  12.875000,   0.000000
K,      108,  15.812500,   0.000000
K,      109,  16.187500,   0.000000
K,      110,  17.593750,   0.000000
K,      111,  20.562500,   0.000000
K,      112,   0.000000,   5.000000
K,      113,   3.000000,   5.000000
K,      114,   9.437500,   5.000000
K,      115,  11.062500,   5.000000
K,      116,  12.875000,   5.000000
K,      117,  15.812500,   5.000000
K,      118,  16.187500,   5.000000
K,      119,  16.187500,   6.875000
K,      120,  17.187500,   6.875000
K,      121,  17.621294,   5.362101
K,      122,  18.101925,   5.000000
K,      123,  19.062500,   5.000000
K,      124,  20.562500,   5.000000
K,      125,  18.101925,   5.500000
K,      126,  16.187500, 129.250000                                    ! Define the keypoints
K,      127,  17.187500, 129.250000
K,      128,  19.062500, 129.250000
K,      129,  20.562500, 129.250000

L,            101,  102                                                ! Define the lines
*REPEAT,       10,    1,    1
L,            112,  113
*REPEAT,        9,    1,    1
LARC,         121,  122,  125,   0.500000
L,            122,  123
L,            123,  124
L,            101,  112
L,            102,  113
L,            104,  114
L,            105,  115
L,            107,  116
L,            108,  117
L,            109,  118
L,            111,  124
L,            126,  127
L,            128,  129
L,            119,  126
L,            120,  127
L,            123,  128
L,            124,  129

AL,             1,   24,   11,   23                                    ! Define the areas
AL,             2,    3,   25,   12,   24
AL,             4,   26,   13,   25
AL,             5,    6,   27,   14,   26
AL,             7,   28,   15,   27
AL,             8,   29,   16,   28
AL,             9,   10,   30,   22,   21,   20,   19,   18,   17,   29
AL,            18,   34,   31,   33
AL,            22,   36,   32,   35

MSHAPE,         0,  2-D                                                ! Mesh the areas into elements
ESIZE,         0.125000
AATT,           1,    1,    1
AMESH,          1,    7,    1
AATT,           1,    1,    2
AMESH,          8
AATT,           1,    1,    3
AMESH,          9

*SET,    PP,           47000                                          ! Puncture bar interface pressure
*SET,   WPC,            8000                                          ! Weight of payload canister
*SET,   WIV,            4023                                          ! Weight of inner vessel
```

```
*SET,   WIL,            2547                                    ! Weight of impact limiter
*SET,    GA,        29.500000                                    ! Inertia load (g's)
*SET,    F1,          -WPC*GA                                    ! Ring load from payload canister weight
*SET,    F2,          -WIV*GA                                    ! Ring load from inner vessel weight
*SET,    F3,          -WIL*GA                                    ! Ring load from impact limiter weight

SFL,      1,       PRES,         PP                             ! Define the puncture bar pressure load
FK,     116,         FY,         F1                             ! Define the payload canister ring force
FK,     117,         FY,         F2                             ! Define the inner vessel ring force
FK,     110,         FY,         F3                             ! Define the impact limiter ring force

DL,      23,     ,   UX,     0.0000                             ! Radial restraint at the axial centerline
DL,      31,     ,   UX,     0.0000                             ! Radial restraint at the shell ends
DL,      32,     ,   UX,     0.0000
DL,      31,     ,   UY,     0.0000                             ! Axial restraint at the shell ends
DL,      32,     ,   UY,     0.0000

SBCTRAN                                                         ! Transfer all loads from keypoints to nodes

ACEL,          0.000000,   386.0*GA,   0.000000                 ! Apply a vertical acceleration

WSORT,        ALL                                               ! Reduce the solution wavefront

/RGB,       INDEX,  100,  100,  100,    0                       ! Invert colors (white background for output plot files)
/RGB,       INDEX,   80,   80,   80,   13
/RGB,       INDEX,   60,   60,   60,   14
/RGB,       INDEX,    0,    0,    0,   15

/DEV,        FONT,    1,Courier*New,  400,    0,  -16,    0,    0        Set the font sizes
/DEV,        FONT,    2,      Arial,  400,    0,  -13,    0,    0
/DEV,        FONT,    3,      Arial,  400,    0,  -13,    0,    0

PNGR,        COMP,    1                                         ! Set the graphics file parameters
PNGR,       ORIEN,HORIZ
PNGR,       COLOR,    2
PNGR,        TMOD,    1
/GFILE,      1800

/WINDOW,        1,    -1.0000,     1.6700,    -0.9260,     0.9260       ! Set the graphics window size to 9.00 x 6.25 ratio

/PNUM,       TYPE,    1                                         ! Show the elements types as different colors
/NUMBER,        1                                              ! Turn on element colors only
/PSF,        PRES, NORM,    2,    0,    1                      ! Show surface load symbols (pressure)
/PBC,         ALL,     ,    1                                  ! Show boundary condition symbols
/PLOPTS,     LEG3,    0                                        ! Turn off pressure contour legend

/FOCUS,         1,     9.0800,    61.4800,     0.0000          ! Set the graphics window parameters
/DIST,          1,    70.0000
/VIEW,          1,     0.0000,     0.0000,     1.0000
/ANGLE,         1,     0.0000
/EDGE,          1,    1                                         ! Plot only edge lines

EPLOT                                                           ! Plot elements to the screen
/SHOW,        PNG
EPLOT                                                           ! Plot elements to a file
/SHOW,      CLOSE

/FOCUS,         1,    11.3800,     7.3550,     0.0000          ! Set the graphics window parameters
/DIST,          1,     8.5000
/VIEW,          1,     0.0000,     0.0000,     1.0000
/ANGLE,         1,     0.0000
/EDGE,          1,    0                                         ! Plot edge and interior lines

EPLOT                                                           ! Plot elements to the screen
/SHOW,        PNG
EPLOT                                                           ! Plot elements to a file
/SHOW,      CLOSE

FINISH

/SOLUTION                                                       ! Enter the solution module

ANTYPE, STATIC                                                  ! Specify a static problem
SOLCONTROL,    ON,   ON                                         ! Set solution controls

SOLVE                                                           ! Solve the problem

FINISH

/POST1                                                          ! Enter the post-processing module

SET,   LAST                                                     ! Retrieve the final load step's data

/GROPT,      AXDV,   ON                                         ! Define linerized stress graph parameters
/GROPT,      AXNM,   ON
/GROPT,     AXNSC,    1
/GROPT,     ASCAL,   ON
/GROPT,      LOGX,  OFF
/GROPT,      LOGY,  OFF
/GROPT,      FILL,  OFF
/GROPT,     CGRID,   ON
/GROPT,      DIG1,    6
/GROPT,      DIG2,    0
/GROPT,      REVX,  OFF
/GROPT,      REVY,  OFF
/GROPT,      DIVX,   10
/GROPT,      DIVY,   12
/GROPT,      LTYP,    0
/AXLAB,         X
/AXLAB,         Y
/GTHK,       AXIS,    2
/GTHK,       GRID,    1
/GTHK,      CURVE,    3
/GRTYP,             0
/GRID,              1
/XRANGE,        DEFAULT
/YRANGE,            0,72000,    0
```

```
PATH,          P1,    2,   30,   20                          ! Linerized stress intensity at bottom center
*GET,          N1,   KP,  101, ATTR, NODE                   ! Get the node number at keypoint 101
PPATH,          1,   N1
*GET,          N2,   KP,  112, ATTR, NODE                   ! Get the node number at keypoint 112
PPATH,          2,   N2
PMAP,          ACCURATE
/OUTPUT,         OCPUNC,  OUT                               ! Write output to a file
PRSECT                                                      ! Print path stresses at this location
/OUTPUT
PLSECT,         S,  INT                                    ! Plot linearized stress intensity to the screen
/SHOW,        PNG
PLSECT,         S,  INT                                    ! Plot linearized stress intensity to a file
/SHOW,      CLOSE

/NUMBER,        0                                          ! Turn on element numbers and colors
/PLOPTS,     LEG3,    1                                    ! Turn on contour legend
/GRAPHICS,   FULL                                           ! Disable PowerGraphics

/FOCUS,         1,    10.4500,     6.8600,     0.0000      ! Set the graphics window parameters
/DIST,          1,     7.5000
/VIEW,          1,     0.0000,     0.0000,     1.0000
/ANGLE,         1,     0.0000

PLNSOL,        SI                                           ! Plot stress intensity to the screen
/SHOW,        PNG
PLNSOL,        SI                                           ! Plot stress intensity to a file
/SHOW,      CLOSE
```

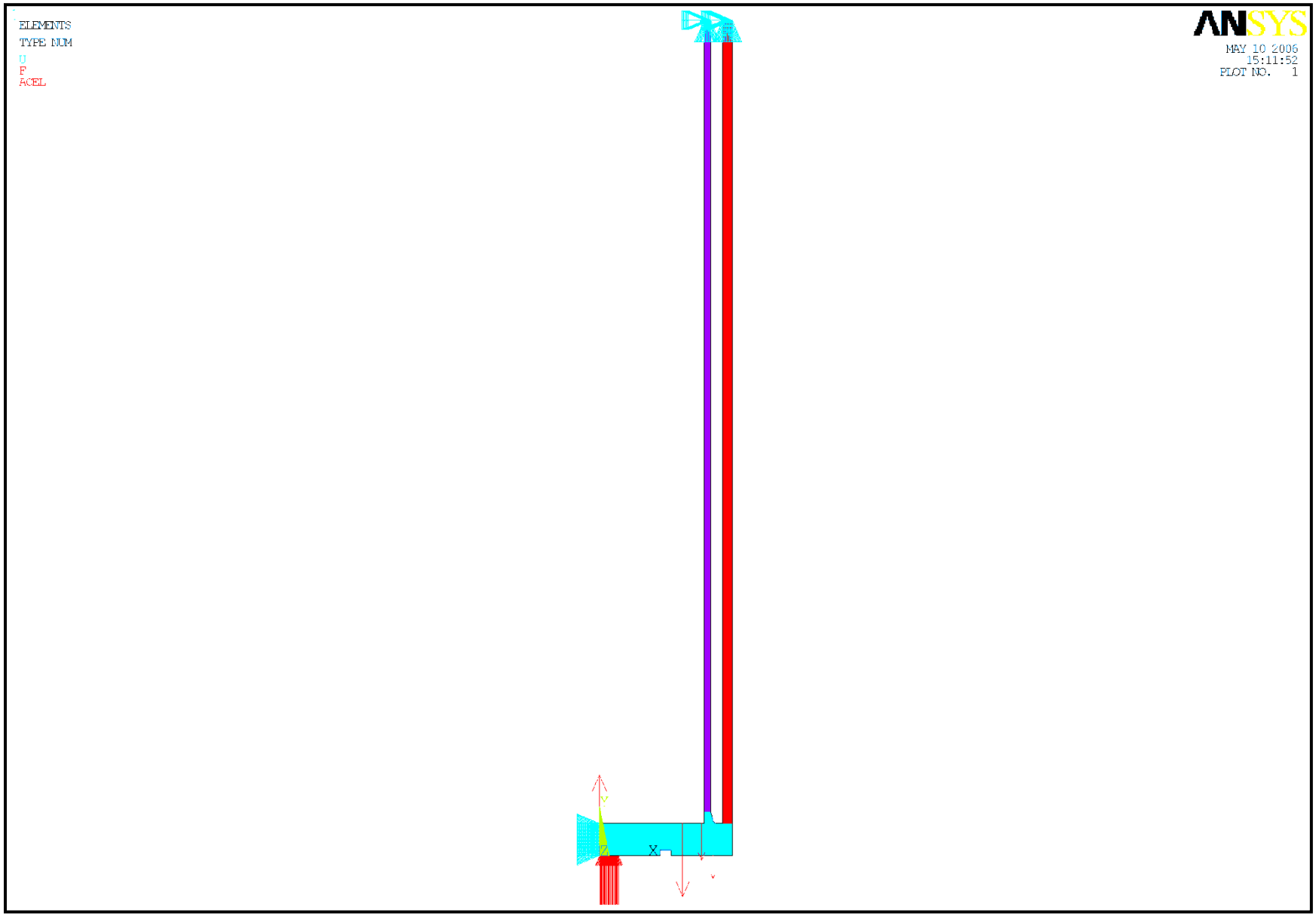

Figure 2.10.1-10 – Finite Element Analysis Model of the OC Bottom Due to Puncture

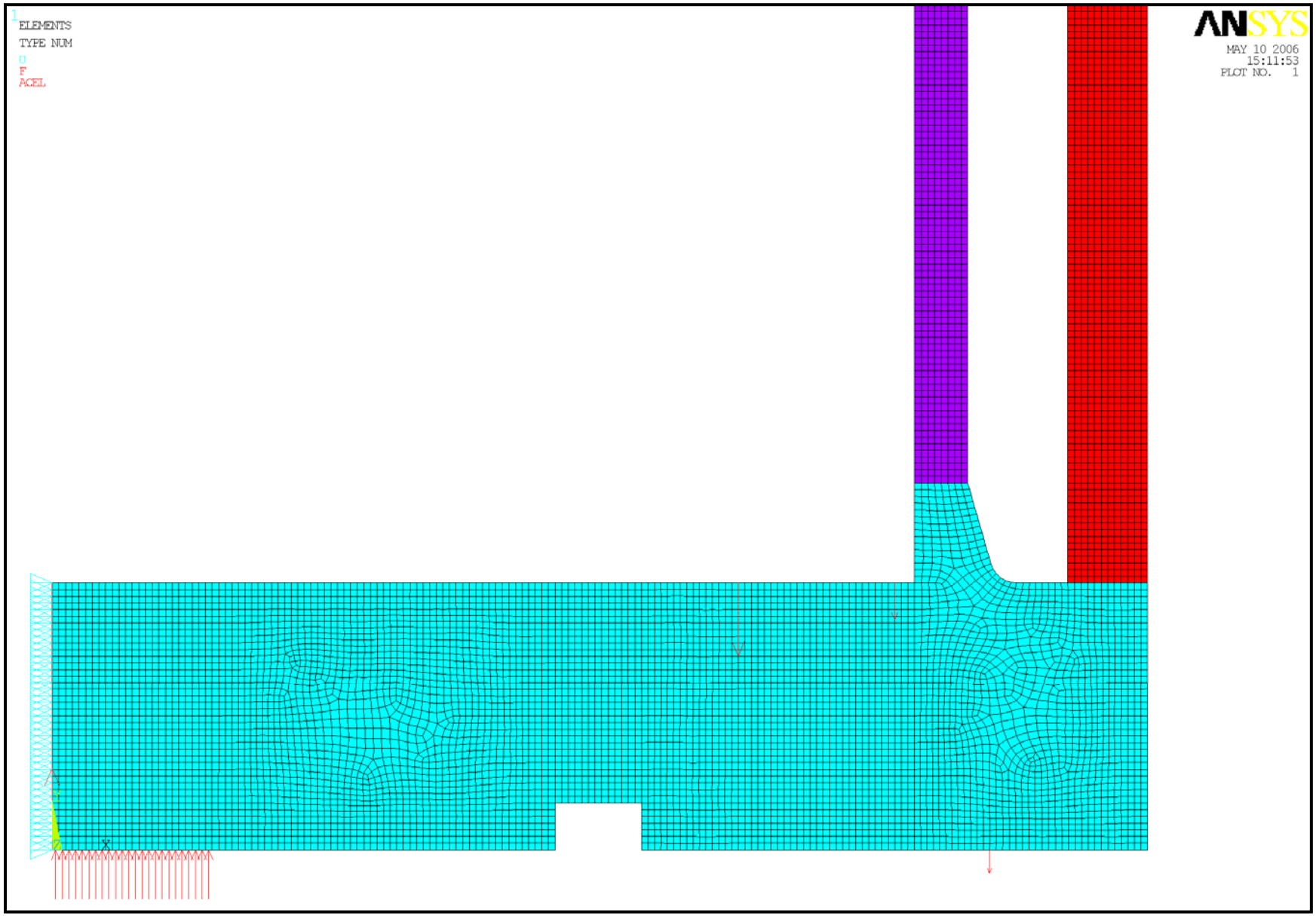

Figure 2.10.1-11 – Finite Element Analysis Model of the OC Bottom Due to Puncture (Close-up)

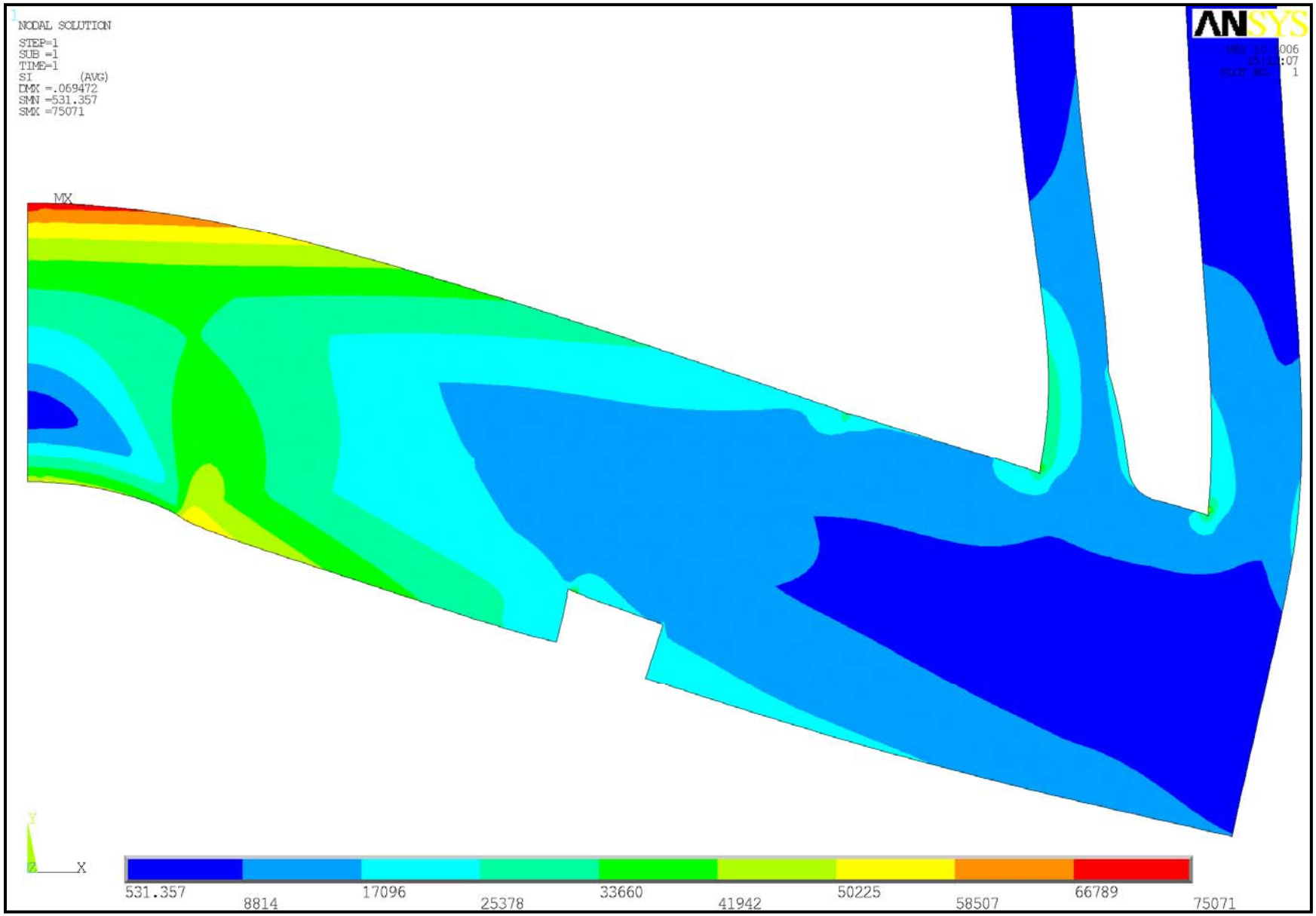

Figure 2.10.1-12 – OC Bottom Stress Intensities Due to Puncture

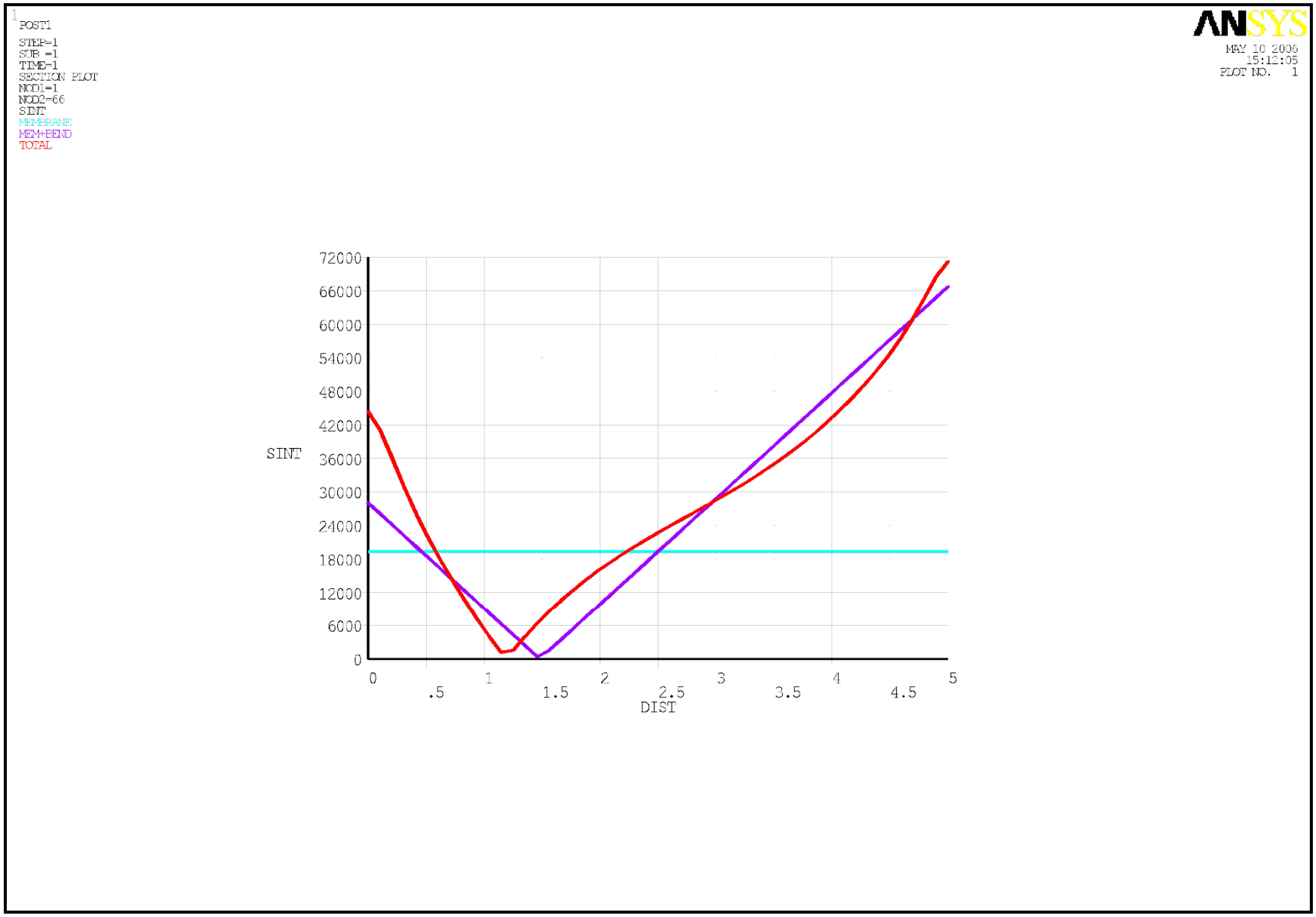

Figure 2.10.1-13 – Linearized Stress Intensities at the OC Bottom Centerline

2.10.2 Drop Analysis Codes Description

2.10.2.1 Description of the CASKDROP Computer Code

This section briefly documents the methodology employed by the PacTec computer code CASKDROP. The computer program CASKDROP is used to demonstrate compliance of the package with 10 CFR §71.71(c)(7)[1] and 10 CFR §71.73(c)(1)[1] for normal conditions of transport (NCT) and hypothetical accident conditions (HAC) free drop analyses, respectively.

A summary of the appendix subsections is as follows:

- describes the CASKDROP analysis methodology.
- provides an example problem with input and output.

2.10.2.1.1 Using CASKDROP to Determine Impact Limiter Deformation Behavior

The package is protected by polyurethane foam-filled, energy absorbing end buffers, called impact limiters. For purposes of the regulatory free drop analyses using the CASKDROP computer program, the impact limiters are assumed to absorb, in plastic deformation of the polyurethane foam, all of the potential energy of the drop event. In other words, the drop analyses assume that none of the potential energy of the free drop event is transferred to kinetic or strain energy of the target (i.e., the "unyielding" surface assumption of 10 CFR 71), nor strain energy in the package body itself.

CASKDROP evaluates all angles of drop from 0º (horizontal) to 90º (vertical) by performing a quasi-static analysis that ignores rotational effects. At orientations where rotational effects are important, use of a dynamic analysis computer program such as SCANS[2] or SLAPDOWN[3] is required utilizing the force-deflection data developed by CASKDROP. Three orientations where rotational motions (or pitch) play no role in the evaluation of the free drop analyses are:

- END DROP on the circular end surface of the impact limiter,
- SIDE DROP on the cylindrical side surfaces of the impact limiters, and
- CORNER DROP with the package center of gravity directly over the impact limiter corner.

For all orientations of impact, the prediction of impact limiter deformation behavior can be approached from straightforward energy balance principles:

$$E = W(h + \delta) = \int_0^{\delta} F_x dx$$

[1] Title 10, Code of Federal Regulations, Part 71 (10 CFR 71), *Packaging and Transportation of Radioactive Material*, 01-01-14 Edition.

[2] *SCANS (Shipping Package ANalysis System), a Microcomputer Based Analysis System for Shipping Package Design Review*, NUREG/CR-4554, Version 1A, Lawrence Livermore National Laboratory, Livermore, California.

[3] G. D. Sjaardema, G. W. Wellman, *Numerical and Analytical Methods for Approximating the Eccentric Impact Response (Slapdown) of Deformable Bodies*, SAND 88-0616, Sandia National Laboratories, Albuquerque, New Mexico, March 1988.

where the package gross weight is W, the drop height is h, the maximum impact limiter deformation is δ, and the force imposed on target at an impact limiter deformation of x is F_x. The left-hand term represents the potential energy of the free drop. The right-hand term represents the strain energy of the deformed impact limiter(s).

Given a specific drop angle, θ, and impact limiter deformation, δ, as illustrated in Figure 2.10.2-1, the result is an impact limiter crush plane "footprint." Integration of the impact limiter crush plane yields a total crush force and centriodal distance of:

$$F = \iint \sigma\{\varepsilon\} dA$$

and,

$$\overline{X} = \left(\frac{1}{F}\right) \iint \overline{x} \sigma\{\varepsilon\} dA$$

respectively, where the total integrated force is F, the differential stress as a function of strain is $\sigma\{\varepsilon\}$, the differential area is dA (i.e., dA is a function of the "x" and "y" directions, or dx and dy), the total integrated centriodal distance from the package center of gravity is $\overline{X}$, and the differential centriodal distance from the package center of gravity is $\overline{x}$.

With reference to Figure 2.10.2-1, the geometric calculations for the impact surface (crush plane) and the associated strains are carried out using a translating X'-Y'-Z' coordinate system, with the X'-Y' plane corresponding to the crush plane. Due to the cylindrical nature of the problem, the overall crush plane is comprised of a segment of an ellipse corresponding to the outside surface of the impact limiter. The optional end hole requires removal of its associated elliptical segment. Similarly, the optional conical surface is an elliptical, parabolic, or hyperbolic segment depending on both the drop angle, θ, and angle of the cone.

Calculation of the differential strain is somewhat more complex. As illustrated in Figure 2.10.2-2, the differential strain, $\varepsilon\{x,y\}$, is calculated at the center of the differential area, dA. The differential strain is determined by calculating the amount of vertical deformation at the (x, y) location on the crush plane. The vertical distance from point (x, y) on the impact surface to the package or upper impact limiter surface is found and denoted z_{TOP}. Similarly, the vertical distance from point (x, y) on the impact surface to the undeformed lower impact limiter surface is found and denoted z_{BOT}. In equation format the differential strain at location (x, y) is simply:

$$\varepsilon = \frac{z_{BOT}}{z_{BOT} + z_{TOP}}$$

This strain is used to determine the corresponding crush stress from an implicit tabular definition of the crushable media stress-strain characteristics. For each differential area, dA, the differential force, dF, is found. The total force, F, is therefore the summation of the differential forces. Similarly, the centroidal distance, $\overline{X}$, is the summation of the moments, $\overline{x} \times dF$, divided by the total force, F.

Unbacked regions are defined as having an (x, y) location where z_{TOP} is calculated to occur outside the package's "shadow" (i.e., or backing, occurring on the impact limiter surface). Unbacked regions usually utilize the nominal crush strength of the crushable media (typically at

10% strain for polyurethane foam material) for integrated force purposes. The crush strength for unbacked regions is user-definable in the program CASKDROP.

For most drop angles, θ, and impact limiter deformations, δ, the impact limiter crush force, F, is transmitted to the package body in direct compression. Hence, the forces transmitted to the circumferential impact limiter attachments are essentially zero. However, for nearly vertical or horizontal orientations at small deformations where the crush force occurs beyond the edge of the package, the forces transmitted to the impact limiter attachments can be substantially large. It is important to note that only the nearly vertical or nearly horizontal orientations are required to produce the prying motion; all other orientations will always compress the impact limiter onto the package body. Figure 2.10.2-3 illustrates the near-vertical and near-horizontal orientations producing impact limiter separation forces.

For the near vertical orientation, the moment about point "a" determines whether a separation force exists at the impact limiter attachments. Assuming for this case that a counterclockwise moment is positive (i.e., will tend to "pry" the impact limiter off the package), the equation for the moment about point "a," M_a, is:

$$M_a = Fx_F + F_{IL}x_{IL}$$

Similarly, for the near horizontal orientation, the moment about point "b" determines whether a separation force exists at the impact limiter attachments. Assuming for this case that a clockwise moment is positive (i.e., will tend to "pry" the impact limiter off the package), the equation for the moment about point "b," M_b, is:

$$M_b = Fx_F - F_{IL}x_{IL}$$

If M_a or M_b are positive, a separation force will occur at the impact limiter attachments whereas if M_a or M_b are zero or negative, a separation force will not occur. Note that use of a conically shaped impact limiter typically eliminates the impact limiter separation force by causing the crush force, F, to almost always occur between points "a" and "b."

2.10.2.1.2 Example Problem for the CASKDROP Program

An example problem is illustrated in Figure 2.10.2-4. The CASKDROP program utilizes a variety of physical input data to determine package and impact limiter geometry. In all cases, the package and impact limiter are assumed axisymmetric. The package is cylindrical, as is the impact limiter. Two fundamental variations in the basic cylindrical shape of the impact limiter are an optional end hole and optional conical end. The end hole may extend part or all of the way from the outside surface of the impact limiter to the package end. The conical end may be a truncated or fully developed cone, defined by a cone diameter and a cone length at the outside surface of the impact limiter. By varying the impact limiter dimensions the result is a wide variety of possible impact limiter shapes, from a totally enclosing "overpack" to pointed end-only buffers.

The CASKDROP program was primarily developed as an impact limiter design tool. Geometry and analysis control input to the CASKDROP program is fully interactive allowing changes "on the fly." The top screenshot in Figure 2.10.2-5 illustrates the CASKDROP screen for data entry into the Input Window.

The CASKDROP program allows for three types of crushable media definition:

1. CONSTANT: a constant crush stress independent of calculated strain.
2. VARIABLE: a variable, user-defined stress-strain definition.
3. POLYFOAM: a built-in polyurethane foam database providing accurate stress-strain definition for 5 to 25 pound per cubic foot (pcf) density and temperatures of -20 ºF to +300 ºF based on extensive sample testing.

The example problem assumes 20-pcf polyurethane foam at a temperature of -20 ºF. A +60% bias is applied to the temperature-corrected stress-strain data to account for dynamic strain rate effects for the example problem. The bottom screenshot in Figure 2.10.2-5 illustrates the CASKDROP input screen for the polyurethane foam crush media for the example problem.

For the example problem, the CASKDROP program utilizes polyurethane foam where "parallel-to-rise" foam curing occurs in the axial direction and "perpendicular-to-rise" foam curing occurs in the radial direction, although the difference between these two directions is small. The user may optionally select the "parallel-to-rise" or "perpendicular-to-rise" properties to be reversed or global for all drop orientations. For orientations other than axial (end drop) and radial (side drop), the CASKDROP program interpolates foam properties using an ellipse function. For the case where crush stress "parallel-to-rise" is in the axial direction, σ_{PAR}, and crush stress "perpendicular-to-rise" is in the radial direction, σ_{PER}, the interpolation equation at drop angle, θ, is:

$$\sigma_\theta = \sqrt{\frac{1}{\frac{\sin^2\theta}{\sigma_{PAR}^2} + \frac{\cos^2\theta}{\sigma_{PER}^2}}}$$

Similarly, for the case where crush stress "perpendicular-to-rise" is in the axial direction, σ_{PER}, and crush stress "parallel-to-rise" is in the radial direction, σ_{PAR}, the interpolation equation is:

$$\sigma_\theta = \sqrt{\frac{1}{\frac{\sin^2\theta}{\sigma_{PER}^2} + \frac{\cos^2\theta}{\sigma_{PAR}^2}}}$$

The Control Window allows the user to specify various analysis and output controls. The Control Window is separated into Analysis, Crush, Angle, Static, Dynamic, Print, and File.

Three Analysis options are available: "dXY" defines the number of integration elements in the crush plane, 25 for the example problem; "Sln" defines the analysis methodology ("Global" versus "Local Strain Theory"), "Global" for the example problem; "ε/σ" defines the strain (or crush stress) value to be utilized in unbacked regions (e.g., if a value is specified between 0 and 1, it is assumed a strain value and the corresponding crush stress at that strain is used; if a value is specified greater than 1, it is assumed to be a crush stress), 0.1 for the example problem corresponding to a crush stress at 10% strain from the polyurethane foam database.

The "Crush" options define the incremental deformations to be analyzed. The example problem specifies analyzing for crush deformations from 0.25 inches to 20 inches in 0.25-inch increments. Specifying a "Max" value greater than the actual maximum available crush depth (as determined geometrically) flags the CASKDROP program not to exceed the maximum available crush depth.

Similarly, the "Angle" options define the incremental angular orientations to be analyzed. The example problem specifies analyzing for drop angles from 0º to 90º in 15º increments.

The "Static" options allow the user to specify quasi-static analyses providing "Full" display output, "Smry" (summary) output, or "Both". The example problem specifies "Full" output to the display only. Similarly, the "Dynamic" options allow the user to specify dynamic analyses providing "Full" display output, "Smry" (summary) output, or "Both". The example problem does not specify a dynamic analysis as that module is not completed in the CASKDROP program.

The "Print" and "File" options allow the user to specify "Full" display output, "Smry" (summary) output, or "Both" to the printer or a file. The example problem specifies "Full" output to an output file only.

The Output Window provides the location for Static and Dynamic display output. A quasi-static solution is achieved when the strain energy of the crushable media (SE) is equal to the free-falling kinetic energy of the package (KE), or SE/KE = 1. Table 2.10.2-1 provides a sample file output at 0º (side drop), at 45º, and at 90º (end drop).

2.10.2.2 Description of the SLAPDOWN Computer Code

Impact limiter deflections and package accelerations are calculated using the Sandia National Laboratories developed computer code SLAPDOWN[3]. This program solves the rigid-body equations of motion for a transportation package, given parameters such as weight, rotational moment of inertia, geometric relationships, and impact limiter force-deflection curves. The output consists of maximum impact limiter deformations and a time history of the parameters of motion (of principal interest, the acceleration at the center of gravity and angular acceleration). From these outputs, accelerations at any point on the package are found. Figure 2.10.2-6 shows a sample of geometric parameters, and Table 2.10.2-2 lists the required input parameters for the sample geometry.

To bound the dynamic impact analyses, the lower values of package weight and mass moment of inertia are used conservatively with the upper bound force-deflection curves to calculate the maximum impact accelerations, the condition for which the impact velocity of the secondary impact is greatest. The higher values of package weight and mass moment of inertia are used with the lower bound force-deflection curves to calculate the maximum crush distances. The center of gravity (CG) is taken as the geometric center of the package. Friction is assigned a value of zero, since this maximizes the impact forces and deflections for the secondary (slapdown) impact limiter.

The original VMS-based SLAPDOWN FORTRAN computer code is now IBM-PC compatible through the use of a PC-based FORTRAN compiler. Using a test input file, the current PC version gives identical results to the original VMS version running at Sandia National Laboratories.

Table 2.10.2-2 shows a listing of sample input for the SLAPDOWN program. Table 2.10.2-3 shows a listing of sample force-deflection data for the SLAPDOWN program. Table 2.10.2-4 shows a sample output of the SLAPDOWN program from the general output file. This is performed for a 15º primary oblique orientation. Note that the angle of secondary contact with a the ground surface is displayed at the end of the output list ("Tail Impact Angle"). The angle is

nearly zero, which is true in almost all cases. Table 2.10.2-5 shows a portion of the corresponding time history output file, showing the results only through the end of the primary impact. The time variable is given in the first column. In the second, third and fourth columns are given the results at the package center of gravity (SLAPDOWN node 2): the vertical position is in the column headed POSY(2) (inches), the velocity is in the column headed VELY(2) (in/s), and the acceleration is in the column headed ACCY(2) (in/s^2). The last three columns give the rotational parameters of angular position: the angle THETA (radians, horizontal is zero), the angular velocity OMEGA (rad/s) and the angular acceleration ALPHA (rad/s^2). Table 2.10.2-5 is an excerpt from the time history output file, and shows the beginning (primary portion) of the impact.

As further confirmation of the SLAPDOWN code analysis methodology, the sample problem described above is compared to output from the public domain program SCANS[2]. The results compare well, as demonstrated in Table 2.10.2-6. Input data for the comparison is taken from Table 2.10.2-2. A 15º initial impact angle is used for direct comparison.

Table 2.10.2-1 – CASKDROP Sample Problem Output Files

Side Drop *** PACKAGING TECHNOLOGY *** CASKDROP, v2.21
05-16-1995, 15:38:39 Jul 01, 1994

SAMPLE PROBLEM FOR QUALITY ASSURANCE CHECK (AREAS AND VOLUMES)	
Impact Limiter Weight (each) - 1,000 lbs	Cask and Payload Weight - 10,000 lbs
Impact Limiter Outside Diameter - 60.0000 in	Cask Outside Diameter - 40.0000 in
Impact Limiter Overall Length - 24.0000 in	Cask Overall Length - 48.0000 in
Impact Limiter Conical Diameter - 48.0000 in	Dynamic Unloading Modulus - 1.000E+07 lbs/in
Impact Limiter Conical Length - 10.0000 in	Rad Mass Moment of Inertia - 12,235 lb-in-s^2
Impact Limiter End Thickness - 12.0000 in	Frictional Coefficient - 0.0000
Impact Limiter Hole Diameter - 20.0000 in	Drop Height - 30.0000 ft
Impact Limiter Hole Length - 8.0000 in	Drop Angle from Horizontal - 0.0000°
Unbacked Area Threshhold Strain - 0.1000 in/in	Crush Analysis Theory - Global
Unbacked Area Crush Stress - 2,675 psi	Number of Integration Incs - 25

POLYFOAM CRUSH STRESS (Axial: "∥" to rise)	
Density = 20.000 pcf	
Temp = -20.000 °F	
σ-yield = 2,552.3 psi	
Bias = 60.000%	
ε (in/in)	σ (psi)
0.000	0.0
0.100	2,552.3
0.200	2,687.0
0.300	2,868.8
0.400	3,302.9
0.500	4,115.1
0.600	6,074.3
0.650	7,942.0
0.700	10,925.0
0.750	15,001.8
0.800	26,829.5

POLYFOAM CRUSH STRESS (Radial: "⊥" to rise)	
Density = 20.000 pcf	
Temp = -20.000 °F	
σ-yield = 2,675.0 psi	
Bias = 60.000%	
ε (in/in)	σ (psi)
0.000	0.0
0.100	2,675.0
0.200	2,785.4
0.300	2,959.9
0.400	3,345.9
0.500	4,147.7
0.600	6,062.8
0.650	7,868.8
0.700	10,180.0
0.750	15,554.4
0.800	29,704.8

POLYFOAM CRUSH STRESS (Actual Data @ 0.0°)	
Density = 20.000 pcf	
Temp = -20.000 °F	
σ-yield = 2,675.0 psi	
Bias = 60.000%	
ε (in/in)	σ (psi)
0.000	0.0
0.100	2,675.0
0.200	2,785.4
0.300	2,959.9
0.400	3,345.9
0.500	4,147.7
0.600	6,062.8
0.650	7,868.8
0.700	10,180.0
0.750	15,554.4
0.800	29,704.8

DEFL (in)	MAX ε (%)	AREA (in^2)	VOLUME (in^3)	XBAR (in)	IMPACT FORCE (lbs)	ACCEL (g's)	I/L MOMENT (in-lbs)	STRAIN ENERGY (in-lbs)	KINETIC ENERGY (in-lbs)	SE/KE RATIO
0.250	2.50	221	37	0.00	106,881	8.9	0	13,360	4,323,000	0.00
0.500	5.00	318	105	0.00	289,508	24.1	0	62,909	4,326,000	0.01
0.750	7.50	396	194	0.00	518,875	43.2	0	163,957	4,329,000	0.04
1.000	10.00	465	302	0.00	733,200	61.1	0	320,466	4,332,000	0.07
1.250	12.49	528	425	0.00	955,009	79.6	0	531,492	4,335,000	0.12
1.500	14.99	587	565	0.00	1,107,366	92.3	0	789,289	4,338,000	0.18
1.750	17.49	644	719	0.00	1,270,225	105.9	0	1,086,488	4,341,000	0.25
2.000	19.99	699	886	0.00	1,371,441	114.3	0	1,416,697	4,344,000	0.33
2.250	22.49	752	1,068	0.00	1,509,207	125.8	0	1,776,778	4,347,000	0.41
2.500	24.99	804	1,262	0.00	1,668,937	139.1	0	2,174,046	4,350,000	0.50
2.750	27.49	855	1,469	0.00	1,761,221	146.8	0	2,602,815	4,353,000	0.60
3.000	29.99	906	1,690	0.00	1,946,101	162.2	0	3,066,230	4,356,000	0.70
3.250	32.49	955	1,921	0.00	2,044,813	170.4	0	3,565,095	4,359,000	0.82
3.500	34.98	1,005	2,167	0.00	2,249,052	187.4	0	4,101,828	4,362,000	0.94
3.614	36.13	1,027	2,285	0.00	2,326,676	193.9	0	4,363,372	4,363,372	1.00
3.750	37.48	1,053	2,424	0.00	2,419,003	201.6	0	4,956,582	4,365,000	1.14
4.000	39.98	1,101	2,692	0.00	2,640,297	220.0	0	5,588,994	4,368,000	1.28
4.250	42.48	1,149	2,975	0.00	2,759,520	230.0	0	6,263,971	4,371,000	1.43
4.500	44.98	1,197	3,267	0.00	2,956,003	246.3	0	6,978,412	4,374,000	1.60
4.750	47.48	1,244	3,571	0.00	3,208,534	267.4	0	7,748,979	4,377,000	1.77
5.000	49.98	1,292	3,889	0.00	3,357,376	279.8	0	8,569,718	4,380,000	1.96
5.250	52.48	1,339	4,219	0.00	3,603,141	300.3	0	9,439,782	4,383,000	2.15
5.500	54.97	1,385	4,556	0.00	3,906,997	325.6	0	10,378,550	4,386,000	2.37
5.750	57.47	1,432	4,909	0.00	4,215,273	351.3	0	11,393,833	4,389,000	2.60
6.000	59.97	1,479	5,275	0.00	4,573,066	381.1	0	12,492,376	4,392,000	2.84
6.250	62.47	1,520	5,650	0.00	4,961,100	413.4	0	13,684,147	4,395,000	3.11

Side Drop *** PACKAGING TECHNOLOGY *** CASKDROP, v2.21
05-16-1995, 15:38:39 (continued...) Jul 01, 1994

DEFL (in)	MAX ε (%)	AREA (in^2)	VOLUME (in^3)	XBAR (in)	IMPACT FORCE (lbs)	ACCEL (g's)	I/L MOMENT (in-lbs)	STRAIN ENERGY (in-lbs)	KINETIC ENERGY (in-lbs)	SE/KE RATIO
6.500	64.97	1,559	6,035	0.00	5,404,072	450.3	0	14,979,793	4,398,000	3.41
6.750	67.47	1,597	6,430	0.00	5,893,283	491.1	0	16,391,963	4,401,000	3.72
7.000	69.97	1,632	6,834	0.00	6,440,254	536.7	0	17,933,655	4,404,000	4.07
7.250	72.47	1,666	7,246	0.00	7,087,717	590.6	0	19,624,651	4,407,000	4.45
7.500	74.96	1,698	7,667	0.00	8,001,352	666.8	0	21,510,785	4,410,000	4.88
7.750	77.46	1,730	8,095	0.00	9,446,226	787.2	0	23,691,732	4,413,000	5.37
8.000	79.96	1,760	8,532	0.00	11,484,412	957.0	0	26,308,062	4,416,000	5.96
8.250	82.46	1,790	8,976	0.00	13,964,555	1,163.7	0	29,489,183	4,419,000	6.67
8.500	84.96	1,818	9,427	0.00	16,801,077	1,400.1	0	33,334,887	4,422,000	7.54
8.750	87.46	1,846	9,885	0.00	19,931,256	1,660.9	0	37,926,428	4,425,000	8.57
9.000	89.96	1,873	10,350	0.00	23,276,639	1,939.7	0	43,327,415	4,428,000	9.78
9.250	92.45	1,899	10,822	0.00	26,896,391	2,241.4	0	49,599,044	4,431,000	11.19
9.500	94.95	1,925	11,300	0.00	30,724,250	2,560.4	0	56,801,624	4,434,000	12.81
9.750	97.45	1,950	11,784	0.00	34,740,688	2,895.1	0	64,984,741	4,437,000	14.65
10.000	99.95	1,974	12,275	0.00	38,887,797	3,240.6	0	74,188,302	4,440,000	16.71

Corner Drop *** PACKAGING TECHNOLOGY *** CASKDROP, v2.21
05-16-1995, 15:38:39 Jul 01, 1994

SAMPLE PROBLEM FOR QUALITY ASSURANCE CHECK (AREAS AND VOLUMES)			
Impact Limiter Weight (each) -	1,000 lbs	Cask and Payload Weight -	10,000 lbs
Impact Limiter Outside Diameter -	60.0000 in	Cask Outside Diameter -	40.0000 in
Impact Limiter Overall Length -	24.0000 in	Cask Overall Length -	48.0000 in
Impact Limiter Conical Diameter -	48.0000 in	Dynamic Unloading Modulus -	1.000E+07 lbs/in
Impact Limiter Conical Length -	10.0000 in	Rad Mass Moment of Inertia -	12,235 lb-in-s²
Impact Limiter End Thickness -	12.0000 in	Frictional Coefficient -	0.0000
Impact Limiter Hole Diameter -	20.0000 in	Drop Height -	30.0000 ft
Impact Limiter Hole Length -	8.0000 in	Drop Angle from Horizontal -	45.0000°
Unbacked Area Threshhold Strain -	0.1000 in/in	Crush Analysis Theory -	Global
Unbacked Area Crush Stress -	2,611 psi	Number of Integration Incs -	25

POLYFOAM CRUSH STRESS (Axial: "‖" to rise)

Density = 20.000 pcf
Temp = -20.000 °F
σ-yield = 2,552.3 psi
Bias = 60.000%

ε (in/in)	σ (psi)
0.000	0.0
0.100	2,552.3
0.200	2,687.0
0.300	2,868.8
0.400	3,302.9
0.500	4,115.1
0.600	6,074.3
0.650	7,942.0
0.700	10,925.0
0.750	15,001.8
0.800	26,829.5

POLYFOAM CRUSH STRESS (Radial: "⊥" to rise)

Density = 20.000 pcf
Temp = -20.000 °F
σ-yield = 2,675.0 psi
Bias = 60.000%

ε (in/in)	σ (psi)
0.000	0.0
0.100	2,675.0
0.200	2,785.4
0.300	2,959.9
0.400	3,345.9
0.500	4,147.7
0.600	6,062.8
0.650	7,868.8
0.700	10,180.0
0.750	15,554.4
0.800	29,704.8

POLYFOAM CRUSH STRESS (Actual Data @ 45.0°)

Density = 20.000 pcf
Temp = -20.000 °F
σ-yield = 2,611.5 psi
Bias = 60.000%

ε (in/in)	σ (psi)
0.000	0.0
0.100	2,611.5
0.200	2,734.9
0.300	2,913.3
0.400	3,324.2
0.500	4,131.3
0.600	6,068.5
0.650	7,905.2
0.700	10,532.8
0.750	15,270.6
0.800	28,157.6

DEFL (in)	MAX ε (%)	AREA (in²)	VOLUME (in³)	XBAR (in)	IMPACT FORCE (lbs)	ACCEL (g's)	I/L MOMENT (in-lbs)	STRAIN ENERGY (in-lbs)	KINETIC ENERGY (in-lbs)	SE/KE RATIO
0.250	1.44	7	1	-8.30	1,351	0.1	0	169	4,323,000	0.00
0.500	2.88	20	4	-8.11	7,756	0.6	0	1,307	4,326,000	0.00
0.750	4.33	36	11	-7.90	21,631	1.8	0	4,981	4,329,000	0.00
1.000	5.79	55	22	-7.68	44,807	3.7	0	13,286	4,332,000	0.00
1.250	7.25	78	39	-7.44	78,737	6.6	0	28,729	4,335,000	0.01
1.500	8.71	102	61	-7.19	124,483	10.4	0	54,131	4,338,000	0.01
1.750	10.18	129	90	-6.92	182,320	15.2	0	92,481	4,341,000	0.02
2.000	11.66	158	126	-6.65	250,919	20.9	0	146,636	4,344,000	0.03
2.250	13.14	189	169	-6.39	327,791	27.3	0	218,975	4,347,000	0.05
2.500	14.63	222	221	-6.15	409,985	34.2	0	311,197	4,350,000	0.07
2.750	16.12	256	280	-5.92	495,229	41.3	0	424,349	4,353,000	0.10
3.000	17.64	290	349	-5.70	581,988	48.5	0	559,001	4,356,000	0.13
3.250	19.14	321	425	-5.53	666,955	55.6	0	715,119	4,359,000	0.16
3.500	21.04	350	509	-5.39	750,161	62.5	0	892,258	4,362,000	0.20
3.750	23.53	379	600	-5.30	832,241	69.4	0	1,090,058	4,365,000	0.25
4.000	26.04	407	698	-5.24	913,114	76.1	0	1,308,228	4,368,000	0.30
4.250	28.58	435	804	-5.21	993,967	82.8	0	1,546,613	4,371,000	0.35
4.500	31.14	462	916	-5.20	1,075,026	89.6	0	1,805,237	4,374,000	0.41
4.750	33.55	490	1,035	-5.22	1,157,389	96.4	0	2,084,289	4,377,000	0.48
5.000	35.86	517	1,161	-5.24	1,240,678	103.4	0	2,384,048	4,380,000	0.54
5.250	38.16	545	1,293	-5.27	1,325,202	110.4	0	2,704,783	4,383,000	0.62
5.500	40.44	573	1,433	-5.30	1,413,119	117.8	0	3,047,073	4,386,000	0.69
5.750	42.71	600	1,579	-5.33	1,503,231	125.3	0	3,411,616	4,389,000	0.78
6.000	44.96	628	1,733	-5.37	1,596,230	133.0	0	3,799,049	4,392,000	0.86
6.250	47.21	656	1,894	-5.40	1,692,397	141.0	0	4,210,127	4,395,000	0.96
6.359	48.17	668	1,966	-5.41	1,735,814	144.7	0	4,396,303	4,396,303	1.00
6.500	49.43	684	2,061	-5.42	1,792,981	149.4	0	4,837,403	4,398,000	1.10
6.750	51.75	711	2,236	-5.44	1,897,584	158.1	0	5,298,723	4,401,000	1.20
7.000	54.19	739	2,417	-5.46	2,009,560	167.5	0	5,787,116	4,404,000	1.31
7.250	56.65	767	2,605	-5.47	2,128,316	177.4	0	6,304,351	4,407,000	1.43

Corner Drop
05-16-1995, 15:38:39

*** PACKAGING TECHNOLOGY ***
(continued...)

CASKDROP, v2.21
Jul 01, 1994

DEFL (in)	MAX ε (%)	AREA (in^2)	VOLUME (in^3)	XBAR (in)	IMPACT FORCE (lbs)	ACCEL (g's)	I/L MOMENT (in-lbs)	STRAIN ENERGY (in-lbs)	KINETIC ENERGY (in-lbs)	SE/KE RATIO
7.500	59.12	795	2,800	-5.48	2,255,709	188.0	0	6,852,354	4,410,000	1.55
7.750	61.60	824	3,002	-5.48	2,392,365	199.4	0	7,433,363	4,413,000	1.68
8.000	64.10	852	3,212	-5.47	2,538,941	211.6	0	8,049,776	4,416,000	1.82
8.250	66.60	881	3,429	-5.47	2,701,943	225.2	0	8,704,887	4,419,000	1.97
8.500	69.12	909	3,652	-5.45	2,882,629	240.2	0	9,402,959	4,422,000	2.13
8.750	71.65	938	3,883	-5.43	3,079,002	256.6	0	10,148,162	4,425,000	2.29
9.000	74.19	967	4,121	-5.38	3,300,885	275.1	0	10,945,648	4,428,000	2.47
9.250	76.75	995	4,367	-5.32	3,573,055	297.8	0	11,804,891	4,431,000	2.66
9.500	79.31	1,024	4,619	-5.26	3,901,592	325.1	0	12,739,222	4,434,000	2.87
9.750	81.89	1,053	4,879	-5.17	4,292,510	357.7	0	13,763,484	4,437,000	3.10
10.000	84.49	1,082	5,146	-5.06	4,763,070	396.9	0	14,895,432	4,440,000	3.35
10.250	87.09	1,109	5,419	-4.95	5,316,128	443.0	0	16,155,332	4,443,000	3.64
10.500	89.71	1,134	5,698	-4.83	5,947,562	495.6	0	17,563,293	4,446,000	3.95
10.750	92.34	1,161	5,985	-4.74	6,665,548	555.5	0	19,139,932	4,449,000	4.30
11.000	94.98	1,184	6,270	-4.63	7,465,195	622.1	0	20,906,275	4,452,000	4.70
11.250	97.64	1,206	6,563	-4.54	8,360,345	696.7	0	22,884,467	4,455,000	5.14

End Drop *** PACKAGING TECHNOLOGY *** CASKDROP, v2.21
05-16-1995, 15:38:39 Jul 01, 1994

SAMPLE PROBLEM FOR QUALITY ASSURANCE CHECK (AREAS AND VOLUMES)			
Impact Limiter Weight (each) -	1,000 lbs	Cask and Payload Weight -	10,000 lbs
Impact Limiter Outside Diameter -	60.0000 in	Cask Outside Diameter -	40.0000 in
Impact Limiter Overall Length -	24.0000 in	Cask Overall Length -	48.0000 in
Impact Limiter Conical Diameter -	48.0000 in	Dynamic Unloading Modulus -	1.000E+07 lbs/in
Impact Limiter Conical Length -	10.0000 in	Rad Mass Moment of Inertia -	12,235 lb-in-s²
Impact Limiter End Thickness -	12.0000 in	Frictional Coefficient -	0.0000
Impact Limiter Hole Diameter -	20.0000 in	Drop Height -	30.0000 ft
Impact Limiter Hole Length -	8.0000 in	Drop Angle from Horizontal -	90.0000°
Unbacked Area Threshhold Strain -	0.1000 in/in	Crush Analysis Theory -	Global
Unbacked Area Crush Stress -	2,552 psi	Number of Integration Incs -	25

POLYFOAM CRUSH STRESS (Axial: "‖" to rise)

Density = 20.000 pcf
Temp = -20.000 °F
σ-yield = 2,552.3 psi
Bias = 60.000%

ε (in/in)	σ (psi)
0.000	0.0
0.100	2,552.3
0.200	2,687.0
0.300	2,868.8
0.400	3,302.9
0.500	4,115.1
0.600	6,074.3
0.650	7,942.0
0.700	10,925.0
0.750	15,001.8
0.800	26,829.5

POLYFOAM CRUSH STRESS (Radial: "⊥" to rise)

Density = 20.000 pcf
Temp = -20.000 °F
σ-yield = 2,675.0 psi
Bias = 60.000%

ε (in/in)	σ (psi)
0.000	0.0
0.100	2,675.0
0.200	2,785.4
0.300	2,959.9
0.400	3,345.9
0.500	4,147.7
0.600	6,062.8
0.650	7,868.8
0.700	10,180.0
0.750	15,554.4
0.800	29,704.8

POLYFOAM CRUSH STRESS (Actual Data @ 90.0°)

Density = 20.000 pcf
Temp = -20.000 °F
σ-yield = 2,552.3 psi
Bias = 60.000%

ε (in/in)	σ (psi)
0.000	0.0
0.100	2,552.3
0.200	2,687.0
0.300	2,868.8
0.400	3,302.9
0.500	4,115.1
0.600	6,074.3
0.650	7,942.0
0.700	10,925.0
0.750	15,001.8
0.800	26,829.5

DEFL (in)	MAX ε (%)	AREA (in²)	VOLUME (in³)	XBAR (in)	IMPACT FORCE (lbs)	ACCEL (g's)	I/L MOMENT (in-lbs)	STRAIN ENERGY (in-lbs)	KINETIC ENERGY (in-lbs)	SE/KE RATIO
0.250	2.08	1,518	377	0.00	810,360	67.5	0	101,295	4,323,000	0.02
0.500	4.17	1,541	759	0.00	1,592,808	132.7	0	401,691	4,326,000	0.09
0.750	6.25	1,564	1,147	0.00	2,311,804	192.7	0	889,768	4,329,000	0.21
1.000	8.33	1,587	1,541	0.00	2,931,701	244.3	0	1,545,206	4,332,000	0.36
1.250	10.42	1,610	1,941	0.00	3,416,844	284.7	0	2,338,774	4,335,000	0.54
1.500	12.50	1,634	2,346	0.00	3,752,646	312.7	0	3,234,960	4,338,000	0.75
1.750	14.58	1,657	2,758	0.00	3,971,661	331.0	0	4,200,498	4,341,000	0.97
1.785	14.88	1,661	2,816	0.00	3,995,461	333.0	0	4,341,425	4,341,425	1.00
2.000	16.67	1,681	3,175	0.00	4,112,712	342.7	0	5,354,946	4,344,000	1.23
2.250	18.75	1,705	3,598	0.00	4,214,497	351.2	0	6,395,847	4,347,000	1.47
2.500	20.83	1,729	4,027	0.00	4,287,704	357.3	0	7,458,622	4,350,000	1.71
2.750	22.92	1,753	4,462	0.00	4,351,294	362.6	0	8,538,497	4,353,000	1.96
3.000	25.00	1,777	4,904	0.00	4,445,683	370.5	0	9,638,119	4,356,000	2.21
3.250	27.08	1,801	5,351	0.00	4,562,636	380.2	0	10,764,159	4,359,000	2.47
3.500	29.17	1,826	5,804	0.00	4,693,990	391.2	0	11,921,237	4,362,000	2.73
3.750	31.25	1,851	6,264	0.00	4,831,784	402.6	0	13,111,959	4,365,000	3.00
4.000	33.33	1,875	6,730	0.00	4,973,522	414.5	0	14,337,622	4,368,000	3.28
4.250	35.42	1,900	7,202	0.00	5,120,673	426.7	0	15,599,396	4,371,000	3.57
4.500	37.50	1,925	7,680	0.00	5,274,868	439.6	0	16,898,839	4,374,000	3.86
4.750	39.58	1,951	8,164	0.00	5,437,800	453.2	0	18,237,922	4,377,000	4.17
5.000	41.67	1,976	8,655	0.00	5,611,685	467.6	0	19,619,108	4,380,000	4.48
5.250	43.75	2,002	9,152	0.00	5,802,397	483.5	0	21,045,868	4,383,000	4.80
5.500	45.83	2,027	9,656	0.00	6,018,789	501.6	0	22,523,516	4,386,000	5.14
5.750	47.92	2,053	10,166	0.00	6,268,472	522.4	0	24,059,424	4,389,000	5.48
6.000	50.00	2,079	10,682	0.00	6,560,063	546.7	0	25,662,991	4,392,000	5.84
6.250	52.08	2,105	11,205	0.00	6,900,740	575.1	0	27,345,591	4,395,000	6.22
6.500	54.17	2,131	11,735	0.00	7,296,837	608.1	0	29,120,288	4,398,000	6.62
6.750	56.25	2,158	12,271	0.00	7,751,903	646.0	0	31,001,381	4,401,000	7.04
7.000	58.33	2,184	12,814	0.00	8,272,373	689.4	0	33,004,415	4,404,000	7.49
7.250	60.42	2,211	13,363	0.00	8,862,880	738.6	0	35,146,322	4,407,000	7.98

End Drop *** PACKAGING TECHNOLOGY *** CASKDROP, v2.21
05-16-1995, 15:38:39 (continued...) Jul 01, 1994

DEFL (in)	MAX ε (%)	AREA (in^2)	VOLUME (in^3)	XBAR (in)	IMPACT FORCE (lbs)	ACCEL (g's)	I/L MOMENT (in-lbs)	STRAIN ENERGY (in-lbs)	KINETIC ENERGY (in-lbs)	SE/KE RATIO
7.500	62.50	2,238	13,919	0.00	9,556,877	796.4	0	37,448,792	4,410,000	8.49
7.750	64.58	2,265	14,482	0.00	10,454,871	871.2	0	39,950,260	4,413,000	9.05
8.000	66.67	2,606	15,051	0.00	11,632,851	969.4	0	42,711,226	4,416,000	9.67
8.250	68.75	2,633	15,706	0.00	13,506,993	1,125.6	0	45,853,706	4,419,000	10.38
8.500	70.83	2,660	16,368	0.00	14,954,954	1,246.2	0	49,411,449	4,422,000	11.17
8.750	72.92	2,688	17,037	0.00	16,218,008	1,351.5	0	53,308,070	4,425,000	12.05
9.000	75.00	2,715	17,712	0.00	18,519,890	1,543.3	0	57,650,307	4,428,000	13.02
9.250	77.08	2,743	18,394	0.00	22,571,268	1,880.9	0	62,786,702	4,431,000	14.17
9.500	79.17	2,771	19,084	0.00	27,794,818	2,316.2	0	69,082,462	4,434,000	15.58
9.750	81.25	2,799	19,780	0.00	33,405,583	2,783.8	0	76,732,513	4,437,000	17.29
10.000	83.33	2,827	20,483	0.00	39,286,171	3,273.8	0	85,818,982	4,440,000	19.33
10.250	85.42	2,827	21,190	0.00	45,050,964	3,754.2	0	96,361,124	4,443,000	21.69
10.500	87.50	2,827	21,897	0.00	51,018,884	4,251.6	0	108,369,855	4,446,000	24.37
10.750	89.58	2,827	22,604	0.00	57,507,705	4,792.3	0	121,935,678	4,449,000	27.41
11.000	91.67	2,827	23,311	0.00	64,451,479	5,371.0	0	137,180,576	4,452,000	30.81
11.250	93.75	2,827	24,017	0.00	74,690,773	6,224.2	0	154,573,358	4,455,000	34.70
11.500	95.83	2,827	24,724	0.00	85,563,336	7,130.3	0	174,605,121	4,458,000	39.17
11.750	97.92	2,827	25,431	0.00	96,435,898	8,036.3	0	197,355,026	4,461,000	44.24
12.000	100.00	2,827	26,138	0.00	107,308,461	8,942.4	0	222,823,071	4,464,000	49.92

Table 2.10.2-2 – Sample Inputs to the SLAPDOWN Program

Parameter	Description	Sample Value
Z1, Z2	Length from primary end to CG, and from CG to secondary end, respectively①	90.38 inches (both sides)
R1, R2	Length from package axis to impact limiter contact point, primary and secondary ends, respectively	63.0 inches (both ends)
$\mu 1, \mu 2$	Coefficient of friction, primary and secondary ends, respectively	0.0 (both ends)
M	Overall package mass	611.0 lb-s^2/in
I_{cg}	Radial mass moment of inertia about the package CG	$3.1(10)^6$ in-lb-s^2
v_o	Impact velocity	-527.5 in/s (30-ft drop)
Θ	Angle with respect to horizontal of primary impact	0º, 15º, etc, as required
K	Elastic rebound stiffness of the impact limiter material	10^7 lb/in

Notes:

① This dimension is measured from the package CG to the center of the cylindrical portion of the impact limiter, which is the location of the line of action of side drop impact force.

Table 2.10.2-3 – Sample Force-Deflection to the SLAPDOWN Program

Primary Impact Limiter		Secondary Impact Limiter	
Deflection (in)	**Force (lb)**	**Deflection (in)**	**Force (lb)**
0	0	0	0
1	207,100	1	2,383,000
2	583,900	2	3,363,000
3	1,069,000	3	3,963,000
4	1,640,000	4	4,450,000
5	2,285,000	5	4,885,000
6	2,998,000	6	5,289,000
7	3,767,000	7	5,671,000
8	4,444,000	8	6,041,000
9	5,146,000	9	6,310,000
10	5,756,000	10	6,513,000
11	6,304,000	11	6,721,000
12	6,818,000	12	6,936,000
13	7,223,000	13	7,157,000
14	7,573,000	14	7,384,000
15	7,926,000	15	7,614,000

Table 2.10.2-4 – Sample of SLAPDOWN General Output

```
SAMPLE PACKAGE, 15 DEGREE OBLIQUE

 ****** SEQUENCE OF EVENTS ******

 ** NOSE HIT     AT TIME  0.000E+00, VELOCITY = -5.275E+02, RATIO =  1.00
 ** NOSE REBOUND AT TIME  3.311E-02, VELOCITY =  1.507E+01, RATIO =  -.03
 ** NOSE UNLOAD  AT TIME  4.008E-02, VELOCITY =  1.346E+02, RATIO =  -.26
 ** TAIL HIT     AT TIME  7.318E-02, VELOCITY = -7.061E+02, RATIO =  1.34
 ** TAIL REBOUND AT TIME  1.037E-01, VELOCITY =  2.410E+01, RATIO =  -.05
 ** TAIL UNLOAD  AT TIME  1.106E-01, VELOCITY =  1.422E+02, RATIO =  -.27


 ****** RESULTS ******

 Event over at time    1.115E-01, Time step size  8.712E-04
 Time step multiplier  1.000E-01,  129 Plot times written to database


            DISPLACEMENT     VELOCITY     ACCELERATION

   NOSE      1.159E+01      1.346E+02      2.732E+04 (MAX)
                           -5.275E+02     -7.297E+03 (MIN)

   TAIL      1.206E+01      1.422E+02      2.927E+04 (MAX)
                           -7.061E+02     -6.478E+03 (MIN)

     CG                    2.781E+01      1.099E+04 (MAX)
                           -5.277E+02     -3.860E+02 (MIN)

 ANGULAR                   1.266E+00      2.025E+02 (MAX)
                           -4.623E+00     -1.880E+02 (MIN)

 MAXIMUM ENERGIES:  3.488E+07 (NOSE),  5.947E+07 (TAIL)
  IMPACT AT 80 IN FROM C.G. =       65.677830  (NOSE)
  IMPACT AT 80 IN FROM C.G. =       70.322280  (TAIL)
  TAIL IMPACT ANGLE =        1.906593 DEG.
```

Table 2.10.2-5 – Sample of SLAPDOWN Time History Output

```
TITLE:  SAMPLE PACKAGE, 15 DEGREE OBLIQUE
02/20/1996     13:17:05
TIME,S     POSY(2)      VELY(2)      ACCY(2)       THETA        OMEGA        ALPHA
.0000,    .864E+02,   -.527E+03,   -.386E+03,    .262E+00,    .000E+00,    .000E+00,
.0009,    .859E+02,   -.528E+03,   -.230E+03,    .262E+00,   -.234E-02,   -.268E+01,
.0017,    .855E+02,   -.528E+03,   -.744E+02,    .262E+00,   -.701E-02,   -.536E+01,
.0026,    .850E+02,   -.528E+03,    .186E+03,    .262E+00,   -.156E-01,   -.985E+01,
.0035,    .846E+02,   -.527E+03,    .469E+03,    .262E+00,   -.284E-01,   -.147E+02,
.0044,    .841E+02,   -.526E+03,    .803E+03,    .262E+00,   -.462E-01,   -.205E+02,
.0052,    .836E+02,   -.525E+03,    .116E+04,    .262E+00,   -.695E-01,   -.267E+02,
.0061,    .832E+02,   -.524E+03,    .155E+04,    .262E+00,   -.985E-01,   -.333E+02,
.0070,    .827E+02,   -.522E+03,    .197E+04,    .262E+00,   -.134E+00,   -.406E+02,
.0078,    .823E+02,   -.520E+03,    .240E+04,    .261E+00,   -.176E+00,   -.479E+02,
.0087,    .818E+02,   -.518E+03,    .286E+04,    .261E+00,   -.224E+00,   -.559E+02,
.0096,    .814E+02,   -.515E+03,    .332E+04,    .261E+00,   -.280E+00,   -.638E+02,
.0105,    .809E+02,   -.512E+03,    .382E+04,    .261E+00,   -.343E+00,   -.723E+02,
.0113,    .805E+02,   -.508E+03,    .431E+04,    .261E+00,   -.413E+00,   -.808E+02,
.0122,    .800E+02,   -.504E+03,    .481E+04,    .260E+00,   -.491E+00,   -.894E+02,
.0131,    .796E+02,   -.499E+03,    .531E+04,    .260E+00,   -.577E+00,   -.981E+02,
.0139,    .792E+02,   -.494E+03,    .580E+04,    .259E+00,   -.669E+00,   -.107E+03,
.0148,    .787E+02,   -.489E+03,    .622E+04,    .259E+00,   -.769E+00,   -.114E+03,
.0157,    .783E+02,   -.483E+03,    .663E+04,    .258E+00,   -.874E+00,   -.121E+03,
.0166,    .779E+02,   -.477E+03,    .703E+04,    .257E+00,   -.985E+00,   -.128E+03,
.0174,    .775E+02,   -.470E+03,    .742E+04,    .256E+00,   -.110E+01,   -.134E+03,
.0183,    .771E+02,   -.463E+03,    .779E+04,    .255E+00,   -.122E+01,   -.141E+03,
.0192,    .766E+02,   -.456E+03,    .813E+04,    .254E+00,   -.135E+01,   -.147E+03,
.0200,    .762E+02,   -.449E+03,    .843E+04,    .253E+00,   -.149E+01,   -.152E+03,
.0209,    .759E+02,   -.441E+03,    .870E+04,    .252E+00,   -.162E+01,   -.157E+03,
.0218,    .755E+02,   -.434E+03,    .896E+04,    .250E+00,   -.176E+01,   -.161E+03,
.0227,    .751E+02,   -.426E+03,    .919E+04,    .249E+00,   -.191E+01,   -.165E+03,
.0235,    .747E+02,   -.417E+03,    .939E+04,    .247E+00,   -.205E+01,   -.169E+03,
.0244,    .744E+02,   -.409E+03,    .958E+04,    .245E+00,   -.220E+01,   -.172E+03,
.0253,    .740E+02,   -.401E+03,    .975E+04,    .244E+00,   -.236E+01,   -.175E+03,
.0261,    .737E+02,   -.392E+03,    .990E+04,    .242E+00,   -.251E+01,   -.178E+03,
.0270,    .733E+02,   -.383E+03,    .100E+05,    .239E+00,   -.267E+01,   -.180E+03,
.0279,    .730E+02,   -.374E+03,    .101E+05,    .237E+00,   -.283E+01,   -.182E+03,
.0287,    .727E+02,   -.365E+03,    .102E+05,    .235E+00,   -.299E+01,   -.184E+03,
.0296,    .723E+02,   -.356E+03,    .103E+05,    .232E+00,   -.315E+01,   -.185E+03,
.0305,    .720E+02,   -.347E+03,    .104E+05,    .229E+00,   -.331E+01,   -.186E+03,
.0314,    .717E+02,   -.338E+03,    .104E+05,    .226E+00,   -.347E+01,   -.187E+03,
.0322,    .714E+02,   -.329E+03,    .104E+05,    .223E+00,   -.364E+01,   -.188E+03,
.0331,    .711E+02,   -.320E+03,    .104E+05,    .220E+00,   -.380E+01,   -.188E+03,
.0340,    .709E+02,   -.311E+03,    .104E+05,    .217E+00,   -.397E+01,   -.188E+03,
.0348,    .706E+02,   -.303E+03,    .966E+04,    .213E+00,   -.412E+01,   -.175E+03,
.0357,    .703E+02,   -.295E+03,    .879E+04,    .210E+00,   -.426E+01,   -.160E+03,
.0366,    .701E+02,   -.288E+03,    .763E+04,    .206E+00,   -.438E+01,   -.140E+03,
.0375,    .698E+02,   -.283E+03,    .621E+04,    .202E+00,   -.448E+01,   -.115E+03,
.0383,    .696E+02,   -.279E+03,    .459E+04,    .198E+00,   -.455E+01,   -.870E+02,
.0392,    .693E+02,   -.277E+03,    .281E+04,    .194E+00,   -.460E+01,   -.559E+02,
.0401,    .691E+02,   -.276E+03,    .935E+03,    .190E+00,   -.462E+01,   -.231E+02,
.0409,    .688E+02,   -.276E+03,   -.386E+03,    .186E+00,   -.462E+01,    .000E+00,
```

Table 2.10.2-6 – Comparison of SLAPDOWN and SCANS Results

Parameter	SLAPDOWN Result	SCANS Result
Primary Impact Limiter Deflection, inches	11.6	11.6
Secondary Impact Limiter Deflection, inches	12.1	12.1
Primary Vertical Acceleration (CG), in/s^2	26.9	26.8
Secondary Vertical Acceleration (CG), in/s^2	28.5	28.5
Primary Angular Acceleration, $radians/s^2$	-188	-186
Secondary Angular Acceleration, $radians/s^2$	202	218

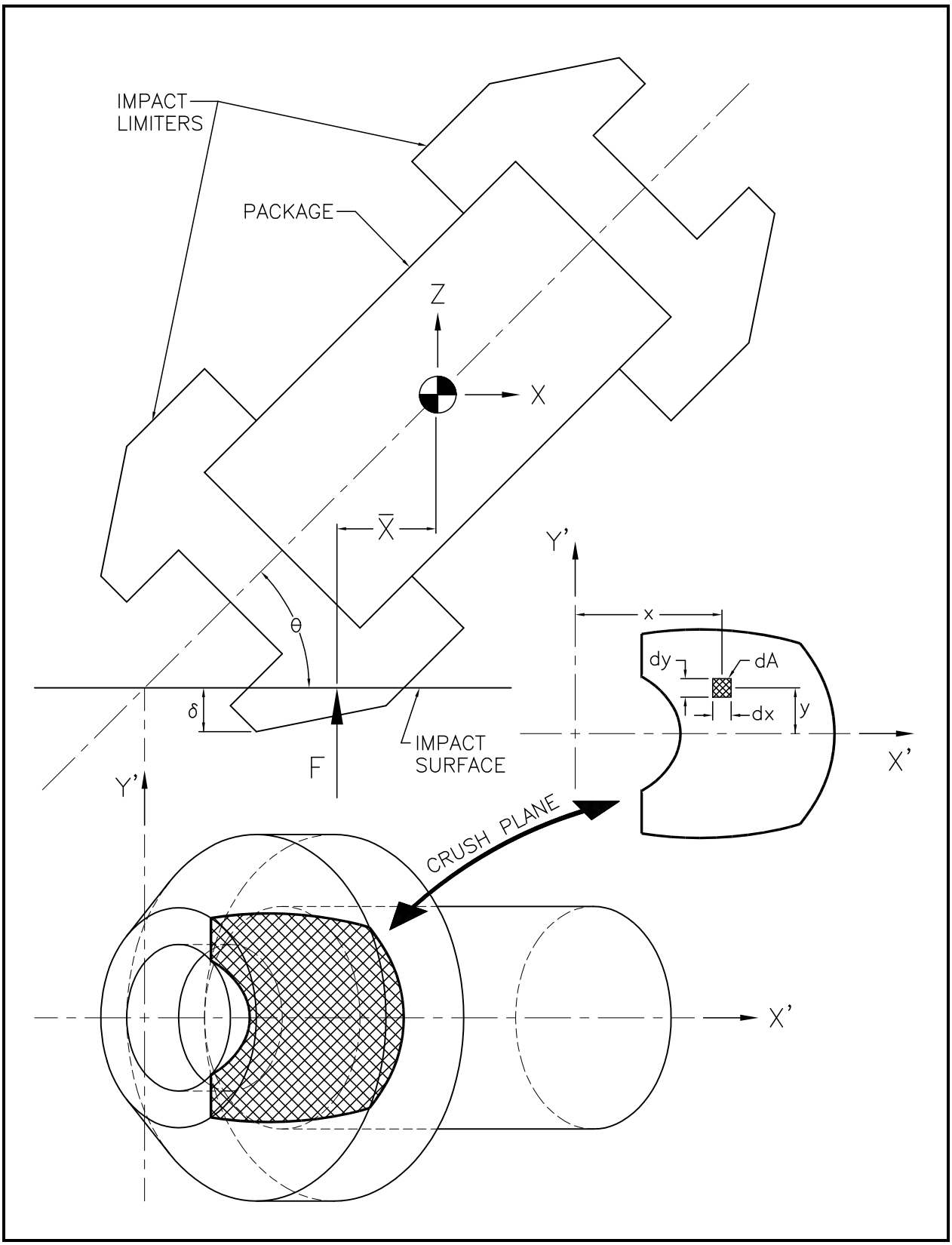

Figure 2.10.2-1 – Impact Limiter Force and Centroid Development

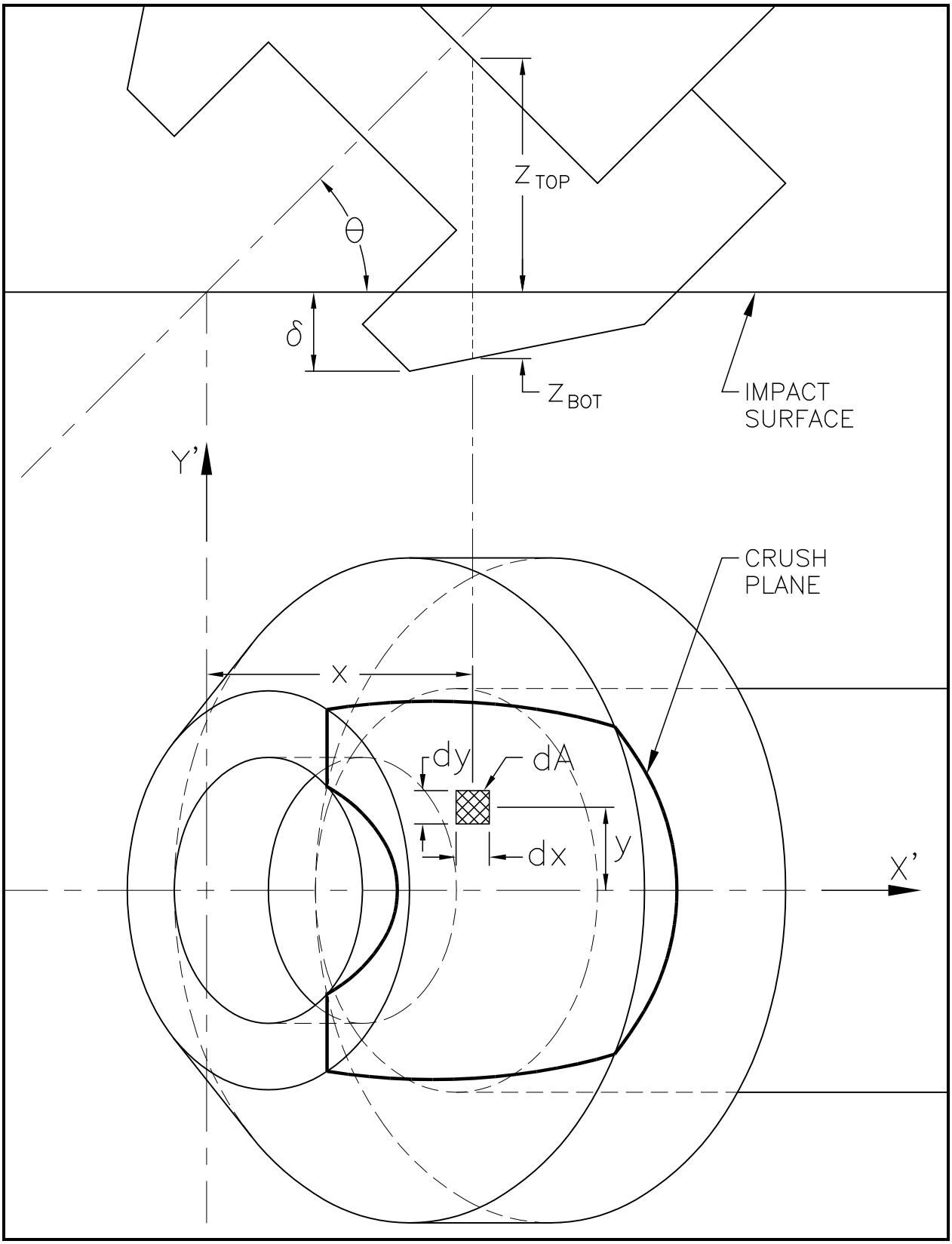

Figure 2.10.2-2 – Strain Determination

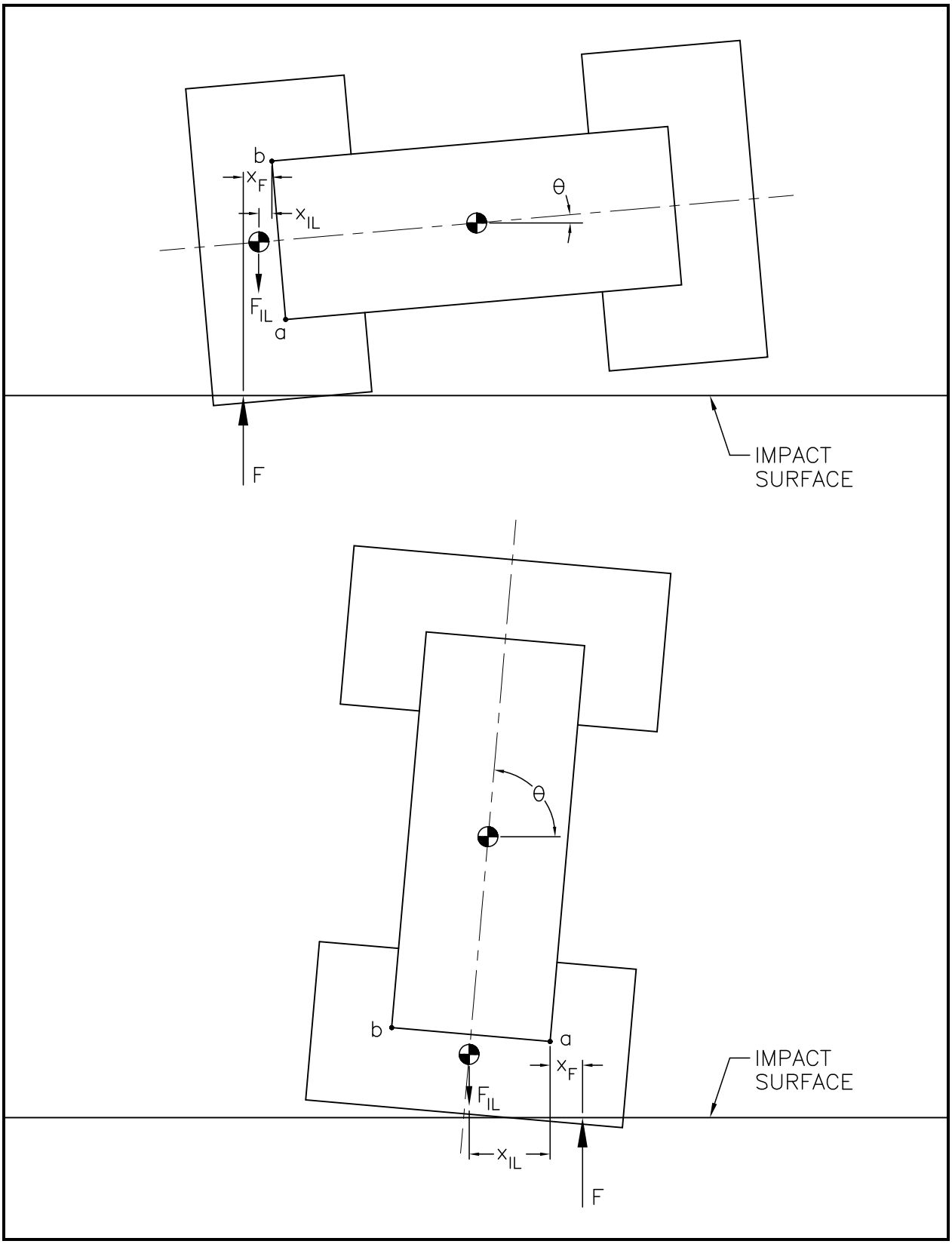

Figure 2.10.2-3 – Determination of Impact Limiter Separation Moments

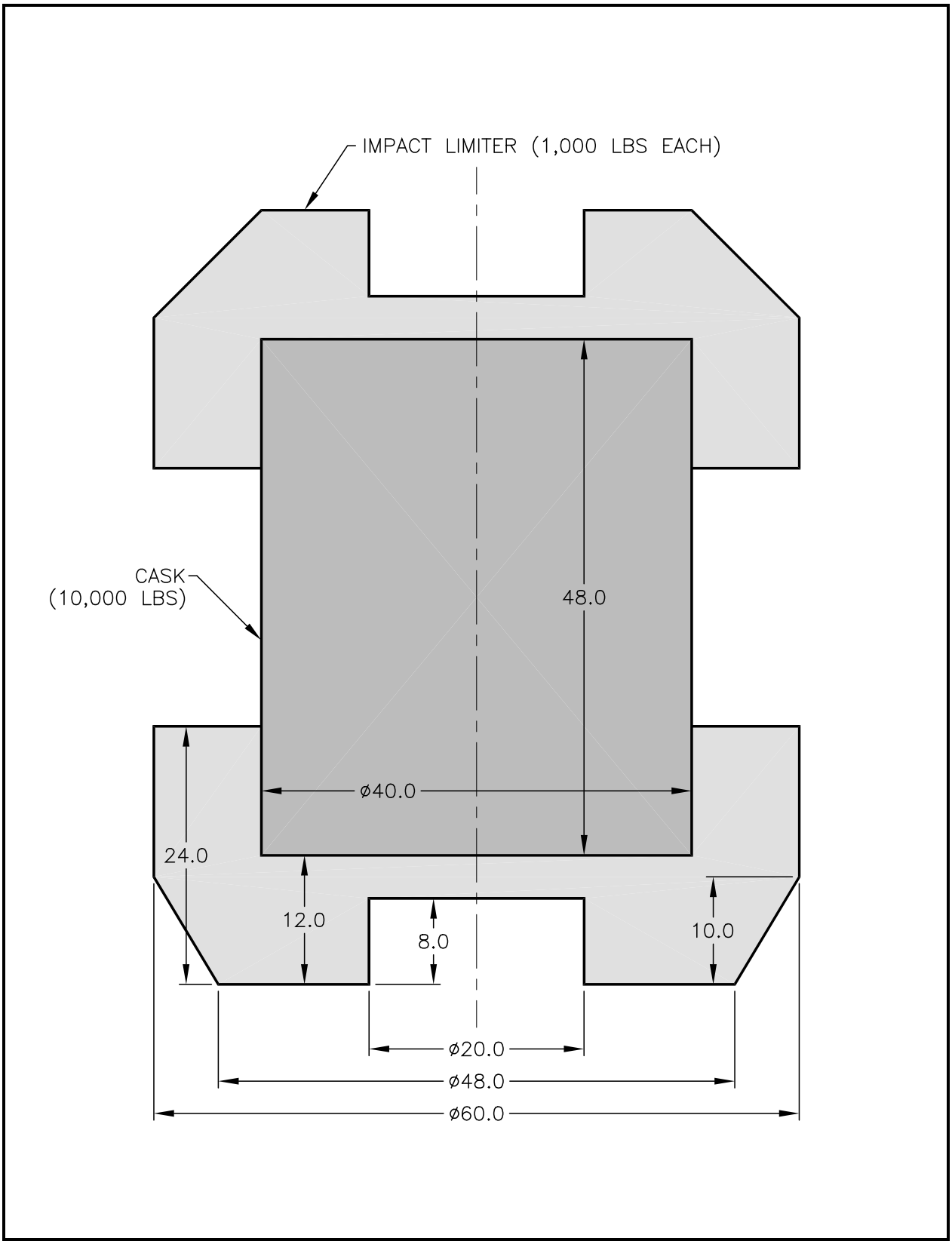

Figure 2.10.2-4 – Example Problem

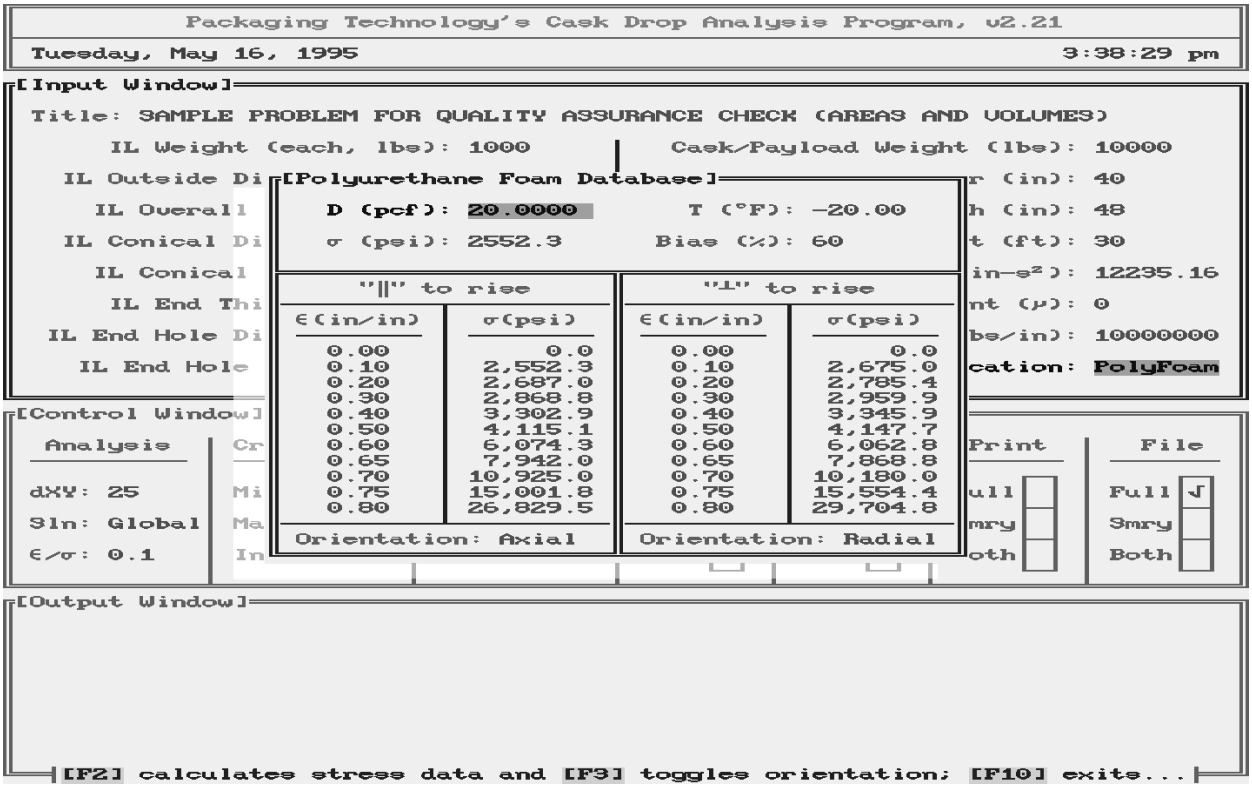

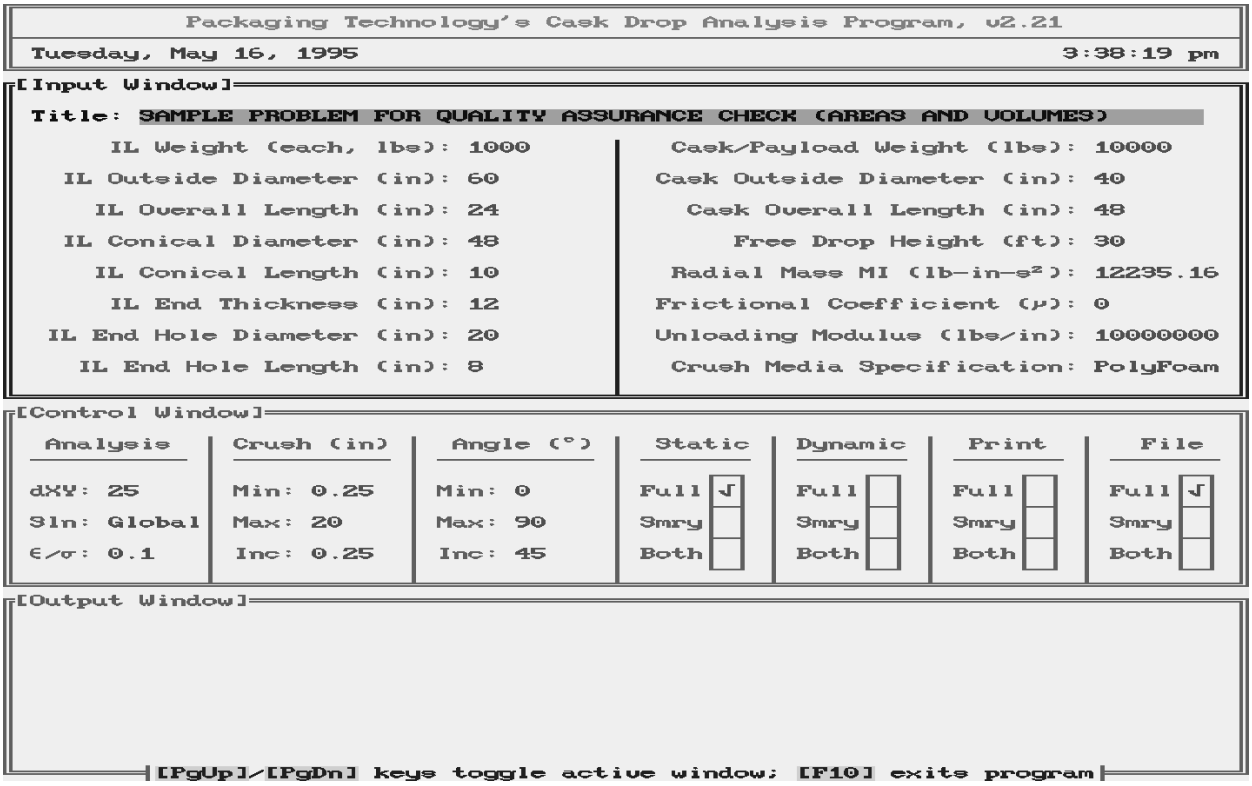

Figure 2.10.2-5 – CASKDROP Program Input Windows

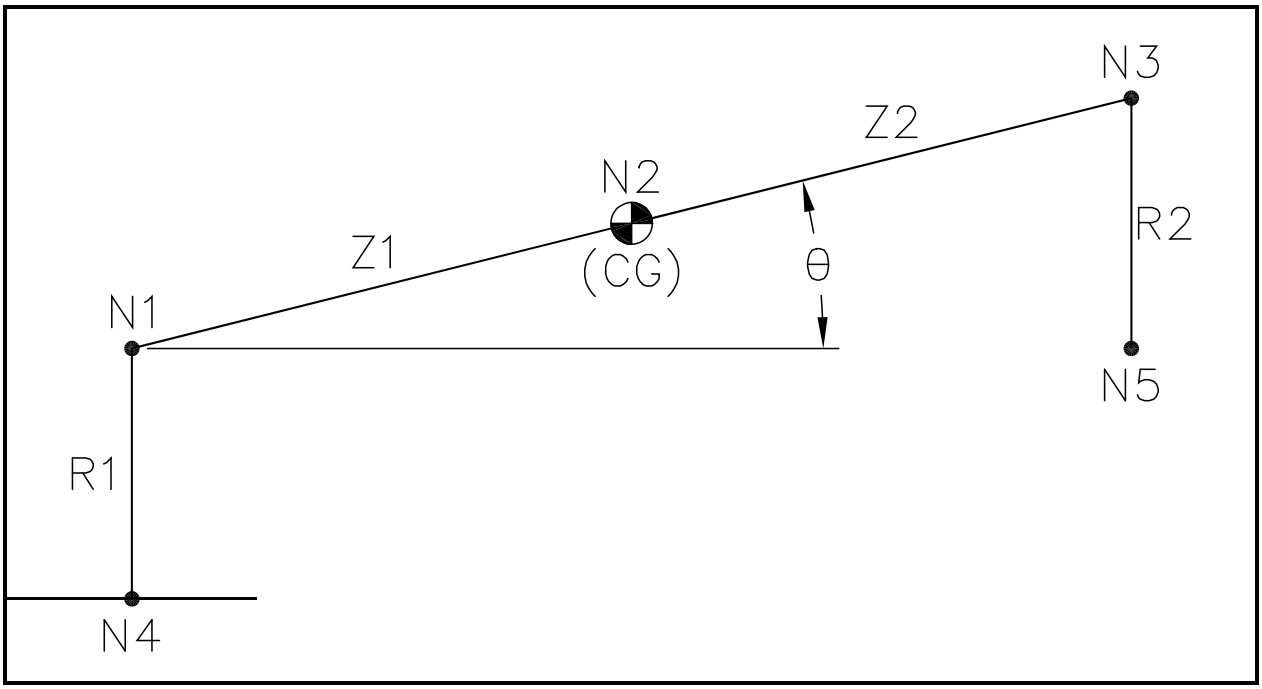

Figure 2.10.2-6 – SLAPDOWN Analytical Model

2.10.3 Drop Impact Evaluation Results

This appendix presents the impact analysis of the RH-TRU 72-B package for normal conditions of transport (NCT) 1-foot drops and hypothetical accident condition (HAC) 30-foot drops. The results are used in Section 2.6.7, *Free Drop*, and Section 2.7.1, *Free Drop*. Given the RH-TRU 72-B package and impact limiter geometry, and the impact limiter's foam material properties, the computer codes CASKDROP (described in Appendix 2.10.2.1, *Description of the CASKDROP Computer Code*) and SLAPDOWN (described in Appendix 2.10.2.2, *Description of the SLAPDOWN Computer Code*) are used to predict results for a combination of bounding foam strengths, orientations, and drop heights. Geometric inputs include limiter outside diameter, limiter overall length, limiter end thickness, package diameter, package length, package mass, and package mass moment of inertia. Mass properties are obtained from Section 2.2, *Weights and Centers of Gravity*.

Impact calculations are performed for end drop, side drop, and oblique angles from five to 85º from horizontal (in 5º increments). If the orientation is stable i.e., where the package center of gravity is supported such that no package rotation occurs, the program CASKDROP is used to report the impact results in the following tables. If the orientation is not stable, such that a secondary impact occurs, the program SLAPDOWN is used to calculate impact results. Program SLAPDOWN uses impact limiter force deflection data calculated by CASKDROP. For angles to the horizontal of 65º to 90º, package rotation is relatively small, and is conservatively neglected by using CASKDROP outputs. For these cases, CASKDROP conservatively overpredicts primary impact results. Secondary slapdown impacts are only important for relatively shallow angles, as discussed in Section 2.10.4, *Slapdown Assessment*.

Impact calculations use the upper- and lower-bound foam stress-strain data given in Table 2.3-3 in Section 2.3, *Mechanical Properties of Materials*. Lower-bound foam properties lead to maximum deflections and strains, and upper-bound properties lead to maximum impacts and stresses. Both parallel-to-rise and perpendicular-to-rise data is used. The parallel-to-rise direction is axial to the package. Depending on impact orientation, the parallel- and perpendicular-to-rise stress-strain data is combined using interpolation, as described in Appendix 2.10.2.1, *Description of the CASKDROP Computer Code*.

For HAC 30-foot drop cases, the foam strength is adjusted by a multiplying factor of 1.52 to bring the calculations into agreement with test results, as discussed in Appendix 2.10.7.3, *Correction Factors*. The factor of 1.52 was developed using 30-foot drop test data, and it includes a dynamic effect. Since the NCT 1-foot drop has a much smaller impact velocity and, therefore, a negligible dynamic effect, the foam strength data for NCT free drops is adjusted by the static factor of 1.19, rather than the full dynamic factor of 1.52. Table 2.10.3-1 summarizes all parallel-to-rise and perpendicular-to-rise stress data for NCT/HAC and warm/cold conditions.

Special circumstances are encountered in the modeling of end and side drop orientations. In the end drop, shear of some of the foam occurs, as described in Appendix 2.10.7.1, *Static Test Program*. To properly account for the shear, the diameter of the inner shell of the package is assumed to be equal to the whole diameter of the impact limiter, namely 75.9 inches (the full diameter is 76 inches). This approach was successful in predicting end orientation crush force-deflection curves in static testing.

Shear of the foam also occurs to a lesser extent in the side drop, as described in Appendix 2.10.7.1, *Static Test Program*. Thus, the inner shell is lengthened somewhat for purposes of calculation. The true end distance is 22.5 inches, but for side drop impacts, a half-effective end length of 11.25 inches is assumed. As before, this approach was successful in predicting side orientation crush force-deflection curves in static testing. These modeling modifications are designated "fully effective," and they are aids to bring the test and modeling results into better agreement. For orientation angles of 5º – 85º, no change to the impact limiter actual dimensions is made.

Significant results from the NCT 1-foot drop analyses are summarized in the following tables and figures:

- Table 2.10.3-2 – CASKDROP Output File for NCT End Drop, Cold (-20 ºF)
- Table 2.10.3-3 – CASKDROP Output File for NCT End Drop, Warm (140 ºF)
- Figure 2.10.3-1 – Impact Limiter Deflection and Residual Clearance for the NCT Oblique Drop, Cold (-20 ºF)
- Figure 2.10.3-2 – Impact Limiter Separation Moments for the NCT Oblique Drop, Cold (-20 ºF)
- Figure 2.10.3-3 – Impact Limiter Deflection and Residual Clearance for the NCT Oblique Drop, Warm (140 ºF)
- Figure 2.10.3-4 – Impact Limiter Separation Moments for the NCT Oblique Drop, Warm (140 ºF)
- Table 2.10.3-4 – CASKDROP Output File for NCT Side Drop, Cold (-20 ºF)
- Table 2.10.3-5 – CASKDROP Output File for NCT Side Drop, Warm (140 ºF)

Significant results from the HAC 30-foot drop analyses are summarized in the following tables and figures:

- Table 2.10.3-6 – CASKDROP Output File for HAC End Drop, Cold (-20 ºF)
- Table 2.10.3-7 – CASKDROP Output File for HAC End Drop, Warm (140 ºF)
- Figure 2.10.3-5 – Impact Limiter Deflection and Residual Clearance for the HAC Oblique Drop, Cold (-20 ºF)
- Figure 2.10.3-6 – Impact Limiter Separation Moments for the HAC Oblique Drop, Cold (-20 ºF)
- Figure 2.10.3-7 – Impact Limiter Deflection and Residual Clearance for the HAC Oblique Drop, Warm (140 ºF)
- Figure 2.10.3-8 – Impact Limiter Separation Moments for the HAC Oblique Drop, Warm (140 ºF)
- Table 2.10.3-8 – CASKDROP Output File for HAC Side Drop, Cold (-20 ºF)
- Table 2.10.3-9 – CASKDROP Output File for HAC Side Drop, Warm (140 ºF)

Maximum impact limiter deflections and residual clearances, and impact limiter separation moments given in Figure 2.10.3-1 though Figure 2.10.3-8 are presented as a function of the initial package impact angle, measured from horizontal.

A summary of the impact limiter deformations and package accelerations for the end and side impact orientations is represented in Table 2.10.3-10. A summary of the maximum package responses as a function of initial impact angle is presented in Table 2.10.3-11 and Table 2.10.3-12. A summary of the maximum impact limiter separation moments as a function of initial impact angle is represented in Table 2.10.3-13.

As shown in Table 2.10.3-13, the maximum impact limiter separation moments are similar for both normal and accident conditions. This is because the maximum moment occurs at a relatively small crush depth, i.e., the moment arm decreases with additional crush depth at a higher rate than the crush force increases.

Finally, Table 2.10.3-14 and Table 2.10.3-15 summarize the time-history from the upper bound (cold) foam strength SLAPDOWN analyses at the time of maximum impact force, F_{max}. The remaining values in the table come from the SLAPDOWN output file.

Table 2.10.3-1 – Polyurethane Foam Data used in CASKDROP

	NCT① (psi)				HAC② (psi)			
	Cold		Warm		Cold		Warm	
Strain	PAR	PER	PAR	PER	PAR	PER	PAR	PER
5%	683	594	336	292	872	758	429	373
10%	689	638	339	314	879	815	433	401
20%	692	665	340	327	883	849	435	418
30%	740	712	364	350	946	910	465	448
40%	824	800	405	393	1,052	1,022	518	503
50%	994	979	489	482	1,270	1,251	625	615
60%	1,385	1,392	681	685	1,768	1,778	870	875
65%	1,767	1,819	869	895	2,257	2,324	1,111	1,143
70%	2,441	2,554	1,201	1,256	3,118	3,262	1,534	1,605
75%	3,668	3,808	1,805	1,873	4,686	4,864	2,305	2,393
80%	—	—	3,226	3,235	—	—	4,120	4,133
87%	—	—	10,539	10,944	—	—	13,462	13,979

Notes:

① NCT data equal to data from Table 2.3-3 in Section 2.3, *Mechanical Properties of Materials*, multiplied by a 1.19 static factor.

② HAC data equal to data from Table 2.3-3 in Section 2.3, *Mechanical Properties of Materials*, multiplied by a 1.52 dynamic factor.

Table 2.10.3-2 – CASKDROP Output File for NCT End Drop, Cold (-20 ºF)

End Drop *** PACKAGING TECHNOLOGY *** CASKDROP, v2.31
02-01-1999, 09:42:06 Nov 13, 1997

72-B End Drop Analysis FULL SCALE SAR PREDICTION (One Foot)			
Impact Limiter Weight (each) -	2,547 lbs	Cask and Payload Weight -	39,906 lbs
Impact Limiter Outside Diameter -	76.0000 in	Cask Outside Diameter -	79.5000 in
Impact Limiter Overall Length -	46.0000 in	Cask Overall Length -	141.7500 in
Impact Limiter Conical Diameter -	0.0000 in	Dynamic Unloading Modulus -	1.000E+07 lbs/in
Impact Limiter Conical Length -	0.0000 in	Rad Mass Moment of Inertia -	304,239 lb-in-s²
Impact Limiter End Thickness -	22.5000 in	Frictional Coefficient -	0.0000
Impact Limiter Hole Diameter -	0.0000 in	Drop Height -	1.0000 ft
Impact Limiter Hole Length -	0.0000 in	Drop Angle from Horizontal -	90.0000°
Unbacked Area Threshhold Strain -	0.1000 in/in	Crush Analysis Theory -	Global
Unbacked Area Crush Stress -	689 psi	Number of Integration Incs -	50

VARIABLE CRUSH STRESS	
ε (in/in)	σ (psi)
0.000	0.0
0.050	683.0
0.100	689.0
0.200	692.0
0.300	740.0
0.400	824.0
0.500	994.0
0.600	1,385.0
0.650	1,767.0
0.700	2,441.0
0.750	3,668.0

DEFL (in)	MAX ε (%)	AREA (in²)	VOLUME (in³)	XBAR (in)	IMPACT FORCE (lbs)	ACCEL (g's)	I/L MOMENT (in-lbs)	STRAIN ENERGY (in-lbs)	KINETIC ENERGY (in-lbs)	SE/KE RATIO
0.500	2.22	4,536	2,268	0.00	1,661,112	36.9	0	415,278	562,500	0.74
0.585	2.60	4,536	2,652	0.00	1,911,833	42.5	0	566,304	566,304	1.00
1.000	4.44	4,536	4,536	0.00	2,900,495	64.5	0	1,555,680	585,000	2.66
1.500	6.67	4,536	6,805	0.00	3,360,835	74.7	0	3,121,012	607,500	5.14
2.000	8.89	4,536	9,073	0.00	3,245,452	72.1	0	4,772,584	630,000	7.58
2.500	11.11	4,536	11,341	0.00	3,035,136	67.4	0	6,342,731	652,500	9.72
3.000	13.33	4,536	13,609	0.00	2,955,584	65.7	0	7,840,411	675,000	11.62
3.500	15.56	4,536	15,878	0.00	2,975,047	66.1	0	9,323,069	697,500	13.37
4.000	17.78	4,536	18,146	0.00	3,050,583	67.8	0	10,829,476	720,000	15.04
4.500	20.00	4,536	20,414	0.00	3,139,253	69.8	0	12,376,935	742,500	16.67
5.000	22.22	4,536	22,682	0.00	3,207,174	71.3	0	13,963,542	765,000	18.25
5.500	24.44	4,536	24,951	0.00	3,255,426	72.3	0	15,579,192	787,500	19.78
6.000	26.67	4,536	27,219	0.00	3,294,103	73.2	0	17,216,574	810,000	21.26

Table 2.10.3-3 – CASKDROP Output File for NCT End Drop, Warm (140 ºF)

End Drop *** PACKAGING TECHNOLOGY *** CASKDROP, v2.31
02-09-1999, 16:42:40 Nov 13, 1997

72-B 90 Deg Drop FULL SCALE SAR PREDICTION (1 ft)			
Impact Limiter Weight (each) -	2,547 lbs	Cask and Payload Weight -	39,906 lbs
Impact Limiter Outside Diameter -	76.0000 in	Cask Outside Diameter -	75.9000 in
Impact Limiter Overall Length -	46.0000 in	Cask Overall Length -	141.8000 in
Impact Limiter Conical Diameter -	0.0000 in	Dynamic Unloading Modulus -	1.000E+07 lbs/in
Impact Limiter Conical Length -	0.0000 in	Rad Mass Moment of Inertia -	304,415 lb-in-s²
Impact Limiter End Thickness -	22.5000 in	Frictional Coefficient -	0.0000
Impact Limiter Hole Diameter -	0.0000 in	Drop Height -	1.0000 ft
Impact Limiter Hole Length -	0.0000 in	Drop Angle from Horizontal -	90.0000°
Unbacked Area Threshhold Strain -	0.1000 in/in	Crush Analysis Theory -	Global
Unbacked Area Crush Stress -	339 psi	Number of Integration Incs -	50

VARIABLE CRUSH STRESS	
ε (in/in)	σ (psi)
0.000	0.0
0.050	336.0
0.100	339.0
0.200	340.0
0.300	364.0
0.400	405.0
0.500	489.0
0.600	681.0
0.650	869.0
0.700	1,201.0
0.750	1,805.0
0.800	3,226.0
0.870	10,539.0

DEFL (in)	MAX ε (%)	AREA (in²)	VOLUME (in³)	XBAR (in)	IMPACT FORCE (lbs)	ACCEL (g's)	I/L MOMENT (in-lbs)	STRAIN ENERGY (in-lbs)	KINETIC ENERGY (in-lbs)	SE/KE RATIO
0.500	2.22	4,536	2,268	0.00	817,125	18.2	0	204,281	562,500	0.36
0.856	3.80	4,536	3,884	0.00	1,284,766	28.6	0	578,525	578,525	1.00
1.000	4.44	4,536	4,536	0.00	1,426,862	31.7	0	765,278	585,000	1.31
1.500	6.67	4,536	6,805	0.00	1,653,486	36.7	0	1,535,365	607,500	2.53
2.000	8.89	4,536	9,073	0.00	1,596,849	35.5	0	2,347,949	630,000	3.73
2.500	11.11	4,536	11,341	0.00	1,493,202	33.2	0	3,120,461	652,500	4.78
3.000	13.33	4,536	13,609	0.00	1,453,542	32.3	0	3,857,147	675,000	5.71
3.500	15.56	4,536	15,878	0.00	1,462,459	32.5	0	4,586,147	697,500	6.58
4.000	17.78	4,536	18,146	0.00	1,499,051	33.3	0	5,326,525	720,000	7.40
4.500	20.00	4,536	20,414	0.00	1,542,413	34.3	0	6,086,891	742,500	8.20
5.000	22.22	4,536	22,682	0.00	1,576,022	35.0	0	6,866,500	765,000	8.98
5.500	24.44	4,536	24,951	0.00	1,600,256	35.6	0	7,660,570	787,500	9.73
6.000	26.67	4,536	27,219	0.00	1,619,852	36.0	0	8,465,597	810,000	10.45

Table 2.10.3-4 – CASKDROP Output File for NCT Side Drop, Cold (-20 ºF)

Side Drop *** PACKAGING TECHNOLOGY *** CASKDROP, v2.31
02-11-1999, 10:19:49 Nov 13, 1997

72-B Side Drop Analysis FULL SCALE SAR PREDICTION (One Foot)			
Impact Limiter Weight (each) -	2,547 lbs	Cask and Payload Weight -	39,906 lbs
Impact Limiter Outside Diameter -	76.0000 in	Cask Outside Diameter -	42.1000 in
Impact Limiter Overall Length -	46.0000 in	Cask Overall Length -	141.7500 in
Impact Limiter Conical Diameter -	0.0000 in	Dynamic Unloading Modulus -	1.000E+07 lbs/in
Impact Limiter Conical Length -	0.0000 in	Rad Mass Moment of Inertia -	241,355 lb-in-s²
Impact Limiter End Thickness -	11.2500 in	Frictional Coefficient -	0.0000
Impact Limiter Hole Diameter -	0.0000 in	Drop Height -	1.0000 ft
Impact Limiter Hole Length -	0.0000 in	Drop Angle from Horizontal -	0.0000°
Unbacked Area Threshhold Strain -	0.1000 in/in	Crush Analysis Theory -	Global
Unbacked Area Crush Stress -	638 psi	Number of Integration Incs -	50

VARIABLE CRUSH STRESS	
ε (in/in)	σ (psi)
0.000	0.0
0.050	594.0
0.100	638.0
0.200	665.0
0.300	712.0
0.400	800.0
0.500	979.0
0.600	1,392.0
0.650	1,819.0
0.700	2,554.0
0.750	3,808.0

DEFL (in)	MAX ε (%)	AREA (in²)	VOLUME (in³)	XBAR (in)	IMPACT FORCE (lbs)	ACCEL (g's)	I/L MOMENT (in-lbs)	STRAIN ENERGY (in-lbs)	KINETIC ENERGY (in-lbs)	SE/KE RATIO
0.500	2.95	1,131	377	0.00	254,185	5.6	0	63,546	562,500	0.11
1.000	5.90	1,593	1,065	0.00	618,411	13.7	0	281,696	585,000	0.48
1.435	8.46	1,903	1,828	0.00	866,688	19.3	0	604,567	604,567	1.00
1.500	8.85	1,945	1,953	0.00	896,815	19.9	0	660,502	607,500	1.09
2.000	11.80	2,238	3,001	0.00	1,094,295	24.3	0	1,158,280	630,000	1.84
2.500	14.75	2,494	4,185	0.00	1,273,629	28.3	0	1,750,261	652,500	2.68
3.000	17.70	2,723	5,491	0.00	1,452,846	32.3	0	2,431,880	675,000	3.60
3.500	20.65	2,931	6,905	0.00	1,630,952	36.2	0	3,202,829	697,500	4.59
4.000	23.60	3,123	8,419	0.00	1,800,623	40.0	0	4,060,723	720,000	5.64
4.500	26.55	3,300	10,026	0.00	1,959,027	43.5	0	5,000,636	742,500	6.73
5.000	29.50	3,467	11,718	0.00	2,107,610	46.8	0	6,017,295	765,000	7.87
5.500	32.44	3,623	13,491	0.00	2,249,786	50.0	0	7,106,644	787,500	9.02
6.000	35.39	3,771	15,340	0.00	2,388,758	53.1	0	8,266,280	810,000	10.21
6.500	38.34	3,911	17,261	0.00	2,526,373	56.1	0	9,495,063	832,500	11.41
7.000	41.29	4,044	19,250	0.00	2,656,249	59.0	0	10,790,718	855,000	12.62
7.500	44.24	4,171	21,304	0.00	2,773,831	61.6	0	12,148,238	877,500	13.84
8.000	47.19	4,292	23,420	0.00	2,912,379	64.7	0	13,569,791	900,000	15.08
8.500	50.14	4,407	25,595	0.00	3,068,230	68.2	0	15,064,943	922,500	16.33
9.000	53.09	4,518	27,826	0.00	3,248,041	72.2	0	16,644,011	945,000	17.61
9.500	56.04	4,625	30,112	0.00	3,461,662	76.9	0	18,321,437	967,500	18.94
10.000	58.99	4,727	32,451	0.00	3,720,944	82.7	0	20,117,089	990,000	20.32
10.500	61.94	4,825	34,839	0.00	4,038,789	89.8	0	22,057,022	1,012,500	21.78
11.000	64.89	4,920	37,276	0.00	4,430,555	98.5	0	24,174,358	1,035,000	23.36
11.500	67.84	5,011	39,759	0.00	4,917,330	109.3	0	26,511,329	1,057,500	25.07
12.000	70.79	5,099	42,287	0.00	5,559,781	123.6	0	29,130,607	1,080,000	26.97
12.500	73.74	5,184	44,858	0.00	6,415,572	142.6	0	32,124,445	1,102,500	29.14
13.000	76.69	5,266	47,471	0.00	7,466,055	165.9	0	35,594,852	1,125,000	31.64
13.500	79.64	5,345	50,124	0.00	8,652,713	192.3	0	39,624,544	1,147,500	34.53
14.000	82.58	5,421	52,815	0.00	9,954,562	221.2	0	44,276,363	1,170,000	37.84
14.500	85.53	5,495	55,545	0.00	11,346,716	252.1	0	49,601,683	1,192,500	41.59
15.000	88.48	5,566	58,310	0.00	12,826,362	285.0	0	55,644,952	1,215,000	45.80
15.500	91.43	5,635	61,110	0.00	14,372,946	319.4	0	62,444,779	1,237,500	50.46
16.000	94.38	5,701	63,945	0.00	15,991,266	355.4	0	70,035,832	1,260,000	55.58
16.500	97.33	5,765	66,812	0.00	17,668,073	392.6	0	78,450,667	1,282,500	61.17

Table 2.10.3-5 – CASKDROP Output File for NCT Side Drop, Warm (140 ºF)

Side Drop *** PACKAGING TECHNOLOGY *** CASKDROP, v2.31
02-09-1999, 15:29:19 Nov 13, 1997

72-B 0 degrees (Full Scale) TAIL (One foot)			
Impact Limiter Weight (each) -	2,547 lbs	Cask and Payload Weight -	39,906 lbs
Impact Limiter Outside Diameter -	76.0000 in	Cask Outside Diameter -	42.1000 in
Impact Limiter Overall Length -	46.0000 in	Cask Overall Length -	141.8000 in
Impact Limiter Conical Diameter -	0.0000 in	Dynamic Unloading Modulus -	1.000E+07 lbs/in
Impact Limiter Conical Length -	0.0000 in	Rad Mass Moment of Inertia -	241,517 lb-in-s²
Impact Limiter End Thickness -	11.2500 in	Frictional Coefficient -	0.0000
Impact Limiter Hole Diameter -	0.0000 in	Drop Height -	1.0000 ft
Impact Limiter Hole Length -	0.0000 in	Drop Angle from Horizontal -	0.0000°
Unbacked Area Threshhold Strain -	0.1000 in/in	Crush Analysis Theory -	Global
Unbacked Area Crush Stress -	314 psi	Number of Integration Incs -	50

VARIABLE CRUSH STRESS	
ε (in/in)	σ (psi)
0.000	0.0
0.050	292.0
0.100	314.0
0.200	327.0
0.300	350.0
0.400	393.0
0.500	482.0
0.600	685.0
0.650	895.0
0.700	1,256.0
0.750	1,873.0
0.800	3,235.0
0.870	10,944.0

DEFL (in)	MAX ε (%)	AREA (in²)	VOLUME (in³)	XBAR (in)	IMPACT FORCE (lbs)	ACCEL (g's)	I/L MOMENT (in-lbs)	STRAIN ENERGY (in-lbs)	KINETIC ENERGY (in-lbs)	SE/KE RATIO
0.500	2.95	1,131	377	0.00	124,918	2.8	0	31,230	562,500	0.06
1.000	5.90	1,593	1,065	0.00	303,986	6.8	0	138,456	585,000	0.24
1.500	8.85	1,945	1,953	0.00	441,013	9.8	0	324,705	607,500	0.53
2.000	11.80	2,238	3,001	0.00	538,294	12.0	0	569,532	630,000	0.90
2.120	12.51	2,303	3,273	0.00	559,706	12.4	0	635,399	635,399	1.00
2.500	14.75	2,494	4,185	0.00	626,550	13.9	0	860,743	652,500	1.32
3.000	17.70	2,723	5,491	0.00	714,637	15.9	0	1,196,040	675,000	1.77
3.500	20.65	2,931	6,905	0.00	802,125	17.8	0	1,575,231	697,500	2.26
4.000	23.60	3,123	8,419	0.00	885,491	19.7	0	1,997,135	720,000	2.77
4.500	26.55	3,300	10,026	0.00	963,353	21.4	0	2,459,346	742,500	3.31
5.000	29.50	3,467	11,718	0.00	1,036,383	23.0	0	2,959,280	765,000	3.87
5.500	32.44	3,623	13,491	0.00	1,106,199	24.6	0	3,494,925	787,500	4.44
6.000	35.39	3,771	15,340	0.00	1,174,375	26.1	0	4,065,069	810,000	5.02
6.500	38.34	3,911	17,261	0.00	1,241,904	27.6	0	4,669,138	832,500	5.61
7.000	41.29	4,044	19,250	0.00	1,305,781	29.0	0	5,306,060	855,000	6.21
7.500	44.24	4,171	21,304	0.00	1,363,848	30.3	0	5,973,467	877,500	6.81
8.000	47.19	4,292	23,420	0.00	1,432,346	31.8	0	6,672,515	900,000	7.41
8.500	50.14	4,407	25,595	0.00	1,509,262	33.5	0	7,407,917	922,500	8.03
9.000	53.09	4,518	27,826	0.00	1,597,651	35.5	0	8,184,646	945,000	8.66
9.500	56.04	4,625	30,112	0.00	1,702,457	37.8	0	9,009,672	967,500	9.31
10.000	58.99	4,727	32,451	0.00	1,829,920	40.7	0	9,892,767	990,000	9.99
10.500	61.94	4,825	34,839	0.00	1,986,897	44.2	0	10,846,971	1,012,500	10.71
11.000	64.89	4,920	37,276	0.00	2,179,962	48.4	0	11,888,686	1,035,000	11.49
11.500	67.84	5,011	39,759	0.00	2,417,147	53.7	0	13,037,963	1,057,500	12.33
12.000	70.79	5,099	42,287	0.00	2,734,368	60.8	0	14,325,842	1,080,000	13.26
12.500	73.74	5,184	44,858	0.00	3,163,581	70.3	0	15,800,329	1,102,500	14.33
13.000	76.69	5,266	47,471	0.00	3,670,030	81.6	0	17,508,732	1,125,000	15.56
13.500	79.64	5,345	50,124	0.00	4,441,159	98.7	0	19,536,529	1,147,500	17.03
14.000	82.58	5,421	52,815	0.00	6,132,302	136.3	0	22,179,894	1,170,000	18.96
14.500	85.53	5,495	55,545	0.00	9,078,839	201.8	0	25,982,679	1,192,500	21.79
15.000	88.48	5,566	58,310	0.00	13,103,071	291.2	0	31,528,157	1,215,000	25.95
15.500	91.43	5,635	61,110	0.00	17,894,737	397.7	0	39,277,609	1,237,500	31.74
16.000	94.38	5,701	63,945	0.00	23,299,209	517.8	0	49,576,095	1,260,000	39.35
16.500	97.33	5,765	66,812	0.00	29,219,382	649.3	0	62,705,743	1,282,500	48.89

Table 2.10.3-6 – CASKDROP Output File for HAC End Drop, Cold (-20 ºF)

End Drop *** PACKAGING TECHNOLOGY *** CASKDROP, v2.31
02-09-1999, 10:29:48 Nov 13, 1997

72-B End Drop Analysis FULL SCALE SAR PREDICTION (30 ft)			
Impact Limiter Weight (each) -	2,547 lbs	Cask and Payload Weight -	39,906 lbs
Impact Limiter Outside Diameter -	76.0000 in	Cask Outside Diameter -	79.5000 in
Impact Limiter Overall Length -	46.0000 in	Cask Overall Length -	141.7500 in
Impact Limiter Conical Diameter -	0.0000 in	Dynamic Unloading Modulus -	1.000E+07 lbs/in
Impact Limiter Conical Length -	0.0000 in	Rad Mass Moment of Inertia -	304,239 lb-in-s²
Impact Limiter End Thickness -	22.5000 in	Frictional Coefficient -	0.0000
Impact Limiter Hole Diameter -	0.0000 in	Drop Height -	30.0000 ft
Impact Limiter Hole Length -	0.0000 in	Drop Angle from Horizontal -	90.0000°
Unbacked Area Threshhold Strain -	0.1000 in/in	Crush Analysis Theory -	Global
Unbacked Area Crush Stress -	879 psi	Number of Integration Incs -	50

VARIABLE CRUSH STRESS	
ε (in/in)	σ (psi)
0.000	0.0
0.050	872.0
0.100	879.0
0.200	883.0
0.300	946.0
0.400	1,052.0
0.500	1,270.0
0.600	1,768.0
0.650	2,257.0
0.700	3,118.0
0.750	4,686.0

DEFL (in)	MAX ε (%)	AREA (in²)	VOLUME (in³)	XBAR (in)	IMPACT FORCE (lbs)	ACCEL (g's)	I/L MOMENT (in-lbs)	STRAIN ENERGY (in-lbs)	KINETIC ENERGY (in-lbs)	SE/KE RATIO
0.500	2.22	4,536	2,268	0.00	2,121,086	47.1	0	530,271	16,222,500	0.03
1.000	4.44	4,536	4,536	0.00	3,703,284	82.3	0	1,986,364	16,245,000	0.12
1.500	6.67	4,536	6,805	0.00	4,290,028	95.3	0	3,984,692	16,267,500	0.24
2.000	8.89	4,536	9,073	0.00	4,141,244	92.0	0	6,092,510	16,290,000	0.37
2.500	11.11	4,536	11,341	0.00	3,871,467	86.0	0	8,095,688	16,312,500	0.50
3.000	13.33	4,536	13,609	0.00	3,769,226	83.8	0	10,005,861	16,335,000	0.61
3.500	15.56	4,536	15,878	0.00	3,794,042	84.3	0	11,896,678	16,357,500	0.73
4.000	17.78	4,536	18,146	0.00	3,891,134	86.5	0	13,817,972	16,380,000	0.84
4.500	20.00	4,536	20,414	0.00	4,005,722	89.0	0	15,792,186	16,402,500	0.96
4.653	20.68	4,536	21,110	0.00	4,036,322	89.7	0	16,409,407	16,409,407	1.00
5.000	22.22	4,536	22,682	0.00	4,094,493	91.0	0	17,817,239	16,425,000	1.08
5.500	24.44	4,536	24,951	0.00	4,158,401	92.4	0	19,880,463	16,447,500	1.21
6.000	26.67	4,536	27,219	0.00	4,209,808	93.6	0	21,972,515	16,470,000	1.33
6.500	28.89	4,536	29,487	0.00	4,261,154	94.7	0	24,090,255	16,492,500	1.46
7.000	31.11	4,536	31,755	0.00	4,324,629	96.1	0	26,236,701	16,515,000	1.59
7.500	33.33	4,536	34,023	0.00	4,406,678	97.9	0	28,419,528	16,537,500	1.72
8.000	35.56	4,536	36,292	0.00	4,508,003	100.2	0	30,648,198	16,560,000	1.85
8.500	37.78	4,536	38,560	0.00	4,629,057	102.9	0	32,932,463	16,582,500	1.99
9.000	40.00	4,536	40,828	0.00	4,770,292	106.0	0	35,282,300	16,605,000	2.12
9.500	42.22	4,536	43,096	0.00	4,933,137	109.6	0	37,708,157	16,627,500	2.27
10.000	44.44	4,536	45,365	0.00	5,122,922	113.8	0	40,222,171	16,650,000	2.42

Table 2.10.3-7 – CASKDROP Output File for HAC End Drop, Warm (140 ºF)

End Drop *** PACKAGING TECHNOLOGY *** CASKDROP, v2.31
02-09-1999, 15:06:40 Nov 13, 1997

72-B 90 Deg Drop FULL SCALE SAR PREDICTION (30 ft)			
Impact Limiter Weight (each) -	2,547 lbs	Cask and Payload Weight -	39,906 lbs
Impact Limiter Outside Diameter -	76.0000 in	Cask Outside Diameter -	79.5000 in
Impact Limiter Overall Length -	46.0000 in	Cask Overall Length -	141.8000 in
Impact Limiter Conical Diameter -	0.0000 in	Dynamic Unloading Modulus -	1.000E+07 lbs/in
Impact Limiter Conical Length -	0.0000 in	Rad Mass Moment of Inertia -	304,415 lb-in-s²
Impact Limiter End Thickness -	22.5000 in	Frictional Coefficient -	0.0000
Impact Limiter Hole Diameter -	0.0000 in	Drop Height -	30.0000 ft
Impact Limiter Hole Length -	0.0000 in	Drop Angle from Horizontal -	90.0000°
Unbacked Area Threshhold Strain -	0.1000 in/in	Crush Analysis Theory -	Global
Unbacked Area Crush Stress -	433 psi	Number of Integration Incs -	50

VARIABLE CRUSH STRESS	
ε (in/in)	σ (psi)
0.000	0.0
0.050	429.0
0.100	433.0
0.200	435.0
0.300	465.0
0.400	518.0
0.500	625.0
0.600	870.0
0.650	1,111.0
0.700	1,534.0
0.750	2,305.0
0.800	4,120.0
0.870	13,462.0

DEFL (in)	MAX ε (%)	AREA (in²)	VOLUME (in³)	XBAR (in)	IMPACT FORCE (lbs)	ACCEL (g's)	I/L MOMENT (in-lbs)	STRAIN ENERGY (in-lbs)	KINETIC ENERGY (in-lbs)	SE/KE RATIO
0.500	2.22	4,536	2,268	0.00	1,043,255	23.2	0	260,814	16,222,500	0.02
1.000	4.44	4,536	4,536	0.00	1,821,777	40.5	0	977,072	16,245,000	0.06
1.500	6.67	4,536	6,805	0.00	2,111,263	46.9	0	1,960,332	16,267,500	0.12
2.000	8.89	4,536	9,073	0.00	2,039,305	45.3	0	2,997,974	16,290,000	0.18
2.500	11.11	4,536	11,341	0.00	1,907,653	42.4	0	3,984,714	16,312,500	0.24
3.000	13.33	4,536	13,609	0.00	1,857,962	41.3	0	4,926,117	16,335,000	0.30
3.500	15.56	4,536	15,878	0.00	1,870,313	41.6	0	5,858,186	16,357,500	0.36
4.000	17.78	4,536	18,146	0.00	1,917,764	42.6	0	6,805,205	16,380,000	0.42
4.500	20.00	4,536	20,414	0.00	1,973,373	43.9	0	7,777,990	16,402,500	0.47
5.000	22.22	4,536	22,682	0.00	2,015,887	44.8	0	8,775,305	16,425,000	0.53
5.500	24.44	4,536	24,951	0.00	2,046,019	45.5	0	9,790,781	16,447,500	0.60
6.000	26.67	4,536	27,219	0.00	2,070,140	46.0	0	10,819,821	16,470,000	0.66
6.500	28.89	4,536	29,487	0.00	2,094,660	46.5	0	11,861,021	16,492,500	0.72
7.000	31.11	4,536	31,755	0.00	2,125,852	47.2	0	12,916,149	16,515,000	0.78
7.500	33.33	4,536	34,023	0.00	2,166,877	48.2	0	13,989,331	16,537,500	0.85
8.000	35.56	4,536	36,292	0.00	2,217,782	49.3	0	15,085,496	16,560,000	0.91
8.500	37.78	4,536	38,560	0.00	2,278,476	50.6	0	16,209,560	16,582,500	0.98
8.666	38.52	4,536	39,314	0.00	2,300,796	51.1	0	16,589,977	16,589,977	1.00
9.000	40.00	4,536	40,828	0.00	2,348,872	52.2	0	17,366,397	16,605,000	1.05
9.500	42.22	4,536	43,096	0.00	2,429,426	54.0	0	18,560,972	16,627,500	1.12
10.000	44.44	4,536	45,365	0.00	2,522,773	56.1	0	19,799,021	16,650,000	1.19
10.500	46.67	4,536	47,633	0.00	2,632,097	58.5	0	21,087,739	16,672,500	1.26
11.000	48.89	4,536	49,901	0.00	2,760,578	61.3	0	22,435,908	16,695,000	1.34
11.500	51.11	4,536	52,169	0.00	2,911,590	64.7	0	23,853,950	16,717,500	1.43
12.000	53.33	4,536	54,438	0.00	3,092,917	68.7	0	25,355,076	16,740,000	1.51
12.500	55.56	4,536	56,706	0.00	3,316,754	73.7	0	26,957,494	16,762,500	1.61
13.000	57.78	4,536	58,974	0.00	3,595,488	79.9	0	28,685,555	16,785,000	1.71
13.500	60.00	4,536	61,242	0.00	3,941,507	87.6	0	30,569,803	16,807,500	1.82
14.000	62.22	4,536	63,510	0.00	4,367,345	97.1	0	32,647,016	16,830,000	1.94
14.500	64.44	4,536	65,779	0.00	4,886,139	108.6	0	34,960,387	16,852,500	2.07
15.000	66.67	4,536	68,047	0.00	5,521,128	122.7	0	37,562,204	16,875,000	2.23
15.500	68.89	4,536	70,315	0.00	6,382,208	141.8	0	40,538,038	16,897,500	2.40
16.000	71.11	4,536	72,583	0.00	7,615,724	169.2	0	44,037,521	16,920,000	2.60
16.500	73.33	4,536	74,852	0.00	9,180,523	204.0	0	48,236,582	16,942,500	2.85
17.000	75.56	4,536	77,120	0.00	10,854,594	241.2	0	53,245,362	16,965,000	3.14

Table 2.10.3-8 – CASKDROP Output File for HAC Side Drop, Cold (-20 ºF)

72-B Side Drop Analysis FULL SCALE SAR PREDICTION (30 Foot)			
Impact Limiter Weight (each) -	2,547 lbs	Cask and Payload Weight -	39,906 lbs
Impact Limiter Outside Diameter -	76.0000 in	Cask Outside Diameter -	42.1000 in
Impact Limiter Overall Length -	46.0000 in	Cask Overall Length -	141.7500 in
Impact Limiter Conical Diameter -	0.0000 in	Dynamic Unloading Modulus -	1.000E+07 lbs/in
Impact Limiter Conical Length -	0.0000 in	Rad Mass Moment of Inertia -	241,355 lb-in-s²
Impact Limiter End Thickness -	11.2500 in	Frictional Coefficient -	0.0000
Impact Limiter Hole Diameter -	0.0000 in	Drop Height -	30.0000 ft
Impact Limiter Hole Length -	0.0000 in	Drop Angle from Horizontal -	0.0000°
Unbacked Area Threshhold Strain -	0.1000 in/in	Crush Analysis Theory -	Global
Unbacked Area Crush Stress -	815 psi	Number of Integration Incs -	50

VARIABLE CRUSH STRESS	
ε (in/in)	σ (psi)
0.000	0.0
0.050	758.0
0.100	815.0
0.200	849.0
0.300	910.0
0.400	1,022.0
0.500	1,251.0
0.600	1,778.0
0.650	2,324.0
0.700	3,262.0
0.750	4,864.0

DEFL (in)	MAX ε (%)	AREA (in²)	VOLUME (in³)	XBAR (in)	IMPACT FORCE (lbs)	ACCEL (g's)	I/L MOMENT (in-lbs)	STRAIN ENERGY (in-lbs)	KINETIC ENERGY (in-lbs)	SE/KE RATIO
0.500	2.95	1,131	377	0.00	324,284	7.2	0	81,071	16,222,500	0.00
1.000	5.90	1,593	1,065	0.00	789,118	17.5	0	359,422	16,245,000	0.02
1.500	8.85	1,945	1,953	0.00	1,144,778	25.4	0	842,896	16,267,500	0.05
2.000	11.80	2,238	3,001	0.00	1,397,243	31.0	0	1,478,401	16,290,000	0.09
2.500	14.75	2,494	4,185	0.00	1,626,309	36.1	0	2,234,289	16,312,500	0.14
3.000	17.70	2,723	5,491	0.00	1,855,001	41.2	0	3,104,616	16,335,000	0.19
3.500	20.65	2,931	6,905	0.00	2,082,242	46.3	0	4,088,927	16,357,500	0.25
4.000	23.60	3,123	8,419	0.00	2,298,917	51.1	0	5,184,217	16,380,000	0.32
4.500	26.55	3,300	10,026	0.00	2,501,445	55.6	0	6,384,308	16,402,500	0.39
5.000	29.50	3,467	11,718	0.00	2,691,558	59.8	0	7,682,558	16,425,000	0.47
5.500	32.44	3,623	13,491	0.00	2,873,426	63.9	0	9,073,804	16,447,500	0.55
6.000	35.39	3,771	15,340	0.00	3,051,045	67.8	0	10,554,922	16,470,000	0.64
6.500	38.34	3,911	17,261	0.00	3,226,824	71.7	0	12,124,389	16,492,500	0.74
7.000	41.29	4,044	19,250	0.00	3,392,747	75.4	0	13,779,282	16,515,000	0.83
7.500	44.24	4,171	21,304	0.00	3,543,103	78.7	0	15,513,244	16,537,500	0.94
7.788	45.94	4,241	22,516	0.00	3,654,879	81.2	0	16,550,469	16,550,469	1.00
8.000	47.19	4,292	23,420	0.00	3,720,284	82.7	0	17,329,091	16,560,000	1.05
8.500	50.14	4,407	25,595	0.00	3,919,504	87.1	0	19,239,038	16,582,500	1.16
9.000	53.09	4,518	27,826	0.00	4,149,136	92.2	0	21,256,198	16,605,000	1.28
9.500	56.04	4,625	30,112	0.00	4,421,782	98.3	0	23,398,928	16,627,500	1.41
10.000	58.99	4,727	32,451	0.00	4,752,752	105.6	0	25,692,561	16,650,000	1.54
10.500	61.94	4,825	34,839	0.00	5,158,773	114.6	0	28,170,443	16,672,500	1.69
11.000	64.89	4,920	37,276	0.00	5,659,424	125.8	0	30,874,992	16,695,000	1.85
11.500	67.84	5,011	39,759	0.00	6,281,177	139.6	0	33,860,142	16,717,500	2.03
12.000	70.79	5,099	42,287	0.00	7,101,512	157.8	0	37,205,814	16,740,000	2.22
12.500	73.74	5,184	44,858	0.00	8,194,556	182.1	0	41,029,831	16,762,500	2.45
13.000	76.69	5,266	47,471	0.00	9,536,501	211.9	0	45,462,595	16,785,000	2.71
13.500	79.64	5,345	50,124	0.00	11,052,547	245.6	0	50,609,857	16,807,500	3.01
14.000	82.58	5,421	52,815	0.00	12,715,792	282.6	0	56,551,942	16,830,000	3.36
14.500	85.53	5,495	55,545	0.00	14,494,454	322.1	0	63,354,504	16,852,500	3.76
15.000	88.48	5,566	58,310	0.00	16,384,939	364.1	0	71,074,352	16,875,000	4.21
15.500	91.43	5,635	61,110	0.00	18,360,939	408.0	0	79,760,821	16,897,500	4.72
16.000	94.38	5,701	63,945	0.00	20,428,655	454.0	0	89,458,220	16,920,000	5.29
16.500	97.33	5,765	66,812	0.00	22,571,122	501.6	0	100,208,164	16,942,500	5.91

Table 2.10.3-9 – CASKDROP Output File for HAC Side Drop, Warm (140 ºF)

72-B 0 degrees (Full Scale) TAIL			
Impact Limiter Weight (each) -	2,547 lbs	Cask and Payload Weight -	39,906 lbs
Impact Limiter Outside Diameter -	76.0000 in	Cask Outside Diameter -	42.1000 in
Impact Limiter Overall Length -	46.0000 in	Cask Overall Length -	141.8000 in
Impact Limiter Conical Diameter -	0.0000 in	Dynamic Unloading Modulus -	1.000E+07 lbs/in
Impact Limiter Conical Length -	0.0000 in	Rad Mass Moment of Inertia -	241,517 lb-in-s²
Impact Limiter End Thickness -	11.2500 in	Frictional Coefficient -	0.0000
Impact Limiter Hole Diameter -	0.0000 in	Drop Height -	30.0000 ft
Impact Limiter Hole Length -	0.0000 in	Drop Angle from Horizontal -	0.0000°
Unbacked Area Threshhold Strain -	0.1000 in/in	Crush Analysis Theory -	Global
Unbacked Area Crush Stress -	401 psi	Number of Integration Incs -	50

VARIABLE CRUSH STRESS	
ε (in/in)	σ (psi)
0.000	0.0
0.050	373.0
0.100	401.0
0.200	418.0
0.300	448.0
0.400	503.0
0.500	615.0
0.600	875.0
0.650	1,143.0
0.700	1,605.0
0.750	2,393.0
0.800	4,133.0
0.870	13,979.0

DEFL (in)	MAX ε (%)	AREA (in²)	VOLUME (in³)	XBAR (in)	IMPACT FORCE (lbs)	ACCEL (g's)	I/L MOMENT (in-lbs)	STRAIN ENERGY (in-lbs)	KINETIC ENERGY (in-lbs)	SE/KE RATIO
0.500	2.95	1,131	377	0.00	159,582	3.5	0	39,895	16,222,500	0.00
1.000	5.90	1,593	1,065	0.00	388,316	8.6	0	176,870	16,245,000	0.01
1.500	8.85	1,945	1,953	0.00	563,302	12.5	0	414,774	16,267,500	0.03
2.000	11.80	2,238	3,001	0.00	687,524	15.3	0	727,481	16,290,000	0.04
2.500	14.75	2,494	4,185	0.00	800,286	17.8	0	1,099,433	16,312,500	0.07
3.000	17.70	2,723	5,491	0.00	912,911	20.3	0	1,527,732	16,335,000	0.09
3.500	20.65	2,931	6,905	0.00	1,024,839	22.8	0	2,012,170	16,357,500	0.12
4.000	23.60	3,123	8,419	0.00	1,131,547	25.1	0	2,551,266	16,380,000	0.16
4.500	26.55	3,300	10,026	0.00	1,231,260	27.4	0	3,141,968	16,402,500	0.19
5.000	29.50	3,467	11,718	0.00	1,324,837	29.4	0	3,780,992	16,425,000	0.23
5.500	32.44	3,623	13,491	0.00	1,414,346	31.4	0	4,465,788	16,447,500	0.27
6.000	35.39	3,771	15,340	0.00	1,501,758	33.4	0	5,194,814	16,470,000	0.32
6.500	38.34	3,911	17,261	0.00	1,588,246	35.3	0	5,967,315	16,492,500	0.36
7.000	41.29	4,044	19,250	0.00	1,669,847	37.1	0	6,781,838	16,515,000	0.41
7.500	44.24	4,171	21,304	0.00	1,743,728	38.7	0	7,635,232	16,537,500	0.46
8.000	47.19	4,292	23,420	0.00	1,830,733	40.7	0	8,528,847	16,560,000	0.52
8.500	50.14	4,407	25,595	0.00	1,928,488	42.9	0	9,468,653	16,582,500	0.57
9.000	53.09	4,518	27,826	0.00	2,041,121	45.4	0	10,461,055	16,605,000	0.63
9.500	56.04	4,625	30,112	0.00	2,174,985	48.3	0	11,515,081	16,627,500	0.69
10.000	58.99	4,727	32,451	0.00	2,337,898	52.0	0	12,643,302	16,650,000	0.76
10.500	61.94	4,825	34,839	0.00	2,538,382	56.4	0	13,862,372	16,672,500	0.83
11.000	64.89	4,920	37,276	0.00	2,784,839	61.9	0	15,193,178	16,695,000	0.91
11.500	67.84	5,011	39,759	0.00	3,087,936	68.6	0	16,661,371	16,717,500	1.00
11.518	67.95	5,015	39,851	0.00	3,100,628	68.9	0	16,718,328	16,718,328	1.00
12.000	70.79	5,099	42,287	0.00	3,493,463	77.6	0	18,306,721	16,740,000	1.09
12.500	73.74	5,184	44,858	0.00	4,041,833	89.8	0	20,190,545	16,762,500	1.20
13.000	76.69	5,266	47,471	0.00	4,688,811	104.2	0	22,373,206	16,785,000	1.33
13.500	79.64	5,345	50,124	0.00	5,673,939	126.1	0	24,963,893	16,807,500	1.49
14.000	82.58	5,421	52,815	0.00	7,834,174	174.1	0	28,340,922	16,830,000	1.68
14.500	85.53	5,495	55,545	0.00	11,597,645	257.7	0	33,198,876	16,852,500	1.97
15.000	88.48	5,566	58,310	0.00	16,737,524	371.9	0	40,282,669	16,875,000	2.39
15.500	91.43	5,635	61,110	0.00	22,857,434	507.9	0	50,181,408	16,897,500	2.97
16.000	94.38	5,701	63,945	0.00	29,760,073	661.3	0	63,335,785	16,920,000	3.74
16.500	97.33	5,765	66,812	0.00	37,321,340	829.4	0	80,106,138	16,942,500	4.73

Table 2.10.3-10 – Summary of End and Side Drop Impact Accelerations and Impact Limiter Deflections

Drop Height (ft)	Drop Orientation	Impact Limiter Temperature (ºF)	Impact Acceleration (*g*)	Impact Limiter Deflection (in)
1	End	-20	42.5	0.59
		140	28.6	0.86
	Side	-20	19.3	1.44
		140	12.4	2.12
30	End	-20	89.7	4.65
		140	51.1	8.67
	Side	-20	81.2	7.79
		140	68.9	11.52

Table 2.10.3-11 – Maximum Package Responses as a Function of Initial Impact Angle (-20 ºF Cases)

Drop Height (ft)	Package Orientation (degrees from horizontal)	Impact Acceleration (*g*)	Impact Force (lb)
1	0	19.3	$8.69(10)^5$
	5	5.2	$2.34(10)^5$
	10	4.2	$1.89(10)^5$
	15	3.9	$1.76(10)^5$
	20	3.8	$1.71(10)^5$
	25	3.7	$1.67(10)^5$
	30	3.8	$1.71(10)^5$
	35	4.1	$1.85(10)^5$
	40	4.4	$1.98(10)^5$
	45	4.8	$2.16(10)^5$
	50	5.3	$2.39(10)^5$
	55	5.9	$2.66(10)^5$
	60	6.5	$2.93(10)^5$
	65	8.2	$3.69(10)^5$
	70	9.3	$4.19(10)^5$
	75	10.9	$4.91(10)^5$
	80	13.2	$5.94(10)^5$
	85	17.9	$8.06(10)^5$
	90	42.5	$1.91(10)^6$
30	0	81.2	$3.65(10)^6$
	5	48.1	$2.16(10)^6$
	10	33.1	$1.49(10)^6$
	15	32.3	$1.45(10)^6$
	20	30.5	$1.37(10)^6$
	25	30.3	$1.36(10)^6$
	30	31.1	$1.40(10)^6$
	35	32.9	$1.48(10)^6$
	40	35.5	$1.60(10)^6$
	45	38.6	$1.74(10)^6$
	50	42.4	$1.91(10)^6$
	55	46.3	$2.08(10)^6$
	60	50.7	$2.28(10)^6$
	65	56.2	$2.53(10)^6$
	70	60.1	$2.70(10)^6$
	75	66.7	$3.00(10)^6$
	80	77.5	$3.49(10)^6$
	85	90.7	$4.08(10)^6$
	90	89.7	$4.04(10)^6$

Table 2.10.3-12 – Maximum Package Responses as a Function of Initial Impact Angle (140 ºF Cases)

Drop Height (ft)	Package Orientation (degrees from horizontal)	Impact Acceleration (*g*)	Impact Force (lb)
1	0	12.4	$5.58(10)^5$
	5	4.0	$1.82(10)^5$
	10	3.3	$1.49(10)^5$
	15	3.0	$1.36(10)^5$
	20	2.8	$1.26(10)^5$
	25	2.7	$1.21(10)^5$
	30	2.8	$1.25(10)^5$
	35	3.0	$1.33(10)^5$
	40	3.3	$1.47(10)^5$
	45	3.6	$1.63(10)^5$
	50	3.8	$1.72(10)^5$
	55	4.3	$1.94(10)^5$
	60	5.1	$2.29(10)^5$
	65	6.6	$2.97(10)^5$
	70	7.2	$3.24(10)^5$
	75	8.2	$3.69(10)^5$
	80	10.1	$4.55(10)^5$
	85	14.0	$6.30(10)^5$
	90	28.6	$1.29(10)^6$
30	0	68.9	$3.10(10)^6$
	5	44.3	$1.99(10)^6$
	10	21.8	$9.79(10)^5$
	15	22.5	$1.01(10)^6$
	20	23.6	$1.06(10)^6$
	25	24.9	$1.12(10)^6$
	30	26.1	$1.18(10)^6$
	35	28.2	$1.27(10)^6$
	40	31.3	$1.41(10)^6$
	45	35.2	$1.58(10)^6$
	50	39.6	$1.78(10)^6$
	55	42.4	$1.91(10)^6$
	60	46.1	$2.07(10)^6$
	65	49.9	$2.25(10)^6$
	70	48.9	$2.20(10)^6$
	75	50.1	$2.25(10)^6$
	80	48.5	$2.18(10)^6$
	85	46.9	$2.11(10)^6$
	90	51.1	$2.30(10)^6$

Table 2.10.3-13 – Summary of Impact Limiter Separation Moments

Drop Height (ft)	Impact Limiter Temperature (ºF)	Limiter Separation Moment (in-lb)
1	-20	$2.16(10)^6$
	140	$1.06(10)^6$
30	-20	$2.76(10)^6$
	140	$1.36(10)^6$

Table 2.10.3-14 – Time-History Details from the Maximum Impact Force Condition SLAPDOWN Analyses (NCT, -20 ºF, 1-foot Drop)

θ_o (degrees)	θ (radians)①	$\partial\theta/\partial t$ (rad/sec)②	$\partial^2\theta/\partial t^2$ (rad/sec^2)③	$\partial^2 y/\partial t^2$ (in/sec^2)④	F_{max} (lb)⑤
5	0.0762	-1.10	-68.4	$2.02(10)^3$	$2.34(10)^5$
10	0.159	-1.17	-54.2	$1.62(10)^3$	$1.89(10)^5$
15	0.242	-1.22	-48.2	$1.51(10)^3$	$1.76(10)^5$
20	0.327	-1.26	-43.7	$1.46(10)^3$	$1.71(10)^5$
25	0.411	-1.30	-39.6	$1.43(10)^3$	$1.67(10)^5$
30	0.495	-1.32	-37.0	$1.48(10)^3$	$1.71(10)^5$
35	0.580	-1.33	-34.7	$1.57(10)^3$	$1.85(10)^5$
40	0.667	-1.30	-32.5	$1.70(10)^3$	$1.98(10)^5$
45	0.754	-1.23	-29.8	$1.85(10)^3$	$2.16(10)^5$
50	0.844	-1.11	-26.8	$2.05(10)^3$	$2.39(10)^5$
55	0.937	-0.917	-22.9	$2.28(10)^3$	$2.66(10)^5$
60⑥	1.031	-0.656	-17.9	$2.53(10)^3$	$2.93(10)^5$

Notes:

① Package orientation at moment of maximum force.

② Rotational velocity.

③ Rotational acceleration.

④ Linear acceleration.

⑤ Maximum impact force.

⑥ For orientation angles greater than 60º, the quasi-static program CASKDROP was conservatively used.

Table 2.10.3-15 – Time-History Details from the Maximum Impact Force Condition SLAPDOWN Analyses (HAC, -20 ºF, 30-foot Drop)

θ_o (degrees)	θ (radians)①	$\partial\theta/\partial t$ (rad/sec)②	$\partial^2\theta/\partial t^2$ (rad/sec^2)③	$\partial^2 y/\partial t^2$ (in/sec^2)④	F_{max} (lb)⑤
5	0.0442	-5.16	$-1.74(10)^2$	$1.86(10)^4$	$2.16(10)^6$
10	0.130	-5.34	$-3.66(10)^2$	$1.28(10)^4$	$1.49(10)^6$
15	0.210	-5.48	$-3.44(10)^2$	$1.25(10)^4$	$1.45(10)^6$
20	0.288	-5.62	$-3.01(10)^2$	$1.18(10)^4$	$1.37(10)^6$
25	0.368	-5.74	$-2.94(10)^2$	$1.17(10)^4$	$1.36(10)^6$
30	0.449	-5.87	$-2.85(10)^2$	$1.20(10)^4$	$1.40(10)^6$
35	0.532	-5.99	$-2.83(10)^2$	$1.27(10)^4$	$1.48(10)^6$
40	0.617	-6.07	$-2.85(10)^2$	$1.37(10)^4$	$1.60(10)^6$
45	0.702	-6.16	$-2.88(10)^2$	$1.49(10)^4$	$1.74(10)^6$
50	0.788	-6.26	$-2.88(10)^2$	$1.61(10)^4$	$1.91(10)^6$
55	0.879	-6.14	$-2.94(10)^2$	$1.79(10)^4$	$2.08(10)^6$
60⑥	0.970	-6.05	$-2.96(10)^2$	$1.96(10)^4$	$2.28(10)^6$

Notes:

① Package orientation at moment of maximum force.

② Rotational velocity.

③ Rotational acceleration.

④ Linear acceleration.

⑤ Maximum impact force.

⑥ For orientation angles greater than 60º, the quasi-static program CASKDROP was conservatively used.

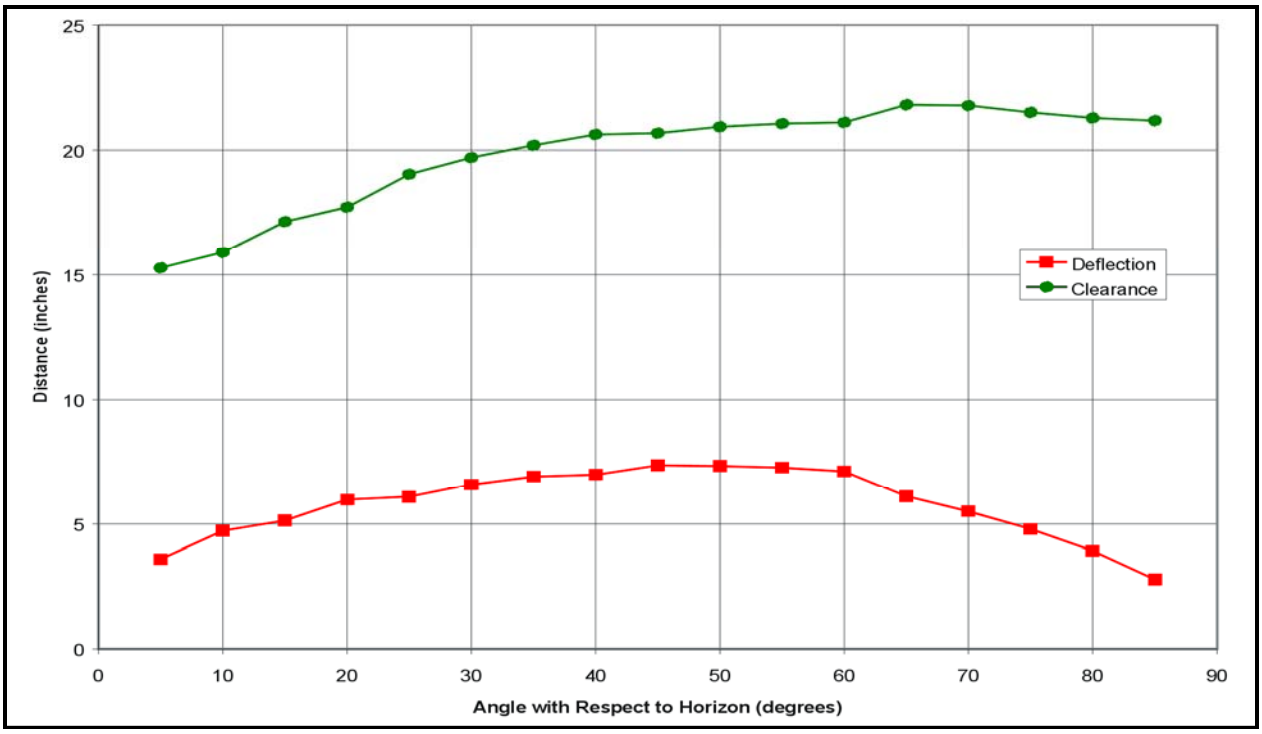

Figure 2.10.3-1 – Impact Limiter Deflection and Residual Clearance for the NCT Oblique Drop, Cold (-20 ºF)

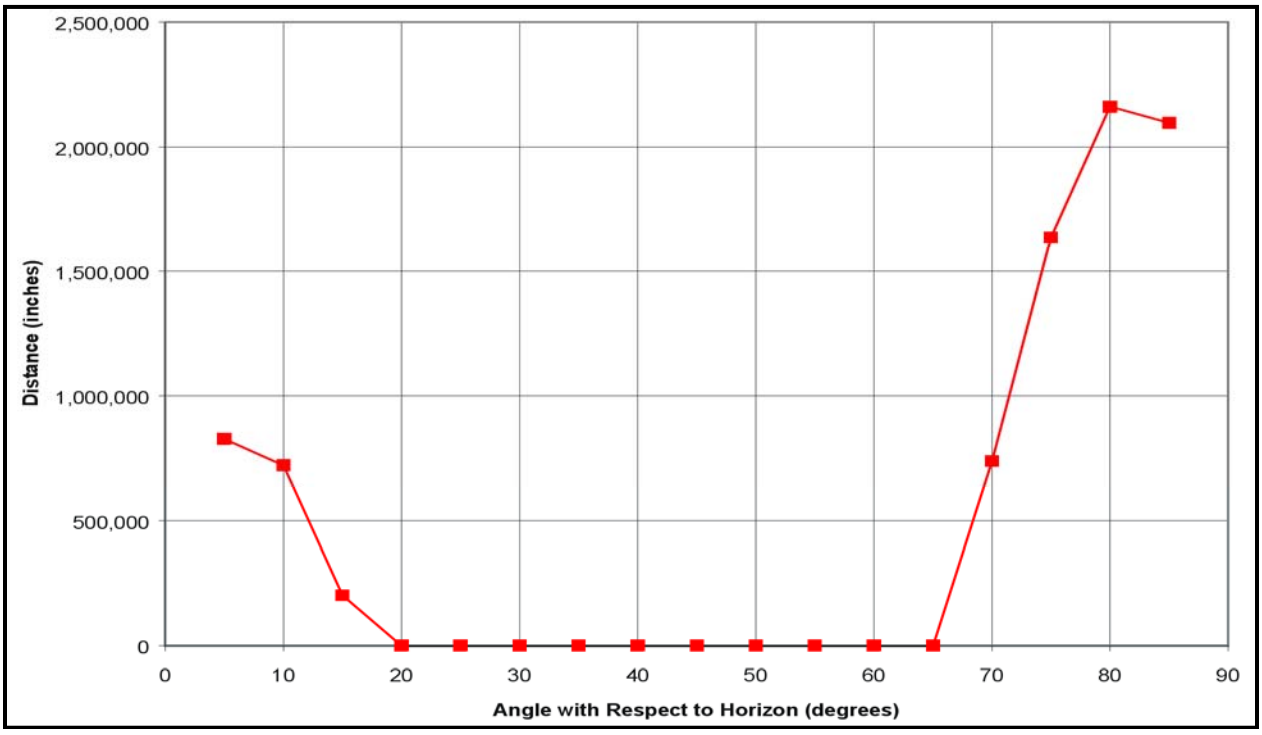

Figure 2.10.3-2 – Impact Limiter Separation Moments for the NCT Oblique Drop, Cold (-20 ºF)

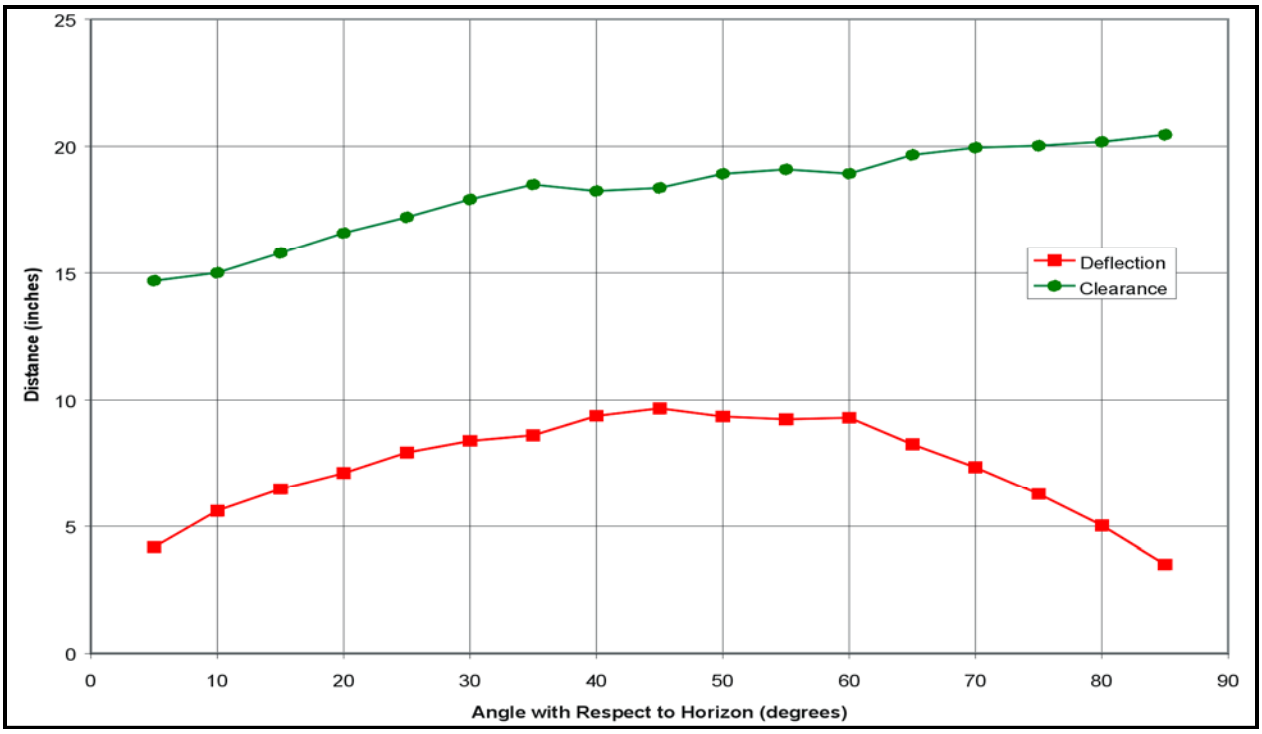

Figure 2.10.3-3 – Impact Limiter Deflection and Residual Clearance for the NCT Oblique Drop, Warm (140 ºF)

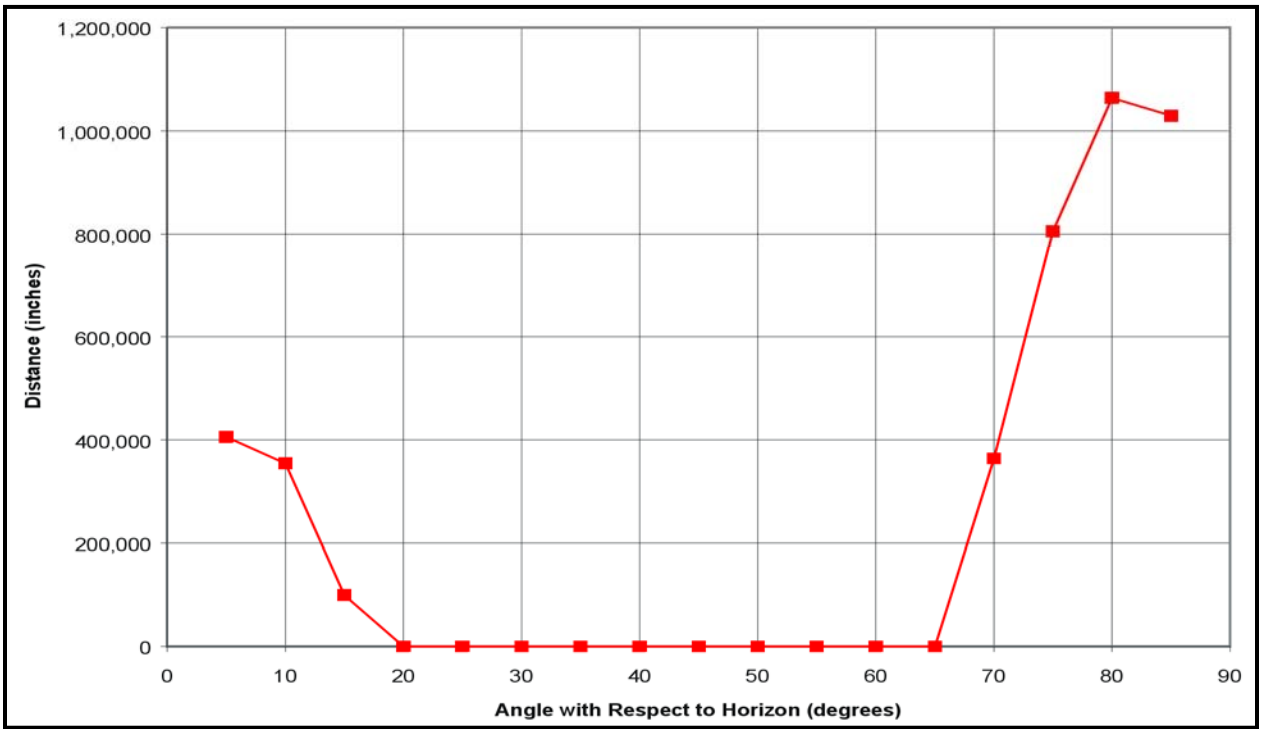

Figure 2.10.3-4 – Impact Limiter Separation Moments for the NCT Oblique Drop, Warm (140 ºF)

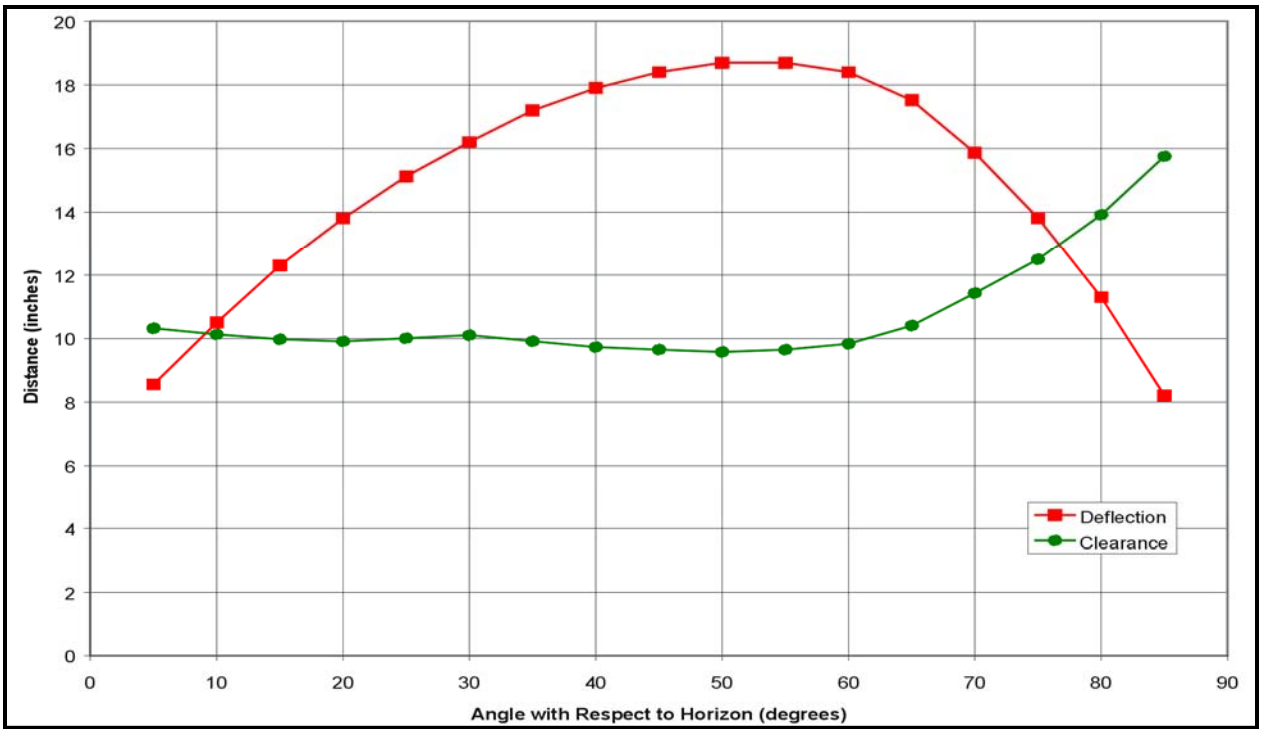

Figure 2.10.3-5 – Impact Limiter Deflection and Residual Clearance for the HAC Oblique Drop, Cold (-20 ºF)

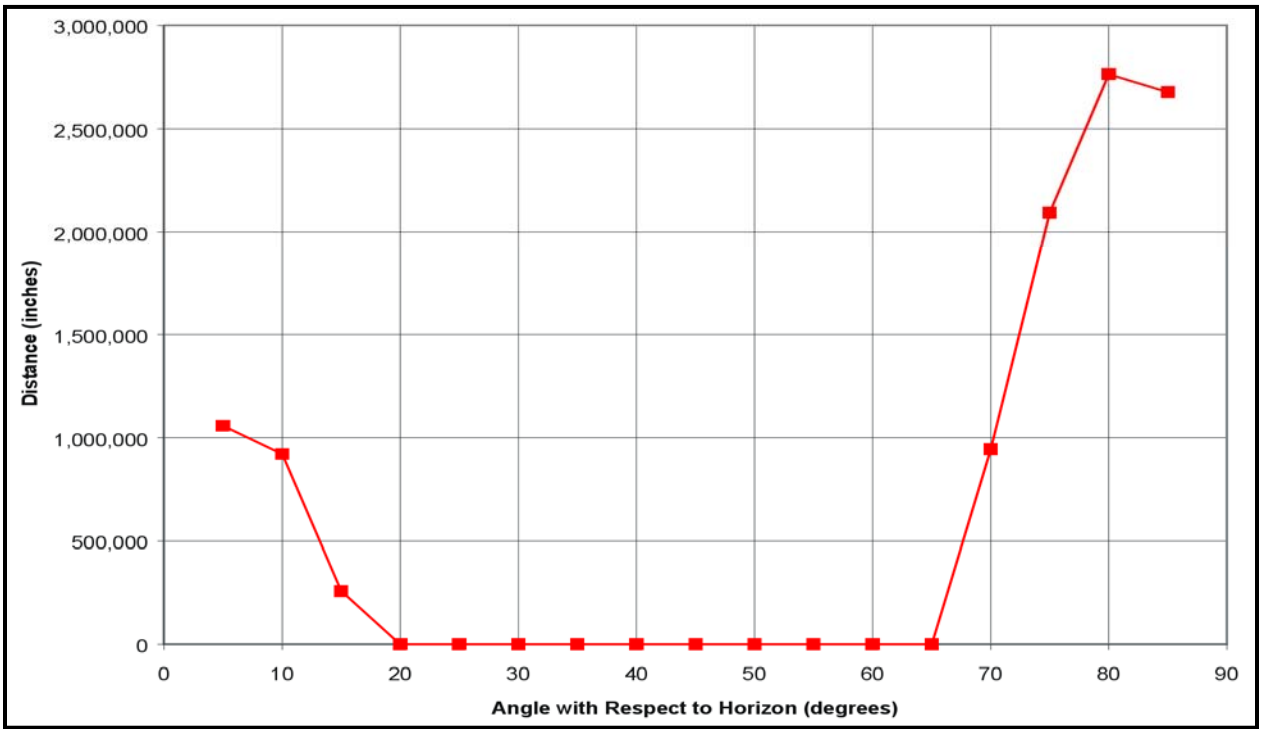

Figure 2.10.3-6 – Impact Limiter Separation Moments for the HAC Oblique Drop, Cold (-20 ºF)

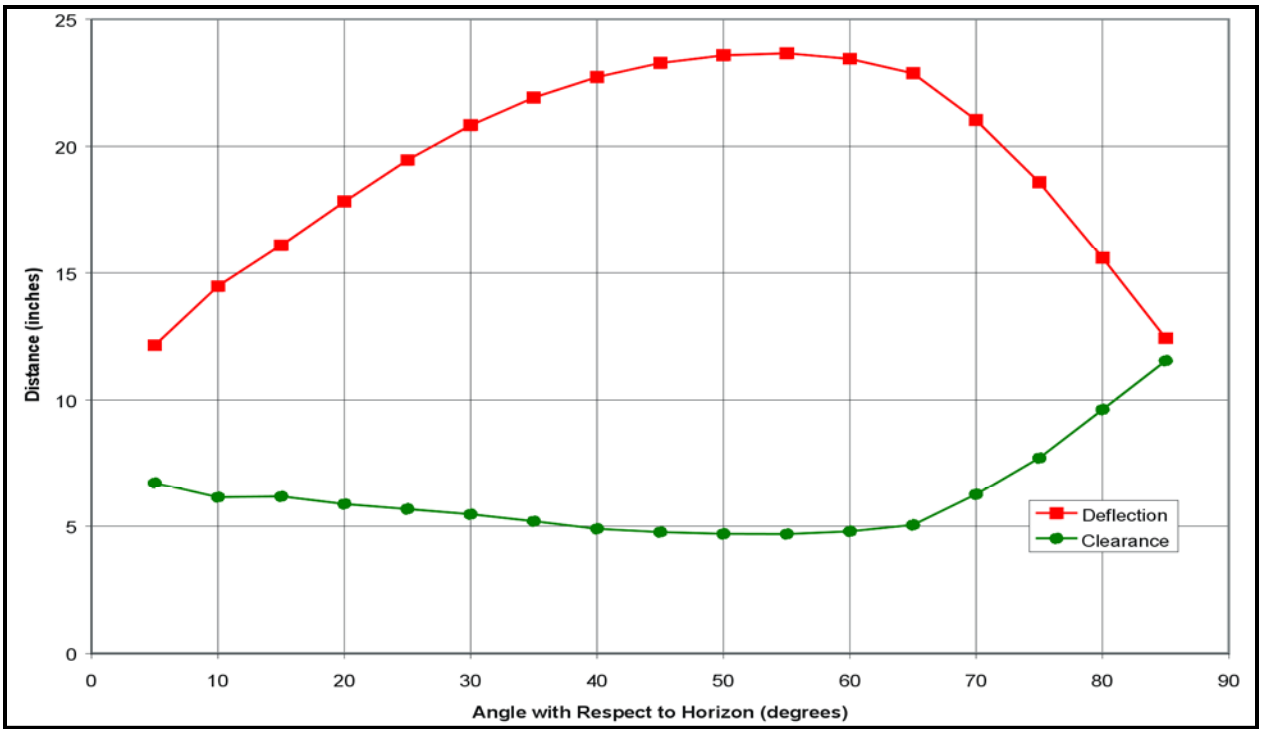

Figure 2.10.3-7 – Impact Limiter Deflection and Residual Clearance for the HAC Oblique Drop, Warm (140 ºF)

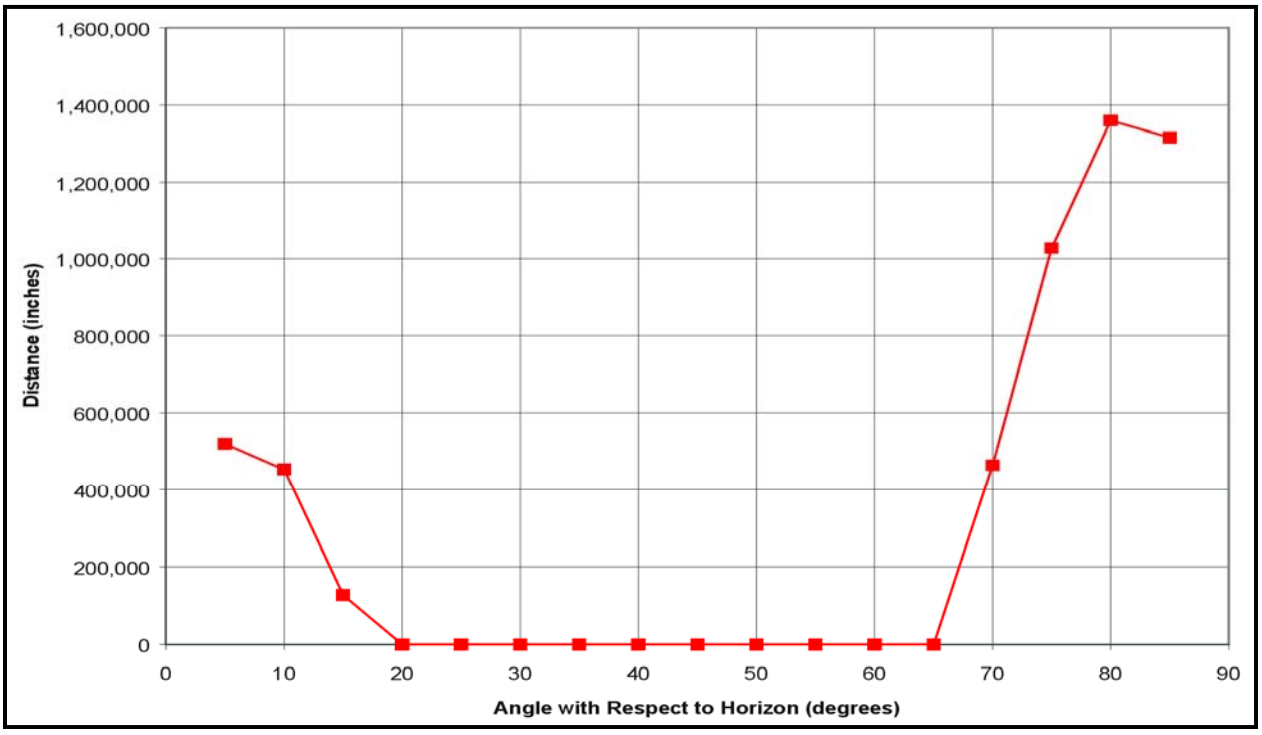

Figure 2.10.3-8 – Impact Limiter Separation Moments for the HAC Oblique Drop, Warm (140 ºF)

2.10.4 Slapdown Assessment

This appendix presents an evaluation of the RH-TRU 72-B package for potential secondary impacts, or slapdowns, following the primary impacts associated with 30-foot corner or oblique drop events. The conclusion reached is that stresses associated with slapdown are within allowable hypothetical accident condition (HAC) stresses. Additionally, impact limiter deformations resulting from slapdown are acceptable as they will not allow "bottoming out" on any package external surface (i.e., trunnions and the package body itself). The basic analytic approach is summarized in Section 2.10.2.2, *Description of the SLAPDOWN Computer Code*.

2.10.4.1 Slapdown Response – Force and Deflection

After an initial impact on the primary limiter, slapdown occurs on the secondary limiter. The secondary impact occurs at an angle very close to horizontal, so the side drop (0º) force deflection curve (calculated by CASKDROP) is used in the analysis. Therefore, the maximum impact force can be obtained by interpolating on the force-deflection curve for the maximum deflection calculated by SLAPDOWN.

Table 2.10.4-1 and Table 2.10.4-2 show secondary impact deformations for 5º, 10º, 15º, and 20º primary impact angles, and corresponding maximum impact forces based on the force-deflection curve for horizontal impact (see Table 2.10.4-3). Calculations are for both cold and warm HAC.

2.10.4.2 Slapdown Response – Maximum Bending Moment

Considering the free-body diagram in Figure 2.10.4-1, the maximum moment occurring in the package as a result of slapdown can be determined.

From force equilibrium:

$$F = m\ddot{y} = \omega_1 L_2$$

or,

$$\omega_1 = \frac{F}{L_2}$$

From moment equilibrium:

$$\frac{FL_2}{2} = 2\left(\frac{\omega_2}{2}\right)\left(\frac{L_2}{2}\right)\left(\frac{2}{3}\right)\left(\frac{L_2}{2}\right) = \frac{\omega_2 L_2^2}{6} = I\ddot{\Theta}$$

or,

$$\omega_2 = \frac{3F}{L_2}$$

Shear and moment as a function of position, x, are given in Table 2.10.4-4. The corresponding shear and moment diagrams are shown in Figure 2.10.4-2 and Figure 2.10.4-3.

The maximum moment is seen to occur at 2/3 the package length, and is equal to $(4/27)FL_2$. The results of this analysis are used in Section 2.10.4.4, *Slapdown Response – Deflections Versus*

Allowable Stress Limits, to show that package stresses associated with this maximum bending moment, as well as axial thrust, are within allowable stress limits.

2.10.4.3 Slapdown Response – Thrust Loadings and Package Stresses

As the previous sections considered slapdown orientations slightly off horizontal, a slight amount of axial thrust can develop in the package. This thrust loading, T, is equal to the slapdown force, F, times the sine of the slapdown orientation angle. In addition, the slapdown moment, $(4/27)FL_2$, determined in Section 2.10.4.2, *Slapdown Response – Maximum Bending Moment*, can be multiplied by the cosine of the slapdown orientation angle. Using these formulas and the impact limiter force data from Section 2.10.4.1, *Slapdown Response – Force and Deflection*, the thrusts and moments due to slapdown are calculated and given in Table 2.10.4-5 and Table 2.10.4-6.

For shallow angle cases, calculated time histories show that primary and secondary impacts overlap during the impact event. Thus, the slapdown force is a superposition of the primary and secondary impacts. For remaining angles, only secondary impact forces are used.

By considering the outer cask (OC) geometry, the effect of the thrust loading on the overall response of the package can be seen to be small. For the OC, per Paragraph (3) in Section 2.6.7.2, *Corner and Oblique Drops*, the cross-sectional area, $A = 292$ in^2, the moment of inertia, $I = 51{,}334$ in^4, and $c = 20.565$ inches.

Per Table 2.1-1 in Section 2.1.2.1.1, *Containment Structures*, the HAC allowable membrane-plus-bending stress, σ_a, is the lesser of $3.6S_m$ (72,000 psi) or S_u (72,600 psi) at 160 ºF. Thus, the allowable stress, σ_a, = 72,000 psi.

Converting the tabulated thrust and moment data to a stress magnitude ($\sigma = T/A + Mc/I$) and computing the margin of safety ($MS = \sigma_a/\sigma - 1$) yields the results given in Table 2.10.4-7 and Table 2.10.4-8.

The lowest margin of safety is +2.60, therefore, the RH-TRU 72-B package is within allowable stress limits for slapdown.

2.10.4.4 Slapdown Response – Deflections Versus Allowable Stress Limits

The impact limiter deflections required to absorb the available slapdown energy were determined in Section 2.10.4.1, *Slapdown Response – Force and Deflection*. A maximum allowable deformation can be established which guarantees that the package body and trunnions are not directly impacted in a slapdown event. This allowable deformation will conservatively equal the distance between the ground and a bottom positioned trunnion during a 0º impact. This allowable can be conservatively applied to all slapdown orientation angles. Based on the package geometry, the maximum allowable deformation will equal 38.000 – 23.695 = 14.305 inches, where 38.000 inches is the impact limiter radius and 23.695 inches is the half-distance across trunnions.

Table 2.10.4-9 compares the allowable deformation with the predicted deformations found in Section 2.10.4.3, *Slapdown Response – Thrust Loadings and Package Stresses*. Only the warm foam case is considered as it results in the maximum impact limiter deformations.

Table 2.10.4-1 – Impact Force and Maximum Deflections for Cold (-20 ºF) HAC Slapdown Cases

Slapdown Orientation (degrees from horizontal)	5º	10º	15º	20º
Force (lb)	$2.13(10)^6$	$2.08(10)^6$	$2.07(10)^6$	$2.06(10)^6$
Deflection (in)	9.23	9.02	9.01	8.95

Table 2.10.4-2 – Impact Force and Maximum Deflections for Warm (140 ºF) HAC Slapdown Cases

Slapdown Orientation (degrees from horizontal)	5º	10º	15º	20º
Force (lb)	$2.30(10)^6$	$2.25(10)^6$	$2.19(10)^6$	$2.20(10)^6$
Deflection (in)	12.93	12.86	12.76	12.77

Table 2.10.4-3 – Force-Deflection Data for Cold (-20 ºF) and Warm (140 ºF) HAC 0º Slapdowns

Deflection (in)	Force at -20 ºF (lb)	Force at 140 ºF (lb)
0.0	0	0
0.5	$1.62(10)^5$	$7.98(10)^4$
1.0	$3.95(10)^5$	$1.94(10)^5$
1.5	$5.72(10)^5$	$2.82(10)^5$
2.0	$6.99(10)^5$	$3.44(10)^5$
2.5	$8.13(10)^5$	$4.00(10)^5$
3.0	$9.28(10)^5$	$4.56(10)^5$
3.5	$1.04(10)^6$	$5.12(10)^5$
4.0	$1.15(10)^6$	$5.66(10)^5$
4.5	$1.25(10)^6$	$6.16(10)^5$
5.0	$1.35(10)^6$	$6.62(10)^5$
5.5	$1.44(10)^6$	$7.07(10)^5$
6.0	$1.53(10)^6$	$7.51(10)^5$
6.5	$1.61(10)^6$	$7.94(10)^5$
7.0	$1.70(10)^6$	$8.35(10)^5$
7.5	$1.77(10)^6$	$8.72(10)^5$
8.0	$1.86(10)^6$	$9.15(10)^5$
8.5	$1.96(10)^6$	$9.64(10)^5$
9.0	$2.07(10)^6$	$1.02(10)^6$
9.5	$2.21(10)^6$	$1.09(10)^6$
10.0	$2.38(10)^6$	$1.17(10)^6$
10.5	$2.58(10)^6$	$1.27(10)^6$
11.0	$2.83(10)^6$	$1.39(10)^6$
11.5	$3.14(10)^6$	$1.54(10)^6$
12.0	$3.55(10)^6$	$1.75(10)^6$
12.5	$4.10(10)^6$	$2.02(10)^6$
13.0	$4.77(10)^6$	$2.34(10)^6$
13.5	$5.53(10)^6$	$2.84(10)^6$
14.0	$6.36(10)^6$	$3.92(10)^6$
14.5	$7.25(10)^6$	$5.80(10)^6$
15.0	$8.19(10)^6$	$8.37(10)^6$
15.5	$9.18(10)^6$	$1.14(10)^7$
16.0	$1.02(10)^7$	$1.49(10)^7$
16.5	$1.13(10)^7$	$1.87(10)^7$

Table 2.10.4-4 – Shear and Moment During Slapdown

Position, x	Shear	Moment
0	0	0
$L_2/6$	(0.2500)F	$(0.02315)FL_2$
$L_2/3$	(0.3333)F	$(0.07407)FL_2$
$L_2/2$	(0.2500)F	$(0.12500)FL_2$
$2L_2/3$	0	$(0.14815)FL_2$
$5L_2/6$	(-0.4166)F	$(0.11574)FL_2$
L_2	(-1.0000)F	0

Table 2.10.4-5 – Thrust and Moment Due to HAC Cold (-20 ºF) Slapdown Cases

θ (degrees from horizontal)	5º	10º	15º	20º
Impact Limiter Force, F, lb	$2.13(10)^6$	$2.08(10)^6$	$2.07(10)^6$	$2.06(10)^6$
Thrust, T = F(sin θ), lb	$1.86(10)^5$	$3.61(10)^5$	$5.36(10)^5$	$7.05(10)^5$
Moment, $M = (0.14815)FL_2(\cos\theta)$, in-lb①	$4.46(10)^7$	$4.30(10)^7$	$4.20(10)^7$	$4.07(10)^7$

Notes:

① $L_2 = 141.75$ inches.

Table 2.10.4-6 – Thrust and Moment Due to HAC Warm (140 ºF) Slapdown Cases

θ (degrees from horizontal)	5º	10º	15º	20º
Impact Limiter Force, F, lb	$2.30(10)^6$	$2.25(10)^6$	$2.19(10)^6$	$2.20(10)^6$
Thrust, T = F(sin θ), lb	$2.00(10)^5$	$3.91(10)^5$	$5.67(10)^5$	$7.52(10)^5$
Moment, $M = (0.14815)FL_2(\cos\theta)$, in-lb①	$4.81(10)^7$	$4.65(10)^7$	$4.44(10)^7$	$4.34(10)^7$

Notes:

① $L_2 = 141.75$ inches.

Table 2.10.4-7 – Stresses and Margins of Safety Due to HAC Cold (-20 ºF) Slapdown

θ (degrees from horizontal)	5º	10º	15º	20º
T/A, psi	636	$1.24(10)^3$	$1.83(10)^3$	$2.41(10)^3$
Mc/I, psi	$1.79(10)^4$	$1.72(10)^4$	$1.68(10)^4$	$1.63(10)^4$
σ = T/A + Mc/I, psi	$1.85(10)^4$	$1.85(10)^4$	$1.87(10)^4$	$1.87(10)^4$
MS = $\sigma_a/\sigma - 1$	+2.89	+2.90	+2.86	+2.85

Table 2.10.4-8 – Stresses and Margins of Safety Due to HAC Warm (140 ºF) Slapdown

θ (degrees from horizontal)	5º	10º	15º	20º
T/A, psi	687	$1.34(10)^3$	$1.94(10)^3$	$2.58(10)^3$
Mc/I, psi	$1.93(10)^4$	$1.86(10)^4$	$1.78(10)^4$	$1.74(10)^4$
σ = T/A + Mc/I, psi	$2.00(10)^4$	$2.00(10)^4$	$1.97(10)^4$	$2.00(10)^4$
MS = $\sigma_a/\sigma - 1$	+2.61	+2.60	+2.65	+2.61

Table 2.10.4-9 – Comparison of Allowable and Predicted Deformations for Warm (140 ºF) Slapdown

θ (degrees from horizontal)	5º	10º	15º	20º
Allowable Deformation, inches	14.305	14.305	14.305	14.305
Deformation, inches	12.93	12.86	12.760	12.77
Clearance, inches	1.375	1.445	1.545	1.535

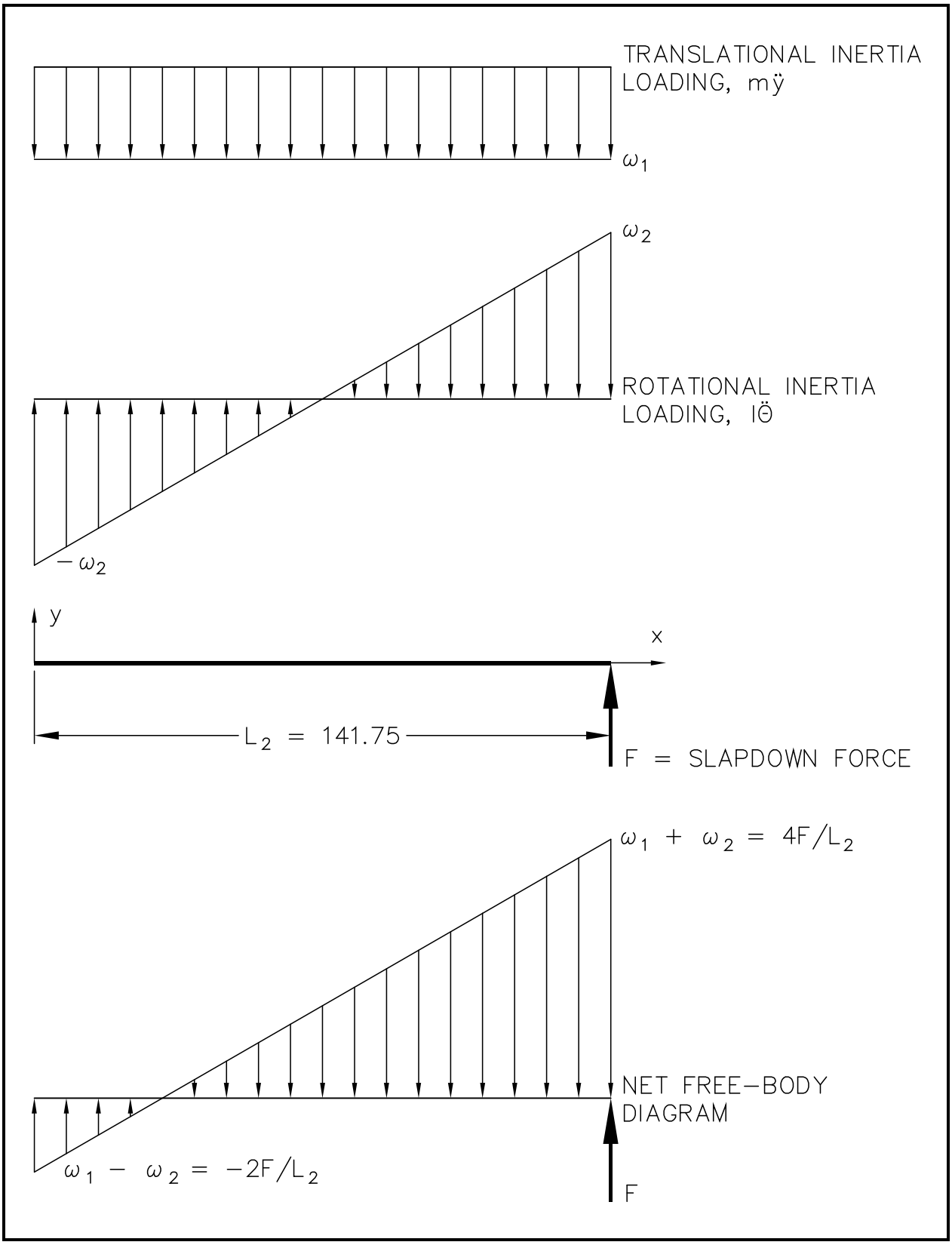

Figure 2.10.4-1 – Free-Body Diagram for Slapdown Loads

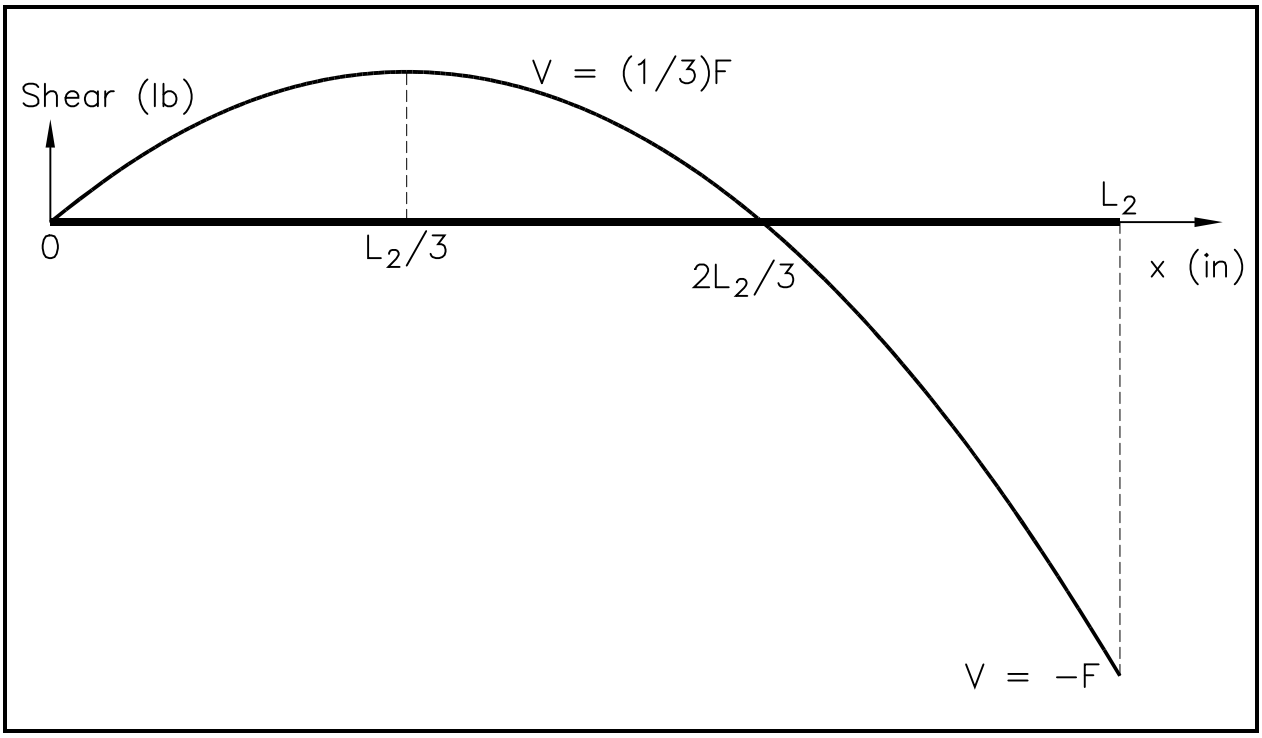

Figure 2.10.4-2 – Shear Diagram for Package During Slapdown

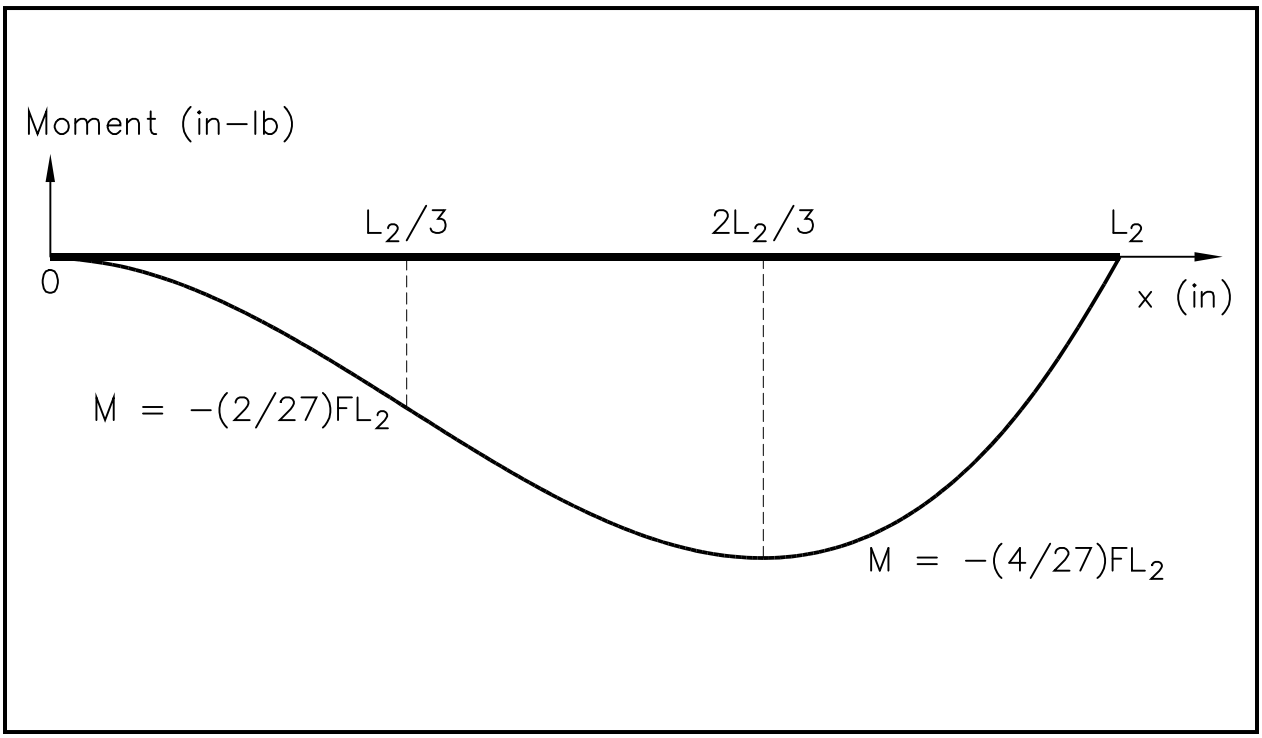

Figure 2.10.4-3 – Moment Diagram for Package During Slapdown

2.10.5 Buckling Design Criteria and Detailed Evaluation

The buckling criteria selected for use in analyzing the RH-TRU 72-B package is that presented in Code Case N-284[1] of the ASME Boiler and Pressure Vessel Code. By demonstrating that the requirements specified in ASME Code Case N-284[1] are met, the buckling requirement of Paragraph C.5 of Regulatory Guide 7.6[2] (i.e., buckling should not occur as the result of any normal or accident condition loading) is considered to have been satisfied. Consistent with Regulatory Guide 7.6 philosophy, ASME Code Level A service condition allowables are used for Regulatory Guide 7.6 defined normal conditions of transport (NCT), and ASME Level D service condition allowables are used for hypothetical accident conditions (HAC) in performing the buckling assessment. It is also noted that Paragraph F-1331.5(c) in Appendix F of the ASME Code[3] (for Level D Service Loadings) specifically identifies use of "a Code Case for metal containment shell buckling" as an acceptable means of addressing buckling issues.

ASME Code Case N-284 addresses both elastic and inelastic buckling and employs a factor of safety of 2.0 for Level A (NCT) conditions and a factor of safety of 1.34 for Level D (HAC) conditions. Interaction equations are employed which account for the effect of combined hoop compressive, axial compressive, and in plane shear loadings. The basic analytic approach is summarized as follows.

1. Theoretical elastic buckling stresses are determined using classical theory.

2. Capacity reduction factors are applied which account for the difference between classical theory and predicted instability stresses for fabricated shells.

3. Plasticity reduction factors are applied for those cases where elastically determined buckling stresses are above the proportional limit.

4. Elastic and inelastic buckling checks which employ appropriate factors of safety and appropriate interaction equations are made using worst case applied compressive and in-plane shear stresses.

All terminology used herein is consistent with that in ASME Code Case N-284[1].

2.10.5.1 Theoretical Elastic Buckling Stresses

The geometry and geometric parameters and the material property data required to carry out the buckling evaluation are presented in Table 2.10.5-1 and Table 2.10.5-2. Using this data, Table 2.10.5-3 and Table 2.10.5-4 are developed to give stress values as a function of the modulus of elasticity, E, as a temperature-dependent property, and Table 2.10.5-4 gives the stresses at the temperatures of interest. The basic equations used in the development of these two tables are

[1] American Society of Mechanical Engineers (ASME) Boiler and Pressure Vessel Code, Section III, *Rules for Construction of Nuclear Power Plant Components*, Division 1, Class MC, Code Case N-284, *Metal Containment Shell Buckling Design Methods*, August 25, 1980.

[2] U. S. Nuclear Regulatory Commission, Regulatory Guide 7.6, *Design Criteria for the Structural Analysis of Shipping Package Containment Vessels*, Revision 1, March 1978.

[3] American Society of Mechanical Engineers (ASME) Boiler and Pressure Vessel Code, Section III, *Rules for Construction of Nuclear Power Plant Components*, Division 1, Subsection NB and Appendices, 1986 Edition.

directly available from Paragraph –1712 of ASME Code Case N-284[1], and are summarized below (note the capacity reduction factors, C_i, are geometric dependent parameters).

a) For Axial Compression, the theoretical axial buckling stress, $\sigma_{\phi eL}$, is:

$$\sigma_{\phi eL} = C_\phi \frac{Et}{R}$$

where:

$$C_\phi = \frac{0.904}{M_\phi^2} + (0.1013)M_\phi^2 \qquad \text{if } 1.5 \le M_\phi < 1.73$$

$$C_\phi = 0.605 \qquad \text{if } M_\phi \ge 1.73$$

Note: The theoretical elastic buckling stress for axial compression of cylinders is also directly applicable for the case of bending of cylinders per ASME Code Case N-284[1].

b) For External Pressure:

i) No End Pressure ($\sigma_\phi = 0$), the theoretical hoop buckling stress for case of no end pressure, $\sigma_{\theta eL}$, is:

$$\sigma_{\theta eL} = \sigma_{reL} = C_{\theta r} \frac{Et}{R}$$

where:

$$C_{\theta r} = \frac{2.41}{M_\phi^{1.49} - 0.338} \qquad \text{if } 1.5 \le M_\phi < 3.0$$

$$C_{\theta r} = \frac{0.92}{M_\phi - 1.17} \qquad \text{if } 3.0 \le M_\phi < (1.65)(R/t)$$

$$C_{\theta r} = (0.275)\left(\frac{t}{R}\right) + \left(\frac{2.1}{M_\phi^4}\right)\left(\frac{R}{t}\right)^3 \qquad \text{if } M_\phi \ge (1.65)(R/t)$$

ii) ii. End Pressure Included ($\sigma_\phi = ½\sigma_\theta$), the theoretical hoop buckling stress for case of end pressure included, $\sigma_{\theta eL}$, is:

$$\sigma_{\theta eL} = \sigma_{heL} = C_{\theta h} \frac{Et}{R}$$

where:

$$C_{\theta h} = \frac{1.08}{M_\phi^{1.07} - 0.45} \qquad \text{if } 1.5 \le M_\phi < 3.0$$

$$C_{\theta h} = \frac{0.92}{M_\phi - 0.636} \qquad \text{if } 3.0 \le M_\phi < (1.65)(R/t)$$

$$C_{\theta h} = (0.275)\left(\frac{t}{R}\right) + \left(\frac{2.1}{M_\phi^4}\right)\left(\frac{R}{t}\right)^3 \quad \text{if } M_\phi \geq (1.65)(R/t)$$

c) For Shear, the theoretical in-plane shear buckling stress, $\sigma_{\phi\theta eL}$, is:

$$\sigma_{\phi\theta eL} = C_{\phi\theta}\frac{Et}{R}$$

where:

$$C_{\phi\theta} = \left(\frac{4.82}{M_\phi^2}\right)\sqrt{1+(0.0239)M_\phi^3} \quad \text{if } 1.5 \leq M_\phi < 26$$

$$C_{\phi\theta} = \frac{0.746}{\sqrt{M_\phi}} \quad \text{if } 26 \leq M_\phi < (8.69)(R/t)$$

$$C_{\phi\theta} = 0.253\sqrt{\frac{t}{R}} \quad \text{if } M_\phi \geq (8.69)(R/t)$$

2.10.5.2 Capacity Reduction Factors

Capacity reduction factors which account for the difference between classical theory and predicted instability stresses for fabricated shells are directly determined using Paragraph –1500 of ASME Code Case N-284[1]. For the RH-TRU 72-B package shell geometries, the basic governing equations are as follows.

a) For Axial Compression, the larger of (i) or (ii) is used:

i) Effect of R/t:

$$\alpha_{\phi L} = 0.207 \quad \text{if } R/t \geq 600$$

$$\alpha_{\phi L} = 1.52 - (0.473)\log_{10}(R/t) \quad \text{if } R/t < 600 \text{ (use smaller value)}$$

$$\alpha_{\phi L} = (10^{-5})\sigma_y - 0.033 \quad \text{if } R/t < 600 \text{ (use smaller value)}$$

ii) Effect of Length:

$$\alpha_{\phi L} = 0.837 - (0.14)M \quad \text{if } 1.5 \leq M < 1.73$$

$$\alpha_{\phi L} = \frac{0.837}{M^{0.6}} \quad \text{if } 1.73 \leq M < 10$$

$$\alpha_{\phi L} = 0.207 \quad \text{if } M \geq 10$$

Note: The capacity reduction factor for cylinders under axial compression is also employed for the case of bending of cylinders. This is slightly conservative based on an inspection of Figure 10-9 and Figure 10-13 of ASME Code Case N-284[1]. In other words, advantage is not taken of the fact that the critical buckling stress for cylinders under axial compression is slightly less than the critical buckling stress for cylinders in bending.

b) For Hoop Compression:

$$\alpha_{\theta L} = 0.8$$

c) For Shear:

$$\alpha_{\phi\theta L} = 0.8 \qquad \text{if } R/t \le 250$$

$$\alpha_{\phi\theta L} = 1.323 - (0.218)\log_{10}(R/t) \qquad \text{if } 250 < R/t < 1000$$

Direct application of these equations results in the capacity reduction factors presented in Table 2.10.5-5 as a function of temperature.

In order to directly use the above defined capacity reduction factors, the tolerance requirements of Paragraph NE-4220 of the ASME Code[4] must be met. Per Paragraph NE-4221.1 and Paragraph NE-4221.2, limits on "maximum difference in cross-sectional diameters" and "maximum deviation from true theoretical form for external pressure" must be met. Per the general arrangement drawing in Appendix 1.3.1, *Packaging General Arrangement Drawings*, these requirements are met for the outer cask (OC) outer and inner shells, and inner vessel (IV) shell.

2.10.5.3 Plasticity Reduction Factors

Plasticity reduction factors for cases where the elastically determined buckling stresses are above the proportional limit are directly determined using Paragraph –1600 of ASME Code Case N-284[1]. The magnitude of the reduction factor is directly related to the magnitude of the applied compressive or in-plane shear stress, σ_i, as indicated by the applicable equations below.

a) For Axial Compression:

$$\eta_\phi = 1.0 \qquad \text{if } \sigma_\phi(FS)/\sigma_y \le 0.55$$

$$\eta_\phi = \frac{0.18}{1 - \dfrac{(0.45)\sigma_y}{(FS)\sigma_\phi}} \qquad \text{if } 0.55 < \sigma_\phi(FS)/\sigma_y \le 0.738$$

$$\eta_\phi = 1.31 - \frac{(1.15)\sigma_\phi(FS)}{\sigma_y} \qquad \text{if } 0.738 < \sigma_\phi(FS)/\sigma_y \le 1.0$$

b) For Hoop Compression:

$$\eta_\theta = 1.0 \qquad \text{if } \sigma_\theta(FS)/\sigma_y \le 0.67$$

$$\eta_\theta = 2.53 - \frac{(2.29)\sigma_\theta(FS)}{\sigma_y} \qquad \text{if } 0.67 < \sigma_\theta(FS)/\sigma_y \le 1.0$$

c) For Shear:

$$\eta_{\phi\theta} = 1.0 \qquad \text{if } \sigma_{\phi\theta}(FS)/\sigma_y \le 0.48$$

[4] American Society of Mechanical Engineers (ASME) Boiler and Pressure Vessel Code, Section III, *Rules for Construction of Nuclear Power Plant Components*, Division 1, Subsection NE, 1986 Edition.

$$\eta_{\phi\theta} = \frac{0.1}{1 - \frac{(0.43)\sigma_y}{(FS)\sigma_{\phi\theta}}} \qquad \text{if } 0.48 < \sigma_{\phi\theta}(FS)/\sigma_y \leq 0.6$$

As plasticity reduction factors depend directly on applied compressive or in-plane shear stress magnitudes, numerical values for reduction factors cannot be presented at this point in the evaluation.

2.10.5.4 Development of Upper-Bound Magnitudes for Compressive Stresses and In-Plane Shear Stresses

Per Paragraph –1600 of ASME Code Case N-284[1], as an upper limit, σ_ϕ and σ_θ must be less than σ_y divided by the applicable Factor of Safety (FS). Similarly, for shear, $\sigma_{\phi\theta}$ must be less than or equal to $(0.6)\sigma_y$ divided by the applicable Factor of Safety (FS). With a Factor of Safety of 2.0 for NCT, and 1.34 for HAC, the maximum (upper-bound) permitted values for elastically determined axial, σ_ϕ, or hoop, σ_θ, compressive stresses, and for shear, $\sigma_{\phi\theta}$, are presented in Table 2.10.5-6. Under no circumstances can these upper-bound limits be exceeded. However, satisfying these limits alone is not sufficient to demonstrate that buckling will not occur. As discussed in Section 2.10.5.5, *Interaction Equations*, interaction equations must also be satisfied.

2.10.5.5 Interaction Equations

Elastic and inelastic interaction equations must be satisfied for all states of compressive and in-plane shear stress. The interaction equations for cylindrical shells are directly available from Paragraphs –1713.1.1 and –1713.2.1 of ASME Code Case N-284[1]. Once a stress state is established for a specific shell, plasticity reduction factors can be determined and all appropriate interaction equations checked.

Elastic interaction equations must be satisfied, and if any of the uniaxial critical stress values exceed the proportional limit of the fabricated material, the inelastic interaction equations must also be satisfied.

2.10.5.6 Stress Summary

Applied compressive membrane and in-plane shear stresses for each load condition and for each shell of the RH-TRU 72-B package are summarized in Table 2.10.5-7, Table 2.10.5-8, and Table 2.10.5-9. Appropriate worst-case combinations of these stresses are provided in Table 2.10.5-10, Table 2.10.3-11, and Table 2.10.5-12, thus allowing plasticity reduction factors to be explicitly determined and interaction equations to be checked.

In general, stresses provided in the tables correspond to cold condition (-20 ºF) impact loadings, whereas buckling checks are conservatively performed at upper bound shell temperatures of 160 ºF. The only exceptions to this are for the cases of HAC oblique and side drops, where for the OC outer shell and IV shell, advantage is taken of the lower impact loadings associated with hot conditions. For these two cases, both hot and cold conditions are specifically checked for potential buckling. In addition, with one exception (see below), all buckling checks of the OC shells ignore lead shrinkage induced stresses. This is done recognizing the displacement limited nature of these stresses (i.e., if buckling modes were to initiate, lead-induced stresses would be relieved). More

significantly, if lead is in direct contact with a shell, the shell buckling modes are significantly altered and the presence of the surrounding lead is actually of much more benefit to increasing the buckling resistance of the shell than are the detrimental effects of any imposed displacement limited stresses. This is especially true for the RH-TRU 72-B OC, given the relatively low magnitude of lead shrinkage-induced stresses reported in Appendix 2.10.8, *Fabrication Stresses Due to Lead Pour* (as summarized in Appendix 2.10.8.8, *Summary*). Further, due to creep effects, the actual initial stress state for the OC shells associated with differential expansion of the lead and shells is dependent on the specific thermal cycle history of a package. As such, any beneficial lead shrinkage-induced shell support may have fully crept away prior to a hypothesized drop event. Given the above, lead shrinkage-induced stresses are generally ignored herein, and no benefit is taken for the presence of lead improving buckling resistance. The only exception is for the case of end drop, where the stress analyses from Section 2.6.7, *Free Drop*, and Section 2.7.1, *Free Drop*, do not readily allow removal of lead-induced axial stresses. Thus, for end drop, lead-induced axial compressive stresses are conservatively included, without taking any advantage of their beneficial effect on increased buckling resistance.

2.10.5.7 Detailed Buckling Evaluations, Plasticity Reduction Factor Determinations, and Interaction Equation Checks

By using the worst-case load combinations available in Table 2.10.5-10, Table 2.10.3-11, and Table 2.10.5-12, and the various data available in previous sections, the methods outlined in ASME Code Case N-284[1] can be directly applied to the RH-TRU 72-B package shells. By way of example, Load Combination 6 for the OC inner shell (Table 2.10.5-10) is considered as follows. The step-by-step procedure is that specified in Paragraph –1800 of ASME Code Case N-284[1].

Step 1: Stresses for each specified loading are per Table 2.10.5-7 herein. The specified loadings for Load Combination 6 are NCT differential expansion and HAC oblique drop at 160 ºF.

Step 2: Combined stresses are per Table 2.10.5-10 herein. For Load Combination 6, the combined stresses are:

$$\sigma_\phi = 17{,}049 \text{ psi}$$
$$\sigma_\theta = 724 \text{ psi}$$
$$\sigma_{\phi\theta} = 4{,}796 \text{ psi}$$

Step 3: For HAC, the Factor of Safety (FS) is 1.34. Multiplying the stress components by this Factor of Safety yields:

$$(FS)\sigma_\phi = 22{,}846 \text{ psi}$$
$$(FS)\sigma_\theta = 970 \text{ psi}$$
$$(FS)\sigma_{\phi\theta} = 6{,}427 \text{ psi}$$

Step 4: Capacity reduction factors are available from Section 2.10.5.2, *Capacity Reduction Factors*, and are as follows for Load Combination 6 at a temperature of 160 ºF.

$$\alpha_{\phi L} = 0.237$$
$$\alpha_{\theta L} = 0.8$$
$$\alpha_{\phi\theta L} = 0.8$$

Step 5: Plasticity reduction factors are determined using the equations presented in Section 2.10.5.3, *Plasticity Reduction Factors*, as follows, (the yield strength, σ_y, at 160 ºF is available from Table 2.10.5-2).

a) For axial compression:

$$\frac{(FS)\sigma_\phi}{\sigma_y} = \frac{22{,}846}{27{,}000} = 0.846 \Rightarrow \eta_\phi = 1.31 - \frac{(1.15)(FS)\sigma_\phi}{\sigma_y} = 1.31 - \frac{(1.15)(22{,}846)}{27{,}000} = 0.337$$

b) For hoop compression:

$$\frac{(FS)\sigma_\theta}{\sigma_y} = \frac{970}{27{,}000} = 0.036 \quad \Rightarrow \quad \eta_\theta = 1.0$$

c) For shear:

$$\frac{(FS)\sigma_{\phi\theta}}{\sigma_y} = \frac{6{,}427}{27{,}000} = 0.238 \quad \Rightarrow \quad \eta_\theta = 1.0$$

Step 6: Compute the elastic stress components:

$$\sigma_{\phi s} = \frac{(FS)\sigma_\phi}{\alpha_{\phi L}} = \frac{22{,}846}{0.237} = 96{,}397 \text{ psi}$$

$$\sigma_{\theta s} = \frac{(FS)\sigma_\theta}{\alpha_{\theta L}} = \frac{970}{0.8} = 1{,}213 \text{ psi}$$

$$\sigma_{\phi\theta s} = \frac{(FS)\sigma_{\phi\theta}}{\alpha_{\phi\theta L}} = \frac{6{,}427}{0.8} = 8{,}034 \text{ psi}$$

Step 7: Compute the inelastic stress components:

$$\sigma_{\phi p} = \frac{\sigma_{\phi s}}{\eta_\phi} = \frac{96{,}397}{0.337} = 286{,}045 \text{ psi}$$

$$\sigma_{\theta p} = \frac{\sigma_{\theta s}}{\eta_\theta} = \frac{1{,}213}{1.0} = 1{,}213 \text{ psi}$$

$$\sigma_{\phi\theta p} = \frac{\sigma_{\phi\theta s}}{\eta_{\phi\theta}} = \frac{8{,}034}{1.0} = 8{,}034 \text{ psi}$$

Step 8: For the RH-TRU 72-B package, the buckling evaluation approach consistent with the vessel design and method of analysis is that of Paragraph –1710 of ASME Code Case N-284[1].

Step 9: The following assumptions apply to the buckling analyses:

a) Discontinuity stresses from NCT differential expansion are included and conservatively used without any modification.

b) No corrections are made for discontinuity stresses.

c) Classical uniaxial buckling values are available from Section 2.10.5.1, *Theoretical Elastic Buckling Stresses*. For the OC inner shell at 160 ºF, these classical values are as follows:

$$\sigma_{\phi eL} = 1{,}007{,}722 \text{ psi}$$
$$\sigma_{\theta eL} = \sigma_{reL} = 48{,}400 \text{ psi}$$
$$\sigma_{\theta eL} = \sigma_{heL} = 48{,}400 \text{ psi}$$
$$\sigma_{\phi\theta eL} = 228{,}071 \text{ psi}$$

d) Applicable elastic and inelastic interaction equations in Paragraph –1713.1.1 and Paragraph –1713.2.1 of ASME Code Case N-284[1] are checked as follows:

i) Elastic buckling per Paragraph –1713.1.1 of ASME Code Case N-284[1]:

(a) Axial compression-plus-hoop compression ($\sigma_{\phi s} < \frac{1}{2}\sigma_{\theta s}$):

Not Applicable (n/a)

(b) Axial compression-plus-hoop compression ($\sigma_{\phi s} \geq \frac{1}{2}\sigma_{\theta s}$):

$$\frac{\sigma_{\phi s} - \frac{1}{2}\sigma_{heL}}{\sigma_{\phi eL} - \frac{1}{2}\sigma_{heL}} + \left(\frac{\sigma_{\theta s}}{\sigma_{heL}}\right)^2 \leq 1.0$$

$$\frac{96{,}397 - \frac{1}{2}(48{,}400)}{1{,}007{,}722 - \frac{1}{2}(48{,}400)} + \left(\frac{1{,}213}{48{,}400}\right)^2 = 0.074 \leq 1.0$$

(c) Axial compression-plus-shear:

$$\frac{\sigma_{\phi s}}{\sigma_{\phi eL}} + \left(\frac{\sigma_{\phi\theta s}}{\sigma_{\phi\theta eL}}\right)^2 \leq 1.0$$

$$\frac{96{,}397}{1{,}007{,}722} + \left(\frac{8{,}034}{228{,}071}\right)^2 = 0.097 \leq 1.0$$

(d) Hoop compression-plus-shear:

$$\frac{\sigma_{\theta s}}{\sigma_{reL}} + \left(\frac{\sigma_{\phi\theta s}}{\sigma_{\phi\theta eL}}\right)^2 \leq 1.0$$

$$\frac{1{,}213}{48{,}400} + \left(\frac{8{,}034}{228{,}071}\right)^2 = 0.026 \leq 1.0$$

(e) Axial compression-plus-hoop compression-plus-shear:

$$K = 1 - \left(\frac{\sigma_{\varphi\theta s}}{\sigma_{\varphi\theta eL}}\right)^2 = 1 - \left(\frac{8{,}034}{228{,}071}\right)^2 \approx 1.00$$

and equations **(a)** and **(b)** above remain unchanged.

ii) Inelastic buckling per Paragraph –1713.2.1 of ASME Code Case N-284[1]:

(a) Axial compression:

$$\frac{\sigma_{\phi p}}{\sigma_{\phi eL}} \le 1.0 \quad \Rightarrow \quad \frac{286{,}045}{1{,}007{,}722} = 0.284 \le 1.0$$

(b) Hoop compression:

$$\frac{\sigma_{\theta p}}{\sigma_{\theta eL}} \le 1.0 \quad \Rightarrow \quad \frac{1{,}213}{48{,}400} = 0.025 \le 1.0$$

(c) Axial compression-plus-shear:

$$\left(\frac{\sigma_{\phi p}}{\sigma_{\phi eL}}\right)^2 + \left(\frac{\sigma_{\phi\theta p}}{\sigma_{\phi\theta eL}}\right)^2 \le 1.0$$

$$\left(\frac{286{,}045}{1{,}007{,}722}\right)^2 + \left(\frac{8{,}034}{228{,}071}\right)^2 = 0.082 \le 1.0$$

(d) Hoop compression-plus-shear:

$$\left(\frac{\sigma_{\theta p}}{\sigma_{reL}}\right)^2 + \left(\frac{\sigma_{\phi\theta p}}{\sigma_{\phi\theta eL}}\right)^2 \le 1.0$$

$$\left(\frac{1{,}213}{48{,}400}\right)^2 + \left(\frac{8{,}034}{228{,}071}\right)^2 = 0.002 \le 1.0$$

(e) Stiffeners not needed:

As all interaction equations are satisfied and there are no concentrated loads on the shell that cause localized buckling, buckling of the OC inner shell will not occur.

Table 2.10.5-13 summarizes results from the interaction equations for all shells under the worst-case load combinations. As shown, all interaction equations yield values less than 1.0; thus, it is concluded that buckling will not occur for any RH-TRU 72-B package shell component.

Table 2.10.5-1 – Geometry, Geometric Parameters, and Material Data Used in Buckling Evaluations

Parameter	Outer Cask		Inner Vessel
	Outer Shell	Inner Shell	
R (radius, inches)	19.815	16.69	15.8125
t (thickness, inches)	1.5	1.0	0.375
$(Rt)^{0.5}$	5.45	4.085	2.435
L_ϕ (length, inches)	121.62	121.25	111.75
$L_\theta = 2\pi R$ (circumference, inches)	124.5	104.87	99.35
$M_\phi = L_\phi/(Rt)^{0.5}$	22.31	29.68	45.89
$M_\theta = L_\theta/(Rt)^{0.5}$	22.84	25.67	40.80
M (lesser of M_ϕ or M_θ)	22.31	25.67	40.80
μ (Poisson's ratio)	0.3	0.3	0.3
E (Young's modulus, psi)	Temperature Dependent①		
σ_y (yield strength, psi)	Temperature Dependent①		

Notes:

① Potential temperatures of interest are -20 ºF, 70 ºF, and 160 ºF (see Table 2.10.5-2).

Table 2.10.5-2 – Temperature Dependent Material Properties for Type 304 Stainless Steel

Parameter	Temperature		
	-20 ºF	70 ºF	160 ºF
E (Young's modulus, psi)	$28.8(10)^6$	$28.3(10)^6$	$27.8(10)^6$
σ_y (yield strength, psi)	36,000①	31,500①	27,000

Notes:

① The yield strength, σ_y, at -20 ºF and 70 ºF is linearly extrapolated from Table 2.3-1 in Section 2.3, *Mechanical Properties of Materials*

Table 2.10.5-3 – Theoretical Elastic Buckling Stress Values (General Temperature Independent Form)

Elastic Buckling Stress①	Outer Cask		Inner Vessel
	Outer Shell	Inner Shell	
$\sigma_{\phi eL} = C_{\phi}Et/R$ (axial)	(0.045799)E	(0.036249)E	(0.014348)E
$\sigma_{\theta eL} = \sigma_{reL} = C_{\theta r}Et/R$ (hoop, without end pressure)	(0.003052)E	(0.001741)E	(0.000488)E
$\sigma_{\theta eL} = \sigma_{heL} = C_{\theta h}Et/R$ (hoop, with end pressure)	(0.003052)E	(0.001741)E	(0.000482)E
$\sigma_{\phi\theta eL} = C_{\phi\theta}Et/R$ (shear)	(0.011962)E	(0.008204)E	(0.002612)E

Notes:

① Elastic buckling stress formulas are given in Appendix 2.10.5.1, *Theoretical Elastic Buckling Stresses*. The tabulated values are the resultant numerical values with the modulus of elasticity, E, retained as a temperature dependent parameter, and C_i, t, and R are geometric parameters.

Table 2.10.5-4 – Temperature Dependent Theoretical Elastic Buckling Stresses for Each RH-TRU 72-B Package Shell

Shell	Temperature		
	-20 ºF	70 ºF	160 ºF
$\sigma_{\phi eL}$ = theoretical axial buckling stress (psi)			
Outer Cask Outer Shell	1,319,011	1,296,112	1,273,212
Outer Cask Inner Shell	1,043,971	1,025,847	1,007,722
Inner Vessel	413,222	406,048	398,874
$\sigma_{\theta eL} = \sigma_{reL}$ = theoretical hoop buckling stress with no end pressure (psi)			
Outer Cask Outer Shell	87,898	86,372	84,846
Outer Cask Inner Shell	50,141	49,270	48,400
Inner Vessel	14,054	13,810	13,566
$\sigma_{\theta eL} = \sigma_{heL}$ = theoretical hoop buckling stress with end pressure (psi)			
Outer Cask Outer Shell	87,898	86,372	84,846
Outer Cask Inner Shell	50,141	49,270	48,400
Inner Vessel	13,882	13,641	13,400
$\sigma_{\phi\theta eL}$ = theoretical in-plane shear buckling stress (psi)			
Outer Cask Outer Shell	344,506	338,525	332,544
Outer Cask Inner Shell	236,275	232,173	228,071
Inner Vessel	75,226	73,920	72,614

Table 2.10.5-5 – Temperature Dependent Capacity Reduction Factors

Capacity Reduction Factor	Temperature		
	-20 ºF	70 ºF	160 ºF
$\alpha_{\phi L}$ (axial)	0.327	0.282	0.237
$\alpha_{\theta L}$ (hoop)	0.8	0.8	0.8
$\alpha_{\phi\theta L}$(shear)	0.8	0.8	0.8

Table 2.10.5-6 – Upper Bounds for Compressive Stresses and In-Plane Shear Stresses

Stress Condition	Load Condition	Temperature		
		-20 ºF	70 ºF	160 ºF
Upper-bound permitted compressive stress σ_ϕ or σ_θ (psi)	NCT	18,000	15,750	13,500
	HAC	26,866	23,507	20,149
Upper-bound permitted in-plane shear stress $\sigma_{\phi\theta}$ (psi)	NCT	10,800	9,450	8,100
	HAC	16,120	14,104	12,089

Table 2.10.5-7 – Compressive Membrane and In-Plane Shear Stress Summary for the Outer Cask Inner Shell

Load Condition	σ_{axial}	σ_{hoop}	τ	Reference
(a) NCT Differential Thermal Expansion	0	724	0	§2.6.1.2
(b) NCT End Drop at 160 ºF①	6,067	0	0	§2.6.7.1, ¶(6)
(c) NCT Oblique Drop (85º from horizontal) at 160 ºF	6,463	0	608	§2.6.7.2, ¶(4)
(d) NCT Side Drop Maximum Moment Location at 160 ºF	3,881	0	0	§2.6.7.3, ¶(4)
(e) NCT Side Drop Maximum Shear Location at 160 ºF	0	0	1,255	§2.6.7.3, ¶(4)
(f) HAC End Drop at 160 ºF①	12,801	0	0	§2.7.1.1, ¶(6)
(g) HAC Oblique Drop (5º from horizontal) at 160 ºF	17,049	0	4,796	§2.7.1.2, ¶(4)
(h) HAC Side Drop Maximum Moment Location at 160 ºF	16,331	0	0	§2.7.1.3, ¶(4)
(i) HAC Side Drop Maximum Shear Location at 160 ºF	0	0	5,554	§2.7.1.3, ¶(4)
(j) Side Pin Punch Maximum Moment Location at 160 ºF	8,526	0	0	§2.7.3.2
(k) Side Pin Punch Maximum Shear Location at 160 ºF	0	0	4,546	§2.7.3.2

Notes:

① The lead is assumed to be initially shrunk onto the OC inner shell which, for the OC inner shell, is worse than assuming the lead is initially stress-free.

Table 2.10.5-8 – Compressive Membrane and In-Plane Shear Stress Summary for the Outer Cask Outer Shell

Load Condition	σ_{axial}	σ_{hoop}	τ	Reference
(a) NCT Differential Thermal Expansion	0	724	0	§2.6.1.2
(b) NCT End Drop at 160 ºF①	3,550	0	0	§2.6.7.1, ¶(7)
(c) NCT Oblique Drop (85º from horizontal) at 160 ºF	7,348	0	608	§2.6.7.2, ¶(4)
(d) NCT Side Drop Maximum Moment Location at 160 ºF	4,607	0	0	§2.6.7.3, ¶(4)
(e) NCT Side Drop Maximum Shear Location at 160 ºF	0	0	1,255	§2.6.7.3, ¶(4)
(f) HAC End Drop at 160 ºF①	7,493	0	0	§2.7.1.1, ¶(7)
(g1) HAC Oblique Drop (5º from horizontal) at -20 ºF	20,212	0	4,796	§2.7.1.2, ¶(4)
(g2) HAC Oblique Drop (5º from horizontal) at 160 ºF	18,615②	0	4,796	§2.7.1.2, ¶(4)
(h1) HAC Side Drop Maximum Moment Location at -20 ºF	19,388	0	0	§2.7.1.3, ¶(4)
(h2) HAC Side Drop Maximum Moment Location at 160 ºF	16,460③	0	0	§2.7.1.3, ¶(4)
(i) HAC Side Drop Maximum Shear Location at 160 ºF	0	0	5,554	§2.7.1.3, ¶(4)
(j) Side Pin Punch Maximum Moment Location at 160 ºF	10,119	0	0	§2.7.3.2
(k) Side Pin Punch Maximum Shear Location at 160 ºF	0	0	4,546	§2.7.3.2

Notes:

① The lead is assumed to be initially stress-free which, for the OC outer shell, is worse than assuming the lead is initially shrunk onto the OC inner shell.

② For the 160 ºF oblique drop case, the axial stress component from the -20 ºF case is multiplied by the ratio of impact accelerations at temperature; from Table 2.10.3-11 and Table 2.10.3-12 in Appendix 2.10.3, *Drop Impact Evaluation Results*, the appropriate ratio for a 5º oblique drop is 44.3/48.1 = 0.921. Although shear stress could have been similarly reduced, it is conservatively left at the higher magnitude associated with the -20 ºF conditions.

③ For the 160 ºF side drop case, the axial stress component from the -20 ºF case is multiplied by the ratio of impact accelerations at temperature; from Table 2.10.3-11 and Table 2.10.3-12 in Appendix 2.10.3, *Drop Impact Evaluation Results*, the appropriate ratio for a 0º side drop is 68.9/81.2 = 0.849.

Table 2.10.5-9 – Compressive Membrane and In-Plane Shear Stress Summary for the Inner Vessel

Load Condition	σ_{axial}	σ_{hoop}	τ	Reference
(a) NCT Differential Thermal Expansion	0	1,208	0	§2.6.1.2
(b) NCT End Drop at 160 ºF①	4,185	0	0	§2.6.7.1, ¶(5)
(c) NCT Oblique Drop (85º from horizontal) at 160 ºF	5,247	0	2,099	§2.6.7.2, ¶(5)
(d) NCT Side Drop Maximum Moment Location at 160 ºF	4,661	0	0	§2.6.7.3, ¶(5)
(e) NCT Side Drop Maximum Shear Location at 160 ºF	0	0	2,214	§2.6.7.3, ¶(5)
(f) HAC End Drop at 160 ºF①	11,995	0	0	§2.7.1.1, ¶(5)
(g1) HAC Oblique Drop (5º from horizontal) at -20 ºF	21,372	0	7,503	§2.7.1.2, ¶(5)
(g2) HAC Oblique Drop (5º from horizontal) at 160 ºF	18,194②	0	7,503	§2.7.1.2, ¶(5)
(h1) HAC Side Drop Maximum Moment Location at -20 ºF	19,611	0	0	§2.7.1.3, ¶(5)
(h2) HAC Side Drop Maximum Moment Location at 160 ºF	16,650③	0	0	§2.7.1.3, ¶(5)
(i) HAC Side Drop Maximum Shear Location at 160 ºF	0	0	9,317	§2.7.1.3, ¶(5)

Notes:

① The bottom end drop is the worst case for the IV.

② Axial stress for this 160 ºF case is reduced from the value of 21,372 psi presented in Paragraph (5) of Section 2.7.1.2, *Corner and Oblique Drops*, which corresponds to -20 ºF conditions. The reduction recognizes the lower impact acceleration of 44.3*g* at 160 ºF compared to 48.1*g* at -20 ºF (see Note 2 of Table 2.10.5-8). More significantly, from an inspection of Figure 2.10.1-9 in Appendix 2.10.1.4, *Containment Assembly Analysis for Oblique Drops*, and Figure 2.7-11, Figure 2.7-12, and Figure 2.7-13 in Paragraph (3) of Section 2.7.1.2, *Corner and Oblique Drops*, it is clear that the maximum moment of 44.3/48.1 × 4,260,000 = 3,923,451 in-lb (where 4,260,000 in-lb is from the last paragraph of Paragraph (3) of Section 2.7.1.2, *Corner and Oblique Drops*) occurs at IV node 211, which corresponds to the centerline of the 10-inch wide payload canister support ring. However, the nearest location where buckling of the IV shell can actually occur is 5 inches away (i.e., at the outer edge of the payload canister support ring); that location is addressed as follows. From Figure 2.7-12, the shear force at the point of maximum moment is approximately -60,000 pounds. As such, at a point 5 inches away, the bending moment becomes 3,923,451 – 5(60,000) = 3,623,451 in-lb. Finally, as was done in Paragraph (3) of Section 2.7.1.2, *Corner and Oblique Drops*, the 3,623,451 in-lb moment must be increased by a factor of 1.49 to 5,398,942 in-lb. Repeating the IV membrane stress calculation in Paragraph (5) of Section 2.7.1.2, *Corner and Oblique Drops*, using a bending moment of 5,398,942 in-lb instead of 6,347,400 in-lb, results in an axial stress of 18,194 psi. Although stresses due to shear and thrust loads could have been similarly reduced, they are conservatively left at the higher magnitudes associated with the -20 ºF conditions.

③ For the 160 ºF side drop case, the axial stress component from the -20 ºF case is multiplied by the ratio of impact accelerations at temperature; from Table 2.10.3-11 and Table 2.10.3-12 in Appendix 2.10.3, *Drop Impact Evaluation Results*, the appropriate ratio for a 0º side drop is 68.9/81.2 = 0.849.

Table 2.10.5-10 – Worst-Case Load Combinations for the Outer Cask Inner Shell

Combination① (Table 2.10.5-7)	Regulatory Condition	Shell Temperature (ºF)	σ_ϕ (psi)	σ_θ (psi)	$\sigma_{\theta\phi}$ (psi)
(1) (a) + (b)	NCT	160	6,067	724	0
(2) (a) + (c)	NCT	160	6,463	724	608
(3) (a) + (d)	NCT	160	3,881	724	0
(4) (a) + (e)	NCT	160	0	724	1,255
(5) (a) + (f)	HAC	160	12,801	724	0
(6) (a) + (g)	HAC	160	17,049	724	4,796
(7) (a) + (h)	HAC	160	16,331	724	0
(8) (a) + (i)	HAC	160	0	724	5,554

Notes:

① Combining load condition (a) with load conditions (j) or (k) would not result in a governing worst-case.

Table 2.10.5-11 – Worst-Case Load Combinations for the Outer Cask Outer Shell

Combination① (Table 2.10.5-8)	Regulatory Condition	Shell Temperature (ºF)	σ_ϕ (psi)	σ_θ (psi)	$\sigma_{\theta\phi}$ (psi)
(1) (a) + (b)	NCT	160	3,550	724	0
(2) (a) + (c)	NCT	160	7,348	724	608
(3) (a) + (e)	NCT	160	0	724	1,255
(4) (a) + (f)	HAC	160	7,493	724	0
(5a) (a) + (g_1)	HAC	-20	20,212	724	4,796
(5b) (a) + (g_2)	HAC	160	18,615	724	4,796
(6) (a) + (i)	HAC	160	0	724	5,554

Notes:

① Combining load condition (a) with load conditions (d), (h1), (h2), (j), or (k) would not result in a governing worst-case.

Table 2.10.5-12 – Worst-Case Load Combinations for the Inner Vessel

Combination① (Table 2.10.5-9)	Regulatory Condition	Shell Temperature (ºF)	σ_ϕ (psi)	σ_θ (psi)	$\sigma_{\theta\phi}$ (psi)
(1) (a) + (c)	NCT	160	5,247	1,208	2,099
(2) (a) + (e)	NCT	160	0	1,208	2,214
(3a) (a) + (g_1)	HAC	-20	21,372	1,208	7,503
(3b) (a) + (g_2)	HAC	160	18,194	1,208	7,503
(4) (a) + (i)	HAC	160	0	1,208	9,317

Notes:

① Combining load condition (a) with load conditions (b), (d), (f), (h1), or (h2) would not result in a governing worst-case.

Table 2.10.5-13 – Interaction Equation Checks

Combination		Elastic Interaction per –1713.1.1						Inelastic Interaction per –1713.1.2			
		(a)[1]	(b)[2]	(c)[3]	(d)[4]	(e)(1)[5]	(e)(2)[6]	(a)[7]	(b)[8]	(c)[3]	(d)[4]
Outer Cask Inner Shell per Table 2.10.5-10											
(1)	(a) + (b)	n/a	0.029	0.051	0.037	n/a	0.029	⑩	⑩	⑨	⑨
(2)	(a) + (c)	n/a	0.032	0.054	0.037	n/a	0.032	⑩	⑩	⑩	⑩
(3)	(a) + (d)	n/a	0.010	0.032	0.037	n/a	0.010	⑩	⑩	⑨	⑨
(4)	(a) + (e)	n/a	n/a	0.000	0.038	n/a	n/a	⑩	⑩	⑩	⑩
(5)	(a) + (f)	n/a	0.050	0.072	0.025	n/a	0.050	0.116	0.025	0.014	0.001
(6)	(a) + (g)	n/a	0.074	0.097	0.026	n/a	0.074	0.284	0.025	0.082	0.002
(7)	(a) + (h)	n/a	0.070	0.092	0.025	n/a	0.070	0.242	0.025	0.059	0.001
(8)	(a) + (i)	n/a	n/a	0.002	0.027	n/a	n/a	⑩	⑩	⑩	⑩
Outer Cask Outer Shell per Table 2.10.3-11											
(1)	(a) + (b)	n/a	n/a	0.024	0.021	n/a	n/a	⑩	⑩	⑨	⑨
(2)	(a) + (c)	n/a	0.016	0.049	0.021	n/a	0.016	⑩	⑩	⑩	⑩
(3)	(a) + (e)	n/a	n/a	0.000	0.021	n/a	n/a	⑩	⑩	⑩	⑩
(4)	(a) + (f)	n/a	n/a	0.033	0.013	n/a	n/a	⑩	⑩	⑨	⑨
(5a)	(a) + (g_1)	n/a	0.031	0.063	0.014	n/a	0.031	0.141	0.014	0.020	0.001
(5b)	(a) + (g_2)	n/a	0.051	0.083	0.015	n/a	0.051	0.334	0.014	0.112	0.001
(6)	(a) + (i)	n/a	n/a	0.001	0.015	n/a	n/a	⑩	⑩	⑩	⑩
Inner Vessel per Table 2.10.5-12											
(1)	(a) + (c)	n/a	0.147	0.116	0.228	n/a	0.148	⑩	⑩	⑩	⑩
(2)	(a) + (e)	n/a	n/a	0.006	0.228	n/a	n/a	⑩	⑩	⑩	⑩
(3a)	(a) + (g_1)	n/a	0.220	0.240	0.172	n/a	0.227	0.536	0.144	0.316	0.049
(3b)	(a) + (g_2)	n/a	0.268	0.288	0.179	n/a	0.278	0.950	0.149	0.932	0.052
(4)	(a) + (i)	n/a	n/a	0.046	0.195	n/a	n/a	⑩	⑩	⑩	⑩

Notes for Table 2.10.5-13:

① Axial Compression + Hoop Compression ($\sigma_{\phi s} < (0.5)\sigma_{\theta s}$)

② Axial Compression + Hoop Compression ($\sigma_{\phi s} \geq (0.5)\sigma_{\theta s}$)

③ Axial Compression + Shear

④ Hoop Compression + Shear

⑤ Axial Compression + Hoop Compression + Shear ($\sigma_{\phi s} < (0.5)\sigma_{\theta s}$)

⑥ Axial Compression + Hoop Compression + Shear ($\sigma_{\phi s} \geq (0.5)\sigma_{\theta s}$)

⑦ Axial Compression

⑧ Hoop Compression

⑨ No Shear

⑩ Elastic Stresses Only

2.10.6 Closure Bolt Stress Evaluations

2.10.6.1 Analysis Results

The closure bolt stress analyses consider impact loads, pressure loads and bolt preloads. Bolt stress analysis results are summarized in the following eight tables:

- Table 2.10.6-1 – Outer Cask NCT Bolt Stresses, Torque Coefficient = 0.13
- Table 2.10.6-2 – Outer Cask NCT Bolt Stresses, Torque Coefficient = 0.20
- Table 2.10.6-3 – Inner Vessel NCT Bolt Stresses, Torque Coefficient = 0.13
- Table 2.10.6-4 – Inner Vessel NCT Bolt Stresses, Torque Coefficient = 0.20
- Table 2.10.6-5 – Outer Cask HAC Bolt Stresses, Torque Coefficient = 0.13
- Table 2.10.6-6 – Outer Cask HAC Bolt Stresses, Torque Coefficient = 0.20
- Table 2.10.6-7 – Inner Vessel HAC Bolt Stresses, Torque Coefficient = 0.13
- Table 2.10.6-8 – Inner Vessel HAC Bolt Stresses, Torque Coefficient = 0.20

Each table is preceded by an explicit listing of relevant geometry, taken directly from Appendix 1.3.1, *Packaging General Arrangement Drawings*, and loading data (torque, pressure).

Impact loads are expressed in acceleration *g*-loads, as given within Appendix 2.10.3, *Drop Impact Evaluation Results*. For conservatism, these loads are based upon the -20 ºF "cold" foam stress-strain relations, and bolt allowable stresses are taken at the "hot" temperature of 160 ºF.

Consistent with the ASME Code[1], the normal conditions of transport (NCT) allowable stress, $S_a = 2.0S_m$, and the hypothetical accident conditions (HAC) allowable stress, $S_a = 3.0S_m$ per Paragraph NB-3232 of the ASME Code[1]. For conservatism, external energy absorber reaction forces, which resist separation of the outer cask lid and body, are completely neglected in all calculations.

Analysis methodology, allowable stresses, and basic assumptions used are consistent with conventional design/analysis codes, such as AISC[2] and Section III of the ASME Code[1], specifically Appendix F (Paragraph F-1335). However, the analysis presented herein is more conservative, including stresses associated with preloads. Conventional design/analysis codes consider only externally applied loads and ignore preloads.

Like the ASME Code methodology given in Paragraph F-1335, this analysis uses nominal tensile and shear stresses based upon the tabulated "stress area" of the bolts. It should be noted that the elliptic interaction equations of Paragraph F-1335 and the approach used here give nearly identical results when adjustments in loadings are made to account for the differing treatment of preload tension (ASME ignores preload effects, while this method includes them).

The structural adequacy of the internally threaded base material, when Type 304 stainless steel (S_y = 30,000 psi) or the optional plated carbon steel threaded inserts (Sy = 140,000 psi), to resist the shear loads due to the worst-case bolt tensile loads is easily demonstrated. Of the two, the

[1] American Society of Mechanical Engineers (ASME) Boiler and Pressure Vessel Code, Section III, *Rules for Construction of Nuclear Power Plant Components*, Division 1, Subsection NB and Appendices, 1986 Edition.

[2] American Institute of Steel Construction, *Manual of Steel Construction*, Eighth Edition, American Institute of Steel Construction, Chicago, IL, 1980.

weakest configuration is threading directly into the Type 304 stainless steel base material. Since the optional threaded inserts have a larger outer diameter and a finer thread pitch, the insert/base material interface will be stronger than threading directly into the base metal.

From Table 2.10.6-1 through Table 2.10.6-8, the maximum NCT tensile bolt loads for the outer cask (OC) and inner vessel (IV) for all load combinations and torque coefficients are 54,945 pounds and 21,871 pounds, respectively, and the maximum HAC tensile bolt loads for the OC and IV are 75,794 pounds and 21,871 pounds, respectively.

Per Table 2.1-1 in Section 2.1.2.1.1, *Containment Structures*, the allowable shear stress for NCT is $0.6S_m = (0.6)(20,000) = 12,000$ psi at 160 ºF, and the allowable shear stress for HAC is $0.42S_u = (0.42)(67,700) = 28,430$ psi, where material properties for Type F304 stainless steel is taken from Table 2.3-1 in Section 2.3, *Mechanical Properties of Materials*. Each closure bolt hole is analyzed separately.

OC Closure Bolt Hole (1¼-7UNC-2B): From Table 2.10.6-1, the maximum NCT tensile bolt load is 54,945 pounds. For a 1¼-7 UNC-2B thread, the minimum shear area for an internal thread is 2.9441 in^2/in of engagement[3]. The OC closure bolts have a minimum engagement length of 1.75 inches. Therefore, the maximum shear stress, τ, and resulting margin of safety, MS, is:

$$\tau = \frac{54,945}{(2.9441)(1.75)} = 10,664 \text{ psi}$$

$$MS = \frac{12,000}{10,664} - 1.0 = +0.13$$

From Table 2.10.6-5, the maximum HAC tensile bolt load is 75,794 pounds. For a 1¼-7 UNC-2B thread, the minimum shear area for an internal thread is 2.9441 in^2/in of engagement. The OC closure bolts have a minimum engagement length of 1.75 inches. Therefore, the maximum shear stress, τ, and resulting margin of safety, MS, is:

$$\tau = \frac{75,794}{(2.9441)(1.75)} = 14,711 \text{ psi}$$

$$MS = \frac{28,430}{14,711} - 1.0 = +0.93$$

IV Closure Bolt Hole (7/8-9UNC-2B): From Table 2.10.6-3, the maximum NCT tensile bolt load is 21,871 pounds. For a 7/8-9UNC-2B thread, the minimum shear area for an internal thread is 2.0252 in^2/in of engagement[3]. The IV closure bolts have an engagement length of 1.06 inches. Therefore, the maximum shear stress, τ, and resultant minimum margin of safety, MS, is:

$$\tau = \frac{21,871}{(2.0252)(1.06)} = 10,188 \text{ psi}$$

$$MS = \frac{12,000}{10,188} - 1.0 = +0.18$$

[3] Raymond C. Boucher, *Table Speeds Calculation of Strength of Threads*, Product Engineering, November 27, 1961, Pages 41-49.

From Table 2.10.6-7, the maximum HAC tensile bolt load is 21,871 pounds. For a 7/8-9UNC-2B thread, the minimum shear area for an internal thread is 2.0252 in^2/in of engagement[3]. The IV closure bolts have an engagement length of 1.06 inches. Therefore, the maximum shear stress, τ, and resultant minimum margin of safety, MS, is:

$$\tau = \frac{21,871}{(2.0252)(1.06)} = 10,188 \text{ psi}$$

$$MS = \frac{28,430}{10,188} - 1.0 = +1.79$$

As demonstrated by these results, the internal threads for the RH-TRU 72-B package closure bolts have sufficient strength for all NCT and HAC.

2.10.6.2 Analysis Methodology

A description of terms and the methodology used in Table 2.10.6-1 through Table 2.10.6-8 is described in detail below. The data from Table 2.10.6-1 for the OC with a torque coefficient of 0.13 is used for the following descriptions:

a) Longitudinal Weight, W_A: the weight acting in the longitudinal (axial) direction, and reacted by the lid bolts.

i) OC: W_A includes the OC lid (1,667 pounds), IV (4,023 pounds), and a fully-loaded canister (8,000 pounds):

$$W_A = 1,667 + 4,023 + 8,000 = 13,690 \text{ lb}$$

ii) IV: Longitudinal loads are transferred directly to OC lid. Both are flat and parallel, and the OC lid is thicker and stiffer; thus, $W_A = 0$.

b) Lateral Weight, W_L: the weight acting in the lateral (transverse) direction, and amounts to the lid weight only (1,667 pounds for OC, and 1,382 pounds for IV). The IV bolt analysis conservatively ignores lateral support of the IV lid by the OC inner shell.

c) Bolt Preload, F_i: the bolt preload calculated from the torque relation for cadmium plated bolts (i.e., torque coefficient = 0.13[4]). Each bolt analysis is also calculated for non-cadmium plated bolts in successive tables (i.e., torque coefficient = 0.20[5]).

$$F_i = \frac{12T}{(0.13)d} = 51,692 \text{ lb}$$

[4] Unbrako Manufacturer's Catalog, *Unbrako Socket Screws*, SPS Technologies, Jenkintown, PA, 1980, pp. 8–9, when ratioing the recommended torques for non-plated and cadmium plated bolts results in a torque coefficient of 0.15; Fastenal's *Technical Reference Guide*, S7028, Rev. 4, Fastenal Company, Winona, MN, reports torque coefficients for cadmium plated bolts of 0.11 – 0.15, and torque coefficients for lubricated bolts of 0.15; thus, a value of 0.13 is reasonable (see http://www.fastenal.com/content/documents/FastenalTechnicalReferenceGuide.pdf).

[5] A torque coefficient of 0.20 is also considered in order to bound a wide variety of bolt conditions, platings, and/or lubrications. Specific to the chrome plating option identified in Drawing Note 31, per http://raskcycle.com/techtip/webdoc14.html, cadmium plating reduces the torque coefficient by 25% more than does chrome plating. Using this relationship and a torque coefficient of 0.13 for cadmium plating results in a value of 0.173 for chrome plating, which falls within the analysis-assumed range of 0.13 to 0.20.

where the preload torque, T = 700 lb-ft, and the nominal bolt diameter, d = 1.25 inches.

d) Bolt Pressure Load, F_P:

$$F_P = \frac{P_P A_P}{N} = 7{,}083 \text{ pounds for 18 bolts}$$

where the internal pressure, P_P = 150 psig, the pressure area, A_P = 850 in^2 (based on a seal diameter of 32.896 inches), and the number of bolts, N = 18.

e) Bolt Stiffness, K_b:

$$K_b = \frac{A_b E}{L} = 1.44(10)^7 \text{ lb/in}$$

where the bolt cross-sectional area, A_b = 1.23 in^2, the elastic modulus, E = 27.3(10)^6 psi at 160 ºF (see Table 2.3-1 in Section 2.3, *Mechanical Properties of Materials*, for ASTM A320, Grade L43, fasteners), and the effective bolt length, L = (grip length, L_g) + ½(nominal bolt diameter, D) = 1.70 + ½(1.25) = 2.33 inches.

f) Lid Stiffness, K_m:

$$K_m = \frac{A_L E}{L_g} = 1.61(10)^8 \text{ lb/in}$$

where the assumed cross-sectional area is equal to a cylinder with an inside diameter equal to the nominal bolt diameter, D, and an outside diameter equal to three times the nominal bolt diameter, $A_L = (\pi/4)[(3D)^2 - D^2] = 2\pi D^2 = 2\pi(1.25)^2 = 9.8175$ in^2, the elastic modulus, E = 27.8(10)^6 psi at 160 ºF (see Table 2.3-1 in Section 2.3, *Mechanical Properties of Materials*, for Type 304 stainless steel, and the bolt grip length, L_g = 1.70 inches.

g) Impact Acceleration, n_g: based on impact force predictions with a total package weight of 45,000 pounds per Appendix 2.10.3, *Drop Impact Evaluation Results*.

h) Tensile Impact Loads – Uniform Bolt Force Distribution, F_A: only applicable to the 90º end impact case for the OC for NCT.

$$F_A = \frac{P_A}{N} = \frac{n_g W_A (\sin\theta)}{N} = 32{,}324 \text{ lb}$$

where the impact acceleration, $n_g = 42.5g$, the longitudinal weight, W_A = 13,690 pounds, the impact angle, θ = 90º, and the number of bolts, N = 18.

i) Tensile Impact Load – Triangular Bolt Force Distribution, F_A:

$$F_A = P_A\left(\frac{R_L(R_L + R_B)}{I_o}\right)A_B = n_g W_A(\sin\theta)\left(\frac{R_L(R_L + R_B)}{I_o}\right)A_B = 18{,}258 \text{ lb}$$

where the impact acceleration, $n_g = 17.9g$, the longitudinal weight, W_A = 13,690 pounds, the impact angle, θ = 85º, the lid radius, R_L = ½(37.60) = 18.80 inches, the bolt circle radius, R_B = ½(35.20) = 17.60 inches, the bolt shank area, A_B = 0.969 in^2, and the bolt circle moment of inertia, I_o, is:

$$I_o = \pi R_B^3 t + A_b N R_L^2 = \pi(17.60)^3(0.158) + (0.969)(18)(18.80)^2 = 8{,}866 \text{ in}^4$$

where the number of bolts, N = 18, and the equivalent ring thickness, t, is:

$$t = \frac{A_b N}{2\pi R_B} = \frac{(0.969)(18)}{2\pi(17.60)} = 0.158 \text{ inches}$$

The derivation of the triangular force distribution relationship is as follows.

Tensile bolt stresses are calculated by assuming the lid pivots about the outer edge of the lid, point "o", and assuming the bolts are approximated as a thin, circular ring with the thickness equivalent to the total bolt area (ring area).

The equivalent ring thickness, t, is derived from:

$$A = A_b N = 2\pi R_B t \quad \Rightarrow \quad t = \frac{A_b N}{2\pi R_B} = \frac{(0.969)(18)}{2\pi(17.60)} = 0.158 \text{ inches}$$

The moment of inertia of the bolt ring about point "o" is:

$$I_o = I_{cg} A d^2 = \pi R_B^3 t + A_b N R_L^2 = \pi(17.60)^3(0.158) + (0.969)(18)(18.80)^2 = 8{,}866 \text{ in}^4$$

The applied bending moment about point "o" due to the impact force, P_A, is $M_o = P_A R_L$. Thus, the maximum tensile stress in the bolt, f_a, is found as:

$$f_A = \frac{Mc}{I} = P_A \left(\frac{R_L (R_L + R_B)}{I_o} \right)$$

and,

$$F_A = P_A \left(\frac{R_L (R_L + R_B)}{I_o} \right) A_B = 18{,}258 \text{ lb}$$

Note: In this analysis, which sweeps from vertical, or end impacts through side impacts, there is a transition from one bolt tension relation to the other at some orientation angle. Both conservatively neglect restoring reaction forces from external energy absorbers. This neglect is extraordinarily conservative for near vertical impacts, but becomes more realistic as the package approaches side impact orientations. Specifically, the center of pressure of the external energy absorber reaction force upon the lid moves from the center of the lid towards the impacting corner of the package as the impact orientation moves from near-vertical to near-horizontal.

j) Lateral (Shear) Bolt Load, F_L:

$$F_L = \frac{P_L}{N} = \frac{n_g W_L (\cos\theta)}{N} = 144 \text{ lb}$$

where the impact acceleration, $n_g = 17.9g$, the lateral weight, W_L = 1,667 pounds, the impact angle, $\theta = 85^\circ$, and the number of bolts, N = 18.

k) Total External Bolt Load, P:

$$P = F_P + F_A = 25{,}341 \text{ lb}$$

where the pressure load, F_P = 7,083 pounds, and the impact load, F_A = 18,258 pounds at an impact angle of 85º.

l) Net Bolt Tension, F_b: the net bolt tension, considering applied external loads and pretension loads.

$$F_b = P\left(\frac{K_b}{K_b + K_m}\right) + F_i \qquad F_m < 0$$

$$F_b = P \qquad F_m \geq 0$$

where the total external bolt load, P = 25,341 pounds at an impact angle of 85º, the bolt stiffness, $K_b = 1.44(10)^7$ lb/in, the lid stiffness, $K_m = 1.61(10)^8$ lb/in, the preload, F_i = 51,692 pounds, and the clamping force, F_m, is:

$$F_m = P\left(\frac{K_m}{K_b + K_m}\right) - F_i = -28{,}431 \text{ lb}$$

Since $F_m < 0$, the net bolt tension, F_b, is:

$$F_b = P\left(\frac{K_b}{K_b + K_m}\right) + F_i = 53{,}784 \text{ lb}$$

m) Bolt Tensile Stress, f_b:

$$f_b = \frac{F_b}{A_b} = 55{,}504 \text{ psi}$$

where the net bolt tension, F_b = 53,784 pounds, and the bolt area, $A_b = 0.969$ in^2, is the lesser of the shank area (1.23 in^2) and the tensile stress area (0.969 in^2).

n) Nominal Bolt Shear Stress, f_v:

$$f_v = \frac{F_L}{A_b} = 149 \text{ psi}$$

where the lateral bolt load, F_L = 144 pounds, and the bolt area, $A_b = 0.969$ in^2, is the lesser of the shank area (1.23 in^2) and the tensile stress area (0.969 in^2).

o) Principal Stresses, σ_1 and σ_2:

$$\sigma_{1,2} = \frac{f_b}{2} \pm \sqrt{\left(\frac{f_b}{2}\right)^2 + f_v^2} = 0,\ 55{,}505 \text{ psi (at } \theta = 85º)$$

where the bolt tensile stress, f_b = 55,504 psi, and the nominal bolt shear stress, f_v = 149 psi.

p) Stress Intensity, SI:

$$SI = |\sigma_1 - \sigma_2| = 55{,}505 \text{ psi (at } \theta = 85^\circ)$$

where the principal stresses, $\sigma_1 = 0$ psi, and $\sigma_2 = 55{,}505$ psi.

q) Margin of Safety, MS:

$$MS = \frac{S_a}{SI} - 1 = \frac{2.0S_m}{SI} - 1 = \frac{67{,}600}{55{,}505} - 1 = +0.22$$

This page intentionally left blank.

Table 2.10.6-1 – Outer Cask NCT Bolt Stresses, Torque Coefficient = 0.13

Parameter	Value	Parameter	Value	Parameter	Value
Nominal Thread Diameter (in)	1.25	Preload Torque (lb-ft)	700	Package Weight (lb)	45,000
Number of Bolts	18	Bolt Circle Diameter (in)	35.2	Longitudinal Weight (lb)	13,690
Allowable Stress, $2S_m$ (psi)	67,600	Lid Diameter (in)	37.6	Lateral Weight (lb)	1,667
Shank Area (in^2)	1.23	Impact Limiter Radius (in)	38.0	Torque Coefficient, K	0.13
Stress Area (in^2)	0.969	Package Radius (in)	20.8	Bolt Preload (lb)	51,692
Grip Length (in)	1.7	Bolt Circle Moment of Inertia (in^4)	8,866	Bolt Pressure Load (lb)	7,083
Maximum Pressure (psi)	150	Bolt Elastic Modulus (psi)	$2.73(10)^7$	Bolt Stiffness (lb/in)	14,442,581
Seal Diameter (in)	32.896	Lid Elastic Modulus (psi)	$2.78(10)^7$	Lid Stiffness (lb/in)	$1.61(10)^8$

Angle from Horizontal (degrees)	Impact Acceleration (*g*)	Bolt Force Distribution	Impact Forces		Bolt Tensions		Direct Stresses		Principal Stresses		Stress Intensity	MS
			Tension	Shear	Applied	Net	Tension	Shear	σ_1	σ_2		
90	42.5	Uniform	32,324	0	39,406	54,945	56,702	0	56,702	0	56,702	+0.19
85	17.9	Triangular	18,258	144	25,341	53,784	55,504	149	55,505	0	55,505	+0.22
80	13.2	Triangular	13,310	212	20,393	53,375	55,083	219	55,084	-1	55,085	+0.23
75	10.9	Triangular	10,780	261	17,863	53,167	54,868	270	54,869	-1	54,870	+0.23
70	9.3	Triangular	8,948	295	16,031	53,015	54,711	304	54,713	-2	54,715	+0.24
65	8.2	Triangular	7,609	321	14,692	52,905	54,597	331	54,599	-2	54,601	+0.24
60	6.5	Triangular	5,764	301	12,846	52,753	54,440	311	54,442	-2	54,444	+0.24
55	5.9	Triangular	4,948	313	12,031	52,685	54,371	323	54,373	-2	54,375	+0.24
50	5.3	Triangular	4,157	316	11,240	52,620	54,303	326	54,305	-2	54,307	+0.24
45	4.8	Triangular	3,475	314	10,558	52,564	54,245	324	54,247	-2	54,249	+0.25
40	4.4	Triangular	2,896	312	9,978	52,516	54,196	322	54,198	-2	54,200	+0.25
35	4.1	Triangular	2,408	311	9,490	52,476	54,154	321	54,156	-2	54,158	+0.25
30	3.8	Triangular	1,945	305	9,028	52,437	54,115	315	54,117	-2	54,119	+0.25
25	3.7	Triangular	1,601	311	8,684	52,409	54,086	320	54,088	-2	54,089	+0.25
20	3.8	Triangular	1,331	331	8,413	52,387	54,063	341	54,065	-2	54,067	+0.25
15	3.9	Triangular	1,034	349	8,116	52,362	54,037	360	54,040	-2	54,042	+0.25
10	4.2	Triangular	747	383	7,829	52,339	54,013	395	54,016	-3	54,019	+0.25
5	5.2	Triangular	464	480	7,547	52,315	53,989	495	53,993	-5	53,998	+0.25
0	19.3	Triangular	0	1,787	7,083	52,277	53,949	1,845	54,012	-63	54,075	+0.25

Table 2.10.6-2 – Outer Cask NCT Bolt Stresses, Torque Coefficient = 0.20

Parameter	Value	Parameter	Value	Parameter	Value
Nominal Thread Diameter (in)	1.25	Preload Torque (lb-ft)	700	Package Weight (lb)	45,000
Number of Bolts	18	Bolt Circle Diameter (in)	35.2	Longitudinal Weight (lb)	13,690
Allowable Stress, $2S_m$ (psi)	67,600	Lid Diameter (in)	37.6	Lateral Weight (lb)	1,667
Shank Area (in^2)	1.23	Impact Limiter Radius (in)	38.0	Torque Coefficient, K	0.20
Stress Area (in^2)	0.969	Package Radius (in)	20.8	Bolt Preload (lb)	33,600
Grip Length (in)	1.7	Bolt Circle Moment of Inertia (in^4)	8,866	Bolt Pressure Load (lb)	7,083
Maximum Pressure (psi)	150	Bolt Elastic Modulus (psi)	$2.73(10)^7$	Bolt Stiffness (lb/in)	14,442,581
Seal Diameter (in)	32.896	Lid Elastic Modulus (psi)	$2.78(10)^7$	Lid Stiffness (lb/in)	$1.61(10)^8$

Angle from Horizontal (degrees)	Impact Acceleration (*g*)	Bolt Force Distribution	Impact Forces		Bolt Tensions		Direct Stresses		Principal Stresses		Stress Intensity	MS
			Tension	Shear	Applied	Net	Tension	Shear	σ_1	σ_2		
90	42.5	Uniform	32,324	0	39,406	39,406	40,667	0	40,667	0	40,667	+0.66
85	17.9	Triangular	18,258	144	25,341	35,691	36,833	149	36,834	0	36,835	+0.84
80	13.2	Triangular	13,310	212	20,393	35,283	36,412	219	36,413	-1	36,415	+0.86
75	10.9	Triangular	10,780	261	17,863	35,074	36,196	270	36,198	-2	36,200	+0.87
70	9.3	Triangular	8,948	295	16,031	34,923	36,040	304	36,043	-3	36,045	+0.88
65	8.2	Triangular	7,609	321	14,692	34,813	35,926	331	35,929	-3	35,932	+0.88
60	6.5	Triangular	5,764	301	12,846	34,660	35,769	311	35,772	-3	35,775	+0.89
55	5.9	Triangular	4,948	313	12,031	34,593	35,700	323	35,703	-3	35,706	+0.89
50	5.3	Triangular	4,157	316	11,240	34,528	35,632	326	35,635	-3	35,638	+0.90
45	4.8	Triangular	3,475	314	10,558	34,471	35,574	324	35,577	-3	35,580	+0.90
40	4.4	Triangular	2,896	312	9,978	34,424	35,525	322	35,528	-3	35,531	+0.90
35	4.1	Triangular	2,408	311	9,490	34,383	35,483	321	35,486	-3	35,489	+0.90
30	3.8	Triangular	1,945	305	9,028	34,345	35,444	315	35,447	-3	35,449	+0.91
25	3.7	Triangular	1,601	311	8,684	34,317	35,415	320	35,417	-3	35,420	+0.91
20	3.8	Triangular	1,331	331	8,413	34,294	35,392	341	35,395	-3	35,398	+0.91
15	3.9	Triangular	1,034	349	8,116	34,270	35,366	360	35,370	-4	35,374	+0.91
10	4.2	Triangular	747	383	7,829	34,246	35,342	395	35,346	-4	35,351	+0.91
5	5.2	Triangular	464	480	7,547	34,223	35,318	495	35,325	-7	35,332	+0.91
0	19.3	Triangular	0	1,787	7,083	34,185	35,278	1,845	35,374	-96	35,471	+0.91

Table 2.10.6-3 – Inner Vessel NCT Bolt Stresses, Torque Coefficient = 0.13

Parameter	Value	Parameter	Value	Parameter	Value
Nominal Thread Diameter (in)	0.875	Preload Torque (lb-ft)	200	Package Weight (lb)	45,000
Number of Bolts	8	Bolt Circle Diameter (in)	30.0	Longitudinal Weight (lb)	0
Allowable Stress, $2S_m$ (psi)	67,600	Lid Diameter (in)	32.0	Lateral Weight (lb)	1,382
Shank Area (in^2)	0.407	Impact Limiter Radius (in)	38.0	Torque Coefficient, K	0.13
Stress Area (in^2)	0.407	Package Radius (in)	20.8	Bolt Preload (lb)	21,099
Grip Length (in)	2.75	Bolt Circle Moment of Inertia (in^4)	1,200	Bolt Pressure Load (lb)	11,545
Maximum Pressure (psi)	150	Bolt Elastic Modulus (psi)	$2.73(10)^7$	Bolt Stiffness (lb/in)	3,485,835
Seal Diameter (in)	28.0	Lid Elastic Modulus (psi)	$2.78(10)^7$	Lid Stiffness (lb/in)	$4.86(10)^7$

Angle from Horizontal (degrees)	Impact Acceleration (*g*)	Bolt Force Distribution	Impact Forces		Bolt Tensions		Direct Stresses		Principal Stresses		Stress Intensity	MS
			Tension	Shear	Applied	Net	Tension	Shear	σ_1	σ_2		
90	42.5	Uniform	0	0	11,545	21,871	53,737	0	53,737	0	53,737	+0.26
85	17.9	Uniform	0	270	11,545	21,871	53,737	662	53,746	-8	53,754	+0.26
80	13.2	Uniform	0	396	11,545	21,871	53,737	973	53,755	-18	53,773	+0.26
75	10.9	Uniform	0	487	11,545	21,871	53,737	1,197	53,764	-27	53,791	+0.26
70	9.3	Uniform	0	549	11,545	21,871	53,737	1,350	53,771	-34	53,805	+0.26
65	8.2	Uniform	0	599	11,545	21,871	53,737	1,471	53,778	-40	53,818	+0.26
60	6.5	Uniform	0	561	11,545	21,871	53,737	1,379	53,773	-35	53,808	+0.26
55	5.9	Uniform	0	585	11,545	21,871	53,737	1,436	53,776	-38	53,814	+0.26
50	5.3	Uniform	0	589	11,545	21,871	53,737	1,446	53,776	-39	53,815	+0.26
45	4.8	Uniform	0	586	11,545	21,871	53,737	1,441	53,776	-39	53,815	+0.26
40	4.4	Uniform	0	582	11,545	21,871	53,737	1,431	53,775	-38	53,814	+0.26
35	4.1	Uniform	0	580	11,545	21,871	53,737	1,426	53,775	-38	53,813	+0.26
30	3.8	Uniform	0	569	11,545	21,871	53,737	1,397	53,774	-36	53,810	+0.26
25	3.7	Uniform	0	579	11,545	21,871	53,737	1,423	53,775	-38	53,813	+0.26
20	3.8	Uniform	0	617	11,545	21,871	53,737	1,516	53,780	-43	53,823	+0.26
15	3.9	Uniform	0	651	11,545	21,871	53,737	1,599	53,785	-48	53,832	+0.26
10	4.2	Uniform	0	715	11,545	21,871	53,737	1,756	53,795	-57	53,852	+0.26
5	5.2	Uniform	0	895	11,545	21,871	53,737	2,199	53,827	-90	53,917	+0.25
0	19.3	Uniform	0	3,334	11,545	21,871	53,737	8,192	54,958	-1,221	56,179	+0.20

Table 2.10.6-4 – Inner Vessel NCT Bolt Stresses, Torque Coefficient = 0.20

Parameter	Value	Parameter	Value	Parameter	Value
Nominal Thread Diameter (in)	0.875	Preload Torque (lb-ft)	200	Package Weight (lb)	45,000
Number of Bolts	8	Bolt Circle Diameter (in)	30.0	Longitudinal Weight (lb)	0
Allowable Stress, $2S_m$ (psi)	67,600	Lid Diameter (in)	32.0	Lateral Weight (lb)	1,382
Shank Area (in^2)	0.407	Impact Limiter Radius (in)	38.0	Torque Coefficient, K	0.20
Stress Area (in^2)	0.407	Package Radius (in)	20.8	Bolt Preload (lb)	13,714
Grip Length (in)	2.75	Bolt Circle Moment of Inertia (in^4)	1,200	Bolt Pressure Load (lb)	11,545
Maximum Pressure (psi)	150	Bolt Elastic Modulus (psi)	$2.73(10)^7$	Bolt Stiffness (lb/in)	3,485,835
Seal Diameter (in)	28.0	Lid Elastic Modulus (psi)	$2.78(10)^7$	Lid Stiffness (lb/in)	$4.86(10)^7$

Angle from Horizontal (degrees)	Impact Acceleration (*g*)	Bolt Force Distribution	Impact Forces		Bolt Tensions		Direct Stresses		Principal Stresses		Stress Intensity	MS
			Tension	Shear	Applied	Net	Tension	Shear	σ_1	σ_2		
90	42.5	Uniform	0	0	11,545	14,487	35,593	0	35,593	0.00	35,593	+0.90
85	17.9	Uniform	0	270	11,545	14,487	35,593	662	35,606	-12	35,618	+0.90
80	13.2	Uniform	0	396	11,545	14,487	35,593	973	35,620	-27	35,647	+0.90
75	10.9	Uniform	0	487	11,545	14,487	35,593	1,197	35,634	-40	35,674	+0.89
70	9.3	Uniform	0	549	11,545	14,487	35,593	1,350	35,645	-51	35,696	+0.89
65	8.2	Uniform	0	599	11,545	14,487	35,593	1,471	35,654	-61	35,715	+0.89
60	6.5	Uniform	0	561	11,545	14,487	35,593	1,379	35,647	-53	35,700	+0.89
55	5.9	Uniform	0	585	11,545	14,487	35,593	1,436	35,651	-58	35,709	+0.89
50	5.3	Uniform	0	589	11,545	14,487	35,593	1,446	35,652	-59	35,711	+0.89
45	4.8	Uniform	0	586	11,545	14,487	35,593	1,441	35,652	-58	35,710	+0.89
40	4.4	Uniform	0	582	11,545	14,487	35,593	1,431	35,651	-57	35,708	+0.89
35	4.1	Uniform	0	580	11,545	14,487	35,593	1,426	35,650	-57	35,707	+0.89
30	3.8	Uniform	0	569	11,545	14,487	35,593	1,397	35,648	-55	35,703	+0.89
25	3.7	Uniform	0	579	11,545	14,487	35,593	1,423	35,650	-57	35,707	+0.89
20	3.8	Uniform	0	617	11,545	14,487	35,593	1,516	35,658	-64	35,722	+0.89
15	3.9	Uniform	0	651	11,545	14,487	35,593	1,599	35,665	-72	35,737	+0.89
10	4.2	Uniform	0	715	11,545	14,487	35,593	1,756	35,680	-86	35,766	+0.89
5	5.2	Uniform	0	895	11,545	14,487	35,593	2,199	35,729	-135	35,864	+0.88
0	19.3	Uniform	0	3,334	11,545	14,487	35,593	8,192	37,388	-1,795	39,183	+0.73

Table 2.10.6-5 – Outer Cask HAC Bolt Stresses, Torque Coefficient = 0.13

Parameter	Value	Parameter	Value	Parameter	Value
Nominal Thread Diameter (in)	1.25	Preload Torque (lb-ft)	700	Package Weight (lb)	45,000
Number of Bolts	18	Bolt Circle Diameter (in)	35.2	Longitudinal Weight (lb)	13,690
Allowable Stress, $3S_m$ (psi)	101,400	Lid Diameter (in)	37.6	Lateral Weight (lb)	1,667
Shank Area (in^2)	1.23	Impact Limiter Radius (in)	38.0	Torque Coefficient, K	0.13
Stress Area (in^2)	0.969	Package Radius (in)	20.8	Bolt Preload (lb)	51,692
Grip Length (in)	1.7	Bolt Circle Moment of Inertia (in^4)	8,866	Bolt Pressure Load (lb)	7,074
Maximum Pressure (psi)	150	Bolt Elastic Modulus (psi)	$2.73(10)^7$	Bolt Stiffness (lb/in)	14,442,581
Seal Diameter (in)	32.876	Lid Elastic Modulus (psi)	$2.78(10)^7$	Lid Stiffness (lb/in)	$1.61(10)^8$

Angle from Horizontal (degrees)	Impact Acceleration (*g*)	Bolt Force Distribution	Impact Forces		Bolt Tensions		Direct Stresses		Principal Stresses		Stress Intensity	MS
			Tension	Shear	Applied	Net	Tension	Shear	σ_1	σ_2		
90	89.7	Uniform	68,222	0	75,296	75,296	77,705	0	77,705	0	77,705	+0.30
85	90.7	Uniform	68,720	732	75,794	75,794	78,219	756	78,226	-7	78,233	+0.30
80	77.5	Uniform	58,048	1,246	65,122	65,122	67,205	1,286	67,230	-25	67,254	+0.51
75	66.7	Triangular	65,966	1,599	73,040	73,040	75,377	1,650	75,413	-36	75,449	+0.34
70	60.1	Triangular	57,825	1,904	64,899	64,899	66,975	1,965	67,033	-58	67,090	+0.51
65	56.2	Triangular	52,151	2,200	59,225	59,225	61,120	2,270	61,204	-84	61,288	+0.65
60	50.7	Triangular	44,956	2,348	52,030	55,987	57,778	2,423	57,879	-101	57,981	+0.75
55	46.3	Triangular	38,833	2,459	45,907	55,481	57,256	2,538	57,368	-112	57,481	+0.76
50	42.4	Triangular	33,256	2,524	40,330	55,021	56,781	2,605	56,900	-119	57,020	+0.78
45	38.6	Triangular	27,946	2,528	35,020	54,583	56,329	2,609	56,449	-121	56,570	+0.79
40	35.5	Triangular	23,364	2,519	30,438	54,205	55,939	2,599	56,059	-121	56,180	+0.80
35	32.9	Triangular	19,321	2,496	26,395	53,871	55,594	2,576	55,713	-119	55,832	+0.82
30	31.1	Triangular	15,921	2,494	22,996	53,590	55,305	2,574	55,424	-120	55,544	+0.83
25	30.3	Triangular	13,111	2,543	20,185	53,358	55,065	2,625	55,190	-125	55,315	+0.83
20	30.5	Triangular	10,681	2,654	17,755	53,158	54,858	2,739	54,995	-136	55,131	+0.84
15	32.3	Triangular	8,560	2,889	15,634	52,983	4,678	2,982	54,840	-162	55,002	+0.84
10	33.1	Triangular	5,885	3,019	12,959	52,762	54,450	3,115	54,628	-178	54,805	+0.85
5	48.1	Triangular	4,292	4,438	11,366	52,630	54,314	4,580	54,698	-383	55,081	+0.84
0	81.2	Triangular	0	7,520	7,074	52,276	53,949	7,761	55,043	-1,094	56,137	+0.81

Table 2.10.6-6 – Outer Cask HAC Bolt Stresses, Torque Coefficient = 0.20

Parameter	Value	Parameter	Value	Parameter	Value
Nominal Thread Diameter (in)	1.25	Preload Torque (lb-ft)	700	Package Weight (lb)	45,000
Number of Bolts	18	Bolt Circle Diameter (in)	35.2	Longitudinal Weight (lb)	13,690
Allowable Stress, $3S_m$ (psi)	101,400	Lid Diameter (in)	37.6	Lateral Weight (lb)	1,667
Shank Area (in^2)	1.23	Impact Limiter Radius (in)	38.0	Torque Coefficient, K	0.20
Stress Area (in^2)	0.969	Package Radius (in)	20.8	Bolt Preload (lb)	33,600
Grip Length (in)	1.7	Bolt Circle Moment of Inertia (in^4)	8,866	Bolt Pressure Load (lb)	7,074
Maximum Pressure (psi)	150	Bolt Elastic Modulus (psi)	$2.73(10)^7$	Bolt Stiffness (lb/in)	14,442,581
Seal Diameter (in)	32.876	Lid Elastic Modulus (psi)	$2.78(10)^7$	Lid Stiffness (lb/in)	$1.61(10)^8$

Angle from Horizontal (degrees)	Impact Acceleration (*g*)	Bolt Force Distribution	Impact Forces		Bolt Tensions		Direct Stresses		Principal Stresses		Stress Intensity	MS
			Tension	Shear	Applied	Net	Tension	Shear	σ_1	σ_2		
90	89.7	Uniform	68,222	0	75,296	75,296	77,705	0	77,705	0	77,705	+0.30
85	90.7	Uniform	68,720	732	75,794	75,794	78,219	756	78,226	-7	78,233	+0.30
80	77.5	Uniform	58,048	1,246	65,122	65,122	67,205	1,286	67,230	-25	67,254	+0.51
75	66.7	Triangular	65,966	1,599	73,040	73,040	75,377	1,650	75,413	-36.10	75,449	+0.34
70	60.1	Triangular	57,825	1,904	64,899	64,899	66,975	1,965	67,033	-58	67,090	+0.51
65	56.2	Triangular	52,151	2,200	59,225	59,225	61,120	2,270	61,204	-84	61,288	+0.65
60	50.7	Triangular	44,956	2,348	52,030	52,030	53,695	2,423	53,804	-109	53,913	+0.88
55	46.3	Triangular	38,833	2,459	45,907	45,907	47,375	2,538	47,511	-136	47,647	+1.13
50	42.4	Triangular	33,256	2,524	40,330	40,330	41,620	2,605	41,783	-162	41,945	+1.42
45	38.6	Triangular	27,946	2,528	35,020	36,490	37,658	2,609	37,838	-180	38,017	+1.67
40	35.5	Triangular	23,364	2,519	30,438	36,112	37,268	2,599	37,448	-180	37,628	+1.69
35	32.9	Triangular	19,321	2,496	26,395	35,779	36,923	2,576	37,102	-179	37,281	+1.72
30	31.1	Triangular	15,921	2,494	22,996	35,498	36,634	2,574	36,814	-180	36,994	+1.74
25	30.3	Triangular	13,111	2,543	20,185	35,266	36,394	2,625	36,583	-188	36,771	+1.76
20	30.5	Triangular	10,681	2,654	17,755	35,065	36,187	2,739	36,393	-206	36,600	+1.77
15	32.3	Triangular	8,560	2,889	15,634	34,890	36,007	2,982	36,252	-245	36,497	+1.78
10	33.1	Triangular	5,885	3,019	12,959	34,670	35,779	3,115	36,048	-269	36,317	+1.79
5	48.1	Triangular	4,292	4,438	11,366	34,538	35,643	4,580	36,222	-579	36,801	+1.76
0	81.2	Triangular	0	7,520	7,074	34,184	35,277	7,761	36,909	-1,632	38,541	+1.63

Table 2.10.6-7 – Inner Vessel HAC Bolt Stresses, Torque Coefficient = 0.13

Parameter	Value	Parameter	Value	Parameter	Value
Nominal Thread Diameter (in)	0.875	Preload Torque (lb-ft)	200	Package Weight (lb)	45,000
Number of Bolts	8	Bolt Circle Diameter (in)	30.0	Longitudinal Weight (lb)	0
Allowable Stress, $3S_m$ (psi)	101,400	Lid Diameter (in)	32.0	Lateral Weight (lb)	1,382
Shank Area (in^2)	0.407	Impact Limiter Radius (in)	38.0	Torque Coefficient, K	0.13
Stress Area (in^2)	0.407	Package Radius (in)	20.8	Bolt Preload (lb)	21,099
Grip Length (in)	2.75	Bolt Circle Moment of Inertia (in^4)	1,200	Bolt Pressure Load (lb)	11,545
Maximum Pressure (psi)	150	Bolt Elastic Modulus (psi)	$2.73(10)^7$	Bolt Stiffness (lb/in)	3,485,835
Seal Diameter (in)	28.0	Lid Elastic Modulus (psi)	$2.78(10)^7$	Lid Stiffness (lb/in)	$4.86(10)^7$

Angle from Horizontal (degrees)	Impact Acceleration (*g*)	Bolt Force Distribution	Impact Forces		Bolt Tensions		Direct Stresses		Principal Stresses		Stress Intensity	MS
			Tension	Shear	Applied	Net	Tension	Shear	σ_1	σ_2		
90	89.7	Uniform	0	0	11,545	21,871	53,737	0	53,737	0	53,737	+0.89
85	90.7	Uniform	0	1,366	11,545	21,871	53,737	3,355	53,946	-209	54,155	+0.87
80	77.5	Uniform	0	2,325	11,545	21,871	53,737	5,712	54,338	-600	54,938	+0.85
75	66.7	Triangular	0	2,982	11,545	21,871	53,737	7,327	54,719	-981	55,700	+0.82
70	60.1	Triangular	0	3,551	11,545	21,871	53,737	8,725	55,118	-1,381	56,499	+0.79
65	56.2	Triangular	0	4,103	11,545	21,871	53,737	10,081	55,566	-1,829	57,395	+0.77
60	50.7	Triangular	0	4,379	11,545	21,871	53,737	10,760	55,812	-2,074	57,886	+0.75
55	46.3	Triangular	0	4,588	11,545	21,871	53,737	11,272	56,006	-2,269	58,275	+0.74
50	42.4	Triangular	0	4,708	11,545	21,871	53,737	11,568	56,122	-2,384	58,506	+0.73
45	38.6	Triangular	0	4,715	11,545	21,871	53,737	11,585	56,129	-2,391	58,520	+0.73
40	35.5	Triangular	0	4,698	11,545	21,871	53,737	11,543	56,112	-2,374	58,486	+0.73
35	32.9	Triangular	0	4,656	11,545	21,871	53,737	11,439	56,071	-2,334	58,405	+0.74
30	31.1	Triangular	0	4,653	11,545	21,871	53,737	11,432	56,068	-2,331	58,399	+0.74
25	30.3	Triangular	0	4,744	11,545	21,871	53,737	11,656	56,157	-2,419	58,576	+0.73
20	30.5	Triangular	0	4,951	11,545	21,871	53,737	12,165	56,363	-2,626	58,989	+0.72
15	32.3	Triangular	0	5,390	11,545	21,871	53,737	13,242	56,824	-3,086	59,910	+0.69
10	33.1	Triangular	0	5,631	11,545	21,871	53,737	13,836	57,090	-3,353	60,444	+0.68
5	48.1	Triangular	0	8,278	11,545	21,871	53,737	20,338	60,567	-6,830	67,396	+0.50
0	81.2	Triangular	0	14,027	11,545	21,871	53,737	34,465	70,570	-16,832	87,402	+0.16

Table 2.10.6-8 – Inner Vessel HAC Bolt Stresses, Torque Coefficient = 0.20

Parameter	Value	Parameter	Value	Parameter	Value
Nominal Thread Diameter (in)	0.875	Preload Torque (lb-ft)	200	Package Weight (lb)	45,000
Number of Bolts	8	Bolt Circle Diameter (in)	30.0	Longitudinal Weight (lb)	0
Allowable Stress, $3S_m$ (psi)	101,400	Lid Diameter (in)	32.0	Lateral Weight (lb)	1,382
Shank Area (in^2)	0.407	Impact Limiter Radius (in)	38.0	Torque Coefficient, K	0.20
Stress Area (in^2)	0.407	Package Radius (in)	20.8	Bolt Preload (lb)	13,714
Grip Length (in)	2.75	Bolt Circle Moment of Inertia (in^4)	1,200	Bolt Pressure Load (lb)	11,545
Maximum Pressure (psi)	150	Bolt Elastic Modulus (psi)	$2.73(10)^7$	Bolt Stiffness (lb/in)	3,485,835
Seal Diameter (in)	28.0	Lid Elastic Modulus (psi)	$2.78(10)^7$	Lid Stiffness (lb/in)	$4.86(10)^7$

Angle from Horizontal (degrees)	Impact Acceleration (*g*)	Bolt Force Distribution	Impact Forces		Bolt Tensions		Direct Stresses		Principal Stresses		Stress Intensity	MS
			Tension	Shear	Applied	Net	Tension	Shear	σ_1	σ_2		
90	89.7	Uniform	0	0	11,545	14,487	35,593	0	35,593	0	35,593	+1.85
85	90.7	Uniform	0	1,366	11,545	14,487	35,593	3,355	35,907	-314	36,220	+1.80
80	77.5	Uniform	0	2,325	11,545	14,487	35,593	5,712	36,488	-894	37,382	+1.71
75	66.7	Triangular	0	2,982	11,545	14,487	35,593	7,327	37,043	-1,449	38,492	+1.63
70	60.1	Triangular	0	3,551	11,545	14,487	35,593	8,725	37,617	-2,024	39,640	+1.56
65	56.2	Triangular	0	4,103	11,545	14,487	35,593	10,081	38,250	-2,657	40,907	+1.48
60	50.7	Triangular	0	4,379	11,545	14,487	35,593	10,760	38,593	-3,000	41,593	+1.44
55	46.3	Triangular	0	4,588	11,545	14,487	35,593	11,272	38,863	-3,269	42,132	+1.41
50	42.4	Triangular	0	4,708	11,545	14,487	35,593	11,568	39,023	-3,429	42,452	+1.39
45	38.6	Triangular	0	4,715	11,545	14,487	35,593	11,585	39,032	-3,439	42,470	+1.39
40	35.5	Triangular	0	4,698	11,545	14,487	35,593	11,543	39,009	-3,415	42,424	+1.39
35	32.9	Triangular	0	4,656	11,545	14,487	35,593	11,439	38,953	-3,359	42,312	+1.40
30	31.1	Triangular	0	4,653	11,545	14,487	35,593	11,432	38,949	-3,355	42,304	+1.40
25	30.3	Triangular	0	4,744	11,545	14,487	35,593	11,656	39,071	-3,477	42,548	+1.38
20	30.5	Triangular	0	4,951	11,545	14,487	35,593	12,165	39,354	-3,760	43,114	+1.35
15	32.3	Triangular	0	5,390	11,545	14,487	35,593	13,242	39,980	-4,386	44,366	+1.29
10	33.1	Triangular	0	5,631	11,545	14,487	35,593	13,836	40,339	-4,746	45,084	+1.25
5	48.1	Triangular	0	8,278	11,545	14,487	35,593	20,338	44,822	-9,229	54,051	+0.88
0	81.2	Triangular	0	14,027	11,545	14,487	35,593	34,465	56,585	-20,992	77,577	+0.31

2.10.7 Static and Dynamic Testing

This section describes the testing performed on the RH-TRU 72-B impact limiters. Testing was performed to verify that the impact analyses documented in Appendix 2.10.3, *Drop Impact Evaluation Results*, properly predict the performance of the impact limiters during normal conditions of transport (NCT) and hypothetical accident conditions (HAC). The test program included both static and dynamic tests on half-scale, prototypic test specimens. Static testing is documented in Appendix 2.10.7.1, *Static Test Program*, and dynamic testing in Appendix 2.10.7.2, *Dynamic Test Program*.

2.10.7.1 Static Test Program

Static testing was performed by crushing half-scale impact limiter test articles at a fixed orientation in a laboratory test machine. Two prototypic test articles were tested in a total of three crush orientations. Test results were in the form of static force-deflection curves for crush at the tested orientation.

The purpose of static testing was to confirm that the analytical tools used to calculate impact limiter performance possess adequate accuracy. To the degree that test results and analysis predictions differed, a correction factor was formed, which was used to adjust analytical results. The correction factor formed on the basis of static testing was combined with a similar factor formed on the basis of dynamic testing, as discussed in Appendix 2.10.7.2, *Dynamic Test Program*. Impact magnitudes are calculated in Appendix 2.10.3, *Drop Impact Evaluation Results*.

An additional purpose of testing was to confirm the acceptable behavior of the impact limiters, including the ability to adequately predict such behavior, at relatively high foam strains, i.e., between 80% – 90%. Testing was performed at the University of Washington Structures Research Laboratory in Seattle, Washington, on January 6th, 1999.

2.10.7.1.1 Test Article Configuration

The test was conducted using half-scale, prototypic test articles, including attachment bolts. Therefore, all test article dimensions were half of those given in Appendix 1.3.1, *Packaging General Arrangement Drawings*. Drawings of the test articles are provided in Appendix 2.10.7.4, *Drawings*. Only two differences existed between the test articles and the full-scale prototypic impact limiters:

1. The bolt access hole debris ring was not used in testing. This component is an annular disk made of 11-gage sheet metal, held to the limiter using quarter-turn screws, and that is used to cover the impact limiter attachment bolt holes. The omission of this component had no effect on the crush strength of the impact limiters.
2. The polyurethane foam used in the test articles was nominally 12.5 lb/ft^3 density, whereas the density of the foam used in the full-scale production limiters is 11.5 lb/ft^3. This small difference came about as a consequence of the test program. As described in this appendix, the impact limiters exhibited a greater strength than expected, necessitating a small reduction in the full-scale production foam nominal density to 11.5 lb/ft^3. The test program was not repeated with the lighter foam since the difference in foam strength is modest. Furthermore,

it is of secondary importance, since the results of testing are not utilized directly, but rather as an adjustment factor that can be applied to foam strengths which are not necessarily identical to the one actually tested[1].

The test articles were designated No. 1 and No. 2.

2.10.7.1.2 Test Facilities

Testing was performed using a Baldwin test machine capable of 2.4 million pounds of crush force, and was calibrated for the purposes of this test to a load of 1.2 million pounds. The test fixture, with the test article mounted in the desired orientation, was placed within the test machine. The test fixture rested on the lower platen of the machine at floor level, and the upper platen was used to load the test article. The actual configuration of test article, test fixture, and test machine platens depended on the test orientation, and is discussed in further detail below. The test machine operated at a crush deflection rate of approximately one inch per minute.

The test articles were mounted to a massive steel test fixture which was capable of reconfiguration into each of the required orientations. The fixture was designed to have negligible deflection under test loads. The mandrel of the fixture (the component of the fixture which simulated the package and which interfaced with the test article) had a diameter of 20.8 inches, which was half of the full-scale package diameter of 41⅝ inches. This difference is negligible and had no effect on testing. The mandrel was fully engaged with the test articles, and provided for prototypic attachment of the test articles.

The crush deflection was measured using linear variable-differential transformer (LVDT) measuring devices. The instantaneous deflection values from the LVDTs, along with force values from the test machine, were sampled by a PC-based data acquisition system and recorded as force-deflection pairs.

2.10.7.1.3 Technical Basis for Tests

The orientations chosen for static testing were taken from the overall governing analysis cases. As shown in Table 2.10.3-11 in Appendix 2.10.3, *Drop Impact Evaluation Results*, the governing orientations for maximum impact are the end (85º to 90º from horizontal) and side (0º from horizontal). As shown in Figure 2.10.3-7 (oblique impact deflection) in Appendix 2.10.3, *Drop Impact Evaluation Results*, and Table 2.10.3-12 (hot side drop results) in Appendix 2.10.3, *Drop Impact Evaluation Results*, the governing cases for maximum deflection are the 55º from the horizontal orientation and the side orientation[2]. Combining all of these orientations, static tests of end, side, and 55º from the horizontal were performed. Due to the interest in maximum deflection cases, each test was carried out to the maximum practicable deflection. To prevent excessive accumulation of damage on a single test article, two test articles were used. Test article No. 1 was tested in the end orientation and test article No. 2 was tested in the side and oblique (55º) orientations. In the latter case, the damage was separated by 180º of azimuth. The tests and orientations are summarized in Table 2.10.7-1.

[1] Note that nominal density is utilized as a convenient means of designating a particular foam's general strength level; however, actual foam behavior is ultimately determined only by its individual stress-strain characteristics.

[2] Maximum impacts assume upper-bound foam properties and maximum deflections assume lower-bound foam properties.

2.10.7.1.4 Test Description and Results

Details pertaining to each test orientation and test results are discussed below. After testing was completed, the test data was plotted against the corresponding analysis-generated prediction. It was found that, for all three tests, an increase factor on foam crush stress of 1.19 was needed to bring the test results and predictions into good agreement. The "static factor" of 1.19 was applied universally as a multiplying factor to all polyurethane foam crush stress values, and the same factor was found to apply to each of the three tests. As discussed below, the application of the static factor led to extremely good agreement between test results and test predictions. Due to the good agreement and universal applicability of the static factor, it is used consistently in all of the impact analyses performed in Appendix 2.10.3, *Drop Impact Evaluation Results*[3].

Analytical predictions were prepared using the computer program CASKDROP, documented in Appendix 2.10.2.1.1, *Using CASKDROP to Determine Impact Limiter Deformation Behavior*. The basic polyurethane foam stress-strain data was taken from the foam pour records of the test articles. For the end orientation, the prediction was prepared using the parallel-to-rise[4] data from test article No. 1, pour 1, since only pour 1 foam was crushed in the test. For the side orientation, the perpendicular-to-rise data for pour 2 in test article No. 2 was used. Use of data from a single pour was sufficient since the stress-strain difference between the pours was negligible. For the oblique orientation, a combination of parallel-to-rise and perpendicular-to-rise data for pour 2 was used. The data was combined using interpolation, as described in Appendix 2.10.2.1.1, *Using CASKDROP to Determine Impact Limiter Deformation Behavior*. This stress-strain data, taken from test article acceptance test records, is given in Table 2.10.7-2. The stress-strain properties used in the analytical predictions (as adjusted for temperature) are shown in Table 2.10.7-3, Table 2.10.7-4, and Table 2.10.7-5.

The ambient temperature and the temperature of the foam within the test articles during all of the testing was approximately 65 ºF to 70 ºF.

2.10.7.1.4.1 End Orientation

Figure 2.10.7-1 shows the configuration of the end orientation static test. As shown, the only part of the test fixture needed for the test was the mandrel portion; the main framework of the fixture was not used. The mandrel was placed, axis vertical, in the test machine, and test article No. 1 was placed on top of it, with the flat, outer end of the article facing upward toward the upper platen. To avoid contact between the deformed impact limiter and the flange of the mandrel, solid steel spacers (equaling a thickness of three inches) were placed on top of the mandrel before installing the test article as shown. Furthermore, since in the end orientation there is no loading applied to the attachment bolts (since the load is applied parallel to the mandrel axis), the test article was not bolted to the mandrel. Non-prototypic bolts were used to attach the test article only to the steel spacer plates. These differences in attachment had no effect on the test. The mounted test article was placed in the approximate center of the test machine. A steel plate of 3/8-inch thickness was used to cover the upper platen. The LVDT measured the change in distance between the upper and lower platens of the test machine.

[3] Note that a "dynamic factor" is also used, based on the results of dynamic testing. The total combined static and dynamic factor, used to increase the foam crush stress for all orientations, is 1.52. Details of the dynamic test results, and a further discussion of these correction factors, are given in Section 2.10.7.3, *Correction Factors*.

[4] Rise direction is defined to be the vertical direction during foam pour, i.e., the axial direction for all test articles.

The post-test configuration of the test article is shown in a side view in Figure 2.10.7-2. As shown, the deformation exhibited by the impact limiter was completely of an inside-out nature. That is, the mandrel pushed into the impact limiter from the inside, rather than the flat bottom of the limiter crushing down from the outside. This mode of deformation means that the inner shell of the limiter moved axially relative to the outer shell, drawing the end annular shell down into the impact limiter opening as shown in Figure 2.10.7-3. As the end annular shell was drawn into the opening, it developed the radial wrinkles shown in the figure. Eventually, at a crush deflection of approximately 5.9 inches (52.4% foam crush), the seam between the end annular shell and the inner cylindrical shell of the test article separated adjacent to the weld, extending over an arc of approximately 200º around the circumference of the seam as shown in Figure 2.10.7-3. The crush test was continued to a total of 7.25 inches (65% foam strain), but due to a higher than expected crush strength, the force measuring equipment saturated at a crush of approximately 6.6 inches (59% foam strain). Note that the maximum predicted foam strain in the end drop for lower bound foam properties is 38.5%, which is less than the point at which the seam separated (see Table 2.10.3-7 in Appendix 2.10.3, *Drop Impact Evaluation Results*). The vertical height of the test article and fixture before testing was 35.5 inches, and after load removal after the test was 29 inches, for a difference of 6.5 inches.

As shown by Figure 2.10.7-2, the end annular shell of the test article came in contact with the ribs of the mandrel flange. However, as seen in Figure 2.10.7-3, the impression of the ribs is slight (less than 1/4-inch), demonstrating that this occurred late in the test, in fact, after the force measuring instrumentation had saturated. Therefore, the interference with the ribs had no effect on the data collected.

One feature of an inside-out crush deformation is that the foam undergoes two kinds of deformation: 1) ordinary compressive crush within the diameter of the inner shell of the limiter, and 2) shear cutting around the circumference of the inner shell. Only the former type of deformation is accounted for directly in the analysis software used. To account for the shear force developed, an equivalent increase in the diameter of the inner shell is assumed. Therefore, for purposes of analysis, the inner shell is assumed to have a diameter essentially equal to the outer diameter of the impact limiter, or for the case of the half-scale test article, a diameter of 37.9 inches (the outer diameter of the limiter is 38 inches). This assumption is designated the "end fully effective" case, and accounts for all of the energy absorption actually occurring in the impact limiter. When combined with the 19% increase in foam strength (the static factor of 1.19), the analysis prediction is in good agreement with test results, as shown in Figure 2.10.7-4. The CASKDROP end crush prediction results are given in Table 2.10.7-3.

2.10.7.1.4.2 Side Orientation

Figure 2.10.7-5 shows the configuration of the side orientation static test. Test article No. 2 was placed, axis horizontal, on the mandrel and attached with six, prototypic attachment bolts tightened to the appropriate half-scale torque value of 80±5 lb-ft. As shown, an upper platen load fixture was used due to the design of the test fixture. The upper platen load fixture was rigid and completely covered the crush plane of the test article. The LVDT measured the change in distance between the upper platen and the top of the main test fixture.

The post-test configuration is shown in an end view in Figure 2.10.7-6. In this case, the deformation was largely of the outside-in variety. Some shearing of the foam did occur, but not

as much as in the end orientation. In this case, the end thickness of the limiter (the portion which extends beyond, and is unsupported by, the mandrel) did not crush as much as did the annular portion (surrounding the mandrel). Instead, this portion underwent both partial crush and partial shear, with the shear plane being the plane of the bottom of the inner shell. Other than the expected deformations, there was no damage to the shells or welds, except that the welds which connected the bottom shell to the two bolt access tubes nearest the crush zone separated. The amount of exposed foam was negligible. The crush was carried out for a total crush distance of approximately 7.1 inches (84% foam strain). Upon unloading, the force-deflection curve did not reach zero force until the displacement had returned to approximately 6 inches.

As in the case of the end orientation, the crush force prediction must account for both the crush and the shearing action of the foam. For the side orientation, a fictitious increase in the inner shell is again considered, but in this case the length, rather than the diameter, is increased. The end distance of the half-scale test article, i.e., the thickness of foam beyond the end of the inner shell, is 11.25 inches. For the purposes of analysis, however, the inner shell is assumed to lengthen through half of this distance, so that the end distance is 11.25/2 = 5.625 inches. This assumption is designated the "side fully effective" case, and analytically accounts for all of the energy absorption actually occurring in the impact limiter. When combined with the 19% increase in foam strength (the static factor of 1.19), the analysis prediction is in good agreement with test results, as shown in Figure 2.10.7-7. The CASKDROP side crush prediction results are given in Table 2.10.7-4.

Examination of Figure 2.10.7-7 shows that above a crush of approximately 6 inches in the half-scale (70% foam strain), the analysis force-deflection curve diverges significantly from the test data curve. This difference is conservative, however, since it leads to an overprediction of crush force (i.e., impact) levels while at the same time conservatively overpredicting deflection. This is possible since the analytical prediction curve represents a lower rate of energy absorption than the test data curve. In fact, the energy beneath the curves becomes equivalent only at the end of the test, at a crush of 7 inches (82% foam strain). At that point, the test data curve represents $2.29(10)^6$ in-lb of energy, and the analytical prediction curve $2.24(10)^6$ in-lb. At any lesser crush, the analysis (since it underestimates absorbed energy) will overpredict deflection. Whether the crush force is overpredicted depends on the deflection distance. Below the curve crossover point at 5.5 inches (65% foam strain), the greater predicted deflection will lead to crush force levels approximately on par with the test data. Above the crossover point, the crush force levels will be conservatively overpredicted.

2.10.7.1.4.3 Oblique Orientation

Figure 2.10.7-8 shows the configuration of the oblique orientation static test. The same test article used in the side orientation, No. 2, was used for this test also. Since several of the attachment bolthole access tubes were deformed in the side orientation crush, making access to the attachment bolts impossible, the bolts were left undisturbed and the limiter was re-oriented by rotating the mandrel on the fixture through 180º. In this way, the crush began on the outer corner of the test article farthest away from the side orientation test damage. With a reconfiguration of the main test fixture, the axis of the test article was oriented at an angle of 55º from the plane of the upper platen[5]. For this test, the upper platen load fixture was removed and

[5] The test fixture and inner shell were oriented at 55º from horizontal; due to prior damage in the side test, the outer shell was oriented at approximately 60º from horizontal.

the 3/8 inch thick plate reinstalled. Since the total deflection in this test exceeded the stroke of a single LVDT, two were arranged in parallel, with an adequate offset. The second LVDT was set to begin readings before the first one reached the end of its stroke. In this way, the entire range of test travel was accommodated. The LVDTs measured the change in distance between the upper platen and the top of the main test fixture.

The post-test configuration is shown in Figure 2.10.7-9 and Figure 2.10.7-10. (Figure 2.10.7-9 shows the relative juxtaposition of the side and oblique crush damage zones.) In this orientation, essentially all the crush was of the outside-in variety. As seen in the post-test figures, the crush damage caused the welds between the bottom shell and the bolt access tubes to separate, but exposure of foam was negligible. The crush was continued for a total distance of 13.8 inches (97% foam strain). Upon unloading, the force-deflection curve did not reach zero force until the displacement had returned to approximately 12 inches.

Unlike the other two orientations, no alteration to the inner shell dimensions is necessary for the oblique case. Using the 19% increase in foam strength (static factor of 1.19), the analysis prediction is in good agreement with test results, as shown in Figure 2.10.7-11. The CASKDROP oblique crush prediction results are given in Table 2.10.7-5.

2.10.7.1.4.4 Summary

The RH-TRU 72-B package impact limiters were statically crush tested in half-scale, and force-deflection curves were developed. Two test articles were tested in end, side, and 55º from horizontal oblique orientations to deflections that were larger than the maximum deflections predicted for the worst case HAC drop events. Analytical tools were used to predict the test results, and with the utilization of a correction factor of 1.19 on the basic input foam crush stress levels, the agreement between test and predictions is good.

2.10.7.2 Dynamic Test Program

Dynamic testing was performed by dropping half-scale impact limiter test articles from a height of 30 feet onto a flat, horizontal, essentially unyielding surface, in accordance with 10 CFR 71.73(c)(1)[6]. Two test articles were used together with a test package, and were dropped in a total of three orientations, which corresponded to the orientations used in static testing. The test package possessed prototypic weight and impact limiter attachment features. Test results took the form of measured impact deformations. The purpose of dynamic testing was to confirm that the analytical tools used to calculate impact limiter performance possess adequate accuracy. To the degree that test results and analysis predictions differed, a correction factor was formed, which was used to adjust analytical results. The correction factor formed on the basis of dynamic testing was inclusive of the factor formed on the basis of static testing as discussed in Section 2.10.7.1, *Static Test Program*. Impact magnitudes are calculated in Appendix 2.10.3, *Drop Impact Evaluation Results*.

An additional purpose of testing was to confirm the dynamic integrity of the impact limiter in an impact event, and to demonstrate that impact limiter attachments are adequate to prevent loss of

[6] Title 10, Code of Federal Regulations, Part 71 (10 CFR 71), *Packaging and Transportation of Radioactive Material*, 01-01-14 Edition.

a limiter due to impact. Testing was performed in Richland, Washington, on January 18 and February 4, 1999.

2.10.7.2.1 Test Article Configuration

A description of the test articles is given in Section 2.10.7.1.1, *Test Article Configuration*. Dynamic testing was performed using test articles designated No. 3 and No. 4. These articles had the same construction and polyurethane foam specification as did the test articles used in static testing (No. 1 and No. 2). The bolt access hole debris ring was not used in dynamic testing. This omission had no effect on test results. Drawings of the test articles are provided in Appendix 2.10.7.4, *Drawings*.

2.10.7.2.2 Test Facilities

Free drop testing was performed using the drop pad located in the 300 Area of the Department of Energy Hanford Site in Richland, Washington. The pad is made of highly reinforced concrete and covered with an 8½-inch thick steel plate. The pad weighs an estimated 110 tons, which is more than 38 times the weight of the test package, and easily qualifies as an essentially unyielding surface.

The free drop height was 30 feet, +3/-0 inches, measured from the point of the impact limiter nearest the ground. The orientation of the test package for all drops was verified using an inclinometer. When necessary due to wind conditions, guy ropes were used to control the position of the package prior to release to ensure that the package struck within the boundaries of the pad's steel top plate. However, inclination to the horizontal was not affected by wind. The drop from the specified height was completely free.

The test package was made from a thick walled, mild steel pipe with thick end plates, as shown on the drawings included in Appendix 2.10.7.4, *Drawings*. To attain the necessary weight, solid steel bars were securely welded to the inside of the pipe. One additional bar was located in the center of the pipe, and securely welded to one end plate. The space between the steel bars was packed with sand. The test package was 20.8 inches in diameter, which was half of the full-scale package diameter of 41⅝ inches. This difference is negligible and had no effect on testing. The length of the package was 70.9 inches. The impact limiter test articles were attached to the package using prototypic attachment bolts tightened to 80±5 lb-ft. If impact distortion did not render the bolt heads inaccessible, this torque was restored between separate drop tests. For the end drop, only a lower impact limiter test article was needed, and therefore a test plate, which simulated the weight of an impact limiter, was attached to the upper end of the test package in place of an impact limiter. The total weight of the test package in the end drop case was 5,736 pounds. In the side and oblique drop cases, both impact limiter test articles were in place, and the weight of the test package in these drop cases was 5,781 pounds. These weights are within 3% of the half-scale maximum package weight of 45,000 × 1/8 = 5,625 pounds, where 45,000 pounds is the full-scale weight from Section 2.2, *Weights and Centers of Gravity*, and the 1/8 factor is the scale factor on weight, equal to $(1/2)^3$.

A complete record of all drop test activities was made using still and conventional speed video photography.

2.10.7.2.3 Technical Basis for Tests

The orientations chosen for dynamic testing were based on the orientations used in static testing. As discussed in Section 2.10.7.1.3, *Technical Basis for Tests*, these orientations are chosen based on the overall governing analysis cases. The dynamic tests further confirm the adequacy of the analytical methods to properly predict maximum impacts and deformations presented in Appendix 2.10.3, *Drop Impact Evaluation Results*. Another reason for including the end drop among the free drops performed is because the end drop orientation represents the largest[7] impact level, and thus caused the greatest amount of damage to the impact limiter. To prevent excessive accumulation of damage on a single test article, two test articles were used. Test article No. 3 was tested in the end drop and test article No. 4 was tested in the side and oblique (55º) drops. (Test article No. 3 was also present as a prop for the side and oblique drops). As for the static testing, the side and the oblique impact damage zones were separated by 180º of azimuth. The tests and orientations are summarized in Table 2.10.7-6.

2.10.7.2.4 Test Description and Results

Details pertaining to each test orientation and test results are discussed below. Aside from ordinary physical examination, noting types and degree of impact damage, the principal form of free drop test result was the measurement of impact deflection. Due to the presence of significant elastic recovery of the polyurethane foam, crush gages were used in the end and side drop cases to accurately record the maximum crush deflection of the test articles, as described in more detail below. (Measurement of the oblique impact deflection was made using physical measurements of the test article). The measured maximum deflection was used to formulate a correction factor for use with the analytical prediction method ("dynamic factor"). Discussion of the dynamic factor, and its relationship to the static factor, is given in Appendix 2.10.7.3, *Correction Factors*.

Analytical predictions of maximum deflection were prepared using the code CASKDROP, documented in Appendix 2.10.2.1.1, *Using CASKDROP to Determine Impact Limiter Deformation Behavior*. The basic polyurethane foam stress-strain data was taken from the foam pour records of the test articles. For the end drop, the prediction was prepared using the parallel-to-rise data from test article No. 3, pour 1, since only pour 1 foam was crushed in the test. For the side drop, the perpendicular-to-rise data in test article No. 4 for pour 3 was used. (Use of data from a single pour was sufficient since the stress-strain difference between the pours was negligible). For the oblique orientation, a combination of parallel-to-rise and perpendicular-to-rise data for pour 3 was used. The data was combined using interpolation, as described in Appendix 2.10.2.1.1, *Using CASKDROP to Determine Impact Limiter Deformation Behavior*. The stress-strain data, taken from test article acceptance test records, is given in Table 2.10.7-7.

Prior to each test, the temperature of the foam in the test article was measured using short holes drilled into the foam beneath each of the three plastic pipe plug ports. In preparing the test predictions, the properties of the foam were adjusted for temperature using factors developed using the General Plastics foam property database. Since the pour's stress-strain data was taken at room temperature (approximately 73 ºF), the adjustment factor was equal to the ratio of the strength at test temperature to the strength at 73 ºF.

[7] The 85º oblique drop has a very slightly higher impact than the end drop: 90.7*g* vs 89.7*g* (see Table 2.10.3-11 in Appendix 2.10.3, *Drop Impact Evaluation Results*).

The database foam chosen to create this ratio had a strength level essentially the same as the test article foam.

2.10.7.2.4.1 End Free Drop

Figure 2.10.7-12 shows the configuration of the end drop. Test article No. 3 was attached to the bottom of the test package using 6 prototypic bolts, tightened as discussed in Appendix 2.10.7.2.2, *Test Facilities*. The test plate, simulating the weight of a half-scale impact limiter, was attached to the top of the test package. The axis of the test package was at an angle of 90º from horizontal. To ensure that a record of maximum deflection would be made, independent of elastic recovery, measurement of the bolt access tubes was made both prior to and after the test. The tubes are located on the bottom of the inner shell and are positioned parallel to the package axis (the direction of crush). During impact, the tubes deform by crippling, with essentially no change in their overall position. To ensure that the elastic recovery of the foam did not re-lengthen the deformed tubes, the weld connecting the tube to the bottom shell of test article No. 3 was severed on three of the six tubes. In this way, a tensile load could not be applied to the deformed tube after the maximum deflection had occurred. Therefore, the maximum deflection of the impact limiter was the difference between the length of the deformed and undeformed tubes. The average temperature of the foam in the test article was 42 ºF.

Figure 2.10.7-13 shows the post-test configuration of the end drop test. As in the static end orientation case, the deformation is completely inside-out. That is, the test package pushed into the impact limiter from the inside, rather than the flat bottom of the limiter crushing in from the outside. In fact, the deformation pattern and nature was identical to the static end test, but with a lesser magnitude. There was no failure of the shell anywhere on the test article.

The average length of the three tubes before testing (measured from the flat end of the limiter to the attachment bolt head) was 8.57 inches. After testing, the average length was 6.05 inches, for a difference equal to the maximum deflection of 8.57 – 6.05 = 2.52 inches. To obtain this same deflection value using the CASKDROP code using test article foam data adjusted for a temperature of 42 ºF required that an increase factor of 1.52 be applied to the input foam stress-strain data. Further discussion of this factor is given in Appendix 2.10.7.3, *Correction Factors*. The CASKDROP end drop prediction results are given in Table 2.10.7-8.

Immediately after impact, the elastic recovery in the foam caused the ends of the three gage tubes to recede below the bottom surface of the impact limiter. The difference in length between the top of the three gage tubes and the bottom of the limiter was an average of 1.4 inches. The amount of elastic recovery, or “springback”, was therefore 1.4/2.52 × 100 = 56%.

2.10.7.2.4.2 Side Free Drop

Figure 2.10.7-14 shows the configuration of the side drop. Test article No. 3 was attached to the bottom of the package as in the end drop. Since the bolt tubes were crippled, retightening of the attachment bolts was not possible. Test article No. 4 was attached to the top end of the package using 6 prototypic bolts and tightened, as discussed in Appendix 2.10.7.2.2, *Test Facilities*. The axis of the package was horizontal. The damage to test article No. 3 from the end drop was modest, and did not significantly affect the impact behavior of the new test article, No. 4. To ensure that a record of maximum deflection would be made, independent of elastic recovery, two independent crush gages were secured to the lower side of the test package, as shown in Figure

2.10.7-15[8]. The gages consisted of square tubes, approximately 3.5 inches on a side, made from 1/16 inch thick soft aluminum sheet. The axis of the tubes was parallel to the direction of deflection of the impact limiters during impact. During impact, the gages crippled and retained the maximum deflection of the limiters. The force required to deform the gages was negligible. The average temperature of the foam in the test article was 45 ºF.

Figure 2.10.7-16 shows the post-test configuration of the side drop test. In this case, the nature of the deflection is essentially all outside-in. As for the end drop, the deformation of the test article was similar to that from the corresponding static test, but of a lesser magnitude. The only (minimal) exposure of foam was from the separation of the weld between the two bolt access tubes nearest the ground and the bottom sheet of the limiter.

Figure 2.10.7-16 also shows the post-test configuration of the test article No. 4 crush gage. The gages had an undeformed length of 7.0 inches. There was also a clearance between the end of the gage and the ground of 1.5 inches. After the test, the test article No. 4 gage had a length of 4.94 inches. Thus, the maximum deflection of test article No. 4 in the side drop was $7.0 - 4.94 + 1.5 = 3.56$ inches. (In the side drop, test article No. 3 was considered only as a backup, due to the prior damage it received in the end drop. Therefore, since good data was collected from test article No. 4, no further consideration of test article No. 3 was needed.) CASKDROP predicted, using test article foam data corrected for temperature and using the dynamic factor of 1.52 as a multiplying factor on foam strength, a deflection of 4.04 inches, which is in reasonable agreement with the test results. The CASKDROP side drop prediction results are given in Table 2.10.7-9.

However, note is taken of the fact that, as seen in Figure 2.10.7-7 in Appendix 2.10.7.1.4.2, *Side Orientation*, the static test force-deflection curve in the region below 4 – 5 inches of deflection lies somewhat above the CASKDROP predicted curve. Therefore, the actual test force-deflection curve could be expected to absorb the drop test energy with slightly less deflection than the predicted curve. In fact, when the actual static test force-deflection curve is used to form the dynamic prediction, the deflection result is identical with the test data. How this was done is now briefly described.

First, the static test force-deflection curve was adjusted for temperature, which was done the same way as for foam strength as described above. Next, the curve was adjusted for the dynamic effect. In the end drop, an overall factor (including both static and dynamic effects) was found to be 1.52. The dynamic share of this factor is $1.52/1.19 = 1.277$, where 1.19 is the static factor found in Appendix 2.10.7.1.4, *Test Description and Results*. The static force-deflection curve is then increased by the "temperature factor" × "dynamic factor".

The resulting curve is integrated to give the total absorbed energy of crush. When the absorbed energy equals the kinetic energy of the test package, the solution is reached. (This is the same quasi-static approach utilized in the CASKDROP code). The total kinetic energy of the test package is $W \times (360 + \delta)$, where W is the weight of the test package, 360 is the drop height in inches, and δ is the crush deflection of the impact limiters. The solution for δ is 3.56 inches, identical with the test data, and an impact of 155.9*g*. Although less accurate, the CASKDROP prediction is still conservative for both deflection and impact, since it predicts 4.04 inches and 156.4*g*.

[8] For clarity in the photograph, the test package has been rolled so that the axis of the gages is horizontal. During the drop, the axis of the gages is vertical.

Measurements of the post-test flat on test article No. 4 were also made to compare with the crush gage. Using the package body as a reference, the apparent deflection in the side drop was 1.87 inches. The elastic recovery, or "springback", was therefore (3.56 – 1.87)/3.56 × 100 = 47%.

2.10.7.2.4.3 Oblique Free Drop

Figure 2.10.7-17 shows the configuration of the oblique drop. Test articles No. 3 and No. 4 were attached to the test package as in the side drop. Since five of the attachment bolts of test article No. 4 were still accessible, they were retightened to specification. The amount of retightening needed was modest. The primary impact occurred on test article No. 4, at the corner of the limiter which was 180º opposite the side drop damage. A slapdown occurred on test article No. 3. The axis of the test package was actually 53º from horizontal. The average temperature of the foam in the test article was again 45 ºF.

Figure 2.10.7-18 and Figure 2.10.7-19 show the post-test configuration of the oblique drop test. In this case, no separate crush gages were used, since the nature of the oblique impact damage made determination of the maximum deflection somewhat more straightforward. In the oblique case, there is a reduction in surface area over the impact plane, and this accounts for the strongly wrinkled state of the impact surface. In addition, the same reduction in surface area causes local scrubbing of the steel drop pad, transferring a heavy coat of rust to the test article, and making the actual extent of the maximum impact surface quite distinct.

Figure 2.10.7-20 shows how the maximum deflection was calculated using the edges of contact. The maximum deflection, measured along the direction of crush, was 7.3 inches. The corresponding prediction was prepared using both CASKDROP and SLAPDOWN, the latter code (see Appendix 2.10.2.2, *Description of the SLAPDOWN Computer Code*) being necessary since the impact is unstable with some of the drop energy going into package rotation. As in the previous two cases, the basic test article foam data was corrected for temperature and increased by the dynamic factor of 1.52 as a multiplying factor on foam strength. The force-deflection curve produced by CASKDROP was fed into SLAPDOWN, which performed a dynamic analysis. The resulting maximum predicted deflection of the primary impact limiter (test article No. 4), was 8.76 inches, which is in reasonable agreement with the test results, and again represents a conservative overprediction of deflection. The CASKDROP and SLAPDOWN oblique drop prediction results are given in Table 2.10.7-10 and Table 2.10.7-11, respectively.

After the oblique drop test, of the four remaining accessible bolts, only one had less than full torque.

2.10.7.2.5 Summary

The RH-TRU 72-B impact limiters were tested in half-scale, 30-foot free drop tests. Two test articles were tested in end, side, and 55º from horizontal oblique orientations. Based on a correction factor developed on the basis of the end drop test, the predictions of the side and oblique drops were in good to excellent agreement with the test results, as summarized in Table 2.10.7-12.

A further result of testing was to demonstrate the structural integrity of both limiter shells and attachments, in a range of impact orientations.

2.10.7.3 Correction Factors

As discussed in Appendix 2.10.7.1.4, *Test Description and Results*, a factor was developed which was used to bring the static test results and test predictions into good agreement. The fact that the same factor (1.19) could be applied to all cases gives confidence that the basic prediction technique is acceptable. However, as described in Appendix 2.10.7.2.4, *Test Description and Results*, further adjustments to the results due to dynamic effects are also necessary. The adjustment factor in that case was found to be 1.52. This was developed on the basis of the end drop test, but when applied to the side and oblique drop cases, good agreement to test results was again obtained. Similar to the static factor, the universal applicability of the dynamic factor gives confidence that the analysis predictions are correct.

These correction factors are used in the impact predictions in Appendix 2.10.3, *Drop Impact Evaluation Results*, in the following way. For HAC drops from 30 feet, the overall factor of 1.52 is used, consistent with the test results discussed in this section. (The static factor of 1.19 is contained within the overall factor, and therefore does not need to be separately applied). For NCT free drops from 1 foot, only the static factor of 1.19 is applied. This is because the strain rate (and therefore, any dynamic effect) in the 1-foot drop is negligible compared to the 30-foot drop. The development of the foam strength used in the impact predictions, including the application of the correction factors, is discussed in Appendix 2.10.3, *Drop Impact Evaluation Results*.

2.10.7.4 Drawings

The following drawings are included in this section:

- 9715-015, *RH-72B Dummy Package*, Sheet 1 (Figure 2.10.7-21)
- 9715-015, *RH-72B Dummy Package*, Sheet 2 (Figure 2.10.7-22)
- 9715-010, *Impact Limiter Test Article RH-72B*, Sheet 1 (Figure 2.10.7-23)
- 9715-010, *Impact Limiter Test Article RH-72B*, Sheet 2 (Figure 2.10.7-24)
- 9715-010, *Impact Limiter Test Article RH-72B*, Sheet 3 (Figure 2.10.7-25)
- 9715-010, *Impact Limiter Test Article RH-72B*, Sheet 4 (Figure 2.10.7-26)

Table 2.10.7-1 – Static Crush Test Summary

Test No.	Unit No.	Orientation from Horizontal	Azimuth Orientation	Purpose of Test
1	1	End (90º)	—	Maximum Impact Case
2	2	Side (0º)	0º	High Impact Case (Cold), High Deflections (Warm)
3	2	Oblique (55º)	180º	Maximum Deflection Case (Warm)

Table 2.10.7-2 – Static Test Article Stress-Strain Properties

Strain, %	Crush Stress at 73ºF (psi)		
	No. 1, Pour 1 Parallel-to-Rise	No. 2, Pour 2 Parallel-to-Rise	No. 2, Pour 2 Perpendicular-to-Rise
5	488	420	363
10	516	423	390
20	510	438	415
30	544	479	458
40	630	549	534
50	822	683	674
60	1,187	972	972
65	1,533	1,278	1,292
70	2,078	1,762	1,864
75	—	2,625	2,750
80	—	4,509	4,849
87	—	14,731	16,403

Table 2.10.7-3 – End Crush CASKDROP Output

End Drop *** PACKAGING TECHNOLOGY *** CASKDROP, v2.31
02-02-1999, 14:00:20 Nov 13, 1997

72-B End Crush Test Prediction (Half Scale), fully effective			
Impact Limiter Weight (each) -	313 lbs	Cask and Payload Weight -	5,000 lbs
Impact Limiter Outside Diameter -	38.0000 in	Cask Outside Diameter -	37.9000 in
Impact Limiter Overall Length -	23.0000 in	Cask Overall Length -	70.9000 in
Impact Limiter Conical Diameter -	0.0000 in	Dynamic Unloading Modulus -	1.000E+07 lbs/in
Impact Limiter Conical Length -	0.0000 in	Rad Mass Moment of Inertia -	9,468 lb-in-s²
Impact Limiter End Thickness -	11.2500 in	Frictional Coefficient -	0.0000
Impact Limiter Hole Diameter -	0.0000 in	Drop Height -	30.0000 ft
Impact Limiter Hole Length -	0.0000 in	Drop Angle from Horizontal -	90.0000°
Unbacked Area Threshhold Strain -	0.0000 in/in	Crush Analysis Theory -	Global
Unbacked Area Crush Stress -	0 psi	Number of Integration Incs -	50

VARIABLE CRUSH STRESS	
ε (in/in)	σ (psi)
0.000	0.0
0.050	580.0
0.060	610.0
0.100	614.0
0.120	612.6
0.150	610.5
0.200	607.0
0.300	647.0
0.400	750.0
0.500	979.0
0.600	1,412.0
0.650	1,824.0
0.700	2,473.0

DEFL (in)	MAX ε (%)	AREA (in²)	VOLUME (in³)	XBAR (in)	IMPACT FORCE (lbs)	ACCEL (g's)	I/L MOMENT (in-lbs)	STRAIN ENERGY (in-lbs)	KINETIC ENERGY (in-lbs)	SE/KE RATIO
0.500	4.44	1,134	567	0.00	618,243	109.9	0	30,912	2,027,813	0.02
0.600	5.33	1,134	680	0.00	669,350	119.0	0	95,292	2,028,375	0.05
0.700	6.22	1,134	794	0.00	692,297	123.1	0	163,374	2,028,938	0.08
0.800	7.11	1,134	907	0.00	701,658	124.7	0	233,072	2,029,500	0.11
0.900	8.00	1,134	1,021	0.00	702,463	124.9	0	303,278	2,030,063	0.15
1.000	8.89	1,134	1,134	0.00	698,515	124.2	0	373,327	2,030,625	0.18
1.500	13.33	1,134	1,701	0.00	690,652	122.8	0	719,470	2,033,438	0.35
2.000	17.78	1,134	2,268	0.00	685,219	121.8	0	1,063,448	2,036,250	0.52
2.500	22.22	1,134	2,835	0.00	688,517	122.4	0	1,406,225	2,039,063	0.69
3.000	26.67	1,134	3,402	0.00	707,622	125.8	0	1,754,699	2,041,875	0.86
3.500	31.11	1,134	3,969	0.00	738,526	131.3	0	2,115,848	2,044,688	1.03
4.000	35.56	1,134	4,536	0.00	781,508	138.9	0	2,495,203	2,047,500	1.22
4.500	40.00	1,134	5,104	0.00	846,115	150.4	0	2,901,032	2,050,313	1.41
5.000	44.44	1,134	5,671	0.00	941,113	167.3	0	3,346,559	2,053,125	1.63
5.500	48.89	1,134	6,238	0.00	1,067,868	189.8	0	3,847,543	2,055,938	1.87
6.000	53.33	1,134	6,805	0.00	1,228,583	218.4	0	4,420,013	2,058,750	2.15
6.500	57.78	1,134	7,372	0.00	1,448,800	257.6	0	5,086,229	2,061,563	2.47
7.000	62.22	1,134	7,939	0.00	1,768,481	314.4	0	5,885,487	2,064,375	2.85
7.500	66.67	1,134	8,506	0.00	2,279,317	405.2	0	6,887,367	2,067,188	3.33
8.000	71.11	1,134	9,073	0.00	2,966,120	527.3	0	8,196,035	2,070,000	3.96
8.500	75.56	1,134	9,640	0.00	3,670,901	652.6	0	9,855,290	2,072,813	4.75
9.000	80.00	1,134	10,207	0.00	4,375,682	777.9	0	11,866,936	2,075,625	5.72
9.500	84.44	1,134	10,774	0.00	5,080,464	903.2	0	14,230,973	2,078,438	6.85
10.000	88.89	1,134	11,341	0.00	5,785,245	1,028.5	0	16,947,400	2,081,250	8.14
10.500	93.33	1,134	11,908	0.00	6,490,026	1,153.8	0	20,016,218	2,084,063	9.60
11.000	97.78	1,134	12,475	0.00	7,194,808	1,279.1	0	23,437,426	2,086,875	11.23

Note: For the purpose of this analysis, only the indicated columns are relevant.

Table 2.10.7-4 – Side Crush CASKDROP Output

Side Drop *** PACKAGING TECHNOLOGY *** CASKDROP, v2.31
02-24-1999, 13:54:29 Nov 13, 1997

72-B Side Crush Prediction (Half Scale), fully effective			
Impact Limiter Weight (each) -	313 lbs	Cask and Payload Weight -	5,000 lbs
Impact Limiter Outside Diameter -	38.0000 in	Cask Outside Diameter -	21.0000 in
Impact Limiter Overall Length -	23.0000 in	Cask Overall Length -	70.9000 in
Impact Limiter Conical Diameter -	0.0000 in	Dynamic Unloading Modulus -	1.000E+07 lbs/in
Impact Limiter Conical Length -	0.0000 in	Rad Mass Moment of Inertia -	7,526 lb-in-s²
Impact Limiter End Thickness -	5.6250 in	Frictional Coefficient -	0.0000
Impact Limiter Hole Diameter -	0.0000 in	Drop Height -	30.0000 ft
Impact Limiter Hole Length -	0.0000 in	Drop Angle from Horizontal -	0.0000°
Unbacked Area Threshhold Strain -	0.1000 in/in	Crush Analysis Theory -	Global
Unbacked Area Crush Stress -	464 psi	Number of Integration Incs -	50

VARIABLE CRUSH STRESS	
ε (in/in)	σ (psi)
0.000	0.0
0.050	431.0
0.100	464.0
0.200	494.0
0.300	545.0
0.400	635.0
0.500	802.0
0.600	1,157.0
0.650	1,537.0
0.700	2,218.0
0.750	3,273.0
0.800	5,770.0
0.870	19,520.0

DEFL (in)	MAX ε (%)	AREA (in²)	VOLUME (in³)	XBAR (in)	IMPACT FORCE (lbs)	ACCEL (g's)	I/L MOMENT (in-lbs)	STRAIN ENERGY (in-lbs)	KINETIC ENERGY (in-lbs)	SE/KE RATIO
0.500	5.88	398	133	0.00	112,001	19.9	0	28,000	2,027,813	0.01
1.000	11.76	560	375	0.00	198,795	35.3	0	105,699	2,030,625	0.05
1.500	17.65	681	686	0.00	265,260	47.2	0	221,713	2,033,438	0.11
2.000	23.53	781	1,052	0.00	331,071	58.9	0	370,796	2,036,250	0.18
2.500	29.41	867	1,465	0.00	390,680	69.5	0	551,233	2,039,063	0.27
3.000	35.29	943	1,917	0.00	446,952	79.5	0	760,641	2,041,875	0.37
3.500	41.17	1,011	2,406	0.00	502,477	89.3	0	997,999	2,044,688	0.49
4.000	47.05	1,073	2,927	0.00	558,063	99.2	0	1,263,134	2,047,500	0.62
4.500	52.93	1,130	3,478	0.00	629,479	111.9	0	1,560,019	2,050,313	0.76
5.000	58.82	1,182	4,056	0.00	727,804	129.4	0	1,899,340	2,053,125	0.93
5.205	61.23	1,202	4,301	0.00	781,000	138.8	0	2,054,280	2,054,280	1.00
5.500	64.70	1,230	4,659	0.00	876,240	155.8	0	2,300,351	2,055,938	1.12
6.000	70.58	1,275	5,286	0.00	1,121,838	199.4	0	2,799,870	2,058,750	1.36
6.500	76.46	1,316	5,934	0.00	1,524,711	271.1	0	3,461,508	2,061,563	1.68
7.000	82.34	1,355	6,602	0.00	2,568,055	456.5	0	4,484,699	2,064,375	2.17
7.500	88.22	1,391	7,289	0.00	5,588,834	993.6	0	6,523,921	2,067,188	3.16
8.000	94.10	1,425	7,993	0.00	10,065,785	1,789.5	0	10,437,576	2,070,000	5.04
8.500	99.99	1,457	8,714	0.00	15,477,921	2,751.6	0	16,823,502	2,072,813	8.12

Note: The column labeled "Impact Force" represents the sum of two identical forces on each impact limiter. For the purpose of this analysis, only the indicated columns are relevant.

Table 2.10.7-5 – Oblique Crush CASKDROP Output

Corner Drop *** PACKAGING TECHNOLOGY *** CASKDROP, v2.31
02-05-1999, 17:00:46 Nov 13, 1997

72-B 55 Deg Crush Prediction (Half Scale), fully effective			
Impact Limiter Weight (each) -	313 lbs	Cask and Payload Weight -	5,000 lbs
Impact Limiter Outside Diameter -	38.0000 in	Cask Outside Diameter -	21.0000 in
Impact Limiter Overall Length -	23.0000 in	Cask Overall Length -	70.9000 in
Impact Limiter Conical Diameter -	0.0000 in	Dynamic Unloading Modulus -	1.000E+07 lbs/in
Impact Limiter Conical Length -	0.0000 in	Rad Mass Moment of Inertia -	8,136 lb-in-s²
Impact Limiter End Thickness -	11.2500 in	Frictional Coefficient -	0.0000
Impact Limiter Hole Diameter -	0.0000 in	Drop Height -	30.0000 ft
Impact Limiter Hole Length -	0.0000 in	Drop Angle from Horizontal -	55.0000°
Unbacked Area Threshhold Strain -	0.1000 in/in	Crush Analysis Theory -	Global
Unbacked Area Crush Stress -	489 psi	Number of Integration Incs -	50
		Maximum Non-Convergence -	0.0000%

VARIABLE CRUSH STRESS	
ε (in/in)	σ (psi)
0.000	0.0
0.050	474.0
0.100	489.0
0.200	512.0
0.300	561.0
0.400	647.0
0.500	809.0
0.600	1,157.0
0.650	1,526.0
0.700	2,134.0
0.750	3,170.0
0.800	5,489.0
0.870	18,116.0

DEFL (in)	MAX ε (%)	AREA (in²)	VOLUME (in³)	XBAR (in)	IMPACT FORCE (lbs)	ACCEL (g's)	I/L MOMENT (in-lbs)	STRAIN ENERGY (in-lbs)	KINETIC ENERGY (in-lbs)	SE/KE RATIO
0.500	69.32	8	2	-11.64	6,847	1.2	0	1,712	2,027,813	0.00
1.000	69.25	23	9	-12.05	19,199	3.4	0	8,223	2,030,625	0.00
1.500	69.17	42	25	-12.45	34,960	6.2	0	21,763	2,033,438	0.01
2.000	69.09	64	51	-12.86	53,340	9.5	0	43,838	2,036,250	0.02
2.500	69.01	88	89	-13.26	73,842	13.1	0	75,634	2,039,063	0.04
3.000	68.97	115	140	-13.66	96,056	17.1	0	118,108	2,041,875	0.06
3.500	68.95	144	204	-14.05	119,686	21.3	0	172,044	2,044,688	0.08
4.000	68.95	174	284	-14.43	144,505	25.7	0	238,092	2,047,500	0.12
4.500	68.95	206	379	-14.81	170,324	30.3	0	316,799	2,050,313	0.15
5.000	68.96	240	490	-15.18	196,936	35.0	0	408,614	2,053,125	0.20
5.500	68.96	274	619	-15.55	224,255	39.9	0	513,911	2,055,938	0.25
6.000	68.96	310	765	-15.90	252,107	44.8	0	633,002	2,058,750	0.31
6.500	68.95	347	929	-16.25	280,412	49.9	0	766,131	2,061,563	0.37
7.000	68.93	384	1,112	-16.60	309,061	54.9	0	913,499	2,064,375	0.44
7.500	68.90	422	1,313	-16.93	337,933	60.1	0	1,075,248	2,067,188	0.52
8.000	68.86	461	1,534	-17.25	366,846	65.2	0	1,251,443	2,070,000	0.60
8.500	68.81	500	1,774	-17.57	395,795	70.4	0	1,442,103	2,072,813	0.70
9.000	68.74	540	2,034	-17.87	424,614	75.5	0	1,647,206	2,075,625	0.79
9.500	68.67	580	2,314	-18.16	453,147	80.6	0	1,866,646	2,078,438	0.90
10.000	69.84	620	2,614	-18.34	485,247	86.3	0	2,101,245	2,081,250	1.01
10.500	73.59	660	2,934	-18.22	533,409	94.8	0	2,355,909	2,084,063	1.13
11.000	77.36	701	3,274	-18.09	589,096	104.7	0	2,636,535	2,086,875	1.26
11.500	81.11	741	3,635	-17.80	664,802	118.2	0	2,950,010	2,089,688	1.41
12.000	84.64	781	4,015	-17.32	782,469	139.1	0	3,311,827	2,092,500	1.58
12.500	88.17	822	4,416	-16.59	978,863	174.0	0	3,752,160	2,095,313	1.79
13.000	91.69	861	4,837	-15.86	1,282,291	228.0	0	4,317,449	2,098,125	2.06
13.500	95.22	901	5,277	-15.26	1,713,019	304.5	0	5,066,277	2,100,938	2.41
14.000	98.75	940	5,737	-14.85	2,279,355	405.2	0	6,064,370	2,103,750	2.88

Note: For the purpose of this analysis, only the indicated columns are relevant.

Table 2.10.7-6 – Dynamic Drop Test Summary

Test No.	Unit No.	Orientation from Horizontal	Azimuth Orientation	Purpose of Test
1	3	End (90º)	—	Maximum Impact Case, Structural Integrity Case
2	4	Side (0º)	0º	High Impact Case (Cold), High Deflections (Warm)
3	4	Oblique (55º)	180º	Maximum Deflection Case (Warm)

Table 2.10.7-7 – Dynamic Test Article Stress-Strain Properties

Strain, %	Crush Stress at 73ºF (psi)		
	No. 3, Pour 1 Parallel-to-Rise	No. 4, Pour 3 Parallel-to-Rise	No. 4, Pour 3 Perpendicular-to-Rise
5	438	459	384
10	458	457	426
20	473	467	446
30	513	505	483
40	585	565	548
50	734	703	685
60	1,055	994	994
65	1,341	1,265	1,305
70	1,850	1,709	1,788
75	2,689	2,475	2,578

Table 2.10.7-8 – End Drop CASKDROP Output

End Drop *** PACKAGING TECHNOLOGY *** CASKDROP, v2.31
02-02-1999, 09:38:21 Nov 13, 1997

72-B End Drop Analysis (Half Scale @ 42 Deg F, incl. nec. factors)			
Impact Limiter Weight (each) -	0 lbs	Cask and Payload Weight -	5,736 lbs
Impact Limiter Outside Diameter -	38.0000 in	Cask Outside Diameter -	37.9000 in
Impact Limiter Overall Length -	23.0000 in	Cask Overall Length -	70.9000 in
Impact Limiter Conical Diameter -	0.0000 in	Dynamic Unloading Modulus -	1.000E+07 lbs/in
Impact Limiter Conical Length -	0.0000 in	Rad Mass Moment of Inertia -	7,552 lb-in-s²
Impact Limiter End Thickness -	11.2500 in	Frictional Coefficient -	0.0000
Impact Limiter Hole Diameter -	0.0000 in	Drop Height -	30.0000 ft
Impact Limiter Hole Length -	0.0000 in	Drop Angle from Horizontal -	90.0000°
Unbacked Area Threshhold Strain -	0.1000 in/in	Crush Analysis Theory -	Global
Unbacked Area Crush Stress -	813 psi	Number of Integration Incs -	50

VARIABLE CRUSH STRESS	
ε (in/in)	σ (psi)
0.000	0.0
0.050	778.0
0.100	813.0
0.200	838.0
0.300	907.0
0.400	1,030.0

DEFL (in)	MAX ε (%)	AREA (in²)	VOLUME (in³)	XBAR (in)	IMPACT FORCE (lbs)	ACCEL (g's)	I/L MOMENT (in-lbs)	STRAIN ENERGY (in-lbs)	KINETIC ENERGY (in-lbs)	SE/KE RATIO
0.500	4.44	1,134	567	0.00	823,303	143.5	0	205,826	2,067,900	0.10
1.000	8.89	1,134	1,134	0.00	948,200	165.3	0	648,702	2,070,768	0.31
1.500	13.33	1,134	1,701	0.00	888,817	154.9	0	1,107,956	2,073,636	0.53
2.000	17.78	1,134	2,268	0.00	923,511	161.0	0	1,561,038	2,076,504	0.75
2.500	22.22	1,134	2,835	0.00	971,329	169.3	0	2,034,748	2,079,373	0.98
2.546	22.63	1,134	2,888	0.00	974,589	169.9	0	2,079,637	2,079,637	1.00
3.000	26.67	1,134	3,402	0.00	1,002,104	174.7	0	2,528,106	2,082,241	1.21
3.500	31.11	1,134	3,969	0.00	1,039,374	181.2	0	3,038,476	2,085,109	1.46
4.000	35.56	1,134	4,536	0.00	1,097,285	191.3	0	3,572,641	2,087,977	1.71
4.500	40.00	1,134	5,104	0.00	1,166,845	203.4	0	4,138,673	2,090,845	1.98
5.000	44.44	1,134	5,671	0.00	1,238,346	215.9	0	4,739,971	2,093,713	2.26
5.500	48.89	1,134	6,238	0.00	1,309,846	228.3	0	5,377,019	2,096,581	2.56
6.000	53.33	1,134	6,805	0.00	1,381,347	240.8	0	6,049,817	2,099,449	2.88
6.500	57.78	1,134	7,372	0.00	1,452,848	253.3	0	6,758,366	2,102,317	3.21
7.000	62.22	1,134	7,939	0.00	1,524,349	265.7	0	7,502,665	2,105,185	3.56
7.500	66.67	1,134	8,506	0.00	1,595,850	278.2	0	8,282,715	2,108,054	3.93
8.000	71.11	1,134	9,073	0.00	1,667,351	290.7	0	9,098,515	2,110,922	4.31
8.500	75.56	1,134	9,640	0.00	1,738,851	303.1	0	9,950,065	2,113,790	4.71
9.000	80.00	1,134	10,207	0.00	1,810,352	315.6	0	10,837,366	2,116,658	5.12
9.500	84.44	1,134	10,774	0.00	1,881,853	328.1	0	11,760,418	2,119,526	5.55
10.000	88.89	1,134	11,341	0.00	1,953,354	340.5	0	12,719,219	2,122,394	5.99
10.500	93.33	1,134	11,908	0.00	2,024,855	353.0	0	13,713,771	2,125,262	6.45
11.000	97.78	1,134	12,475	0.00	2,096,355	365.5	0	14,744,074	2,128,130	6.93

Table 2.10.7-9 – Side Drop CASKDROP Output

Side Drop *** PACKAGING TECHNOLOGY *** CASKDROP, v2.31
02-05-1999, 09:45:29 Nov 13, 1997

72-B Side Drop Analysis (Half Scale @ 45 Deg F, incl. harder foam)			
Impact Limiter Weight (each) -	0 lbs	Cask and Payload Weight -	5,736 lbs
Impact Limiter Outside Diameter -	38.0000 in	Cask Outside Diameter -	21.0500 in
Impact Limiter Overall Length -	23.0000 in	Cask Overall Length -	70.9000 in
Impact Limiter Conical Diameter -	0.0000 in	Dynamic Unloading Modulus -	1.000E+07 lbs/in
Impact Limiter Conical Length -	0.0000 in	Rad Mass Moment of Inertia -	6,630 lb-in-s²
Impact Limiter End Thickness -	5.6250 in	Frictional Coefficient -	0.0000
Impact Limiter Hole Diameter -	0.0000 in	Drop Height -	30.0000 ft
Impact Limiter Hole Length -	0.0000 in	Drop Angle from Horizontal -	0.0000°
Unbacked Area Threshhold Strain -	0.1000 in/in	Crush Analysis Theory -	Global
Unbacked Area Crush Stress -	776 psi	Number of Integration Incs -	50

VARIABLE CRUSH STRESS	
ε (in/in)	σ (psi)
0.000	0.0
0.050	699.0
0.100	776.0
0.200	808.0
0.300	870.0
0.400	979.0
0.500	1,221.0
0.600	1,762.0
0.650	2,311.0
0.700	3,154.0
0.750	4,559.0

DEFL (in)	MAX ε (%)	AREA (in²)	VOLUME (in³)	XBAR (in)	IMPACT FORCE (lbs)	ACCEL (g's)	I/L MOMENT (in-lbs)	STRAIN ENERGY (in-lbs)	KINETIC ENERGY (in-lbs)	SE/KE RATIO
0.500	5.90	398	133	0.00	181,706	31.7	0	45,426	2,067,900	0.02
1.000	11.80	560	375	0.00	328,211	57.2	0	172,906	2,070,768	0.08
1.500	17.70	681	686	0.00	437,973	76.4	0	364,452	2,073,636	0.18
2.000	23.60	781	1,052	0.00	542,231	94.5	0	609,503	2,076,504	0.29
2.500	29.50	867	1,465	0.00	636,048	110.9	0	904,073	2,079,373	0.43
3.000	35.39	943	1,917	0.00	722,512	126.0	0	1,243,713	2,082,241	0.60
3.500	41.29	1,011	2,406	0.00	805,517	140.4	0	1,625,720	2,085,109	0.78
4.000	47.19	1,073	2,927	0.00	887,891	154.8	0	2,049,072	2,087,977	0.98
4.044	47.71	1,078	2,975	0.00	897,107	156.4	0	2,088,228	2,088,228	1.00
4.500	53.09	1,130	3,478	0.00	995,265	173.5	0	2,519,861	2,090,845	1.21
5.000	58.99	1,182	4,056	0.00	1,145,686	199.7	0	3,055,099	2,093,713	1.46
5.500	64.89	1,230	4,659	0.00	1,373,480	239.4	0	3,684,890	2,096,581	1.76
6.000	70.79	1,275	5,286	0.00	1,716,836	299.3	0	4,457,469	2,099,449	2.12
6.500	76.69	1,316	5,934	0.00	2,270,132	395.8	0	5,454,211	2,102,317	2.59
7.000	82.58	1,355	6,602	0.00	2,982,596	520.0	0	6,767,394	2,105,185	3.21
7.500	88.48	1,391	7,289	0.00	3,799,797	662.4	0	8,462,992	2,108,054	4.01
8.000	94.38	1,425	7,993	0.00	4,697,081	818.8	0	10,587,212	2,110,922	5.02

Table 2.10.7-10 – Oblique Drop CASKDROP Output

Corner Drop *** PACKAGING TECHNOLOGY *** CASKDROP, v2.31
02-09-1999, 09:22:12 Nov 13, 1997

72-B Oblique Analysis (Half Scale @ 50 Deg F, incl. harder foam)			
Impact Limiter Weight (each) -	313 lbs	Cask and Payload Weight -	5,736 lbs
Impact Limiter Outside Diameter -	38.0000 in	Cask Outside Diameter -	20.8000 in
Impact Limiter Overall Length -	23.0000 in	Cask Overall Length -	70.9000 in
Impact Limiter Conical Diameter -	0.0000 in	Dynamic Unloading Modulus -	1.000E+07 lbs/in
Impact Limiter Conical Length -	0.0000 in	Rad Mass Moment of Inertia -	6,621 lb-in-s²
Impact Limiter End Thickness -	11.2500 in	Frictional Coefficient -	0.0000
Impact Limiter Hole Diameter -	0.0000 in	Drop Height -	30.0000 ft
Impact Limiter Hole Length -	0.0000 in	Drop Angle from Horizontal -	55.0000°
Unbacked Area Threshhold Strain -	0.1000 in/in	Crush Analysis Theory -	Global
Unbacked Area Crush Stress -	784 psi	Number of Integration Incs -	50

VARIABLE CRUSH STRESS	
ε (in/in)	σ (psi)
0.000	0.0
0.050	762.0
0.100	784.0
0.200	811.0
0.300	877.0
0.400	986.0
0.500	1,224.0
0.600	1,755.0
0.650	2,266.0
0.700	3,067.0
0.750	4,527.0

DEFL (in)	MAX ε (%)	AREA (in²)	VOLUME (in³)	XBAR (in)	IMPACT FORCE (lbs)	ACCEL (g's)	I/L MOMENT (in-lbs)	STRAIN ENERGY (in-lbs)	KINETIC ENERGY (in-lbs)	SE/KE RATIO
0.500	3.33	8	2	-11.43	2,016	0.4	0	504	2,067,900	0.00
1.000	6.66	23	9	-11.66	10,144	1.8	0	3,544	2,070,768	0.00
1.500	9.99	42	25	-11.92	22,992	4.0	0	11,828	2,073,636	0.01
2.000	13.33	64	51	-12.20	38,254	6.7	0	27,140	2,076,504	0.01
2.500	16.66	88	89	-12.47	55,384	9.7	0	50,549	2,079,373	0.02
3.000	20.00	115	140	-12.73	74,452	13.0	0	83,008	2,082,241	0.04
3.500	23.33	144	204	-12.99	95,586	16.7	0	125,518	2,085,109	0.06
4.000	26.67	174	284	-13.25	118,742	20.7	0	179,100	2,087,977	0.09
4.500	30.01	206	379	-13.50	143,787	25.1	0	244,732	2,090,845	0.12
5.000	33.37	240	490	-13.76	170,586	29.7	0	323,325	2,093,713	0.15
5.500	36.96	274	619	-14.01	199,086	34.7	0	415,743	2,096,581	0.20
6.000	40.59	310	765	-14.25	229,343	40.0	0	522,850	2,099,449	0.25
6.500	44.26	347	929	-14.48	261,478	45.6	0	645,556	2,102,317	0.31
7.000	47.85	384	1,112	-14.71	295,700	51.5	0	784,850	2,105,185	0.37
7.500	51.27	422	1,313	-14.93	332,210	57.9	0	941,827	2,108,054	0.45
8.000	54.69	461	1,534	-15.13	371,510	64.8	0	1,117,757	2,110,922	0.53
8.500	58.11	500	1,774	-15.32	414,175	72.2	0	1,314,179	2,113,790	0.62
9.000	61.66	540	2,034	-15.49	461,292	80.4	0	1,533,045	2,116,658	0.72
9.500	65.31	580	2,314	-15.64	514,169	89.6	0	1,776,911	2,119,526	0.84
10.000	68.98	620	2,614	-15.75	574,167	100.1	0	2,048,995	2,122,394	0.97
10.127	69.92	630	2,693	-15.78	591,060	103.0	0	2,123,124	2,123,124	1.00
10.500	72.67	660	2,934	-15.83	644,808	112.4	0	2,353,739	2,125,262	1.11
11.000	76.39	701	3,274	-15.85	730,237	127.3	0	2,697,500	2,128,130	1.27
11.500	80.14	741	3,635	-15.84	833,472	145.3	0	3,088,427	2,130,998	1.45
12.000	83.91	781	4,015	-15.81	956,356	166.7	0	3,535,884	2,133,866	1.66
12.500	87.71	822	4,416	-15.76	1,100,030	191.8	0	4,049,981	2,136,735	1.90
13.000	91.53	861	4,837	-15.71	1,265,463	220.6	0	4,641,354	2,139,603	2.17
13.500	95.22	901	5,277	-15.69	1,455,425	253.7	0	5,321,576	2,142,471	2.48
14.000	98.75	940	5,737	-15.68	1,670,416	291.2	0	6,103,036	2,145,339	2.84

Note: Only the force-deflection relationship from this output is relevant to the oblique test; the dynamic result is given in Table 2.10.7-11.

Table 2.10.7-11 – Oblique Drop SLAPDOWN Output

```
PROGRAM SLAPDOWN  VERSION 2.1
 TITLE: 72-B 55 DEG OBLIQUE DROP TEST PREDICTION

 02/18/1999     10:59:08

 ****** NOSE PROPERTIES ******

 LENGTH FROM NOSE TO CG (Z1)            3.545E+01
 RADIUS OF PACKAGE AT NOSE (R1)            1.040E+01
 SQUARE END
 COEFFICIENT OF FRICTION AT NOSE (CF1)  0.000E+00

       NOSE SPRING DEFINITION

       DISPLACEMENT     FORCE
         0.000E+00    0.000E+00
         5.000E-01    2.016E+03
         1.000E+00    1.014E+04
         1.500E+00    2.299E+04
         2.000E+00    3.825E+04
         2.500E+00    5.538E+04
         3.000E+00    7.445E+04
         3.500E+00    9.559E+04
         4.000E+00    1.187E+05
         4.500E+00    1.438E+05
         5.000E+00    1.706E+05
         5.500E+00    1.991E+05
         6.000E+00    2.293E+05
         6.500E+00    2.615E+05
         7.000E+00    2.957E+05
         7.500E+00    3.322E+05
         8.000E+00    3.715E+05
         8.500E+00    4.142E+05
         9.000E+00    4.613E+05
         9.500E+00    5.142E+05
         1.000E+01    5.742E+05
         1.050E+01    6.448E+05
         1.100E+01    7.302E+05
         1.150E+01    8.335E+05
         1.200E+01    9.564E+05
         1.250E+01    1.100E+06
         1.300E+01    1.265E+06
         1.350E+01    1.455E+06
         1.400E+01    1.670E+06

 UNLOADING MODULUS FOR NOSE SPRING      1.000E+07


 ****** TAIL PROPERTIES ******

 LENGTH FROM TAIL TO CG (Z2)            3.545E+01
 RADIUS OF PACKAGE AT TAIL (R2)            1.040E+01
 COEFFICIENT OF FRICTION AT TAIL (CF2)  0.000E+00
 ROUND END

       TAIL SPRING DEFINITION

       DISPLACEMENT     FORCE
         0.000E+00    0.000E+00
         5.000E-01    9.135E+04
         1.000E+00    1.616E+05
         1.500E+00    2.143E+05
         2.000E+00    2.658E+05
         2.500E+00    3.122E+05
         3.000E+00    3.551E+05
         3.500E+00    3.960E+05
         4.000E+00    4.358E+05
         4.500E+00    4.896E+05
         5.000E+00    5.673E+05
         5.500E+00    6.816E+05
         6.000E+00    8.506E+05
         6.500E+00    1.129E+06
         7.000E+00    1.491E+06
         7.500E+00    1.908E+06
         8.000E+00    2.366E+06

 UNLOADING MODULUS FOR TAIL SPRING      1.000E+07
****** MASS, MOMENT OF INERTIA, AND INITIAL CONDITION DATA ******
```

```
MASS OF BODY                          1.484E+01
MOMENT OF INERTIA                     8.706E+03
RADIUS OF GYRATION                    2.422E+01
INITIAL VERTICAL VELOCITY (pos. up)  -5.275E+02
GRAVITATIONAL ACCELERATION (pos. up) -3.860E+02
INITIAL ANGLE (positive CCW)          5.500E+01

TIME STEP SCALE FACTOR                1.000E-02
FRICTION SCALE FACTOR                 0.000E+00
WRITE PLOT DATA EVERY STEP


72-B 55 DEG OBLIQUE DROP TEST PREDICTION

****** SEQUENCE OF EVENTS ******

** NOSE HIT     AT TIME  0.000E+00, VELOCITY = -5.275E+02, RATIO =  1.00
** NOSE REBOUND AT TIME  2.312E-02, VELOCITY =  1.050E+02, RATIO =  -.20
** NOSE UNLOAD  AT TIME  2.449E-02, VELOCITY =  1.636E+02, RATIO =  -.31
** TAIL HIT     AT TIME  8.990E-02, VELOCITY = -6.965E+02, RATIO =  1.32
** TAIL REBOUND AT TIME  1.001E-01, VELOCITY =  2.625E-01, RATIO =   .00
** TAIL UNLOAD  AT TIME  1.012E-01, VELOCITY =  6.767E+01, RATIO =  -.13


****** RESULTS ******

Event over at time    1.012E-01, Time step size  1.177E-05
Time step multiplier  1.000E-02, 8601 Plot times written to database


           DISPLACEMENT     VELOCITY     ACCELERATION

   NOSE      8.756E+00      3.152E+02      6.270E+04 (MAX)
                           -5.278E+02     -3.477E+04 (MIN)

   TAIL      4.331E+00      6.767E+01      9.753E+04 (MAX)
                           -6.967E+02     -5.843E+03 (MIN)

     CG                    4.987E+01      3.138E+04 (MAX)
                           -5.279E+02     -3.860E+02 (MIN)

ANGULAR                    5.094E-01      1.893E+03 (MAX)
                           -1.425E+01     -1.270E+03 (MIN)

MAXIMUM ENERGIES:  1.423E+06 (NOSE),  1.157E+06 (TAIL)
TAIL IMPACT ANGLE =       -4.363187 DEG.
```

Table 2.10.7-12 – Free Drop Test Result Summary

Drop Test Case	Test Result Deflection (inches)	Analytical Prediction (inches)	Comment
End Drop (90º)	2.52	2.52	Basis of Dynamic Correction Factor
Side Drop (0º)	3.56	4.04	Using Analytical Tools
—	—	3.56	Using Static Force-deflection Curve
Oblique Drop (55º)	7.30	8.76	Using Analytical Tools

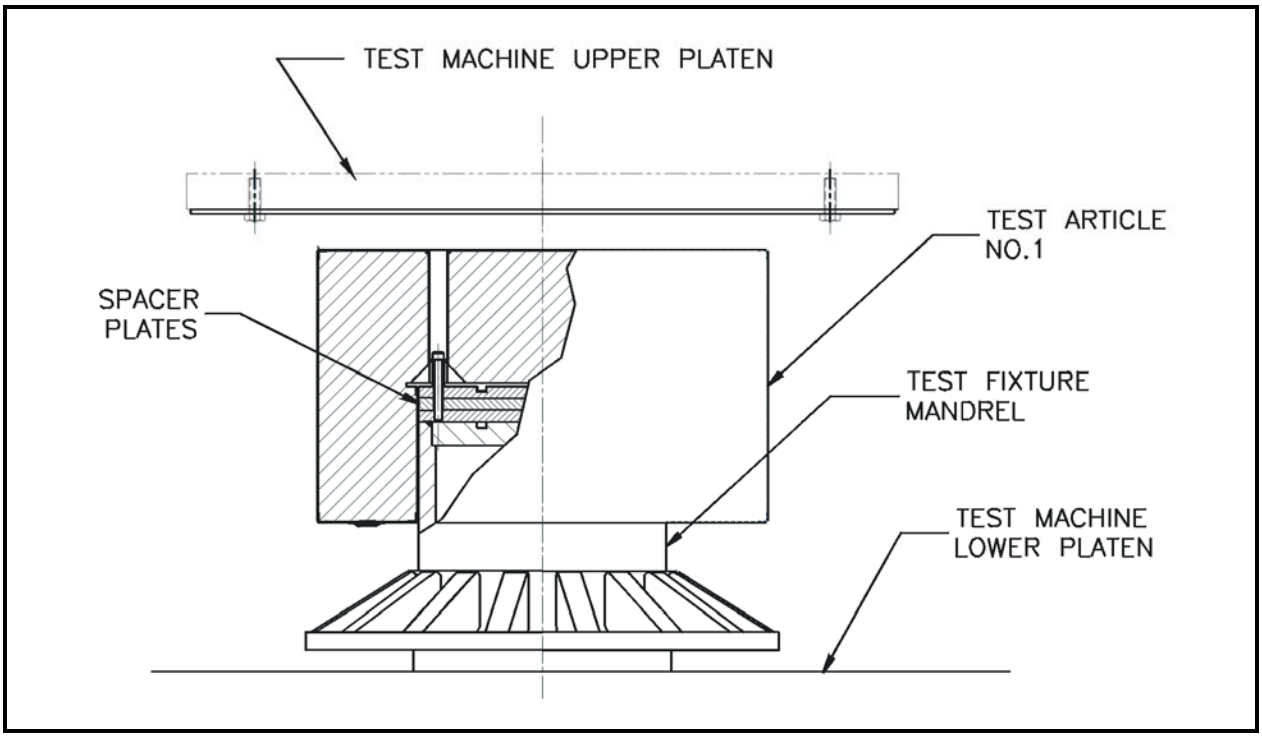

Figure 2.10.7-1 – End Orientation Test

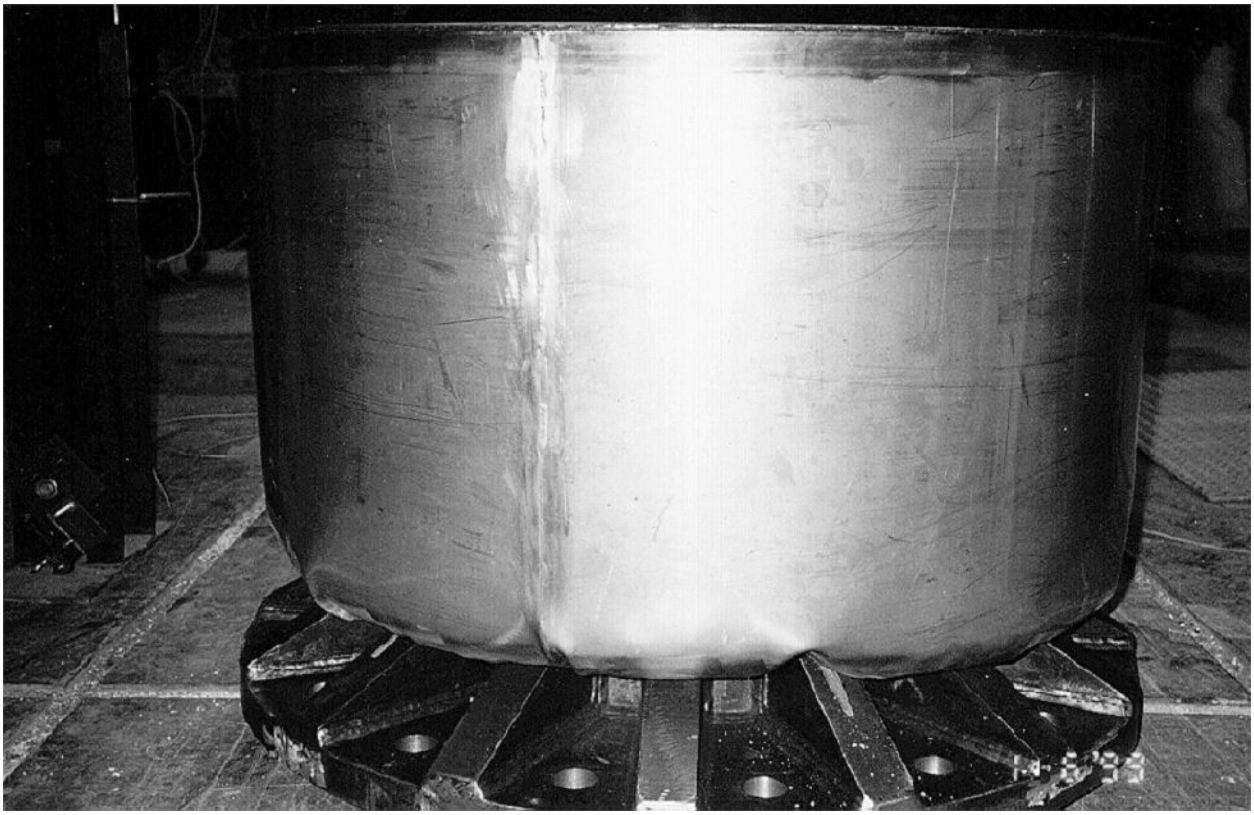

Figure 2.10.7-2 – End Orientation, Post-Test Configuration



Figure 2.10.7-3 – End Orientation, View of Open End

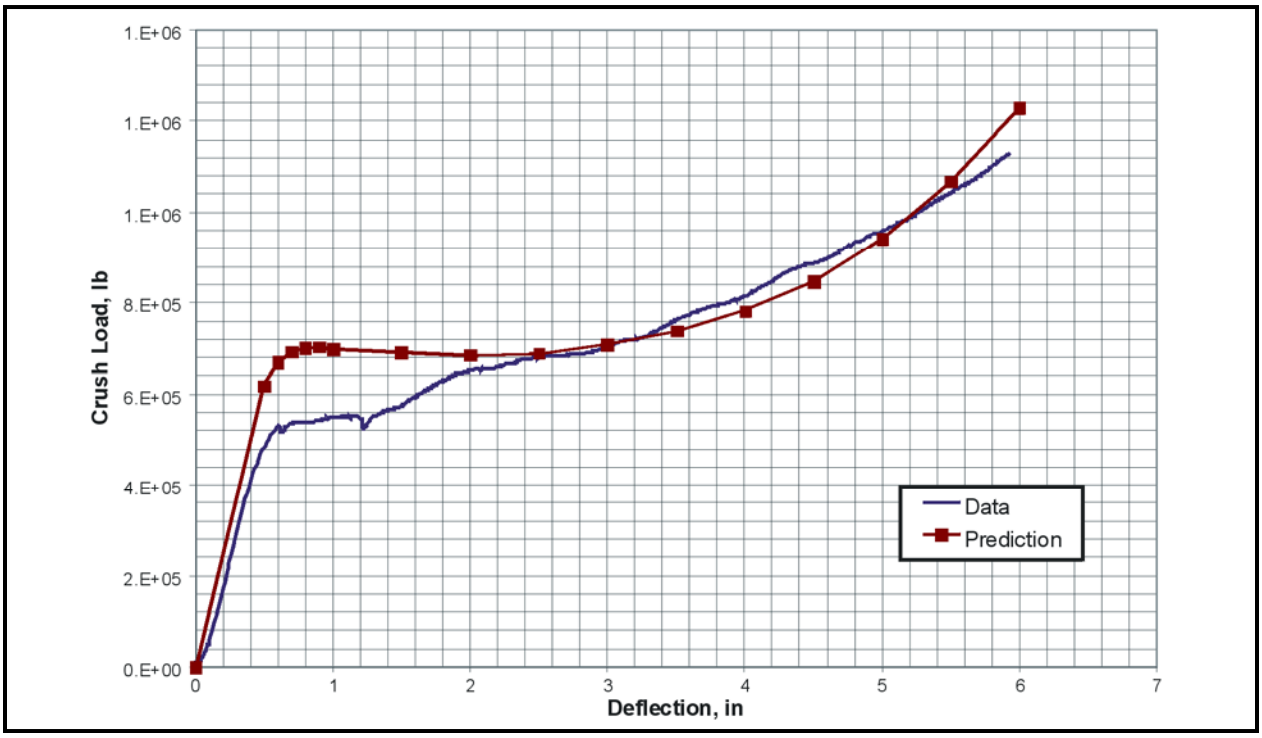

Figure 2.10.7-4 – End Crush Data Versus Prediction

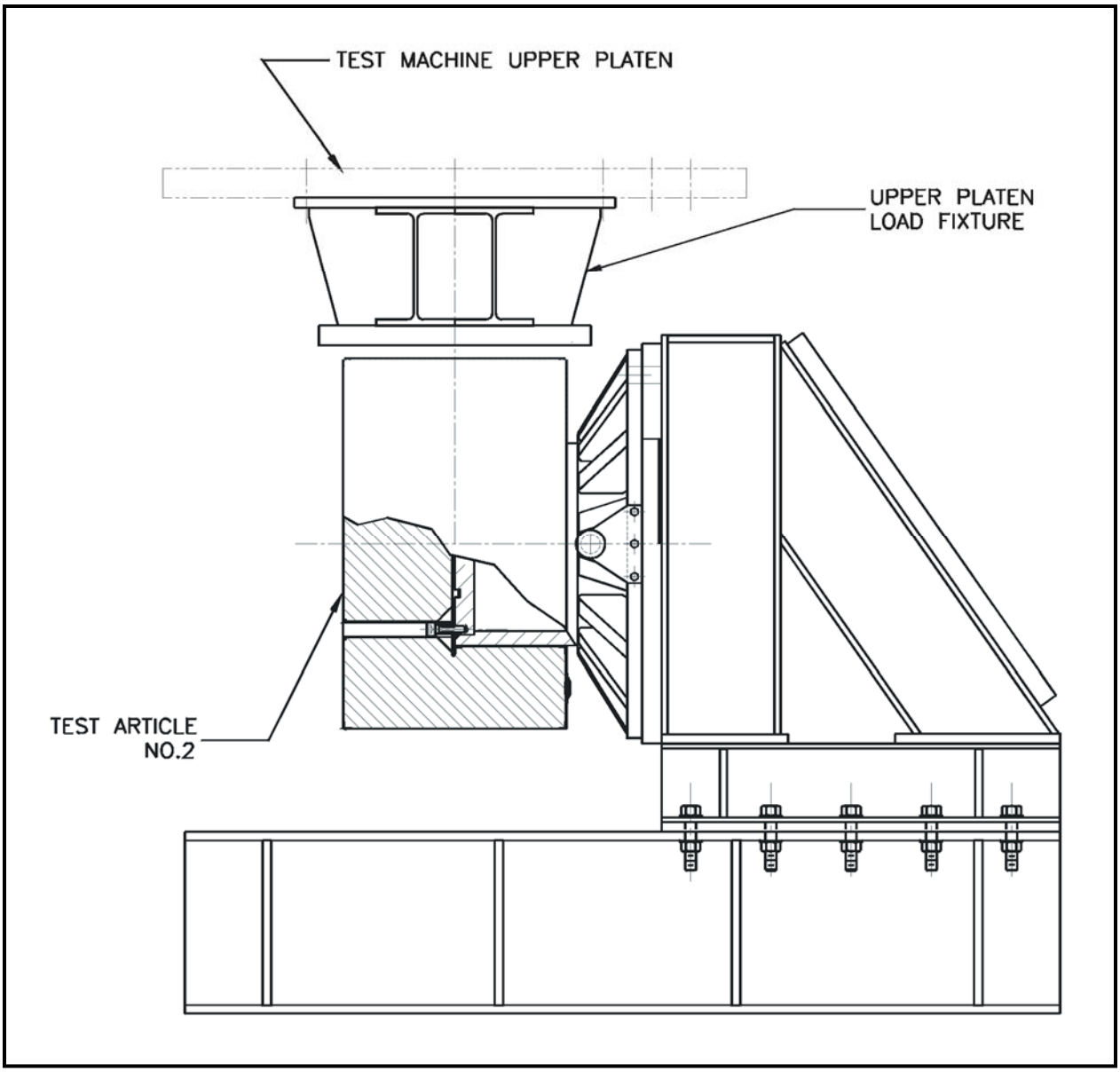

Figure 2.10.7-5 – Side Orientation Test

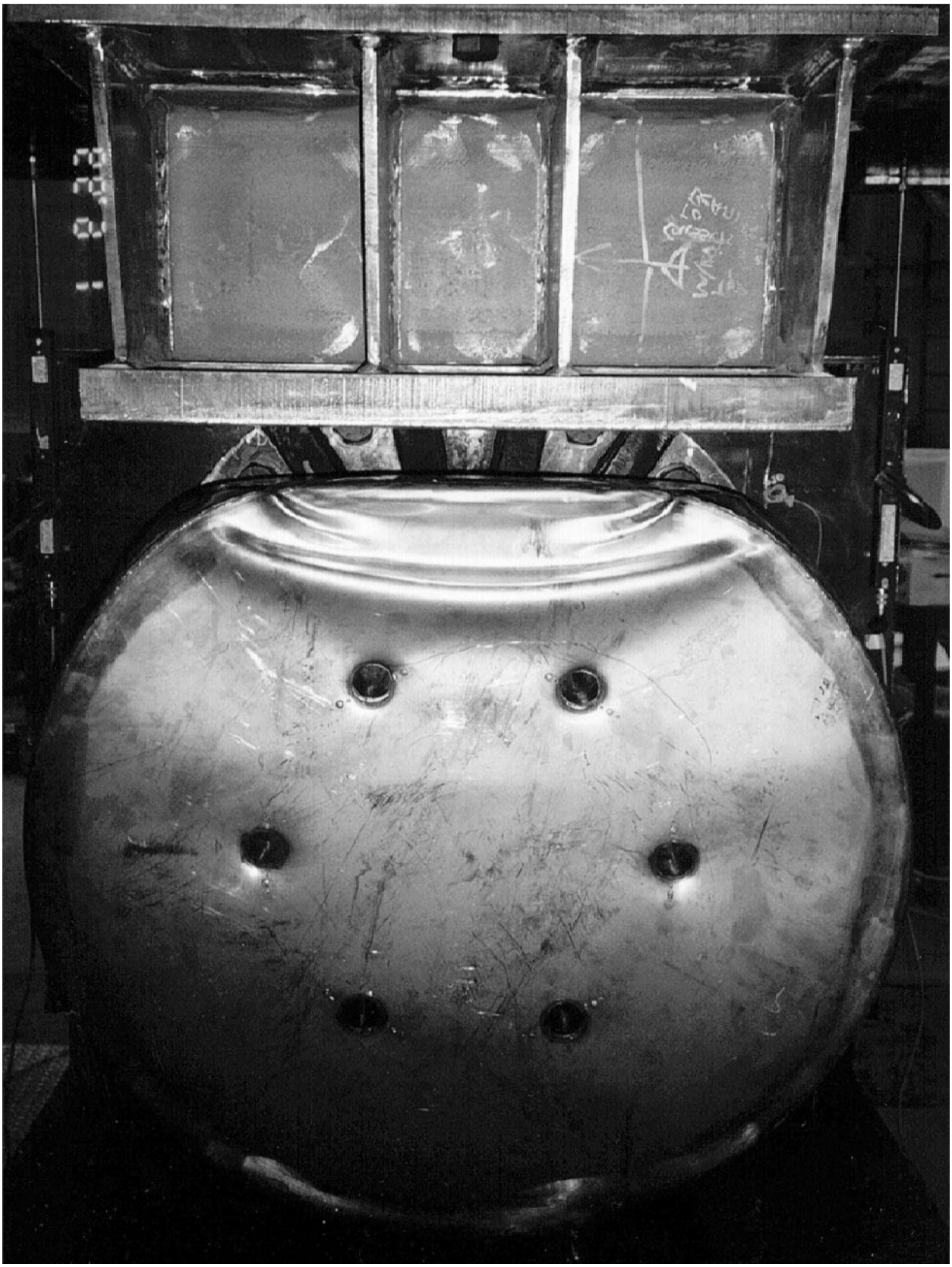

Figure 2.10.7-6 – Side Orientation, Post-Test Configuration

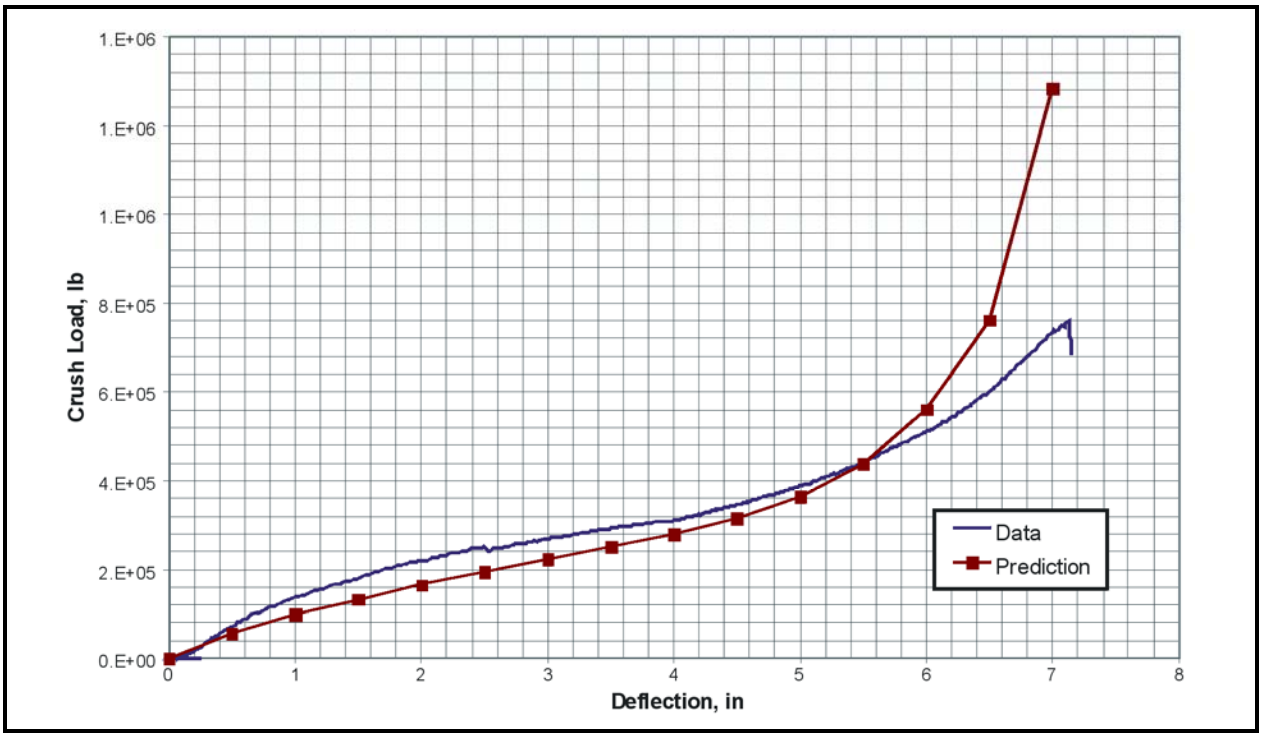

Figure 2.10.7-7 – Side Crush Data Versus Prediction

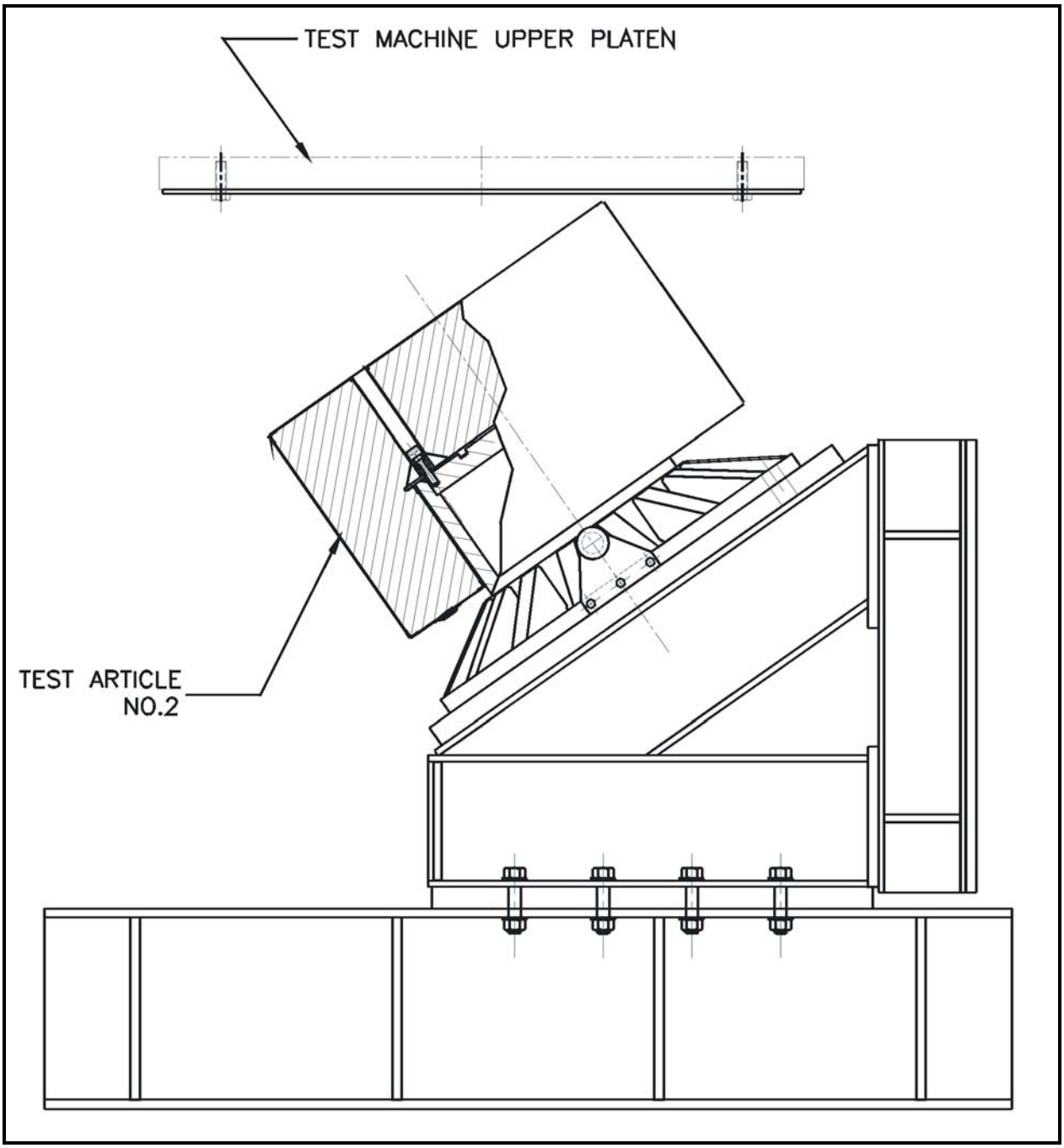

Figure 2.10.7-8 – Oblique Orientation Test



Figure 2.10.7-9 – Oblique Orientation, Post-Test Configuration

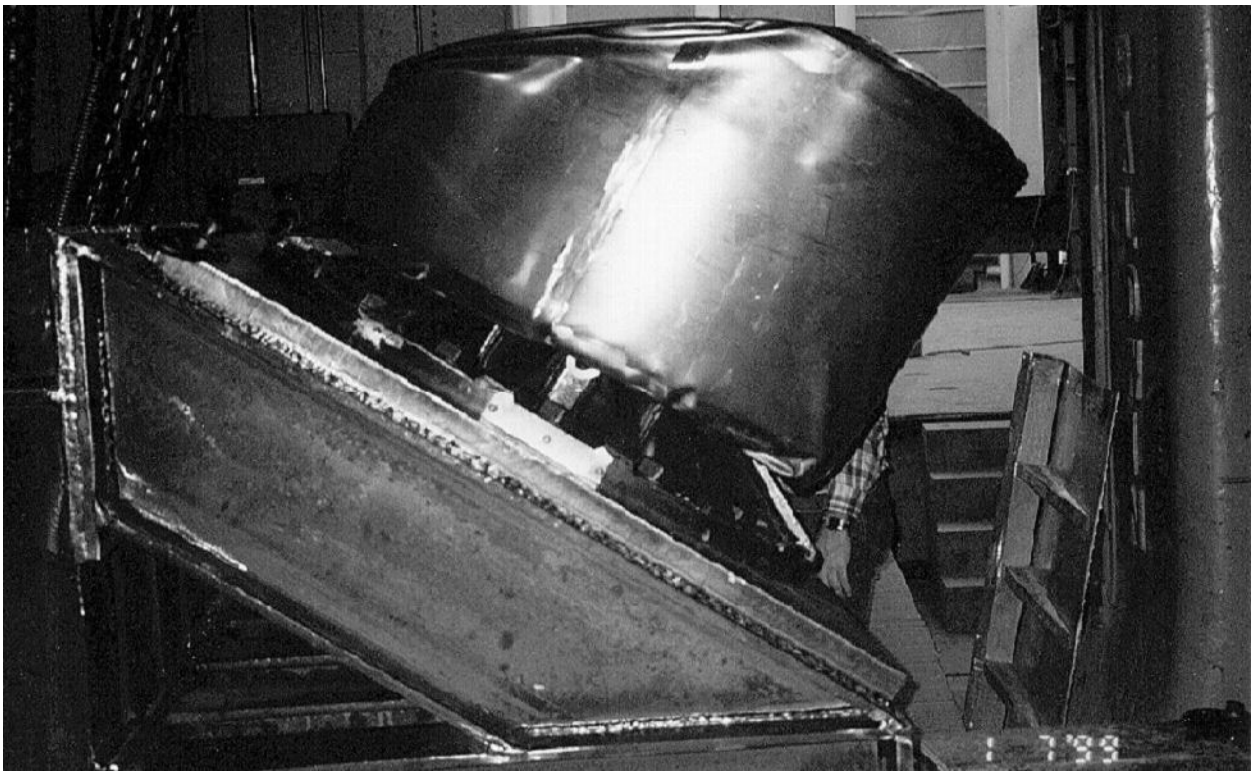

Figure 2.10.7-10 – Oblique Orientation, Post-Test Side View

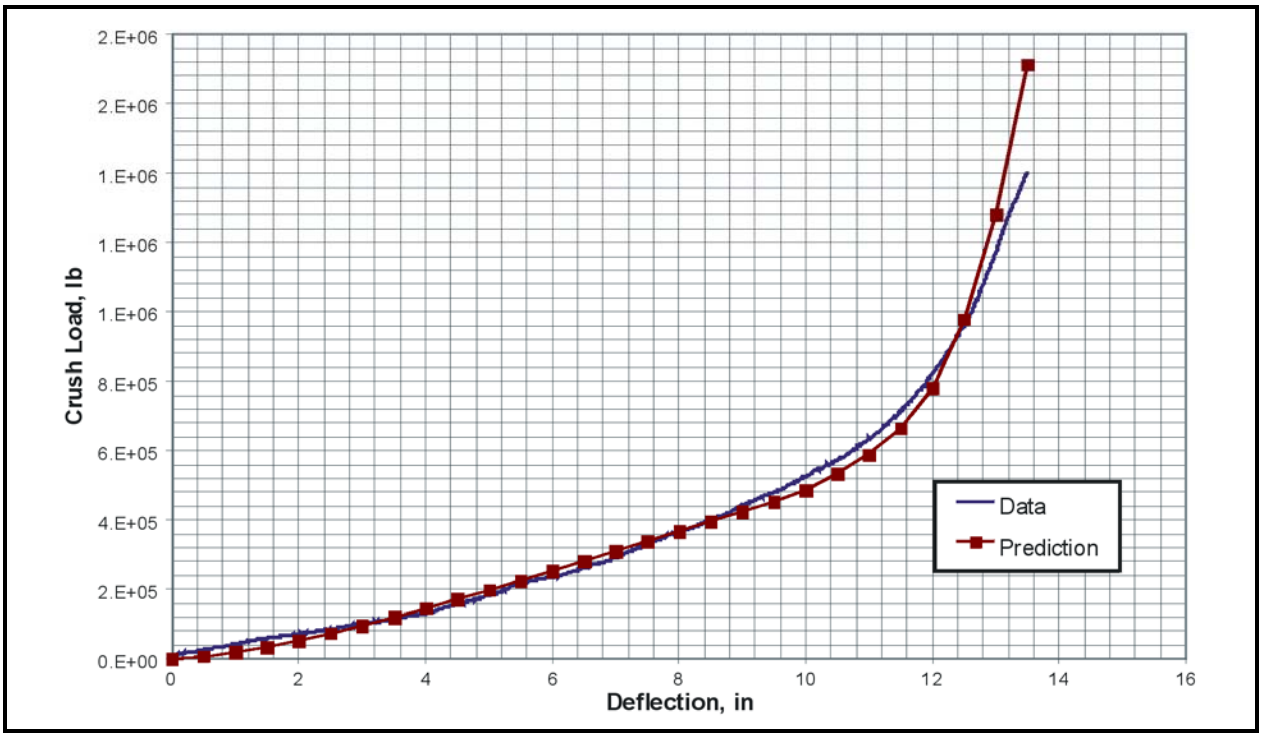

Figure 2.10.7-11 – Oblique Crush Data Versus Prediction

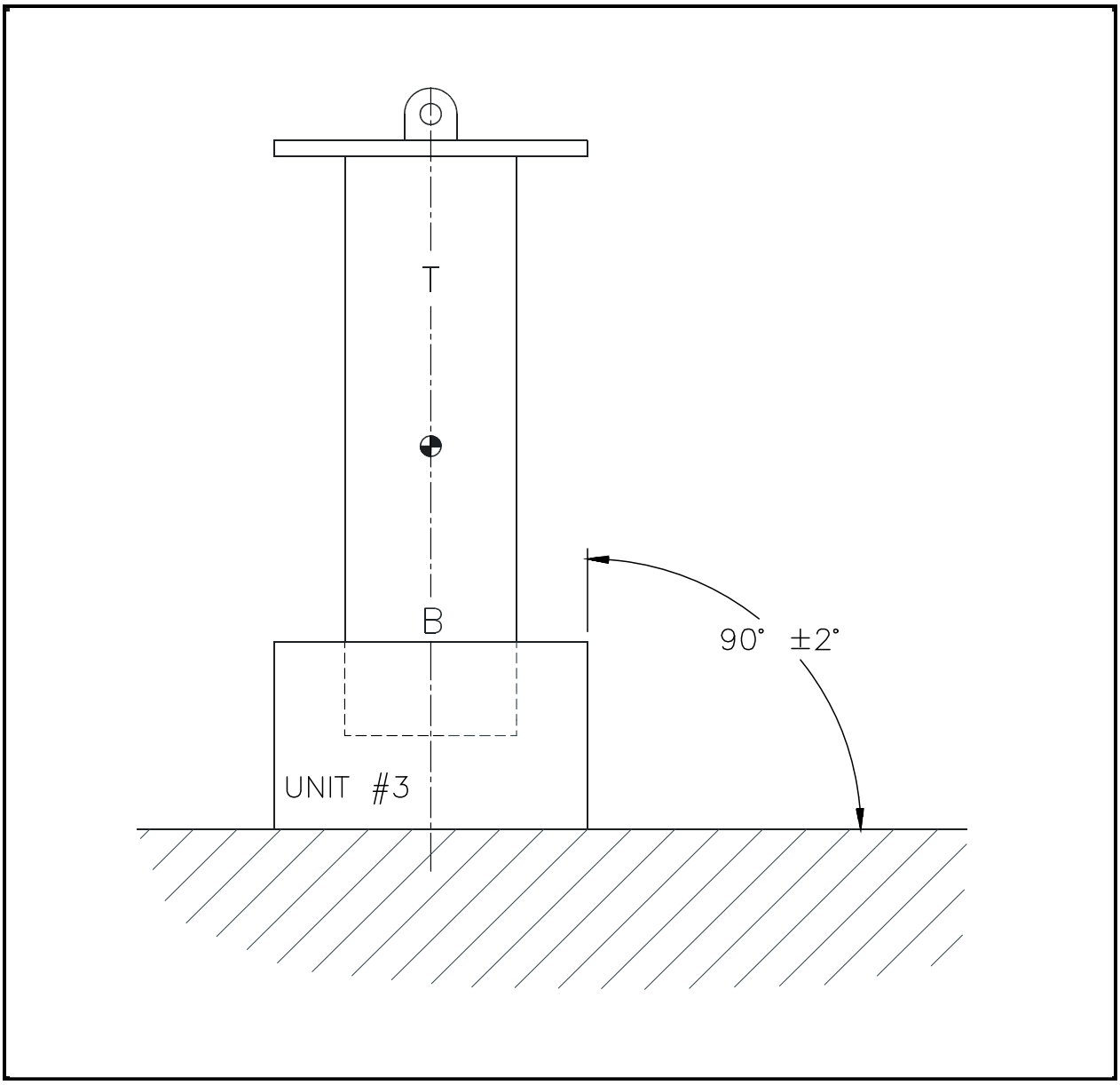

Figure 2.10.7-12 – End Drop Configuration

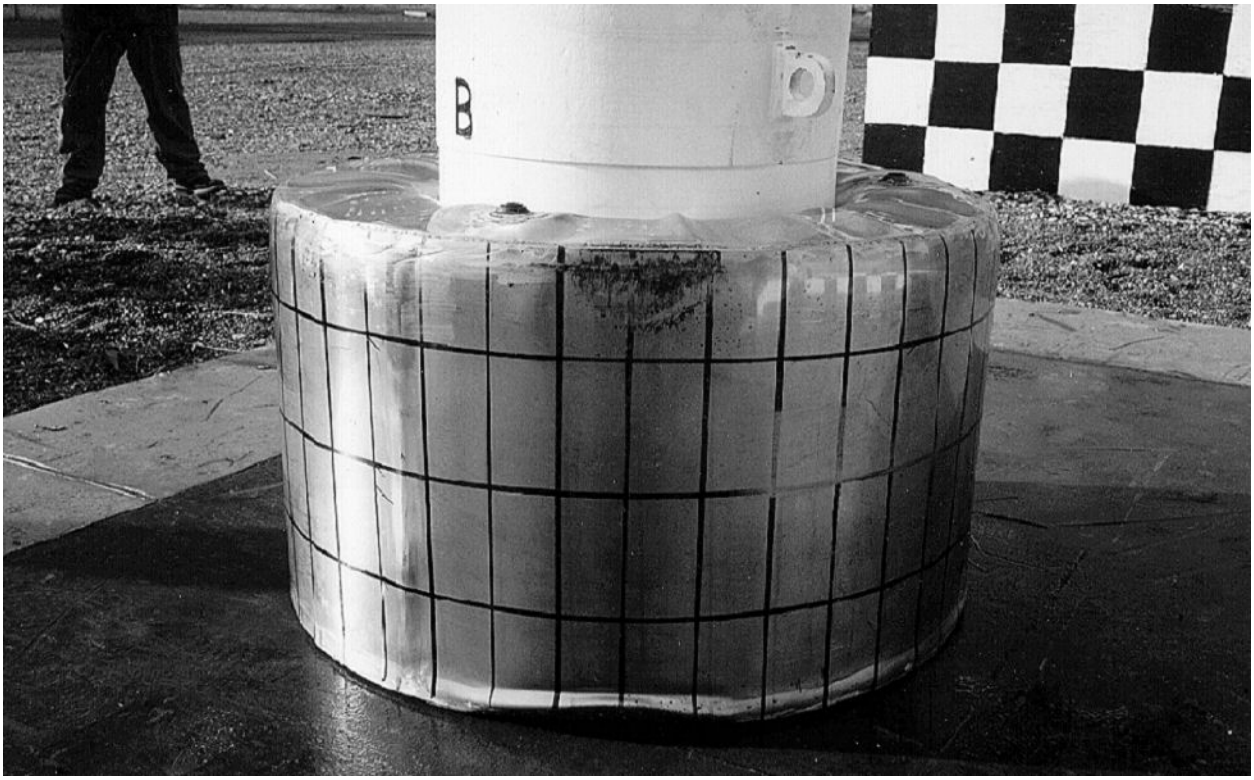

Figure 2.10.7-13 – End Drop, Post-Test Configuration

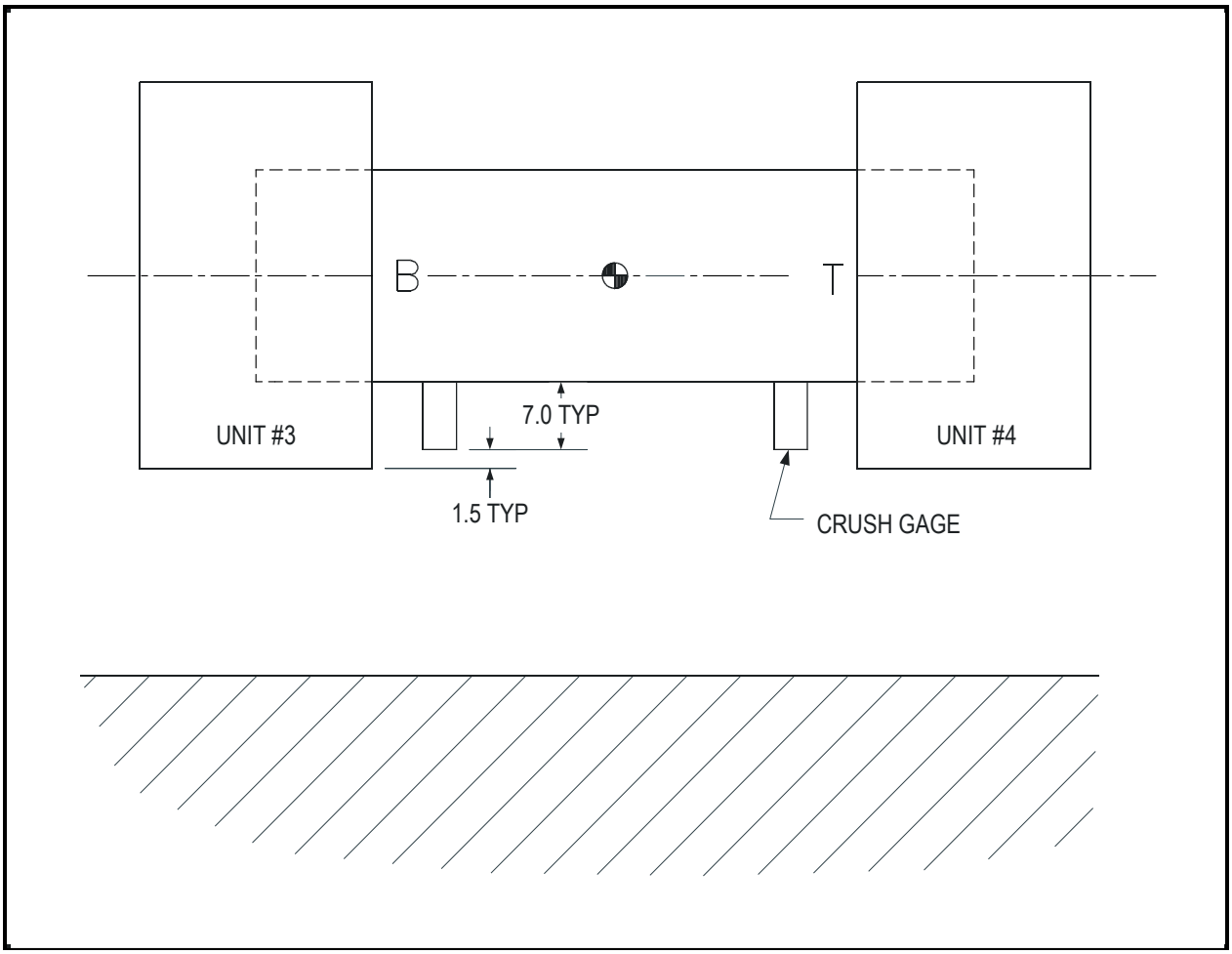

Figure 2.10.7-14 – Side Drop Configuration

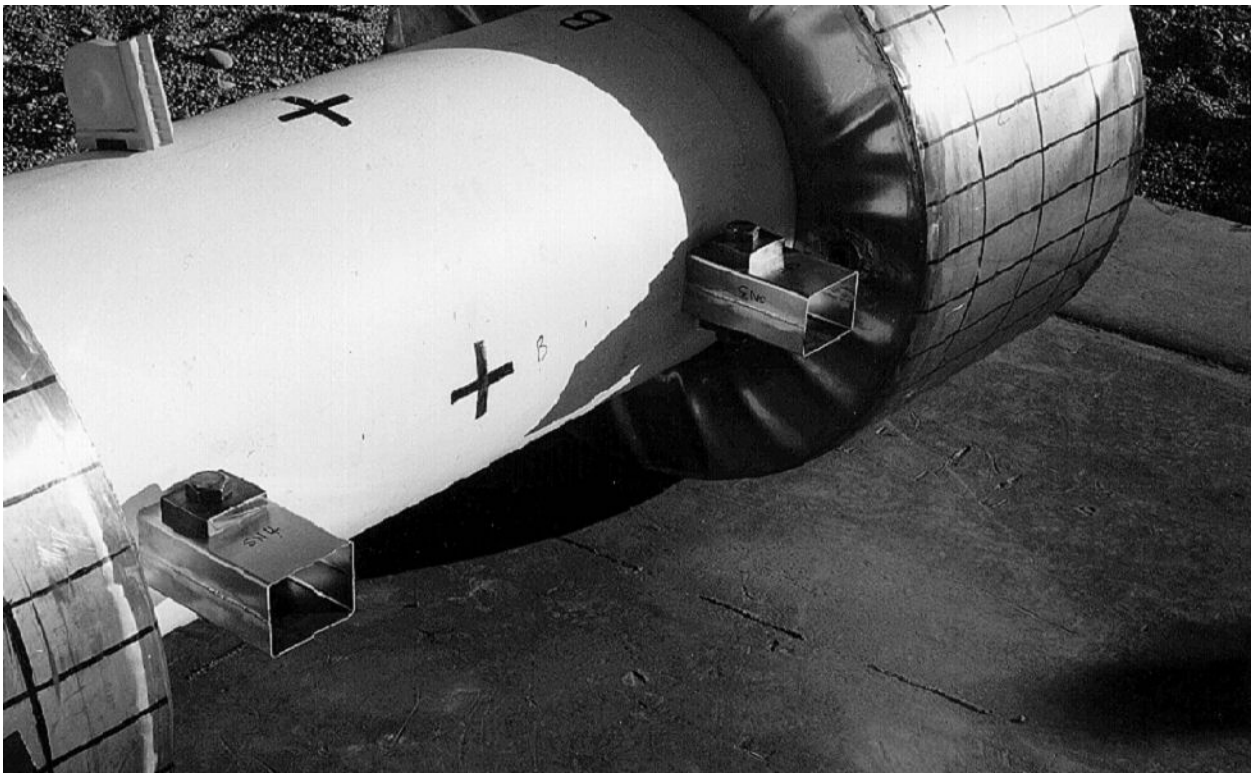

Figure 2.10.7-15 – Side Drop, Crush Gage Detail (Before Test)

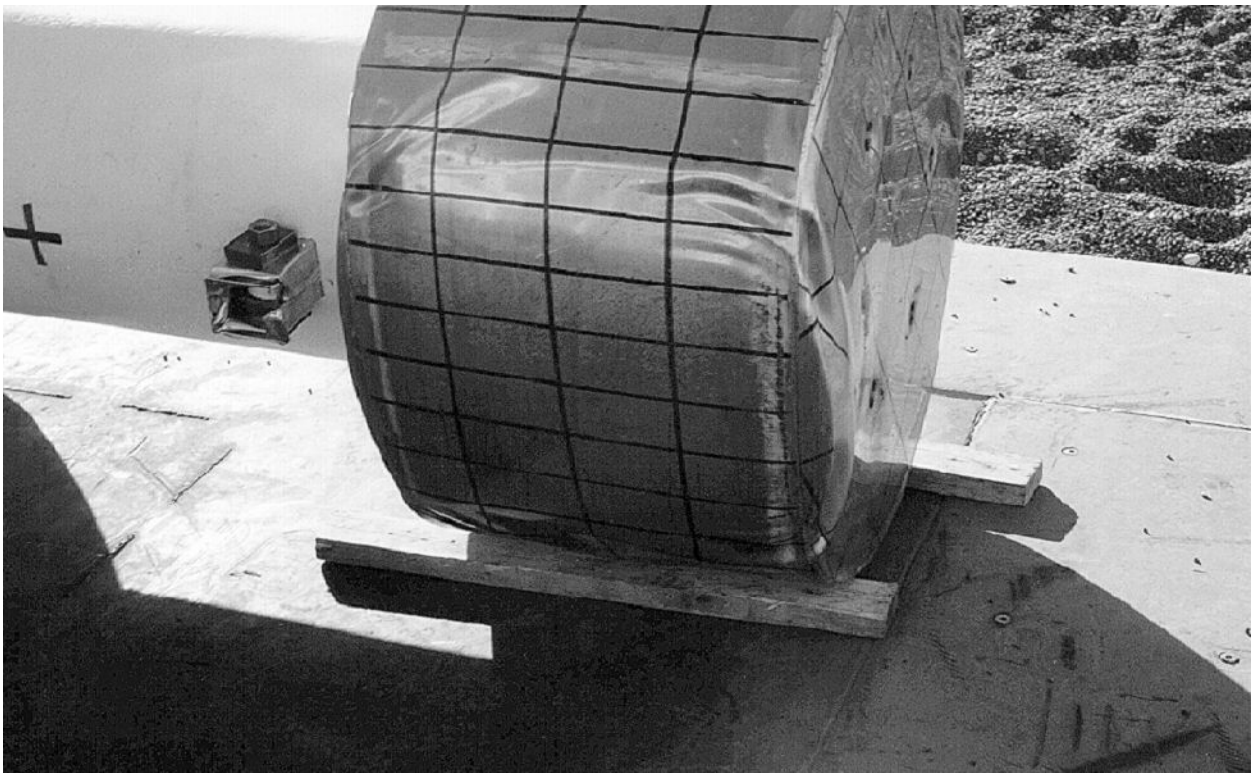

Figure 2.10.7-16 – Side Drop, Post-Test Configuration

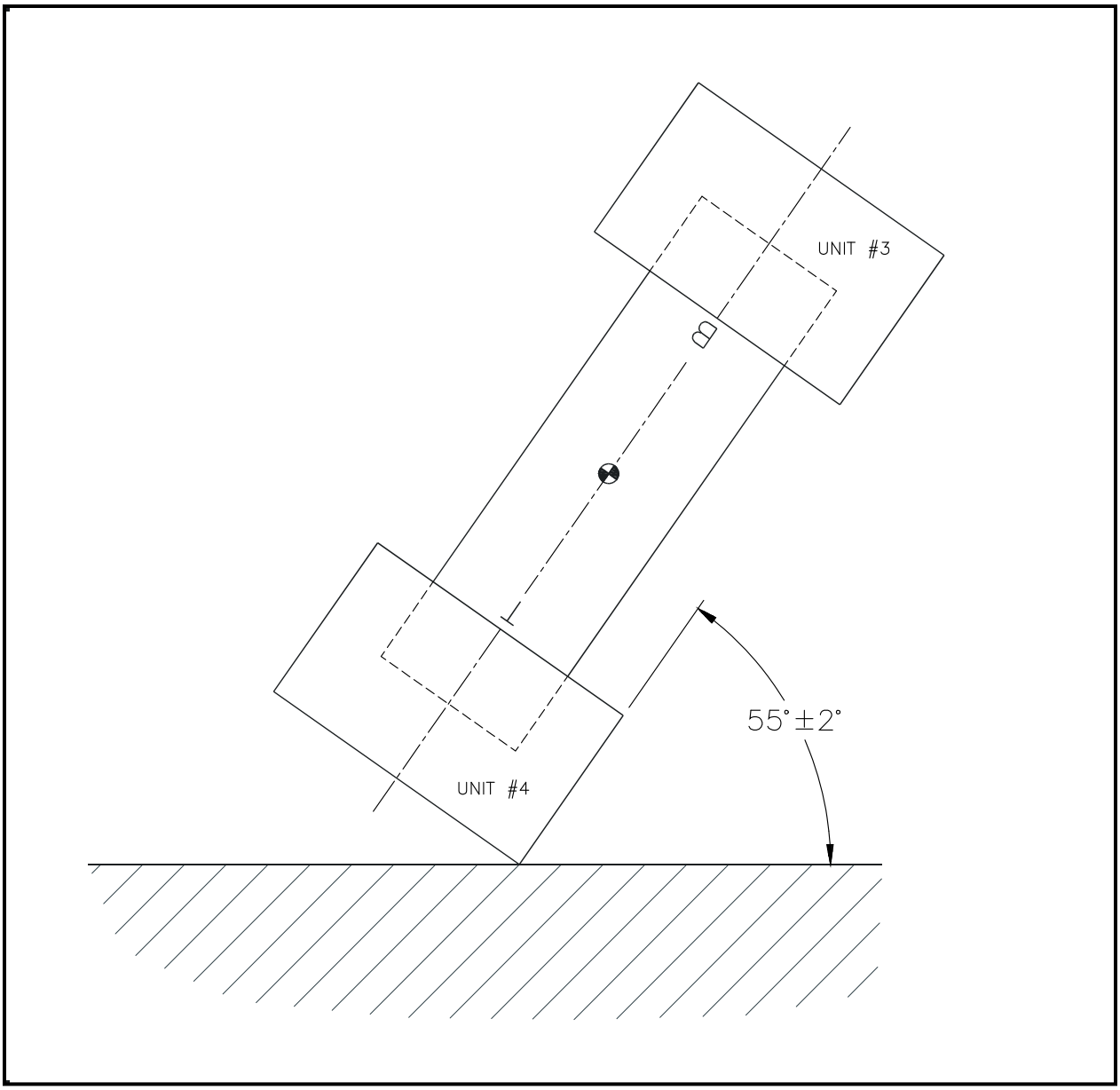

Figure 2.10.7-17 – Oblique Drop Configuration

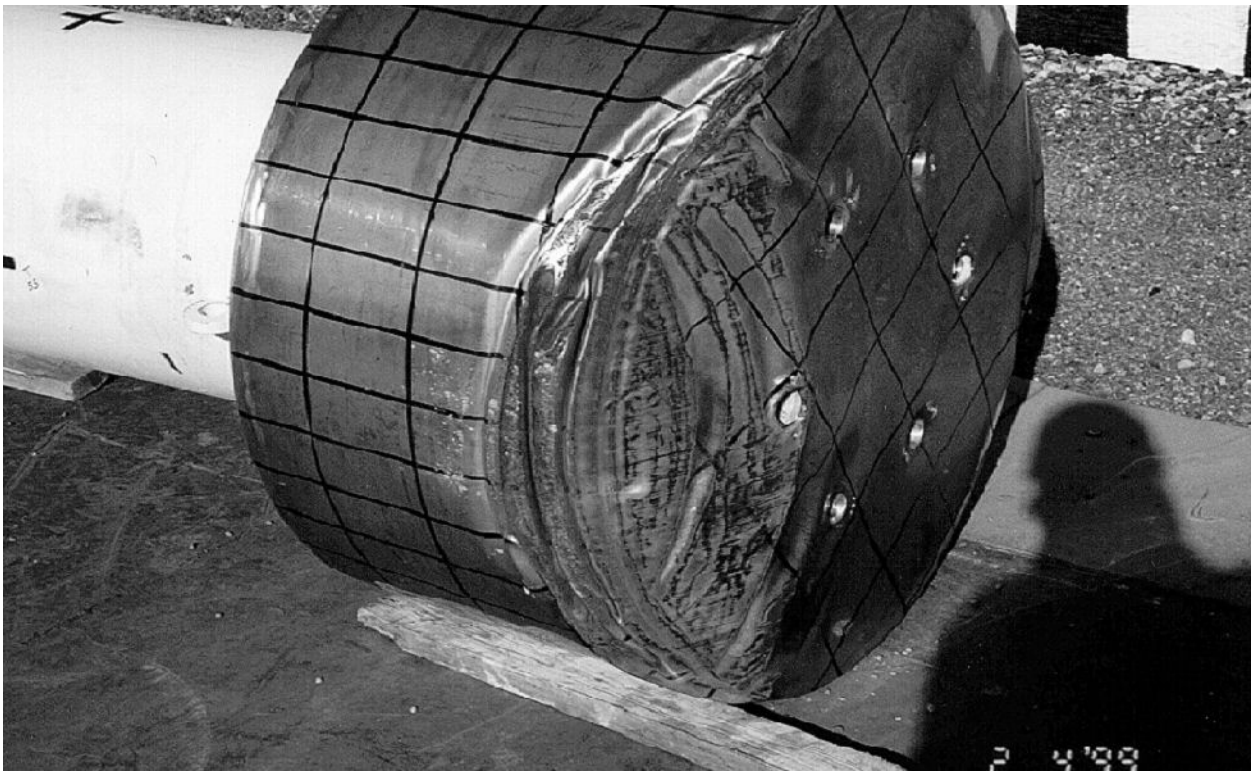

Figure 2.10.7-18 – Oblique Drop, Post-Test Configuration

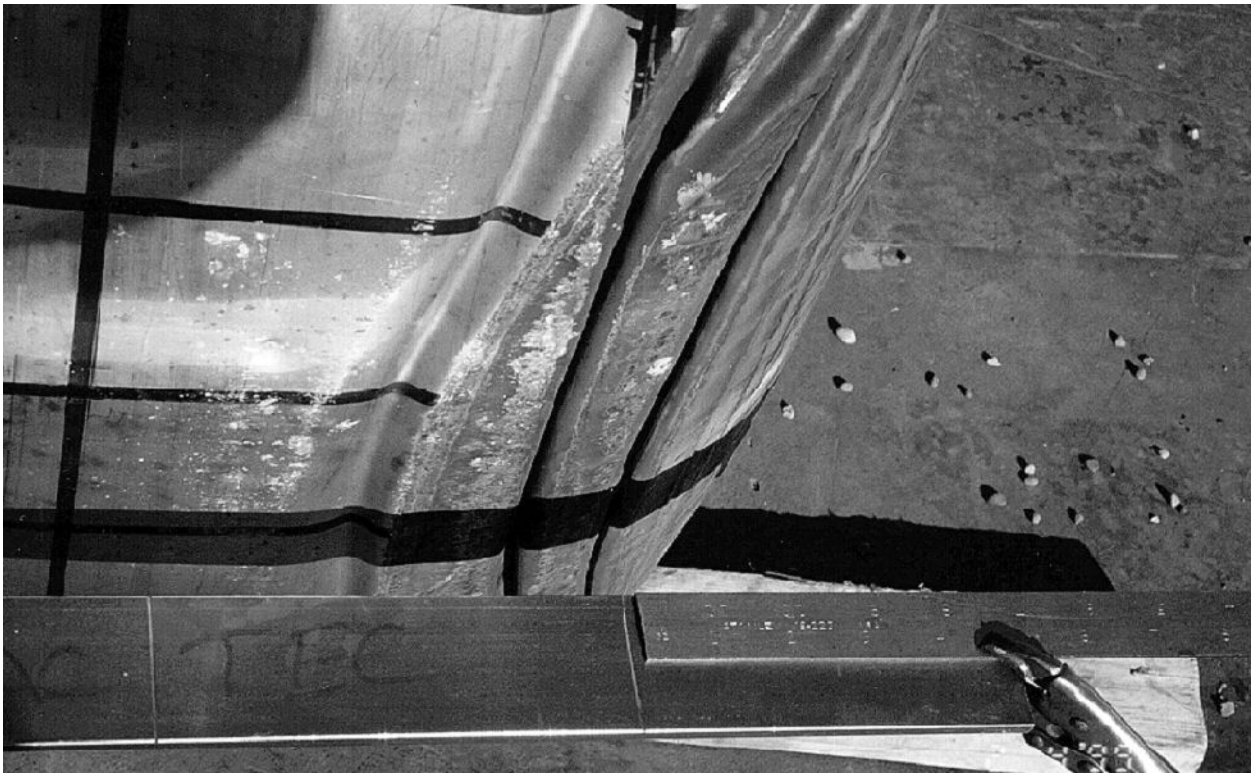

Figure 2.10.7-19 – Oblique Drop, Post-Test Configuration (Detail)

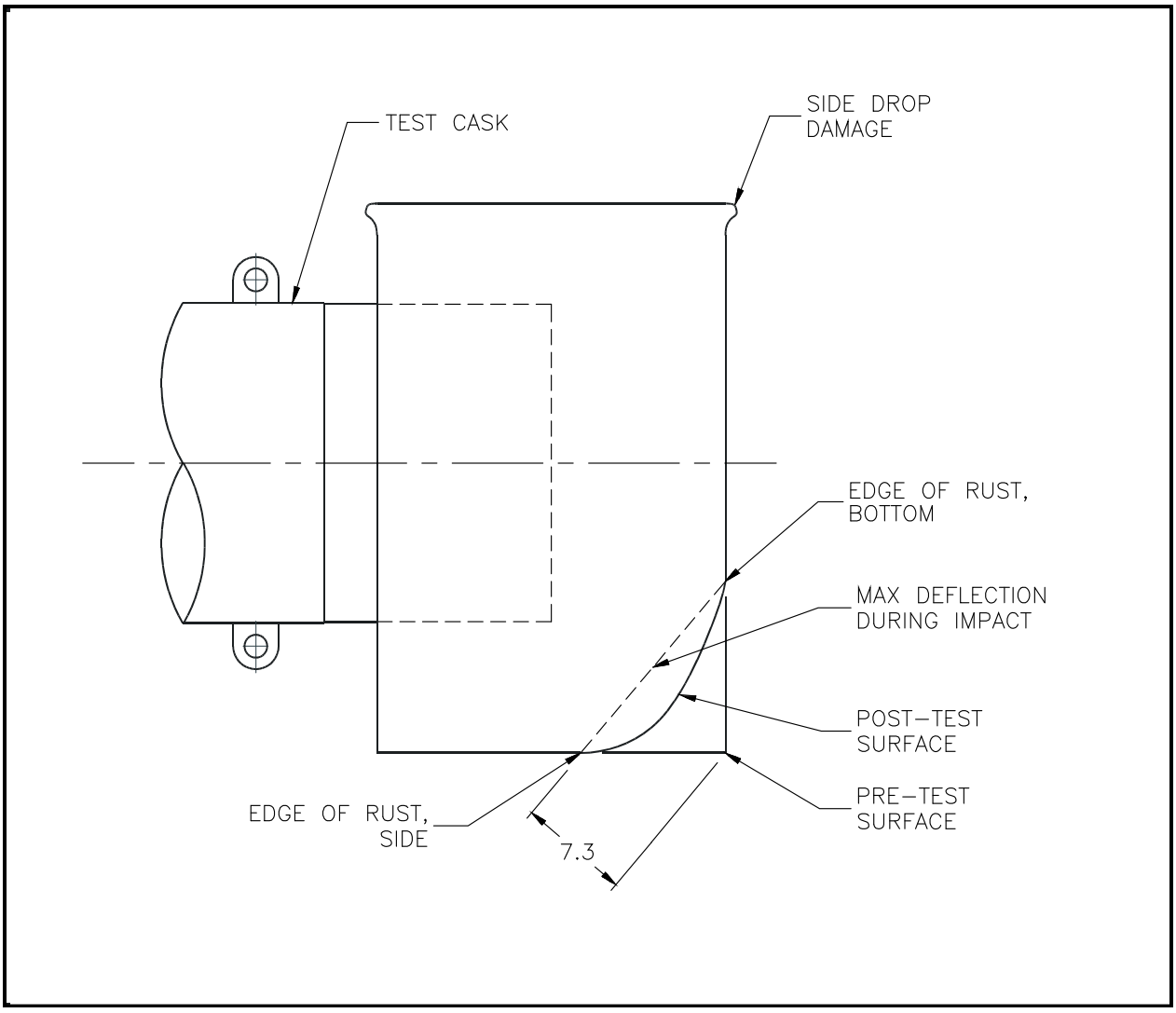

Figure 2.10.7-20 – Oblique Free Drop, Measurement of Deflection

This page intentionally left blank.

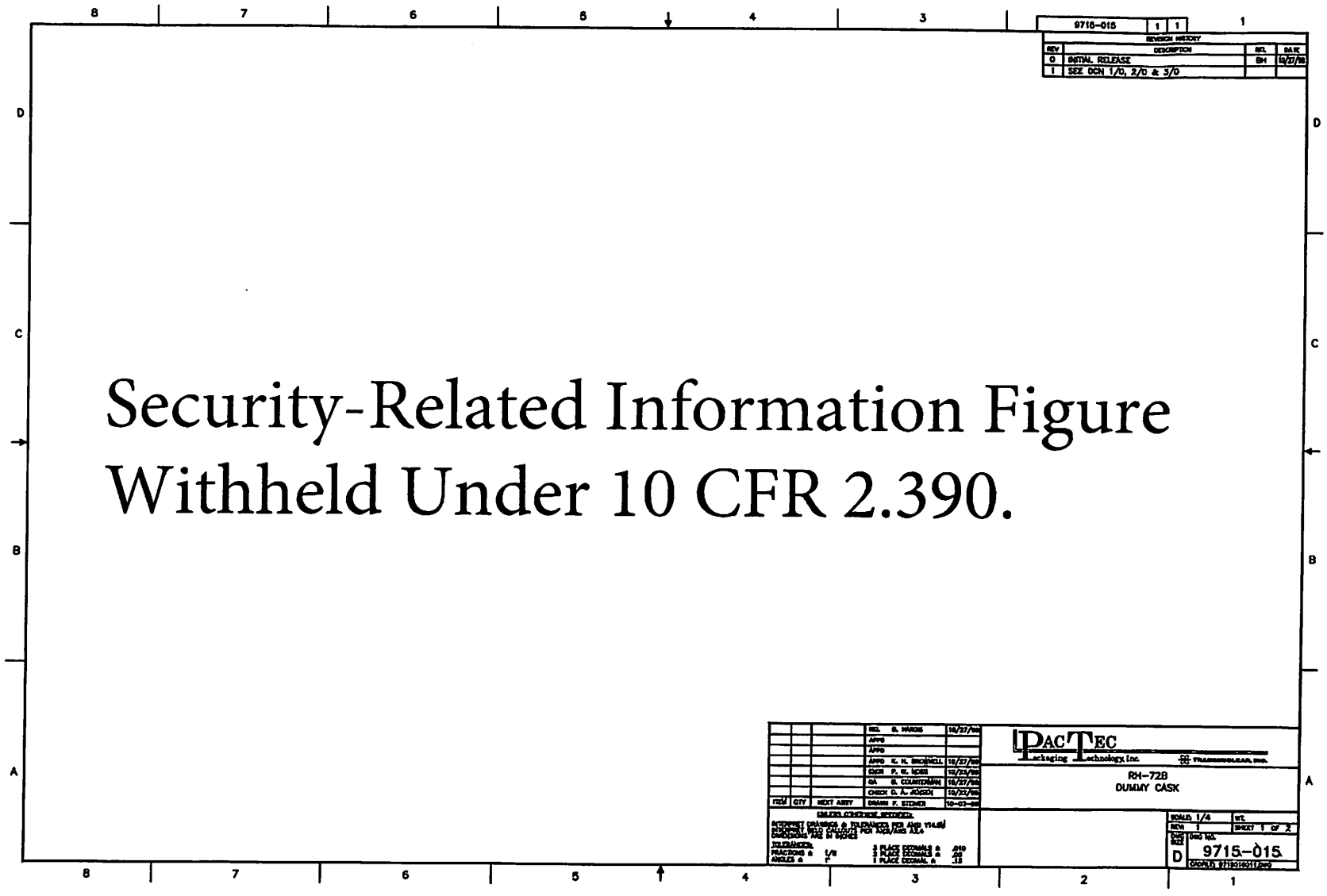

Figure 2.10.7-21 – Drawing 9715-015, *RH-72B Dummy Package*, Sheet 1

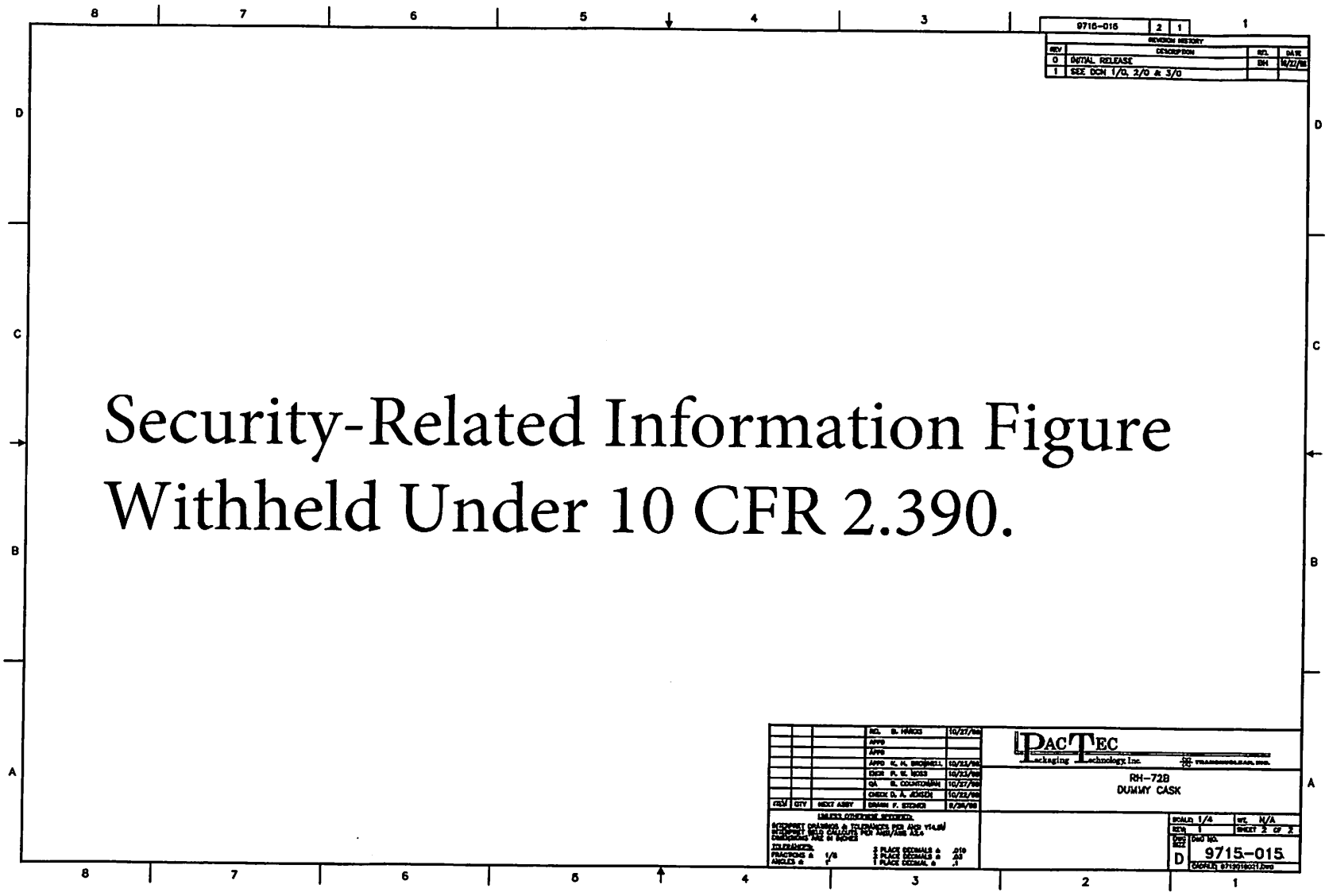

Figure 2.10.7-22 – Drawing 9715-015, *RH-72B Dummy Package*, Sheet 2

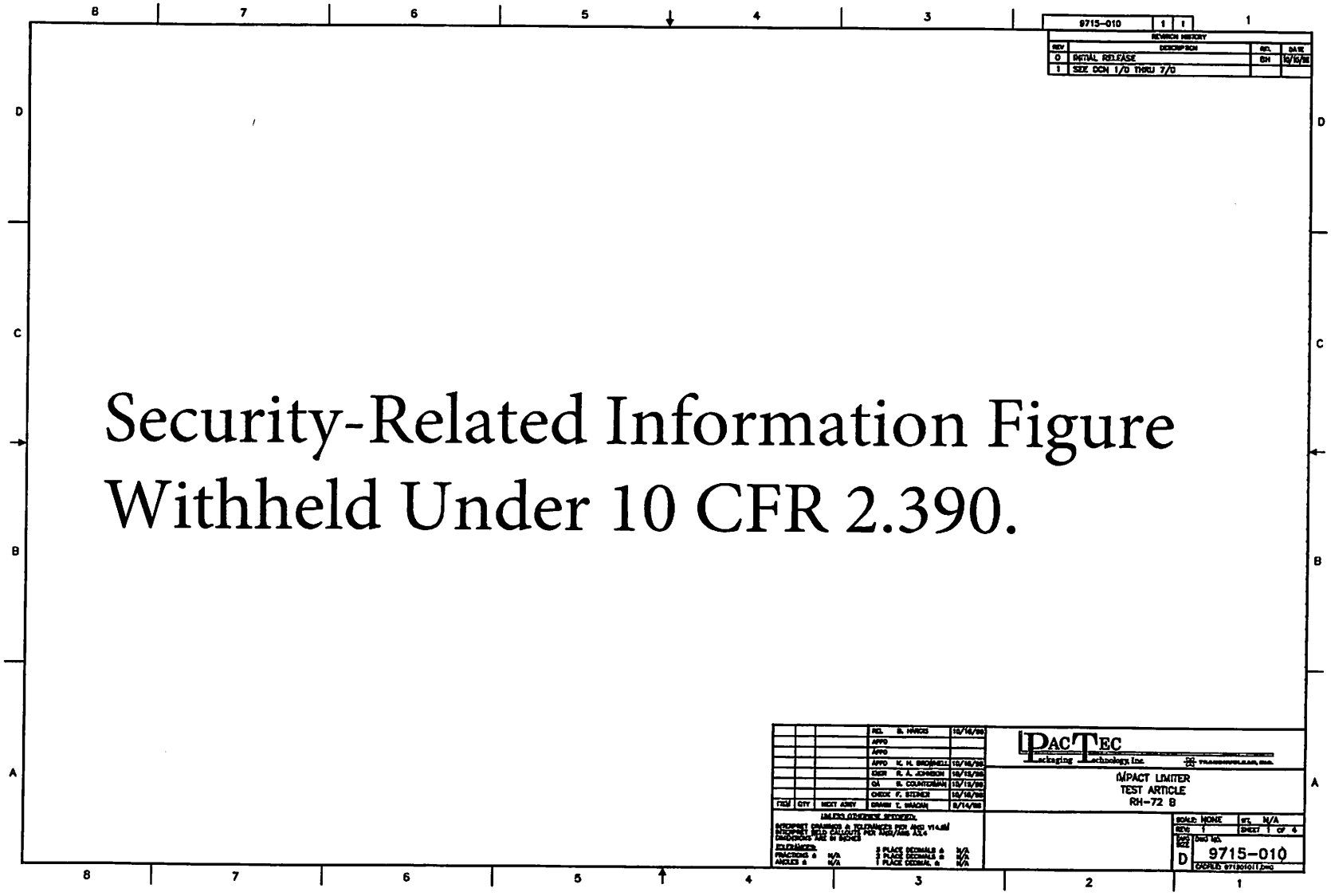

Figure 2.10.7-23 – Drawing 9715-010, *Impact Limiter Test Article RH-72B*, Sheet 1

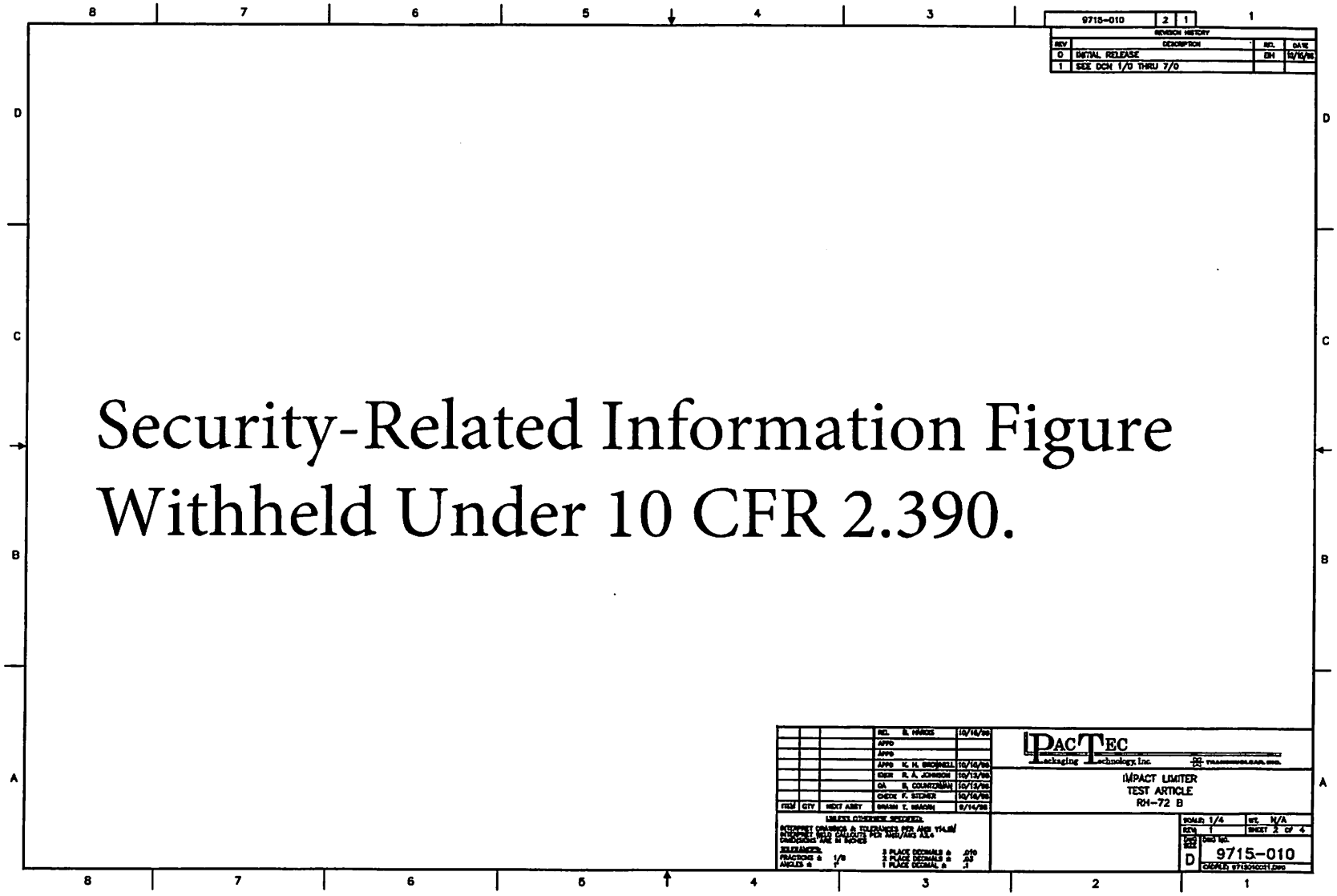

Figure 2.10.7-24 – Drawing 9715-010, *Impact Limiter Test Article RH-72B*, Sheet 2

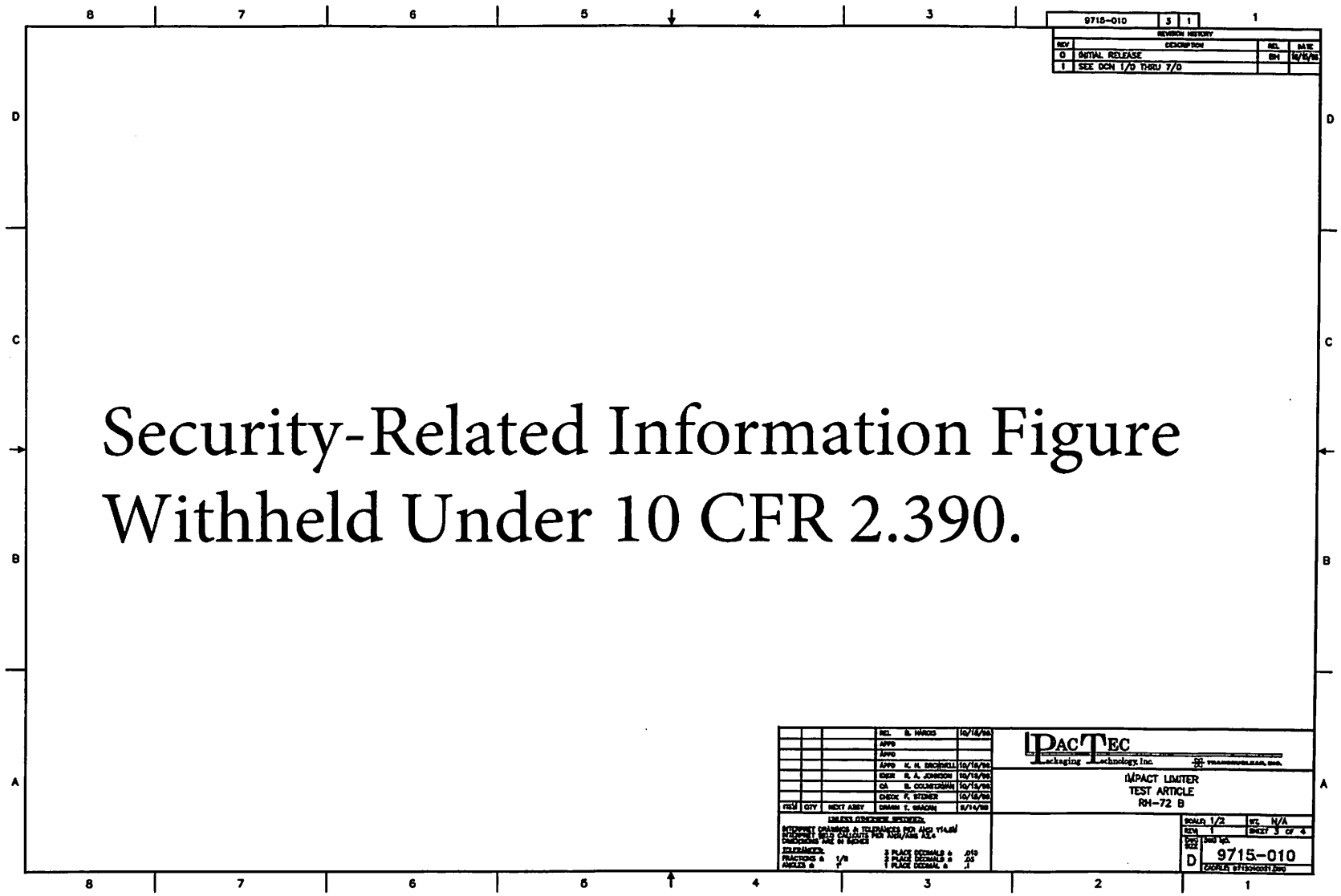

Figure 2.10.7-25 – Drawing 9715-010, *Impact Limiter Test Article RH-72B*, Sheet 3

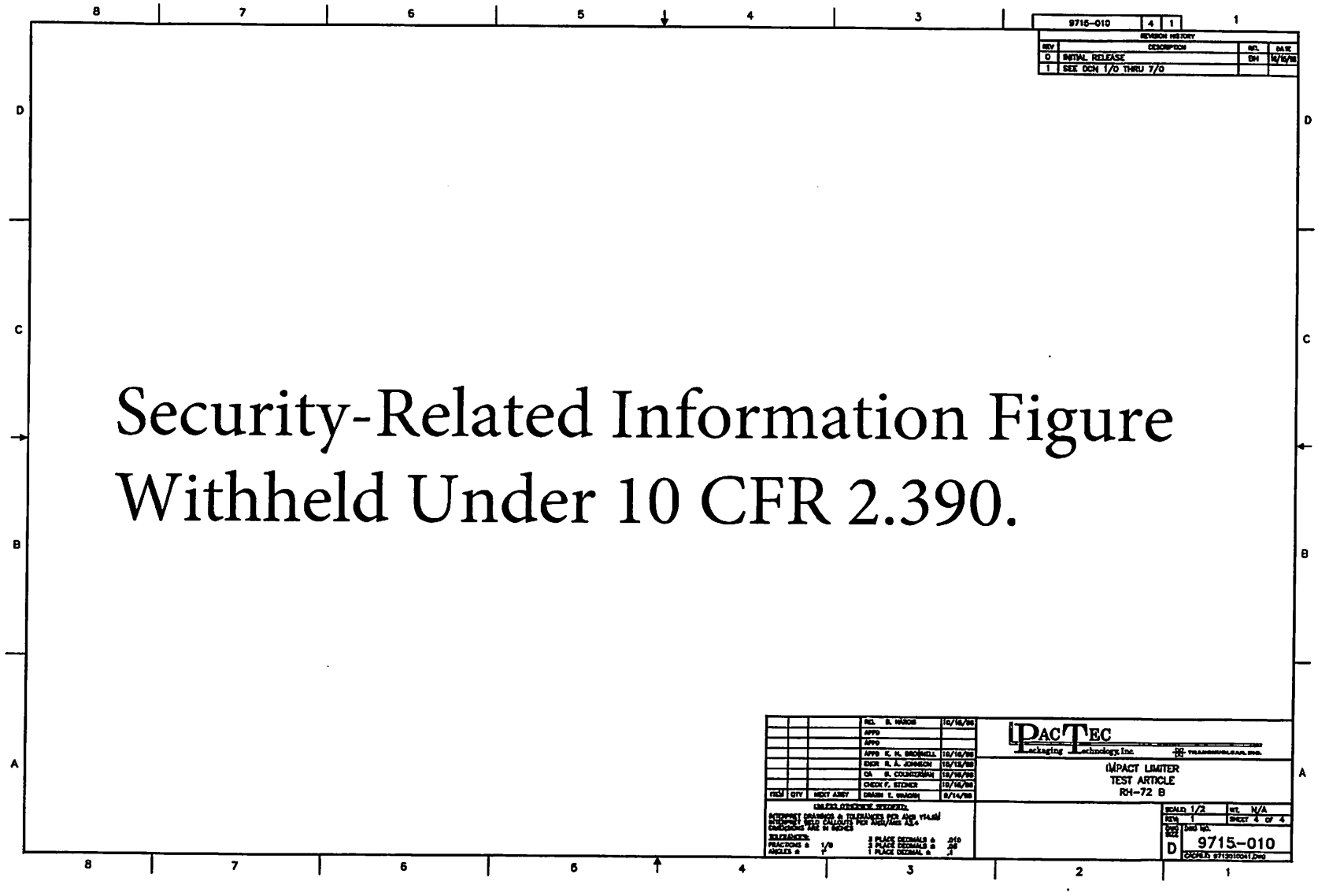

Figure 2.10.7-26 – Drawing 9715-010, *Impact Limiter Test Article RH-72B*, Sheet 4

2.10.8 Fabrication Stresses Due to Lead Pour

To determine fabrication stresses due to lead pour, assume a uniform steel and lead temperature of 620 ºF. The static head (pressure) due to a column of lead, p, is simply:

$$p = \gamma h = 54.1 \text{ psi}$$

where the specific weight of liquid lead, $\gamma = 0.386$ lb/in^3, and the height of the lead column, assuming an additional 11.0 inches for the overflow standpipe, h = 129.25 + 11.0 = 140.25 inches.

The physical properties of ASTM A240, Type 304, stainless steel used for the outer cask (OC) inner and outer shells are extracted from Table 2.3-1 in Section 2.3, *Mechanical Properties of Materials*, and are given in Table 2.10.8-1. The physical properties of lead (copperized) are extracted from Table 2.3-2 in Section 2.3, *Mechanical Properties of Materials*, and are given in Table 2.10.8-2. In the tables, E is Young's (elasticity) modulus, α is the coefficient of thermal expansion (mean from 70 ºF), and μ is Poisson's ratio.

At 70 ºF, the steel shell geometry is presented in Table 2.10.8-3.

2.10.8.1 Hoop Stress Evaluation after Heatup from 70 ºF to 620 ºF

At 620 ºF, without lead, the shells grow in radius and thickness in the following manner:

$$R' = R(1 + \alpha\Delta T)$$
$$t' = t(1 + \alpha\Delta T)$$

where the mean radius is R, the thickness is t, the coefficient of thermal expansion for stainless steel, $\alpha = 9.56(10)^{-6}$ in/in/ºF at 620 ºF, and the change in temperature, $\Delta T = 620 - 70 = 550$ ºF. Then, for each shell, given the dimensions in Table 2.10.8-3, the resulting dimensions are:

$$R'_i = (16.69)[(1 + 9.56(10)^{-6}(550)] = 16.778 \text{ in}$$
$$t'_i = (1.00)[(1 + 9.56(10)^{-6}(550)] = 1.005 \text{ in}$$
$$R'_o = (19.813)[(1 + 9.56(10)^{-6}(550)] = 19.917 \text{ in}$$
$$t'_o = (1.50)[(1 + 9.56(10)^{-6}(550)] = 1.508 \text{ in}$$

When filled with lead, the inner and outer OC shells are subjected to the 54.1 psi pressure head. This pressure head decreases the radius of the inner shell and increases the radius of the outer shell. Utilizing Table 29, Case 1b, of Roark[1], the change in radius of each shell, ΔR, is:

$$\Delta R'_i = \frac{q(R'_i)^2}{Et'_i} = \frac{(-54.1)(16.778)^2}{[25.2(10)^6](1.005)} = -0.00060 \text{ in}$$

$$\Delta R'_o = \frac{q(R'_o)^2}{Et'_o} = \frac{(54.1)(19.917)^2}{[25.2(10)^6](1.508)} = 0.000565 \text{ in}$$

[1] R. J. Roark, W. C. Young, *Formulas for Stress and Strain*, 5th Edition, McGraw-Hill, Inc., New York, NY, 1975.

In summary, as given in Table 2.10.8-4, the initial condition of the steel shells just before lead solidification at 620 ºF is:

$$R = R' + \Delta R' \pm \frac{t'}{2}$$

Lead experiences a decrease in volume of approximently 3.85% upon solidification. The lead pour fabrication process in Appendix 8.3.1, *Lead Installation Procedure*, carefully controls the solidification process such that lead solidification progresses upward from the bottom of the column. As the lead solidifies, it shrinks and liquid lead from above fills in between the solidifying lead and the OC inner and outer shells, thus maintaining a 54.1 psi pressure on the shells.

Eventually, the full annular region between the stainless steel shells is filled with lead, subjected to a pressure loading, as illustrated in Figure 2.10.8-1. (Note: the 54.1 psi pressure actually only exists at the base of the lead column, and linearly decreases to 6.2 psi at the top of the column; use of a uniform 54.1 psi pressure is, therefore, conservative.)

Under this loading, the outer radius of the inner shell, R_{iL} = 17.280 inches, and the inner radius of the outer shell, R_{oL} = 19.164 inches. The geometry of the unloaded lead shell is determined as follows:

$$R_{oL} = a + \Delta a \;\Rightarrow\; \Delta a = R_{oL} - a$$

$$R_{iL} = b + \Delta b \;\Rightarrow\; \Delta b = R_{iL} - b$$

$$t = L + \Delta L \;\Rightarrow\; \Delta L = t - L$$

where a, b, and L, are determined by superimposing Cases 1b and 1d from Table 32 of Roark[1]:

$$\Delta a = \frac{qab^2(2-\mu)}{E(a^2-b^2)} - \frac{qa\left[a^2(1-2\mu)+b^2(1+\mu)\right]}{E(a^2-b^2)} = R_{oL} - a$$

$$\Delta b = \frac{qb\left[a^2(1+\mu)+b^2(1-2\mu)\right]}{E(a^2-b^2)} - \frac{qa^2b(2-\mu)}{E(a^2-b^2)} = R_{iL} - b$$

$$\Delta L = \frac{qLb^2(1-2\mu)}{E(a^2-b^2)} - \frac{qLa^2(1-2\mu)}{E(a^2-b^2)} = t - L$$

Solving simultaneously,

$$a = 19.164076 \text{ in} \;\Rightarrow\; \Delta a = -7.6(10)^{-5} \text{ in}$$

$$b = 17.280069 \text{ in} \;\Rightarrow\; \Delta b = -6.9(10)^{-5} \text{ in}$$

$$L = 1.0000040 \text{ in} \;\Rightarrow\; \Delta L = -4.0(10)^{-6} \text{ in}$$

where, at 620 ºF, the pressure, q = 54.1 psi, the elastic modulus of lead, $E = 1.36(10)^6$ psi, Poisson's ratio, μ = 0.45, R_{oL} = 19.164 inches, R_{iL} = 17.280 inches, and t = 1.0 inch. These displacements are negligible, and are therefore subsequently ignored.

At this point, the hoop stress in the OC inner stainless steel shell, σ_i, is:

$$\sigma_i = \frac{pR_i}{t_i} = \frac{p\left(\frac{R_{iL} + R_{iS}}{2}\right)}{R_{iL} - R_{iS}} = -903 \text{ psi}$$

where the pressure, p = 54.1 psi, the inner shell outer radius, R_{iL} = 17.280 inches, and the inner shell inner radius, R_{iS} = 16.275 inches.

The hoop stress in the OC outer stainless steel shell, σ_o, is:

$$\sigma_o = \frac{pR_o}{t_o} = \frac{p\left(\frac{R_{oS} + R_{oL}}{2}\right)}{R_{oS} - R_{oL}} = 715 \text{ psi}$$

where the pressure, p = 54.1 psi, the outer shell outer radius, R_{oS} = 20.672 inches, and the outer shell inner radius, R_{oL} = 19.164 inches.

2.10.8.2 Hoop Stress Evaluation after Cooldown from 620 ºF to 70 ºF

In cooling from lead solidification at 620 ºF to a nominal ambient temperature of 70 ºF, the lead shell, with its greater coefficient of thermal expansion/contraction, tends to shrink onto the inner stainless steel shell. If the lead is allowed to cool freely and there is no interference, the cooling lead shell would assume the following geometry:

$$R_L' = R_L(1 + \alpha\Delta T) = 18.018 \text{ in}$$
$$t_L' = t_L(1 + \alpha\Delta T) = 1.863 \text{ in}$$

and,

$$R_{oL}' = R_L' + \frac{t_L'}{2} = 18.950 \text{ in}$$
$$R_{iL}' = R_L' - \frac{t_L'}{2} = 17.087 \text{ in}$$

where the coefficient of thermal expansion for lead, $\alpha = 20.39(10)^{-6}$ in/in/ºF at 620 ºF (a conservative value), the change in temperature, $\Delta T = 70 - 620 = -550$ ºF, the lead mean radius, $R_L = \frac{1}{2}(R_{oL} + R_{iL}) = 18.222$ inches, and the lead thickness, $t_L = R_{oL} - R_{iL} = 1.884$ inches.

Stress-free dimensions for the OC inner shell have been previously determined and are repeated once again for convenience in Table 2.10.8-5.

The interference between the lead and stainless steel inner shell, δ, is thus the difference between the unstressed lead inner radius and the unstressed inner shell outer radius at 70 ºF:

$$\delta = 17.190 - 17.087 = 0.103 \text{ in}$$

Using a press (interference) fit equation, Equation 7.33 of Juvinall[2], the interference pressure, p, at a temperature of 70 ºF is:

[2] Robert C. Juvinall, *Engineering Considerations of Stress, Strain, and Strength*, McGraw-Hill Book Company, New York, NY, 1967.

$$\delta = \frac{b_L p}{E_L}\left(\frac{c^2 + b_L^2}{c^2 - b_L^2} + \mu_L\right) + \frac{b_S p}{E_S}\left(\frac{b_S^2 + a^2}{b_S^2 - a^2} - \mu_S\right)$$

Rearranging terms,

$$p = \frac{\delta}{\frac{b_L p}{E_L}\left(\frac{c^2 + b_L^2}{c^2 - b_L^2} + \mu_L\right) + \frac{b_S p}{E_S}\left(\frac{b_S^2 + a^2}{b_S^2 - a^2} - \mu_S\right)} = 1{,}225 \text{ psi}$$

where, from Table 2.10.8-5, the inner stainless steel shell inner radius, a = 16.190 inches, the inner stainless steel shell outer radius, b_S = 17.190 inches, the lead shell inner radius, b_L = 17.087 inches, the lead shell outer radius, c = 18.950 inches, the stainless steel elastic modulus and Poisson's ratio, $E_S = 28.3(10)^6$ psi and $\mu_S = 0.3$, respectively (from Table 2.10.8-1) at 70 ºF, the lead elastic modulus and Poisson's ratio, $E_L = 2.34(10)^6$ psi and $\mu_L = 0.45$, respectively (from Table 2.10.8-2) at 70 ºF, and the interface deflection, $\delta = b_S - b_L = 0.103$ inches.

An interface pressure of 1,225 psi corresponds to a lead shell hoop stress, σ_L, of:

$$\sigma_L = p\left(\frac{c^2 + b_L^2}{c^2 - b_L^2}\right) = 11{,}881 \text{ psi}$$

Because of lead's low yield strength, this stress level cannot be sustained.

To fully accommodate the 0.103-inch radial interference, the lead would be required to see a strain of 0.103/17.087 = 0.00603 in/in, or 0.603%. Extrapolating from Figure 2.3-5 in Section 2.3, *Mechanical Properties of Materials*, a hoop stress of approximately 820 psi would exist in the lead for this strain. With this hoop stress, the effective interface pressure, p, would then be:

$$p = \frac{\sigma_L}{\left(\frac{c^2 + b_L^2}{c^2 - b_L^2}\right)} = 84.6 \text{ psi}$$

Note that the deflection, δ, for the inner stainless steel shell with a pressure of -84.6 psi is:

$$\delta = \frac{b_S p}{E_S}\left(\frac{b_S^2 + a^2}{b_S^2 - a^2} - \mu_S\right) = -0.00084 \text{ in}$$

which can be conservatively neglected for the inner stainless steel shell hoop stress calculations.

For a pressure of -84.6 psi at 70 ºF, the hoop stress in the inner stainless steel shell, σ_S, is:

$$\sigma_S = p\left(\frac{b_S^2 + a^2}{b_S^2 - a^2}\right) = -1{,}413 \text{ psi}$$

From Figure 2.3-8 in Section 2.3, *Mechanical Properties of Materials*, it is concluded that in 2-to-3 weeks, at 70 ºF, the lead hoop stress, σ_L, would creep to a value of approximately 300 psi

(holding an essentially constant 0.603% strain in the lead). The corresponding interface pressure, p, and inner stainless steel shell hoop stress, σ_S, would be:

$$p = \frac{\sigma_L}{\left(\frac{c^2 + b_L^2}{c^2 - b_L^2}\right)} = 31.0 \text{ psi}$$

$$\sigma_S = -p\left(\frac{b_S^2 + a^2}{b_S^2 - a^2}\right) = -518 \text{ psi}$$

To determine the stress-free temperature, T_o, unloading with heat-up would be elastic and, thus, using the previous interference fit equation:

$$\delta = \frac{b_L p}{E_L}\left(\frac{c^2 + b_L^2}{c^2 - b_L^2} + \mu_L\right) + \frac{b_S p}{E_S}\left(\frac{b_S^2 + a^2}{b_S^2 - a^2} - \mu_S\right) = R(\alpha_L - \alpha_S)(T_o - 70)$$

Rewriting the equation in terms of the stress-free temperature, T_o, gives:

$$T_o = \frac{\frac{b_L p}{E_L}\left(\frac{c^2 + b_L^2}{c^2 - b_L^2} + \mu_L\right) + \frac{b_S p}{E_S}\left(\frac{b_S^2 + a^2}{b_S^2 - a^2} - \mu_S\right)}{R(\alpha_L - \alpha_S)} + 70 = 89.9\,^{\circ}\text{F}$$

where, as before, from Table 2.10.8-5, the inner stainless steel shell inner radius, a = 16.190 inches, the inner stainless steel shell outer radius, b_S = 17.190 inches, the lead shell inner radius, b_L = 17.087 inches, the lead shell outer radius, c = 18.950 inches, the stainless steel elastic modulus, Poisson's ratio, and coefficient of thermal expansion, $E_S = 28.3(10)^6$ psi, $\mu_S = 0.3$, and $\alpha_S = 8.46(10)^{-6}$ in/in/ºF, respectively (from Table 2.10.8-1) at 70 ºF, the lead elastic modulus, Poisson's ratio, and coefficient of thermal expansion, $E_L = 2.34(10)^6$ psi, $\mu_L = 0.45$, and $\alpha_L = 16.07(10)^{-6}$ in/in/ºF, respectively (from Table 2.10.8-2) at 70 ºF, the inner steel/lead interface radius, $R = b_s = 17.190$ inches, and the interface pressure, p = 31.0 psi.

2.10.8.3 Hoop Stress Evaluation after Cooldown from 90 ºF to -20 ºF

Next, consider cooling to -20 ºF (ΔT = 110 ºF) for determining the worst-case hoop stress on the inner stainless steel shell during all regulatory drop events. The stainless steel and lead shell initial conditions are determined based on the previously defined dimensions of a, b_S, b_L, and c at 70 ºF as follows:

$$a = (16.190)(1 + \alpha_s \Delta T) = 16.175 \text{ in}$$

$$b_s = (17.190)(1 + \alpha_s \Delta T) = 17.174 \text{ in}$$

$$b_L = (17.087)(1 + \alpha_L \Delta T) = 17.058 \text{ in}$$

$$c = (18.950)(1 + \alpha_L \Delta T) = 18.917 \text{ in}$$

$$\delta = b_s - b_L = 0.116 \text{ in}$$

where the thermal expansion coefficient for stainless steel, $\alpha_S = 8.21(10)^{-6}$ in/in/ºF (extrapolated from Table 2.10.8-1) at -20 ºF, and the thermal expansion coefficient for lead, $\alpha_L = 15.7(10)^{-6}$ in/in/ºF (extrapolated from Table 2.10.8-2) at -20 ºF.

To fully accommodate the 0.116-inch radial interference, the lead would be required to see a strain of 0.116/17.058 = 0.00680 in/in, or 0.680%. Extrapolating from Figure 2.3-5 in Section 2.3, *Mechanical Properties of Materials*, a hoop stress, σ_L, of approximately 1,060 psi would exist in the lead for this strain. With this hoop stress, the effective interface pressure, p, would then be:

$$p = \frac{\sigma_L}{\left(\frac{c^2 + b_L^2}{c^2 - b_L^2}\right)} = 109 \text{ psi}$$

For a pressure of -109 psi at -20 ºF, and conservatively neglecting the beneficial effects of lead creep, the hoop stress in the inner stainless steel shell, σ_S, is:

$$\sigma_S = -p\left(\frac{b_S^2 + a^2}{b_S^2 - a^2}\right) = -1{,}821 \text{ psi}$$

2.10.8.4 Hoop Stress Evaluation after Cooldown from 90 ºF to -40 ºF

Finally, consider cooling to -40 ºF (ΔT = 130 ºF) for determining the worst-case hoop stress on the inner stainless steel shell. The stainless steel and lead shell initial conditions are determined based on the previously defined dimensions of a, b_S, b_L, and c at 70 ºF as follows:

$$a = (16.190)(1 + \alpha_s \Delta T) = 16.173 \text{ in}$$

$$b_s = (17.190)(1 + \alpha_s \Delta T) = 17.172 \text{ in}$$

$$b_L = (17.087)(1 + \alpha_L \Delta T) = 17.052 \text{ in}$$

$$c = (18.950)(1 + \alpha_L \Delta T) = 18.912 \text{ in}$$

$$\delta = b_s - b_L = 0.120 \text{ in}$$

where the thermal expansion coefficient for stainless steel, $\alpha_S = 8.15(10)^{-6}$ in/in/ºF (extrapolated from Table 2.10.8-1) at -40 ºF, and the thermal expansion coefficient for lead, $\alpha_L = 15.6(10)^{-6}$ in/in/ºF (extrapolated from Table 2.10.8-2) at -40 ºF.

To fully accommodate the 0.120-inch radial interference, the lead would be required to see a strain of 0.120/17.052 = 0.00704 in/in, or 0.704%. Extrapolating from Figure 2.3-5 in Section 2.3, *Mechanical Properties of Materials*, a hoop stress, σ_L, of approximately 1,070 psi would exist in the lead for this strain. With this hoop stress, the effective interface pressure, p, would then be:

$$p = \frac{\sigma_L}{\left(\frac{c^2 + b_L^2}{c^2 - b_L^2}\right)} = 110 \text{ psi}$$

For a pressure of -110 psi at -40 ºF, and conservatively neglecting the beneficial effects of lead creep, the hoop stress in the inner stainless steel shell, σ_S, is:

$$\sigma_S = p\left(\frac{b_S^2 + a^2}{b_S^2 - a^2}\right) = -1{,}837 \text{ psi}$$

2.10.8.5 Axial Stress Evaluation after Cooldown from 620 ºF to -20 ºF

The preceeding calculations deal only with the determination of hoop stresses. Axial stresses will also develop in the inner stainless steel shell and lead shell due to axial shrinkage of the lead. In cooling from 620 ºF to 90 ºF (stress-free condition of the lead), then from 90 ºF to -20 ºF, the axial strain in the lead, ε, assuming bonding of the lead to the inner stainless steel shell, would be:

$$\varepsilon = [(\alpha_L - \alpha_s)\Delta T]_{620} + [(\alpha_L - \alpha_s)\Delta T]_{-20} = 0.00656 \text{ in/in} = 0.656\% \text{ strain (tensile)}$$

where, for cooldown from 620 ºF to 90 ºF, the lead and stainless steel coefficients of thermal expansion, $\alpha_S = 9.56(10)^{-6}$ in/in/ºF (from Table 2.10.8-1) and $\alpha_L = 20.39(10)^{-6}$ in/in/ºF (from Table 2.10.8-2), respectively, and $\Delta T = 620 - 90 = 530$ ºF, and for cooldown from 90 ºF to -20 ºF, the lead and stainless steel coefficients of thermal expansion, $\alpha_S = 8.21(10)^{-6}$ in/in/ºF (extrapolated from Table 2.10.8-1) and $\alpha_L = 15.7(10)^{-6}$ in/in/ºF (extrapolated from Table 2.10.8-2), respectively, and $\Delta T = 90 - (-20) = 110$ ºF.

Extrapolating from Figure 2.3-5 in Section 2.3, *Mechanical Properties of Materials*, an axial stress, σ_L, of approximately 1,040 psi would exist in the lead for this strain. The effective axial force in the lead shell, P_a, would then be:

$$P_a = \sigma_L A_L = 205{,}532 \text{ lb}$$

where the cross-sectional area of the lead shell, $A_L = \pi(c^2 - b_S^2) = 197.627$ in^2, the outer lead shell radius, c = 18.917 inches, and the inner stainless steel shell outer radius, $b_S = 17.174$ inches, respectively (from Appendix 2.10.8.3, *Hoop Stress Evaluation after Cooldown from 90 ºF to -20 ºF*).

From equilibrium, this same force could develop in the inner stainless steel shell. Thus, at a temperature of -20 ºF, the compressive axial stress in the inner steel shell would be:

$$\sigma_a = \frac{P_a}{A_S} = -1{,}963 \text{ psi}$$

where the axial force, $P_a = -205{,}532$ lb, and the cross-sectional area of the inner stainless steel shell, $A_S = \pi(b_S^2 - a^2) = 104.664$ in^2, and the inner and outer lead shell radii, $b_S = 17.174$ inches and a = 16.175 inches, respectively (from Appendix 2.10.8.3, *Hoop Stress Evaluation after Cooldown from 90 ºF to -20 ºF*.

This stress value is a conservative estimate in that it assumes the OC inner shell is incompressible under axial load and that no load would develop in the outer shell (i.e., any compressibility of the inner shell would reduce the lead strain and resultant axial forces and stresses).

2.10.8.6 Axial Stress Evaluation after Cooldown from 620 ºF to -40 ºF

In cooling from 620 ºF to 90 ºF (stress-free condition of the lead), then from 90 ºF to -40 ºF, the axial strain in the lead, ε, assuming bonding of the lead to the inner stainless steel shell, would be:

$$\varepsilon = [(\alpha_L - \alpha_s)\Delta T]_{620} + [(\alpha_L - \alpha_s)\Delta T]_{-40} = 0.00671 \text{ in/in} = 0.671\% \text{ strain (tensile)}$$

where, for cooldown from 620 ºF to 90 ºF, the lead and stainless steel coefficients of thermal expansion, $\alpha_S = 9.56(10)^{-6}$ in/in/ºF (from Table 2.10.8-1) and $\alpha_L = 20.39(10)^{-6}$ in/in/ºF (from Table 2.10.8-2), respectively, and $\Delta T = 620 - 90 = 530$ ºF, and for cooldown from 90 ºF to -40 ºF, the lead and stainless steel coefficients of thermal expansion, $\alpha_S = 8.15(10)^{-6}$ in/in/ºF (extrapolated from Table 2.10.8-1) and $\alpha_L = 15.6(10)^{-6}$ in/in/ºF (extrapolated from Table 2.10.8-2), respectively, and $\Delta T = 90 - (-40) = 130$ ºF.

Extrapolating from Figure 2.3-5 in Section 2.3, *Mechanical Properties of Materials*, an axial stress, σ_L, of approximately 1,050 psi would exist in the lead for this strain. The effective axial force in the lead shell, P_a, would then be:

$$P_a = \sigma_L A_L = 207{,}111 \text{ lb}$$

where the cross-sectional area of the lead shell, $A_L = \pi(c^2 - b_S^2) = 197.248$ in^2, the outer lead shell radius, $c = 18.912$ inches, and the inner stainless steel shell outer radius, $b_S = 17.172$ inches, respectively (from Appendix 2.10.8.4, *Hoop Stress Evaluation after Cooldown from 90 ºF to -40 ºF*).

From equilibrium, this same force could develop in the inner stainless steel shell. Thus, at a temperature of -40 ºF, the compressive axial stress in the inner steel shell would be:

$$\sigma_a = \frac{P_a}{A_S} = -1{,}979 \text{ psi}$$

where the axial force, $P_a = -207{,}111$ lb, and the cross-sectional area of the inner stainless steel shell, $A_S = \pi(b_S^2 - a^2) = 104.652$ in^2, and the inner and outer lead shell radii, $b_S = 17.172$ inches and $a = 16.173$ inches, respectively (from Appendix 2.10.8.4, *Hoop Stress Evaluation after Cooldown from 90 ºF to -40 ºF*.

Again, this calculation conservatively assumes that the OC inner shell is incompressible under an axial load and that no load develops in the outer shell.

2.10.8.7 Transient Effects

The preceding calculations in this appendix are based on the assumption that the OC inner and outer shells and the lead between them are always at the same temperature during cooldown. Although this ideal condition could never be fully achieved in practice, the procedures used for lead pour (see Appendix 8.3.1, *Lead Installation Procedure*) are set up to minimize the temperature differences that could occur. To control the cooldown process, thermocouples are used to monitor temperatures of the OC inner and outer shells. Thermocouples on the outer shell are located directly opposite those on the inner shell, and the maximum acceptable temperature difference indicated by any opposing pair of thermocouples is limited to 300 ºF. Temperature differences are not expected to ever be this great in practice, but even if they were, the following calculations indicate that they would be acceptable. An additional control is placed on the thermocouple readings so that no single thermocouple reading may change by more than 100 ºF

in any 30-minute period. Recognizing the good conductivity exhibited by stainless steel and lead, this control essentially eliminates the consequences of transient effects.

Temperature differences between the inner and outer shells are of little consequence since the axial tie between the shells is made after lead cooldown, when a uniform temperature exists throughout the OC. By welding the outer shell to the base after the cooldown process, temperature differences between the two shells will not cause axial stresses to develop in the shells during cooldown. It can be shown that if the weld were made prior to lead pour, a condition where the inner shell is 300 ºF hotter than the outer shell will result in elastically calculated axial stresses that would be unacceptable, thus establishing the need for final welding after cooldown.

The remaining issue to be addressed is that of temperature differences between the inner shell and the lead. The 300 ºF maximum difference in temperature between the inner and outer shells could conservatively be used as the maximum temperature difference between the inner shell and the lead. Furthermore, if the inner shell is cooler than the lead, the previous calculations will remain conservative. Specifically, with lower temperatures for the inner shell than for the lead, the interference and associated contact pressure between the shell and lead would be reduced, thus reducing the stresses within the inner shell.

When a uniform temperature is finally achieved throughout the OC, the lead would have "caught up" with the inner shell and the previous calculations would be directly applicable.

The remaining case of the inner shell being 300 ºF hotter than the lead is addressed as follows, but considering the lead as being at 70 ºF and the inner shell as being at 370 ºF. The analytical method is identical to the methodology previously used in this appendix.

Per Table 2.10.8-5, the lead inner radius at 70 ºF, assuming no interference with the inner shell, is $b_L = 17.087$ inches. The outer radius of the inner shell at 370 ºF, b_S, and the inner radius of the inner shell at 370 ºF, a, assuming no interference with the lead, are:

$$b_s = (17.190)(1 + \alpha_s \Delta T) = 17.237 \text{ in}$$

$$a = (16.190)(1 + \alpha_s \Delta T) = 16.234 \text{ in}$$

where the thermal expansion coefficient for stainless steel, $\alpha_S = 9.133(10)^{-6}$ in/in/ºF (interpolated from Table 2.10.8-1) at 370 ºF, and $\Delta T = 300$ ºF.

The resulting interference, δ, is:

$$\delta = b_s - b_L = 0.150 \text{ in}$$

and the maximum strain in the lead, ε, therefore becomes:

$$\varepsilon = \frac{\delta}{b_L} = 0.00878 \text{ in/in} = 0.878\% \text{ strain (tensile)}$$

Extrapolating from Figure 2.3-5 in Section 2.3, *Mechanical Properties of Materials*, a hoop stress, σ, of approximately 900 psi would exist in the lead for this strain. The effective interface pressure, p, would then be:

$$p = \frac{\sigma}{\left(\frac{c^2 + b_L^2}{c^2 - b_L^2}\right)} = 92.8 \text{ psi}$$

where, from Table 2.10.8-5, the outer and inner lead shell radii, c = 18.950 inches and b_L = 17.087 inches, respectively.

For a pressure of 92.8 psi at 370 ºF, and conservatively neglecting the beneficial effects of lead creep, the hoop stress in the inner stainless steel shell, σ_S, is:

$$\sigma_S = -p\left(\frac{b_S^2 + a^2}{b_S^2 - a^2}\right) = -1{,}551 \text{ psi}$$

where, from above, the outer and inner radii of the inner stainless steel shell, b_S = 17.237 inches and a = 16.234 inches, respectively.

The -1,551 psi hoop stress compares with the previously determined hoop stress in the inner shell of -1,413 psi, and only would exist during the fabrication cooldown process (i.e., when the shell is 300 ºF hotter than the lead). When the inner shell continues to cool, this hoop stress would reduce, and it is concluded that the -1,551 psi hoops stress case is independent and would not combine with other loads such as those resulting from hypothesized drop events.

Regarding axial stresses, with the lead at 70 ºF and the inner shell at 370 ºF, and interpolating data from Table 2.10.8-1 and Table 2.10.8-2, the axial strain in the lead, ε_a, assuming bonding, would be:

$$\varepsilon = [(\alpha_L - \alpha_s)\Delta T]_{620} + [\alpha_s \Delta T]_{370} = 0.00870 \text{ in/in} = 0.870\% \text{ strain (tensile)}$$

where, for cooldown from 620 ºF to 70 ºF, the lead and stainless steel coefficients of thermal expansion, $\alpha_S = 9.56(10)^{-6}$ in/in/ºF (from Table 2.10.8-1) and $\alpha_L = 20.39(10)^{-6}$ in/in/ºF (from Table 2.10.8-2), respectively, and ΔT = 620 – 70 = 550 ºF, and for heatup from 70 ºF to 370 ºF, the stainless steel coefficient of thermal expansion, $\alpha_S = 9.133(10)^{-6}$ in/in/ºF (interpolated from Table 2.10.8-1), and ΔT = 370 – 70 = 300 ºF.

Extrapolating from Figure 2.3-5 in Section 2.3, *Mechanical Properties of Materials*, an axial stress, σ_L, of approximately 900 psi would exist in the lead for this strain.

The corresponding axial stressing the inner shell, σ_a = -1,662 psi. Continued cooling of the inner stell to 70 ºF would reduce this axial compressive stress. Further cooling of the lead and inner shell to -20 ºF or -40 ºF would result in axial stresses no worse than previously determined for these temperatures.

2.10.8.8 Summary

The preceding calculations indicate that stress levels resulting from lead pour and subsequent cooldown would be relatively small. In particular, with compressive stress magnitudes in the neighborhood of 1,500 psi to 2,000 psi, as calculated herein, it is concluded that buckling of the OC inner shell should not occur due to the lead pour procedure (i.e., critical buckling stresses, as determined in Appendix 2.10.5, *Buckling Design Criteria and Detailed Evaluation*, for the OC inner shell, are well above the predicted stress levels).

Table 2.10.8-1 – Mechanical Properties of Stainless Steel (Type 304)

Temperature (ºF)	E (10^6 psi)	α (10^{-6} in/in/ºF)	μ
70	28.3	8.46	0.3
100	28.2	8.55	0.3
200	27.6	8.79	0.3
300	27.0	9.00	0.3
400	26.5	9.19	0.3
500	25.8	9.37	0.3
600	25.3	9.53	0.3
620	25.2	9.56	0.3

Table 2.10.8-2 – Mechanical Properties of Lead (Copperized)

Temperature (ºF)	E (10^6 psi)	α (10^{-6} in/in/ºF)	μ
70	2.34	16.07	0.45
100	2.30	16.21	0.45
200	2.16	16.70	0.45
300	2.00	17.34	0.45
400	1.82	18.17	0.45
500	1.61	19.13	0.45
600	1.40	20.18	0.45
620	1.36	20.39	0.45

Table 2.10.8-3 – Steel Shell Geometry at 70 ºF

Geometry (at 70 ºF)	Inner Shell (in)	Outer Shell (in)
Inside Diameter, D_i	32.38	38.13
Outside Diameter, D_o	34.38	41.13
Shell Thickness, t	1.00	1.50

Table 2.10.8-4 – Initial Shell Conditions Before Lead Solidification

Shell	Inner Radius (in)	Outer Radius (in)
Inner	16.275	17.280
Outer	19.164	20.672

Table 2.10.8-5 – Stress-Free OC Inner Shell Dimensions

Item	Radius (in)		
	620 ºF	70 ºF	ΔR
Stainless Steel Inner Shell Inner Radius	16.275	16.190	0.085
Stainless Steel Inner Shell Outer Radius	17.280	17.190	0.090
Lead Inner Radius	17.280	17.087	0.193
Lead Outer Radius	19.164	18.950	0.214

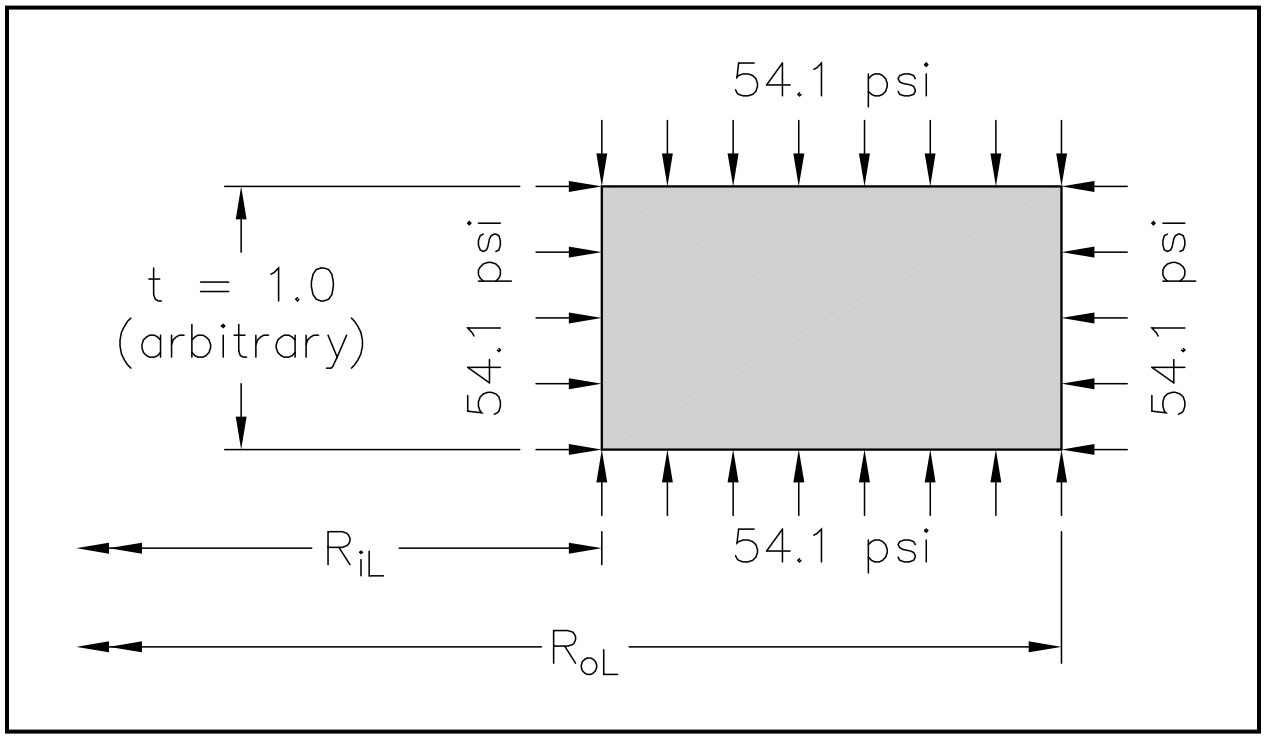

Figure 2.10.8-1 – Free-Body Diagram of Molten Lead in the Lead Column

3.0 THERMAL EVALUATION

This section identifies and describes the principal thermal engineering design aspects of the RH-TRU 72-B package important to compliance with the thermal performance requirements of 10 CFR 71[1]. For a more detailed discussion of the package and its key features, see Chapter 1.0, *General Information*.

3.1 Discussion

The following subsections present the RH-TRU 72-B packaging and payload configurations. The RH-TRU 72-B package, with an RH-TRU waste canister payload, is illustrated in Figure 1.1-1 and Figure 1.1-2 from Chapter 1.0, *General Information*.

3.1.1 Packaging Configuration

As described in Section 1.2.1, *Packaging*, the RH-TRU 72-B package is designed with a totally passive thermal system. The principal physical characteristics of this system consist of an external thermal fire shield surrounding the outer cask (OC) outer shell. The thermal fire shield is a 10-gauge (0.1406-inch thick) stainless steel cylinder offset from the OC body by a 12-gauge (0.1094-inch diameter) stainless steel wire wrap on a 3-inch pitch. The OC consists of a 1½-inch thick, 41⅛-inch outside diameter stainless steel outer shell surrounding a 1⅞-inch thick lead shield and a 1-inch thick, 32⅜-inch inside diameter stainless steel inner shell. The OC bottom end plate is 5-inch thick stainless steel, while the OC lid is 6-inch thick stainless steel that is attached via 18, 1¼-7UNC socket head cap screws. Two, 18-inch × 28-inch main trunnion blocks and six, 6-inch diameter lifting and handling trunnions penetrate the thermal shield and attach directly to the OC outer shell.

The 32-inch outside diameter inner vessel (IV) is constructed of 3/8-inch thick stainless steel, with a 1½-inch thick stainless steel bottom end plate and a 6½-inch thick stainless steel lid that is attached via eight, 7/8-9UNC flange head cap screws.

The impact limiters are fabricated of stainless steel shells filled with 11½-lb/ft^3 polyurethane foam for impact and thermal protection. The outer cylindrical shell and inner and outer plates are 11-gauge (0.125-inch thick) stainless steel, the inner cylindrical shell is 3/16-inch thick stainless steel, and the impact limiter base plate is 1/2-inch thick stainless steel. Six, 3¼-inch diameter, 1/8-inch thick stainless steel bolt tubes allow access to the impact limiter attachment bolts.

Further discussion regarding the packaging configuration used for the thermal analysis model is provided in Section 3.4.1.1.1, *Packaging Model*.

3.1.2 Payload Configurations

RH-TRU waste may be loaded directly into a 120½-inch long payload canister, or into inner containers (e.g., 30-gallon or 55-gallon drums) within the payload canister. The payload canister

[1] Title 10, *Code of Federal Regulations*, Part 71 (10 CFR 71), *Packaging and Transportation of Radioactive Material*, 01-01-14 Edition.

is basically a one- or two-piece construction unit (fixed or removable lid versions, respectively, either of which may be configured with a through-pintle fill port and plug). The two payload canister versions are essentially identical in overall configuration, but the removable lid canister (RLC) configuration is used for the thermal analysis to address both configurations.

The payload canister is a 26-inch outside diameter, 1/4-inch thick, minimum, cylinder fabricated of painted carbon steel (only exterior surfaces are painted) or stainless steel, with a 1/4-inch thick, minimum, base and lid. A lift pintle is integrated into the lid plate. The payload canister may be directly loaded with waste or may contain waste in up to three, 30-gallon or 55-gallon drums. The RLC with a 30-gallon drum payload is illustrated in Figure 3.1-1.

The RLC may be utilized as a neutron shielded canister (NSC) in two configurations, NS15 and NS30, that incorporate neutron shielding components to provide neutron shielding for approximately 15-gallon drum and 30-gallon drum inner containers, respectively, as illustrated in Figure 3.1-2 and Figure 3.1-3.

Further discussion regarding the payload configurations used for the thermal analysis models is provided in Section 3.4.1.1.2, *Payload Models*.

3.1.3 Boundary Conditions

The thermal characteristics of the RH-TRU 72-B package are evaluated for the payload configurations based on three thermal boundary conditions for Normal Conditions of Transport (NCT):

1. Steady-state conditions at an ambient temperature of 100 ºF without insolation in still air, as defined in 10 CFR §71.43(g), for limiting the maximum accessible package surface temperature to not exceed 185 ºF for exclusive use shipments,
2. Transient conditions at an ambient temperature of 100 ºF with insolation in still air, as defined in 10 CFR §71.71(c)(1), and
3. Steady-state conditions at an ambient temperature of -40 ºF without insolation in still air, as described in 10 CFR §71.71(c)(2).

The thermal characteristics of the RH-TRU 72-B package are also evaluated for the payload configurations based on the following sequence of thermal boundary conditions for Hypothetical Accident Conditions (HAC):

1. Transient, pre-fire conditions at an ambient temperature of 100 ºF in still air, as defined in 10 CFR §71.73(b), with insolation,
2. Transient conditions in sufficiently quiescent ambient conditions to provide an average emissivity coefficient of at least 0.9 at an ambient temperature of 1,475 ºF, without insolation, for 30 minutes and with a package surface emissivity of at least 0.8 and an external convection coefficient based on a fire environment, as defined in 10 CFR §71.73(c)(4), and
3. Transient, post-fire conditions at an ambient temperature of 100 ºF with insolation in still air, as described in 10 CFR §71.73(c)(4), until maximum temperatures for all package components have been achieved.

Further discussion regarding boundary conditions is provided in Section 3.4.2, *Package Conditions and Environment*, for NCT and Section 3.5.2, *Package Conditions and Environment*, for HAC.

3.1.4 Analysis Summary

The primary heat transfer mechanisms utilized in the RH-TRU 72-B thermal analyses are component-to-component from conduction and radiation within the package, and free convection and radiation from the exterior of the package to the ambient. Due to the relatively close coupling of the bodies within the packaging, convective heat transfer in spaces within the package is conservatively ignored.

Maximum allowed decay heat loads were developed for a range of payload densities from 12 to 100 lb/ft^3 using the thermal properties of polyurethane foam as a surrogate payload material (see Table 3.2-8 in Section 3.2, *Summary of Thermal Properties of Materials*) based on use of an allowable average payload temperature of 302 ºF and an allowable peak payload temperature of 402 ºF (see Section 3.3.3, *Payload Material*; the allowable temperatures apply to both NCT and HAC). Worst-case payload temperatures occur for HAC. As discussed in Appendix 3.6.1.4, *Determination of Density-Dependent Payload Decay Heat Limits*, the maximum allowed RH-TRU waste canister decay heat for a low-density (i.e., up to 12 lb/ft^3) payload is 90 watts total, and the maximum allowed RH-TRU waste canister decay heat for a high-density (i.e., 100 lb/ft^3 and greater) payload is 270 watts total. Appendix 3.6.1.4 also demonstrates how use of the density-dependent decay heat limit based on an RH-TRU waste canister containing three, 30-gallon drums is conservatively bounding for use with other authorized RH TRU waste canister payload configurations (i.e., containing three, 55-gallon drum payloads or directly loaded).

The maximum decay heat load for the NS15 and NS30 neutron shielded canister is 50 watts conservatively based on a low-density payload (i.e., up to 12 lb/ft^3). Higher density payloads result in correspondingly higher payload thermal conductivity that distributes decay heat more evenly and results in lower overall packaging and payload temperatures; therefore, use of low-density payload material is bounding for all temperature predictions.

Details of the applicable normal conditions of transport (NCT) analyses and their results are presented in Section 3.4, *Thermal Evaluation for Normal Conditions of Transport*, and details of the applicable hypothetical accident condition (HAC) thermal response is addressed in Section 3.5, *Thermal Evaluation for Hypothetical Accident Conditions*. Maximum NCT and HAC temperatures are summarized in Table 3.1-1 and Table 3.1-2, respectively.

In summary, the combined thermal performance of the RLC and NSCs within the RH-TRU 72-B packaging was evaluated for the applicable NCT and HAC conditions, and for a variety of decay heat distributions within the packaging. The evaluations found that the resulting component temperatures remained within their specified allowable limits for all cases.

Table 3.1-1 – Maximum NCT Temperatures with Insolation (ºF)

Location	RLC		NS15	NS30	Allowable Limit①
	12 lb/ft³ Payload (90 W)	100 lb/ft³ Payload (270 W)	12 lb/ft³ Payload (50 W)	12 lb/ft³ Payload (50 W)	
Lower Drum Contents Peak	331.8	312.1	258.6	245.2	402
Lower Drum Contents Average	225.7	253.1	194.7	185.9	302
Lower Drum Wall Peak	180.1	252.0	166.9	160.8	—
Middle Drum Contents Peak	338.8	326.3	263.5	249.5	402
Middle Drum Contents Average	233.6	271.1	200.8	190.9	302
Middle Drum Wall Peak	180.3	252.4	167.0	160.9	—
Upper Drum Contents Peak	331.2	310.7	258.4	245.0	402
Upper Drum Contents Average	224.9	250.8	194.5	185.7	302
Upper Drum Wall Peak	180.1	251.4	166.9	160.8	—
HDPE Shielding Wall Peak	—	—	158.7	154.3	170
HDPE Shielding Wall Average	—	—	149.7	148.5	150
RLC Shell Peak	159.3	202.2	148.4	147.8	210②
RLC Lid Peak	141.9	161.6	136.0	136.2	212
IV Shell Peak	145.1	158.2	142.3	142.2	160②
IV Base Peak	138.6	152.2	135.0	135.1	160②
IV Upper Forging Peak	137.1	147.1	134.7	134.7	160②
IV Lid Peak	136.1	145.7	133.7	133.8	160②
IV Lid O-ring Seal Peak	136.1	145.7	133.7	133.8	225
IV Lid Ports O-ring Seals Peak	136.1	145.7	133.7	133.8	225
OC Inner Shell Peak	143.8	150.4	142.5	142.5	160②
OC Lead Shield Peak	143.9	150.3	142.6	142.6	160②
OC Outer Shell Peak	144.0	150.4	142.7	142.7	160②
OC Base Peak	136.7	145.7	134.6	134.6	160②
OC Upper Forging Peak	136.7	142.6	135.3	135.3	160②
OC Lid Peak	135.0	141.2	133.5	133.5	160②
OC Lid O-ring Seal Peak	134.9	141.2	133.3	133.4	225
OC Lid Port O-ring Seal Peak	135.0	141.2	133.5	133.5	225
OC Thermal Shield Peak	146.8	151.9	145.7	145.7	185③
OC Main Trunnions Peak	144.0	149.7	142.8	142.7	153②
OC Small Trunnions Peak	144.5	149.7	143.5	143.5	153②
Impact Limiter Foam Peak	157.7	157.7	157.7	157.7	260
Impact Limiter Foam Average	133.5	136.4	132.8	132.8	140②
Impact Limiter Shell Peak	157.7	157.7	157.7	157.7	185③

Notes:

① Allowable temperature limits are discussed in Section 3.3, *Technical Specifications of Components*.

② Allowable temperature limits correspond to temperatures used in the structural evaluations in Chapter 2.0, *Structural Evaluation*.

③ The allowable temperature limit of 185 ºF for external surfaces of the package is based on the maximum accessible surface temperature without insolation for exclusive use shipments per 10 CFR §71.43(g),[1] but is also conservatively being used here.

Table 3.1-2 – Maximum HAC Fire Transient Temperatures (ºF)

Location	RLC		NS15	NS30	Allowable Limit①
	12 lb/ft^3 Payload (90 W)	100 lb/ft^3 Payload (270 W)	12 lb/ft^3 Payload (50 W)	12 lb/ft^3 Payload (50 W)	
Lower Drum Contents Peak	370.4	331.5	286.5	276.9	402
Lower Drum Contents Average	273.1	275.6	223.2	219.3	302
Lower Drum Wall Peak	258.4	280.9	199.3	208.3	—
Middle Drum Contents Peak	381.2	345.3	293.6	284.5	402
Middle Drum Contents Average	287.8	293.7	231.2	229.3	302
Middle Drum Wall Peak	264.8	283.0	201.6	211.8	—
Upper Drum Contents Peak	370.4	330.5	287.5	277.8	402
Upper Drum Contents Average	273.7	274.1	223.9	220.9	302
Upper Drum Wall Peak	264.7	282.5	201.4	211.9	—
HDPE Shielding Wall Peak	—	—	194.9	208.6	256
HDPE Shielding Wall Average	—	—	182.2	195.1	—
RLC Shell Peak	266.9	284.2	227.9	226.7	650/256③
RLC Minimum	149.8	163.2	137.6	145.8	—
RLC Lid Peak	188.9	200.4	170.4	172.1	650/256③
IV Shell Peak	374.6	384.4	372.2	372.2	390②
IV Base Peak	196.1	204.7	186.4	186.9	300②
IV Upper Forging Peak	183.1	190.4	177.0	177.3	300②
IV Lid Peak	179.6	186.7	174.1	174.5	300②
IV Lid O-ring Seal Peak	179.4	186.4	173.7	174.1	360
IV Lid Ports O-ring Seals Peak	179.6	186.7	174.1	174.5	360
OC Inner Shell Peak	542.5	546.8	541.6	541.7	550②
OC Lead Shield Peak	565.7	570.4	564.7	564.8	620
OC Outer Shell Peak	697.9	701.5	697.4	696.9	705②
OC Base Peak	195.3	202.4	192.7	192.7	500②
OC Upper Forging Peak	237.2	242.2	231.4	231.3	500②
OC Lid Peak	192.7	197.5	191.4	191.3	500②
OC Lid O-ring Seal Peak	188.9	193.9	187.3	187.4	360
OC Lid Port O-ring Seal Peak	192.7	197.5	191.4	191.3	360
OC @ Puncture Damage Peak	441.1	448.6	435.8	442.6	500②
OC Thermal Shield Peak	1,322	1,323	1,322	1,322	2,600
OC Main Trunnions Peak	1,068	1,070	1,068	1,068	2,600
OC Small Trunnions Peak	1,094	1,096	1,094	1,094	2,600
Impact Limiter Foam Peak	1,473	1,473	1,473	1,473	—
Impact Limiter Foam Average	—	—	—	—	—
Impact Limiter Shell Peak	1,474	1,474	1,474	1,474	2,600

Notes:

① Allowable temperature limits are discussed in Section 3.3, *Technical Specifications of Components*.

② Allowable temperature limits correspond to temperatures used in the structural evaluations in Chapter 2.0, *Structural Evaluation*.

③ The allowable temperature limit of the RLC components for the NSC configuration is based on the HDPE shield insert temperature limitation of 256 ºF; otherwise, the allowable temperature limit is based on carbon steel.

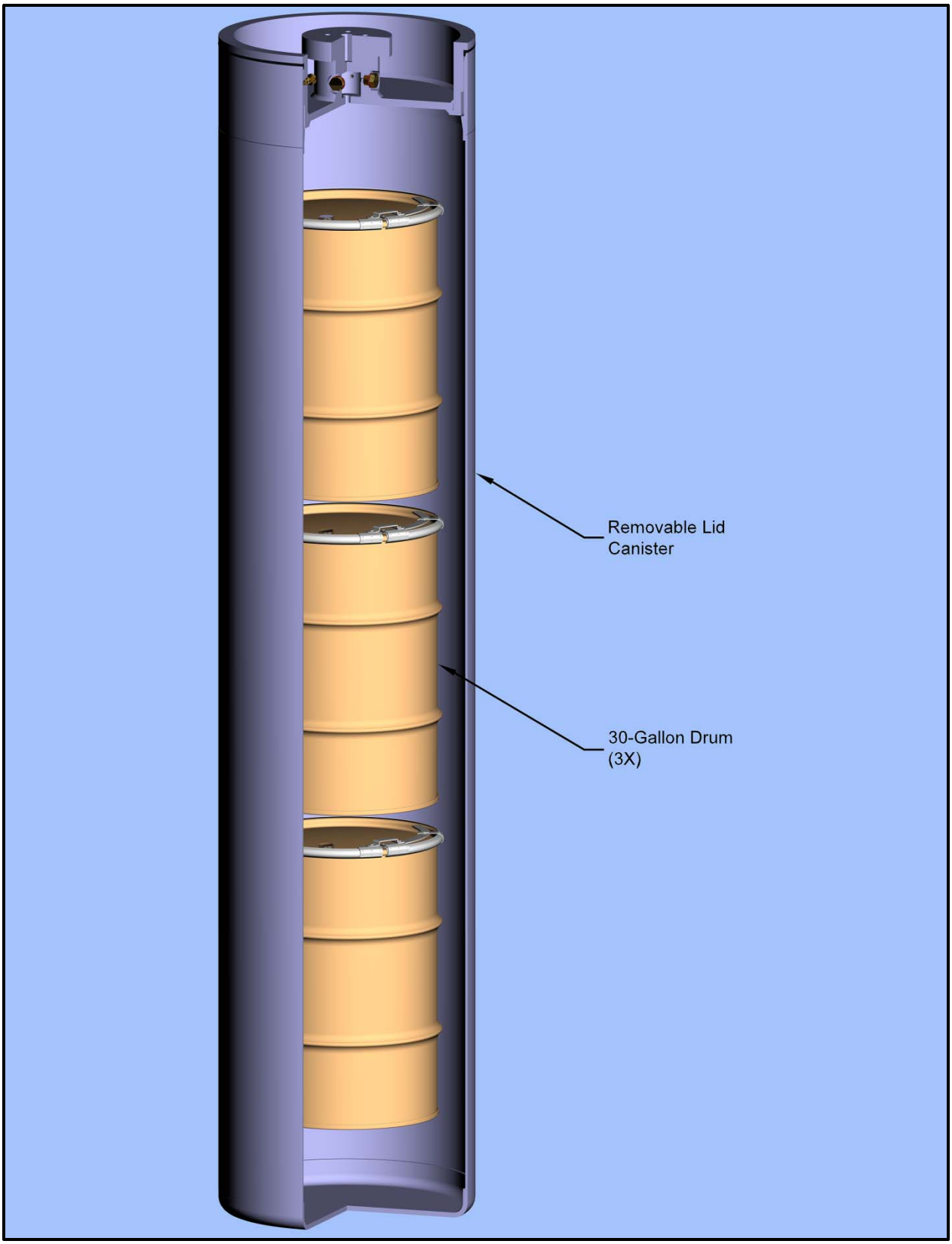

Figure 3.1-1 – RLC with Three, 30-Gallon Drums

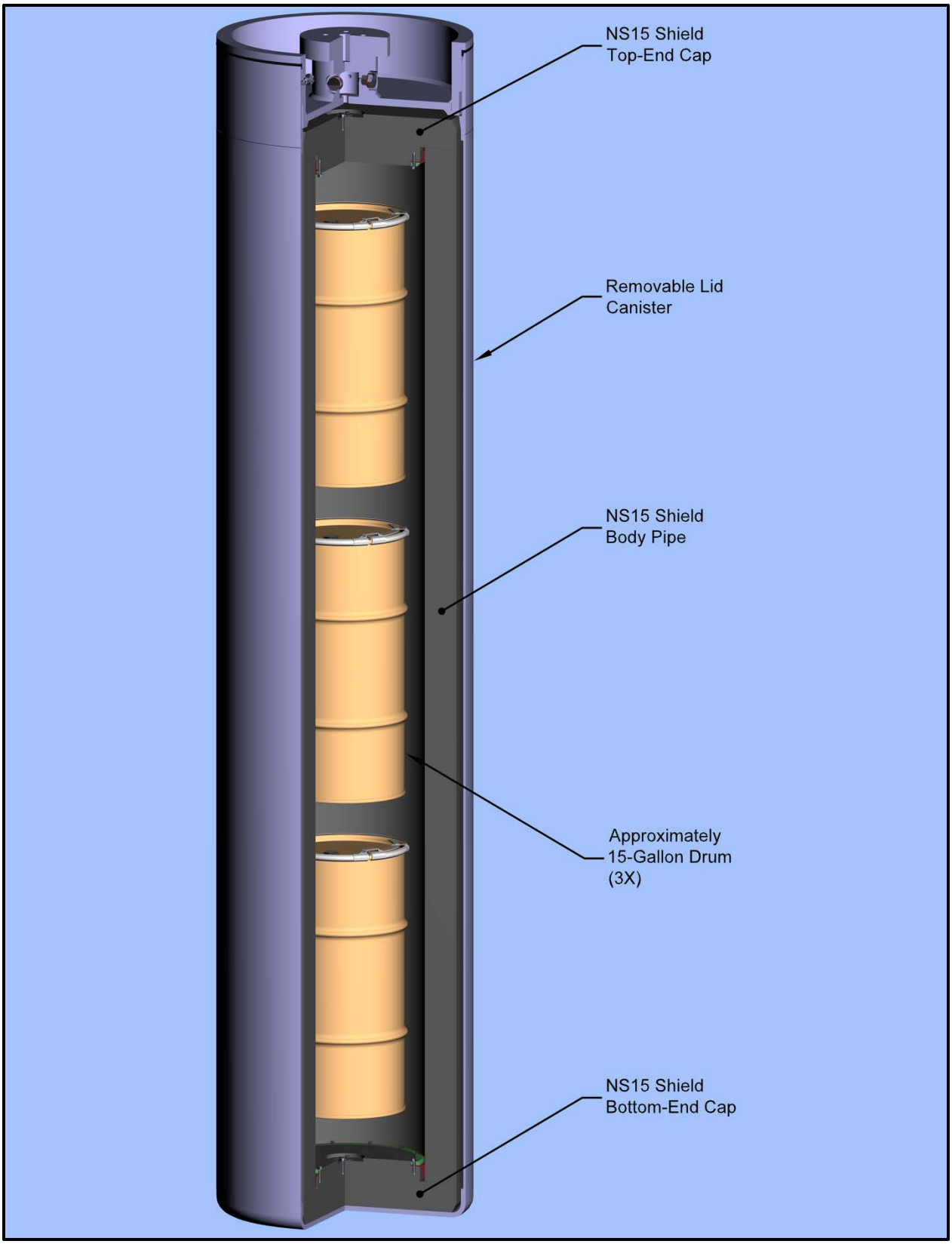

Figure 3.1-2 – NS15 NSC with Three, Approximately 15-Gallon Drums

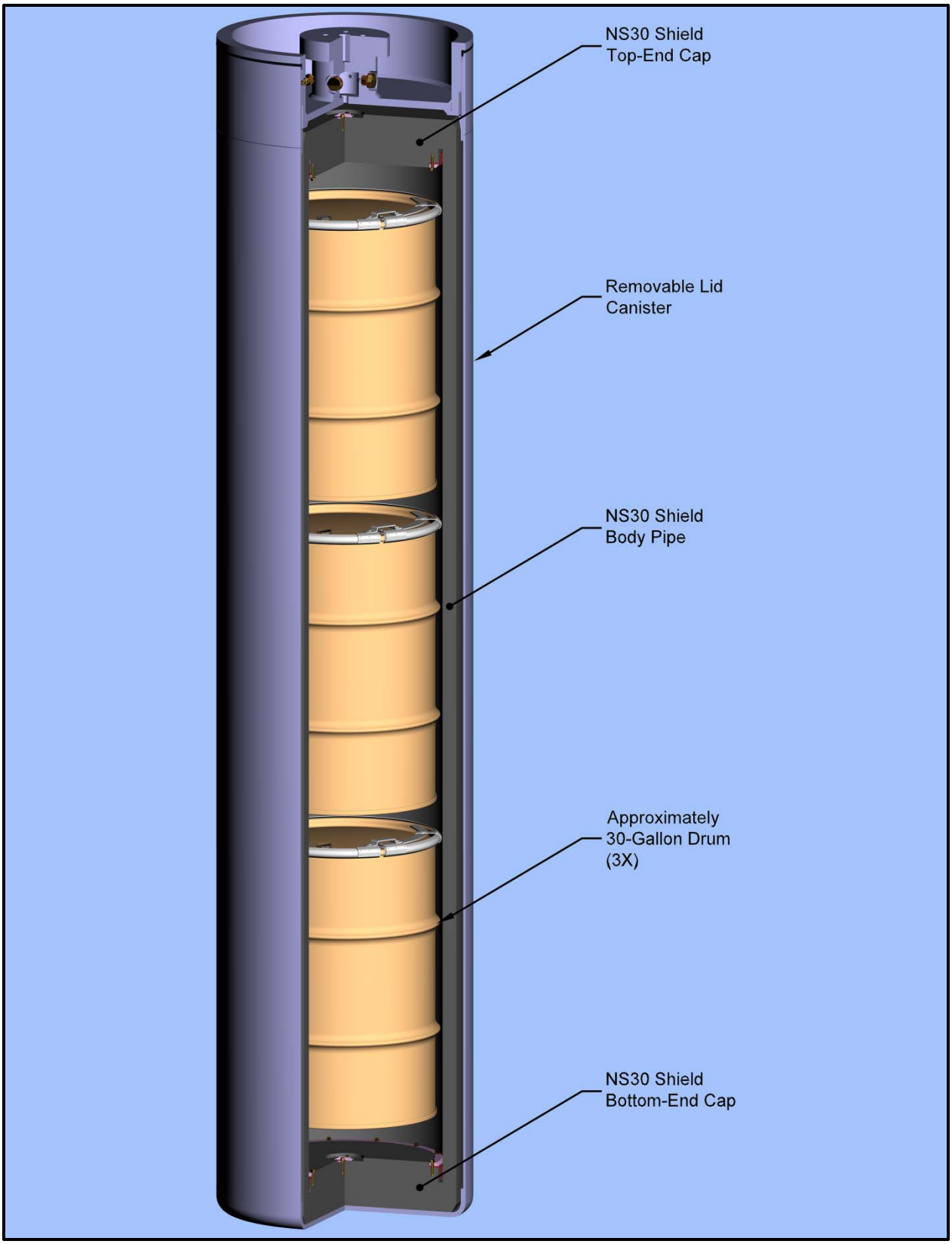

Figure 3.1-3 – NS30 NSC with Three, Approximately 30-Gallon Drums

3.2 Summary of Thermal Properties of Materials

The RH-TRU 72-B packaging is fabricated primarily of Type 304 stainless steel for the IV, OC, and impact limiter structures, lead shielding within the OC sidewall, and polyurethane foam within the impact limiter's shells. The RH-TRU waste canister (fixed and removable lid) may be fabricated of either carbon or stainless steel; the bounding lower conductivity and emissivity properties of stainless steel are conservatively used herein. The inner containers (i.e., the 30-gallon and 55-gallon drums) within an RH-TRU waste canister, if used, are constructed of carbon steel, and painted externally and unpainted internally. Similarly, the approximately 15-gallon and 30-gallon drums used within neutron shielded canisters (NSCs) are constructed of carbon steel, and painted externally and unpainted internally. The NSCs also include a high-density polyethylene (HDPE) neutron shield insert.

Dry air at one atmosphere is assumed to fill the regions between the OC and IV, the IV and RLC, and the RLC and drums. For the NSC payloads, air is assumed to fill the regions between the RLC and the HDPE shield insert, and between the HDPE shield insert and the drums. Air is also included in the radial gap and small axial gap between the OC and inner surfaces of the impact limiters.

The following list of tables present thermophysical properties for the various materials in the package (note that all thermal analyses utilize a density at a temperature of 70 ºF for all materials):

- Table 3.2-1 – Thermophysical Properties of Air at One Atmosphere
- Table 3.2-2 – Thermophysical Properties of Type 304 Stainless Steel
- Table 3.2-3 – Thermophysical Properties of Carbon Steel
- Table 3.2-4 – Thermophysical Properties of ASTM B29 Lead
- Table 3.2-5 – Thermophysical Properties of the Thermal Shield Gap
- Table 3.2-6 – Thermophysical Properties of High-Density Polyethylene (HDPE)
- Table 3.2-7 – Thermophysical Properties of 11½ lb/ft³ Polyurethane Foam
- Table 3.2-8 – Thermophysical Properties of the Payload Material

The calculational methodology used to determine the effective thermophysical properties of the thermal shield gap, as used in Table 3.2-5, is presented in Appendix 3.6.1.1, *Calculation to Determine the Thermophysical Properties of the Thermal Shield Gap*.

The calculational methodology used for determining the effective density of the damaged impact limiter regions due to the HAC side drop, as used in Table 3.2-7 to determine the increased thermal conductivity in those regions for the HAC fire analysis, is presented in Appendix 3.6.1.2, *Calculation to Determine the Effective Density in the Impact Limiter's Damaged Region*. Note that the closed-cell polyurethane foam used in the impact limiters retains its compressive strength and charring characteristics over time. Foam samples aged for twenty years have been tested and the compressive strength, elastic modulus, and charring ability compare favorably with nominal design values.[1]

[1] General Plastics, *Last-a-Foam FR 3700® for Crash and Fire Protection of Nuclear Material Shipping Containers*, General Plastics Manufacturing Company, 4910 Burlington Way, Tacoma, Washington, February 1990.

The payload may consist of organic or inorganic waste of varying decay heat loadings as described in the *Remote-Handled Transuranic Waste Authorized Methods for Payload Control* (RH-TRAMPAC).[2] Analyses utilize the thermal properties of polyurethane foam as a surrogate material to simulate the varied density of the payload material and its effect on allowable decay heat. Further discussion is provided in Table 3.2-8.

Finally, Table 3.2-9 presents the important optical properties for radiative heat transfer, i.e., infrared emissivity (ε) for the interior and exterior radiating surfaces, and solar absorptivity (α) for the exterior package surfaces, both for NCT and HAC. The RLC's optionally painted exterior that results in a significantly higher emissivity to aid in internal heat rejection is conservatively ignored.

[2] U.S. Department of Energy (DOE), *Remote-Handled Transuranic Waste Authorized Methods for Payload Control* (RH-TRAMPAC), U.S. Department of Energy, Carlsbad Field Office, Carlsbad, New Mexico.

Table 3.2-1 – Thermophysical Properties of Air at One Atmosphere

Temperature (ºF)	Density① (lb/in^3)	Thermal Conductivity① (Btu/hr-in-ºF)	Specific Heat① (Btu/lb-ºF)
70	$4.2768(10)^{-5}$	$1.2452(10)^{-3}$	0.2405
100	—	$1.3058(10)^{-3}$	0.2406
150	—	$1.4041(10)^{-3}$	0.2408
200	—	$1.5049(10)^{-3}$	0.2413
250	—	$1.6069(10)^{-3}$	0.2420
300	—	$1.7033(10)^{-3}$	0.2429
350	—	$1.7954(10)^{-3}$	0.2439
400	—	$1.8870(10)^{-3}$	0.2450
450	—	$1.9768(10)^{-3}$	0.2463
500	—	$2.0630(10)^{-3}$	0.2476
550	—	$2.1462(10)^{-3}$	0.2490
600	—	$2.2265(10)^{-3}$	0.2504
650	—	$2.3034(10)^{-3}$	0.2520
700	—	$2.3778(10)^{-3}$	0.2536
750	—	$2.4512(10)^{-3}$	0.2552
800	—	$2.5226(10)^{-3}$	0.2567
850	—	$2.5904(10)^{-3}$	0.2583
900	—	$2.6560(10)^{-3}$	0.2599
950	—	$2.7207(10)^{-3}$	0.2615
1,000	—	$2.7832(10)^{-3}$	0.2631
1,050	—	$2.8444(10)^{-3}$	0.2645
1,100	—	$2.9076(10)^{-3}$	0.2660
1,150	—	$2.9722(10)^{-3}$	0.2675
1,200	—	$3.0343(10)^{-3}$	0.2688
1,250	—	$3.0956(10)^{-3}$	0.2701
1,300	—	$3.1592(10)^{-3}$	0.2715
1,350	—	$3.2241(10)^{-3}$	0.2728
1,400	—	$3.2886(10)^{-3}$	0.2740
1,450	—	$3.3527(10)^{-3}$	0.2752
1,500	—	$3.4167(10)^{-3}$	0.2764

Notes:

① Density, thermal conductivity, and specific heat for 100 K to 3,000 K are taken from Table A.4 of Incropera, DeWitt, Bergman, and Lavine, *Fundamentals of Heat and Mass Transfer*, 6th Edition.

Table 3.2-2 – Thermophysical Properties of Type 304 Stainless Steel

Temperature (ºF)	Density① (lb/in^3)	Thermal Conductivity② (Btu/hr-in-ºF)	Specific Heat② (Btu/lb-ºF)
70	0.2860	0.7167	0.1152
100	—	0.7250	0.1159
150	—	0.7500	0.1185
200	—	0.7750	0.1210
250	—	0.8000	0.1235
300	—	0.8167	0.1247
350	—	0.8417	0.1272
400	—	0.8667	0.1287
450	—	0.8833	0.1298
500	—	0.9083	0.1321
550	—	0.9250	0.1324
600	—	0.9417	0.1335
650	—	0.9667	0.1349
700	—	0.9833	0.1359
750	—	1.0000	0.1362
800	—	1.0250	0.1383
850	—	1.0417	0.1393
900	—	1.0583	0.1394
950	—	1.0750	0.1404
1,000	—	1.0917	0.1406
1,100	—	1.1333	0.1435
1,200	—	1.1667	0.1446
1,300	—	1.2083	0.1467
1,400	—	1.2417	0.1484
1,500	—	1.2750	0.1501

Notes:

① Density at 70 ºF is from Table 2.7.1.0(b) of MIL-HDBK-5J, *Metallic Materials and Elements for Aerospace Vehicle Structures*.

② Specific heat as a function of temperature is determined using $C(T) = TC(T)/[\delta(T)TD(T)]$ from the ASME Boiler and Pressure Vessel Code, Section II – *Materials*, Part D – *Properties*, Subpart 2 – *Physical Properties Tables*, Table TCD, General Note (a). Thermal diffusivity as a function of temperature, TD(T), and thermal conductivity as a function of temperature, TC(T), are from the ASME Boiler and Pressure Vessel Code, Section II – *Materials*, Part D – *Properties (Customary)*, Subpart 2 – *Physical Properties Tables*, Table TCD, Material Group J. Density as a function of temperature is determined using the volumetric change of a 70 ºF unit cube, $\delta(T) = \delta(70)/\{1 + \alpha(T)[T - 70]\}^3$. Thermal expansion coefficients as a function of temperature, $\alpha(T)$, are from ASME Boiler and Pressure Vessel Code, Section II – *Materials*, Part D – *Properties (Customary)*, Subpart 2 – *Physical Properties Tables*, Table TE-1, Material Group 3, Coefficient B, where Coefficient B is the mean coefficient of thermal expansion in going from 70 ºF to the indicated temperature.

Table 3.2-3 – Thermophysical Properties of Carbon Steel

Temperature (ºF)	Density① (lb/in^3)	Thermal Conductivity② (Btu/hr-in-ºF)	Specific Heat② (Btu/lb-ºF)
70	0.2840	2.9083	0.1016
100	—	2.8917	0.1047
150	—	2.8500	0.1089
200	—	2.8083	0.1127
250	—	2.7500	0.1154
300	—	2.6917	0.1181
350	—	2.6333	0.1206
400	—	2.5750	0.1229
450	—	2.5083	0.1249
500	—	2.4500	0.1276
550	—	2.3917	0.1302
600	—	2.3333	0.1333
650	—	2.2750	0.1361
700	—	2.2167	0.1396
750	—	2.1667	0.1435
800	—	2.1083	0.1473
850	—	2.0500	0.1515
900	—	1.9833	0.1555
950	—	1.9250	0.1597
1,000	—	1.8667	0.1650
1,100	—	1.7417	0.1754
1,200	—	1.6167	0.1891
1,300	—	1.4917	0.2102
1,400	—	1.3833	0.4214
1,500	—	1.2917	0.1972

Notes:

① Density at 70 ºF is from Table 2.2.1.0(b) of MIL-HDBK-5J, *Metallic Materials and Elements for Aerospace Vehicle Structures*.

② Specific heat as a function of temperature is determined using $C(T) = TC(T)/[\delta(T)TD(T)]$ from the ASME Boiler and Pressure Vessel Code, Section II – *Materials*, Part D – *Properties*, Subpart 2 – *Physical Properties Tables*, Table TCD, General Note (a). Thermal diffusivity as a function of temperature, TD(T), and thermal conductivity as a function of temperature, TC(T), are from the ASME Boiler and Pressure Vessel Code, Section II – *Materials*, Part D – *Properties (Customary)*, Subpart 2 – *Physical Properties Tables*, Table TCD, Material Group A. Density as a function of temperature is determined using the volumetric change of a 70 ºF unit cube, $\delta(T) = \delta(70)/\{1 + \alpha(T)[T - 70]\}^3$. Thermal expansion coefficients as a function of temperature, $\alpha(T)$, are from ASME Boiler and Pressure Vessel Code, Section II – *Materials*, Part D – *Properties (Customary)*, Subpart 2 – *Physical Properties Tables*, Table TE-1, Material Group 1, Coefficient B, where Coefficient B is the mean coefficient of thermal expansion in going from 70 ºF to the indicated temperature.

Table 3.2-4 – Thermophysical Properties of ASTM B29 Lead

Temperature (ºF)	Density① (lb/in^3)	Thermal Conductivity② (Btu/hr-in-ºF)	Specific Heat③ (Btu/lb-ºF)
70	0.4095	1.6979	0.0308
100	—	1.6891	0.0309
150	—	1.6733	0.0311
200	—	1.6538	0.0313
250	—	1.6318	0.0315
300	—	1.6118	0.0317
350	—	1.5942	0.0320
400	—	1.5779	0.0323
450	—	1.5617	0.0327
500	—	1.5448	0.0330
550	—	1.5273	0.0334
600	—	1.5095	0.0338
620.33④	—	1.5023	0.0339

Notes:

① Density at 70 ºF is 11,340 kg/m^3 (0.4095 lb/in^3) at 300 K (67.73 ºF; assume 70 ºF) is from Table A.1 of Incropera, DeWitt, Bergman, and Lavine, *Fundamentals of Heat and Mass Transfer*, 6th Edition.

② Thermal conductivity is taken Figure No. 26R and Table No. 26R of Touloukian, Y.S., Powell, R.W., Ho, C.Y., and Klemens, P.C., *Thermophysical Properties of Matter*, Volume 1, *Thermal Conductivity – Metallic Elements and Alloys*, 1970.

③ Specific heat from 100 K to 600 K is taken from Table A.1 of Incropera, DeWitt, Bergman, and Lavine, *Fundamentals of Heat and Mass Transfer*, 6th Edition.

④ Melting point of lead.

Table 3.2-5 – Thermophysical Properties of the Thermal Shield Gap

Temperature (ºF)	Density① (lb/in^3)	Thermal Conductivity① (Btu/hr-in-ºF)	Specific Heat① (Btu/lb-ºF)
70	$8.2329(10)^{-3}$	$3.5080(10)^{-3}$	0.1159
100	—	$3.6337(10)^{-3}$	0.1165
150	—	$3.8559(10)^{-3}$	0.1190
200	—	$4.0819(10)^{-3}$	0.1215
250	—	$4.3092(10)^{-3}$	0.1240
300	—	$4.5104(10)^{-3}$	0.1251
350	—	$4.7186(10)^{-3}$	0.1275
400	—	$4.9257(10)^{-3}$	0.1291
450	—	$5.1135(10)^{-3}$	0.1302
500	—	$5.3105(10)^{-3}$	0.1325
550	—	$5.4860(10)^{-3}$	0.1327
600	—	$5.6563(10)^{-3}$	0.1338
650	—	$5.8369(10)^{-3}$	0.1352
700	—	$5.9966(10)^{-3}$	0.1362
750	—	$6.1544(10)^{-3}$	0.1364
800	—	$6.3253(10)^{-3}$	0.1385
850	—	$6.4735(10)^{-3}$	0.1395
900	—	$6.6179(10)^{-3}$	0.1397
950	—	$6.7606(10)^{-3}$	0.1406
1,000	—	$6.8996(10)^{-3}$	0.1408
1,100	—	$7.1935(10)^{-3}$	0.1437
1,200	—	$7.4738(10)^{-3}$	0.1448
1,300	—	$7.7685(10)^{-3}$	0.1469
1,400	—	$8.0532(10)^{-3}$	0.1486
1,500	—	$8.3355(10)^{-3}$	0.1503

Notes:

① See Appendix 3.6.1.1, *Calculation to Determine the Thermophysical Properties of the Thermal Shield Gap*, for determination of the thermophysical properties.

Table 3.2-6 – Thermophysical Properties of High-Density Polyethylene (HDPE)

Temperature (ºF)	Density① (lb/in^3)	Thermal Conductivity① (Btu/hr-in-ºF)	Specific Heat① (Btu/lb-ºF)
70	$3.4667(10)^{-2}$	$1.6363(10)^{-2}$	0.4133
100	—	$1.6475(10)^{-2}$	0.4445
150	—	$1.6663(10)^{-2}$	0.5107
200	—	$1.6667(10)^{-2}$	0.5761
250	—	$1.6667(10)^{-2}$	0.9772

Notes:

① Density, thermal conductivity, and specific heat are from Chapter 3 of *Handbook of Polyethylene Pipe*, 2nd Edition, Plastic Pipe Institute, Irving, TX.

Table 3.2-7 – Thermophysical Properties of 11½ lb/ft³ Polyurethane Foam

Region①	Density① (lb/ft^3)	Density① (lb/in^3)	Thermal Conductivity② (Btu/hr-in-ºF)	Specific Heat② (Btu/lb-ºF)
Undamaged	11½	$6.6551(10)^{-3}$	$1.6415(10)^{-3}$	0.3530
Compressed & Unbacked	20	$1.1574(10)^{-2}$	$2.4236(10)^{-3}$	
Compressed & Backed	30	$1.7361(10)^{-2}$	$3.3194(10)^{-3}$	

Notes:

① Thermal conductivity in the compressed regions is determined based on the effective density increase from Appendix 3.6.1.2, *Calculation to Determine the Effective Density in the Impact Limiter's Damaged Region*.

② Thermal conductivity and specific heat are from Table 3 of *Design Guide for Use of LAST-A-FOAM® FR-3700 for Crash & Fire Protection of Radioactive Material Shipping Containers*, Revision 02-20-2012, and Technical Data Sheet for 30 lb/ft³ *LAST-A-FOAM® FR-3700*, Revision 04-07-2004, General Plastics Manufacturing Company, Tacoma, WA.

Table 3.2-8 – Thermophysical Properties of the Payload Material

Density①		Thermal Conductivity①②	Specific Heat②
(lb/ft^3)	(lb/in^3)	(Btu/hr-in-ºF)	(Btu/lb-ºF)
≤12	$\leq 6.9444(10)^{-3}$	$1.7083(10)^{-3}$	
23	$1.3310(10)^{-2}$	$2.6924(10)^{-3}$	
34	$1.9676(10)^{-2}$	$3.6738(10)^{-3}$	
45	$2.6042(10)^{-2}$	$4.6571(10)^{-3}$	
56	$3.2407(10)^{-2}$	$5.6389(10)^{-3}$	0.3530
67	$3.8773(10)^{-2}$	$6.6208(10)^{-3}$	
78	$4.5139(10)^{-2}$	$7.6027(10)^{-3}$	
89	$5.1505(10)^{-2}$	$8.5845(10)^{-3}$	
≥100	$\geq 5.7870(10)^{-2}$	$9.5664(10)^{-3}$	

Notes:

① Polyurethane foam is ideal as a surrogate payload material because of uniformly distributed gas-filled cells in a relatively low conductivity polymer matrix. The thermal conductivity for 12 lb/ft³ polyurethane foam of $1.7083(10)^{-3}$ Btu/hr-in-ºF (0.0205 Btu/hr-ft-ºF) is essentially identical to the Sandia derived lower-bound thermal conductivity of 0.02 Btu/hr-ft-ºF based on testing of randomly filled, loose-packed drums of paper wipes (6.30 lb/ft³ effective density), disposable paper/plastic clothing (4.85 lb/ft³ effective density), and plastic sheeting (6.73 lb/ft³ effective density), with measured lower-bound thermal conductivity values for the three waste forms of 0.04 W/m-K (0.023 Btu/hr-ft-ºF), 0.06 W/m-K (0.034 Btu/hr-ft-ºF), and 0.05W/m-K (0.027 Btu/hr-ft-ºF), respectively.[3] These three typical low-density waste forms all exhibit thermal conductivity values that exceed the value for 12 lb/ft³ polyurethane foam used herein thereby demonstrating that radiation heat transfer between surfaces within "real world" waste forms is still significant. The thermal conductivity for low-density payloads up to 12 lb/ft³ may therefore be represented by 12 lb/ft³ polyurethane foam since it exhibits a thermal conductivity less than the tested waste forms. High-density payloads equal to or greater than 100 lb/ft³ may be represented by the use of a 100 lb/ft³ payload density since a higher density material will have a higher thermal conductivity and correspondingly result in lower payload temperatures. For intermediate densities between 12 and 100 lb/ft³, use of the conductivity of polyurethane foam is also appropriate since over this range it is representative of the lowest conductivity materials in existence.

② Thermal conductivity and specific heat are from Table 3 of *Design Guide for Use of LAST-A-FOAM® FR-3700 for Crash & Fire Protection of Radioactive Material Shipping Containers*, Revision 02-20-2012, and Technical Data Sheets for 12, 15, 18, 20, 25, 30, and 40 lb/ft³ *LAST-A-FOAM® FR-3700*, Revision 04-07-2004, from General Plastics Manufacturing Company, Tacoma, WA. Because thermal conductivity for polyurethane foam is found to be directly proportional to density between 12 and 40 lb/ft³, thermal conductivity for densities above 40 lb/ft³ are linearly extrapolated. Similar to the General Plastics data, other polyurethane foam test data[4] demonstrates a linear relationship between thermal conductivity and density.

[3] Letter from M. M. Warrant, Sandia National Laboratories, to C. Ozaki, Westinghouse, *Effective Conductivity of Waste Forms*, March 4, 1988; the letter references a memo from J. Moya, D. Schulze, and R. Acton, Sandia National Laboratories, to J. M. Freedman, Sandia National Laboratories, *Effective Thermal Conductivity of Waste Forms* (R804877), February 26, 1988, Sandia National Laboratories, Albuquerque, NM.

[4] Rudolf Boetes, *Heat Transfer Reduction in Closed Cell Polyurethane Foams*, Ph.D. Thesis Technische Hogeschool, Delft (Netherlands), TR diss 1498; Figure 7.3.

Table 3.2-9 – Optical Properties of Package Materials

Material	Emissivity (ε)	Absorptivity (α)	Reference Notes
NCT and HAC Pre-Fire Optical Properties			
Type 304 Stainless Steel (Interior Surfaces)	0.25	—	①, ②
Type 304 Stainless Steel (Exterior Surfaces)	0.25	0.50	①, ②
Carbon Steel (Bare)	0.50	—	③
Carbon Steel (Painted)	0.90	—	④
High-Density Polyethylene (Black)	0.92	—	⑤
Polyurethane Foam Cavity Surfaces	0.99	—	⑥
HAC Fire Optical Properties			
Type 304 Stainless Steel (Exterior Surfaces)	0.80	—	⑦
Fire Environment	0.90	—	⑦
HAC Post-Fire Optical Properties			
Type 304 Stainless Steel (Exterior Surfaces)	0.62	0.87	⑧

Notes:

① W. D. Wood, H. W. Deem, and C. F. Lucks, *Thermal Radiation Properties of Selected Materials*, Volume I, DMIC Report 177; normal total emmittance and total solar absorptance for Type 301 stainless steel for the clean-and-smooth surface condition (p56 and p58, respectively).

② *Emissivity of Metal Surfaces*, Report No. 2-2623-2-RF-C86-349, August 21, 1986; lower-bound emissivity data for the average of three specimens from three sets of ASTM A240, Type 304, stainless steel samples.

③ *Emissivity of Metal Surfaces*, Report No. 2-2623-2-RF-C86-349, August 21, 1986; emissivity data for the average of three specimens for commercially sandblasted and white metal blasted ASTM A516, Grade 70, carbon steel (these conditions reasonably represent clean carbon steel).

④ Omega Engineering, Inc., Technical Reference Section, *Table of Total Emissivity*; minimum emissivity for paints at 75 ºF.

⑤ Electro Optical Industries, Inc., *Emissivity of Materials*; emissivity for black polyethylene plastic.

⑥ The assumed upper-bound emissivity of impact limiter foam cavity surfaces, both plastic and metallic, based on flat-black char.

⑦ Emissivity per 10 CFR §71.73(c)(4).

⑧ W. D. Wood, H. W. Deem, and C. F. Lucks, *Thermal Radiation Properties of Selected Materials*, Volume I, DMIC Report 177; normal total emmittance and total solar absorptance for Type 301 stainless steel for the clean-and-smooth surface condition after heating to 1,475 ºF and cooling to 100 ºF (p56 and p58, respectively).

3.3 Technical Specifications of Components

3.3.1 Packaging Components

The materials used for the RH-TRU 72-B packaging that are considered temperature sensitive are the butyl rubber used for the O-ring seals and polyurethane foam used in the impact limiters.

The butyl rubber O-ring seal material is Rainier Rubber compound R0405-70,[1] or equivalent, per Appendix 3.6.4, *Containment O-ring Seal Material Tests*. With reference to Appendix 3.6.4, the butyl rubber O-ring seals have an allowable short duration (8-hour) temperature limit of 360 ºF. The allowable long-term temperature range of -40 ºF to 225 ºF is conservatively bounded by data in Figure 2-25 of the Parker O-ring Handbook[2] for butyl rubber and by Rainier Rubber Company for butyl rubber compound R0405-70.

The minimum operational temperature of polyurethane foam is -20 ºF since this is the lowest initial temperature at which the packaging must perform. Polyurethane foam has an operating temperature range of -20 ºF to 260 ºF during impact loadings.[3] In addition, temperature excursions to -40 ºF for the polyurethane foam will not permanently degrade its properties. Polyurethane foam performance under hypothetical accident condition (HAC) transient conditions is discussed in Section 3.5.2, *Package Conditions and Environment*, and polyurethane foam strength sensitivity to temperature is addressed in Chapter 2.0, *Structural Evaluation*.

Other package materials are stainless steel and lead. The melting points for these materials are approximately 2,600 ºF and 620 ºF, respectively.

In compliance with the ASME Boiler and Pressure Vessel Code,[4] the allowable temperature for stainless steel under NCT conditions is limited to 800 ºF if the component serves a structural purpose (e.g., the IV shell, the OC inner and outer shell, lid, and trunnions).

3.3.2 Payload Canister Components

The materials used for the RH-TRU 72-B payload canister components that are considered temperature sensitive are the removable lid canister (RLC) filter vents and the high-density polyethylene (HDPE) shielding inserts in the neutron shielded canisters (NSC).

The RLC filter vent is limited to a temperature of 100 ºC (212 ºF) per Section 2.4 of the *Remote-Handled Transuranic Waste Authorized Methods for Payload Control* (RH-TRAMPAC).[5]

---

[1] Rainier Rubber Company, *Company Standard Compounds*, Seattle, WA (Rainier Rubber Company).

[2] ORD 5700, *Parker O-ring Handbook*, Parker Hannifin Corporation, Cleveland, OH, 2007 (Parker O-ring Handbook - ORD 5700).

[3] *Design Guide – LAST-A-FOAM® FR-3700 – Crash & Fire Protection of Radioactive Material Shipping Containers*, General Plastics Manufacturing Company, Tacoma, WA, Rev. 02.20.12 (General Plastics Design Guide).

[4] American Society of Mechanical Engineers (ASME) Boiler and Pressure Vessel Code, Section III, *Rules for Construction of Nuclear Facility Components*, Division 1, Subsection NB, *Class 1 Components*, Subsection NG, *Core Support Structures*, and Section II, *Materials*, Part D, *Properties (Customary)*, Subpart 1, *Stress Tables*, 2010.

[5] U.S. Department of Energy (DOE), *Remote-Handled Transuranic Waste Authorized Methods for Payload Control* (RH-TRAMPAC), U.S. Department of Energy, Carlsbad Field Office, Carlsbad, New Mexico.

Full-scale drop HAC testing was performed for the NSC with the HDPE neutron shielding at a temperature of at least 150 ºF and with a test configuration that produced a 204*g* side-oriented impact acceleration[6] compared to the applicable HAC hot side drop acceleration of 68.9*g* per Table 2.10.3-9 and Table 2.10.3-10 from Appendix 2.10.3, *Drop Impact Evaluation Results*; thus the acceleration margin based on testing is 204/68.9 = 3.0. HDPE pipe exhibits a temperature reduction factor of 1.00 at 73 ºF and 0.50 at 140 ºF;[7] the linearized temperature reduction factor is 0.43 at 150 ºF and 0.28 at 170 ºF, resulting in a strength reduction factor of 0.43/0.28 = 1.5 had testing been performed at 170 ºF. Since the tested acceleration margin of 3.0 exceeds the strength reduction factor of 1.5, a peak temperature of 170 ºF in the HDPE shield inserts is acceptable. Therefore, for consistency with conditions used for HAC free drop testing, the NCT temperature limits for HDPE are taken as an average sidewall temperature of 150 ºF and a maximum peak sidewall temperature of 170 ºF. HDPE pipe has a Vicat softening temperature of 256 ºF;[8] this defines the HAC temperature limit for the NS15 and NS30 HDPE shielding inserts.

The primary payload canister material is carbon or stainless steel. Conservatively assuming carbon steel, the allowable temperature under NCT conditions is limited to 650 ºF based on the ASME Boiler and Pressure Vessel Code.[4] Carbon steel has a melting temperature of approximately 2,750 ºF, and stainless steel has a melting temperature of approximately 2,600 ºF.

3.3.3 Payload Material

As discussed in Appendix 4.6 of the *RH-TRU Payload Appendices*,[9] the generation of gas due to thermal decomposition of worst-case, organically-based waste materials does not occur at temperatures below 302 ºF (150 ºC), and gas generation due to thermal degradation of materials is negligible even at much higher temperatures (up to 100 ºF) above the threshold decomposition temperature of 302 ºF. Therefore, the allowable average payload temperature is conservatively taken as 302 ºF, and the allowable peak payload temperature is conservatively taken as 402 ºF, both for NCT and HAC.

[6] Engineering Report 7953-R-027, *30-foot Free Drop Post-Test Summary Report for the NS30 Neutron Shielded Canister*, Rev. 0, Petersen Incorporated, November 2009.

[7] *Design and Engineering Guide for Polyethylene Piping*, PolyPipe, Inc., Gainsville, TX, Rev. 05/05; Figure A-2.

[8] Performance Pipe DriscoPlex 5300 Series PE3608/(PE3408), *Geothermal Systems Data Sheet*, Bulletin PP102, Chevron Phillips Chemical Company, Plano, TX, September 2006.

[9] U.S. Department of Energy (DOE), *RH-TRU Payload Appendices*, U.S. Department of Energy, Carlsbad Field Office, Carlsbad, New Mexico.

3.4 Thermal Evaluation for Normal Conditions of Transport

This section presents the thermal analyses of the RH-TRU 72-B package for normal conditions of transport (NCT). The thermal conditions considered are those specified in 10 CFR §71.71.[1] Per 10 CFR §71.71(c)(1), a 100 ºF ambient temperature with insolation values per Table 3.4-1 are used for heat input to the exterior package surfaces.

3.4.1 Thermal Model

3.4.1.1 Analytical Model

The analysis models were constructed and evaluated using Cullimore and Ring Technologies' Thermal Desktop with RadCAD, Version 5.6, and SINDA/FLUINT, Version 5.6.[2] RadCAD allows radiation heat transfer analysis using one of two methods: progressive radiosity or Monte Carlo ray-tracing. Monte Carlo ray-tracing was used for its superior accuracy due to the relative complexity of the packaging configuration in the regions where radiation exchange occurs.

For a removable lid canister (RLC) with drums, radiation exchange occurs for six distinct regions: 1) within the gap between the 30-gallon drums and the RLC, 2) within the gap between the RLC and inner vessel (IV), 3) within the gap between the IV and outer cask (OC), 4) within the gap between the OC and the thermal shield, and 5) within the radial gap and small axial gap between the OC and the impact limiters, and 6) from external outer cask and impact limiter surfaces to ambient. For a neutron shielded canister (NSC) that includes a high-density polyethylene (HDPE) shield insert within the RLC, radiation exchange occurs in two distinct sub-regions: 1a) between the drums and the HDPE shield insert, and 1b) between the HDPE shield insert and the RLC.

All empty spaces within the package are assumed to be filled with dry air at one atmosphere pressure. Both radial and axial contactors are used to generate the air conductors between surfaces. Unless otherwise specified, all bodies are assumed to be radially and axially centered. Appendix 3.6.2, *Sensitivity Studies*, addresses the effects that shifting components axially and radially has on maximum component temperatures. As discussed in Appendix 3.6.2.4, *Effect of Internal Convection Heat Transfer*, the impact of internal convection between components is negligible.

To encompass the greatest amount of analysis flexibility, the thermal models are three-dimensional, half-symmetry (180º) representations of the package system, as shown in Figure 3.4-1. The global coordinate system axis is located at the center of the OC base with the x-axis radially along the axis of symmetry, the y-axis normal to the axis of symmetry, and the z-axis aligned with the package's axial centerline. A reflective planar surface is defined at the symmetry face to properly model radiation exchange in regions bisected by the symmetry plane.

---

[1] Title 10, Code of Federal Regulations, Part 71 (10 CFR 71), *Packaging and Transportation of Radioactive Material*, 01-01-14 Edition.

[2] Thermal Desktop with RadCAD, *CAD Based Thermal Analysis and Design*, Version 5.6, and SINDA/FLUINT, *General Purpose Thermal/Fluid Network Analyzer*, Version 5.6, Cullimore and Ring Technologies, Inc., Boulder, CO.

As presented in Section 3.2, *Summary of Thermal Properties of Materials*, temperature-dependent values for thermal conductivity and specific heat are used whenever data is available, and optical properties are assumed to be constant with varying temperature.

As discussed in Table 3.2-8 in Section 3.2, *Summary of Thermal Properties of Materials*, the thermal properties (i.e., conductivity and specific heat) of polyurethane foam are used as a surrogate for the payload material. For each thermal run, the payload canister decay heat load is uniformly distributed within the three drums inside an RLC or NSC, as applicable.

Payload models with payload densities of 12 lb/ft^3 and 100 lb/ft^3 represent the bounding conditions for the RH-TRU waste canister, and a payload density of 12 lb/ft^3 is used for the NS15 and NS30 NSC payloads. Allowable decay heat for a low-density payload (≤12 lb/ft^3) is generally limited by satisfaction of HAC thermal decomposition temperature limits whereas the allowable decay heat for a high-density payload (≥100 lb/ft^3) is limited by a consideration of NCT temperatures of packaging components. For NSCs, satisfaction of NCT temperature limits for the HDPE shield inserts is what limits decay heat to 50 watts, and is independent of payload density (i.e., higher density payloads do not increase temperatures for the HDPE shield inserts).

3.4.1.1.1 Packaging Model

3.4.1.1.1.1 Outer Cask (OC) Model

With reference to Figure 3.4-2, the OC is modeled primarily of finite difference (FD) solid elements, with finite elements (FE) only used to transition between the trunnions and the cylindrical OC outer shell. With the exception of the lead shell, the entire OC assembly is stainless steel. The lead shell is assumed to be in direct contact at its inner and outer surfaces, both radially and axially.

The thermal shield is directly connected at each end of the OC body and around the periphery of each trunnion penetration. Both radiation and conduction heat transfer are used within the 12-gauge (0.1094-inch thick) gap between the inside of the cylindrical 10-gauge (0.1406-inch thick) thermal shield and the outside of the outer OC cylindrical shell. The effective conductivity of the thermal shield gap is a composite of air and stainless steel wire, as discussed in Table 3.2-5 from Section 3.2, *Summary of Thermal Properties of Materials*.

Because the upper forging and lid are in close proximity to one another, these components are modeled as a single, monolithic structure, and the OC O-ring seal region and the lid-to-forging contact surface are, therefore, not explicitly modeled. The OC O-ring seal temperature is determined using nodes positioned near the geometric location of the actual O-ring sealing region.

A total of 602 FD solids and 322 FE solids are used to represent the OC thermal model, with entity connectivity accomplished via 7,554 nodes.

3.4.1.1.1.2 Inner Vessel (IV) Model

With reference to Figure 3.4-3, the IV is modeled entirely of FD surface and solid elements. The entire IV assembly is stainless steel.

Since the thermal gradient across the 3/8-inch thick cylindrical sidewall is not important, this component is modeled using FD surfaces. The IV base, upper forging, lid, and center region of the IV spacers use FD solid elements. Radiation and air conduction heat transfer within the two small annular voids under each of the two IV spacers is ignored due to their negligible impact on resulting temperatures.

Because the upper forging and lid are in close proximity to one another, these components are modeled as a single, monolithic structure and the IV O-ring seal region and the lid-to-forging contact surface are, therefore, not explicitly modeled. The IV O-ring seal temperature is determined using nodes positioned near the geometric location of the actual O-ring sealing region.

Both radiation and air conduction are used to transfer heat across the 3/16-inch radial gap between the IV cylindrical shell and the inside surface of the OC inner cylindrical shell. Similarly, both radiation and air conduction are used to transfer heat across the 3/8-inch axial gaps between the outside surface of the IV base and the inside surface of the OC base, and between the outside surface of the IV lid and the inside surface of the OC lid.

A total of 11 FD surfaces and 11 FD solids are used to represent the IV thermal model, with entity connectivity accomplished via 1,060 nodes.

3.4.1.1.1.3 Impact Limiter Model

With reference to Figure 3.4-4, the impact limiters are modeled entirely of FE solids and surfaces. With the exception of polyurethane foam filling the entire cavity, the entire structure is stainless steel.

Since the thermal gradient across the impact limiter shell structures is not important, these components are modeled using a feature of Thermal Desktop that allows the free faces of FE solids to be surface coated with planar elements. These planar elements share the same nodes as the underlying FE solids and are defined by material, thickness, and optical properties for radiation heat transfer, and may also include surface heat loads and convection heat transfer parameters.

The 3¼-inch outside diameter bolt tubes are modeled explicitly, and include 3½-inch high solid elements adjacent to the base plates to represent each bolting interface and attachment bolt. With reference to Figure 3.4-5, the relatively stiff bolting interface (shown in red) is assumed to be in direct steel-to-steel contact with each end of the OC lid and base via a 2-inch wide annular area. Heat transfer from/to the remaining impact limiter base plate surface utilizes radiation and air conduction across an assumed axial air gap of 0.01 inches to account for imperfect flatness of the impact limiter base plate and the OC ends (i.e., base plate and lid). Similarly, radiation and air conduction is assumed across the 9/32-inch radial gap between the outside cylindrical surface of the OC and inside cylindrical surface of the impact limiters.

A total of 2,720 FE planar surfaces and 4,800 FE solids are used to thermally model both impact limiters, with entity connectivity accomplished via 5,944 nodes.

3.4.1.1.2 Payload Models

With reference to Figure 3.4-6, Figure 3.4-7, and Figure 3.4-8, a removable lid canister (RLC) is used as the thermal model for the RH-TRU waste canister, the NS15, and the NS30. For completeness, the lifting pintle is included. The RLC is modeled as a 26-inch outside diameter, 1/4-inch minimum thickness cylinder with a 1/4-inch minimum thickness flat base and flat lid plate; the corresponding internal cavity has a 25½-inch inside diameter and 113-inch length.

Because of its lower thermal conductivity and lower emissivity, stainless steel is conservatively assumed for the RLC material of construction.

Since the thermal gradients across the 1/4-inch thick flat base, cylindrical sidewall, and flat lid plate are not important, these components are modeled using FD surfaces. The upper flange and pintle are modeled using FD solid elements.

Both radiation and air conduction are used to transfer heat across the 2⅝-inch radial gap between the RLC cylindrical shell and the IV cylindrical shell, and across the approximately 1½-inch average radial gap between the RLC cylindrical shell and the two IV spacer rings. Similarly, both radiation and air conduction are used to transfer heat across the 3/4-inch axial gap between the RLC base and the inside surface of the IV base, across the 8¼-inch axial gap between the RLC lid plate and the inside surface of the IV lid, across the 2-inch axial gap between the RLC pintle cap and the inside surface of the IV lid, and across the 3/4-inch axial gap between the RLC flange top and the inside surface of the IV lid.

A total of 3 FD surfaces and 6 FD solids are used to represent the RLC thermal model, with entity connectivity accomplished via 383 nodes.

Three payload cases are evaluated, as summarized in the following subsections:

- **Case 1:** RLC with three, 30-gallon drums loaded with varying density waste, i.e., low- to high-density (12 lb/ft^3 to 100 lb/ft^3) waste; two evaluations are made for the 12 lb/ft^3 and 100 lb/ft^3 waste densities.
- **Case 2:** NSC with an NS15 shield insert and three, approximately 15-gallon drums loaded with low-density (12 lb/ft^3) waste.
- **Case 3:** NSC with an NS30 shield insert and three, approximately 30-gallon drums loaded with low-density (12 lb/ft^3) waste.

3.4.1.1.2.1 RLC Model with a 30-Gallon Drum Payload

With reference to Figure 3.4-6, the three, 30-gallon drums are modeled as simple cylinders with an 18¼-inch diameter and 26¾-inch height. A 2-inch axial spacing between drums is used to account for the rolled top and bottom ends. Since the thermal gradients across the 18-gauge (0.0478-inch thick) cylindrical shell and flat ends are not important, the drums are modeled using FD surfaces. The three drums are assumed to be completely filled with waste modeled using FD solids.

Both radiation and air conduction are used to transfer heat across the 3⅝-inch radial gap between the 30-gallon drum sidewalls and the RLC's cylindrical shell. Similarly, both radiation and air conduction are used to transfer heat across the 2-inch axial gap between drum ends and across

the 14⅜-inch axial gap between the first and third drum ends and the inside surface of the RLC base and lid, respectively.

A total of 9 FD surfaces and 3 FD solids are used to represent the three, 30-gallon drum thermal models, with entity connectivity accomplished via 783 nodes.

3.4.1.1.2.2 NSC Model with an NS15 Shield Insert and an Approximately 15-Gallon Drum Payload

With reference to Figure 3.4-7, the NS15 shield insert is modeled as a 24-inch outside diameter, 3.387-inch nominal thickness cylindrical pipe with 5-inch thick flat ends; the corresponding internal cavity has a 17.226-inch inside diameter and 102-inch length.

The three, approximately 15-gallon drums are modeled as simple cylinders with a 14-inch diameter and 25¾-inch height. A 1½-inch axial spacing between drums is used to account for the rolled top and bottom ends. Since the thermal gradients across the 20-gauge (0.0359-inch thick) cylindrical shell and flat ends are not important, the drums are modeled using FD surfaces. The three drums are assumed to be completely filled with waste modeled using FD solids.

Both radiation and air conduction are used to transfer heat across the 1.613-inch radial gap between the cylindrical drum sidewalls and the inside surface of the NS15 shield insert's cylindrical shell. Similarly, both radiation and air conduction are used to transfer heat across the 1½-inch axial gap between the drum ends, and across the 10⅞-inch axial gap between the first and third drum ends and the inside surface of the NS15 shield insert base and lid, respectively. Finally, both radiation and air conduction are used to transfer heat across the 3/4-inch radial gap between the NS15 shield's cylindrical sidewall and the RLC's cylindrical shell, and across the 1/2-inch axial gap between the NS15 shield's ends and the surface of the RLC base and lid.

A total of 9 FD surfaces and 8 FD solids are used to represent the NS15 shield insert thermal model and three approximately 15-gallon drum thermal models, with entity connectivity accomplished via 1,447 nodes.

3.4.1.1.2.3 NSC Model with an NS30 Shield Insert and an Approximately 30-Gallon Drum Payload

With reference to Figure 3.4-8, the NS30 shield insert is modeled as a 24-inch outside diameter, 1.454-inch nominal thickness cylindrical pipe with 5-inch thick flat ends; the corresponding internal cavity has a 21.092-inch inside diameter and 102-inch length.

The three, approximately 30-gallon drums are modeled as simple cylinders with an 18¼-inch diameter and 26¾-inch height. A 2-inch axial spacing between drums is used to account for the rolled top and bottom ends. Since the thermal gradients across the 18-gauge (0.0478-inch thick) cylindrical shell and flat ends are not important, the drums are modeled using FD surfaces. The three drums are assumed to be completely filled with waste modeled using FD solids.

Both radiation and air conduction are used to transfer heat across the 1.421-inch radial gap between the approximately 30-gallon drum sidewalls and the inside surface of the NS30 shield insert's cylindrical shell. Both radiation and air conduction are also used to transfer heat across the 2-inch axial gap between the drum ends, and across the 8⅞-inch axial gap between the first and third drum ends and the inside surface of the NS30 shield insert base and lid, respectively.

Finally, both radiation and air conduction are used to transfer heat across the 3/4-inch radial gap between the NS30 shield's cylindrical sidewall and the RLC's cylindrical shell, and across the 1/2-inch axial gap between NS30 shield's ends and the surface of the RLC base and lid.

A total of 9 FD surfaces and 8 FD solids are used to represent the NS30 shield insert thermal model and three approximately 30-gallon drum thermal models, with entity connectivity accomplished via 2,276 nodes.

3.4.1.2 Test Model

This section is not applicable as no thermal testing for NCT is performed for the RH-TRU 72-B package.

3.4.2 Package Conditions and Environment

The RH-TRU 72-B package is mounted in a horizontal orientation on its dedicated transport trailer for NCT. This establishes the orientation of the exterior surfaces of the package for determining the free convection heat transfer coefficients and insolation loading. In addition, since the package is supported on its main trunnions, the entire package is exposed to ambient air instead of resting on the trailer or some other non-adiabatic, conducting surface. Thus, heat transfer from the exterior of the entire package to the ambient occurs via free convection and radiation exchange. Thermal Desktop uses temperature dependent, free convection heat transfer coefficients based on equations taken from Chapter 3 of Guyer's *Handbook of Applied Thermal Design*.[3]

Table 3.4-1 presents the insolation values that are used for heat input to the exterior package surfaces for NCT, as specified in 10 CFR §71.71(c)(1).[1] Correspondingly, all vertical flat surfaces (i.e., the impact limiter inside and outside ends and some trunnion surfaces) have an insolation value of 200 gcal/cm^2 (737.5 Btu/ft^2), all curved surfaces (i.e., the OC and impact limiter cylindrical shells, and some trunnion surfaces) have an insolation value of 400 gcal/cm^2 (1,475 Btu/ft^2), and all horizontal flat surfaces (i.e., the remaining trunnion surfaces) have an insolation value of 800 gcal/cm^2 (2,950 Btu/ft^2). Consistent with 10 CFR §71.71(c)(1), a 100 ºF ambient temperature is used.

Table 3.4-1 – Total Insolation for a 12-Hour Period

Form and Location of Surface	Total Insolation for a 12-Hour Period	
	(gcal/cm^2)	(Btu/ft^2)
Flat surfaces transported horizontally:		
• Base	None	None
• Other surfaces	800	2,950
Flat surfaces not transported horizontally	200	737.5
Curved surfaces	400	1,475

[3] Eric C. Guyer, Editor in Chief, *Handbook of Applied Thermal Design*, First Edition, Taylor & Francis, Philadelphia, PA, 1999.

Insolation is applied in "12-hour off"/"12-hour on" steps, i.e., repeating the 12-hour off/12-hour on cycle for a sufficient period of time to allow the hottest location within the package to achieve pseudo-steady state equilibrium. As an example, Figure 3.4-9 illustrates transient temperatures for the first 360 hours (15 days) of the 600-hour (25-day) analysis at the centermost node in three, 30-gallon drums within an RLC for a 12 lb/ft^3 payload density with 90 watts of decay heat. The light-yellow regions in the plots depict the 12-hour periods when insolation is active.

Whereas Figure 3.4-9 illustrates how decoupled the center node temperatures for the three, 30-gallon drums are from the transient 12-hour "off/on" solar heat loads, Figure 3.4-10 illustrates how major components respond to the periodic step loading of the solar heat loads. The impact limiter responds immediately to the application of insolation, as expected, but Figure 3.4-10 also shows that regions further removed from the package surface, as they become more isolated from the ambient, demonstrate a periodic phase shift relative to the application of insolation. With reference to Figure 3.4-9, the center nodes for the waste within the three, 30-gallon drums exhibit peak temperatures that occur 5 hours after the start of a "12-hour on" insolation period. Because of this variability, the absolute maximum temperatures for components are reported in the temperature summary tables regardless of the time in the transient thermal evaluation.

3.4.3 Maximum Temperatures

The maximum NCT temperatures for the major package components with the maximum decay heat loads are presented in Table 3.4-2 for a 100 ºF ambient temperature without insolation and Table 3.4-3 for a 100 ºF ambient temperature with insolation. The following figures illustrate package and packaging NCT temperatures both with and without insolation for the three payload cases:

- **Case 1:** Figure 3.4-11 through Figure 3.4-14 show the package temperatures for a 12 lb/ft^3 payload density with 90 watts of uniformly distributed decay heat in three, 30-gallon drums within an RLC, and Figure 3.4-15 through Figure 3.4-18 show the package temperatures for a 100 lb/ft^3 payload density with 270 watts of uniformly distributed decay heat in three, 30-gallon drums within an RLC.
- **Case 2:** Figure 3.4-19 through Figure 3.4-22 show the package temperatures for a 12 lb/ft^3 payload density with 50 watts of uniformly distributed decay heat in three, approximately 15-gallon drums within an NS15 NSC.
- **Case 3:** Figure 3.4-23 through Figure 3.4-26 show the package temperatures for a 12 lb/ft^3 payload density with 50 watts of uniformly distributed decay heat in three, approximately 30-gallon drums within an NS30 NSC.

The thermal shield, trunnions, and impact limiter shells represent the only accessible surfaces of the RH-TRU 72-B package during transportation. As shown in Table 3.4-2, the maximum temperatures for these components for any payload remain below the regulatory defined maximum temperature of 185 ºF for an exclusive use shipment without insolation per 10 CFR §71.43(g).

Note that for Cases 2 and 3 NSC configurations, higher density payloads would result in correspondingly higher payload thermal conductivity that distributes decay heat more evenly thereby resulting in lower overall payload temperatures; therefore, use of a low-density payload material is bounding for all temperature predictions, i.e., for a given wattage, the average payload temperature at a payload density of 12 lb/ft^3 bounds the average payload temperature at higher payload densities.

3.4.4 Minimum Temperatures

The minimum temperature distribution for the RH-TRU 72-B package will occur with no decay heat load and an ambient air temperature of -40 ºF per 10 CFR §71.71(c)(2)[1]. Since the steady state analysis of these conditions represents a trivial case, no computerized thermal calculations are performed. Instead, it was assumed that all packaging components would reach the -40 ºF temperature under steady state conditions. For a package with the thermal capacitances of the RH-TRU 72-B package, prolonged exposure to low temperature environments is required to significantly depress package temperatures. The -40 ºF temperature is within the package's allowable temperature limits for the temperature sensitive components according to Section 3.3, *Technical Specifications of Components*.

As a potential initial condition for all NCT or HAC events, a -20 ºF minimum uniform temperature is considered in performing the tests of 10 CFR §71.71(b) and §71.73(b).

3.4.5 Maximum Internal Pressure

Evaluation of the maximum internal pressure for the RH-TRU 72-B package considers all factors that affect pressure to demonstrate that pressure increases are below the allowable pressure for the package. Structural loads do not affect the maximum pressure capability of the packaging for NCT.

Decay heat/temperature equations are presented to support internal pressure calculations. Decay heat dependent temperatures for the packaging and payload components used in the internal pressure calculations are based on the following parabolic (i.e., second-order polynomial) equation:

$$T = a + bQ - cQ^2$$

where T is the temperature (degrees Fahrenheit) and Q is the decay heat load (watts). The parabolic equation coefficients for applicable packaging and payload components are presented in Table 3.4-4.

3.4.5.1 Design Pressure and Maximum Normal Operating Pressure

The RH-TRU 72-B package has a design pressure of 150 psig. Assuming an external pressure of 14.7 psia, the maximum normal operating pressure (MNOP) is 164.7 psia for the IV at the maximum normal operating temperature. Chapter 2.0, *Structural Evaluation*, discusses the ability of the package to withstand MNOP for both NCT and HAC.

3.4.5.2 Factors Affecting Pressure

The gauge pressure within the sealed IV of the RH-TRU 72-B package may potentially be changed (increased or decreased) due to one or more of the following factors that can affect pressure:

- Radiolytic gas generation (or consumption),
- Temperature-related pressure change,
- Barometric pressure change,

- Chemical reactions,
- Biological gas generation, and/or
- Thermal decomposition.

Each of these factors is discussed in the following sections. Depending on the payload, the relative contribution from each factor may vary from negligible to a significant fraction of the total pressure change. Section 3.4.5.3, *Maximum Pressure for Normal Conditions of Transport*, evaluates the worst-case combination of conditions for pressure increases within a payload.

3.4.5.2.1 Radiolytic Gas Generation

Radiolytic gas generation (radiolysis of the payload materials by the radioactive contaminants) is a potentially significant factor affecting pressure for some payloads. Radiolytic gases are generated when materials absorb radiation energy and produce gas molecules. Oxygen in the initial atmosphere within an RH-TRU package IV may also be consumed in some radiolytic processes. Gases are generated from radiolysis due to alpha, beta, gamma, or neutron interactions with matter. The radiation breaks chemical bonds in the target (potentially gas producing material) and causes chemical reactions to occur in the payload materials and in the atmosphere of the payload cavity. This may result in the net generation or consumption of gases. During transport, radiolysis of waste materials in the RH-TRU 72-B package payloads could result in either the net increase or decrease of pressure within the IV.

The gas generation rate, n_g (moles/sec), is determined from the following equation (see Appendix 2.1 of the *RH-TRU Payload Appendices*[4]):

$$n_g = W \times F \times G \times C \quad (1)$$

where W is the total decay heat (watts), F is the fraction of total ionizing radiation that is absorbed by target material (potential gas producing material), G is the number of gas molecules generated per unit (100 ev) ionizing radiation absorbed by target material, and C is the conversion factor based on units of measurement.

The gas generation rate depends on the G-value of the material (molecules of gas produced per 100 ev of energy absorbed), the fraction, F, of the emitted energy which is absorbed by the target material, and the emitted energy available from the form of alpha, beta, gamma or neutron radiation. The G-value may be positive (in the case of hydrogen, carbon dioxide, etc.) or negative (often in the case of oxygen). The variable, F, depends on the type of radiation emitted, the spatial distribution of the radioactive contaminants, and the target materials inside the payload container.

In experiments designed to measure the G-values of a material, care is taken to obtain intimate contact between the radionuclides and the target material. The F-factor then approaches 1.0 (100% of the emitted energy is absorbed). In RH-TRU wastes, the F-factor is unlikely to be equal to 1.0 due to the presence of non-target materials and the distribution of source and target materials. Since special care is needed to achieve an F-factor of 1.0 in laboratory conditions, the

[4] U.S. Department of Energy (DOE), *RH-TRU Payload Appendices*, U.S. Department of Energy, Carlsbad Field Office, Carlsbad, New Mexico.

F-factor in actual waste materials will usually be much less than 1.0; hence, the energy absorbed by the target materials will be only a fraction of the energy emitted.

For payloads in the RH-TRU 72-B package, the analysis of potential gas production in the payload materials is based on an effective G-value (or the product of F and G). When several different waste materials may be present and the distribution of RH-TRU radionuclides is not well known, all of the energy is assumed to be absorbed by the material having the highest G-value. By using this approach, if actual values for gas generation are measured from a specific payload container, results would be bounded by the analytic prediction. A detailed discussion of how effective G-values are assigned to content codes is provided in Appendix 2.2 of the *RH-TRU Payload Appendices*[4].

The discussion of effective G-value in Appendix 2.2 of the *RH-TRU Payload Appendices* considers G-values for materials, hydrogen, and net (total). The effective hydrogen gas G-value for each content code is used to determine the allowable gas generation rate to restrict the hydrogen concentration within the innermost confinement volume of the waste to a value less than 5 molar percent and to calculate the decay heat limit for each content code, as discussed in Appendix 2.5 of the *RH-TRU Payload Appendices*[4]. The effective net (total) gas G-value is used in calculating the contribution of total pressure that originates from potential radiolytic gas generation.

Appendix 2.2 of the *RH-TRU Payload Appendices*[4] also discusses the reduction in the rate of hydrogen gas generation (G-value) over time based on the total dose of alpha and beta radiation received by the target matrix in the vicinity of the TRU radionuclides. Over time and with constant exposure to radiation, hydrogen is removed from the hydrogenous waste or packaging material (the matrix), thus decreasing the number of hydrogen bonds available for further radiolytic breakdown (the matrix is depleted). As the amount of available hydrogen is reduced over time, the effective G-value decreases with increasing dose to a value that is defined as the "dose-dependent G-value". Because of the characteristics of alpha, beta, and gamma radiation, only the matrix depletion effects of alpha and beta radiation are considered. No credit is taken for the matrix depletion effects of gamma radiation.

3.4.5.2.2 Temperature Related Pressure Change

Temperature affects package pressure changes in two ways. The first is the thermal expansion of the gases (air, and radiolytic gases) within the IV cavity, caused by an increase in temperature. This increase is calculated utilizing the ideal gas law equation: $PV = nRT$. The temperature, T, of the IV internal gas (essentially air) is calculated by considering an area average surface temperature of IV and payload canister walls. This value varies depending on decay heat wattage assumed in the thermal analysis for the payload. The bounding case for NCT is analyzed at the package limit of 270 watts (indicative of 100 lb/in^3 density). Table 3.4-4 shows the average IV cavity air temperature of 167.9 ºF for the 100 lb/in^3 case at the maximum thermal load of 270 watts. For HAC, and similar calculations, Table 3.5-2 in Section 3.5.3, *Package Temperatures*, shows that the calculated internal gas temperatures would be ½(384.4 + 284.1) = 334.25 ºF for the 100 lb/in^3 case at the maximum thermal load of 270 watts (determined by averaging the peak IV and payload canister shell temperatures, respectively).

The second pressure increase related to temperature is the partial pressure of moisture and potentially volatile chemicals within the IV cavity. The assumption for both payloads is that

sufficient water exists to maintain a saturated atmosphere. The partial pressure exerted by water vapor is combined with other pressure contributions using Dalton's Law. The water vapor pressure is obtained from thermodynamic steam tables based on the coolest IV wall temperature where moisture condenses. The partial pressure contribution from potentially volatile chemicals in the waste is assumed to be insignificant.

Appendix 4.4 of the *RH-TRU Payload Appendices*[4] evaluates the contribution to the overall pressure in the IV by the vapor pressure that might be exerted by potentially flammable VOCs. (Appendix 4.3 of the *RH-TRU Payload Appendices*[4] evaluates the compatibility of VOCs with the butyl-rubber O-ring seals used in the RH-TRU 72-B package.)

3.4.5.2.3 Barometric Pressure Change

The design of the RH-TRU 72-B package meets the regulatory requirement for an external pressure of 3.5 psia per 10 CFR §71.71(c)(3)[1]. This external pressure is well below the maximum barometric pressure decrease expected during transport due to elevation and weather changes. The expected maximum barometric pressure decrease would only result in an external pressure of approximately 8 psia.

The conservative approach of using the regulatory requirement of 3.5 psia reduces the safe pressure increase limit by 11.2 psi for a maximum allowable internal pressure of 150 psig. Thus, barometric pressure changes are accounted for by reducing the maximum allowable internal pressure to 150.0 – 11.2 = 138.8 psig, or adding 11.2 psia to the cumulative pressure increases from other sources.

3.4.5.2.4 Chemical Reactions

Potential pressure increases from gas-producing or exothermic chemical reactions in the payload materials are considered. The chemical compatibility evaluation performed in Appendix 4.1 of the *RH-TRU Payload Appendices*[4] determines the potential for chemical reactions. The chemical list for each content code in the Remote-Handled Transuranic Content Codes (*RH-TRUCON*)[5] is restricted to preclude the occurrence of chemical reactions that produce excessive gas or heat.

These chemical lists are evaluated for potential incompatibilities in accordance with the U.S. Environmental Protection Agency (EPA) method that looks at gas production and exothermic reactions.[6] This method is discussed in Appendix 4.1 of the *RH-TRU Payload Appendices*[4]. Use of the EPA method ensures that incompatible chemicals do not contribute to increased pressures in the IV.

3.4.5.2.5 Biological Gas Generation

Several different types of microorganisms have the potential to cause gas production from biological decomposition of materials in the payload. These include aerobic, anaerobic,

[5] U.S. Department of Energy (DOE), *Remote-Handled Transuranic Content Codes* (RH-TRUCON), DOE/WIPP 90-045, U.S. Department of Energy, Carlsbad Field Office, Carlsbad, New Mexico.

[6] H. K. Hatayama, J. J. Chen, E. R. de Vera, R. D. Stephens, D. L. Storm, *A Method for Determining the Compatibility of Hazardous Wastes*, EPA 600/2 80 076, U.S. Environmental Protection Agency, Cincinnati, Ohio, 1980.

facultative anaerobes, and obligate anaerobes. Each of these microorganisms requires a specific environment to multiply and produce gas.

Cellulosic materials within the payload materials can serve as substrate for microorganisms. However, additional conditions are required for gas generation than just the presence of cellulosic materials. The environment within the payload is hostile and incompatible for these microorganisms due to insufficient nutrients (associated with suitable substrate [nitrogen and phosphorus]), segregation of waste types, a high pH (in some waste types), excess oxygen (for some microorganisms), and/or insufficient water content. These factors will greatly reduce the potential for biological gas generation during the 60-day shipping period. Aerobic bacteria, which are the most likely microorganism to be present, will deplete oxygen and produce CO_2, causing no net increase in pressure. The limited potential for biological gas generation in the RH-TRU 72-B package payload is discussed in Appendix 4.5 of the *RH-TRU Payload Appendices*[4].

3.4.5.2.6 Thermal Decomposition

Thermal decomposition can be a factor affecting pressure. However, as discussed in Appendix 4.6 of the *RH-TRU Payload Appendices*[4], and Section 3.3.3, *Payload Material*, average and peak payload temperatures are limited to values that ensure thermal decomposition will not be a factor affecting internal pressure.

As demonstrated in the NCT thermal evaluation (see Section 3.4.3, *Maximum Temperatures*), the temperatures of the payloads within the RH-TRU 72-B package are relatively low.

3.4.5.3 Maximum Pressure for Normal Conditions of Transport

The maximum pressure within the RH-TRU 72-B package IV under NCT is calculated below based on package temperatures at the bounding payload density of 100 lb/in^3 with 270 watts of decay heat.

As discussed in Section 3.4.5.2, *Factors Affecting Pressure*, the major factors affecting the IV internal pressure are radiolytic gas generation, thermal expansion of gases, and the vapor pressure of water within the IV cavity. Barometric changes that affect external pressure and, hence, the gauge pressure of the IV, are bound by the regulatory condition of 3.5 psia external pressure. Thus, upon loading at standard conditions of 14.7 psia, the internal pressure rise allowed is the package design pressure difference, 150 psig less 11.2 psia (14.7 – 3.5), or 138.8 psig; or barometric pressure contributes an administrative 11.2 psia before the other physical factors mentioned above are added. Subsequently, it will become obvious that barometric pressure effects are negligible based upon the low increases in pressure determined due to the other factors. IV internal pressure does not increase significantly due to chemical reactions, biological gas generation, or thermal decomposition (see Appendices 4.1, 4.5, and 4.6 of the *RH-TRU Payload Appendices*[4]).

Calculation of maximum pressure in the IV considers immediate release of gases from the innermost confinement containers to the IV. The payload canister and IV void volumes are assumed to be filled with air at 70 ºF and 14.7 psia when the IV is sealed for transport. Sufficient water is assumed to be present for saturated water vapor at any temperature. The

pressure increase due to water vapor is obtained from the tabulated thermodynamic properties of saturated water and steam.

The maximum pressure in the IV is calculated for the maximum quantity of gas generated by the end of the shipping period. The maximum allowable shipping period is 60 days per Appendix 2.3 of the *RH-TRU Payload Appendices*[4], while the maximum normal shipping period will be less than 60 days by a large margin of safety. As described in Appendix 2.3 of the *RH-TRU Payload Appendices*[4], routine monitoring of shipments includes the use of the TRANSCOM system at the Waste Isolation Pilot Plant which provides continuous tracking of shipments from the shipping site to its destination. The use of a 60-day shipping period in the calculation of MNOP is consistent with 10 CFR §71.41(c)[1]. As specified in 10 CFR §71.41(c), this section shows that the "…controls proposed to be exercised by the shipper are demonstrated to be adequate to provide equivalent safety of the shipment."

The calculated pressure increase for the bounding case is below the limit for the RH-TRU 72-B package. For the bounding decay heat of 270 watts at a payload density of 100 lb/in^3, the pressure increase at the end of a shipping period is 8.995 psig, well below the design limit, $P_{allow\text{-}NCT}$ = 138.8 psig. Hydrogen gas concentration, and the corresponding total gas generated, will always be bounded by what is assumed in this analysis.

The methodology used to calculate the maximum IV pressure is summarized below. Appendix 2.2 in the *RH-TRU Payload Appendices*[4] summarizes both hydrogen and net (total) gas G-values for bounding waste material. The payloads within the package are always limited to 5 molar percent of hydrogen in the innermost confinement layer, and this analysis conservatively assumes that no layers of confinement exist such that all of the generated hydrogen gas is within the IV headspace. Therefore, the maximum possible partial pressure of hydrogen gas within the headspace of the IV at the end of the shipping period, P_{H2}, is:

$$P_{H2} = P_{atm} \times C_{H2} = 0.735 \text{ psia}$$

where P_{atm} is the atmospheric pressure at the start of the shipment in the IV (14.7psia), and C_{H2} is the maximum allowed concentration of hydrogen in the innermost layer of confinement at the end of the shipping period (5 molar percent).

For the purposes of pressure calculations, total gas generation must be considered. Based on the proportion of hydrogen G-values to net (total) G-values, the bounding ratio of G-values, $R_{G\text{-value}}$, is based on the bounding waste material Polyvinyl Chloride (PVC):

$$R_{G-value} = \frac{G_{net}}{G_{H2}} = \frac{2.6 \text{ molecules}/100 \text{ eV}}{0.7 \text{ molecules}/100 \text{ eV}} = 3.714$$

where the net (total) gas G-value for PVC, G_{Net} = 2.6 molecules/100 eV, and the hydrogen gas G-value for PVC, G_{H2} = 0.7 molecules/100 eV.

Utilizing the ratio $R_{G\text{-value}}$ and the partial pressure for the maximum allowed generated hydrogen gas P_{H2}, the maximum partial pressure of generated net (total) gas, P_{net}, is:

$$P_{net} = P_{H2} \times R_{G\text{-value}} = 0.735 \times 3.714 = 2.730 \text{ psia}$$

Thus, using the ideal gas law, the total pressure within the IV cavity due to net (total) gas generation, the atmosphere of initial pressure, and the heating of those gases up to the average IV

cavity air temperature of 167.9 ºF from Table 3.4-4 at the maximum 270-watt decay heat load, P_{hu_NCT}, is:

$$P_{hu_NCT} = (P_{net} + P_{atm}) \times \left(\frac{167.9\,^{\circ}F + 460\,^{\circ}R}{70\,^{\circ}F + 460\,^{\circ}R} \right) = 20.650 \text{ psia}$$

The water vapor pressure is based on the minimum IV cavity surface temperature where moisture will condense; 142.0 ºF from Table 3.4-4 at the maximum 270-watt decay head load. The water vapor pressure from thermodynamic steam tables is P_{wv_NCT} = 3.045 psia. Therefore, the maximum IV pressure at the end of a shipment for a bounding maximum thermal load of 270 watts, P_{max_NCT}, is:

$$P_{max_NCT} = P_{hu_NCT} + P_{wv_NCT} - P_{atm} = 20.650 + 3.045 - 14.7 = 8.995 \text{ psia}$$

Thus, the margin of safety against the NCT design pressure limit, MS_{MNOP_NCT}, is:

$$MS_{MNOP_NCT} = \left(\frac{P_{allow_NCT}}{P_{max_NCT}} \right) - 1 = \left(\frac{138.8}{8.995} \right) - 1 = +14.4$$

3.4.6 Maximum Thermal Stresses

Maximum NCT thermal stresses are determined using the temperature results from Section 3.4.3, *Maximum Temperatures*, and Section 3.4.4, *Minimum Temperatures*. NCT thermal stresses are discussed in Section 2.6.1, *Heat*, and Section 2.6.2, *Cold*. As input to Chapter 2.0, *Structural Evaluation*, the minimum temperature is taken as -40 ºF (-20 ºF when combined with any other load cases) and, unless otherwise stated, the maximum temperature is taken as 160 ºF.

3.4.7 Evaluation of Package Performance for Normal Conditions of Transport

The thermal performance of the RH-TRU 72-B packaging was evaluated for the applicable NCT conditions and for a variety of decay heat distributions within the packaging based on the various payload configurations. The evaluations found that the resulting component temperatures remained within their specified temperature limits for all cases.

Table 3.4-2 – Maximum NCT Temperatures without Insolation (ºF)

Location	RLC		NS15	NS30	Allowable Limit①
	12 lb/ft^3 Payload (90 W)	100 lb/ft^3 Payload (270 W)	12 lb/ft^3 Payload (50 W)	12 lb/ft^3 Payload (50 W)	
Lower Drum Contents Peak	306.0	292.4	230.9	217.3	402
Lower Drum Contents Average	199.2	232.9	166.9	157.8	302
Lower Drum Wall Peak	153.0	232.7	139.2	132.5	—
Middle Drum Contents Peak	313.5	307.5	236.1	221.9	402
Middle Drum Contents Average	207.5	252.0	173.2	163.0	302
Middle Drum Wall Peak	153.2	233.2	139.4	132.7	—
Upper Drum Contents Peak	305.1	290.9	230.6	216.9	402
Upper Drum Contents Average	198.1	230.4	166.5	157.3	302
Upper Drum Wall Peak	152.8	232.1	139.1	132.4	—
HDPE Shielding Wall Peak	—	—	130.3	125.3	170
HDPE Shielding Wall Average	—	—	120.9	119.4	150
RLC Shell Peak	129.1	177.8	117.7	117.1	210②
RLC Lid Peak	112.8	135.6	106.4	106.6	212
IV Shell Peak	109.3	125.5	105.5	105.5	160②
IV Base Peak	109.2	125.2	105.0	105.1	160②
IV Upper Forging Peak	107.1	119.2	103.9	104.0	160②
IV Lid Peak	106.9	118.5	103.7	103.8	160②
IV Lid O-ring Seal Peak	106.9	118.5	103.7	103.8	225
IV Lid Ports O-ring Seals Peak	106.9	118.5	103.7	103.8	225
OC Inner Shell Peak	106.6	117.6	103.8	103.8	160②
OC Lead Shield Peak	106.6	117.6	103.8	103.8	160②
OC Outer Shell Peak	106.5	117.5	103.7	103.8	160②
OC Base Peak	106.8	118.2	103.8	103.9	160②
OC Upper Forging Peak	105.0	113.2	102.8	102.9	160②
OC Lid Peak	105.1	113.5	102.9	102.9	160②
OC Lid O-ring Seal Peak	105.0	113.2	102.8	102.9	225
OC Lid Port O-ring Seal Peak	105.1	113.5	102.9	102.9	225
OC Thermal Shield Peak	106.5	117.6	103.7	103.8	185③
OC Main Trunnions Peak	105.1	113.2	103.1	103.1	153②
OC Small Trunnions Peak	105.7	114.9	103.4	103.4	153②
Impact Limiter Foam Peak	106.7	118.0	103.8	103.9	260
Impact Limiter Foam Average	102.3	106.0	101.3	101.3	140②
Impact Limiter Shell Peak	106.7	118.0	103.8	103.9	185③

Notes:

① Allowable temperature limits are discussed in Section 3.3, *Technical Specifications of Components*.

② Allowable temperature limits correspond to temperatures used in the structural evaluations in Chapter 2.0, *Structural Evaluation*.

③ The allowable temperature limit of 185 ºF for external surfaces of the package is based on the maximum accessible surface temperature without insolation for exclusive use shipments per 10 CFR §71.43(g).

Table 3.4-3 – Maximum NCT Temperatures with Insolation (ºF)

Location	RLC		NS15	NS30	Allowable Limit①
	12 lb/ft^3 Payload (90 W)	100 lb/ft^3 Payload (270 W)	12 lb/ft^3 Payload (50 W)	12 lb/ft^3 Payload (50 W)	
Lower Drum Contents Peak	331.8	312.1	258.6	245.2	402
Lower Drum Contents Average	225.7	253.1	194.7	185.9	302
Lower Drum Wall Peak	180.1	252.0	166.9	160.8	—
Middle Drum Contents Peak	338.8	326.3	263.5	249.5	402
Middle Drum Contents Average	233.6	271.1	200.8	190.9	302
Middle Drum Wall Peak	180.3	252.4	167.0	160.9	—
Upper Drum Contents Peak	331.2	310.7	258.4	245.0	402
Upper Drum Contents Average	224.9	250.8	194.5	185.7	302
Upper Drum Wall Peak	180.1	251.4	166.9	160.8	—
HDPE Shielding Wall Peak	—	—	158.7	154.3	170
HDPE Shielding Wall Average	—	—	149.7	148.5	150
RLC Shell Peak	159.3	202.2	148.4	147.8	210②
RLC Lid Peak	141.9	161.6	136.0	136.2	212
IV Shell Peak	145.1	158.2	142.3	142.2	160②
IV Base Peak	138.6	152.2	135.0	135.1	160②
IV Upper Forging Peak	137.1	147.1	134.7	134.7	160②
IV Lid Peak	136.1	145.7	133.7	133.8	160②
IV Lid O-ring Seal Peak	136.1	145.7	133.7	133.8	225
IV Lid Ports O-ring Seals Peak	136.1	145.7	133.7	133.8	225
OC Inner Shell Peak	143.8	150.4	142.5	142.5	160②
OC Lead Shield Peak	143.9	150.3	142.6	142.6	160②
OC Outer Shell Peak	144.0	150.4	142.7	142.7	160②
OC Base Peak	136.7	145.7	134.6	134.6	160②
OC Upper Forging Peak	136.7	142.6	135.3	135.3	160②
OC Lid Peak	135.0	141.2	133.5	133.5	160②
OC Lid O-ring Seal Peak	134.9	141.2	133.3	133.4	225
OC Lid Port O-ring Seal Peak	135.0	141.2	133.5	133.5	225
OC Thermal Shield Peak	146.8	151.9	145.7	145.7	185③
OC Main Trunnions Peak	144.0	149.7	142.8	142.7	153②
OC Small Trunnions Peak	144.5	149.7	143.5	143.5	153②
Impact Limiter Foam Peak	157.7	157.7	157.7	157.7	260
Impact Limiter Foam Average	133.5	136.4	132.8	132.8	140②
Impact Limiter Shell Peak	157.7	157.7	157.7	157.7	185③

Notes:

① Allowable temperature limits are discussed in Section 3.3, *Technical Specifications of Components*.

② Allowable temperature limits correspond to temperatures used in the structural evaluations in Chapter 2.0, *Structural Evaluation*.

③ The allowable temperature limit of 185 ºF for external surfaces of the package is based on the maximum accessible surface temperature without insolation for exclusive use shipments per 10 CFR §71.43(g).[1]

Table 3.4-4 – Equation Coefficients for NCT Temperatures (ºF) Based on Decay Heat Load (W)

RLC 12 lb/ft^3 Payload Density	Temperature (ºF)				Equation Coefficients①		
	0 W	30 W	60 W	90 W	a	b	c
Average Contents	132.3	166.8	200.5	233.6	132.3	1.1620	4.0E-04
Average RLC Wall	133.3	139.2	145.0	150.6	133.3	0.2000	7.5E-05
Average IV Wall	135.8	137.9	140.0	142.0	135.8	0.0715	2.8E-05
Average IV Cavity Air	134.5	138.5	142.5	146.3	134.5	0.1363	5.5E-05
Minimum IV Wall	123.8	126.0	128.1	130.2	123.8	0.0735	2.8E-05

RLC 100 lb/ft^3 Payload Density	Temperature (ºF)				Equation Coefficients①		
	0 W	90 W	180 W	270 W	a	b	c
Average Contents	131.4	183.0	229.0	271.1	131.4	0.5955	2.9E-04
Average RLC Wall	132.9	150.2	166.4	181.7	132.9	0.1973	6.2E-05
Average IV Wall	135.8	142.1	148.2	154.2	135.8	0.0706	9.3E-06
Average IV Cavity Air	134.4	146.2	157.3	167.9	134.4	0.1340	3.7E-05
Minimum IV Wall	123.7	130.1	136.2	142.0	123.7	0.0730	2.0E-05

NS15 12 lb/ft^3 Payload Density	Temperature (ºF)				Equation Coefficients①		
	0 W	16.7 W	33.3 W	50 W	a	b	c
Average Contents	131.3	154.8	177.8	200.8	131.3	1.4150	5.4E-04
Average RLC Wall	132.6	135.9	139.2	142.4	132.6	0.2000	9.0E-05
Average IV Wall	135.8	137.0	138.1	139.3	135.8	0.0700	0
Average IV Cavity Air	134.2	136.4	138.7	140.8	134.2	0.1370	9.0E-05
Minimum IV Wall	123.8	125.0	126.3	127.5	123.8	0.0744	0

NS30 12 lb/ft^3 Payload Density	Temperature (ºF)				Equation Coefficients①		
	0 W	16.7 W	33.3 W	50 W	a	b	c
Average Contents	131.6	151.6	171.3	190.9	131.6	1.2070	4.1E-04
Average RLC Wall	132.5	135.9	139.1	142.3	132.5	0.2030	1.3E-04
Average IV Wall	135.8	137.0	138.1	139.3	135.8	0.0700	0
Average IV Cavity Air	134.2	136.4	138.6	140.8	134.2	0.1350	4.4E-05
Minimum IV Wall	123.8	125.0	126.3	127.5	123.8	0.0744	0

Notes:

① The parabolic equation coefficients for the payload and packaging components used for gas generation and/or internal pressure calculations are based on the equation $T = a + bQ - cQ^2$, where T is the temperature (ºF) and Q is the decay heat load (watts).

This page intentionally left blank.

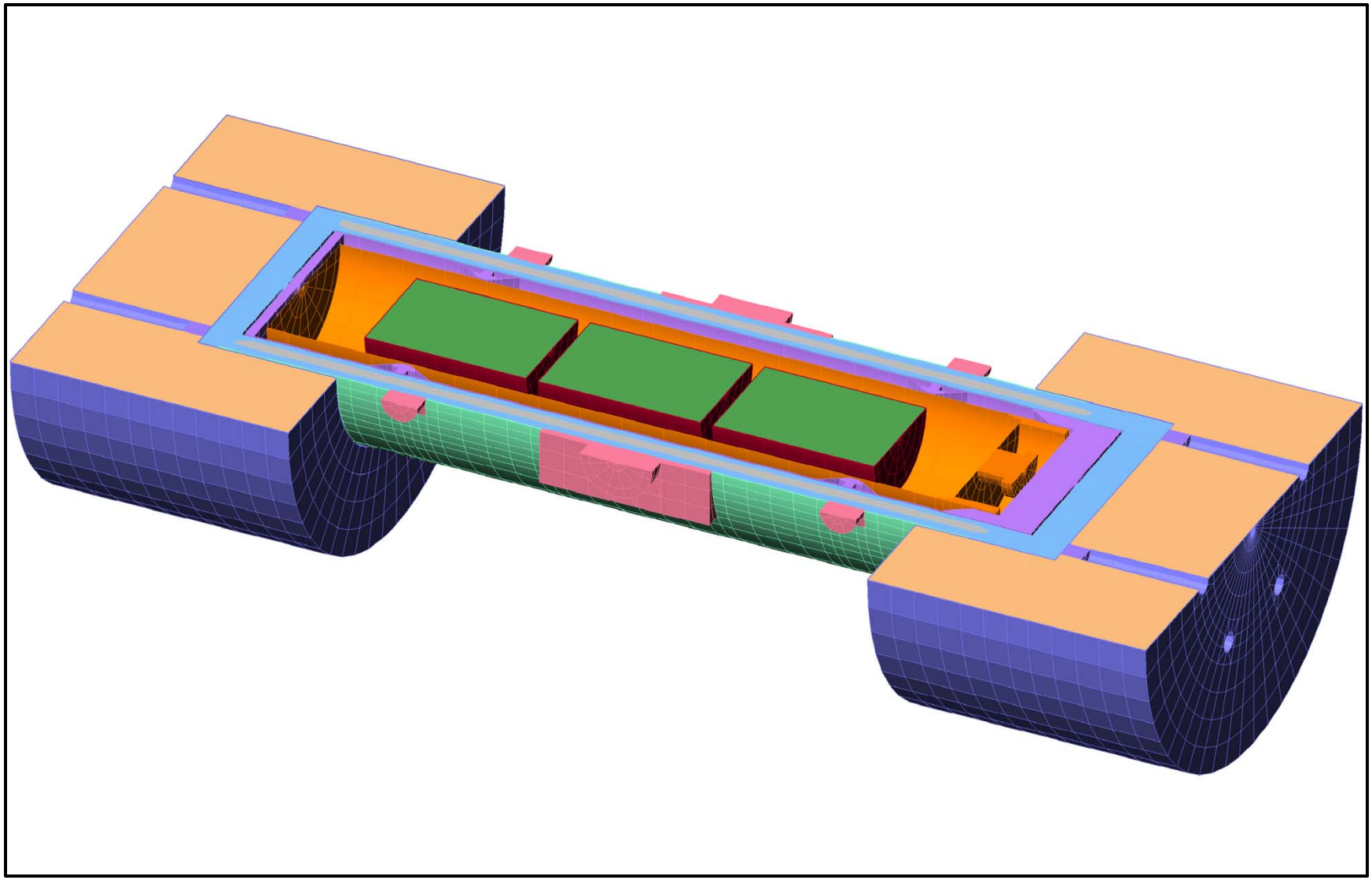

Figure 3.4-1 – NCT Package Thermal Model with an RLC

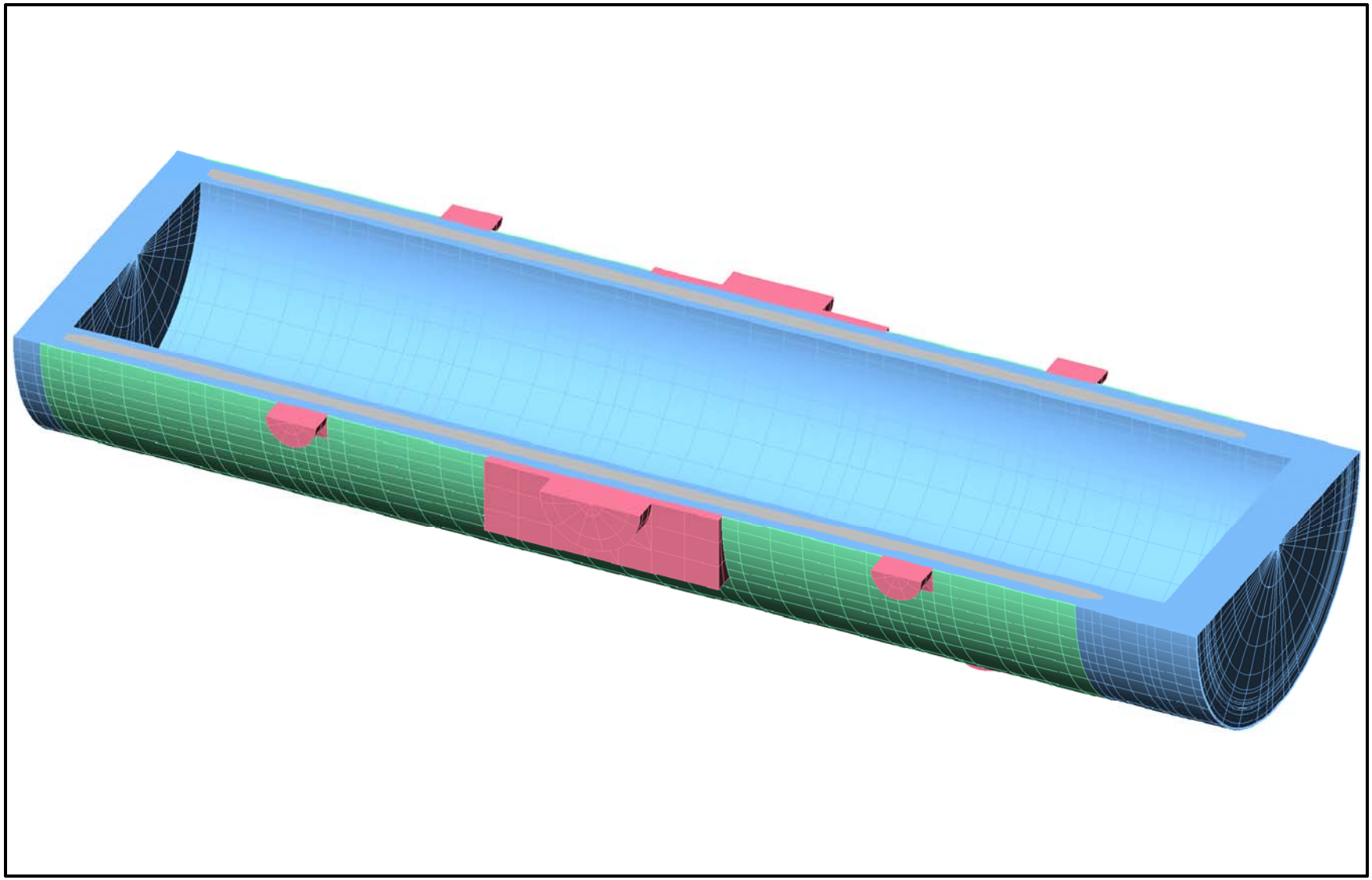

Figure 3.4-2 – OC Thermal Model

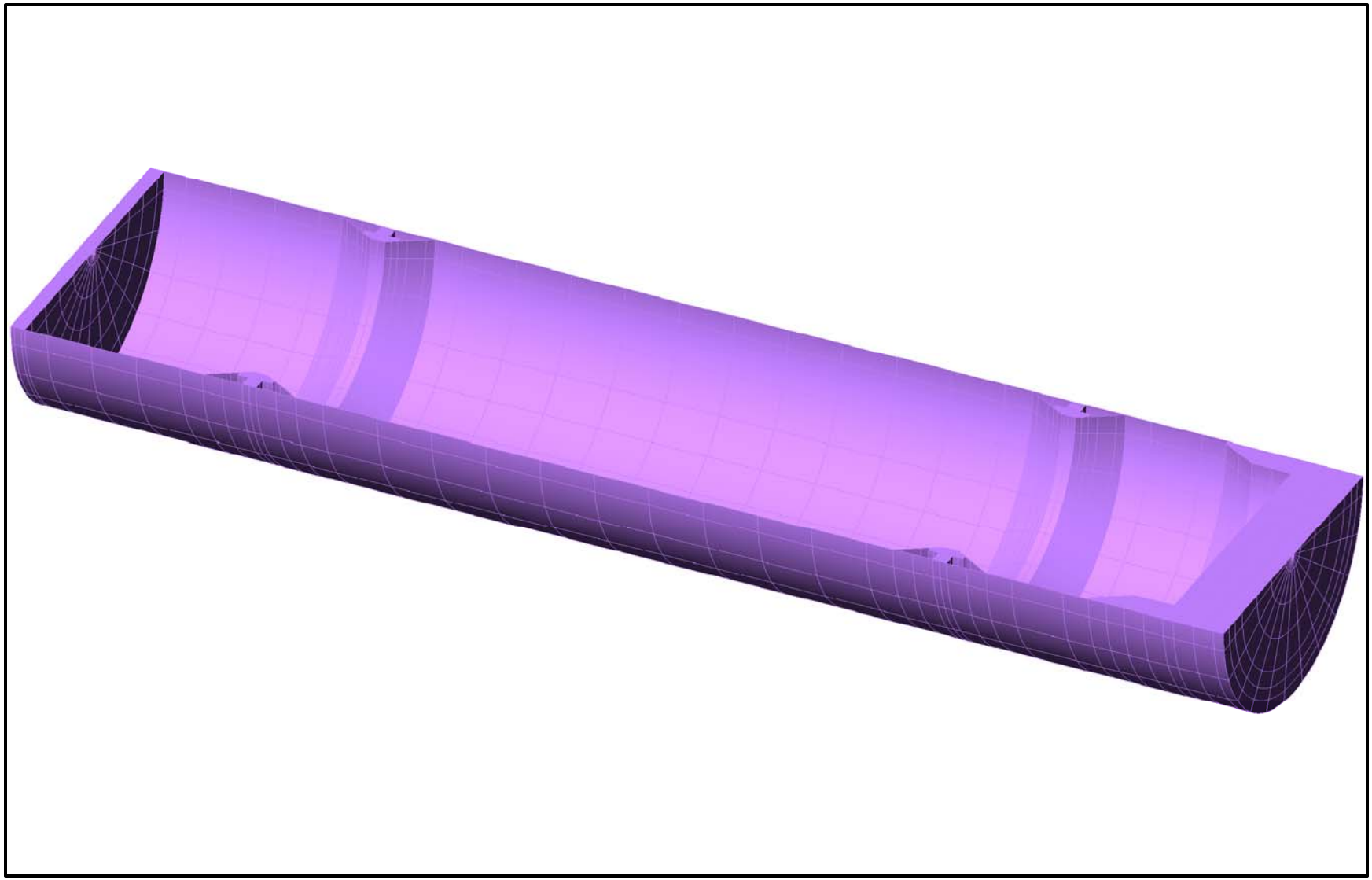

Figure 3.4-3 – IV Thermal Model

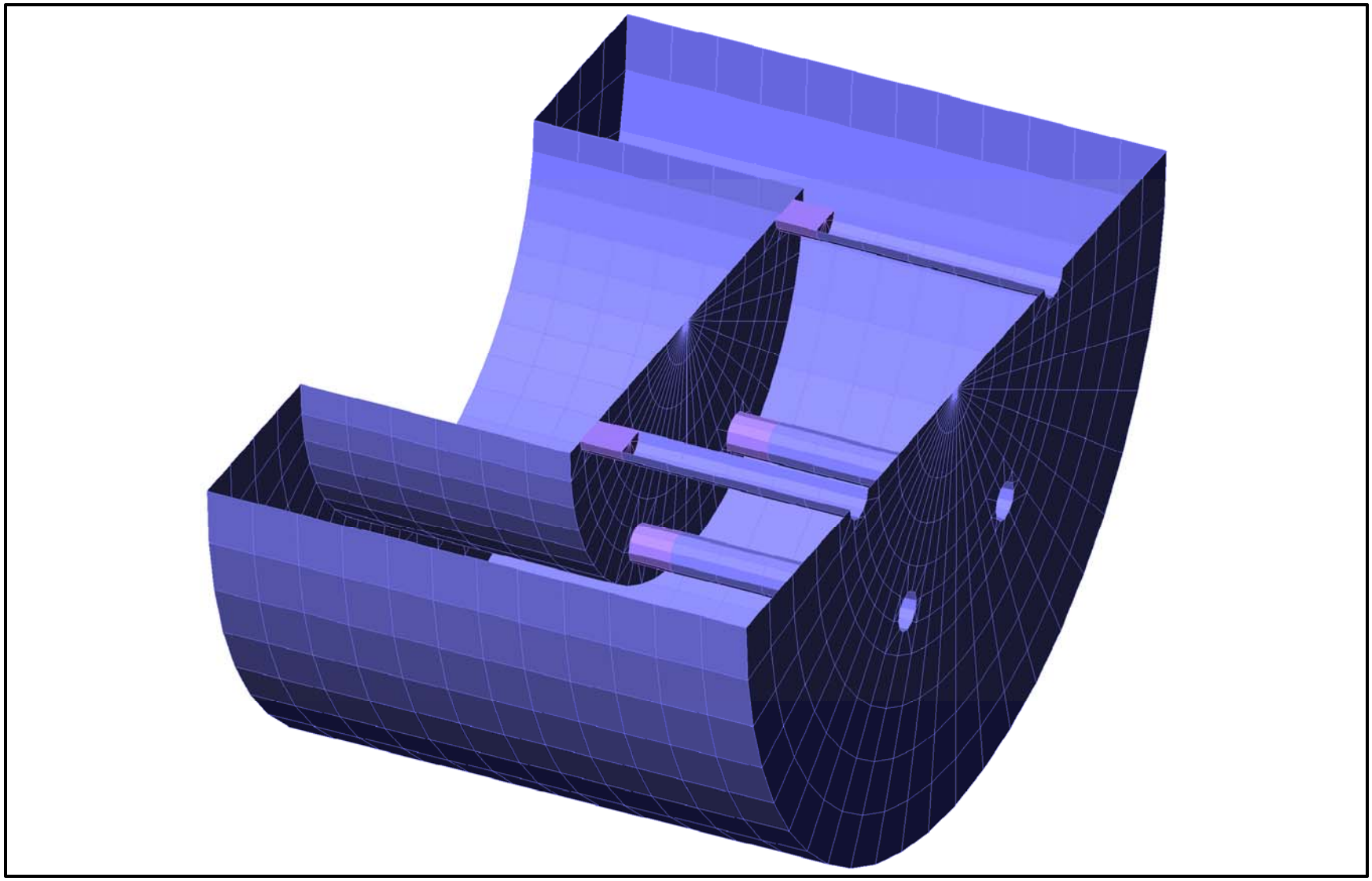

Figure 3.4-4 – NCT Impact Limiter Thermal Model (Polyurethane Foam Hidden)

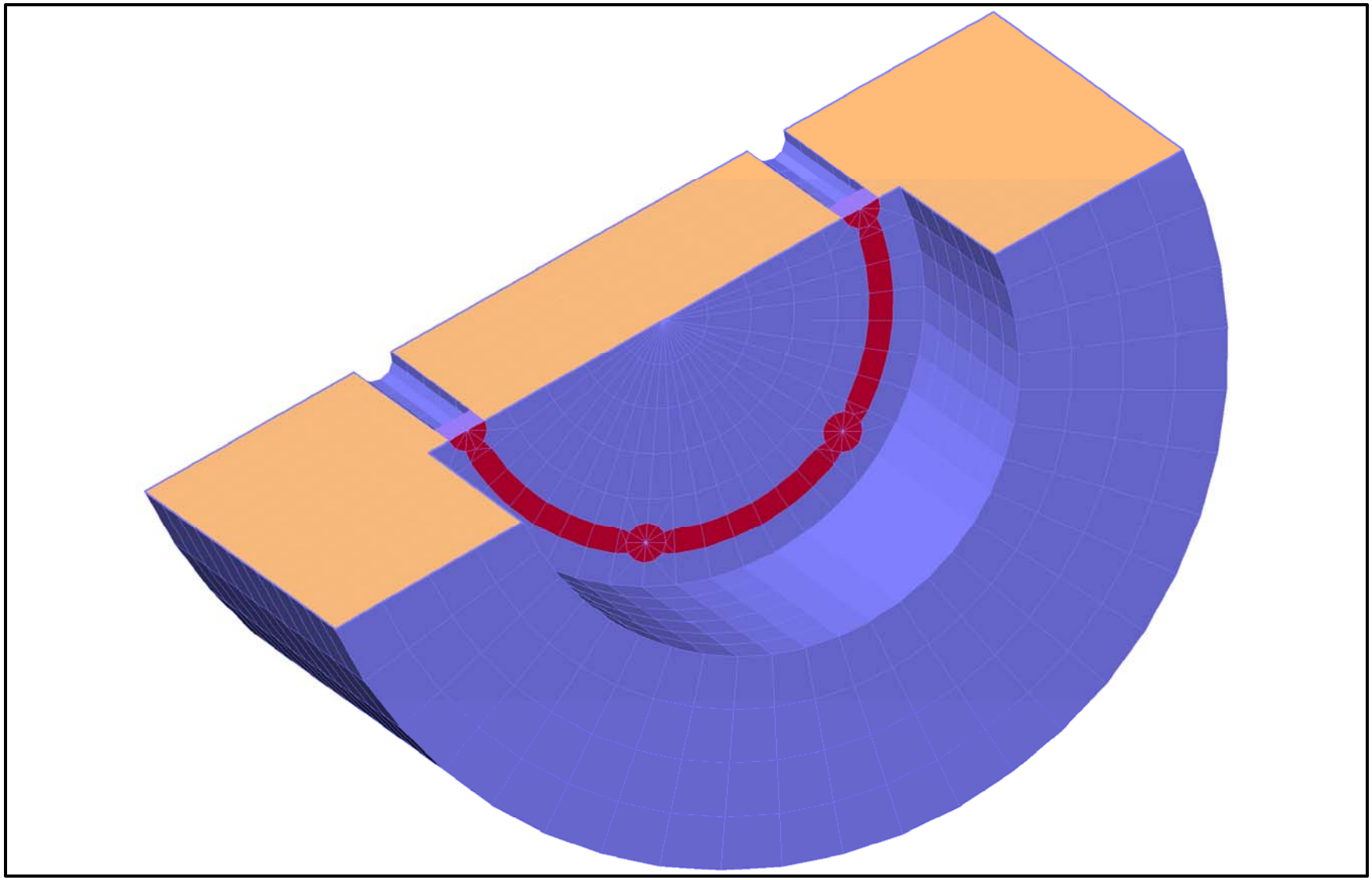

Figure 3.4-5 – NCT Impact Limiter Thermal Model (Steel Contactor Region Shown in Red)

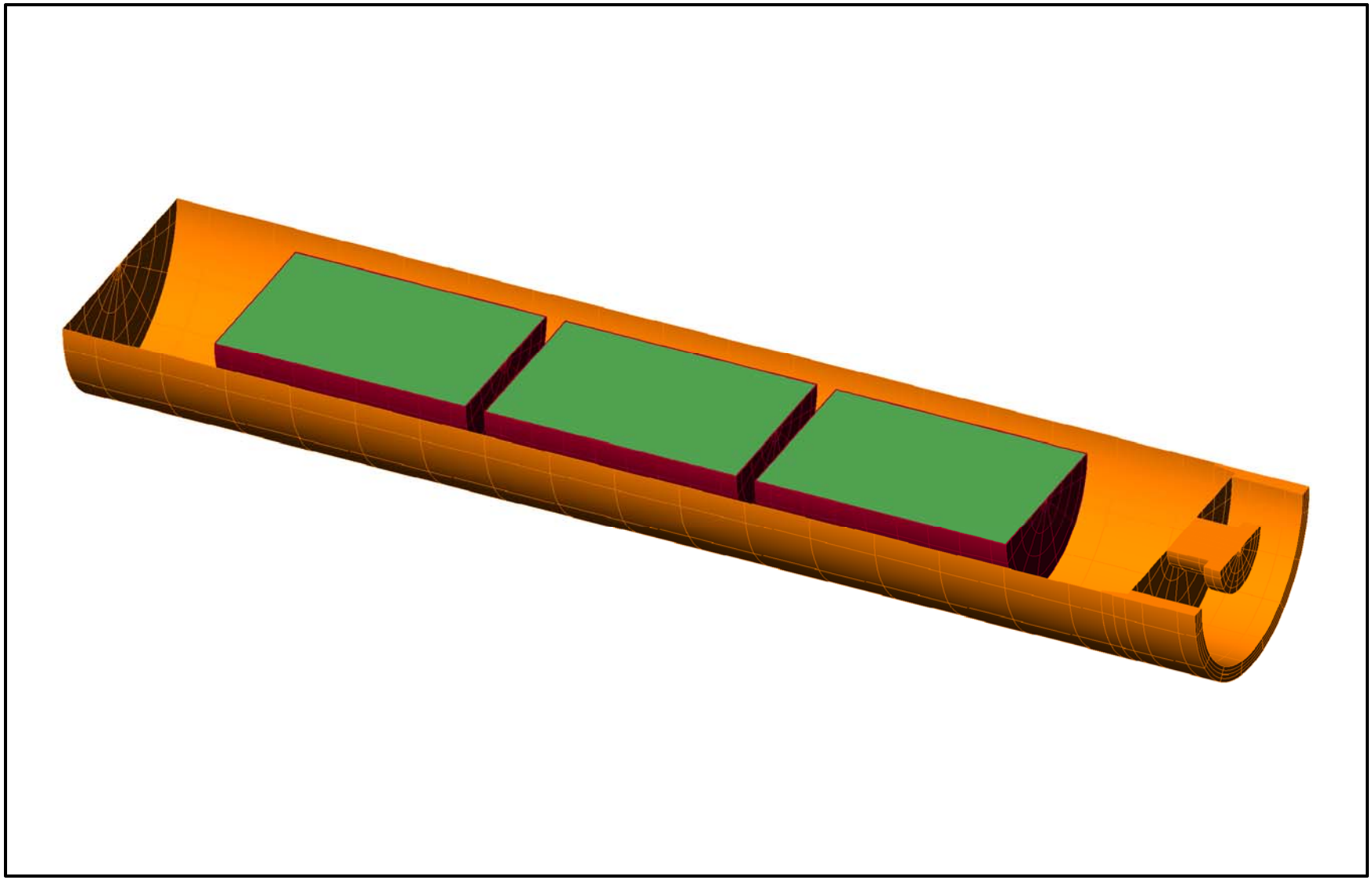

Figure 3.4-6 – RLC Thermal Model with a 30-Gallon Drum Payload

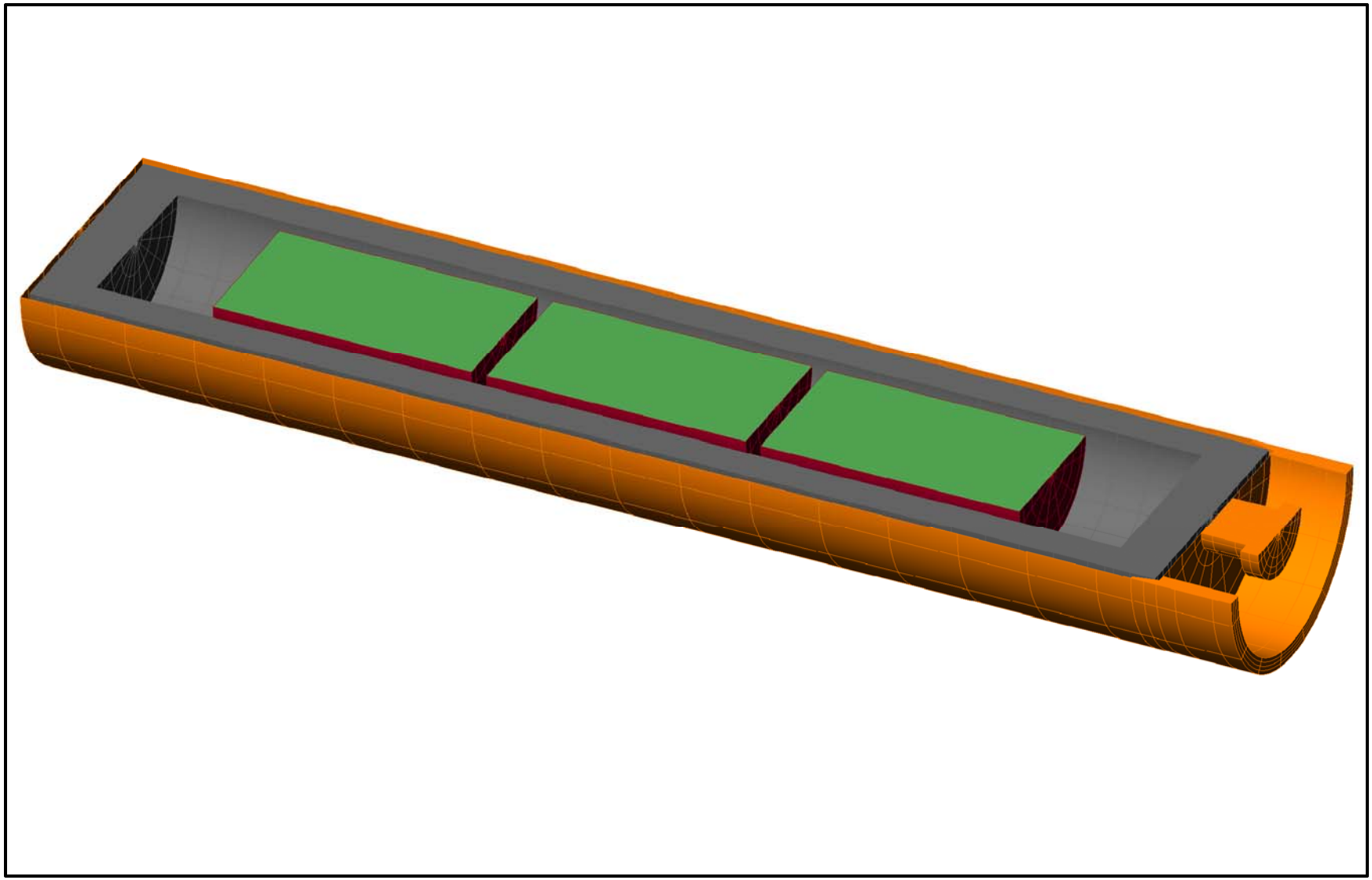

Figure 3.4-7 – NS15 Thermal Model with an Approximately 15-Gallon Drum Payload

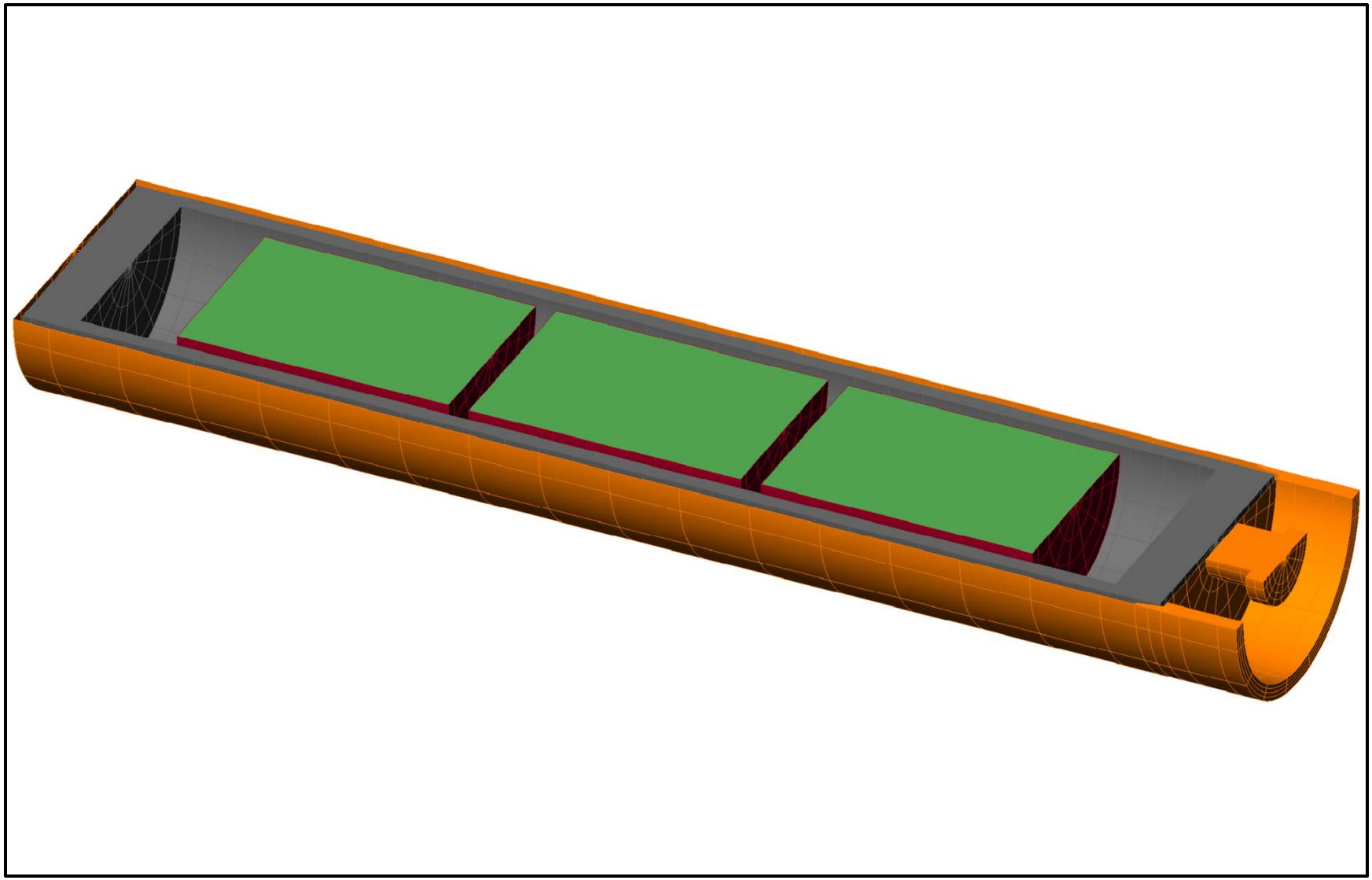

Figure 3.4-8 – NS30 Thermal Model with an Approximately 30-Gallon Drum Payload

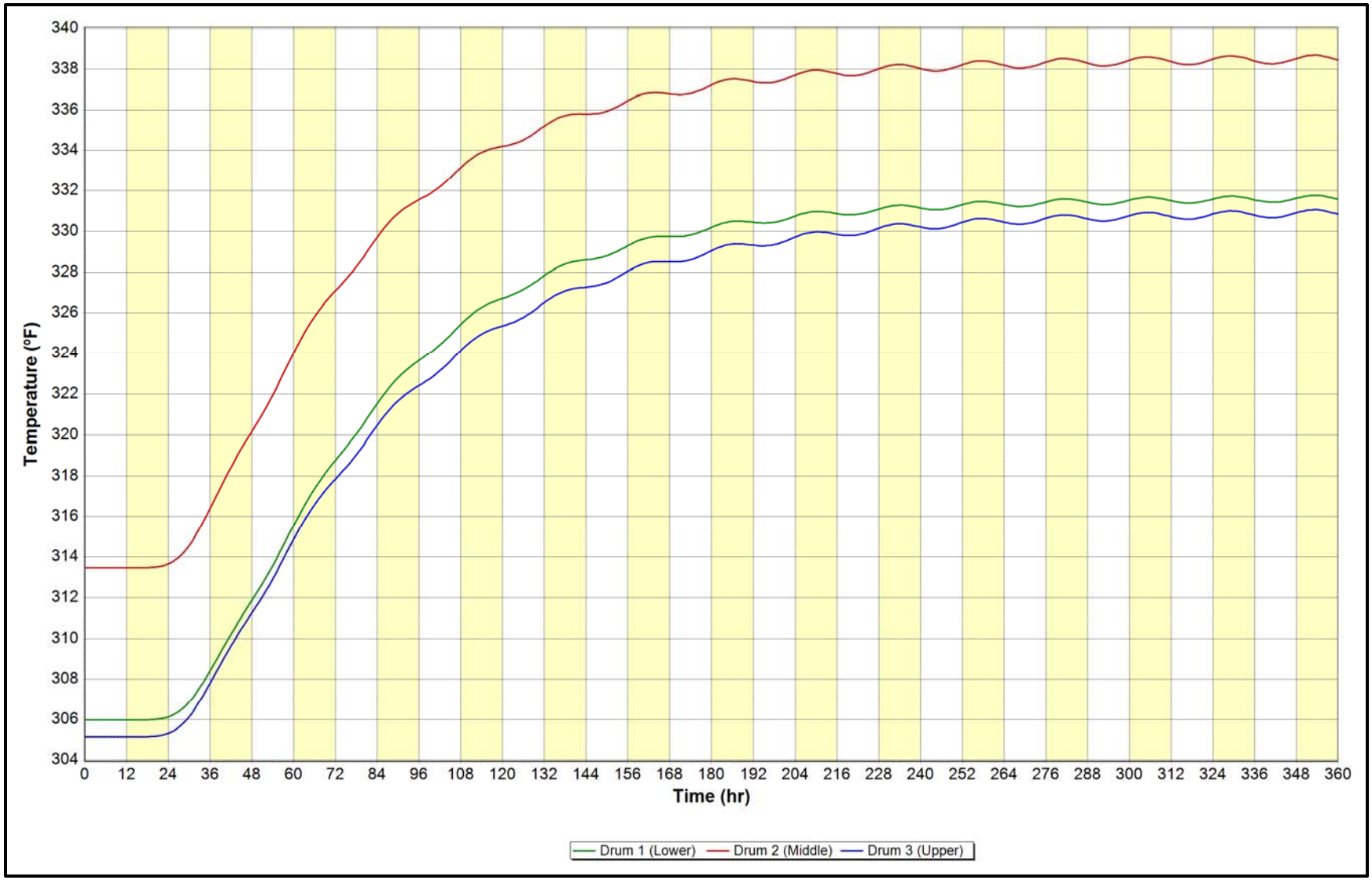

Figure 3.4-9 – NCT Case 1 Maximum Temperature for the Drum Contents Center Nodes; 12 lb/ft³ Waste with 90 Watts Decay Heat

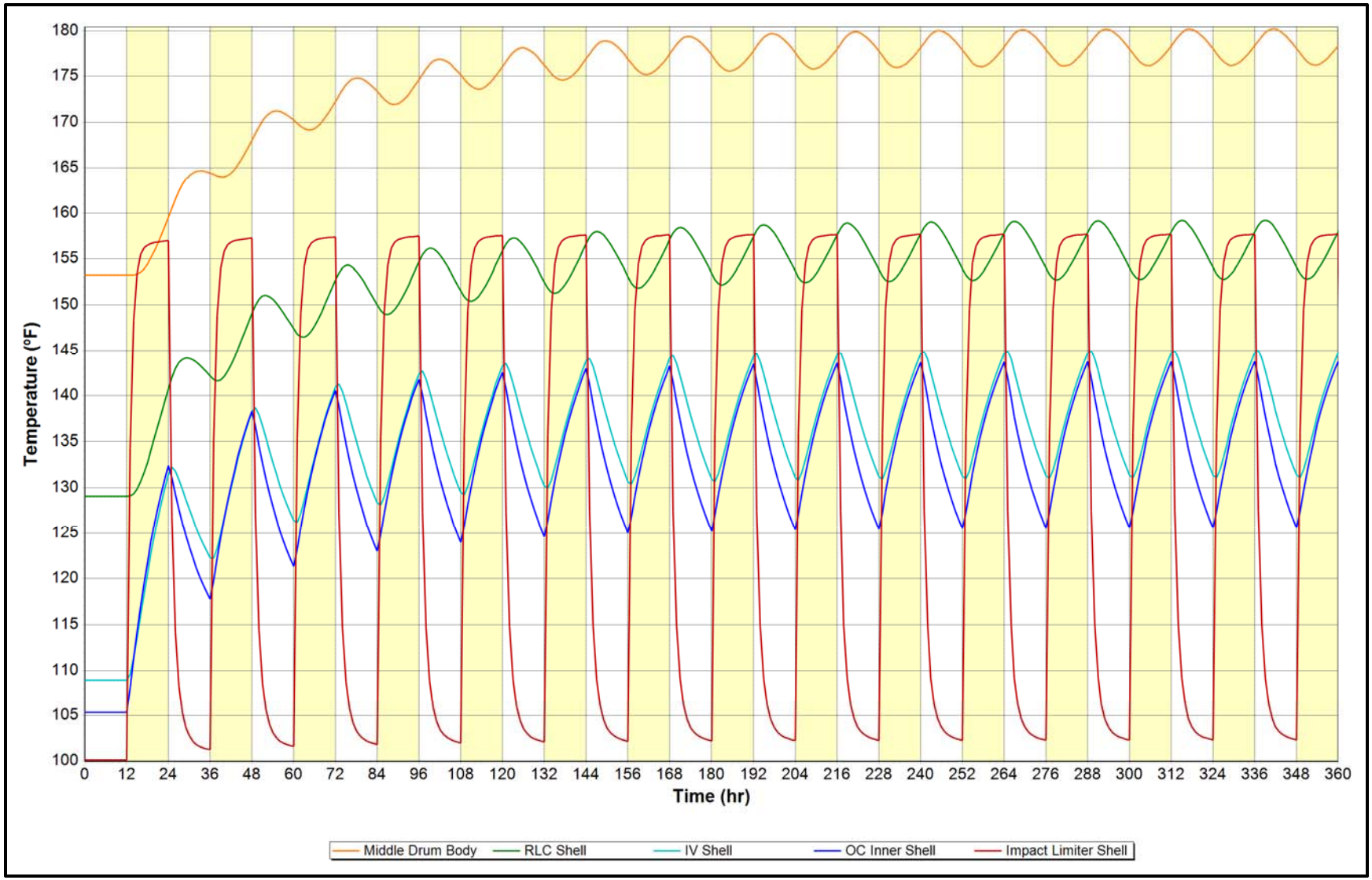

Figure 3.4-10 – NCT Case 1 Transient Temperatures for the Major Package Components; 12 lb/ft³ Waste with 90 Watts Decay Heat

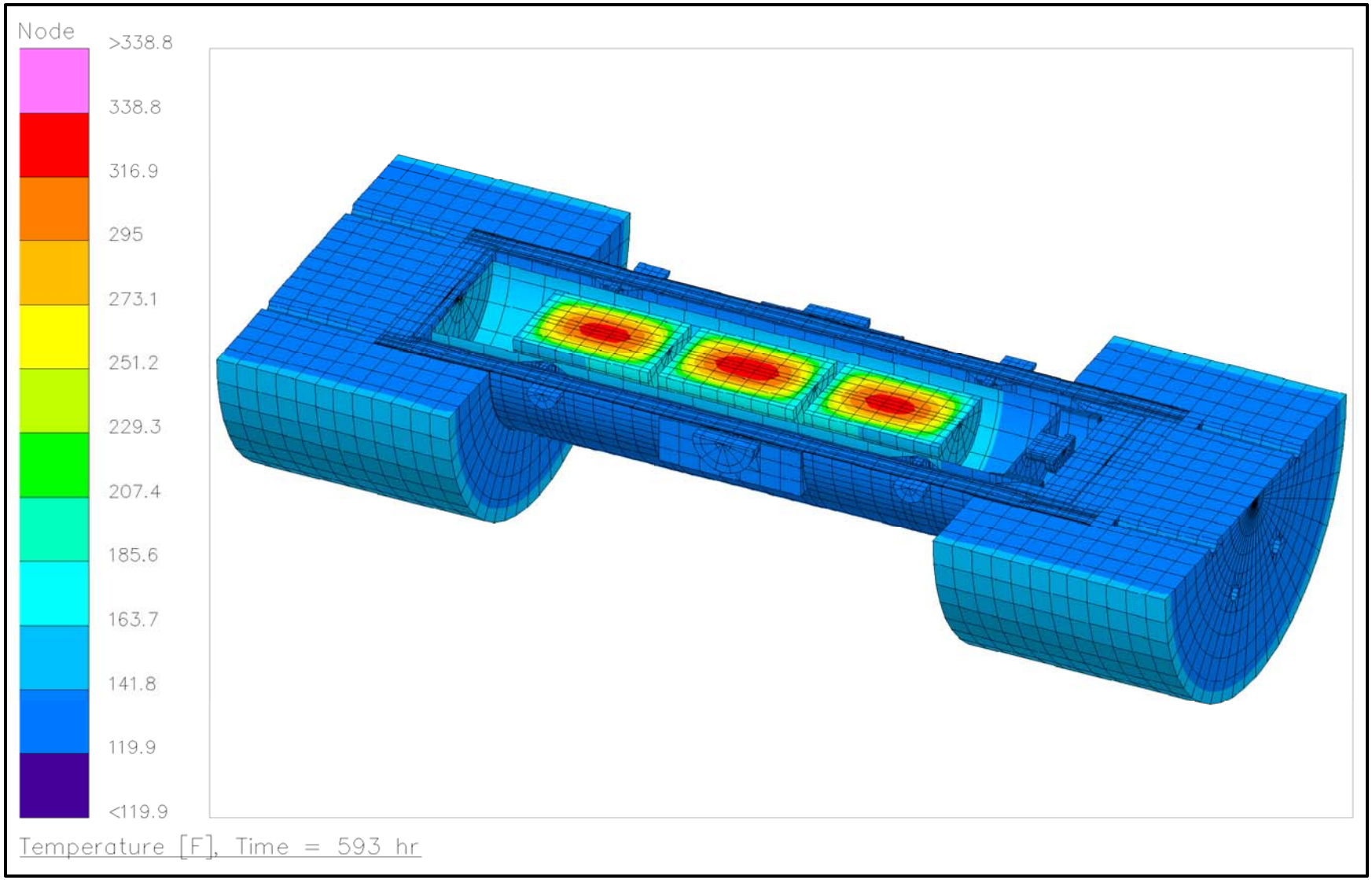

Figure 3.4-11 – NCT Case 1 – Package with RLC; 12 lb/ft³ Waste with 90 Watts Decay Heat and Insolation

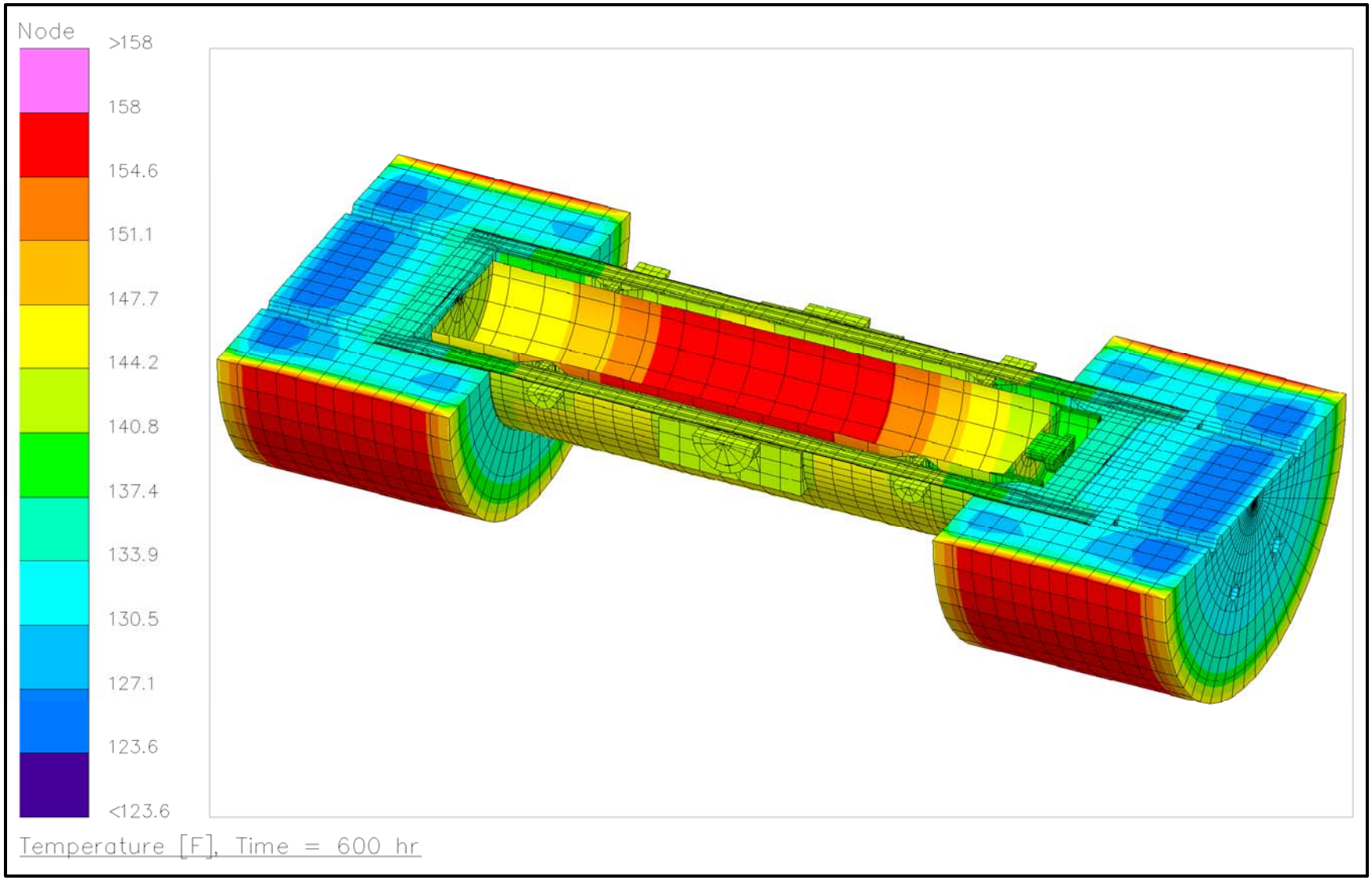

Figure 3.4-12 – NCT Case 1 – Package with RLC; 12 lb/ft³ Waste with 90 Watts Decay Heat and Insolation (Drums Hidden)

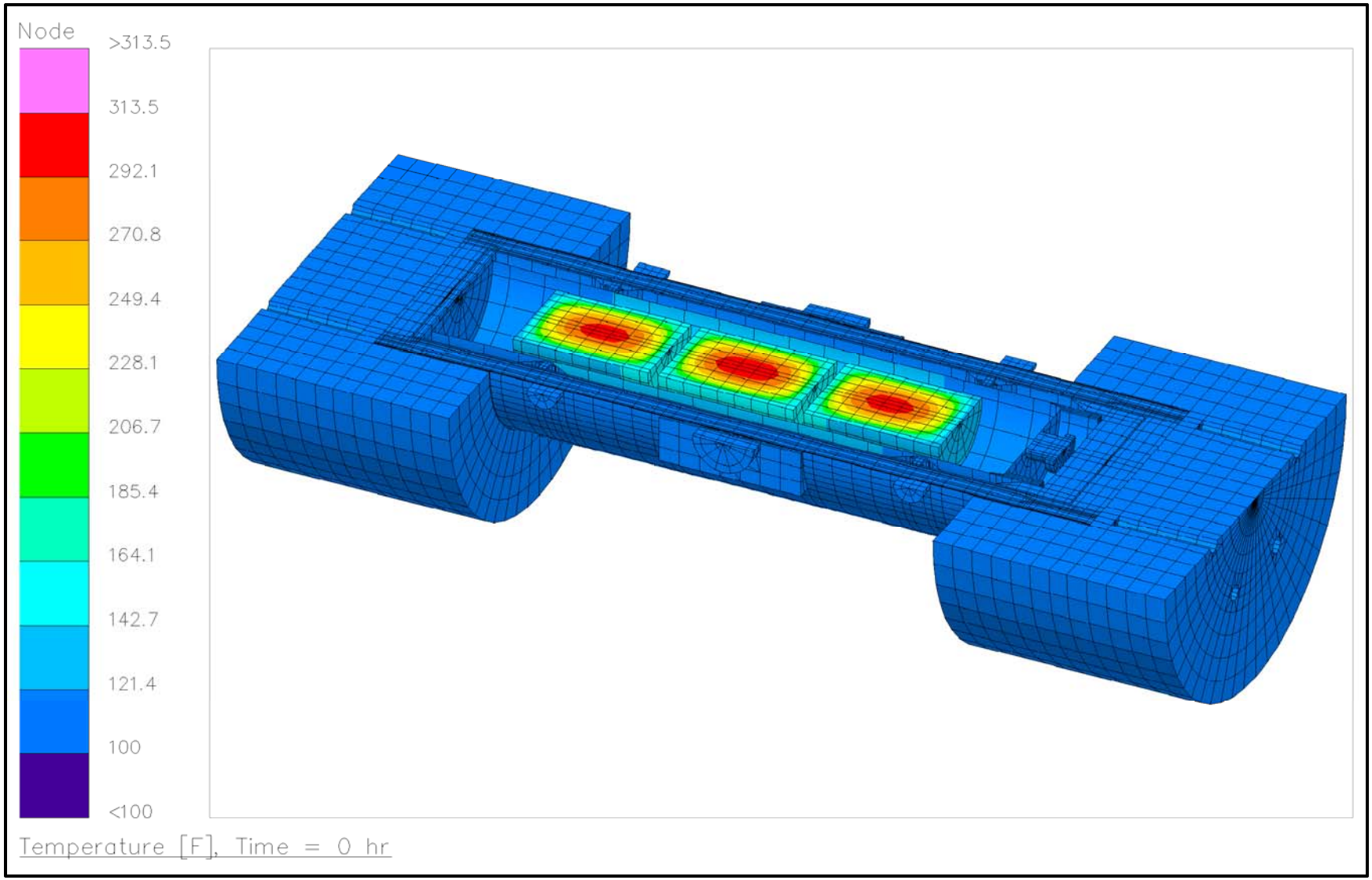

Figure 3.4-13 – NCT Case 1 – Package with RLC; 12 lb/ft³ Waste with 90 Watts Decay Heat and No Insolation

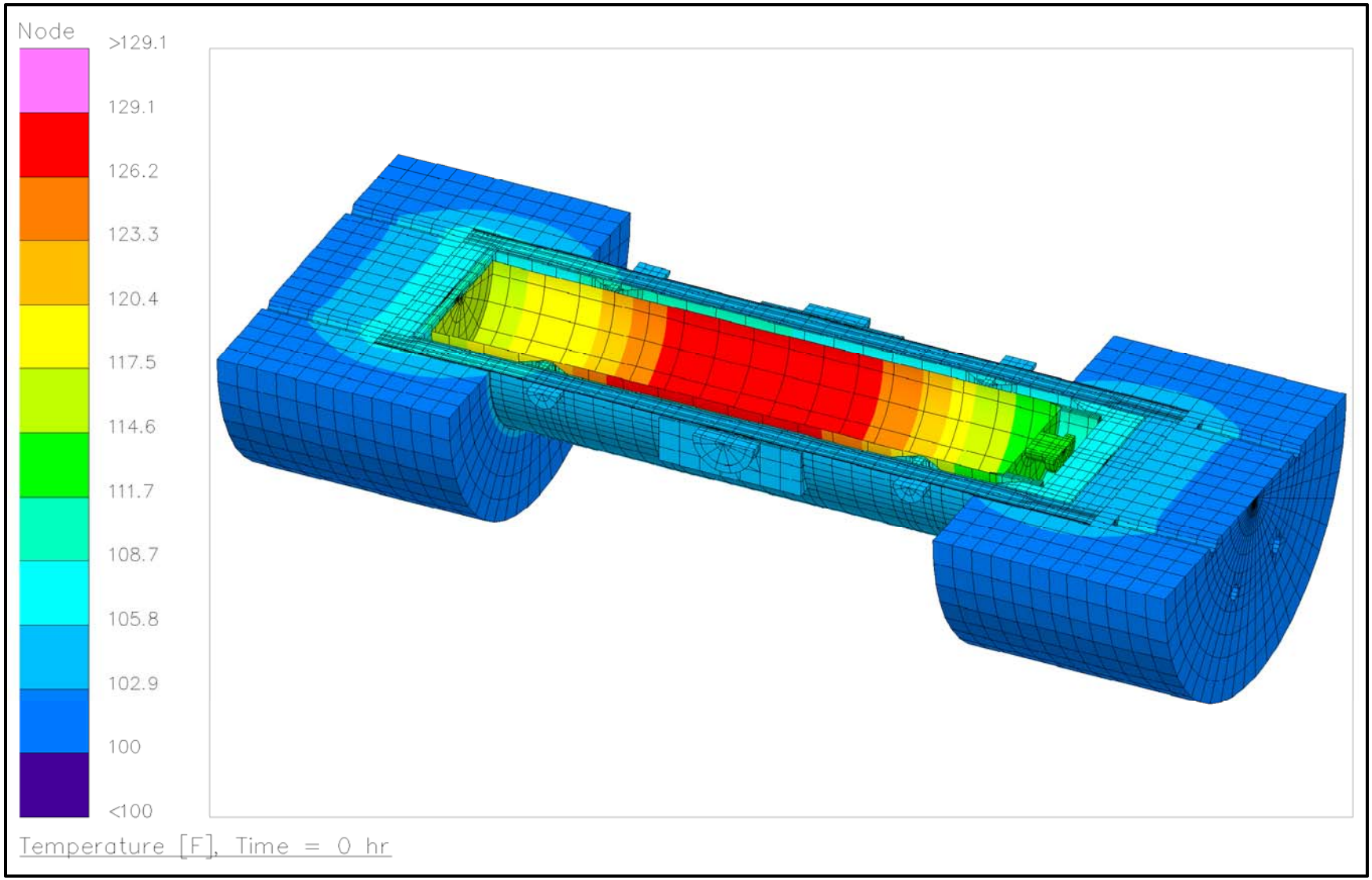

Figure 3.4-14 – NCT Case 1 – Package with RLC; 12 lb/ft³ Waste with 90 Watts Decay Heat and No Insolation (Drums Hidden)

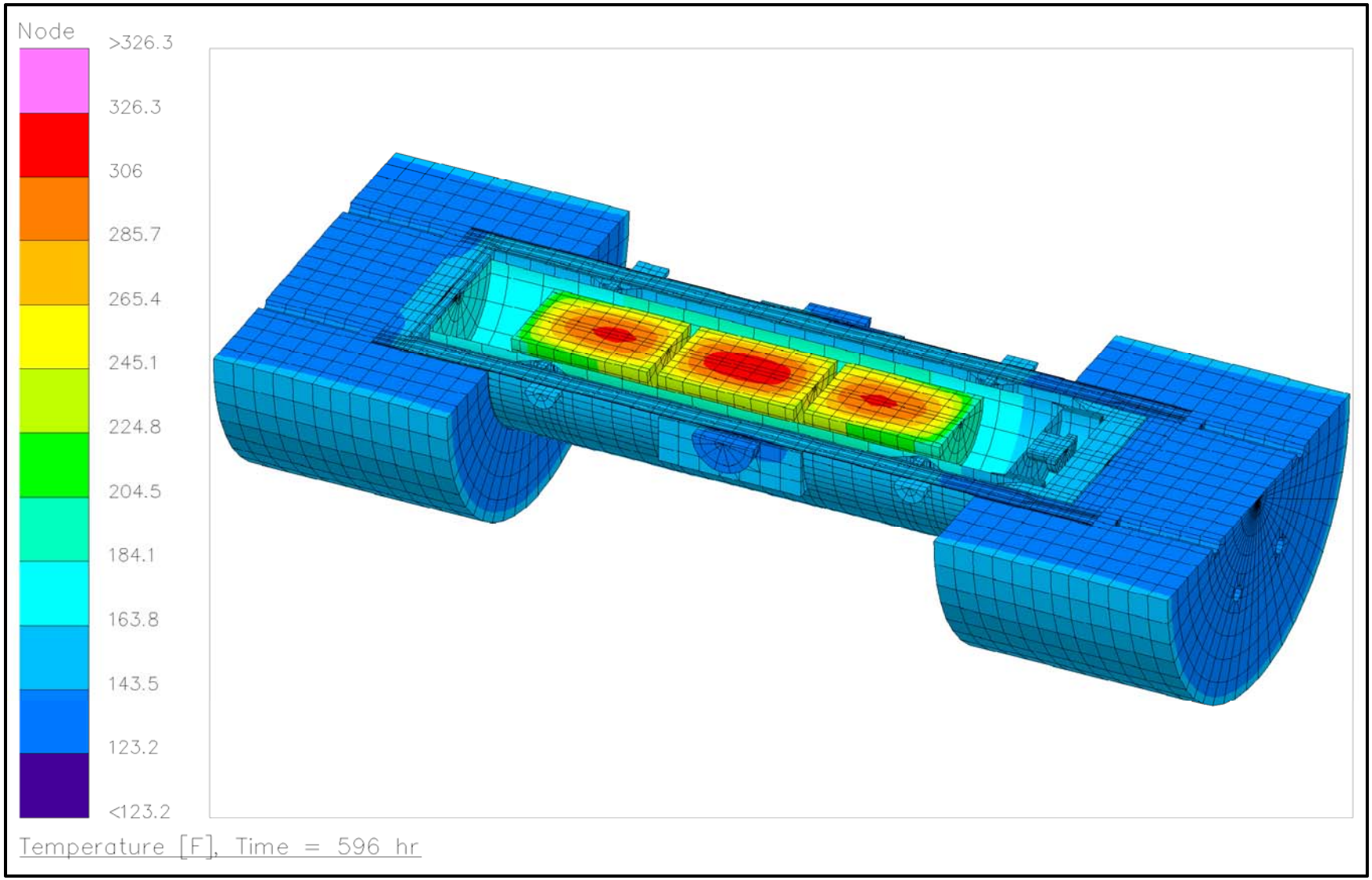

Figure 3.4-15 – NCT Case 1 – Package with RLC; 100 lb/ft³ Waste with 270 Watts Decay Heat and Insolation

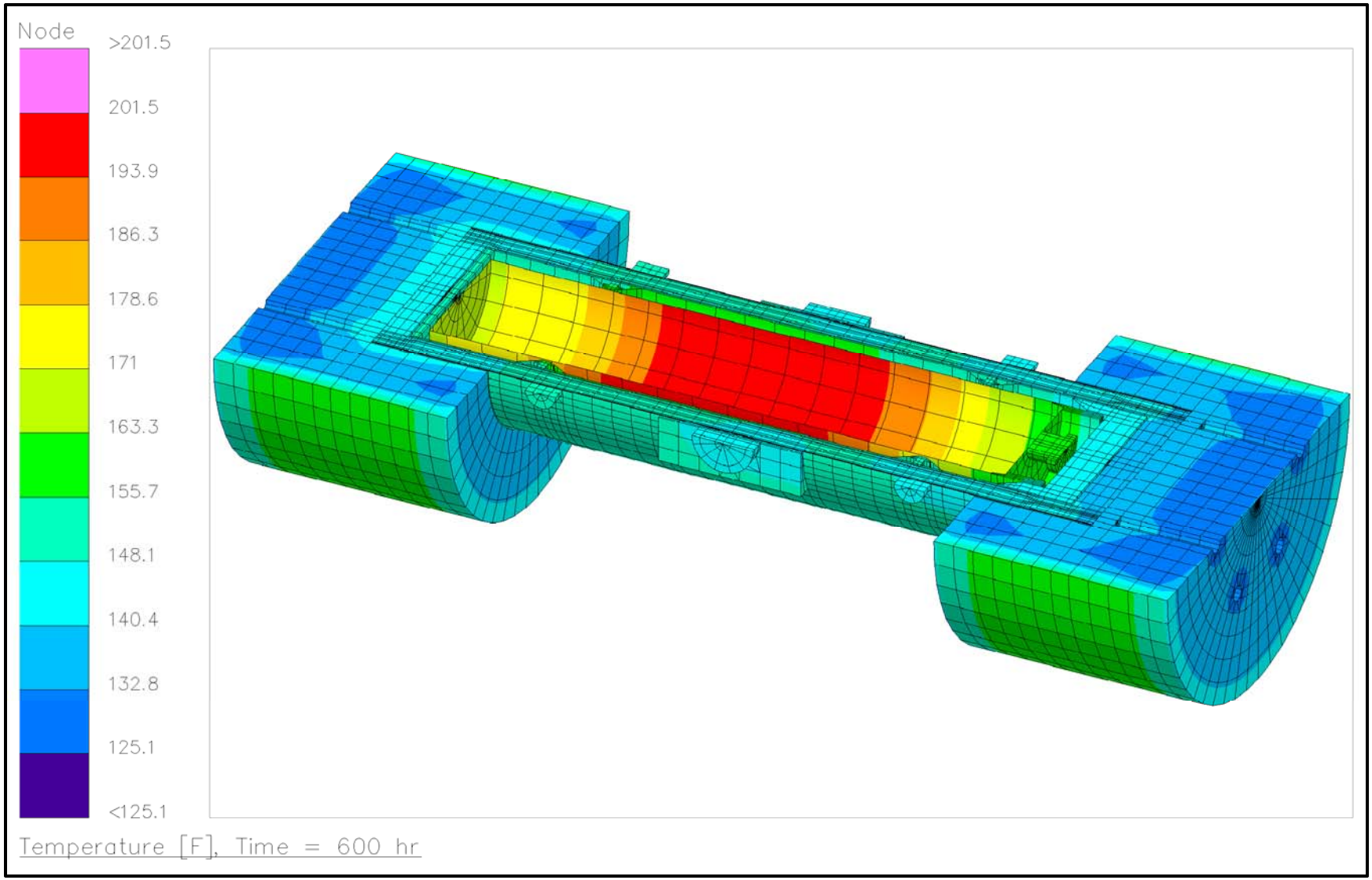

Figure 3.4-16 – NCT Case 1 – Package with RLC; 100 lb/ft³ Waste with 270 Watts Decay Heat and Insolation (Drums Hidden)

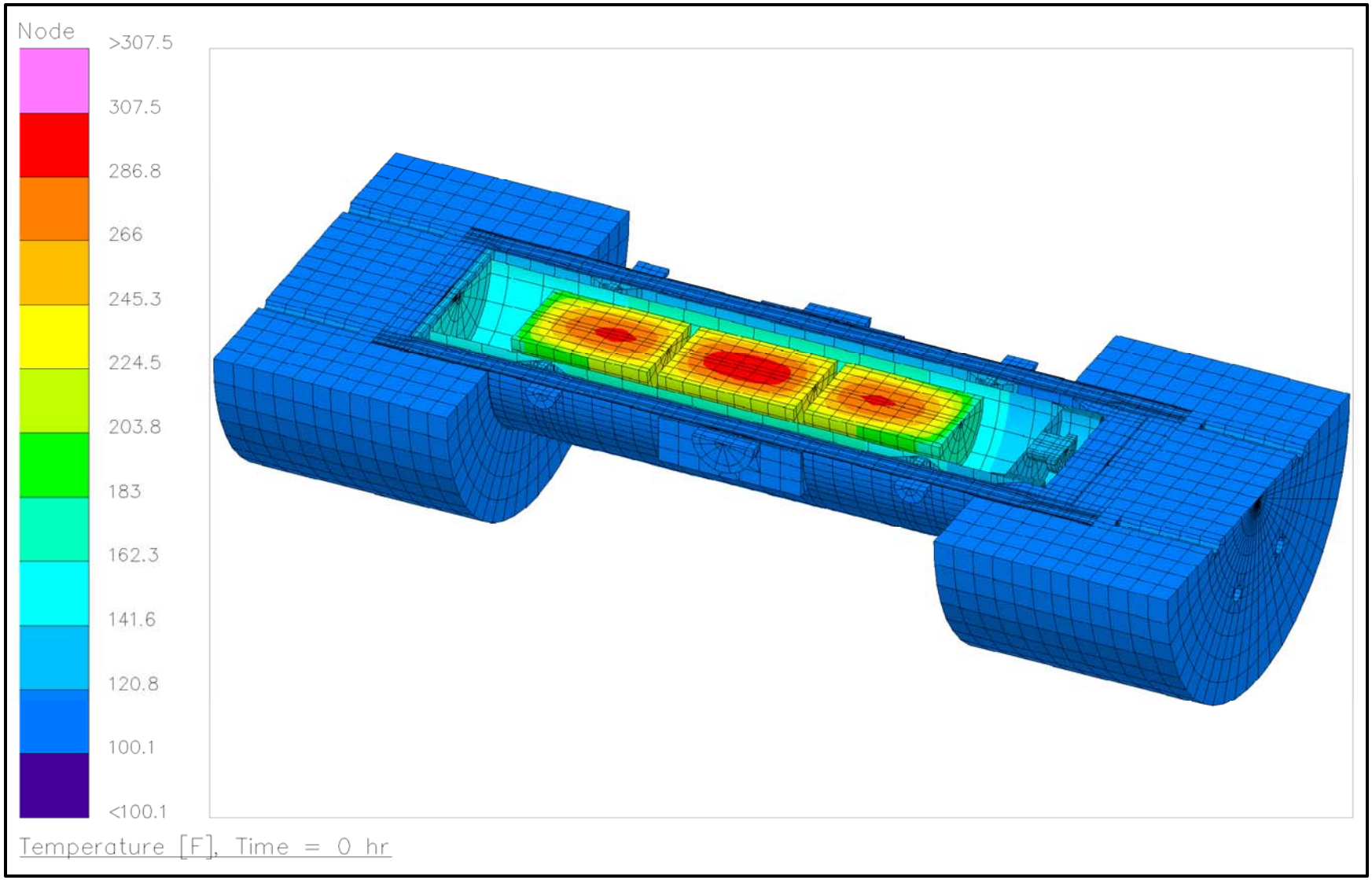

Figure 3.4-17 – NCT Case 1 – Package with RLC; 100 lb/ft³ Waste with 270 Watts Decay Heat and No Insolation

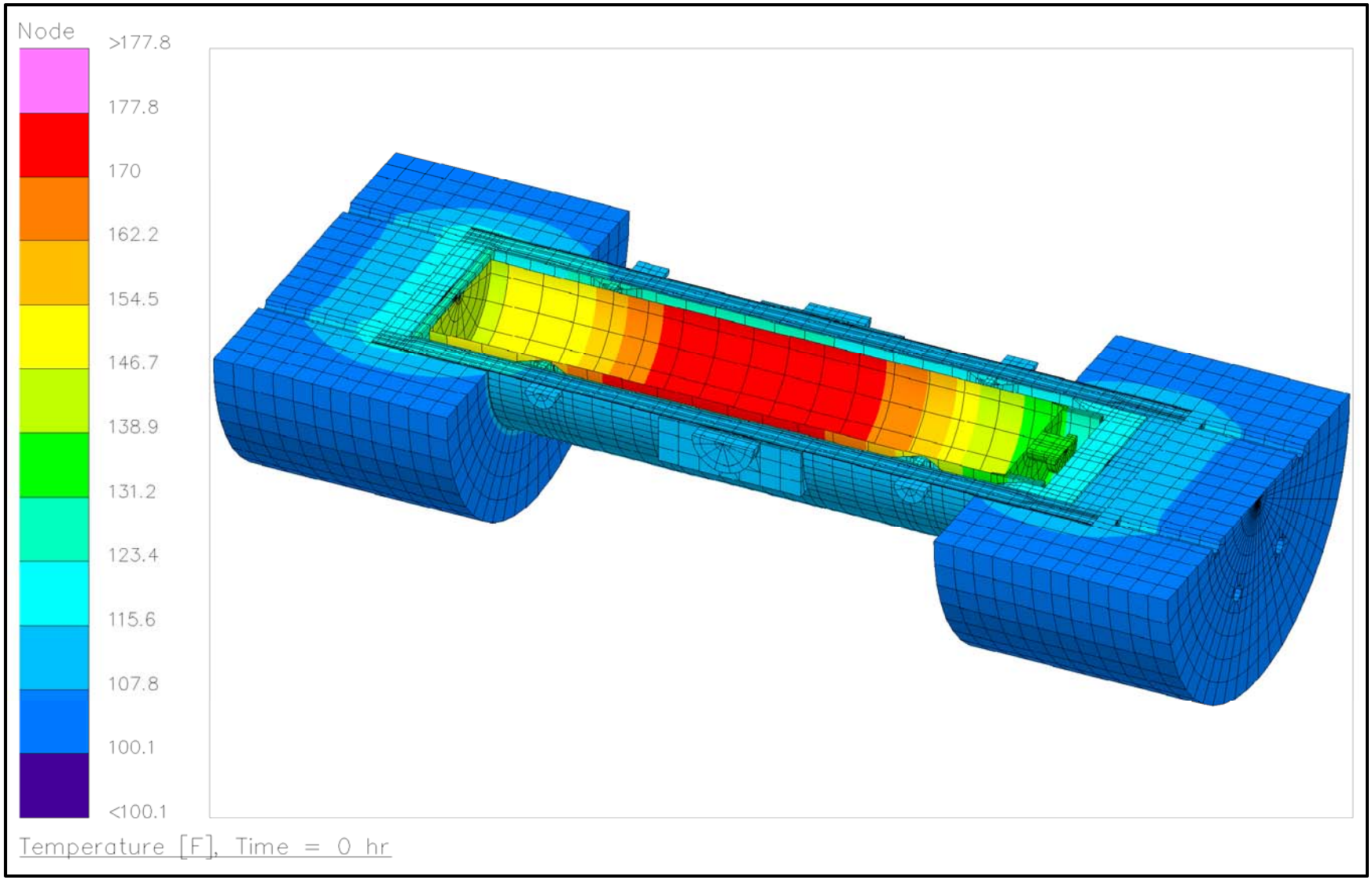

Figure 3.4-18 – NCT Case 1 – Package with RLC; 100 lb/ft³ Waste with 270 Watts Decay Heat and No Insolation (Drums Hidden)

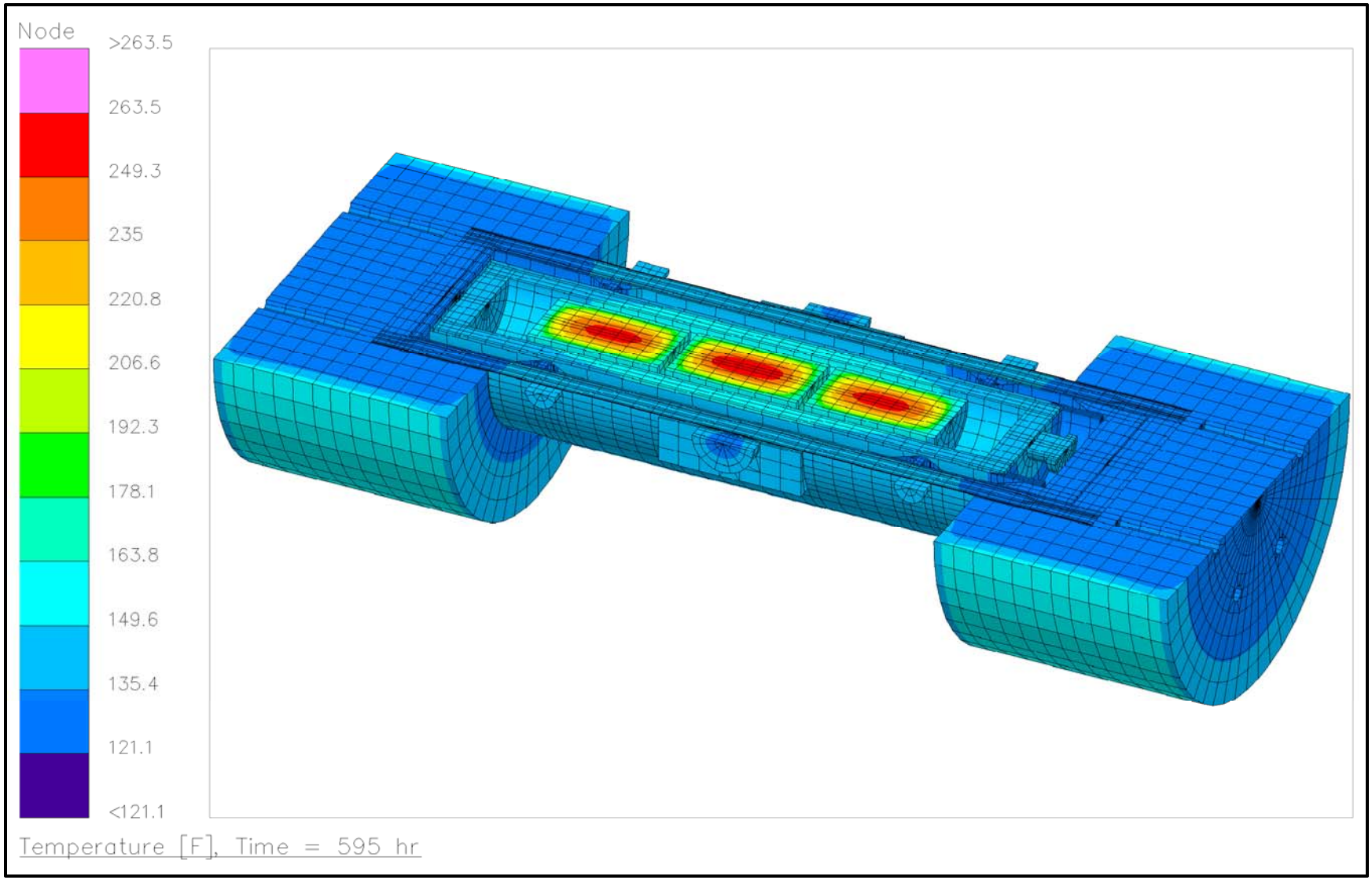

Figure 3.4-19 – NCT Case 2 – Package with NS15; 12 lb/ft³ Waste with 50 Watts Decay Heat and Insolation

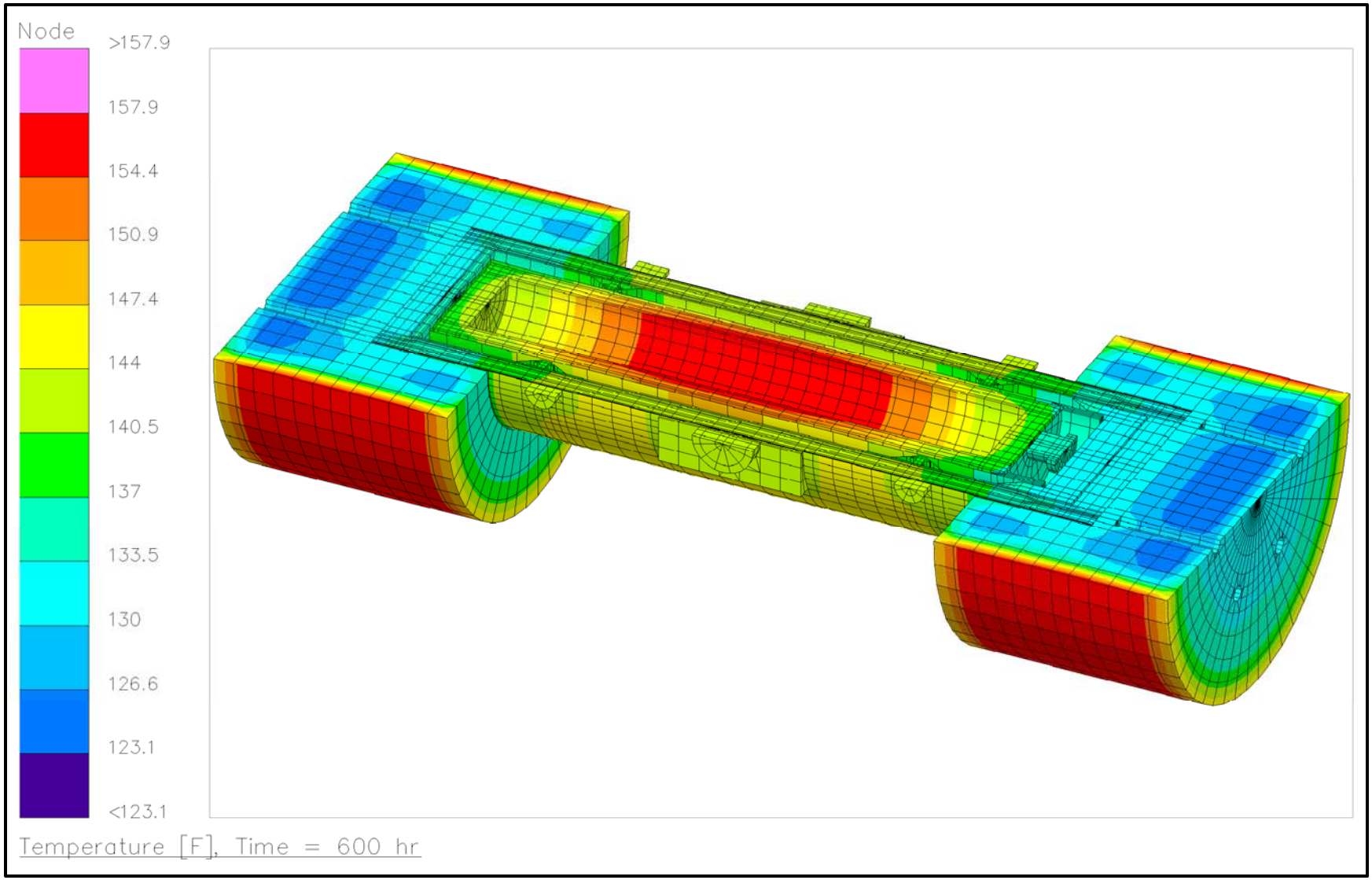

Figure 3.4-20 – NCT Case 2 – Package with NS15; 12 lb/ft³ Waste with 50 Watts Decay Heat and Insolation (Drums Hidden)

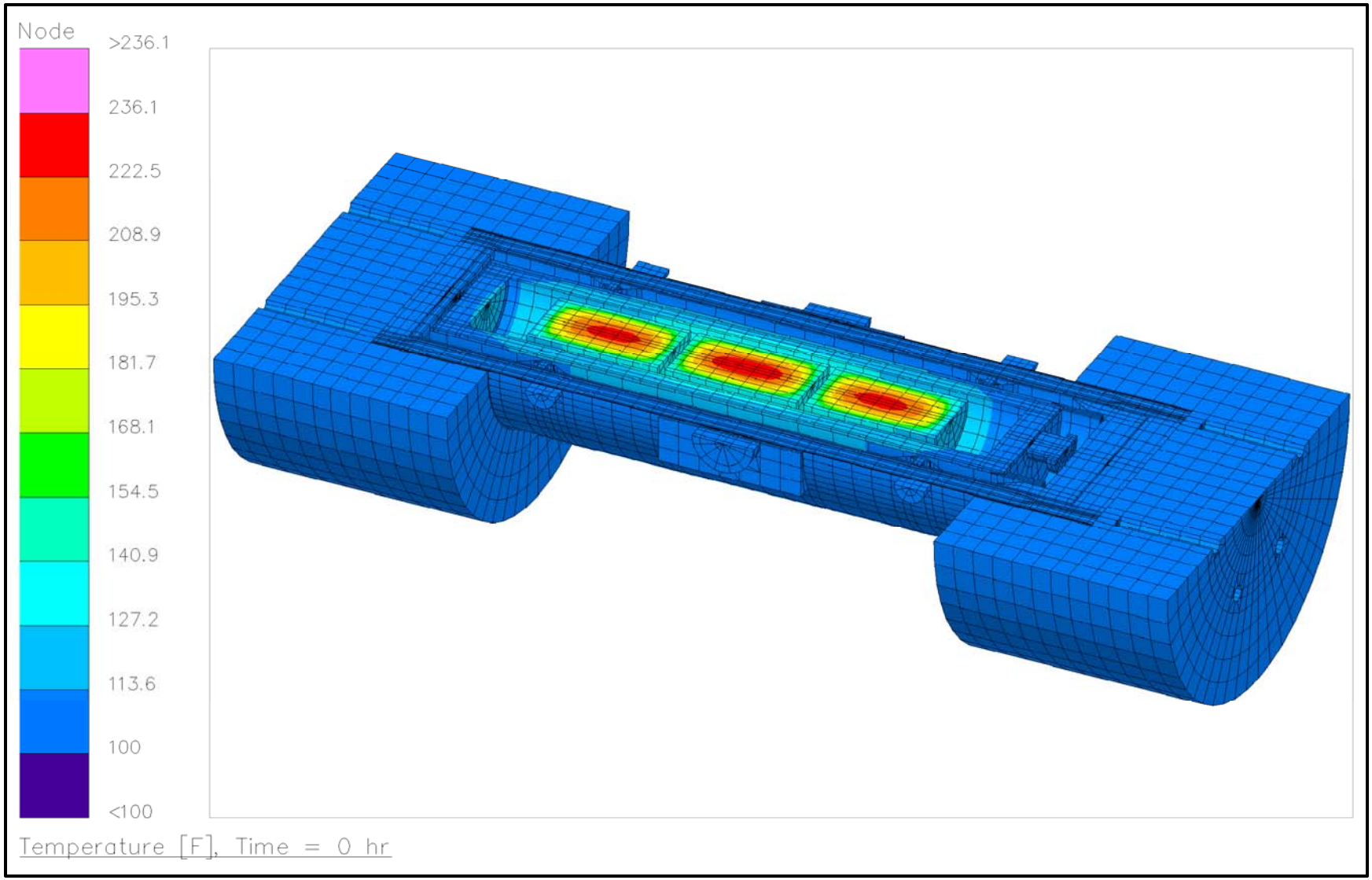

Figure 3.4-21 – NCT Case 2 – Package with NS15; 12 lb/ft³ Waste with 50 Watts Decay Heat and No Insolation

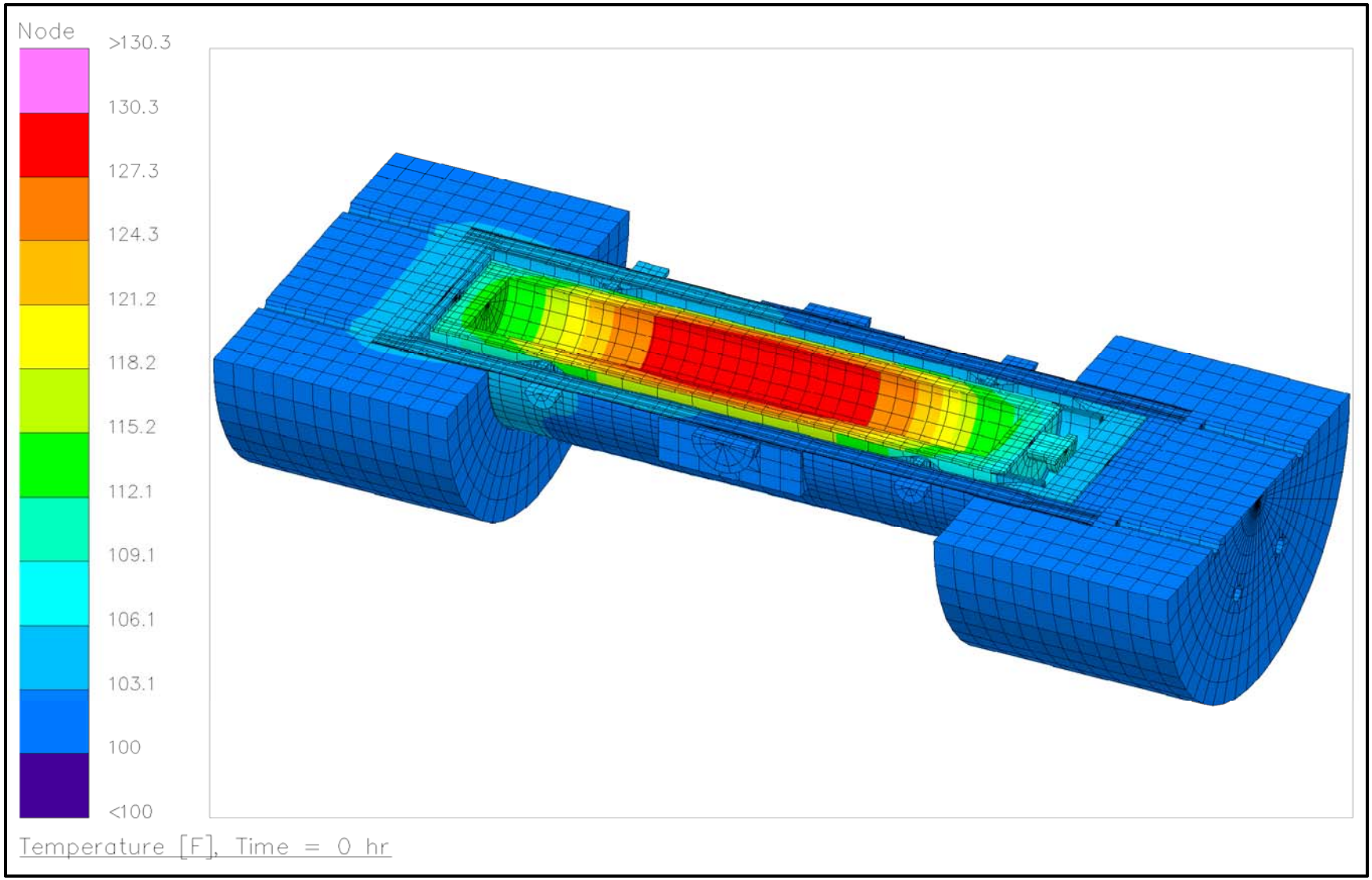

Figure 3.4-22 – NCT Case 2 – Package with NS15; 12 lb/ft³ Waste with 50 Watts Decay Heat and No Insolation (Drums Hidden)

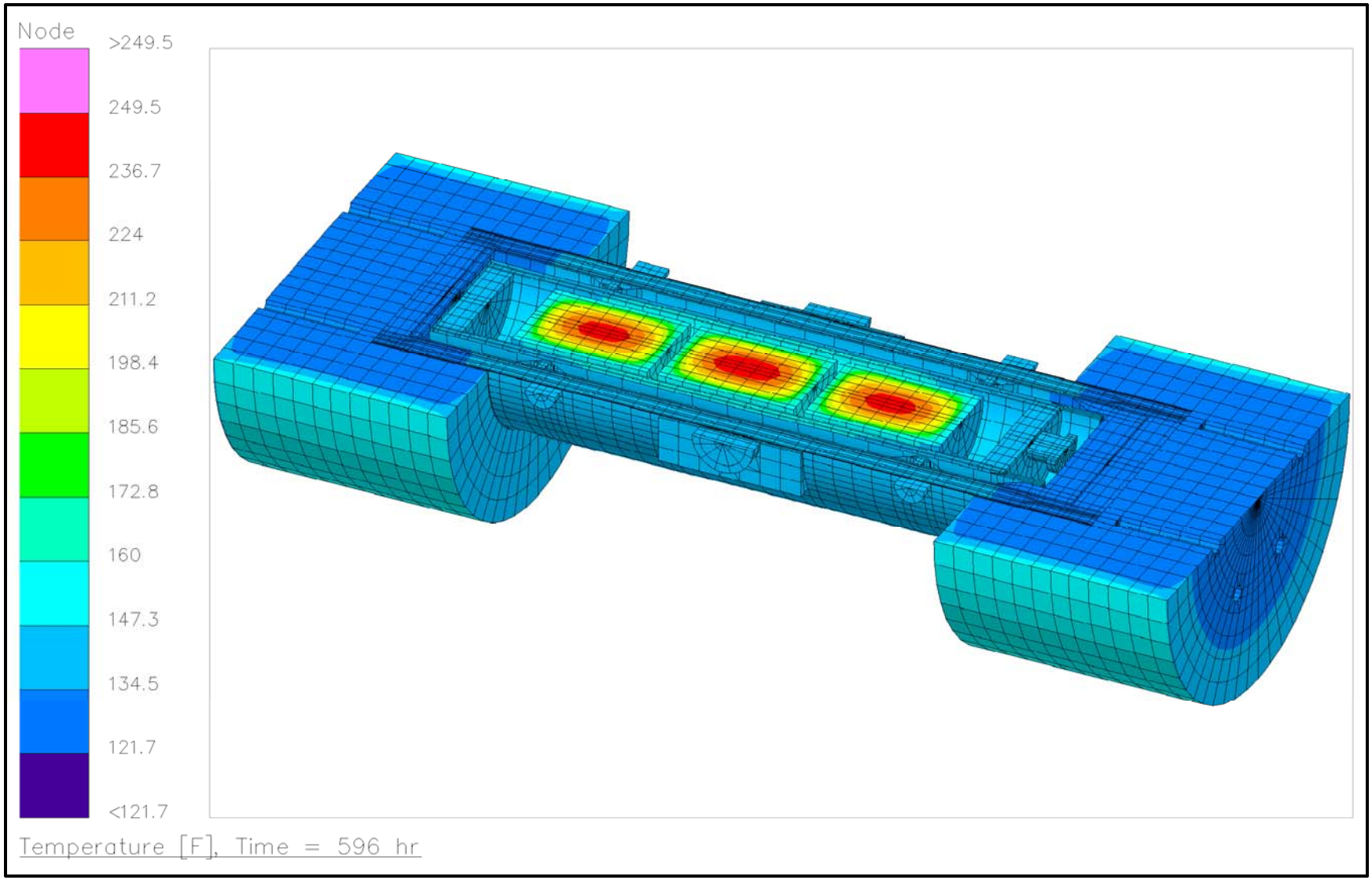

Figure 3.4-23 – NCT Case 3 – Package with NS30; 12 lb/ft³ Waste with 50 Watts Decay Heat and Insolation

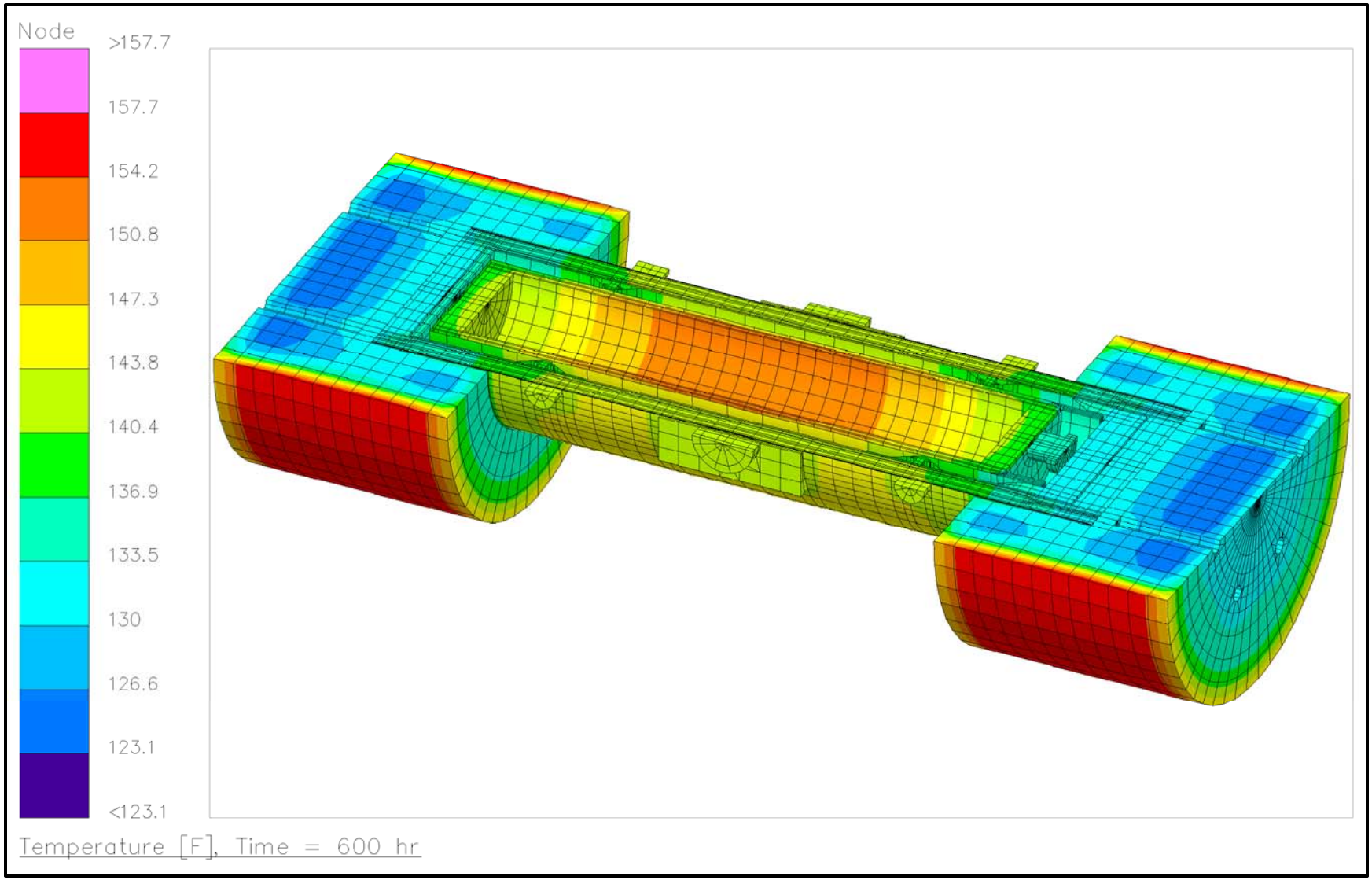

Figure 3.4-24 – NCT Case 3 – Package with NS30; 12 lb/ft³ Waste with 50 Watts Decay Heat and Insolation (Drums Hidden)

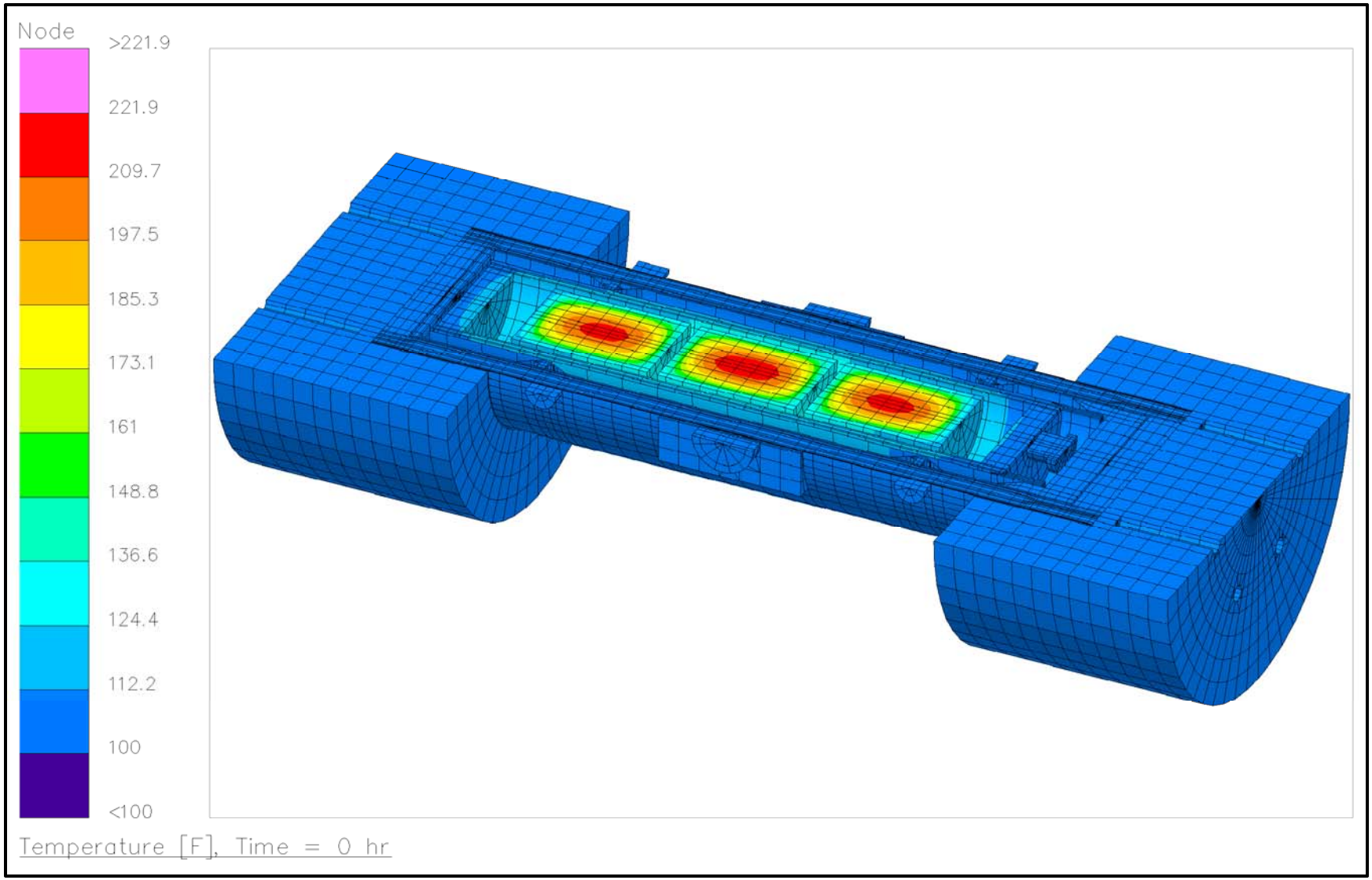

Figure 3.4-25 – NCT Case 3 – Package with NS30; 12 lb/ft³ Waste with 50 Watts Decay Heat and No Insolation

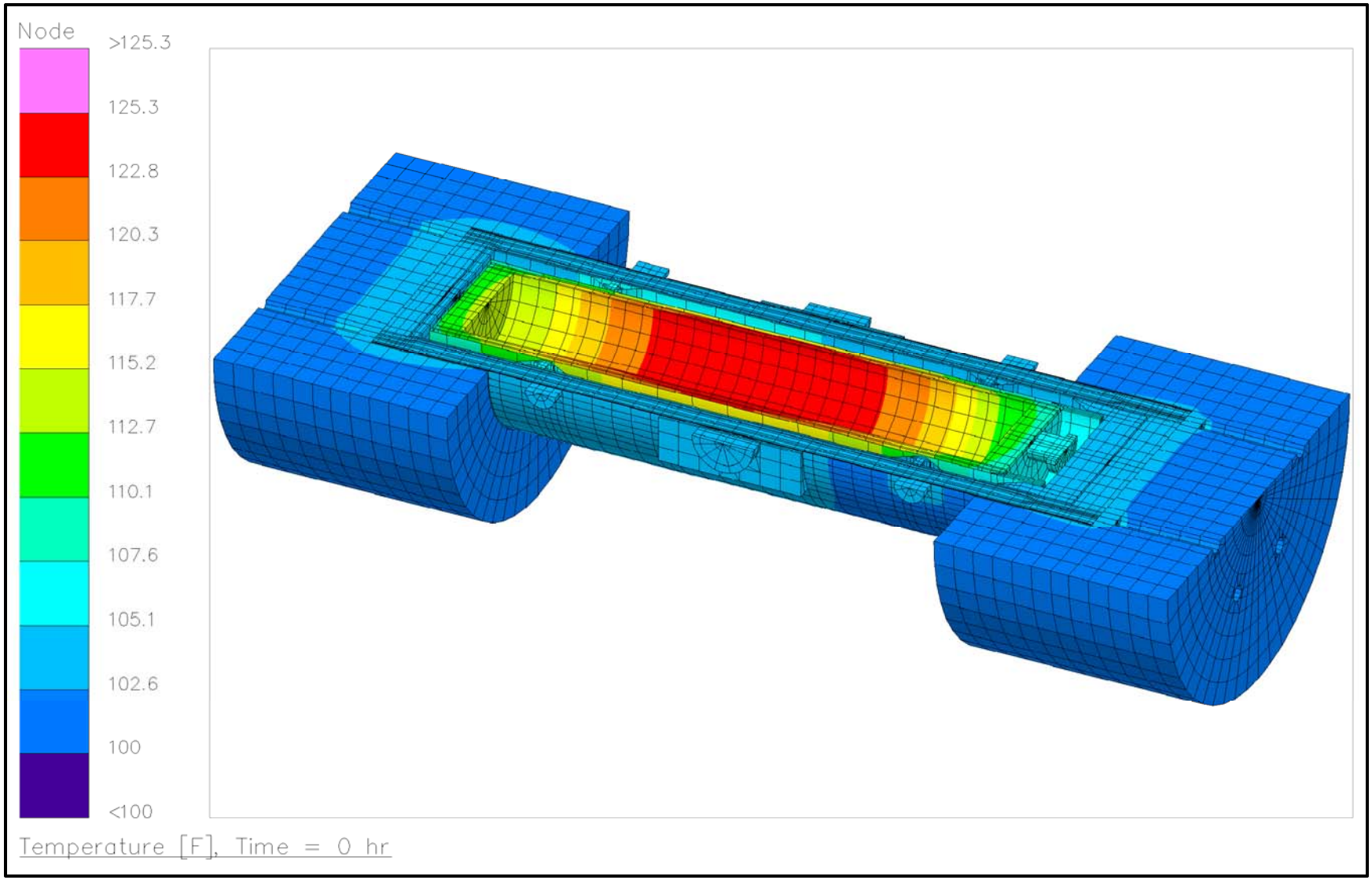

Figure 3.4-26 – NCT Case 3 – Package with NS30; 12 lb/ft³ Waste with 50 Watts Decay Heat and No Insolation (Drums Hidden)

3.5 Thermal Evaluation for Hypothetical Accident Conditions

This section presents the thermal analyses of the RH-TRU 72-B package for the hypothetical accident condition (HAC) specified in 10 CFR §71.73(c)(4)[1]. The initial temperature distribution within the package prior to the HAC fire is based on an ambient temperature of 100 ºF in still air, as defined in 10 CFR §71.73(b), and includes the "12-hour on/12-hour off" insolation cycle that was used for NCT. The pre-fire transient analysis is continued for sufficient time until a pseudo-steady state condition is achieved (600 hours, i.e., 25 days). To determine the effect of the HAC fire event, the package is then analytically exposed to a 1,475 ºF radiation and forced convection environment for 30 minutes. Finally, the thermal boundary is returned to the 100 ºF ambient air condition and again continues the "12-hour on/12-hour off" insolation cycle that was used for the pre-fire condition. The post-fire transient analysis is continued for sufficient time until a pseudo-steady state condition is once again achieved (ending time is 1,200 hours).

Two HAC fire analyses are performed for each case: 1) the 30-minute fire starts immediately following a "12-hour on" insolation cycle, and 2) the 30-minute fire starts 30-minutes before the start of the next "12-hour on" insolation cycle. The summary tables in this section report the highest temperatures for each payload and packaging component considering each of these two bounding analyses.

3.5.1 Thermal Model

3.5.1.1 Analytical Model

The analytical model used to evaluate the HAC fire event is essentially identical to the model described in Section 3.4.1.1, *Analytical Model*, for NCT. The notable exception is the application of 30-foot free drop and 1-meter puncture drop damage to the impact limiters. In addition, the HAC thermal model addresses the effect of foam thermal degradation and resulting external char layer. Damage from these two HAC drop scenarios and char reduction of the polyurethane foam are included in a single model, with an HAC analysis performed for each of the four payload configurations. Further discussion of these damage conditions is provided in Section 3.5.2, *Package Conditions and Environment*. The HAC thermal model is illustrated in Figure 3.5-1 and Figure 3.5-2.

If the package's exterior surfaces are optionally painted, the relatively high emissivity of paint ($\varepsilon \geq 0.90$[2]) compared to that of bare stainless steel ($\varepsilon = 0.25$[3]) would briefly result in higher heat flow into the package during the HAC fire event, but the net effect is negligible since the paint burns away very shortly after the start of the fire. If the packaging's exterior surfaces are

[1] Title 10, Code of Federal Regulations, Part 71 (10 CFR 71), *Packaging and Transportation of Radioactive Material*, 01-01-14 Edition.

[2] Omega Engineering, Inc., Technical Reference Section, *Table of Total Emissivity*; minimum emissivity for paints at 75 ºF (see http://www.omega.com/temperature/Z/pdf/z088-089.pdf).

[3] *Emissivity of Metal Surfaces*, Report No. 2-2623-2-RF-C86-349, August 21, 1986; lower-bound emissivity data for the average of three specimens for "As Received" ASTM A240, Type 304, stainless steel.

optionally abrasively blasted, the increased emissivity from abrasive-blasting ($\varepsilon = 0.40$[4]) is still well below the required fire event emissivity of 0.8 per 10 CFR §71.73(c) and, therefore, is not limiting.

3.5.1.2 Test Model

HAC thermal testing was not performed for the RH-TRU 72-B package. However, thermal tests to evaluate the polyurethane foam used in the impact limiters were performed as part of the NuPac 125-B cask certification[5]. Results of these tests are documented in Appendix 3.6.3, *Polyurethane Foam Performance Tests*. These tests, covering a range of boundary condition assumptions, demonstrate three major findings:

1. Foam char under direct flame impingement on exposed foam amounts to approximately 4 inches, completely consistent with thermal modeling assumptions. Importantly, these tests were conducted with a flame temperature of approximately 1,800 ºF, significantly higher than the regulatory requirement of 1475 ºF.
2. Following termination of the impinging flame, the combustion process is self-extinguishing, regardless of thermal boundary conditions in the tests.
3. Minor tears or ruptures of the energy absorbing impact limiter shells (up to approximately 3/4-inch) are of no thermal consequence because the intumescent character of the foam char tends to seal and heal the opening in the impact limiter shell by the extrusion of a char "plug".

3.5.2 Package Conditions and Environment

To model the HAC fire environment, the entire package model is surrounded by a hemispherical surface with an assigned emissivity of 0.9 and temperature of 1,475 ºF per 10 CFR §71.73(c)(4). An external emissivity of 0.8 and forced convection are applied to all exposed package external surfaces. Forced convection coefficients are determined in Appendix 3.6.1.3, *Calculation of Forced Convection Coefficients for HAC*, and range between 1.40 and 2.05 Btu/hr-ft^2-ºF; for conservatism, an upper-bound convection coefficient of 2.1 Btu/hr-ft^2-ºF is applied.

Two damage conditions, further discussed in subsequent paragraphs, are imposed on the thermal model for the HAC thermal evaluation: 1) damage to the impact limiters from a 30-foot free drop, and 2) damage to the impact limiters from a 1-meter puncture drop.

The first damage condition is imposed by the 30-foot side drop. Compared to the HAC end and corner drop orientations, the HAC side drop orientation damages both impact limiters nearer to the OC and IV containment seals. As summarized in Table 2.10.3-9 from Appendix 2.10.3, *Drop Impact Evaluation Results*, the resulting side drop deformation is 11.518 inches, corresponding to a minimum residual centerline thickness of 5.388 inches. The HAC package thermal model with side drop damage is illustrated in Figure 3.5-1 and Figure 3.5-2.

---

[4] *Emissivity of Metal Surfaces*, Report No. 2-2623-2-RF-C86-349, August 21, 1986; lower-bound emissivity data for the average of three specimens each for "Commercial Sand Blast" and "White Metal Blast" ASTM A240, Type 304, stainless steel.

[5] Nuclear Packaging, Inc., *Safety Analysis Report for the NuPac 125-B Fuel Shipping Package*, USNRC Certificate of Compliance 71-9200, U.S. Department of Energy, Washington, D.C.

As discussed earlier in Section 3.2, *Summary of Thermal Properties of Materials*, and summarized in Table 3.2-7, the effective polyurethane foam density is 30 lb/in^3 for the compressed foam in the impact limiter's damaged region that is backed by the OC, 20 lb/in^3 for the compressed foam in the impact limiter's damaged region that is unbacked by the OC, and 11½ lb/in^3 for all other undamaged regions. The polyurethane foam's thermal conductivity in those compressed regions is correspondingly increased.

The second damage condition results from a 1-meter drop onto a 6-inch diameter puncture bar. For the purposes of these analyses, puncture bar damage is conservatively assumed to consist of a 6-inch square hole in the impact limiter side, conservatively projecting completely through the outer cylindrical shell, polyurethane foam, and inner cylindrical shell, as shown in Figure 3.5-2. The puncture bar damage is aligned adjacent to the OC and IV lids to maximize heat transmission from the HAC fire event into the O-ring seal regions. Note also that the puncture bar damage is circumferentially aligned with the side drop-damaged region. Assuming complete penetration through the impact limiter maximizes heat input into the package's O-ring seal regions.

In addition to the free drop and puncture damage, a prescribed thickness of the impact limiter's outermost foam is conservatively assumed to be consumed prior to the start of the HAC fire event. Based on a series of thermal performance testing conducted by the polyurethane foam vendor, a foam density of 10 lb/in^3 (i.e., the nominal design foam density of 11½ lb/in^3 less the 15% fabrication tolerance) will char to a depth of 3.3 inches after 30 minutes of exposure to the HAC fire event.[6] This predicted char depth is consistent with the foam loss observed from a series of experimental tests (see Appendix 3.6.3, *Polyurethane Foam Performance Tests*). A minimum foam thickness of 4 inches is required to prevent the foam backside temperature from exceeding 300 ºF after 30 minutes of exposure. An initial foam thickness of 5 inches or greater at this density will prevent any significant backside temperature rise due to HAC fire exposure. Since the undamaged RH-TRU 72-B impact limiters provide a foam thickness of approximately 23 inches in the axial direction and approximately 17 inches in the radial direction, no significant heat from the fire event will reach the OC surface through the undamaged region of the impact limiter. Consistent with the above test results, a 4-inch thickness of polyurethane foam, as shown in Figure 3.5-1 and Figure 3.5-2, is assumed to be removed from the side and ends of the impact limiters. As a further conservatism, all surfaces inside the impact limiter's char region are assigned an emissivity of 0.99.

As discussed in Section 3.4.1.1.1.1, *Outer Cask (OC) Model*, the thermal shield is directly connected at each end of the OC body and around the periphery of each trunnion penetration. Both radiation and conduction heat transfer are used within the 12-gauge (0.1094-inch thick) gap between the inside of the cylindrical 10-gauge (0.1406-inch thick) thermal shield and the outside of the OC outer cylindrical shell. The thermal shield, however, is not attached to the 12-gauge wire wrap. Application of the HAC fire's 1,475 ºF environment to the thermal shield will cause this relatively thin shell to heat quickly and expand radially outward away from the much cooler OC outer shell and wire wrap (Figure 3.5-3 shows the thermal shield's temperature exceeding 1,000 ºF in less than 3 minutes). Consequently, HAC analyses assume the wire wrap is present both before and after, but not during, the 30-minute fire event, i.e., air replaces the wire/air composite within the thermal shield gap during the 30-minute fire event.

[6] C. Williamson and Z. Iams, *Thermal Assault and Polyurethane Foam – Evaluating Protective Mechanisms*, General Plastics Manufacturing Company, Tacoma, WA; presented at PATRAM International Symposium, Berlin, Germany, 2004.

3.5.3 Package Temperatures

The maximum pre-fire, fire, and post-fire temperatures are presented in Table 3.5-1, Table 3.5-2, and Table 3.5-3, respectively, for the major components of the RH-TRU 72-B package. As expected, the package's HAC pre-fire temperatures, with insolation, that are presented in Table 3.5-1 compare closely with the package's NCT temperatures, with insolation, that are presented in Table 3.4-3 from Section 3.4.3, *Maximum Temperatures*.

The following figures illustrate package and packaging HAC temperatures for the three payload cases:

- **Case 1:** Figure 3.5-3 through Figure 3.5-6 show transient temperature plots for the major components of the packaging and payload when the HAC fire occurs immediately following the end of a "12-hour on" insolation cycle, and Figure 3.5-7 through Figure 3.5-10 show transient temperature plots for the major components of the packaging and payload when the HAC fire occurs immediately prior to the start of a "12-hour on" insolation cycle. Figure 3.5-11 through Figure 3.5-21 illustrate the package temperatures throughout the HAC pre-fire, fire, and post-fire events for three, 30-gallon drums within an RLC for a 12 lb/ft^3 payload density with 90 watts of uniformly distributed decay heat, and Figure 3.5-22 through Figure 3.5-32 illustrate the package temperatures throughout the HAC pre-fire, fire, and post-fire events for three, 30-gallon drums within an RLC for a 100 lb/ft^3 payload density with 270 watts of uniformly distributed decay heat.
- **Case 2:** Because of the lower payload decay heat for Case 2 compared to Case 1, the package component temperatures for Case 1 bound the package component temperatures for Case 2. As such, Figure 3.5-33 through Figure 3.5-35 only illustrate the payload component temperatures for the HAC fire event for three, approximately 15-gallon drums within an NS15 NSC for a 12 lb/ft^3 payload density with 50 watts of uniformly distributed decay heat.
- **Case 3:** Because of the lower payload decay heat for Case 3 compared to Case 1, the package component temperatures for Case 1 bound the package component temperatures for Case 3. As such, Figure 3.5-36 through Figure 3.5-38 only illustrate the payload component temperatures for the HAC fire event for three, approximately 30-gallon drums within an NS30 NSC for a 12 lb/ft^3 payload density with 50 watts of uniformly distributed decay heat.

Note that the light-red region in the transient temperature plots (Figure 3.5-3 through Figure 3.5-10) depicts the 30-minute fire, and the light-yellow region(s) in the plots depict the 12-hour periods when insolation is active.

3.5.4 Maximum Internal Pressure

3.5.4.1 Temperature Control

The maximum HAC fire event pressure increase compared to NCT is primarily due to increased temperature and water vapor. Radiolytic gas generation effects are negligible because the period of the HAC fire event is relatively short. All other factors, as discussed in Section 3.4.5, *Maximum Internal Pressure*, are negligible. Furthermore, the internal pressure rises and falls

during the HAC fire event along with, and driven by, local IV and payload canister surface temperature transients. Thus, peak internal pressure occurs with peak surrounding temperatures during the HAC fire transient. Structural loads do not affect the maximum pressure capability of the RH-TRU 72-B packaging for HAC.

Table 3.5-2 lists peak IV and RLC shell temperatures of 384.4 ºF and 284.1 ºF, respectively, for a bounding payload density of 100 lb/ft^3 with 270 watts of decay heat. The peak IV air cavity temperature, based on the average of the peak IV and RLC wall temperatures, is ½(384.4 + 284.1) = 334.25 ºF. Calculation of water vapor pressure employs thermodynamic steam tables and the minimum IV cavity surface temperature of 163.2 ºF (from Table 3.5-2 for the RLC shell). Calculation of increased internal air temperature employs the Ideal Gas Law, as calculated below.

The initial pressure of air present in the IV cavity is 14.7 psia at 70 ºF. As determined in Section 3.4.5.3, *Maximum Pressure for Normal Conditions of Transport*, the initial partial pressure of net (total) gas generated at the end of the shipping period, P_{net} = 2.73 psia. The increased pressure associated with the increase in temperature for HAC from 70 ºF to 334.25 ºF, P_{hu_HAC}, is:

$$P_{hu_HAC} = \left(P_{net} + P_{atm}\right)\left(\frac{334.25\ ^\circ F + 460\ ^\circ F}{70\ ^\circ F + 460\ ^\circ F}\right) = 26.12\ \text{psia}$$

Water vapor pressure, P_{wv}, is based on the temperature of the coolest surface where water will condense in the IV cavity. From thermodynamic steam tables, P_{wv_HAC} = 5.12 psia, for a minimum IV cavity surface temperature of 163.2 ºF. Therefore, the maximum IV pressure, P_{max_HAC}, at the end of a shipment is:

$$P_{max_HAC} = P_{hu_HAC} + P_{wv_HAC} - P_{atm} = 26.12 + 5.12 - 14.7 = 16.54\ \text{psig}$$

The above is the worst-case possible transient pressure rise due to a HAC fire event at the end of the shipping period for a bounding maximum thermal load of 270 watts, and is still appreciably below the HAC analysis pressure, P_{allow_HAC} = 300 psig, used in Section 2.7.4, *Thermal*. Thus, the margin of safety against the HAC design pressure limit, MS_{MNOP_HAC}, is:

$$MS_{MNOP_HAC} = \left(\frac{P_{allow_HAC}}{P_{max_HAC}}\right) - 1 = \left(\frac{300}{16.54}\right) - 1 = +17.1$$

3.5.4.2 Flammable Gas Control

Radiolytic gas generation effects are negligible because the period of the HAC thermal event is relatively short. All other factors, as mentioned in Section 3.4.5, *Maximum Internal Pressure*, are negligible. Thus, flammable gas generation during the HAC fire event is no more severe than for NCT. It is assumed that RH-TRU waste materials breach the layers of confinement and also the payload containers under HAC.

From a hydrogen concentration viewpoint, the worst case is when the layers of internal confinement and the payload containers are intact under NCT. In this case, the maximum number of barriers to the release of gases generated within the innermost layer will be present, and flammable gas concentrations will increase from the outside of the payload container to the innermost layer of confinement. If breaching the payload containers and layers of confinement

occurred during HAC, the result would be a decrease in the number of barriers to release of generated gases. This scenario would result in more mixing of the gases between layers of confinement and reduced concentrations in each. Hence, the controls placed on the payload to ensure flammability limits are met for NCT also ensure compliance for HAC.

3.5.5 Maximum Thermal Stresses

Thermal stresses associated with the HAC fire event may be classified as secondary, displacement limited stresses. The ANSYS® finite element program[7] was used to determine thermal stresses. The analysis utilized three-dimensional solid elements representing the OC inner and outer shells, upper forging, lid, base, and external trunnion assemblies. Because the package's lead shielding is poured into the cavity between the OC inner and outer shells at a temperature of approximately 620 ºF, the lead shrinks both radially and longitudinally as it cools and solidifies. This shrinkage produces slight radial and axial gaps between the lead and the OC outer and inner shells, forging, and base. The lead will absorb heat and expand during the HAC fire event, but will not close the gaps until the 620 ºF solidification temperature is reached. Since the maximum reported lead temperature is 570.4 ºF per Table 3.5-2, thermal expansion of the lead will not contribute to the stress state in the OC structure. Consequently, the lead is not included in this evaluation of OC thermal stresses for the HAC fire event.

As shown in Figure 3.5-40, the OC structural model is identical to the OC thermal model and is represented by a refined mesh of approximately 12,000 solid elements. Symmetry boundary conditions are applied to the cut face to ensure the correct structural response. Temperatures from the HAC thermal analysis, shown in Figure 3.5-41, are mapped into the thermal stress model (see Figure 3.5-42) and show excellent correlation. Temperature-dependent elastic moduli and mean coefficients of thermal expansion for Type 304 stainless steel are presented in Table 3.5-4, and based on a stress-free temperature of 70 ºF.

Thermal stress evaluations were performed in three-minute intervals from the start of the HAC fire until 30 minutes after the end of the fire based on the Case 1 model with 270 watts of decay heat that resulted in the highest peak structural temperatures (i.e., the HAC 30-minute fire immediately following a "12-hour on" solar cycle). The maximum stress intensity for each of the 21 time intervals is plotted as Figure 3.5-39. The peak stress intensity of 118,570 psi occurs 15 minutes after fire start, as shown in Figure 3.5-43 and Figure 3.5-44, and occurs in the main trunnion block. As shown in Figure 3.5-45, the peak stress intensity in the OC outer shell is 76,600 psi, and occurs adjacent to the main trunnion block.

3.5.6 Evaluation of Package Performance for the Hypothetical Accident Thermal Conditions

None of the temperatures noted from the HAC fire transient analyses exceed the temperature limitations of the respective materials, as defined in Section 3.3, *Technical Specifications of Components*. The highest lead temperature noted, 570.4 ºF per Table 3.5-2, is 50 ºF below the melting point of lead. As expected, the highest OC shell temperatures are adjacent to the

[7] ANSYS® Workbench 2.0 Framework, Revision 14.5.1; ANSYS, Inc., 275 Technology Drive, Canonsburg, PA 15317.

trunnions due to the presence of these direct heat paths into the shell structure (as an example, see Figure 3.5-14).

The package's O-ring seal regions see modest temperature rises during the HAC fire transient due to a combination of the thermal protection provided by the impact limiter, the physical distance of the O-ring seals from the high temperature regions near the trunnions, and the relatively large mass (i.e., high heat capacity) of the package. With reference to Table 3.5-2, the highest O-ring seal temperature reported, 193.9 ºF for the OC lid seals, is more than 30 ºF below the recommended long-term upper operating limit for the butyl O-ring seal material of 225 ºF, and 165 ºF below the short-term operating limit of 360 ºF.

With reference to Table 3.5-2, the peak temperatures of 208.6 ºF and 195.1 ºF for the NS15 and NS30 HDPE neutron shield inserts, respectively, are shown to remain below the design limit based on the Vicat softening temperature of 256 ºF[8]. Further, since the RLC shell also remains below this temperature limit, it is clear that the HDPE temperature limit would not have been exceeded even if direct contact occurred between these two components.

Finally, with reference to Section 3.5.5, *Maximum Thermal Stresses*, thermal stresses are shown to be well below the maximum allowable alternating stress intensity, as determined in Section 2.7.4, *Thermal*.

In summary, the thermal performance of the RH-TRU 72-B packaging was evaluated for the applicable HAC conditions and for a variety of decay heat distributions within the packaging based on the various payload configurations. The evaluations found that the resulting component temperatures remained within their specified allowable limits for all cases. Thus, the defined payloads will not impact the safety basis of the RH-TRU 72-B package for HAC.

Table 3.5-1 – HAC Pre-Fire Steady State Temperatures with Insolation (ºF)

Location	RLC		NS15	NS30	Allowable Limit①
	12 lb/ft³ Payload (90 W)	100 lb/ft³ Payload (270 W)	12 lb/ft³ Payload (50 W)	12 lb/ft³ Payload (50 W)	
Lower Drum Contents Peak	331.7	311.8	258.5	245.5	402
Lower Drum Contents Average	225.5	252.7	194.6	186.3	302
Lower Drum Wall Peak	180.0	251.7	166.8	161.3	—
Middle Drum Contents Peak	338.7	326.1	263.5	249.7	402
Middle Drum Contents Average	233.5	270.9	200.7	191.2	302
Middle Drum Wall Peak	180.2	252.2	167.0	161.5	—
Upper Drum Contents Peak	331.1	310.5	258.7	245.4	402
Upper Drum Contents Average	224.9	250.6	194.5	186.2	302
Upper Drum Wall Peak	180.0	251.2	166.9	161.3	—
HDPE Shielding Wall Peak	—	—	158.6	154.4	170
HDPE Shielding Wall Average	—	—	149.6	148.5	150
RLC Shell Peak	159.2	201.9	148.4	147.9	210②
RLC Lid Peak	142.0	161.3	136.2	136.2	212
IV Shell Peak	145.1	158.0	142.4	142.3	160②
IV Base Peak	138.3	151.5	134.9	134.9	160②
IV Upper Forging Peak	137.3	146.8	134.9	134.9	160②
IV Lid Peak	136.3	145.4	134.0	134.0	160②
IV Lid O-ring Seal Peak	136.3	145.4	133.9	134.0	225
IV Lid Ports O-ring Seals Peak	136.3	145.4	134.0	134.0	225
OC Inner Shell Peak	143.8	150.2	142.5	142.5	160②
OC Lead Shield Peak	143.8	150.1	142.5	142.5	160②
OC Outer Shell Peak	144.0	150.2	142.7	142.7	160②
OC Base Peak	136.6	144.9	134.6	134.6	160②
OC Upper Forging Peak	138.1	143.6	136.7	136.8	160②
OC Lid Peak	138.1	143.6	136.7	136.8	160②
OC Lid O-ring Seal Peak	135.6	141.3	134.2	134.2	225
OC Lid Port O-ring Seal Peak	138.1	143.6	136.7	136.8	225
OC Thermal Shield Peak	146.7	151.6	145.6	145.6	185③
OC Main Trunnions Peak	143.9	149.5	142.7	142.7	153③
OC Small Trunnions Peak	144.6	149.4	143.6	143.6	153③
Impact Limiter Foam Peak	156.1	156.2	156.1	156.1	260
Impact Limiter Foam Average	135.2	138.0	134.5	134.5	140②
Impact Limiter Shell Peak	157.1	157.2	157.1	157.1	185③

Notes:

① Allowable temperature limits are discussed in Section 3.3, *Technical Specifications of Components*.

② Allowable temperature limits correspond to temperatures used in the structural evaluations in Chapter 2.0, *Structural Evaluation*.

③ The allowable temperature limit of 185 ºF for external surfaces of the package is based on the maximum accessible surface temperature without insolation for exclusive use shipments per 10 CFR §71.43(g), but is also conservatively being used here.

Table 3.5-2 – HAC Fire Temperatures (T) and Time (t) After End-of-Fire

Location	RLC				NS15		NS30		Allowable Limit①
	12 lb/ft³ Payload (90 W)		100 lb/ft³ Payload (270 W)		12 lb/ft³ Payload (50 W)		12 lb/ft³ Payload (50 W)		
	T (ºF)	*t (hr)*	T (ºF)	*t (hr)*	T (ºF)	*t (hr)*	T (ºF)	*t (hr)*	
Lower Drum Contents Peak	370.4	*37.5*	331.5	*59.0*	286.5	*54.0*	276.9	*54.5*	402
Lower Drum Contents Average	273.1	*16.0*	275.6	*22.5*	223.2	*44.0*	219.3	*38.0*	302
Lower Drum Wall Peak	258.4	*9.6*	280.9	*18.0*	199.3	*25.0*	208.3	*19.0*	—
Middle Drum Contents Peak	381.2	*33.5*	345.3	*55.5*	293.6	*48.5*	284.5	*49.0*	402
Middle Drum Contents Average	287.8	*13.5*	293.7	*19.0*	231.2	*34.0*	229.3	*24.5*	302
Middle Drum Wall Peak	264.8	*9.0*	283.0	*17.0*	201.6	*24.0*	211.8	*18.0*	—
Upper Drum Contents Peak	370.4	*35.0*	330.5	*56.5*	287.5	*50.5*	277.8	*51.0*	402
Upper Drum Contents Average	273.7	*14.5*	274.1	*20.0*	223.9	*41.0*	220.9	*26.0*	302
Upper Drum Wall Peak	264.7	*9.0*	282.5	*17.0*	201.4	*24.0*	211.9	*18.0*	—
HDPE Shielding Wall Peak	—	—	—	—	194.9	*21.5*	208.6	*15.5*	256
HDPE Shielding Wall Average	—	—	—	—	182.2	*21.0*	195.1	*14.5*	—
RLC Shell Peak	266.9	*5.25*	284.2	*3.85*	227.9	*3.75*	226.7	*4.45*	650/256③
RLC Minimum	149.8	*5.25*	163.2	*3.85*	137.6	*3.75*	145.8	*4.45*	—
RLC Lid Peak	188.9	*16.5*	200.4	*19.5*	170.4	*20.5*	172.1	*21.5*	650/256③
IV Shell Peak	374.6	*1.4*	384.4	*1.4*	372.2	*1.4*	372.2	*1.4*	390②
IV Base Peak	196.1	*17.5*	204.7	*17.5*	186.4	*14.5*	186.9	*15.0*	300②
IV Upper Forging Peak	183.1	*12.5*	190.4	*12.5*	177.0	*12.0*	177.3	*12.5*	300②
IV Lid Peak	179.6	*22.5*	186.7	*22.0*	174.1	*20.0*	174.5	*20.0*	300②
IV Lid O-ring Seal Peak	179.4	*20.5*	186.4	*20.0*	173.7	*20.0*	174.1	*20.0*	360
IV Lid Ports O-ring Seals Peak	179.6	*22.5*	186.7	*22.0*	174.1	*20.0*	174.5	*20.0*	360
OC Inner Shell Peak	542.5	*0.4*	546.8	*0.4*	541.6	*0.4*	541.7	*0.4*	550②
OC Lead Shield Peak	565.7	*0.1*	570.4	*0.1*	564.7	*0.1*	564.8	*0.1*	620
OC Outer Shell Peak	697.9	*0*	701.5	*0*	697.4	*0*	696.9	*0*	705②
OC Base Peak	195.3	*11.3*	202.4	*10.0*	192.7	*5.45*	192.7	*9.85*	500②
OC Upper Forging Peak	237.2	*1.1*	242.2	*1.2*	231.4	*1.1*	231.3	*1.45*	500②
OC Lid Peak	192.7	*9.7*	197.5	*9.15*	191.4	*9.35*	191.3	*9.55*	500②
OC Lid O-ring Seal Peak	188.9	*12.0*	193.9	*12.0*	187.3	*12.00*	187.4	*12.00*	360
OC Lid Port O-ring Seal Peak	192.7	*9.7*	197.5	*9.15*	191.4	*9.35*	191.3	*9.55*	360
OC @ Puncture Damage Peak	441.1	*0*	448.6	*0*	435.8	*0*	442.6	*0*	500②
OC Thermal Shield Peak	1,322	*0*	1,323	*0*	1,322	*0*	1,322	*0*	2,600
OC Main Trunnions Peak	1,068	*0*	1,070	*0*	1,068	*0*	1,068	*0*	2,600
OC Small Trunnions Peak	1,094	*0*	1,096	*0*	1,094	*0*	1,094	*0*	2,600
Impact Limiter Foam Peak	1,473	*0*	1,473	*0*	1,473	*0*	1,473	*0*	—
Impact Limiter Foam Average	—	—	—	—	—	—	—	—	—
Impact Limiter Shell Peak	1,474	*0*	1,474	*0*	1,474	*0*	1,474	*0*	2,600

Notes:

① Allowable temperature limits are discussed in Section 3.3, *Technical Specifications of Components*.

② Allowable temperature limits correspond to temperatures used in the structural evaluations in Chapter 2.0, *Structural Evaluation*.

③ The allowable temperature limit of the RLC components for the NSC configuration is based on the 256 ºF temperature limitation of the HDPE shield insert; otherwise, the allowable temperature limit is based on carbon steel.

Table 3.5-3 – HAC Post-Fire Steady State Temperatures with Insolation (ºF)

Location	RLC		NS15	NS30	Allowable Limit①
	12 lb/ft³ Payload (90 W)	100 lb/ft³ Payload (270 W)	12 lb/ft³ Payload (50 W)	12 lb/ft³ Payload (50 W)	
Lower Drum Contents Peak	335.7	313.9	263.0	250.1	402
Lower Drum Contents Average	230.0	255.1	199.2	191.0	302
Lower Drum Wall Peak	185.1	254.0	171.4	166.1	—
Middle Drum Contents Peak	342.6	328.2	267.9	254.2	402
Middle Drum Contents Average	238.0	273.2	205.2	195.8	302
Middle Drum Wall Peak	185.5	254.5	171.7	166.4	—
Upper Drum Contents Peak	335.4	312.9	263.2	250.2	402
Upper Drum Contents Average	229.7	253.3	199.3	191.1	302
Upper Drum Wall Peak	185.4	253.7	171.6	166.3	—
HDPE Shielding Wall Peak	—	—	163.4	159.4	256
HDPE Shielding Wall Average	—	—	154.6	153.7	—
RLC Shell Peak	165.2	205.8	154.3	153.7	650/256③
RLC Lid Peak	147.4	165.3	141.7	141.7	650/256③
IV Shell Peak	153.4	164.7	151.0	150.9	390②
IV Base Peak	143.4	154.9	140.3	140.3	300②
IV Upper Forging Peak	143.3	151.5	141.2	141.3	300②
IV Lid Peak	141.8	149.7	139.8	139.9	300②
IV Lid O-ring Seal Peak	141.8	149.7	139.8	139.8	360
IV Lid Ports O-ring Seals Peak	141.8	149.7	139.8	139.9	360
OC Inner Shell Peak	153.0	157.6	152.1	152.1	550②
OC Lead Shield Peak	153.0	157.6	152.2	152.2	620
OC Outer Shell Peak	153.7	157.7	152.9	152.9	705②
OC Base Peak	142.0	148.9	140.5	140.5	500②
OC Upper Forging Peak	146.9	151.2	145.9	145.9	500②
OC Lid Peak	146.9	151.2	145.9	145.9	500②
OC Lid O-ring Seal Peak	142.3	146.9	141.2	141.2	360
OC Lid Port O-ring Seal Peak	146.9	151.2	145.9	145.9	360
OC Thermal Shield Peak	156.7	160.0	156.1	156.1	2,600
OC Main Trunnions Peak	154.0	157.9	153.2	153.2	2,600
OC Small Trunnions Peak	156.6	159.6	155.9	155.9	2,600
Impact Limiter Foam Peak	164.3	164.3	164.3	164.3	—
Impact Limiter Foam Average	140.2	144.0	139.6	139.6	—
Impact Limiter Shell Peak	165.3	165.3	165.3	165.3	2,600

Notes:

① Allowable temperature limits are discussed in Section 3.3, *Technical Specifications of Components*.

② Allowable temperature limits correspond to temperatures used in the structural evaluations in Chapter 2.0, *Structural Evaluation*.

③ The allowable temperature limit of the RLC components for the NSC configuration is based on the 256 ºF temperature limitation of the HDPE shield insert; otherwise, the allowable temperature limit is based on carbon steel.

Table 3.5-4 – Temperature-Dependent Physical Properties of Type 304 Stainless Steel

Temperature (ºF)	Elastic Modulus① ($\times 10^6$ psi)	Mean Coefficient of Thermal Expansion② ($\times 10^{-6}$ in/in)
70	28.3	8.5
100	—	8.6
150	—	8.8
200	27.5	8.9
250	—	9.1
300	27.0	9.2
350	—	9.4
400	26.4	9.5
450	—	9.6
500	25.9	9.7
550	—	9.8
600	25.3	9.9
650	—	9.9
700	24.8	10.0
750	—	10.0
800	24.1	10.1
850	—	10.2
900	23.5	10.2
950	—	10.3
1,000	22.8	10.3
1,050	—	10.4
1,100	22.0	10.4
1,150	—	10.5
1,200	21.2	10.6
1,250	—	10.6
1,300	20.3	10.7
1,350	—	10.7
1,400	19.2	10.8
1,450	—	10.8
1,500	18.1	10.8

Notes:

① ASME Boiler and Pressure Vessel Code, Section II – *Materials*, Part D – *Properties (Customary)*, Subpart 2 – *Physical Properties Tables*, Table TM-1, Material Group G, 2010.

② ASME Boiler and Pressure Vessel Code, Section II – *Materials*, Part D – *Properties (Customary)*, Subpart 2 – *Physical Properties Tables*, Table TE-1, Material Group 3, Coefficient A, 2010.

This page intentionally left blank.

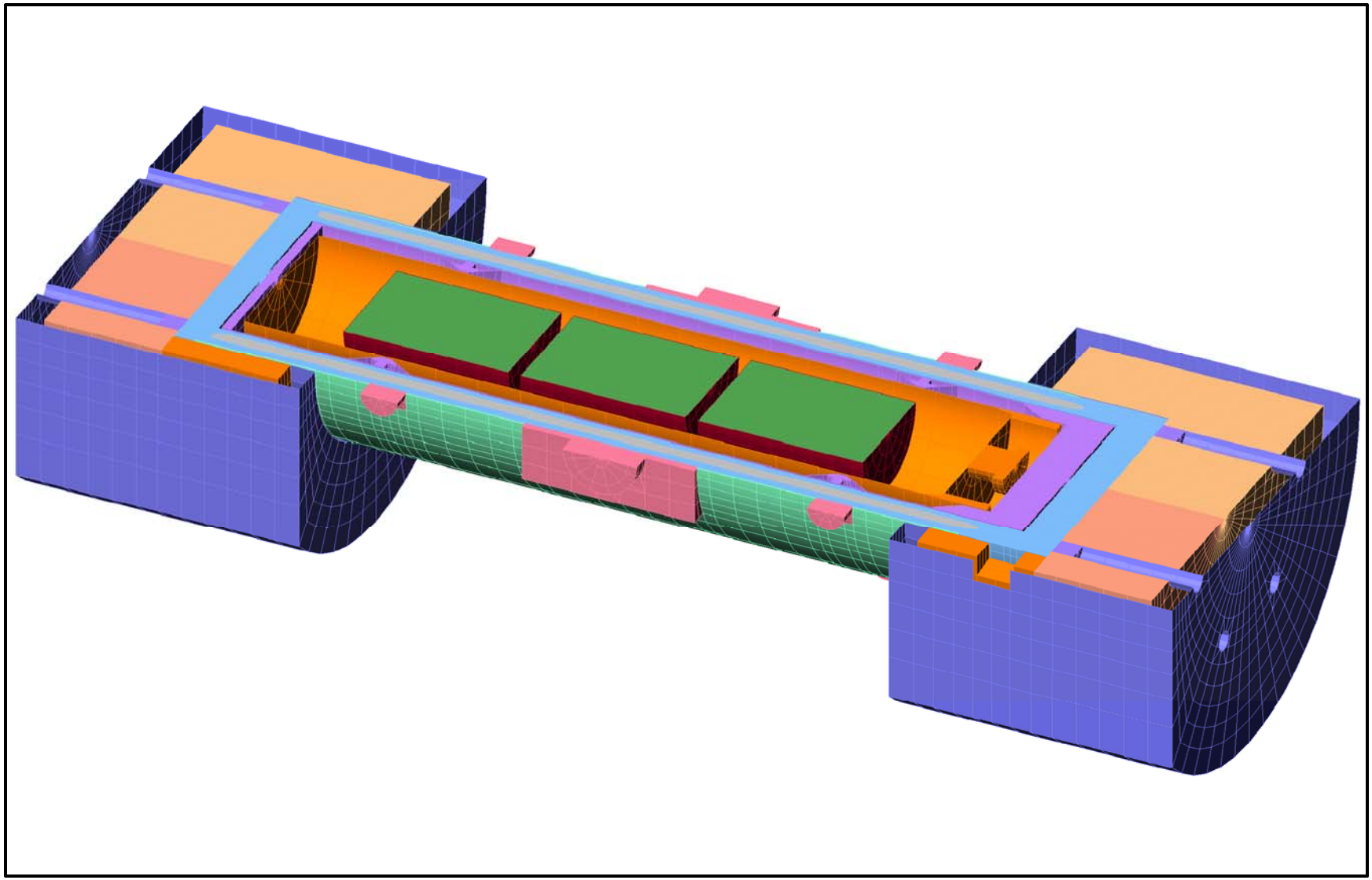

Figure 3.5-1 – HAC Package Thermal Model with an RLC

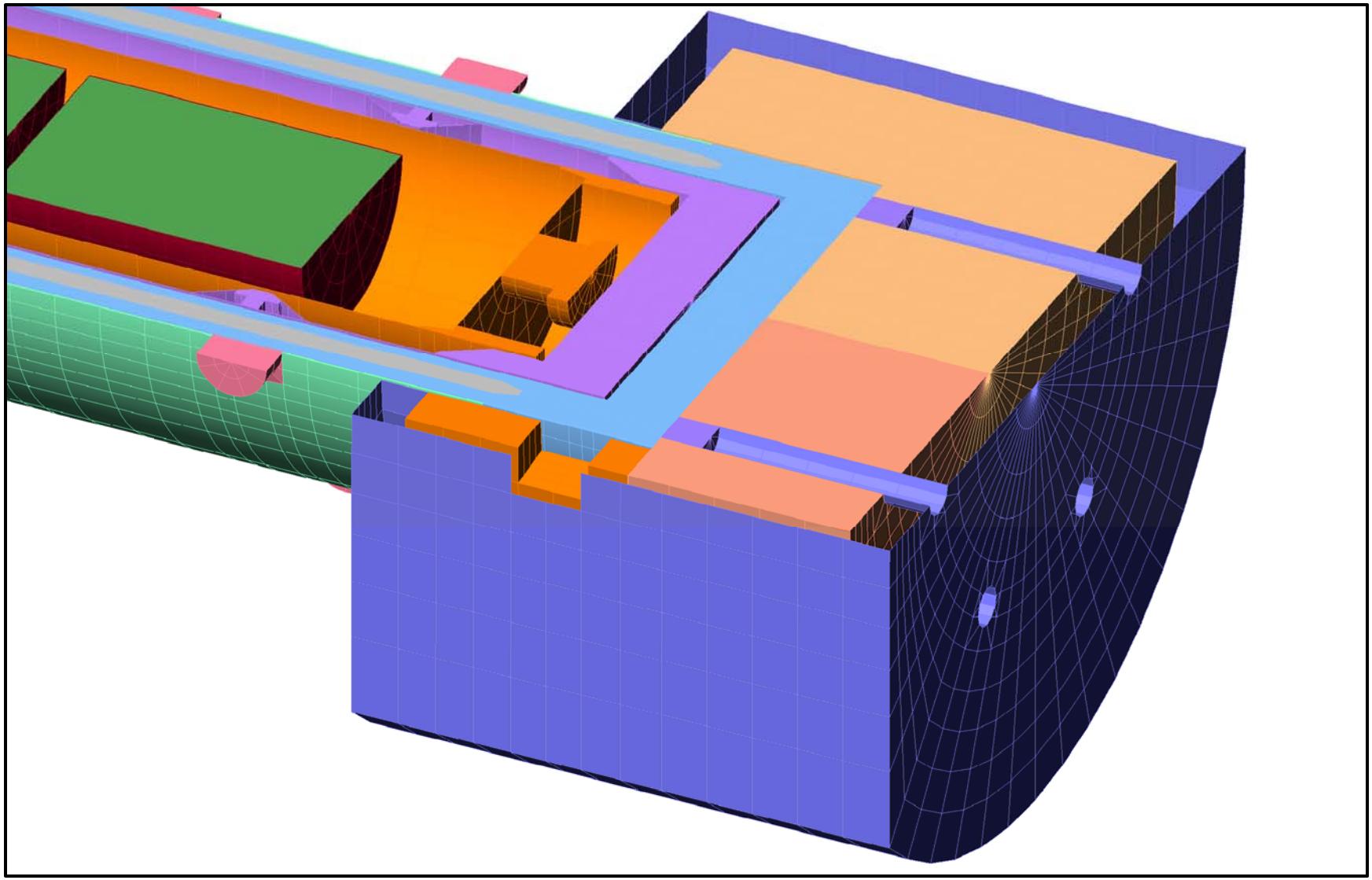

Figure 3.5-2 – HAC Package Thermal Model with an RLC (Upper Impact Limiter Close-Up)

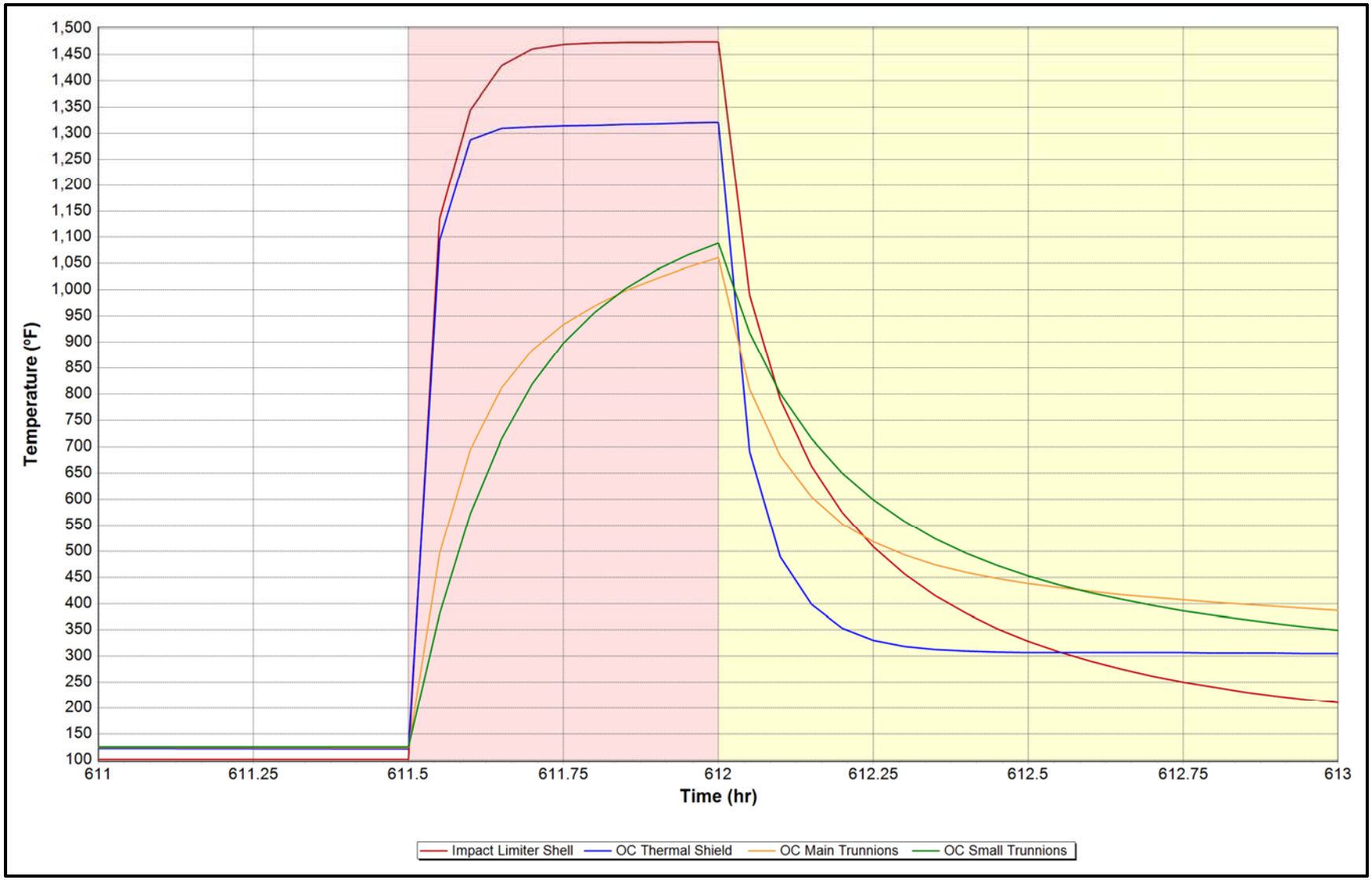

Figure 3.5-3 – HAC Case 1 Temperatures of External Package Surfaces; 12 lb/ft³ Waste with 90 Watts Decay Heat – Fire *Before* Insolation

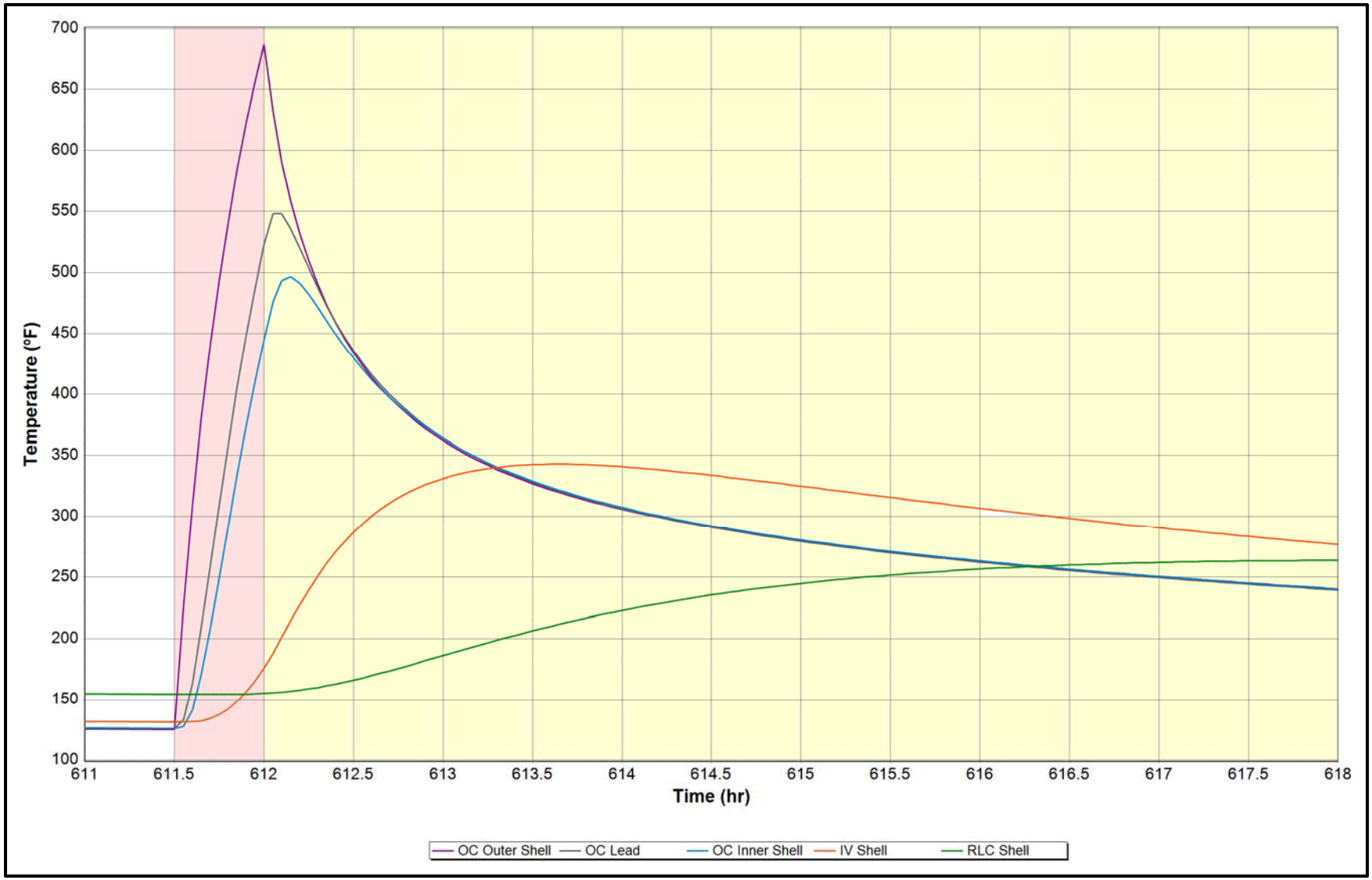

Figure 3.5-4 – HAC Case 1 Temperatures of Internal Package Surfaces; 12 lb/ft³ Waste with 90 Watts Decay Heat – Fire *Before* Insolation

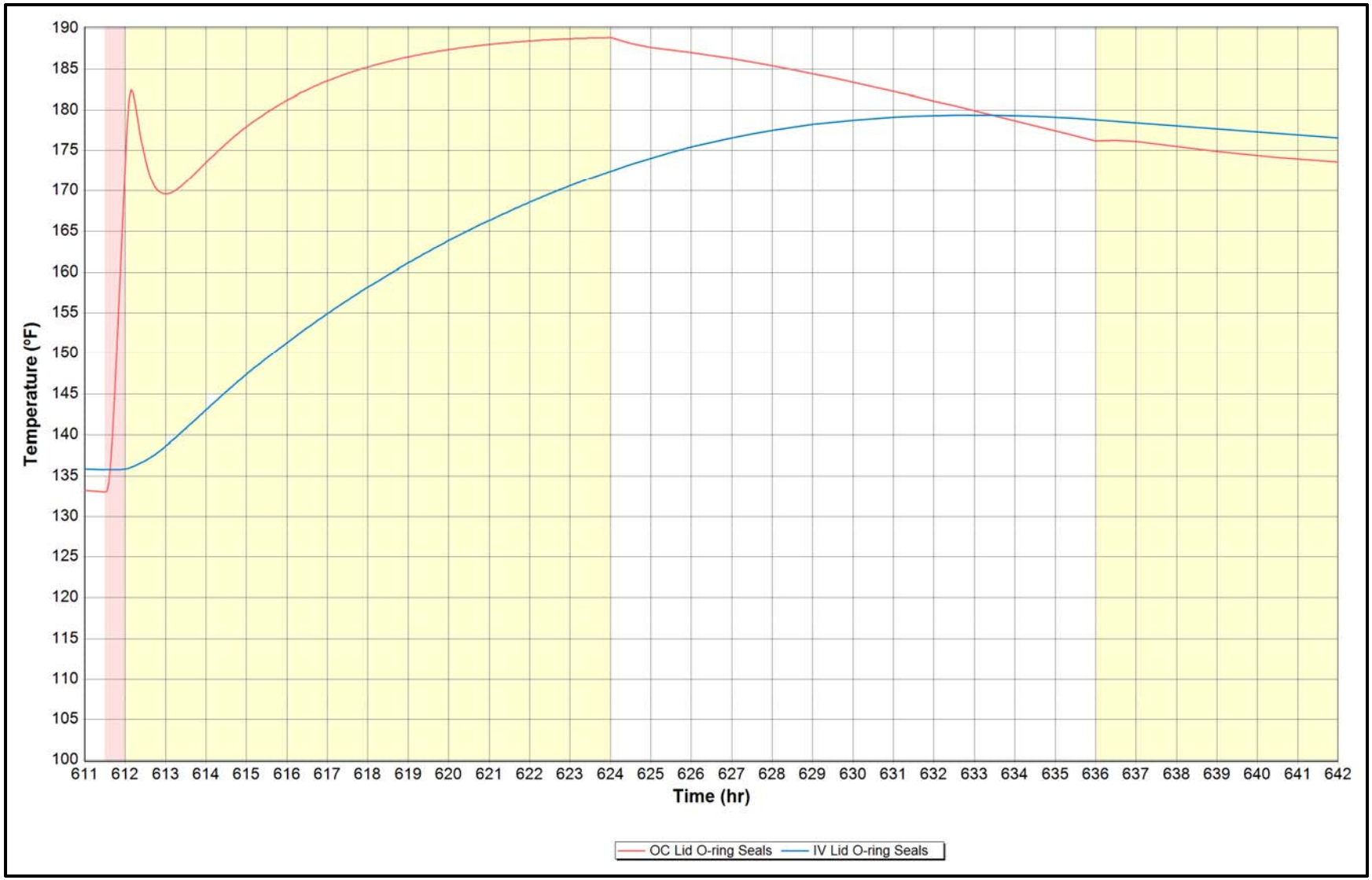

Figure 3.5-5 – HAC Case 1 Temperatures of the OC and IV O-ring Seals; 12 lb/ft³ Waste with 90 Watts Decay Heat – Fire *Before* Insolation

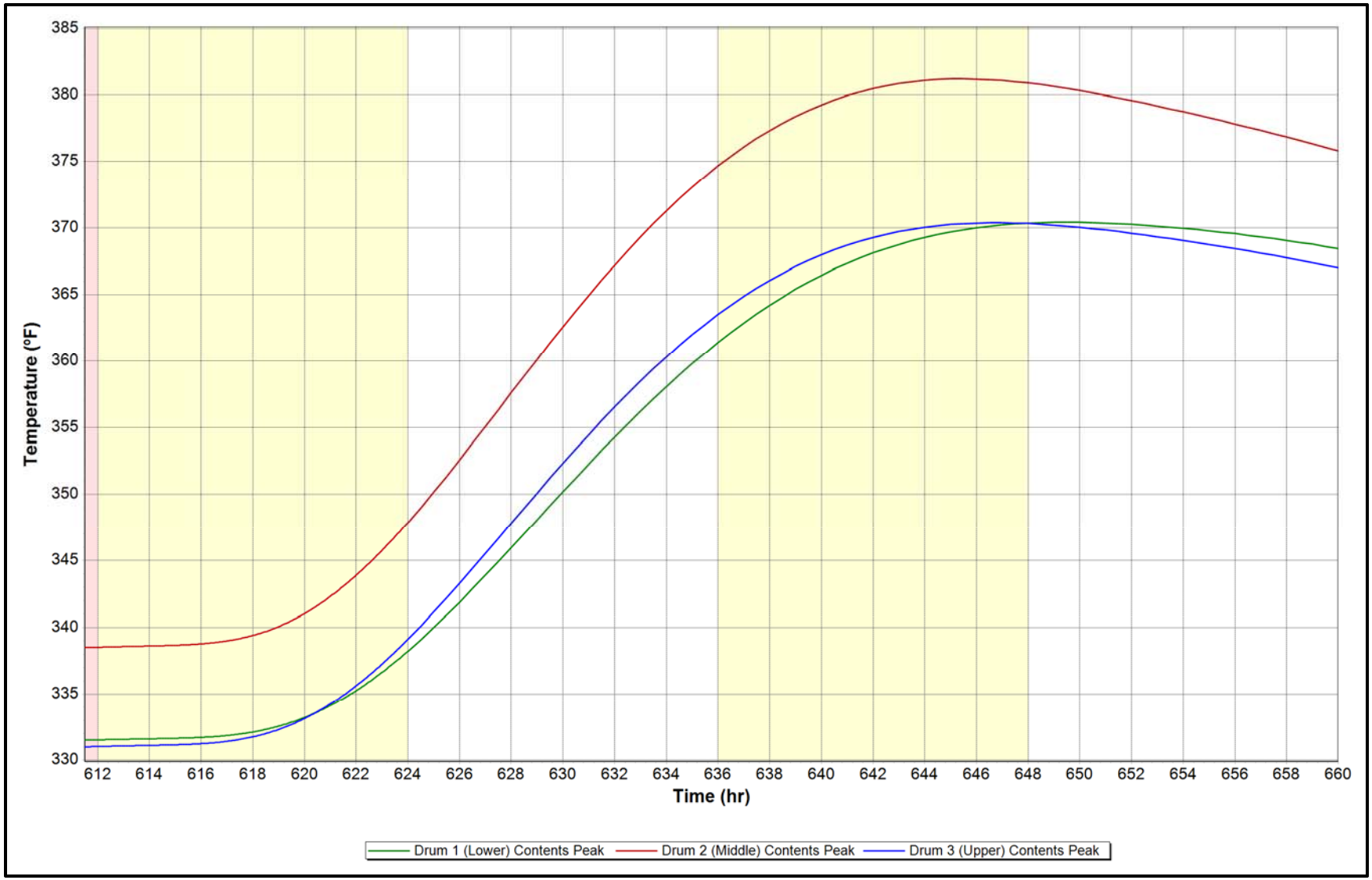

Figure 3.5-6 – HAC Case 1 Temperatures of the Drum Contents Center Nodes; 12 lb/ft³ Waste with 90 Watts Decay Heat – Fire *Before* Insolation

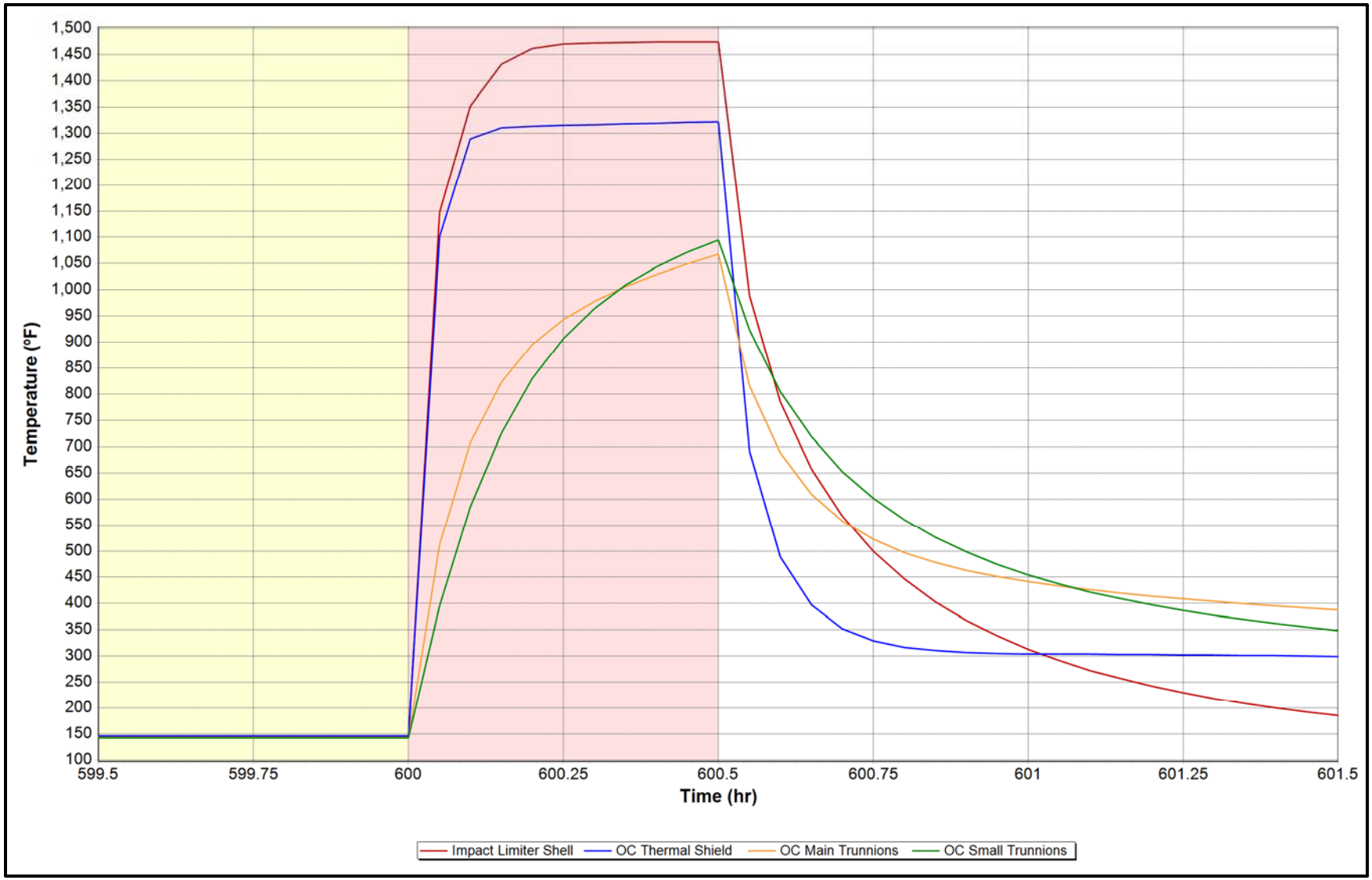

Figure 3.5-7 – HAC Case 1 Temperatures of External Package Surfaces; 12 lb/ft³ Waste with 90 Watts Decay Heat – Fire *After* Insolation

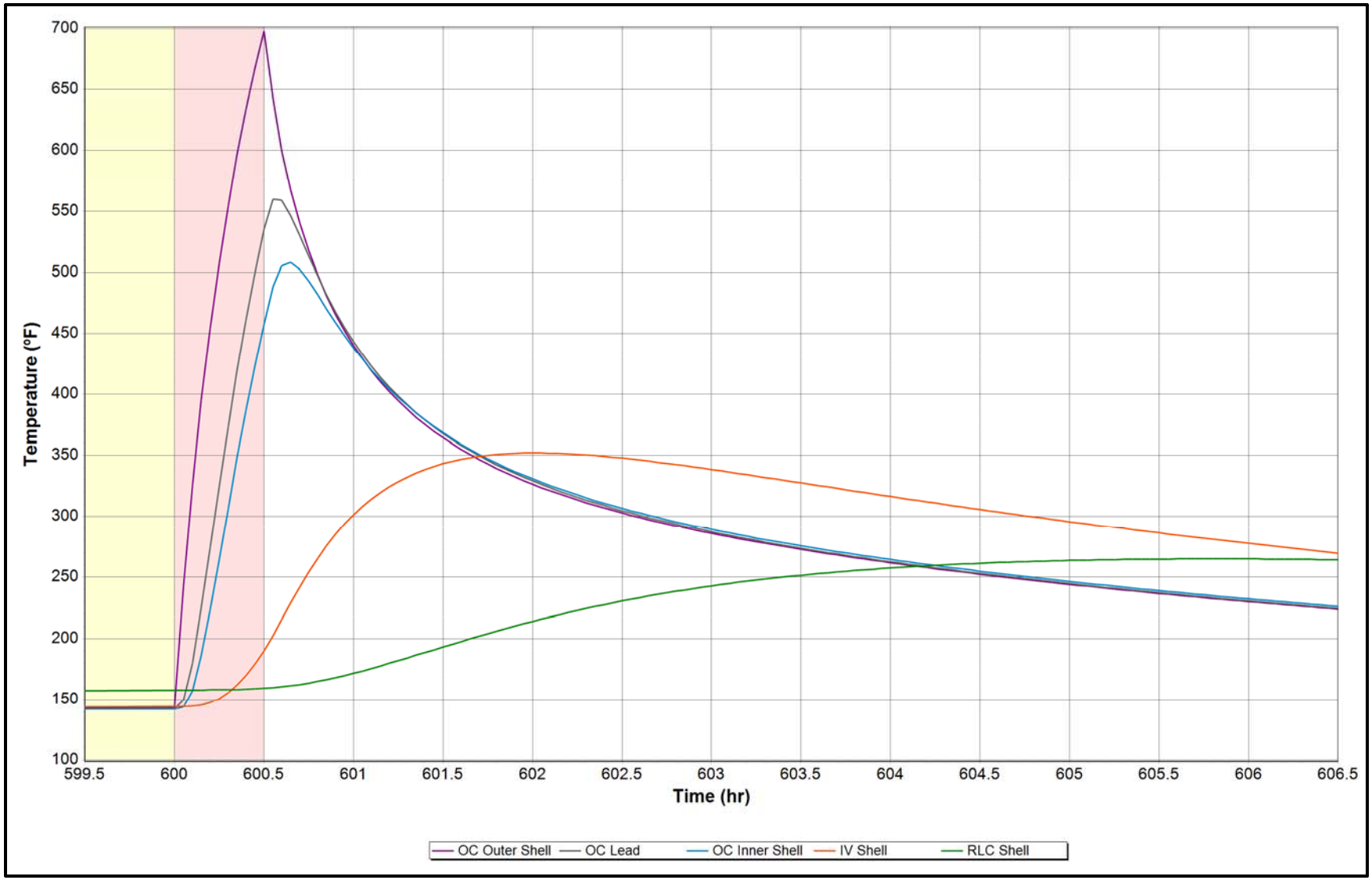

Figure 3.5-8 – HAC Case 1 Temperatures of Internal Package Surfaces; 12 lb/ft³ Waste with 90 Watts Decay Heat – Fire *After* Insolation

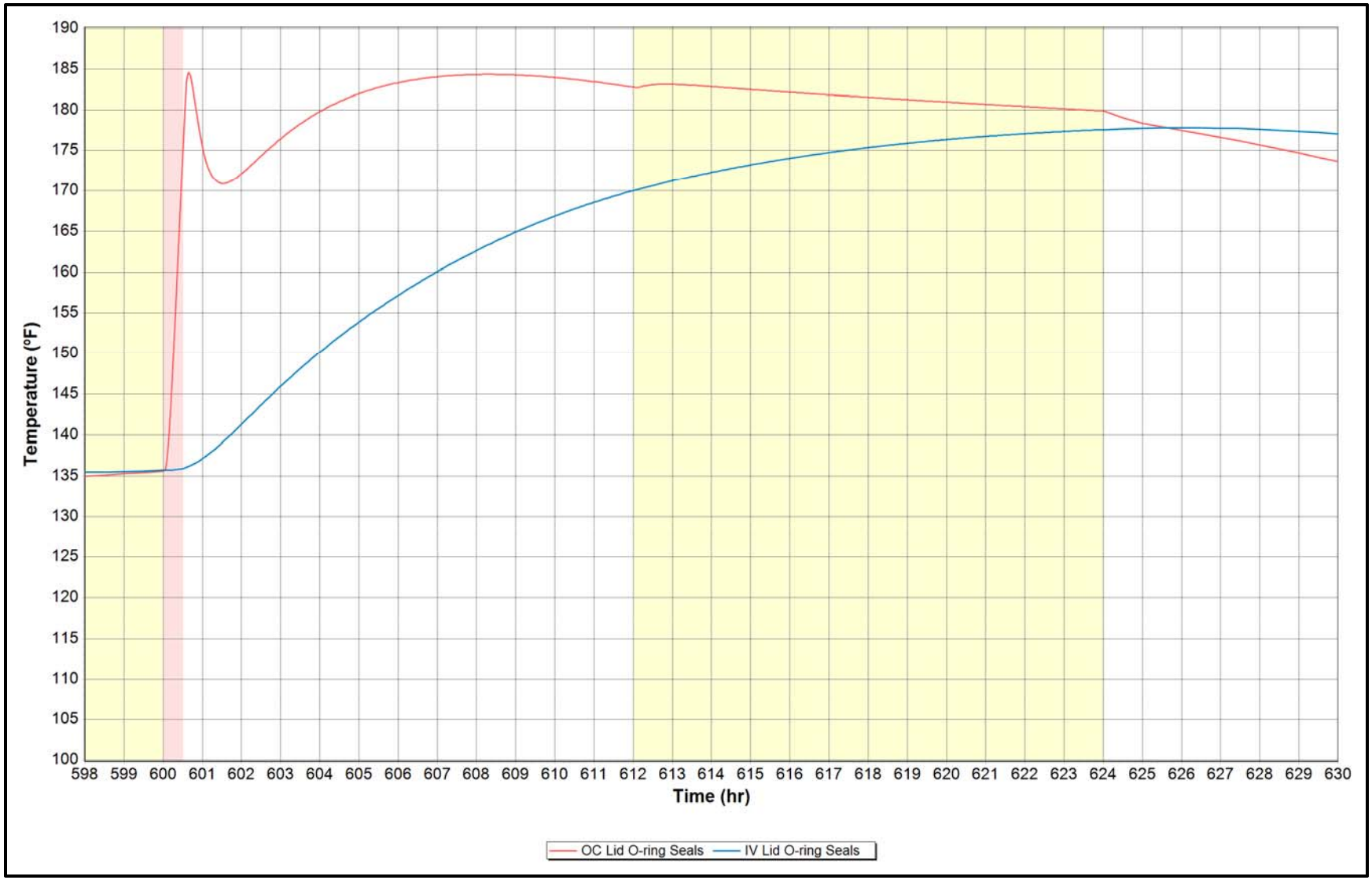

Figure 3.5-9 – HAC Case 1 Temperatures of the OC and IV O-ring Seals; 12 lb/ft³ Waste with 90 Watts Decay Heat – Fire *After* Insolation

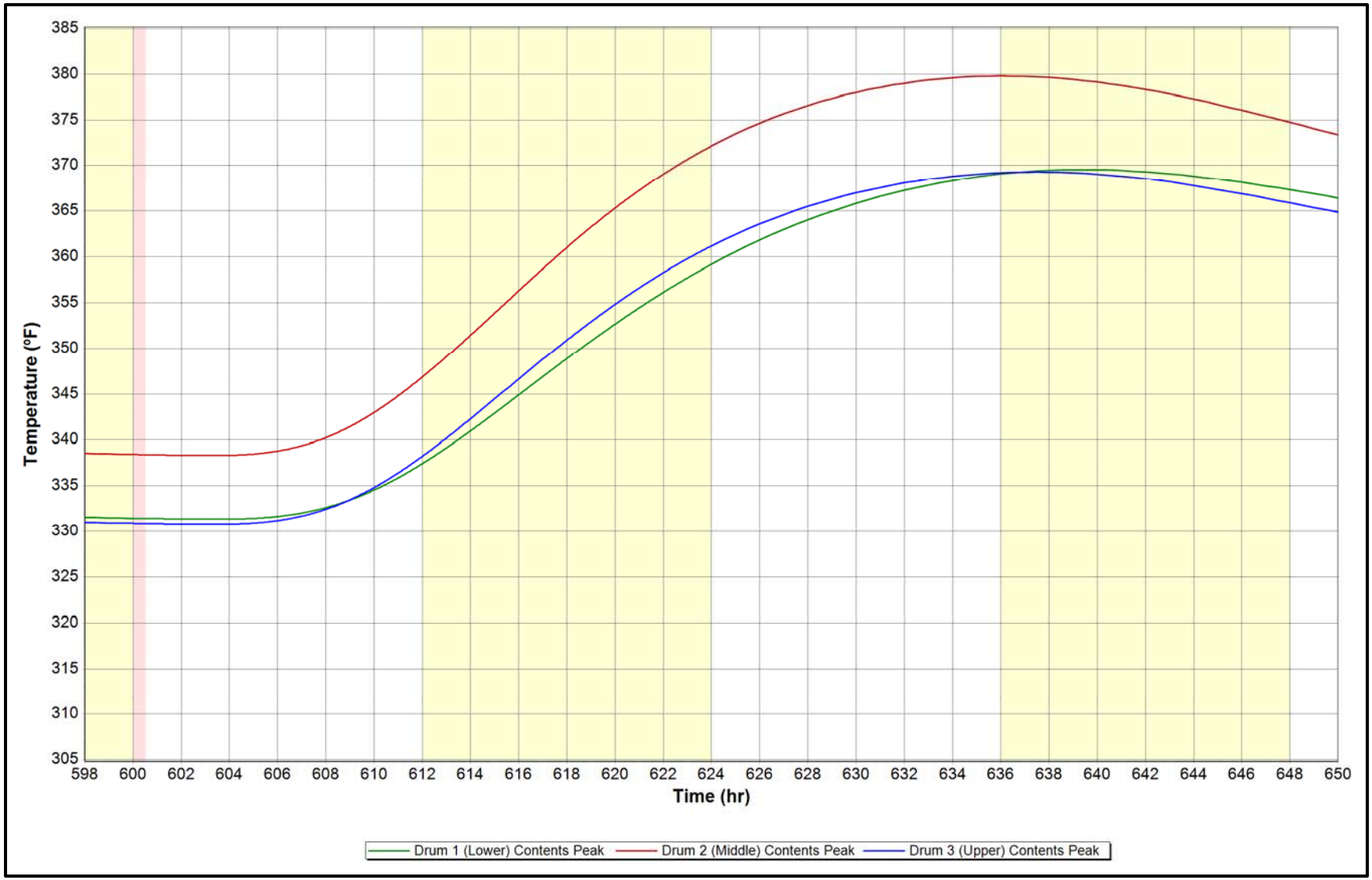

Figure 3.5-10 – HAC Case 1 Temperatures of the Drum Contents Center Nodes; 12 lb/ft³ Waste with 90 Watts Decay Heat – Fire *After* Insolation

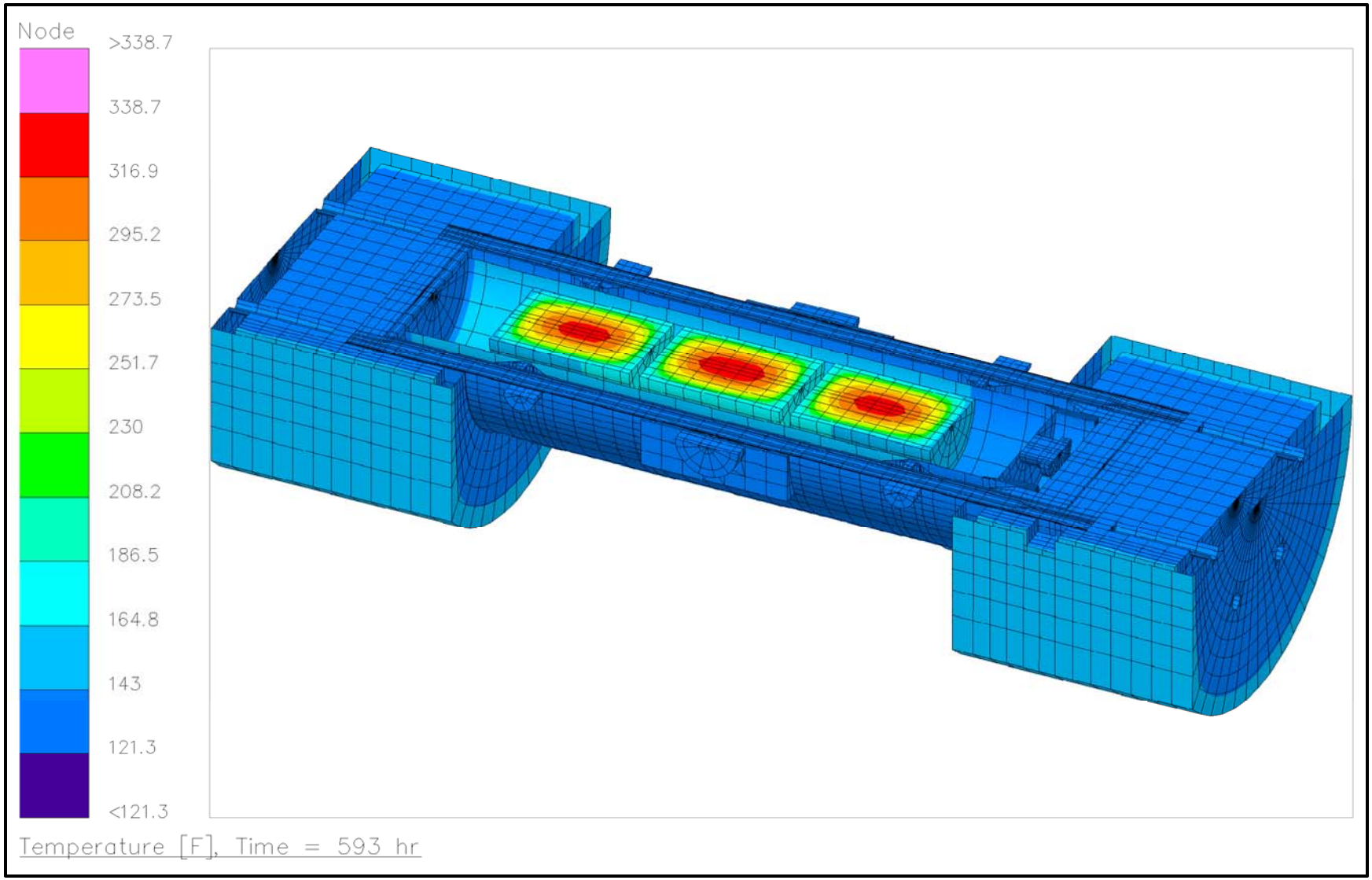

Figure 3.5-11 – HAC Case 1 – Package with RLC; 12 lb/ft³ Waste with 90 Watts Decay Heat and Insolation – Pre-Fire Temperatures

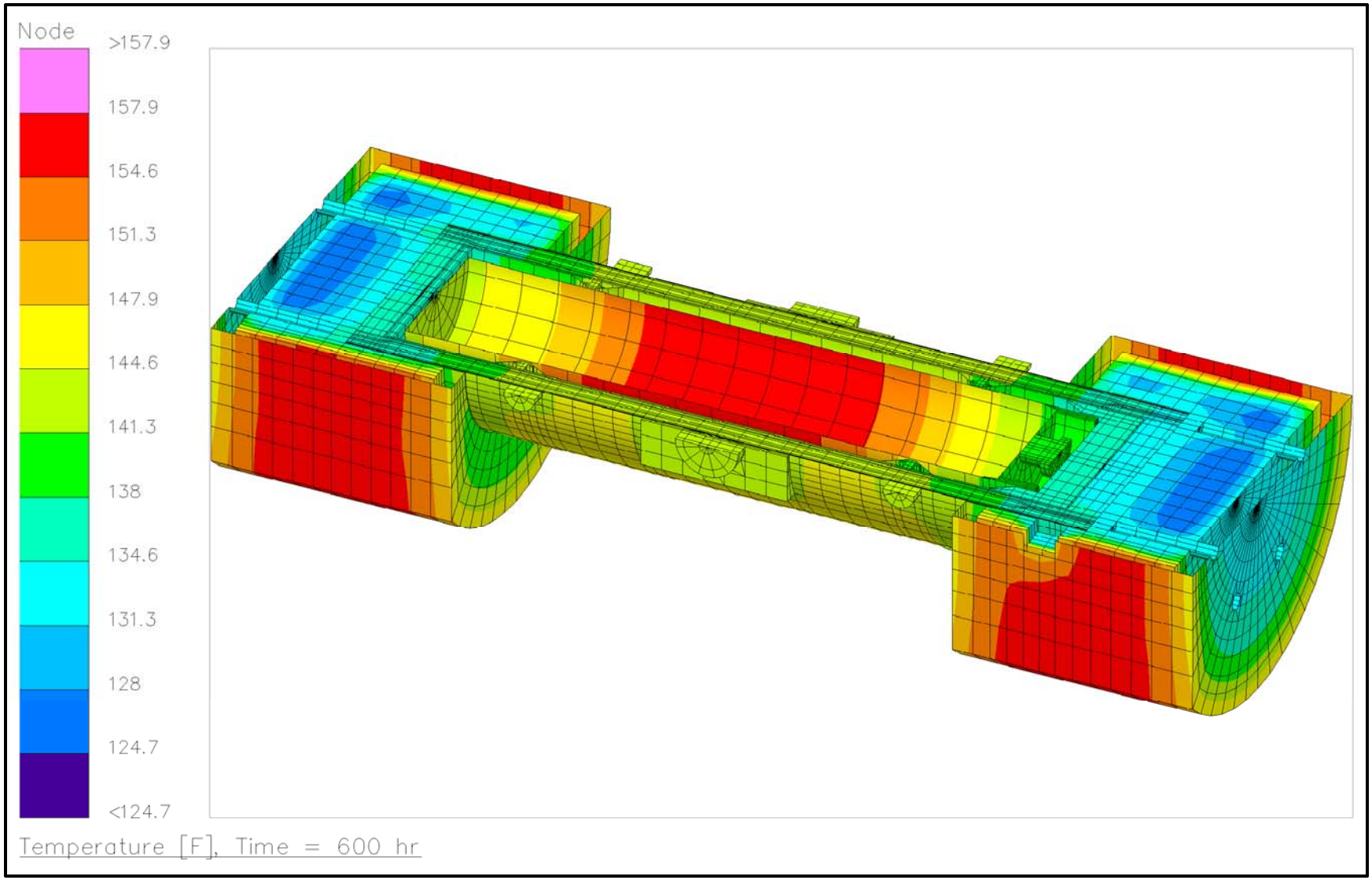

Figure 3.5-12 – HAC Case 1 – Package with RLC; 12 lb/ft³ Waste with 90 Watts Decay Heat and Insolation – Pre-Fire Temperatures (Drums Hidden)

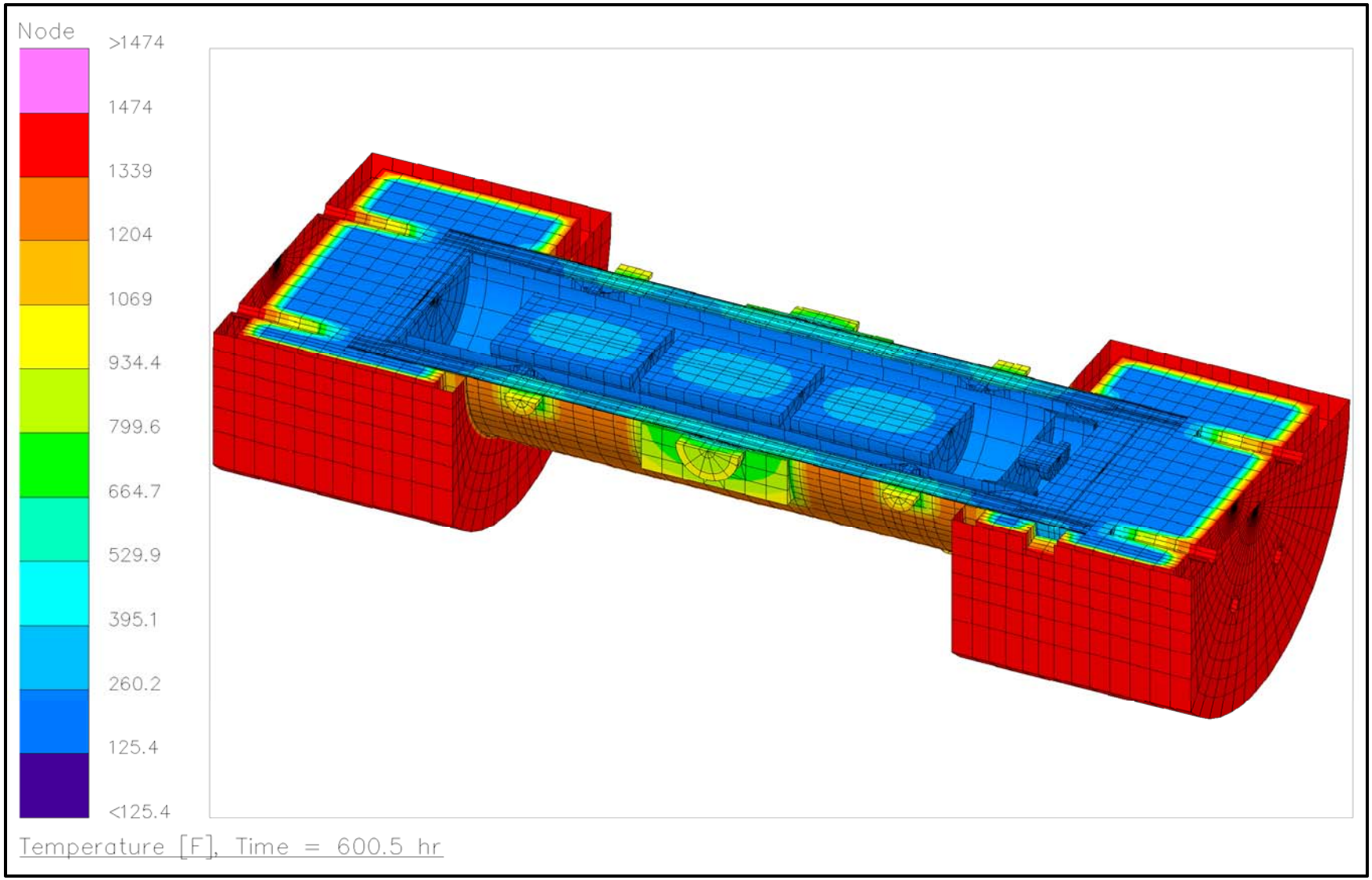

Figure 3.5-13 – HAC Case 1 – Package with RLC; 12 lb/ft³ Waste with 90 Watts Decay Heat – Package Fire Temperatures

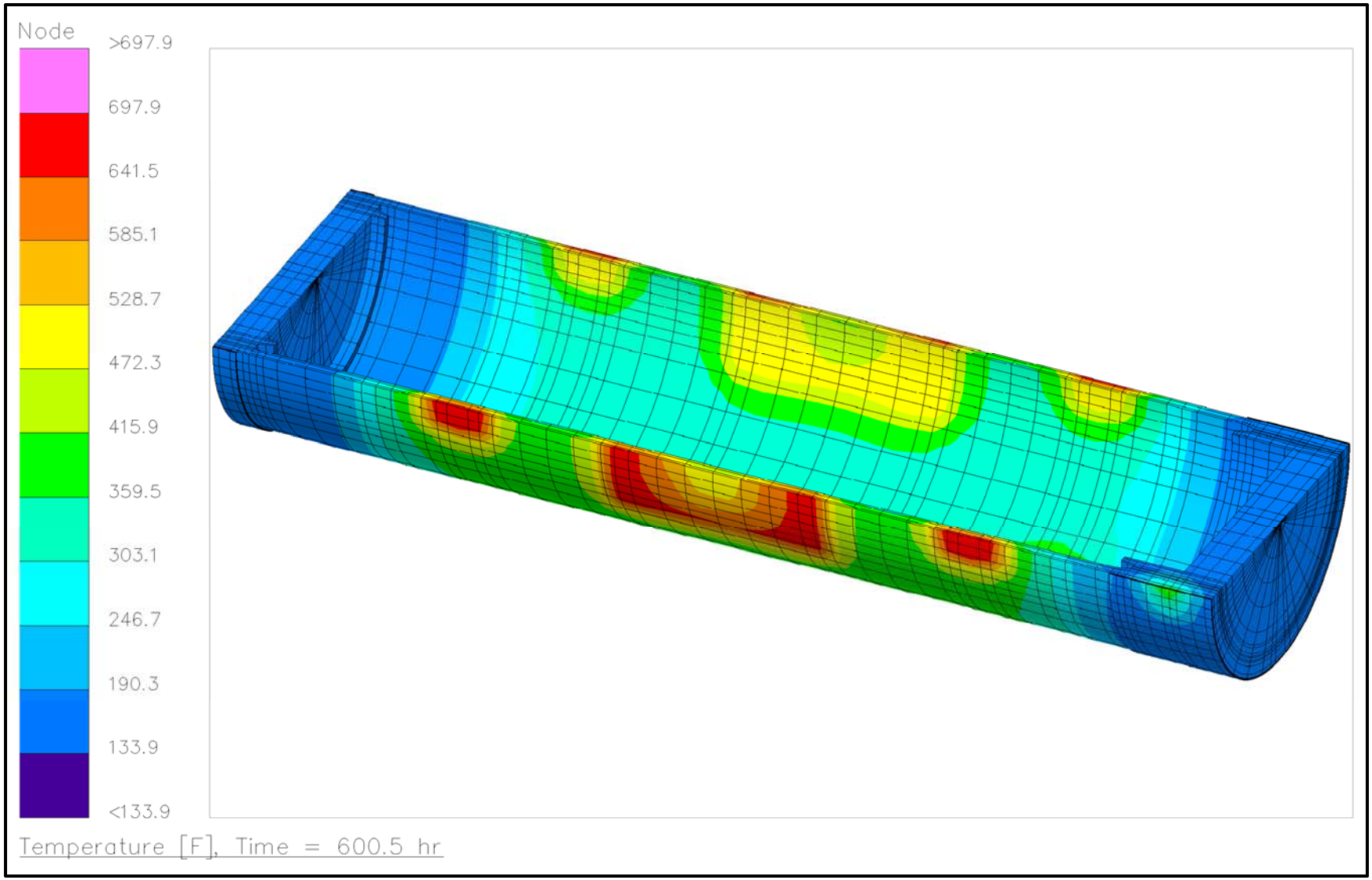

Figure 3.5-14 – HAC Case 1 – Package with RLC; 12 lb/ft³ Waste with 90 Watts Decay Heat – OC Outer Shell Fire Temperatures

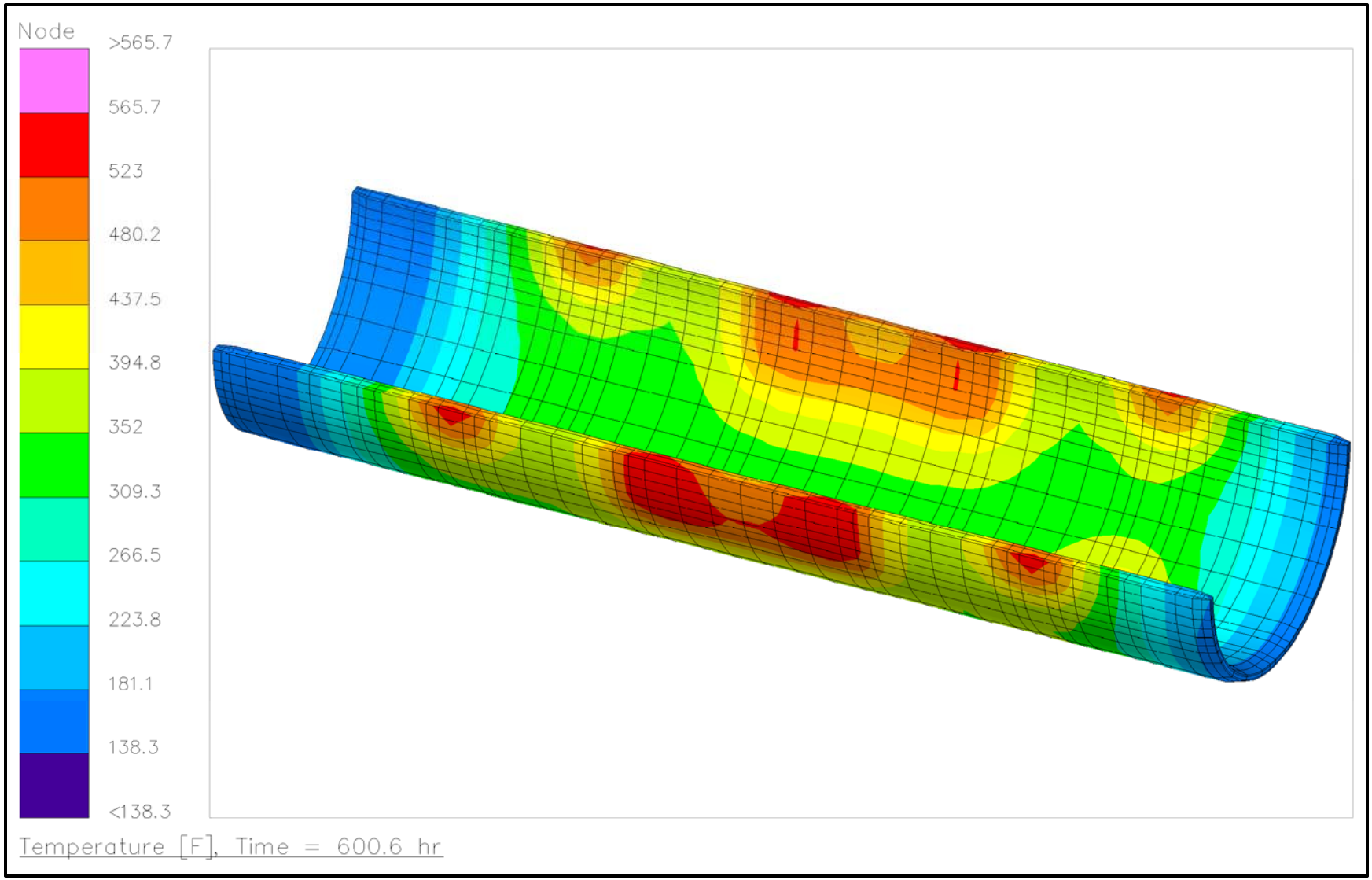

Figure 3.5-15 – HAC Case 1 – Package with RLC; 12 lb/ft³ Waste with 90 Watts Decay Heat – OC Lead Fire Temperatures

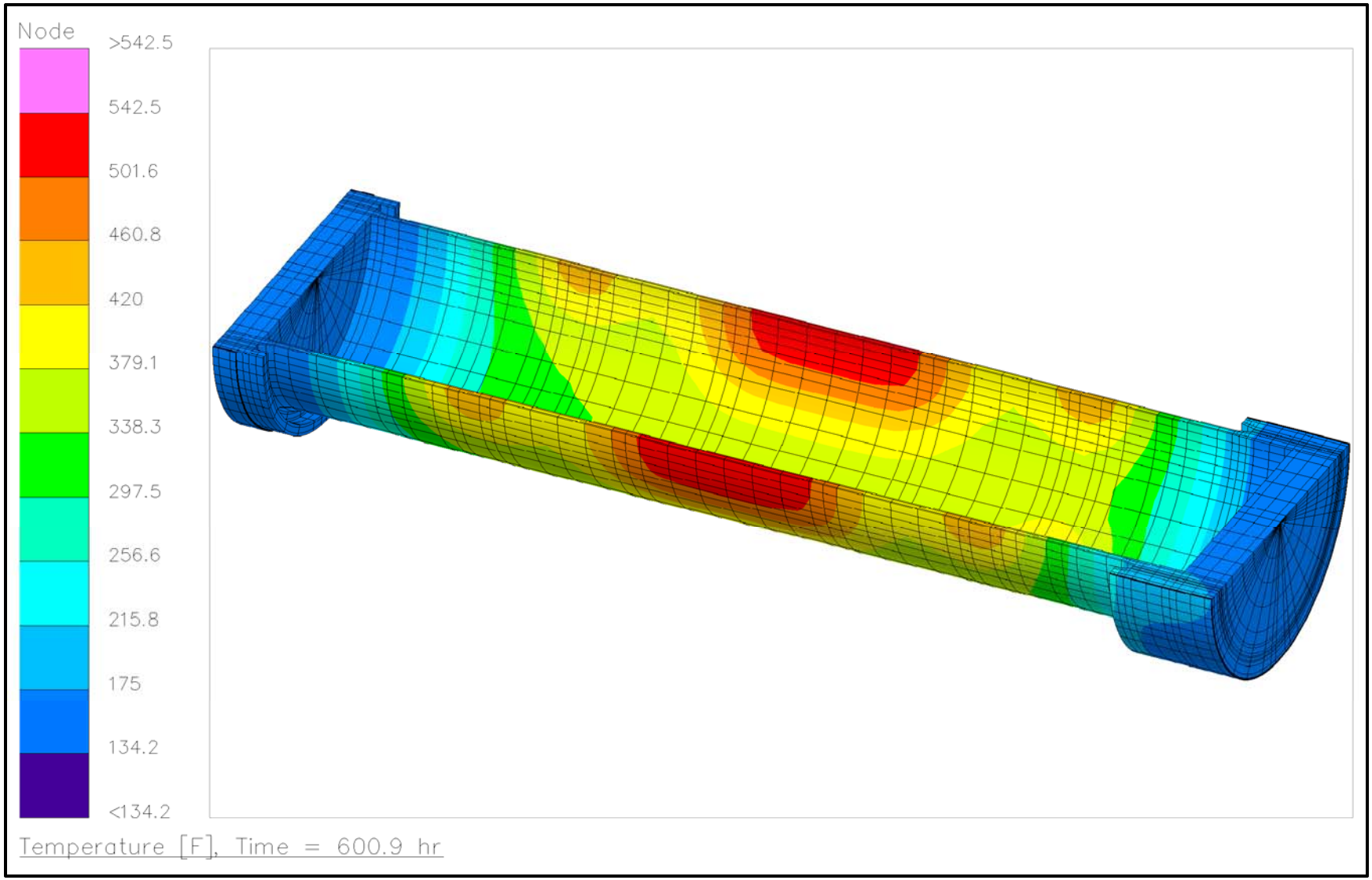

Figure 3.5-16 – HAC Case 1 – Package with RLC; 12 lb/ft³ Waste with 90 Watts Decay Heat – OC Inner Shell Fire Temperatures

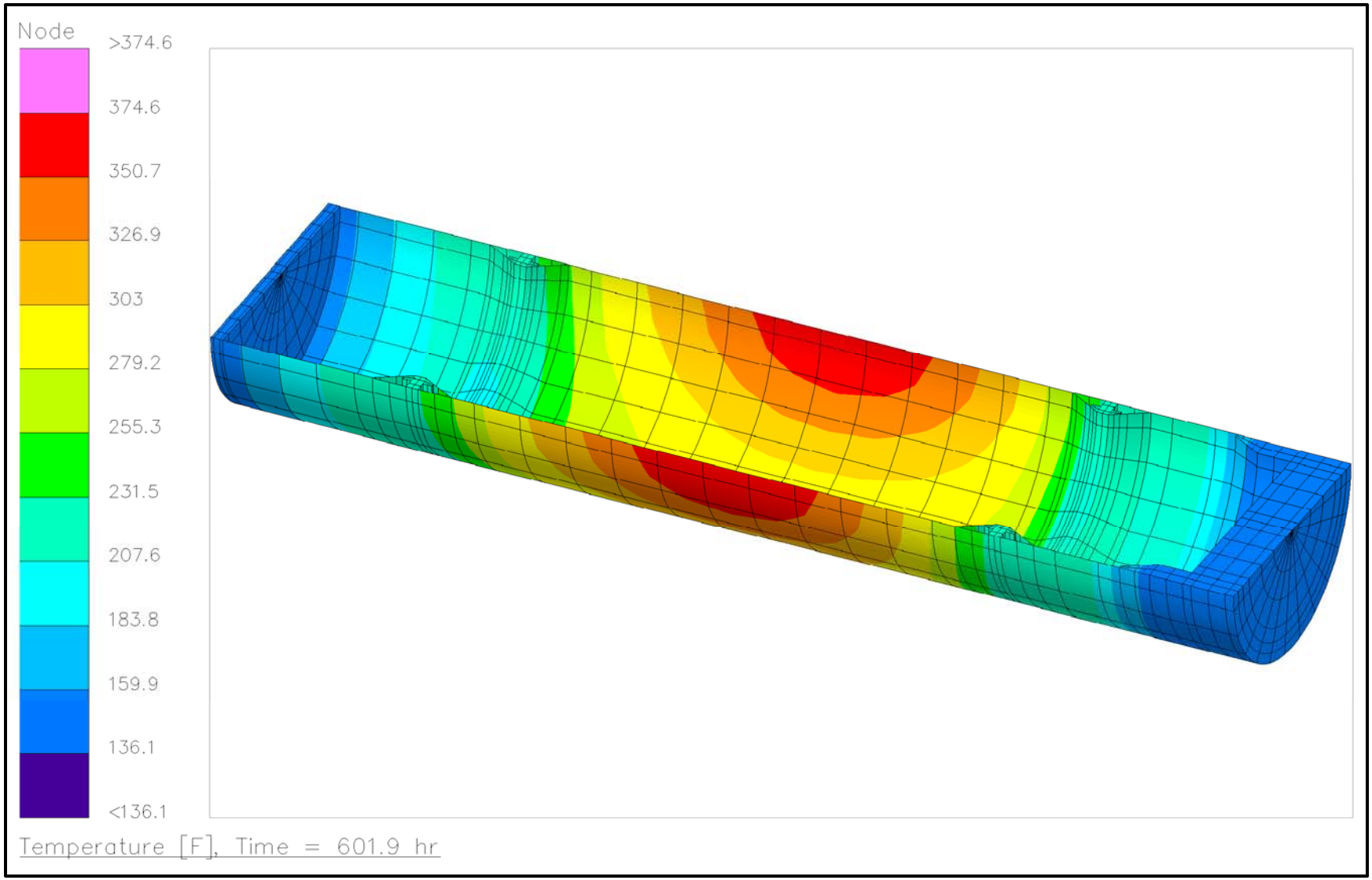

Figure 3.5-17 – HAC Case 1 – Package with RLC; 12 lb/ft³ Waste with 90 Watts Decay Heat – IV Fire Temperatures

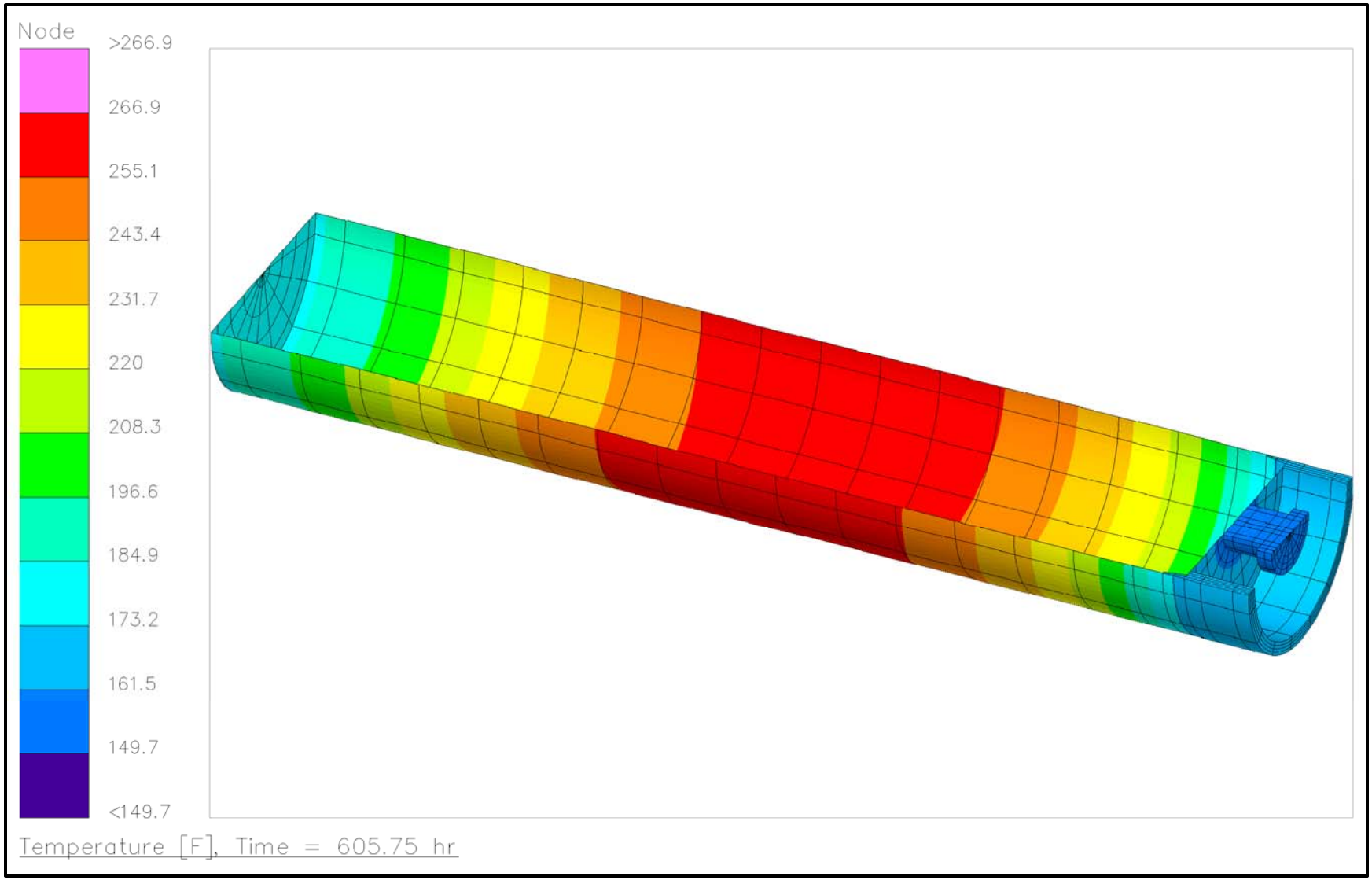

Figure 3.5-18 – HAC Case 1 – Package with RLC; 12 lb/ft³ Waste with 90 Watts Decay Heat – RLC Fire Temperatures

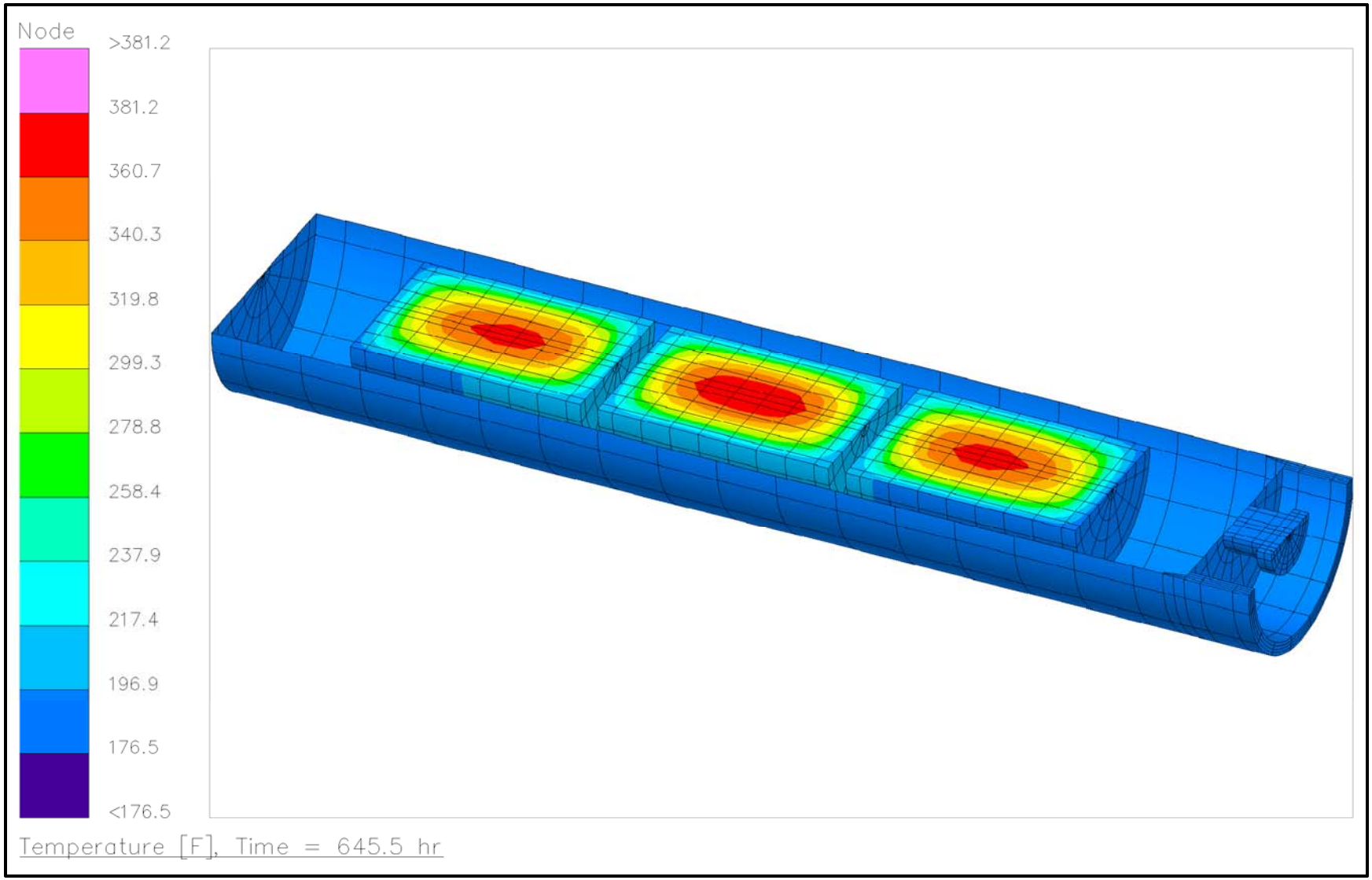

Figure 3.5-19 – HAC Case 1 – Package with RLC; 12 lb/ft³ Waste with 90 Watts Decay Heat – Drum and Waste Fire Temperatures

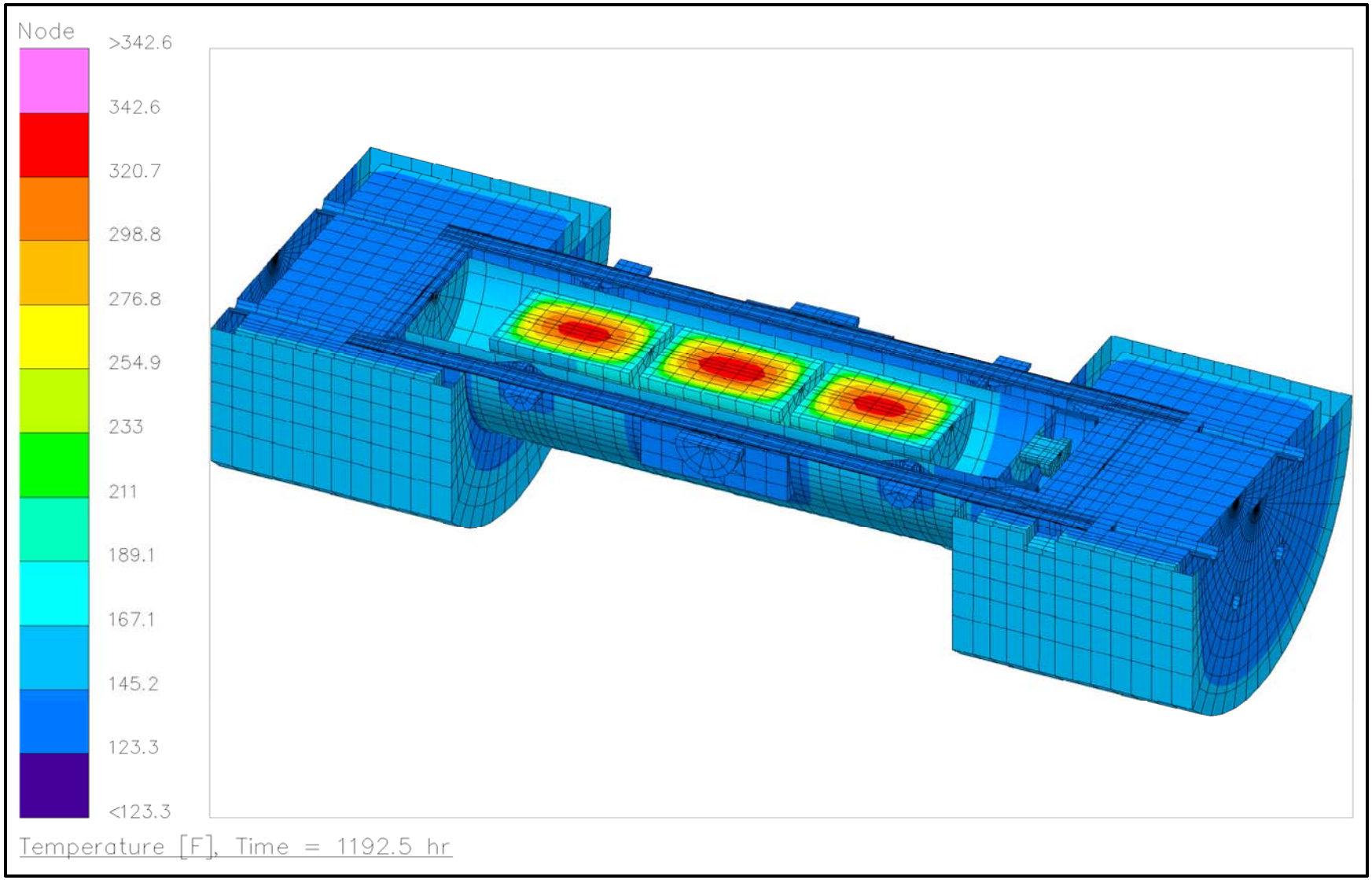

Figure 3.5-20 – HAC Case 1 – Package with RLC; 12 lb/ft³ Waste with 90 Watts Decay Heat and Insolation – Post-Fire Temperatures

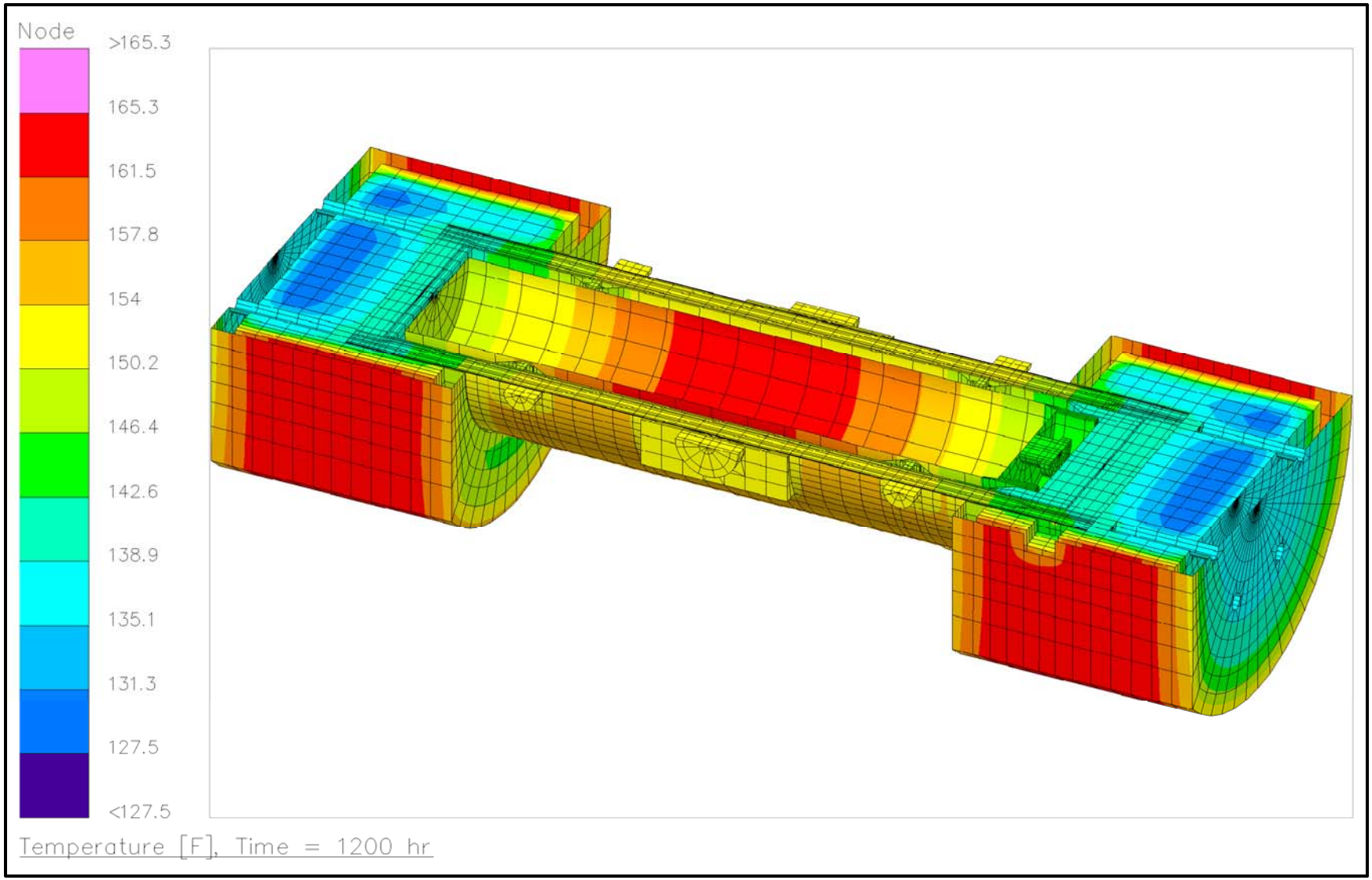

Figure 3.5-21 – HAC Case 1 – Package with RLC; 12 lb/ft³ Waste with 90 Watts Decay Heat and Insolation – Post-Fire Temperatures (Drums Hidden)

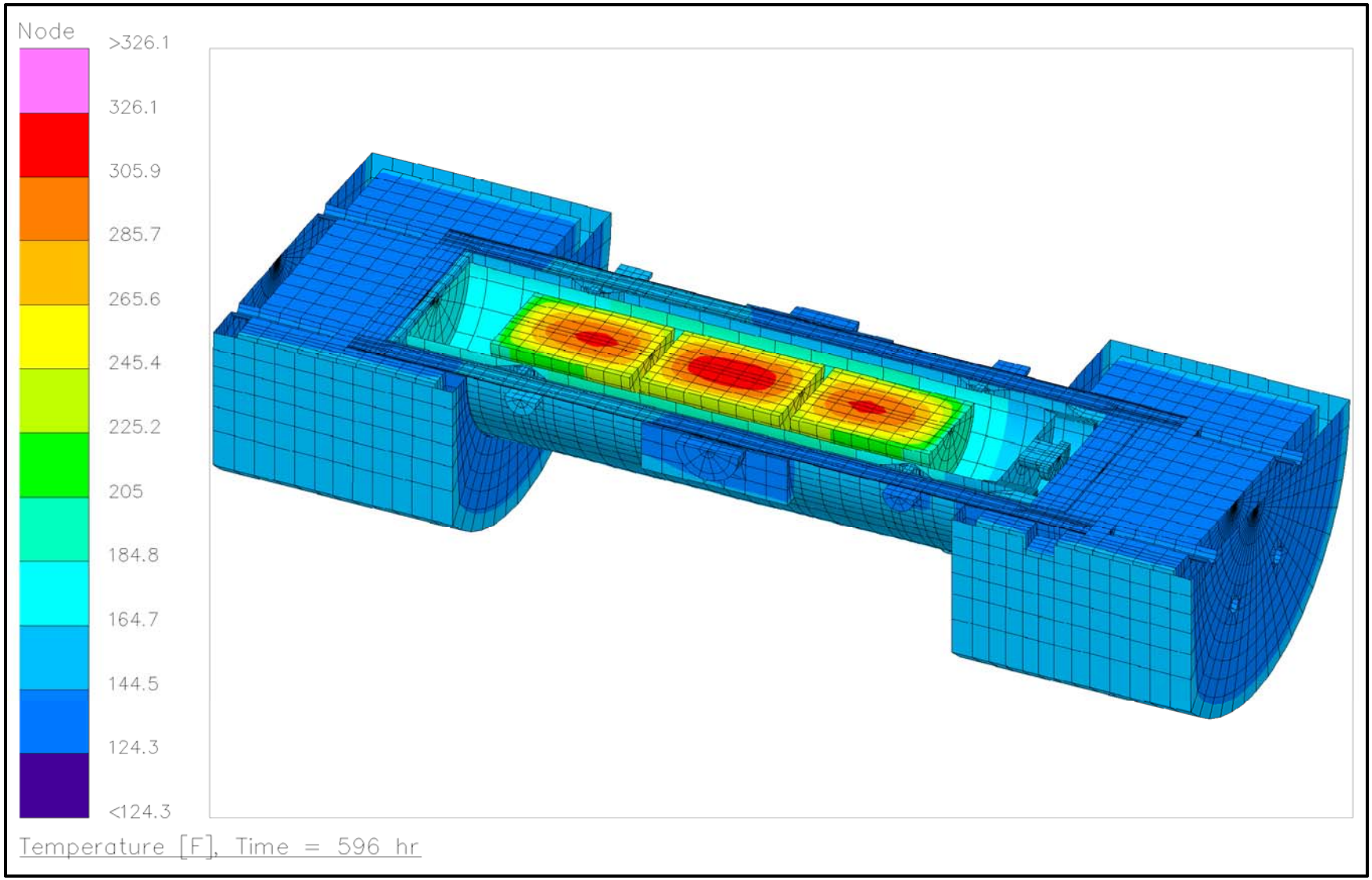

Figure 3.5-22 – HAC Case 1 – Package with RLC; 100 lb/ft³ Waste with 270 Watts Decay Heat and Insolation – Pre-Fire Temperatures

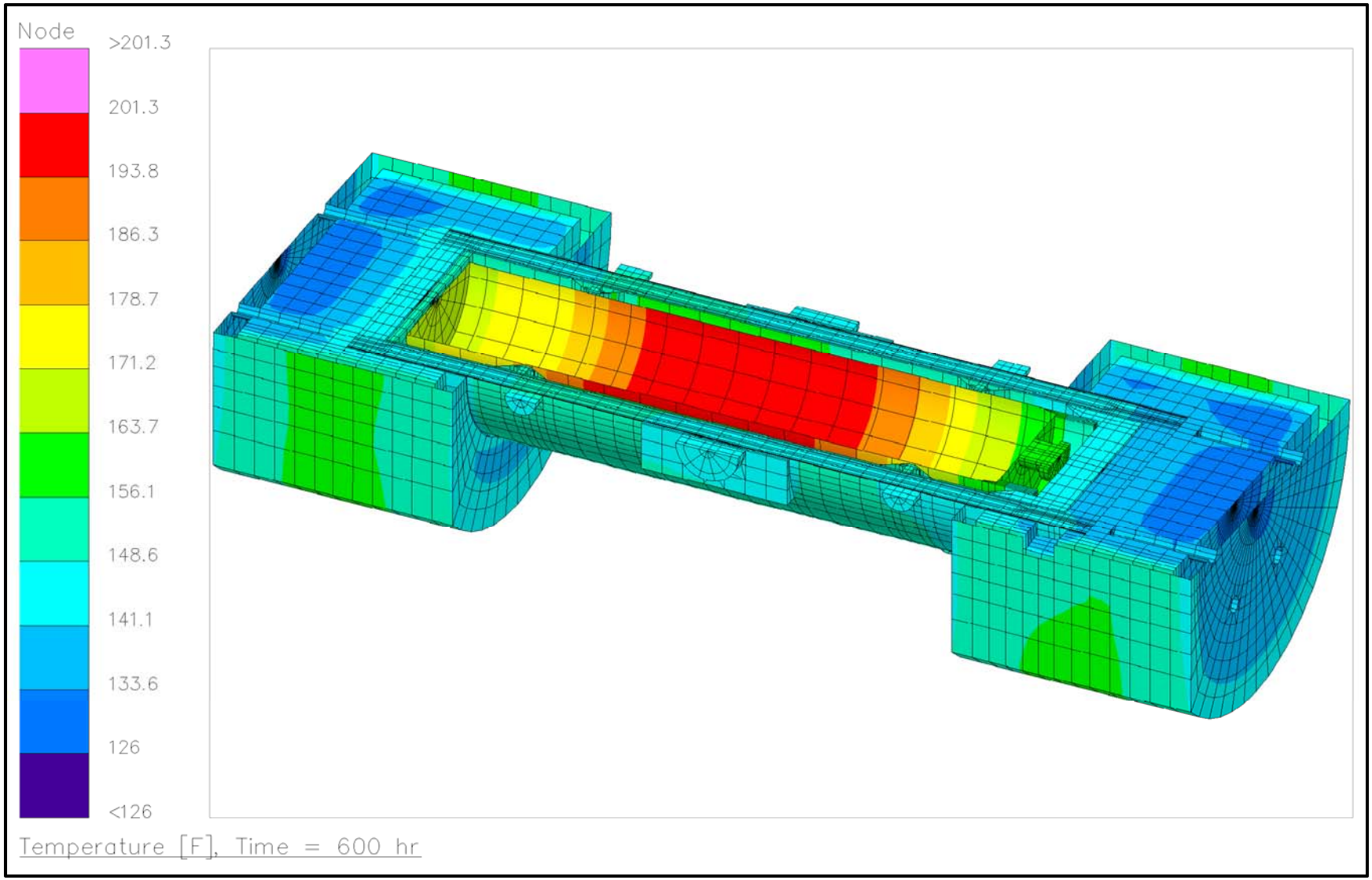

Figure 3.5-23 – HAC Case 1 – Package with RLC; 100 lb/ft³ Waste with 270 Watts Decay Heat and Insolation – Pre-Fire Temperatures (Drums Hidden)

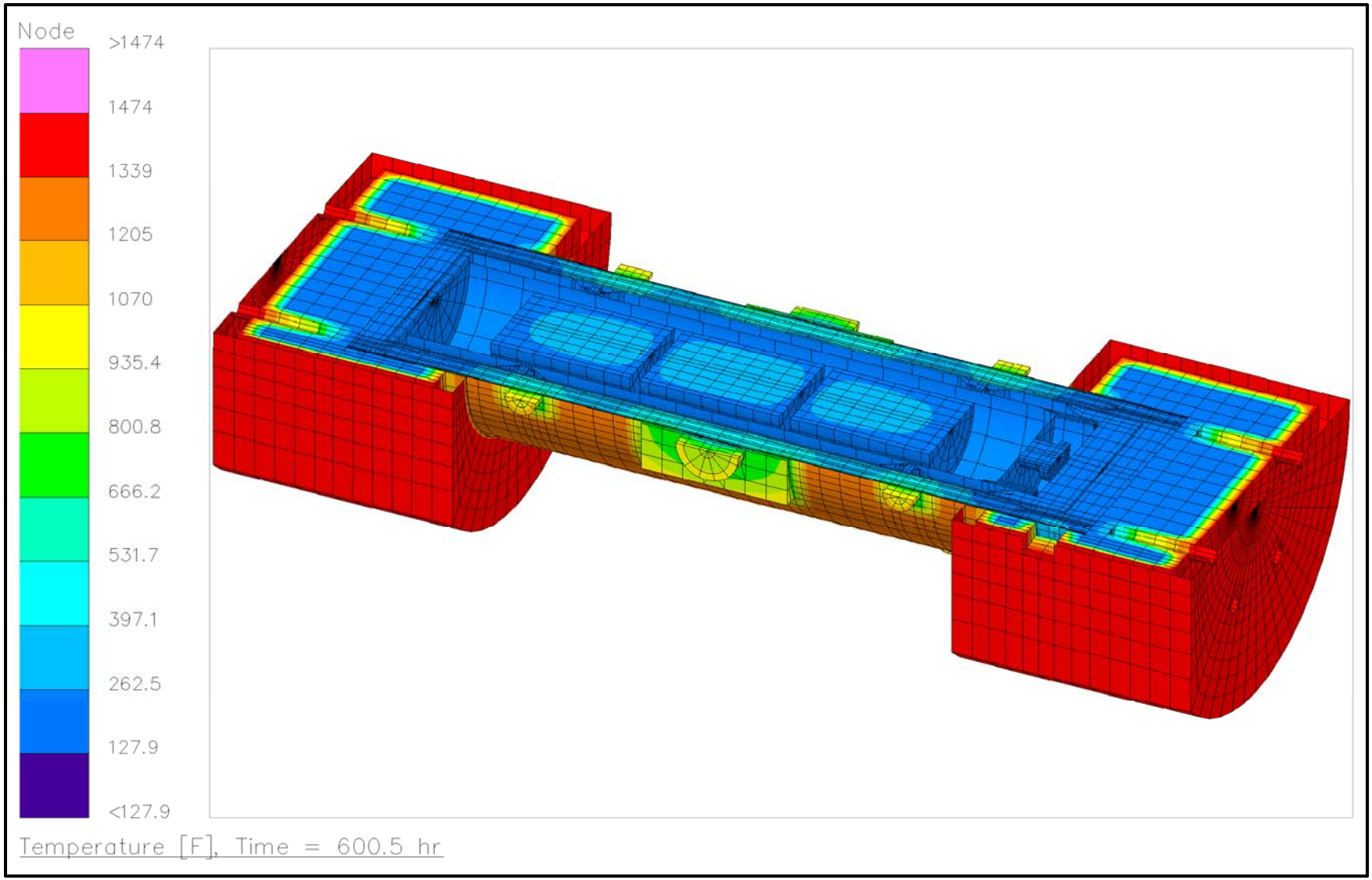

Figure 3.5-24 – HAC Case 1 – Package with RLC; 100 lb/ft³ Waste with 270 Watts Decay Heat – Package Fire Temperatures

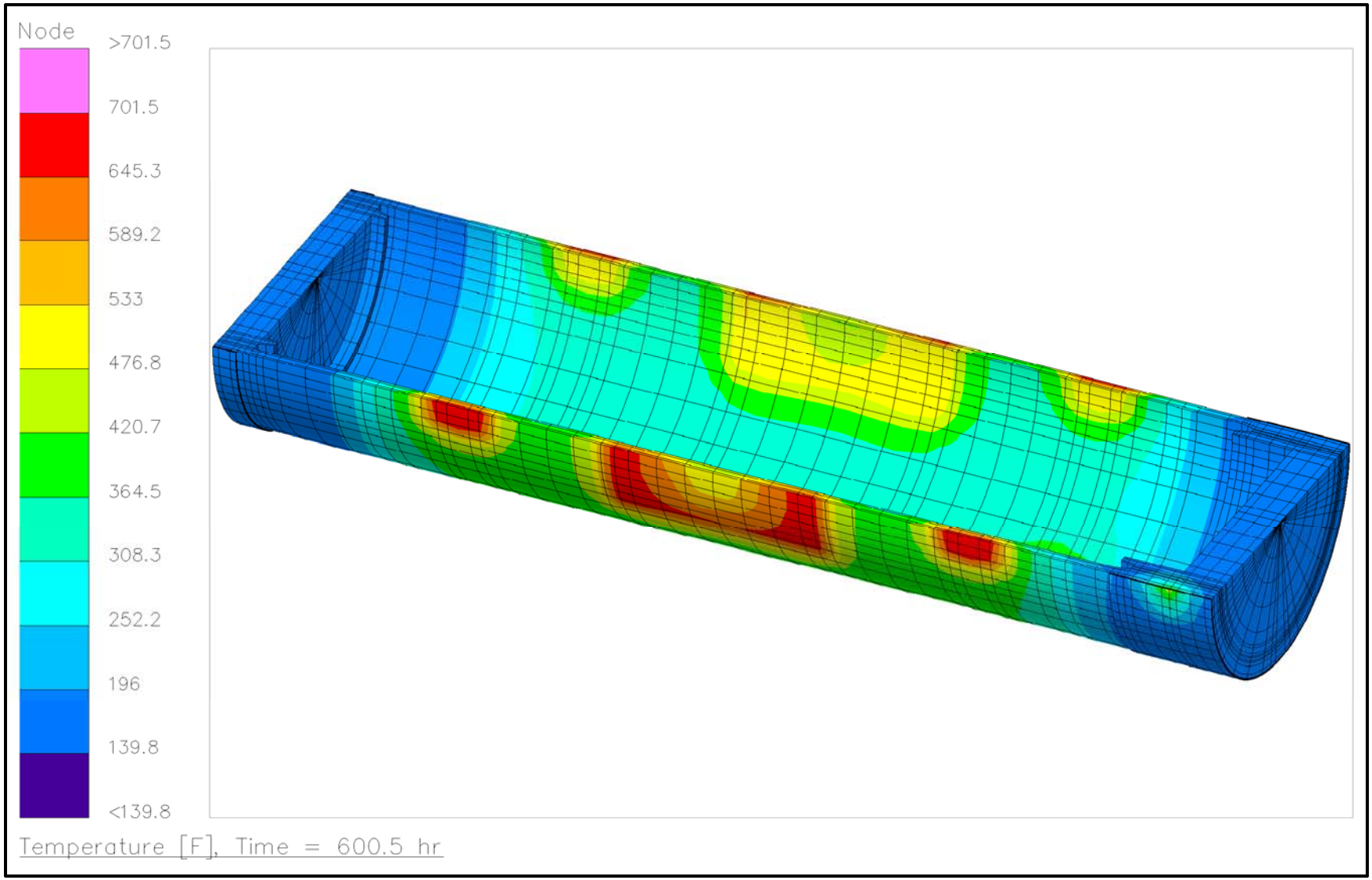

Figure 3.5-25 – HAC Case 1 – Package with RLC; 100 lb/ft³ Waste with 270 Watts Decay Heat – OC Outer Shell Fire Temperatures

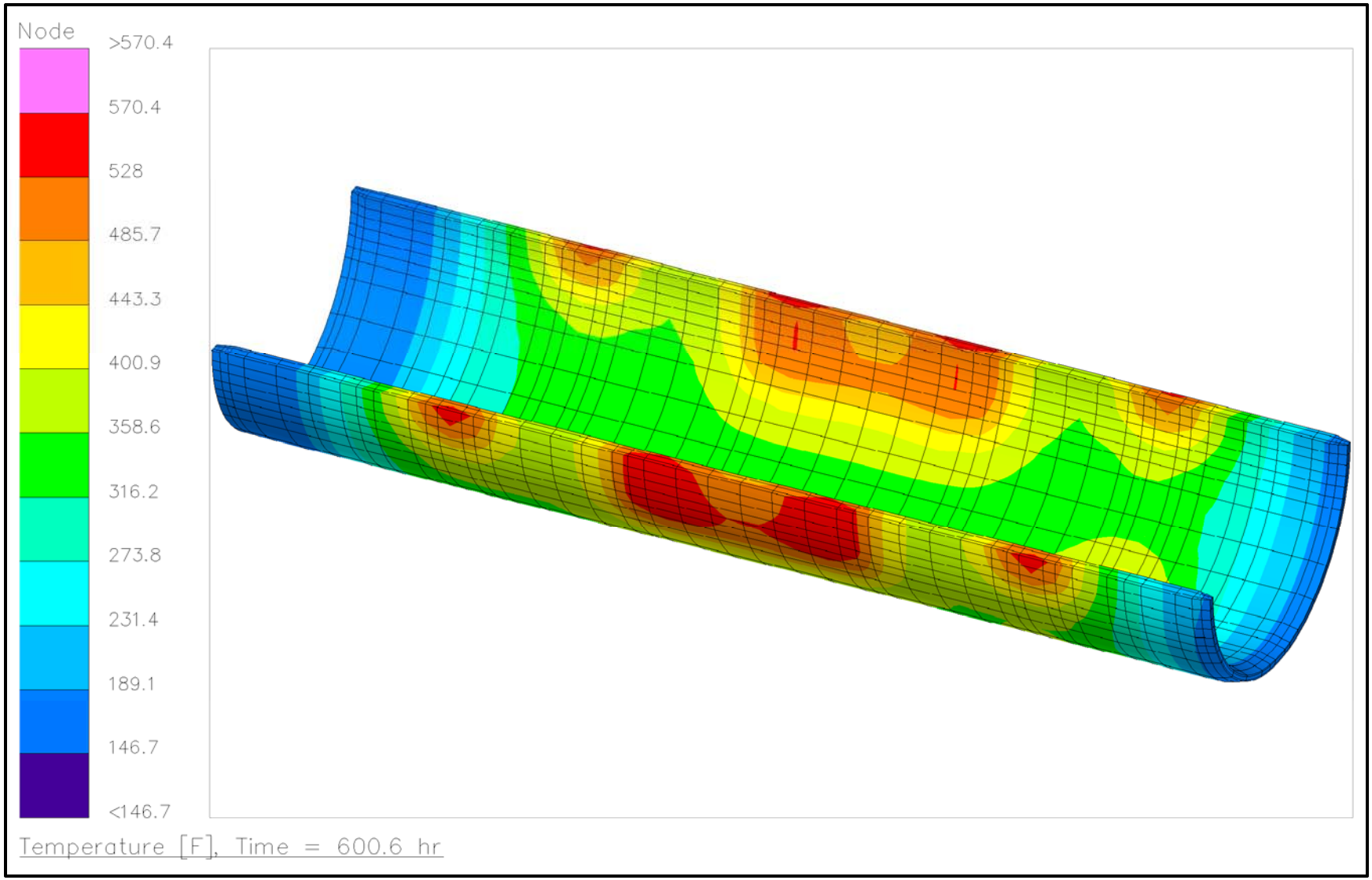

Figure 3.5-26 – HAC Case 1 – Package with RLC; 100 lb/ft³ Waste with 270 Watts Decay Heat – OC Lead Fire Temperatures

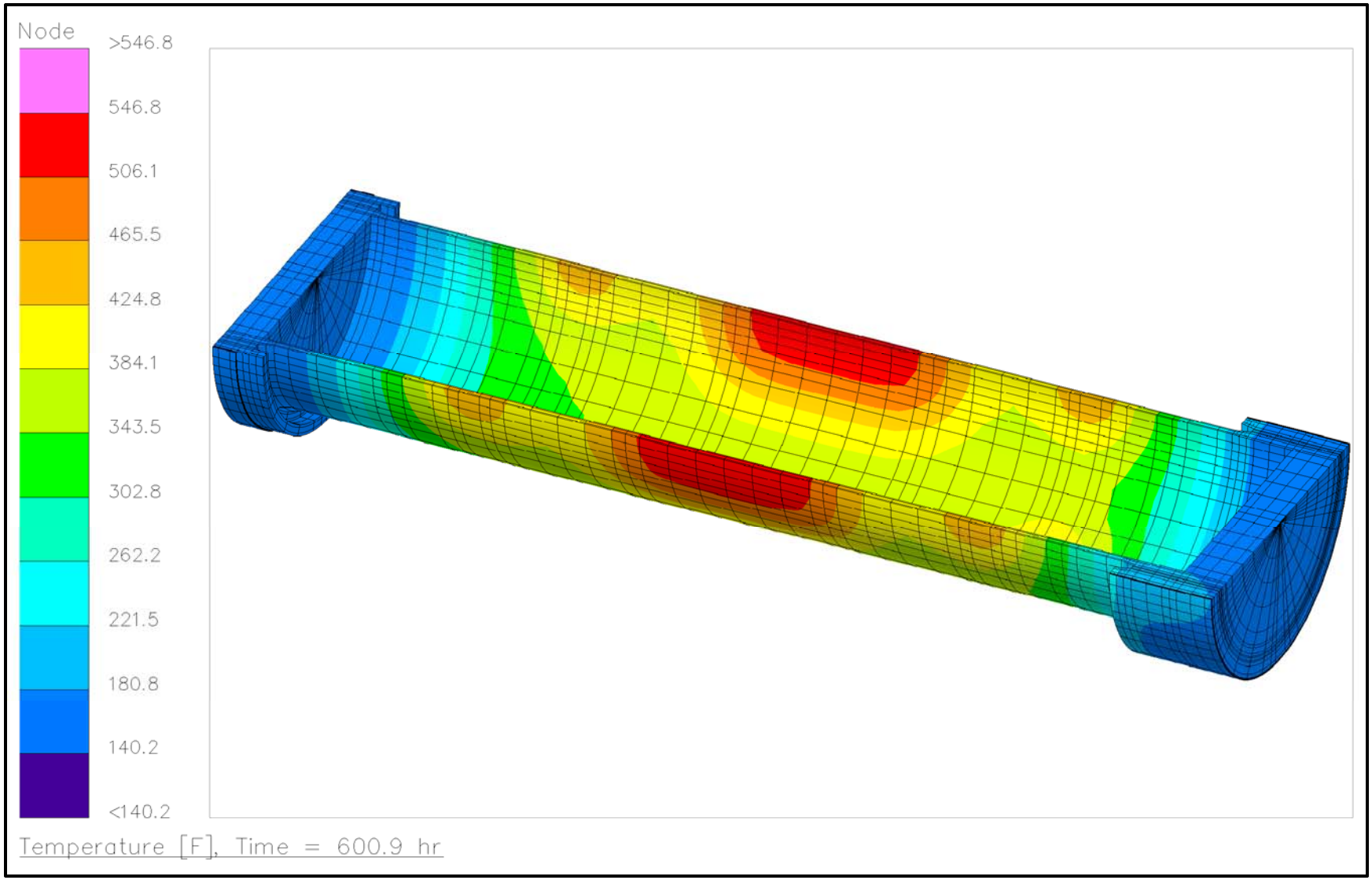

Figure 3.5-27 – HAC Case 1 – Package with RLC; 100 lb/ft³ Waste with 270 Watts Decay Heat – OC Inner Shell Fire Temperatures

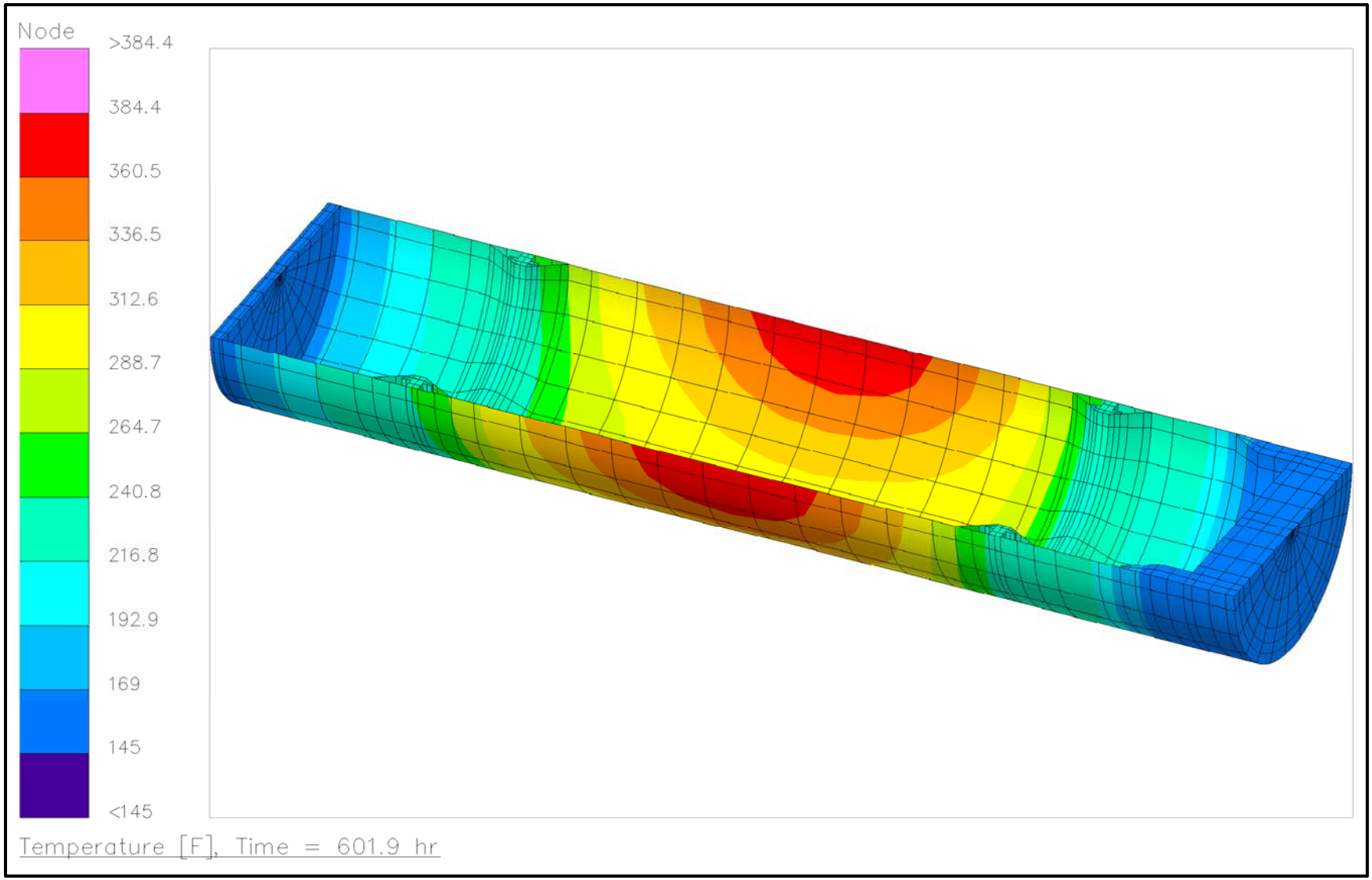

Figure 3.5-28 – HAC Case 1 – Package with RLC; 100 lb/ft³ Waste with 270 Watts Decay Heat – IV Fire Temperatures

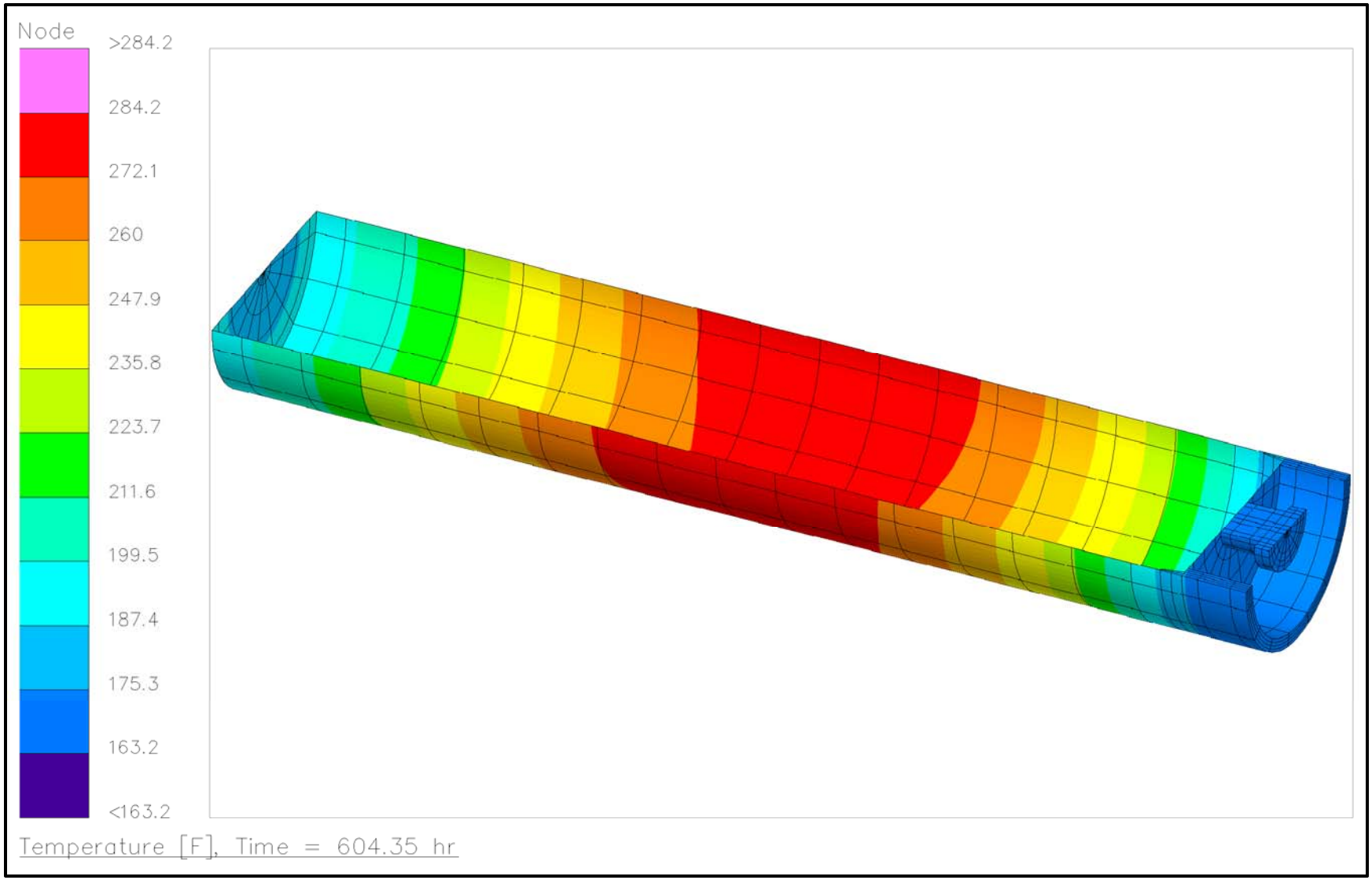

Figure 3.5-29 – HAC Case 1 – Package with RLC; 100 lb/ft³ Waste with 270 Watts Decay Heat – RLC Fire Temperatures

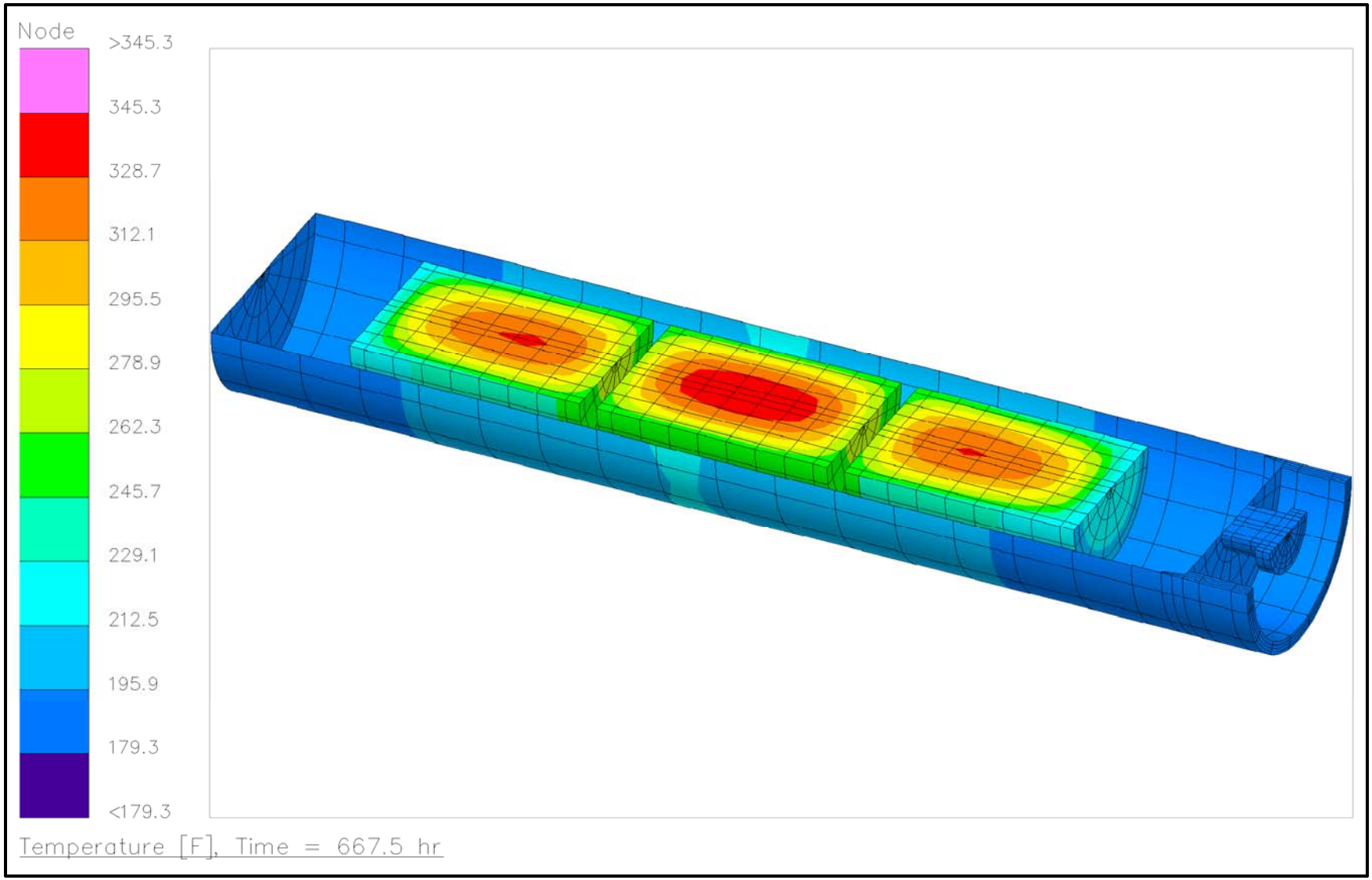

Figure 3.5-30 – HAC Case 1 – Package with RLC; 100 lb/ft³ Waste with 270 Watts Decay Heat – Drum and Waste Fire Temperatures

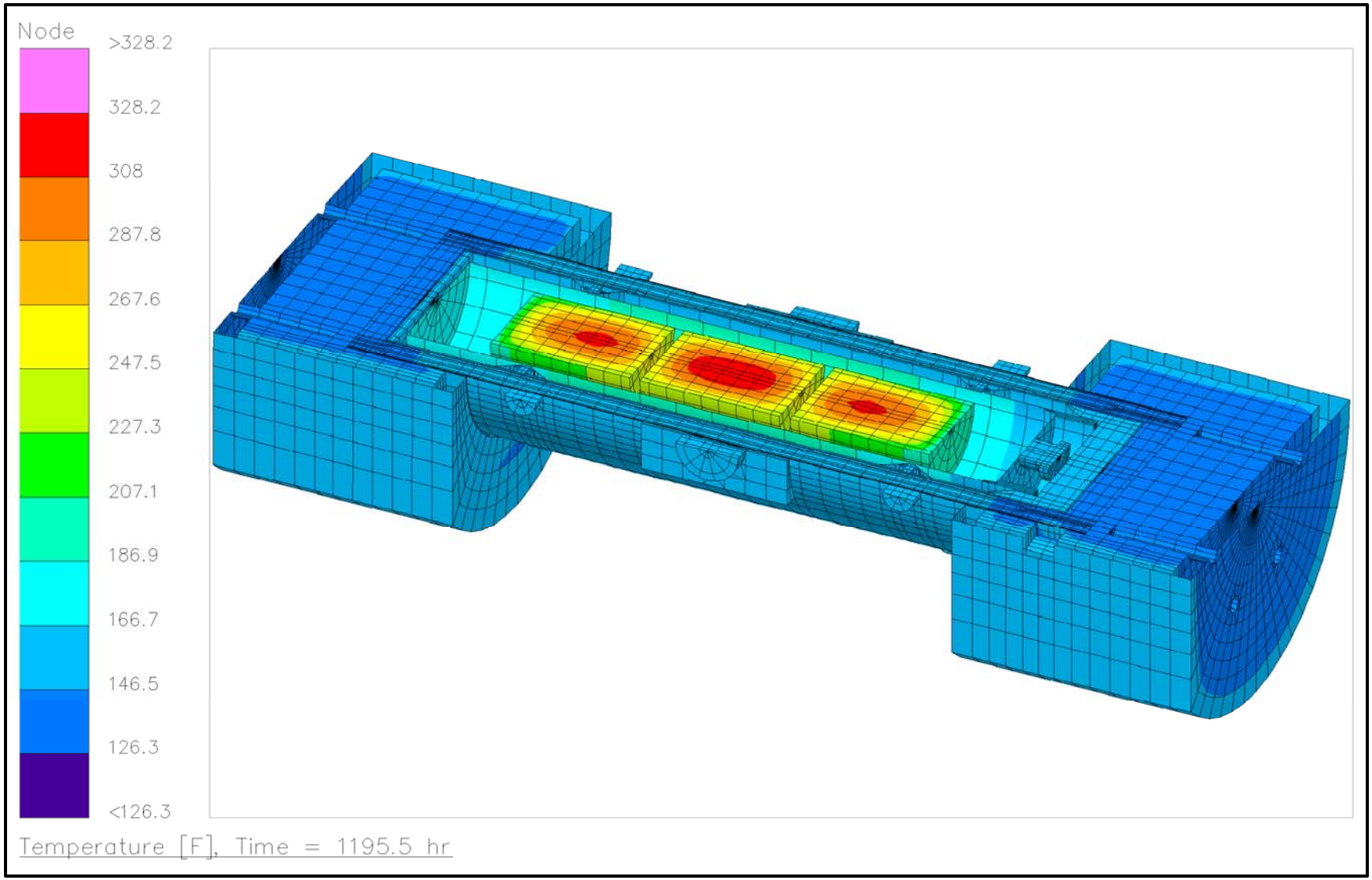

Figure 3.5-31 – HAC Case 1 – Package with RLC; 100 lb/ft³ Waste with 270 Watts Decay Heat and Insolation – Post-Fire Temperatures

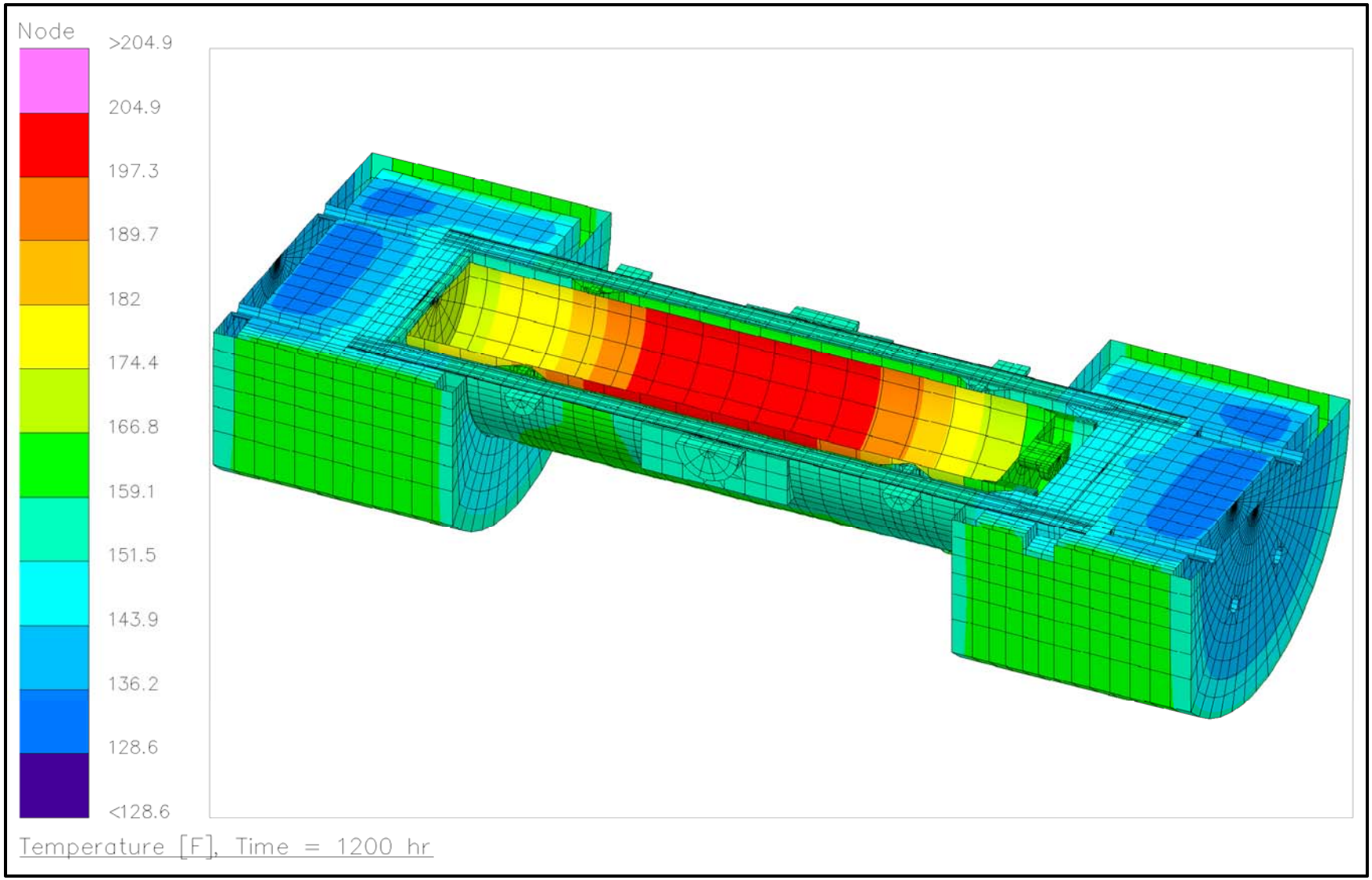

Figure 3.5-32 – HAC Case 1 – Package with RLC; 100 lb/ft³ Waste with 270 Watts Decay Heat and Insolation – Post-Fire Temperatures (Drums Hidden)

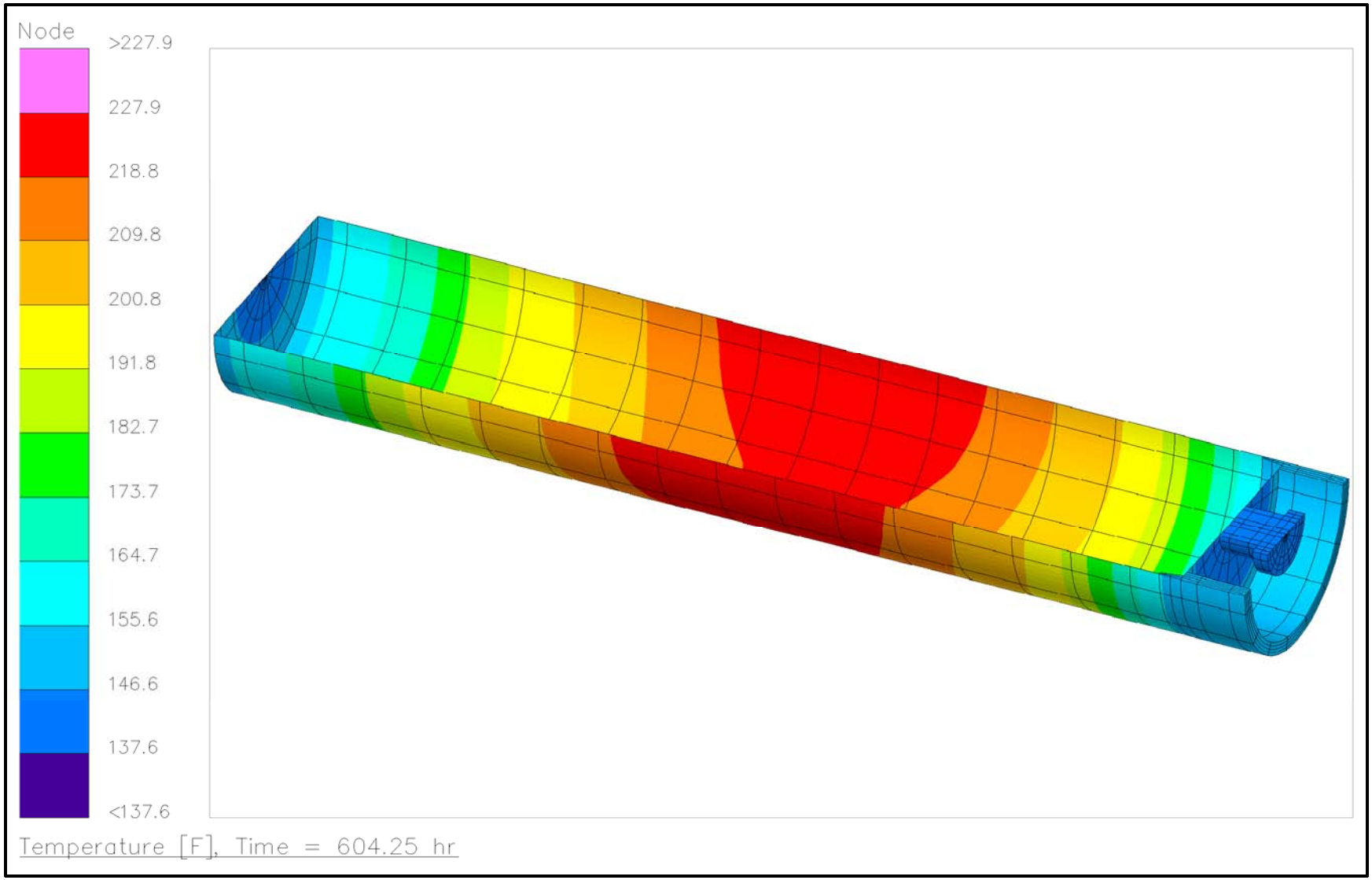

Figure 3.5-33 – HAC Case 2 – Package with NS15; 12 lb/ft³ Waste with 50 Watts Decay Heat – RLC (NSC) Fire Temperatures

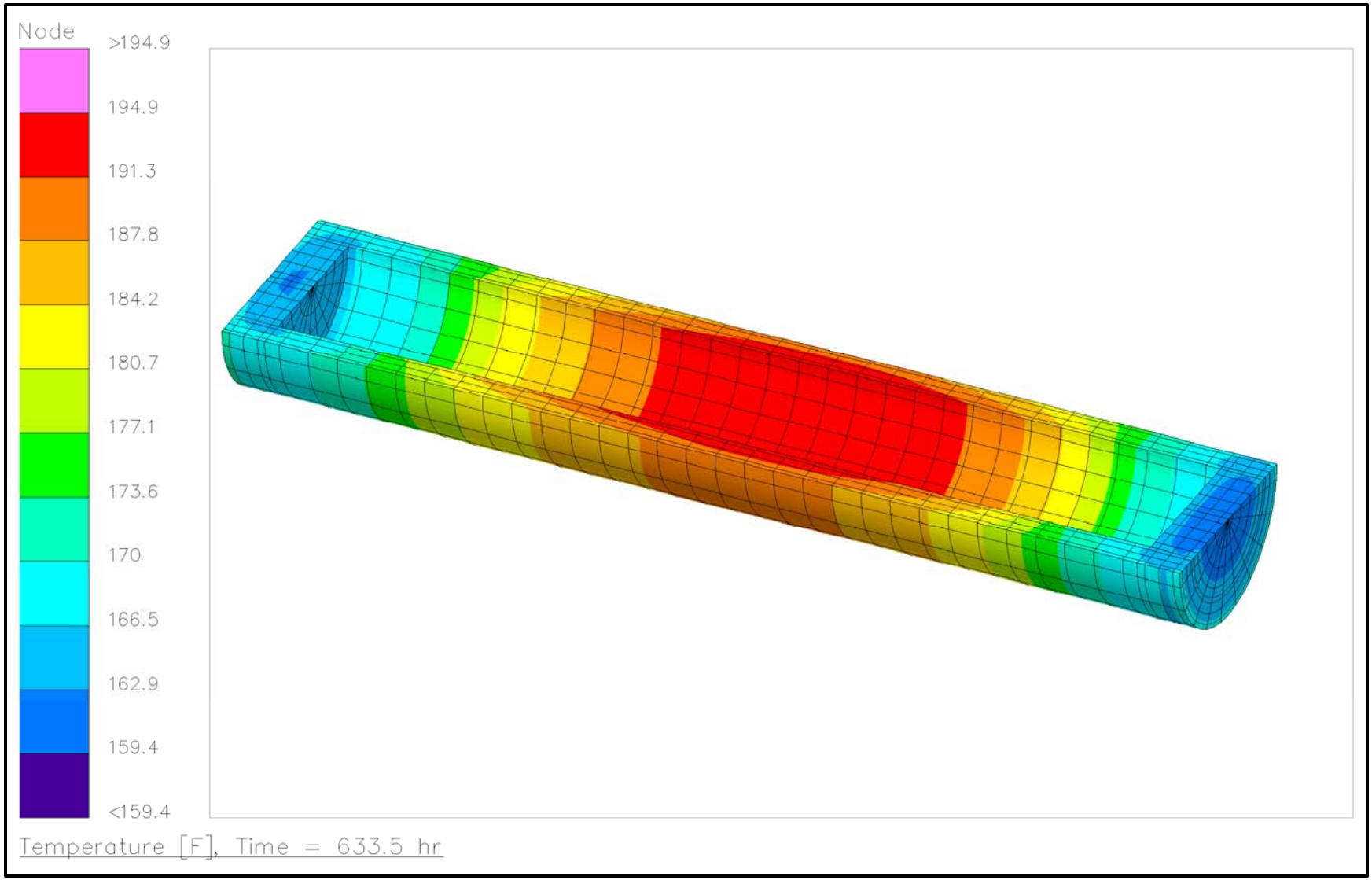

Figure 3.5-34 – HAC Case 2 – Package with NS15; 12 lb/ft³ Waste with 50 Watts Decay Heat – HDPE Shield Insert Fire Temperatures

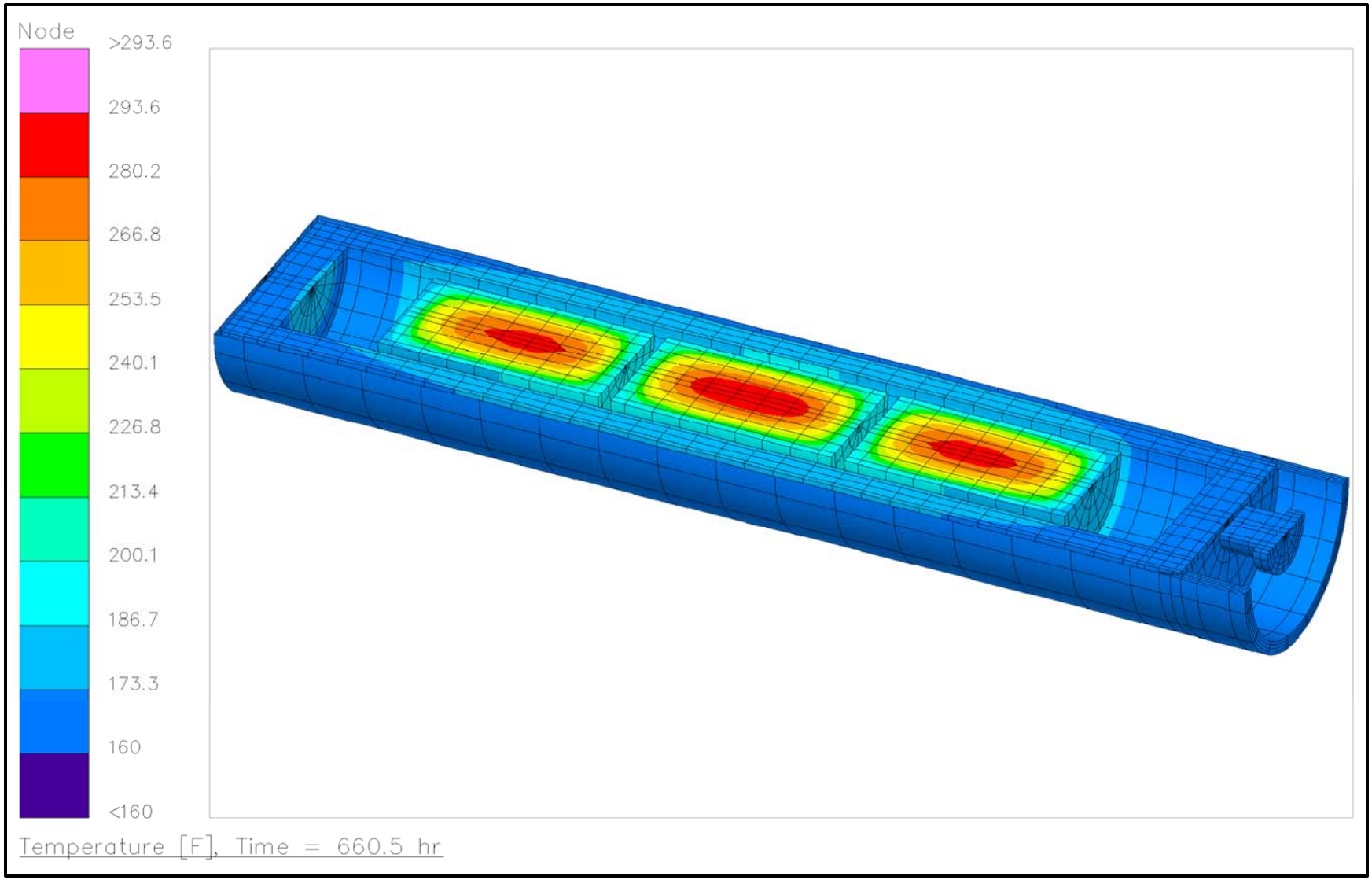

Figure 3.5-35 – HAC Case 2 – Package with NS15; 12 lb/ft³ Waste with 50 Watts Decay Heat – Drum and Waste Fire Temperatures

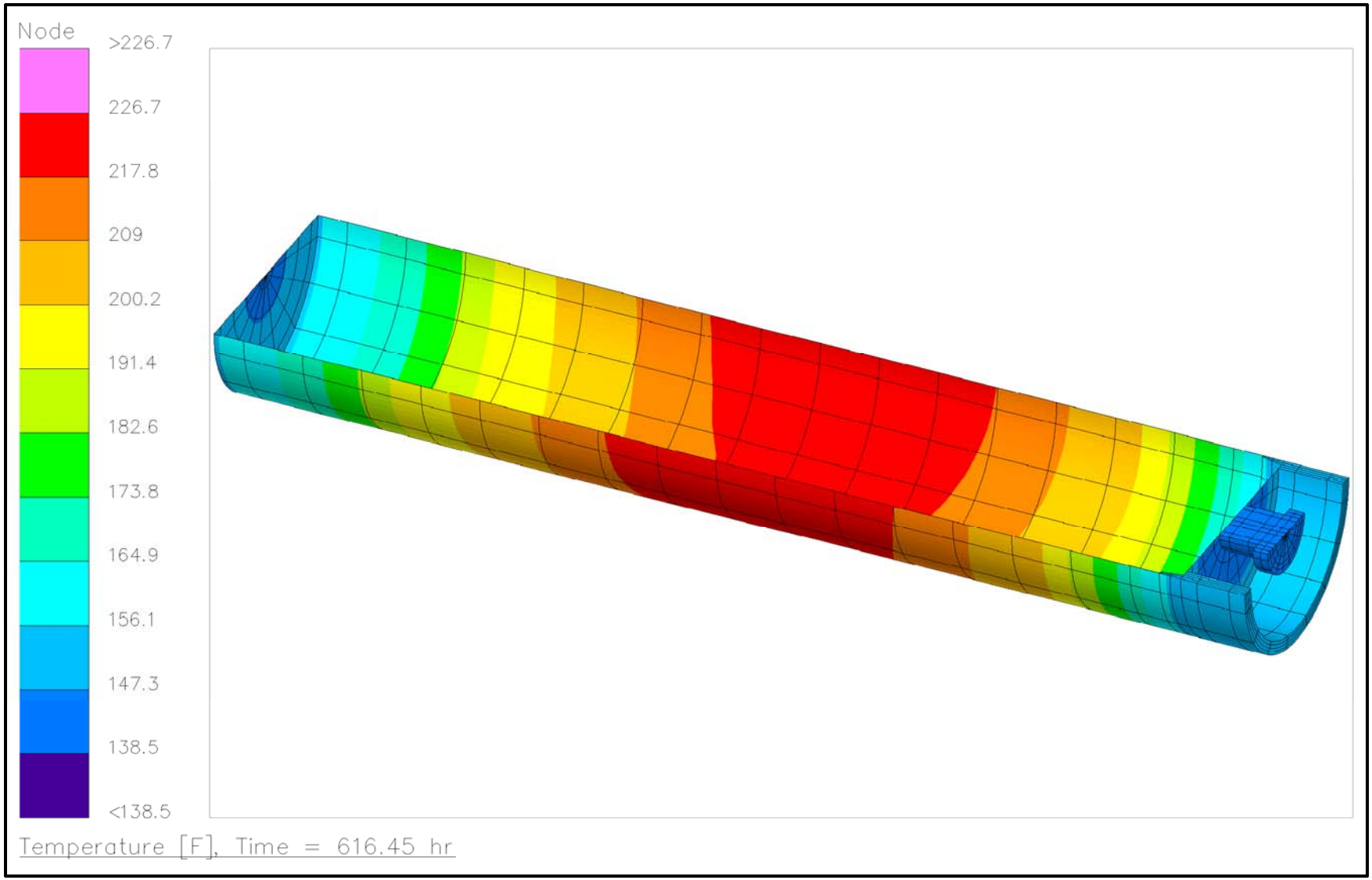

Figure 3.5-36 – HAC Case 3 – Package with NS30; 12 lb/ft³ Waste with 50 Watts Decay Heat – RLC (NSC) Fire Temperatures

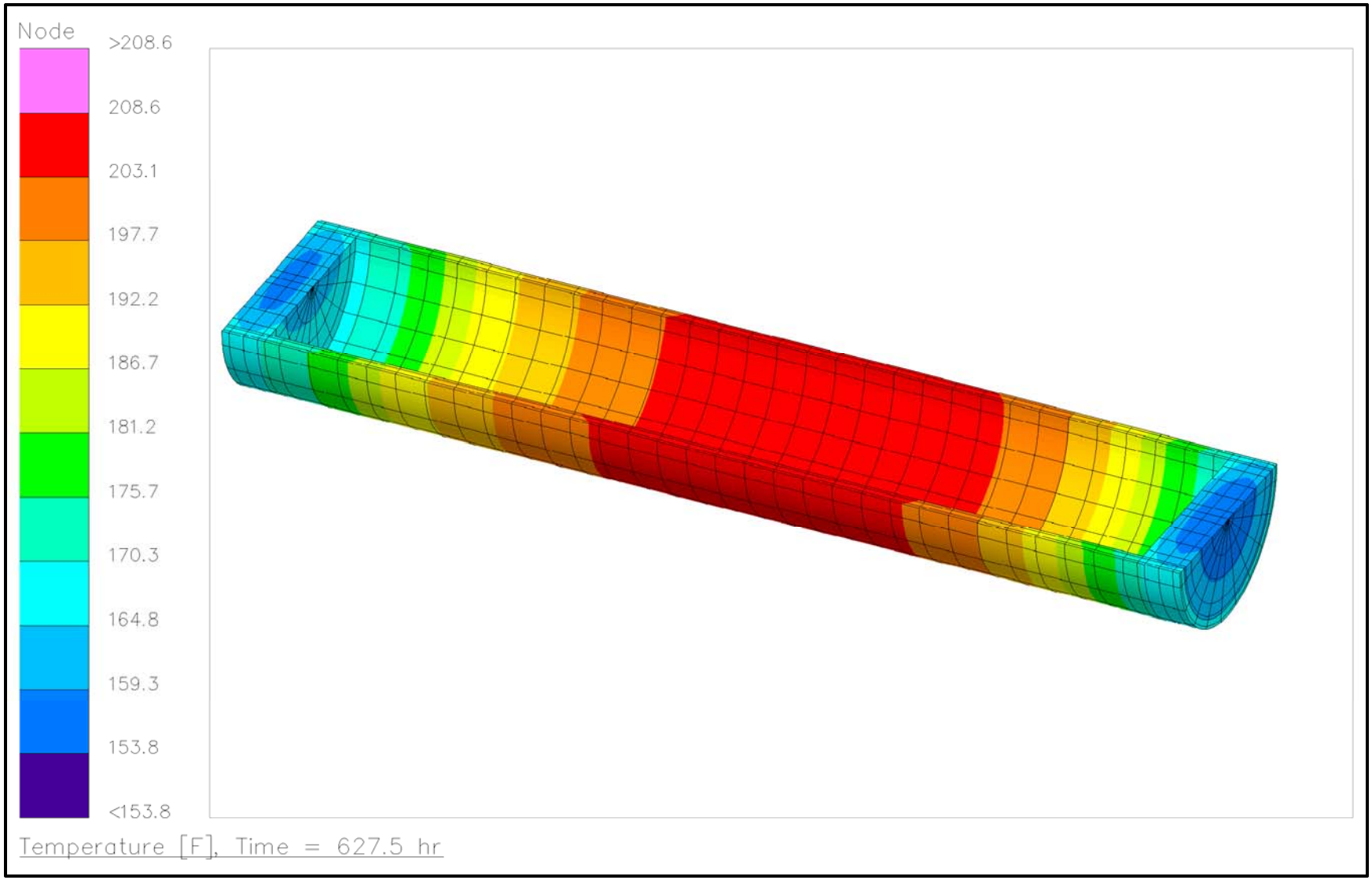

Figure 3.5-37 – HAC Case 3 – Package with NS30; 12 lb/ft³ Waste with 50 Watts Decay Heat – HDPE Shield Insert Fire Temperatures

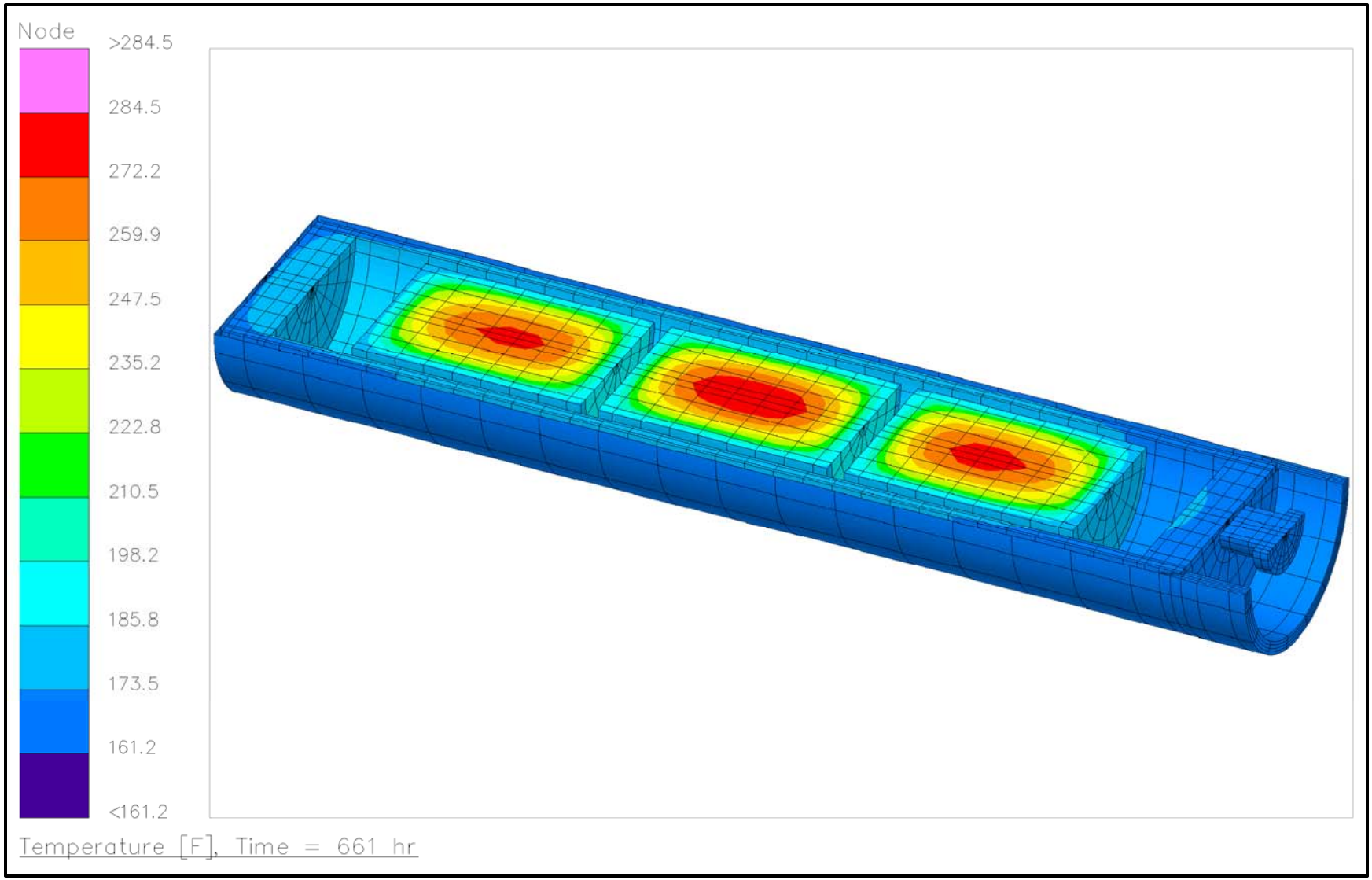

Figure 3.5-38 – HAC Case 3 – Package with NS30; 12 lb/ft³ Waste with 50 Watts Decay Heat – Drum and Waste Fire Temperatures

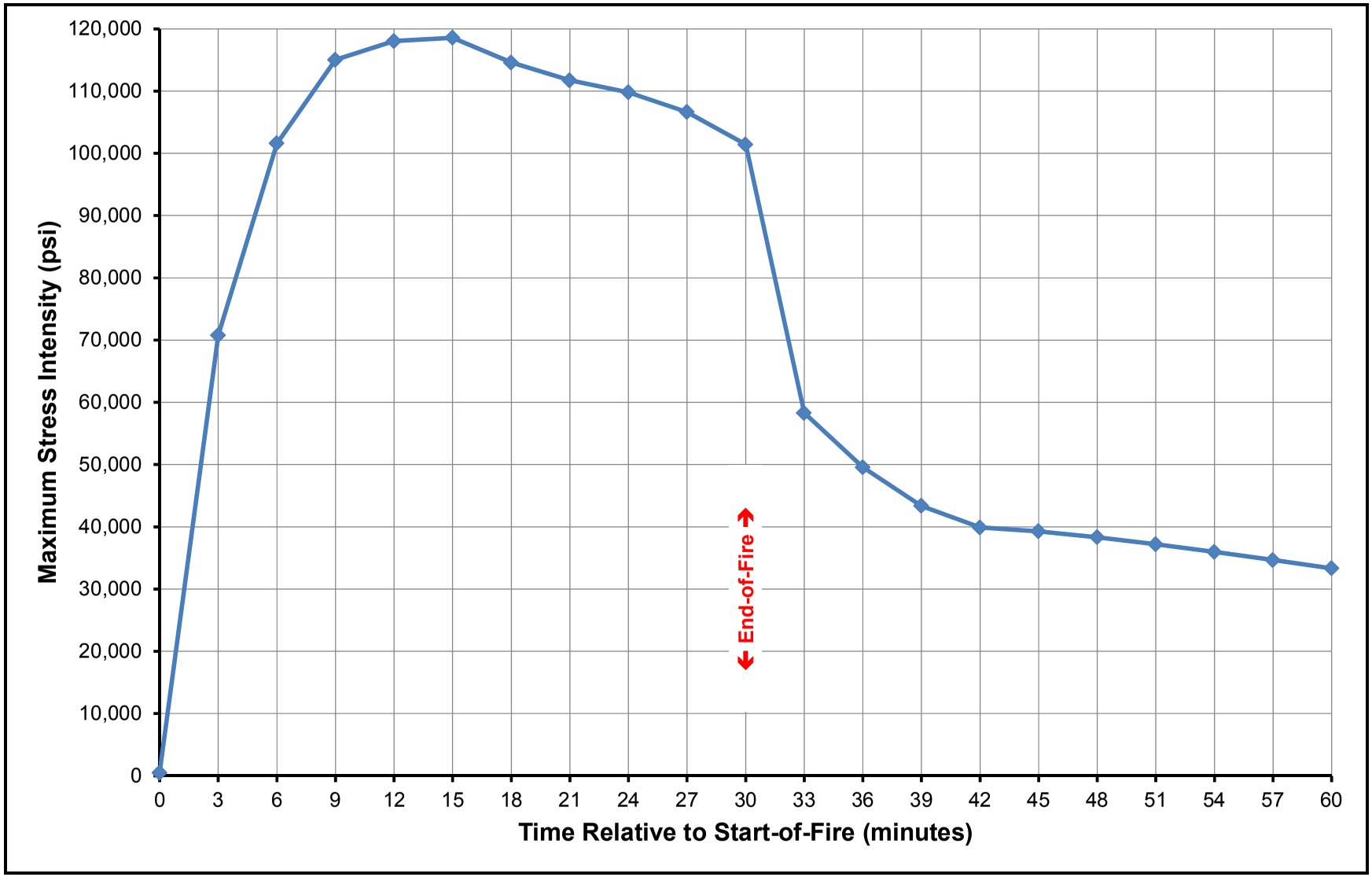

Figure 3.5-39 – Maximum OC Thermal Stress Intensity vs. Time Relative to Start-of-Fire

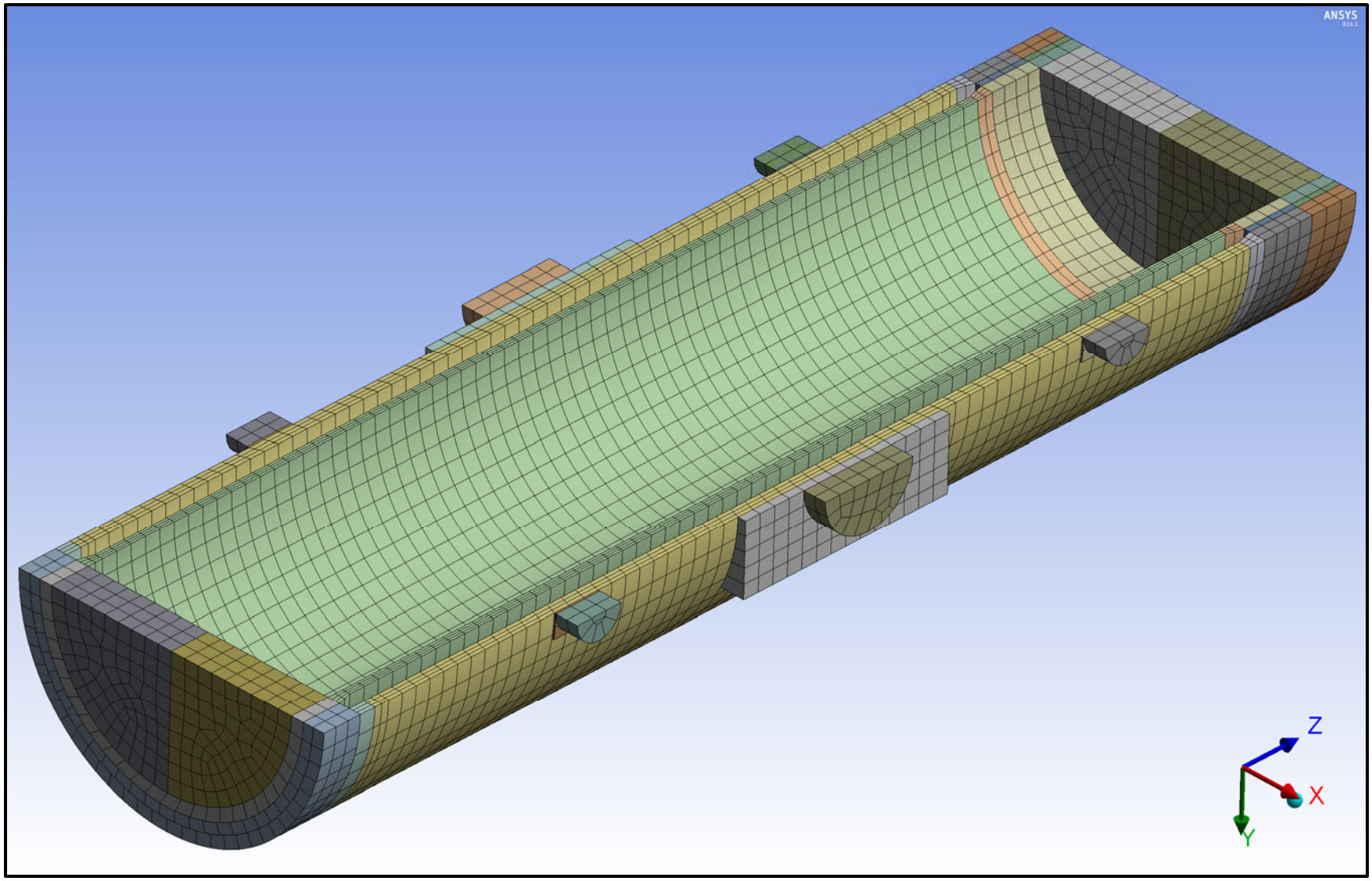

Figure 3.5-40 – ANSYS HAC Thermal Stress Model

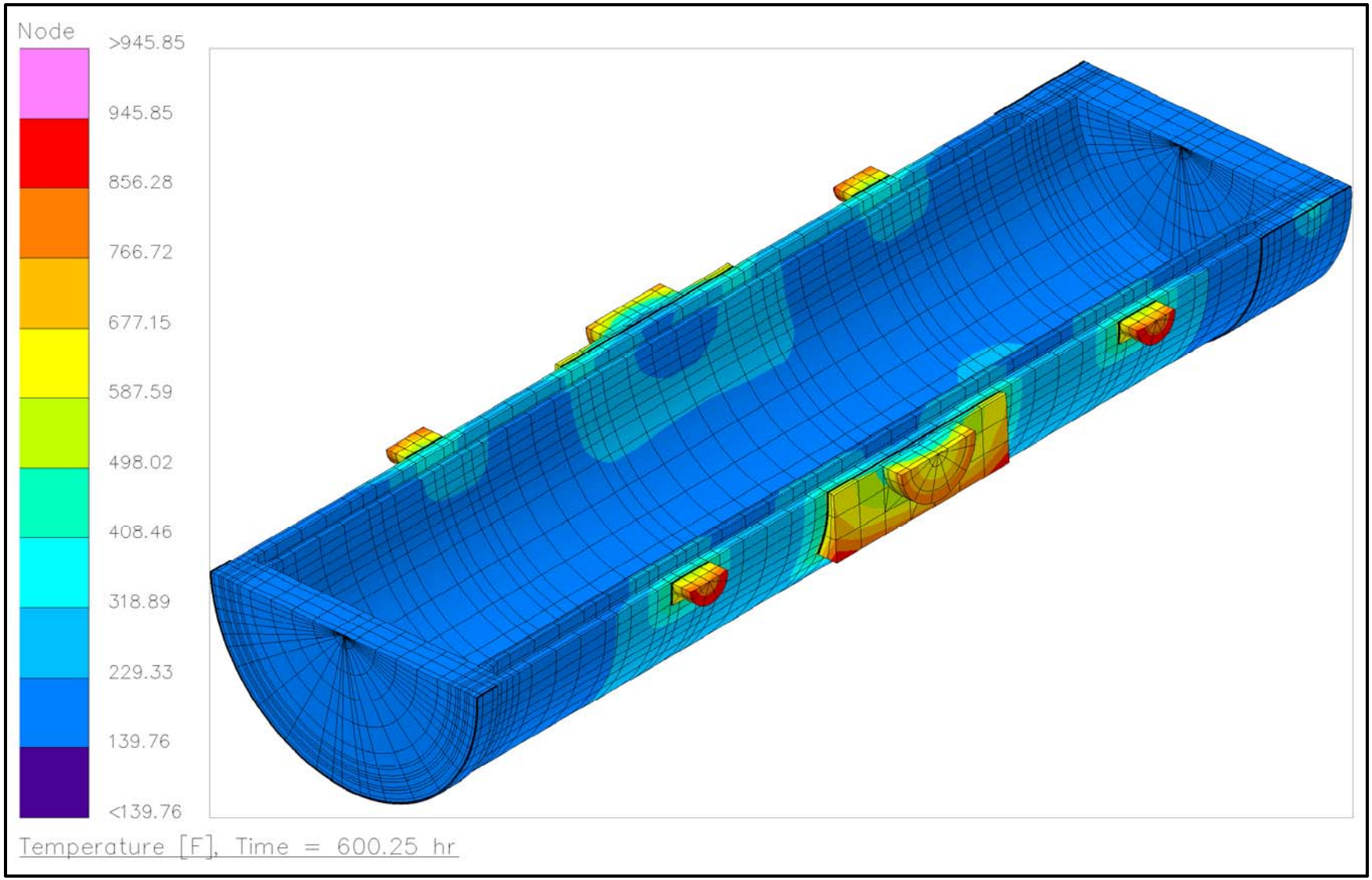

Figure 3.5-41 – HAC Case 1 – OC Temperatures @ 15m after Start-of-Fire; 100 lb/ft³ Waste with 270 Watts Decay Heat

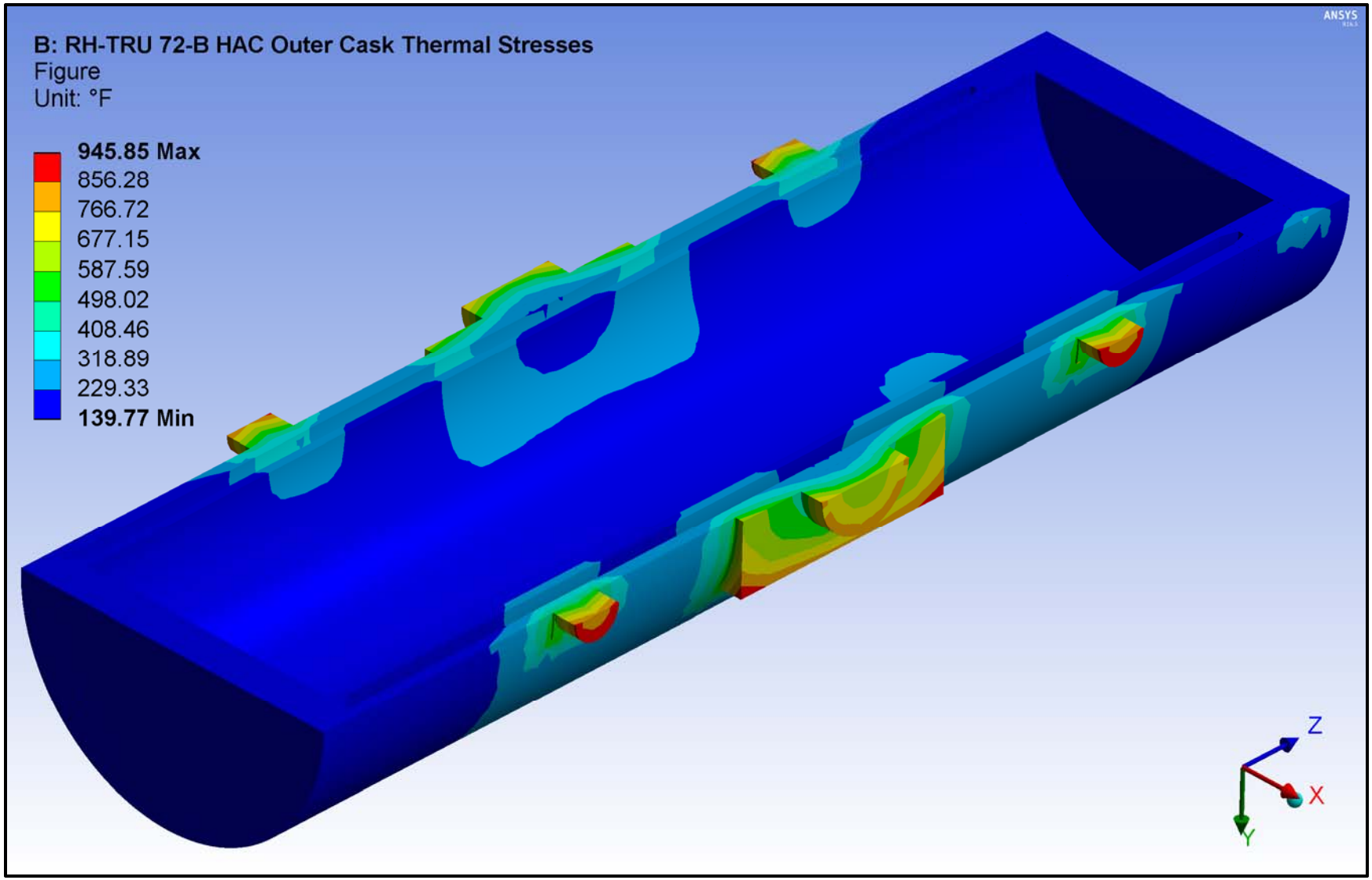

Figure 3.5-42 – ANSYS HAC Thermal Stress Model – OC Temperatures @ 15m after Start-of-Fire for Comparison

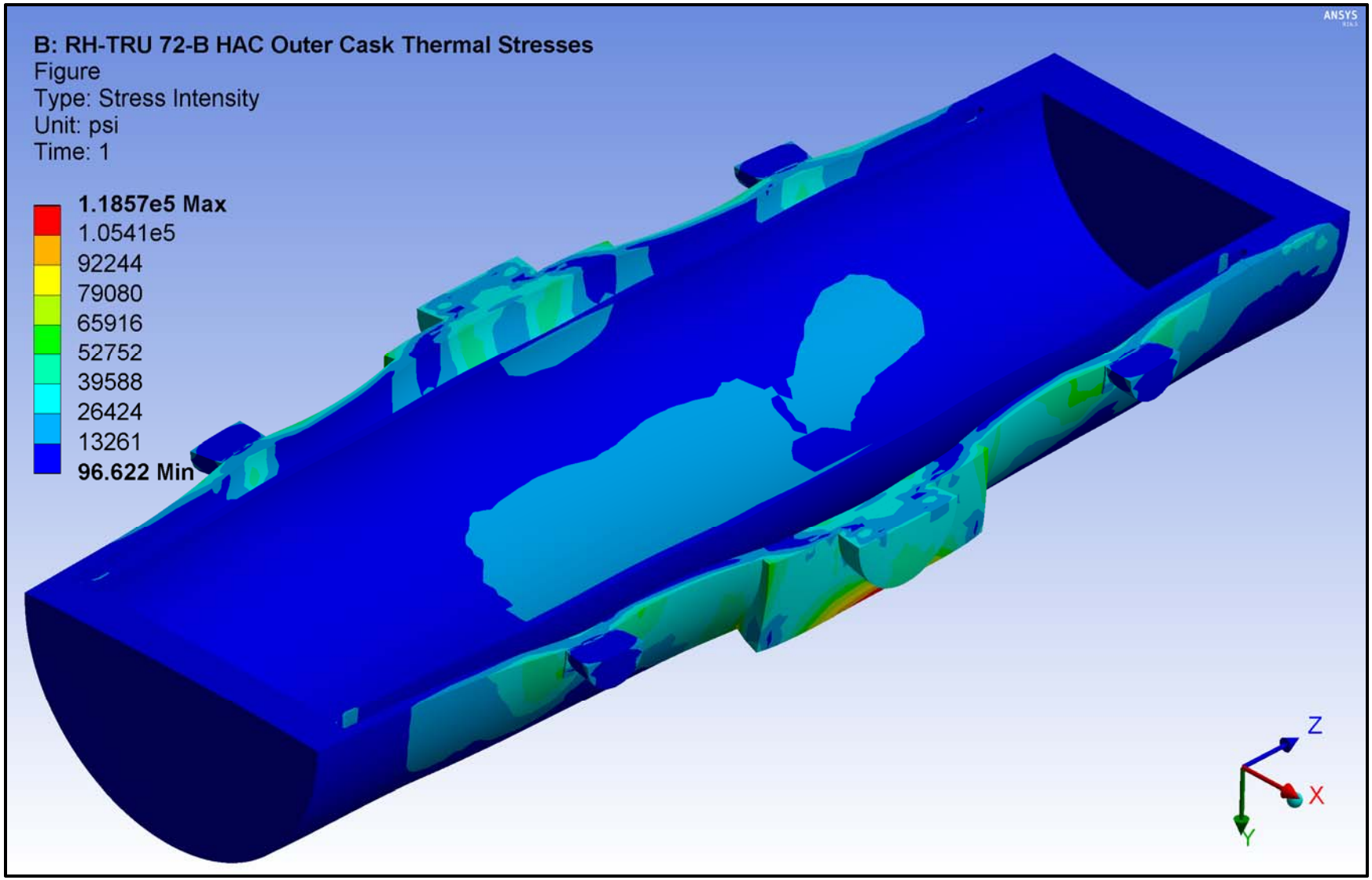

Figure 3.5-43 – ANSYS HAC Thermal Stress Model – Maximum Thermal Stress Intensity @ 15m after Start-of-Fire

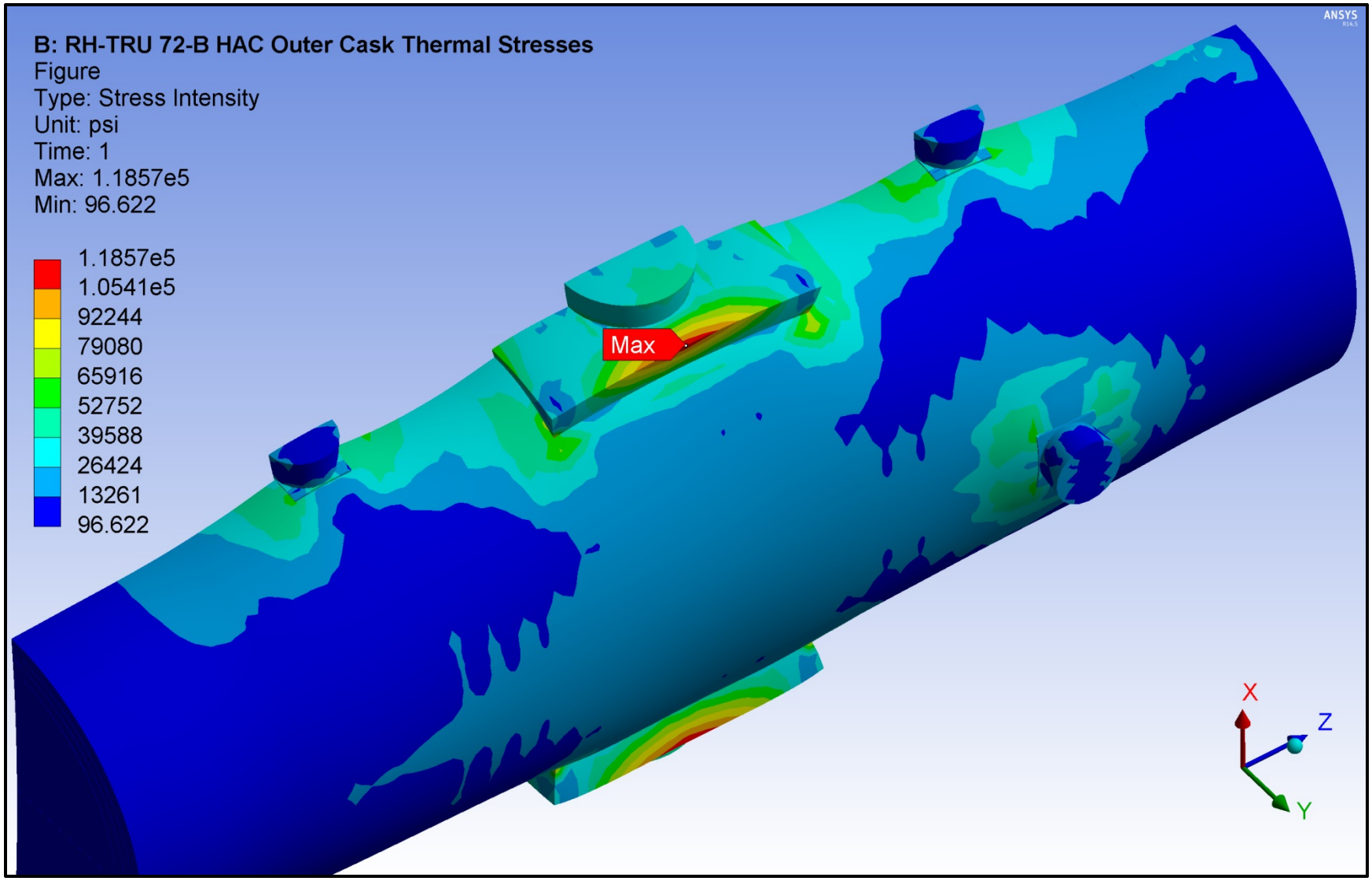

Figure 3.5-44 – ANSYS HAC Thermal Stress Model – Maximum Thermal Stress Intensity @ 15m after Start-of-Fire (Rotated)

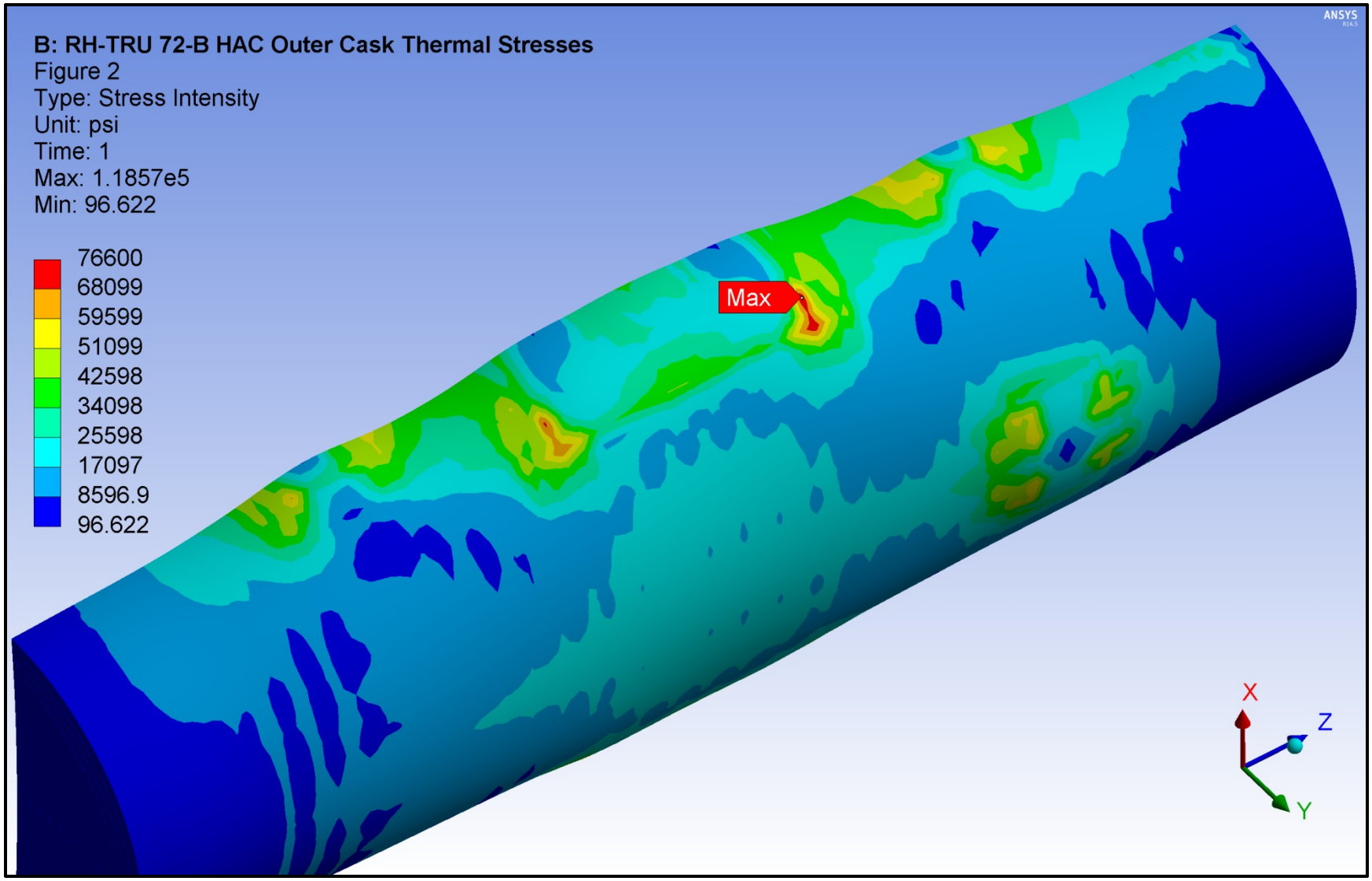

Figure 3.5-45 – ANSYS HAC Thermal Stress Model – Maximum Thermal Stress Intensity @ 15m after Start-of-Fire (Rotated without Trunnions)

This page intentionally left blank.

3.6 Appendices

3.6.1 *Thermal Model Details*

3.6.2 *Sensitivity Studies*

3.6.3 *Polyurethane Foam Performance Tests*

3.6.4 *Containment O-ring Seal Material Tests*

This page intentionally left blank.

3.6.1 Thermal Model Details

Additional thermal model details are provided in this section.

3.6.1.1 Calculation to Determine the Thermophysical Properties of the Thermal Shield Gap

The OC thermal shield is designed to reduce the transfer of heat from the external surface of the package to the underlying OC structure during the HAC fire event. As shown in Figure 3.6.1-1, 12-gauge (0.1094-inch diameter) wire is positioned between the OC thermal shield and OC outer shell on a 3-inch pitch. Wire effectively presents a line contact on each surface, and assembly of the relatively thin OC thermal shield (10-gauge; 0.1406-inch thick) onto the wire wrap results in an imperfect line contact with the wire. For the purpose of this calculation, however, the wire is assumed to be in full line contact with each surface.

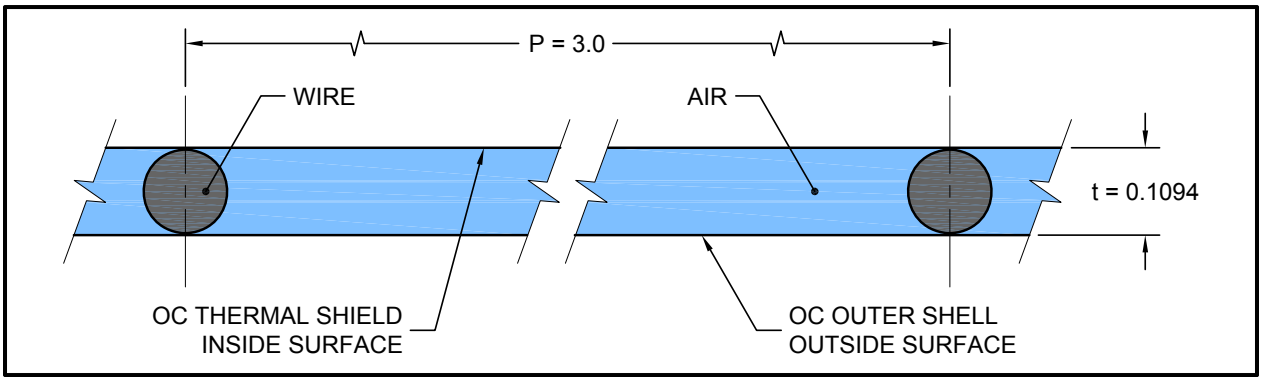

Figure 3.6.1-1 – Thermal Shield Gap Configuration

The thermal properties of the thermal shield gap are derived from the properties of air and stainless steel from Table 3.2-1 and Table 3.2-2, respectively, in Section 3.2, *Summary of Thermal Properties of Materials*.

Given a thermal shield gap thickness, t = 0.1094 inches and a wire pitch, P = 3.0 inches, the calculated thermal properties are determined using the proportion of the cross-sectional area of the stainless steel wire, X_{sst}, and air, X_{air}, for the 3-inch pitch spacing:

$$X_{sst} = \frac{(\pi/4)t^2}{tP} = \frac{(\pi/4)(0.1094)^2}{(0.1094)(3.0)} = 2.8641\%$$

$$X_{air} = \frac{tP - (\pi/4)t^2}{tP} = \frac{(0.1094)(3.0) - (\pi/4)(0.1094)^2}{(0.1094)(3.0)} = 97.1359\%$$

The effective density, $\delta(T)$, of the wire/air composite as a function of temperature, T, is then:

$$\delta(T) = \delta_{sst}(T)X_{sst} + \delta_{air}(T)X_{air}$$

The effective thermal conductivity, k(T), of the wire/air composite as a function of temperature, T, is determined by integration of the conductive path through the circular wire in parallel with the conductive path through the air based on the 3-inch pitch spacing:

$$k(T) = \left(\frac{t}{P}\right)\int_{-t/2}^{t/2}\left(\frac{\sqrt{t^2-4x^2}}{k_{sst}(T)} + \frac{t-\sqrt{t^2-4x^2}}{k_{air}(T)}\right)^{-1} dx + \left(\frac{P-t}{P}\right)k_{air}(T)$$

Finally, the effective specific heat, C(T), of the wire/air composite as a function of temperature, T, is based on mass proportions:

$$C(T) = \left(\frac{X_{sst}\delta_{sst}(T)}{X_{air}\delta_{air}(T) + X_{sst}\delta_{sst}(T)}\right)C_{sst}(T) + \left(\frac{X_{air}\delta_{air}(T)}{X_{air}\delta_{air}(T) + X_{sst}\delta_{sst}(T)}\right)C_{air}(T)$$

3.6.1.2 Calculation to Determine the Effective Density in the Impact Limiter's Damaged Region

As summarized in Table 2.10.3-9 from Appendix 2.10.3, *Drop Impact Evaluation Results*, the HAC side drop analysis determined a maximum impact limiter radial deformation of 11.518 inches. The underlying polyurethane foam in the damaged region becomes compressed, and the resulting increase in effective density may be reasonably determined by assuming the affected region is a circular sector, as shown in Figure 3.6.1-2.

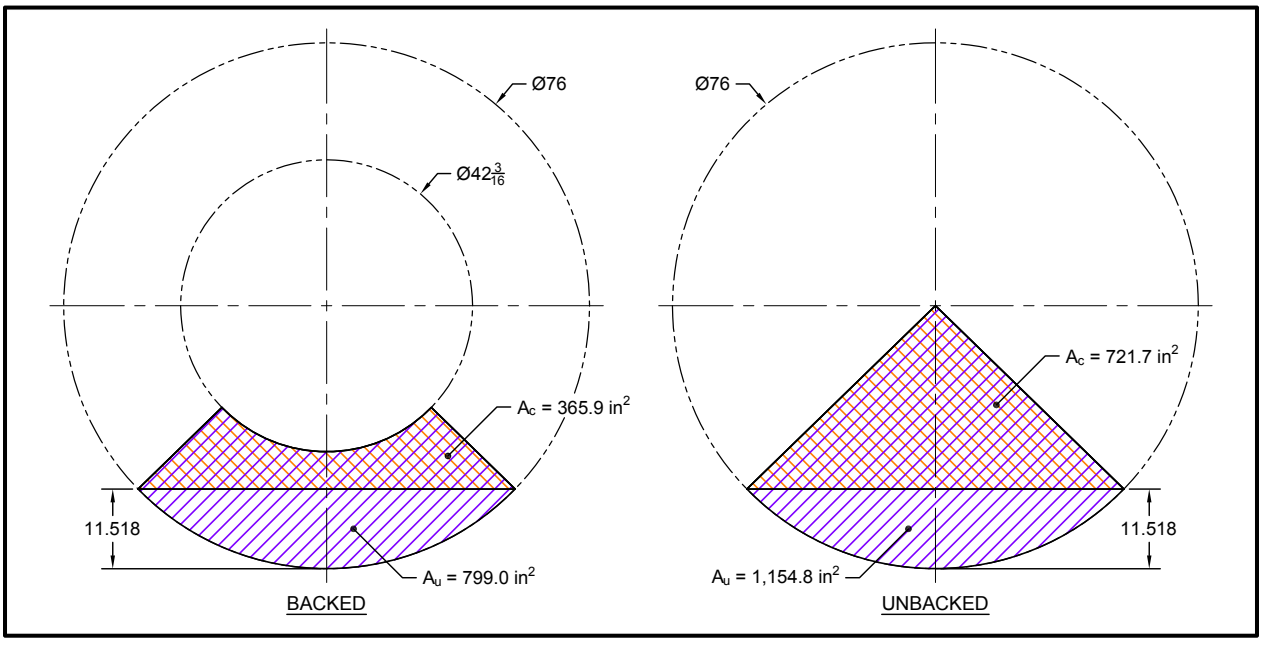

Figure 3.6.1-2 – Impact Limiter Compressed Foam Geometry

With reference to Figure 3.6.1-2, the "backed" region corresponds to the polyurethane foam in the impact limiter that is backed by the outer cask body, whereas the "unbacked" region corresponds to the polyurethane foam in the overhanging end region of the impact limiter.

The density compression factor for the backed region, f_b, is simply the ratio of the area of the original undamaged foam to the area of the residual compressed foam:

$$f_b = \frac{A_u}{A_c} = \frac{799.0}{365.9} = 2.2$$

Thus, for a nominal impact limiter polyurethane foam density, δ_f = 11½ lb/ft^3, the increase in effective density in the backed region of the impact limiter, δ_b, becomes:

$$\delta_b = f_b \delta_f = (2.2)(11.5) = 25.3 \text{ lb/ft}^3 \text{ (use 30 lb/ft}^3\text{)}$$

Similarly, the density compression factor for the unbacked region, f_u, is:

$$f_u = \frac{A_u}{A_c} = \frac{1{,}154.8}{721.7} = 1.6$$

Similarly, for a nominal impact limiter polyurethane foam density, δ_f = 11½ lb/ft^3, the increase in effective density in the unbacked region of the impact limiter, δ_u, is:

$$\delta_u = f_u \delta_f = (1.6)(11.5) = 18.4 \text{ lb/ft}^3 \text{ (use 20 lb/ft}^3\text{)}$$

3.6.1.3 Calculation of Forced Convection Coefficients for HAC

During the HAC fire event, the heated gases surrounding the RH-TRU 72-B package achieve significant velocities, sufficient to induce forced convection on all external surfaces. Measurements taken during actual hydrocarbon-fueled fire tests resulted in average induced gas velocities of between 6 and 9 m/s (19.7 – 29.5 ft/s).[1] Although the report noted that a peak gas velocity as high as 15 m/s (49.2 ft/s) was measured 6.1 meters (20 feet) above the fire surface, the gas velocities 2.2 meters above the fire surface (7.2 feet), a location more commensurate with the hottest region of the fire, were all under 10 m/s.[2] Therefore, a representative upper-bound gas velocity, V = 9 m/s (29.5 ft/s), is used for all calculations.

3.6.1.3.1 Cylindrical Surfaces

The convection coefficient, h_D, for a cylindrical surface in cross flow is:

$$h_D = Nu_D \frac{k}{D}$$

where the Nusselt number, Nu_D, thermal conductivity of the gas at film temperature, k, and diameter of the cylinder, D, are known. When $Re_D Pr \geq 0.2$ for a cylindrical surface in cross flow, the Nusselt number from Equation 7.54 of *Fundamentals of Heat and Mass Transfer*[3] is:

$$Nu_D = 0.3 + \frac{0.62\, Re_D^{1/2}\, Pr^{1/3}}{[1 + (0.4/Pr)^{2/3}]^{1/4}} \left[1 + \left(\frac{Re_D}{282{,}000}\right)^{5/8}\right]^{4/5}$$

[1] J. J. Gregory, R. Mata, and N. R. Keltner, *Thermal Measurements in a Series of Large Pool Fires*, SAND85-0196, TTC-0659, Sandia National Laboratories, Albuquerque, NM, August 1987.

[2] M. E. Schneider, L. A. Kent, *Measurement of Gas Velocities and Temperatures in a Large Open Pool Fire*, Heat and Mass Transfer in Fire, HTD Volume 73.

[3] Incropera, DeWitt, Bergman, and Lavine, *Fundamentals of Heat and Mass Transfer*, 6th Edition, John Wiley & Sons, 2006.

For a gas velocity, V, diameter of the cylinder, D, and kinematic viscosity, ν, the Reynolds number for a cylindrical surface, Re_D, is:

$$Re_D = \frac{VD}{\nu}$$

All properties for air presented in the following subsections are linearly interpolated from data presented in Table A.4 of *Fundamentals of Heat and Mass Transfer* at the specified gas film temperature.

3.6.1.3.1.1 OC Thermal Shield

The convection coefficient for the 41⅝-inch (3.47-foot) outside diameter thermal shield may be determined using the equations presented in Appendix 3.6.1.3.1, *Cylindrical Surfaces*.

With reference to Figure 3.5-3 from Section 3.5.3, *Package Temperatures*, the thermal shield's temperature reaches 1,200 ºF within 10 minutes; therefore, a gas film temperature of ½(1,200 ºF + 1,475 ºF) = 1,337.5 ºF is appropriate. Using a gas film temperature of 1,337.5 ºF, the Reynolds number, Re_D, is:

$$Re_D = \frac{(29.5)(3.47)}{1.309(10)^{-3}} = 78{,}200$$

where the gas velocity, V = 29.5 ft/s, the diameter, D = 3.47 ft, and the kinematic viscosity, $\nu = 1.309(10)^{-3}$ ft^2/s, for air at 1,337.5 ºF. As a check, $Re_D Pr = 56{,}700 \geq 0.2$, where the Prandtl number, Pr = 0.7255, for air at 1,337.5 ºF.

With a Reynolds number, Re_D = 78,200, and Prandtl number, Pr = 0.7255, the corresponding Nusselt number, Nu_D, is:

$$Nu_D = 0.3 + \frac{0.62(78{,}200)^{1/2}(0.7255)^{1/3}}{[1+(0.4/0.7255)^{2/3}]^{1/4}}\left[1+\left(\frac{78{,}200}{282{,}000}\right)^{5/8}\right]^{4/5} = 184.6$$

Finally, with a thermal conductivity, $k = 3.849(10)^{-2}$ Btu/hr-ft-ºF for air at 1,337.5 ºF, the convection coefficient, h_D, for the thermal shield's cylindrical surface is:

$$h_D = (184.6)\left(\frac{3.849(10)^{-2}}{3.47}\right) = 2.05 \text{ Btu/hr-ft}^2\text{-}^\circ\text{F}$$

3.6.1.3.1.2 Impact Limiter Cylindrical Shell

The convection coefficient for the 76-inch (6.33-foot) outside diameter, impact limiter cylindrical shell may be determined using the equations presented in Appendix 3.6.1.3.1, *Cylindrical Surfaces*. With reference to Figure 3.5-3 from Section 3.5.3, *Package Temperatures*, the impact limiter's outer shell temperature reaches 1,400 ºF within 10 minutes; therefore, a gas film temperature of ½(1,400 ºF + 1,475 ºF) = 1,437.5 ºF is appropriate. Using a gas film temperature of 1,437.5 ºF, the Reynolds number, Re_D, is:

$$Re_D = \frac{(29.5)(6.33)}{1.428(10)^{-3}} = 130{,}800$$

where the gas velocity, V = 29.5 ft/s, the diameter, D = 6.33 ft, and the kinematic viscosity, $\nu = 1.428(10)^{-3}$ ft^2/s, for air at 1,437.5 ºF. As a check, $Re_D Pr = 95{,}000 \geq 0.2$, where the Prandtl number, Pr = 0.7265, for air at 1,437.5 ºF.

With a Reynolds number, Re_D = 130,800, and Prandtl number, Pr = 0.7265, the corresponding Nusselt number, Nu_D, is:

$$Nu_D = 0.3 + \frac{0.62(130{,}800)^{1/2}(0.7265)^{1/3}}{[1+(0.4/0.7265)^{2/3}]^{1/4}}\left[1+\left(\frac{130{,}800}{282{,}000}\right)^{5/8}\right]^{4/5} = 260.9$$

Finally, with a thermal conductivity, $k = 4.004(10)^{-2}$ Btu/hr-ft-ºF for air at 1,437.5 ºF, the convection coefficient, h_D, for the impact limiter's cylindrical shell is:

$$h_D = (260.9)\left(\frac{4.004(10)^{-2}}{6.33}\right) = 1.65 \text{ Btu/hr-ft}^2\text{-}^\circ\text{F}$$

3.6.1.3.2 Impact Limiter Flat Ends

The convection coefficient, h_L, for a flat surface in parallel flow is:

$$h_L = Nu_L \frac{k}{L}$$

where the Nusselt number, Nu_x, thermal conductivity of the gas at film temperature, k, and length of the flat plate, L, are known. When $0.6 \leq Pr \leq 60$ for a flat surface in parallel flow, the Nusselt number from Equation 7.49 of *Fundamentals of Heat and Mass Transfer*[3] is:

$$Nu_L = (0.680)(Re_L)^{1/2}(Pr)^{1/3}$$

For a gas velocity, V, length of the flat surface, L, and kinematic viscosity, ν, the Reynolds number for a flat surface, Re_L, is:

$$Re_L = \frac{VL}{\nu}$$

All properties for air are linearly interpolated from data presented in Table A.4 of *Fundamentals of Heat and Mass Transfer* at the specified gas film temperature.

Using the same gas film temperature of 1,437.5 ºF for the impact limiter surface as determined in Appendix 3.6.1.3.1.2, *Impact Limiter Cylindrical Shell*, the Reynolds number, Re_D, is:

$$Re_L = \frac{(29.5)(6.33)}{1.428(10)^{-3}} = 130{,}800$$

where the gas velocity, V = 29.5 ft/s, the diameter, L = 6.33 ft (i.e., the diameter of the impact limiter), and the kinematic viscosity, $\nu = 1.428(10)^{-3}$ ft^2/s, for air at 1,437.5 ºF. As a check, Pr > 0.6, where the Prandtl number, Pr = 0.7265, for air at 1,437.5 ºF.

With a Reynolds number, Re_L = 130,800, and Prandtl number, Pr = 0.7265, the corresponding Nusselt number, Nu_D, is:

$$Nu_L = (0.680)(130{,}800)^{1/2}(0.7265)^{1/3} = 221.1$$

With a thermal conductivity, $k = 4.004(10)^{-2}$ Btu/hr-ft-ºF for air at 1,437.5 ºF, the convection coefficient, h_L, for the impact limiter's flat ends is:

$$h_L = (221.1)\left(\frac{4.004(10)^{-2}}{6.33}\right) = 1.40 \text{ Btu/hr-ft}^2\text{-}^\circ\text{F}$$

3.6.1.4 Determination of Density-Dependent Payload Decay Heat Limits

For potential use with RH-TRU waste canister (fixed or removable lid canister, FLC or RLC, respectively) shipments, maximum decay heat loads were developed for a variety of 30-gallon drum payload densities from 12 to 100 lb/ft^3 using the thermal properties of polyurethane foam as a surrogate payload material (see Table 3.2-8 in Section 3.2, *Summary of Thermal Properties of Materials*, for a detailed discussion) based on an average payload temperature limit of 302 ºF and a peak payload temperature limit of 402 ºF (see Section 3.3.3, *Payload Material*; the temperature limits apply to both NCT and HAC). Worst-case 30-gallon drum payload temperatures occur for HAC.

The maximum payload decay heat for a given density was found by imposing the more restrictive of two payload temperature limits, i.e., an average payload temperature of 302 ºF and a peak payload temperature of 402 ºF. Table 3.6.1-1 and Figure 3.6.1-3 present the calculated maximum decay heat that is based on satisfying these allowable temperature limits using the worst-case HAC evaluation. For conservatism, the calculated decay heat limit is reduced by a 6% to 10% administrative margin resulting in an adjusted allowable decay heat limit curve that is defined by the following fourth-order polynomial equation:

$$Q_{adj}(\delta) = (2.83215E{+}01) + (5.96476E{+}00)\delta - (7.55983E{-}02)\delta^2 + (5.94706E{-}04)\delta^3 - (1.93520E{-}06)\delta^4$$

where Q_{adj} is the decay heat limit (watts) and δ is the payload density (lb/ft^3).

Therefore, the allowable payload canister decay heat limit is 90 watts (conservatively based on a payload density of ≤12 lb/ft^3). For payloads with densities >12 lb/ft^3, a higher decay heat limit (up to 270 watts based on a payload density of ≥100 lb/ft^3) determined from the aforementioned polynomial equation is applicable.

For a constant mass of payload material, a larger volume will result in lower payload temperatures. For example, this effect is clearly demonstrated in Table 3.6.1-2 for an assumed payload mass of 600 pounds, payload canister volume of 942 liters (33.3 ft^3), 55-gallon drum volume of 208 liters (7.35 ft^3), and 30-gallon drum volume of 114 liters (4.03 ft^3). Correspondingly, estimated payload densities are 600/33.3 ≈ 18 lb/ft^3 for a direct-filled payload canister, 600/(3 × 7.35) ≈ 27 lb/ft^3 for a 55-gallon drum payload, and 600/(3 × 4.03) ≈ 50 lb/ft^3 for a 30-gallon drum payload, and interpolating the calculated decay heat curve from Table 3.6.1-1 results in a maximum decay heat of 126 watts, 159 watts, and 216 watts, respectively, based on the 302 ºF bulk average temperature limit and 402 ºF peak temperature limit discussed in Section 3.3.3, *Payload Material*.

As shown in Table 3.6.1-2, using the 30-gallon decay heat-versus-density curve for the greater payload volume configurations conservatively results in greater thermal margins for the payload. Thermal margins are shown to be only slightly greater for the packaging components. This is as expected since packaging response is driven by the external, HAC fire environment and is insensitive to the configuration and, to a lesser extent, the wattage of the waste within the payload canister. Temperature results for the three payload configurations are illustrated in Figure 3.6.1-4, Figure 3.6.1-5, and Figure 3.6.1-6.

Table 3.6.1-1 – Calculated and Adjusted Maximum Decay Heat vs. Payload Density

Payload Density (lb/ft^3)	Calculated Decay Heat (W)	Adjusted Decay Heat (W)	Administrative Reduction
≤12	99.3	90.0	9.4%
23	146.4	132.2	9.7%
34	179.2	164.5	8.2%
45	205.7	189.9	7.7%
56	227.7	210.7	7.5%
67	246.4	228.5	7.3%
78	262.5	244.2	7.0%
89	276.6	258.2	6.7%
≥100	289.0	270.0	6.6%

Table 3.6.1-2 – Maximum HAC Temperatures (ºF) with Insolation for Various Payload Configurations with a Constant Payload Mass of 600 Pounds and Proportional Density, and Decay Heat Adjusted to the Maximum Calculated Limit

Location	30-Gallon Drum Model (216 W; 50 lb/ft^3)	55-Gallon Drum Model (159 W; 27 lb/ft^3)	ΔT	Direct-Filled RLC Model (126 W; 18 lb/ft^3)	ΔT
Lower Drum Contents Peak	364.4	336.1	-28.3	—	—
Lower Drum Contents Average	284.2	256.8	-27.4	—	—
Lower Drum Wall Peak	278.6	250.4	-28.2	—	—
Middle Drum Contents Peak	378.5	345.6	-32.9	325.9	-52.6
Middle Drum Contents Average	301.9	268.4	-33.5	244.9	-57.0
Middle Drum Wall Peak	281.9	257.4	-24.5	—	—
Upper Drum Contents Peak	363.7	334.6	-29.1	—	—
Upper Drum Contents Average	283.4	254.6	-28.8	—	—
Upper Drum Wall Peak	281.7	253.5	-28.2	—	—
RLC Shell Peak	279.1	263.8	-15.3	266.1	-13.0
RLC Lid Peak	197.7	189.9	-7.8	184.9	-12.8
IV Shell Peak	381.5	377.8	-3.7	375.9	-5.6
IV Base Peak	202.6	193.3	-9.3	195.5	-7.1
IV Upper Forging Peak	188.4	183.8	-4.6	183.4	-5.0
IV Lid Peak	184.7	180.9	-3.8	179.9	-4.8
IV Lid O-ring Seal Peak	184.5	180.9	-3.6	179.7	-4.8
IV Lid Ports O-ring Seals Peak	184.7	180.9	-3.8	179.9	-4.8
OC Inner Shell Peak	545.5	544.1	-1.4	543.3	-2.2
OC Lead Shield Peak	568.8	567.4	-1.4	566.5	-2.3
OC Outer Shell Peak	700.2	698.9	-1.3	698.6	-1.6
OC Base Peak	200.3	196.1	-4.2	196.8	-3.5
OC Upper Forging Peak	240.6	239.6	-1.0	238.4	-2.2
OC Lid Peak	196.1	190.2	-5.9	193.9	-2.2
OC Lid O-ring Seal Peak	192.4	187.4	-5.0	190.1	-2.3
OC Lid Port O-ring Seal Peak	196.1	190.2	-5.9	193.9	-2.2
OC Thermal Shield Peak	1,323	1,323	0.0	1,323	0.0
OC Main Trunnions Peak	1,069	1,069	0.0	1,068	-1.0
OC Small Trunnions Peak	1,096	1,095	-1.0	1,094	-2.0
Impact Limiter Foam Peak	1,473	1,473	0.0	1,473	0.0
Impact Limiter Foam Average	—	—	—	—	—
Impact Limiter Shell Peak	1,474	1,474	0.0	1,474	0.0

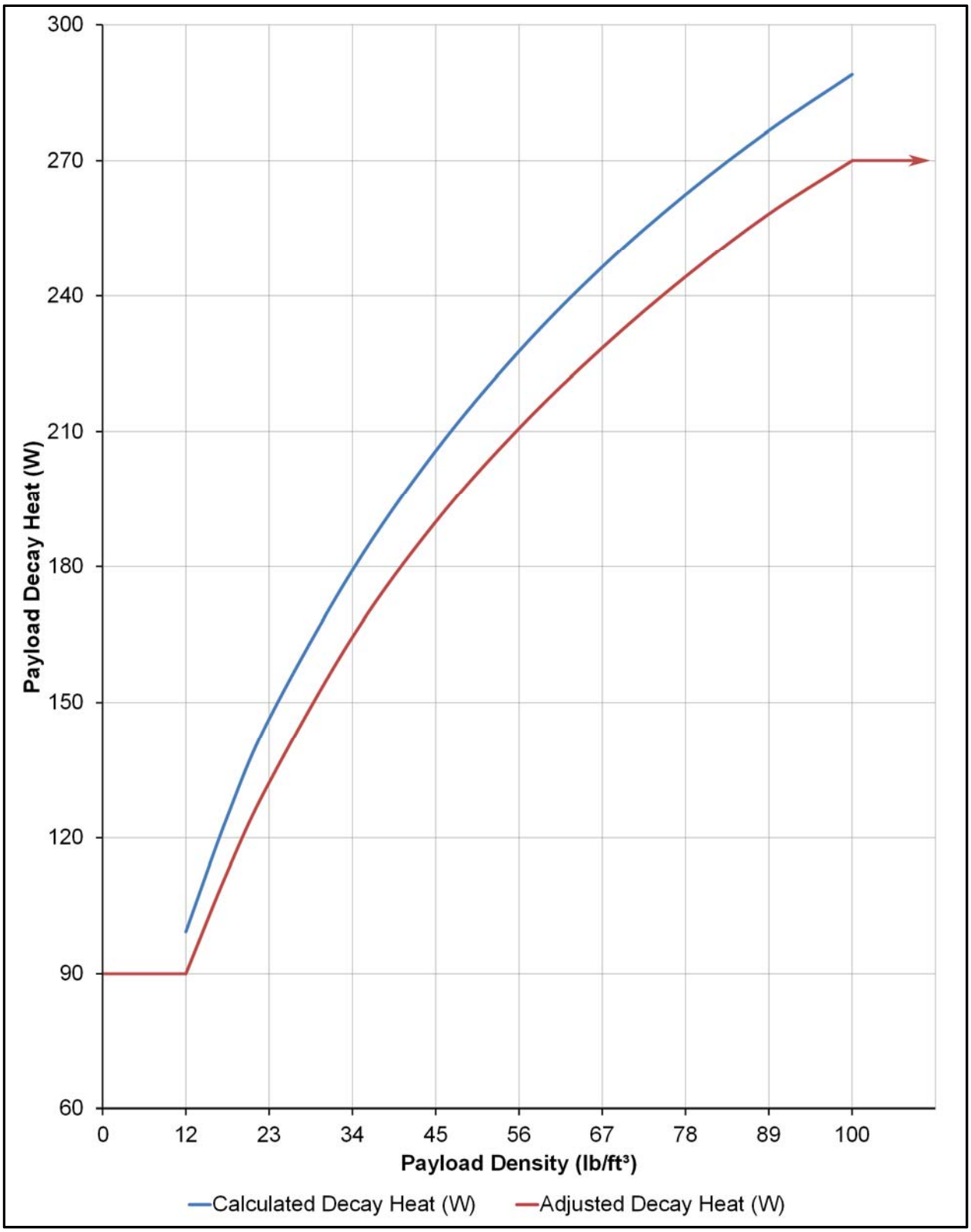

Figure 3.6.1-3 – Calculated and Adjusted Maximum Decay Heat vs. Payload Density

This page intentionally left blank.

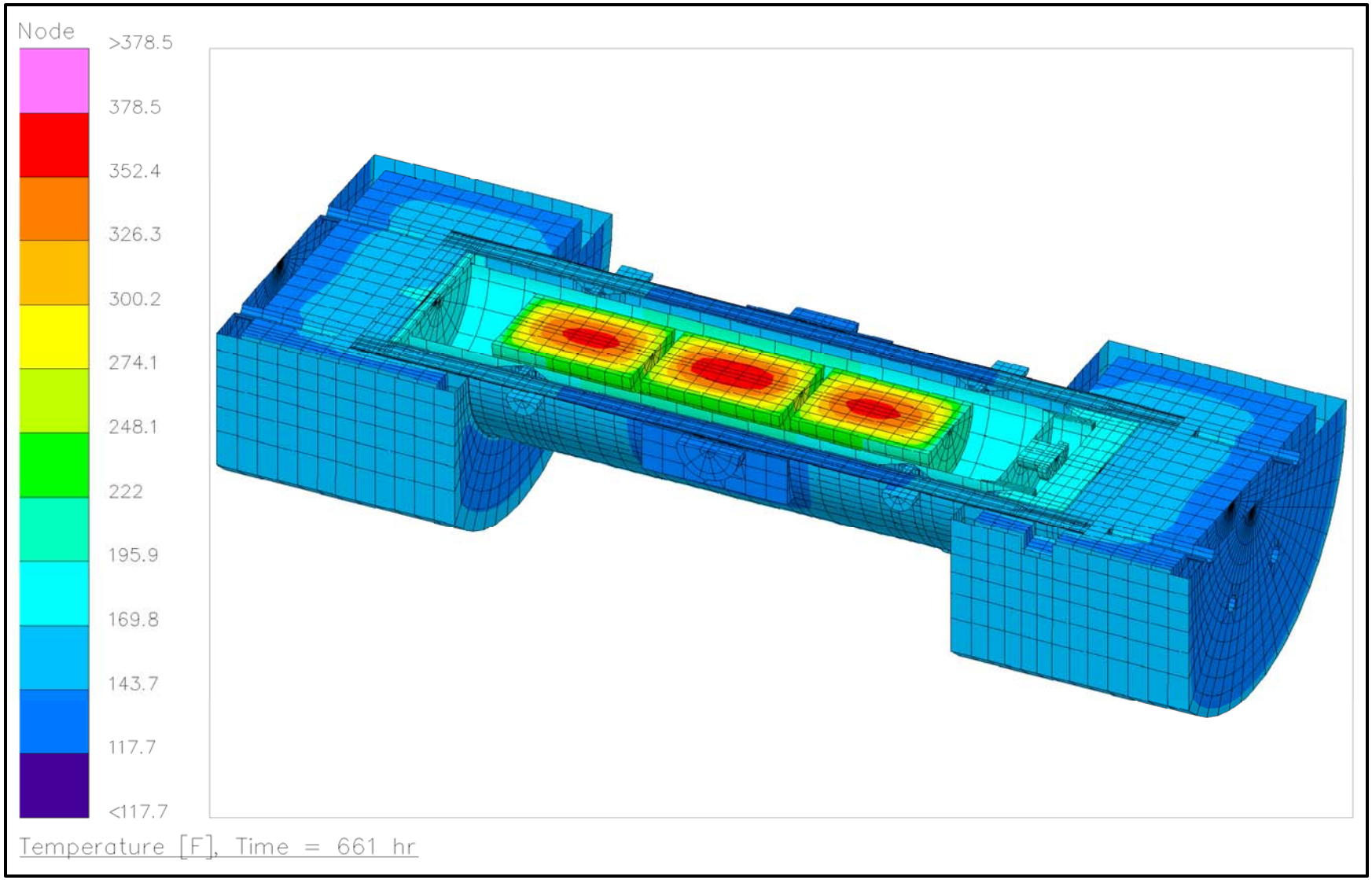

Figure 3.6.1-4 – HAC Case 1 – Package with RLC; 50 lb/ft³ Waste with 216 Watts Decay Heat and Insolation – 30-Gallon Drum Payload

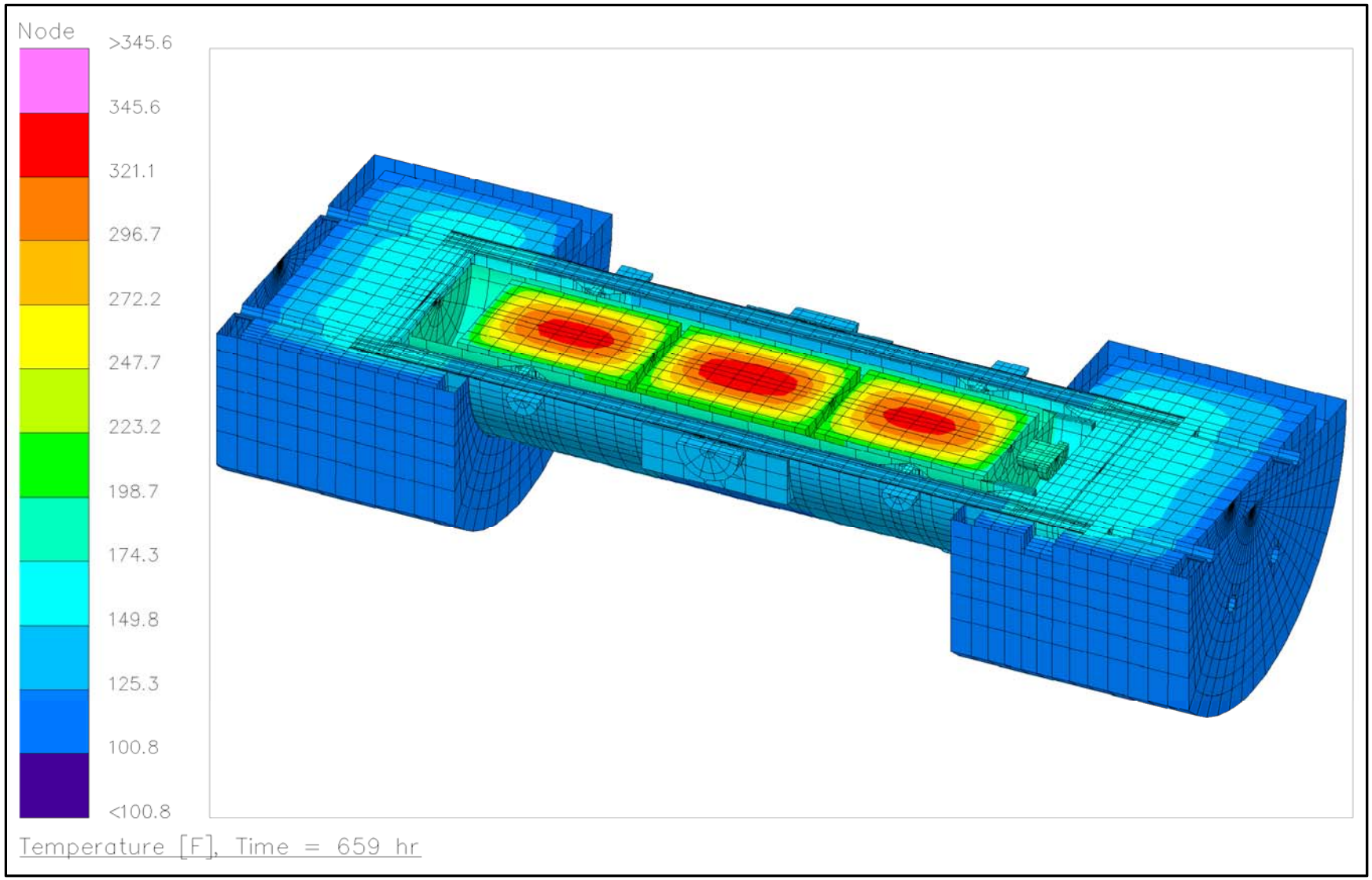

Figure 3.6.1-5 – HAC Case 1 – Package with RLC; 27 lb/ft³ Waste with 159 Watts Decay Heat and Insolation – 55-Gallon Drum Payload

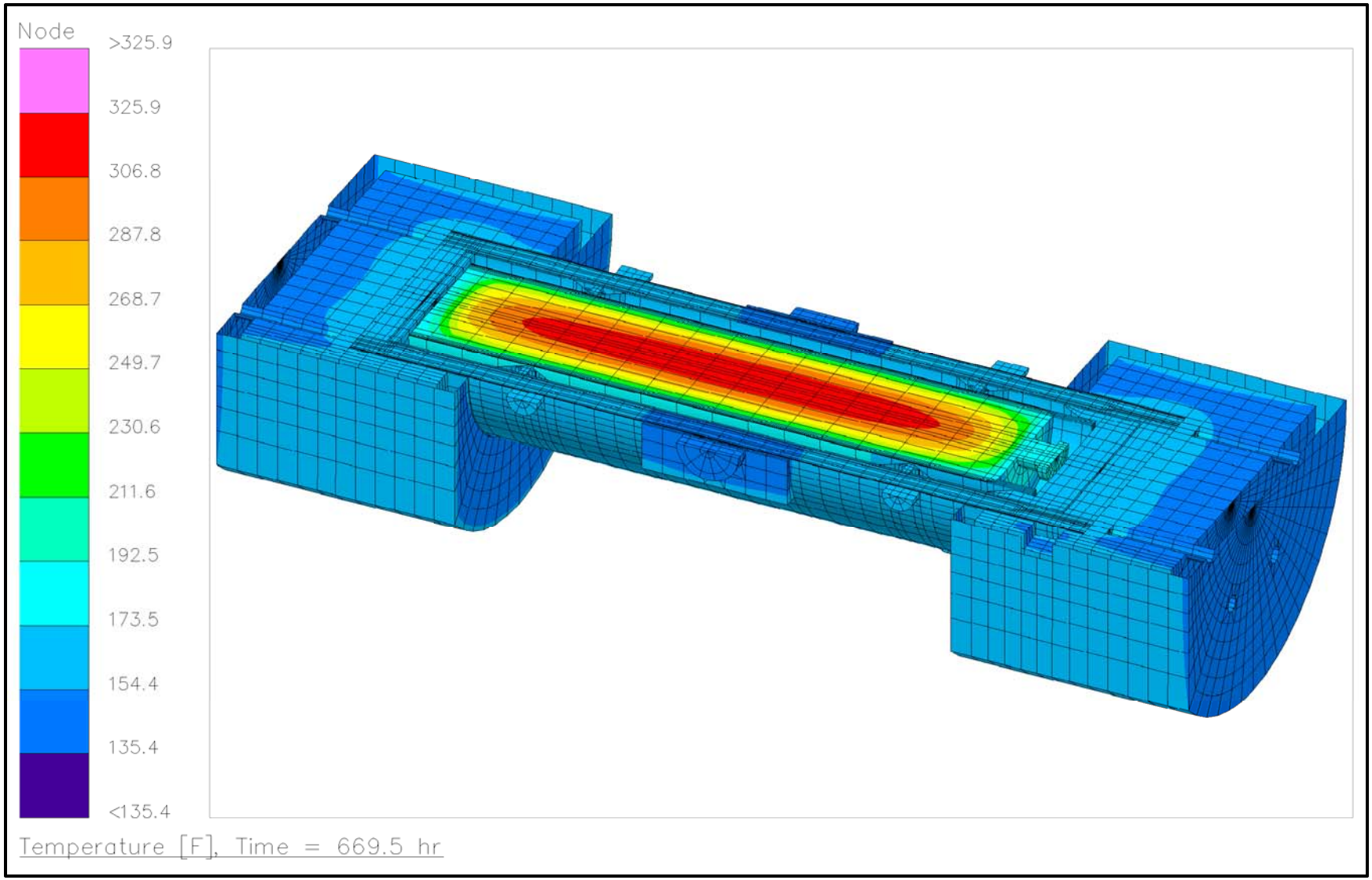

Figure 3.6.1-6 – HAC Case 1 – Package with RLC; 18 lb/ft³ Waste with 126 Watts Decay Heat and Insolation – Direct-Filled RLC

This page intentionally left blank.

3.6.2 Sensitivity Studies

Sensitivity studies were performed to determine the effects of model resolution, axial component offsets, radial component offsets, and the effect of internal convection in the thermal models.

3.6.2.1 Model Resolution

An evaluation was performed to determine if the models are of sufficient resolution to present reasonable temperature results. This evaluation uses the Case 1 baseline NCT model (i.e., a payload density of 12 lb/ft^3 with 90 watts of decay heat uniformly distributed in three, 30-gallon drums) for comparison.

The Case 1 baseline model is comprised of 15,725 nodes and 115,415 conductors, and the Case 1 high-resolution model contains 53,235 nodes and 516,697 conductors. The high-resolution model increased the radial, circumferential, and axial resolution of the model by $(53{,}235/15{,}725)^{1/3} \approx 50\%$ based on the number of nodes, and $(516{,}697/115{,}415)^{1/3} \approx 65\%$ based on the number of conductors. Maximum temperatures for comparison, both with and without insolation, are shown in Figure 3.6.2-1 to Figure 3.6.2-4.

Table 3.6.2-1 summarizes the comparison of packaging and payload component temperatures, and shows that the maximum payload temperature difference does not exceed 2 ºF (~1%). Most packaging temperature differences are less than 0.3 ºF (~0.1%). Of these differences resulting in increased temperatures, the maximum increase is only 0.1 ºF and may be attributed to numeric round-off. Therefore, the baseline models are of sufficient resolution to accurately predict maximum temperatures for packaging and payload components.

3.6.2.2 Axial Component Offsets

The baseline analyses all assume that packaging and payload components are axially centered within each other. Since the RLC-to-IV nominal axial gap is only 3/4 inches at each end and the IV-to-OC nominal axial gap is only 3/8 inches at each end, axially closing the RLC-to-IV gap and the IV-to-OC gap will have a negligible effect on payload and packaging temperatures, especially since the primary heat path is radial and both packaging ends are set within the highly insulating impact limiters. Axially shifting the heated 30-gallon drums within the RLC, however, will have a somewhat greater effect since the drum-to-RLC axial gap is 14⅜ inches when the drums are centered.

An evaluation was performed to determine the effect of axially shifting the drums downward and upward 13⅜ inches from their axially centered position (a 1-inch axial gap between the end drums and the corresponding RLC end surface is assumed to account for the rolled top and bottom drum ends). This evaluation uses the Case 1 baseline NCT configuration (i.e., a payload density of 12 lb/ft^3 with 90 watts of decay heat uniformly distributed in three, 30-gallon drums) for comparison. Maximum temperatures for comparison, both with and without insolation, are shown in Figure 3.6.2-5 to Figure 3.6.2-8 with the drums biased downward, and Figure 3.6.2-9 to Figure 3.6.2-12 with the drums biased upward.

Table 3.6.2-2 summarizes the maximum NCT temperatures for packaging and payload components as compared to the baseline temperatures. The maximum temperature difference is 7.2 ºF for the RLC lid without insolation, and 5.2 ºF for the OC base with insolation. The largest increases occur for the components at the ends (e.g., bases, upper forgings, and lids). Since the

regions of highest stress occur in the cylindrical shells at elevated temperatures (i.e., with insolation applied), a 0.2 ºF increase in the RLC, IV, and OC shells is considered insignificant. Increases in end components are also considered insignificant because they occur either for temperatures without insolation or in end components that are not subject to limiting stresses. Therefore, the models with axially centered drums are reasonable for predicting maximum temperatures for packaging and payload components.

3.6.2.3 Radial Component Offsets

The use of a uniform radial gap is appropriate for NCT and HAC evaluations even though the RH-TRU 72-B package is transported horizontally since the decrease in the radial gap on one side of a component will be offset by a corresponding increase in gap on the opposite side.

An evaluation was performed to determine the effect of radially shifting the 30-gallon drums, RLC, and IV until surface contact was achieved (i.e., cylinder-to-cylinder line contact). Stainless steel paired with stainless steel under moderate contact interface pressure exhibits a typical thermal contact conductance of approximately 1,900 W/m^2-K (2.324 Btu/hr-in^2-ºF).[1] This value was used to define the node-to-node conductors between adjacent components to model radial heat flow across contact surfaces.

This evaluation uses the Case 1 baseline configuration (i.e., a low-density payload density of 12 lb/ft^3 with 90 watts of decay heat uniformly distributed in three, 30-gallon drums) for comparison. The NCT payload temperatures are worse with all components centered within one another since radial shifting will improve the ability to transfer heat out of the package (the pre-fire temperature results in Table 3.6.2-3 are essentially NCT temperatures). Therefore, this evaluation compares temperatures for HAC, with maximum HAC temperatures listed in Table 3.6.2-3 and illustrated in Figure 3.6.2-13 to Figure 3.6.2-20.

Table 3.6.2-3 presents the HAC temperature summary demonstrating, with only two exceptions, that radial contact results in negligible changes to packaging and payload component temperatures. The two exceptions are the IV shell and upper forging that result in temperature increases of 46.3 ºF and 18.1 ºF, respectively, and is due to their contact with the hot (540.3 ºF) OC inner shell. However, as illustrated in Figure 3.6.2-17, these two IV temperature increases are very much localized and have negligible effect on other component temperatures within the packaging or payload.

With the exception of the IV shell, HAC temperature limits are not exceeded. Per Table 3.5-2 in Section 3.5.3, *Package Temperatures*, the allowable temperature for the IV shell is 390 ºF, and is exceeded with a temperature of 420.9 ºF for the radially-shifted configuration (i.e., Δ = 30.9 ºF). The 420.9 ºF localized IV shell temperature is acceptable because of the very large design margins determined in Section 2.7, *Hypothetical Accident Conditions*, based on the 390 ºF temperature limit. The very large design margins readily offset the modest reduction in material strength due to the 30.9 ºF temperature increase thereby maintaining positive design margins.

Therefore, the models with radially centered packaging and payload components are reasonable for predicting maximum temperatures for packaging and payload components.

[1] Yunus A. Çengel, *Introduction to Thermodynamics and Heat Transfer*, Second Edition, The McGraw−Hill Companies, 2008; Chapter 10, Section 10-2, *Thermal Contact Resistance*, Table 10-2.

3.6.2.4 Effect of Internal Convection Heat Transfer

The RH-TRU 72-B waste shipping package is transported horizontally. Natural convection heat transfer across a gap between two long, horizontal concentric cylinders may be evaluated using Equations 3.101 through 3.104 from Guyer's *Handbook of Applied Thermal Design*.[2] When sufficient radial gap is present between the two concentric cylindrical surfaces, and when buoyancy forces are able to overcome viscous forces, natural convection heat transfer will establish a convective flow pattern as shown in the accompanying illustration.

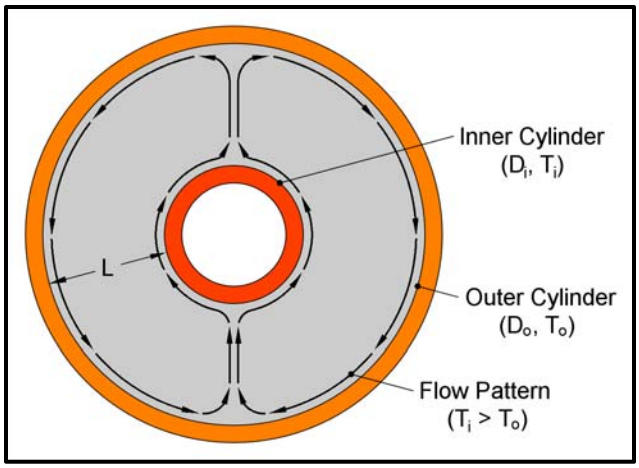

The illustration depicts a condition where the inside cylinder is hotter than the outside cylinder; if the reverse is true, then the convective flow pattern would be reversed from what is shown.

From Equation 3.101 of Guyer, the natural convection heat transfer, q′, across the gap between two long, horizontal concentric cylinders, where the annulus contains air and the inside cylinder is hotter than the outside cylinder, is given as:

$$q' = \frac{2\pi k_{air} Nu}{\ln(D_o/D_i)}(T_i - T_o) \qquad \text{(3.101 from Guyer)}$$

where k_{air} is the temperature dependent thermal conductivity of air, Nu is the temperature dependent Nusselt number, D_o is the diameter of the outer cylinder's inside surface, D_i is the diameter of the inner cylinder's outside surface, and $T_i - T_o$ is the temperature differential between the inner and outer cylindrical surfaces, respectively.

Substituting k_{eff} for $k_{air} \times Nu$ in Equation 3.101 reduces the equation to simple thermal conduction between two concentric cylinders:

$$q' = \frac{2\pi k_{eff}}{\ln(D_o/D_i)}(T_i - T_o)$$

Thus, the Nusselt number, $Nu = k_{eff}/k_{air}$, and k_{eff} becomes the effective thermal conductivity of air for heat transfer across the radial cylindrical gap. Equation 3.102 from Guyer, defines the Nusselt number, Nu, as:

$$Nu = 0.386\left(\frac{Pr}{0.861 + Pr}\right)^{1/4}(Ra_c)^{1/4} \qquad \text{(3.102 from Guyer)}$$

where the Prandtl number for air, Pr = 0.7, and Ra_c is the critical Rayleigh number. Equation 3.102 is valid for $Pr \geq 0.7$ and $100 < Ra_c < 10^8$, and establishes the following limits:

[2] Eric C. Guyer, Editor in Chief, *Handbook of Applied Thermal Design*, First Edition, Taylor & Francis, Philadelphia, PA, 1999.

$$Ra_c < 100 \quad \Rightarrow \quad Nu = \frac{k_{eff}}{k_{air}} = 1$$

$$100 < Ra_c < 10^8 \quad \Rightarrow \quad Nu = 0.386\left(\frac{Pr}{0.861 + Pr}\right)^{1/4} (Ra_c)^{1/4}$$

From Equation 3.103, the critical Rayleigh number, Ra_c, is

$$Ra_c = \frac{\left[\ln(D_o/D_i)\right]^4}{L^3\left(D_i^{-3/5} + D_o^{-3/5}\right)^5} Ra \qquad \text{(3.103 from Guyer)}$$

where the characteristic length, $L = (D_o - D_i)/2$, and Ra is the Rayleigh number. From Equation 3.104, the Rayleigh number, Ra, is:

$$Ra = \frac{g\beta L^3}{\nu\alpha}(T_i - T_o) \qquad \text{(3.104 from Guyer)}$$

where the gravitational constant, $g = 386.0886$ in/s^2, β is the thermal expansion coefficient for air, ν is the kinematic viscosity of air, α is the thermal diffusivity of air, and $T_i - T_o$ is the maximum average temperature differential between the two cylindrical surfaces. The coefficients β, ν, and α are determined using the average temperature of the two surfaces at the time when the maximum average temperature differential occurs, with values linearly interpolated from Table A.4 of Incropera.[3]

Determining the convective heat transfer coefficients is an iterative process. The heat transfer coefficients reported in Table 3.6.2-4 are taken from the final iteration of the HAC thermal analyses that use the calculated Nusselt numbers as coefficients for the effective radial thermal conductivity of air in the annulus between the outer cask and inner vessel (OC/IV), in the annulus between the inner vessel and removable lid canister (IV/RLC), and in the annulus between removable lid canister and payload drums (RLC/Drum). As summarized in Table 3.6.2-4, the coefficients in the OC/IV annulus are unity because the radial gap is insufficient to support a convective flow pattern, and the same is true for the gap between the OC thermal shield and the OC outer shell since the radial gap there is even less.

Table 3.6.2-5 and Table 3.6.2-6 summarize temperatures from the final iteration of the HAC pre-fire and HAC fire/post-fire analyses that used the coefficient discussed above, and compare these results to the original results without internal convection. With a few negligible exceptions, temperatures are lower when internal convection is included in the evaluations. These temperature reductions occur because under normal conditions, any convective modes of heat transfer that exist internal to the package will reduce initial condition, pre-fire temperatures, and because the two regions that are most affected by the HAC fire event, the OC thermal shield air gap and OC/IV air gap, are too closely coupled to support an internal convection flow pattern. Therefore, the original analyses with all package components centered, but without internal convection, are reasonable for determining worst-case package temperatures and pressures.

[3] Incropera, DeWitt, Bergman, and Lavine, *Fundamentals of Heat and Mass Transfer*, 6th Edition.

Table 3.6.2-1 – Maximum NCT Temperatures (ºF) for the Baseline vs. High-Resolution RLC Models with 12 lb/ft³ Payload Density and 90 Watts of Decay Heat

Location	Without Insolation			With Insolation		
	Baseline	Hi-Res	ΔT	Baseline	Hi-Res	ΔT
Lower Drum Contents Peak	306.0	306.8	+0.8	331.8	332.7	+0.9
Lower Drum Wall Peak	153.0	154.7	+1.7	180.1	181.7	+1.6
Middle Drum Contents Peak	313.5	314.9	+1.4	338.8	340.1	+1.3
Middle Drum Wall Peak	153.2	154.9	+1.7	180.3	182.1	+1.8
Upper Drum Contents Peak	305.1	306.3	+1.2	331.2	332.3	+1.1
Upper Drum Wall Peak	152.8	154.7	+1.9	180.1	181.9	+1.8
RLC Shell Peak	129.1	130.1	+1.0	159.3	160.3	+1.0
RLC Lid Peak	112.8	112.5	-0.3	141.9	141.5	-0.4
IV Shell Peak	109.3	109.4	+0.1	145.1	145.2	+0.1
IV Base Peak	109.2	109.0	-0.2	138.6	138.5	-0.1
IV Upper Forging Peak	107.1	107.0	-0.1	137.1	137.1	0.0
IV Lid Peak	106.9	106.7	-0.2	136.1	136.1	0.0
IV Lid O-ring Seal Peak	106.9	106.7	-0.2	136.1	135.9	-0.2
IV Lid Ports O-ring Seals Peak	106.9	106.7	-0.2	136.1	136.1	0.0
OC Inner Shell Peak	106.6	106.6	0.0	143.8	143.9	+0.1
OC Lead Shield Peak	106.6	106.5	-0.1	143.9	143.9	0.0
OC Outer Shell Peak	106.5	106.5	0.0	144.0	144.1	+0.1
OC Base Peak	106.8	106.7	-0.1	136.7	136.5	-0.2
OC Upper Forging Peak	105.0	105.0	0.0	136.7	136.4	-0.3
OC Lid Peak	105.1	105.1	0.0	135.0	135.0	0.0
OC Lid O-ring Seal Peak	105.0	105.1	+0.1	134.9	134.7	-0.2
OC Lid Port O-ring Seal Peak	105.1	105.1	0.0	135.0	135.0	0.0
OC Thermal Shield Peak	106.5	106.5	0.0	146.8	146.8	0.0
OC Main Trunnions Peak	105.1	105.2	+0.1	144.0	144.0	0.0
OC Small Trunnions Peak	105.7	105.7	0.0	144.5	144.6	+0.1
Impact Limiter Foam Peak	106.7	106.7	0.0	157.7	157.4	-0.3
Impact Limiter Foam Average	102.3	102.1	-0.2	133.5	132.7	-0.8
Impact Limiter Shell Peak	106.7	106.7	0.0	157.7	157.4	-0.3

Table 3.6.2-2 – Maximum NCT Temperatures (ºF) for Centered vs. Axially-Shifted RLC Models with 12 lb/ft³ Payload Density and 90 Watts of Decay Heat

Location	Without Insolation			With Insolation		
	Centered	Shifted	ΔT	Centered	Shifted	ΔT
Lower Drum Contents Peak	306.0	309.8 ▼	+3.8	331.8	335.3 ▼	+3.5
Lower Drum Wall Peak	153.0	153.8 ▼	+0.8	180.1	180.4 ▼	+0.3
Middle Drum Contents Peak	313.5	313.8 ▼	+0.3	338.8	339.0 ▼	+0.2
Middle Drum Wall Peak	153.2	153.9 ▼	+0.7	180.3	180.5 ▼	+0.2
Upper Drum Contents Peak	305.1	306.5 ▲	+1.4	331.2	332.4 ▲	+1.2
Upper Drum Wall Peak	152.8	153.0 ▼	+0.2	180.1	180.3 ▼	+0.2
RLC Shell Peak	129.1	129.4 ▼	+0.3	159.3	159.3 ▼	0.0
RLC Lid Peak	112.8	120.0 ▲	+7.2	141.9	144.3 ▲	+2.4
IV Shell Peak	109.3	111.6 ▼	+2.3	145.1	145.3 ▼	+0.2
IV Base Peak	109.2	112.8 ▼	+3.6	138.6	141.9 ▼	+3.3
IV Upper Forging Peak	107.1	109.8 ▲	+2.7	137.1	139.5 ▲	+2.4
IV Lid Peak	106.9	109.4 ▲	+2.5	136.1	138.4 ▲	+2.3
IV Lid O-ring Seal Peak	106.9	109.4 ▲	+2.5	136.1	138.4 ▲	+2.3
IV Lid Ports O-ring Seals Peak	106.9	109.4 ▲	+2.5	136.1	138.4 ▲	+2.3
OC Inner Shell Peak	106.6	108.3 ▼	+1.7	143.8	144.0 ▼	+0.2
OC Lead Shield Peak	106.6	108.3 ▼	+1.7	143.9	144.1 ▼	+0.2
OC Outer Shell Peak	106.5	108.3 ▼	+1.8	144.0	144.2 ▼	+0.2
OC Base Peak	106.8	112.8 ▼	+6.0	136.7	141.9 ▼	+5.2
OC Upper Forging Peak	105.0	106.4 ▲	+1.4	136.7	137.8 ▲	+1.1
OC Lid Peak	105.1	106.6 ▲	+1.5	135.0	136.2 ▲	+1.2
OC Lid O-ring Seal Peak	105.0	106.4 ▲	+1.4	134.9	136.1 ▲	+1.2
OC Lid Port O-ring Seal Peak	105.1	106.6 ▲	+1.5	135.0	136.2 ▲	+1.2
OC Thermal Shield Peak	106.5	108.3 ▼	+1.8	146.8	147.0 ▼	+0.2
OC Main Trunnions Peak	105.1	105.4 ▼	+0.3	144.0	144.1 ▼	+0.1
OC Small Trunnions Peak	105.7	106.8 ▼	+1.1	144.5	145.2 ▲	+0.7
Impact Limiter Foam Peak	106.7	108.6 ▼	+1.9	157.7	157.7 –	0.0
Impact Limiter Foam Average	102.3	102.4 ▼	+0.1	133.5	133.7 ▼	+0.2
Impact Limiter Shell Peak	106.7	108.6 ▼	+1.9	157.7	157.7 –	0.0

Notes:

① The ▲ symbol indicates the temperature occurred for the upwardly shifted payload.

② The ▼ symbol indicates the temperature occurred for the downwardly shifted payload.

③ The – symbol indicates the same temperature occurred for all three axial payload positions.

Table 3.6.2-3 – Maximum HAC Temperatures (ºF) for Centered vs. Radially-Shifted RLC Models with 12 lb/ft³ Payload Density and 90 Watts of Decay Heat

Location	Pre-Fire			Fire		
	Centered	Shifted	ΔT	Centered	Shifted	ΔT
Lower Drum Contents Peak	331.7	329.3	-2.4	370.4	368.9	-1.5
Lower Drum Wall Peak	180.0	178.1	-1.9	258.4	258.3	-0.1
Middle Drum Contents Peak	338.7	336.6	-2.1	381.2	380.1	-1.1
Middle Drum Wall Peak	180.2	178.4	-1.8	264.8	266.7	+1.9
Upper Drum Contents Peak	331.1	329.4	-1.7	370.4	369.8	-0.6
Upper Drum Wall Peak	180.0	178.3	-1.7	264.7	265.4	+0.7
RLC Shell Peak	159.2	165.2	+6.0	266.9	268.1	+1.2
RLC Lid Peak	142.0	141.2	-0.8	188.9	189.4	+0.5
IV Shell Peak	145.1	145.1	0.0	374.6	420.9	+46.3
IV Base Peak	138.3	137.5	-0.8	196.2	196.6	+0.4
IV Upper Forging Peak	137.3	137.6	+0.3	183.2	201.3	+18.1
IV Lid Peak	136.3	136.2	-0.1	179.7	180.9	+1.2
IV Lid O-ring Seal Peak	136.3	136.2	-0.1	179.5	180.9	+1.4
IV Lid Ports O-ring Seals Peak	136.3	136.2	-0.1	179.7	180.9	+1.2
OC Inner Shell Peak	143.8	143.8	0.0	542.5	540.3	-2.2
OC Lead Shield Peak	143.8	143.8	0.0	565.9	565.2	-0.7
OC Outer Shell Peak	144.0	144.0	0.0	697.3	697.8	+0.5
OC Base Peak	136.6	136.6	0.0	195.5	195.2	-0.3
OC Upper Forging Peak	138.1	138.0	-0.1	238.7	232.8	-5.9
OC Lid Peak	138.1	138.0	-0.1	192.9	191.1	-1.8
OC Lid O-ring Seal Peak	135.6	135.5	-0.1	189.1	186.9	-2.2
OC Lid Port O-ring Seal Peak	138.1	138.0	-0.1	192.9	191.1	-1.8
OC Thermal Shield Peak	146.7	146.6	-0.1	1,322	1,322	0.0
OC Main Trunnions Peak	143.9	144.0	+0.1	1,068	1,068	0.0
OC Small Trunnions Peak	144.6	144.6	0.0	1,095	1,094	-1.0
Impact Limiter Foam Peak	156.1	156.1	0.0	1,473	1,473	0.0
Impact Limiter Foam Average	135.2	135.2	0.0	—	—	—
Impact Limiter Shell Peak	157.1	157.1	0.0	1,474	1,474	0.0

Table 3.6.2-4 – HAC Pre-Fire and HAC Fire/Post-Fire Internal Convection Coefficient Calculations

HAC Pre-Fire Internal Convection Coefficients			
Variable	**OC/IV**	**IV/RLC**	**RLC/Drum**
D_o (in)	32.375	31.250	25.500
D_i (in)	32.000	26.000	18.250
L (in)	0.1875	2.6250	3.6250
ΔT (ºF)	10.6	28.1	34.3
T_{avg} (ºF)	139.2	158.3	189.3
β ($ºF^{-1}$)	$1.6719(10)^{-3}$	$1.6196(10)^{-3}$	$1.5425(10)^{-3}$
ν (in^2/s)	$2.9662(10)^{-2}$	$3.1354(10)^{-2}$	$3.4178(10)^{-2}$
α (in^2/s)	$4.2245(10)^{-2}$	$4.4759(10)^{-2}$	$4.9024(10)^{-2}$
Ra	$3.5994(10)^{1}$	$2.2647(10)^{5}$	$5.8073(10)^{5}$
Ra_c	$1.0483(10)^{-1}$	$1.0291(10)^{4}$	$4.6703(10)^{4}$
Nu	1.00	3.18	4.64
HAC Fire/Post-Fire Internal Convection Coefficients			
Variable	**OC/IV**	**IV/RLC**	**RLC/Drum**
D_o (in)	32.375	31.250	25.500
D_i (in)	32.000	26.000	18.250
L (in)	0.1875	2.6250	3.6250
ΔT (ºF)	145.1	45.2	33.3
T_{avg} (ºF)	261.8	226.8	190.0
β ($ºF^{-1}$)	$1.3872(10)^{-3}$	$1.4587(10)^{-3}$	$1.5408(10)^{-3}$
ν (in^2/s)	$4.1104(10)^{-2}$	$3.7709(10)^{-2}$	$3.4242(10)^{-2}$
α (in^2/s)	$5.9599(10)^{-2}$	$5.4422(10)^{-2}$	$4.9120(10)^{-2}$
Ra	$2.0911(10)^{2}$	$2.2437(10)^{5}$	$5.6103(10)^{5}$
Ra_c	$6.0904(10)^{-1}$	$1.0195(10)^{4}$	$4.5117(10)^{4}$
Nu	1.00	3.17	4.60

Table 3.6.2-5 – HAC Pre-Fire Steady State Temperatures with Insolation (ºF) for an RLC with 30-Gallon Drums Containing a 100 lb/ft³ Payload with 270 Watts Decay Heat; without and with Internal Convection

Location	No Internal Convection	Internal Convection	ΔT	Allowable Limit
Lower Drum Contents Peak	311.8	295.5	-16.3	402
Lower Drum Contents Average	252.7	234.1	-18.6	302
Lower Drum Wall Peak	251.7	237.8	-13.9	—
Middle Drum Contents Peak	326.1	306.7	-19.4	402
Middle Drum Contents Average	270.9	252.0	-18.9	302
Middle Drum Wall Peak	252.2	234.5	-17.7	—
Upper Drum Contents Peak	310.5	294.2	-16.3	402
Upper Drum Contents Average	250.6	235.9	-14.7	302
Upper Drum Wall Peak	251.2	233.6	-17.6	—
HDPE Shielding Wall Peak	—	—	—	170
HDPE Shielding Wall Average	—	—	—	150
RLC Shell Peak	201.9	189.2	-12.7	210
RLC Lid Peak	161.3	155.8	-5.5	212
IV Shell Peak	158.0	158.5	+0.5	160
IV Base Peak	151.5	149.6	-1.9	160
IV Upper Forging Peak	146.8	144.6	-2.2	160
IV Lid Peak	145.4	143.0	-2.4	160
IV Lid O-ring Seal Peak	145.4	143.0	-2.4	225
IV Lid Ports O-ring Seals Peak	145.4	143.0	-2.4	225
OC Inner Shell Peak	150.2	150.3	+0.1	160
OC Lead Shield Peak	150.1	150.3	+0.2	160
OC Outer Shell Peak	150.2	150.3	+0.1	160
OC Base Peak	144.9	144.5	-0.4	160
OC Upper Forging Peak	143.6	143.0	-0.6	160
OC Lid Peak	143.6	143.0	-0.6	160
OC Lid O-ring Seal Peak	141.3	140.7	-0.6	225
OC Lid Port O-ring Seal Peak	143.6	143.0	-0.6	225
OC Thermal Shield Peak	151.6	151.8	+0.2	185
OC Main Trunnions Peak	149.5	149.6	+0.1	153
OC Small Trunnions Peak	149.4	149.4	0.0	153
Impact Limiter Foam Peak	156.2	156.2	0.0	260
Impact Limiter Foam Average	138.0	137.8	-0.2	140
Impact Limiter Shell Peak	157.2	157.2	0.0	185

Table 3.6.2-6 – HAC Fire Transient Temperatures (T) and Time (t) after End-of-Fire for an RLC with 30-Gallon Drums Containing a 100 lb/ft³ Payload with 270 Watts Decay Heat; without and with Internal Convection

Location	No Internal Convection		Internal Convection		ΔT	Allowable Limit
	T (ºF)	*t (hr)*	T (ºF)	*t (hr)*	(ºF)	(ºF)
Lower Drum Contents Peak	331.5	*59.0*	317.9	*56.5*	-13.6	402
Lower Drum Contents Average	275.6	*22.5*	264.1	*20.5*	-11.5	302
Lower Drum Wall Peak	280.9	*18.0*	269.4	*17.0*	-11.5	—
Middle Drum Contents Peak	345.3	*55.5*	329.2	*53.0*	-16.1	402
Middle Drum Contents Average	293.7	*19.0*	279.7	*17.5*	-14.0	302
Middle Drum Wall Peak	283.0	*17.0*	272.0	*16.0*	-11.0	—
Upper Drum Contents Peak	330.5	*56.5*	317.3	*54.0*	-13.2	402
Upper Drum Contents Average	274.1	*20.0*	263.7	*18.0*	-10.4	302
Upper Drum Wall Peak	282.5	*17.0*	271.6	*16.0*	-10.9	—
HDPE Shielding Wall Peak	—	—	—	—	—	256
HDPE Shielding Wall Average	—	—	—	—	—	—
RLC Shell Peak	284.2	*3.85*	282.6	*3.50*	-1.6	650/256
RLC Minimum	163.2	*3.85*	158.1	*3.50*	-5.1	—
RLC Lid Peak	200.4	*19.5*	200.0	*16.0*	-0.4	650/256
IV Shell Peak	384.4	*1.4*	377.7	*1.4*	-6.7	390
IV Base Peak	204.7	*17.5*	203.2	*17.0*	-1.5	300
IV Upper Forging Peak	190.4	*12.5*	193.3	*12.0*	+2.9	300
IV Lid Peak	186.7	*22.0*	187.7	*17.5*	+1.0	300
IV Lid O-ring Seal Peak	186.4	*20.0*	187.7	*17.5*	+1.3	360
IV Lid Ports O-ring Seals Peak	186.7	*22.0*	187.7	*17.5*	+1.0	360
OC Inner Shell Peak	546.8	*0.4*	546.8	*0.4*	+0.0	550
OC Lead Shield Peak	570.4	*0.1*	570.5	*0.1*	+0.1	620
OC Outer Shell Peak	701.5	*0*	701.0	*0*	-0.5	705
OC Base Peak	202.4	*10.0*	201.7	*10.0*	-0.7	500
OC Upper Forging Peak	242.2	*1.2*	235.2	*1.2*	-7.0	500
OC Lid Peak	197.5	*9.15*	195.7	*10.0*	-1.8	500
OC Lid O-ring Seal Peak	193.9	*12.0*	192.3	*12.0*	-1.6	360
OC Lid Port O-ring Seal Peak	197.5	*9.15*	195.7	*10.0*	-1.8	360
OC Thermal Shield Peak	1,323	*0*	1,323	*0*	0.0	2,600
OC Main Trunnions Peak	1,070	*0*	1,070	*0*	0.0	2,600
OC Small Trunnions Peak	1,096	*0*	1,096	*0*	0.0	2,600
Impact Limiter Foam Peak	1,473	*0*	1,473	*0*	0.0	—
Impact Limiter Foam Average	—	—	—	—	—	—
Impact Limiter Shell Peak	1,474	*0*	1,474	*0*	0.0	2,600

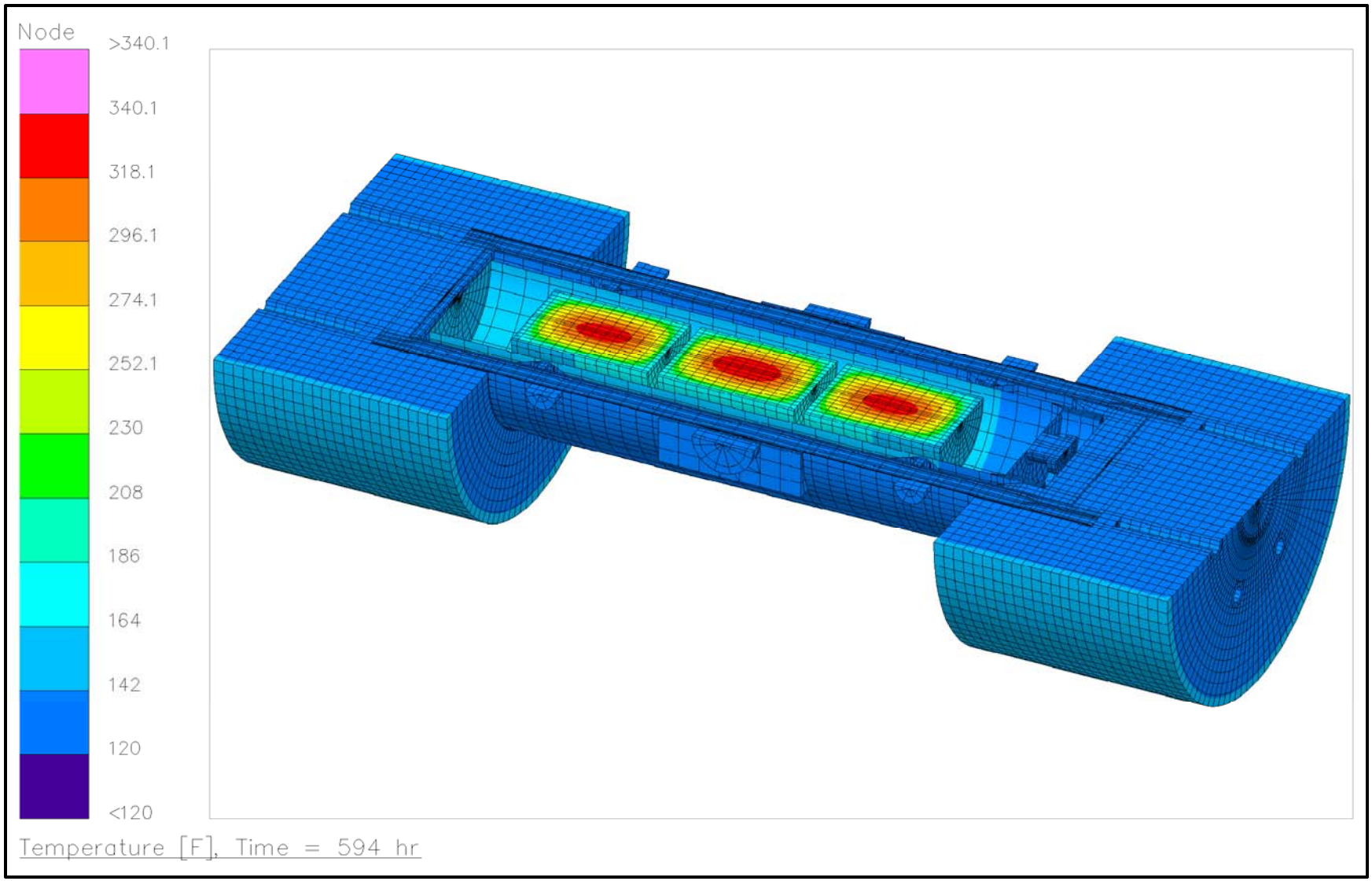

Figure 3.6.2-1 – NCT Case 1 – Package with RLC; 12 lb/ft³ Waste with 90 Watts Decay Heat and Insolation – High-Resolution Model

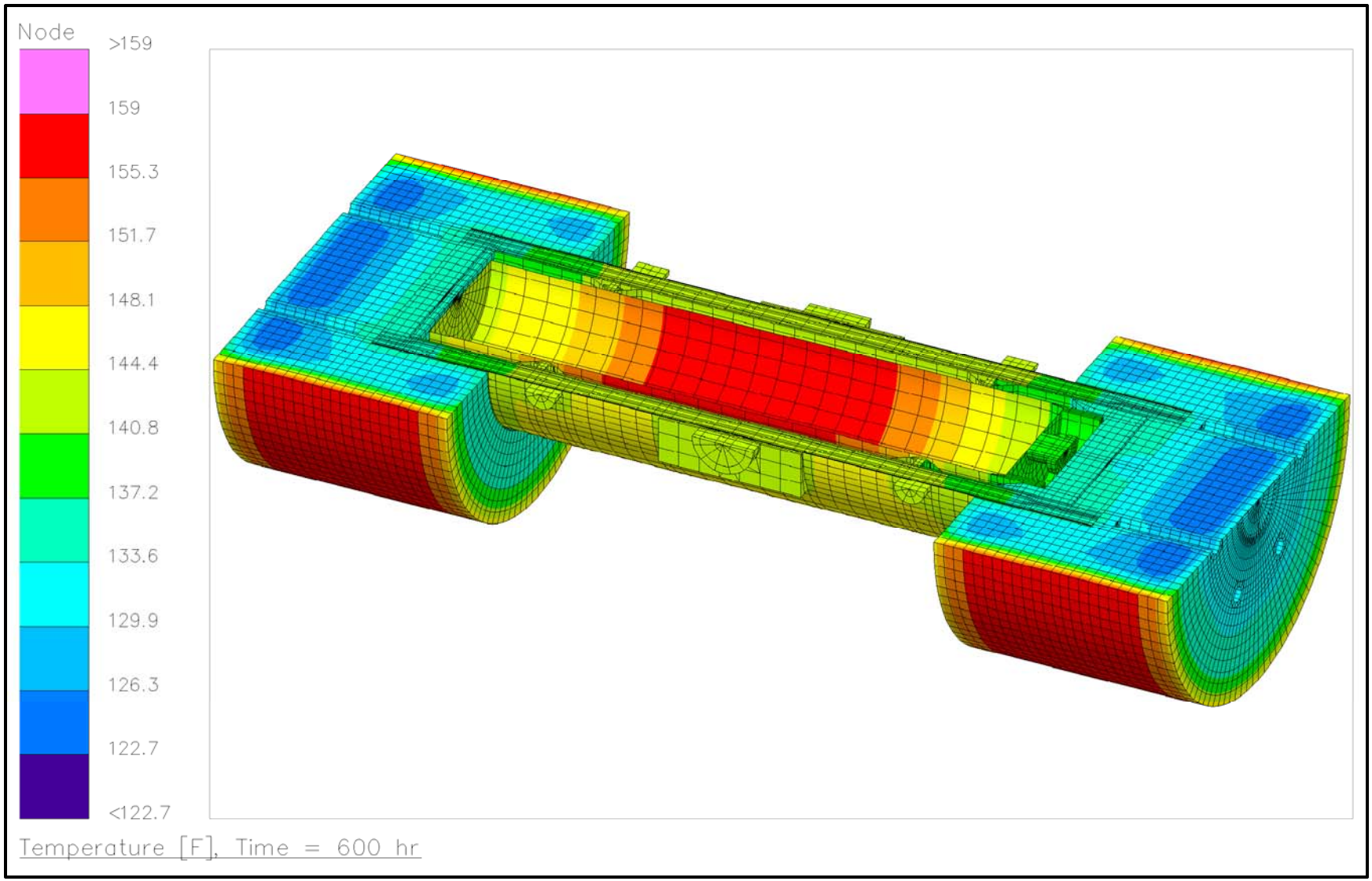

Figure 3.6.2-2 – NCT Case 1 – Package with RLC; 12 lb/ft³ Waste with 90 Watts Decay Heat and Insolation – High-Resolution Model (Drums Hidden)

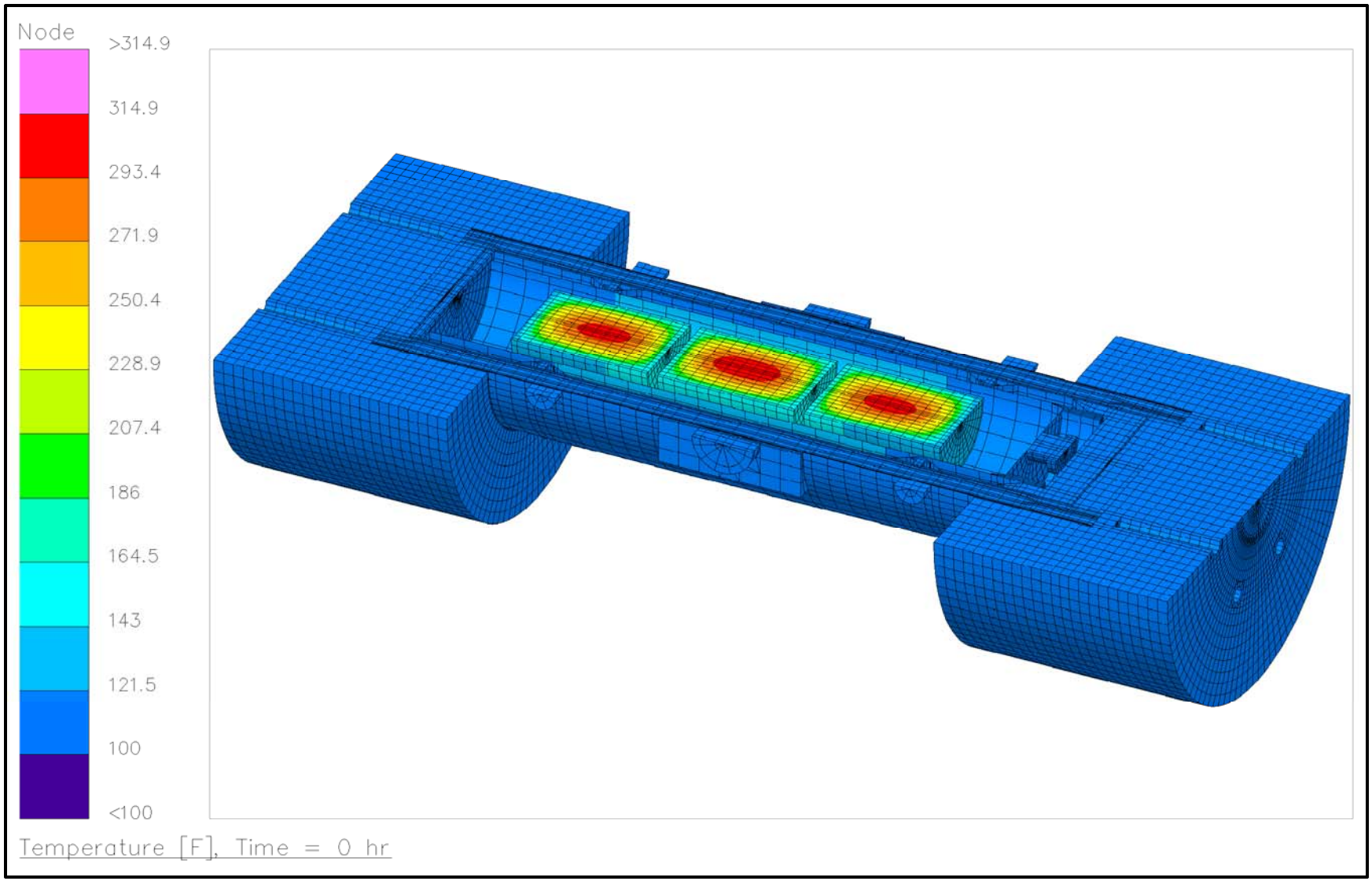

Figure 3.6.2-3 – NCT Case 1 – Package with RLC; 12 lb/ft³ Waste with 90 Watts Decay Heat and No Insolation – High-Resolution Model

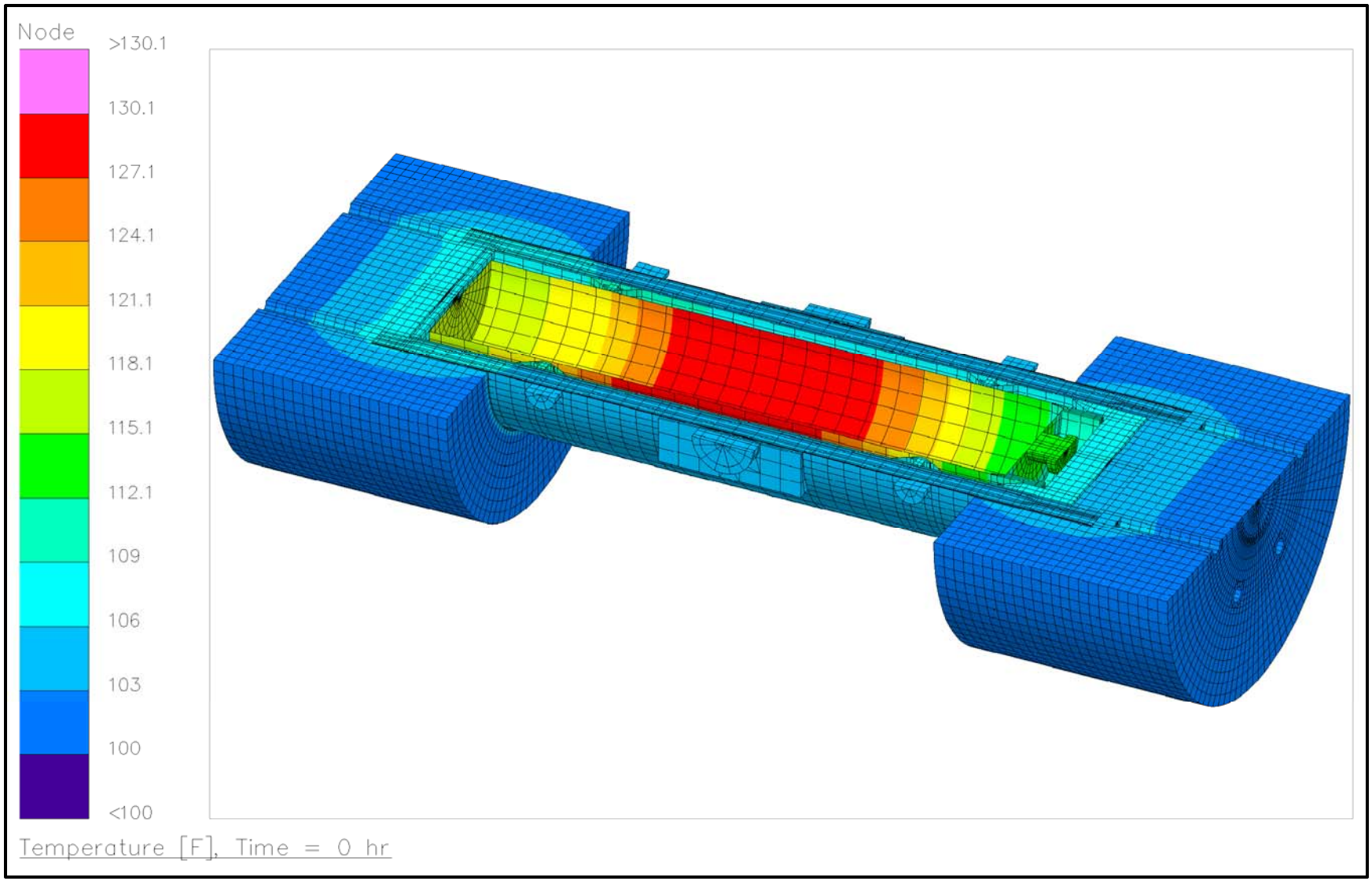

Figure 3.6.2-4 – NCT Case 1 – Package with RLC; 12 lb/ft³ Waste with 90 Watts Decay Heat and No Insolation – High-Resolution Model (Drums Hidden)

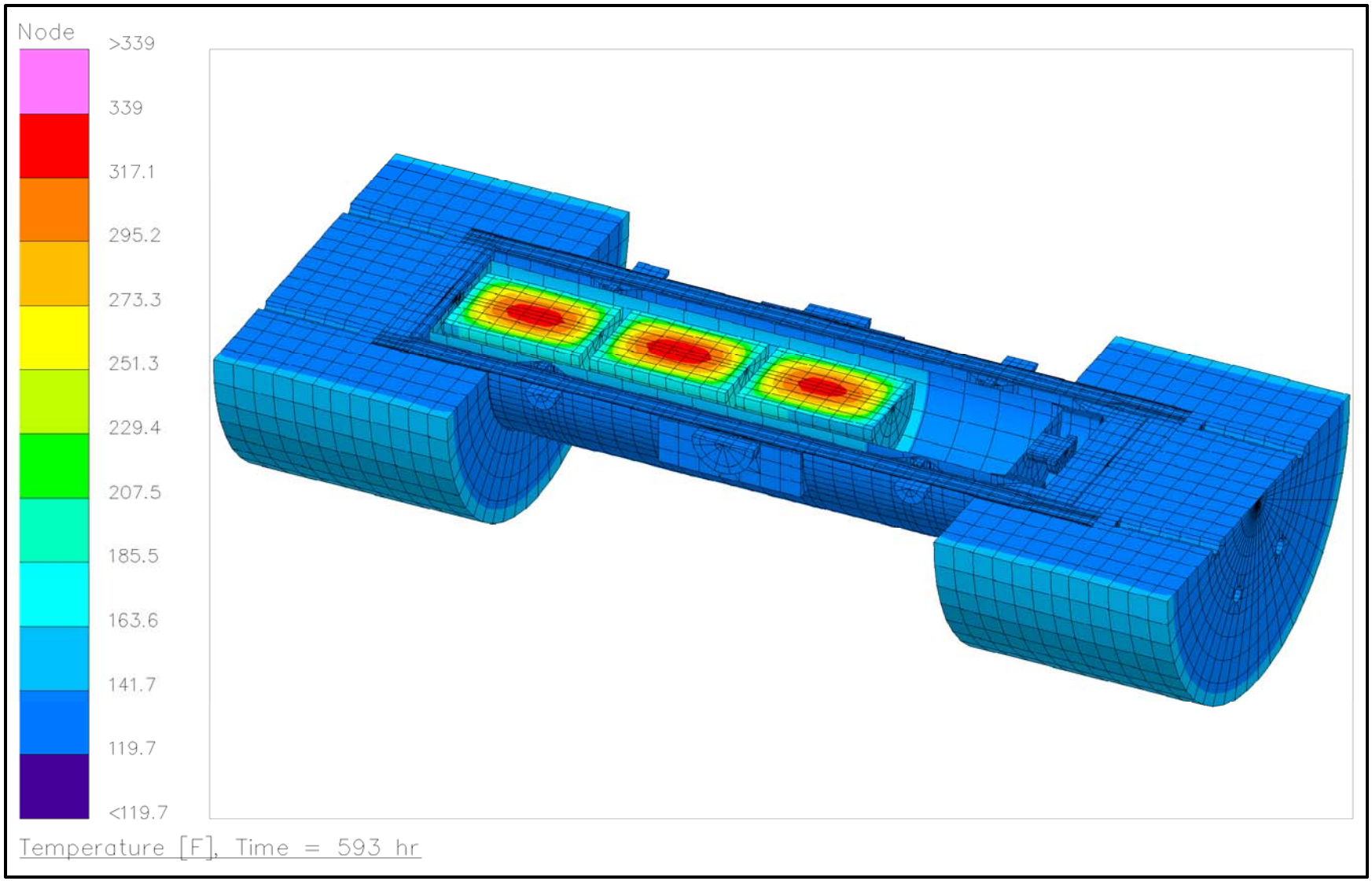

Figure 3.6.2-5 – NCT Case 1 – Package with RLC; 12 lb/ft³ Waste with 90 Watts Decay Heat and Insolation – Downward Axial Bias

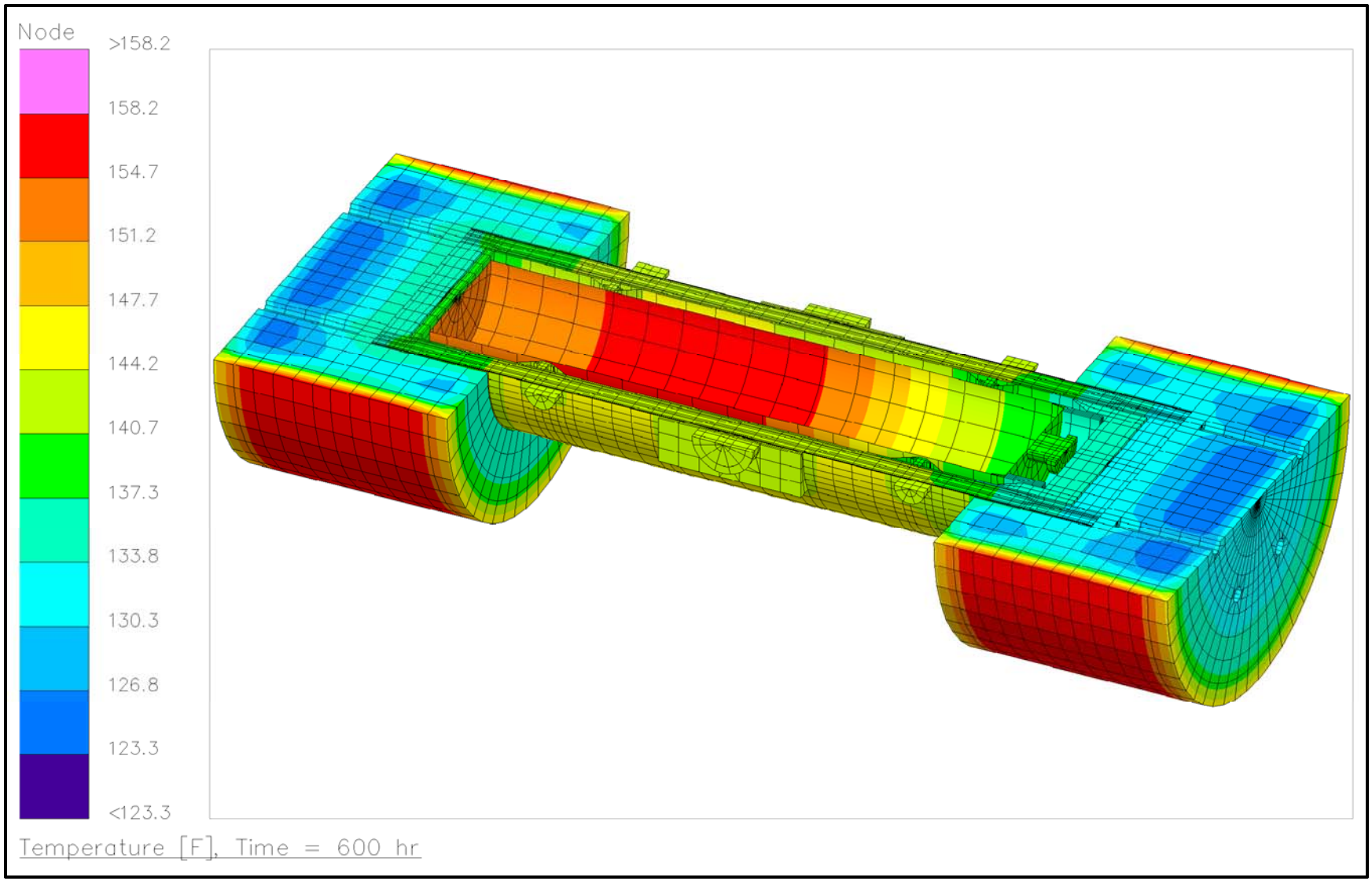

Figure 3.6.2-6 – NCT Case 1 – Package with RLC; 12 lb/ft³ Waste with 90 Watts Decay Heat and Insolation – Downward Axial Bias (Drums Hidden)

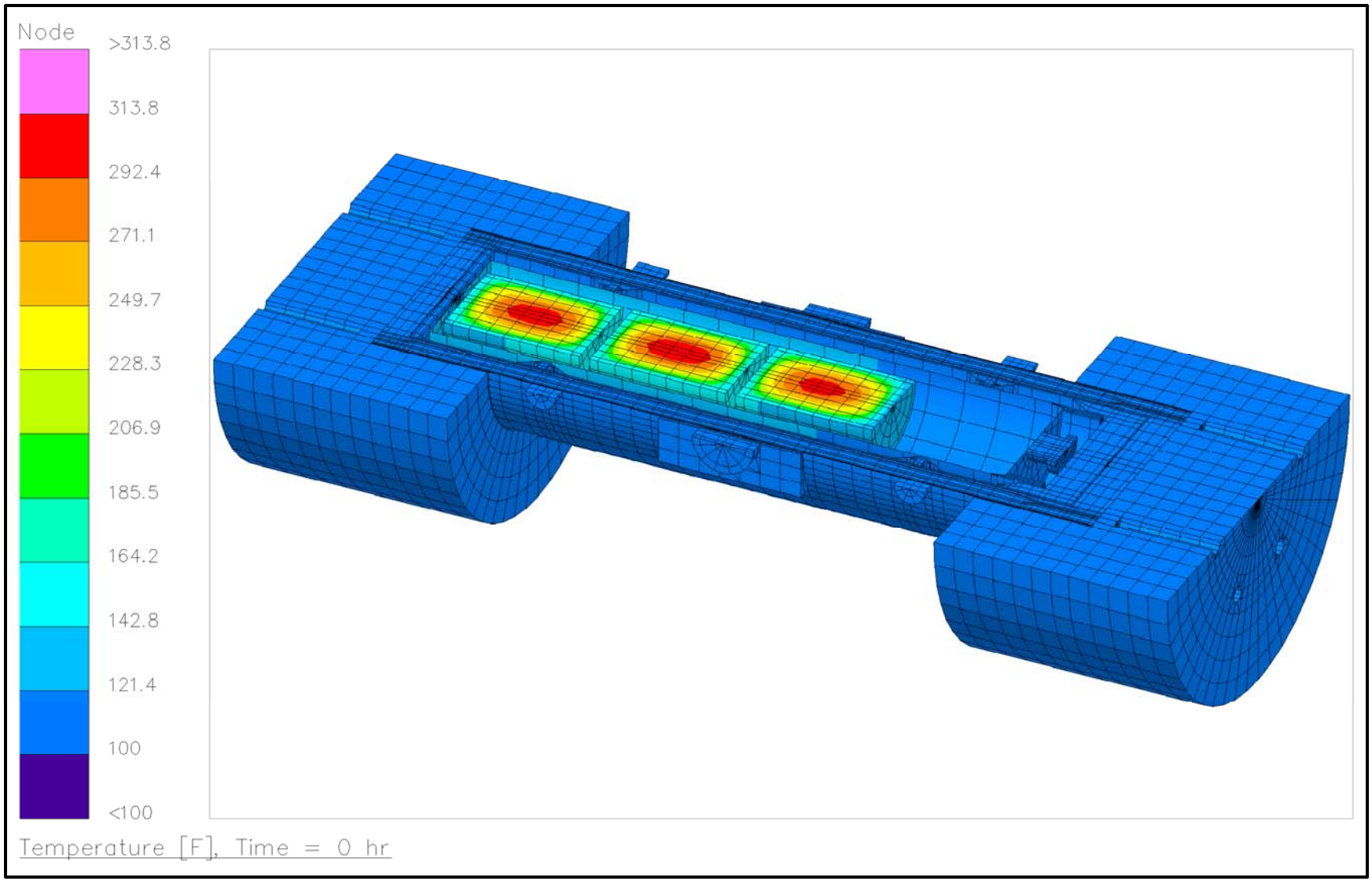

Figure 3.6.2-7 – NCT Case 1 – Package with RLC; 12 lb/ft³ Waste with 90 Watts Decay Heat and No Insolation – Downward Axial Bias

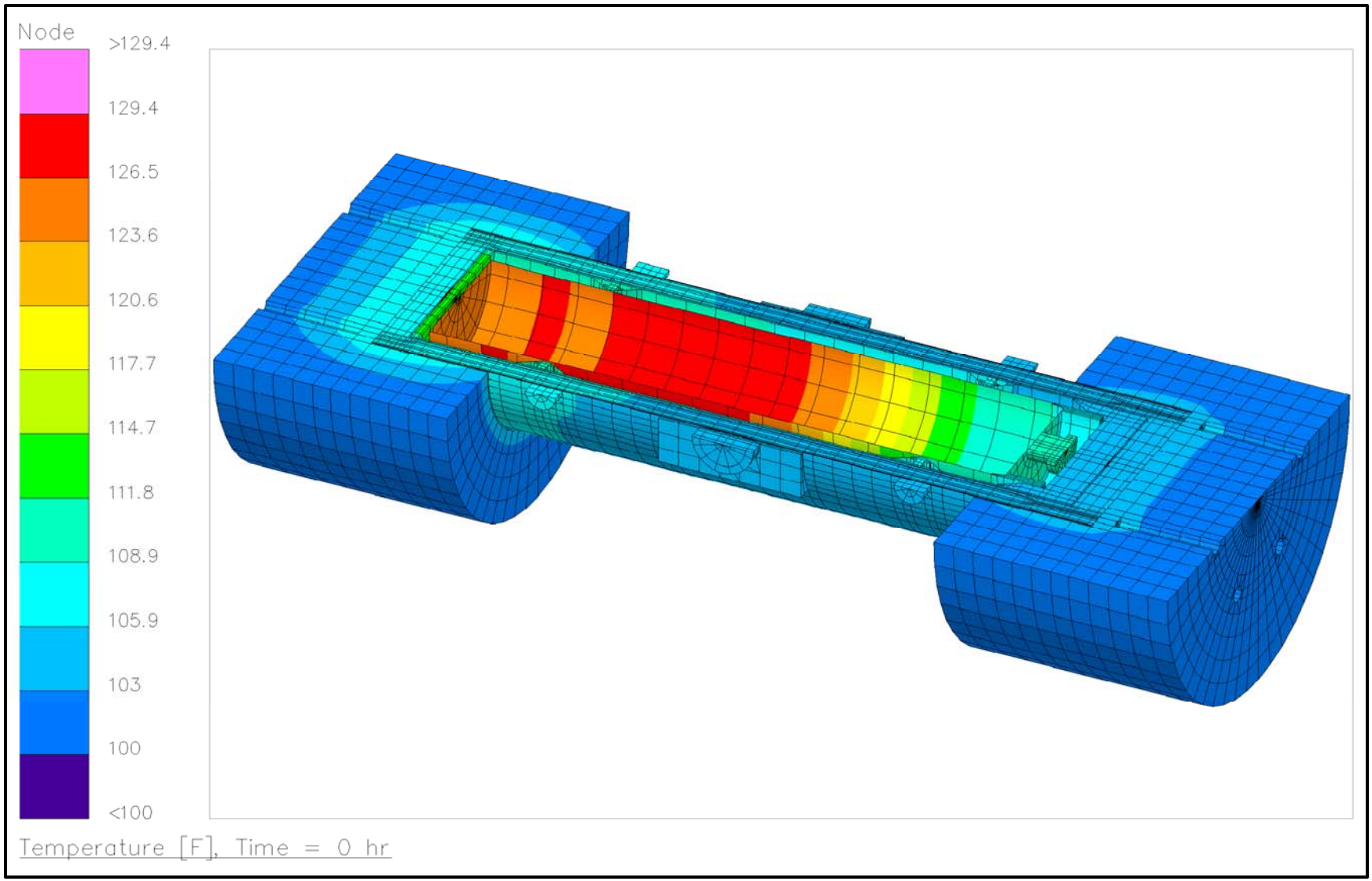

Figure 3.6.2-8 – NCT Case 1 – Package with RLC; 12 lb/ft³ Waste with 90 Watts Decay Heat and No Insolation – Downward Axial Bias (Drums Hidden)

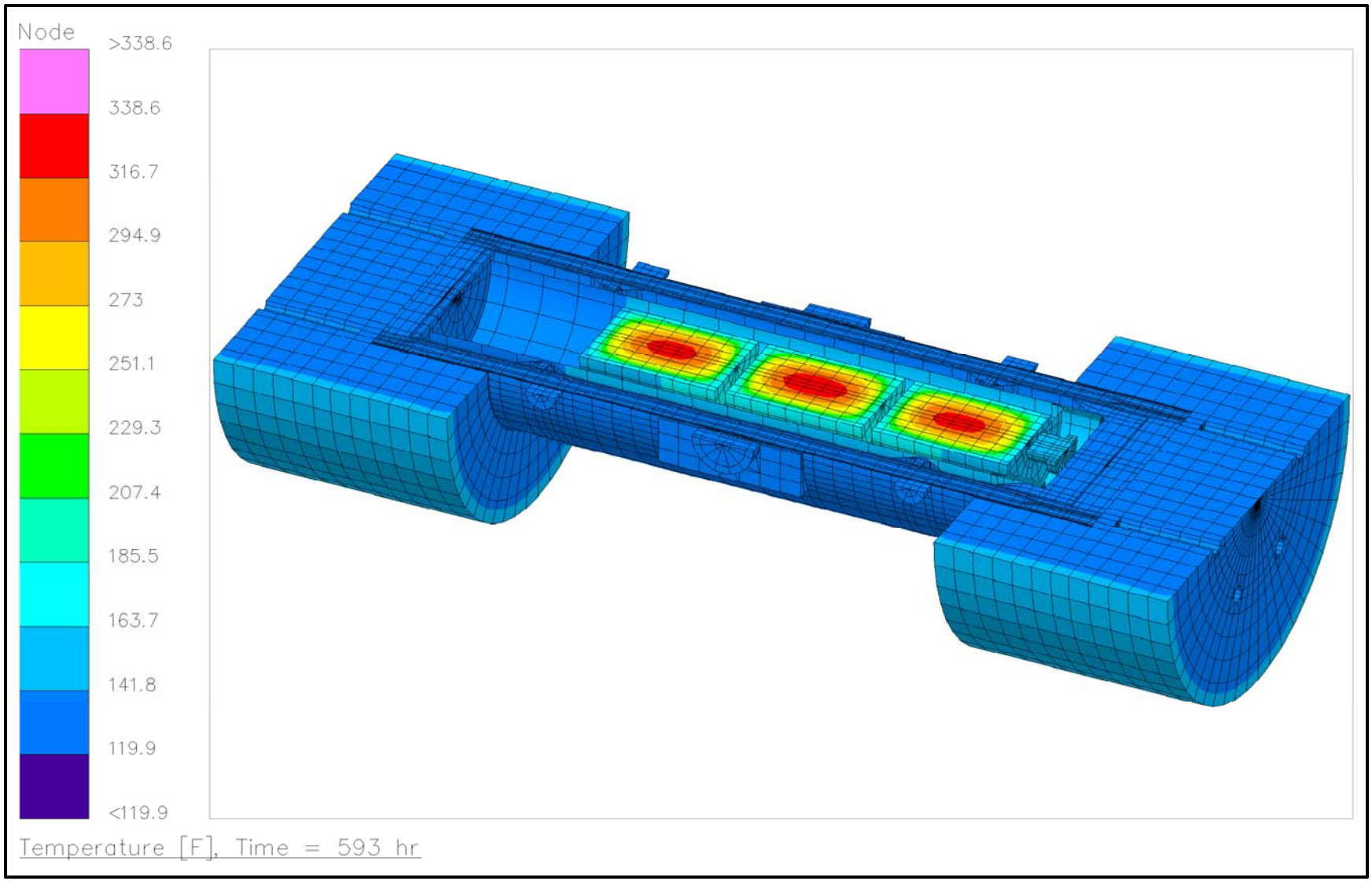

Figure 3.6.2-9 – NCT Case 1 – Package with RLC; 12 lb/ft³ Waste with 90 Watts Decay Heat and Insolation – Upward Axial Bias

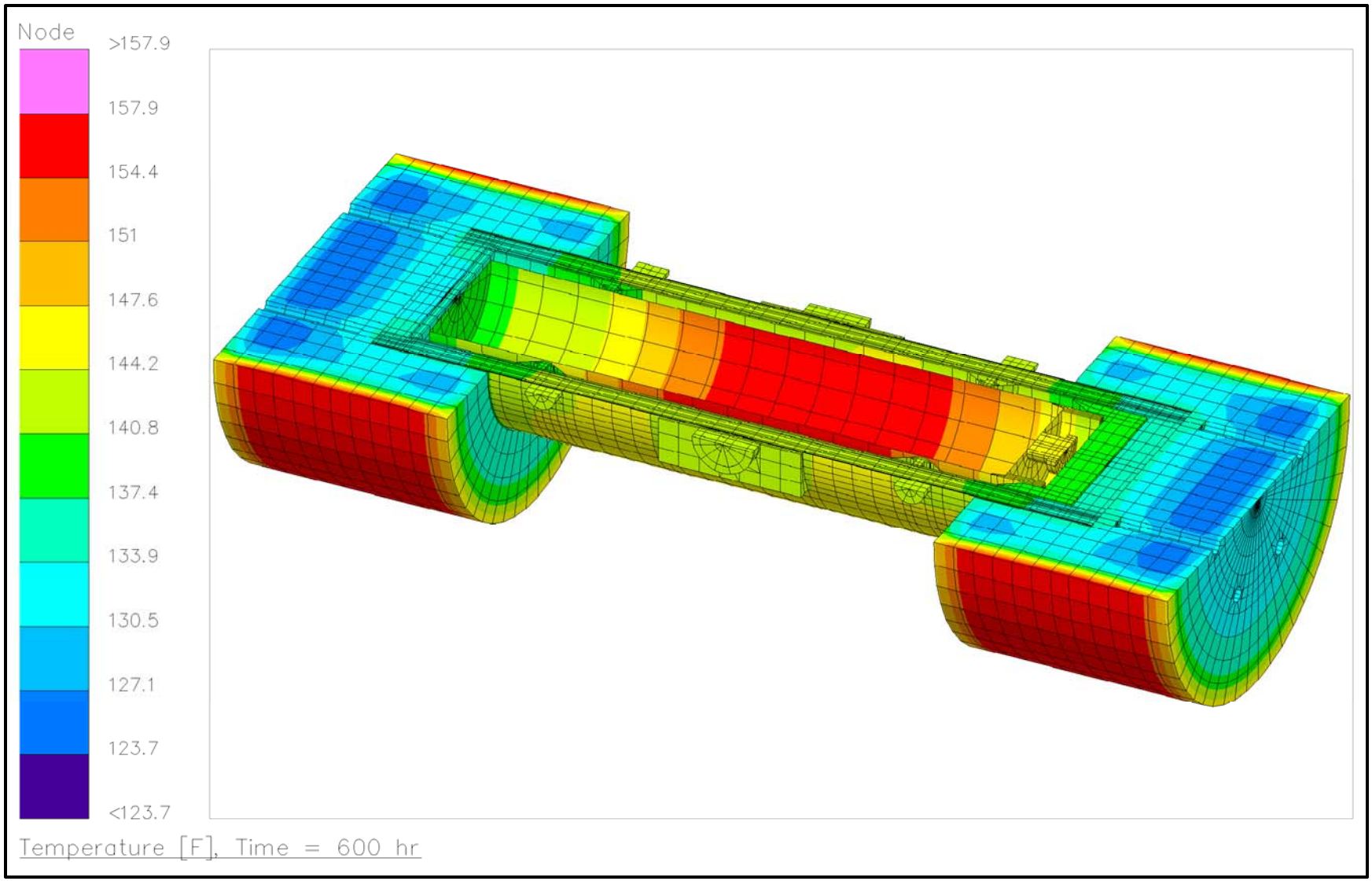

Figure 3.6.2-10 – NCT Case 1 – Package with RLC; 12 lb/ft³ Waste with 90 Watts Decay Heat and Insolation – Upward Axial Bias (Drums Hidden)

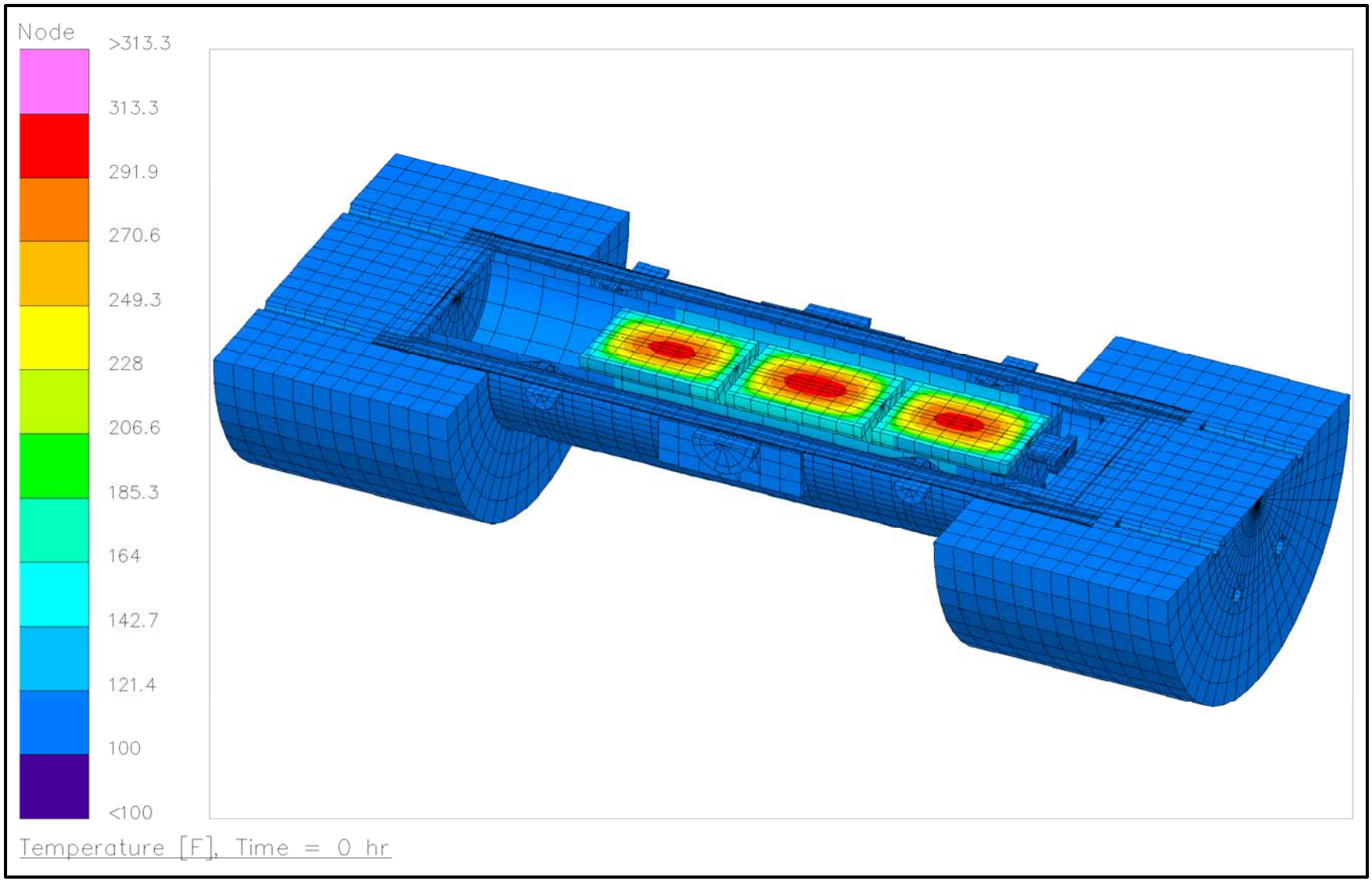

Figure 3.6.2-11 – NCT Case 1 – Package with RLC; 12 lb/ft³ Waste with 90 Watts Decay Heat and No Insolation – Upward Axial Bias

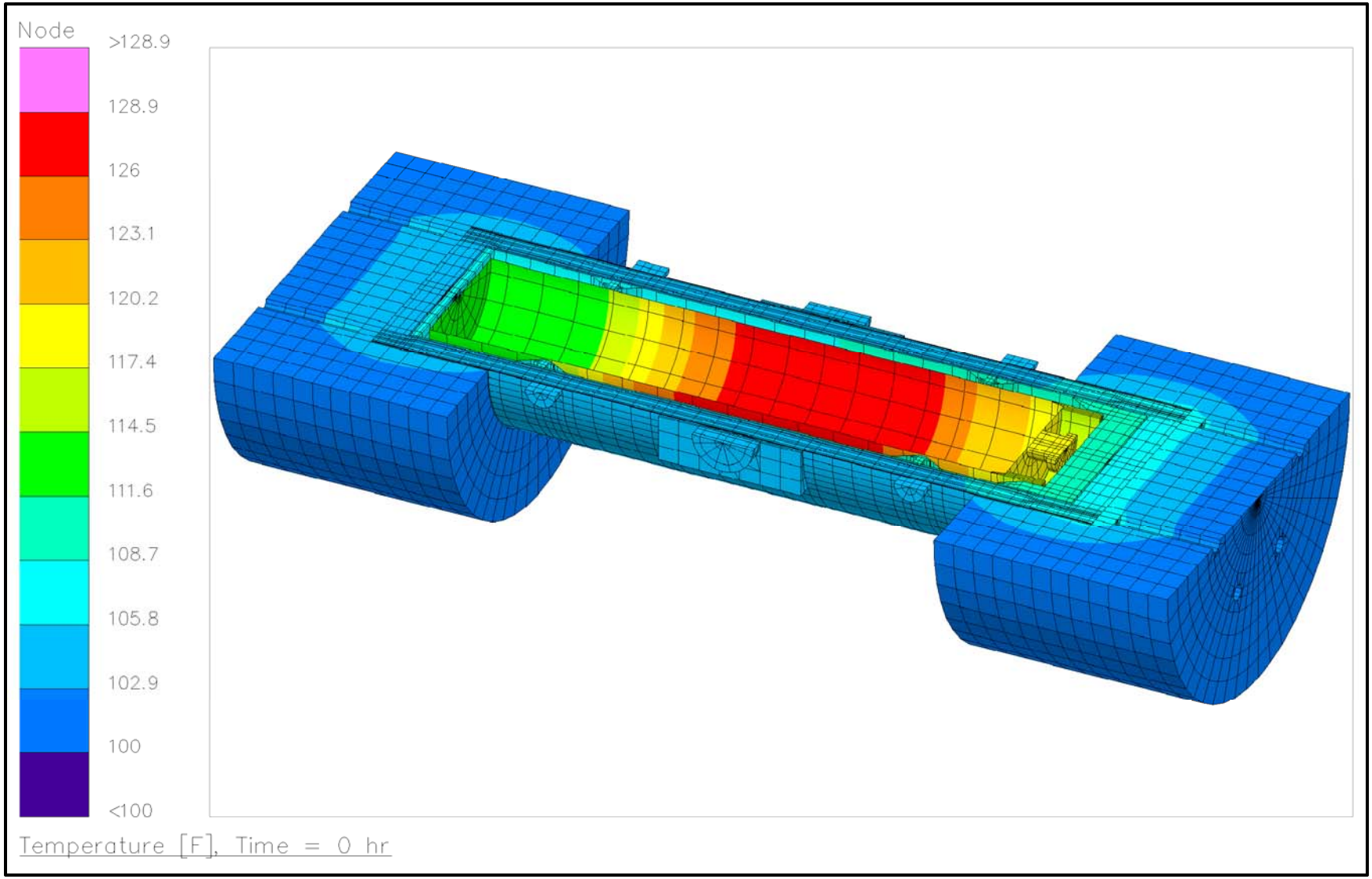

Figure 3.6.2-12 – NCT Case 1 – Package with RLC; 12 lb/ft³ Waste with 90 Watts Decay Heat and No Insolation – Upward Axial Bias (Drums Hidden)

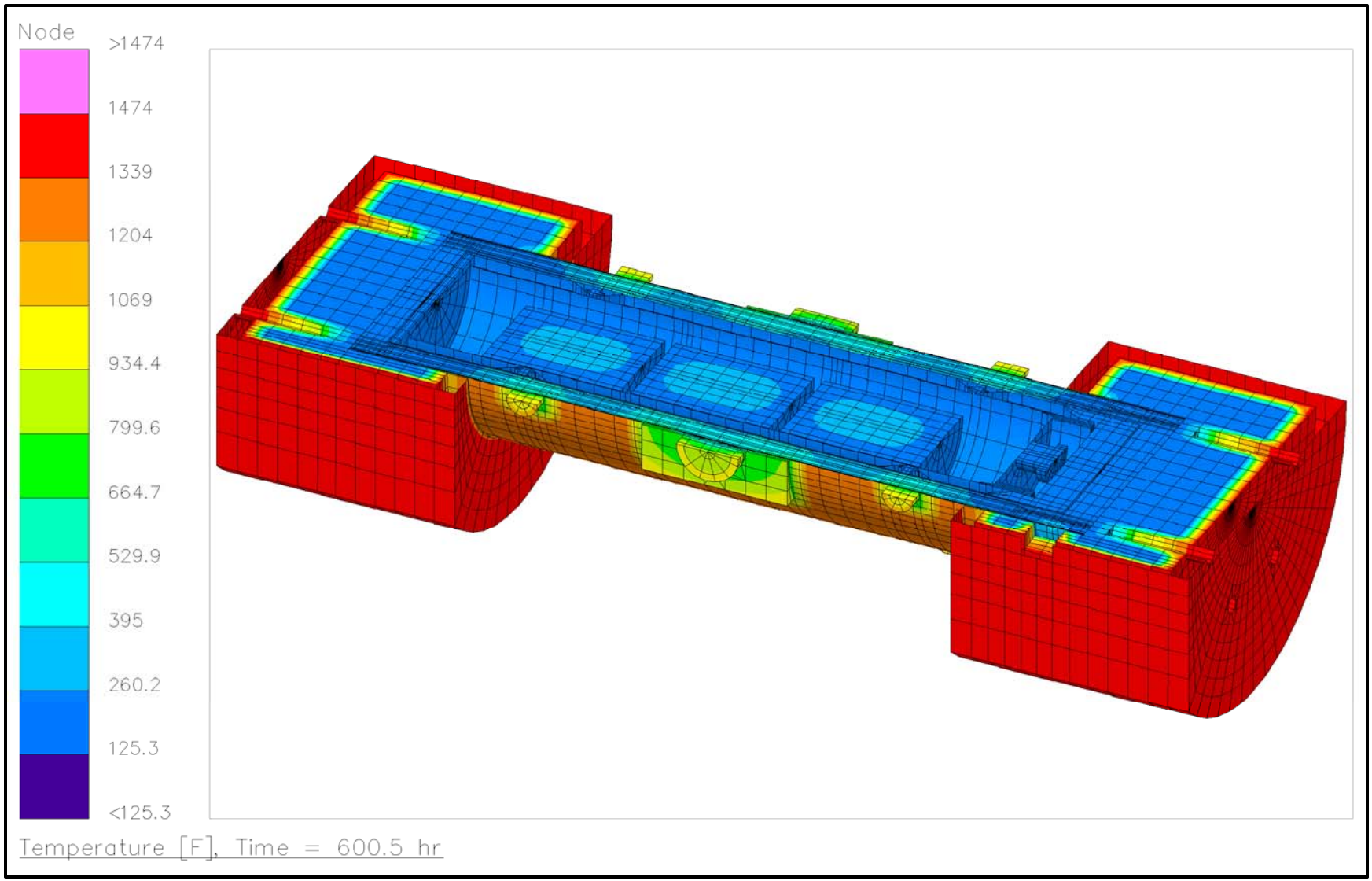

Figure 3.6.2-13 – HAC Case 1 – Package with RLC; 12 lb/ft³ Waste with 90 Watts Decay Heat – Radial Bias – Package Temperatures

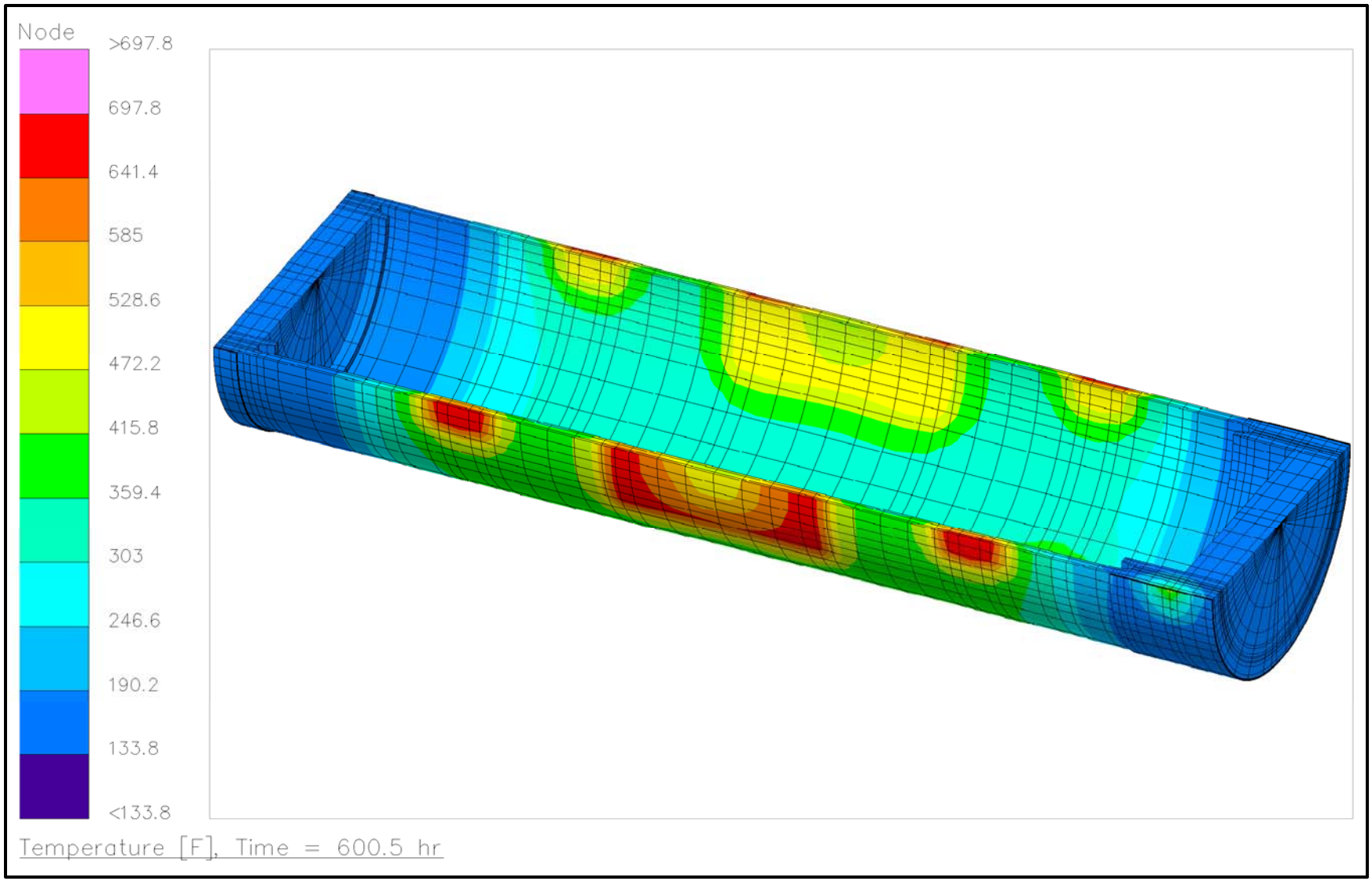

Figure 3.6.2-14 – HAC Case 1 – Package with RLC; 12 lb/ft³ Waste with 90 Watts Decay Heat – Radial Bias – OC Outer Shell Temperatures

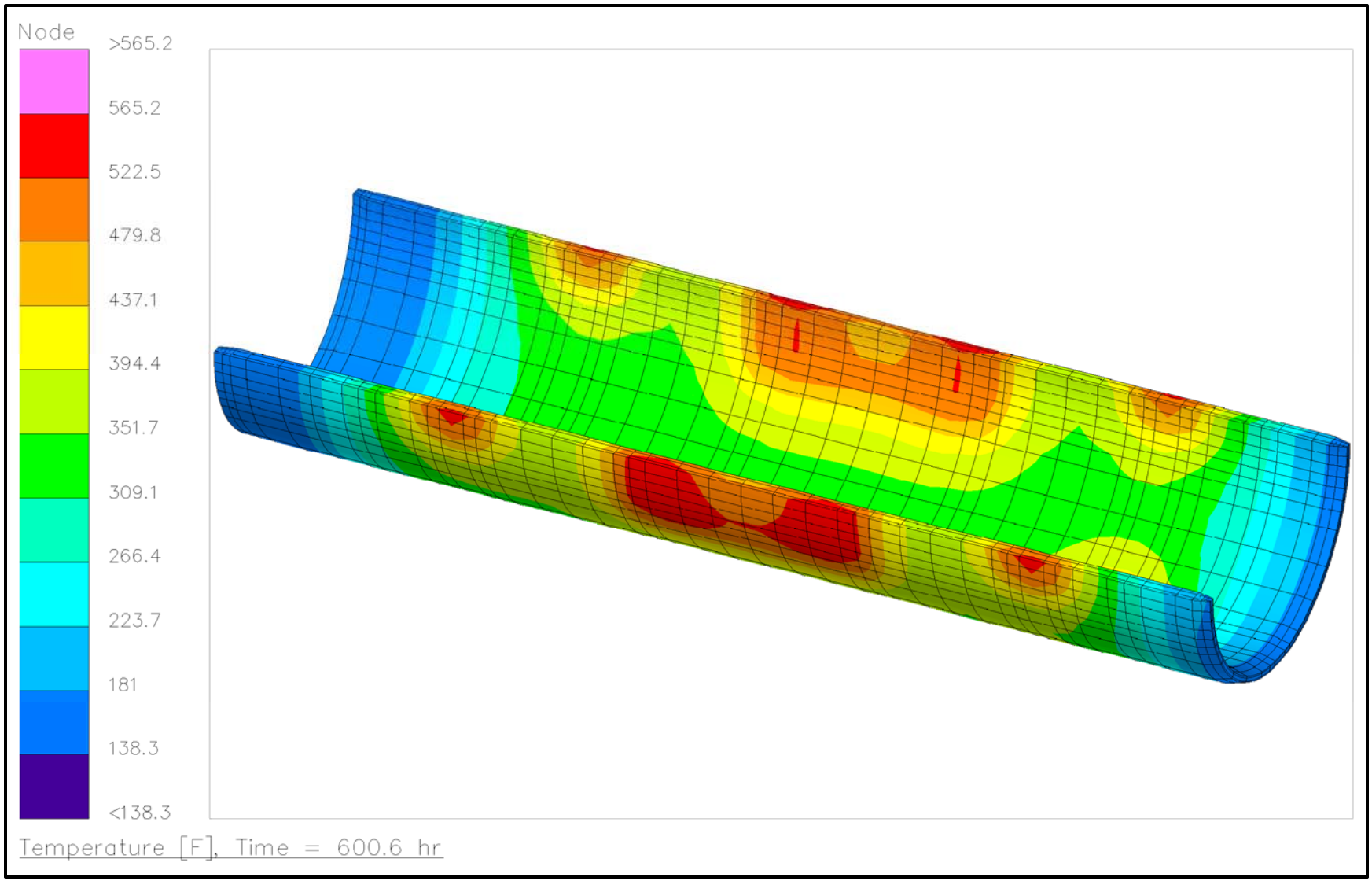

Figure 3.6.2-15 – HAC Case 1 – Package with RLC; 12 lb/ft³ Waste with 90 Watts Decay Heat – Radial Bias – OC Lead Temperatures

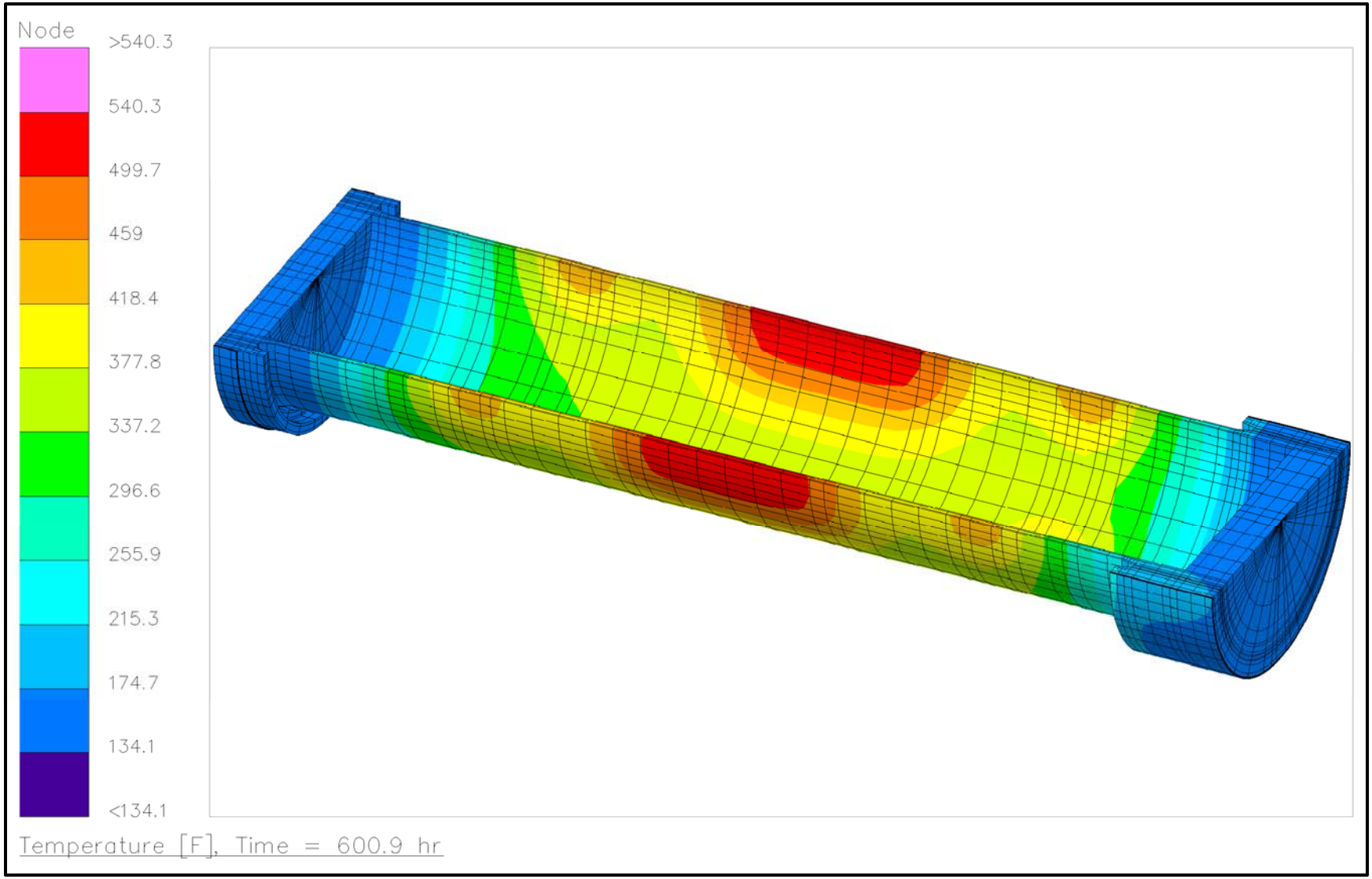

Figure 3.6.2-16 – HAC Case 1 – Package with RLC; 12 lb/ft³ Waste with 90 Watts Decay Heat – Radial Bias – OC Inner Shell Temperatures

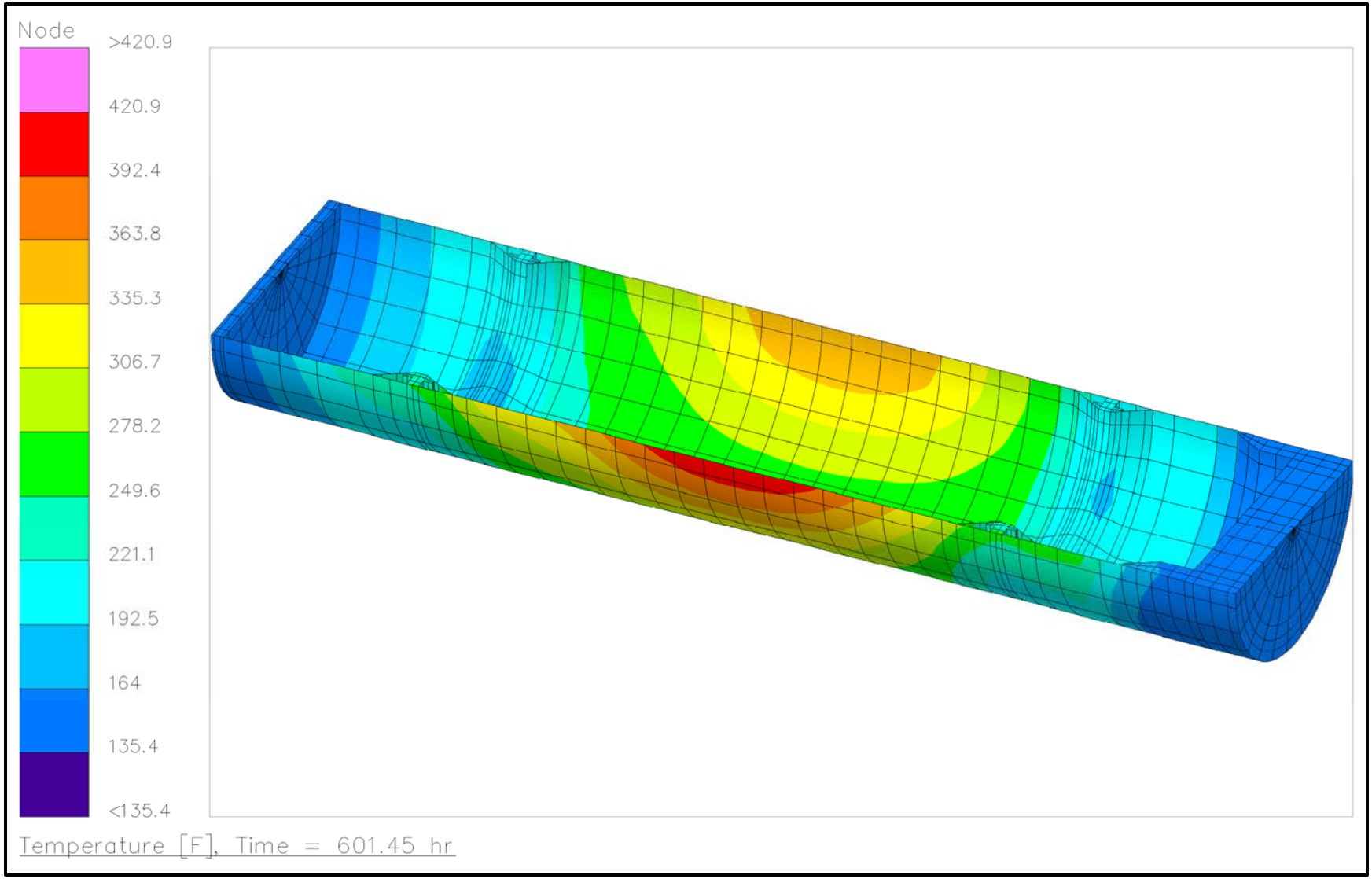

Figure 3.6.2-17 – HAC Case 1 – Package with RLC; 12 lb/ft³ Waste with 90 Watts Decay Heat – Radial Bias – IV Temperatures

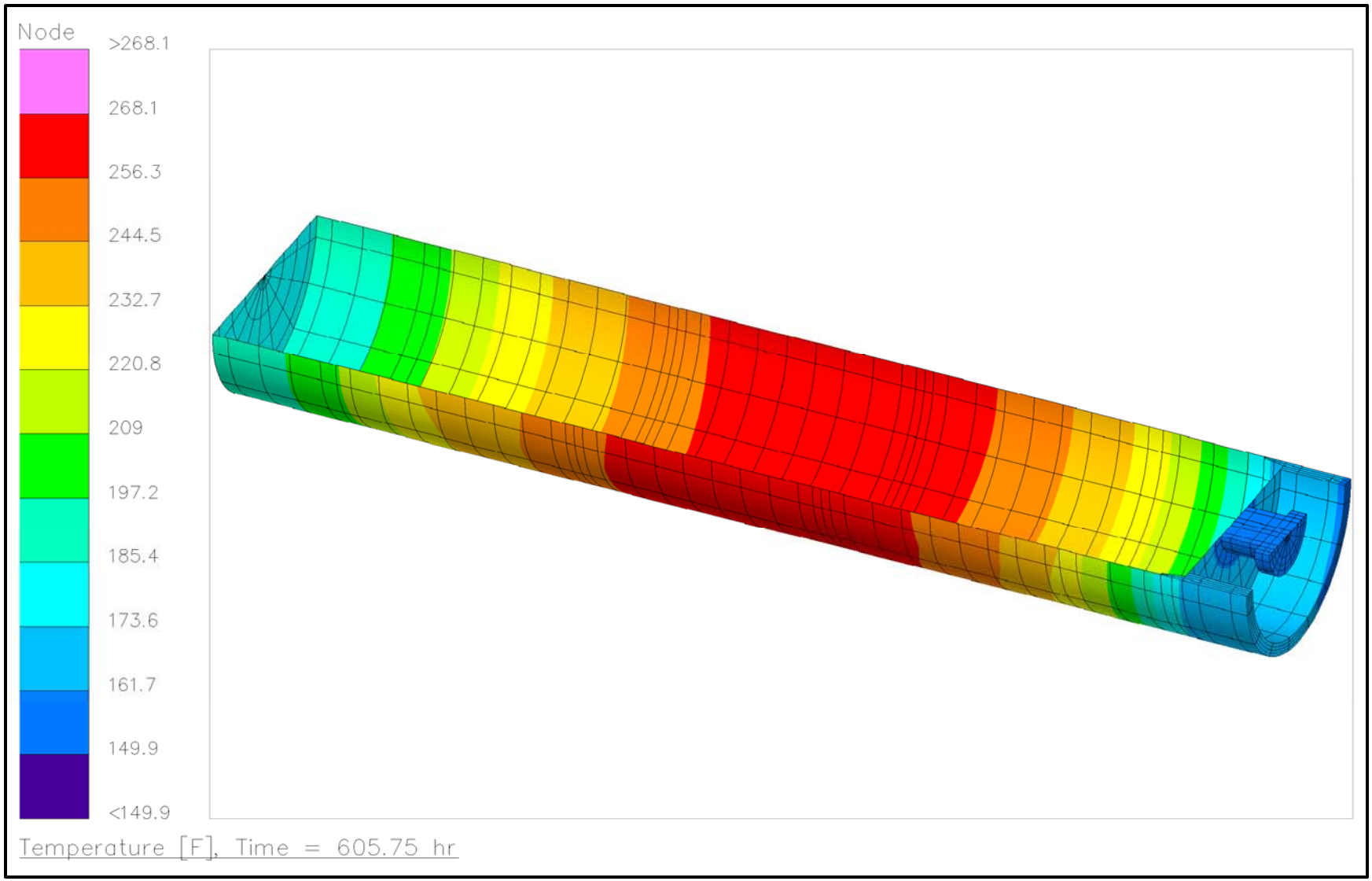

Figure 3.6.2-18 – HAC Case 1 – Package with RLC; 12 lb/ft³ Waste with 90 Watts Decay Heat – Radial Bias – RLC Temperatures

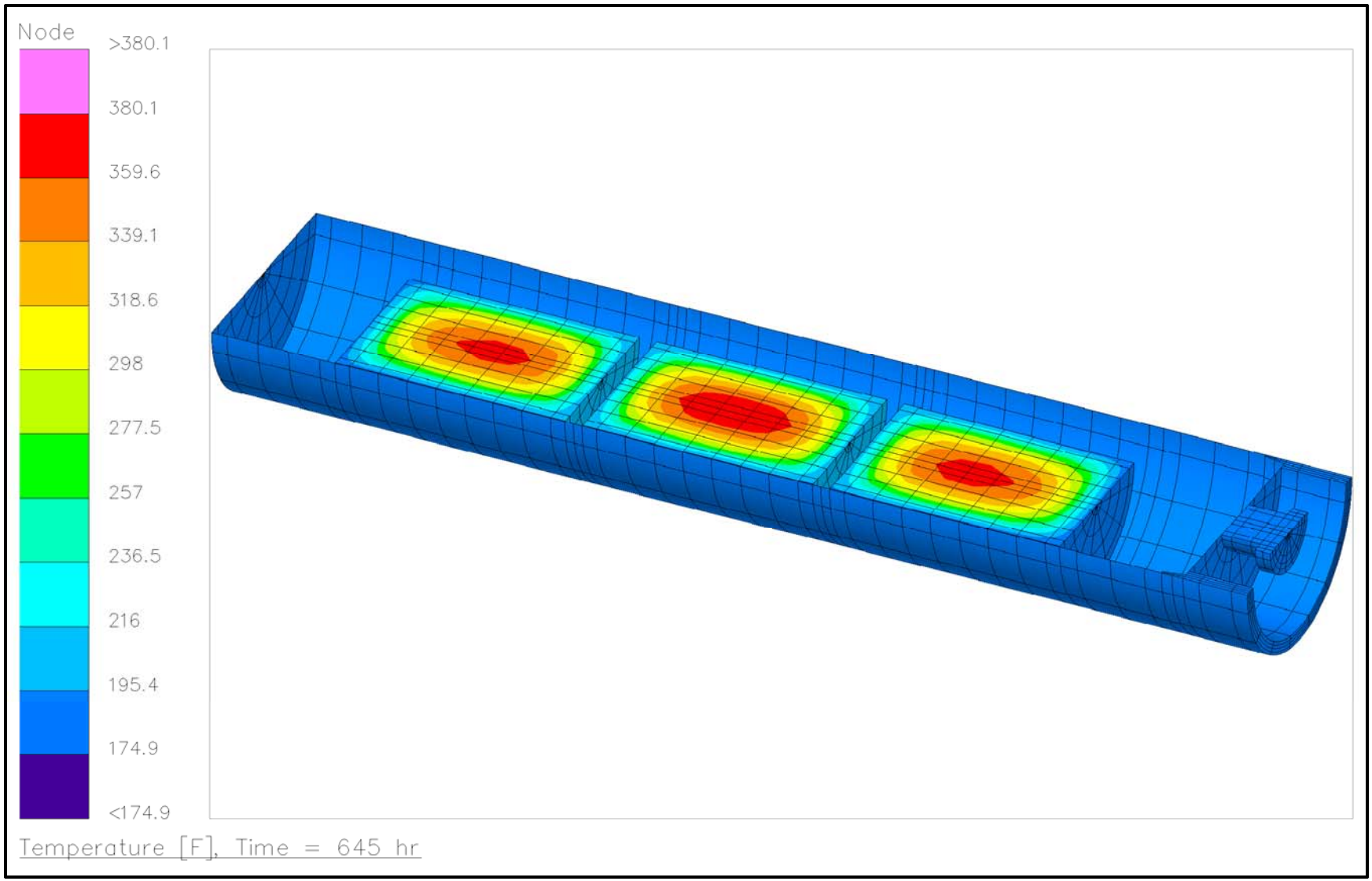

Figure 3.6.2-19 – HAC Case 1 – Package with RLC; 12 lb/ft³ Waste with 90 Watts Decay Heat – Radial Bias – Drum Temperatures

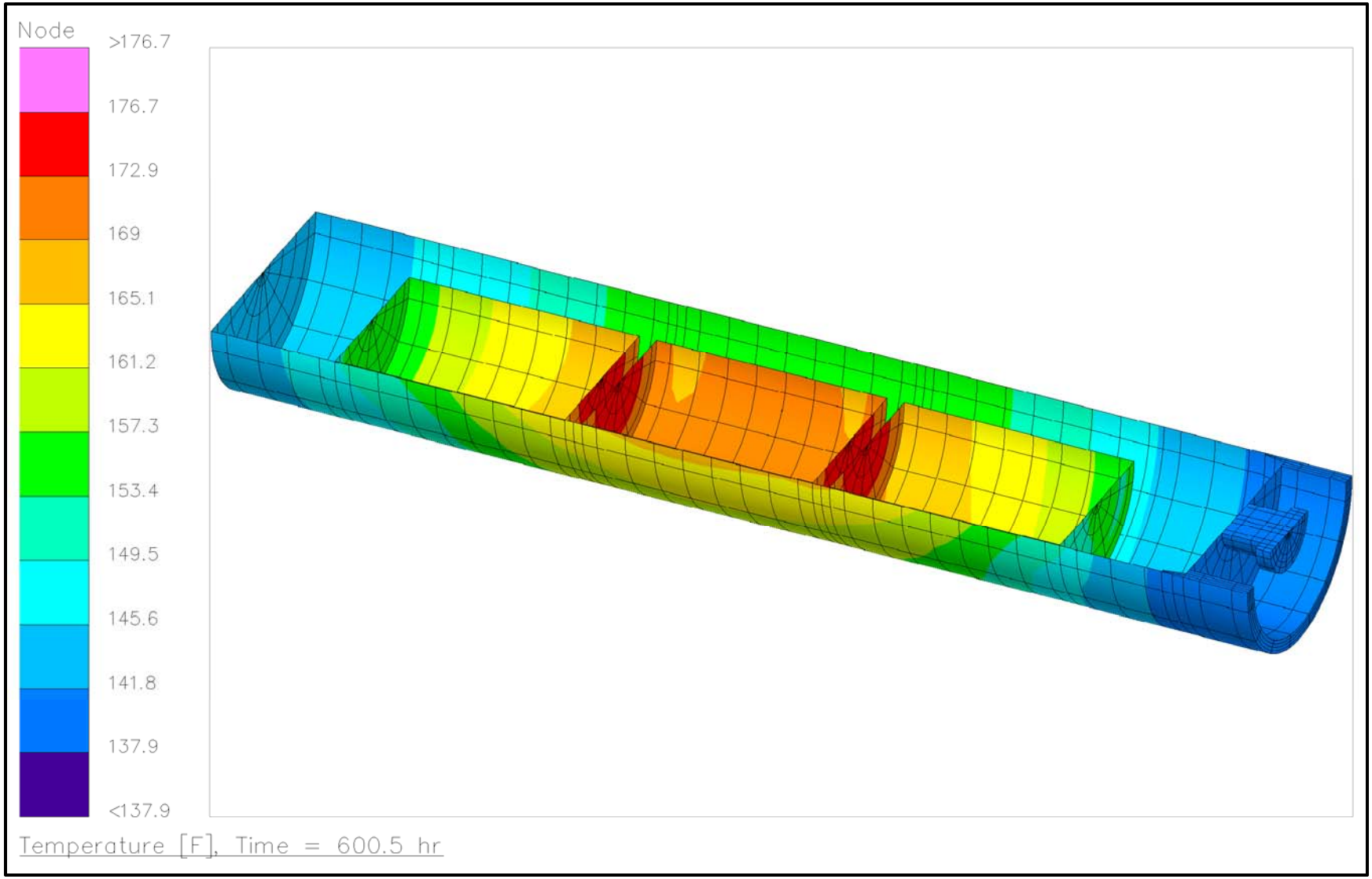

Figure 3.6.2-20 – HAC Case 1 – Package with RLC; 12 lb/ft³ Waste with 90 Watts Decay Heat – Radial Bias – RLC Shell Depicting Radial Bias

3.6.3 Polyurethane Foam Performance Tests

3.6.3.1 Introduction

(1) During the design phase of the NuPac 125-B cask[1], a rigid unicellular polyurethane foam was selected for the impact absorption medium in the overpacks. The specific product, *LAST-A-FOAM* FR-3700, with a nominal density of 12 lb/ft^3 . The foam, when at a 12 lb/ft^3 density, was designated as "FR-3712".

(2) The NuPac 125-B quarter-scale impact limiters were filled with this product and performed well during the engineering development drop test series. Therefore, the foam in the stated density was selected as the primary impact limiting medium for the full-scale impact limiters.

(3) A series of thermal evaluation tests were conducted on May 2, 1985, to evaluate the foam's performance when subjected to high-temperature thermal input and flame impingement[2]. This was done to assure that the foam would allow the impact limiter to survive the fire test and protect the containment seals from degradation as required by 10 CFR 71[3].

(4) The tests were conducted in accordance with the referenced NuPac test procedure.

3.6.3.2 Test Discussion

(1) A total of three (3) new 5-gallon steel cans were filled with the FR-3712 foam under the same process controls utilized in production. The steel cans were selected to simulate a general impact limiter configuration (the foam encased in a steel shell).

(2) The three (3) foamed cans were then configured for the test series as follows:

(a) One can was left in the as-foamed configuration with the end uncovered. This configuration was selected to simulate a basically undamaged impact limiter with a single opening to expose the foam to flame impingement.

(b) One can was crushed to elongate it approximately 20% at the can diameter. The can was then punctured approximately halfway down one side to a depth of 2 – 3 inches into the foam with a hole approximately 1¼ inches in diameter. The opposite side was cut and the steel shell torn away to expose the foam over a 3/4-inch wide by 3-inch long by 1/4-inch deep area. The can opening was left uncovered. The foam was cracked longitudinally from one end to the other due to crushing. The crack opening was from 1/8-inch to 1/2-inch in width.

This configuration was selected to simulate a severely damaged impact limiter.

---

[1] Nuclear Packaging, Inc., *Safety Analysis Report for the NuPac 125-B Fuel Shipping Package*, USNRC Certificate of Compliance 71-9200, U.S. Department of Energy, Washington, D.C.

[2] General Plastics, *Last-a-Foam FR-3700® for Crash and Fire Protection of Nuclear Material Shipping Containers*, General Plastics Manufacturing Company, 4910 Burlington Way, Tacoma, Washington, February 1990.

[3] Title 10, Code of Federal Regulations, Part 71 (10 CFR 71), *Packaging and Transportation of Radioactive Material*, 01-01-14 Edition.

(c) One can was left undamaged and wrapped with two (2) layers of thick fiberglass mat. The can was then closed off with a steel lid. The lid was punctured to exposed the foam to the atmosphere over an area approximately 3 square inches. The puncture extended approximately 2 inches deep into the foam.

This configuration was selected to subject the foam to a high level of heat retention and gas production within the foamed impact limiter. This was done to simulate a relatively undamaged, but highly heated impact limiter.

(3) The foam height was 13¼ inches to 13½ inches in each can.

(4) Each can was instrumented with a thermocouple at the end farthest from the flame.

(5) Each can was then subjected to a 1,800 to 1,850 ºF flame for thirty (30) minutes.

(6) All tests were fully documented with video equipment.

3.6.3.3 Test Results

(1) The undamaged can described in Paragraph (2)(a) of Appendix 3.6.3.2, *Test Discussion*, performed well during the flame test. The test can was sectioned after the flame test. Inspection of the sectioned specimen indicated that the foam exposed to the flame developed a char layer approximately 6 inches high. However, the undamaged foam height only decreased from 13½ inches to 10½ inches. The foam below the char line exhibited no damage, discoloration, or other degradation.

The temperature at the back of the foam opposite the flame increased to 134 ºF during the test. This indicated very good thermal insulation properties for the foam. When the flame was removed, the foam self-extinguished very quickly.

A summary of the test results follows:

- Final Temperature in the Foam at the End Opposite the Flame: 134 ºF
- Remaining Foam Height: 10½ inches
- Char Height: 6 inches
- Duration of Foam Burn after Flame Removal: 1 minute, 26 seconds

(2) The damaged can as described in Paragraph (2)(b) of Appendix 3.6.3.2, *Test Discussion*, also performed well during the flame test. Due to the crushing of the can, the foam was highly cracked. This provided a number of routes for flame progression into the foam. Inspection of the sectioned can showed that the flame had progressed all the way to the bottom of the can. However, observation during the test indicated that about 10 minutes into the 30-minute test many of the flame routes had been closed down by the self-healing properties of the developing char layer.

In particular, the foam char pushing out of the penetrations on the sides of the can completely closed off the flow of flame to the inside of the can at those locations after 10 minutes of the test. This resulted in self-healing of the foam and no further foam damage below the char line in those areas.

The basic foam height remaining after the flame test was 9½ inches of the original 13½ inches. Foam under the char at the various crack lines exhibited no damage or discoloration.

The foam self-extinguished just as quickly after flame removal as the undamaged can discussed in Paragraph (1).

Thermal insulation performance was excellent. Even though the 1,850 ºF flame traveled down the crack network and charred the foam until a distance approximately 3/4 inches from the thermocouple, the temperature at the back of the foam did not exceed 482 ºF.

A summary of the test results follows:

- Final Temperature in the Foam at the End Opposite the Flame: 482 ºF
- Remaining Foam Height: 9½ inches
- Char Height: 6 inches
- Duration of Foam Burn after Flame Removal: 1 minute, 31 seconds

(3) The undamaged and fiberglass-wrapped can described in Paragraph (2)(c) of Appendix 3.6.3.2, *Test Discussion*, performed better than predicted during the flame test. This configuration performed very well in the area of thermal insulation. The maximum temperature noted at the back of the foam was 89 ºF.

The foam continued to burn very slowly through the one hole in the can cover for approximately 5 minutes after the flame was removed. This was due to the gases generated by the retained heat within the foam inside the can. However, the amount of gas, the intensity of the burn and its duration were all lower than expected and therefore, very satisfactory.

Inspection of the sectioned can showed that the char was only 3 inches high due to the restraint provided by the can cover. The remaining foam height was 10¼ inches from a pretest height of 13¼ inches. The foam below the char line was totally undamaged and intact, and appeared as new.

A summary of the test results follows:

- Final Temperature in the Foam at the End Opposite the Flame: 89 ºF
- Remaining Foam Height: 10¼ inches
- Char Height: 2⅜ inches
- Duration of Foam Burn after Flame Removal: 4 minute, 58 seconds

3.6.3.4 Summary

(1) The foam performed very well in the thermal performance evaluation series. The highly damaged sample sustained greater damage due to the cracking and resulting additional flame impingement and convection routes they presented. However, the damaged sample still demonstrated good temperature attenuation and quick self-extinguishing after the flame removal.

The final can, with the fiberglass wrap, was configured to present the worst-case for flame self-extinguishing. It did take the longest to self-extinguish, but still performed far better than expected in the areas of thermal insulation, self-extinguishing, and foam condition after test.

(2) Foam char performance was very good in all cases, with less than 30% of the foam turning to char in the worst case.

(3) Therefore, it is recommended that the FR-3700 series of rigid polyurethane foam be approved for use as the impact absorbing medium in impact limiters subjected to the fire test requirements of 10 CFR 71[3] for Type B containers.

Details of this test program have been incorporated into General Plastics', *Last-a-Foam FR-3700® for Crash and Fire Protection of Nuclear Material Shipping Containers*[2].

3.6.4 Containment O-ring Seal Material Tests

3.6.4.1 Introduction

Each containment O-ring seal material formulation shall be initially qualified for use in the RH-TRU 72-B packaging through the application of performance tests that demonstrate the material's ability to achieve and maintain a leaktight[1] seal at or beyond extremes for temperature, duration, minimum seal compression, and maximum seal compression change in a prototypical test fixture. The basis for formulation qualification test conditions applicable to the RH-TRU 72-B packaging is provided in Section 3.6.4.2, *Limits of O-ring Seal Compression and Temperature for RH-TRU 72-B*. Section 3.6.4.3, *Formulation Qualification Test Fixture and Procedure*, defines the test fixture and test procedure for O-ring seal material qualification tests. Section 3.6.4.4, *Rainier Rubber R0405-70 Formulation Qualification Test Results,* summarizes the results of qualification testing successfully performed on Rainier Rubber[2] butyl compound R0405-70.

Each batch of containment O-ring seal material shall additionally be required to satisfy the requirements of ASTM D2000[3] M4AA710 A13 B13 F17 F48 Z Trace Element. Section 3.6.4.5, *ASTM D2000 Standardized Batch Material Tests*, summarizes the industry standardized batch tests and correlates the ASTM D2000 designator to specific O-ring performance characteristics.

3.6.4.2 Limits of O-ring Seal Compression and Temperature for RH-TRU 72-B

3.6.4.2.1 Inner Vessel Containment O-ring Seal

The inner vessel (IV) closure seal configuration consists of three O-ring bore seals, each located on a different diameter of the IV lid (see Appendix 1.3.1, *Packaging General Arrangement Drawings*, for details). The middle O-ring seal is defined as the containment boundary (the inner O-ring seal retains the test gas for helium leak testing, while the outer O-ring seal provides an annulus in which to establish a vacuum for leak testing). In order to determine the minimum compression that may occur on the IV containment O-ring seal, the largest tolerance stack-up on the lid, flange, and O-ring seal groove dimensions are utilized.

1. O-ring Stretch for Minimum Compression

The minimum IV containment O-ring seal groove diameter is 27.368 inches, and the maximum upper flange diameter at this location is 27.806 inches. With a cross-sectional diameter tolerance of ±0.003 inches, the minimum IV O-ring seal cross-sectional diameter in an uninstalled condition is 0.275 – 0.003 = 0.272 inches. With a diametral tolerance of ±1%, the minimum inside diameter of the O-ring seal in an uninstalled condition is 26.300 × (1 – 0.01) = 26.037 inches. In an installed

[1] Leaktight is defined as leakage of 1×10^{-7} standard cubic centimeters per second (scc/sec), air, or less, per Section 2.1, *Definitions – "Leaktight"*, of ANSI N14.5-2014, *American National Standard for Radioactive Materials – Leakage Tests on Packages for Shipment,* American National Standards Institute, Inc. (ANSI).

[2] Rainier Rubber Company, Seattle, WA.

[3] ASTM D2000-08, *Standard Classification System for Rubber Products in Automotive Applications,* American Society for Testing and Materials, Philadelphia, PA, Volume 09.02, 2008.

condition, the O-ring seal's cross-sectional diameter is reduced due to inside diameter stretch of [(27.368 – 26.037) / 26.037] × 100 = 5.11%.

2. Reduction in O-ring Seal Cross-Sectional Diameter Due to Stretch

From Figure 3-3 of the *Parker O-ring Handbook*[4], the O-ring seal cross-sectional diameter is reduced by {0.56 + [0.59 × 5.11] – [0.0046 × $(5.11)^2$]} = 3.45%. Therefore, the installed minimum O-ring cross-sectional diameter is 0.272 × (1 – 0.0345) = 0.263 inches.

3. Minimum O-ring Seal Compression with a Centered Lid

The minimum O-ring seal compression is {[0.263 – ½(27.806 – 27.368)] / 0.263} × 100 = 16.73% with a centered lid. This is the normal, as-installed configuration, since the presence of the O-ring seal will inherently self-center the lid.

4. Minimum O-ring Seal Compression with an Offset Lid

The smallest radial gap occurs at the location of the upper O-ring seal. The maximum upper flange inside diameter at this location is 28.006 inches, and the minimum IV lid diameter at the same location is 27.990 – 0.005 (tolerance) = 27.985 inches. With the lid shifted until metal-to-metal contact occurs at the upper O-ring seal location, the minimum IV containment O-ring seal compression is {[0.263 – ½(27.806 – 27.368) – ½(28.006 – 27.985)] / 0.263} × 100 = 12.74%. This is the worst case possible as a result of the HAC free drop.

5. Maximum Change in O-ring Seal Compression from a Centered Lid to an Offset Lid

The maximum change in compression resulting in a minimally compressed IV containment O-ring seal is 16.73% – 12.74% = 3.99%. This is the maximum change in compression of the O-ring seal as a result of the HAC free drop.

3.6.4.2.2 Outer Cask Containment O-ring Seal

The outer cask (OC) closure seal configuration consists of two O-ring bore seals, both at the same diameter on the OC lid (see Appendix 1.3.1, *Packaging General Arrangement Drawings*, for details). The inner O-ring seal is defined as the containment seal (the outer O-ring seal provides a vacuum annulus for helium leak testing, where the test gas is contained in the void space between the IV and OC). In order to determine the minimum compression that may occur on the OC containment O-ring seal, the largest tolerance stack-up on the lid, flange, and O-ring seal groove dimensions are utilized.

1. O-ring Stretch for Minimum Compression

The minimum OC containment O-ring seal groove diameter is 32.265 inches, and the maximum upper flange diameter is 32.896 inches. With a cross-sectional diameter tolerance of ±0.006 inches, the minimum OC O-ring seal cross-sectional diameter in an uninstalled condition is 0.393 – 0.006 = 0.387 inches. With a diametral tolerance of ±1%, the minimum inside diameter of the O-ring seal in an uninstalled condition is 31.000 × (1 – 0.01) = 30.690 inches. In an installed condition, the O-ring seal's cross-sectional diameter is reduced due to inside diameter stretch of [(32.265 – 30.690) / 30.690] × 100 = 5.13%.

[4] ORD 5700, *Parker O-ring Handbook*, Parker Hannifin Corporation, Cleveland, OH. The *Parker O-ring Handbook* is available at http://www.parker.com/literature/ORD%205700%20Parker_O-Ring_Handbook.pdf.

2. Reduction in O-ring Seal Cross-Sectional Diameter Due to Stretch

The resulting reduction in O-ring seal cross-sectional diameter, again from Parker, is $\{0.56 + [0.59 \times 5.13] - [0.0046 \times (5.13)^2]\} = 3.47\%$. The installed minimum O-ring cross-sectional diameter is therefore $0.387 \times (1 - 0.0347) = 0.374$ inches.

3. Minimum O-ring Seal Compression with a Centered Lid

The minimum O-ring seal compression is $\{[0.374 - ½(32.896 - 32.265)] / 0.374\} \times 100 = 15.64\%$ with a centered lid. This is the normal, as-installed configuration, since the presence of the O-ring seal will inherently self-center the lid.

4. Minimum O-ring Seal Compression with an Offset Lid

The smallest radial gap occurs at the location of the upper O-ring seal. The maximum upper flange inside diameter is 32.896 inches, and the minimum OC lid diameter is 32.861 inches. With the lid shifted until metal-to-metal contact with the upper flange occurs, the minimum O-ring seal compression is $\{[0.374 - ½(32.896 - 32.265) - ½(32.896 - 32.861)] / 0.374\} \times 100 = 10.96\%$. This is the worst case possible as a result of the HAC free drop.

5. Maximum Change in O-ring Seal Compression from a Centered Lid to an Offset Lid

The maximum change in compression resulting in a minimally compressed OC containment O-ring seal is 15.64% – 10.96% = 4.68%. This is the maximum change in compression of the O-ring seal as a result of the HAC free drop.

3.6.4.2.3 Containment O-ring Seal Qualification Temperature

Per Section 3.4.4, *Minimum Temperatures*, the minimum IV and OC containment O-ring seal temperature is -40 ºF for normal conditions of transport (NCT) and -20 ºF for hypothetical accident conditions (HAC). Per Section 3.4.3, *Maximum Temperatures*, Table 3.4-3 summarizes the maximum IV and OC O-ring temperatures under NCT as 145.7 ºF and 141.2 ºF, respectively. The duration of O-ring seal material exposure to elevated temperatures under NCT can conservatively be assumed as 1 year based on the replacement frequency of the O-ring seals. Per Section 3.5.3, *Package Temperatures*, Table 3.5-2 summarizes the maximum IV and OC O-ring seal temperatures under HAC as 186.4 ºF and 193.9 ºF, respectively. Evaluating the time-history of O-ring seal temperatures provided in Figure 3.5-5 and Figure 3.5-9, the duration of O-ring seal material exposure to elevated temperatures within 90% of the reported maximum is approximately 48 hours.

An Arrhenius correlation for butyl material with an activation energy of 80 kJ/mol for butyl rubber has been developed to account for diffusion limited oxidation effects.[5] Use of the Arrhenius correlation allows the effects of both NCT and HAC elevated temperature/duration conditions identified above to be conservatively enveloped by a single, 360 ºF, 8-hour test.

Based on the above evaluations, the minimum O-ring seal qualification test parameters required for initial formulation testing of IV and OC containment O-ring seal materials is summarized in Table 3.6.4-1.

[5]Gillen, K. T., Mathias C., and Keenan M. R., *Methods for Predicting More Confident Lifetimes of Seals in Air Environments*, SAND99-0553J, Sandia National Laboratories, March 1999.

Table 3.6.4-1 – Formulation Qualification Test O-ring Seal Compression and Temperature Parameters

Component / Simulated Condition	Required Compression (%)	Required Compression Change (%)	Required Temperature (ºF)	Required Temperature Duration (hours)
IV / NCT Cold	≤16.73	N/A	≤-40	N/A
IV / HAC Free Drop	≤12.74	≥3.99	≤-20	N/A
IV / HAC Fire		N/A	≥360	≥8
OC / NCT Cold	≤15.64	N/A	≤-40	N/A
OC / HAC Free Drop	≤10.96	≥4.68	≤-20	N/A
OC / HAC Fire		N/A	≥360	≥8

3.6.4.3 Formulation Qualification Test Fixture and Procedure

A bore-type test fixture shall be used to test the containment O-ring seals, representative of the bore seal configuration of the RH-TRU 72-B packaging. The fixture shall include an inner disk containing two, side-by-side O-ring seal grooves. An O-ring seal of prototypic cross-section for either the IV or OC and butyl material, as delineated on the drawings in Appendix 1.3.1, *Packaging General Arrangement Drawings*, shall be placed into each seal groove, and the assembly then placed within a mating bore component. The test fixture shall employ jacking screws or equivalent devices to displace the disk radially relative to the bore, affecting the required O-ring compression on one side of the test fixture. Figure 3.6.4-1 conceptually illustrates the O-ring seal test fixture.

The sizes of all sealing components and O-ring seals utilized in the test fixture, including the amount of O-ring seal stretch, may be adjusted along with the amount of radial displacement to ensure that the parameters in Table 3.6.4-1 can be achieved. The test fixture's overall diameter may be reduced relative to a full-scale RH-TRU 72-B package to achieve a practical size for testing. A reduction in relative diameter is acceptable since the O-ring seal compression, compression change, and temperature are the parameters of primary importance relative to evaluating an O-ring material's ability to maintain a leaktight seal.

All test specimens may be coated lightly with vacuum grease prior to installation into the test fixture. The fully assembled test fixture shall be placed within an environmental test chamber for both heating and cooling with thermocouples attached to the fixture used to confirm the O-ring seal temperature.

The region between the two O-ring seals constitutes a test volume. To perform a leak test, the test volume shall be connected to a helium mass spectrometer leak detector, then evacuated to an appropriate level of vacuum and the outside of the test fixture surrounded with a contained and highly concentrated environment of helium gas, consistent with the guidelines of *Appendix A,*

Section A.5.3, Gas Filled Envelope – Gas Detector, of ANSI N14.5[6]. An O-ring seal test shall be successful if the leakage between the seals is 1×10^{-7} standard cubic centimeters per second (scc/sec), air, or less (i.e., "leaktight").

Test conditions shall be selected to simulate temperature/duration and minimum compression for the prototypic O-ring seals under NCT and HAC conditions. Each set of two test O-ring seals shall be subjected to an initial test at NCT Cold conditions with the inner disk offset as necessary to achieve the NCT required compression, to a second test at HAC Free Drop conditions with the inner disk initially positioned and then radially offset as necessary to achieve the HAC required compression and compression change magnitudes, to a third test at HAC Fire conditions after the required soak duration with the inner disk remaining offset, and to a fourth test at HAC Cold conditions with the inner disk remaining offset (see Table 3.6.4-1).

Helium leakage rate tests shall be performed at each cold temperature test configuration, either at -40 ºF for the NCT Cold condition case, or at -20 ºF for all other cases. Helium leakage rate testing is not practical at hot condition temperatures due to the rapid permeation and saturation of helium gas through the elastomeric material at high temperatures; a fully saturated O-ring seal test specimen results in a measured leakage in excess of 1×10^{-7} scc/sec, air. In lieu of leakage rate testing at the hot temperature test configuration, the ability to establish a rapid, hard vacuum between the O-ring seals shall be used as the basis for acceptance at elevated temperatures, with leaktightness proven subsequent to the elevated temperature phase by the final leakage rate test at -20 ºF. The duration of each of the cold temperature phases of the test shall be defined by the time required to achieve the requisite cold temperatures whereas the duration of the hot phase shall be defined by the required elevated temperature and associated temperature duration given in Table 3.6.4-1.

3.6.4.3.1 Formulation Qualification Test Procedure

The process of formulation qualification leak testing O-ring seal material is given below.

1. Assemble the test fixture with two test O-ring seals.

2. Radially shift the disk inside the bore to establish reduced O-ring seal compression on one side of the test fixture, ensuring the NCT Cold compression requirements are met per Table 3.6.4-1.

3. Cool the test fixture to ≤-40 ºF, continuing to restrain the disk in the NCT offset position relative to the bore.

4. Perform a helium leakage rate test with the test fixture temperature at ≤-40 ºF.

5. Reposition the disk inside the bore to establish an appropriate starting position for the HAC Free Drop test with the test fixture temperature at ≤-20 ºF.

6. Radially shift the disk inside the bore to establish a reduced O-ring seal compression on one side of the test fixture, ensuring the HAC Cold compression and compression change requirements are met per Table 3.6.4-1.

7. Perform a helium leakage rate test with the test fixture temperature at ≤-20 ºF.

[6] ANSI N14.5-2014, *American National Standard for Radioactive Materials – Leakage Tests on Packages for Shipment,* American National Standards Institute, Inc. (ANSI).

8. Warm the test fixture to the elevated test temperature (i.e., HAC Fire temperature per Table 3.6.4-1), continuing to restrain the disk in the HAC offset position relative to the bore.

9. Maintain the elevated temperature for ≥8-hour duration.

10. At the end of the elevated temperature duration, confirm that a rapid, hard vacuum can be achieved and maintained in the test volume between the two, test O-ring seals at the elevated temperature.

11. Cool the test fixture to ≤-20 ºF, continuing to restrain the disk in the HAC offset position relative to the bore.

12. Perform a helium leakage rate test with the test fixture temperature at ≤-20 ºF.

3.6.4.4 Rainier Rubber R0405-70 Formulation Qualification Test Results

Test results are summarized in Table 3.6.4-2, as referenced from GEN-REP-0001.[7] As shown in the table, the Rainier Rubber compound R0405-70 butyl rubber material is capable of maintaining a leaktight seal when subjected to worst-case seal compressions beyond the range of NCT and HAC cold and hot temperatures applicable to the RH-TRU 72-B package. For comparison, the minimum O-ring seal compression applicable for the NCT Cold condition (see Table 3.6.4-1) is 16.73% for the IV and 15.64% for the OC. The NCT Cold tests summarized in Table 3.6.4-2 were conservatively performed with the disk in its full offset position, thus showing leaktight capability at NCT Cold conditions to as low as 10.38%. For the remaining tests, the applicable minimum compression is 12.74% for the IV and 10.96% for the OC whereas the tests were all performed in the full offset position, thus showing leaktight capability to as low as 10.38%. For the HAC Free Drop test, the disk was initially centered and then shifted as much as 10.74%, which very conservatively enveloped the applicable worst-case shifts of 3.99% for the IV and 4.68% for the OC. For the HAC Fire test, again per Table 3.6.4-1, a test temperature of at least 360 ºF for at least 8 hours is applicable, whereas the actual test was conservatively performed at 400 ºF for 8 hours, as noted in Table 3.6.4-2. Therefore, formulation qualification testing of Rainier Rubber compound R0405-70 bounds the minimum O-ring seal compressions for the RH-TRU 72-B package.

3.6.4.5 ASTM D2000 Standardized Batch Material Tests

Based on successfully demonstrating the ability to remain leaktight when subject to the formulation qualification tests, Rainier Rubber R0405-70 butyl rubber compound was selected to benchmark material performance parameters that can be evaluated using available industry standardized tests. Correlation of the R0405-70 butyl rubber compound performance to industry standard performance specifications establishes a standard quality and performance benchmark that is suitable for use in material batch testing. Note that a "formulation" represents a controlled chemical recipe and production process as defined by the material supplier, a "batch" represents the chemical compounding of a production quantity of material before vulcanizing, and a "lot" refers to the quantity of finished product made at any one time.

Qualification testing identified certain key parameters that are important to seal performance. Of these, two important parameters for this application are resistance to helium permeation and acceptable

[7] *Formulation Qualification Testing of Rainier Rubber Butyl Compound RR0405-70*, GEN-REP-0001, Rev. 0, Washington TRU Solutions, February 2010.

resiliency at cold temperatures. Butyl rubber performs very well resisting helium permeation, and the TR-10 test in ASTM D1329[8] provides an acceptable method for determining cold temperature material resiliency, with the properties of the R0405-70 butyl rubber acting as a baseline for the required resiliency.

The ability of the compound to withstand elevated temperatures while not having significant reduction in material properties is also required to maintain seal integrity after the hypothetical accident condition thermal event. Material properties in elastomers are reduced through the process of de-polymerization, an aging phenomenon. Elastomer aging can be accelerated by the application of energy (heat). The effect of aging can be quantified by measuring the reduction of physical properties after maintaining the seal material at an elevated temperature for a specific length of time. For the same amount of reduction in properties, a shorter time can be used at a higher temperature, or a longer time can be used at a lower temperature. ASTM D573[9] provides an acceptable method for determining the effects of temperature aging on elastomeric compounds.

ASTM D395[10] provides an acceptable method for determining the effects of compression set. R0405-70 butyl rubber compound uses an acceptance criterion of less than 25% compression set for 22 hours at an elevated temperature of 70 ºC.

ASTM D2137[11] provides an acceptable method for determining an elastomeric material's ability to withstand cold temperatures and remain pliable. Although the TR-10 test in ASTM D1329 demonstrates the seal material's resiliency at a much lower temperature, this test verifies the seal material's lack of brittleness at the minimum regulatory temperature of -40 ºC.

Hardness or durometer along with tensile strength and elongation are defined and checked to ensure durability of the seal material during operation. ASTM D2240[12] provides an acceptable method for determining the required 70 ±5 durometer, and ASTM D412[13] provides an acceptable method for determining the required minimum 10 MPa (1,450 psi) tensile strength and minimum 250% elongation, with the properties of the R0405-70 butyl rubber acting as a baseline for the required hardness, tensile strength, and elongation.

For proprietary seal materials that have fairly demanding requirements such as the R0405-70 butyl rubber compound, the compound is commonly specified by a company designator and subsequently checked against exacting performance standards. Specifying an elastomeric compound by its chemistry alone is difficult considering the shear number of parameters that affect seal performance. However, by applying the above nationally recognized standards to a material batch, the important parameters are defined for verifying the performance of the seal material.

---

[8] ASTM D1329-88 (re-approved 1998), *Standard Test Method for Evaluating Rubber Property – Retraction at Lower Temperatures (TR Test),* American Society for Testing and Materials, Philadelphia, PA, Volume 09.01, 2001.

[9] ASTM D573-99, *Standard Test Method for Rubber – Deterioration in an Air Oven,* American Society for Testing and Materials, Philadelphia, PA, Volume 09.01, 2001.

[10] ASTM D395-01, *Standard Test Methods for Rubber Property – Compression Set,* American Society for Testing and Materials, Philadelphia, PA, Volume 09.01, 2001.

[11] ASTM D2137-94 (re-approved 2000), *Standard Test Methods for Rubber Property – Brittleness Point of Flexible Polymers and Coated Fabrics,* American Society for Testing and Materials, Philadelphia, PA, Volume 09.02, 2001.

[12] ASTM D2240-00, *Standard Test Method for Rubber Property – Durometer Hardness,* American Society for Testing and Materials, Philadelphia, PA, Volume 09.01, 2002.

[13] ASTM D412-98a, *Standard Test Methods for Vulcanized Rubber and Thermoplastic Rubbers and Thermoplastic Elastomers – Tension,* American Society for Testing and Materials, Philadelphia, PA, Volume 09.01, 2001.

ASTM D1414[14] is the standard method for testing O-ring seals, and covers most, but not all, of the required testing delineated above. However, due to the overall size of the O-ring seals and the additional testing specified, ASTM D2000[3] provides a better standard classification system.

Using the ASTM D2000 designator, O-ring seals with properties equivalent to R0405-70 butyl rubber material are classified as follows and summarized in the table below:

M4AA710 A13 B13 F17 F48 Z Trace Element

Designator	Condition
M	Metric units designator (default condition)
4	Grade 4 acceptance criteria for the tests specified
AA	Butyl rubber compound
7	70 Shore A durometer hardness per ASTM D2240
10	Tensile strength and elongation per ASTM D 412; acceptance criteria are a minimum 10 MPa (1,450 psi) tensile strength and a minimum 250% elongation
A13	Heat resistance test per ASTM D573; the acceptance criteria are a maximum 10 Shore A durometer hardness increase, a maximum reduction in tensile strength of 25%, and a maximum reduction in ultimate elongation of 25% at 70 ºC
B13	Compression set per Method B of ASTM D395; acceptance criterion is a maximum 25% compression set after 22 hours at 70 ºC
F17	Cold temperature resistance specifying low temperature brittleness per Method A, 9.3.2, of ASTM D2137; non-brittle after 3 minutes at -40 ºC
F48	Cold temperature resiliency, where F is for cold temperature resistance, and 4 specifies testing to the TR-10 test of ASTM D1329; 8 indicates a TR-10 temperature of -50 ºC (-58 ºF), or less
Z Trace Element	Z designator allows specific notes to be added; “Z Trace Element” allows trace elements to be added to the elastomeric compound to meet the seal material requirements

[14] ASTM D1414-94 (re-approved 1999), *Standard Test Methods for Rubber O-Rings,* American Society for Testing and Materials, Philadelphia, PA, Volume 09.02, 2001.

Table 3.6.4-2 – Rainier Rubber R0405-70 Formulation Qualification O-ring Seal Test Results

Test Number①	O-ring Seal Number①	O-ring Seal Inside Diameter, D_s (in)	O-ring Seal Cross-Sectional Diameter, d_{cs} (in)		O-ring Seal Stretch, S (%)③	O-ring Seal Reduction in Cross-Sectional Diameter, R (%)④	Minimum O-ring Seal Cross-Sectional Diameter, d_{csr} (in)⑤	O-ring Seal Compression (%)⑥⑦			Temperature for "Leaktight" Leak Test (≤ 8.8×10^{-8} scc/sec, He)⑧			
			Max	Min				Center Disk	Offset Disk	Change	-40 °F	-20 °F	400 °F⑨	-20 °F
1	1	11.368	0.396	0.394	6.80	4.36	0.377	21.12	10.38	10.74	Yes	Yes	Yes	Yes
	4	11.500	0.396	0.392	5.58	3.71	0.377	21.12	10.38	10.74				
2	2	11.417	0.396	0.395	6.34	4.12	0.379	21.54	10.85	10.69	Yes	Yes	Yes	Yes
	3	11.465	0.395	0.394	5.90	3.88	0.379	21.54	10.85	10.69				

Notes:

① The test fixture's pertinent dimensions are taken in line with the direction of offset, which is also the position where the minimum cross-sectional diameter of the O-ring seals are placed: bore inside diameter, D_i = 12.736 inches; disk outside diameter, D_o = 12.655 inches; and the O-ring seal groove diameter, D_g = 12.14125 inches (based on the average of fixture measurements taken along the axis of offset). All tests are performed using WTS Test Fixture No. 4.

② Material for all O-ring seal test specimens is butyl rubber compound R-0405-70, Rainier Rubber Co., Seattle, WA.

③ Given the O-ring seal inside diameter, D_s, the percent of O-ring seal stretch, $S = 100 \times (D_g - D_s)/D_s$.

④ From Figure 3-3 of the *Parker O-ring Handbook*[4] and based on the O-ring seal cross-sectional diameter, d_{cs}, the percent reduction in O-ring seal cross-sectional diameter, $R = -0.005 + 1.19S - 0.19S^2 - 0.001S^3 + 0.008S^4$ for $0 \le S \le 3\%$, and $R = 0.56 + 0.59S - 0.0046S^2$ for $3\% < S \le 25\%$.

⑤ The reduced O-ring seal cross-sectional diameter, $d_{csr} = d_{cs}(1 - R/100)$.

⑥ The percent O-ring seal compression with the disk *centered* is $100 \times [d_{csr} - \frac{1}{2}(D_i - D_g)]/d_{csr}$.

⑦ The percent O-ring seal compression with the disk *offset* is $100 \times [d_{csr} - (D_i - D_o) - \frac{1}{2}(D_o - D_g)]/d_{csr}$.

⑧ A "Yes" response indicates that helium leakage testing demonstrated that the leakage rate was $\le 1.0 \times 10^{-7}$ scc/sec, air (i.e., "leaktight" per ANSI N14.5). In all cases, measured leakage rates were $\le 8.8 \times 10^{-8}$ scc/sec, helium, for tests with a "Yes" response.

⑨ No helium leak tests were performed at elevated temperatures due to O-ring seal permeation and saturation by helium gas. The ability of the test fixture to establish a rapid, hard vacuum between the O-ring seals was used as the basis for leak test acceptance at elevated temperatures. A "Yes" response indicates that all tests rapidly developed a hard vacuum.

This page intentionally left blank.

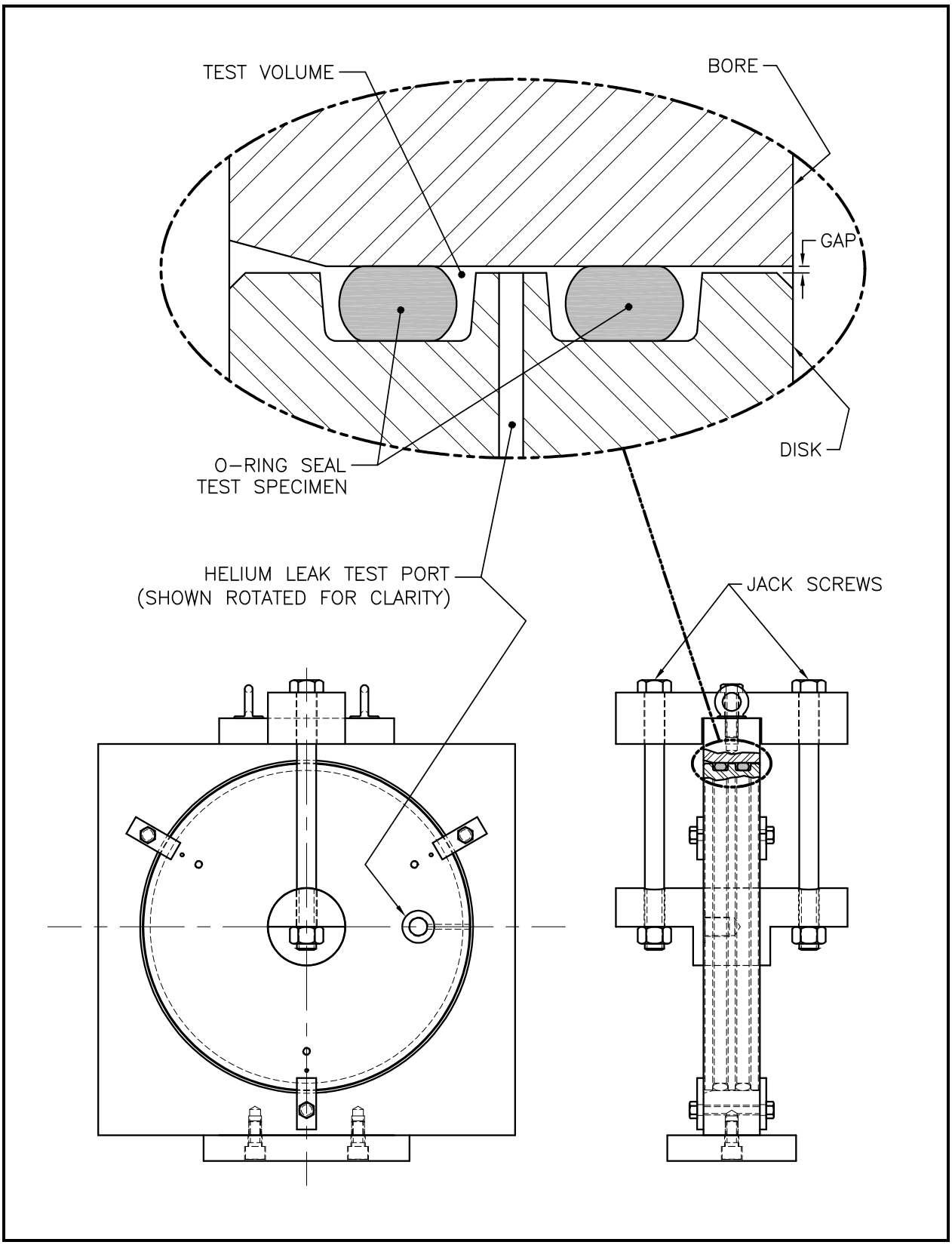

Figure 3.6.4-1 – Test Fixture for O-ring Seal Performance Testing

This page intentionally left blank.

4.0 CONTAINMENT

4.1 Containment Boundary

This section identifies the containment boundary considered for the RH-TRU 72-B package.

4.1.1 Containment Vessel

Up to two independent levels of containment are established within the RH-TRU 72-B package. In general, each containment vessel is constructed primarily of ASTM A240, Type 304, austenitic stainless steel for the shells, and ASTM A240, Type 304, or ASTM A182, Type F304, austenitic stainless steel for the lids and end closures. The exceptions are so noted in the following detailed descriptions.

4.1.1.1 Inner Vessel

The inner vessel (IV) containment boundary is identified as the 32-inch outside diameter by 3/8-inch thick shell, the 1½-inch thick bottom closure, the lid-end forging, and the 6½-inch thick IV lid, complete with the lid's middle O-ring seal, the gas sampling port closure bolt with the closure bolt outer O-ring seal, and the backfill port closure bolt with the closure bolt O-ring seal. The sealing surfaces are machined to a maximum of 125 RMS micro-finish for sealing reliability. As discussed in Chapter 1.0, *General Information*, credit for this containment boundary can only be taken when an optional, preshipment leakage rate test is successfully performed.

With reference to Appendix 1.3.1, *Packaging General Arrangement Drawings*, the IV includes the following containment boundary components:

1. A 1½-inch thick, Type 304 or Type F304 stainless steel bottom closure,

2. A 3/8-inch thick, 32-inch outside diameter, Type 304 stainless steel shell, with a full length, full penetration seam weld,

3. A full-penetration girth weld joining the shell to the bottom forging,

4. An upper end (lid-end), Type F304 stainless steel ring forging,

5. A full-penetration girth weld joining the upper end ring forging to the shell,

6. A 6½-inch thick, Type 304 or Type F304 stainless steel lid,

7. A butyl containment O-ring seal that forms the seal between the upper end forging and the lid (the containment O-ring seal is the middle of the three IV closure seals),

8. A Type 304 or Type 316 stainless steel gas sampling port insert, containing a Nitronic 60 closure bolt with butyl O-ring seal (the upper O-ring seal is the containment seal),

9. A 1/4-inch bevel weld which seals the gas sampling port insert to the lid,

10. A Type 304 or Type 316 stainless steel backfill port insert, containing a Nitronic 60 closure bolt with butyl O-ring seal,

11. A 1/4-inch bevel weld which seals the backfill port insert to the lid,

12. A Type 304 or Type 316 stainless steel test port insert, and

13. A 1/4-inch bevel weld which seals the test port insert to the lid.

The inside diameter of the IV is 31¼ inches. Two (2) intermediate support rings and a pair of optional guide rails are located inside the IV for payload canister support. Including the support rings, guide rails, and upper forging, a 26½-inch diameter by 121½-inch long cavity is provided within the IV for the packaging payload.

The specific IV containment components are illustrated in Figure 4.1-1.

The weight of the IV is approximately 4,023 pounds (1,825 kg), the overall length is 130 inches, and the outside diameter is 32 inches.

The non-Type 304 stainless steel components utilized in the IV containment boundary are the butyl O-ring seals (containment seals for the gas sampling port closure bolt, backfill port closure bolt, and the lid), and the Nitronic 60 gas sampling port and backfill port closure bolts.

4.1.1.2 Outer Cask

The outer cask (OC) containment boundary is identified as the 32 3/8-inch inside diameter by 1-inch thick inner shell, the 5-inch thick OC bottom end plate, the closure end forging, and the 6-inch thick OC lid, complete with the lid inner O-ring seal and the gas sampling port closure bolt with closure bolt O-ring seal. The sealing surfaces are machined to a maximum of 125 RMS micro-finish for sealing reliability.

With reference to Appendix 1.3.1, *Packaging General Arrangement Drawings*, the OC containment boundary consists of the following components:

1. A 5-inch thick, Type 304 or Type F304 stainless steel bottom closure,

2. A 1-inch thick, 34⅜-inch outside diameter, Type 304 stainless steel inner shell, with a full length, full penetration seam weld,

3. A full-penetration girth weld joining the inner shell to the bottom forging,

4. An upper end (lid-end), Type F304 stainless steel ring forging,

5. A full-penetration girth weld joining the upper end ring forging to the inner shell,

6. A 6-inch thick, Type 304 or Type F304 stainless steel lid,

7. A butyl containment O-ring seal that forms the seal between the upper end forging and the lid (the containment O-ring seal is the innermost of the two OC closure seals),

8. A Type 304 or Type 316 stainless steel gas sampling port insert, containing a Nitronic 60 closure bolt with butyl O-ring seal,

9. A 1/4-inch bevel weld which seals the gas sampling port insert to the lid,

10. A Type 304 or Type 316 stainless steel test port insert, and

11. A 1/4-inch bevel weld which seals the test port insert to the lid,

12. A 32⅜-inch diameter by 130¾-inch long cavity is provided within the OC for the IV.

The specific OC containment components are illustrated in Figure 4.1-2.

The non-Type 304 stainless steel components utilized in the OC containment boundary are the butyl O-ring seals (containment seals for the gas sampling port closure bolt and the lid), and the Nitronic 60 gas sampling port closure bolt.

Inadvertent opening of the package closures cannot occur for the RH-TRU 72-B package. Following installation of the packaging payload, the IV lid is secured via eight (8), 7/8-9UNC bolts. The OC closure lid is then secured via eighteen (18), 1¼-7UNC bolts, thus eliminating access to the IV closure. The closure-end impact limiter is attached using six (6), 1¼-7UNC bolts. When installed, the impact limiter eliminates access to the OC closure. With this double closure design coupled with the presence of the impact limiter, inadvertent opening of the package cannot occur.

4.1.2 Containment Penetrations

The only containment penetrations into each of the two containment vessels, the IV and OC, are the test and gas sampling ports, and the lids themselves. In addition, the IV has a backfill port. The detail of each penetration is shown in Appendix 1.3.1, *Packaging General Arrangement Drawings*. Each penetration is designed to maintain a leakage rate not to exceed 1×10^{-7} standard cubic centimeters per second (scc/sec), air, so defined as "leaktight" per ANSI N14.5[1], for all normal conditions of transport (NCT) and hypothetical accident conditions (HAC). All IV penetrations are covered by the OC lid, and all OC penetrations are covered by the impact limiters. These coverings, along with tamper-indicating lock wires, ensure that unauthorized operation is precluded.

4.1.3 Seals and Welds

4.1.3.1 Seals

Seals affecting containment are described above. A summary of seal testing prior to first use, during routine maintenance, and upon assembly for transportation is as follows.

4.1.3.1.1 Fabrication Leakage Rate Test

During fabrication, following the pressure testing per Section 8.1.2.2, *Inner Vessel and Outer Cask Pressure Testing*, both the OC and IV shall be individually tested per the *Fabrication Leakage Rate Test*, delineated in Section 8.1.3, *Fabrication Leakage Rate Tests*. This test verifies the containment integrity of the RH-TRU 72-B package to a leakage rate not to exceed 1×10^{-7} scc/sec, air.

4.1.3.1.2 Maintenance Leakage Rate Tests

The *Maintenance Leakage Rate Test* delineated in Section 8.2.2, *Maintenance/Periodic Leakage Rate Tests*, shall be performed on the package annually. Additionally, upon repair of an O-ring sealing surface, and/or replacement of a containment O-ring seal, a gas sampling port closure bolt, or a backfill port closure bolt (IV only), the appropriate section of the *Maintenance Leakage*

[1] ANSI N14.5-2014, *American National Standard for Radioactive Materials – Leakage Tests on Packages for Shipment,* American National Standards Institute, Inc. (ANSI).

Rate Test delineated in Section 8.2.2, *Maintenance/Periodic Leakage Rate Tests*, shall be performed to verify that the repaired or replaced component is maintained to be "leaktight" per ANSI N14.5[1]. This test verifies the sealing integrity of the RH-TRU 72-B package to a leakage rate not to exceed 1×10^{-7} scc/sec, air.

4.1.3.1.3 Preshipment Leakage Rate Test

Prior to shipment of the loaded RH-TRU 72-B package, the OC shall be leakage rate tested per the *Preshipment Leakage Rate Test* delineated in Appendix 7.4.1, *Preshipment Leakage Rate Test*. As an option, the IV may also be leakage rate tested per the *Preshipment Leakage Rate Test* delineated in Appendix 7.4.1, *Preshipment Leakage Rate Test*.

As an option for both the OC and IV, the *Maintenance Leakage Rate Test* delineated in Section 8.2.2, *Maintenance/Periodic Leakage Rate Tests*, may be performed in lieu of the *Preshipment Leakage Rate Tests*. Optional use of the *Maintenance Leakage Rate Tests* applies to each containment seal test individually, i.e., it is acceptable to test some containment seals following the *Preshipment Leakage Rate Test* procedure while testing others following the *Maintenance/Periodic Leakage Rate Test* procedure.

4.1.3.2 Welds

All containment vessel welds are full penetration welds that have been radiographic or ultrasonic test inspected to ensure structural integrity. All containment boundary welds are confirmed to be leaktight per the *Fabrication Leakage Rate Test*, delineated in Section 8.1.3, *Fabrication Leakage Rate Tests*.

4.1.4 Closure

4.1.4.1 Outer Cask Closure

Closure of the OC is effected by eighteen (18), ASTM A320, Grade L43, alloy steel, 1¼-7UNC cap screws tightened to 600 – 700 lb-ft torque.

4.1.4.2 Inner Vessel Closure

Closure of the IV is effected by the eight (8), ASTM A320, Grade L43, alloy steel, 7/8-9UNC cap screws tightened to 100 – 200 lb-ft torque.

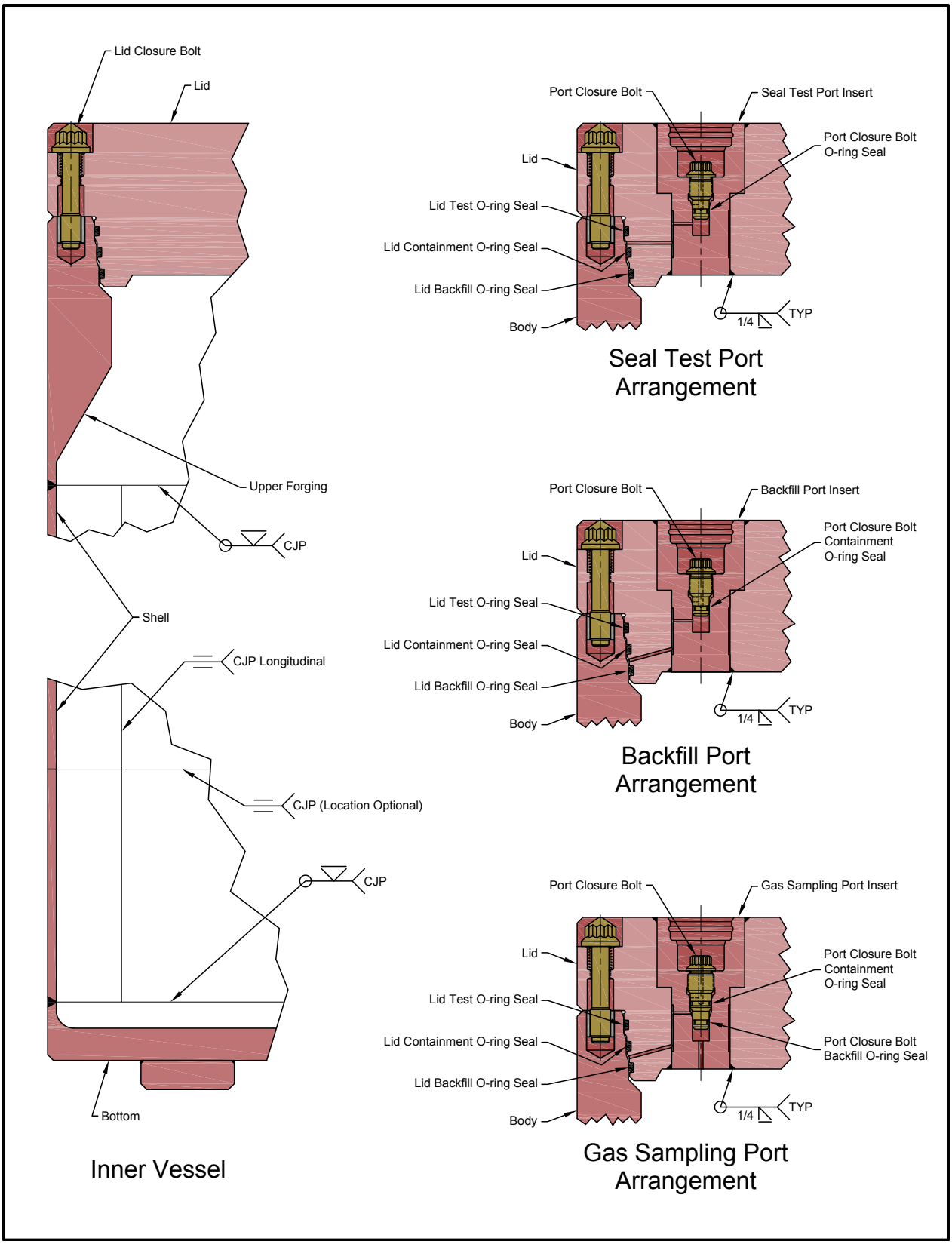

Figure 4.1-1 – Inner Vessel Containment Components

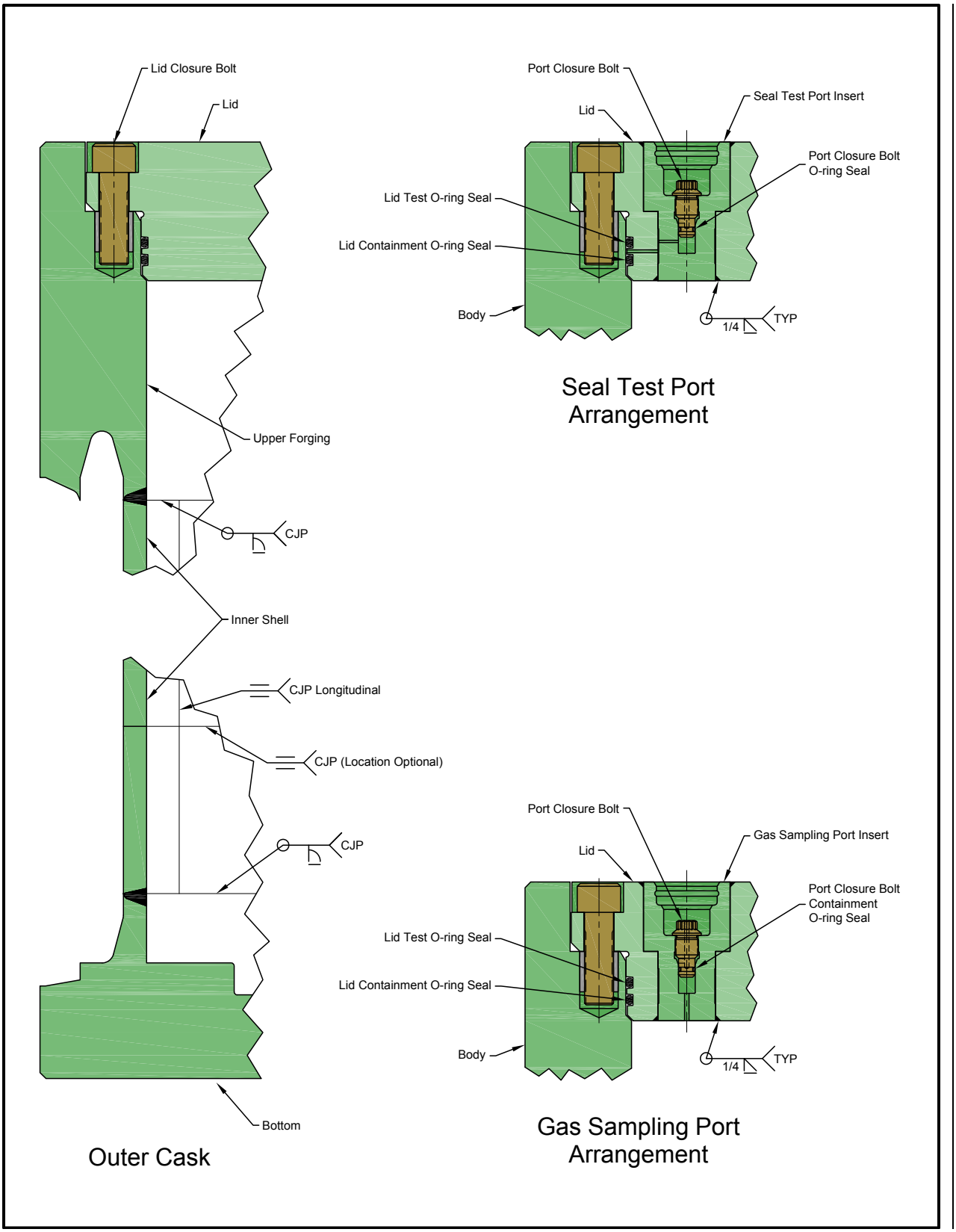

Figure 4.1-2 – Outer Cask Containment Components

4.2 Requirements for Normal Conditions of Transport

The results of the structural analyses performed in Chapter 2.0, *Structural Evaluation*, and the thermal analyses performed in Chapter 3.0, *Thermal Evaluation*, verify that there will be no release of radioactive materials per the "leaktight" criterion of ANSI N14.5[1] under any of the normal conditions of transport (NCT).

4.2.1 Containment of Radioactive Material

The "leaktight" containment criterion of ANSI N14.5[1] specified for the structure and seals of the RH-TRU 72-B package ensures that the requirements of 10 CFR §71.51[2] are satisfied under NCT.

4.2.2 Pressurization of Containment Vessel

The design pressure of both the RH-TRU 72-B package's inner vessel (IV) and outer cask (OC) is 150 psig. Results from the analyses presented in Section 3.4.5, *Maximum Internal Pressure*, verify that any increase in pressure, due to an increase in temperature of the initial package gas atmosphere or due to the water vapor pressure from the water assumed present in the vessel cavity, will be equal to or less than 150 psig within both the IV and OC. A pressure increase to 150 psig in either containment vessel will not reduce the effectiveness of the RH-TRU 72-B package to maintain containment integrity per Section 4.2.1, *Containment of Radioactive Material*.

4.2.3 Containment Criterion

The IV and OC shall be leakage rate tested as described in Section 4.1.3.1.1, *Fabrication Leakage Rate Test*, Section 4.1.3.1.2, *Maintenance Leakage Rate Tests*, and Section 4.1.3.1.3, *Preshipment Leakage Rate Test*, to demonstrate the containment criterion of Section 4.2.1, *Containment of Radioactive Material*, at the completion of fabrication, for maintenance, or for assembly verification prior to transport, respectively.

[1] ANSI N14.5-2014, *American National Standard for Radioactive Materials – Leakage Tests on Packages for Shipment,* American National Standards Institute, Inc. (ANSI).

[2] Title 10, Code of Federal Regulations, Part 71 (10 CFR 71), *Packaging and Transportation of Radioactive Material*, 01-01-14 Edition.

This page intentionally left blank.

4.3 Containment Requirements for the Hypothetical Accident Conditions

The results of the structural analyses performed in Chapter 2.0, *Structural Evaluation*, and the thermal analyses performed in Chapter 3.0, *Thermal Evaluation*, verify that there will be no release of radioactive materials per the "leaktight" criterion of ANSI N14.5[1] under any of the hypothetical accident conditions (HAC).

The RH-TRU 72-B package containment O-ring seals are fabricated from Rainier Rubber butyl compound R0405-70[2], or equivalent, per Appendix 3.6.4, *Containment O-ring Seal Material Tests*.

The inner vessel (IV) closure seal configuration consists of three O-ring bore seals, each located on a different diameter of the IV lid (see Appendix 1.3.1, *Packaging General Arrangement Drawings*, for details). The middle O-ring seal is defined as the containment boundary (the inner O-ring seal retains the test gas for helium leakchecking, while the outer O-ring seal provides an annulus in which to establish a vacuum for leakchecking). As determined in Section 3.6.4.2.1, *Inner Vessel Containment O-ring Seal*, the minimum IV containment O-ring seal compression is 12.74%.

The outer cask (OC) closure seal configuration consists of two O-ring bore seals, both at the same diameter on the OC lid (see Appendix 1.3.1, *Packaging General Arrangement Drawings*, for details). The inner O-ring seal is defined as the containment seal (the outer O-ring seal provides a vacuum annulus for helium leakchecking, where the test gas is contained in the void space between the IV and OC). As determined in Section 3.6.4.2.2, *Outer Cask Containment O-ring Seal*, the minimum OC containment O-ring seal compression is 10.96%.

Two test series, discussed in detail in Section 3.6.4.3, *Formulation Qualification Test Fixture and Procedure*, and Section 3.6.4.4, *Rainier Rubber R0405-70 Formulation Qualification Test Results*, demonstrate the ability of Rainier Rubber butyl compound R0405-70 to successfully pass leak tests with O-ring seal compressions of 10.38% and 10.85%, respectively. Similar formulation qualification testing is also required for any other butyl compound prior to its use on the RH-TRU 72-B packaging. Thus, the sealing material is adequate to maintain containment integrity for HAC.

4.3.1 Fission Gas Products

There are no fission gas products in the RH-TRU 72-B package.

4.3.2 Containment of Radioactive Material

The "leaktight" containment criterion of ANSI N14.5[1] specified for the structure and seals of the RH-TRU 72-B package ensures that the requirements of 10 CFR §71.51[3] are satisfied under

[1] ANSI N14.5-2014, *American National Standard for Radioactive Materials – Leakage Tests on Packages for Shipment,* American National Standards Institute, Inc. (ANSI).

[2] Rainier Rubber Company, Seattle, WA.

[3] Title 10, Code of Federal Regulations, Part 71 (10 CFR 71), *Packaging and Transportation of Radioactive Material*, 01-01-14 Edition.

HAC. The "leaktight" containment design will be verified by the fabrication leak checks of the initial production packaging (refer to Section 8.1.3, *Fabrication Leakage Rate Tests*, for details).

4.3.3 Containment Criterion

The RH-TRU 72-B package has been designed, constructed, and verified by leakage rate testing to meet the "leaktight" criterion established in ANSI N14.5[1].

The results of the structural analyses performed in Chapter 2.0, *Structural Evaluation*, and the thermal analyses performed in Chapter 3.0, *Thermal Evaluation*, verify that the RH-TRU 72-B package will meet the "leaktight" criterion of ANSI N14.5[1] under HAC (refer specifically to Section 2.7.8, *Summary of Damage*). These results verify, structurally, there is no compromise of the containment boundary for HAC. These results verify, thermally, that seal surface temperatures remain low enough to prevent deformation of the sealing materials such that the "leaktight" criterion is maintained.

The only damage arising from normal conditions of transport (NCT) involves minor deformations to the impact limiter(s) that have no effect on packaging containment ability. The analyses presented in Section 2.7.1, *Free Drop*, through Section 2.7.7, *Deep Water Immersion Test*, show that the HAC test sequence will not result in any significant structural damage to the RH-TRU 72 B packaging. Nearly all permanent damage occurs in the external impact limiters, as desired. Minor amounts of damage can occur to packaging components as follows:

In the HAC 30-foot free drop event, no lead slump will occur as delineated in Paragraph (9) of Section 2.7.1.1, *Flat End Drop*. For the 40-inch drop on a 6-inch diameter puncture bar, occurring on the side of the package at midlength, localized OC damage can occur at the impact point. However, overall bending response of the package remains elastic. Additionally, the OC outer shell will not be perforated, and no melting of the lead shielding would occur in the ensuing HAC fire event.

Localized puncture damage would occur in the form of a reduction in lead thickness adjacent to the point of impact of the puncture bar. Pin punch results from the NuPac 125-B quarter-scale drop tests[4] were analyzed to provide a conservative estimate of similar damage that could be expected for the RH-TRU 72-B package. It was determined that a 40-inch side drop on the puncture bar causes, at most, a 35% localized reduction in the thickness of the lead shielding on the NuPac 125-B cask. This estimate is conservative for the RH-TRU 72-B package because it is significantly lighter in weight than the NuPac 125-B cask, and therefore puncture-induced deformations would be expected to be less.

As documented in Section 2.7.3, *Puncture*, puncture on the lid-end of the package can result in a slight, permanent inward deformation of the OC lid. However, stress levels remain modest, and the inward deformation is very small and has been shown to increase containment O-ring seal compression. As such, the lid-end puncture event does not adversely affect containment integrity.

These permanent deformations are of little consequence for the RH-TRU 72-B package as they represent only minor changes in packaging geometry. In particular, damage is not sufficient to

[4] Nuclear Packaging, Inc., *Safety Analysis Report for the NuPac 125-B Fuel Shipping Package*, USNRC Certificate of Compliance 71-9200, U.S. Department of Energy, Washington, D.C.

compromise "leaktightness" of the IV or OC containment boundaries. Lead deformation is only of concern relative to shielding. The worst-case puncture damage is therefore addressed in the shielding evaluation in Chapter 5.0, *Shielding Evaluation*. For these reasons, the integrity of the package is not considered to be compromised by the HAC test sequence set forth in 10 CFR 71[3].

Finally, as detailed in Appendix 3.6.4, *Containment O-ring Seal Material Tests*, full lateral offset of the IV and OC lids that might result from side drop or side puncture will not compromise the containment seals leaktight capability. This is because, as demonstrated in the referenced appendix, O-ring seal compression remains at or above the minimum 10.96% compression required for qualification of the O-ring seal material.

This page intentionally left blank.

5.0 SHIELDING EVALUATION

The analyses in this chapter demonstrate that the RH-TRU 72-B package complies with the requirements of 10 CFR §71.47[1] and §71.51. The analyses show that the dose rate requirements are satisfied when limiting the activity of the RH-TRU 72-B package in accordance with the methodology defined in Section 5.5.4, *Determination of Acceptable Activity*.

The acceptable gamma and/or neutron source term is determined for the RH-TRU 72-B package when transporting the RH-TRU waste canister (fixed or removable lid) and neutron shielded canisters (NS15 and NS30). The evaluations consider both normal conditions of transport (NCT) and hypothetical accident condition (HAC) regulatory dose rate limits under exclusive use requirements.

The removable and fixed lid canisters are generically grouped for evaluation due to the commonality of their thin-wall steel construction and corresponding minimal dose rate attenuation. Separate analyses are performed for the NS15 and NS30 neutron shielded canisters to evaluate the dose rate attenuation provided by their materials of construction (including supplemental extra-high molecular weight polyethylene neutron shielding inserts) and geometry.

The shielding analyses for the above listed cases utilize a ^{60}Co gamma source and a ^{252}Cf neutron source for NCT and HAC under exclusive use conditions. Dose rates on the package surface and 2 meters from the package surface are shown to be less than the 10 CFR 71 limits of 200 mrem/hr and 10 mrem/hr, respectively. The 2-meter dose rate is established at the 2 meters from the package surface in lieu of the outer edge of the conveyance for conservatism and convenience. For hypothetical accident conditions (HAC), the dose rates are shown to be less than 1,000 mrem/hr at 1 meter.

Additionally, the maximum allowable gamma and neutron source strength (as a function of particle energy) for concentrated and distributed sources with varying density is determined to ensure compliance with the most restrictive regulatory dose rate requirement of 10 mrem/hr at 2 meters from the package surface. Compliance with the 2-meter NCT requirement ensures all other NCT and HAC dose rate requirements are met.

5.1 Description of Shielding Design

5.1.1 Design Features

5.1.1.1 RH-TRU 72-B

The RH-TRU 72-B packaging is designed to provide significant gamma and negligible neutron shielding. The packaging is comprised of an outer cask (OC) that provides free drop, shielding, and thermal protection when fitted at each end with impact limiters, and an inner vessel (IV) that provides a secondary containment function. A complete description of the packaging is provided in Chapter 1.0, *General Information*.

[1] Title 10, Code of Federal Regulations, Part 71 (10 CFR 71), *Packaging and Transportation of Radioactive Material*, 01-01-14 Edition.

As illustrated in Figure 1.1-1, the principal shielding characteristic of the RH-TRU 72-B packaging is associated with the structural materials of the OC and IV, including OC inner and outer shells, OC lid and base, OC annular lead, OC thermal shield, and IV shells, lid, and base. The OC body radially utilizes a composite steel/lead/steel structure with thicknesses of 1 inch, 1⅞ inch, and 1½ inch, respectively, surrounded by a 10-gauge thermal shield offset from the outer shell by a 12-gauge wire wrap. The OC lid and base are 6 and 5 inches thick, respectively. The IV shell, lid, and base component thicknesses are 3/8 inch, 6½ inch, and 1½ inch, respectively. All packaging shells, lids, and bases are constructed of Type 304 stainless steel. Lead shielding is cast in place and conforms to the material requirements of QQ-L-171e, Grade A or C, or ASTM B29-92 pure or chemical copper lead. Lead shielding installation is confirmed to be of a minimum acceptable thickness and absent of significant voids through a post-installation gamma scan procedure. The IV has a 32-inch outside diameter and an overall length of 130 inches. The OC outer shell has a 41⅛-inch outside diameter and the OC inner shell has a 32⅜-inch inside diameter; the overall length of the OC is 141¾ inches. The payload canister is located within the IV by an upper forging and two v-shaped locating rings on the IV shell interior with inside diameters of 26½ inches.

Under NCT, material and distance attenuation credit is taken for the RH-TRU 72-B OC and IV with only distance attenuation credited for the impact limiters. This is the same under HAC, but puncture damage to the OC which reduces material and distance attenuation is considered along with conservatively ignoring the distance attenuation provided by the IV upper forging and V-shaped locating rings (IV spacers) which centralize the payload canister within the IV.

5.1.1.2 RH-TRU Waste Canister

As illustrated in Figure 5.1-1, the RH-TRU waste canister is a 26-inch outside diameter, 120½-inch overall height, cylindrical canister with nominally 1/4-inch thick or greater carbon or stainless steel shell, lid, and base components.

Under NCT and HAC, material and distance attenuation credit is taken for the canister shells, lid, and base. Drums are not credited for material attenuation under NCT or HAC conditions.

5.1.1.3 NS15 Neutron Shielded Canister

As illustrated in Figure 5.1-2, the NS15 neutron shielded canister is a 26-inch diameter, 120½-inch tall removable lid canister with a high-density polyethylene (HDPE) neutron shield insert. It is designed to carry three approximately 15-gallon steel drums with internal lever-lock closures. The NS15 neutron shielded canister incorporates the NS15 neutron shield insert which consists of HDPE top and bottom end caps (nominally 5 inches thick) with an integral open-cell urethane filter/gasket and a 24-inch outside diameter cylindrical pipe body (nominally 3.387 inches thick). The minimum thickness of HDPE neutron shielding provided by the body is 3.288 inches.

Under NCT, material and distance attenuation credit is taken for the canister steel shell, lid, and base components and the HDPE shield insert end caps and body. Under HAC, material and distance attenuation credit is taken for the canister steel and HDPE shield insert components with a maximum 1/4-inch HDPE scratch-and-gouge criterion conservatively accounting for the minimum material thickness due to HAC damage. Drums are not credited for material attenuation under NCT or HAC conditions.

5.1.1.4 NS30 Neutron Shielded Canister

As illustrated in Figure 5.1-3, the NS30 neutron shielded canister is a 26-inch diameter, 120½-inch tall removable lid canister with a high-density polyethylene (HDPE) neutron shield insert. It is designed to carry three approximately 30-gallon steel drums with internal lever-lock closures. The NS30 neutron shielded canister incorporates the NS30 neutron shield insert which consists of HDPE top and bottom end caps (nominally 5 inches thick) with an integral open-cell urethane filter/gasket and a 24-inch outside diameter cylindrical pipe body (nominally 1.454 inches thick). The minimum thickness of HDPE neutron shielding provided by the body is 1.412 inches.

Under NCT, material and distance attenuation credit is taken for the canister steel shell, lid, and base components and the HDPE shield insert end caps and body. Under HAC, material and distance attenuation credit is taken for the canister steel and HDPE shield insert components with a maximum 1/4-inch HDPE scratch-and-gouge criterion conservatively accounting for the minimum material thickness due to HAC damage. Drums are not credited for material attenuation under NCT or HAC conditions.

Security-Related Information Figure Withheld Under 10 CFR 2.390.

Figure 5.1-1 – RH-TRU Waste Canister

Security-Related Information Figure
Withheld Under 10 CFR 2.390.

Figure 5.1-2 – NS15 Neutron Shielded Canister

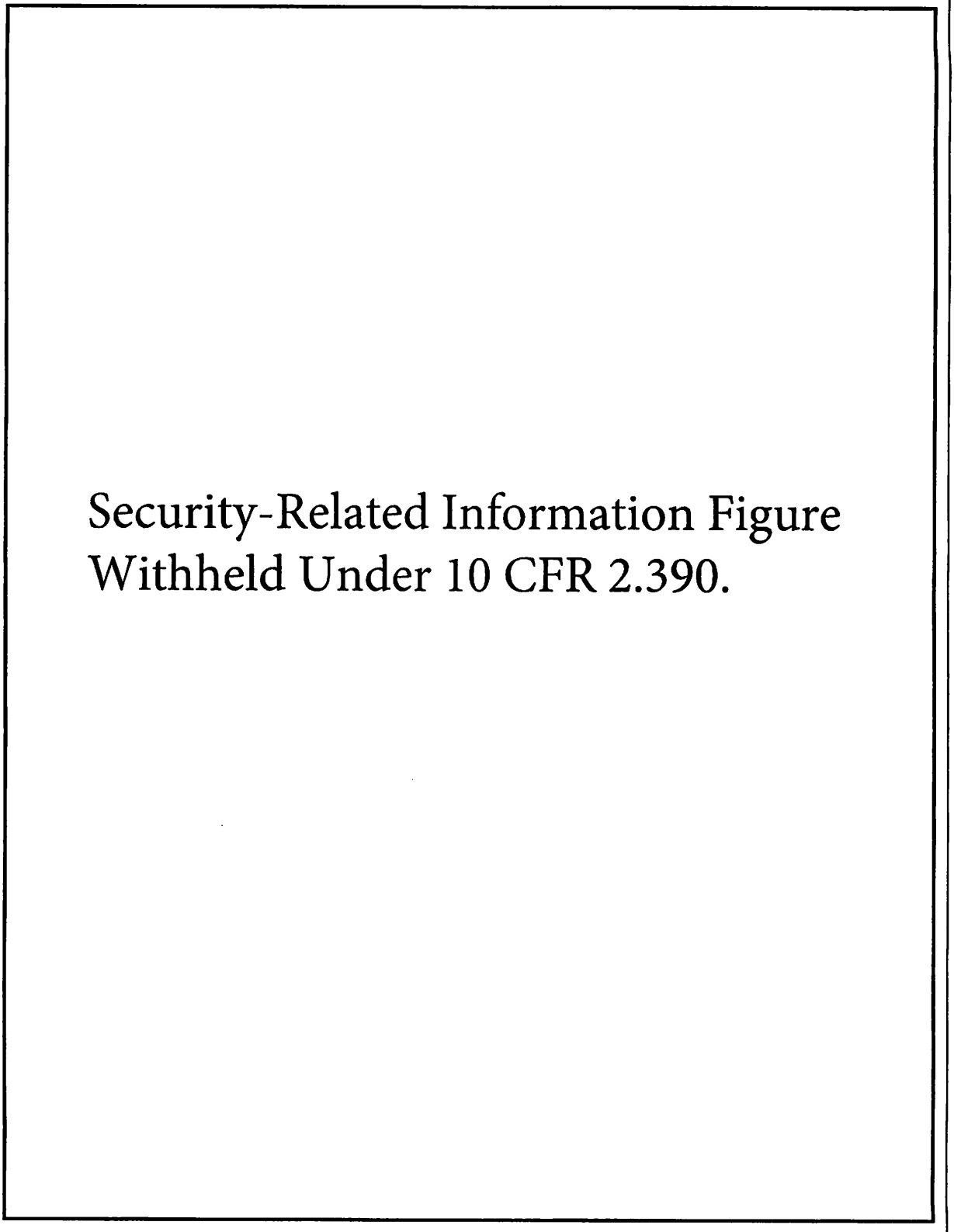

Figure 5.1-3 – NS30 Neutron Shielded Canister

5.1.2 Summary Table of Maximum Radiation Levels

Table 5.1-1 through Table 5.1-3 summarize the NCT and HAC dose rates resulting from a concentrated ^{60}Co gamma and a ^{252}Cf neutron source for each of the analyzed payload canister configurations. The activity (Ci) listed for each configuration is for the loaded package.

Table 5.1-1 – RH-TRU 72-B with RH-TRU Waste Canister Summary of Maximum Dose Rates (mrem/hr)

Condition	Activity (Ci)	Package Surface	1m from Surface	2m from Surface
NCT				
Gamma	10.444	117.62	NA	9.96
Neutron	0.022	129.62	NA	9.98
HAC				
Gamma	10.444	NA	157.40	NA
Neutron	0.022	NA	61.07	NA
Allowable	NA	200	1000	10

Table 5.1-2 – RH-TRU 72-B with NS15 Neutron Shielded Canister Summary of Maximum Dose Rates (mrem/hr)

Condition	Activity (Ci)	Package Surface	1m from Surface	2m from Surface
NCT				
Gamma	16.167	119.10	NA	9.95
Neutron	0.143	136.88	NA	9.93
HAC				
Gamma	16.167	NA	136.88	NA
Neutron	0.143	NA	72.44	NA
Allowable	NA	200	1000	10

Table 5.1-3 – RH-TRU 72-B with NS30 Neutron Shielded Canister Summary of Maximum Dose Rates (mrem/hr)

Condition	Activity (Ci)	Package Surface	1m from Surface	2m from Surface
NCT				
Gamma	12.662	119.91	NA	9.95
Neutron	0.058	142.29	NA	9.94
HAC				
Gamma	12.662	NA	153.70	NA
Neutron	0.058	NA	76.10	NA
Allowable	NA	200	1000	10

5.2 Source Specification

5.2.1 Gamma Source

The concentrated gamma source utilized for evaluation of the RH-TRU 72-B payloads is ^{60}Co with the following photon energies and associated intensities:[1]

Radionuclide	Photon Energy (MeV)	Intensity (%)
^{60}Co	3.469300E-01	7.600000E-03
	8.262800E-01	7.600000E-03
	1.173237E+00	9.997360E+01
	1.332501E+00	9.998560E+01
	2.158770E+00	1.110000E-03
	2.505000E+00	2.000000E-06
Total Source Strength (γ/s/Ci)	7.3991E+10	

[1] R.R. Kinsey, *et al.*, *The NUDAT/PCNUDAT Program for Nuclear Data,* paper submitted to the 9th International Symposium of Capture Gamma-Ray Spectroscopy and Related Topics, Budapest, Hungary, October 1996; data extracted from the NUDAT database, version September 7, 2000, CD-ROM.

5.2.2 Neutron Source

The concentrated neutron source utilized for evaluation of the RH-TRU 72-B payloads is determined using the SOURCES-4A[2] computer program as documented in report ED-042.[3] The neutron source is modeled with a representative UO_2 target material. The total neutron source strength (α/n plus spontaneous fission) for 1 g of ^{252}Cf, as a function of energy, is provided below:

Radionuclide	Neutron Energy Interval (MeV)	Neutrons/s/g
^{252}Cf Specific Activity = 536 Ci/g	0.0 – 0.1	0.00E+00
	0.1 – 0.5	1.80E+11
	0.5 – 1.0	2.71E+11
	1.0 – 2.0	5.36E+11
	2.0 – 3.0	4.10E+11
	3.0 – 4.0	2.73E+11
	4.0 – 6.0	2.66E+11
	6.0 – 8.0	8.53E+10
	8.0 – 10.0	2.44E+10
	10.0 – 15.0	8.36E+09
	Total	2.0541E+12
Total Source Strength (n/s/Ci)	3.8322E+09	

[2] Los Alamos National Laboratory, *SOURCES 4A: A Code for Calculating (α,n), Spontaneous Fission, and Delayed Neutron Sources and Spectra*, LA-13639-MS, Los Alamos, New Mexico, September 1999.

[3] Packaging Technology, Inc., *Neutron Source Rates for TRU Waste*, ED-042, Tacoma, WA, November 2000.

5.3 Shielding Model

5.3.1 Configuration of Source and Shielding

Under NCT, the sources are modeled as evenly distributed to, and centralized within, each of the internal payload containers inside the payload canister. Under HAC, these concentrated sources are coalesced to a single location just inside the confinement boundary for the RH-TRU waste canister and coalesced to two locations (98% of the coalesced sources is located just inside the shield insert and 2% is located just outside of the shield insert next to the confinement boundary for the canister) for the NS15 and NS30 neutron shielded canisters to conservatively bound NSC test results. NCT assumptions maximize the distance from the source(s) to the nearest detector whereas HAC assumptions minimize the distance from the source(s) to the nearest detector. This approach is conservative: maximizing the content activity to satisfy the most restrictive NCT dose rate requirement (a 10-mrem/hr dose rate limit at 2 meters from the package surface is conservatively used for establishing NCT activitity limits, whereas 2 meters from the side of the convenyance is actually 2.7 meters from the package surface) while also demonstrating that the contents meet the HAC dose rate requirement (1-meter from package surface dose rate ≤1,000 mrem/hr) even when reconfigured to the maximum extent theoretically possible.

With reference to Figure 5.3-1, that utilizes distance-squared relationships to establish maximum NCT dose rates possible under various source configurations/reconfigurations, several conclusions can be drawn as follows. For the 2-meter dose point, worst-case deviations from the analytically assumed NCT starting configuration (i.e., source evenly distributed to 3 drums) are readily accommodated by having conservatively considered a 10 mrem/hr limit at 2 meters from the package surface when establishing NCT activity limits (i.e., A_2 = 10 mrem/hr in Figure 5.3-1). From Figure 5.3-1, it is shown that even under extreme axial and radial reconfigurations of the source, the exclusive use limit of 10 mrem/hr at 2 meters from the side of the conveyance would still be satisfied (i.e., C_3 = 8.01 mrem/hr). It is also noted that the 2-meter dose rate is insensitive to axial consolidation of the entire source at the center of the package (e.g., B_3 is only 3.5% greater than A_3).

As demonstrated in Section 5.1.2, *Summary Table of Maximum Radiation Levels*, satisfaction of the 200 mrem/hr surface dose rate requirement is ensured for the analytically assumed NCT starting configuration. However, as shown in Figure 5.3-1, unlike the situation at the 2-meter dose point, axial consolidation of the entire source into a single drum has a much more significant effect on the surface dose rate (i.e., B_1 is 79% greater than A_1). To address this situation, in addition to satisfying the activity limit placed on the payload canister, the contribution from any single drum to the activity limit fraction for the entire payload canister will be limited to no more than half of the total activity limit fraction allowed for the payload canister. This approach effectively reduces the B_1 dose rate shown in Figure 5.3-1 to 121 mrem/hr. The margin this provides against the 200 mrem/hr limit combined with the use of a 10% administrative margin in the compliance evaluation (see Step 10 of Section 5.5.4, *Determination of Acceptable Activity*), reasonably accommodates potential radial movement of the source during transport. Although Figure 5.3-1 is specific to the RLC, its conclusions are conservative for the NS15 and NS30 configurations in that the presence of the HDPE sleeve further limits the maximum possible radial movement of the source material.

Pre-shipment dose rate surveys are used as final validation that source activities and distributions are reasonably consistent with the analytic evaluation. Note that even without the preshipment measurement confirmation and administrative margin, HAC dose rate requirements are ensured by the NCT centralized source analysis assumptions, and NCT 2-meter dose rate requirements are ensured by use of a conservative detector location when establishing NCT activity limits.

5.3.1.1 RH-TRU 72-B

Damage to the packaging under NCT conditions is negligible (i.e., confined to the impact limiters), so the SAR drawing dimensions for the packaging are utilized with the following exception: 1) IV overall height is reduced by 1/2 inch to neglect the inset in the IV lid. The rigid urethane foam filled impact limiters are not explicitly modeled, but credit for the spacing provided by the limiters ensures that the radial package dose rates are the most limiting. Due to the greater material thickness of the IV and OC lids and bases (as compared to the radial shells) and axial distances to detectors, only radial shielding configurations and dose rates are necessarily evaluated.

HAC packaging models utilize dimensions from NCT with the following exceptions: 1) pin puncture damage to the OC thermal shield, outer shell, and lead is accounted for by conservatively assuming a 7.9-inch diameter punch that closes all gaps between the thermal shield and OC outer shell and reduces the lead thickness by 0.656 inches resulting in a 1.219-inch lead thickness at the puncture location, and 2) the IV is assumed to translate radially 0.187 inches in contact with the OC inner shell. Consistent with structural drop impact evaluations, no lead slump is present or evaluated.

5.3.1.2 RH-TRU Waste Canister

The RH-TRU 72-B NCT and HAC package models with a RH-TRU waste canister payload utilize the package dimensions and materials discussed in Section 5.3.1.1, *RH-TRU 72-B*, and are illustrated in Figure 5.3-2 through Figure 5.3-4. The source that represents the contents for the 30-gallon drums, 55-gallon drums, or direct-load waste (as applicable) is modeled as a 1-inch stub-cylinder (equal diameter and height) centralized in each of three drums under NCT conditions. The sources are coalesced to a 1/2-inch stub-cylinder and located adjacent to the inner surface of the canister shell nearest the receptor under HAC conditions. For convenience and consistency with models developed to evaluate distributed sources with variable-density self-shielding properties discussed later in Section 5.5, *Activity Limits*, the stub-cylinder source is modeled as embedded in zirconium. For the small concentrated sources, this assumption has an insignificant effect on model results.

Damage to the RH-TRU waste canister under NCT conditions is negligible, so the SAR drawing dimensions for the Removable Lid Canister (RLC) are utilized to account for all unshielded variants of the RH-TRU waste canister designs. Each drum is utilized to spatially locate its centralized source within the RLC. Each drum is centered within the RLC and only the 1/4-inch thick RLC body shell, 3/4-inch thick lid, and 1/2-inch thick bottom head are credited for material attenuation (1/4-inch is the minimum shell/lid/head thickness required). The outside diameter of the RLC body shell is modeled as 26 inches. The RLC is modeled with an 113-inch cavity height. Due to the equivalent minimum material thickness of the RLC lid/base/body and greater

axial distances to detectors, only radial shielding configurations and dose rates are necessarily evaluated.

HAC RLC payload models utilize dimensions from NCT with the following exception: the RLC is radially offset 2.624 inches in contact with the IV inner shell (IV spacers ignored).

5.3.1.3 NS15 Neutron Shielded Canister

The RH-TRU 72-B NCT and HAC package models with a NS15 canister payload utilize the package and waste canister dimensions and materials discussed in Section 5.3.1.1, *RH-TRU 72-B*, and Section 5.3.1.2, *RH-TRU Waste Canister*, and are illustrated in Figure 5.3-5 through Figure 5.3-7. The source that represents the contents for the approximately 15-gallon drums is modeled as a 1-inch stub-cylinder centralized in each of three drums under NCT conditions. The sources are coalesced into two 1/2-inch stub-cylinders, one (98%) located adjacent to the inner surface of the shield insert and the other (2%) located adjacent to the inner surface of the canister shell nearest the receptor under HAC conditions.[1]

Damage to the NS15 canister under NCT conditions is negligible, so the SAR drawing dimensions are utilized. Each drum is utilized to spatially locate its centralized source within the NS15. Each drum is centered within the NS15 shield insert and only the RLC, 3.387-inch thick shield insert body, and 5-inch thick shield insert end caps are credited for material attenuation. The outside diameter of the NS15 shield insert body is modeled as 24 inches. The NS15 is modeled with a 102-inch cavity height. Due to the greater material thickness of the NS15 shield insert end caps (as compared to the body) and axial distances to detectors, only radial shielding configurations and dose rates are necessarily evaluated.

HAC NS15 payload models utilize dimensions from NCT with the following exceptions: 1) the RLC is radially offset 2.624 inches in contact with the IV inner shell (IV spacers ignored) and 2) the NS15 shield insert body is radially offset 0.24 inches toward the RLC body shell.[1]

5.3.1.4 NS30 Neutron Shielded Canister

The RH-TRU 72-B NCT and HAC package models with a NS30 canister payload utilize the package and waste canister dimensions and materials discussed in Section 5.3.1.1, *RH-TRU 72-B*, and Section 5.3.1.2, *RH-TRU Waste Canister*, and are illustrated in Figure 5.3-8 through Figure 5.3-10. The source that represents the contents for the approximately 30-gallon drums is modeled as a 1-inch stub-cylinder centralized in each of three drums under NCT conditions. The sources are coalesced into two 1/2-inch stub-cylinders, one (98%) located adjacent to the inner surface of the shield insert and the other (2%) located adjacent to the inner surface of the canister shell nearest the receptor under HAC conditions.[1]

Damage to the NS30 canister under NCT conditions is negligible, so the SAR drawing dimensions are utilized. Each drum is utilized to spatially locate its centralized source within the NS30. Each drum is centered within the NS30 shield insert and only the RLC, 1.454-inch thick shield insert body, and 5-inch thick shield insert end caps are credited for material attenuation. The outside diameter of the NS30 shield insert body is modeled as 24 inches. The NS30 is

[1] Petersen Inc., *30-foot Free Drop Post-Test Summary Report for the NS30 Neutron Shielded Canister*, Engineering Report 7953-R-027, Rev. 0, Ogden UT, November 2009.

modeled with a 102-inch cavity height. Due to the greater material thickness of the NS30 shield insert end caps (as compared to the body) and axial distances to detectors, only radial shielding configurations and dose rates are necessarily evaluated.

HAC NS30 payload models utilize dimensions from NCT with the following exceptions: 1) the RLC is radially offset 2.624 inches in contact with the IV inner shell (IV spacers ignored) and 2) the NS30 shield insert body is radially offset 0.24 inches toward the RLC body shell.[1]

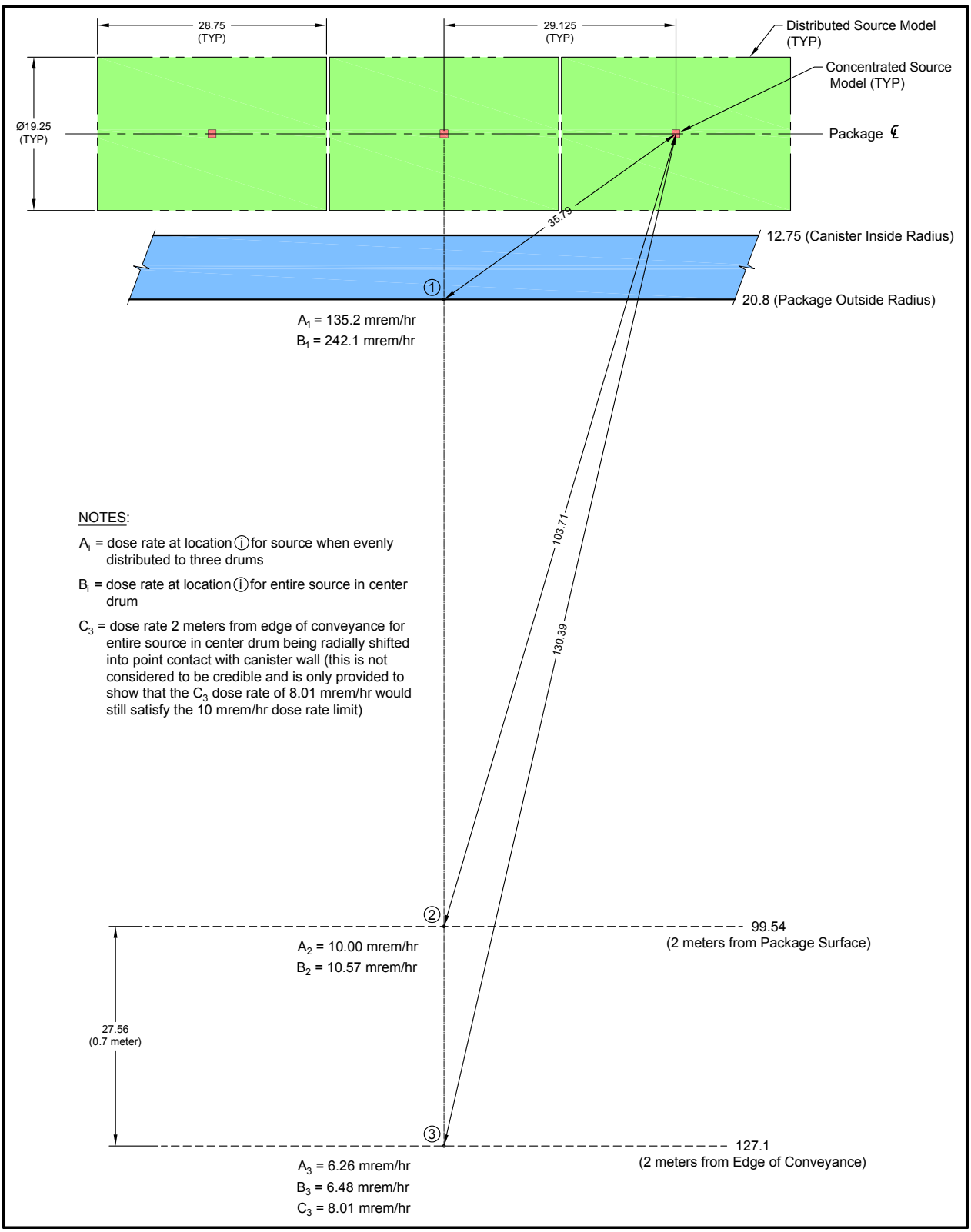

Figure 5.3-1 – Analytic Model Distance Squared Relationships Satisfying A_2 = 10 mrem/hr at 2 meters from the Package Surface

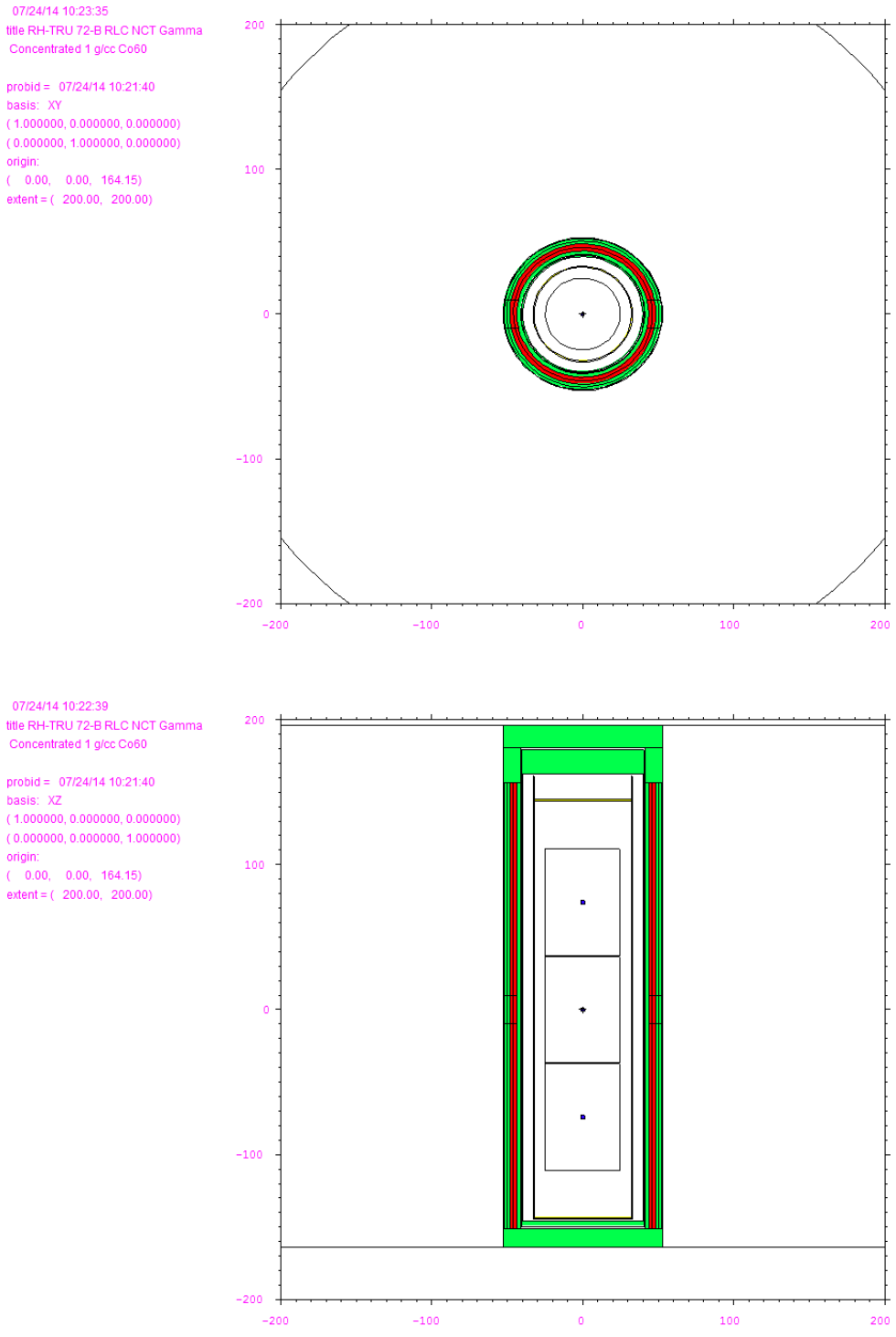

Figure 5.3-2 – RH-TRU 72-B RLC Payload MCNP Model for NCT

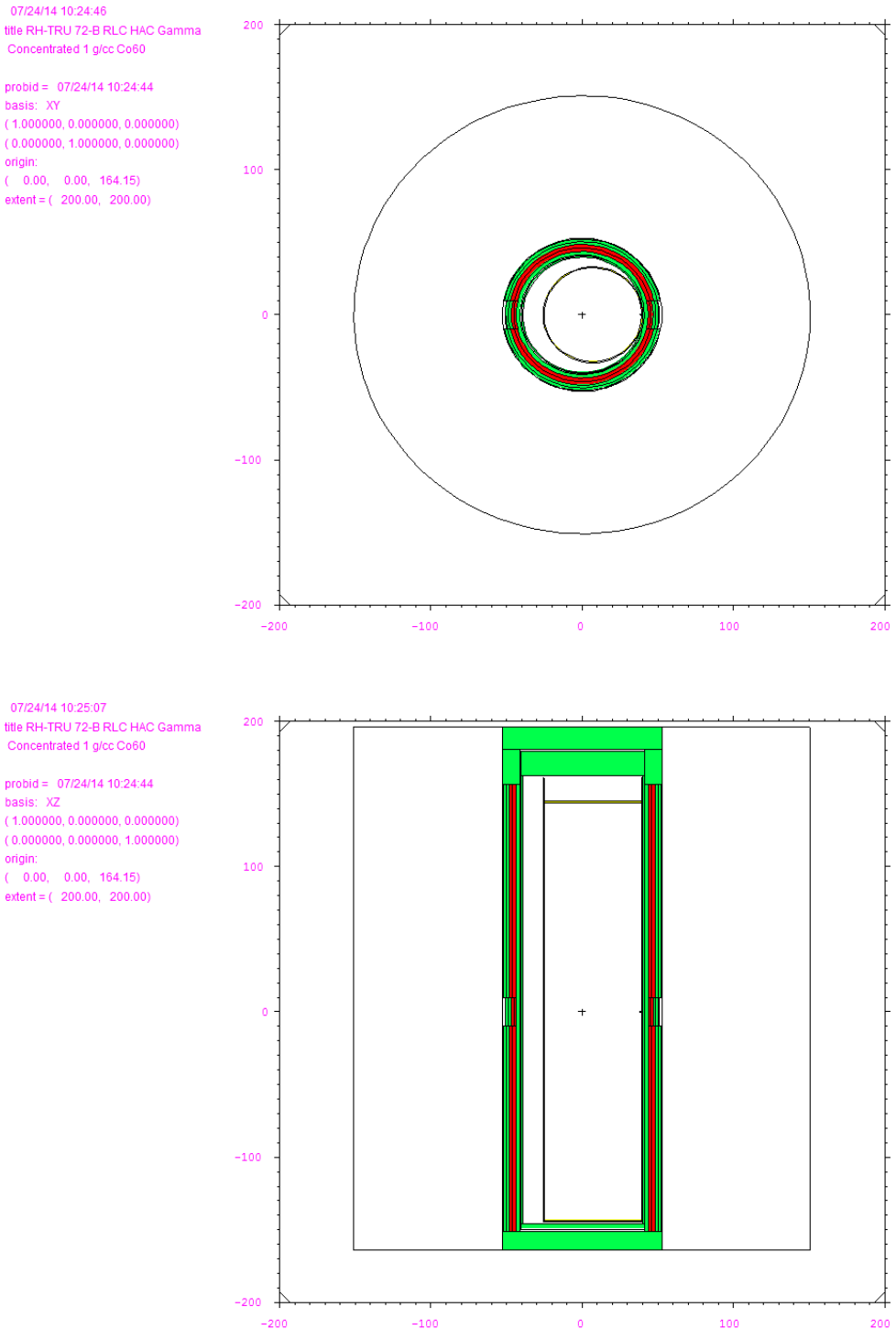

Figure 5.3-3 – RH-TRU 72-B RLC Payload MCNP Model for HAC

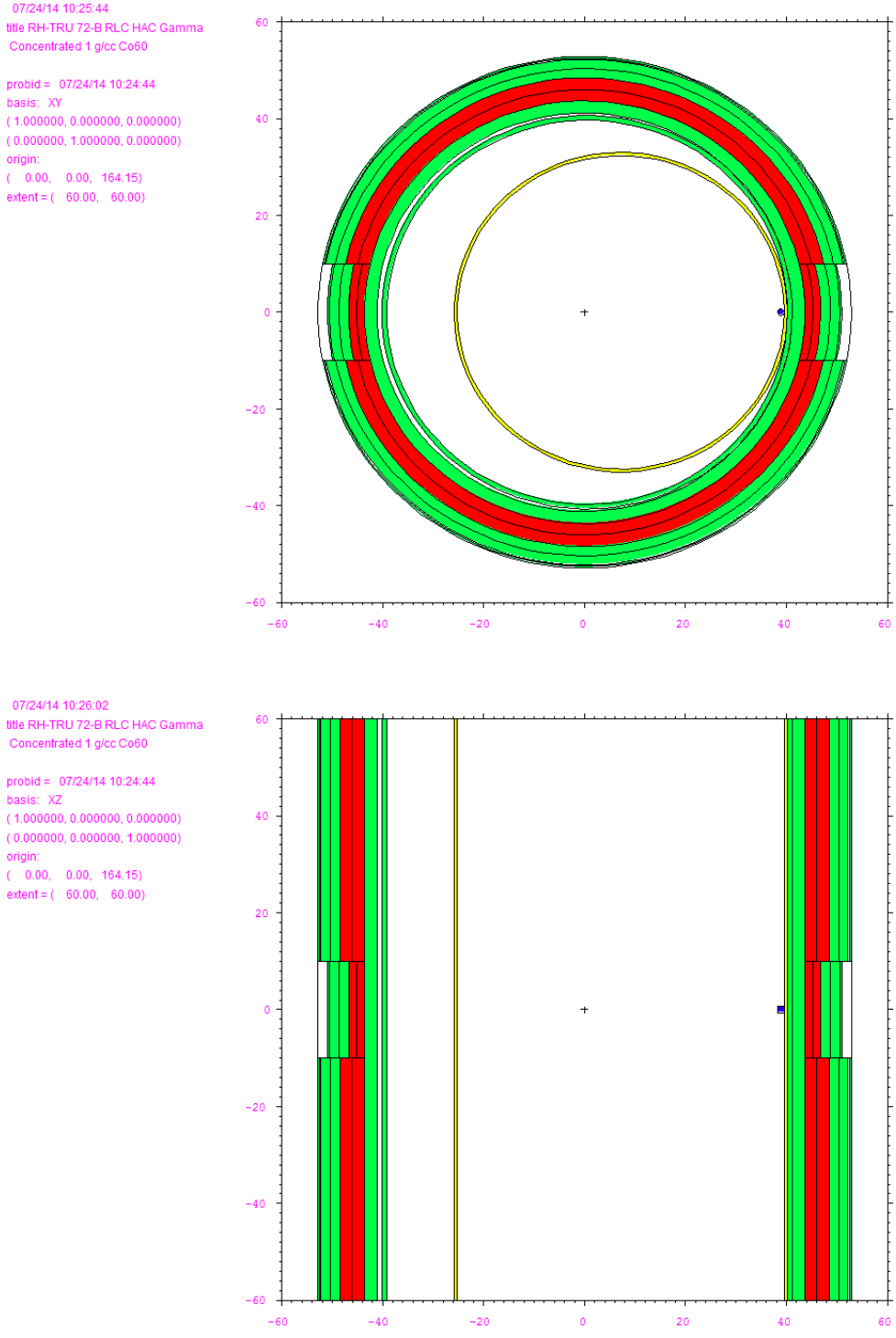

Figure 5.3-4 – RH-TRU 72-B RLC Payload MCNP Model for HAC (close-up)

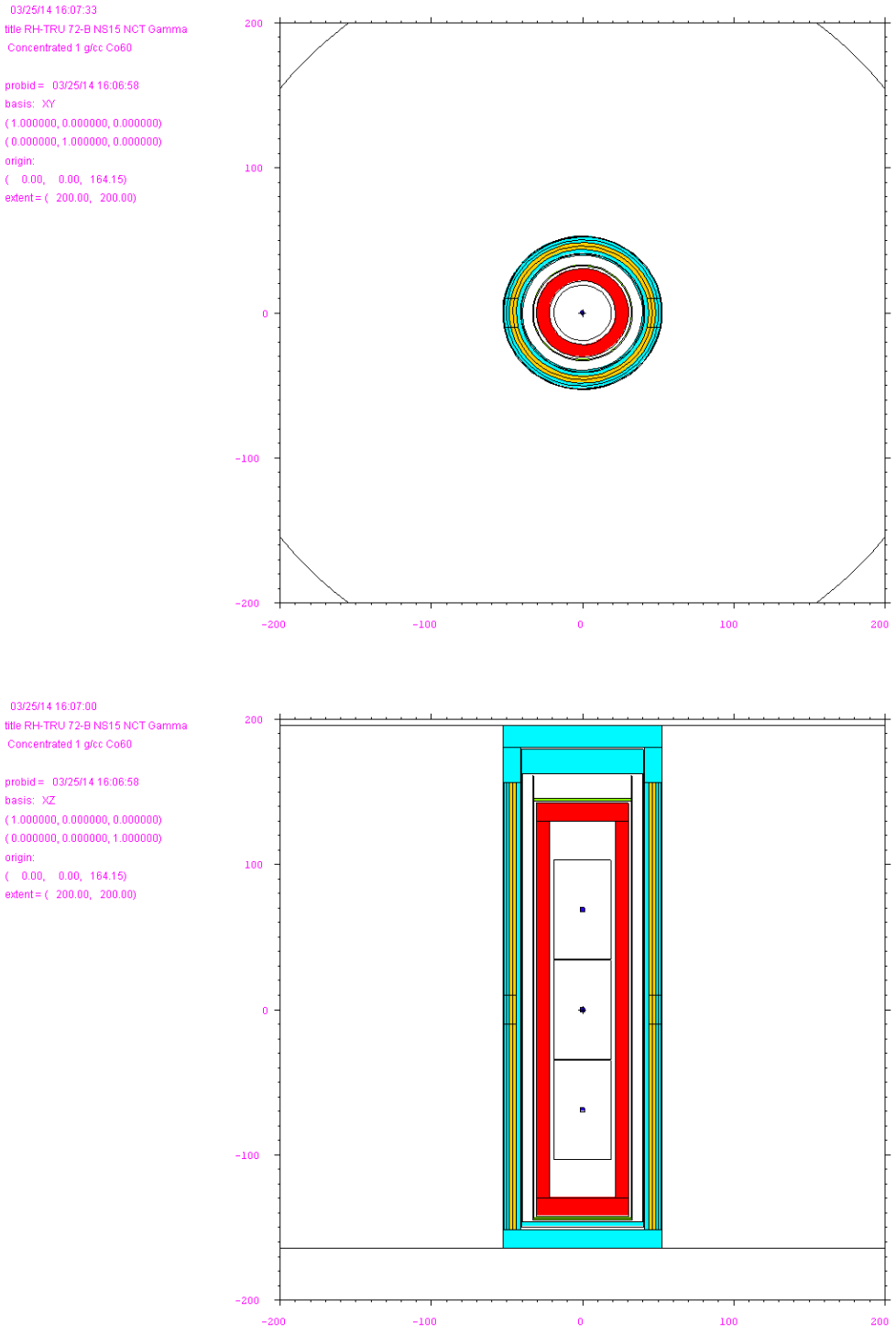

Figure 5.3-5 – RH-TRU 72-B NS15 Payload MCNP Model for NCT

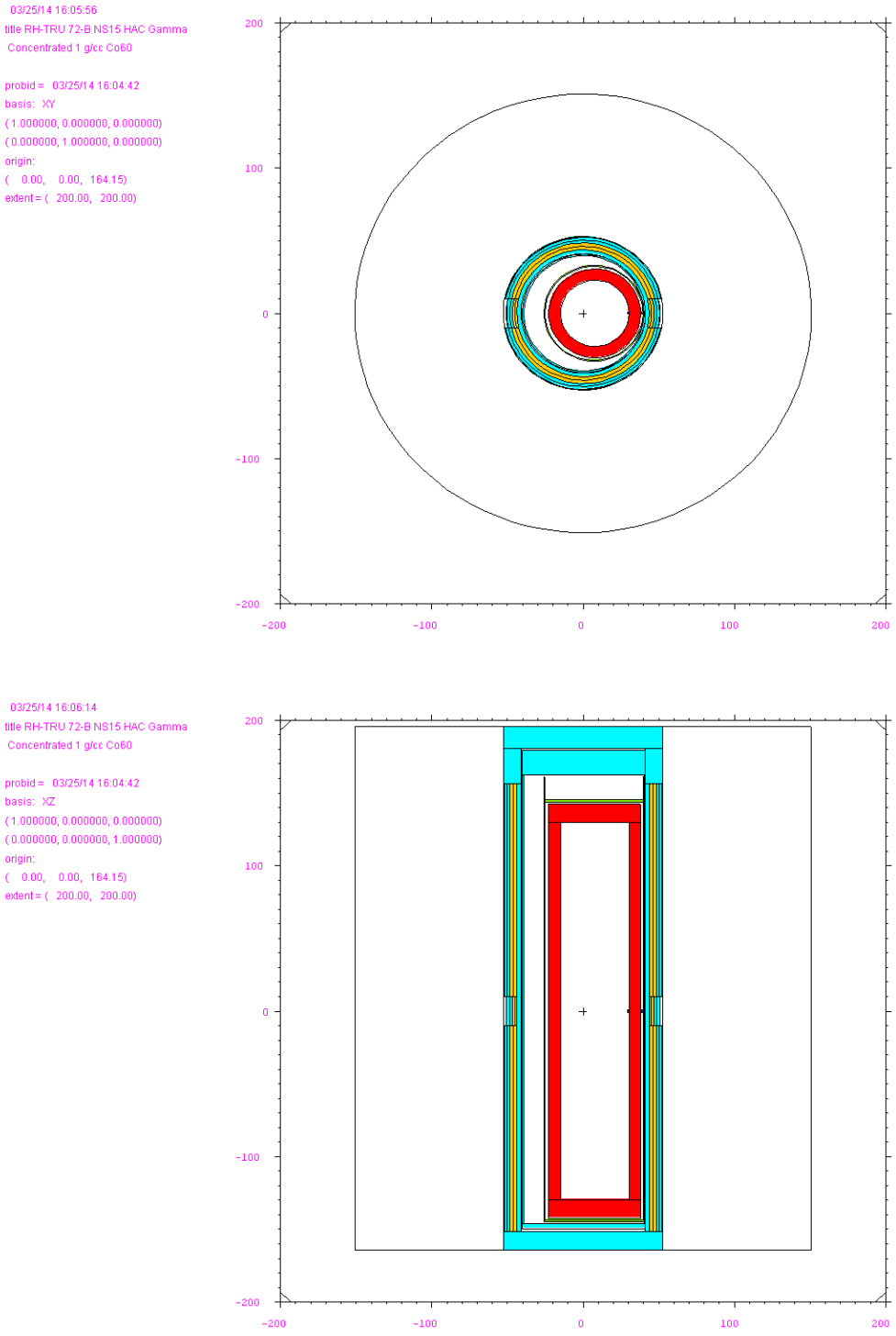

Figure 5.3-6 – RH-TRU 72-B NS15 Payload MCNP Model for HAC

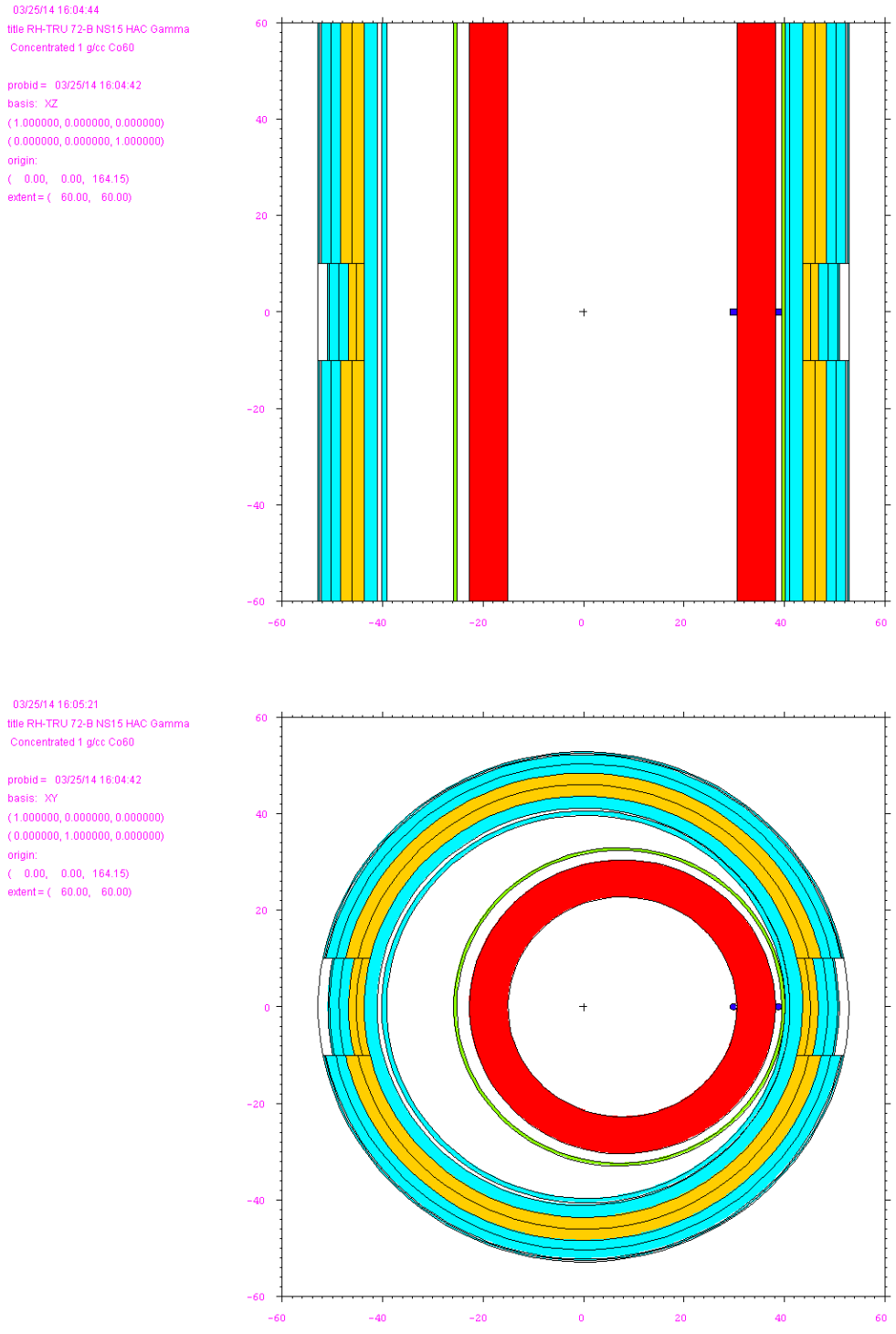

Figure 5.3-7 – RH-TRU 72-B NS15 Payload MCNP Model for HAC (close-up)

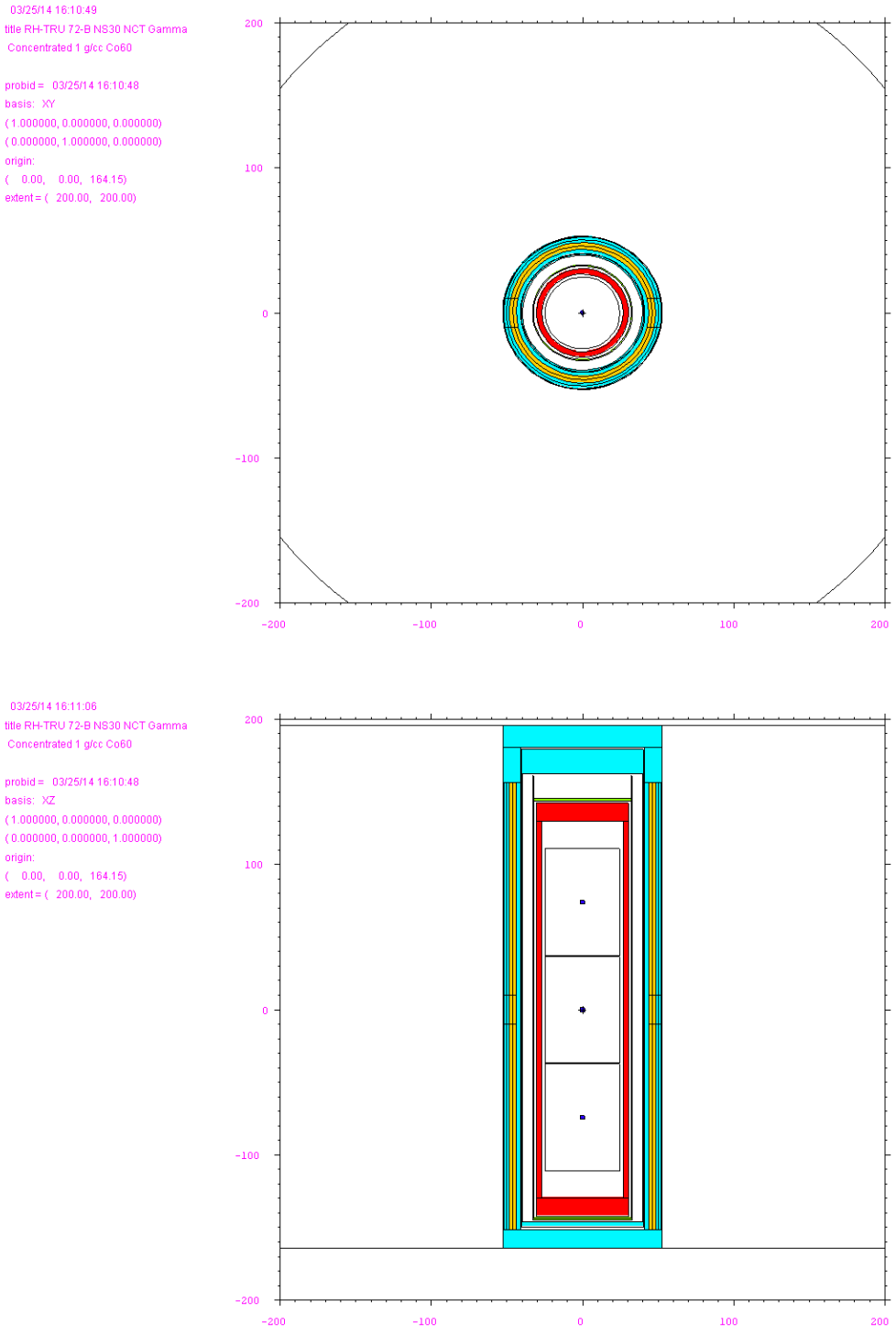

Figure 5.3-8 – RH-TRU 72-B NS30 Payload MCNP Model for NCT

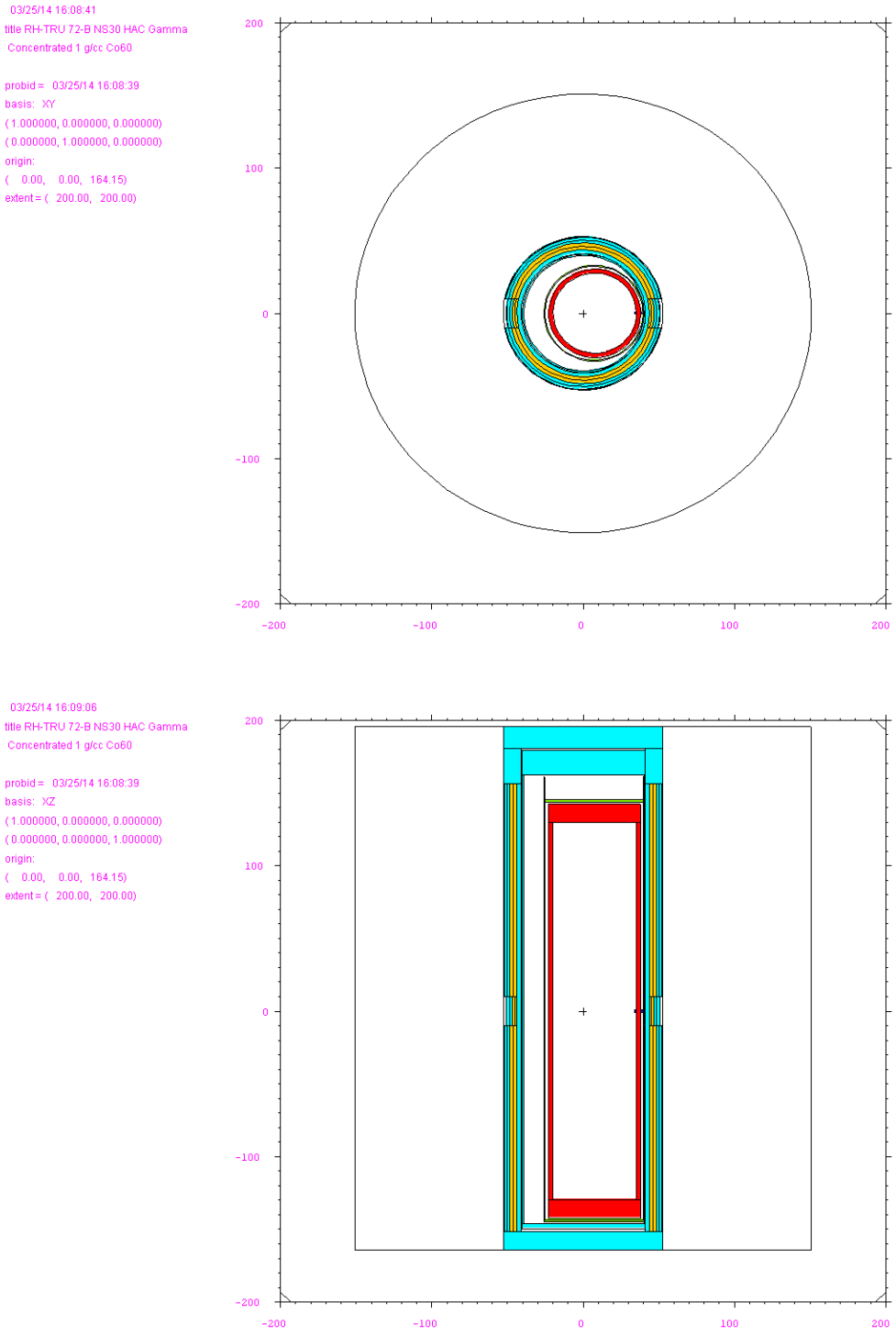

Figure 5.3-9 – RH-TRU 72-B NS30 Payload MCNP Model for HAC

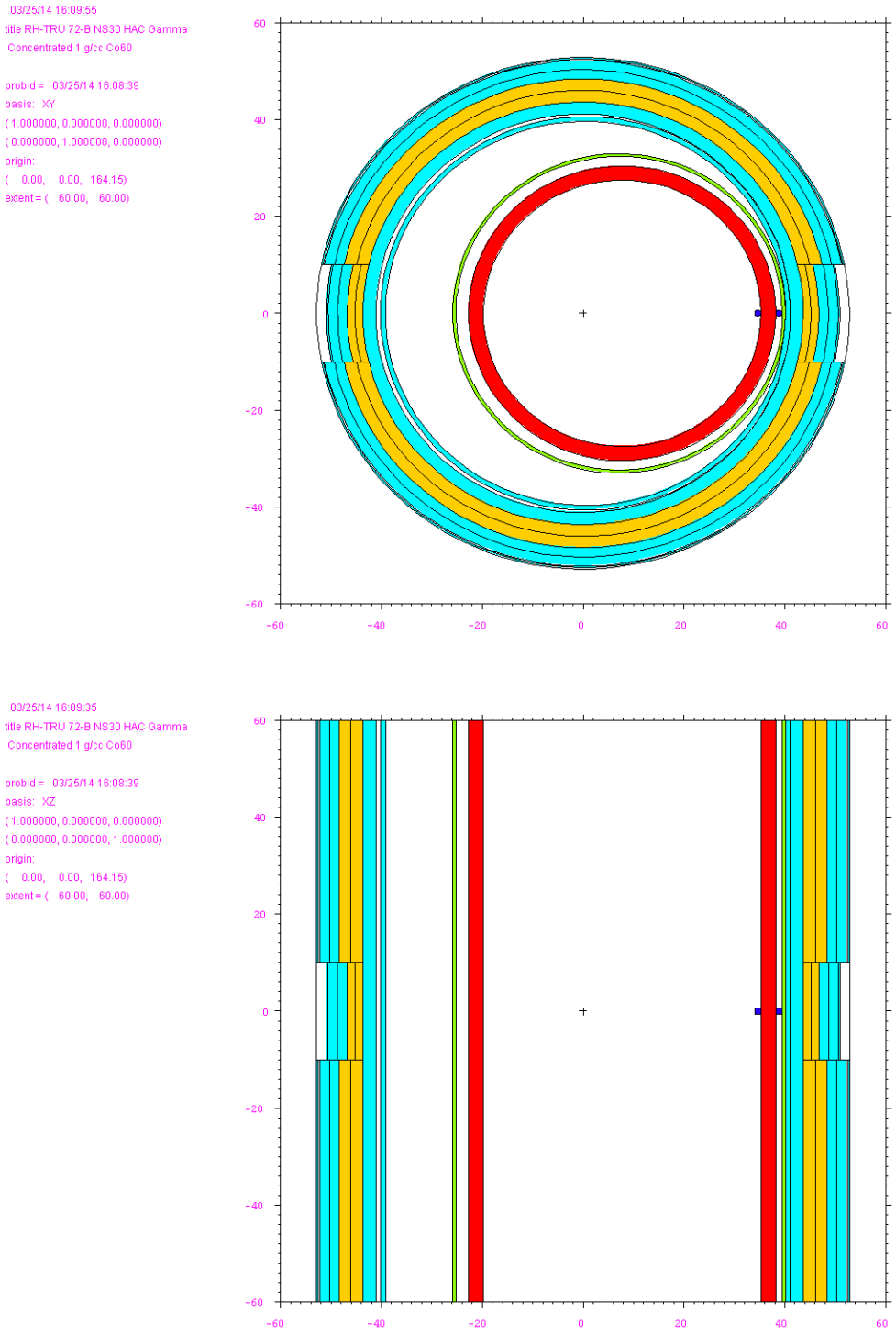

Figure 5.3-10 – RH-TRU 72-B NS30 Payload MCNP Model for HAC (close-up)

5.3.2 Material Properties

The shielding models are comprised of plain carbon steel, Type 304 stainless steel, lead, and extra-high molecular weight high density polyethylene (EHMW-HDPE); with material densities of 490 lb/ft³ (7.8526 g/cc), 500 lb/ft³ (8.0128 g/cc), 708 lb/ft³ (11.3500 g/cc), and 58.68 lb/ft^3 (0.9400 g/cc), respectively. Table 5.3-1 summarizes the shield regional densities for each of these attenuating materials. Zirconium is modeled in the source region at densities ranging from 0.1 to 8 g/cc to represent a conservative basis for self-shielding in distributed sources discussed in Section 5.5, *Activity Limits*. For convenience, Zirconium at 1 g/cc was also modeled in the source region for concentrated 1-inch stub-cylinder sources.

Table 5.3-1 – Summary of Shield Regional Densities

	Carbon Steel		Type 304 Stainless Steel		Lead		EHMW-HDPE	
Element	Percent	Partial Density (g/cc)	Percent	Partial Density (g/cc)	Percent	Partial Density (g/cc)	Percent	Partial Density (g/cc)
Silicon	—	—	1%	0.0801	—	—	—	—
Chromium	—	—	19%	1.5224	—	—	—	—
Manganese	—	—	2%	0.1603	—	—	—	—
Iron	100%	7.8526	68%	5.4487	—	—	—	—
Nickel	—	—	10%	0.8013	—	—	—	—
Lead	—	—	—	—	100%	11.3500	—	—
Hydrogen	—	—	—	—	—	—	14%	0.1316
Carbon	—	—	—	—	—	—	86%	0.8084
Nitrogen	—	—	—	—	—	—	—	—
Oxygen	—	—	—	—	—	—	—	—
Total	100%	7.8526	100%	8.0128	100%	11.3500	100%	0.9400

This page intentionally left blank.

5.4 Shielding Evaluation

5.4.1 Methods

MCNP5 v1.60 is used for the shielding analysis.[1] MCNP5 is a standard, well-accepted shielding program utilized to compute dose rates for shielding licenses. Three-dimensional models are developed to capture all of the relevant design parameters of the RH-TRU 72-B package and the associated payload canister configurations. Dose rates are calculated by tallying the neutron and gamma fluxes over surfaces of interest and converting these fluxes to dose rates. The models are run in either a photon or neutron mode, depending upon the radionuclide being evaluated. Combined photon/neutron mode evaluations were not employed for the neutron analyses as multiple test runs demonstrated that the gamma dose rate due to the interaction of neutrons in the shielding materials contributes a statistically insignificant (<1%) change in the dose rate as compared to the neutron dose rate. This is because secondary gamma production due to thermalized neutrons occurs inside the RH-TRU 72-B gamma shield such that affects to gamma dose rate outside of the package are insignificant. The gamma energies and intensities for ^{252}Cf were similarly ignored based on the same logic.

5.4.2 Input and Output Data

Four input/output cases are used to generate the results for each packaging/payload combination. Case naming conventions are defined in Table 5.4-1. Sample input files are provided in Appendix 5.7.1. All cases are run with a 1 particle/second (par/s) source and the results are scaled to the desired source activity to meet the most restrictive NCT and HAC dose rate limit.

[1] LA-CP-03-0245, MCNP – A General Monte Carlo N-Particle Transport Code, Version 5, Vol. 2: User's Guide, Los Alamos National Laboratory, February 2008.

Table 5.4-1 – Case Naming Conventions

Input file = .i extension	Output file = .io extension	Tally file = .it extension	Runtpe file = .ir extension
Case Name	**Description**	**Case Name Variable, X**	**Packaging / Payload**
Xng001	Gamma, ^{60}Co, NCT	7	RH-TRU 72-B / RLC
Xhg001	Gamma, ^{60}Co, HAC	8	RH-TRU 72-B / NS30
Xnn001	Neutron, ^{252}Cf, NCT	9	RH-TRU 72-B / NS15
Xhn001	Neutron, ^{252}Cf, HAC		

5.4.3 Flux-to-Dose Conversion

ANSI/ANS-6.1.1-1977 flux-to-dose-rate conversion factors are utilized for both neutron and gamma radiation. These factors are provided in Table 5.4-2 and Table 5.4-3.

Table 5.4-2 – Neutron Flux-to-Dose Rate Conversion Factors from ANSI/ANS-6.1.1-1977

n-Energy (MeV)	DFg(E) (n/cm²-s to mrem/hr)	Quality Factor	n-Energy (MeV)	DFg(E) (n/cm²-s to mrem/hr)	Quality Factor
2.50E-08	3.67E-03	2.0	0.5	9.26E-02	11.0
1.00E-07	3.67E-03	2.0	1.0	1.32E-01	11.0
1.00E-06	4.46E-03	2.0	2.5	1.25E-01	9.0
1.00E-05	4.54E-03	2.0	5	1.56E-01	8.0
1.00E-04	4.18E-03	2.0	7	1.47E-01	7.0
0.001	3.76E-03	2.0	10	1.47E-01	6.5
0.01	3.56E-03	2.5	14	2.08E-01	7.5
0.1	2.17E-02	7.5	20	2.27E-01	8.0

Table 5.4-3 – Gamma Flux-to-Dose Rate Conversion Factors from ANSI/ANS-6.1.1-1977

γ-Energy (MeV)	DFg(E) (γ/cm²-s to mrem/hr)	γ-Energy (MeV)	DFg(E) (γ/cm²-s to mrem/hr)
0.01	3.96E-03	1.4	2.51E-03
0.03	5.82E-04	1.8	2.99E-03
0.05	2.90E-04	2.2	3.42E-03
0.07	2.58E-04	2.6	3.82E-03
0.10	2.83E-04	2.8	4.01E-03
0.15	3.79E-04	3.25	4.41E-03
0.20	5.01E-04	3.75	4.83E-03
0.25	6.31E-04	4.25	5.23E-03
0.30	7.59E-04	4.75	5.60E-03
0.35	8.78E-04	5	5.80E-03
0.40	9.85E-04	5.25	6.01E-03
0.45	1.08E-03	5.75	6.37E-03
0.50	1.17E-03	6.25	6.74E-03
0.55	1.27E-03	6.75	7.11E-03
0.60	1.36E-03	7.5	7.66E-03
0.65	1.44E-03	9	8.77E-03
0.70	1.52E-03	11	1.03E-02
0.80	1.68E-03	13	1.18E-02
1	1.98E-03	15	1.33E-02

5.4.4 External Radiation Levels

The MCNP5 models used to determine external radiation levels use segmented surface detectors to calculate the radial dose rates on the surface of the package and at 2 meters from the surface of the package for NCT and at 1 meter from the surface of the package for HAC. The surface detectors for NCT are either axially aligned with the source centerline when a single source exists or axially aligned with a plane that is at the centroid of multiple sources. The axial alignment of the surface detectors is to minimize the aggregate distance from the source(s) to the detector and to report the maximum dose rate.

Dose rates and the associated statistical error are computed based on a 1 par/s source strength. The source strengths for 1 Curie (Ci) of ^{60}Co and ^{252}Cf are 7.3991E+10 γ/s and 3.8322E+09 n/s, respectively, based on the data provided in Section 5.2, *Source Specification*. Conservatively accounting for the statistical error, an activity allowable (par/s) is then determined for the gamma and neutron sources to meet each of the regulatory dose rate limits by dividing the allowable

dose rate by the product of the calculated dose rate and one plus the error. The activity limit (Ci) to meet each regulatory dose rate limit is then determined by dividing the allowable activity (par/s) by the source strength (par/s/Ci). Finally, the NCT and HAC dose rates associated with the limiting activity are then determined by multiplying the allowable dose rate by the ratio of the limiting allowable activity to the allowable activity for each case (NCT at surface, NCT at 2 meters, HAC at 1 meter).

5.4.4.1 RH-TRU Waste Canister

The RH-TRU 72-B dose rates and statistical errors computed for the RH-TRU Waste Canister concentrated gamma and neutron sources with 1 par/s source strength are provided in Table 5.4-4. The dose rates based on the limiting allowable activity (i.e., the NCT at 2 meters values) are provided in Table 5.1-1.

Table 5.4-4 – RH-TRU 72-B – RH-TRU Waste Canister Dose Rates for 1 par/s Source

Case	Nuclide	Source Strength (par/s/Ci)	Calculated Dose Rate (mrem/hr)	Tally Error	Allowable Activity (par/s)	Allowable Activity (Ci)
NCT @ surface						
7ng001.i	^{60}Co	7.3991E+10	1.51E-10	0.7%	1.31E+12	17.758
7nn001.i	^{252}Cf	3.8322E+09	1.54E-06	0.2%	1.30E+08	0.034
NCT @ 2m						
7ng001.i	^{60}Co	7.3991E+10	1.29E-11	0.4%	7.73E+11	**10.444**
7nn001.i	^{252}Cf	3.8322E+09	1.19E-07	0.2%	8.41E+07	**0.022**
HAC @ 1m						
7hg001.i	^{60}Co	7.3991E+10	2.00E-10	1.9%	4.91E+12	66.351
7hn001.i	^{252}Cf	3.8322E+09	7.20E-07	0.9%	1.38E+09	0.359

5.4.4.2 NS15 Neutron Shielded Canister

The RH-TRU 72-B dose rates and statistical errors computed for the NS15 neutron shielded canister concentrated gamma and neutron sources with 1 par/s source strength are provided in Table 5.4-5. The dose rates based on the limiting allowable activity (i.e., the NCT at 2 meters values) are provided in Table 5.1-2.

Table 5.4-5 – RH-TRU 72-B – NS15 Neutron Shielded Canister Dose Rates for 1 par/s Source

Case	Nuclide	Source Strength (par/s/Ci)	Calculated Dose Rate (mrem/hr)	Tally Error	Allowable Activity (par/s)	Allowable Activity (Ci)
NCT @ surface						
9ng001.i	^{60}Co	7.3991E+10	9.88E-11	0.8%	2.01E+12	27.148
9nn001.i	^{252}Cf	3.8322E+09	2.72E-07	0.6%	7.30E+08	0.190
NCT @ 2m						
9ng001.i	^{60}Co	7.3991E+10	8.32E-12	0.5%	1.20E+12	**16.167**
9nn001.i	^{252}Cf	3.8322E+09	1.81E-08	0.7%	5.48E+08	**0.143**
HAC @ 1m						
9hg001.i	^{60}Co	7.3991E+10	1.12E-10	1.7%	8.74E+12	118.106
9hn001.i	^{252}Cf	3.8322E+09	1.29E-07	2.1%	7.57E+09	1.974

5.4.4.3 NS30 Neutron Shielded Canister

The RH-TRU 72-B dose rates and statistical errors computed for the NS30 neutron shielded canister concentrated gamma and neutron sources with 1 par/s source strength are provided in Table 5.4-6. The dose rates based on the limiting allowable activity (i.e., the NCT at 2 meters values) are provided in Table 5.1-3.

Table 5.4-6 – RH-TRU 72-B – NS30 Neutron Shielded Canister Dose Rates for 1 par/s Source

Case	Nuclide	Source Strength (par/s/Ci)	Calculated Dose Rate (mrem/hr)	Tally Error	Allowable Activity (par/s)	Allowable Activity (Ci)
NCT @ surface						
8ng001.i	^{60}Co	7.3991E+10	1.27E-10	0.8%	1.56E+12	21.118
8nn001.i	^{252}Cf	3.8322E+09	6.34E-07	0.6%	3.14E+08	0.082
NCT @ 2m						
8ng001.i	^{60}Co	7.3991E+10	1.06E-11	0.5%	9.37E+11	**12.662**
8nn001.i	^{252}Cf	3.8322E+09	4.45E-08	0.6%	2.23E+08	**0.058**
HAC @ 1m						
8hg001.i	^{60}Co	7.3991E+10	1.61E-10	1.9%	6.10E+12	82.376
8hn001.i	^{252}Cf	3.8322E+09	3.37E-07	1.1%	2.93E+09	0.766

5.4.4.4 Summary

As shown in Table 5.4-4 through Table 5.4-6, each packaging/payload configuration is defined by a limiting allowable activity to meet the NCT at 2 meters from the surface dose rate of 10 mrem/hr. The tally errors are all less than or equal to 2.1%, demonstrating a well-converged solution. All allowable activity calculations conservatively add the error associated with the Monte-Carlo simulation to determine the activity that meets the regulatory dose rate requirement. The limiting NCT activity and the limiting HAC activity are graphically summarized in Figure 5.4-1.

Generally, when at the NCT at 2 meter dose rate limit, the NCT package surface dose rate is at least a factor of approximately 1.33 below the regulatory allowable (200 mrem/hr) and the HAC at 1 meter dose rate is at least a factor of approximately 6.35 below the regulatory allowable (1000 mrem/hr) for all packaging/payload configurations.

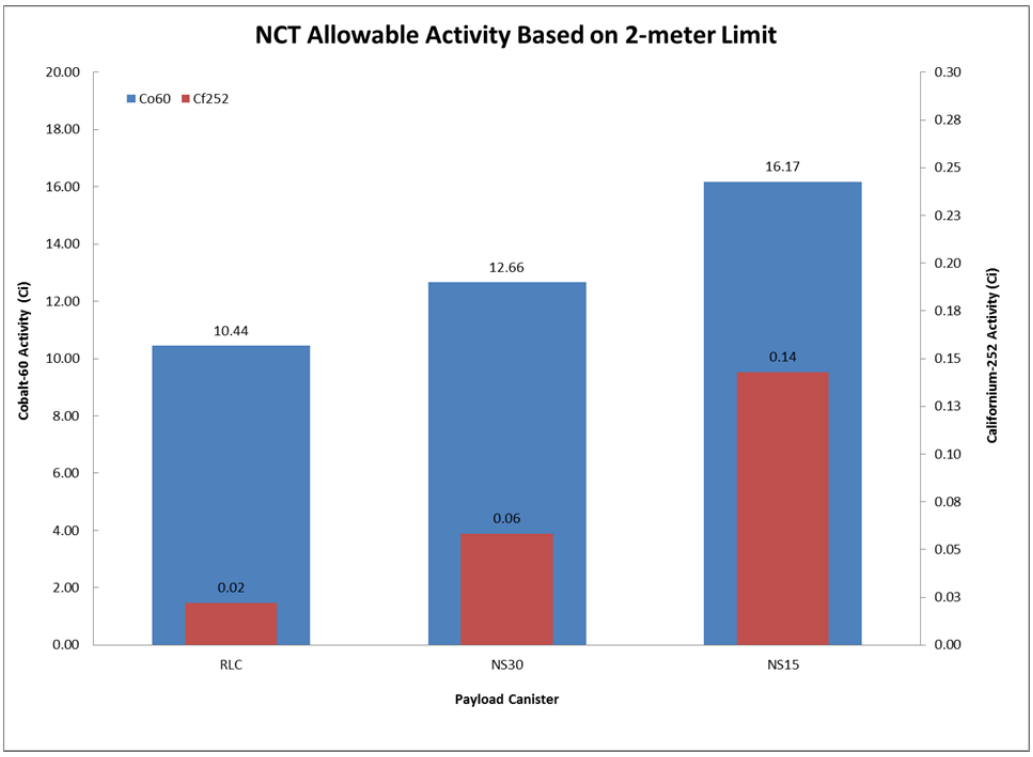

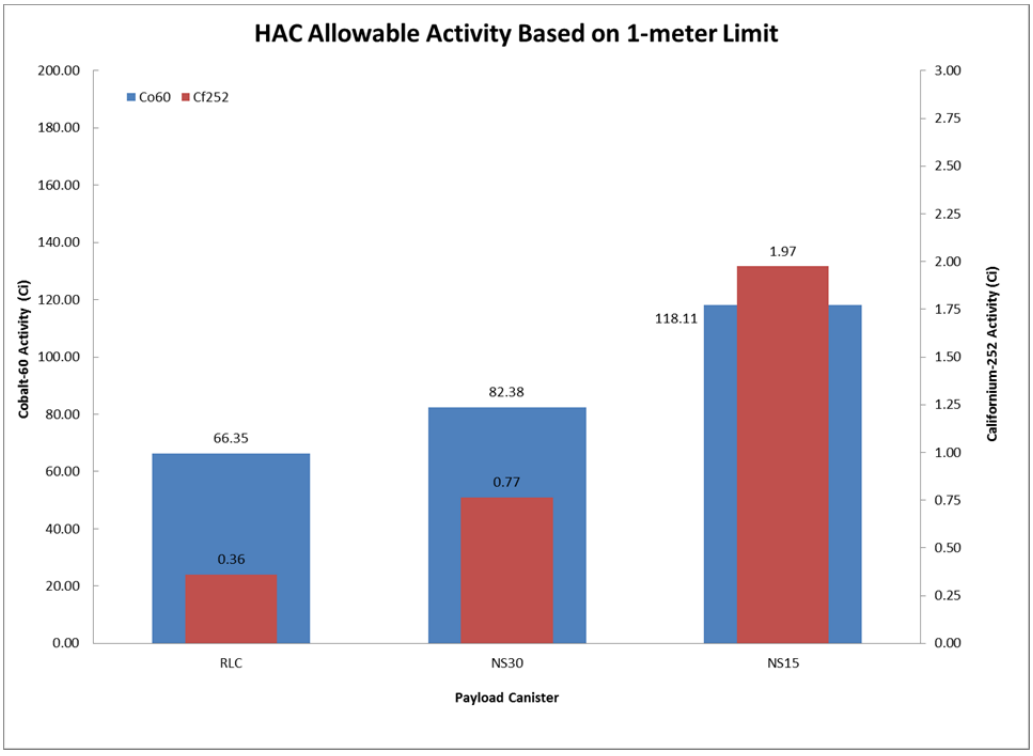

Figure 5.4-1 – Allowable Activity Comparison for Concentrated Sources

This page intentionally left blank.

5.5 Activity Limits

The calculations summarized in Section 5.4, *Shielding Evaluation*, were associated with a ^{60}Co gamma and a ^{252}Cf neutron source term, but TRU waste can be comprised of a multitude of radionuclides. Therefore, a generalized method for determining compliance with 10 CFR §71.47 and §71.51 is required to accommodate any mixture of gamma and/or neutron-emitting radionuclides. Using the packaging models described in Section 5.3, *Shielding Model*, additional calculations were performed to determine the maximum activity that can be contained in the RH-TRU 72-B while meeting the requirements of 10 CFR §71.47. Since the results in Section 5.4, *Shielding Evaluation*, demonstrate that contents meeting the NCT limits at 2 meters will meet NCT surface and HAC at 1 meter limits, maximum activity was determined only for NCT.

For each of the packaging and payload configurations considered in Section 5.4, *Shielding Evaluation*, two source configurations were evaluated as follows. Of note, the discussions and associated Figure 5.3-1 provided in Section 5.3.1, *Configuration of Source and Shielding*, are equally applicable to both configurations.

- *Concentrated Source* – activity in a stub-cylinder with dimensions of 1 inch in diameter by 1 inch in height centered in the payload cavity of drums within the canister.
- *Distributed Source* – activity homogenously distributed in a right-circular cylinder centered in the payload cavity of drums within the canister. The size of the distributed source is dependent upon the available size of the drums and the maximum allowed weight of the contents. To conservatively model the source (i.e., minimize the effects of self-attenuation and distance), the diameter of the source region is maintained at the drum diameter (minus an 1/8-inch radial and axial clearance) and the source height is varied based on the assumed density of the contents ranging from 0.1 to 8 g/cc. The material for the source region was selected as Zr (Z=40); multiple calculations with various materials showed a material selection of Zr was reasonably representative of TRU waste for gamma calculations and inconsequential to neutron calculations.

Dose rates were calculated at 2 meters from the surface of the package for a range of discrete gamma (0.5 to 10 MeV) and neutron (0.1 to 15 MeV) energies provided in Table 5.5-1 with a source strength of 1 par/s. Dose rates were determined with segmented surface detectors axially aligned with a plane that is at the centroid of multiple sources. The axial alignment of the surface detectors is to minimize the aggregate distance from the source(s) to the detector and to report the maximum dose rate. The flux-to-dose rate conversion factors are the same as used previously and listed in Table 5.4-2 and Table 5.4-3.

The maximum allowed gamma and neutron activity in par/s, for each discrete energy, was determined by multiplying the modeled source activity (1 par/s) by the ratio of the dose rate limit (10 mrem/hr) to the calculated dose rate after conservatively adjusting for statistical error. The concentrated source results were determined for a 1 g/cc source density but apply to all concentrated gamma and neutron sources as the assumed source material had no statistically significant effect on the results.

The distributed source results were determined for a range of source densities from 0.1 to 8 g/cc. The 1 g/cc results were evaluated for each discrete gamma and neutron energy listed in Table

5.5-1. For distributed gamma sources, the 1 g/cc (unit density) results are utilized along with a density correction factor (DCF) to apply the distributed gamma unit-density source results to any source density in the range. For distributed neutron sources, the source was evaluated at a single density, 1 g/cc, which applies to any density in the source range without the use of a DCF since the Zr material does not attenuate neutrons. Therefore, the distributed neutron source has an activity allowable that differs from the concentrated neutron source due to distance attenuation effects alone whereas the distributed gamma source has an activity allowable that differs from the concentrated gamma source due to distance and material attenuation effects.

The gamma DCFs were determined by first calculating the maximum allowable activity for gamma energies in the range of 0.5 to 10.0 MeV over the 0.1 to 8 g/cc density range. The gamma DCF is the ratio of the maximum activity at a density other than 1 to the maximum activity for the unit-density source. A 3rd order polynomial curve-fit of the minimum DCF, determined as the smallest DCF for all evaluated energies at each source density, was produced to facilitate calculation of a DCF for any density of contents.

Table 5.5-1 – Discrete Gamma and Neutron Energies

γ-Energy (MeV)	***n*-Energy (MeV)**
0.500	0.100
0.600	0.200
0.800	0.300
1.000	0.500
1.250	0.750
1.500	1.000
1.750	1.250
2.000	1.500
2.500	1.750
4.000	2.000
6.000	2.500
10.000	5.000
–	10.000
–	15.000

5.5.1 RH-TRU Waste Canister

The maximum allowed gamma and neutron activity for a concentrated and distributed unit-density source in a RH-TRU 72-B with a RH-TRU waste canister payload is given in Table 5.5-2 and Table 5.5-3, respectively. Figure 5.5-1 illustrates the source models for the unit-density distributed source with the RH-TRU waste canister payload. The DCF for the RH-TRU 72-B with the RH-TRU waste canister payload and polynomial curve fit of the minimum value is provided in Figure 5.5-2.

Application of the maximum activity limits provided in Table 5.5-2 and Table 5.5-3 and the DCF summarized below can conveniently be used to ensure compliance with 10 CFR §71.47 and §71.51 dose rate requirements for the RH-TRU 72-B with a RH-TRU waste canister payload through the process defined in Section 5.5.4, *Determination of Acceptable Activity*:

$$DCF_{RLC} = (0.00002)\,\rho^3 - (0.0048)\,\rho^2 + (0.6322)\,\rho + 0.3065$$

where ρ is the density of the source region in units of grams per cubic centimeter (g/cc).

Table 5.5-2 – RH-TRU 72-B – RH-TRU Waste Canister Gamma Activity Limits

Case	Source Type	Energy (MeV)	Calculated Dose Rate (mrem/hr)	Tally Error	Allowable Activity (γ/s)
7ng100.i	Concentrated	0.5	4.86E-15	0.8%	2.04E+15
7ng101.i	Concentrated	0.6	5.93E-14	0.3%	1.68E+14
7ng102.i	Concentrated	0.8	8.90E-13	0.3%	1.12E+13
7ng103.i	Concentrated	1	3.93E-12	0.3%	2.54E+12
7ng104.i	Concentrated	1.25	1.25E-11	0.4%	7.99E+11
7ng105.i	Concentrated	1.5	2.58E-11	0.5%	3.85E+11
7ng106.i	Concentrated	1.75	4.20E-11	0.6%	2.37E+11
7ng107.i	Concentrated	2	5.91E-11	0.7%	1.68E+11
7ng108.i	Concentrated	2.5	9.44E-11	0.8%	1.05E+11
7ng109.i	Concentrated	4	1.76E-10	0.9%	5.65E+10
7ng110.i	Concentrated	6	2.33E-10	1.0%	4.25E+10
7ng111.i	Concentrated	10	2.98E-10	1.0%	3.32E+10
7ng120.i	Distributed	0.5	1.02E-15	0.8%	9.72E+15
7ng121.i	Distributed	0.6	1.46E-14	0.4%	6.83E+14
7ng122.i	Distributed	0.8	2.66E-13	0.3%	3.76E+13
7ng123.i	Distributed	1	1.35E-12	0.3%	7.40E+12
7ng124.i	Distributed	1.25	4.79E-12	0.4%	2.08E+12
7ng125.i	Distributed	1.5	1.09E-11	0.5%	9.17E+11
7ng126.i	Distributed	1.75	1.85E-11	0.6%	5.37E+11
7ng127.i	Distributed	2	2.77E-11	0.6%	3.59E+11
7ng128.i	Distributed	2.5	4.61E-11	0.7%	2.16E+11
7ng129.i	Distributed	4	9.17E-11	0.8%	1.08E+11
7ng130.i	Distributed	6	1.21E-10	0.9%	8.23E+10
7ng131.i	Distributed	10	1.53E-10	0.9%	6.47E+10

Table 5.5-3 – RH-TRU 72-B – RH-TRU Waste Canister Neutron Activity Limits

Case	Source Type	Energy (MeV)	Calculated Dose Rate (mrem/hr)	Tally Error	Allowable Activity (n/s)
7nn100.i	Concentrated	0.1	8.42E-09	0.3%	1.18E+09
7nn101.i	Concentrated	0.2	1.84E-08	0.3%	5.40E+08
7nn102.i	Concentrated	0.3	4.45E-08	0.3%	2.24E+08
7nn103.i	Concentrated	0.5	7.60E-08	0.3%	1.31E+08
7nn104.i	Concentrated	0.75	1.03E-07	0.3%	9.69E+07
7nn105.i	Concentrated	1	1.19E-07	0.2%	8.36E+07
7nn106.i	Concentrated	1.25	1.35E-07	0.2%	7.40E+07
7nn107.i	Concentrated	1.5	1.33E-07	0.2%	7.48E+07
7nn108.i	Concentrated	1.75	1.22E-07	0.3%	8.16E+07
7nn109.i	Concentrated	2	1.26E-07	0.2%	7.92E+07
7nn110.i	Concentrated	2.5	1.28E-07	0.2%	7.82E+07
7nn111.i	Concentrated	5	1.33E-07	0.2%	7.53E+07
7nn112.i	Concentrated	10	1.54E-07	0.2%	6.48E+07
7nn113.i	Concentrated	15	2.19E-07	0.2%	4.55E+07
7nn120.i	Distributed	0.1	7.89E-09	0.4%	1.26E+09
7nn121.i	Distributed	0.2	1.68E-08	0.4%	5.93E+08
7nn122.i	Distributed	0.3	4.30E-08	0.3%	2.32E+08
7nn123.i	Distributed	0.5	7.42E-08	0.3%	1.34E+08
7nn124.i	Distributed	0.75	1.02E-07	0.3%	9.74E+07
7nn125.i	Distributed	1	1.18E-07	0.3%	8.42E+07
7nn126.i	Distributed	1.25	1.30E-07	0.2%	7.70E+07
7nn127.i	Distributed	1.5	1.30E-07	0.2%	7.70E+07
7nn128.i	Distributed	1.75	1.19E-07	0.3%	8.35E+07
7nn129.i	Distributed	2	1.20E-07	0.3%	8.32E+07
7nn130.i	Distributed	2.5	1.19E-07	0.3%	8.38E+07
7nn131.i	Distributed	5	1.27E-07	0.3%	7.88E+07
7nn132.i	Distributed	10	1.50E-07	0.3%	6.64E+07
7nn133.i	Distributed	15	2.15E-07	0.3%	4.63E+07

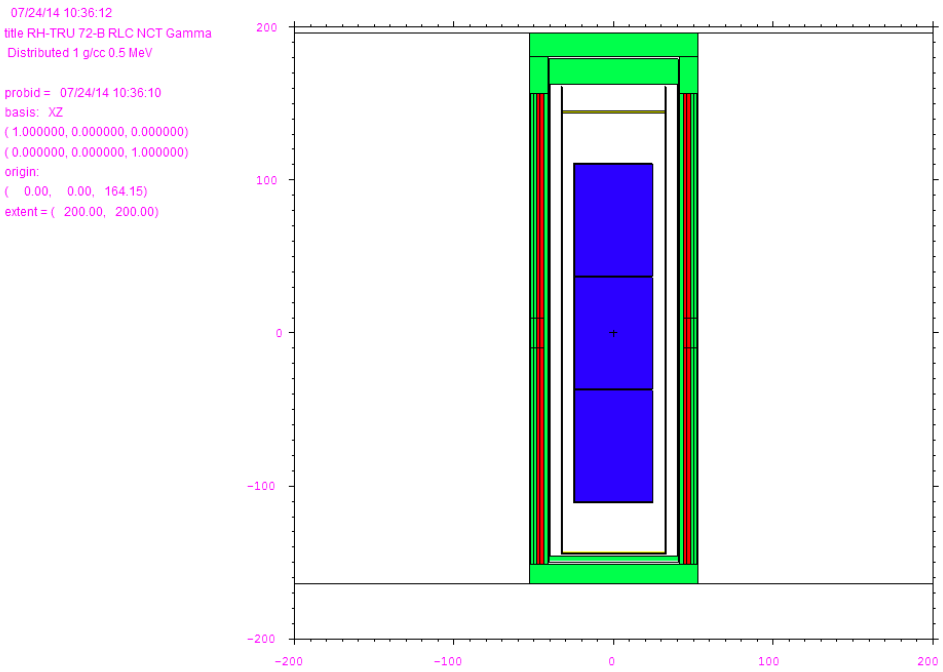

Figure 5.5-1 – RH-TRU 72-B – RH-TRU Waste Canister MCNP Model for Distributed Source at Unit Density

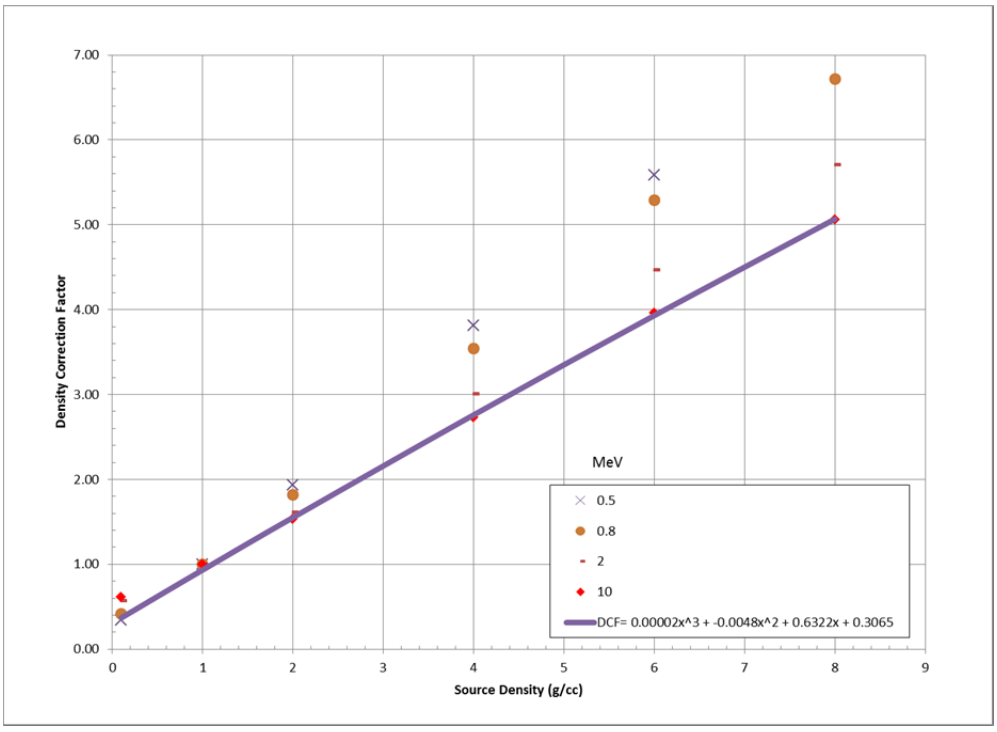

Figure 5.5-2 – RH-TRU 72-B – RH-TRU Waste Canister DCF

5.5.2 NS15 Neutron Shielded Canister

The maximum allowed gamma and neutron activity for a concentrated and distributed unit-density source in a RH-TRU 72-B with a NS15 neutron shielded canister payload is given in Table 5.5-4 and Table 5.5-5, respectively. Figure 5.5-3 illustrates the source models for the unit-density distributed source with the NS15 neutron shielded canister payload. The DCF for the RH-TRU 72-B with the NS15 neutron shielded canister payload and polynomial curve fit of the minimum value is provided in Figure 5.5-4.

Application of the maximum activity limits provided in Table 5.5-4 and Table 5.5-5 and the DCF summarized below can conveniently be used to ensure compliance with 10 CFR §71.47 and §71.51 dose rate requirements for the RH-TRU 72-B with a NS15 neutron shielded canister payload through the process defined in Section 5.5.4, *Determination of Acceptable Activity*:

$$DCF_{NS15} = (0.0035)\,\rho^3 - (0.0554)\,\rho^2 + (0.6338)\,\rho + 0.3698$$

where ρ is the density of the source region in units of grams per cubic centimeter (g/cc).

Table 5.5-4 – RH-TRU 72-B – NS15 Neutron Shielded Canister Gamma Activity Limits

Case	Source Type	Energy (MeV)	Calculated Dose Rate (mrem/hr)	Tally Error	Allowable Activity (γ/s)
9ng100.i	Concentrated	0.5	2.32E-15	1.1%	4.26E+15
9ng101.i	Concentrated	0.6	3.01E-14	0.4%	3.31E+14
9ng102.i	Concentrated	0.8	4.99E-13	0.3%	2.00E+13
9ng103.i	Concentrated	1	2.36E-12	0.3%	4.22E+12
9ng104.i	Concentrated	1.25	8.00E-12	0.5%	1.24E+12
9ng105.i	Concentrated	1.5	1.72E-11	0.6%	5.79E+11
9ng106.i	Concentrated	1.75	2.94E-11	0.6%	3.38E+11
9ng107.i	Concentrated	2	4.33E-11	0.6%	2.30E+11
9ng108.i	Concentrated	2.5	7.25E-11	0.7%	1.37E+11
9ng109.i	Concentrated	4	1.46E-10	0.9%	6.78E+10
9ng110.i	Concentrated	6	2.02E-10	1.0%	4.91E+10
9ng111.i	Concentrated	10	2.71E-10	1.1%	3.66E+10
9ng120.i	Distributed	0.5	6.91E-16	1.0%	1.43E+16
9ng121.i	Distributed	0.6	9.96E-15	0.5%	9.99E+14
9ng122.i	Distributed	0.8	1.95E-13	0.3%	5.12E+13
9ng123.i	Distributed	1	1.03E-12	0.3%	9.71E+12
9ng124.i	Distributed	1.25	3.80E-12	0.8%	2.61E+12
9ng125.i	Distributed	1.5	8.72E-12	0.5%	1.14E+12
9ng126.i	Distributed	1.75	1.56E-11	0.6%	6.39E+11
9ng127.i	Distributed	2	2.35E-11	0.6%	4.22E+11
9ng128.i	Distributed	2.5	4.09E-11	0.7%	2.43E+11
9ng129.i	Distributed	4	8.62E-11	0.9%	1.15E+11
9ng130.i	Distributed	6	1.21E-10	1.0%	8.20E+10
9ng131.i	Distributed	10	1.58E-10	1.0%	6.28E+10

Table 5.5-5 – RH-TRU 72-B – NS15 Neutron Shielded Canister Neutron Activity Limits

Case	Source Type	Energy (MeV)	Calculated Dose Rate (mrem/hr)	Tally Error	Allowable Activity (n/s)
9nn100.i	Concentrated	0.1	2.99E-11	1.8%	3.29E+11
9nn101.i	Concentrated	0.2	5.70E-11	1.8%	1.72E+11
9nn102.i	Concentrated	0.3	1.34E-10	2.2%	7.30E+10
9nn103.i	Concentrated	0.5	6.02E-10	1.9%	1.63E+10
9nn104.i	Concentrated	0.75	1.93E-09	1.3%	5.10E+09
9nn105.i	Concentrated	1	4.12E-09	1.2%	2.40E+09
9nn106.i	Concentrated	1.25	7.28E-09	1.1%	1.36E+09
9nn107.i	Concentrated	1.5	1.04E-08	0.9%	9.57E+08
9nn108.i	Concentrated	1.75	1.21E-08	0.8%	8.21E+08
9nn109.i	Concentrated	2	1.55E-08	0.7%	6.41E+08
9nn110.i	Concentrated	2.5	1.95E-08	0.6%	5.10E+08
9nn111.i	Concentrated	5	4.03E-08	0.4%	2.47E+08
9nn112.i	Concentrated	10	6.69E-08	0.3%	1.49E+08
9nn113.i	Concentrated	15	1.05E-07	0.3%	9.53E+07
9nn120.i	Distributed	0.1	2.69E-11	1.8%	3.65E+11
9nn121.i	Distributed	0.2	4.88E-11	1.7%	2.02E+11
9nn122.i	Distributed	0.3	1.10E-10	2.3%	8.89E+10
9nn123.i	Distributed	0.5	4.81E-10	2.1%	2.04E+10
9nn124.i	Distributed	0.75	1.62E-09	1.5%	6.08E+09
9nn125.i	Distributed	1	3.54E-09	1.2%	2.79E+09
9nn126.i	Distributed	1.25	5.87E-09	1.2%	1.68E+09
9nn127.i	Distributed	1.5	8.41E-09	1.0%	1.18E+09
9nn128.i	Distributed	1.75	1.01E-08	0.9%	9.82E+08
9nn129.i	Distributed	2	1.25E-08	0.8%	7.91E+08
9nn130.i	Distributed	2.5	1.58E-08	0.7%	6.28E+08
9nn131.i	Distributed	5	3.27E-08	0.5%	3.04E+08
9nn132.i	Distributed	10	5.53E-08	0.4%	1.80E+08
9nn133.i	Distributed	15	8.88E-08	0.3%	1.12E+08

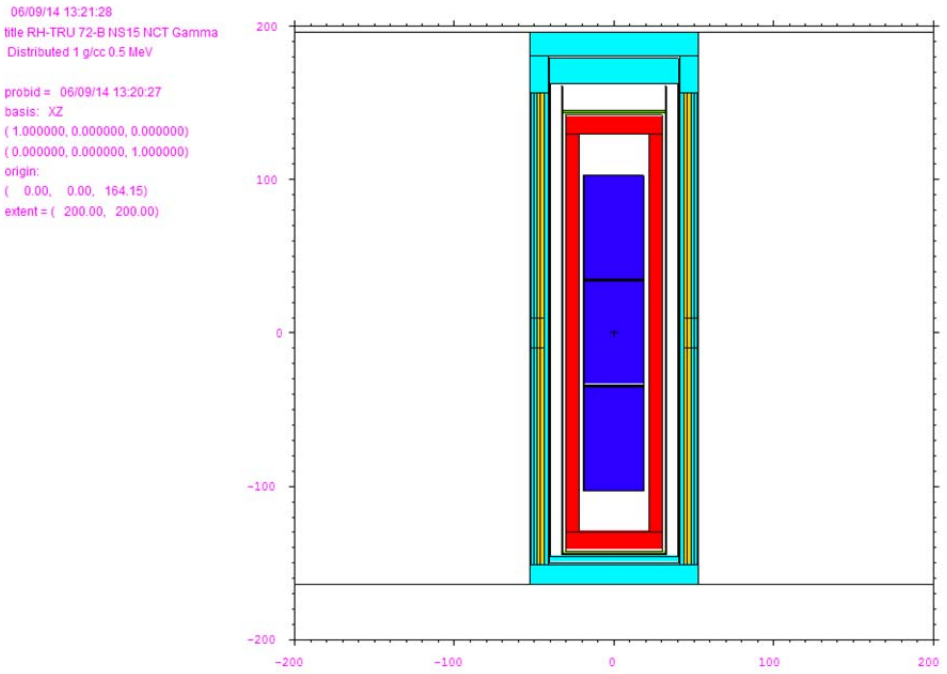

Figure 5.5-3 – RH-TRU 72-B – NS15 Neutron Shielded Canister MCNP Model for Distributed Source at Unit Density

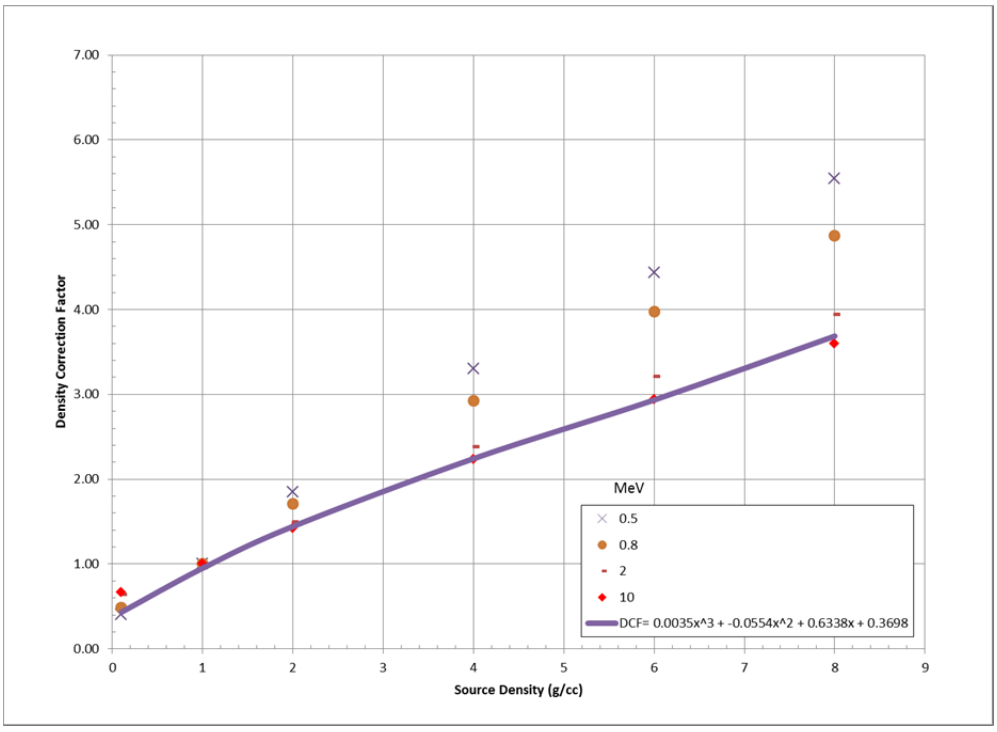

Figure 5.5-4 – RH-TRU 72-B – NS15 Neutron Shielded Canister DCF

5.5.3 NS30 Neutron Shielded Canister

The maximum allowed gamma and neutron activity for a concentrated and distributed unit-density source in a RH-TRU 72-B with a NS30 neutron shielded canister payload is given in Table 5.5-6 and Table 5.5-7, respectively. Figure 5.5-5 illustrates the source models for the unit-density distributed source with the NS30 neutron shielded canister payload. The DCF for the RH-TRU 72-B with the NS30 neutron shielded canister payload and polynomial curve fit of the minimum value is provided in Figure 5.5-6.

Application of the maximum activity limits provided in Table 5.5-6 and Table 5.5-7 and the DCF summarized below can conveniently be used to ensure compliance with 10 CFR §71.47 and §71.51 dose rate requirements for the RH-TRU 72-B with a NS30 neutron shielded canister payload through the process defined in Section 5.5.4, *Determination of Acceptable Activity*:

$$DCF_{NS30} = (0.0013)\,\rho^3 - (0.0430)\,\rho^2 + (0.6786)\,\rho + 0.2942$$

where ρ is the density of the source region in units of grams per cubic centimeter (g/cc).

Table 5.5-6 – RH-TRU 72-B – NS30 Neutron Shielded Canister Gamma Activity Limits

Case	Source Type	Energy (MeV)	Calculated Dose Rate (mrem/hr)	Tally Error	Allowable Activity (γ/s)
8ng100.i	Concentrated	0.5	3.48E-15	0.9%	2.85E+15
8ng101.i	Concentrated	0.6	4.39E-14	0.4%	2.27E+14
8ng102.i	Concentrated	0.8	6.84E-13	0.3%	1.46E+13
8ng103.i	Concentrated	1	3.12E-12	0.3%	3.19E+12
8ng104.i	Concentrated	1.25	1.02E-11	0.5%	9.78E+11
8ng105.i	Concentrated	1.5	2.13E-11	0.6%	4.67E+11
8ng106.i	Concentrated	1.75	3.58E-11	0.6%	2.78E+11
8ng107.i	Concentrated	2	5.15E-11	0.7%	1.93E+11
8ng108.i	Concentrated	2.5	8.28E-11	0.7%	1.20E+11
8ng109.i	Concentrated	4	1.61E-10	0.9%	6.15E+10
8ng110.i	Concentrated	6	2.18E-10	1.0%	4.55E+10
8ng111.i	Concentrated	10	2.82E-10	1.1%	3.51E+10
8ng120.i	Distributed	0.5	7.18E-16	1.0%	1.38E+16
8ng121.i	Distributed	0.6	1.04E-14	0.5%	9.54E+14
8ng122.i	Distributed	0.8	2.00E-13	0.3%	4.99E+13
8ng123.i	Distributed	1	1.05E-12	0.3%	9.52E+12
8ng124.i	Distributed	1.25	3.80E-12	0.4%	2.62E+12
8ng125.i	Distributed	1.5	8.75E-12	0.5%	1.14E+12
8ng126.i	Distributed	1.75	1.54E-11	0.5%	6.46E+11
8ng127.i	Distributed	2	2.33E-11	0.6%	4.26E+11
8ng128.i	Distributed	2.5	4.02E-11	0.7%	2.47E+11
8ng129.i	Distributed	4	8.17E-11	0.9%	1.21E+11
8ng130.i	Distributed	6	1.11E-10	0.9%	8.92E+10
8ng131.i	Distributed	10	1.44E-10	1.0%	6.86E+10

Table 5.5-7 – RH-TRU 72-B – NS30 Neutron Shielded Canister Neutron Activity Limits

Case	Source Type	Energy (MeV)	Calculated Dose Rate (mrem/hr)	Tally Error	Allowable Activity (n/s)
8nn100.i	Concentrated	0.1	6.28E-10	0.8%	1.58E+10
8nn101.i	Concentrated	0.2	1.14E-09	0.9%	8.72E+09
8nn102.i	Concentrated	0.3	2.81E-09	1.0%	3.52E+09
8nn103.i	Concentrated	0.5	8.13E-09	0.8%	1.22E+09
8nn104.i	Concentrated	0.75	1.54E-08	0.9%	6.42E+08
8nn105.i	Concentrated	1	2.42E-08	0.8%	4.10E+08
8nn106.i	Concentrated	1.25	3.50E-08	0.7%	2.84E+08
8nn107.i	Concentrated	1.5	4.14E-08	0.6%	2.40E+08
8nn108.i	Concentrated	1.75	4.06E-08	0.6%	2.45E+08
8nn109.i	Concentrated	2	4.77E-08	0.6%	2.08E+08
8nn110.i	Concentrated	2.5	5.17E-08	0.5%	1.93E+08
8nn111.i	Concentrated	5	7.29E-08	0.4%	1.37E+08
8nn112.i	Concentrated	10	9.60E-08	0.4%	1.04E+08
8nn113.i	Concentrated	15	1.42E-07	0.4%	7.01E+07
8nn120.i	Distributed	0.1	5.72E-10	0.8%	1.73E+10
8nn121.i	Distributed	0.2	9.67E-10	0.9%	1.02E+10
8nn122.i	Distributed	0.3	2.34E-09	1.0%	4.22E+09
8nn123.i	Distributed	0.5	6.80E-09	0.8%	1.46E+09
8nn124.i	Distributed	0.75	1.39E-08	1.0%	7.12E+08
8nn125.i	Distributed	1	2.20E-08	0.8%	4.51E+08
8nn126.i	Distributed	1.25	2.95E-08	0.7%	3.37E+08
8nn127.i	Distributed	1.5	3.52E-08	0.7%	2.82E+08
8nn128.i	Distributed	1.75	3.58E-08	0.7%	2.77E+08
8nn129.i	Distributed	2	3.97E-08	0.6%	2.50E+08
8nn130.i	Distributed	2.5	4.28E-08	0.6%	2.32E+08
8nn131.i	Distributed	5	6.10E-08	0.5%	1.63E+08
8nn132.i	Distributed	10	8.14E-08	0.4%	1.22E+08
8nn133.i	Distributed	15	1.24E-07	0.4%	8.03E+07

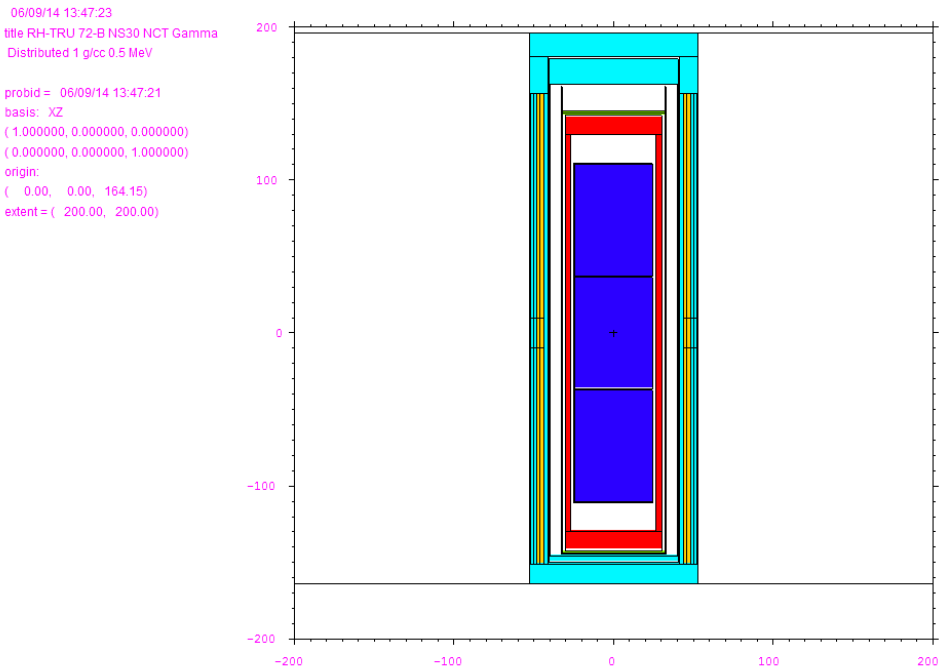

Figure 5.5-5 – RH-TRU 72-B – NS30 Neutron Shielded Canister MCNP Model for Distributed Source at Unit Density

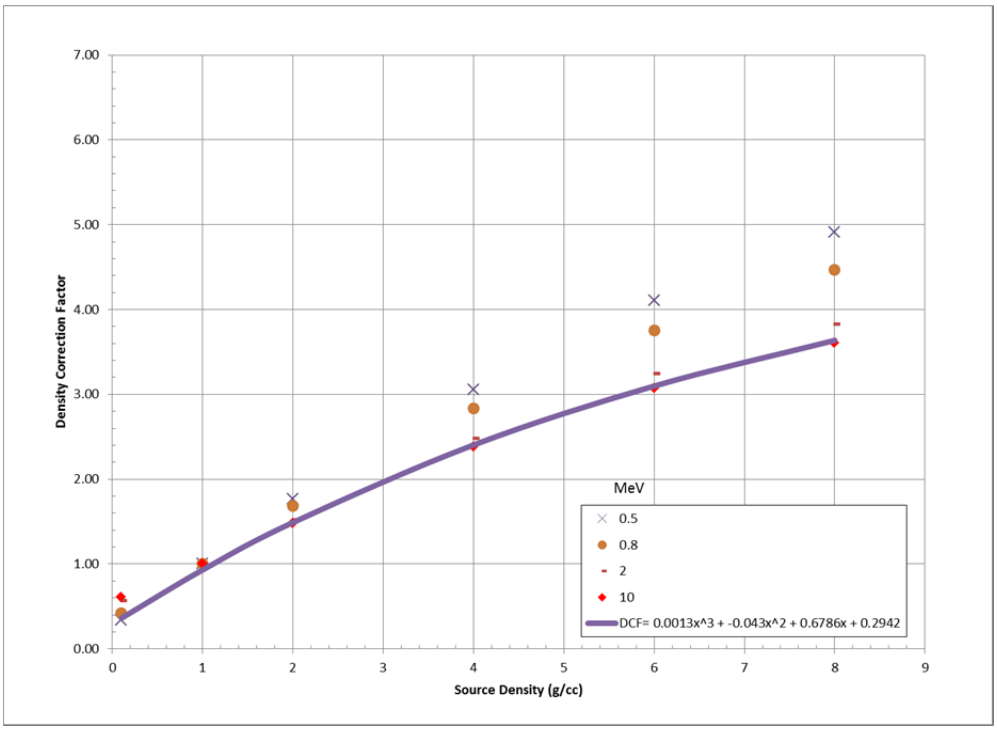

Figure 5.5-6 – RH-TRU 72-B – NS30 Neutron Shielded Canister DCF

5.5.4 Determination of Acceptable Activity

The RH-TRU 72-B package activity limits for the RH-TRU waste canister, NS15 neutron shielded canister, and NS30 neutron shielded canister payloads shall be determined per the following to ensure compliance with 10 CFR §71.47 and §71.51:

1. Determine the list of radionuclides and associated activity (Ci) for the package contents.

2. Optionally determine if the package contents are eligible to utilize results obtained from a distributed source model when determining acceptable activity levels as follows:

Case A: For drums overpacked in a payload canister, the canister contents may always be considered sufficiently distributed to utilize results obtained from a distributed source model. This is primarily because differences in distance attenuation effects for a source that is evenly distributed to and throughout three drums (i.e., per a distributed source model) versus it being evenly distributed to, but centered in the three drums (i.e., per a concentrated source model), are insignificant. Quantitatively, with reference to Table 5.5-3,[1] the maximum difference in allowable activity between distributed and concentrated source types at a given energy level is 9.8% at 0.2 MeV. This difference is considered to be acceptable as it falls within the 10% administrative margin adopted in Step 10, below.

Case B: For waste direct-loaded into a payload canister, the canister contents may only utilize the results obtained from the distributed source model if the contents of the canister meet the definition of "distributed throughout" from NUREG-1608[2]. This is primarily because differences in distance attenuation effects for a source that is distributed throughout a canister versus it being concentrated in the center of the canister are very significant.

3. If eligible to utilize results obtained from a distributed source model, optionally determine the density (ρ, g/cc) of the contents in the payload canister (utilize the minimum density value in the case of multiple drums overpacked in a payload canister).

4. For each gamma-emitting radionuclide in the contents, obtain all discrete gamma energies and intensities from Kinsey[3] (or an equivalent nuclear structure and decay database), ignoring energies less than 0.5 MeV or energies with associated intensities less than 0.1%. Radionuclides with photon energies above 10 MeV with intensities greater than or equal to 0.1% are not acceptable for transport.

5. For each discrete gamma energy, determine its source strength (γ/s).

6. For each discrete gamma energy, determine the ratio of its source strength to the allowable activity determined by logarithmically interpolating from Table 5.5-2, Table 5.5-4, or Table

[1] Table 5.5-3 is considered here because it corresponds to the only case where, as indicated at the end of the next-to-last paragraph of Section 5.5, *Activity Limits*, the distributed source has an activity allowable that differs from that of the concentrated source due to distance attenuation effects only.

[2] J. Cook, R. Lewis, E. Easton, NRC, R. Boyle, DOT, R. Pope, ORNL, *Categorizing and Transporting Low Specific Activity Materials and Surface Contaminated Objects*, NUREG-1608, RAMREG-003, June 1998.

[3] R.R. Kinsey, *et al.*, *The NUDAT/PCNUDAT Program for Nuclear Data,* paper submitted to the 9th International Symposium of Capture Gamma-Ray Spectroscopy and Related Topics, Budapest, Hungary, October 1996; data extracted from the NUDAT database, version September 7, 2000, CD-ROM.

5.5-6, as applicable to the configuration (payload canister and source type). Calculate the sum of fractions for the gamma source term by adding the ratios defined above. If the source qualifies as distributed, optionally obtain the allowable activity by calculating the DCF based on the minimum density value and multiplying the unit-density allowable activity by the DCF.

7. For each neutron-emitting radionuclide in the contents, obtain the neutron source spectrum from ED-042[4] (or an equivalent nuclear reference or Sources[5] analysis), ignoring energies less than 0.10 MeV or energies that contribute less than 1% of the total source strength. Radionuclides with neutron energies above 15 MeV that contribute greater than or equal to 1% of the total source strength are not acceptable for transport.

8. For each neutron energy interval, determine its source strength (n/s).

9. For each neutron energy interval, determine the ratio of its source strength to the allowable activity determined by logarithmically interpolating from Table 5.5-3, Table 5.5-5, or Table 5.5-7, as applicable to the configuration (payload canister and source type). Calculate the sum of fractions for the neutron source term by adding the ratios defined above.

10. For the payload, ensure that the combined sum of the sum of fractions for the gamma and the neutron source term is less than or equal to 0.9.[6] However, if the canister is direct-loaded and its contents do not meet the definition of "distributed throughout" per NUREG-1608, ensure that the combined sum of fractions is less than or equal to 0.45.

11. If the canister contains overpacked drums, ensure that the combined sum of the sum of fractions for the gamma and neutron source term for each drum is less than or equal to 0.45, if Steps 3 through 9, above, are repeated specific to that drum.

5.5.4.1 Acceptable Activity Examples

5.5.4.1.1 Concentrated ^{60}Co Source in RLC in RH-TRU 72-B

A RLC payload consists of a concentrated ^{60}Co source of 7 Ci in the form of a metal capsule 1 cm in diameter and 3 cm long.

1. The radionuclide is ^{60}Co with a total activity of 7 Ci.

2. The content is not a distributed source.

3. NA

4. See Table 5.5-8.

5. See Table 5.5-8.

---

[4] Packaging Technology, Inc., *Neutron Source Rates for TRU Waste*, ED-042, Tacoma, WA, November 2000.

[5] Los Alamos National Laboratory, *SOURCES 4A: A Code for Calculating (α,n), Spontaneous Fission, and Delayed Neutron Sources and Spectra*, LA-13639-MS, Los Alamos, New Mexico, September 1999.

[6] The 10% administrative margin, in conjunction with the conservative use of determining source limits at two meters from the edge of the package versus two meters from the edge of the conveyance and imposition of an individual drum activity limit (identified in Section 5.3.1, *Configuration of Source and Shielding*), accounts for potential source movement during NCT.

6. See Table 5.5-8 (using Table 5.5-2 values).

7. NA

8. NA

9. NA

10. The sum of fractions is equal to 0.652, so the package does not meet the allowable canister activity limit fraction of 0.45, which is applicable for direct-loaded canisters containing contents that do not qualify as "distributed throughout" per NUREG-1608.

11. NA

Table 5.5-8 – Acceptable Activity Example #1

Gamma Energy (MeV)	Intensity (%)	Strength (γ/s)	Allowable Fraction	Comment
0.34693	7.6000E-03	0.0000E+00	0.00E+00	Ignored: Intensity < 0.1%
0.82628	7.6000E-03	0.0000E+00	0.00E+00	Ignored: Intensity < 0.1%
1.173237	9.9974E+01	2.5893E+11	2.33E-01	
1.332501	9.9986E+01	2.5896E+11	4.19E-01	
2.15877	1.1100E-03	0.0000E+00	0.00E+00	Ignored: Intensity < 0.1%
2.505	2.0000E-06	0.0000E+00	0.00E+00	Ignored: Intensity < 0.1%
Total			6.52E-01	Not Authorized for Transport, F > 0.45

5.5.4.1.2 Distributed ^{252}Cf Source in NS30 in RH-TRU 72-B

A NS30 payload consists of three 30-gallon drums containing debris waste contaminated with a ^{252}Cf source term totaling 0.05 Ci. The dose rates of the drums range from 50 to 100 mrem/hr.

1. The radionuclide is ^{252}Cf with a total activity of 0.05 Ci.

2. The content is a distributed source under Case A.

3. Minimum contents weight of an individual drum is 150 lb with a fill volume of 50%. Minimum density is $[(150 \text{ lb})/(3{,}569 \text{ in}^3)] \times [(27.68 \text{ g/cm}^3)/(1 \text{ lb/in}^3)] = 1.16 \text{ g/cm}^3$.

4. See Table 5.5-9.

5. See Table 5.5-9.

6. See Table 5.5-9 (using Table 5.5-6 values):

$$DCF = (0.0013)\,\rho^3 - (0.0430)\,\rho^2 + (0.6786)\,\rho + 0.2942 = 1.03$$

7. See Table 5.5-9.

8. See Table 5.5-9:

Specific Activity = 536 Ci/g

9. See Table 5.5-9 (using Table 5.5-7 values).

10. The sum of fractions is equal to 0.839, so the package meets the allowable canister activity limit fraction of 0.9.

11. Since the dose rate of the drums range from 50 to 100 mrem/hr, the contribution from the worst-case drum can only be twice the least-case drum. Therefore, the sum of fractions for the worst-case drum will be no more than 0.839/2 = 0.42, so the package meets the allowable individual drum activity limit fraction of 0.45.

Table 5.5-9 – Acceptable Activity Example #2

Gamma Energy (MeV)	Intensity (%)	Strength (γ/s)	Allowable Fraction	Comment
0.0434	1.4800E-02	0.0000E+00	0.00E+00	Ignored: Energy < 0.5 MeV Intensity < 0.1%
0.1002	1.3000E-02	0.0000E+00	0.00E+00	Ignored: Energy < 0.5 MeV Intensity < 0.1%
0.1545	5.0400E-04	0.0000E+00	0.00E+00	Ignored: Energy < 0.5 MeV Intensity < 0.1%
Total Gamma			0.00E+00	DCF has no effect due to screening
Neutron Energy (MeV)	**Strength (n/s/g)**	**Strength (n/s)**	**Allowable Fraction**	**Comment**
0.5	1.8000E+11	1.6791E+07	1.15E-02	
1	2.7100E+11	2.5280E+07	5.60E-02	
2	5.3600E+11	5.0000E+07	2.00E-01	
3	4.1000E+11	3.8246E+07	1.81E-01	
4	2.7300E+11	2.5466E+07	1.39E-01	
6	2.6600E+11	2.4813E+07	1.64E-01	
8	8.5300E+10	7.9571E+06	5.93E-02	
10	2.4400E+10	2.2761E+06	1.86E-02	
15	8.3600E+09	7.7985E+05	9.71E-03	
Total Neutron			8.39E-01	DCF not applicable to neutrons
Total Gamma & Neutron			8.39E-01	Authorized for Transport, F ≤ 0.9

5.5.4.1.3 Concentrated ^{137}Cs and ^{239}Pu Sources in NS15 in RH-TRU 72-B

A RH-TRU 72-B payload consists of an NS15, containing one 15-gallon drum of debris waste (with two dunnage drums) contaminated with a ^{137}Cs source term totaling 500 Ci and 323 grams of ^{239}Pu (20 Ci).

1. The radionuclides are ^{137}Cs and ^{239}Pu with a total activity of 500 and 20 Ci, respectively.

2. The content qualifies as a distributed source under Case A, but is conservatively treated as a concentrated source.

3. NA

4. See Table 5.5-10.

5. See Table 5.5-10 (using Table 5.5-4 values).

6. See Table 5.5-10.

7. See Table 5.5-10.

8. See Table 5.5-10:

^{239}Pu Specific Activity = 0.062 Ci/g

9. See Table 5.5-10 (using Table 5.5-5 values).

10. The sum of fractions is equal to 0.124, so the package meets the allowable canister activity limit fraction of 0.9.

11. The sum of fractions is equal to 0.124, so the package also meets the allowable individual drum activity limit fraction of 0.45.

Table 5.5-10 – Acceptable Activity Example #3

Gamma Energy (MeV)	Intensity (%)	Strength (γ/s)	Allowable Fraction	Comment
0.2835	5.8000E-04	0.0000E+00	0.00E+00	^{137}Cs – Ignored: Energy < 0.5 MeV Intensity < 0.1%
0.661657	8.5100E+01	1.5744E+13	1.24E-01	^{137}Cs
0.129296	6.3100E-03	0.0000E+00	0.00E+00	^{239}Pu – Ignored: Energy < 0.5 MeV Intensity < 0.1%
0.375054	1.5540E-03	0.0000E+00	0.00E+00	^{239}Pu – Ignored: Energy < 0.5 MeV Intensity < 0.1%
0.413713	1.4660E-03	0.0000E+00	0.00E+00	^{239}Pu – Ignored: Energy < 0.5 MeV Intensity < 0.1%
Total Gamma			1.24E-01	
Neutron Energy (MeV)	**Strength (n/s/g)**	**Strength (n/s)**	**Allowable Fraction**	**Comment**
0.5	1.7300E+00	5.5806E+02	4.57E-07	
1	1.7100E+00	5.5161E+02	1.34E-06	
2	9.2900E+00	2.9968E+03	1.44E-05	
3	1.8800E+01	6.0645E+03	3.45E-05	
4	6.8400E+00	2.2065E+03	1.45E-05	
6	2.8500E-01	9.1935E+01	7.24E-07	
8	4.5800E-04	1.4774E-01	1.30E-09	
10	9.6600E-05	3.1161E-02	3.00E-10	
15	2.2800E-05	7.3548E-03	1.05E-10	
Total Neutron			6.58E-05	
Total Gamma & Neutron			1.24E-01	Authorized for Transport, F ≤ 0.45

Note: For conciseness, only ^{239}Pu gamma energies greater than 0.1 MeV with associated intensities greater than 0.001% were listed in the above table.

This page intentionally left blank.

5.6 Conclusions

Based on the geometry, materials of construction, and configuration of the RH-TRU 72-B packaging, the NCT dose rate requirement at 2 meters from the surface of the package is the most limiting for all analyzed payload configurations. Establishing compliance with a limiting NCT dose rate requirement of ≤10 mrem/hr at 2 meters from the package surface ensures compliance with the surface dose rate requirement of ≤200 mrem/hr under NCT and the ≤1,000 mrem/hr at 1 meter dose rate requirement under HAC. Therefore, application of the methodology defined in Section 5.5, *Activity Limits*, for the RH-TRU 72-B, confirmed by the preshipment dose rate measurement, ensures compliance with 10 CFR §71.47 and §71.51.

This page intentionally left blank.

5.7 Appendices

5.7.1 *Sample MCNP Input Files*
5.7.1.1 *RH-TRU 72-B – RH-TRU Waste Canister*
5.7.1.1.1 *NCT Concentrated 60Co Gamma Source – 7ng001.i*
5.7.1.1.2 *NCT Concentrated 252Cf Neutron Source – 7nn001.i*
5.7.1.1.3 *NCT Distributed 0.5 MeV Gamma Source – 7ng120.i*
5.7.1.1.4 *NCT Distributed 0.1 MeV Neutron Source – 7nn120.i*
5.7.1.1.5 *HAC 60Co Gamma Source – 7hg001.i*
5.7.1.1.6 *HAC 252Cf Neutron Source – 7hn001.i*
5.7.1.2 *RH-TRU 72-B – NS15 Neutron Shielded Canister*
5.7.1.2.1 *NCT Distributed 0.5 MeV Gamma Source – 9ng120.i*
5.7.1.2.2 *HAC 60Co Gamma Source – 9hg001.i*
5.7.1.3 *RH-TRU 72-B – NS30 Neutron Shielded Canister*
5.7.1.3.1 *NCT Concentrated 60Co Gamma Source – 8ng001.i*
5.7.1.3.2 *HAC 252Cf Neutron Source – 8hn001.i*
5.7.2 *Sample MCNP Output Files*
5.7.2.1 *RH-TRU 72-B – RH-TRU Waste Canister*
5.7.2.1.1 *NCT Concentrated 60Co Gamma Source – 7ng001.io*
5.7.2.1.2 *NCT Concentrated 252Cf Neutron Source – 7nn001.io*
5.7.2.1.3 *NCT Distributed 0.5 MeV Gamma Source – 7ng120.io*
5.7.2.1.4 *NCT Distributed 0.1 MeV Neutron Source – 7nn120.io*
5.7.2.1.5 *HAC 60Co Gamma Source – 7hg001.io*
5.7.2.1.6 *HAC 252Cf Neutron Source – 7hn001.io*
5.7.2.2 *RH-TRU 72-B – NS15 Neutron Shielded Canister*
5.7.2.2.1 *NCT Distributed 0.5 MeV Gamma Source – 9ng120.io*
5.7.2.2.2 *HAC 60Co Gamma Source – 9hg001.io*
5.7.2.3 *RH-TRU 72-B – NS30 Neutron Shielded Canister*
5.7.2.3.1 *NCT Concentrated 60Co Gamma Source – 8ng001.io*
5.7.2.3.2 *HAC 252Cf Neutron Source – 8hn001.io*

This page intentionally left blank.

5.7.1 Sample MCNP Input Files

5.7.1.1 RH-TRU 72-B – RH-TRU Waste Canister

5.7.1.1.1 NCT Concentrated 60Co Gamma Source – 7ng001.i

```
title RH-TRU 72-B RLC NCT Gamma Concentrated 1 g/cc Co60
C
C Cell Cards
C
10  1 -1         10  -11  -16                 imp:p=1    $ Source #1
11  1 -1         12  -13  -17                 imp:p=1    $ Source #2
12  1 -1         14  -15  -18                 imp:p=1    $ Source #3
20  0            20  -21  -26
              (-10:  11:  16)                 imp:p=1    $ Drum #1 cavity
21  0            22  -23  -27
              (-12:  13:  17)                 imp:p=1    $ Drum #2 cavity
22  0            24  -25  -28
              (-14:  15:  18)                 imp:p=1    $ Drum #3 cavity
40  0            41  -45  -43
               #10  #11  #12
               #20  #21  #22                  imp:p=1    $ RLC cavity
41  3 -7.85260   40  -41  -42                 imp:p=1    $ RLC base
42  3 -7.85260   41  -46   43  -42            imp:p=1    $ RLC shell
43  3 -7.85260   45  -44  -43                 imp:p=1    $ RLC lid
50  0            51  -53  -55
              (-40:  42:  46)
             :( 44  -46  -43)                 imp:p=1    $ IV cavity
51  2 -8.01280   50  -51  -52                 imp:p=1    $ IV base
52  2 -8.01280   51  -55   53  -52            imp:p=2    $ IV shell
53  2 -8.01280   55  -54  -52                 imp:p=1    $ IV lid
60  0            61  -63  -65
              (-50:  52:  54)                 imp:p=2    $ OC cavity
61  2 -8.01280   60  -61  -69                 imp:p=1    $ OC base
62  2 -8.01280   61  -66   65  -64            imp:p=5    $ OC ishell
63  4 -11.3500   61  -66   64  -76  71        imp:p=3E1  $ OC lead in
64  4 -11.3500   61  -66   76  -68  71        imp:p=3E2  $ OC lead out
65  2 -8.01280   61  -66   68  -77  71        imp:p=3E3  $ OC oshell in
66  2 -8.01280   61  -66   77  -67  71        imp:p=6E3  $ OC oshell out
67  0            61  -66   67  -70  71        imp:p=1E5  $ OC airgap
68  2 -8.01280   61  -66   70  -69  71        imp:p=2E5  $ OC tshell
69  2 -8.01280   66  -63   65  -69            imp:p=1    $ OC flange
70  2 -8.01280   63  -62  -69                 imp:p=1    $ OC lid
71  4 -11.3500   64  -78  -71                 imp:p=3E1  $ OC lead punct in
72  4 -11.3500   78  -73  -71                 imp:p=3E2  $ OC lead punct out
73  2 -8.01280   73  -79  -71                 imp:p=3E3  $ OC oshell punct in
74  2 -8.01280   79  -72  -71                 imp:p=6E3  $ OC oshell punct out
75  0            72  -75  -71                 imp:p=1E5  $ OC airgap punct
76  2 -8.01280   75  -74  -71                 imp:p=2E5  $ OC tshell punct
777 0            69  -80   60  -62            imp:p=2E5  $ Outside to tally
888 0           -999
              (-60:  80:  62)                 imp:p=1E1  $ Outside pkg
999 0            999                          imp:p=0    $ Outside world

C
C Geometry Cards
C
10  pz 88.9                                                $ Source #1 bottom
11  pz 91.44                                                 $ Source #1 top
12  pz 162.878                                              $ Source #2 bottom
13  pz 165.418                                              $ Source #2 top
14  pz 236.855                                              $ Source #3 bottom
15  pz 239.395                                              $ Source #3 top
16  c/z 0 0 1.27                                            $ Source #1 radius
17  c/z 0 0 1.27                                            $ Source #2 radius
18  c/z 0 0 1.27                                            $ Source #3 radius
C
20  pz 53.34                                                 $ Drum #1 bottom
21  pz 127                                                 $ Drum #1 top
22  pz 127.318                                              $ Drum #2 bottom
23  pz 200.978                                              $ Drum #2 top
24  pz 201.295                                              $ Drum #3 bottom
25  pz 274.955                                              $ Drum #3 top
26  c/z 0 0 24.765                                           $ Drum #1 radius
```

```
27  c/z 0 0 24.765                                  $ Drum #2 radius
28  c/z 0 0 24.765                                  $ Drum #3 radius
C
40  pz 19.368                                       $ RLC base (outside)
41  pz 20.638                                       $ RLC base (inside)
42  c/z 0 0 33.02                                   $ RLC shell (outside)
43  c/z 0 0 32.385                                  $ RLC shell (inside)
44  pz 309.563                                      $ RLC lid (outside)
45  pz 307.658                                      $ RLC lid (inside)
46  pz 325.438                                      $ RLC top (outside)
C
50  pz 14.288                                       $ IV base (outside)
51  pz 18.098                                       $ IV base (inside)
52  c/z 0 0 40.64                                   $ IV shell (outside)
53  c/z 0 0 39.688                                  $ IV shell (inside)
54  pz 343.218                                      $ IV top (outside)
55  pz 326.708                                      $ IV top (inside)
C
60  pz 0                                            $ OC bottom (outside)
61  pz 12.7                                         $ OC bottom (inside)
62  pz 360.045                                      $ OC top (outside)
63  pz 344.805                                      $ OC top (inside)
64  cz 43.656                                       $ OC ishell (outside)
65  cz 41.116                                       $ OC ishell (inside)
66  pz 320.675                                      $ OC lead (upper)
67  cz 52.229                                       $ OC oshell (outside)
68  cz 48.419                                       $ OC oshell (inside)
69  cz 52.838                                       $ OC therm (outside)
70  cz 52.495                                       $ OC therm (inside)
71  c/x 0 164.148 10.033                            $ OC puncture radius
72  cz 52.229                                       $ OC oshell punct (out)
73  cz 48.419                                       $ OC oshell punct (in)
74  cz 52.838                                       $ OC therm punct (out)
75  cz 52.495                                       $ OC therm punct (in)
76  cz 46.038                                       $ OC lead (mid)
77  cz 50.324                                       $ OC oshell (mid)
78  cz 46.038                                       $ OC lead punct (mid)
79  cz 50.324                                       $ OC oshell punct (mid)
C
80  cz 252.838                                      $ 2-meter from OC therm
C
777 pz 161.608                                      $ Ring tally (lower)
888 pz 166.688                                      $ Ring tally (upper)
999 sz 164.148 379.838                              $ Outside world

C
C Physics Cards
C
mode p
C
C Source Cards
C
C Cylindrical Sources
sdef pos=d1 erg=d2 par=2 axs=0 0 1 rad=d3 ext=d4
sc1 Co60
C Source Position and Fraction
si1 L 0 0 90.17
      0 0 164.148
      0 0 238.125
sp1   1 1 1
C Source Energy (MeV) and Intensity (%)
si2 L 3.469300E-01 8.262800E-01 1.173237E+00 1.332501E+00
     2.158770E+00 2.505000E+00
sp2 7.600000E-03 7.600000E-03 9.997360E+01 9.998560E+01
     1.110000E-03 2.000000E-06
C Source Radius
si3 0 1.27
sp3 -21 1
C Source Extent
si4 -1.27 1.27
sp4 -21 0
C
C Tally Cards
C
f2:p 69
fc2 Surface Dose (mrem/hr)                          $ Surface detector
fs2 888 777 t
sd2 1.0 1686.525 1.0 1.0                            $ Surface tally area
f22:p 80
fc22 2-meter Dose (mrem/hr)                         $ 2-m detector
fs22 888 777 t
```

```
sd22 1.0 8070.229 1.0 1.0                                   $ Surface tally area
C
C ANSI/ANS-6.1.1-1977 Gamma Flux to Dose Factors (mrem/hr)
de0 1.0e-02 3.0e-02 5.0e-02 7.0e-02 1.0e-01                 $ Energy (Mev)
     1.5e-01 2.0e-01 2.5e-01 3.0e-01 3.5e-01
     4.0e-01 4.5e-01 5.0e-01 5.5e-01 6.0e-01
     6.5e-01 7.0e-01 8.0e-01 1.00 1.40
     1.80 2.20 2.60 2.80 3.25
     3.75 4.25 4.75 5.00 5.25
     5.75 6.25 6.75 7.50 9.00
     11.00 13.00 15.0000
df0 3.96e-03 5.82e-04 2.90e-04 2.58e-04 2.83e-04            $ Conversion (mrem/hr)
     3.79e-04 5.01e-04 6.31e-04 7.59e-04 8.78e-04
     9.85e-04 1.08e-03 1.17e-03 1.27e-03 1.36e-03
     1.44e-03 1.52e-03 1.68e-03 1.98e-03 2.51e-03
     2.99e-03 3.42e-03 3.82e-03 4.01e-03 4.41e-03
     4.83e-03 5.23e-03 5.60e-03 5.80e-03 6.01e-03
     6.37e-03 6.74e-03 7.11e-03 7.66e-03 8.77e-03
     1.03e-02 1.18e-02 1.33e-02
C
C Material Cards
C
m1   40000 -1.00                                           $ Zirconium
m2   14000 -0.01                                           $ Stainless Steel
     24000 -0.19
     25000 -0.02
     26000 -0.68
     28000 -0.10
m3   26000 -1.00                                           $ Carbon Steel (iron)
m4   82000 -1.00                                           $ Lead
C
C Runtime and Print Cards
C
prdmp j j 1 2
ctme 120
```

5.7.1.1.2 NCT Concentrated 252Cf Neutron Source – 7nn001.i

```
title RH-TRU 72-B RLC NCT Neutron Concentrated 1 g/cc Cf252
C
C Cell Cards
C
10  1 -1         10  -11  -16                imp:n=1    $ Source #1
11  1 -1         12  -13  -17                imp:n=1    $ Source #2
12  1 -1         14  -15  -18                imp:n=1    $ Source #3
20  0            20  -21  -26
              (-10:  11:  16)                imp:n=1    $ Drum #1 cavity
21  0            22  -23  -27
              (-12:  13:  17)                imp:n=1    $ Drum #2 cavity
22  0            24  -25  -28
              (-14:  15:  18)                imp:n=1    $ Drum #3 cavity
40  0            41  -45  -43
              #10  #11  #12
              #20  #21  #22                  imp:n=1    $ RLC cavity
41  3 -7.85260   40  -41  -42                imp:n=1    $ RLC base
42  3 -7.85260   41  -46   43  -42           imp:n=1    $ RLC shell
43  3 -7.85260   45  -44  -43                imp:n=1    $ RLC lid
50  0            51  -53  -55
             (-40:  42:  46)
            :( 44  -46  -43)                 imp:n=1    $ IV cavity
51  2 -8.01280   50  -51  -52                imp:n=1    $ IV base
52  2 -8.01280   51  -55   53  -52           imp:n=1    $ IV shell
53  2 -8.01280   55  -54  -52                imp:n=1    $ IV lid
60  0            61  -63  -65
             (-50:  52:  54)                 imp:n=1    $ OC cavity
61  2 -8.01280   60  -61  -69                imp:n=1    $ OC base
62  2 -8.01280   61  -66   65  -64           imp:n=1    $ OC ishell
63  4 -11.3500   61  -66   64  -76  71       imp:n=1    $ OC lead in
64  4 -11.3500   61  -66   76  -68  71       imp:n=1    $ OC lead out
65  2 -8.01280   61  -66   68  -77  71       imp:n=1    $ OC oshell in
66  2 -8.01280   61  -66   77  -67  71       imp:n=1    $ OC oshell out
67  0            61  -66   67  -70  71       imp:n=1    $ OC airgap
68  2 -8.01280   61  -66   70  -69  71       imp:n=1    $ OC tshell
69  2 -8.01280   66  -63   65  -69           imp:n=1    $ OC flange
70  2 -8.01280   63  -62  -69                imp:n=1    $ OC lid
71  4 -11.3500   64  -78  -71                imp:n=1    $ OC lead punct in
72  4 -11.3500   78  -73  -71                imp:n=1    $ OC lead punct out
73  2 -8.01280   73  -79  -71                imp:n=1    $ OC oshell punct in
74  2 -8.01280   79  -72  -71                imp:n=1    $ OC oshell punct out
```

```
75  0           72  -75  -71                imp:n=1    $ OC airgap punct
76  2 -8.01280  75  -74  -71                imp:n=1    $ OC tshell punct
777 0           69  -80   60  -62            imp:n=1    $ Outside to tally
888 0          -999
              (-60:  80:  62)                imp:n=1    $ Outside pkg
999 0           999                           imp:n=0    $ Outside world

C
C Geometry Cards
C
10  pz 88.9                                                $ Source #1 bottom
11  pz 91.44                                                 $ Source #1 top
12  pz 162.878                                              $ Source #2 bottom
13  pz 165.418                                              $ Source #2 top
14  pz 236.855                                              $ Source #3 bottom
15  pz 239.395                                              $ Source #3 top
16  c/z 0 0 1.27                                            $ Source #1 radius
17  c/z 0 0 1.27                                            $ Source #2 radius
18  c/z 0 0 1.27                                            $ Source #3 radius
C
20  pz 53.34                                                 $ Drum #1 bottom
21  pz 127                                                $ Drum #1 top
22  pz 127.318                                              $ Drum #2 bottom
23  pz 200.978                                              $ Drum #2 top
24  pz 201.295                                              $ Drum #3 bottom
25  pz 274.955                                              $ Drum #3 top
26  c/z 0 0 24.765                                           $ Drum #1 radius
27  c/z 0 0 24.765                                           $ Drum #2 radius
28  c/z 0 0 24.765                                           $ Drum #3 radius
C
40  pz 19.368                                               $ RLC base (outside)
41  pz 20.638                                               $ RLC base (inside)
42  c/z 0 0 33.02                                           $ RLC shell (outside)
43  c/z 0 0 32.385                                          $ RLC shell (inside)
44  pz 309.563                                              $ RLC lid (outside)
45  pz 307.658                                              $ RLC lid (inside)
46  pz 325.438                                              $ RLC top (outside)
C
50  pz 14.288                                               $ IV base (outside)
51  pz 18.098                                               $ IV base (inside)
52  c/z 0 0 40.64                                           $ IV shell (outside)
53  c/z 0 0 39.688                                          $ IV shell (inside)
54  pz 343.218                                              $ IV top (outside)
55  pz 326.708                                              $ IV top (inside)
C
60  pz 0                                                    $ OC bottom (outside)
61  pz 12.7                                                 $ OC bottom (inside)
62  pz 360.045                                              $ OC top (outside)
63  pz 344.805                                              $ OC top (inside)
64  cz 43.656                                               $ OC ishell (outside)
65  cz 41.116                                               $ OC ishell (inside)
66  pz 320.675                                              $ OC lead (upper)
67  cz 52.229                                               $ OC oshell (outside)
68  cz 48.419                                               $ OC oshell (inside)
69  cz 52.838                                               $ OC therm (outside)
70  cz 52.495                                               $ OC therm (inside)
71  c/x 0 164.148 10.033                                    $ OC puncture radius
72  cz 52.229                                               $ OC oshell punct (out)
73  cz 48.419                                               $ OC oshell punct (in)
74  cz 52.838                                               $ OC therm punct (out)
75  cz 52.495                                               $ OC therm punct (in)
76  cz 46.038                                               $ OC lead (mid)
77  cz 50.324                                               $ OC oshell (mid)
78  cz 46.038                                               $ OC lead punct (mid)
79  cz 50.324                                               $ OC oshell punct (mid)
C
80  cz 252.838                                              $ 2-meter from OC therm
C
777 pz 161.608                                              $ Ring tally (lower)
888 pz 166.688                                              $ Ring tally (upper)
999 sz 164.148 379.838                                      $ Outside world

C
C Physics Cards
C
mode n
C
C Source Cards
C
C Cylindrical Sources
sdef pos=d1 erg=d2 par=1 axs=0 0 1 rad=d3 ext=d4
```

```
sc1 Cf252
C Source Position and Fraction
si1 L 0 0 90.17
      0 0 164.148
      0 0 238.125
sp1   1 1 1
C Source Energy (MeV) and Fraction
si2 0.1 0.5 1.0 2.0 3.0
     4.0 6.0 8.0 10.0 15.0
sp2 0.00E+00 1.80E+11 2.71E+11 5.36E+11 4.10E+11
     2.73E+11 2.66E+11 8.53E+10 2.44E+10 8.36E+09
C Source Radius
si3 0 1.27
sp3 -21 1
C Source Extent
si4 -1.27 1.27
sp4 -21 0
C
C Tally Cards
C
f2:n 69
fc2 Surface Dose (mrem/hr)                              $ Surface detector
fs2 888 777 t
sd2 1.0 1686.525 1.0 1.0                                $ Surface tally area
f22:n 80
fc22 2-meter Dose (mrem/hr)                             $ 2-m detector
fs22 888 777 t
sd22 1.0 8070.229 1.0 1.0                               $ Surface tally area
C
C ANSI/ANS-6.1.1-1977 Neutron Flux to Dose Factors (mrem/hr)
de0  2.5e-08 1.0e-07 1.0e-06 1.0e-05 1.0e-04            $ Energy (Mev)
     1.0e-03 1.0e-02 1.0e-01 5.0e-01 1.0
     2.5 5.0 7.0 10.0 14.0 20.0
df0  3.67e-03 3.67e-03 4.46e-03 4.54e-03 4.18e-03       $ Conversion (mrem/hr)
     3.76e-03 3.56e-03 2.17e-02 9.26e-02 1.32e-01
     1.25e-01 1.56e-01 1.47e-01 1.47e-01 2.08e-01 2.27e-01
C
C Material Cards
C
m1   40000.60c -1.00                                    $ Zirconium
m2   14000.60c -0.01                                    $ Stainless Steel
     24052.60c -0.19
     25055.60c -0.02
     26057.60c -0.68
     28058.60c -0.10
m3   26057.60c -1.00                                    $ Carbon Steel (iron)
m4   82000.50c -1.00                                    $ Lead
C
C Runtime and Print Cards
C
prdmp j j 1 2
ctme 30
```

5.7.1.1.3 NCT Distributed 0.5 MeV Gamma Source – 7ng120.i

```
title RH-TRU 72-B RLC NCT Gamma Distributed 1 g/cc 0.5 MeV
C
C Cell Cards
C
10  1 -1        10  -11  -16                imp:p=1    $ Source #1
11  1 -1        12  -13  -17                imp:p=1    $ Source #2
12  1 -1        14  -15  -18                imp:p=1    $ Source #3
20  0           20  -21  -26
              (-10:  11:  16)               imp:p=1    $ Drum #1 cavity
21  0           22  -23  -27
              (-12:  13:  17)               imp:p=1    $ Drum #2 cavity
22  0           24  -25  -28
              (-14:  15:  18)               imp:p=1    $ Drum #3 cavity
40  0           41  -45  -43
               #10  #11  #12
               #20  #21  #22                imp:p=1    $ RLC cavity
41  3 -7.85260  40  -41  -42                imp:p=1    $ RLC base
42  3 -7.85260  41  -46   43  -42            imp:p=1    $ RLC shell
43  3 -7.85260  45  -44  -43                imp:p=1    $ RLC lid
50  0           51  -53  -55
             (-40:  42:  46)
            :( 44  -46  -43)                imp:p=1    $ IV cavity
51  2 -8.01280  50  -51  -52                imp:p=1    $ IV base
52  2 -8.01280  51  -55   53  -52            imp:p=2    $ IV shell
```

```
53  2 -8.01280  55  -54  -52                imp:p=1    $ IV lid
60  0           61  -63  -65
             (-50:  52:  54)                imp:p=2    $ OC cavity
61  2 -8.01280  60  -61  -69                imp:p=1    $ OC base
62  2 -8.01280  61  -66   65  -64           imp:p=5    $ OC ishell
63  4 -11.3500  61  -66   64  -76  71       imp:p=3E1  $ OC lead in
64  4 -11.3500  61  -66   76  -68  71       imp:p=3E2  $ OC lead out
65  2 -8.01280  61  -66   68  -77  71       imp:p=3E3  $ OC oshell in
66  2 -8.01280  61  -66   77  -67  71       imp:p=6E3  $ OC oshell out
67  0           61  -66   67  -70  71       imp:p=1E5  $ OC airgap
68  2 -8.01280  61  -66   70  -69  71       imp:p=2E5  $ OC tshell
69  2 -8.01280  66  -63   65  -69           imp:p=1    $ OC flange
70  2 -8.01280  63  -62  -69                imp:p=1    $ OC lid
71  4 -11.3500  64  -78  -71                imp:p=3E1  $ OC lead punct in
72  4 -11.3500  78  -73  -71                imp:p=3E2  $ OC lead punct out
73  2 -8.01280  73  -79  -71                imp:p=3E3  $ OC oshell punct in
74  2 -8.01280  79  -72  -71                imp:p=6E3  $ OC oshell punct out
75  0           72  -75  -71                imp:p=1E5  $ OC airgap punct
76  2 -8.01280  75  -74  -71                imp:p=2E5  $ OC tshell punct
777 0           69  -80   60  -62           imp:p=2E5  $ Outside to tally
888 0          -999
             (-60:  80:  62)                imp:p=1E1  $ Outside pkg
999 0           999                         imp:p=0    $ Outside world

C
C Geometry Cards
C
10  pz 53.658                                          $ Source #1 bottom
11  pz 126.683                                           $ Source #1 top
12  pz 127.635                                        $ Source #2 bottom
13  pz 200.66                                       $ Source #2 top
14  pz 201.613                                        $ Source #3 bottom
15  pz 274.638                                        $ Source #3 top
16  c/z 0 0 24.448                                      $ Source #1 radius
17  c/z 0 0 24.448                                      $ Source #2 radius
18  c/z 0 0 24.448                                      $ Source #3 radius
C
20  pz 53.34                                          $ Drum #1 bottom
21  pz 127                                          $ Drum #1 top
22  pz 127.318                                        $ Drum #2 bottom
23  pz 200.978                                        $ Drum #2 top
24  pz 201.295                                        $ Drum #3 bottom
25  pz 274.955                                        $ Drum #3 top
26  c/z 0 0 24.765                                     $ Drum #1 radius
27  c/z 0 0 24.765                                     $ Drum #2 radius
28  c/z 0 0 24.765                                     $ Drum #3 radius
C
40  pz 19.368                                         $ RLC base (outside)
41  pz 20.638                                         $ RLC base (inside)
42  c/z 0 0 33.02                                     $ RLC shell (outside)
43  c/z 0 0 32.385                                    $ RLC shell (inside)
44  pz 309.563                                        $ RLC lid (outside)
45  pz 307.658                                        $ RLC lid (inside)
46  pz 325.438                                        $ RLC top (outside)
C
50  pz 14.288                                         $ IV base (outside)
51  pz 18.098                                         $ IV base (inside)
52  c/z 0 0 40.64                                     $ IV shell (outside)
53  c/z 0 0 39.688                                    $ IV shell (inside)
54  pz 343.218                                        $ IV top (outside)
55  pz 326.708                                        $ IV top (inside)
C
60  pz 0                                              $ OC bottom (outside)
61  pz 12.7                                           $ OC bottom (inside)
62  pz 360.045                                        $ OC top (outside)
63  pz 344.805                                        $ OC top (inside)
64  cz 43.656                                         $ OC ishell (outside)
65  cz 41.116                                         $ OC ishell (inside)
66  pz 320.675                                        $ OC lead (upper)
67  cz 52.229                                         $ OC oshell (outside)
68  cz 48.419                                         $ OC oshell (inside)
69  cz 52.838                                         $ OC therm (outside)
70  cz 52.495                                         $ OC therm (inside)
71  c/x 0 164.148 10.033                              $ OC puncture radius
72  cz 52.229                                         $ OC oshell punct (out)
73  cz 48.419                                         $ OC oshell punct (in)
74  cz 52.838                                         $ OC therm punct (out)
75  cz 52.495                                         $ OC therm punct (in)
76  cz 46.038                                         $ OC lead (mid)
77  cz 50.324                                         $ OC oshell (mid)
78  cz 46.038                                         $ OC lead punct (mid)
```

```
79  cz 50.324                                           $ OC oshell punct (mid)
C
80  cz 252.838                                          $ 2-meter from OC therm
C
777 pz 161.608                                          $ Ring tally (lower)
888 pz 166.688                                          $ Ring tally (upper)
999 sz 164.148 379.838                                  $ Outside world

C
C Physics Cards
C
mode p
C
C Source Cards
C
C Cylindrical Sources
sdef pos=d1 erg=d2 par=2 axs=0 0 1 rad=d3 ext=d4
sc1 0.5 MeV
C Source Position and Fraction
si1 L 0 0 90.17
      0 0 164.148
      0 0 238.125
sp1   1 1 1
C Source Energy (MeV) and Intensity (%)
si2 L 0.5
sp2 1
C Source Radius
si3 0 24.448
sp3 -21 1
C Source Extent
si4 -36.513 36.513
sp4 -21 0
C
C Tally Cards
C
f2:p 69
fc2 Surface Dose (mrem/hr)                              $ Surface detector
fs2 888 777 t
sd2 1.0 1686.525 1.0 1.0                                $ Surface tally area
f22:p 80
fc22 2-meter Dose (mrem/hr)                             $ 2-m detector
fs22 888 777 t
sd22 1.0 8070.229 1.0 1.0                               $ Surface tally area
C
C ANSI/ANS-6.1.1-1977 Gamma Flux to Dose Factors (mrem/hr)
de0 1.0e-02 3.0e-02 5.0e-02 7.0e-02 1.0e-01             $ Energy (Mev)
     1.5e-01 2.0e-01 2.5e-01 3.0e-01 3.5e-01
     4.0e-01 4.5e-01 5.0e-01 5.5e-01 6.0e-01
     6.5e-01 7.0e-01 8.0e-01 1.00 1.40
     1.80 2.20 2.60 2.80 3.25
     3.75 4.25 4.75 5.00 5.25
     5.75 6.25 6.75 7.50 9.00
     11.00 13.00 15.0000
df0 3.96e-03 5.82e-04 2.90e-04 2.58e-04 2.83e-04        $ Conversion (mrem/hr)
     3.79e-04 5.01e-04 6.31e-04 7.59e-04 8.78e-04
     9.85e-04 1.08e-03 1.17e-03 1.27e-03 1.36e-03
     1.44e-03 1.52e-03 1.68e-03 1.98e-03 2.51e-03
     2.99e-03 3.42e-03 3.82e-03 4.01e-03 4.41e-03
     4.83e-03 5.23e-03 5.60e-03 5.80e-03 6.01e-03
     6.37e-03 6.74e-03 7.11e-03 7.66e-03 8.77e-03
     1.03e-02 1.18e-02 1.33e-02
C
C Material Cards
C
m1   40000 -1.00                                        $ Zirconium
m2   14000 -0.01                                        $ Stainless Steel
     24000 -0.19
     25000 -0.02
     26000 -0.68
     28000 -0.10
m3   26000 -1.00                                        $ Carbon Steel (iron)
m4   82000 -1.00                                        $ Lead
C
C Runtime and Print Cards
C
prdmp j j 1 2
ctme 240
```

5.7.1.1.4 NCT Distributed 0.1 MeV Neutron Source – 7nn120.i

```
title RH-TRU 72-B RLC NCT Neutron Distributed 1 g/cc 0.1 MeV
C
C Cell Cards
C
10  1 -1         10  -11  -16                 imp:n=1    $ Source #1
11  1 -1         12  -13  -17                 imp:n=1    $ Source #2
12  1 -1         14  -15  -18                 imp:n=1    $ Source #3
20  0            20  -21  -26
              (-10:  11:  16)                 imp:n=1    $ Drum #1 cavity
21  0            22  -23  -27
              (-12:  13:  17)                 imp:n=1    $ Drum #2 cavity
22  0            24  -25  -28
              (-14:  15:  18)                 imp:n=1    $ Drum #3 cavity
40  0            41  -45  -43
                #10  #11  #12
                #20  #21  #22                 imp:n=1    $ RLC cavity
41  3 -7.85260   40  -41  -42                 imp:n=1    $ RLC base
42  3 -7.85260   41  -46   43  -42            imp:n=1    $ RLC shell
43  3 -7.85260   45  -44  -43                 imp:n=1    $ RLC lid
50  0            51  -53  -55
              (-40:  42:  46)
             :( 44  -46  -43)                 imp:n=1    $ IV cavity
51  2 -8.01280   50  -51  -52                 imp:n=1    $ IV base
52  2 -8.01280   51  -55   53  -52            imp:n=1    $ IV shell
53  2 -8.01280   55  -54  -52                 imp:n=1    $ IV lid
60  0            61  -63  -65
              (-50:  52:  54)                 imp:n=1    $ OC cavity
61  2 -8.01280   60  -61  -69                 imp:n=1    $ OC base
62  2 -8.01280   61  -66   65  -64            imp:n=1    $ OC ishell
63  4 -11.3500   61  -66   64  -76  71        imp:n=1    $ OC lead in
64  4 -11.3500   61  -66   76  -68  71        imp:n=1    $ OC lead out
65  2 -8.01280   61  -66   68  -77  71        imp:n=1    $ OC oshell in
66  2 -8.01280   61  -66   77  -67  71        imp:n=1    $ OC oshell out
67  0            61  -66   67  -70  71        imp:n=1    $ OC airgap
68  2 -8.01280   61  -66   70  -69  71        imp:n=1    $ OC tshell
69  2 -8.01280   66  -63   65  -69            imp:n=1    $ OC flange
70  2 -8.01280   63  -62  -69                 imp:n=1    $ OC lid
71  4 -11.3500   64  -78  -71                 imp:n=1    $ OC lead punct in
72  4 -11.3500   78  -73  -71                 imp:n=1    $ OC lead punct out
73  2 -8.01280   73  -79  -71                 imp:n=1    $ OC oshell punct in
74  2 -8.01280   79  -72  -71                 imp:n=1    $ OC oshell punct out
75  0            72  -75  -71                 imp:n=1    $ OC airgap punct
76  2 -8.01280   75  -74  -71                 imp:n=1    $ OC tshell punct
777 0            69  -80   60  -62            imp:n=1    $ Outside to tally
888 0          -999
              (-60:  80:  62)                 imp:n=1    $ Outside pkg
999 0            999                          imp:n=0    $ Outside world

C
C Geometry Cards
C
10  pz 53.658                                              $ Source #1 bottom
11  pz 126.683                                               $ Source #1 top
12  pz 127.635                                            $ Source #2 bottom
13  pz 200.66                                           $ Source #2 top
14  pz 201.613                                            $ Source #3 bottom
15  pz 274.638                                            $ Source #3 top
16  c/z 0 0 24.448                                          $ Source #1 radius
17  c/z 0 0 24.448                                          $ Source #2 radius
18  c/z 0 0 24.448                                          $ Source #3 radius
C
20  pz 53.34                                              $ Drum #1 bottom
21  pz 127                                              $ Drum #1 top
22  pz 127.318                                            $ Drum #2 bottom
23  pz 200.978                                            $ Drum #2 top
24  pz 201.295                                            $ Drum #3 bottom
25  pz 274.955                                            $ Drum #3 top
26  c/z 0 0 24.765                                          $ Drum #1 radius
27  c/z 0 0 24.765                                          $ Drum #2 radius
28  c/z 0 0 24.765                                          $ Drum #3 radius
C
40  pz 19.368                                             $ RLC base (outside)
41  pz 20.638                                             $ RLC base (inside)
42  c/z 0 0 33.02                                         $ RLC shell (outside)
43  c/z 0 0 32.385                                        $ RLC shell (inside)
44  pz 309.563                                            $ RLC lid (outside)
45  pz 307.658                                            $ RLC lid (inside)
46  pz 325.438                                            $ RLC top (outside)
```

```
C
50  pz 14.288                                          $ IV base (outside)
51  pz 18.098                                          $ IV base (inside)
52  c/z 0 0 40.64                                      $ IV shell (outside)
53  c/z 0 0 39.688                                     $ IV shell (inside)
54  pz 343.218                                         $ IV top (outside)
55  pz 326.708                                         $ IV top (inside)
C
60  pz 0                                               $ OC bottom (outside)
61  pz 12.7                                            $ OC bottom (inside)
62  pz 360.045                                         $ OC top (outside)
63  pz 344.805                                         $ OC top (inside)
64  cz 43.656                                          $ OC ishell (outside)
65  cz 41.116                                          $ OC ishell (inside)
66  pz 320.675                                         $ OC lead (upper)
67  cz 52.229                                          $ OC oshell (outside)
68  cz 48.419                                          $ OC oshell (inside)
69  cz 52.838                                          $ OC therm (outside)
70  cz 52.495                                          $ OC therm (inside)
71  c/x 0 164.148 10.033                               $ OC puncture radius
72  cz 52.229                                          $ OC oshell punct (out)
73  cz 48.419                                          $ OC oshell punct (in)
74  cz 52.838                                          $ OC therm punct (out)
75  cz 52.495                                          $ OC therm punct (in)
76  cz 46.038                                          $ OC lead (mid)
77  cz 50.324                                          $ OC oshell (mid)
78  cz 46.038                                          $ OC lead punct (mid)
79  cz 50.324                                          $ OC oshell punct (mid)
C
80  cz 252.838                                         $ 2-meter from OC therm
C
777 pz 161.608                                         $ Ring tally (lower)
888 pz 166.688                                         $ Ring tally (upper)
999 sz 164.148 379.838                                 $ Outside world

C
C Physics Cards
C
mode n
C
C Source Cards
C
C Cylindrical Sources
sdef pos=d1 erg=d2 par=1 axs=0 0 1 rad=d3 ext=d4
sc1 0.1 MeV
C Source Position and Fraction
si1 L 0 0 90.17
      0 0 164.148
      0 0 238.125
sp1   1 1 1
C Source Energy (MeV) and Fraction
si2 L 0.1
sp2 1
C Source Radius
si3 0 24.448
sp3 -21 1
C Source Extent
si4 -36.513 36.513
sp4 -21 0
C
C Tally Cards
C
f2:n 69
fc2 Surface Dose (mrem/hr)                             $ Surface detector
fs2 888 777 t
sd2 1.0 1686.525 1.0 1.0                               $ Surface tally area
f22:n 80
fc22 2-meter Dose (mrem/hr)                            $ 2-m detector
fs22 888 777 t
sd22 1.0 8070.229 1.0 1.0                              $ Surface tally area
C
C ANSI/ANS-6.1.1-1977 Neutron Flux to Dose Factors (mrem/hr)
de0  2.5e-08 1.0e-07 1.0e-06 1.0e-05 1.0e-04           $ Energy (Mev)
     1.0e-03 1.0e-02 1.0e-01 5.0e-01 1.0
     2.5 5.0 7.0 10.0 14.0 20.0
df0  3.67e-03 3.67e-03 4.46e-03 4.54e-03 4.18e-03      $ Conversion (mrem/hr)
     3.76e-03 3.56e-03 2.17e-02 9.26e-02 1.32e-01
     1.25e-01 1.56e-01 1.47e-01 1.47e-01 2.08e-01 2.27e-01
C
C Material Cards
C
```

```
m1   40000.60c -1.00                                    $ Zirconium
m2   14000.60c -0.01                                    $ Stainless Steel
     24052.60c -0.19
     25055.60c -0.02
     26057.60c -0.68
     28058.60c -0.10
m3   26057.60c -1.00                                    $ Carbon Steel (iron)
m4   82000.50c -1.00                                    $ Lead
C
C Runtime and Print Cards
C
prdmp j j 1 2
ctme 30
```

5.7.1.1.5 HAC 60Co Gamma Source – 7hg001.i

```
title RH-TRU 72-B RLC HAC Gamma Concentrated 1 g/cc Co60
C
C Cell Cards
C
10  1 -1        10  -11  -16                imp:p=1    $ Source #1
20  0           20  -21  -26
              (-10:  11:  16)               imp:p=1    $ Drum #1 cavity
40  0           41  -45  -43
             #10  #20                       imp:p=1    $ RLC cavity
41  3 -7.85260  40  -41  -42                imp:p=1    $ RLC base
42  3 -7.85260  41  -46   43  -42           imp:p=1    $ RLC shell
43  3 -7.85260  45  -44  -43                imp:p=1    $ RLC lid
50  0           51  -53  -55
             (-40:  42:  46)
            :( 44  -46  -43)                imp:p=1    $ IV cavity
51  2 -8.01280  50  -51  -52                imp:p=1    $ IV base
52  2 -8.01280  51  -55   53  -52           imp:p=2    $ IV shell
53  2 -8.01280  55  -54  -52                imp:p=1    $ IV lid
60  0           61  -63  -65
             (-50:  52:  54)                imp:p=2    $ OC cavity
61  2 -8.01280  60  -61  -69                imp:p=1    $ OC base
62  2 -8.01280  61  -66   65  -64           imp:p=5    $ OC ishell
63  4 -11.3500  61  -66   64  -76  71       imp:p=3E1  $ OC lead in
64  4 -11.3500  61  -66   76  -68  71       imp:p=3E2  $ OC lead out
65  2 -8.01280  61  -66   68  -77  71       imp:p=3E3  $ OC oshell in
66  2 -8.01280  61  -66   77  -67  71       imp:p=6E3  $ OC oshell out
67  0           61  -66   67  -70  71       imp:p=1E5  $ OC airgap
68  2 -8.01280  61  -66   70  -69  71       imp:p=2E5  $ OC tshell
69  2 -8.01280  66  -63   65  -69           imp:p=1    $ OC flange
70  2 -8.01280  63  -62  -69                imp:p=1    $ OC lid
71  4 -11.3500  64  -78  -71                imp:p=3E1  $ OC lead punct in
72  4 -11.3500  78  -73  -71                imp:p=3E2  $ OC lead punct out
73  2 -8.01280  73  -79  -71                imp:p=3E3  $ OC oshell punct in
74  2 -8.01280  79  -72  -71                imp:p=6E3  $ OC oshell punct out
75  0           74  -69  -71                imp:p=1E5  $ OC airgap punct
76  2 -8.01280  75  -74  -71                imp:p=2E5  $ OC tshell punct
777 0           69  -80   60  -62           imp:p=2E5  $ Outside to tally
888 0          -999
             (-60:  80:  62)                imp:p=1E1  $ Outside pkg
999 0           999                         imp:p=0    $ Outside world

C
C Geometry Cards
C
10  pz 163.513                                        $ Source #1 bottom
11  pz 164.783                                        $ Source #1 top
16  c/z 38.885 0 0.635                                $ Source #1 radius
C
20  pz 163.511                                        $ Drum #1 bottom
21  pz 164.784                                        $ Drum #1 top
26  c/z 38.885 0 0.636                                $ Drum #1 radius
C
40  pz 19.368                                         $ RLC base (outside)
41  pz 20.638                                         $ RLC base (inside)
42  c/z 7.139 0 33.02                                 $ RLC shell (outside)
43  c/z 7.139 0 32.385                                $ RLC shell (inside)
44  pz 309.563                                        $ RLC lid (outside)
45  pz 307.658                                        $ RLC lid (inside)
46  pz 325.438                                        $ RLC top (outside)
C
50  pz 14.288                                         $ IV base (outside)
51  pz 18.098                                         $ IV base (inside)
52  c/z 0.474 0 40.64                                 $ IV shell (outside)
```

```
53  c/z 0.474 0 39.688                                  $ IV shell (inside)
54  pz 343.218                                          $ IV top (outside)
55  pz 326.708                                          $ IV top (inside)
C
60  pz 0                                                $ OC bottom (outside)
61  pz 12.7                                             $ OC bottom (inside)
62  pz 360.045                                          $ OC top (outside)
63  pz 344.805                                          $ OC top (inside)
64  cz 43.656                                           $ OC ishell (outside)
65  cz 41.116                                           $ OC ishell (inside)
66  pz 320.675                                          $ OC lead (upper)
67  cz 52.229                                           $ OC oshell (outside)
68  cz 48.419                                           $ OC oshell (inside)
69  cz 52.838                                           $ OC therm (outside)
70  cz 52.495                                           $ OC therm (inside)
71  c/x 0 164.148 10.033                                $ OC puncture radius
72  cz 50.563                                           $ OC oshell punct (out)
73  cz 46.753                                           $ OC oshell punct (in)
74  cz 50.905                                           $ OC therm punct (out)
75  cz 50.563                                           $ OC therm punct (in)
76  cz 46.038                                           $ OC lead (mid)
77  cz 50.324                                           $ OC oshell (mid)
78  cz 45.204                                           $ OC lead punct (mid)
79  cz 48.658                                           $ OC oshell punct (mid)
C
80  cz 150.905                                          $ 1-meter from OC therm
C
777 c/x 0 164.148 2.54                                  $ Tally cylinder
888 px 0                                                $ Tally truncation
999 sz 164.148 277.905                                  $ Outside world

C
C Physics Cards
C
mode p
C
C Source Cards
C
C Cylindrical Sources
sdef pos=d1 erg=d2 par=2 axs=0 0 1 rad=d3 ext=d4
sc1 Co60
C Source Position and Fraction
si1 L 38.885 0 164.148
      0 0 0
sp1   98 2
C Source Energy (MeV) and Intensity (%)
si2 L 3.469300E-01 8.262800E-01 1.173237E+00 1.332501E+00
     2.158770E+00 2.505000E+00
sp2 7.600000E-03 7.600000E-03 9.997360E+01 9.998560E+01
     1.110000E-03 2.000000E-06
C Source Radius
si3 0 0.635
sp3 -21 1
C Source Extent
si4 -0.635 0.635
sp4 -21 0
C
C Tally Cards
C
f2:p 69
fc2 Surface Dose (mrem/hr)                              $ Surface detector
fs2 -888 -777 t
sd2 1.0 20.268 1.0 1.0                                  $ Surface tally area
f22:p 80
fc22 1-meter Dose (mrem/hr)                             $ 1-m detector
fs22 -888 -777 t
sd22 1.0 20.268 1.0 1.0                                 $ Surface tally area
C
C ANSI/ANS-6.1.1-1977 Gamma Flux to Dose Factors (mrem/hr)
de0 1.0e-02 3.0e-02 5.0e-02 7.0e-02 1.0e-01             $ Energy (Mev)
     1.5e-01 2.0e-01 2.5e-01 3.0e-01 3.5e-01
     4.0e-01 4.5e-01 5.0e-01 5.5e-01 6.0e-01
     6.5e-01 7.0e-01 8.0e-01 1.00 1.40
     1.80 2.20 2.60 2.80 3.25
     3.75 4.25 4.75 5.00 5.25
     5.75 6.25 6.75 7.50 9.00
     11.00 13.00 15.0000
df0 3.96e-03 5.82e-04 2.90e-04 2.58e-04 2.83e-04        $ Conversion (mrem/hr)
     3.79e-04 5.01e-04 6.31e-04 7.59e-04 8.78e-04
     9.85e-04 1.08e-03 1.17e-03 1.27e-03 1.36e-03
     1.44e-03 1.52e-03 1.68e-03 1.98e-03 2.51e-03
```

```
     2.99e-03 3.42e-03 3.82e-03 4.01e-03 4.41e-03
     4.83e-03 5.23e-03 5.60e-03 5.80e-03 6.01e-03
     6.37e-03 6.74e-03 7.11e-03 7.66e-03 8.77e-03
     1.03e-02 1.18e-02 1.33e-02
C
C Material Cards
C
m1   40000 -1.00                                          $ Zirconium
m2   14000 -0.01                                          $ Stainless Steel
     24000 -0.19
     25000 -0.02
     26000 -0.68
     28000 -0.10
m3   26000 -1.00                                          $ Carbon Steel (iron)
m4   82000 -1.00                                          $ Lead
C
C Runtime and Print Cards
C
prdmp j j 1 2
ctme 360
```

5.7.1.1.6 HAC 252Cf Neutron Source – 7hn001.i

```
title RH-TRU 72-B RLC HAC Neutron Concentrated 1 g/cc Cf252
C
C Cell Cards
C
10  1 -1        10  -11  -16                imp:n=1    $ Source #1
20  0           20  -21  -26
              (-10:  11:  16)                imp:n=1    $ Drum #1 cavity
40  0           41  -45  -43
             #10  #20                        imp:n=1    $ RLC cavity
41  3 -7.85260  40  -41  -42                 imp:n=1    $ RLC base
42  3 -7.85260  41  -46   43  -42            imp:n=1    $ RLC shell
43  3 -7.85260  45  -44  -43                 imp:n=1    $ RLC lid
50  0           51  -53  -55
            (-40:  42:  46)
           :( 44  -46  -43)                  imp:n=1    $ IV cavity
51  2 -8.01280  50  -51  -52                 imp:n=1    $ IV base
52  2 -8.01280  51  -55   53  -52            imp:n=1    $ IV shell
53  2 -8.01280  55  -54  -52                 imp:n=1    $ IV lid
60  0           61  -63  -65
            (-50:  52:  54)                  imp:n=1    $ OC cavity
61  2 -8.01280  60  -61  -69                 imp:n=1    $ OC base
62  2 -8.01280  61  -66   65  -64            imp:n=1    $ OC ishell
63  4 -11.3500  61  -66   64  -76  71        imp:n=1    $ OC lead in
64  4 -11.3500  61  -66   76  -68  71        imp:n=1    $ OC lead out
65  2 -8.01280  61  -66   68  -77  71        imp:n=1    $ OC oshell in
66  2 -8.01280  61  -66   77  -67  71        imp:n=1    $ OC oshell out
67  0           61  -66   67  -70  71        imp:n=1    $ OC airgap
68  2 -8.01280  61  -66   70  -69  71        imp:n=1    $ OC tshell
69  2 -8.01280  66  -63   65  -69            imp:n=1    $ OC flange
70  2 -8.01280  63  -62  -69                 imp:n=1    $ OC lid
71  4 -11.3500  64  -78  -71                 imp:n=1    $ OC lead punct in
72  4 -11.3500  78  -73  -71                 imp:n=1    $ OC lead punct out
73  2 -8.01280  73  -79  -71                 imp:n=1    $ OC oshell punct in
74  2 -8.01280  79  -72  -71                 imp:n=1    $ OC oshell punct out
75  0           74  -69  -71                 imp:n=1    $ OC airgap punct
76  2 -8.01280  75  -74  -71                 imp:n=1    $ OC tshell punct
777 0           69  -80   60  -62            imp:n=1    $ Outside to tally
888 0          -999
              (-60:  80:  62)                imp:n=1    $ Outside pkg
999 0           999                           imp:n=0    $ Outside world

C
C Geometry Cards
C
10  pz 163.513                                          $ Source #1 bottom
11  pz 164.783                                          $ Source #1 top
16  c/z 38.885 0 0.635                                  $ Source #1 radius
C
20  pz 163.511                                          $ Drum #1 bottom
21  pz 164.784                                          $ Drum #1 top
26  c/z 38.885 0 0.636                                  $ Drum #1 radius
C
40  pz 19.368                                           $ RLC base (outside)
41  pz 20.638                                           $ RLC base (inside)
42  c/z 7.139 0 33.02                                   $ RLC shell (outside)
43  c/z 7.139 0 32.385                                  $ RLC shell (inside)
```

```
44  pz 309.563                                          $ RLC lid (outside)
45  pz 307.658                                          $ RLC lid (inside)
46  pz 325.438                                          $ RLC top (outside)
C
50  pz 14.288                                           $ IV base (outside)
51  pz 18.098                                           $ IV base (inside)
52  c/z 0.474 0 40.64                                   $ IV shell (outside)
53  c/z 0.474 0 39.688                                  $ IV shell (inside)
54  pz 343.218                                          $ IV top (outside)
55  pz 326.708                                          $ IV top (inside)
C
60  pz 0                                                $ OC bottom (outside)
61  pz 12.7                                             $ OC bottom (inside)
62  pz 360.045                                          $ OC top (outside)
63  pz 344.805                                          $ OC top (inside)
64  cz 43.656                                           $ OC ishell (outside)
65  cz 41.116                                           $ OC ishell (inside)
66  pz 320.675                                          $ OC lead (upper)
67  cz 52.229                                           $ OC oshell (outside)
68  cz 48.419                                           $ OC oshell (inside)
69  cz 52.838                                           $ OC therm (outside)
70  cz 52.495                                           $ OC therm (inside)
71  c/x 0 164.148 10.033                                $ OC puncture radius
72  cz 50.563                                           $ OC oshell punct (out)
73  cz 46.753                                           $ OC oshell punct (in)
74  cz 50.905                                           $ OC therm punct (out)
75  cz 50.563                                           $ OC therm punct (in)
76  cz 46.038                                           $ OC lead (mid)
77  cz 50.324                                           $ OC oshell (mid)
78  cz 45.204                                           $ OC lead punct (mid)
79  cz 48.658                                           $ OC oshell punct (mid)
C
80  cz 150.905                                          $ 1-meter from OC therm
C
777 c/x 0 164.148 2.54                                  $ Tally cylinder
888 px 0                                                $ Tally truncation
999 sz 164.148 277.905                                  $ Outside world

C
C Physics Cards
C
mode n
C
C Source Cards
C
C Cylindrical Sources
sdef pos=d1 erg=d2 par=1 axs=0 0 1 rad=d3 ext=d4
sc1 Cf252
C Source Position and Fraction
si1 L 38.885 0 164.148
      0 0 0
sp1   98 2
C Source Energy (MeV) and Fraction
si2 0.1 0.5 1.0 2.0 3.0
     4.0 6.0 8.0 10.0 15.0
sp2 0.00E+00 1.80E+11 2.71E+11 5.36E+11 4.10E+11
     2.73E+11 2.66E+11 8.53E+10 2.44E+10 8.36E+09
C Source Radius
si3 0 0.635
sp3 -21 1
C Source Extent
si4 -0.635 0.635
sp4 -21 0
C
C Tally Cards
C
f2:n 69
fc2 Surface Dose (mrem/hr)                              $ Surface detector
fs2 -888 -777 t
sd2 1.0 20.268 1.0 1.0                                  $ Surface tally area
f22:n 80
fc22 1-meter Dose (mrem/hr)                             $ 1-m detector
fs22 -888 -777 t
sd22 1.0 20.268 1.0 1.0                                 $ Surface tally area
C
C ANSI/ANS-6.1.1-1977 Neutron Flux to Dose Factors (mrem/hr)
de0  2.5e-08 1.0e-07 1.0e-06 1.0e-05 1.0e-04            $ Energy (Mev)
     1.0e-03 1.0e-02 1.0e-01 5.0e-01 1.0
     2.5 5.0 7.0 10.0 14.0 20.0
df0  3.67e-03 3.67e-03 4.46e-03 4.54e-03 4.18e-03       $ Conversion (mrem/hr)
     3.76e-03 3.56e-03 2.17e-02 9.26e-02 1.32e-01
```

```
     1.25e-01 1.56e-01 1.47e-01 1.47e-01 2.08e-01 2.27e-01
C
C Material Cards
C
m1   40000.60c -1.00                                    $ Zirconium
m2   14000.60c -0.01                                    $ Stainless Steel
     24052.60c -0.19
     25055.60c -0.02
     26057.60c -0.68
     28058.60c -0.10
m3   26057.60c -1.00                                    $ Carbon Steel (iron)
m4   82000.50c -1.00                                    $ Lead
C
C Runtime and Print Cards
C
prdmp j j 1 2
ctme 120
```

5.7.1.2 RH-TRU 72-B – NS15 Neutron Shielded Canister

5.7.1.2.1 NCT Distributed 0.5 MeV Gamma Source – 9ng120.i

```
title RH-TRU 72-B NS15 NCT Gamma Distributed 1 g/cc 0.5 MeV
C
C Cell Cards
C
10  1 -1         10  -11  -16                 imp:p=1    $ Source #1
11  1 -1         12  -13  -17                 imp:p=1    $ Source #2
12  1 -1         14  -15  -18                 imp:p=1    $ Source #3
20  0            20  -21  -26
              (-10:  11:  16)                 imp:p=1    $ Drum #1 cavity
21  0            22  -23  -27
              (-12:  13:  17)                 imp:p=1    $ Drum #2 cavity
22  0            24  -25  -28
              (-14:  15:  18)                 imp:p=1    $ Drum #3 cavity
30  0            31  -35  -33
              #10  #11  #12
              #20  #21  #22                   imp:p=1    $ NS15 cavity
31  5 -0.94000   30  -31  -32                 imp:p=1    $ NS15 botcap
32  5 -0.94000   31  -35   33  -32            imp:p=1    $ NS15 body
33  5 -0.94000   35  -34  -32                 imp:p=1    $ NS15 topcap
40  0            41  -45  -43
              (-30:  32:  34)                 imp:p=1    $ RLC cavity
41  3 -7.85260   40  -41  -42                 imp:p=1    $ RLC base
42  3 -7.85260   41  -46   43  -42            imp:p=1    $ RLC shell
43  3 -7.85260   45  -44  -43                 imp:p=1    $ RLC lid
50  0            51  -53  -55
              (-40:  42:  46)
             ⊗ 44  -46  -43)                 imp:p=1    $ IV cavity
51  2 -8.01280   50  -51  -52                 imp:p=1    $ IV base
52  2 -8.01280   51  -55   53  -52            imp:p=2    $ IV shell
53  2 -8.01280   55  -54  -52                 imp:p=1    $ IV lid
60  0            61  -63  -65
              (-50:  52:  54)                 imp:p=2    $ OC cavity
61  2 -8.01280   60  -61  -69                 imp:p=1    $ OC base
62  2 -8.01280   61  -66   65  -64            imp:p=5    $ OC ishell
63  4 -11.3500   61  -66   64  -76  71        imp:p=3E1  $ OC lead in
64  4 -11.3500   61  -66   76  -68  71        imp:p=3E2  $ OC lead out
65  2 -8.01280   61  -66   68  -77  71        imp:p=3E3  $ OC oshell in
66  2 -8.01280   61  -66   77  -67  71        imp:p=6E3  $ OC oshell out
67  0            61  -66   67  -70  71        imp:p=1E5  $ OC airgap
68  2 -8.01280   61  -66   70  -69  71        imp:p=2E5  $ OC tshell
69  2 -8.01280   66  -63   65  -69            imp:p=1    $ OC flange
70  2 -8.01280   63  -62  -69                 imp:p=1    $ OC lid
71  4 -11.3500   64  -78  -71                 imp:p=3E1  $ OC lead punct in
72  4 -11.3500   78  -73  -71                 imp:p=3E2  $ OC lead punct out
73  2 -8.01280   73  -79  -71                 imp:p=3E3  $ OC oshell punct in
74  2 -8.01280   79  -72  -71                 imp:p=6E3  $ OC oshell punct out
75  0            72  -75  -71                 imp:p=1E5  $ OC airgap punct
76  2 -8.01280   75  -74  -71                 imp:p=2E5  $ OC tshell punct
777 0            69  -80   60  -62            imp:p=2E5  $ Outside to tally
888 0          -999
              (-60:  80:  62)                 imp:p=1E1  $ Outside pkg
999 0            999                         imp:p=0    $ Outside world

C
C Geometry Cards
```

```
C
10  pz 61.278                                   $ Source #1 bottom
11  pz 129.223                                  $ Source #1 top
12  pz 130.175                                $ Source #2 bottom
13  pz 198.12                                 $ Source #2 top
14  pz 199.073                                $ Source #3 bottom
15  pz 267.018                                $ Source #3 top
16  c/z 0 0 18.733                              $ Source #1 radius
17  c/z 0 0 18.733                              $ Source #2 radius
18  c/z 0 0 18.733                              $ Source #3 radius
C
20  pz 60.96                                  $ Drum #1 bottom
21  pz 129.54                                    $ Drum #1 top
22  pz 129.858                                $ Drum #2 bottom
23  pz 198.438                                $ Drum #2 top
24  pz 198.755                                $ Drum #3 bottom
25  pz 267.335                                $ Drum #3 top
26  c/z 0 0 19.05                             $ Drum #1 radius
27  c/z 0 0 19.05                             $ Drum #2 radius
28  c/z 0 0 19.05                             $ Drum #3 radius
C
30  pz 21.908                                 $ NS15 botcap (outside)
31  pz 34.608                                 $ NS15 botcap (inside)
32  c/z 0 0 30.48                             $ NS15 body (outside)
33  c/z 0 0 21.877                            $ NS15 body (inside)
34  pz 306.388                                $ NS15 topcap (outside)
35  pz 293.688                                $ NS15 topcap (inside)
C
40  pz 19.368                                 $ RLC base (outside)
41  pz 20.638                                 $ RLC base (inside)
42  c/z 0 0 33.02                             $ RLC shell (outside)
43  c/z 0 0 32.385                            $ RLC shell (inside)
44  pz 309.563                                $ RLC lid (outside)
45  pz 307.658                                $ RLC lid (inside)
46  pz 325.438                                $ RLC top (outside)
C
50  pz 14.288                                 $ IV base (outside)
51  pz 18.098                                 $ IV base (inside)
52  c/z 0 0 40.64                             $ IV shell (outside)
53  c/z 0 0 39.688                            $ IV shell (inside)
54  pz 343.218                                $ IV top (outside)
55  pz 326.708                                $ IV top (inside)
C
60  pz 0                                      $ OC bottom (outside)
61  pz 12.7                                   $ OC bottom (inside)
62  pz 360.045                                $ OC top (outside)
63  pz 344.805                                $ OC top (inside)
64  cz 43.656                                 $ OC ishell (outside)
65  cz 41.116                                 $ OC ishell (inside)
66  pz 320.675                                $ OC lead (upper)
67  cz 52.229                                 $ OC oshell (outside)
68  cz 48.419                                 $ OC oshell (inside)
69  cz 52.838                                 $ OC therm (outside)
70  cz 52.495                                 $ OC therm (inside)
71  c/x 0 164.148 10.033                      $ OC puncture radius
72  cz 52.229                                 $ OC oshell punct (out)
73  cz 48.419                                 $ OC oshell punct (in)
74  cz 52.838                                 $ OC therm punct (out)
75  cz 52.495                                 $ OC therm punct (in)
76  cz 46.038                                 $ OC lead (mid)
77  cz 50.324                                 $ OC oshell (mid)
78  cz 46.038                                 $ OC lead punct (mid)
79  cz 50.324                                 $ OC oshell punct (mid)
C
80  cz 252.838                                $ 2-meter from OC therm
C
777 pz 161.608                                $ Ring tally (lower)
888 pz 166.688                                $ Ring tally (upper)
999 sz 164.148 379.838                        $ Outside world

C
C Physics Cards
C
mode p
C
C Source Cards
C
C Cylindrical Sources
sdef pos=d1 erg=d2 par=2 axs=0 0 1 rad=d3 ext=d4
sc1 0.5 MeV
C Source Position and Fraction
```

```
si1 L 0 0 95.25
      0 0 164.148
      0 0 233.045
sp1   1 1 1
C Source Energy (MeV) and Intensity (%)
si2 L 0.5
sp2 1
C Source Radius
si3 0 18.733
sp3 -21 1
C Source Extent
si4 -33.973 33.973
sp4 -21 0
C
C Tally Cards
C
f2:p 69
fc2 Surface Dose (mrem/hr)                                  $ Surface detector
fs2 888 777 t
sd2 1.0 1686.525 1.0 1.0                                    $ Surface tally area
f22:p 80
fc22 2-meter Dose (mrem/hr)                                 $ 2-m detector
fs22 888 777 t
sd22 1.0 8070.229 1.0 1.0                                   $ Surface tally area
C
C ANSI/ANS-6.1.1-1977 Gamma Flux to Dose Factors (mrem/hr)
de0 1.0e-02 3.0e-02 5.0e-02 7.0e-02 1.0e-01                 $ Energy (Mev)
     1.5e-01 2.0e-01 2.5e-01 3.0e-01 3.5e-01
     4.0e-01 4.5e-01 5.0e-01 5.5e-01 6.0e-01
     6.5e-01 7.0e-01 8.0e-01 1.00 1.40
     1.80 2.20 2.60 2.80 3.25
     3.75 4.25 4.75 5.00 5.25
     5.75 6.25 6.75 7.50 9.00
     11.00 13.00 15.0000
df0 3.96e-03 5.82e-04 2.90e-04 2.58e-04 2.83e-04            $ Conversion (mrem/hr)
     3.79e-04 5.01e-04 6.31e-04 7.59e-04 8.78e-04
     9.85e-04 1.08e-03 1.17e-03 1.27e-03 1.36e-03
     1.44e-03 1.52e-03 1.68e-03 1.98e-03 2.51e-03
     2.99e-03 3.42e-03 3.82e-03 4.01e-03 4.41e-03
     4.83e-03 5.23e-03 5.60e-03 5.80e-03 6.01e-03
     6.37e-03 6.74e-03 7.11e-03 7.66e-03 8.77e-03
     1.03e-02 1.18e-02 1.33e-02
C
C Material Cards
C
m1   40000 -1.00                                           $ Zirconium
m2   14000 -0.01                                           $ Stainless Steel
     24000 -0.19
     25000 -0.02
     26000 -0.68
     28000 -0.10
m3   26000 -1.00                                           $ Carbon Steel (iron)
m4   82000 -1.00                                           $ Lead
m5   1000   2                                             $ EHMW Polyethylene
     6000   1
C
C Runtime and Print Cards
C
prdmp j j 1 2
ctme 240
```

5.7.1.2.2 HAC 60Co Gamma Source – 9hg001.i

```
title RH-TRU 72-B NS15 HAC Gamma Concentrated 1 g/cc Co60
C
C Cell Cards
C
10  1 -1        10  -11  -16                imp:p=1    $ Source #1
11  1 -1        12  -13  -17                imp:p=1    $ Source #2
20  0           20  -21  -26
              (-10:  11:  16)               imp:p=1    $ Drum #1 cavity
21  0           22  -23  -27
              (-12:  13:  17)               imp:p=1    $ Drum #2 cavity
30  0           31  -35  -33
               #10  #20                     imp:p=1    $ NS15 cavity
31  5 -0.94000  30  -31  -32                imp:p=1    $ NS15 botcap
32  5 -0.94000  31  -35   33  -32           imp:p=1    $ NS15 body
33  5 -0.94000  35  -34  -32                imp:p=1    $ NS15 topcap
40  0           41  -45  -43
```

```
             (-30:  32:  34) #11  #21       imp:p=1    $ RLC cavity
41  3 -7.85260  40  -41  -42                 imp:p=1    $ RLC base
42  3 -7.85260  41  -46   43  -42            imp:p=1    $ RLC shell
43  3 -7.85260  45  -44  -43                 imp:p=1    $ RLC lid
50  0           51  -53  -55
             (-40:  42:  46)
            ☹ 44  -46  -43)                imp:p=1    $ IV cavity
51  2 -8.01280  50  -51  -52                 imp:p=1    $ IV base
52  2 -8.01280  51  -55   53  -52            imp:p=2    $ IV shell
53  2 -8.01280  55  -54  -52                 imp:p=1    $ IV lid
60  0           61  -63  -65
             (-50:  52:  54)                 imp:p=2    $ OC cavity
61  2 -8.01280  60  -61  -69                 imp:p=1    $ OC base
62  2 -8.01280  61  -66   65  -64            imp:p=5    $ OC ishell
63  4 -11.3500  61  -66   64  -76  71        imp:p=3E1  $ OC lead in
64  4 -11.3500  61  -66   76  -68  71        imp:p=3E2  $ OC lead out
65  2 -8.01280  61  -66   68  -77  71        imp:p=3E3  $ OC oshell in
66  2 -8.01280  61  -66   77  -67  71        imp:p=6E3  $ OC oshell out
67  0           61  -66   67  -70  71        imp:p=1E5  $ OC airgap
68  2 -8.01280  61  -66   70  -69  71        imp:p=2E5  $ OC tshell
69  2 -8.01280  66  -63   65  -69            imp:p=1    $ OC flange
70  2 -8.01280  63  -62  -69                 imp:p=1    $ OC lid
71  4 -11.3500  64  -78  -71                 imp:p=3E1  $ OC lead punct in
72  4 -11.3500  78  -73  -71                 imp:p=3E2  $ OC lead punct out
73  2 -8.01280  73  -79  -71                 imp:p=3E3  $ OC oshell punct in
74  2 -8.01280  79  -72  -71                 imp:p=6E3  $ OC oshell punct out
75  0           74  -69  -71                 imp:p=1E5  $ OC airgap punct
76  2 -8.01280  75  -74  -71                 imp:p=2E5  $ OC tshell punct
777 0           69  -80   60  -62            imp:p=2E5  $ Outside to tally
888 0          -999
             (-60:  80:  62)                 imp:p=1E1  $ Outside pkg
999 0           999                          imp:p=0    $ Outside world

C
C Geometry Cards
C
10  pz 163.513                                          $ Source #1 bottom
11  pz 164.783                                          $ Source #1 top
12  pz 163.513                                          $ Source #2 bottom
13  pz 164.783                                          $ Source #2 top
16  c/z 29.873 0 0.635                                   $ Source #1 radius
17  c/z 38.885 0 0.635                                   $ Source #2 radius
C
20  pz 163.511                                          $ Drum #1 bottom
21  pz 164.784                                          $ Drum #1 top
22  pz 163.511                                          $ Drum #2 bottom
23  pz 164.784                                          $ Drum #2 top
26  c/z 29.873 0 0.636                                  $ Drum #1 radius
27  c/z 38.885 0 0.636                                  $ Drum #2 radius
C
30  pz 21.908                                           $ NS15 botcap (outside)
31  pz 34.608                                           $ NS15 botcap (inside)
32  c/z 7.748 0 30.48                                   $ NS15 body (outside)
33  c/z 7.748 0 22.763                                  $ NS15 body (inside)
34  pz 306.388                                          $ NS15 topcap (outside)
35  pz 293.688                                          $ NS15 topcap (inside)
C
40  pz 19.368                                           $ RLC base (outside)
41  pz 20.638                                           $ RLC base (inside)
42  c/z 7.139 0 33.02                                   $ RLC shell (outside)
43  c/z 7.139 0 32.385                                  $ RLC shell (inside)
44  pz 309.563                                          $ RLC lid (outside)
45  pz 307.658                                          $ RLC lid (inside)
46  pz 325.438                                          $ RLC top (outside)
C
50  pz 14.288                                           $ IV base (outside)
51  pz 18.098                                           $ IV base (inside)
52  c/z 0.474 0 40.64                                   $ IV shell (outside)
53  c/z 0.474 0 39.688                                  $ IV shell (inside)
54  pz 343.218                                          $ IV top (outside)
55  pz 326.708                                          $ IV top (inside)
C
60  pz 0                                                $ OC bottom (outside)
61  pz 12.7                                             $ OC bottom (inside)
62  pz 360.045                                          $ OC top (outside)
63  pz 344.805                                          $ OC top (inside)
64  cz 43.656                                           $ OC ishell (outside)
65  cz 41.116                                           $ OC ishell (inside)
66  pz 320.675                                          $ OC lead (upper)
67  cz 52.229                                           $ OC oshell (outside)
68  cz 48.419                                           $ OC oshell (inside)
```

```
69  cz 52.838                                          $ OC therm (outside)
70  cz 52.495                                          $ OC therm (inside)
71  c/x 0 164.148 10.033                               $ OC puncture radius
72  cz 50.563                                          $ OC oshell punct (out)
73  cz 46.753                                          $ OC oshell punct (in)
74  cz 50.905                                          $ OC therm punct (out)
75  cz 50.563                                          $ OC therm punct (in)
76  cz 46.038                                          $ OC lead (mid)
77  cz 50.324                                          $ OC oshell (mid)
78  cz 45.204                                          $ OC lead punct (mid)
79  cz 48.658                                          $ OC oshell punct (mid)
C
80  cz 150.905                                         $ 1-meter from OC therm
C
777 c/x 0 164.148 2.54                                 $ Tally cylinder
888 px 0                                               $ Tally truncation
999 sz 164.148 277.905                                 $ Outside world

C
C Physics Cards
C
mode p
C
C Source Cards
C
C Cylindrical Sources
sdef pos=d1 erg=d2 par=2 axs=0 0 1 rad=d3 ext=d4
sc1 Co60
C Source Position and Fraction
si1 L 29.873 0 164.148
      38.885 0 164.148
sp1   98 2
C Source Energy (MeV) and Intensity (%)
si2 L 3.469300E-01 8.262800E-01 1.173237E+00 1.332501E+00
     2.158770E+00 2.505000E+00
sp2 7.600000E-03 7.600000E-03 9.997360E+01 9.998560E+01
     1.110000E-03 2.000000E-06
C Source Radius
si3 0 0.635
sp3 -21 1
C Source Extent
si4 -0.635 0.635
sp4 -21 0
C
C Tally Cards
C
f2:p 69
fc2 Surface Dose (mrem/hr)                             $ Surface detector
fs2 -888 -777 t
sd2 1.0 20.268 1.0 1.0                                 $ Surface tally area
f22:p 80
fc22 1-meter Dose (mrem/hr)                            $ 1-m detector
fs22 -888 -777 t
sd22 1.0 20.268 1.0 1.0                                $ Surface tally area
C
C ANSI/ANS-6.1.1-1977 Gamma Flux to Dose Factors (mrem/hr)
de0 1.0e-02 3.0e-02 5.0e-02 7.0e-02 1.0e-01            $ Energy (Mev)
     1.5e-01 2.0e-01 2.5e-01 3.0e-01 3.5e-01
     4.0e-01 4.5e-01 5.0e-01 5.5e-01 6.0e-01
     6.5e-01 7.0e-01 8.0e-01 1.00 1.40
     1.80 2.20 2.60 2.80 3.25
     3.75 4.25 4.75 5.00 5.25
     5.75 6.25 6.75 7.50 9.00
     11.00 13.00 15.0000
df0 3.96e-03 5.82e-04 2.90e-04 2.58e-04 2.83e-04       $ Conversion (mrem/hr)
     3.79e-04 5.01e-04 6.31e-04 7.59e-04 8.78e-04
     9.85e-04 1.08e-03 1.17e-03 1.27e-03 1.36e-03
     1.44e-03 1.52e-03 1.68e-03 1.98e-03 2.51e-03
     2.99e-03 3.42e-03 3.82e-03 4.01e-03 4.41e-03
     4.83e-03 5.23e-03 5.60e-03 5.80e-03 6.01e-03
     6.37e-03 6.74e-03 7.11e-03 7.66e-03 8.77e-03
     1.03e-02 1.18e-02 1.33e-02
C
C Material Cards
C
m1   40000 -1.00                                       $ Zirconium
m2   14000 -0.01                                       $ Stainless Steel
     24000 -0.19
     25000 -0.02
     26000 -0.68
     28000 -0.10
```

```
m3   26000 -1.00                                          $ Carbon Steel (iron)
m4   82000 -1.00                                          $ Lead
m5   1000   2                                            $ EHMW Polyethylene
     6000   1
C
C Runtime and Print Cards
C
prdmp j j 1 2
ctme 480
```

5.7.1.3 RH-TRU 72-B – NS30 Neutron Shielded Canister

5.7.1.3.1 NCT Concentrated 60Co Gamma Source – 8ng001.i

```
title RH-TRU 72-B NS30 NCT Gamma Concentrated 1 g/cc Co60
C
C Cell Cards
C
10  1 -1         10  -11  -16                imp:p=1    $ Source #1
11  1 -1         12  -13  -17                imp:p=1    $ Source #2
12  1 -1         14  -15  -18                imp:p=1    $ Source #3
20  0            20  -21  -26
              (-10:  11:  16)                imp:p=1    $ Drum #1 cavity
21  0            22  -23  -27
              (-12:  13:  17)                imp:p=1    $ Drum #2 cavity
22  0            24  -25  -28
              (-14:  15:  18)                imp:p=1    $ Drum #3 cavity
30  0            31  -35  -33
              #10  #11  #12
              #20  #21  #22                  imp:p=1    $ NS30 cavity
31  5 -0.94000  30  -31  -32                 imp:p=1    $ NS30 botcap
32  5 -0.94000  31  -35   33  -32            imp:p=1    $ NS30 body
33  5 -0.94000  35  -34  -32                 imp:p=1    $ NS30 topcap
40  0            41  -45  -43
              (-30:  32:  34)                imp:p=1    $ RLC cavity
41  3 -7.85260  40  -41  -42                 imp:p=1    $ RLC base
42  3 -7.85260  41  -46   43  -42            imp:p=1    $ RLC shell
43  3 -7.85260  45  -44  -43                 imp:p=1    $ RLC lid
50  0            51  -53  -55
             (-40:  42:  46)
            ☹ 44  -46  -43)                 imp:p=1    $ IV cavity
51  2 -8.01280  50  -51  -52                 imp:p=1    $ IV base
52  2 -8.01280  51  -55   53  -52            imp:p=2    $ IV shell
53  2 -8.01280  55  -54  -52                 imp:p=1    $ IV lid
60  0            61  -63  -65
              (-50:  52:  54)                imp:p=2    $ OC cavity
61  2 -8.01280  60  -61  -69                 imp:p=1    $ OC base
62  2 -8.01280  61  -66   65  -64            imp:p=5    $ OC ishell
63  4 -11.3500  61  -66   64  -76  71        imp:p=3E1  $ OC lead in
64  4 -11.3500  61  -66   76  -68  71        imp:p=3E2  $ OC lead out
65  2 -8.01280  61  -66   68  -77  71        imp:p=3E3  $ OC oshell in
66  2 -8.01280  61  -66   77  -67  71        imp:p=6E3  $ OC oshell out
67  0           61  -66   67  -70  71        imp:p=1E5  $ OC airgap
68  2 -8.01280  61  -66   70  -69  71        imp:p=2E5  $ OC tshell
69  2 -8.01280  66  -63   65  -69            imp:p=1    $ OC flange
70  2 -8.01280  63  -62  -69                 imp:p=1    $ OC lid
71  4 -11.3500  64  -78  -71                 imp:p=3E1  $ OC lead punct in
72  4 -11.3500  78  -73  -71                 imp:p=3E2  $ OC lead punct out
73  2 -8.01280  73  -79  -71                 imp:p=3E3  $ OC oshell punct in
74  2 -8.01280  79  -72  -71                 imp:p=6E3  $ OC oshell punct out
75  0           72  -75  -71                 imp:p=1E5  $ OC airgap punct
76  2 -8.01280  75  -74  -71                 imp:p=2E5  $ OC tshell punct
777 0           69  -80   60  -62            imp:p=2E5  $ Outside to tally
888 0          -999
              (-60:  80:  62)                imp:p=1E1  $ Outside pkg
999 0           999                           imp:p=0    $ Outside world

C
C Geometry Cards
C
10  pz 88.9                                               $ Source #1 bottom
11  pz 91.44                                              $ Source #1 top
12  pz 162.878                                            $ Source #2 bottom
13  pz 165.418                                            $ Source #2 top
14  pz 236.855                                            $ Source #3 bottom
15  pz 239.395                                            $ Source #3 top
16  c/z 0 0 1.27                                          $ Source #1 radius
```

```
17  c/z 0 0 1.27                                $ Source #2 radius
18  c/z 0 0 1.27                                $ Source #3 radius
C
20  pz 53.34                                    $ Drum #1 bottom
21  pz 127                                      $ Drum #1 top
22  pz 127.318                                  $ Drum #2 bottom
23  pz 200.978                                  $ Drum #2 top
24  pz 201.295                                  $ Drum #3 bottom
25  pz 274.955                                  $ Drum #3 top
26  c/z 0 0 24.765                              $ Drum #1 radius
27  c/z 0 0 24.765                              $ Drum #2 radius
28  c/z 0 0 24.765                              $ Drum #3 radius
C
30  pz 21.908                                   $ NS30 botcap (outside)
31  pz 34.608                                   $ NS30 botcap (inside)
32  c/z 0 0 30.48                               $ NS30 body (outside)
33  c/z 0 0 26.787                              $ NS30 body (inside)
34  pz 306.388                                  $ NS30 topcap (outside)
35  pz 293.688                                  $ NS30 topcap (inside)
C
40  pz 19.368                                   $ RLC base (outside)
41  pz 20.638                                   $ RLC base (inside)
42  c/z 0 0 33.02                               $ RLC shell (outside)
43  c/z 0 0 32.385                              $ RLC shell (inside)
44  pz 309.563                                  $ RLC lid (outside)
45  pz 307.658                                  $ RLC lid (inside)
46  pz 325.438                                  $ RLC top (outside)
C
50  pz 14.288                                   $ IV base (outside)
51  pz 18.098                                   $ IV base (inside)
52  c/z 0 0 40.64                               $ IV shell (outside)
53  c/z 0 0 39.688                              $ IV shell (inside)
54  pz 343.218                                  $ IV top (outside)
55  pz 326.708                                  $ IV top (inside)
C
60  pz 0                                        $ OC bottom (outside)
61  pz 12.7                                     $ OC bottom (inside)
62  pz 360.045                                  $ OC top (outside)
63  pz 344.805                                  $ OC top (inside)
64  cz 43.656                                   $ OC ishell (outside)
65  cz 41.116                                   $ OC ishell (inside)
66  pz 320.675                                  $ OC lead (upper)
67  cz 52.229                                   $ OC oshell (outside)
68  cz 48.419                                   $ OC oshell (inside)
69  cz 52.838                                   $ OC therm (outside)
70  cz 52.495                                   $ OC therm (inside)
71  c/x 0 164.148 10.033                        $ OC puncture radius
72  cz 52.229                                   $ OC oshell punct (out)
73  cz 48.419                                   $ OC oshell punct (in)
74  cz 52.838                                   $ OC therm punct (out)
75  cz 52.495                                   $ OC therm punct (in)
76  cz 46.038                                   $ OC lead (mid)
77  cz 50.324                                   $ OC oshell (mid)
78  cz 46.038                                   $ OC lead punct (mid)
79  cz 50.324                                   $ OC oshell punct (mid)
C
80  cz 252.838                                  $ 2-meter from OC therm
C
777 pz 161.608                                  $ Ring tally (lower)
888 pz 166.688                                  $ Ring tally (upper)
999 sz 164.148 379.838                          $ Outside world

C
C Physics Cards
C
mode p
C
C Source Cards
C
C Cylindrical Sources
sdef pos=d1 erg=d2 par=2 axs=0 0 1 rad=d3 ext=d4
sc1 Co60
C Source Position and Fraction
si1 L 0 0 90.17
      0 0 164.148
      0 0 238.125
sp1   1 1 1
C Source Energy (MeV) and Intensity (%)
si2 L 3.469300E-01 8.262800E-01 1.173237E+00 1.332501E+00
     2.158770E+00 2.505000E+00
sp2 7.600000E-03 7.600000E-03 9.997360E+01 9.998560E+01
```

```
     1.110000E-03 2.000000E-06
C Source Radius
si3 0 1.27
sp3 -21 1
C Source Extent
si4 -1.27 1.27
sp4 -21 0
C
C Tally Cards
C
f2:p 69
fc2 Surface Dose (mrem/hr)                                  $ Surface detector
fs2 888 777 t
sd2 1.0 1686.525 1.0 1.0                                    $ Surface tally area
f22:p 80
fc22 2-meter Dose (mrem/hr)                                 $ 2-m detector
fs22 888 777 t
sd22 1.0 8070.229 1.0 1.0                                   $ Surface tally area
C
C ANSI/ANS-6.1.1-1977 Gamma Flux to Dose Factors (mrem/hr)
de0 1.0e-02 3.0e-02 5.0e-02 7.0e-02 1.0e-01                 $ Energy (Mev)
     1.5e-01 2.0e-01 2.5e-01 3.0e-01 3.5e-01
     4.0e-01 4.5e-01 5.0e-01 5.5e-01 6.0e-01
     6.5e-01 7.0e-01 8.0e-01 1.00 1.40
     1.80 2.20 2.60 2.80 3.25
     3.75 4.25 4.75 5.00 5.25
     5.75 6.25 6.75 7.50 9.00
     11.00 13.00 15.0000
df0 3.96e-03 5.82e-04 2.90e-04 2.58e-04 2.83e-04            $ Conversion (mrem/hr)
     3.79e-04 5.01e-04 6.31e-04 7.59e-04 8.78e-04
     9.85e-04 1.08e-03 1.17e-03 1.27e-03 1.36e-03
     1.44e-03 1.52e-03 1.68e-03 1.98e-03 2.51e-03
     2.99e-03 3.42e-03 3.82e-03 4.01e-03 4.41e-03
     4.83e-03 5.23e-03 5.60e-03 5.80e-03 6.01e-03
     6.37e-03 6.74e-03 7.11e-03 7.66e-03 8.77e-03
     1.03e-02 1.18e-02 1.33e-02
C
C Material Cards
C
m1   40000 -1.00                                           $ Zirconium
m2   14000 -0.01                                           $ Stainless Steel
     24000 -0.19
     25000 -0.02
     26000 -0.68
     28000 -0.10
m3   26000 -1.00                                           $ Carbon Steel (iron)
m4   82000 -1.00                                           $ Lead
m5   1000   2                                             $ EHMW Polyethylene
     6000   1
C
C Runtime and Print Cards
C
prdmp j j 1 2
ctme 120
```

5.7.1.3.2 HAC 252Cf Neutron Source – 8hn001.i

```
title RH-TRU 72-B NS30 HAC Neutron Concentrated 1 g/cc Cf252
C
C Cell Cards
C
10  1 -1         10  -11  -16                imp:n=1    $ Source #1
11  1 -1         12  -13  -17                imp:n=1    $ Source #2
20  0            20  -21  -26
              (-10:  11:  16)                imp:n=1    $ Drum #1 cavity
21  0            22  -23  -27
              (-12:  13:  17)                imp:n=1    $ Drum #2 cavity
30  0            31  -35  -33
               #10  #20                      imp:n=1    $ NS30 cavity
31  5 -0.94000   30  -31  -32                imp:n=1    $ NS30 botcap
32  5 -0.94000   31  -35   33  -32           imp:n=1    $ NS30 body
33  5 -0.94000   35  -34  -32                imp:n=1    $ NS30 topcap
40  0            41  -45  -43
              (-30:  32:  34) #11  #21       imp:n=1    $ RLC cavity
41  3 -7.85260   40  -41  -42                imp:n=1    $ RLC base
42  3 -7.85260   41  -46   43  -42           imp:n=1    $ RLC shell
43  3 -7.85260   45  -44  -43                imp:n=1    $ RLC lid
50  0            51  -53  -55
              (-40:  42:  46)
```

```
             ⊗ 44  -46  -43)                imp:n=1    $ IV cavity
51  2 -8.01280  50  -51  -52                 imp:n=1    $ IV base
52  2 -8.01280  51  -55   53  -52            imp:n=1    $ IV shell
53  2 -8.01280  55  -54  -52                 imp:n=1    $ IV lid
60  0           61  -63  -65
            (-50:  52:  54)                  imp:n=1    $ OC cavity
61  2 -8.01280  60  -61  -69                 imp:n=1    $ OC base
62  2 -8.01280  61  -66   65  -64            imp:n=1    $ OC ishell
63  4 -11.3500  61  -66   64  -76  71        imp:n=1    $ OC lead in
64  4 -11.3500  61  -66   76  -68  71        imp:n=1    $ OC lead out
65  2 -8.01280  61  -66   68  -77  71        imp:n=1    $ OC oshell in
66  2 -8.01280  61  -66   77  -67  71        imp:n=1    $ OC oshell out
67  0           61  -66   67  -70  71        imp:n=1    $ OC airgap
68  2 -8.01280  61  -66   70  -69  71        imp:n=1    $ OC tshell
69  2 -8.01280  66  -63   65  -69            imp:n=1    $ OC flange
70  2 -8.01280  63  -62  -69                 imp:n=1    $ OC lid
71  4 -11.3500  64  -78  -71                 imp:n=1    $ OC lead punct in
72  4 -11.3500  78  -73  -71                 imp:n=1    $ OC lead punct out
73  2 -8.01280  73  -79  -71                 imp:n=1    $ OC oshell punct in
74  2 -8.01280  79  -72  -71                 imp:n=1    $ OC oshell punct out
75  0           74  -69  -71                 imp:n=1    $ OC airgap punct
76  2 -8.01280  75  -74  -71                 imp:n=1    $ OC tshell punct
777 0           69  -80   60  -62            imp:n=1    $ Outside to tally
888 0          -999
            (-60:  80:  62)                  imp:n=1    $ Outside pkg
999 0           999                          imp:n=0    $ Outside world

C
C Geometry Cards
C
10  pz 163.513                                          $ Source #1 bottom
11  pz 164.783                                          $ Source #1 top
12  pz 163.513                                          $ Source #2 bottom
13  pz 164.783                                          $ Source #2 top
16  c/z 34.638 0 0.635                                  $ Source #1 radius
17  c/z 38.885 0 0.635                                  $ Source #2 radius
C
20  pz 163.511                                          $ Drum #1 bottom
21  pz 164.784                                          $ Drum #1 top
22  pz 163.511                                          $ Drum #2 bottom
23  pz 164.784                                          $ Drum #2 top
26  c/z 34.638 0 0.636                                  $ Drum #1 radius
27  c/z 38.885 0 0.636                                  $ Drum #2 radius
C
30  pz 21.908                                           $ NS30 botcap (outside)
31  pz 34.608                                           $ NS30 botcap (inside)
32  c/z 7.748 0 30.48                                   $ NS30 body (outside)
33  c/z 7.748 0 27.529                                  $ NS30 body (inside)
34  pz 306.388                                          $ NS30 topcap (outside)
35  pz 293.688                                          $ NS30 topcap (inside)
C
40  pz 19.368                                           $ RLC base (outside)
41  pz 20.638                                           $ RLC base (inside)
42  c/z 7.139 0 33.02                                   $ RLC shell (outside)
43  c/z 7.139 0 32.385                                  $ RLC shell (inside)
44  pz 309.563                                          $ RLC lid (outside)
45  pz 307.658                                          $ RLC lid (inside)
46  pz 325.438                                          $ RLC top (outside)
C
50  pz 14.288                                           $ IV base (outside)
51  pz 18.098                                           $ IV base (inside)
52  c/z 0.474 0 40.64                                   $ IV shell (outside)
53  c/z 0.474 0 39.688                                  $ IV shell (inside)
54  pz 343.218                                          $ IV top (outside)
55  pz 326.708                                          $ IV top (inside)
C
60  pz 0                                                $ OC bottom (outside)
61  pz 12.7                                             $ OC bottom (inside)
62  pz 360.045                                          $ OC top (outside)
63  pz 344.805                                          $ OC top (inside)
64  cz 43.656                                           $ OC ishell (outside)
65  cz 41.116                                           $ OC ishell (inside)
66  pz 320.675                                          $ OC lead (upper)
67  cz 52.229                                           $ OC oshell (outside)
68  cz 48.419                                           $ OC oshell (inside)
69  cz 52.838                                           $ OC therm (outside)
70  cz 52.495                                           $ OC therm (inside)
71  c/x 0 164.148 10.033                                $ OC puncture radius
72  cz 50.563                                           $ OC oshell punct (out)
73  cz 46.753                                           $ OC oshell punct (in)
74  cz 50.905                                           $ OC therm punct (out)
```

```
75  cz 50.563                                          $ OC therm punct (in)
76  cz 46.038                                          $ OC lead (mid)
77  cz 50.324                                          $ OC oshell (mid)
78  cz 45.204                                          $ OC lead punct (mid)
79  cz 48.658                                          $ OC oshell punct (mid)
C
80  cz 150.905                                         $ 1-meter from OC therm
C
777 c/x 0 164.148 2.54                                 $ Tally cylinder
888 px 0                                               $ Tally truncation
999 sz 164.148 277.905                                 $ Outside world

C
C Physics Cards
C
mode n
C
C Source Cards
C
C Cylindrical Sources
sdef pos=d1 erg=d2 par=1 axs=0 0 1 rad=d3 ext=d4
sc1 Cf252
C Source Position and Fraction
si1 L 34.638 0 164.148
      38.885 0 164.148
sp1   98 2
C Source Energy (MeV) and Fraction
si2 0.1 0.5 1.0 2.0 3.0
     4.0 6.0 8.0 10.0 15.0
sp2 0.00E+00 1.80E+11 2.71E+11 5.36E+11 4.10E+11
     2.73E+11 2.66E+11 8.53E+10 2.44E+10 8.36E+09
C Source Radius
si3 0 0.635
sp3 -21 1
C Source Extent
si4 -0.635 0.635
sp4 -21 0
C
C Tally Cards
C
f2:n 69
fc2 Surface Dose (mrem/hr)                             $ Surface detector
fs2 -888 -777 t
sd2 1.0 20.268 1.0 1.0                                 $ Surface tally area
f22:n 80
fc22 1-meter Dose (mrem/hr)                            $ 1-m detector
fs22 -888 -777 t
sd22 1.0 20.268 1.0 1.0                                $ Surface tally area
C
C ANSI/ANS-6.1.1-1977 Neutron Flux to Dose Factors (mrem/hr)
de0  2.5e-08 1.0e-07 1.0e-06 1.0e-05 1.0e-04           $ Energy (Mev)
     1.0e-03 1.0e-02 1.0e-01 5.0e-01 1.0
     2.5 5.0 7.0 10.0 14.0 20.0
df0  3.67e-03 3.67e-03 4.46e-03 4.54e-03 4.18e-03      $ Conversion (mrem/hr)
     3.76e-03 3.56e-03 2.17e-02 9.26e-02 1.32e-01
     1.25e-01 1.56e-01 1.47e-01 1.47e-01 2.08e-01 2.27e-01
C
C Material Cards
C
m1   40000.60c -1.00                                   $ Zirconium
m2   14000.60c -0.01                                   $ Stainless Steel
     24052.60c -0.19
     25055.60c -0.02
     26057.60c -0.68
     28058.60c -0.10
m3   26057.60c -1.00                                   $ Carbon Steel (iron)
m4   82000.50c -1.00                                   $ Lead
m5   1001.60c   2                                      $ EHMW Polyethylene
     6000.60c   1
mt5  poly.60t
C
C Runtime and Print Cards
C
prdmp j j 1 2
ctme 360
```

This page intentionally left blank.

5.7.2 Sample MCNP Output Files

5.7.2.1 RH-TRU 72-B – RH-TRU Waste Canister

5.7.2.1.1 NCT Concentrated 60Co Gamma Source – 7ng001.io

```
          Thread Name & Version = MCNP5, 1.60

            _ _   _  _   _    _
           |_|_|  (_  |_|  |_)  _)
                        |

  +------------------------------------------------------------------+
  | Copyright 2010. Los Alamos National Security, LLC.  All rights   |
  | reserved.                                                        |
  |   This material was produced under U.S. Government contract      |
  | DE-AC52-06NA25396 for Los Alamos National Laboratory, which is   |
  | operated by Los Alamos National Security, LLC, for the U.S.      |
  | Department of Los Energy. The Government is granted for itself and |
  | others acting on its behalf a paid-up, nonexclusive, irrevocable |
  | worldwide license in this material to reproduce, prepare derivative |
  | works, and perform publicly and display publicly. Beginning five |
  | (5) years after 2010, subject to additional five-year worldwide  |
  | renewals, the Government is granted for itself and others acting on |
  | its behalf a paid-up, nonexclusive, irrevocable worldwide license |
  | in this material to reproduce, prepare derivative works, distribute |
  | copies to the public, perform publicly and display publicly, and to |
  | permit others to do so. NEITHER THE UNITED STATES NOR THE UNITED |
  | STATES DEPARTMENT OF ENERGY, NOR LOS ALAMOS NATIONAL SECURITY, LLC, |
  | NOR ANY OF THEIR EMPLOYEES, MAKES ANY WARRANTY, EXPRESS OR IMPLIED, |
  | OR ASSUMES ANY LEGAL LIABILITY OR RESPONSIBILITY FOR THE ACCURACY, |
  | COMPLETENESS, OR USEFULNESS OF ANY INFORMATION, APPARATUS, PRODUCT, |
  | OR PROCESS DISCLOSED, OR REPRESENTS THAT ITS USE WOULD NOT INFRINGE |
  | PRIVATELY OWNED RIGHTS.                                          |
  +------------------------------------------------------------------+

1mcnp     version 5     ld=09282010                    07/22/14 18:57:53
 ***********************************************************************                    probid =  07/22/14 18:57:53
 inp=7ng001.i

         1-       title RH-TRU 72-B RLC NCT Gamma Concentrated 1 g/cc Co60
         2-       C
         3-       C Cell Cards
         4-       C
         5-       10  1 -1        10  -11  -16                imp:p=1    $ Source #1
         6-       11  1 -1        12  -13  -17                imp:p=1    $ Source #2
         7-       12  1 -1        14  -15  -18                imp:p=1    $ Source #3
         8-       20  0           20  -21  -26
         9-                     (-10:  11:  16)              imp:p=1    $ Drum #1 cavity
        10-       21  0           22  -23  -27
        11-                     (-12:  13:  17)              imp:p=1    $ Drum #2 cavity
        12-       22  0           24  -25  -28
```

```
      13-                      (-14:  15:  18)                imp:p=1    $ Drum #3 cavity
      14-       40  0           41  -45  -43
      15-                       #10  #11  #12
      16-                       #20  #21  #22                 imp:p=1    $ RLC cavity
      17-       41  3 -7.85260  40  -41  -42                 imp:p=1    $ RLC base
      18-       42  3 -7.85260  41  -46   43  -42            imp:p=1    $ RLC shell
      19-       43  3 -7.85260  45  -44  -43                 imp:p=1    $ RLC lid
      20-       50  0           51  -53  -55
      21-                      (-40:  42:  46)
      22-                     :( 44  -46  -43)               imp:p=1    $ IV cavity
      23-       51  2 -8.01280  50  -51  -52                 imp:p=1    $ IV base
      24-       52  2 -8.01280  51  -55   53  -52            imp:p=2    $ IV shell
      25-       53  2 -8.01280  55  -54  -52                 imp:p=1    $ IV lid
      26-       60  0           61  -63  -65
      27-                      (-50:  52:  54)               imp:p=2    $ OC cavity
      28-       61  2 -8.01280  60  -61  -69                 imp:p=1    $ OC base
      29-       62  2 -8.01280  61  -66   65  -64            imp:p=5    $ OC ishell
      30-       63  4 -11.3500  61  -66   64  -76  71        imp:p=3E1  $ OC lead in
      31-       64  4 -11.3500  61  -66   76  -68  71        imp:p=3E2  $ OC lead out
      32-       65  2 -8.01280  61  -66   68  -77  71        imp:p=3E3  $ OC oshell in
      33-       66  2 -8.01280  61  -66   77  -67  71        imp:p=6E3  $ OC oshell out
      34-       67  0           61  -66   67  -70  71        imp:p=1E5  $ OC airgap
      35-       68  2 -8.01280  61  -66   70  -69  71        imp:p=2E5  $ OC tshell
      36-       69  2 -8.01280  66  -63   65  -69            imp:p=1    $ OC flange
      37-       70  2 -8.01280  63  -62  -69                 imp:p=1    $ OC lid
      38-       71  4 -11.3500  64  -78  -71                 imp:p=3E1  $ OC lead punct in
      39-       72  4 -11.3500  78  -73  -71                 imp:p=3E2  $ OC lead punct out
      40-       73  2 -8.01280  73  -79  -71                 imp:p=3E3  $ OC oshell punct in
      41-       74  2 -8.01280  79  -72  -71                 imp:p=6E3  $ OC oshell punct out
      42-       75  0           72  -75  -71                 imp:p=1E5  $ OC airgap punct
      43-       76  2 -8.01280  75  -74  -71                 imp:p=2E5  $ OC tshell punct
      44-       777 0           69  -80   60  -62            imp:p=2E5  $ Outside to tally
      45-       888 0         -999
      46-                      (-60:  80:  62)               imp:p=1E1  $ Outside pkg
      47-       999 0           999                         imp:p=0    $ Outside world
      48-
      49-       C
      50-       C Geometry Cards
      51-       C
      52-       10  pz 88.9                                                $ Source #1 bottom
      53-       11  pz 91.44                                                 $ Source #1 top
      54-       12  pz 162.878                                              $ Source #2 bottom
      55-       13  pz 165.418                                              $ Source #2 top
      56-       14  pz 236.855                                              $ Source #3 bottom
      57-       15  pz 239.395                                              $ Source #3 top
      58-       16  c/z 0 0 1.27                                            $ Source #1 radius
warning.  this surface has been replaced by a surface of type cz
      59-       17  c/z 0 0 1.27                                            $ Source #2 radius
warning.  this surface has been replaced by a surface of type cz
      60-       18  c/z 0 0 1.27                                            $ Source #3 radius
      61-       C
warning.  this surface has been replaced by a surface of type cz
      62-       20  pz 53.34                                                $ Drum #1 bottom
      63-       21  pz 127                                                $ Drum #1 top
      64-       22  pz 127.318                                              $ Drum #2 bottom
      65-       23  pz 200.978                                              $ Drum #2 top
      66-       24  pz 201.295                                              $ Drum #3 bottom
      67-       25  pz 274.955                                              $ Drum #3 top
```

```
      68-       26  c/z 0 0 24.765                                    $ Drum #1 radius
warning.  this surface has been replaced by a surface of type cz
      69-       27  c/z 0 0 24.765                                    $ Drum #2 radius
warning.  this surface has been replaced by a surface of type cz
      70-       28  c/z 0 0 24.765                                    $ Drum #3 radius
      71-       C
warning.  this surface has been replaced by a surface of type cz
      72-       40  pz 19.368                                        $ RLC base (outside)
      73-       41  pz 20.638                                        $ RLC base (inside)
      74-       42  c/z 0 0 33.02                                    $ RLC shell (outside)
warning.  this surface has been replaced by a surface of type cz
      75-       43  c/z 0 0 32.385                                   $ RLC shell (inside)
warning.  this surface has been replaced by a surface of type cz
      76-       44  pz 309.563                                       $ RLC lid (outside)
      77-       45  pz 307.658                                       $ RLC lid (inside)
      78-       46  pz 325.438                                       $ RLC top (outside)
      79-       C
      80-       50  pz 14.288                                        $ IV base (outside)
      81-       51  pz 18.098                                        $ IV base (inside)
      82-       52  c/z 0 0 40.64                                    $ IV shell (outside)
warning.  this surface has been replaced by a surface of type cz
      83-       53  c/z 0 0 39.688                                   $ IV shell (inside)
warning.  this surface has been replaced by a surface of type cz
      84-       54  pz 343.218                                       $ IV top (outside)
      85-       55  pz 326.708                                       $ IV top (inside)
      86-       C
      87-       60  pz 0                                             $ OC bottom (outside)
      88-       61  pz 12.7                                          $ OC bottom (inside)
      89-       62  pz 360.045                                       $ OC top (outside)
      90-       63  pz 344.805                                       $ OC top (inside)
      91-       64  cz 43.656                                        $ OC ishell (outside)
      92-       65  cz 41.116                                        $ OC ishell (inside)
      93-       66  pz 320.675                                       $ OC lead (upper)
      94-       67  cz 52.229                                        $ OC oshell (outside)
      95-       68  cz 48.419                                        $ OC oshell (inside)
      96-       69  cz 52.838                                        $ OC therm (outside)
      97-       70  cz 52.495                                        $ OC therm (inside)
      98-       71  c/x 0 164.148 10.033                             $ OC puncture radius
      99-       72  cz 52.229                                        $ OC oshell punct (out)
     100-       73  cz 48.419                                        $ OC oshell punct (in)
     101-       74  cz 52.838                                        $ OC therm punct (out)
     102-       75  cz 52.495                                        $ OC therm punct (in)
     103-       76  cz 46.038                                        $ OC lead (mid)
     104-       77  cz 50.324                                        $ OC oshell (mid)
     105-       78  cz 46.038                                        $ OC lead punct (mid)
     106-       79  cz 50.324                                        $ OC oshell punct (mid)
     107-       C
     108-       80  cz 252.838                                       $ 2-meter from OC therm
     109-       C
     110-       777 pz 161.608                                       $ Ring tally (lower)
     111-       888 pz 166.688                                       $ Ring tally (upper)
     112-       999 sz 164.148 379.838                               $ Outside world
     113-
     114-       C
     115-       C Physics Cards
     116-       C
     117-       mode p
     118-       C
```

```
C Source Cards
C
C Cylindrical Sources
sdef pos=d1 erg=d2 par=2 axs=0 0 1 rad=d3 ext=d4
sc1 Co60
C Source Position and Fraction
si1 L 0 0 90.17
      0 0 164.148
      0 0 238.125
sp1   1 1 1
C Source Energy (MeV) and Intensity (%)
si2 L 3.469300E-01 8.262800E-01 1.173237E+00 1.332501E+00
     2.158770E+00 2.505000E+00
sp2 7.600000E-03 7.600000E-03 9.997360E+01 9.998560E+01
     1.110000E-03 2.000000E-06
C Source Radius
si3 0 1.27
sp3 -21 1
C Source Extent
si4 -1.27 1.27
sp4 -21 0
C
C Tally Cards
C
f2:p 69
fc2 Surface Dose (mrem/hr)                              $ Surface detector
fs2 888 777 t
sd2 1.0 1686.525 1.0 1.0                                $ Surface tally area
f22:p 80
fc22 2-meter Dose (mrem/hr)                             $ 2-m detector
fs22 888 777 t
sd22 1.0 8070.229 1.0 1.0                               $ Surface tally area
C
C ANSI/ANS-6.1.1-1977 Gamma Flux to Dose Factors (mrem/hr)
de0 1.0e-02 3.0e-02 5.0e-02 7.0e-02 1.0e-01             $ Energy (Mev)
     1.5e-01 2.0e-01 2.5e-01 3.0e-01 3.5e-01
     4.0e-01 4.5e-01 5.0e-01 5.5e-01 6.0e-01
     6.5e-01 7.0e-01 8.0e-01 1.00 1.40
     1.80 2.20 2.60 2.80 3.25
     3.75 4.25 4.75 5.00 5.25
     5.75 6.25 6.75 7.50 9.00
     11.00 13.00 15.0000
df0 3.96e-03 5.82e-04 2.90e-04 2.58e-04 2.83e-04        $ Conversion (mrem/hr)
     3.79e-04 5.01e-04 6.31e-04 7.59e-04 8.78e-04
     9.85e-04 1.08e-03 1.17e-03 1.27e-03 1.36e-03
     1.44e-03 1.52e-03 1.68e-03 1.98e-03 2.51e-03
     2.99e-03 3.42e-03 3.82e-03 4.01e-03 4.41e-03
     4.83e-03 5.23e-03 5.60e-03 5.80e-03 6.01e-03
     6.37e-03 6.74e-03 7.11e-03 7.66e-03 8.77e-03
     1.03e-02 1.18e-02 1.33e-02
C
C Material Cards
C
m1   40000 -1.00                                        $ Zirconium
m2   14000 -0.01                                        $ Stainless Steel
     24000 -0.19
     25000 -0.02
     26000 -0.68
```

```
      177-            28000 -0.10
      178-       m3   26000 -1.00                                    $ Carbon Steel (iron)
      179-       m4   82000 -1.00                                    $ Lead
      180-       C
      181-       C Runtime and Print Cards
      182-       C
      183-       prdmp j j 1 2
      184-       ctme 120

 surface       16   and surface       17   are the same.       17   will be deleted.

 surface       16   and surface       18   are the same.       18   will be deleted.

 surface       26   and surface       27   are the same.       27   will be deleted.

 surface       26   and surface       28   are the same.       28   will be deleted.

 surface       67   and surface       72   are the same.       72   will be deleted.

 surface       68   and surface       73   are the same.       73   will be deleted.

 surface       69   and surface       74   are the same.       74   will be deleted.

 surface       70   and surface       75   are the same.       75   will be deleted.

 surface       76   and surface       78   are the same.       78   will be deleted.

 surface       77   and surface       79   are the same.       79   will be deleted.

  comment.          10 surfaces were deleted for being the same as others.

  warning.  sum of segment sizes differs from total in   2 cases.
1cells                                                                  print table 60

                          atom        gram                                      photon
            cell     mat  density     density     volume       mass            pieces importance

       1      10       1  6.60141E-03 1.00000E+00 1.28704E+01 1.28704E+01          1  1.0000E+00
       2      11       1  6.60141E-03 1.00000E+00 1.28704E+01 1.28704E+01          1  1.0000E+00
       3      12       1  6.60141E-03 1.00000E+00 1.28704E+01 1.28704E+01          1  1.0000E+00
       4      20       0  0.00000E+00 0.00000E+00 1.41912E+05 0.00000E+00          1  1.0000E+00
       5      21       0  0.00000E+00 0.00000E+00 1.41912E+05 0.00000E+00          1  1.0000E+00
       6      22       0  0.00000E+00 0.00000E+00 1.41912E+05 0.00000E+00          1  1.0000E+00
       7      40       0  0.00000E+00 0.00000E+00 5.19918E+05 0.00000E+00          1  1.0000E+00
       8      41       3  8.46757E-02 7.85260E+00 4.35019E+03 3.41603E+04          1  1.0000E+00
       9      42       3  8.46757E-02 7.85260E+00 3.97694E+04 3.12294E+05          1  1.0000E+00
      10      43       3  8.46757E-02 7.85260E+00 6.27672E+03 4.92886E+04          1  1.0000E+00
      11      50       0  0.00000E+00 0.00000E+00 5.31049E+05 0.00000E+00          1  1.0000E+00
      12      51       2  8.80825E-02 8.01280E+00 1.97689E+04 1.58404E+05          1  1.0000E+00
      13      52       2  8.80825E-02 8.01280E+00 7.41419E+04 5.94084E+05          1  2.0000E+00
      14      53       2  8.80825E-02 8.01280E+00 8.56652E+04 6.86418E+05          1  1.0000E+00
      15      60       0  0.00000E+00 0.00000E+00 5.70765E+04 0.00000E+00          1  2.0000E+00
      16      61       2  8.80825E-02 8.01280E+00 1.11390E+05 8.92546E+05          1  1.0000E+00
      17      62       2  8.80825E-02 8.01280E+00 2.08330E+05 1.66931E+06          1  5.0000E+00
      18      63       4  3.29849E-02 1.13500E+01 0.00000E+00 0.00000E+00          0  3.0000E+01
      19      64       4  3.29849E-02 1.13500E+01 0.00000E+00 0.00000E+00          0  3.0000E+02
      20      65       2  8.80825E-02 8.01280E+00 0.00000E+00 0.00000E+00          0  3.0000E+03
      21      66       2  8.80825E-02 8.01280E+00 0.00000E+00 0.00000E+00          0  6.0000E+03
```

```
       22       67        0  0.00000E+00 0.00000E+00 0.00000E+00 0.00000E+00          0  1.0000E+05
       23       68        2  8.80825E-02 8.01280E+00 0.00000E+00 0.00000E+00          0  2.0000E+05
       24       69        2  8.80825E-02 8.01280E+00 8.34880E+04 6.68973E+05          1  1.0000E+00
       25       70        2  8.80825E-02 8.01280E+00 1.33668E+05 1.07106E+06          1  1.0000E+00
       26       71        4  3.29849E-02 1.13500E+01 0.00000E+00 0.00000E+00          0  3.0000E+01
       27       72        4  3.29849E-02 1.13500E+01 0.00000E+00 0.00000E+00          0  3.0000E+02
       28       73        2  8.80825E-02 8.01280E+00 0.00000E+00 0.00000E+00          0  3.0000E+03
       29       74        2  8.80825E-02 8.01280E+00 0.00000E+00 0.00000E+00          0  6.0000E+03
       30       75        0  0.00000E+00 0.00000E+00 0.00000E+00 0.00000E+00          0  1.0000E+05
       31       76        2  8.80825E-02 8.01280E+00 0.00000E+00 0.00000E+00          0  2.0000E+05
       32      777        0  0.00000E+00 0.00000E+00 6.91509E+07 0.00000E+00          1  2.0000E+05
       33      888        0  0.00000E+00 0.00000E+00 1.57245E+08 0.00000E+00          1  1.0000E+01
       34      999        0  0.00000E+00 0.00000E+00 0.00000E+00 0.00000E+00          0  0.0000E+00

 total                                                2.28696E+08 6.13657E+06

    minimum source weight = 1.0000E+00    maximum source weight = 1.0000E+00

 ************************************************
 * Random Number Generator  =                   1 *
 * Random Number Seed       =       19073486328125 *
 * Random Number Multiplier =       19073486328125 *
 * Random Number Adder      =                   0 *
 * Random Number Bits Used  =                  48 *
 * Random Number Stride     =              152917 *
 ************************************************


        11 warning messages so far.
1cross-section tables                                                                  print table 100

     table    length

                         tables from file mcplib04

  14000.04p     4792  ENDF/B-VI Release 8 Photoatomic Data for 14-SI                  mat1400      02/07/03
  24000.04p     5682  ENDF/B-VI Release 8 Photoatomic Data for 24-CR                  mat2400      02/07/03
  25000.04p     5598  ENDF/B-VI Release 8 Photoatomic Data for 25-MN                  mat2500      02/07/03
  26000.04p     5718  ENDF/B-VI Release 8 Photoatomic Data for 26-FE                  mat2600      02/07/03
  28000.04p     5826  ENDF/B-VI Release 8 Photoatomic Data for 28-NI                  mat2800      02/07/03
  40000.04p     7703  ENDF/B-VI Release 8 Photoatomic Data for 40-ZR                  mat4000      02/07/03
  82000.04p    10010  ENDF/B-VI Release 8 Photoatomic Data for 82-PB                  mat8200      02/07/03

  total        45329

 maximum photon energy set to  100.0 mev (maximum electron energy)

                         tables from file el03

  14000.03e     2339                                                                                6/6/98
  24000.03e     2345                                                                                6/6/98
  25000.03e     2345                                                                                6/6/98
  26000.03e     2345                                                                                6/6/98
  28000.03e     2347                                                                                6/6/98
  40000.03e     2353                                                                                6/6/98
  82000.03e     2373                                                                                6/6/98

  warning.  material        1 has been set to a conductor.
```

```
  warning.  material        2 has been set to a conductor.

  warning.  material        3 has been set to a conductor.

  warning.  material        4 has been set to a conductor.

 ************************************************************************************************************************

 dump no.    1 on file runtpe     nps =           0     coll =              0     ctm =        0.00   nrn =
    0

       15 warning messages so far.

 ************************************************************************************************************************

 dump no.    2 on file runtpe     nps =      968316     coll =      662303549     ctm =       60.01   nrn =
 9549144901
1problem summary

      run terminated when it had used  120  minutes of computer time.
+                                                                                                  07/22/14 20:57:55
      title RH-TRU 72-B RLC NCT Gamma Concentrated 1 g/cc Co60                              probid =  07/22/14 18:57:53
0
 photon creation     tracks      weight        energy            photon loss         tracks      weight        energy
                                 (per source particle)                                           (per source particle)

 source             1936616    1.0000E+00    1.2528E+00          escape          1483514441    3.9546E-03    3.0892E-03
                                                                 energy cutoff             0    0.            1.6116E-04
                                                                 time cutoff               0    0.            0.
 weight window             0    0.            0.                weight window             0    0.            0.
 cell importance  1784639430    2.3319E-01    1.0758E-01        cell importance   132762830    2.3320E-01    1.0765E-01
 weight cutoff             0    0.            0.                weight cutoff             0    0.            0.
 e or t importance         0    0.            0.                e or t importance         0    0.            0.
 dxtran                    0    0.            0.                dxtran                    0    0.            0.
 forced collisions         0    0.            0.                forced collisions         0    0.            0.
 exp. transform            0    0.            0.                exp. transform            0    0.            0.
 from neutrons             0    0.            0.                compton scatter           0    0.            9.8822E-01
 bremsstrahlung    115833074    6.8753E-01    2.4037E-02        capture           402410258    2.4377E+00    3.0949E-01
 p-annihilation       624160    5.2331E-03    2.6741E-03        pair production      312080    2.6165E-03    3.4200E-03
 photonuclear              0    0.            0.                photonuclear abs          0    0.            0.
 electron x-rays           0    0.            0.
 1st fluorescence  106347660    6.7614E-01    2.4130E-02
 2nd fluorescence    9618669    7.5373E-02    8.4823E-04
     total        2018999609    2.6775E+00    1.4120E+00              total        2018999609    2.6775E+00    1.4120E+00

   number of photons banked                239570416        average time of (shakes)              cutoffs
   photon tracks per source particle      1.0425E+03          escape            1.2868E+00        tco   1.0000E+33
   photon collisions per source particle  6.8327E+02          capture           1.6197E-01        eco   1.0000E-03
   total photon collisions                1323238326          capture or escape 1.6379E-01        wc1  -5.0000E-01
                                                              any termination   1.6357E-01        wc2  -2.5000E-01

 computer time so far in this run   120.02 minutes            maximum number ever in bank        13
 computer time in mcrun             120.01 minutes            bank overflows to backup file       0
 source particles per minute            1.6137E+04
 random numbers generated              19078044321            most random numbers used was     1731204 in history     1619895

  warning.   random number stride   152917 exceeded       42 times.
```

```
 range of sampled source weights = 1.0000E+00 to 1.0000E+00

  warning.  importance function may be poor.  see print table 120.
1photon   activity in each cell                                                print table 126
```

cell	tracks entering	population	collisions	collisions * weight (per history)	number weighted energy	flux weighted energy	average track weight (relative)	average track mfp (cm)
1 10	646876	659362	51816	2.6756E-02	1.2192E+00	1.2192E+00	1.0000E+00	1.9064E+01
2 11	645386	657722	51865	2.6781E-02	1.2190E+00	1.2190E+00	1.0000E+00	1.9062E+01
3 12	645087	657376	51321	2.6500E-02	1.2191E+00	1.2191E+00	1.0000E+00	1.9064E+01
4 20	790214	745240	0	0.0000E+00	1.0986E+00	1.0986E+00	1.0000E+00	0.0000E+00
5 21	849806	800273	0	0.0000E+00	1.0852E+00	1.0852E+00	1.0000E+00	0.0000E+00
6 22	788812	743660	0	0.0000E+00	1.0983E+00	1.0983E+00	1.0000E+00	0.0000E+00
7 40	2766323	2012357	0	0.0000E+00	9.1375E-01	9.1375E-01	1.0000E+00	0.0000E+00
8 41	66681	66150	93257	4.8155E-02	7.2229E-01	7.2229E-01	1.0000E+00	1.6539E+00
9 42	2423987	2179714	1905795	9.8409E-01	8.4894E-01	8.4894E-01	1.0000E+00	1.8264E+00
10 43	62469	66971	123028	6.3527E-02	7.2377E-01	7.2377E-01	1.0000E+00	1.6606E+00
11 50	2588758	2174668	0	0.0000E+00	8.0455E-01	8.0455E-01	8.1824E-01	0.0000E+00
12 51	61252	69644	217609	1.1237E-01	6.5505E-01	6.5505E-01	1.0000E+00	1.5443E+00
13 52	4301893	4250381	5336851	1.3779E+00	7.5235E-01	7.5235E-01	1.0000E+00	1.6658E+00
14 53	35283	44202	186717	9.6414E-02	6.1184E-01	6.1184E-01	1.0000E+00	1.4905E+00
15 60	4179889	3591399	0	0.0000E+00	7.1834E-01	7.1834E-01	7.7526E-01	0.0000E+00
16 61	18883	23422	100454	5.1871E-02	5.7951E-01	5.7951E-01	1.0000E+00	1.4504E+00
17 62	7508032	8697721	21584111	2.2291E+00	6.9191E-01	6.9191E-01	1.0000E+00	1.5984E+00
18 63	19700906	39742559	75104210	1.2927E+00	9.0566E-01	9.0566E-01	1.0000E+00	1.0820E+00
19 64	31527697	67917300	127029460	2.1865E-01	9.4386E-01	9.4386E-01	1.0000E+00	1.1351E+00
20 65	75052111	82017286	161597370	2.7814E-02	7.0313E-01	7.0313E-01	1.0000E+00	1.6304E+00
21 66	92685759	102976520	210395510	1.8107E-02	6.2836E-01	6.2836E-01	1.0000E+00	1.5283E+00
22 67	167235007	162348133	0	0.0000E+00	6.4147E-01	6.4147E-01	3.1410E+00	0.0000E+00
23 68	1658441323	1699861996	703438701	1.8162E-03	6.6086E-01	6.6086E-01	1.0000E+00	1.5917E+00
24 69	6437	7550	29217	1.5087E-02	5.6453E-01	5.6453E-01	1.0000E+00	1.4268E+00
25 70	157	187	787	4.0638E-04	5.1001E-01	5.1001E-01	1.0000E+00	1.3571E+00
26 71	261570	512144	935568	1.6103E-02	9.1339E-01	9.1339E-01	1.0000E+00	1.0917E+00
27 72	441139	912429	1647868	2.8363E-03	9.4904E-01	9.4904E-01	1.0000E+00	1.1410E+00
28 73	1092898	1173273	2087675	3.5933E-04	7.0896E-01	7.0896E-01	1.0000E+00	1.6369E+00
29 74	1307271	1423555	2641774	2.2735E-04	6.3465E-01	6.3465E-01	1.0000E+00	1.5361E+00
30 75	2140196	2082818	0	0.0000E+00	6.4924E-01	6.4924E-01	3.2052E+00	0.0000E+00
31 76	21345938	21855708	8627362	2.2274E-05	6.6789E-01	6.6789E-01	1.0000E+00	1.6008E+00
32 777	1483514228	1483514228	0	0.0000E+00	7.7451E-01	7.7451E-01	1.0026E+00	0.0000E+00
33 888	1483514441	1483514441	0	0.0000E+00	7.7321E-01	7.7321E-01	5.3100E-05	0.0000E+00
total	5066646709	5177300389	1323238326	6.6375E+00				

```
1tally        2        nps =     1936616
+                                Surface Dose (mrem/hr)                          $ Surface detector
          tally type 2    particle flux averaged over a surface.
          tally for  photons

          this tally is modified by a dose function.

          areas
               surface:      69
              segment
                1       1.00000E+00
                2       1.68653E+03
```

```
               3       1.00000E+00
           whole       1.00000E+00

 surface  69
 segment:           888
               3.77313E-06 0.0023

 surface  69
 segment:          -888         777
               1.51112E-10 0.0073

 surface  69
 segment:          -888        -777
               3.79285E-06 0.0022

 surface  69
 segment:   whole surface
               7.82084E-06 0.0015

 ============================================================================================================================================

          results of 10 statistical checks for the estimated answer for the tally fluctuation chart (tfc) bin of tally        2

 tfc bin     --mean--      ---------relative error---------      ----variance of the variance----      --figure of merit--     -pdf-
 behavior    behavior      value    decrease   decrease rate      value    decrease   decrease rate       value     behavior     slope

 desired      random       <0.10      yes      1/sqrt(nps)       <0.10      yes        1/nps           constant    random      >3.00
 observed     random        0.00      yes          yes            0.00      yes         yes            constant    random       1.59
 passed?        yes          yes      yes          yes             yes      yes         yes               yes        yes          no

 ============================================================================================================================================


 warning.  the tally in the tally fluctuation chart bin did not pass  1 of the 10 statistical checks.

1analysis of the results in the tally fluctuation chart bin (tfc) for tally        2 with nps=     1936616 print table 160


 normed average tally per history  = 7.82084E-06          unnormed average tally per history  = 7.82084E-06
 estimated tally relative error    = 0.0015               estimated variance of the variance  = 0.0047
 relative error from zero tallies  = 0.0008               relative error from nonzero scores  = 0.0012

 number of nonzero history tallies =      824405          efficiency for the nonzero tallies  = 0.4257
 history number of largest  tally  =      361002          largest  unnormalized history tally = 5.43613E-03
 (largest  tally)/(average tally)  = 6.95083E+02          (largest  tally)/(avg nonzero tally)= 2.95892E+02

 (confidence interval shift)/mean  = 0.0000               shifted confidence interval center  = 7.82100E-06


 if the largest  history score sampled so far were to occur on the next history, the tfc bin quantities would change as follows:

      estimated quantities           value at nps           value at nps+1           value(nps+1)/value(nps)-1.

      mean                            7.82084E-06            7.82364E-06                    0.000358
      relative error                  1.48033E-03            1.52255E-03                    0.028522
      variance of the variance        4.69287E-03            7.25340E-03                    0.545622
      shifted center                  7.82100E-06            7.82107E-06                    0.000009
```

```
      figure of merit                 3.80255E+03             3.59458E+03                     -0.054692

 the estimated inverse power slope of the 198 largest  tallies starting at 1.31998E-04 is 1.5925
 the history score probability density function appears to have an unsampled region at the largest  history scores:
 please examine. see print table 161.

 fom = (histories/minute)*(f(x) signal-to-noise ratio)**2 = (1.614E+04)*( 4.854E-01)**2 = (1.614E+04)*(2.356E-01) = 3.803E+03

1unnormed tally density for tally        2          nonzero tally mean(m) = 1.837E-05   nps =     1936616  print table 161

 abscissa              ordinate   log plot of tally probability density function in tally fluctuation chart bin(d=decade,slope= 1.6)
  tally  number num den log den:d----------d----------d----------d----------d----------d----------d----------d----------d-
 3.98-09      2 7.03+02   2.847 **********|**********|**********|**********|**********|**********|*******   |          |
 6.31-09      4 8.87+02   2.948 **********|**********|**********|**********|**********|**********|********  |          |
 1.00-08      9 1.26+03   3.100 **********|**********|**********|**********|**********|**********|********** |          |
 1.58-08     14 1.24+03   3.092 **********|**********|**********|**********|**********|**********|********** |          |
 2.51-08     31 1.73+03   3.237 **********|**********|**********|**********|**********|**********|**********|          |
 3.98-08     95 3.34+03   3.524 **********|**********|**********|**********|**********|**********|**********|****      |
 6.31-08    262 5.81+03   3.764 **********|**********|**********|**********|**********|**********|**********|*******   |
 1.00-07    565 7.91+03   3.898 **********|**********|**********|**********|**********|**********|**********|********  |
 1.58-07   1227 1.08+04   4.035 **********|**********|**********|**********|**********|**********|**********|********** |
 2.51-07   2276 1.27+04   4.103 **********|**********|**********|**********|**********|**********|**********|********** |
 3.98-07   3984 1.40+04   4.146 **********|**********|**********|**********|**********|**********|**********|********** |
 6.31-07   7879 1.75+04   4.242 **********|**********|**********|**********|**********|**********|**********|**********|
 1.00-06  15224 2.13+04   4.328 **********|**********|**********|**********|**********|**********|**********|**********|*
 1.58-06  26487 2.34+04   4.369 **********|**********|**********|**********|**********|**********|**********|**********|*
 2.51-06  40491 2.26+04   4.353 **********|**********|**********|**********|**********|**********|**********|**********|*
 3.98-06  55574 1.95+04   4.291 **********|**********|**********|**********|**********|**********|**********|**********|
 6.31-06  78004 1.73+04   4.238 **********|**********|**********|**********|**********|**********|**********|**********|
 1.00-05 106024 1.48+04   4.171 **********|**********|**********|**********|**********|**********|**********|**********|
 1.58-05 130499 1.15+04   4.061 **********|**********|**********|**********|**********|**********|**********|********** |
 2.51-05 141480 7.88+03   3.897 mmmmmmmmmmm|mmmmmmmmmmmm|mmmmmmmmmmm|mmmmmmmmmmm|mmmmmmmmmmmm|mmmmmmmmmmm|mmmmmmmmmm|mmmmmmmm  |
 3.98-05 122059 4.29+03   3.632 **********|**********|**********|**********|**********|**********|**********|*****     |
 6.31-05  69867 1.55+03   3.190 **********|**********|**********|**********|**********|**********|**********|          |
 1.00-04  20417 2.86+02   2.456 **********|**********|**********|**********|**********|**********|**        |          |
 1.58-04   1882 1.66+01   1.220 **********|**********|**********|**********|**********|         s|          |          |
 2.51-04     16 8.91-02  -1.050 **********|**********|********  |          |          |     s    |          |          |
 3.98-04      0 0.00+00   0.000           |          |          |          |          |s         |          |          |
 6.31-04      6 1.33-02  -1.876 **********|**********|          |          |         s|          |          |          |
 1.00-03      8 1.12-02  -1.951 **********|**********|          |          |      s   |          |          |          |
 1.58-03      9 7.95-03  -2.100 **********|*********|          |          |    s     |          |          |          |
 2.51-03      6 3.34-03  -2.476 **********|****      |          |         s|          |          |          |          |
 3.98-03      3 1.05-03  -2.977 *********  |          |          |     s    |          |          |          |          |
 6.31-03      1 2.22-04  -3.654 *          |          |          |  s       |          |          |          |          |
  total  824405 4.26-01         d----------d----------d----------d----------d----------d----------d----------d----------d-

1tally       22        nps =     1936616
+                                 2-meter Dose (mrem/hr)                                $ 2-m detector
           tally type 2    particle flux averaged over a surface.
           tally for  photons

           this tally is modified by a dose function.

           areas
                surface:      80
               segment
                 1       1.00000E+00
                 2       8.07023E+03
```

```
               3       1.00000E+00
           whole       1.00000E+00

 surface  80
 segment:           888
               2.79305E-06 0.0018

 surface  80
 segment:          -888         777
               1.28858E-11 0.0043

 surface  80
 segment:          -888        -777
               2.56585E-06 0.0018

 surface  80
 segment:   whole surface
               5.46290E-06 0.0015

 ================================================================================================================================

          results of 10 statistical checks for the estimated answer for the tally fluctuation chart (tfc) bin of tally       22

 tfc bin     --mean--      ---------relative error---------      ----variance of the variance----      --figure of merit--     -pdf-
 behavior    behavior      value    decrease   decrease rate      value    decrease   decrease rate       value     behavior     slope

 desired      random       <0.10      yes      1/sqrt(nps)       <0.10      yes        1/nps           constant    random      >3.00
 observed     random        0.00      yes          yes            0.00      yes         yes            constant    random       1.94
 passed?        yes          yes      yes          yes              yes     yes         yes               yes         yes          no

 ================================================================================================================================

 warning.  the tally in the tally fluctuation chart bin did not pass  1 of the 10 statistical checks.

1analysis of the results in the tally fluctuation chart bin (tfc) for tally       22 with nps=     1936616 print table 160

 normed average tally per history  = 5.46290E-06          unnormed average tally per history  = 5.46290E-06
 estimated tally relative error    = 0.0015               estimated variance of the variance  = 0.0002
 relative error from zero tallies  = 0.0008               relative error from nonzero scores  = 0.0012

 number of nonzero history tallies =      824330          efficiency for the nonzero tallies  = 0.4257
 history number of largest  tally  =      873519          largest  unnormalized history tally = 1.42045E-03
 (largest  tally)/(average tally)  = 2.60017E+02          (largest  tally)/(avg nonzero tally)= 1.10678E+02

 (confidence interval shift)/mean  = 0.0000               shifted confidence interval center  = 5.46291E-06

 if the largest  history score sampled so far were to occur on the next history, the tfc bin quantities would change as follows:

      estimated quantities           value at nps           value at nps+1          value(nps+1)/value(nps)-1.

      mean                            5.46290E-06            5.46363E-06                  0.000134
      relative error                  1.45490E-03            1.46084E-03                  0.004082
      variance of the variance        2.11878E-04            2.78559E-04                  0.314713
      shifted center                  5.46291E-06            5.46292E-06                  0.000001
```

```
     figure of merit                3.93666E+03            3.90472E+03                  -0.008114

 the estimated inverse power slope of the 200 largest  tallies starting at 1.02032E-04 is 1.9412
 the large score tail of the empirical history score probability density function appears to have no unsampled regions.

 fom = (histories/minute)*(f(x) signal-to-noise ratio)**2 = (1.614E+04)*( 4.939E-01)**2 = (1.614E+04)*(2.439E-01) = 3.937E+03

1unnormed tally density for tally       22          nonzero tally mean(m) = 1.283E-05   nps =     1936616  print table 161

 abscissa             ordinate   log plot of tally probability density function in tally fluctuation chart bin(d=decade,slope= 1.9)
  tally  number num den log den:d------------d------------d------------d------------d------------d------------d------------d---
2.00-09     41 2.88+04   4.459 ************|************|************|************|************|************|************|
3.16-09     39 1.73+04   4.237 ************|************|************|************|************|************|***********  |
5.01-09    106 2.96+04   4.471 ************|************|************|************|************|************|************|*
7.94-09    196 3.45+04   4.538 ************|************|************|************|************|************|************|**
1.26-08    339 3.77+04   4.576 ************|************|************|************|************|************|************|**
2.00-08    503 3.53+04   4.547 ************|************|************|************|************|************|************|**
3.16-08    720 3.19+04   4.503 ************|************|************|************|************|************|************|*
5.01-08    897 2.50+04   4.399 ************|************|************|************|************|************|************|
7.94-08   1475 2.60+04   4.415 ************|************|************|************|************|************|************|
1.26-07   2644 2.94+04   4.468 ************|************|************|************|************|************|************|*
2.00-07   5017 3.52+04   4.546 ************|************|************|************|************|************|************|**
3.16-07   8933 3.95+04   4.597 ************|************|************|************|************|************|************|**
5.01-07  15425 4.31+04   4.634 ************|************|************|************|************|************|************|***
7.94-07  24898 4.39+04   4.642 ************|************|************|************|************|************|************|***
1.26-06  37247 4.14+04   4.617 ************|************|************|************|************|************|************|***
2.00-06  50824 3.56+04   4.552 ************|************|************|************|************|************|************|**
3.16-06  65489 2.90+04   4.462 ************|************|************|************|************|************|************|*
5.01-06  82910 2.31+04   4.364 ************|************|************|************|************|************|************|
7.94-06 102646 1.81+04   4.257 ************|************|************|************|************|************|***********  |
1.26-05 117931 1.31+04   4.118 ************|************|************|************|************|************|**********   |
2.00-05 123302 8.65+03   3.937 mmmmmmmmmmmmm|mmmmmmmmmmmmmm|mmmmmmmmmmmmmm|mmmmmmmmmmmmm|mmmmmmmmmmmmmm|mmmmmmmmmmmmmm|mmmmmmm      |
3.16-05 104523 4.62+03   3.665 ************|************|************|************|************|***********  |************|
5.01-05  59382 1.66+03   3.220 ************|************|************|************|************|***********  |            |
7.94-05  17218 3.03+02   2.482 ************|************|************|************|************|*           |            |
1.26-04   1595 1.77+01   1.249 ************|************|************|***********  |        s   |            |            |
2.00-04     11 7.71-02  -1.113 ************|******      |            |            |  s         |            |            |
3.16-04      0 0.00+00   0.000               |            |            |          s |            |            |            |
5.01-04      6 1.68-02  -1.776 ***********   |            |            |     s      |            |            |            |
7.94-04      7 1.23-02  -1.909 *********     |            |          s |            |            |            |            |
1.26-03      4 4.45-03  -2.352 ***           |            |        s   |            |            |            |            |
1.58-03      2 3.17-03  -2.499 *             |            |    s       |            |            |            |            |
 total  824330 4.26-01         d------------d------------d------------d------------d------------d------------d------------d---

1status of the statistical checks used to form confidence intervals for the mean for each tally bin


 tally   result of statistical checks for the tfc bin (the first check not passed is listed) and error magnitude check for all bins

       2   missed  1 of 10 tfc bin checks: the slope of decrease of largest tallies is less than the minimum acceptable value of 3.0
         passed all bin error check:     4 tally bins all have relative errors less than 0.10 with no zero bins

      22   missed  1 of 10 tfc bin checks: the slope of decrease of largest tallies is less than the minimum acceptable value of 3.0
         passed all bin error check:     4 tally bins all have relative errors less than 0.10 with no zero bins


 the 10 statistical checks are only for the tally fluctuation chart bin and do not apply to other tally bins.
```

```
 warning.       2 of the     2 tally fluctuation chart bins did not pass all 10 statistical checks.
1tally fluctuation charts

                          tally        2                          tally       22
         nps      mean     error   vov  slope    fom      mean     error   vov  slope    fom
      128000   7.8083E-06 0.0054 0.0062  4.8    4299   5.4483E-06 0.0055 0.0001 10.0    4099
      256000   7.7725E-06 0.0038 0.0019  3.8    4429   5.4299E-06 0.0040 0.0004  4.8    4047
      384000   7.8021E-06 0.0036 0.0632  2.7    3202   5.4371E-06 0.0032 0.0004  4.3    4011
      512000   7.8072E-06 0.0031 0.0403  2.4    3381   5.4406E-06 0.0028 0.0003  3.6    4041
      640000   7.8083E-06 0.0027 0.0281  2.2    3507   5.4455E-06 0.0025 0.0007  2.8    3950
      768000   7.8277E-06 0.0024 0.0210  2.1    3646   5.4636E-06 0.0023 0.0005  2.6    3952
      896000   7.8332E-06 0.0022 0.0159  1.9    3653   5.4694E-06 0.0022 0.0007  2.4    3871
     1024000   7.8268E-06 0.0021 0.0128  1.9    3735   5.4655E-06 0.0020 0.0006  2.4    3904
     1152000   7.8176E-06 0.0019 0.0105  1.8    3801   5.4610E-06 0.0019 0.0005  2.2    3896
     1280000   7.8156E-06 0.0018 0.0093  1.8    3710   5.4571E-06 0.0018 0.0004  2.3    3914
     1408000   7.8179E-06 0.0018 0.0078  1.7    3722   5.4585E-06 0.0017 0.0004  2.1    3909
     1536000   7.8229E-06 0.0017 0.0067  1.7    3772   5.4637E-06 0.0016 0.0003  2.1    3920
     1664000   7.8235E-06 0.0016 0.0059  1.6    3763   5.4643E-06 0.0016 0.0003  2.0    3914
     1792000   7.8209E-06 0.0015 0.0052  1.6    3803   5.4627E-06 0.0015 0.0002  2.0    3925
     1920000   7.8208E-06 0.0015 0.0048  1.6    3796   5.4629E-06 0.0015 0.0002  2.0    3935
     1936616   7.8208E-06 0.0015 0.0047  1.6    3803   5.4629E-06 0.0015 0.0002  1.9    3937

 ************************************************************************************************************************

 dump no.    3 on file runtpe     nps =     1936616     coll =     1323238326     ctm =      120.01   nrn =
 19078044321
 tally data written to file mctal

        20 warning messages so far.


 run terminated when it had used  120  minutes of computer time.

 computer time =  120.02 minutes

 mcnp     version 5     09282010                     07/22/14 20:57:55                     probid =  07/22/14 18:57:53
```

5.7.2.1.2 NCT Concentrated 252Cf Neutron Source – 7nn001.io

```
          Thread Name & Version = MCNP5, 1.60

                                 _
            ._ _   _  ._  ._    |_
            | | |  (_  | |  |_)   _)
                           |

  +-------------------------------------------------------------------+
  | Copyright 2010. Los Alamos National Security, LLC.  All rights    |
  | reserved.                                                         |
  |   This material was produced under U.S. Government contract       |
  | DE-AC52-06NA25396 for Los Alamos National Laboratory, which is    |
  | operated by Los Alamos National Security, LLC, for the U.S.       |
  | Department of Los Energy. The Government is granted for itself and |
  | others acting on its behalf a paid-up, nonexclusive, irrevocable  |
  | worldwide license in this material to reproduce, prepare derivative |
  | works, and perform publicly and display publicly. Beginning five  |
  | (5) years after 2010, subject to additional five-year worldwide   |
  | renewals, the Government is granted for itself and others acting on |
```

| its behalf a paid-up, nonexclusive, irrevocable worldwide license |
| in this material to reproduce, prepare derivative works, distribute |
| copies to the public, perform publicly and display publicly, and to |
| permit others to do so. NEITHER THE UNITED STATES NOR THE UNITED |
| STATES DEPARTMENT OF ENERGY, NOR LOS ALAMOS NATIONAL SECURITY, LLC, |
| NOR ANY OF THEIR EMPLOYEES, MAKES ANY WARRANTY, EXPRESS OR IMPLIED, |
| OR ASSUMES ANY LEGAL LIABILITY OR RESPONSIBILITY FOR THE ACCURACY, |
| COMPLETENESS, OR USEFULNESS OF ANY INFORMATION, APPARATUS, PRODUCT, |
| OR PROCESS DISCLOSED, OR REPRESENTS THAT ITS USE WOULD NOT INFRINGE |
| PRIVATELY OWNED RIGHTS. |

```
1mcnp     version 5     ld=09282010                    07/23/14 08:58:30
 ******************************************************************************                probid =  07/23/14 08:58:30
 inp=7nn001.i

         1-       title RH-TRU 72-B RLC NCT Neutron Concentrated 1 g/cc Cf252
         2-       C
         3-       C Cell Cards
         4-       C
         5-       10  1 -1        10  -11  -16               imp:n=1    $ Source #1
         6-       11  1 -1        12  -13  -17               imp:n=1    $ Source #2
         7-       12  1 -1        14  -15  -18               imp:n=1    $ Source #3
         8-       20  0           20  -21  -26
         9-                     (-10:  11:  16)              imp:n=1    $ Drum #1 cavity
        10-       21  0           22  -23  -27
        11-                     (-12:  13:  17)              imp:n=1    $ Drum #2 cavity
        12-       22  0           24  -25  -28
        13-                     (-14:  15:  18)              imp:n=1    $ Drum #3 cavity
        14-       40  0           41  -45  -43
        15-                      #10  #11  #12
        16-                      #20  #21  #22               imp:n=1    $ RLC cavity
        17-       41  3 -7.85260  40  -41  -42               imp:n=1    $ RLC base
        18-       42  3 -7.85260  41  -46   43  -42          imp:n=1    $ RLC shell
        19-       43  3 -7.85260  45  -44  -43               imp:n=1    $ RLC lid
        20-       50  0           51  -53  -55
        21-                     (-40:  42:  46)
        22-                    :( 44  -46  -43)              imp:n=1    $ IV cavity
        23-       51  2 -8.01280  50  -51  -52               imp:n=1    $ IV base
        24-       52  2 -8.01280  51  -55   53  -52          imp:n=1    $ IV shell
        25-       53  2 -8.01280  55  -54  -52               imp:n=1    $ IV lid
        26-       60  0           61  -63  -65
        27-                     (-50:  52:  54)              imp:n=1    $ OC cavity
        28-       61  2 -8.01280  60  -61  -69               imp:n=1    $ OC base
        29-       62  2 -8.01280  61  -66   65  -64          imp:n=1    $ OC ishell
        30-       63  4 -11.3500  61  -66   64  -76  71      imp:n=1    $ OC lead in
        31-       64  4 -11.3500  61  -66   76  -68  71      imp:n=1    $ OC lead out
        32-       65  2 -8.01280  61  -66   68  -77  71      imp:n=1    $ OC oshell in
        33-       66  2 -8.01280  61  -66   77  -67  71      imp:n=1    $ OC oshell out
        34-       67  0           61  -66   67  -70  71      imp:n=1    $ OC airgap
        35-       68  2 -8.01280  61  -66   70  -69  71      imp:n=1    $ OC tshell
        36-       69  2 -8.01280  66  -63   65  -69          imp:n=1    $ OC flange
        37-       70  2 -8.01280  63  -62  -69               imp:n=1    $ OC lid
        38-       71  4 -11.3500  64  -78  -71               imp:n=1    $ OC lead punct in
        39-       72  4 -11.3500  78  -73  -71               imp:n=1    $ OC lead punct out
        40-       73  2 -8.01280  73  -79  -71               imp:n=1    $ OC oshell punct in
        41-       74  2 -8.01280  79  -72  -71               imp:n=1    $ OC oshell punct out
        42-       75  0           72  -75  -71               imp:n=1    $ OC airgap punct
```

```
      43-       76  2 -8.01280  75  -74  -71                imp:n=1    $ OC tshell punct
      44-       777 0           69  -80   60  -62            imp:n=1    $ Outside to tally
      45-       888 0          -999
      46-                      (-60:  80:  62)               imp:n=1    $ Outside pkg
      47-       999 0           999                          imp:n=0    $ Outside world
      48-
      49-       C
      50-       C Geometry Cards
      51-       C
      52-       10  pz 88.9                                              $ Source #1 bottom
      53-       11  pz 91.44                                               $ Source #1 top
      54-       12  pz 162.878                                            $ Source #2 bottom
      55-       13  pz 165.418                                            $ Source #2 top
      56-       14  pz 236.855                                            $ Source #3 bottom
      57-       15  pz 239.395                                            $ Source #3 top
      58-       16  c/z 0 0 1.27                                          $ Source #1 radius
warning.  this surface has been replaced by a surface of type cz
      59-       17  c/z 0 0 1.27                                          $ Source #2 radius
warning.  this surface has been replaced by a surface of type cz
      60-       18  c/z 0 0 1.27                                          $ Source #3 radius
      61-       C
warning.  this surface has been replaced by a surface of type cz
      62-       20  pz 53.34                                               $ Drum #1 bottom
      63-       21  pz 127                                               $ Drum #1 top
      64-       22  pz 127.318                                            $ Drum #2 bottom
      65-       23  pz 200.978                                            $ Drum #2 top
      66-       24  pz 201.295                                            $ Drum #3 bottom
      67-       25  pz 274.955                                            $ Drum #3 top
      68-       26  c/z 0 0 24.765                                         $ Drum #1 radius
warning.  this surface has been replaced by a surface of type cz
      69-       27  c/z 0 0 24.765                                         $ Drum #2 radius
warning.  this surface has been replaced by a surface of type cz
      70-       28  c/z 0 0 24.765                                         $ Drum #3 radius
      71-       C
warning.  this surface has been replaced by a surface of type cz
      72-       40  pz 19.368                                            $ RLC base (outside)
      73-       41  pz 20.638                                            $ RLC base (inside)
      74-       42  c/z 0 0 33.02                                        $ RLC shell (outside)
warning.  this surface has been replaced by a surface of type cz
      75-       43  c/z 0 0 32.385                                       $ RLC shell (inside)
warning.  this surface has been replaced by a surface of type cz
      76-       44  pz 309.563                                           $ RLC lid (outside)
      77-       45  pz 307.658                                           $ RLC lid (inside)
      78-       46  pz 325.438                                           $ RLC top (outside)
      79-       C
      80-       50  pz 14.288                                            $ IV base (outside)
      81-       51  pz 18.098                                            $ IV base (inside)
      82-       52  c/z 0 0 40.64                                        $ IV shell (outside)
warning.  this surface has been replaced by a surface of type cz
      83-       53  c/z 0 0 39.688                                       $ IV shell (inside)
warning.  this surface has been replaced by a surface of type cz
      84-       54  pz 343.218                                           $ IV top (outside)
      85-       55  pz 326.708                                           $ IV top (inside)
      86-       C
      87-       60  pz 0                                                 $ OC bottom (outside)
      88-       61  pz 12.7                                              $ OC bottom (inside)
      89-       62  pz 360.045                                           $ OC top (outside)
      90-       63  pz 344.805                                           $ OC top (inside)
```

```
 91-       64  cz 43.656                                  $ OC ishell (outside)
 92-       65  cz 41.116                                  $ OC ishell (inside)
 93-       66  pz 320.675                                 $ OC lead (upper)
 94-       67  cz 52.229                                  $ OC oshell (outside)
 95-       68  cz 48.419                                  $ OC oshell (inside)
 96-       69  cz 52.838                                  $ OC therm (outside)
 97-       70  cz 52.495                                  $ OC therm (inside)
 98-       71  c/x 0 164.148 10.033                       $ OC puncture radius
 99-       72  cz 52.229                                  $ OC oshell punct (out)
100-       73  cz 48.419                                  $ OC oshell punct (in)
101-       74  cz 52.838                                  $ OC therm punct (out)
102-       75  cz 52.495                                  $ OC therm punct (in)
103-       76  cz 46.038                                  $ OC lead (mid)
104-       77  cz 50.324                                  $ OC oshell (mid)
105-       78  cz 46.038                                  $ OC lead punct (mid)
106-       79  cz 50.324                                  $ OC oshell punct (mid)
107-       C
108-       80  cz 252.838                                 $ 2-meter from OC therm
109-       C
110-       777 pz 161.608                                 $ Ring tally (lower)
111-       888 pz 166.688                                 $ Ring tally (upper)
112-       999 sz 164.148 379.838                         $ Outside world
113-
114-       C
115-       C Physics Cards
116-       C
117-       mode n
118-       C
119-       C Source Cards
120-       C
121-       C Cylindrical Sources
122-       sdef pos=d1 erg=d2 par=1 axs=0 0 1 rad=d3 ext=d4
123-       sc1 Cf252
124-       C Source Position and Fraction
125-       si1 L 0 0 90.17
126-             0 0 164.148
127-             0 0 238.125
128-       sp1   1 1 1
129-       C Source Energy (MeV) and Fraction
130-       si2 0.1 0.5 1.0 2.0 3.0
131-            4.0 6.0 8.0 10.0 15.0
132-       sp2 0.00E+00 1.80E+11 2.71E+11 5.36E+11 4.10E+11
133-            2.73E+11 2.66E+11 8.53E+10 2.44E+10 8.36E+09
134-       C Source Radius
135-       si3 0 1.27
136-       sp3 -21 1
137-       C Source Extent
138-       si4 -1.27 1.27
139-       sp4 -21 0
140-       C
141-       C Tally Cards
142-       C
143-       f2:n 69
144-       fc2 Surface Dose (mrem/hr)                     $ Surface detector
145-       fs2 888 777 t
146-       sd2 1.0 1686.525 1.0 1.0                       $ Surface tally area
147-       f22:n 80
148-       fc22 2-meter Dose (mrem/hr)                    $ 2-m detector
```

```
      149-       fs22 888 777 t
      150-       sd22 1.0 8070.229 1.0 1.0                                $ Surface tally area
      151-       C
      152-       C ANSI/ANS-6.1.1-1977 Neutron Flux to Dose Factors (mrem/hr)
      153-       de0  2.5e-08 1.0e-07 1.0e-06 1.0e-05 1.0e-04             $ Energy (Mev)
      154-            1.0e-03 1.0e-02 1.0e-01 5.0e-01 1.0
      155-            2.5 5.0 7.0 10.0 14.0 20.0
      156-       df0  3.67e-03 3.67e-03 4.46e-03 4.54e-03 4.18e-03        $ Conversion (mrem/hr)
      157-            3.76e-03 3.56e-03 2.17e-02 9.26e-02 1.32e-01
      158-            1.25e-01 1.56e-01 1.47e-01 1.47e-01 2.08e-01 2.27e-01
      159-       C
      160-       C Material Cards
      161-       C
      162-       m1   40000.60c -1.00                                      $ Zirconium
      163-       m2   14000.60c -0.01                                      $ Stainless Steel
      164-            24052.60c -0.19
      165-            25055.60c -0.02
      166-            26057.60c -0.68
      167-            28058.60c -0.10
      168-       m3   26057.60c -1.00                                      $ Carbon Steel (iron)
      169-       m4   82000.50c -1.00                                      $ Lead
      170-       C
      171-       C Runtime and Print Cards
      172-       C
      173-       prdmp j j 1 2
      174-       ctme 30

 surface       16   and surface       17   are the same.       17   will be deleted.

 surface       16   and surface       18   are the same.       18   will be deleted.

 surface       26   and surface       27   are the same.       27   will be deleted.

 surface       26   and surface       28   are the same.       28   will be deleted.

 surface       67   and surface       72   are the same.       72   will be deleted.

 surface       68   and surface       73   are the same.       73   will be deleted.

 surface       69   and surface       74   are the same.       74   will be deleted.

 surface       70   and surface       75   are the same.       75   will be deleted.

 surface       76   and surface       78   are the same.       78   will be deleted.

 surface       77   and surface       79   are the same.       79   will be deleted.

  comment.          10 surfaces were deleted for being the same as others.

  warning.  sum of segment sizes differs from total in   2 cases.
1cells                                                                  print table 60

                          atom        gram                                    neutron
             cell     mat    density     density     volume       mass          pieces importance

       1       10        1  6.60141E-03 1.00000E+00 1.28704E+01 1.28704E+01          1  1.0000E+00
       2       11        1  6.60141E-03 1.00000E+00 1.28704E+01 1.28704E+01          1  1.0000E+00
       3       12        1  6.60141E-03 1.00000E+00 1.28704E+01 1.28704E+01          1  1.0000E+00
```

```
        4       20        0  0.00000E+00 0.00000E+00 1.41912E+05 0.00000E+00          1  1.0000E+00
        5       21        0  0.00000E+00 0.00000E+00 1.41912E+05 0.00000E+00          1  1.0000E+00
        6       22        0  0.00000E+00 0.00000E+00 1.41912E+05 0.00000E+00          1  1.0000E+00
        7       40        0  0.00000E+00 0.00000E+00 5.19918E+05 0.00000E+00          1  1.0000E+00
        8       41        3  8.30568E-02 7.85260E+00 4.35019E+03 3.41603E+04          1  1.0000E+00
        9       42        3  8.30568E-02 7.85260E+00 3.97694E+04 3.12294E+05          1  1.0000E+00
       10       43        3  8.30568E-02 7.85260E+00 6.27672E+03 4.92886E+04          1  1.0000E+00
       11       50        0  0.00000E+00 0.00000E+00 5.31049E+05 0.00000E+00          1  1.0000E+00
       12       51        2  8.70856E-02 8.01280E+00 1.97689E+04 1.58404E+05          1  1.0000E+00
       13       52        2  8.70856E-02 8.01280E+00 7.41419E+04 5.94084E+05          1  1.0000E+00
       14       53        2  8.70856E-02 8.01280E+00 8.56652E+04 6.86418E+05          1  1.0000E+00
       15       60        0  0.00000E+00 0.00000E+00 5.70765E+04 0.00000E+00          1  1.0000E+00
       16       61        2  8.70856E-02 8.01280E+00 1.11390E+05 8.92546E+05          1  1.0000E+00
       17       62        2  8.70856E-02 8.01280E+00 2.08330E+05 1.66931E+06          1  1.0000E+00
       18       63        4  3.29849E-02 1.13500E+01 0.00000E+00 0.00000E+00          0  1.0000E+00
       19       64        4  3.29849E-02 1.13500E+01 0.00000E+00 0.00000E+00          0  1.0000E+00
       20       65        2  8.70856E-02 8.01280E+00 0.00000E+00 0.00000E+00          0  1.0000E+00
       21       66        2  8.70856E-02 8.01280E+00 0.00000E+00 0.00000E+00          0  1.0000E+00
       22       67        0  0.00000E+00 0.00000E+00 0.00000E+00 0.00000E+00          0  1.0000E+00
       23       68        2  8.70856E-02 8.01280E+00 0.00000E+00 0.00000E+00          0  1.0000E+00
       24       69        2  8.70856E-02 8.01280E+00 8.34880E+04 6.68973E+05          1  1.0000E+00
       25       70        2  8.70856E-02 8.01280E+00 1.33668E+05 1.07106E+06          1  1.0000E+00
       26       71        4  3.29849E-02 1.13500E+01 0.00000E+00 0.00000E+00          0  1.0000E+00
       27       72        4  3.29849E-02 1.13500E+01 0.00000E+00 0.00000E+00          0  1.0000E+00
       28       73        2  8.70856E-02 8.01280E+00 0.00000E+00 0.00000E+00          0  1.0000E+00
       29       74        2  8.70856E-02 8.01280E+00 0.00000E+00 0.00000E+00          0  1.0000E+00
       30       75        0  0.00000E+00 0.00000E+00 0.00000E+00 0.00000E+00          0  1.0000E+00
       31       76        2  8.70856E-02 8.01280E+00 0.00000E+00 0.00000E+00          0  1.0000E+00
       32      777        0  0.00000E+00 0.00000E+00 6.91509E+07 0.00000E+00          1  1.0000E+00
       33      888        0  0.00000E+00 0.00000E+00 1.57245E+08 0.00000E+00          1  1.0000E+00
       34      999        0  0.00000E+00 0.00000E+00 0.00000E+00 0.00000E+00          0  0.0000E+00

 total                                                2.28696E+08 6.13657E+06

    minimum source weight = 1.0000E+00    maximum source weight = 1.0000E+00

 ************************************************
 * Random Number Generator  =                  1 *
 * Random Number Seed       =       19073486328125 *
 * Random Number Multiplier =       19073486328125 *
 * Random Number Adder      =                    0 *
 * Random Number Bits Used  =                   48 *
 * Random Number Stride     =               152917 *
 ************************************************


        11 warning messages so far.
1cross-section tables                                                                print table 100

     table    length

                         tables from file endf60

  14000.60c   51392  14-si-nat from endf/b-vi                                  mat1400      11/25/93
  24052.60c   66325  24-cr-52 from endf/b-vi.1                                mat2431      11/25/93
  25055.60c   84549  25-mn-55 from endf/b-vi                                  mat2525      11/25/93
  26057.60c   72092  endf/b-vi.1 fe57a                                        mat2634      11/25/93
  28058.60c   83305  28-ni-58 from endf/b-vi.1                                mat2825      11/25/93
```

```
  40000.60c   45269  40-zr-nat from endf-vi.1                                                    mat4000      11/27/93

                        tables from file rmccs

  82000.50c   28695  njoy                                                                     ( 1382)     03/10/82

  total      431627

 ************************************************************************************************************************

 dump no.    1 on file runtpe     nps =           0     coll =             0     ctm =        0.00   nrn =
    0

        11 warning messages so far.
1problem summary

      run terminated when it had used   30  minutes of computer time.
+                                                                                          07/23/14 09:28:34
      title RH-TRU 72-B RLC NCT Neutron Concentrated 1 g/cc Cf252                  probid =  07/23/14 08:58:30
0
 neutron creation    tracks      weight        energy            neutron loss        tracks      weight        energy
                                 (per source particle)                                         (per source particle)

 source            21482123    1.0000E+00    2.5766E+00          escape            21335297    9.3555E-01    7.2771E-01
                                                                 energy cutoff            0    0.            0.
                                                                 time cutoff              0    0.            0.
 weight window            0    0.            0.                weight window            0    0.            0.
 cell importance          0    0.            0.                cell importance          0    0.            0.
 weight cutoff            0    1.5922E-03    1.3397E-06        weight cutoff       219327    1.5925E-03    1.4403E-06
 e or t importance        0    0.            0.                e or t importance        0    0.            0.
 dxtran                   0    0.            0.                dxtran                   0    0.            0.
 forced collisions        0    0.            0.                forced collisions        0    0.            0.
 exp. transform           0    0.            0.                exp. transform           0    0.            0.
 upscattering             0    0.            2.6576E-11        downscattering           0    0.            1.7611E+00
 photonuclear             0    0.            0.                capture                  0    6.7683E-02    5.9090E-02
 (n,xn)              144971    6.4619E-03    7.5353E-03        loss to (n,xn)       72470    3.2303E-03    3.6220E-02
 prompt fission           0    0.            0.                loss to fission          0    0.            0.
 delayed fission          0    0.            0.
     total         21627094    1.0081E+00    2.5841E+00            total         21627094    1.0081E+00    2.5841E+00

   number of neutrons banked                  72501        average time of (shakes)              cutoffs
   neutron tracks per source particle     1.0067E+00         escape            1.9961E+02         tco   1.0000E+33
   neutron collisions per source particle 3.1937E+01         capture           3.5969E+02         eco   0.0000E+00
   total neutron collisions                686064893         capture or escape 2.1041E+02         wc1  -5.0000E-01
   net multiplication              1.0032E+00 0.0000         any termination   2.1445E+02         wc2  -2.5000E-01

 computer time so far in this run    30.03 minutes           maximum number ever in bank         2
 computer time in mcrun              30.01 minutes           bank overflows to backup file       0
 source particles per minute            7.1593E+05
 random numbers generated               5692445901           most random numbers used was        5169 in history    10326245

 range of sampled source weights = 1.0000E+00 to 1.0000E+00
1neutron  activity in each cell                                                                        print table 126

                      tracks     population   collisions   collisions     number        flux        average      average
              cell    entering                             * weight     weighted     weighted   track weight   track mfp
                                                         (per history)    energy       energy     (relative)      (cm)
```

```
         1       10     7177825     7169587      270618    1.2593E-02   1.7662E+00   2.5501E+00   9.9974E-01   3.0944E+01
         2       11     7177612     7170195      270061    1.2567E-02   1.7658E+00   2.5502E+00   9.9973E-01   3.0945E+01
         3       12     7175940     7167863      270845    1.2603E-02   1.7656E+00   2.5499E+00   9.9974E-01   3.0949E+01
         4       20    15415044     9495045           0    0.0000E+00   2.9955E-01   1.5251E+00   9.6676E-01   0.0000E+00
         5       21    16824642    10684525           0    0.0000E+00   3.1174E-01   1.5079E+00   9.6851E-01   0.0000E+00
         6       22    15321915     9502244           0    0.0000E+00   2.9128E-01   1.5333E+00   9.6591E-01   0.0000E+00
         7       40    78727939    21518722           0    0.0000E+00   1.5617E-01   1.0042E+00   9.4750E-01   0.0000E+00
         8       41     3350997     1786680     2806775    1.2196E-01   8.7084E-02   6.4655E-01   9.2521E-01   5.4377E+00
         9       42    78997459    21244221    33557212    1.4831E+00   1.5428E-01   9.5952E-01   9.4776E-01   5.1987E+00
        10       43     2998218     1818549     3603092    1.5537E-01   7.2131E-02   6.4916E-01   9.1361E-01   5.4565E+00
        11       50    92478204    21525080           0    0.0000E+00   1.3207E-01   8.7073E-01   9.4187E-01   0.0000E+00
        12       51     4373279     1985918    13447697    5.6265E-01   6.7851E-02   5.4591E-01   9.1244E-01   3.3468E+00
        13       52    89257865    21130623    66835968    2.8889E+00   1.3539E-01   8.4049E-01   9.4361E-01   3.5242E+00
        14       53     3518501     1555317    42809564    1.6587E+00   2.3378E-02   3.3429E-01   8.3862E-01   3.0963E+00
        15       60    95361467    21528622           0    0.0000E+00   9.5805E-02   7.3674E-01   9.2723E-01   0.0000E+00
        16       61     2742750     1527701    31228871    1.2738E+00   4.3581E-02   3.8819E-01   8.8761E-01   3.2721E+00
        17       62    82468158    21046967   169431517    7.3062E+00   1.2398E-01   7.5394E-01   9.4102E-01   3.5136E+00
        18       63    70571168    20693534    86669002    3.7245E+00   1.1802E-01   6.9787E-01   9.4017E-01   4.3349E+00
        19       64    59614280    20502213    73195856    3.1443E+00   1.1448E-01   6.6312E-01   9.3966E-01   4.3391E+00
        20       65    46336658    20285418    74713679    3.2137E+00   1.1098E-01   6.3128E-01   9.3826E-01   3.4311E+00
        21       66    30807633    20021718    45275852    1.9501E+00   1.1906E-01   6.4891E-01   9.3975E-01   3.6068E+00
        22       67    22804663    19684985           0    0.0000E+00   1.3589E-01   6.9900E-01   9.4327E-01   0.0000E+00
        23       68    21234925    19686699     4602653    1.9930E-01   1.4272E-01   7.1839E-01   9.4457E-01   3.8496E+00
        24       69     2182212     1038384    17079521    6.6379E-01   2.3014E-02   2.9744E-01   8.4100E-01   3.1076E+00
        25       70     1246459      516775    17481396    6.2119E-01   8.4918E-03   1.4958E-01   7.5748E-01   2.8397E+00
        26       71      839732      503938      810788    3.5312E-02   1.5109E-01   7.6947E-01   9.5022E-01   4.4348E+00
        27       72      674761      405520      652350    2.8391E-02   1.4580E-01   7.3152E-01   9.4967E-01   4.4362E+00
        28       73      484224      314658      637824    2.7746E-02   1.3983E-01   6.9212E-01   9.4797E-01   3.4944E+00
        29       74      310803      245223      376210    1.6373E-02   1.4964E-01   7.1107E-01   9.4877E-01   3.6670E+00
        30       75      197081      177154           0    0.0000E+00   1.6762E-01   7.6136E-01   9.5125E-01   0.0000E+00
        31       76      184015      176941       37542    1.6423E-03   1.7828E-01   7.8226E-01   9.5277E-01   3.9001E+00
        32      777    20448409    20448409           0    0.0000E+00   1.5589E-01   7.9051E-01   9.4632E-01   0.0000E+00
        33      888    21335297    21335297           0    0.0000E+00   1.2962E-01   7.5535E-01   9.3810E-01   0.0000E+00

          total     902640135    353894725    686064893    2.9115E+01

1tally        2        nps =    21482123
+                                Surface Dose (mrem/hr)                                $ Surface detector
          tally type 2    particle flux averaged over a surface.
          tally for  neutrons

          this tally is modified by a dose function.

          areas
               surface:      69
              segment
                1       1.00000E+00
                2       1.68653E+03
                3       1.00000E+00
               whole      1.00000E+00

 surface  69
 segment:          888
                5.59455E-02 0.0004

 surface  69
 segment:         -888        777
                1.53799E-06 0.0023
```

```
 surface  69
 segment:          -888       -777
                5.47657E-02 0.0004

 surface  69
 segment:   whole surface
                1.13305E-01 0.0003

 ================================================================================================================================

           results of 10 statistical checks for the estimated answer for the tally fluctuation chart (tfc) bin of tally        2

 tfc bin     --mean--      ---------relative error---------      ----variance of the variance----      --figure of merit--     -pdf-
 behavior    behavior      value   decrease   decrease rate      value   decrease   decrease rate       value     behavior     slope

 desired      random       <0.10      yes      1/sqrt(nps)       <0.10      yes        1/nps           constant    random      >3.00
 observed     random        0.00      yes          yes            0.00      yes         yes            decrease    random       8.47
 passed?        yes          yes      yes          yes              yes      yes         yes                no        yes          yes

 ================================================================================================================================


 warning.  the tally in the tally fluctuation chart bin did not pass  1 of the 10 statistical checks.

1analysis of the results in the tally fluctuation chart bin (tfc) for tally        2 with nps=    21482123 print table 160


 normed average tally per history  = 1.13305E-01          unnormed average tally per history  = 1.13305E-01
 estimated tally relative error    = 0.0003               estimated variance of the variance  = 0.0000
 relative error from zero tallies  = 0.0001               relative error from nonzero scores  = 0.0003

 number of nonzero history tallies =    20382963          efficiency for the nonzero tallies  = 0.9488
 history number of largest  tally  =     2592305          largest  unnormalized history tally = 3.82063E+00
 (largest  tally)/(average tally)  = 3.37198E+01          (largest  tally)/(avg nonzero tally)= 3.19945E+01

 (confidence interval shift)/mean  = 0.0000               shifted confidence interval center  = 1.13305E-01


 if the largest  history score sampled so far were to occur on the next history, the tfc bin quantities would change as follows:

      estimated quantities           value at nps           value at nps+1          value(nps+1)/value(nps)-1.

      mean                            1.13305E-01            1.13305E-01                   0.000002
      relative error                  2.67254E-04            2.67258E-04                   0.000015
      variance of the variance        5.06201E-06            5.06274E-06                   0.000142
      shifted center                  1.13305E-01            1.13305E-01                   0.000000
      figure of merit                 4.66602E+05            4.66588E+05                  -0.000029

 the estimated inverse power slope of the 198 largest  tallies starting at 2.98286E+00 is 8.4748
 the empirical history score probability density function appears to be increasing at the largest  history scores:
 please examine. see print table 161.
 the large score tail of the empirical history score probability density function appears to have no unsampled regions.

 fom = (histories/minute)*(f(x) signal-to-noise ratio)**2 = (7.159E+05)*( 8.073E-01)**2 = (7.159E+05)*(6.517E-01) = 4.666E+05

1unnormed tally density for tally        2          nonzero tally mean(m) = 1.194E-01   nps =    21482123  print table 161
```

```
 abscissa             ordinate   log plot of tally probability density function in tally fluctuation chart bin(d=decade,slope= 8.5)
  tally  number num den log den:d----------d----------d----------d----------d----------d----------d----------d----------d-
 1.00-03     87 1.97-02  -1.706 **********|**********|**********|**********|*********  |          |          |          |
 1.26-03   4625 8.31-01  -0.080 **********|**********|**********|**********|**********|**********|****      |          |
 1.58-03  23452 3.35+00   0.525 **********|**********|**********|**********|**********|**********|**********|          |
 2.00-03  66767 7.57+00   0.879 **********|**********|**********|**********|**********|**********|**********|****      |
 2.51-03 170583 1.54+01   1.187 **********|**********|**********|**********|**********|**********|**********|********  |
 3.16-03 402375 2.88+01   1.459 **********|**********|**********|**********|**********|**********|**********|**********|
 3.98-03 866167 4.92+01   1.692 **********|**********|**********|**********|**********|**********|**********|**********|*
 5.01-03 683407 3.09+01   1.489 **********|**********|**********|**********|**********|**********|**********|**********|
 6.31-03 440971 1.58+01   1.199 **********|**********|**********|**********|**********|**********|**********|********  |
 7.94-03 335002 9.55+00   0.980 **********|**********|**********|**********|**********|**********|**********|*****     |
 1.00-02 227395 5.15+00   0.712 **********|**********|**********|**********|**********|**********|**********|**        |
 1.26-02 257443 4.63+00   0.665 **********|**********|**********|**********|**********|**********|**********|*       |
 1.58-02 299826 4.28+00   0.632 **********|**********|**********|**********|**********|**********|**********|*       |
 2.00-02 306762 3.48+00   0.542 **********|**********|**********|**********|**********|**********|**********|        |
 2.51-02 394628 3.56+00   0.551 **********|**********|**********|**********|**********|**********|**********|        |
 3.16-02 400285 2.86+00   0.457 **********|**********|**********|**********|**********|**********|**********|        |
 3.98-02 439950 2.50+00   0.398 **********|**********|**********|**********|**********|**********|**********  |        |
 5.01-02 608906 2.75+00   0.439 **********|**********|**********|**********|**********|**********|**********|        |
 6.31-02 975439 3.50+00   0.544 **********|**********|**********|**********|**********|**********|**********|        |
 7.94-02 1.3+06 3.59+00   0.555 **********|**********|**********|**********|**********|**********|**********|        |
 1.00-01 1.3+06 2.99+00   0.476 **********|**********|**********|**********|**********|**********|**********|        |
 1.26-01 2.0+06 3.63+00   0.560 mmmmmmmmmmm|mmmmmmmmmmmm|mmmmmmmmmmm|mmmmmmmmmmm|mmmmmmmmmmm|mmmmmmmmmmm|mmmmmmmmmmm|        |
 1.58-01 4.0+06 5.68+00   0.754 **********|**********|**********|**********|**********|**********|**********|**      |
 2.00-01 2.3+06 2.60+00   0.414 **********|**********|**********|**********|**********|**********|**********  |        |
 2.51-01 1.2+06 1.06+00   0.025 **********|**********|**********|**********|**********|**********|*****     |        |
 3.16-01 627929 4.49-01  -0.347 **********|**********|**********|**********|**********|**********|*         |        |
 3.98-01 347017 1.97-01  -0.705 **********|**********|**********|**********|**********|********  |          |        |
 5.01-01 193381 8.73-02  -1.059 **********|**********|**********|**********|**********|****      |          |        |
 6.31-01 107708 3.86-02  -1.413 **********|**********|**********|**********|**********|          |          |        |
 7.94-01  60615 1.73-02  -1.763 **********|**********|**********|**********|********  |          |          |        |
 1.00+00  35452 8.02-03  -2.096 **********|**********|**********|**********|****      |          |          |        |
 1.26+00  20828 3.74-03  -2.427 **********|**********|**********|**********|          |          |          |        |
 1.58+00   6997 9.99-04  -3.000 **********|**********|**********|*****     |          |          |          |        |
 2.00+00   8167 9.26-04  -3.033 **********|**********|**********|*****     |          |          |          |        |
 2.51+00  13639 1.23-03  -2.910 **********|**********|**********|******    |          |          |          |        |
 3.16+00  12404 8.88-04  -3.052 **********|**********|**********|*****     |  s       |          |          |        |
 3.98+00      8 4.55-07  -6.342 *          |          |          |     s    |          |          |          |        |
  total 2.04+07 9.49-01         d----------d----------d----------d----------d----------d----------d----------d----------d-

1tally       22        nps =    21482123
+                                  2-meter Dose (mrem/hr)                                $ 2-m detector
           tally type 2    particle flux averaged over a surface.
           tally for  neutrons

           this tally is modified by a dose function.

           areas
                surface:      80
               segment
                  1       1.00000E+00
                  2       8.07023E+03
                  3       1.00000E+00
              whole       1.00000E+00

 surface  80
```

```
segment:          888
               2.90869E-02 0.0004

surface  80
segment:         -888        777
               1.18658E-07 0.0023

surface  80
segment:         -888       -777
               2.56580E-02 0.0004

surface  80
segment:   whole surface
               5.57025E-02 0.0002

================================================================================================================================

          results of 10 statistical checks for the estimated answer for the tally fluctuation chart (tfc) bin of tally       22

tfc bin     --mean--      ---------relative error---------      ----variance of the variance----      --figure of merit--     -pdf-
behavior    behavior      value   decrease   decrease rate      value   decrease   decrease rate       value     behavior     slope

desired      random       <0.10      yes      1/sqrt(nps)       <0.10      yes        1/nps           constant    random      >3.00
observed     random        0.00      yes          yes            0.00      yes         yes            decrease    random      10.00
passed?        yes          yes      yes          yes             yes      yes         yes                no        yes         yes

================================================================================================================================

 warning.  the tally in the tally fluctuation chart bin did not pass  1 of the 10 statistical checks.

1analysis of the results in the tally fluctuation chart bin (tfc) for tally       22 with nps=    21482123 print table 160

 normed average tally per history  = 5.57025E-02          unnormed average tally per history  = 5.57025E-02
 estimated tally relative error    = 0.0002               estimated variance of the variance  = 0.0000
 relative error from zero tallies  = 0.0001               relative error from nonzero scores  = 0.0002

 number of nonzero history tallies =    14875596          efficiency for the nonzero tallies  = 0.6925
 history number of largest  tally  =     3386680          largest  unnormalized history tally = 4.41459E-01
 (largest  tally)/(average tally)  = 7.92530E+00          (largest  tally)/(avg nonzero tally)= 5.48799E+00

 (confidence interval shift)/mean  = 0.0000               shifted confidence interval center  = 5.57025E-02

 if the largest  history score sampled so far were to occur on the next history, the tfc bin quantities would change as follows:

      estimated quantities           value at nps           value at nps+1          value(nps+1)/value(nps)-1.

      mean                            5.57025E-02            5.57025E-02                  0.000000
      relative error                  2.24722E-04            2.24723E-04                  0.000001
      variance of the variance        3.36314E-08            3.36352E-08                  0.000115
      shifted center                  5.57025E-02            5.57025E-02                  0.000000
      figure of merit                 6.59937E+05            6.59936E+05                 -0.000001

 the estimated slope of the 200 largest  tallies starting at  3.03182E-01 appears to be decreasing at least exponentially.
 the empirical history score probability density function appears to be increasing at the largest  history scores:
```

```
 please examine. see print table 161.
 the large score tail of the empirical history score probability density function appears to have no unsampled regions.

 fom = (histories/minute)*(f(x) signal-to-noise ratio)**2 = (7.159E+05)*( 9.601E-01)**2 = (7.159E+05)*(9.218E-01) = 6.599E+05

1unnormed tally density for tally       22          nonzero tally mean(m) = 8.044E-02   nps =    21482123  print table 161

 abscissa              ordinate   log plot of tally probability density function in tally fluctuation chart bin(d=decade,slope=10.0)
  tally  number num den log den:d----------d----------d----------d----------d----------d----------d----------d----------d--
1.00-03    330 7.47-02  -1.127 **********|**********|**********|**********|**********|****      |          |          |
1.26-03   9494 1.71+00   0.232 **********|**********|**********|**********|**********|**********|********  |          |
1.58-03  35092 5.01+00   0.700 **********|**********|**********|**********|**********|**********|**********|*         |
2.00-03  95038 1.08+01   1.033 **********|**********|**********|**********|**********|**********|**********|*****     |
2.51-03 227326 2.05+01   1.311 **********|**********|**********|**********|**********|**********|**********|*********  |
3.16-03 577546 4.13+01   1.616 **********|**********|**********|**********|**********|**********|**********|**********|*
3.98-03 939601 5.34+01   1.728 **********|**********|**********|**********|**********|**********|**********|**********|**
5.01-03 315459 1.42+01   1.154 **********|**********|**********|**********|**********|**********|**********|*******   |
6.31-03 117965 4.23+00   0.627 **********|**********|**********|**********|**********|**********|**********|          |
7.94-03 131849 3.76+00   0.575 **********|**********|**********|**********|**********|**********|**********|          |
1.00-02  66302 1.50+00   0.176 **********|**********|**********|**********|**********|**********|*******   |          |
1.26-02 250483 4.50+00   0.654 **********|**********|**********|**********|**********|**********|**********|*         |
1.58-02 214085 3.06+00   0.485 **********|**********|**********|**********|**********|**********|**********|          |
2.00-02 272100 3.09+00   0.489 **********|**********|**********|**********|**********|**********|**********|          |
2.51-02 351148 3.16+00   0.500 **********|**********|**********|**********|**********|**********|**********|          |
3.16-02 288547 2.07+00   0.315 **********|**********|**********|**********|**********|**********|*********  |          |
3.98-02 394531 2.24+00   0.351 **********|**********|**********|**********|**********|**********|*********  |          |
5.01-02 643906 2.91+00   0.464 **********|**********|**********|**********|**********|**********|**********  |          |
6.31-02 1.1+06 3.91+00   0.592 **********|**********|**********|**********|**********|**********|**********|          |
7.94-02 1.1+06 3.18+00   0.503 **********|**********|**********|**********|**********|**********|**********|          |
1.00-01 1.1+06 2.55+00   0.406 mmmmmmmmmmm|mmmmmmmmmmmm|mmmmmmmmmmm|mmmmmmmmmmm|mmmmmmmmmmm|mmmmmmmmmmm|mmmmmmmmm  |          |
1.26-01 2.1+06 3.86+00   0.587 **********|**********|**********|**********|**********|**********|**********|          |
1.58-01 3.9+06 5.60+00   0.748 **********|**********|**********|**********|**********|**********|**********|**        |
2.00-01 504327 5.72-01  -0.243 **********|**********|**********|**********|**********|**********|**        |          |
2.51-01  37665 3.39-02  -1.469 **********|**********|**********|**********|**********|          |          |          |
3.16-01   2604 1.86-03  -2.730 **********|**********|**********|********  |          |          |          |          |
3.98-01     94 5.34-05  -4.272 **********|**********|*         |          |          |          |          |          |
5.01-01      1 4.52-07  -6.345 *          |          |          |          |          |          |          |          |
 total 1.49+07 6.92-01         d----------d----------d----------d----------d----------d----------d----------d----------d--

1status of the statistical checks used to form confidence intervals for the mean for each tally bin


 tally   result of statistical checks for the tfc bin (the first check not passed is listed) and error magnitude check for all bins

       2   missed  1 of 10 tfc bin checks: the figure of merit does not appear to be a constant for the last half of the problem
         passed all bin error check:     4 tally bins all have relative errors less than 0.10 with no zero bins

      22   missed  1 of 10 tfc bin checks: the figure of merit does not appear to be a constant for the last half of the problem
         passed all bin error check:     4 tally bins all have relative errors less than 0.10 with no zero bins


 the 10 statistical checks are only for the tally fluctuation chart bin and do not apply to other tally bins.

 warning.       2 of the     2 tally fluctuation chart bins did not pass all 10 statistical checks.
1tally fluctuation charts

                          tally       2                          tally       22
          nps      mean    error   vov  slope    fom      mean    error   vov  slope    fom
```

```
     2048000   1.1319E-01 0.0009 0.0001  1.7  483270   5.5623E-02 0.0007 0.0000 10.0  677727
     4096000   1.1321E-01 0.0006 0.0000 10.0  481210   5.5637E-02 0.0005 0.0000 10.0  677849
     6144000   1.1329E-01 0.0005 0.0000 10.0  483486   5.5670E-02 0.0004 0.0000 10.0  681929
     8192000   1.1329E-01 0.0004 0.0000 10.0  479933   5.5673E-02 0.0004 0.0000 10.0  677735
    10240000   1.1329E-01 0.0004 0.0000 10.0  478418   5.5677E-02 0.0003 0.0000 10.0  676518
    12288000   1.1328E-01 0.0004 0.0000 10.0  476665   5.5688E-02 0.0003 0.0000 10.0  673737
    14336000   1.1330E-01 0.0003 0.0000 10.0  471356   5.5689E-02 0.0003 0.0000 10.0  666886
    16384000   1.1329E-01 0.0003 0.0000 10.0  467180   5.5688E-02 0.0003 0.0000 10.0  660895
    18432000   1.1329E-01 0.0003 0.0000 10.0  465358   5.5697E-02 0.0002 0.0000 10.0  658240
    20480000   1.1330E-01 0.0003 0.0000 10.0  466358   5.5702E-02 0.0002 0.0000 10.0  659732
    21482123   1.1331E-01 0.0003 0.0000  8.5  466602   5.5702E-02 0.0002 0.0000 10.0  659937

************************************************************************************************************************

dump no.    2 on file runtpe     nps =    21482123     coll =      686064893     ctm =       30.01   nrn =
5692445901
tally data written to file mctal

       14 warning messages so far.


run terminated when it had used   30  minutes of computer time.

computer time =   30.03 minutes

mcnp     version 5     09282010                     07/23/14 09:28:34                     probid =  07/23/14 08:58:30
```

5.7.2.1.3 NCT Distributed 0.5 MeV Gamma Source – 7ng120.io

```
         Thread Name & Version = MCNP5, 1.60

                                  _
          _ _      _   _    _    |_
         | | |    (_  | |  |_)    _)
                                  |

 +-------------------------------------------------------------------+
 | Copyright 2010. Los Alamos National Security, LLC.  All rights    |
 | reserved.                                                         |
 |   This material was produced under U.S. Government contract       |
 | DE-AC52-06NA25396 for Los Alamos National Laboratory, which is    |
 | operated by Los Alamos National Security, LLC, for the U.S.       |
 | Department of Los Energy. The Government is granted for itself and |
 | others acting on its behalf a paid-up, nonexclusive, irrevocable  |
 | worldwide license in this material to reproduce, prepare derivative |
 | works, and perform publicly and display publicly. Beginning five  |
 | (5) years after 2010, subject to additional five-year worldwide   |
 | renewals, the Government is granted for itself and others acting on |
 | its behalf a paid-up, nonexclusive, irrevocable worldwide license |
 | in this material to reproduce, prepare derivative works, distribute |
 | copies to the public, perform publicly and display publicly, and to |
 | permit others to do so. NEITHER THE UNITED STATES NOR THE UNITED  |
 | STATES DEPARTMENT OF ENERGY, NOR LOS ALAMOS NATIONAL SECURITY, LLC, |
 | NOR ANY OF THEIR EMPLOYEES, MAKES ANY WARRANTY, EXPRESS OR IMPLIED, |
 | OR ASSUMES ANY LEGAL LIABILITY OR RESPONSIBILITY FOR THE ACCURACY, |
 | COMPLETENESS, OR USEFULNESS OF ANY INFORMATION, APPARATUS, PRODUCT, |
 | OR PROCESS DISCLOSED, OR REPRESENTS THAT ITS USE WOULD NOT INFRINGE |
 | PRIVATELY OWNED RIGHTS.                                           |
```

```
  +--------------------------------------------------------------------+

1mcnp     version 5     ld=09282010                       07/23/14 03:38:07
 ********************************************************************************                probid =  07/23/14 03:38:07
 inp=7ng120.i

         1-       title RH-TRU 72-B RLC NCT Gamma Distributed 1 g/cc 0.5 MeV
         2-       C
         3-       C Cell Cards
         4-       C
         5-       10  1 -1        10  -11  -16                imp:p=1    $ Source #1
         6-       11  1 -1        12  -13  -17                imp:p=1    $ Source #2
         7-       12  1 -1        14  -15  -18                imp:p=1    $ Source #3
         8-       20  0           20  -21  -26
         9-                     (-10:  11:  16)               imp:p=1    $ Drum #1 cavity
        10-       21  0           22  -23  -27
        11-                     (-12:  13:  17)               imp:p=1    $ Drum #2 cavity
        12-       22  0           24  -25  -28
        13-                     (-14:  15:  18)               imp:p=1    $ Drum #3 cavity
        14-       40  0           41  -45  -43
        15-                      #10  #11  #12
        16-                      #20  #21  #22                imp:p=1    $ RLC cavity
        17-       41  3 -7.85260  40  -41  -42                imp:p=1    $ RLC base
        18-       42  3 -7.85260  41  -46   43  -42           imp:p=1    $ RLC shell
        19-       43  3 -7.85260  45  -44  -43                imp:p=1    $ RLC lid
        20-       50  0           51  -53  -55
        21-                     (-40:  42:  46)
        22-                    :( 44  -46  -43)               imp:p=1    $ IV cavity
        23-       51  2 -8.01280  50  -51  -52                imp:p=1    $ IV base
        24-       52  2 -8.01280  51  -55   53  -52           imp:p=2    $ IV shell
        25-       53  2 -8.01280  55  -54  -52                imp:p=1    $ IV lid
        26-       60  0           61  -63  -65
        27-                     (-50:  52:  54)               imp:p=2    $ OC cavity
        28-       61  2 -8.01280  60  -61  -69                imp:p=1    $ OC base
        29-       62  2 -8.01280  61  -66   65  -64           imp:p=5    $ OC ishell
        30-       63  4 -11.3500  61  -66   64  -76  71       imp:p=3E1  $ OC lead in
        31-       64  4 -11.3500  61  -66   76  -68  71       imp:p=3E2  $ OC lead out
        32-       65  2 -8.01280  61  -66   68  -77  71       imp:p=3E3  $ OC oshell in
        33-       66  2 -8.01280  61  -66   77  -67  71       imp:p=6E3  $ OC oshell out
        34-       67  0           61  -66   67  -70  71       imp:p=1E5  $ OC airgap
        35-       68  2 -8.01280  61  -66   70  -69  71       imp:p=2E5  $ OC tshell
        36-       69  2 -8.01280  66  -63   65  -69           imp:p=1    $ OC flange
        37-       70  2 -8.01280  63  -62  -69                imp:p=1    $ OC lid
        38-       71  4 -11.3500  64  -78  -71                imp:p=3E1  $ OC lead punct in
        39-       72  4 -11.3500  78  -73  -71                imp:p=3E2  $ OC lead punct out
        40-       73  2 -8.01280  73  -79  -71                imp:p=3E3  $ OC oshell punct in
        41-       74  2 -8.01280  79  -72  -71                imp:p=6E3  $ OC oshell punct out
        42-       75  0           72  -75  -71                imp:p=1E5  $ OC airgap punct
        43-       76  2 -8.01280  75  -74  -71                imp:p=2E5  $ OC tshell punct
        44-       777 0           69  -80   60  -62           imp:p=2E5  $ Outside to tally
        45-       888 0          -999
        46-                     (-60:  80:  62)               imp:p=1E1  $ Outside pkg
        47-       999 0           999                         imp:p=0    $ Outside world
        48-
        49-       C
        50-       C Geometry Cards
        51-       C
        52-       10  pz 53.658                                          $ Source #1 bottom
```

```
      53-       11  pz 126.683                                          $ Source #1 top
      54-       12  pz 127.635                                        $ Source #2 bottom
      55-       13  pz 200.66                                        $ Source #2 top
      56-       14  pz 201.613                                        $ Source #3 bottom
      57-       15  pz 274.638                                        $ Source #3 top
      58-       16  c/z 0 0 24.448                                     $ Source #1 radius
warning.  this surface has been replaced by a surface of type cz
      59-       17  c/z 0 0 24.448                                     $ Source #2 radius
warning.  this surface has been replaced by a surface of type cz
      60-       18  c/z 0 0 24.448                                     $ Source #3 radius
      61-       C
warning.  this surface has been replaced by a surface of type cz
      62-       20  pz 53.34                                          $ Drum #1 bottom
      63-       21  pz 127                                          $ Drum #1 top
      64-       22  pz 127.318                                        $ Drum #2 bottom
      65-       23  pz 200.978                                        $ Drum #2 top
      66-       24  pz 201.295                                        $ Drum #3 bottom
      67-       25  pz 274.955                                        $ Drum #3 top
      68-       26  c/z 0 0 24.765                                     $ Drum #1 radius
warning.  this surface has been replaced by a surface of type cz
      69-       27  c/z 0 0 24.765                                     $ Drum #2 radius
warning.  this surface has been replaced by a surface of type cz
      70-       28  c/z 0 0 24.765                                     $ Drum #3 radius
      71-       C
warning.  this surface has been replaced by a surface of type cz
      72-       40  pz 19.368                                         $ RLC base (outside)
      73-       41  pz 20.638                                         $ RLC base (inside)
      74-       42  c/z 0 0 33.02                                     $ RLC shell (outside)
warning.  this surface has been replaced by a surface of type cz
      75-       43  c/z 0 0 32.385                                    $ RLC shell (inside)
warning.  this surface has been replaced by a surface of type cz
      76-       44  pz 309.563                                        $ RLC lid (outside)
      77-       45  pz 307.658                                        $ RLC lid (inside)
      78-       46  pz 325.438                                        $ RLC top (outside)
      79-       C
      80-       50  pz 14.288                                         $ IV base (outside)
      81-       51  pz 18.098                                         $ IV base (inside)
      82-       52  c/z 0 0 40.64                                     $ IV shell (outside)
warning.  this surface has been replaced by a surface of type cz
      83-       53  c/z 0 0 39.688                                    $ IV shell (inside)
warning.  this surface has been replaced by a surface of type cz
      84-       54  pz 343.218                                        $ IV top (outside)
      85-       55  pz 326.708                                        $ IV top (inside)
      86-       C
      87-       60  pz 0                                              $ OC bottom (outside)
      88-       61  pz 12.7                                           $ OC bottom (inside)
      89-       62  pz 360.045                                        $ OC top (outside)
      90-       63  pz 344.805                                        $ OC top (inside)
      91-       64  cz 43.656                                         $ OC ishell (outside)
      92-       65  cz 41.116                                         $ OC ishell (inside)
      93-       66  pz 320.675                                        $ OC lead (upper)
      94-       67  cz 52.229                                         $ OC oshell (outside)
      95-       68  cz 48.419                                         $ OC oshell (inside)
      96-       69  cz 52.838                                         $ OC therm (outside)
      97-       70  cz 52.495                                         $ OC therm (inside)
      98-       71  c/x 0 164.148 10.033                              $ OC puncture radius
      99-       72  cz 52.229                                         $ OC oshell punct (out)
     100-       73  cz 48.419                                         $ OC oshell punct (in)
```

```
101-       74  cz 52.838                                          $ OC therm punct (out)
102-       75  cz 52.495                                          $ OC therm punct (in)
103-       76  cz 46.038                                          $ OC lead (mid)
104-       77  cz 50.324                                          $ OC oshell (mid)
105-       78  cz 46.038                                          $ OC lead punct (mid)
106-       79  cz 50.324                                          $ OC oshell punct (mid)
107-       C
108-       80  cz 252.838                                         $ 2-meter from OC therm
109-       C
110-       777 pz 161.608                                         $ Ring tally (lower)
111-       888 pz 166.688                                         $ Ring tally (upper)
112-       999 sz 164.148 379.838                                 $ Outside world
113-
114-       C
115-       C Physics Cards
116-       C
117-       mode p
118-       C
119-       C Source Cards
120-       C
121-       C Cylindrical Sources
122-       sdef pos=d1 erg=d2 par=2 axs=0 0 1 rad=d3 ext=d4
123-       sc1 0.5 MeV
124-       C Source Position and Fraction
125-       si1 L 0 0 90.17
126-             0 0 164.148
127-             0 0 238.125
128-       sp1   1 1 1
129-       C Source Energy (MeV) and Intensity (%)
130-       si2 L 0.5
131-       sp2 1
132-       C Source Radius
133-       si3 0 24.448
134-       sp3 -21 1
135-       C Source Extent
136-       si4 -36.513 36.513
137-       sp4 -21 0
138-       C
139-       C Tally Cards
140-       C
141-       f2:p 69
142-       fc2 Surface Dose (mrem/hr)                             $ Surface detector
143-       fs2 888 777 t
144-       sd2 1.0 1686.525 1.0 1.0                               $ Surface tally area
145-       f22:p 80
146-       fc22 2-meter Dose (mrem/hr)                            $ 2-m detector
147-       fs22 888 777 t
148-       sd22 1.0 8070.229 1.0 1.0                              $ Surface tally area
149-       C
150-       C ANSI/ANS-6.1.1-1977 Gamma Flux to Dose Factors (mrem/hr)
151-       de0 1.0e-02 3.0e-02 5.0e-02 7.0e-02 1.0e-01            $ Energy (Mev)
152-            1.5e-01 2.0e-01 2.5e-01 3.0e-01 3.5e-01
153-            4.0e-01 4.5e-01 5.0e-01 5.5e-01 6.0e-01
154-            6.5e-01 7.0e-01 8.0e-01 1.00 1.40
155-            1.80 2.20 2.60 2.80 3.25
156-            3.75 4.25 4.75 5.00 5.25
157-            5.75 6.25 6.75 7.50 9.00
158-            11.00 13.00 15.0000
```

```
      159-       df0 3.96e-03 5.82e-04 2.90e-04 2.58e-04 2.83e-04        $ Conversion (mrem/hr)
      160-            3.79e-04 5.01e-04 6.31e-04 7.59e-04 8.78e-04
      161-            9.85e-04 1.08e-03 1.17e-03 1.27e-03 1.36e-03
      162-            1.44e-03 1.52e-03 1.68e-03 1.98e-03 2.51e-03
      163-            2.99e-03 3.42e-03 3.82e-03 4.01e-03 4.41e-03
      164-            4.83e-03 5.23e-03 5.60e-03 5.80e-03 6.01e-03
      165-            6.37e-03 6.74e-03 7.11e-03 7.66e-03 8.77e-03
      166-            1.03e-02 1.18e-02 1.33e-02
      167-       C
      168-       C Material Cards
      169-       C
      170-       m1   40000 -1.00                                        $ Zirconium
      171-       m2   14000 -0.01                                        $ Stainless Steel
      172-            24000 -0.19
      173-            25000 -0.02
      174-            26000 -0.68
      175-            28000 -0.10
      176-       m3   26000 -1.00                                        $ Carbon Steel (iron)
      177-       m4   82000 -1.00                                        $ Lead
      178-       C
      179-       C Runtime and Print Cards
      180-       C
      181-       prdmp j j 1 2
      182-       ctme 240

 surface       16   and surface       17   are the same.       17   will be deleted.

 surface       16   and surface       18   are the same.       18   will be deleted.

 surface       26   and surface       27   are the same.       27   will be deleted.

 surface       26   and surface       28   are the same.       28   will be deleted.

 surface       67   and surface       72   are the same.       72   will be deleted.

 surface       68   and surface       73   are the same.       73   will be deleted.

 surface       69   and surface       74   are the same.       74   will be deleted.

 surface       70   and surface       75   are the same.       75   will be deleted.

 surface       76   and surface       78   are the same.       78   will be deleted.

 surface       77   and surface       79   are the same.       79   will be deleted.

  comment.          10 surfaces were deleted for being the same as others.

  warning.  sum of segment sizes differs from total in   2 cases.
1cells                                                                    print table 60

                          atom       gram                                    photon
             cell     mat    density     density     volume       mass          pieces importance

        1       10        1  6.60141E-03 1.00000E+00 1.37122E+05 1.37122E+05          1  1.0000E+00
        2       11        1  6.60141E-03 1.00000E+00 1.37122E+05 1.37122E+05          1  1.0000E+00
        3       12        1  6.60141E-03 1.00000E+00 1.37122E+05 1.37122E+05          1  1.0000E+00
        4       20        0  0.00000E+00 0.00000E+00 4.80248E+03 0.00000E+00          1  1.0000E+00
        5       21        0  0.00000E+00 0.00000E+00 4.80248E+03 0.00000E+00          1  1.0000E+00
```

```
         6       22        0  0.00000E+00 0.00000E+00 4.80248E+03 0.00000E+00          1  1.0000E+00
         7       40        0  0.00000E+00 0.00000E+00 5.19918E+05 0.00000E+00          1  1.0000E+00
         8       41        3  8.46757E-02 7.85260E+00 4.35019E+03 3.41603E+04          1  1.0000E+00
         9       42        3  8.46757E-02 7.85260E+00 3.97694E+04 3.12294E+05          1  1.0000E+00
        10       43        3  8.46757E-02 7.85260E+00 6.27672E+03 4.92886E+04          1  1.0000E+00
        11       50        0  0.00000E+00 0.00000E+00 5.31049E+05 0.00000E+00          1  1.0000E+00
        12       51        2  8.80825E-02 8.01280E+00 1.97689E+04 1.58404E+05          1  1.0000E+00
        13       52        2  8.80825E-02 8.01280E+00 7.41419E+04 5.94084E+05          1  2.0000E+00
        14       53        2  8.80825E-02 8.01280E+00 8.56652E+04 6.86418E+05          1  1.0000E+00
        15       60        0  0.00000E+00 0.00000E+00 5.70765E+04 0.00000E+00          1  2.0000E+00
        16       61        2  8.80825E-02 8.01280E+00 1.11390E+05 8.92546E+05          1  1.0000E+00
        17       62        2  8.80825E-02 8.01280E+00 2.08330E+05 1.66931E+06          1  5.0000E+00
        18       63        4  3.29849E-02 1.13500E+01 0.00000E+00 0.00000E+00          0  3.0000E+01
        19       64        4  3.29849E-02 1.13500E+01 0.00000E+00 0.00000E+00          0  3.0000E+02
        20       65        2  8.80825E-02 8.01280E+00 0.00000E+00 0.00000E+00          0  3.0000E+03
        21       66        2  8.80825E-02 8.01280E+00 0.00000E+00 0.00000E+00          0  6.0000E+03
        22       67        0  0.00000E+00 0.00000E+00 0.00000E+00 0.00000E+00          0  1.0000E+05
        23       68        2  8.80825E-02 8.01280E+00 0.00000E+00 0.00000E+00          0  2.0000E+05
        24       69        2  8.80825E-02 8.01280E+00 8.34880E+04 6.68973E+05          1  1.0000E+00
        25       70        2  8.80825E-02 8.01280E+00 1.33668E+05 1.07106E+06          1  1.0000E+00
        26       71        4  3.29849E-02 1.13500E+01 0.00000E+00 0.00000E+00          0  3.0000E+01
        27       72        4  3.29849E-02 1.13500E+01 0.00000E+00 0.00000E+00          0  3.0000E+02
        28       73        2  8.80825E-02 8.01280E+00 0.00000E+00 0.00000E+00          0  3.0000E+03
        29       74        2  8.80825E-02 8.01280E+00 0.00000E+00 0.00000E+00          0  6.0000E+03
        30       75        0  0.00000E+00 0.00000E+00 0.00000E+00 0.00000E+00          0  1.0000E+05
        31       76        2  8.80825E-02 8.01280E+00 0.00000E+00 0.00000E+00          0  2.0000E+05
        32      777        0  0.00000E+00 0.00000E+00 6.91509E+07 0.00000E+00          1  2.0000E+05
        33      888        0  0.00000E+00 0.00000E+00 1.57245E+08 0.00000E+00          1  1.0000E+01
        34      999        0  0.00000E+00 0.00000E+00 0.00000E+00 0.00000E+00          0  0.0000E+00

 total                                                2.28696E+08 6.54790E+06

    minimum source weight = 1.0000E+00    maximum source weight = 1.0000E+00

 ************************************************
 * Random Number Generator  =                  1 *
 * Random Number Seed       =       19073486328125 *
 * Random Number Multiplier =       19073486328125 *
 * Random Number Adder      =                  0 *
 * Random Number Bits Used  =                 48 *
 * Random Number Stride     =             152917 *
 ************************************************


        11 warning messages so far.
1cross-section tables                                                                print table 100

     table    length

                         tables from file mcplib04

  14000.04p     4792  ENDF/B-VI Release 8 Photoatomic Data for 14-SI                    mat1400      02/07/03
  24000.04p     5682  ENDF/B-VI Release 8 Photoatomic Data for 24-CR                    mat2400      02/07/03
  25000.04p     5598  ENDF/B-VI Release 8 Photoatomic Data for 25-MN                    mat2500      02/07/03
  26000.04p     5718  ENDF/B-VI Release 8 Photoatomic Data for 26-FE                    mat2600      02/07/03
  28000.04p     5826  ENDF/B-VI Release 8 Photoatomic Data for 28-NI                    mat2800      02/07/03
  40000.04p     7703  ENDF/B-VI Release 8 Photoatomic Data for 40-ZR                    mat4000      02/07/03
  82000.04p    10010  ENDF/B-VI Release 8 Photoatomic Data for 82-PB                    mat8200      02/07/03
```

```
  total       45329

 maximum photon energy set to  100.0 mev (maximum electron energy)

                        tables from file el03

  14000.03e    2339                                                                                    6/6/98
  24000.03e    2345                                                                                    6/6/98
  25000.03e    2345                                                                                    6/6/98
  26000.03e    2345                                                                                    6/6/98
  28000.03e    2347                                                                                    6/6/98
  40000.03e    2353                                                                                    6/6/98
  82000.03e    2373                                                                                    6/6/98

  warning.  material        1 has been set to a conductor.

  warning.  material        2 has been set to a conductor.

  warning.  material        3 has been set to a conductor.

  warning.  material        4 has been set to a conductor.

 ************************************************************************************************************************

 dump no.    1 on file runtpe     nps =           0     coll =              0     ctm =        0.00   nrn =
    0

       15 warning messages so far.

 ************************************************************************************************************************

 dump no.    2 on file runtpe     nps =   111158336     coll =     1488478927     ctm =       60.01   nrn =
 18157915849

 ************************************************************************************************************************

 dump no.    3 on file runtpe     nps =   222572923     coll =     2980927790     ctm =      120.02   nrn =
 36364370439

 ************************************************************************************************************************

 dump no.    4 on file runtpe     nps =   333641645     coll =     4467960647     ctm =      180.02   nrn =
 54504895452
1problem summary

      run terminated when it had used  240  minutes of computer time.
+                                                                                    07/23/14 07:38:09
      title RH-TRU 72-B RLC NCT Gamma Distributed 1 g/cc 0.5 MeV                probid =  07/23/14 03:38:07
0
 photon creation     tracks      weight        energy           photon loss         tracks      weight        energy
                                 (per source particle)                                        (per source particle)

 source           444826025    1.0000E+00    5.0000E-01       escape            46448454    1.0167E-06    3.3622E-07
                                                              energy cutoff            0    0.            6.1579E-05
                                                              time cutoff              0    0.            0.
 weight window            0    0.            0.               weight window            0    0.            0.
 cell importance 1131304545    7.2545E-02    1.6582E-02       cell importance  112771460    7.2537E-02    1.6582E-02
```

weight cutoff	0	0.	0.	weight cutoff	0	0.	0.
e or t importance	0	0.	0.	e or t importance	0	0.	0.
dxtran	0	0.	0.	dxtran	0	0.	0.
forced collisions	0	0.	0.	forced collisions	0	0.	0.
exp. transform	0	0.	0.	exp. transform	0	0.	0.
from neutrons	0	0.	0.	compton scatter	0	0.	2.9043E-01
bremsstrahlung	404668911	2.2603E-01	4.2983E-03	capture	3084180798	1.8383E+00	2.2441E-01
p-annihilation	0	0.	0.	pair production	0	0.	0.
photonuclear	0	0.	0.	photonuclear abs	0	0.	0.
electron x-rays	0	0.	0.				
1st fluorescence	1103779722	5.9055E-01	1.0461E-02				
2nd fluorescence	158821509	2.1712E-02	1.4628E-04				
total	3243400712	1.9108E+00	5.3149E-01	total	3243400712	1.9108E+00	5.3149E-01

number of photons banked	1038226086	average time of (shakes)	cutoffs
photon tracks per source particle	7.2914E+00	escape 1.1752E+00	tco 1.0000E+33
photon collisions per source particle	1.3391E+01	capture 6.7038E-02	eco 1.0000E-03
total photon collisions	5956542950	capture or escape 6.7039E-02	wc1 -5.0000E-01
		any termination 6.8808E-02	wc2 -2.5000E-01

computer time so far in this run	240.02 minutes	maximum number ever in bank	11
computer time in mcrun	240.01 minutes	bank overflows to backup file	0
source particles per minute	1.8534E+06		
random numbers generated	72664636898	most random numbers used was	2408533 in history 164504534

warning. random number stride 152917 exceeded 24 times.

range of sampled source weights = 1.0000E+00 to 1.0000E+00

warning. importance function may be poor. see print table 120.

1photon activity in each cell print table 126

cell	tracks entering	population	collisions	collisions * weight (per history)	number weighted energy	flux weighted energy	average track weight (relative)	average track mfp (cm)
1 10	164602623	182633308	400063291	8.9937E-01	4.0972E-01	4.0972E-01	1.0000E+00	9.5524E+00
2 11	174049121	192664329	423147563	9.5127E-01	4.0795E-01	4.0795E-01	1.0000E+00	9.5145E+00
3 12	164574101	182616656	400069680	8.9938E-01	4.0971E-01	4.0971E-01	1.0000E+00	9.5522E+00
4 20	93898347	82849533	0	0.0000E+00	3.9900E-01	3.9900E-01	1.0000E+00	0.0000E+00
5 21	107345601	91838075	0	0.0000E+00	3.9618E-01	3.9618E-01	1.0000E+00	0.0000E+00
6 22	93862352	82824372	0	0.0000E+00	3.9899E-01	3.9899E-01	1.0000E+00	0.0000E+00
7 40	273740911	222861894	0	0.0000E+00	3.7210E-01	3.7210E-01	1.0000E+00	0.0000E+00
8 41	5060980	4864911	9028005	2.0296E-02	3.1711E-01	3.1711E-01	1.0000E+00	1.1080E+00
9 42	227715084	211375265	235930734	5.3039E-01	3.4565E-01	3.4565E-01	1.0000E+00	1.1773E+00
10 43	4746519	4836368	11352143	2.5520E-02	3.1676E-01	3.1676E-01	1.0000E+00	1.1087E+00
11 50	214538673	182530951	0	0.0000E+00	3.3142E-01	3.3142E-01	8.0852E-01	0.0000E+00
12 51	3423442	3584779	12147826	2.7309E-02	2.9942E-01	2.9942E-01	1.0000E+00	1.0520E+00
13 52	350502326	336126720	541345705	6.0849E-01	3.1763E-01	3.1763E-01	1.0000E+00	1.0914E+00
14 53	1591501	1718863	6524644	1.4668E-02	2.8871E-01	2.8871E-01	1.0000E+00	1.0284E+00
15 60	281250387	241571915	0	0.0000E+00	3.0998E-01	3.0998E-01	7.5632E-01	0.0000E+00
16 61	399147	426976	1633397	3.6720E-03	2.8058E-01	2.8058E-01	1.0000E+00	1.0126E+00
17 62	496527488	525871918	1535917109	6.9057E-01	3.0336E-01	3.0336E-01	1.0000E+00	1.0631E+00
18 63	706009909	1106710953	2186314500	1.6383E-01	3.7960E-01	3.7960E-01	1.0000E+00	3.6569E-01
19 64	33181602	56485036	114846678	8.6061E-04	4.3005E-01	4.3005E-01	1.0000E+00	4.4325E-01
20 65	4738623	4876464	11522518	8.6345E-06	3.4395E-01	3.4395E-01	1.0000E+00	1.1543E+00
21 66	4406928	4629295	11207482	4.1992E-06	3.1394E-01	3.1394E-01	1.0000E+00	1.0901E+00
22 67	6615644	6421335	0	0.0000E+00	3.1607E-01	3.1607E-01	2.8154E+00	0.0000E+00

```
       23       68    55793175     56519567     30696747    3.4504E-07   3.2301E-01   3.2301E-01   1.0000E+00   1.1214E+00
       24       69      171782       181792       632886    1.4228E-03   2.7737E-01   2.7737E-01   1.0000E+00   1.0032E+00
       25       70         221          236          826    1.8569E-06   2.6041E-01   2.6041E-01   1.0000E+00   9.6700E-01
       26       71     7432792     11557292     22577022    1.6918E-03   3.7910E-01   3.7910E-01   1.0000E+00   3.6491E-01
       27       72      332176       559439      1123118    8.4162E-06   4.3012E-01   4.3012E-01   1.0000E+00   4.4336E-01
       28       73       46638        47317       103785    7.7772E-08   3.4649E-01   3.4649E-01   1.0000E+00   1.1605E+00
       29       74       42098        43615        98439    3.6883E-08   3.1569E-01   3.1569E-01   1.0000E+00   1.0951E+00
       30       75       59522        57886            0    0.0000E+00   3.1688E-01   3.1688E-01   2.7870E+00   0.0000E+00
       31       76      483993       489978       258852    2.9096E-09   3.2520E-01   3.2520E-01   1.0000E+00   1.1273E+00
       32      777    46448286     46448286            0    0.0000E+00   3.4407E-01   3.4407E-01   1.1739E+00   0.0000E+00
       33      888    46448454     46448454            0    0.0000E+00   3.2049E-01   3.2049E-01   1.3552E-04   0.0000E+00

           total    3570040446   3892673778   5956542950    4.8388E+00

1tally        2        nps =   444826025
+                                Surface Dose (mrem/hr)                                  $ Surface detector
          tally type 2    particle flux averaged over a surface.
          tally for  photons

          this tally is modified by a dose function.

          areas
               surface:      69
              segment
                1       1.00000E+00
                2       1.68653E+03
                3       1.00000E+00
             whole      1.00000E+00

 surface  69
 segment:          888
                4.19262E-10 0.0541

 surface  69
 segment:         -888        777
                8.12006E-15 0.0115

 surface  69
 segment:         -888       -777
                3.13475E-10 0.0235

 surface  69
 segment:   whole surface
                7.46432E-10 0.0319


 ============================================================================================================================

          results of 10 statistical checks for the estimated answer for the tally fluctuation chart (tfc) bin of tally       2

 tfc bin     --mean--      ---------relative error---------      ----variance of the variance----      --figure of merit--     -pdf-
 behavior    behavior      value   decrease   decrease rate      value   decrease   decrease rate       value     behavior     slope

 desired      random       <0.10      yes      1/sqrt(nps)       <0.10      yes        1/nps          constant     random      >3.00
 observed    decrease       0.03      yes          yes            0.20      yes         yes           constant    increase      1.25
 passed?        no           yes      yes          yes              no      yes         yes              yes          no          no

 ============================================================================================================================
```

```
 warning.  the tally in the tally fluctuation chart bin did not pass  4 of the 10 statistical checks.

1analysis of the results in the tally fluctuation chart bin (tfc) for tally        2 with nps=   444826025 print table 160


 normed average tally per history  = 7.46432E-10          unnormed average tally per history  = 7.46432E-10
 estimated tally relative error    = 0.0319               estimated variance of the variance  = 0.2039
 relative error from zero tallies  = 0.0017               relative error from nonzero scores  = 0.0319

 number of nonzero history tallies =      361843          efficiency for the nonzero tallies  = 0.0008
 history number of largest  tally  =   167745863          largest  unnormalized history tally = 6.95145E-03
 (largest  tally)/(average tally)  = 9.31290E+06          (largest  tally)/(avg nonzero tally)= 7.57557E+03

 (confidence interval shift)/mean  = 0.0060               shifted confidence interval center  = 7.50881E-10


 if the largest  history score sampled so far were to occur on the next history, the tfc bin quantities would change as follows:

      estimated quantities           value at nps           value at nps+1           value(nps+1)/value(nps)-1.

      mean                            7.46432E-10            7.62059E-10                  0.020936
      relative error                  3.19273E-02            3.73965E-02                  0.171303
      variance of the variance        2.03895E-01            1.90129E-01                 -0.067516
      shifted center                  7.50881E-10            7.51893E-10                  0.001347
      figure of merit                 4.08738E+00            2.97925E+00                 -0.271110

 the estimated inverse power slope of the 200 largest  tallies starting at 3.48270E-06 is 1.2479
 the history score probability density function appears to have an unsampled region at the largest  history scores:
 please examine. see print table 161.

 fom = (histories/minute)*(f(x) signal-to-noise ratio)**2 = (1.853E+06)*( 1.485E-03)**2 = (1.853E+06)*(2.205E-06) = 4.087E+00

1unnormed tally density for tally       2          nonzero tally mean(m) = 9.176E-07   nps =   444826025  print table 161

 abscissa              ordinate   log plot of tally probability density function in tally fluctuation chart bin(d=decade,slope= 1.2)
  tally  number num den log den:d---------d---------d---------d---------d---------d---------d---------d---------d---------d---------d-
 2.00-09      9 2.75+01   1.439 **********|**********|**********|**********|**********|**********|**********|*******   |          |
 3.16-09      9 1.73+01   1.239 **********|**********|**********|**********|**********|**********|**********|*****     |          |
 5.01-09     13 1.58+01   1.199 **********|**********|**********|**********|**********|**********|**********|*****     |          |
 7.94-09     28 2.15+01   1.332 **********|**********|**********|**********|**********|**********|**********|******    |          |
 1.26-08     60 2.90+01   1.463 **********|**********|**********|**********|**********|**********|**********|*******   |          |
 2.00-08    154 4.70+01   1.672 **********|**********|**********|**********|**********|**********|**********|**********|          |
 3.16-08    409 7.88+01   1.896 **********|**********|**********|**********|**********|**********|**********|**********|*         |
 5.01-08   1202 1.46+02   2.165 **********|**********|**********|**********|**********|**********|**********|**********|****      |
 7.94-08   2923 2.24+02   2.351 **********|**********|**********|**********|**********|**********|**********|**********|******    |
 1.26-07   6775 3.28+02   2.516 **********|**********|**********|**********|**********|**********|**********|**********|********  |
 2.00-07  19477 5.95+02   2.774 **********|**********|**********|**********|**********|**********|**********|**********|**********|
 3.16-07  27457 5.29+02   2.723 **********|**********|**********|**********|**********|**********|**********|**********|**********|
 5.01-07  59240 7.20+02   2.857 **********|**********|**********|**********|**********|**********|**********|**********|**********|*
 7.94-07  98337 7.54+02   2.877 **********|**********|**********|**********|**********|**********|**********|**********|**********|*
 1.26-06  98774 4.78+02   2.679 mmmmmmmmmm|mmmmmmmmmm|mmmmmmmmmm|mmmmmmmmmm|mmmmmmmmmm|mmmmmmmmmm|mmmmmmmmmm|mmmmmmmmmm|mmmmmmmmmm|
 2.00-06  40445 1.23+02   2.092 **********|**********|**********|**********|**********|**********|**********|**********|***       |
 3.16-06   6159 1.19+01   1.074 **********|**********|**********|**********|**********|**********|**********|***       |          |
 5.01-06    294 3.57-01  -0.447 **********|**********|**********|**********|**********|********  |       s  |          |          |
 7.94-06      2 1.53-03  -2.814 **********|**********|**********|****      |          |          |   s      |          |          |
 1.26-05      6 2.90-03  -2.537 **********|**********|**********|*******   |          |          | s        |          |          |
```

```
 2.00-05      3 9.16-04  -3.038 **********|**********|**********|**        |          |         s|          |          |          |
 3.16-05      2 3.85-04  -3.414 **********|**********|********* |          |          |      s   |          |          |          |
 5.01-05      6 7.29-04  -3.137 **********|**********|**********|*         |          |    s     |          |          |          |
 7.94-05      2 1.53-04  -3.814 **********|**********|****      |          |          |  s       |          |          |          |
 1.26-04      1 4.84-05  -4.315 **********|**********|          |          |         s|          |          |          |          |
 2.00-04      2 6.11-05  -4.214 **********|**********|          |          |     s    |          |          |          |          |
 3.16-04      1 1.93-05  -4.715 **********|*****     |          |          |   s      |          |          |          |          |
 5.01-04      3 3.65-05  -4.438 **********|********  |          |          | s        |          |          |          |          |
 7.94-04     19 1.46-04  -3.837 **********|**********|****      |         s|          |          |          |          |          |
 1.26-03     22 1.06-04  -3.973 **********|**********|***       |      s   |          |          |          |          |          |
 2.00-03      5 1.53-05  -4.816 **********|****      |          |   s      |          |          |          |          |          |
 3.16-03      2 3.85-06  -5.414 *********  |          |          | s        |          |          |          |          |          |
 5.01-03      1 1.22-06  -5.915 ***        |          |         s|          |          |          |          |          |          |
 7.94-03      1 7.67-07  -6.115 *          |          |      s   |          |          |          |          |          |          |
  total  361843 8.13-04         d---------d----------d----------d----------d----------d----------d----------d----------d----------d-

1tally       22        nps =   444826025
+                                2-meter Dose (mrem/hr)                          $ 2-m detector
          tally type 2    particle flux averaged over a surface.
          tally for  photons

          this tally is modified by a dose function.

          areas
               surface:      80
              segment
                1       1.00000E+00
                2       8.07023E+03
                3       1.00000E+00
               whole      1.00000E+00

 surface  80
 segment:          888
               2.44881E-10 0.0279

 surface  80
 segment:         -888        777
               1.02051E-15 0.0079

 surface  80
 segment:         -888       -777
               2.09445E-10 0.0225

 surface  80
 segment:   whole surface
               4.62562E-10 0.0180


 ================================================================================================================================

          results of 10 statistical checks for the estimated answer for the tally fluctuation chart (tfc) bin of tally       22

 tfc bin     --mean--      ---------relative error---------      ----variance of the variance----      --figure of merit--     -pdf-
 behavior    behavior      value   decrease   decrease rate      value   decrease   decrease rate       value     behavior     slope

 desired      random       <0.10      yes      1/sqrt(nps)       <0.10      yes        1/nps          constant    random      >3.00
 observed    decrease       0.02      yes          yes            0.05      yes         yes           constant   increase      1.34
 passed?        no           yes      yes          yes             yes      yes         yes              yes        no          no
```

```
 ================================================================================================================================

 warning.  the tally in the tally fluctuation chart bin did not pass  3 of the 10 statistical checks.

1analysis of the results in the tally fluctuation chart bin (tfc) for tally       22 with nps=   444826025 print table 160


 normed average tally per history  = 4.62562E-10          unnormed average tally per history  = 4.62562E-10
 estimated tally relative error    = 0.0180               estimated variance of the variance  = 0.0465
 relative error from zero tallies  = 0.0017               relative error from nonzero scores  = 0.0179

 number of nonzero history tallies =      361564          efficiency for the nonzero tallies  = 0.0008
 history number of largest  tally  =   191085760          largest  unnormalized history tally = 1.17393E-03
 (largest  tally)/(average tally)  = 2.53790E+06          (largest  tally)/(avg nonzero tally)= 2.06286E+03

 (confidence interval shift)/mean  = 0.0019               shifted confidence interval center  = 4.63423E-10


 if the largest  history score sampled so far were to occur on the next history, the tfc bin quantities would change as follows:

      estimated quantities           value at nps           value at nps+1          value(nps+1)/value(nps)-1.

      mean                            4.62562E-10            4.65201E-10                  0.005705
      relative error                  1.80113E-02            1.87861E-02                  0.043021
      variance of the variance        4.65052E-02            4.67260E-02                  0.004747
      shifted center                  4.63423E-10            4.63464E-10                  0.000090
      figure of merit                 1.28434E+01            1.18058E+01                 -0.080791

 the estimated inverse power slope of the 200 largest  tallies starting at 2.50225E-06 is 1.3360
 the history score probability density function appears to have an unsampled region at the largest  history scores:
 please examine. see print table 161.

 fom = (histories/minute)*(f(x) signal-to-noise ratio)**2 = (1.853E+06)*( 2.632E-03)**2 = (1.853E+06)*(6.930E-06) = 1.284E+01

1unnormed tally density for tally       22          nonzero tally mean(m) = 5.691E-07   nps =   444826025  print table 161

 abscissa              ordinate   log plot of tally probability density function in tally fluctuation chart bin(d=decade,slope= 1.3)
  tally  number num den log den:d-----------d-----------d-----------d-----------d-----------d-----------d-----------d-----------
2.00-09    191 5.83+02   2.766 ***********|***********|***********|***********|***********|***********|***********|********
3.16-09    270 5.20+02   2.716 ***********|***********|***********|***********|***********|***********|***********|*******
5.01-09    693 8.42+02   2.925 ***********|***********|***********|***********|***********|***********|***********|***********
7.94-09   1286 9.86+02   2.994 ***********|***********|***********|***********|***********|***********|***********|***********
1.26-08   2116 1.02+03   3.010 ***********|***********|***********|***********|***********|***********|***********|***********
2.00-08   2645 8.08+02   2.907 ***********|***********|***********|***********|***********|***********|***********|*********
3.16-08   2819 5.43+02   2.735 ***********|***********|***********|***********|***********|***********|***********|*******
5.01-08   3676 4.47+02   2.650 ***********|***********|***********|***********|***********|***********|***********|******
7.94-08   6746 5.17+02   2.714 ***********|***********|***********|***********|***********|***********|***********|*******
1.26-07  14592 7.06+02   2.849 ***********|***********|***********|***********|***********|***********|***********|*********
2.00-07  35548 1.09+03   3.036 ***********|***********|***********|***********|***********|***********|***********|***********
3.16-07  47089 9.07+02   2.958 ***********|***********|***********|***********|***********|***********|***********|***********
5.01-07  81807 9.94+02   2.998 ***********|***********|***********|***********|***********|***********|***********|***********
7.94-07  94215 7.23+02   2.859 mmmmmmmmmmm|mmmmmmmmmmm|mmmmmmmmmmm|mmmmmmmmmmm|mmmmmmmmmmm|mmmmmmmmmmm|mmmmmmmmmmm|mmmmmmmmm
1.26-06  55232 2.67+02   2.427 ***********|***********|***********|***********|***********|***********|***********|***
2.00-06  11622 3.55+01   1.550 ***********|***********|***********|***********|***********|***********|****       |
3.16-06    952 1.83+00   0.263 ***********|***********|***********|***********|***********|*          s |           |
5.01-06     13 1.58-02  -1.801 ***********|***********|***********|           |           |       s   |           |
```

```
 7.94-06      4 3.07-03  -2.513 ***********|***********|***        |            |            |   s        |           |
 1.26-05      6 2.90-03  -2.537 ***********|***********|***        |            |            |s           |           |
 2.00-05      2 6.11-04  -3.214 ***********|*******    |           |            |            |        s   |           |
 3.16-05      5 9.63-04  -3.016 ***********|**********  |           |            |        s   |            |           |
 5.01-05      2 2.43-04  -3.614 ***********|**         |           |            |    s       |            |           |
 7.94-05      1 7.67-05  -4.115 *********   |           |           |            |s           |            |           |
 1.26-04      2 9.68-05  -4.014 **********  |           |           |            |     s      |            |           |
 2.00-04      0 0.00+00   0.000             |           |           |        s   |            |            |           |
 3.16-04      1 1.93-05  -4.715 *           |           |           |    s       |            |            |           |
 5.01-04     11 1.34-04  -3.874 ***********|           |           |s           |            |            |           |
 7.94-04     10 7.67-05  -4.115 *********   |           |       s   |            |            |            |           |
 1.26-03      8 3.87-05  -4.412 *****       |           |   s       |            |            |            |           |
  total  361564 8.13-04         d-----------d-----------d-----------d------------d------------d------------d-----------d-----------

1status of the statistical checks used to form confidence intervals for the mean for each tally bin


 tally   result of statistical checks for the tfc bin (the first check not passed is listed) and error magnitude check for all bins

        2   missed  4 of 10 tfc bin checks: the estimated mean has a trend during the last half of the problem
          passed all bin error check:     4 tally bins all have relative errors less than 0.10 with no zero bins

       22   missed  3 of 10 tfc bin checks: the estimated mean has a trend during the last half of the problem
          passed all bin error check:     4 tally bins all have relative errors less than 0.10 with no zero bins


 the 10 statistical checks are only for the tally fluctuation chart bin and do not apply to other tally bins.

 warning.       2 of the     2 tally fluctuation chart bins did not pass all 10 statistical checks.
1tally fluctuation charts

                          tally       2                          tally       22
         nps      mean     error   vov  slope    fom      mean     error   vov  slope    fom
    32768000   6.7991E-10 0.0779 0.6887  2.4 9.3E+00   4.4796E-10 0.0552 0.5124  2.5      18
    65536000   7.4668E-10 0.0821 0.4438  1.7 4.2E+00   4.5169E-10 0.0384 0.2577  2.0      19
    98304000   7.5152E-10 0.0620 0.2750  1.6 4.9E+00   4.7389E-10 0.0433 0.1592  1.7      10
   131072000   7.6734E-10 0.0514 0.1767  1.5 5.4E+00   4.7368E-10 0.0374 0.1211  1.6      10
   163840000   7.6898E-10 0.0474 0.1312  1.4 5.0E+00   4.7351E-10 0.0328 0.0976  1.5      11
   196608000   8.0472E-10 0.0597 0.3161  1.3 2.6E+00   4.8513E-10 0.0327 0.0735  1.4 8.8E+00
   229376000   8.0862E-10 0.0539 0.2569  1.3 2.8E+00   4.8538E-10 0.0300 0.0619  1.4 9.0E+00
   262144000   7.9028E-10 0.0488 0.2466  1.3 3.0E+00   4.7729E-10 0.0267 0.0618  1.4 9.9E+00
   294912000   7.8041E-10 0.0444 0.2352  1.3 3.2E+00   4.7171E-10 0.0242 0.0604  1.4      11
   327680000   7.7101E-10 0.0408 0.2273  1.3 3.4E+00   4.7069E-10 0.0228 0.0550  1.4      11
   360448000   7.6522E-10 0.0378 0.2182  1.3 3.6E+00   4.6962E-10 0.0214 0.0503  1.4      11
   393216000   7.6016E-10 0.0352 0.2093  1.3 3.8E+00   4.6761E-10 0.0200 0.0476  1.3      12
   425984000   7.5113E-10 0.0331 0.2046  1.3 4.0E+00   4.6338E-10 0.0187 0.0475  1.3      12
   444826025   7.4643E-10 0.0319 0.2039  1.2 4.1E+00   4.6256E-10 0.0180 0.0465  1.3      13

 ********************************************************************************************************************************

 dump no.    5 on file runtpe     nps =   444826025     coll =     5956542950     ctm =      240.01   nrn =
 72664636898
 tally data written to file mctal

        20 warning messages so far.


 run terminated when it had used  240  minutes of computer time.
```

```
 computer time =  240.02 minutes
 mcnp     version 5     09282010                    07/23/14 07:38:09                    probid =  07/23/14 03:38:07
```

5.7.2.1.4 NCT Distributed 0.1 MeV Neutron Source – 7nn120.io

```
          Thread Name & Version = MCNP5, 1.60
                                  _
            ._ _   _  ._  ._    |_
            | | |  (_  | |  |_)   _)
                           |
  +-------------------------------------------------------------------+
  | Copyright 2010. Los Alamos National Security, LLC.  All rights    |
  | reserved.                                                         |
  |   This material was produced under U.S. Government contract       |
  | DE-AC52-06NA25396 for Los Alamos National Laboratory, which is    |
  | operated by Los Alamos National Security, LLC, for the U.S.       |
  | Department of Los Energy. The Government is granted for itself and |
  | others acting on its behalf a paid-up, nonexclusive, irrevocable  |
  | worldwide license in this material to reproduce, prepare derivative |
  | works, and perform publicly and display publicly. Beginning five  |
  | (5) years after 2010, subject to additional five-year worldwide   |
  | renewals, the Government is granted for itself and others acting on |
  | its behalf a paid-up, nonexclusive, irrevocable worldwide license |
  | in this material to reproduce, prepare derivative works, distribute |
  | copies to the public, perform publicly and display publicly, and to |
  | permit others to do so. NEITHER THE UNITED STATES NOR THE UNITED  |
  | STATES DEPARTMENT OF ENERGY, NOR LOS ALAMOS NATIONAL SECURITY, LLC, |
  | NOR ANY OF THEIR EMPLOYEES, MAKES ANY WARRANTY, EXPRESS OR IMPLIED, |
  | OR ASSUMES ANY LEGAL LIABILITY OR RESPONSIBILITY FOR THE ACCURACY, |
  | COMPLETENESS, OR USEFULNESS OF ANY INFORMATION, APPARATUS, PRODUCT, |
  | OR PROCESS DISCLOSED, OR REPRESENTS THAT ITS USE WOULD NOT INFRINGE |
  | PRIVATELY OWNED RIGHTS.                                           |
  +-------------------------------------------------------------------+

1mcnp     version 5     ld=09282010                    07/22/14 16:58:39
 ***************************************************************************                    probid =  07/22/14 16:58:39
 inp=7nn120.i

         1-       title RH-TRU 72-B RLC NCT Neutron Distributed 1 g/cc 0.1 MeV
         2-       C
         3-       C Cell Cards
         4-       C
         5-       10  1 -1        10  -11  -16                imp:n=1    $ Source #1
         6-       11  1 -1        12  -13  -17                imp:n=1    $ Source #2
         7-       12  1 -1        14  -15  -18                imp:n=1    $ Source #3
         8-       20  0           20  -21  -26
         9-                     (-10:  11:  16)               imp:n=1    $ Drum #1 cavity
        10-       21  0           22  -23  -27
        11-                     (-12:  13:  17)               imp:n=1    $ Drum #2 cavity
        12-       22  0           24  -25  -28
        13-                     (-14:  15:  18)               imp:n=1    $ Drum #3 cavity
        14-       40  0           41  -45  -43
        15-                      #10  #11  #12
        16-                      #20  #21  #22                imp:n=1    $ RLC cavity
```

```
      17-       41  3 -7.85260  40  -41  -42                imp:n=1    $ RLC base
      18-       42  3 -7.85260  41  -46   43  -42            imp:n=1    $ RLC shell
      19-       43  3 -7.85260  45  -44  -43                imp:n=1    $ RLC lid
      20-       50  0           51  -53  -55
      21-                    (-40:  42:  46)
      22-                   :( 44  -46  -43)                imp:n=1    $ IV cavity
      23-       51  2 -8.01280  50  -51  -52                imp:n=1    $ IV base
      24-       52  2 -8.01280  51  -55   53  -52            imp:n=1    $ IV shell
      25-       53  2 -8.01280  55  -54  -52                imp:n=1    $ IV lid
      26-       60  0           61  -63  -65
      27-                    (-50:  52:  54)                imp:n=1    $ OC cavity
      28-       61  2 -8.01280  60  -61  -69                imp:n=1    $ OC base
      29-       62  2 -8.01280  61  -66   65  -64            imp:n=1    $ OC ishell
      30-       63  4 -11.3500  61  -66   64  -76  71        imp:n=1    $ OC lead in
      31-       64  4 -11.3500  61  -66   76  -68  71        imp:n=1    $ OC lead out
      32-       65  2 -8.01280  61  -66   68  -77  71        imp:n=1    $ OC oshell in
      33-       66  2 -8.01280  61  -66   77  -67  71        imp:n=1    $ OC oshell out
      34-       67  0           61  -66   67  -70  71        imp:n=1    $ OC airgap
      35-       68  2 -8.01280  61  -66   70  -69  71        imp:n=1    $ OC tshell
      36-       69  2 -8.01280  66  -63   65  -69            imp:n=1    $ OC flange
      37-       70  2 -8.01280  63  -62  -69                imp:n=1    $ OC lid
      38-       71  4 -11.3500  64  -78  -71                imp:n=1    $ OC lead punct in
      39-       72  4 -11.3500  78  -73  -71                imp:n=1    $ OC lead punct out
      40-       73  2 -8.01280  73  -79  -71                imp:n=1    $ OC oshell punct in
      41-       74  2 -8.01280  79  -72  -71                imp:n=1    $ OC oshell punct out
      42-       75  0           72  -75  -71                imp:n=1    $ OC airgap punct
      43-       76  2 -8.01280  75  -74  -71                imp:n=1    $ OC tshell punct
      44-       777 0           69  -80   60  -62            imp:n=1    $ Outside to tally
      45-       888 0          -999
      46-                    (-60:  80:  62)                imp:n=1    $ Outside pkg
      47-       999 0           999                         imp:n=0    $ Outside world
      48-
      49-       C
      50-       C Geometry Cards
      51-       C
      52-       10  pz 53.658                                          $ Source #1 bottom
      53-       11  pz 126.683                                           $ Source #1 top
      54-       12  pz 127.635                                        $ Source #2 bottom
      55-       13  pz 200.66                                       $ Source #2 top
      56-       14  pz 201.613                                        $ Source #3 bottom
      57-       15  pz 274.638                                        $ Source #3 top
      58-       16  c/z 0 0 24.448                                      $ Source #1 radius
warning.  this surface has been replaced by a surface of type cz
      59-       17  c/z 0 0 24.448                                      $ Source #2 radius
warning.  this surface has been replaced by a surface of type cz
      60-       18  c/z 0 0 24.448                                      $ Source #3 radius
      61-       C
warning.  this surface has been replaced by a surface of type cz
      62-       20  pz 53.34                                          $ Drum #1 bottom
      63-       21  pz 127                                         $ Drum #1 top
      64-       22  pz 127.318                                        $ Drum #2 bottom
      65-       23  pz 200.978                                        $ Drum #2 top
      66-       24  pz 201.295                                        $ Drum #3 bottom
      67-       25  pz 274.955                                        $ Drum #3 top
      68-       26  c/z 0 0 24.765                                     $ Drum #1 radius
warning.  this surface has been replaced by a surface of type cz
      69-       27  c/z 0 0 24.765                                     $ Drum #2 radius
warning.  this surface has been replaced by a surface of type cz
```

```
      70-       28  c/z 0 0 24.765                                    $ Drum #3 radius
      71-       C
warning.  this surface has been replaced by a surface of type cz
      72-       40  pz 19.368                                        $ RLC base (outside)
      73-       41  pz 20.638                                        $ RLC base (inside)
      74-       42  c/z 0 0 33.02                                    $ RLC shell (outside)
warning.  this surface has been replaced by a surface of type cz
      75-       43  c/z 0 0 32.385                                   $ RLC shell (inside)
warning.  this surface has been replaced by a surface of type cz
      76-       44  pz 309.563                                       $ RLC lid (outside)
      77-       45  pz 307.658                                       $ RLC lid (inside)
      78-       46  pz 325.438                                       $ RLC top (outside)
      79-       C
      80-       50  pz 14.288                                        $ IV base (outside)
      81-       51  pz 18.098                                        $ IV base (inside)
      82-       52  c/z 0 0 40.64                                    $ IV shell (outside)
warning.  this surface has been replaced by a surface of type cz
      83-       53  c/z 0 0 39.688                                   $ IV shell (inside)
warning.  this surface has been replaced by a surface of type cz
      84-       54  pz 343.218                                       $ IV top (outside)
      85-       55  pz 326.708                                       $ IV top (inside)
      86-       C
      87-       60  pz 0                                             $ OC bottom (outside)
      88-       61  pz 12.7                                          $ OC bottom (inside)
      89-       62  pz 360.045                                       $ OC top (outside)
      90-       63  pz 344.805                                       $ OC top (inside)
      91-       64  cz 43.656                                        $ OC ishell (outside)
      92-       65  cz 41.116                                        $ OC ishell (inside)
      93-       66  pz 320.675                                       $ OC lead (upper)
      94-       67  cz 52.229                                        $ OC oshell (outside)
      95-       68  cz 48.419                                        $ OC oshell (inside)
      96-       69  cz 52.838                                        $ OC therm (outside)
      97-       70  cz 52.495                                        $ OC therm (inside)
      98-       71  c/x 0 164.148 10.033                             $ OC puncture radius
      99-       72  cz 52.229                                        $ OC oshell punct (out)
     100-       73  cz 48.419                                        $ OC oshell punct (in)
     101-       74  cz 52.838                                        $ OC therm punct (out)
     102-       75  cz 52.495                                        $ OC therm punct (in)
     103-       76  cz 46.038                                        $ OC lead (mid)
     104-       77  cz 50.324                                        $ OC oshell (mid)
     105-       78  cz 46.038                                        $ OC lead punct (mid)
     106-       79  cz 50.324                                        $ OC oshell punct (mid)
     107-       C
     108-       80  cz 252.838                                       $ 2-meter from OC therm
     109-       C
     110-       777 pz 161.608                                       $ Ring tally (lower)
     111-       888 pz 166.688                                       $ Ring tally (upper)
     112-       999 sz 164.148 379.838                               $ Outside world
     113-
     114-       C
     115-       C Physics Cards
     116-       C
     117-       mode n
     118-       C
     119-       C Source Cards
     120-       C
     121-       C Cylindrical Sources
     122-       sdef pos=d1 erg=d2 par=1 axs=0 0 1 rad=d3 ext=d4
```

```
      123-       sc1 0.1 MeV
      124-       C Source Position and Fraction
      125-       si1 L 0 0 90.17
      126-             0 0 164.148
      127-             0 0 238.125
      128-       sp1   1 1 1
      129-       C Source Energy (MeV) and Fraction
      130-       si2 L 0.1
      131-       sp2 1
      132-       C Source Radius
      133-       si3 0 24.448
      134-       sp3 -21 1
      135-       C Source Extent
      136-       si4 -36.513 36.513
      137-       sp4 -21 0
      138-       C
      139-       C Tally Cards
      140-       C
      141-       f2:n 69
      142-       fc2 Surface Dose (mrem/hr)                              $ Surface detector
      143-       fs2 888 777 t
      144-       sd2 1.0 1686.525 1.0 1.0                                $ Surface tally area
      145-       f22:n 80
      146-       fc22 2-meter Dose (mrem/hr)                             $ 2-m detector
      147-       fs22 888 777 t
      148-       sd22 1.0 8070.229 1.0 1.0                               $ Surface tally area
      149-       C
      150-       C ANSI/ANS-6.1.1-1977 Neutron Flux to Dose Factors (mrem/hr)
      151-       de0  2.5e-08 1.0e-07 1.0e-06 1.0e-05 1.0e-04            $ Energy (Mev)
      152-            1.0e-03 1.0e-02 1.0e-01 5.0e-01 1.0
      153-            2.5 5.0 7.0 10.0 14.0 20.0
      154-       df0  3.67e-03 3.67e-03 4.46e-03 4.54e-03 4.18e-03        $ Conversion (mrem/hr)
      155-            3.76e-03 3.56e-03 2.17e-02 9.26e-02 1.32e-01
      156-            1.25e-01 1.56e-01 1.47e-01 1.47e-01 2.08e-01 2.27e-01
      157-       C
      158-       C Material Cards
      159-       C
      160-       m1   40000.60c -1.00                                    $ Zirconium
      161-       m2   14000.60c -0.01                                    $ Stainless Steel
      162-            24052.60c -0.19
      163-            25055.60c -0.02
      164-            26057.60c -0.68
      165-            28058.60c -0.10
      166-       m3   26057.60c -1.00                                    $ Carbon Steel (iron)
      167-       m4   82000.50c -1.00                                    $ Lead
      168-       C
      169-       C Runtime and Print Cards
      170-       C
      171-       prdmp j j 1 2
      172-       ctme 30

surface       16   and surface       17   are the same.       17   will be deleted.

surface       16   and surface       18   are the same.       18   will be deleted.

surface       26   and surface       27   are the same.       27   will be deleted.

surface       26   and surface       28   are the same.       28   will be deleted.
```

```
 surface       67   and surface       72   are the same.       72   will be deleted.

 surface       68   and surface       73   are the same.       73   will be deleted.

 surface       69   and surface       74   are the same.       74   will be deleted.

 surface       70   and surface       75   are the same.       75   will be deleted.

 surface       76   and surface       78   are the same.       78   will be deleted.

 surface       77   and surface       79   are the same.       79   will be deleted.

  comment.          10 surfaces were deleted for being the same as others.

  warning.  sum of segment sizes differs from total in   2 cases.
1cells                                                                                                print table 60

                                 atom        gram                                                      neutron
             cell     mat     density     density      volume       mass            pieces importance

        1       10        1  6.60141E-03 1.00000E+00 1.37122E+05 1.37122E+05           1  1.0000E+00
        2       11        1  6.60141E-03 1.00000E+00 1.37122E+05 1.37122E+05           1  1.0000E+00
        3       12        1  6.60141E-03 1.00000E+00 1.37122E+05 1.37122E+05           1  1.0000E+00
        4       20        0  0.00000E+00 0.00000E+00 4.80248E+03 0.00000E+00           1  1.0000E+00
        5       21        0  0.00000E+00 0.00000E+00 4.80248E+03 0.00000E+00           1  1.0000E+00
        6       22        0  0.00000E+00 0.00000E+00 4.80248E+03 0.00000E+00           1  1.0000E+00
        7       40        0  0.00000E+00 0.00000E+00 5.19918E+05 0.00000E+00           1  1.0000E+00
        8       41        3  8.30568E-02 7.85260E+00 4.35019E+03 3.41603E+04           1  1.0000E+00
        9       42        3  8.30568E-02 7.85260E+00 3.97694E+04 3.12294E+05           1  1.0000E+00
       10       43        3  8.30568E-02 7.85260E+00 6.27672E+03 4.92886E+04           1  1.0000E+00
       11       50        0  0.00000E+00 0.00000E+00 5.31049E+05 0.00000E+00           1  1.0000E+00
       12       51        2  8.70856E-02 8.01280E+00 1.97689E+04 1.58404E+05           1  1.0000E+00
       13       52        2  8.70856E-02 8.01280E+00 7.41419E+04 5.94084E+05           1  1.0000E+00
       14       53        2  8.70856E-02 8.01280E+00 8.56652E+04 6.86418E+05           1  1.0000E+00
       15       60        0  0.00000E+00 0.00000E+00 5.70765E+04 0.00000E+00           1  1.0000E+00
       16       61        2  8.70856E-02 8.01280E+00 1.11390E+05 8.92546E+05           1  1.0000E+00
       17       62        2  8.70856E-02 8.01280E+00 2.08330E+05 1.66931E+06           1  1.0000E+00
       18       63        4  3.29849E-02 1.13500E+01 0.00000E+00 0.00000E+00           0  1.0000E+00
       19       64        4  3.29849E-02 1.13500E+01 0.00000E+00 0.00000E+00           0  1.0000E+00
       20       65        2  8.70856E-02 8.01280E+00 0.00000E+00 0.00000E+00           0  1.0000E+00
       21       66        2  8.70856E-02 8.01280E+00 0.00000E+00 0.00000E+00           0  1.0000E+00
       22       67        0  0.00000E+00 0.00000E+00 0.00000E+00 0.00000E+00           0  1.0000E+00
       23       68        2  8.70856E-02 8.01280E+00 0.00000E+00 0.00000E+00           0  1.0000E+00
       24       69        2  8.70856E-02 8.01280E+00 8.34880E+04 6.68973E+05           1  1.0000E+00
       25       70        2  8.70856E-02 8.01280E+00 1.33668E+05 1.07106E+06           1  1.0000E+00
       26       71        4  3.29849E-02 1.13500E+01 0.00000E+00 0.00000E+00           0  1.0000E+00
       27       72        4  3.29849E-02 1.13500E+01 0.00000E+00 0.00000E+00           0  1.0000E+00
       28       73        2  8.70856E-02 8.01280E+00 0.00000E+00 0.00000E+00           0  1.0000E+00
       29       74        2  8.70856E-02 8.01280E+00 0.00000E+00 0.00000E+00           0  1.0000E+00
       30       75        0  0.00000E+00 0.00000E+00 0.00000E+00 0.00000E+00           0  1.0000E+00
       31       76        2  8.70856E-02 8.01280E+00 0.00000E+00 0.00000E+00           0  1.0000E+00
       32      777        0  0.00000E+00 0.00000E+00 6.91509E+07 0.00000E+00           1  1.0000E+00
       33      888        0  0.00000E+00 0.00000E+00 1.57245E+08 0.00000E+00           1  1.0000E+00
       34      999        0  0.00000E+00 0.00000E+00 0.00000E+00 0.00000E+00           0  0.0000E+00

 total                                              2.28696E+08 6.54790E+06
```

```
    minimum source weight = 1.0000E+00    maximum source weight = 1.0000E+00

 ************************************************
 * Random Number Generator  =                1 *
 * Random Number Seed       =       19073486328125 *
 * Random Number Multiplier =       19073486328125 *
 * Random Number Adder      =                  0 *
 * Random Number Bits Used  =                 48 *
 * Random Number Stride     =             152917 *
 ************************************************


        11 warning messages so far.
1cross-section tables                                                                                    print table 100

     table    length

                         tables from file endf60

  14000.60c    51392  14-si-nat from endf/b-vi                                                    mat1400      11/25/93
  24052.60c    66325  24-cr-52 from endf/b-vi.1                                                   mat2431      11/25/93
  25055.60c    84549  25-mn-55 from endf/b-vi                                                     mat2525      11/25/93
  26057.60c    72092  endf/b-vi.1 fe57a                                                           mat2634      11/25/93
  28058.60c    83305  28-ni-58 from endf/b-vi.1                                                   mat2825      11/25/93
  40000.60c    45269  40-zr-nat from endf-vi.1                                                    mat4000      11/27/93

                         tables from file rmccs

  82000.50c    28695  njoy                                                                     ( 1382)     03/10/82

  total       431627

 ********************************************************************************************************************************

 dump no.    1 on file runtpe     nps =           0     coll =              0     ctm =        0.00   nrn =
    0

        11 warning messages so far.
1problem summary

      run terminated when it had used   30  minutes of computer time.
+                                                                                                  07/22/14 17:28:45
      title RH-TRU 72-B RLC NCT Neutron Distributed 1 g/cc 0.1 MeV                        probid =  07/22/14 16:58:39
0
 neutron creation    tracks      weight        energy           neutron loss        tracks      weight        energy
                                 (per source particle)                                        (per source particle)

 source             9533660    1.0000E+00    1.0000E-01        escape             9148684    7.9690E-01    1.2142E-02
                                                                energy cutoff            0    0.            0.
                                                                time cutoff              0    0.            0.
 weight window            0    0.            0.                weight window           0    0.            0.
 cell importance          0    0.            0.                cell importance         0    0.            0.
 weight cutoff            0    6.0423E-03    5.7223E-06        weight cutoff      384976    6.0571E-03    5.7557E-06
 e or t importance        0    0.            0.                e or t importance       0    0.            0.
 dxtran                   0    0.            0.                dxtran                  0    0.            0.
 forced collisions        0    0.            0.                forced collisions       0    0.            0.
 exp. transform           0    0.            0.                exp. transform          0    0.            0.
 upscattering             0    0.            9.2982E-11        downscattering          0    0.            8.5433E-02
```

photonuclear	0	0.	0.	capture	0	2.0308E-01	2.4256E-03
(n,xn)	0	0.	0.	loss to (n,xn)	0	0.	0.
prompt fission	0	0.	0.	loss to fission	0	0.	0.
delayed fission	0	0.	0.				
total	9533660	1.0060E+00	1.0001E-01	total	9533660	1.0060E+00	1.0001E-01

number of neutrons banked	0	average time of (shakes)	cutoffs
neutron tracks per source particle	1.0000E+00	escape 8.6043E+02	tco 1.0000E+33
neutron collisions per source particle	8.0328E+01	capture 5.3875E+02	eco 0.0000E+00
total neutron collisions	765817780	capture or escape 7.9510E+02	wc1 -5.0000E-01
net multiplication	1.0000E+00 0.0000	any termination 8.0986E+02	wc2 -2.5000E-01

computer time so far in this run	30.04 minutes	maximum number ever in bank	0
computer time in mcrun	30.01 minutes	bank overflows to backup file	0
source particles per minute	3.1771E+05		
random numbers generated	5967571236	most random numbers used was	4714 in history 5717666

range of sampled source weights = 1.0000E+00 to 1.0000E+00

1neutron activity in each cell print table 126

	cell	tracks entering	population	collisions	collisions * weight (per history)	number weighted energy	flux weighted energy	average track weight (relative)	average track mfp (cm)
1	10	10539385	4550109	20667292	2.0290E+00	2.0498E-02	5.3857E-02	9.2010E-01	1.9425E+01
2	11	12368838	5368724	24218977	2.3842E+00	2.1339E-02	5.3221E-02	9.2367E-01	1.9460E+01
3	12	10394200	4550576	20400396	2.0044E+00	2.0656E-02	5.4322E-02	9.2083E-01	1.9380E+01
4	20	18068993	4564812	0	0.0000E+00	1.6603E-02	4.6452E-02	9.0838E-01	0.0000E+00
5	21	21776905	5392824	0	0.0000E+00	1.8171E-02	4.7462E-02	9.1531E-01	0.0000E+00
6	22	17780223	4565349	0	0.0000E+00	1.6726E-02	4.6933E-02	9.0905E-01	0.0000E+00
7	40	62867283	9533660	0	0.0000E+00	1.3631E-02	4.0707E-02	8.9629E-01	0.0000E+00
8	41	2407300	1066247	3060697	2.9531E-01	7.8127E-03	2.7378E-02	8.5607E-01	4.6613E+00
9	42	62881998	9494026	48736815	4.8075E+00	1.3170E-02	3.8897E-02	8.9515E-01	3.8744E+00
10	43	2068533	1086013	3740030	3.5918E-01	7.1011E-03	2.7026E-02	8.4704E-01	4.6854E+00
11	50	72368662	9533660	0	0.0000E+00	1.1559E-02	3.5783E-02	8.8647E-01	0.0000E+00
12	51	2870113	1085124	12395264	1.1072E+00	5.1447E-03	1.9490E-02	8.2430E-01	2.1865E+00
13	52	69794955	9473322	89720628	8.5284E+00	1.1380E-02	3.4401E-02	8.8704E-01	2.0219E+00
14	53	2029660	858982	26268630	2.0864E+00	1.8212E-03	9.5446E-03	7.2490E-01	2.2727E+00
15	60	71250935	9531954	0	0.0000E+00	8.6091E-03	2.9695E-02	8.6487E-01	0.0000E+00
16	61	1549279	705972	19993987	1.6408E+00	2.2091E-03	8.2007E-03	7.5696E-01	2.3020E+00
17	62	60632560	9430605	205158397	1.9301E+01	9.2587E-03	2.8276E-02	8.7579E-01	2.0807E+00
18	63	48775409	9259859	85434050	7.7895E+00	8.1400E-03	2.4898E-02	8.6922E-01	2.7306E+00
19	64	39784828	9135603	69564271	6.3185E+00	7.5806E-03	2.3064E-02	8.6600E-01	2.7312E+00
20	65	28859410	8992629	74453274	6.8726E+00	6.4600E-03	1.9413E-02	8.5624E-01	2.0756E+00
21	66	16666638	8777705	39353118	3.5840E+00	5.5701E-03	1.6538E-02	8.4610E-01	2.2094E+00
22	67	10764686	8525803	0	0.0000E+00	5.2859E-03	1.5680E-02	8.4163E-01	0.0000E+00
23	68	9634378	8526529	3384695	3.0502E-01	5.2333E-03	1.5564E-02	8.4050E-01	2.3709E+00
24	69	1197599	512526	10029825	7.8509E-01	1.5564E-03	7.0700E-03	7.1748E-01	2.2978E+00
25	70	523213	205012	6728700	4.2848E-01	4.0204E-04	1.6892E-03	5.8914E-01	2.3132E+00
26	71	583489	269588	828591	7.6597E-02	9.3793E-03	2.6283E-02	8.8150E-01	2.7336E+00
27	72	452770	208578	644070	5.9329E-02	8.7086E-03	2.4387E-02	8.7806E-01	2.7331E+00
28	73	302124	155318	668570	6.2355E-02	7.3642E-03	2.0471E-02	8.6830E-01	2.0640E+00
29	74	167267	111681	339510	3.1261E-02	6.3233E-03	1.7389E-02	8.5807E-01	2.2023E+00
30	75	90990	75601	0	0.0000E+00	6.0528E-03	1.6580E-02	8.5380E-01	0.0000E+00
31	76	81615	75553	27993	2.5525E-03	6.0041E-03	1.6461E-02	8.5292E-01	2.3713E+00
32	777	8814174	8814174	0	0.0000E+00	5.1621E-03	1.5718E-02	8.3789E-01	0.0000E+00
33	888	9148684	9148684	0	0.0000E+00	4.4992E-03	1.4746E-02	8.2389E-01	0.0000E+00

```
           total     677497096    163586802    765817780    7.0859E+01

1tally        2        nps =     9533660
+                              Surface Dose (mrem/hr)                                $ Surface detector
           tally type 2    particle flux averaged over a surface.
           tally for  neutrons

           this tally is modified by a dose function.

           areas
                surface:      69
               segment
                  1       1.00000E+00
                  2       1.68653E+03
                  3       1.00000E+00
                whole      1.00000E+00

 surface  69
 segment:           888
                3.76534E-03 0.0007

 surface  69
 segment:          -888         777
                9.83887E-08 0.0038

 surface  69
 segment:          -888        -777
                3.68193E-03 0.0007

 surface  69
 segment:   whole surface
                7.61321E-03 0.0005


 ============================================================================================================================

           results of 10 statistical checks for the estimated answer for the tally fluctuation chart (tfc) bin of tally        2

 tfc bin     --mean--      ---------relative error---------      ----variance of the variance----      --figure of merit--     -pdf-
 behavior    behavior      value   decrease   decrease rate      value   decrease   decrease rate       value     behavior     slope

 desired      random       <0.10      yes      1/sqrt(nps)       <0.10      yes        1/nps           constant    random      >3.00
 observed     random        0.00      yes          yes            0.00      yes         yes            constant    random      10.00
 passed?        yes          yes      yes          yes              yes      yes         yes               yes        yes         yes

 ============================================================================================================================


 this tally meets the statistical criteria used to form confidence intervals: check the tally fluctuation chart to verify.
 the results in other bins associated with this tally may not meet these statistical criteria.

 ----- estimated confidence intervals:  -----

 estimated asymmetric confidence interval(1,2,3 sigma): 7.6097E-03 to 7.6167E-03; 7.6062E-03 to 7.6202E-03; 7.6027E-03 to 7.6237E-03
 estimated  symmetric confidence interval(1,2,3 sigma): 7.6097E-03 to 7.6167E-03; 7.6062E-03 to 7.6202E-03; 7.6027E-03 to 7.6237E-03

1analysis of the results in the tally fluctuation chart bin (tfc) for tally        2 with nps=     9533660 print table 160
```

```
 normed average tally per history  = 7.61321E-03          unnormed average tally per history  = 7.61321E-03
 estimated tally relative error    = 0.0005               estimated variance of the variance  = 0.0000
 relative error from zero tallies  = 0.0001               relative error from nonzero scores  = 0.0005

 number of nonzero history tallies =     8814174          efficiency for the nonzero tallies  = 0.9245
 history number of largest  tally  =      588329          largest  unnormalized history tally = 4.27259E-01
 (largest  tally)/(average tally)  = 5.61208E+01          (largest  tally)/(avg nonzero tally)= 5.18855E+01

 (confidence interval shift)/mean  = 0.0000               shifted confidence interval center  = 7.61321E-03


 if the largest  history score sampled so far were to occur on the next history, the tfc bin quantities would change as follows:

      estimated quantities           value at nps           value at nps+1           value(nps+1)/value(nps)-1.

      mean                            7.61321E-03            7.61325E-03                    0.000006
      relative error                  4.61163E-04            4.61197E-04                    0.000073
      variance of the variance        2.50594E-05            2.50762E-05                    0.000669
      shifted center                  7.61321E-03            7.61321E-03                    0.000000
      figure of merit                 1.56698E+05            1.56675E+05                   -0.000145

 the estimated slope of the 200 largest  tallies starting at  3.87829E-01 appears to be decreasing at least exponentially.
 the empirical history score probability density function appears to be increasing at the largest  history scores:
 please examine. see print table 161.
 the large score tail of the empirical history score probability density function appears to have no unsampled regions.

 fom = (histories/minute)*(f(x) signal-to-noise ratio)**2 = (3.177E+05)*( 7.023E-01)**2 = (3.177E+05)*(4.932E-01) = 1.567E+05

1tally       22        nps =     9533660
+                                  2-meter Dose (mrem/hr)                                  $ 2-m detector
           tally type 2    particle flux averaged over a surface.
           tally for  neutrons

           this tally is modified by a dose function.

           areas
                surface:      80
               segment
                  1       1.00000E+00
                  2       8.07023E+03
                  3       1.00000E+00
              whole       1.00000E+00

 surface  80
 segment:          888
                1.91263E-03 0.0006

 surface  80
 segment:         -888        777
                7.89083E-09 0.0038

 surface  80
 segment:         -888       -777
                1.69176E-03 0.0007

 surface  80
 segment:   whole surface
```

```
                3.66807E-03 0.0004

 ================================================================================================================================

          results of 10 statistical checks for the estimated answer for the tally fluctuation chart (tfc) bin of tally       22

 tfc bin     --mean--      ---------relative error---------      ----variance of the variance----      --figure of merit--     -pdf-
 behavior    behavior      value   decrease   decrease rate      value   decrease   decrease rate      value     behavior     slope

 desired      random       <0.10      yes      1/sqrt(nps)       <0.10      yes        1/nps          constant    random      >3.00
 observed     random        0.00      yes          yes            0.00      yes         yes           constant    random      10.00
 passed?        yes          yes      yes          yes             yes      yes         yes              yes        yes         yes

 ================================================================================================================================


 this tally meets the statistical criteria used to form confidence intervals: check the tally fluctuation chart to verify.
 the results in other bins associated with this tally may not meet these statistical criteria.

 ----- estimated confidence intervals:  -----

 estimated asymmetric confidence interval(1,2,3 sigma): 3.6666E-03 to 3.6695E-03; 3.6652E-03 to 3.6710E-03; 3.6637E-03 to 3.6724E-03
 estimated  symmetric confidence interval(1,2,3 sigma): 3.6666E-03 to 3.6695E-03; 3.6652E-03 to 3.6710E-03; 3.6637E-03 to 3.6724E-03

1analysis of the results in the tally fluctuation chart bin (tfc) for tally       22 with nps=     9533660 print table 160


 normed average tally per history  = 3.66807E-03          unnormed average tally per history  = 3.66807E-03
 estimated tally relative error    = 0.0004               estimated variance of the variance  = 0.0000
 relative error from zero tallies  = 0.0002               relative error from nonzero scores  = 0.0003

 number of nonzero history tallies =     6453739          efficiency for the nonzero tallies  = 0.6769
 history number of largest  tally  =     7981618          largest  unnormalized history tally = 3.74446E-02
 (largest  tally)/(average tally)  = 1.02082E+01          (largest  tally)/(avg nonzero tally)= 6.91039E+00

 (confidence interval shift)/mean  = 0.0000               shifted confidence interval center  = 3.66807E-03


 if the largest  history score sampled so far were to occur on the next history, the tfc bin quantities would change as follows:

      estimated quantities           value at nps           value at nps+1          value(nps+1)/value(nps)-1.

      mean                          3.66807E-03            3.66807E-03                    0.000001
      relative error                3.93574E-04            3.93574E-04                    0.000002
      variance of the variance      6.87553E-07            6.87579E-07                    0.000038
      shifted center                3.66807E-03            3.66807E-03                    0.000000
      figure of merit               2.15140E+05            2.15139E+05                   -0.000004

 the estimated slope of the 198 largest  tallies starting at  3.22707E-02 appears to be decreasing at least exponentially.
 the empirical history score probability density function appears to be increasing at the largest  history scores:
 please examine. see print table 161.
 the large score tail of the empirical history score probability density function appears to have no unsampled regions.

 fom = (histories/minute)*(f(x) signal-to-noise ratio)**2 = (3.177E+05)*( 8.229E-01)**2 = (3.177E+05)*(6.772E-01) = 2.151E+05

1status of the statistical checks used to form confidence intervals for the mean for each tally bin
```

```
 tally   result of statistical checks for the tfc bin (the first check not passed is listed) and error magnitude check for all bins

        2   passed the 10 statistical checks for the tally fluctuation chart bin result
          passed all bin error check:     4 tally bins all have relative errors less than 0.10 with no zero bins

       22   passed the 10 statistical checks for the tally fluctuation chart bin result
          passed all bin error check:     4 tally bins all have relative errors less than 0.10 with no zero bins


 the 10 statistical checks are only for the tally fluctuation chart bin and do not apply to other tally bins.

1tally fluctuation charts

                          tally        2                          tally       22
         nps       mean     error    vov  slope    fom      mean     error    vov  slope    fom
      512000   7.6152E-03 0.0020 0.0005 10.0  157742   3.6671E-03 0.0017 0.0000 10.0  217160
     1024000   7.6066E-03 0.0014 0.0002 10.0  160335   3.6648E-03 0.0012 0.0000 10.0  219263
     1536000   7.6129E-03 0.0011 0.0002 10.0  159853   3.6649E-03 0.0010 0.0000 10.0  219259
     2048000   7.6126E-03 0.0010 0.0001 10.0  158755   3.6651E-03 0.0008 0.0000 10.0  217765
     2560000   7.6112E-03 0.0009 0.0001 10.0  159280   3.6671E-03 0.0008 0.0000 10.0  218159
     3072000   7.6157E-03 0.0008 0.0001 10.0  159117   3.6667E-03 0.0007 0.0000 10.0  218460
     3584000   7.6163E-03 0.0008 0.0001 10.0  158134   3.6676E-03 0.0006 0.0000 10.0  217984
     4096000   7.6165E-03 0.0007 0.0001 10.0  157694   3.6688E-03 0.0006 0.0000 10.0  217225
     4608000   7.6157E-03 0.0007 0.0001 10.0  157600   3.6687E-03 0.0006 0.0000 10.0  217056
     5120000   7.6159E-03 0.0006 0.0000 10.0  157091   3.6685E-03 0.0005 0.0000 10.0  216666
     5632000   7.6145E-03 0.0006 0.0000 10.0  156731   3.6682E-03 0.0005 0.0000 10.0  216390
     6144000   7.6134E-03 0.0006 0.0000 10.0  156927   3.6682E-03 0.0005 0.0000 10.0  216203
     6656000   7.6143E-03 0.0006 0.0000 10.0  157065   3.6688E-03 0.0005 0.0000 10.0  216090
     7168000   7.6150E-03 0.0005 0.0000 10.0  157343   3.6690E-03 0.0005 0.0000 10.0  215844
     7680000   7.6142E-03 0.0005 0.0000 10.0  157057   3.6689E-03 0.0004 0.0000 10.0  215542
     8192000   7.6132E-03 0.0005 0.0000 10.0  156805   3.6690E-03 0.0004 0.0000 10.0  215046
     8704000   7.6131E-03 0.0005 0.0000 10.0  156530   3.6685E-03 0.0004 0.0000 10.0  215029
     9216000   7.6138E-03 0.0005 0.0000 10.0  156650   3.6685E-03 0.0004 0.0000 10.0  215086
     9533660   7.6132E-03 0.0005 0.0000 10.0  156698   3.6681E-03 0.0004 0.0000 10.0  215140

 ************************************************************************************************************************

 dump no.    2 on file runtpe     nps =     9533660     coll =      765817780     ctm =       30.01   nrn =
5967571236
 tally data written to file mctal

        11 warning messages so far.


 run terminated when it had used   30  minutes of computer time.

 computer time =   30.04 minutes

 mcnp     version 5     09282010                    07/22/14 17:28:45                    probid =  07/22/14 16:58:39
```

5.7.2.1.5 HAC 60Co Gamma Source – 7hg001.io

```
          Thread Name & Version = MCNP5, 1.60
```

```
          | | |  (_  | |  |_)   _)
                          |
  +-------------------------------------------------------------------+
  | Copyright 2010. Los Alamos National Security, LLC.  All rights    |
  | reserved.                                                         |
  |   This material was produced under U.S. Government contract       |
  | DE-AC52-06NA25396 for Los Alamos National Laboratory, which is    |
  | operated by Los Alamos National Security, LLC, for the U.S.       |
  | Department of Los Energy. The Government is granted for itself and |
  | others acting on its behalf a paid-up, nonexclusive, irrevocable  |
  | worldwide license in this material to reproduce, prepare derivative |
  | works, and perform publicly and display publicly. Beginning five  |
  | (5) years after 2010, subject to additional five-year worldwide   |
  | renewals, the Government is granted for itself and others acting on |
  | its behalf a paid-up, nonexclusive, irrevocable worldwide license |
  | in this material to reproduce, prepare derivative works, distribute |
  | copies to the public, perform publicly and display publicly, and to |
  | permit others to do so. NEITHER THE UNITED STATES NOR THE UNITED  |
  | STATES DEPARTMENT OF ENERGY, NOR LOS ALAMOS NATIONAL SECURITY, LLC, |
  | NOR ANY OF THEIR EMPLOYEES, MAKES ANY WARRANTY, EXPRESS OR IMPLIED, |
  | OR ASSUMES ANY LEGAL LIABILITY OR RESPONSIBILITY FOR THE ACCURACY, |
  | COMPLETENESS, OR USEFULNESS OF ANY INFORMATION, APPARATUS, PRODUCT, |
  | OR PROCESS DISCLOSED, OR REPRESENTS THAT ITS USE WOULD NOT INFRINGE |
  | PRIVATELY OWNED RIGHTS.                                           |
  +-------------------------------------------------------------------+

1mcnp     version 5     ld=09282010                        07/22/14 10:57:24
 ***********************************************************************                probid =  07/22/14 10:57:24
 inp=7hg001.i

          1-       title RH-TRU 72-B RLC HAC Gamma Concentrated 1 g/cc Co60
          2-       C
          3-       C Cell Cards
          4-       C
          5-       10  1 -1        10  -11  -16                imp:p=1    $ Source #1
          6-       20  0           20  -21  -26
          7-                     (-10:  11:  16)                imp:p=1    $ Drum #1 cavity
          8-       40  0           41  -45  -43
          9-                      #10  #20                      imp:p=1    $ RLC cavity
         10-       41  3 -7.85260  40  -41  -42                imp:p=1    $ RLC base
         11-       42  3 -7.85260  41  -46   43  -42           imp:p=1    $ RLC shell
         12-       43  3 -7.85260  45  -44  -43                imp:p=1    $ RLC lid
         13-       50  0           51  -53  -55
         14-                     (-40:  42:  46)
         15-                    :( 44  -46  -43)                imp:p=1    $ IV cavity
         16-       51  2 -8.01280  50  -51  -52                imp:p=1    $ IV base
         17-       52  2 -8.01280  51  -55   53  -52           imp:p=2    $ IV shell
         18-       53  2 -8.01280  55  -54  -52                imp:p=1    $ IV lid
         19-       60  0           61  -63  -65
         20-                     (-50:  52:  54)                imp:p=2    $ OC cavity
         21-       61  2 -8.01280  60  -61  -69                imp:p=1    $ OC base
         22-       62  2 -8.01280  61  -66   65  -64           imp:p=5    $ OC ishell
         23-       63  4 -11.3500  61  -66   64  -76  71       imp:p=3E1  $ OC lead in
         24-       64  4 -11.3500  61  -66   76  -68  71       imp:p=3E2  $ OC lead out
         25-       65  2 -8.01280  61  -66   68  -77  71       imp:p=3E3  $ OC oshell in
         26-       66  2 -8.01280  61  -66   77  -67  71       imp:p=6E3  $ OC oshell out
         27-       67  0           61  -66   67  -70  71       imp:p=1E5  $ OC airgap
         28-       68  2 -8.01280  61  -66   70  -69  71       imp:p=2E5  $ OC tshell
```

```
69  2 -8.01280  66  -63   65  -69          imp:p=1    $ OC flange
70  2 -8.01280  63  -62  -69               imp:p=1    $ OC lid
71  4 -11.3500  64  -78  -71               imp:p=3E1  $ OC lead punct in
72  4 -11.3500  78  -73  -71               imp:p=3E2  $ OC lead punct out
73  2 -8.01280  73  -79  -71               imp:p=3E3  $ OC oshell punct in
74  2 -8.01280  79  -72  -71               imp:p=6E3  $ OC oshell punct out
75  0           74  -69  -71               imp:p=1E5  $ OC airgap punct
76  2 -8.01280  75  -74  -71               imp:p=2E5  $ OC tshell punct
777 0           69  -80   60  -62          imp:p=2E5  $ Outside to tally
888 0         -999
                (-60:  80:  62)            imp:p=1E1  $ Outside pkg
999 0           999                        imp:p=0    $ Outside world

C
C Geometry Cards
C
10  pz 163.513                                        $ Source #1 bottom
11  pz 164.783                                        $ Source #1 top
16  c/z 38.885 0 0.635                                $ Source #1 radius
C
20  pz 163.511                                        $ Drum #1 bottom
21  pz 164.784                                        $ Drum #1 top
26  c/z 38.885 0 0.636                                $ Drum #1 radius
C
40  pz 19.368                                         $ RLC base (outside)
41  pz 20.638                                         $ RLC base (inside)
42  c/z 7.139 0 33.02                                 $ RLC shell (outside)
43  c/z 7.139 0 32.385                                $ RLC shell (inside)
44  pz 309.563                                        $ RLC lid (outside)
45  pz 307.658                                        $ RLC lid (inside)
46  pz 325.438                                        $ RLC top (outside)
C
50  pz 14.288                                         $ IV base (outside)
51  pz 18.098                                         $ IV base (inside)
52  c/z 0.474 0 40.64                                 $ IV shell (outside)
53  c/z 0.474 0 39.688                                $ IV shell (inside)
54  pz 343.218                                        $ IV top (outside)
55  pz 326.708                                        $ IV top (inside)
C
60  pz 0                                              $ OC bottom (outside)
61  pz 12.7                                           $ OC bottom (inside)
62  pz 360.045                                        $ OC top (outside)
63  pz 344.805                                        $ OC top (inside)
64  cz 43.656                                         $ OC ishell (outside)
65  cz 41.116                                         $ OC ishell (inside)
66  pz 320.675                                        $ OC lead (upper)
67  cz 52.229                                         $ OC oshell (outside)
68  cz 48.419                                         $ OC oshell (inside)
69  cz 52.838                                         $ OC therm (outside)
70  cz 52.495                                         $ OC therm (inside)
71  c/x 0 164.148 10.033                              $ OC puncture radius
72  cz 50.563                                         $ OC oshell punct (out)
73  cz 46.753                                         $ OC oshell punct (in)
74  cz 50.905                                         $ OC therm punct (out)
75  cz 50.563                                         $ OC therm punct (in)
76  cz 46.038                                         $ OC lead (mid)
77  cz 50.324                                         $ OC oshell (mid)
78  cz 45.204                                         $ OC lead punct (mid)
```

```
 87-       79  cz 48.658                                          $ OC oshell punct (mid)
 88-       C
 89-       80  cz 150.905                                         $ 1-meter from OC therm
 90-       C
 91-       777 c/x 0 164.148 2.54                                 $ Tally cylinder
 92-       888 px 0                                               $ Tally truncation
 93-       999 sz 164.148 277.905                                 $ Outside world
 94-
 95-       C
 96-       C Physics Cards
 97-       C
 98-       mode p
 99-       C
100-       C Source Cards
101-       C
102-       C Cylindrical Sources
103-       sdef pos=d1 erg=d2 par=2 axs=0 0 1 rad=d3 ext=d4
104-       sc1 Co60
105-       C Source Position and Fraction
106-       si1 L 38.885 0 164.148
107-             0 0 0
108-       sp1   98 2
109-       C Source Energy (MeV) and Intensity (%)
110-       si2 L 3.469300E-01 8.262800E-01 1.173237E+00 1.332501E+00
111-            2.158770E+00 2.505000E+00
112-       sp2 7.600000E-03 7.600000E-03 9.997360E+01 9.998560E+01
113-            1.110000E-03 2.000000E-06
114-       C Source Radius
115-       si3 0 0.635
116-       sp3 -21 1
117-       C Source Extent
118-       si4 -0.635 0.635
119-       sp4 -21 0
120-       C
121-       C Tally Cards
122-       C
123-       f2:p 69
124-       fc2 Surface Dose (mrem/hr)                             $ Surface detector
125-       fs2 -888 -777 t
126-       sd2 1.0 20.268 1.0 1.0                                 $ Surface tally area
127-       f22:p 80
128-       fc22 1-meter Dose (mrem/hr)                            $ 1-m detector
129-       fs22 -888 -777 t
130-       sd22 1.0 20.268 1.0 1.0                                $ Surface tally area
131-       C
132-       C ANSI/ANS-6.1.1-1977 Gamma Flux to Dose Factors (mrem/hr)
133-       de0 1.0e-02 3.0e-02 5.0e-02 7.0e-02 1.0e-01            $ Energy (Mev)
134-            1.5e-01 2.0e-01 2.5e-01 3.0e-01 3.5e-01
135-            4.0e-01 4.5e-01 5.0e-01 5.5e-01 6.0e-01
136-            6.5e-01 7.0e-01 8.0e-01 1.00 1.40
137-            1.80 2.20 2.60 2.80 3.25
138-            3.75 4.25 4.75 5.00 5.25
139-            5.75 6.25 6.75 7.50 9.00
140-            11.00 13.00 15.0000
141-       df0 3.96e-03 5.82e-04 2.90e-04 2.58e-04 2.83e-04       $ Conversion (mrem/hr)
142-            3.79e-04 5.01e-04 6.31e-04 7.59e-04 8.78e-04
143-            9.85e-04 1.08e-03 1.17e-03 1.27e-03 1.36e-03
144-            1.44e-03 1.52e-03 1.68e-03 1.98e-03 2.51e-03
```

```
      145-            2.99e-03 3.42e-03 3.82e-03 4.01e-03 4.41e-03
      146-            4.83e-03 5.23e-03 5.60e-03 5.80e-03 6.01e-03
      147-            6.37e-03 6.74e-03 7.11e-03 7.66e-03 8.77e-03
      148-            1.03e-02 1.18e-02 1.33e-02
      149-       C
      150-       C Material Cards
      151-       C
      152-       m1   40000 -1.00                                        $ Zirconium
      153-       m2   14000 -0.01                                        $ Stainless Steel
      154-            24000 -0.19
      155-            25000 -0.02
      156-            26000 -0.68
      157-            28000 -0.10
      158-       m3   26000 -1.00                                        $ Carbon Steel (iron)
      159-       m4   82000 -1.00                                        $ Lead
      160-       C
      161-       C Runtime and Print Cards
      162-       C
      163-       prdmp j j 1 2
      164-       ctme 360

 surface       72   and surface       75   are the same.       75   will be deleted.

  comment.           1 surfaces were deleted for being the same as others.

  warning.  sum of segment sizes differs from total in   2 cases.
1cells                                                                                                print table 60

                          atom        gram                                                    photon
             cell     mat    density     density     volume       mass            pieces importance

        1       10        1  6.60141E-03 1.00000E+00 1.60880E+00 1.60880E+00           1  1.0000E+00
        2       20        0  0.00000E+00 0.00000E+00 8.88335E-03 0.00000E+00           1  1.0000E+00
        3       40        0  0.00000E+00 0.00000E+00 0.00000E+00 0.00000E+00           0  1.0000E+00
        4       41        3  8.46757E-02 7.85260E+00 4.35019E+03 3.41603E+04           1  1.0000E+00
        5       42        3  8.46757E-02 7.85260E+00 3.97694E+04 3.12294E+05           1  1.0000E+00
        6       43        3  8.46757E-02 7.85260E+00 6.27672E+03 4.92886E+04           1  1.0000E+00
        7       50        0  0.00000E+00 0.00000E+00 0.00000E+00 0.00000E+00           0  1.0000E+00
        8       51        2  8.80825E-02 8.01280E+00 1.97689E+04 1.58404E+05           1  1.0000E+00
        9       52        2  8.80825E-02 8.01280E+00 7.41419E+04 5.94084E+05           1  2.0000E+00
       10       53        2  8.80825E-02 8.01280E+00 8.56652E+04 6.86418E+05           1  1.0000E+00
       11       60        0  0.00000E+00 0.00000E+00 0.00000E+00 0.00000E+00           0  2.0000E+00
       12       61        2  8.80825E-02 8.01280E+00 1.11390E+05 8.92546E+05           1  1.0000E+00
       13       62        2  8.80825E-02 8.01280E+00 2.08330E+05 1.66931E+06           1  5.0000E+00
       14       63        4  3.29849E-02 1.13500E+01 0.00000E+00 0.00000E+00           0  3.0000E+01
       15       64        4  3.29849E-02 1.13500E+01 0.00000E+00 0.00000E+00           0  3.0000E+02
       16       65        2  8.80825E-02 8.01280E+00 0.00000E+00 0.00000E+00           0  3.0000E+03
       17       66        2  8.80825E-02 8.01280E+00 0.00000E+00 0.00000E+00           0  6.0000E+03
       18       67        0  0.00000E+00 0.00000E+00 0.00000E+00 0.00000E+00           0  1.0000E+05
       19       68        2  8.80825E-02 8.01280E+00 0.00000E+00 0.00000E+00           0  2.0000E+05
       20       69        2  8.80825E-02 8.01280E+00 8.34880E+04 6.68973E+05           1  1.0000E+00
       21       70        2  8.80825E-02 8.01280E+00 1.33668E+05 1.07106E+06           1  1.0000E+00
       22       71        4  3.29849E-02 1.13500E+01 0.00000E+00 0.00000E+00           0  3.0000E+01
       23       72        4  3.29849E-02 1.13500E+01 0.00000E+00 0.00000E+00           0  3.0000E+02
       24       73        2  8.80825E-02 8.01280E+00 0.00000E+00 0.00000E+00           0  3.0000E+03
       25       74        2  8.80825E-02 8.01280E+00 0.00000E+00 0.00000E+00           0  6.0000E+03
       26       75        0  0.00000E+00 0.00000E+00 0.00000E+00 0.00000E+00           0  1.0000E+05
       27       76        2  8.80825E-02 8.01280E+00 0.00000E+00 0.00000E+00           0  2.0000E+05
```

```
      28      777        0  0.00000E+00 0.00000E+00 2.26002E+07 0.00000E+00          1  2.0000E+05
      29      888        0  0.00000E+00 0.00000E+00 6.41456E+07 0.00000E+00          1  1.0000E+01
      30      999        0  0.00000E+00 0.00000E+00 0.00000E+00 0.00000E+00          0  0.0000E+00

 total                                              8.75127E+07 6.13653E+06

    minimum source weight = 1.0000E+00    maximum source weight = 1.0000E+00

 ************************************************
 * Random Number Generator  =                  1 *
 * Random Number Seed       =       19073486328125 *
 * Random Number Multiplier =       19073486328125 *
 * Random Number Adder      =                  0 *
 * Random Number Bits Used  =                 48 *
 * Random Number Stride     =             152917 *
 ************************************************


         1 warning message so far.
1cross-section tables                                                                print table 100

     table    length

                        tables from file mcplib04

  14000.04p    4792  ENDF/B-VI Release 8 Photoatomic Data for 14-SI                  mat1400      02/07/03
  24000.04p    5682  ENDF/B-VI Release 8 Photoatomic Data for 24-CR                  mat2400      02/07/03
  25000.04p    5598  ENDF/B-VI Release 8 Photoatomic Data for 25-MN                  mat2500      02/07/03
  26000.04p    5718  ENDF/B-VI Release 8 Photoatomic Data for 26-FE                  mat2600      02/07/03
  28000.04p    5826  ENDF/B-VI Release 8 Photoatomic Data for 28-NI                  mat2800      02/07/03
  40000.04p    7703  ENDF/B-VI Release 8 Photoatomic Data for 40-ZR                  mat4000      02/07/03
  82000.04p   10010  ENDF/B-VI Release 8 Photoatomic Data for 82-PB                  mat8200      02/07/03

  total       45329

 maximum photon energy set to  100.0 mev (maximum electron energy)

                        tables from file el03

  14000.03e    2339                                                                          6/6/98
  24000.03e    2345                                                                          6/6/98
  25000.03e    2345                                                                          6/6/98
  26000.03e    2345                                                                          6/6/98
  28000.03e    2347                                                                          6/6/98
  40000.03e    2353                                                                          6/6/98
  82000.03e    2373                                                                          6/6/98

  warning.  material        1 has been set to a conductor.

  warning.  material        2 has been set to a conductor.

  warning.  material        3 has been set to a conductor.

  warning.  material        4 has been set to a conductor.

 ********************************************************************************************************************************

 dump no.    1 on file runtpe     nps =           0     coll =              0     ctm =        0.00   nrn =
```

```
    0

         5 warning messages so far.

 ********************************************************************************************************************************

 dump no.    2 on file runtpe     nps =     1007431     coll =      551199301     ctm =       60.01   nrn =
 8041396930

 ********************************************************************************************************************************

 dump no.    3 on file runtpe     nps =     2008171     coll =     1099125638     ctm =      120.01   nrn =
 16036196954

 ********************************************************************************************************************************

 dump no.    4 on file runtpe     nps =     3006986     coll =     1646152044     ctm =      180.02   nrn =
 24017879018

 ********************************************************************************************************************************

 dump no.    5 on file runtpe     nps =     4017714     coll =     2196295684     ctm =      240.02   nrn =
 32043137752

 ********************************************************************************************************************************

 dump no.    6 on file runtpe     nps =     5011340     coll =     2742304804     ctm =      300.02   nrn =
 40010760032
1problem summary

      run terminated when it had used  360  minutes of computer time.
+                                                                                                    07/22/14 16:57:46
      title RH-TRU 72-B RLC HAC Gamma Concentrated 1 g/cc Co60                              probid =  07/22/14 10:57:24
0
 photon creation     tracks      weight        energy            photon loss         tracks      weight        energy
                                 (per source particle)                                          (per source particle)

 source              6006188    1.0000E+00    1.2528E+00         escape          3356878710    1.5061E-02    1.4384E-02
                                                                 energy cutoff             0    0.            1.3942E-04
                                                                 time cutoff               0    0.            0.
 weight window             0    0.            0.                 weight window             0    0.            0.
 cell importance  4362681566    2.5282E-01    1.0617E-01         cell importance   583948382    2.5278E-01    1.0620E-01
 weight cutoff             0    0.            0.                 weight cutoff             0    0.            0.
 e or t importance         0    0.            0.                 e or t importance         0    0.            0.
 dxtran                    0    0.            0.                 dxtran                    0    0.            0.
 forced collisions         0    0.            0.                 forced collisions         0    0.            0.
 exp. transform            0    0.            0.                 exp. transform            0    0.            0.
 from neutrons             0    0.            0.                 compton scatter           0    0.            1.0194E+00
 bremsstrahlung    259326135    5.8296E-01    1.9359E-02         capture           956077624    2.2033E+00    2.5551E-01
 p-annihilation      1262888    4.3354E-03    2.2154E-03         pair production      631444    2.1677E-03    2.8329E-03
 photonuclear              0    0.            0.                 photonuclear abs          0    0.            0.
 electron x-rays           0    0.            0.
 1st fluorescence  248585089    5.8147E-01    1.7302E-02
 2nd fluorescence   19674294    5.1723E-02    5.8229E-04
     total        4897536160    2.4733E+00    1.3985E+00             total        4897536160    2.4733E+00    1.3985E+00

   number of photons banked                 564351151        average time of (shakes)              cutoffs
   photon tracks per source particle      8.1542E+02          escape            5.9305E-01          tco   1.0000E+33
```

```
   photon collisions per source particle  5.4690E+02          capture           1.3715E-01          eco   1.0000E-03
   total photon collisions                3284779356          capture or escape 1.4025E-01          wc1  -5.0000E-01
                                                              any termination   1.3766E-01          wc2  -2.5000E-01

 computer time so far in this run   360.02 minutes            maximum number ever in bank        15
 computer time in mcrun             360.01 minutes            bank overflows to backup file       0
 source particles per minute            1.6683E+04
 random numbers generated              47924508086            most random numbers used was     1122266 in history     5137800

  warning.   random number stride   152917 exceeded    11250 times.

 range of sampled source weights = 1.0000E+00 to 1.0000E+00

  warning.  importance function may be poor.  see print table 120.
1photon   activity in each cell                                                                    print table 126
```

	cell	tracks entering	population	collisions	collisions * weight (per history)	number weighted energy	flux weighted energy	average track weight (relative)	average track mfp (cm)
1	10	5938704	5949900	239410	3.9861E-02	1.2225E+00	1.2225E+00	1.0000E+00	1.9077E+01
2	20	5992492	5898146	0	0.0000E+00	1.2158E+00	1.2158E+00	1.0000E+00	0.0000E+00
3	40	7704584	6216964	0	0.0000E+00	8.8532E-01	8.8532E-01	1.0000E+00	0.0000E+00
4	41	131609	130066	187291	3.1188E-02	6.8617E-01	6.8617E-01	1.0000E+00	1.6064E+00
5	42	8520288	7185901	9222317	1.5355E+00	8.6214E-01	8.6214E-01	1.0000E+00	1.8535E+00
6	43	123556	131886	246276	4.1004E-02	6.8975E-01	6.8975E-01	1.0000E+00	1.6165E+00
7	50	8404633	6750044	0	0.0000E+00	7.0107E-01	7.0107E-01	8.0868E-01	0.0000E+00
8	51	116974	132119	419659	6.9942E-02	6.2853E-01	6.2853E-01	1.0007E+00	1.5099E+00
9	52	13272790	13170811	19892716	1.6560E+00	7.2498E-01	7.2498E-01	1.0000E+00	1.6332E+00
10	53	73950	92415	390823	6.5070E-02	6.0713E-01	6.0713E-01	1.0000E+00	1.4842E+00
11	60	11935537	10072821	0	0.0000E+00	6.4541E-01	6.4541E-01	7.7131E-01	0.0000E+00
12	61	97966	122525	416310	9.4556E-02	7.0798E-01	7.0798E-01	1.3868E+00	1.6198E+00
13	62	20495464	23566343	63226099	2.1054E+00	6.4052E-01	6.4052E-01	1.0000E+00	1.5270E+00
14	63	25026135	48300613	92960712	5.1592E-01	8.5263E-01	8.5263E-01	1.0000E+00	1.0138E+00
15	64	27415785	58757935	111319342	6.1780E-02	9.2097E-01	9.2097E-01	1.0000E+00	1.1077E+00
16	65	64276866	69842121	140134269	7.7772E-03	6.7657E-01	6.7657E-01	1.0000E+00	1.5968E+00
17	66	83471873	92163946	188151436	5.2210E-03	6.0674E-01	6.0674E-01	1.0000E+00	1.5007E+00
18	67	194057847	186099671	0	0.0000E+00	6.1874E-01	6.1874E-01	2.8452E+00	0.0000E+00
19	68	1518742361	1556461926	676013663	5.6276E-04	6.3711E-01	6.3711E-01	1.0000E+00	1.5616E+00
20	69	10214	11796	45480	7.5722E-03	5.2506E-01	5.2506E-01	1.0000E+00	1.3709E+00
21	70	308	366	1502	2.5008E-04	4.8213E-01	4.8213E-01	1.0000E+00	1.3158E+00
22	71	19235048	34889269	61642309	3.4210E-01	8.6709E-01	8.6709E-01	1.0000E+00	1.0317E+00
23	72	42601462	81207378	137862324	7.6511E-02	9.2560E-01	9.2560E-01	1.0000E+00	1.1119E+00
24	73	144905048	158461415	299228131	1.6607E-02	7.0413E-01	7.0413E-01	1.0000E+00	1.6341E+00
25	74	164872546	181227925	353045203	9.7967E-03	6.2106E-01	6.2106E-01	1.0000E+00	1.5186E+00
26	75	2301381226	2297417923	0	0.0000E+00	6.9151E-01	6.9151E-01	5.1228E-01	0.0000E+00
27	76	2663522354	2728290365	1130134084	9.4081E-04	6.4350E-01	6.4350E-01	1.0000E+00	1.5665E+00
28	777	3356813559	3356813559	0	0.0000E+00	7.3337E-01	7.3337E-01	1.0139E+00	0.0000E+00
29	888	3356908685	3356907662	0	0.0000E+00	9.7892E-01	9.7892E-01	3.4038E-04	0.0000E+00
total		14046049864	14286273811	3284779356	6.6835E+00				

```
1tally        2        nps =     6006188
+                                Surface Dose (mrem/hr)                                  $ Surface detector
          tally type 2    particle flux averaged over a surface.
          tally for  photons

          this tally is modified by a dose function.
```

```
          areas
               surface:      69
              segment
                1       1.00000E+00
                2       2.02680E+01
                3       1.00000E+00
             whole      1.00000E+00

 surface  69
 segment:          -888
                1.54489E-06 0.0021

 surface  69
 segment:           888       -777
                1.66987E-08 0.0037

 surface  69
 segment:           888        777
                3.59514E-06 0.0015

 surface  69
 segment:   whole surface
                5.47848E-06 0.0012

 ================================================================================================================================

          results of 10 statistical checks for the estimated answer for the tally fluctuation chart (tfc) bin of tally        2

 tfc bin     --mean--      ---------relative error---------      ----variance of the variance----      --figure of merit--     -pdf-
 behavior    behavior      value   decrease   decrease rate      value   decrease   decrease rate       value     behavior     slope

 desired      random       <0.10      yes      1/sqrt(nps)       <0.10      yes        1/nps           constant    random      >3.00
 observed     random        0.00      yes          yes            0.00       no          no             constant    random       1.75
 passed?        yes          yes      yes          yes             yes       no          no                yes        yes          no

 ================================================================================================================================


 warning.  the tally in the tally fluctuation chart bin did not pass  3 of the 10 statistical checks.

1analysis of the results in the tally fluctuation chart bin (tfc) for tally        2 with nps=     6006188 print table 160


 normed average tally per history  = 5.47848E-06          unnormed average tally per history  = 5.47848E-06
 estimated tally relative error    = 0.0012               estimated variance of the variance  = 0.0003
 relative error from zero tallies  = 0.0007               relative error from nonzero scores  = 0.0010

 number of nonzero history tallies =     1629165          efficiency for the nonzero tallies  = 0.2712
 history number of largest  tally  =     4292958          largest  unnormalized history tally = 4.92859E-03
 (largest  tally)/(average tally)  = 8.99628E+02          (largest  tally)/(avg nonzero tally)= 2.44022E+02

 (confidence interval shift)/mean  = 0.0000               shifted confidence interval center  = 5.47850E-06


 if the largest  history score sampled so far were to occur on the next history, the tfc bin quantities would change as follows:
```

```
      estimated quantities          value at nps          value at nps+1          value(nps+1)/value(nps)-1.

      mean                           5.47848E-06           5.47930E-06                0.000150
      relative error                 1.21614E-03           1.22513E-03                0.007388
      variance of the variance       3.34346E-04           5.46745E-04                0.635267
      shifted center                 5.47850E-06           5.47850E-06                0.000001
      figure of merit                1.87807E+03           1.85062E+03               -0.014615

 the estimated inverse power slope of the 198 largest  tallies starting at 2.33870E-04 is 1.7457
 the history score probability density function appears to have an unsampled region at the largest  history scores:
 please examine. see print table 161.

 fom = (histories/minute)*(f(x) signal-to-noise ratio)**2 = (1.668E+04)*( 3.355E-01)**2 = (1.668E+04)*(1.126E-01) = 1.878E+03

1unnormed tally density for tally       2          nonzero tally mean(m) = 2.020E-05   nps =     6006188  print table 161

 abscissa             ordinate   log plot of tally probability density function in tally fluctuation chart bin(d=decade,slope= 1.7)
  tally  number num den log den:d----------d----------d----------d----------d----------d----------d----------d----------d--
 2.00-09     20 4.52+03   3.655 **********|**********|**********|**********|**********|**********|**********|******    |
 3.16-09     45 6.42+03   3.808 **********|**********|**********|**********|**********|**********|**********|********  |
 5.01-09     85 7.65+03   3.884 **********|**********|**********|**********|**********|**********|**********|********* |
 7.94-09    132 7.50+03   3.875 **********|**********|**********|**********|**********|**********|**********|********  |
 1.26-08    151 5.41+03   3.733 **********|**********|**********|**********|**********|**********|**********|*******   |
 2.00-08    231 5.22+03   3.718 **********|**********|**********|**********|**********|**********|**********|******    |
 3.16-08    310 4.42+03   3.646 **********|**********|**********|**********|**********|**********|**********|******    |
 5.01-08    675 6.08+03   3.784 **********|**********|**********|**********|**********|**********|**********|*******   |
 7.94-08   1612 9.16+03   3.962 **********|**********|**********|**********|**********|**********|**********|********* |
 1.26-07   3393 1.22+04   4.085 **********|**********|**********|**********|**********|**********|**********|**********|
 2.00-07   7271 1.64+04   4.216 **********|**********|**********|**********|**********|**********|**********|**********|*
 3.16-07  11359 1.62+04   4.210 **********|**********|**********|**********|**********|**********|**********|**********|*
 5.01-07  20226 1.82+04   4.260 **********|**********|**********|**********|**********|**********|**********|**********|*
 7.94-07  35534 2.02+04   4.305 **********|**********|**********|**********|**********|**********|**********|**********|**
 1.26-06  59631 2.14+04   4.330 **********|**********|**********|**********|**********|**********|**********|**********|**
 2.00-06  88598 2.00+04   4.302 **********|**********|**********|**********|**********|**********|**********|**********|**
 3.16-06 118346 1.69+04   4.227 **********|**********|**********|**********|**********|**********|**********|**********|*
 5.01-06 149040 1.34+04   4.128 **********|**********|**********|**********|**********|**********|**********|**********|
 7.94-06 180929 1.03+04   4.012 **********|**********|**********|**********|**********|**********|**********|**********|
 1.26-05 204525 7.33+03   3.865 **********|**********|**********|**********|**********|**********|**********|********  |
 2.00-05 211876 4.79+03   3.680 **********|**********|**********|**********|**********|**********|**********|******    |
 3.16-05 201215 2.87+03   3.458 mmmmmmmmmmm|mmmmmmmmmmmm|mmmmmmmmmmm|mmmmmmmmmmm|mmmmmmmmmmm|mmmmmmmmmmm|mmmmmmmmmmm|mmm       |
 5.01-05 163653 1.47+03   3.168 **********|**********|**********|**********|**********|**********|**********|          |
 7.94-05 106916 6.07+02   2.783 **********|**********|**********|**********|**********|**********|*******   |          |
 1.26-04  50282 1.80+02   2.256 **********|**********|**********|**********|**********|**********|*         |          |
 2.00-04  12291 2.78+01   1.444 **********|**********|**********|**********|**********|****      |          |          |
 3.16-04    786 1.12+00   0.050 **********|**********|**********|**********|         s|          |          |          |
 5.01-04      2 1.80-03  -2.745 **********|*         |          |          |    s     |          |          |          |
 7.94-04      7 3.98-03  -2.401 **********|*****     |          |          |s         |          |          |          |
 1.26-03     11 3.94-03  -2.404 **********|*****     |          |        s |          |          |          |          |
 2.00-03      9 2.04-03  -2.691 **********|**        |          |   s      |          |          |          |          |
 3.16-03      2 2.85-04  -3.545 ***       |          |          s          |          |          |          |          |
 5.01-03      2 1.80-04  -3.745 *         |          |       s  |          |          |          |          |          |
  total 1629165 2.71-01         d----------d----------d----------d----------d----------d----------d----------d----------d--

1tally       22        nps =     6006188
+                                1-meter Dose (mrem/hr)                                $ 1-m detector
          tally type 2    particle flux averaged over a surface.
          tally for  photons
```

```
          this tally is modified by a dose function.

          areas
               surface:      80
              segment
                1       1.00000E+00
                2       2.02680E+01
                3       1.00000E+00
             whole      1.00000E+00

 surface  80
 segment:          -888
                1.30533E-06 0.0031

 surface  80
 segment:           888       -777
                1.99974E-10 0.0186

 surface  80
 segment:           888        777
                3.44749E-06 0.0018

 surface  80
 segment:   whole surface
                4.75688E-06 0.0015


 ================================================================================================================================

          results of 10 statistical checks for the estimated answer for the tally fluctuation chart (tfc) bin of tally       22

 tfc bin     --mean--      ---------relative error---------      ----variance of the variance----      --figure of merit--     -pdf-
 behavior    behavior      value   decrease   decrease rate      value   decrease   decrease rate       value     behavior     slope

 desired      random       <0.10      yes      1/sqrt(nps)       <0.10      yes        1/nps           constant    random      >3.00
 observed     random        0.00      yes          yes            0.00      yes         yes            constant    random      10.00
 passed?        yes          yes      yes          yes              yes      yes         yes               yes        yes         yes

 ================================================================================================================================


 this tally meets the statistical criteria used to form confidence intervals: check the tally fluctuation chart to verify.
 the results in other bins associated with this tally may not meet these statistical criteria.

 ----- estimated confidence intervals:  -----

 estimated asymmetric confidence interval(1,2,3 sigma): 4.7497E-06 to 4.7642E-06; 4.7425E-06 to 4.7714E-06; 4.7353E-06 to 4.7786E-06
 estimated  symmetric confidence interval(1,2,3 sigma): 4.7497E-06 to 4.7641E-06; 4.7424E-06 to 4.7713E-06; 4.7352E-06 to 4.7785E-06

1analysis of the results in the tally fluctuation chart bin (tfc) for tally       22 with nps=     6006188 print table 160


 normed average tally per history  = 4.75688E-06          unnormed average tally per history  = 4.75688E-06
 estimated tally relative error    = 0.0015               estimated variance of the variance  = 0.0010
 relative error from zero tallies  = 0.0007               relative error from nonzero scores  = 0.0014

 number of nonzero history tallies =     1629244          efficiency for the nonzero tallies  = 0.2713
 history number of largest  tally  =      123569          largest  unnormalized history tally = 2.42423E-03
```

```
 (largest  tally)/(average tally)  = 5.09626E+02          (largest  tally)/(avg nonzero tally)= 1.38242E+02

 (confidence interval shift)/mean  = 0.0000               shifted confidence interval center  = 4.75695E-06


 if the largest  history score sampled so far were to occur on the next history, the tfc bin quantities would change as follows:

      estimated quantities           value at nps            value at nps+1           value(nps+1)/value(nps)-1.

      mean                            4.75688E-06             4.75728E-06                    0.000085
      relative error                  1.51728E-03             1.51951E-03                    0.001471
      variance of the variance        1.04036E-03             1.04355E-03                    0.003067
      shifted center                  4.75695E-06             4.75695E-06                    0.000000
      figure of merit                 1.20656E+03             1.20302E+03                   -0.002936

 the estimated slope of the 200 largest  tallies starting at  2.34415E-04 appears to be decreasing at least exponentially.
 the empirical history score probability density function appears to be increasing at the largest  history scores:
 please examine. see print table 161.
 the history score probability density function appears to have an unsampled region at the largest  history scores:
 please examine. see print table 161.

 fom = (histories/minute)*(f(x) signal-to-noise ratio)**2 = (1.668E+04)*( 2.689E-01)**2 = (1.668E+04)*(7.232E-02) = 1.207E+03

1status of the statistical checks used to form confidence intervals for the mean for each tally bin


 tally   result of statistical checks for the tfc bin (the first check not passed is listed) and error magnitude check for all bins

        2   missed  3 of 10 tfc bin checks: the variance of the variance does not monotonically decrease over the last half of problem
          passed all bin error check:     4 tally bins all have relative errors less than 0.10 with no zero bins

       22   passed the 10 statistical checks for the tally fluctuation chart bin result
          passed all bin error check:     4 tally bins all have relative errors less than 0.10 with no zero bins


 the 10 statistical checks are only for the tally fluctuation chart bin and do not apply to other tally bins.

 warning.       1 of the     2 tally fluctuation chart bins did not pass all 10 statistical checks.
1tally fluctuation charts

                          tally        2                          tally       22
        nps      mean     error   vov  slope    fom      mean     error   vov  slope    fom
       512000   5.4379E-06 0.0041 0.0008  4.0    1941   4.7211E-06 0.0052 0.0121  2.1    1233
      1024000   5.4807E-06 0.0029 0.0003  2.8    1937   4.7582E-06 0.0037 0.0060  1.7    1229
      1536000   5.4755E-06 0.0024 0.0002  2.7    1949   4.7559E-06 0.0030 0.0041  1.6    1220
      2048000   5.4814E-06 0.0020 0.0001  2.4    1944   4.7608E-06 0.0026 0.0030  1.5    1219
      2560000   5.4771E-06 0.0018 0.0001  2.4    1944   4.7588E-06 0.0023 0.0024  1.4    1204
      3072000   5.4831E-06 0.0017 0.0001  2.1    1923   4.7627E-06 0.0021 0.0020  1.4    1202
      3584000   5.4730E-06 0.0016 0.0001  2.0    1924   4.7528E-06 0.0020 0.0017  1.4    1209
      4096000   5.4738E-06 0.0015 0.0001  2.0    1928   4.7545E-06 0.0018 0.0015  1.4    1205
      4608000   5.4753E-06 0.0014 0.0005  1.9    1888   4.7531E-06 0.0017 0.0013  1.4    1218
      5120000   5.4818E-06 0.0013 0.0004  1.8    1875   4.7568E-06 0.0016 0.0012  1.3    1232
      5632000   5.4811E-06 0.0013 0.0004  1.8    1879   4.7587E-06 0.0016 0.0011 10.0    1213
      6006188   5.4785E-06 0.0012 0.0003  1.7    1878   4.7569E-06 0.0015 0.0010 10.0    1207

 ********************************************************************************************************************************

 dump no.    7 on file runtpe     nps =     6006188     coll =     3284779356     ctm =      360.01   nrn =
```

```
 47924508086
 tally data written to file mctal

         9 warning messages so far.


 run terminated when it had used  360  minutes of computer time.

 computer time =  360.02 minutes

 mcnp     version 5     09282010                    07/22/14 16:57:46                    probid =  07/22/14 10:57:24
```

5.7.2.1.6 HAC 252Cf Neutron Source – 7hn001.io

```
          Thread Name & Version = MCNP5, 1.60

                                  _
            ._ _   _  ._  ._    |_
            | | |  (_  | |  |_)   _)
                           |

  +-------------------------------------------------------------------+
  | Copyright 2010. Los Alamos National Security, LLC.  All rights    |
  | reserved.                                                         |
  |   This material was produced under U.S. Government contract       |
  | DE-AC52-06NA25396 for Los Alamos National Laboratory, which is    |
  | operated by Los Alamos National Security, LLC, for the U.S.       |
  | Department of Los Energy. The Government is granted for itself and |
  | others acting on its behalf a paid-up, nonexclusive, irrevocable  |
  | worldwide license in this material to reproduce, prepare derivative |
  | works, and perform publicly and display publicly. Beginning five  |
  | (5) years after 2010, subject to additional five-year worldwide   |
  | renewals, the Government is granted for itself and others acting on |
  | its behalf a paid-up, nonexclusive, irrevocable worldwide license |
  | in this material to reproduce, prepare derivative works, distribute |
  | copies to the public, perform publicly and display publicly, and to |
  | permit others to do so. NEITHER THE UNITED STATES NOR THE UNITED  |
  | STATES DEPARTMENT OF ENERGY, NOR LOS ALAMOS NATIONAL SECURITY, LLC, |
  | NOR ANY OF THEIR EMPLOYEES, MAKES ANY WARRANTY, EXPRESS OR IMPLIED, |
  | OR ASSUMES ANY LEGAL LIABILITY OR RESPONSIBILITY FOR THE ACCURACY, |
  | COMPLETENESS, OR USEFULNESS OF ANY INFORMATION, APPARATUS, PRODUCT, |
  | OR PROCESS DISCLOSED, OR REPRESENTS THAT ITS USE WOULD NOT INFRINGE |
  | PRIVATELY OWNED RIGHTS.                                           |
  +-------------------------------------------------------------------+

 1mcnp     version 5     ld=09282010                    07/22/14 16:57:46
  ***********************************************************************                    probid =  07/22/14 16:57:46
 inp=7hn001.i

         1-       title RH-TRU 72-B RLC HAC Neutron Concentrated 1 g/cc Cf252
         2-       C
         3-       C Cell Cards
         4-       C
         5-       10  1 -1        10  -11  -16                imp:n=1    $ Source #1
         6-       20  0           20  -21  -26
         7-                      (-10:  11:  16)               imp:n=1    $ Drum #1 cavity
         8-       40  0           41  -45  -43
         9-                       #10  #20                     imp:n=1    $ RLC cavity
```

```
10-       41  3 -7.85260  40  -41  -42                 imp:n=1    $ RLC base
11-       42  3 -7.85260  41  -46   43  -42            imp:n=1    $ RLC shell
12-       43  3 -7.85260  45  -44  -43                 imp:n=1    $ RLC lid
13-       50  0           51  -53  -55
14-                    (-40:  42:  46)
15-                   :( 44  -46  -43)                 imp:n=1    $ IV cavity
16-       51  2 -8.01280  50  -51  -52                 imp:n=1    $ IV base
17-       52  2 -8.01280  51  -55   53  -52            imp:n=1    $ IV shell
18-       53  2 -8.01280  55  -54  -52                 imp:n=1    $ IV lid
19-       60  0           61  -63  -65
20-                    (-50:  52:  54)                 imp:n=1    $ OC cavity
21-       61  2 -8.01280  60  -61  -69                 imp:n=1    $ OC base
22-       62  2 -8.01280  61  -66   65  -64            imp:n=1    $ OC ishell
23-       63  4 -11.3500  61  -66   64  -76  71       imp:n=1    $ OC lead in
24-       64  4 -11.3500  61  -66   76  -68  71       imp:n=1    $ OC lead out
25-       65  2 -8.01280  61  -66   68  -77  71       imp:n=1    $ OC oshell in
26-       66  2 -8.01280  61  -66   77  -67  71       imp:n=1    $ OC oshell out
27-       67  0           61  -66   67  -70  71       imp:n=1    $ OC airgap
28-       68  2 -8.01280  61  -66   70  -69  71       imp:n=1    $ OC tshell
29-       69  2 -8.01280  66  -63   65  -69            imp:n=1    $ OC flange
30-       70  2 -8.01280  63  -62  -69                 imp:n=1    $ OC lid
31-       71  4 -11.3500  64  -78  -71                 imp:n=1    $ OC lead punct in
32-       72  4 -11.3500  78  -73  -71                 imp:n=1    $ OC lead punct out
33-       73  2 -8.01280  73  -79  -71                 imp:n=1    $ OC oshell punct in
34-       74  2 -8.01280  79  -72  -71                 imp:n=1    $ OC oshell punct out
35-       75  0           74  -69  -71                 imp:n=1    $ OC airgap punct
36-       76  2 -8.01280  75  -74  -71                 imp:n=1    $ OC tshell punct
37-       777 0           69  -80   60  -62            imp:n=1    $ Outside to tally
38-       888 0         -999
39-                    (-60:  80:  62)                 imp:n=1    $ Outside pkg
40-       999 0           999                           imp:n=0    $ Outside world
41-
42-       C
43-       C Geometry Cards
44-       C
45-       10  pz 163.513                                          $ Source #1 bottom
46-       11  pz 164.783                                          $ Source #1 top
47-       16  c/z 38.885 0 0.635                                  $ Source #1 radius
48-       C
49-       20  pz 163.511                                          $ Drum #1 bottom
50-       21  pz 164.784                                          $ Drum #1 top
51-       26  c/z 38.885 0 0.636                                  $ Drum #1 radius
52-       C
53-       40  pz 19.368                                           $ RLC base (outside)
54-       41  pz 20.638                                           $ RLC base (inside)
55-       42  c/z 7.139 0 33.02                                   $ RLC shell (outside)
56-       43  c/z 7.139 0 32.385                                  $ RLC shell (inside)
57-       44  pz 309.563                                          $ RLC lid (outside)
58-       45  pz 307.658                                          $ RLC lid (inside)
59-       46  pz 325.438                                          $ RLC top (outside)
60-       C
61-       50  pz 14.288                                           $ IV base (outside)
62-       51  pz 18.098                                           $ IV base (inside)
63-       52  c/z 0.474 0 40.64                                   $ IV shell (outside)
64-       53  c/z 0.474 0 39.688                                  $ IV shell (inside)
65-       54  pz 343.218                                          $ IV top (outside)
66-       55  pz 326.708                                          $ IV top (inside)
67-       C
```

```
 68-       60  pz 0                                          $ OC bottom (outside)
 69-       61  pz 12.7                                       $ OC bottom (inside)
 70-       62  pz 360.045                                    $ OC top (outside)
 71-       63  pz 344.805                                    $ OC top (inside)
 72-       64  cz 43.656                                     $ OC ishell (outside)
 73-       65  cz 41.116                                     $ OC ishell (inside)
 74-       66  pz 320.675                                    $ OC lead (upper)
 75-       67  cz 52.229                                     $ OC oshell (outside)
 76-       68  cz 48.419                                     $ OC oshell (inside)
 77-       69  cz 52.838                                     $ OC therm (outside)
 78-       70  cz 52.495                                     $ OC therm (inside)
 79-       71  c/x 0 164.148 10.033                          $ OC puncture radius
 80-       72  cz 50.563                                     $ OC oshell punct (out)
 81-       73  cz 46.753                                     $ OC oshell punct (in)
 82-       74  cz 50.905                                     $ OC therm punct (out)
 83-       75  cz 50.563                                     $ OC therm punct (in)
 84-       76  cz 46.038                                     $ OC lead (mid)
 85-       77  cz 50.324                                     $ OC oshell (mid)
 86-       78  cz 45.204                                     $ OC lead punct (mid)
 87-       79  cz 48.658                                     $ OC oshell punct (mid)
 88-       C
 89-       80  cz 150.905                                    $ 1-meter from OC therm
 90-       C
 91-       777 c/x 0 164.148 2.54                            $ Tally cylinder
 92-       888 px 0                                          $ Tally truncation
 93-       999 sz 164.148 277.905                            $ Outside world
 94-
 95-       C
 96-       C Physics Cards
 97-       C
 98-       mode n
 99-       C
100-       C Source Cards
101-       C
102-       C Cylindrical Sources
103-       sdef pos=d1 erg=d2 par=1 axs=0 0 1 rad=d3 ext=d4
104-       sc1 Cf252
105-       C Source Position and Fraction
106-       si1 L 38.885 0 164.148
107-             0 0 0
108-       sp1   98 2
109-       C Source Energy (MeV) and Fraction
110-       si2 0.1 0.5 1.0 2.0 3.0
111-            4.0 6.0 8.0 10.0 15.0
112-       sp2 0.00E+00 1.80E+11 2.71E+11 5.36E+11 4.10E+11
113-            2.73E+11 2.66E+11 8.53E+10 2.44E+10 8.36E+09
114-       C Source Radius
115-       si3 0 0.635
116-       sp3 -21 1
117-       C Source Extent
118-       si4 -0.635 0.635
119-       sp4 -21 0
120-       C
121-       C Tally Cards
122-       C
123-       f2:n 69
124-       fc2 Surface Dose (mrem/hr)                        $ Surface detector
125-       fs2 -888 -777 t
```

```
126-       sd2 1.0 20.268 1.0 1.0                                    $ Surface tally area
127-       f22:n 80
128-       fc22 1-meter Dose (mrem/hr)                               $ 1-m detector
129-       fs22 -888 -777 t
130-       sd22 1.0 20.268 1.0 1.0                                   $ Surface tally area
131-       C
132-       C ANSI/ANS-6.1.1-1977 Neutron Flux to Dose Factors (mrem/hr)
133-       de0  2.5e-08 1.0e-07 1.0e-06 1.0e-05 1.0e-04              $ Energy (Mev)
134-            1.0e-03 1.0e-02 1.0e-01 5.0e-01 1.0
135-            2.5 5.0 7.0 10.0 14.0 20.0
136-       df0  3.67e-03 3.67e-03 4.46e-03 4.54e-03 4.18e-03         $ Conversion (mrem/hr)
137-            3.76e-03 3.56e-03 2.17e-02 9.26e-02 1.32e-01
138-            1.25e-01 1.56e-01 1.47e-01 1.47e-01 2.08e-01 2.27e-01
139-       C
140-       C Material Cards
141-       C
142-       m1   40000.60c -1.00                                       $ Zirconium
143-       m2   14000.60c -0.01                                       $ Stainless Steel
144-            24052.60c -0.19
145-            25055.60c -0.02
146-            26057.60c -0.68
147-            28058.60c -0.10
148-       m3   26057.60c -1.00                                       $ Carbon Steel (iron)
149-       m4   82000.50c -1.00                                       $ Lead
150-       C
151-       C Runtime and Print Cards
152-       C
153-       prdmp j j 1 2
154-       ctme 120

 surface       72   and surface       75   are the same.       75   will be deleted.

  comment.           1 surfaces were deleted for being the same as others.

  warning.  sum of segment sizes differs from total in   2 cases.
1cells                                                                                                print table 60

                            atom        gram                                                  neutron
             cell     mat   density     density     volume       mass            pieces importance

        1       10        1  6.60141E-03 1.00000E+00 1.60880E+00 1.60880E+00           1  1.0000E+00
        2       20        0  0.00000E+00 0.00000E+00 8.88335E-03 0.00000E+00           1  1.0000E+00
        3       40        0  0.00000E+00 0.00000E+00 0.00000E+00 0.00000E+00           0  1.0000E+00
        4       41        3  8.30568E-02 7.85260E+00 4.35019E+03 3.41603E+04           1  1.0000E+00
        5       42        3  8.30568E-02 7.85260E+00 3.97694E+04 3.12294E+05           1  1.0000E+00
        6       43        3  8.30568E-02 7.85260E+00 6.27672E+03 4.92886E+04           1  1.0000E+00
        7       50        0  0.00000E+00 0.00000E+00 0.00000E+00 0.00000E+00           0  1.0000E+00
        8       51        2  8.70856E-02 8.01280E+00 1.97689E+04 1.58404E+05           1  1.0000E+00
        9       52        2  8.70856E-02 8.01280E+00 7.41419E+04 5.94084E+05           1  1.0000E+00
       10       53        2  8.70856E-02 8.01280E+00 8.56652E+04 6.86418E+05           1  1.0000E+00
       11       60        0  0.00000E+00 0.00000E+00 0.00000E+00 0.00000E+00           0  1.0000E+00
       12       61        2  8.70856E-02 8.01280E+00 1.11390E+05 8.92546E+05           1  1.0000E+00
       13       62        2  8.70856E-02 8.01280E+00 2.08330E+05 1.66931E+06           1  1.0000E+00
       14       63        4  3.29849E-02 1.13500E+01 0.00000E+00 0.00000E+00           0  1.0000E+00
       15       64        4  3.29849E-02 1.13500E+01 0.00000E+00 0.00000E+00           0  1.0000E+00
       16       65        2  8.70856E-02 8.01280E+00 0.00000E+00 0.00000E+00           0  1.0000E+00
       17       66        2  8.70856E-02 8.01280E+00 0.00000E+00 0.00000E+00           0  1.0000E+00
       18       67        0  0.00000E+00 0.00000E+00 0.00000E+00 0.00000E+00           0  1.0000E+00
```

```
       19       68        2  8.70856E-02 8.01280E+00 0.00000E+00 0.00000E+00           0  1.0000E+00
       20       69        2  8.70856E-02 8.01280E+00 8.34880E+04 6.68973E+05           1  1.0000E+00
       21       70        2  8.70856E-02 8.01280E+00 1.33668E+05 1.07106E+06           1  1.0000E+00
       22       71        4  3.29849E-02 1.13500E+01 0.00000E+00 0.00000E+00           0  1.0000E+00
       23       72        4  3.29849E-02 1.13500E+01 0.00000E+00 0.00000E+00           0  1.0000E+00
       24       73        2  8.70856E-02 8.01280E+00 0.00000E+00 0.00000E+00           0  1.0000E+00
       25       74        2  8.70856E-02 8.01280E+00 0.00000E+00 0.00000E+00           0  1.0000E+00
       26       75        0  0.00000E+00 0.00000E+00 0.00000E+00 0.00000E+00           0  1.0000E+00
       27       76        2  8.70856E-02 8.01280E+00 0.00000E+00 0.00000E+00           0  1.0000E+00
       28      777        0  0.00000E+00 0.00000E+00 2.26002E+07 0.00000E+00           1  1.0000E+00
       29      888        0  0.00000E+00 0.00000E+00 6.41456E+07 0.00000E+00           1  1.0000E+00
       30      999        0  0.00000E+00 0.00000E+00 0.00000E+00 0.00000E+00           0  0.0000E+00

 total                                              8.75127E+07 6.13653E+06

    minimum source weight = 1.0000E+00    maximum source weight = 1.0000E+00

 ************************************************
 * Random Number Generator  =                 1 *
 * Random Number Seed       =       19073486328125 *
 * Random Number Multiplier =       19073486328125 *
 * Random Number Adder      =                 0 *
 * Random Number Bits Used  =                48 *
 * Random Number Stride     =            152917 *
 ************************************************


          1 warning message so far.
1cross-section tables                                                                                print table 100

     table    length

                         tables from file endf60

  14000.60c   51392  14-si-nat from endf/b-vi                                                  mat1400      11/25/93
  24052.60c   66325  24-cr-52 from endf/b-vi.1                                                mat2431      11/25/93
  25055.60c   84549  25-mn-55 from endf/b-vi                                                  mat2525      11/25/93
  26057.60c   72092  endf/b-vi.1 fe57a                                                        mat2634      11/25/93
  28058.60c   83305  28-ni-58 from endf/b-vi.1                                                mat2825      11/25/93
  40000.60c   45269  40-zr-nat from endf-vi.1                                                 mat4000      11/27/93

                         tables from file rmccs

  82000.50c   28695  njoy                                                                  ( 1382)     03/10/82

  total      431627

 ********************************************************************************************************************************

 dump no.    1 on file runtpe     nps =           0     coll =              0     ctm =        0.00   nrn =
    0

          1 warning message so far.

 ********************************************************************************************************************************

 dump no.    2 on file runtpe     nps =    42849093     coll =     1384959356     ctm =       60.01   nrn =
 11505256322
```

```
1problem summary

      run terminated when it had used  120  minutes of computer time.
+                                                                                    07/22/14 18:57:53
      title RH-TRU 72-B RLC HAC Neutron Concentrated 1 g/cc Cf252                 probid =  07/22/14 16:57:46
0
 neutron creation    tracks      weight        energy           neutron loss        tracks      weight        energy
                                 (per source particle)                                        (per source particle)

 source            88924090    1.0000E+00    2.5770E+00         escape            88362675    9.3553E-01    6.7274E-01
                                                                 energy cutoff           0    0.            0.
                                                                 time cutoff             0    0.            0.
 weight window            0    0.            0.                 weight window           0    0.            0.
 cell importance          0    0.            0.                 cell importance         0    0.            0.
 weight cutoff            0    1.4949E-03    1.3641E-06         weight cutoff      861914    1.4891E-03    1.4207E-06
 e or t importance        0    0.            0.                 e or t importance       0    0.            0.
 dxtran                   0    0.            0.                 dxtran                  0    0.            0.
 forced collisions        0    0.            0.                 forced collisions       0    0.            0.
 exp. transform           0    0.            0.                 exp. transform          0    0.            0.
 upscattering             0    0.            2.3823E-11         downscattering          0    0.            1.8144E+00
 photonuclear             0    0.            0.                 capture                 0    6.7689E-02    6.1127E-02
 (n,xn)              600874    6.4319E-03    7.6404E-03         loss to (n,xn)     300375    3.2153E-03    3.6380E-02
 prompt fission           0    0.            0.                 loss to fission         0    0.            0.
 delayed fission          0    0.            0.
     total            89524964    1.0079E+00    2.5847E+00          total          89524964    1.0079E+00    2.5847E+00

   number of neutrons banked                 300499        average time of (shakes)              cutoffs
   neutron tracks per source particle     1.0068E+00         escape            1.6236E+02         tco   1.0000E+33
   neutron collisions per source particle 3.2327E+01         capture           3.5286E+02         eco   0.0000E+00
   total neutron collisions               2874631084         capture or escape 1.7522E+02         wc1  -5.0000E-01
   net multiplication              1.0032E+00 0.0000         any termination   1.7911E+02         wc2  -2.5000E-01

 computer time so far in this run   120.03 minutes           maximum number ever in bank         2
 computer time in mcrun             120.00 minutes           bank overflows to backup file       0
 source particles per minute            7.4101E+05
 random numbers generated              23880258776           most random numbers used was        5082 in history    77007213

 range of sampled source weights = 1.0000E+00 to 1.0000E+00
1neutron  activity in each cell                                                                        print table 126

                  tracks     population   collisions   collisions     number        flux        average      average
             cell entering                              * weight     weighted     weighted    track weight  track mfp
                                                     (per history)   energy       energy      (relative)      (cm)

        1       10   88240877     87149142      1663922    1.8709E-02   1.7820E+00   2.5424E+00   9.9986E-01   3.0910E+01
        2       20   89342257     87149154            0    0.0000E+00   1.7689E+00   2.5319E+00   9.9980E-01   0.0000E+00
        3       40  235744550     87518523            0    0.0000E+00   1.9498E-01   1.1068E+00   9.5546E-01   0.0000E+00
        4       41   11052060      5822867      9521496    9.9015E-02   6.4944E-02   5.3909E-01   9.1145E-01   5.4644E+00
        5       42  359654425     86909567    169267284    1.8192E+00   2.0260E-01   1.1401E+00   9.5632E-01   5.1292E+00
        6       43    9654990      5740601     11902950    1.2284E-01   5.4671E-02   5.4276E-01   8.9973E-01   5.4848E+00
        7       50  401645328     87565366            0    0.0000E+00   1.1194E-01   7.3292E-01   9.3706E-01   0.0000E+00
        8       51   14704489      6618908     46819213    4.6763E-01   5.3220E-02   4.6706E-01   9.0006E-01   3.2536E+00
        9       52  389220228     86500006    306233264    3.2112E+00   1.5175E-01   8.9832E-01   9.4751E-01   3.5587E+00
       10       53   11543386      5121870    141801581    1.3125E+00   2.0084E-02   3.0396E-01   8.2737E-01   3.0402E+00
       11       60  404214295     87632309            0    0.0000E+00   8.2922E-02   6.2204E-01   9.2293E-01   0.0000E+00
       12       61   10338795      6115829    113766302    1.1154E+00   4.3385E-02   4.3298E-01   8.8371E-01   3.2599E+00
       13       62  352339048     86196801    745263614    7.7717E+00   1.2505E-01   7.3406E-01   9.4176E-01   3.5239E+00
       14       63  274095912     76216950    347399961    3.5876E+00   9.9691E-02   5.7898E-01   9.3508E-01   4.2494E+00
```

```
       15       64   232925859     77145814    293760429    3.0330E+00   9.7366E-02   5.5476E-01   9.3469E-01   4.2540E+00
       16       65   180638387     77159512    301744726    3.1213E+00   9.4641E-02   5.3105E-01   9.3328E-01   3.3772E+00
       17       66   119404860     76729580    181177113    1.8758E+00   1.0125E-01   5.4717E-01   9.3466E-01   3.5622E+00
       18       67    87477896     75142622            0    0.0000E+00   1.1562E-01   5.9121E-01   9.3837E-01   0.0000E+00
       19       68    81417063     75305766     18226817    1.8970E-01   1.2151E-01   6.0846E-01   9.3977E-01   3.8237E+00
       20       69     6939707      3257393     55193822    5.1076E-01   1.8374E-02   2.4734E-01   8.2592E-01   3.0243E+00
       21       70     4044104      1674923     56655462    4.8037E-01   7.6147E-03   1.4067E-01   7.4680E-01   2.8134E+00
       22       71    33902479     21823794     19565147    2.1538E-01   5.4869E-01   1.3042E+00   9.8279E-01   4.9082E+00
       23       72    27835536     18081384     15855824    1.7425E-01   4.9816E-01   1.2153E+00   9.8145E-01   4.8985E+00
       24       73    21608951     14984634     22969229    2.5125E-01   4.4256E-01   1.1110E+00   9.7893E-01   3.7954E+00
       25       74    14062372     11331194     14270165    1.5585E-01   4.2853E-01   1.0653E+00   9.7726E-01   3.8945E+00
       26       75     8454366      8250228            0    0.0000E+00   4.8447E-01   1.1332E+00   9.7776E-01   0.0000E+00
       27       76     8791319      8340518      1572763    1.7201E-02   4.7039E-01   1.1079E+00   9.7760E-01   4.0329E+00
       28      777    84003053     84003053            0    0.0000E+00   1.4391E-01   7.0097E-01   9.4450E-01   0.0000E+00
       29      888    88805220     88366172            0    0.0000E+00   1.3970E-01   7.3349E-01   9.4238E-01   0.0000E+00

          total    3652101812   1443854480   2874631084    2.9551E+01

1tally        2        nps =    88924090
+                                Surface Dose (mrem/hr)                                  $ Surface detector
          tally type 2    particle flux averaged over a surface.
          tally for  neutrons

          this tally is modified by a dose function.

          areas
               surface:      69
              segment
                1       1.00000E+00
                2       2.02680E+01
                3       1.00000E+00
             whole      1.00000E+00

 surface  69
 segment:          -888
                4.64229E-02 0.0002

 surface  69
 segment:           888       -777
                4.06323E-05 0.0016

 surface  69
 segment:           888        777
                6.08043E-02 0.0002

 surface  69
 segment:   whole surface
                1.08051E-01 0.0001


 ============================================================================================================================

          results of 10 statistical checks for the estimated answer for the tally fluctuation chart (tfc) bin of tally        2

 tfc bin     --mean--      ---------relative error---------      ----variance of the variance----      --figure of merit--     -pdf-
 behavior    behavior      value   decrease   decrease rate      value   decrease   decrease rate       value     behavior     slope

 desired      random       <0.10      yes      1/sqrt(nps)       <0.10      yes        1/nps           constant    random      >3.00
```

```
observed     random       0.00      yes          yes           0.00      yes         yes            increase   increase      3.72
passed?        yes          yes     yes          yes            yes      yes         yes               no         no          yes

 ================================================================================================================================


 warning.  the tally in the tally fluctuation chart bin did not pass  2 of the 10 statistical checks.

1analysis of the results in the tally fluctuation chart bin (tfc) for tally        2 with nps=    88924090 print table 160


 normed average tally per history  = 1.08051E-01          unnormed average tally per history  = 1.08051E-01
 estimated tally relative error    = 0.0001               estimated variance of the variance  = 0.0000
 relative error from zero tallies  = 0.0000               relative error from nonzero scores  = 0.0001

 number of nonzero history tallies =    83726469          efficiency for the nonzero tallies  = 0.9415
 history number of largest  tally  =    83314056          largest  unnormalized history tally = 4.90053E+00
 (largest  tally)/(average tally)  = 4.53540E+01          (largest  tally)/(avg nonzero tally)= 4.27030E+01

 (confidence interval shift)/mean  = 0.0000               shifted confidence interval center  = 1.08051E-01


 if the largest  history score sampled so far were to occur on the next history, the tfc bin quantities would change as follows:

      estimated quantities           value at nps           value at nps+1          value(nps+1)/value(nps)-1.

      mean                            1.08051E-01            1.08051E-01                0.000000
      relative error                  1.31494E-04            1.31495E-04                0.000007
      variance of the variance        1.24841E-06            1.24858E-06                0.000137
      shifted center                  1.08051E-01            1.08051E-01                0.000000
      figure of merit                 4.81939E+05            4.81933E+05               -0.000013

 the estimated inverse power slope of the 190 largest  tallies starting at 3.04212E+00 is 3.7215
 the empirical history score probability density function appears to be increasing at the largest  history scores:
 please examine. see print table 161.
 the large score tail of the empirical history score probability density function appears to have no unsampled regions.

 fom = (histories/minute)*(f(x) signal-to-noise ratio)**2 = (7.410E+05)*( 8.065E-01)**2 = (7.410E+05)*(6.504E-01) = 4.819E+05

1unnormed tally density for tally        2          nonzero tally mean(m) = 1.148E-01   nps =    88924090  print table 161

 abscissa              ordinate   log plot of tally probability density function in tally fluctuation chart bin(d=decade,slope= 3.7)
  tally   number num den log den:d--------d---------d----------d---------d---------d---------d----------d---------d---------d--------
1.00-03     429 2.35-02  -1.630 *********|*********|**********|*********|*********|*********|*****     |         |         |
1.26-03   18231 7.92-01  -0.101 *********|*********|**********|*********|*********|*********|**********|*********|         |
1.58-03   92158 3.18+00   0.502 *********|*********|**********|*********|*********|*********|**********|*********|******   |
2.00-03  269591 7.39+00   0.869 *********|*********|**********|*********|*********|*********|**********|*********|*********|
2.51-03  702996 1.53+01   1.185 *********|*********|**********|*********|*********|*********|**********|*********|*********|***
3.16-03  1.7+06 2.91+01   1.465 *********|*********|**********|*********|*********|*********|**********|*********|*********|******
3.98-03  3.7+06 5.10+01   1.708 *********|*********|**********|*********|*********|*********|**********|*********|*********|********
5.01-03  2.9+06 3.21+01   1.507 *********|*********|**********|*********|*********|*********|**********|*********|*********|******
6.31-03  1.9+06 1.66+01   1.219 *********|*********|**********|*********|*********|*********|**********|*********|*********|***
7.94-03  1.5+06 1.00+01   1.000 *********|*********|**********|*********|*********|*********|**********|*********|*********|*
1.00-02  989723 5.41+00   0.733 *********|*********|**********|*********|*********|*********|**********|*********|********  |
1.26-02  1.1+06 4.86+00   0.687 *********|*********|**********|*********|*********|*********|**********|*********|********  |
1.58-02  1.3+06 4.52+00   0.655 *********|*********|**********|*********|*********|*********|**********|*********|*******   |
2.00-02  1.3+06 3.67+00   0.565 *********|*********|**********|*********|*********|*********|**********|*********|******    |
2.51-02  1.7+06 3.73+00   0.572 *********|*********|**********|*********|*********|*********|**********|*********|******    |
```

```
 3.16-02 1.7+06 3.01+00   0.478 *********|*********|*********|*********|*********|*********|*********|*********|*****     |
 3.98-02 1.9+06 2.62+00   0.418 *********|*********|*********|*********|*********|*********|*********|*********|*****     |
 5.01-02 2.6+06 2.88+00   0.459 *********|*********|*********|*********|*********|*********|*********|*********|*****     |
 6.31-02 4.2+06 3.66+00   0.563 *********|*********|*********|*********|*********|*********|*********|*********|******    |
 7.94-02 5.5+06 3.75+00   0.574 *********|*********|*********|*********|*********|*********|*********|*********|******    |
 1.00-01 5.7+06 3.09+00   0.490 *********|*********|*********|*********|*********|*********|*********|*********|******    |
 1.26-01 8.5+06 3.69+00   0.567 mmmmmmmmm|mmmmmmmmm|mmmmmmmmmm|mmmmmmmmm|mmmmmmmmm|mmmmmmmmm|mmmmmmmmm|mmmmmmmmm|mmmmmm  |
 1.58-01 1.5+07 5.25+00   0.720 *********|*********|*********|*********|*********|*********|*********|*********|********  |
 2.00-01 9.0+06 2.48+00   0.394 *********|*********|*********|*********|*********|*********|*********|*********|*****     |
 2.51-01 4.6+06 1.01+00   0.004 *********|*********|*********|*********|*********|*********|*********|*********|*         |
 3.16-01 2.4+06 4.23-01  -0.374 *********|*********|*********|*********|*********|*********|*********|*******  |          |
 3.98-01 1.3+06 1.83-01  -0.739 *********|*********|*********|*********|*********|*********|*********|***       |          |
 5.01-01 729309 7.96-02  -1.099 *********|*********|*********|*********|*********|*********|*********|          |          |
 6.31-01 397092 3.44-02  -1.463 *********|*********|*********|*********|*********|*********|*******   |          |          |
 7.94-01 219899 1.51-02  -1.820 *********|*********|*********|*********|*********|*********|***       |          |          |
 1.00+00 127521 6.97-03  -2.157 *********|*********|*********|*********|*********|*********|          |          |          |
 1.26+00  74982 3.26-03  -2.487 *********|*********|*********|*********|*********|******   |          |          |          |
 1.58+00  26981 9.31-04  -3.031 *********|*********|*********|*********|*********|          |          |          |          |
 2.00+00  31931 8.75-04  -3.058 *********|*********|*********|*********|*********|          |          |          |          |
 2.51+00  49682 1.08-03  -2.966 *********|*********|*********|*********|*********|*         |          |          |          |
 3.16+00  41223 7.13-04  -3.147 *********|*********|*********|*********|*********|          s          |          |          |
 3.98+00      7 9.61-08  -7.017 *********|*        |         |         |         |     s    |          |          |          |
 5.01+00      1 1.09-08  -7.962 *        |         |         |         |         | s        |          |          |          |
  total 8.37+07 9.42-01          d--------d---------d---------d---------d---------d--------d----------d---------d---------d--------

1tally       22        nps =    88924090
+                                    1-meter Dose (mrem/hr)                                $ 1-m detector
           tally type 2    particle flux averaged over a surface.
           tally for  neutrons

           this tally is modified by a dose function.

           areas
                surface:      80
               segment
                  1       1.00000E+00
                  2       2.02680E+01
                  3       1.00000E+00
              whole       1.00000E+00

 surface  80
 segment:          -888
                2.98173E-02 0.0002

 surface  80
 segment:           888       -777
                7.19564E-07 0.0093

 surface  80
 segment:           888        777
                4.10799E-02 0.0002

 surface  80
 segment:   whole surface
                7.09118E-02 0.0001


 ============================================================================================================================================
```

```
          results of 10 statistical checks for the estimated answer for the tally fluctuation chart (tfc) bin of tally       22

 tfc bin     --mean--      ---------relative error---------      ----variance of the variance----      --figure of merit--      -pdf-
 behavior    behavior      value   decrease   decrease rate      value   decrease   decrease rate       value     behavior     slope

 desired      random       <0.10      yes      1/sqrt(nps)       <0.10      yes        1/nps           constant    random      >3.00
 observed     random        0.00      yes          yes            0.00      yes         yes            constant    random      10.00
 passed?        yes          yes      yes          yes             yes      yes         yes               yes        yes         yes

 ================================================================================================================================


 this tally meets the statistical criteria used to form confidence intervals: check the tally fluctuation chart to verify.
 the results in other bins associated with this tally may not meet these statistical criteria.

 ----- estimated confidence intervals:  -----

 estimated asymmetric confidence interval(1,2,3 sigma): 7.0912E-02 to 7.0912E-02; 7.0912E-02 to 7.0912E-02; 7.0912E-02 to 7.0912E-02
 estimated  symmetric confidence interval(1,2,3 sigma): 7.0912E-02 to 7.0912E-02; 7.0912E-02 to 7.0912E-02; 7.0912E-02 to 7.0912E-02

1analysis of the results in the tally fluctuation chart bin (tfc) for tally       22 with nps=    88924090 print table 160


 normed average tally per history  = 7.09118E-02          unnormed average tally per history  = 7.09118E-02
 estimated tally relative error    = 0.0000               estimated variance of the variance  = 0.0000
 relative error from zero tallies  = 0.0000               relative error from nonzero scores  = 0.0000

 number of nonzero history tallies =    76176040          efficiency for the nonzero tallies  = 0.8566
 history number of largest  tally  =    31842809          largest  unnormalized history tally = 5.52003E-01
 (largest  tally)/(average tally)  = 7.78437E+00          (largest  tally)/(avg nonzero tally)= 6.66841E+00

 (confidence interval shift)/mean  = 0.0000               shifted confidence interval center  = 7.09118E-02


 if the largest  history score sampled so far were to occur on the next history, the tfc bin quantities would change as follows:

      estimated quantities           value at nps           value at nps+1          value(nps+1)/value(nps)-1.

      mean                            7.09118E-02            7.09118E-02                    0.000000
      relative error                  0.00000E+00            0.00000E+00                    0.000000
      variance of the variance        0.00000E+00            0.00000E+00                    0.000000
      shifted center                  7.09118E-02            7.09118E-02                    0.000000
      figure of merit                 1.00000E+30            1.00000E+30                    0.000000

 the estimated slope of the 200 largest  tallies starting at  4.26588E-01 appears to be decreasing at least exponentially.
 the large score tail of the empirical history score probability density function appears to have no unsampled regions.

 fom = (histories/minute)*(f(x) signal-to-noise ratio)**2 = (7.410E+05)*( 1.162E+12)**2 = (7.410E+05)*(1.350E+24) = 1.000E+30

1status of the statistical checks used to form confidence intervals for the mean for each tally bin


 tally   result of statistical checks for the tfc bin (the first check not passed is listed) and error magnitude check for all bins

        2   missed  2 of 10 tfc bin checks: the figure of merit does not appear to be a constant for the last half of the problem
         passed all bin error check:     4 tally bins all have relative errors less than 0.10 with no zero bins
```

```
      22   passed the 10 statistical checks for the tally fluctuation chart bin result
        passed all bin error check:     4 tally bins all have relative errors less than 0.10 with no zero bins


 the 10 statistical checks are only for the tally fluctuation chart bin and do not apply to other tally bins.

 warning.       1 of the     2 tally fluctuation chart bins did not pass all 10 statistical checks.
1tally fluctuation charts

                          tally        2                          tally       22
         nps      mean     error   vov  slope    fom      mean     error   vov  slope    fom
      8192000   1.0805E-01 0.0004 0.0000 10.0  426640   7.0929E-02 0.0003 0.0000 10.0  890256
     16384000   1.0808E-01 0.0003 0.0000 10.0  422311   7.0909E-02 0.0002 0.0000 10.0  882831
     24576000   1.0806E-01 0.0003 0.0000 10.0  436957   7.0909E-02 0.0002 0.0000 10.0  912740
     32768000   1.0804E-01 0.0002 0.0000 10.0  455996   7.0906E-02 0.0001 0.0000 10.0  951130
     40960000   1.0803E-01 0.0002 0.0000 10.0  463746   7.0904E-02 0.0001 0.0000 10.0  965731
     49152000   1.0804E-01 0.0002 0.0000  9.8  468763   7.0908E-02 0.0001 0.0000 10.0  976671
     57344000   1.0804E-01 0.0002 0.0000  6.3  472854   7.0907E-02 0.0001 0.0000 10.0  985370
     65536000   1.0804E-01 0.0002 0.0000  6.3  476233   7.0909E-02 0.0001 0.0000 10.0  992753
     73728000   1.0805E-01 0.0001 0.0000  6.3  478644   7.0912E-02 0.0000 0.0000 10.0 1.0E+30
     81920000   1.0805E-01 0.0001 0.0000  5.4  480418   7.0913E-02 0.0000 0.0000 10.0 1.0E+30
     88924090   1.0805E-01 0.0001 0.0000  3.7  481939   7.0912E-02 0.0000 0.0000 10.0 1.0E+30

 ************************************************************************************************************************

 dump no.    3 on file runtpe     nps =    88924090     coll =     2874631084     ctm =      120.00   nrn =
 23880258776
 tally data written to file mctal

         3 warning messages so far.


 run terminated when it had used  120  minutes of computer time.

 computer time =  120.03 minutes

 mcnp     version 5     09282010                     07/22/14 18:57:53                     probid =  07/22/14 16:57:46
```

5.7.2.2 RH-TRU 72-B – NS15 Neutron Shielded Canister

5.7.2.2.1 NCT Distributed 0.5 MeV Gamma Source – 9ng120.io

```
          Thread Name & Version = MCNP5, 1.60

            _  _     _  _  _      _
           |_||_|   (_  |_||  |  |_)
                           |

  +-------------------------------------------------------------------+
  | Copyright 2010. Los Alamos National Security, LLC.  All rights    |
  | reserved.                                                         |
  |   This material was produced under U.S. Government contract       |
  | DE-AC52-06NA25396 for Los Alamos National Laboratory, which is    |
  | operated by Los Alamos National Security, LLC, for the U.S.       |
  | Department of Los Energy. The Government is granted for itself and |
```

| others acting on its behalf a paid-up, nonexclusive, irrevocable
| worldwide license in this material to reproduce, prepare derivative
| works, and perform publicly and display publicly. Beginning five
| (5) years after 2010, subject to additional five-year worldwide
| renewals, the Government is granted for itself and others acting on
| its behalf a paid-up, nonexclusive, irrevocable worldwide license
| in this material to reproduce, prepare derivative works, distribute
| copies to the public, perform publicly and display publicly, and to
| permit others to do so. NEITHER THE UNITED STATES NOR THE UNITED
| STATES DEPARTMENT OF ENERGY, NOR LOS ALAMOS NATIONAL SECURITY, LLC,
| NOR ANY OF THEIR EMPLOYEES, MAKES ANY WARRANTY, EXPRESS OR IMPLIED,
| OR ASSUMES ANY LEGAL LIABILITY OR RESPONSIBILITY FOR THE ACCURACY,
| COMPLETENESS, OR USEFULNESS OF ANY INFORMATION, APPARATUS, PRODUCT,
| OR PROCESS DISCLOSED, OR REPRESENTS THAT ITS USE WOULD NOT INFRINGE
| PRIVATELY OWNED RIGHTS.

```
1mcnp     version 5     ld=09282010                    03/01/14 17:49:22
 ***********************************************************************                probid =  03/01/14 17:49:22
 inp=9ng120.i

         1-       title RH-TRU 72-B NS15 NCT Gamma Distributed 1 g/cc 0.5 MeV
         2-       C
         3-       C Cell Cards
         4-       C
         5-       10  1 -1        10  -11  -16                imp:p=1    $ Source #1
         6-       11  1 -1        12  -13  -17                imp:p=1    $ Source #2
         7-       12  1 -1        14  -15  -18                imp:p=1    $ Source #3
         8-       20  0           20  -21  -26
         9-                     (-10:  11:  16)               imp:p=1    $ Drum #1 cavity
        10-       21  0           22  -23  -27
        11-                     (-12:  13:  17)               imp:p=1    $ Drum #2 cavity
        12-       22  0           24  -25  -28
        13-                     (-14:  15:  18)               imp:p=1    $ Drum #3 cavity
        14-       30  0           31  -35  -33
        15-                      #10  #11  #12
        16-                      #20  #21  #22                imp:p=1    $ NS15 cavity
        17-       31  5 -0.94000  30  -31  -32                imp:p=1    $ NS15 botcap
        18-       32  5 -0.94000  31  -35   33  -32           imp:p=1    $ NS15 body
        19-       33  5 -0.94000  35  -34  -32                imp:p=1    $ NS15 topcap
        20-       40  0           41  -45  -43
        21-                     (-30:  32:  34)               imp:p=1    $ RLC cavity
        22-       41  3 -7.85260  40  -41  -42                imp:p=1    $ RLC base
        23-       42  3 -7.85260  41  -46   43  -42           imp:p=1    $ RLC shell
        24-       43  3 -7.85260  45  -44  -43                imp:p=1    $ RLC lid
        25-       50  0           51  -53  -55
        26-                     (-40:  42:  46)
        27-                    :( 44  -46  -43)               imp:p=1    $ IV cavity
        28-       51  2 -8.01280  50  -51  -52                imp:p=1    $ IV base
        29-       52  2 -8.01280  51  -55   53  -52           imp:p=2    $ IV shell
        30-       53  2 -8.01280  55  -54  -52                imp:p=1    $ IV lid
        31-       60  0           61  -63  -65
        32-                     (-50:  52:  54)               imp:p=2    $ OC cavity
        33-       61  2 -8.01280  60  -61  -69                imp:p=1    $ OC base
        34-       62  2 -8.01280  61  -66   65  -64           imp:p=5    $ OC ishell
        35-       63  4 -11.3500  61  -66   64  -76  71       imp:p=3E1  $ OC lead in
        36-       64  4 -11.3500  61  -66   76  -68  71       imp:p=3E2  $ OC lead out
        37-       65  2 -8.01280  61  -66   68  -77  71       imp:p=3E3  $ OC oshell in
```

```
      38-       66  2 -8.01280  61  -66   77  -67  71        imp:p=6E3  $ OC oshell out
      39-       67  0           61  -66   67  -70  71        imp:p=1E5  $ OC airgap
      40-       68  2 -8.01280  61  -66   70  -69  71        imp:p=2E5  $ OC tshell
      41-       69  2 -8.01280  66  -63   65  -69            imp:p=1    $ OC flange
      42-       70  2 -8.01280  63  -62  -69                 imp:p=1    $ OC lid
      43-       71  4 -11.3500  64  -78  -71                 imp:p=3E1  $ OC lead punct in
      44-       72  4 -11.3500  78  -73  -71                 imp:p=3E2  $ OC lead punct out
      45-       73  2 -8.01280  73  -79  -71                 imp:p=3E3  $ OC oshell punct in
      46-       74  2 -8.01280  79  -72  -71                 imp:p=6E3  $ OC oshell punct out
      47-       75  0           72  -75  -71                 imp:p=1E5  $ OC airgap punct
      48-       76  2 -8.01280  75  -74  -71                 imp:p=2E5  $ OC tshell punct
      49-       777 0           69  -80   60  -62            imp:p=2E5  $ Outside to tally
      50-       888 0          -999
      51-                     (-60:  80:  62)                imp:p=1E1  $ Outside pkg
      52-       999 0           999                          imp:p=0    $ Outside world
      53-
      54-       C
      55-       C Geometry Cards
      56-       C
      57-       10  pz 61.278                                            $ Source #1 bottom
      58-       11  pz 129.223                                           $ Source #1 top
      59-       12  pz 130.175                                         $ Source #2 bottom
      60-       13  pz 198.12                                         $ Source #2 top
      61-       14  pz 199.073                                         $ Source #3 bottom
      62-       15  pz 267.018                                         $ Source #3 top
      63-       16  c/z 0 0 18.733                                       $ Source #1 radius
warning.  this surface has been replaced by a surface of type cz
      64-       17  c/z 0 0 18.733                                       $ Source #2 radius
warning.  this surface has been replaced by a surface of type cz
      65-       18  c/z 0 0 18.733                                       $ Source #3 radius
      66-       C
warning.  this surface has been replaced by a surface of type cz
      67-       20  pz 60.96                                          $ Drum #1 bottom
      68-       21  pz 129.54                                           $ Drum #1 top
      69-       22  pz 129.858                                         $ Drum #2 bottom
      70-       23  pz 198.438                                         $ Drum #2 top
      71-       24  pz 198.755                                         $ Drum #3 bottom
      72-       25  pz 267.335                                         $ Drum #3 top
      73-       26  c/z 0 0 19.05                                    $ Drum #1 radius
warning.  this surface has been replaced by a surface of type cz
      74-       27  c/z 0 0 19.05                                    $ Drum #2 radius
warning.  this surface has been replaced by a surface of type cz
      75-       28  c/z 0 0 19.05                                    $ Drum #3 radius
      76-       C
warning.  this surface has been replaced by a surface of type cz
      77-       30  pz 21.908                                         $ NS15 botcap (outside)
      78-       31  pz 34.608                                         $ NS15 botcap (inside)
      79-       32  c/z 0 0 30.48                                     $ NS15 body (outside)
warning.  this surface has been replaced by a surface of type cz
      80-       33  c/z 0 0 21.877                                    $ NS15 body (inside)
warning.  this surface has been replaced by a surface of type cz
      81-       34  pz 306.388                                        $ NS15 topcap (outside)
      82-       35  pz 293.688                                        $ NS15 topcap (inside)
      83-       C
      84-       40  pz 19.368                                         $ RLC base (outside)
      85-       41  pz 20.638                                         $ RLC base (inside)
      86-       42  c/z 0 0 33.02                                     $ RLC shell (outside)
warning.  this surface has been replaced by a surface of type cz
```

```
      87-       43  c/z 0 0 32.385                                      $ RLC shell (inside)
warning.  this surface has been replaced by a surface of type cz
      88-       44  pz 309.563                                          $ RLC lid (outside)
      89-       45  pz 307.658                                          $ RLC lid (inside)
      90-       46  pz 325.438                                          $ RLC top (outside)
      91-       C
      92-       50  pz 14.288                                           $ IV base (outside)
      93-       51  pz 18.098                                           $ IV base (inside)
      94-       52  c/z 0 0 40.64                                       $ IV shell (outside)
warning.  this surface has been replaced by a surface of type cz
      95-       53  c/z 0 0 39.688                                      $ IV shell (inside)
warning.  this surface has been replaced by a surface of type cz
      96-       54  pz 343.218                                          $ IV top (outside)
      97-       55  pz 326.708                                          $ IV top (inside)
      98-       C
      99-       60  pz 0                                                $ OC bottom (outside)
     100-       61  pz 12.7                                             $ OC bottom (inside)
     101-       62  pz 360.045                                          $ OC top (outside)
     102-       63  pz 344.805                                          $ OC top (inside)
     103-       64  cz 43.656                                           $ OC ishell (outside)
     104-       65  cz 41.116                                           $ OC ishell (inside)
     105-       66  pz 320.675                                          $ OC lead (upper)
     106-       67  cz 52.229                                           $ OC oshell (outside)
     107-       68  cz 48.419                                           $ OC oshell (inside)
     108-       69  cz 52.838                                           $ OC therm (outside)
     109-       70  cz 52.495                                           $ OC therm (inside)
     110-       71  c/x 0 164.148 10.033                                $ OC puncture radius
     111-       72  cz 52.229                                           $ OC oshell punct (out)
     112-       73  cz 48.419                                           $ OC oshell punct (in)
     113-       74  cz 52.838                                           $ OC therm punct (out)
     114-       75  cz 52.495                                           $ OC therm punct (in)
     115-       76  cz 46.038                                           $ OC lead (mid)
     116-       77  cz 50.324                                           $ OC oshell (mid)
     117-       78  cz 46.038                                           $ OC lead punct (mid)
     118-       79  cz 50.324                                           $ OC oshell punct (mid)
     119-       C
     120-       80  cz 252.838                                          $ 2-meter from OC therm
     121-       C
     122-       777 pz 161.608                                          $ Ring tally (lower)
     123-       888 pz 166.688                                          $ Ring tally (upper)
     124-       999 sz 164.148 379.838                                  $ Outside world
     125-
     126-       C
     127-       C Physics Cards
     128-       C
     129-       mode p
     130-       C
     131-       C Source Cards
     132-       C
     133-       C Cylindrical Sources
     134-       sdef pos=d1 erg=d2 par=2 axs=0 0 1 rad=d3 ext=d4
     135-       sc1 0.5 MeV
     136-       C Source Position and Fraction
     137-       si1 L 0 0 95.25
     138-             0 0 164.148
     139-             0 0 233.045
     140-       sp1   1 1 1
     141-       C Source Energy (MeV) and Intensity (%)
```

```
      si2 L 0.5
      sp2 1
      C Source Radius
      si3 0 18.733
      sp3 -21 1
      C Source Extent
      si4 -33.973 33.973
      sp4 -21 0
      C
      C Tally Cards
      C
      f2:p 69
      fc2 Surface Dose (mrem/hr)                              $ Surface detector
      fs2 888 777 t
      sd2 1.0 1686.525 1.0 1.0                                $ Surface tally area
      f22:p 80
      fc22 2-meter Dose (mrem/hr)                             $ 2-m detector
      fs22 888 777 t
      sd22 1.0 8070.229 1.0 1.0                               $ Surface tally area
      C
      C ANSI/ANS-6.1.1-1977 Gamma Flux to Dose Factors (mrem/hr)
      de0 1.0e-02 3.0e-02 5.0e-02 7.0e-02 1.0e-01             $ Energy (Mev)
           1.5e-01 2.0e-01 2.5e-01 3.0e-01 3.5e-01
           4.0e-01 4.5e-01 5.0e-01 5.5e-01 6.0e-01
           6.5e-01 7.0e-01 8.0e-01 1.00 1.40
           1.80 2.20 2.60 2.80 3.25
           3.75 4.25 4.75 5.00 5.25
           5.75 6.25 6.75 7.50 9.00
           11.00 13.00 15.0000
      df0 3.96e-03 5.82e-04 2.90e-04 2.58e-04 2.83e-04        $ Conversion (mrem/hr)
           3.79e-04 5.01e-04 6.31e-04 7.59e-04 8.78e-04
           9.85e-04 1.08e-03 1.17e-03 1.27e-03 1.36e-03
           1.44e-03 1.52e-03 1.68e-03 1.98e-03 2.51e-03
           2.99e-03 3.42e-03 3.82e-03 4.01e-03 4.41e-03
           4.83e-03 5.23e-03 5.60e-03 5.80e-03 6.01e-03
           6.37e-03 6.74e-03 7.11e-03 7.66e-03 8.77e-03
           1.03e-02 1.18e-02 1.33e-02
      C
      C Material Cards
      C
      m1   40000 -1.00                                        $ Zirconium
      m2   14000 -0.01                                        $ Stainless Steel
           24000 -0.19
           25000 -0.02
           26000 -0.68
           28000 -0.10
      m3   26000 -1.00                                        $ Carbon Steel (iron)
      m4   82000 -1.00                                        $ Lead
      m5   1000   2                                           $ EHMW Polyethylene
           6000   1
      C
      C Runtime and Print Cards
      C
      prdmp j j 1 2
      ctme 240

surface       16   and surface       17   are the same.       17   will be deleted.
```

```
 surface       16   and surface       18   are the same.       18   will be deleted.

 surface       26   and surface       27   are the same.       27   will be deleted.

 surface       26   and surface       28   are the same.       28   will be deleted.

 surface       67   and surface       72   are the same.       72   will be deleted.

 surface       68   and surface       73   are the same.       73   will be deleted.

 surface       69   and surface       74   are the same.       74   will be deleted.

 surface       70   and surface       75   are the same.       75   will be deleted.

 surface       76   and surface       78   are the same.       78   will be deleted.

 surface       77   and surface       79   are the same.       79   will be deleted.

  comment.          10 surfaces were deleted for being the same as others.

  warning.    1 materials had unnormalized fractions. print table 40.

  warning.  sum of segment sizes differs from total in   2 cases.
1cells                                                                                print table 60

                          atom        gram                                            photon
            cell     mat  density     density     volume       mass            pieces importance

       1      10       1  6.60141E-03 1.00000E+00 7.49069E+04 7.49069E+04          1  1.0000E+00
       2      11       1  6.60141E-03 1.00000E+00 7.49069E+04 7.49069E+04          1  1.0000E+00
       3      12       1  6.60141E-03 1.00000E+00 7.49069E+04 7.49069E+04          1  1.0000E+00
       4      20       0  0.00000E+00 0.00000E+00 3.28056E+03 0.00000E+00          1  1.0000E+00
       5      21       0  0.00000E+00 0.00000E+00 3.28056E+03 0.00000E+00          1  1.0000E+00
       6      22       0  0.00000E+00 0.00000E+00 3.28056E+03 0.00000E+00          1  1.0000E+00
       7      30       0  0.00000E+00 0.00000E+00 1.54984E+05 0.00000E+00          1  1.0000E+00
       8      31       5  1.21068E-01 9.40000E-01 3.70667E+04 3.48427E+04          1  1.0000E+00
       9      32       5  1.21068E-01 9.40000E-01 3.66613E+05 3.44617E+05          1  1.0000E+00
      10      33       5  1.21068E-01 9.40000E-01 3.70667E+04 3.48427E+04          1  1.0000E+00
      11      40       0  0.00000E+00 0.00000E+00 1.15399E+05 0.00000E+00          1  1.0000E+00
      12      41       3  8.46757E-02 7.85260E+00 4.35019E+03 3.41603E+04          1  1.0000E+00
      13      42       3  8.46757E-02 7.85260E+00 3.97694E+04 3.12294E+05          1  1.0000E+00
      14      43       3  8.46757E-02 7.85260E+00 6.27672E+03 4.92886E+04          1  1.0000E+00
      15      50       0  0.00000E+00 0.00000E+00 5.31049E+05 0.00000E+00          1  1.0000E+00
      16      51       2  8.80825E-02 8.01280E+00 1.97689E+04 1.58404E+05          1  1.0000E+00
      17      52       2  8.80825E-02 8.01280E+00 7.41419E+04 5.94084E+05          1  2.0000E+00
      18      53       2  8.80825E-02 8.01280E+00 8.56652E+04 6.86418E+05          1  1.0000E+00
      19      60       0  0.00000E+00 0.00000E+00 5.70765E+04 0.00000E+00          1  2.0000E+00
      20      61       2  8.80825E-02 8.01280E+00 1.11390E+05 8.92546E+05          1  1.0000E+00
      21      62       2  8.80825E-02 8.01280E+00 2.08330E+05 1.66931E+06          1  5.0000E+00
      22      63       4  3.29849E-02 1.13500E+01 0.00000E+00 0.00000E+00          0  3.0000E+01
      23      64       4  3.29849E-02 1.13500E+01 0.00000E+00 0.00000E+00          0  3.0000E+02
      24      65       2  8.80825E-02 8.01280E+00 0.00000E+00 0.00000E+00          0  3.0000E+03
      25      66       2  8.80825E-02 8.01280E+00 0.00000E+00 0.00000E+00          0  6.0000E+03
      26      67       0  0.00000E+00 0.00000E+00 0.00000E+00 0.00000E+00          0  1.0000E+05
      27      68       2  8.80825E-02 8.01280E+00 0.00000E+00 0.00000E+00          0  2.0000E+05
      28      69       2  8.80825E-02 8.01280E+00 8.34880E+04 6.68973E+05          1  1.0000E+00
      29      70       2  8.80825E-02 8.01280E+00 1.33668E+05 1.07106E+06          1  1.0000E+00
      30      71       4  3.29849E-02 1.13500E+01 0.00000E+00 0.00000E+00          0  3.0000E+01
```

```
       31       72        4  3.29849E-02 1.13500E+01 0.00000E+00 0.00000E+00           0  3.0000E+02
       32       73        2  8.80825E-02 8.01280E+00 0.00000E+00 0.00000E+00           0  3.0000E+03
       33       74        2  8.80825E-02 8.01280E+00 0.00000E+00 0.00000E+00           0  6.0000E+03
       34       75        0  0.00000E+00 0.00000E+00 0.00000E+00 0.00000E+00           0  1.0000E+05
       35       76        2  8.80825E-02 8.01280E+00 0.00000E+00 0.00000E+00           0  2.0000E+05
       36      777        0  0.00000E+00 0.00000E+00 6.91509E+07 0.00000E+00           1  2.0000E+05
       37      888        0  0.00000E+00 0.00000E+00 1.57245E+08 0.00000E+00           1  1.0000E+01
       38      999        0  0.00000E+00 0.00000E+00 0.00000E+00 0.00000E+00           0  0.0000E+00

 total                                              2.28696E+08 6.77555E+06

    minimum source weight = 1.0000E+00    maximum source weight = 1.0000E+00

 ************************************************
 * Random Number Generator  =                  1 *
 * Random Number Seed       =       19073486328125 *
 * Random Number Multiplier =       19073486328125 *
 * Random Number Adder      =                  0 *
 * Random Number Bits Used  =                 48 *
 * Random Number Stride     =             152917 *
 ************************************************


        14 warning messages so far.
1cross-section tables                                                                print table 100

     table    length

                         tables from file mcplib04

   1000.04p    1898  ENDF/B-VI Release 8 Photoatomic Data for 1-H                    mat 100      02/07/03
   6000.04p    3152  ENDF/B-VI Release 8 Photoatomic Data for 6-C                    mat 600      02/07/03
  14000.04p    4792  ENDF/B-VI Release 8 Photoatomic Data for 14-SI                  mat1400      02/07/03
  24000.04p    5682  ENDF/B-VI Release 8 Photoatomic Data for 24-CR                  mat2400      02/07/03
  25000.04p    5598  ENDF/B-VI Release 8 Photoatomic Data for 25-MN                  mat2500      02/07/03
  26000.04p    5718  ENDF/B-VI Release 8 Photoatomic Data for 26-FE                  mat2600      02/07/03
  28000.04p    5826  ENDF/B-VI Release 8 Photoatomic Data for 28-NI                  mat2800      02/07/03
  40000.04p    7703  ENDF/B-VI Release 8 Photoatomic Data for 40-ZR                  mat4000      02/07/03
  82000.04p   10010  ENDF/B-VI Release 8 Photoatomic Data for 82-PB                  mat8200      02/07/03

  total       50379

 maximum photon energy set to  100.0 mev (maximum electron energy)

                         tables from file el03

   1000.03e    2329                                                                                6/6/98
   6000.03e    2333                                                                                6/6/98
  14000.03e    2339                                                                                6/6/98
  24000.03e    2345                                                                                6/6/98
  25000.03e    2345                                                                                6/6/98
  26000.03e    2345                                                                                6/6/98
  28000.03e    2347                                                                                6/6/98
  40000.03e    2353                                                                                6/6/98
  82000.03e    2373                                                                                6/6/98

  warning.  material        1 has been set to a conductor.
```

```
  warning.  material        2 has been set to a conductor.

  warning.  material        3 has been set to a conductor.

  warning.  material        4 has been set to a conductor.

 ************************************************************************************************************************

 dump no.    1 on file runtpe     nps =           0     coll =             0     ctm =        0.00   nrn =
    0

       18 warning messages so far.

 ************************************************************************************************************************

 dump no.    2 on file runtpe     nps =   107421008     coll =     1211934896     ctm =       60.00   nrn =
 15389703657

 ************************************************************************************************************************

 dump no.    3 on file runtpe     nps =   214721446     coll =     2422442457     ctm =      120.02   nrn =
 30762413494

 ************************************************************************************************************************

 dump no.    4 on file runtpe     nps =   321966987     coll =     3632284895     ctm =      180.03   nrn =
 46125859996
1problem summary

      run terminated when it had used  240  minutes of computer time.
+                                                                                    03/01/14 21:49:36
      title RH-TRU 72-B NS15 NCT Gamma Distributed 1 g/cc 0.5 MeV                 probid =  03/01/14 17:49:22
0
 photon creation     tracks      weight        energy           photon loss         tracks      weight        energy
                                 (per source particle)                                        (per source particle)

 source           428693066    1.0000E+00    5.0000E-01          escape            28551444    4.5197E-07    1.5707E-07
                                                                 energy cutoff            0    0.            5.2924E-05
                                                                 time cutoff              0    0.            0.
 weight window            0    0.            0.                  weight window            0    0.            0.
 cell importance  740897246    4.9492E-02    1.0730E-02          cell importance   72702556    4.9501E-02    1.0731E-02
 weight cutoff            0    0.            0.                  weight cutoff            0    0.            0.
 e or t importance        0    0.            0.                  e or t importance        0    0.            0.
 dxtran                   0    0.            0.                  dxtran                   0    0.            0.
 forced collisions        0    0.            0.                  forced collisions        0    0.            0.
 exp. transform           0    0.            0.                  exp. transform           0    0.            0.
 from neutrons            0    0.            0.                  compton scatter          0    0.            3.1196E-01
 bremsstrahlung   269924614    1.9250E-01    3.6087E-03          capture         2221866707    1.7723E+00    2.0091E-01
 p-annihilation           0    0.            0.                  pair production          0    0.            0.
 photonuclear             0    0.            0.                  photonuclear abs         0    0.            0.
 electron x-rays          0    0.            0.
 1st fluorescence 781471086    5.6208E-01    9.2103E-03
 2nd fluorescence 102134695    1.7703E-02    1.0327E-04
     total       2323120707    1.8218E+00    5.2365E-01              total       2323120707    1.8218E+00    5.2365E-01

   number of photons banked                694229026        average time of (shakes)              cutoffs
   photon tracks per source particle      5.4191E+00          escape            1.2154E+00          tco   1.0000E+33
   photon collisions per source particle  1.1281E+01          capture           7.7809E-02          eco   1.0000E-03
```

```
   total photon collisions               4836140021          capture or escape 7.7809E-02          wc1  -5.0000E-01
                                                             any termination   7.9033E-02          wc2  -2.5000E-01

 computer time so far in this run   240.02 minutes           maximum number ever in bank        11
 computer time in mcrun             240.00 minutes           bank overflows to backup file       0
 source particles per minute            1.7862E+06
 random numbers generated              61414201720           most random numbers used was      763604 in history   162759129

  warning.   random number stride   152917 exceeded        8 times.

 range of sampled source weights = 1.0000E+00 to 1.0000E+00

  warning.  importance function may be poor.  see print table 120.
1photon   activity in each cell                                                              print table 126
```

cell	tracks entering	population	collisions	collisions * weight (per history)	number weighted energy	flux weighted energy	average track weight (relative)	average track mfp (cm)
1 10	169400592	173672762	358026292	8.3516E-01	4.1062E-01	4.1062E-01	1.0000E+00	9.5558E+00
2 11	178824366	183679884	378593375	8.8313E-01	4.0876E-01	4.0876E-01	1.0000E+00	9.5156E+00
3 12	169375949	173656702	358067612	8.3525E-01	4.1061E-01	4.1061E-01	1.0000E+00	9.5556E+00
4 20	114058049	90674743	0	0.0000E+00	3.6582E-01	3.6582E-01	1.0000E+00	0.0000E+00
5 21	127908764	99838374	0	0.0000E+00	3.6519E-01	3.6519E-01	1.0000E+00	0.0000E+00
6 22	114024118	90650763	0	0.0000E+00	3.6579E-01	3.6579E-01	1.0000E+00	0.0000E+00
7 30	342775863	244550250	0	0.0000E+00	3.2682E-01	3.2682E-01	1.0000E+00	0.0000E+00
8 31	6406667	5598712	16706035	3.8970E-02	2.1246E-01	2.1246E-01	1.0000E+00	7.4412E+00
9 32	267954859	227805976	544787000	1.2708E+00	2.7229E-01	2.7229E-01	1.0000E+00	8.2074E+00
10 33	6397275	5593065	16671190	3.8888E-02	2.1252E-01	2.1252E-01	1.0000E+00	7.4419E+00
11 40	220903861	182031426	0	0.0000E+00	2.6093E-01	2.6093E-01	1.0000E+00	0.0000E+00
12 41	2870374	2693954	5210954	1.2155E-02	2.7536E-01	2.7536E-01	1.0000E+00	9.9191E-01
13 42	205865339	188087328	242002493	5.6451E-01	2.8891E-01	2.8891E-01	1.0000E+00	1.0242E+00
14 43	2748267	2683537	6123106	1.4283E-02	2.7954E-01	2.7954E-01	1.0000E+00	1.0067E+00
15 50	149694353	129092785	0	0.0000E+00	2.9628E-01	2.9628E-01	8.1280E-01	0.0000E+00
16 51	1269592	1324989	4385281	1.0229E-02	2.8350E-01	2.8350E-01	1.0000E+00	1.0152E+00
17 52	250055914	240883404	392198666	4.5744E-01	2.9190E-01	2.9190E-01	1.0000E+00	1.0296E+00
18 53	599538	644945	2396679	5.5907E-03	2.7805E-01	2.7805E-01	1.0000E+00	1.0038E+00
19 60	186338963	161013332	0	0.0000E+00	2.9110E-01	2.9110E-01	7.5668E-01	0.0000E+00
20 61	130078	138875	525876	1.2267E-03	2.7449E-01	2.7449E-01	1.0000E+00	9.9906E-01
21 62	333606313	352137255	1017609058	4.7475E-01	2.8974E-01	2.8974E-01	1.0000E+00	1.0319E+00
22 63	448776574	697973486	1375369547	1.0694E-01	3.7157E-01	3.7157E-01	1.0000E+00	3.5327E-01
23 64	19802064	33684008	68467250	5.3237E-04	4.2886E-01	4.2886E-01	1.0000E+00	4.4129E-01
24 65	2862004	2944645	6962582	5.4138E-06	3.4481E-01	3.4481E-01	1.0000E+00	1.1569E+00
25 66	2673374	2808395	6800486	2.6439E-06	3.1507E-01	3.1507E-01	1.0000E+00	1.0931E+00
26 67	4053827	3933717	0	0.0000E+00	3.1714E-01	3.1714E-01	2.8045E+00	0.0000E+00
27 68	34175357	34618990	18663720	2.1768E-07	3.2445E-01	3.2445E-01	1.0000E+00	1.1253E+00
28 69	50939	53726	182823	4.2647E-04	2.6556E-01	2.6556E-01	1.0000E+00	9.7495E-01
29 70	96	100	369	8.6076E-07	2.5628E-01	2.5628E-01	1.0000E+00	9.6327E-01
30 71	5096011	7871384	15349052	1.1935E-03	3.7140E-01	3.7140E-01	1.0000E+00	3.5302E-01
31 72	215845	363511	729494	5.6722E-06	4.2878E-01	4.2878E-01	1.0000E+00	4.4119E-01
32 73	30807	31367	69415	5.3974E-08	3.4651E-01	3.4651E-01	1.0000E+00	1.1604E+00
33 74	28340	29271	65935	2.5634E-08	3.1413E-01	3.1413E-01	1.0000E+00	1.0913E+00
34 75	39919	38791	0	0.0000E+00	3.1673E-01	3.1673E-01	2.8183E+00	0.0000E+00
35 76	330561	334469	175731	2.0496E-09	3.2393E-01	3.2393E-01	1.0000E+00	1.1239E+00
36 777	28551403	28551403	0	0.0000E+00	3.5799E-01	3.5799E-01	1.0481E+00	0.0000E+00
37 888	28551444	28551444	0	0.0000E+00	3.3718E-01	3.3718E-01	8.2750E-05	0.0000E+00
total	3426447659	3398241768	4836140021	5.5515E+00				

```
1tally        2        nps =   428693066
+                                Surface Dose (mrem/hr)                                  $ Surface detector
          tally type 2    particle flux averaged over a surface.
          tally for  photons

          this tally is modified by a dose function.

          areas
               surface:      69
              segment
                1       1.00000E+00
                2       1.68653E+03
                3       1.00000E+00
               whole      1.00000E+00

 surface  69
 segment:          888
                2.07906E-10 0.0253

 surface  69
 segment:         -888        777
                5.63979E-15 0.0141

 surface  69
 segment:         -888       -777
                1.96690E-10 0.0175

 surface  69
 segment:   whole surface
                4.14108E-10 0.0152

 ============================================================================================================================

          results of 10 statistical checks for the estimated answer for the tally fluctuation chart (tfc) bin of tally        2

 tfc bin     --mean--      ---------relative error---------      ----variance of the variance----      --figure of merit--     -pdf-
 behavior    behavior      value   decrease   decrease rate      value   decrease   decrease rate       value     behavior     slope

 desired      random       <0.10      yes      1/sqrt(nps)       <0.10      yes        1/nps           constant    random      >3.00
 observed     random        0.02      yes          yes            0.12      yes         yes            constant    random       1.65
 passed?        yes          yes      yes          yes              no      yes         yes               yes        yes          no

 ============================================================================================================================

 warning.  the tally in the tally fluctuation chart bin did not pass  2 of the 10 statistical checks.

1analysis of the results in the tally fluctuation chart bin (tfc) for tally        2 with nps=   428693066 print table 160

 normed average tally per history  = 4.14108E-10          unnormed average tally per history  = 4.14108E-10
 estimated tally relative error    = 0.0152               estimated variance of the variance  = 0.1249
 relative error from zero tallies  = 0.0021               relative error from nonzero scores  = 0.0151

 number of nonzero history tallies =      221406         efficiency for the nonzero tallies  = 0.0005
 history number of largest  tally  =   197018165         largest  unnormalized history tally = 1.30384E-03
```

```
 (largest  tally)/(average tally)  = 3.14854E+06          (largest  tally)/(avg nonzero tally)= 1.62612E+03

 (confidence interval shift)/mean  = 0.0026               shifted confidence interval center  = 4.15170E-10


 if the largest  history score sampled so far were to occur on the next history, the tfc bin quantities would change as follows:

      estimated quantities           value at nps           value at nps+1          value(nps+1)/value(nps)-1.

      mean                            4.14108E-10            4.17150E-10                0.007345
      relative error                  1.52065E-02            1.67641E-02                0.102432
      variance of the variance        1.24869E-01            1.17877E-01               -0.056001
      shifted center                  4.15170E-10            4.15257E-10                0.000209
      figure of merit                 1.80187E+01            1.48259E+01               -0.177196

 the estimated inverse power slope of the 200 largest  tallies starting at 3.19484E-06 is 1.6499
 the history score probability density function appears to have an unsampled region at the largest  history scores:
 please examine. see print table 161.

 fom = (histories/minute)*(f(x) signal-to-noise ratio)**2 = (1.786E+06)*( 3.176E-03)**2 = (1.786E+06)*(1.009E-05) = 1.802E+01

1unnormed tally density for tally       2          nonzero tally mean(m) = 8.018E-07   nps =   428693066  print table 161

 abscissa              ordinate   log plot of tally probability density function in tally fluctuation chart bin(d=decade,slope= 1.6)
  tally  number num den log den:d-----------d-----------d-----------d-----------d-----------d-----------d-----------d-----------
 2.51-09      5 1.26+01   1.100 ************|***********|***********|***********|***********|***********|****       |
 3.98-09      2 3.18+00   0.502 ************|***********|***********|***********|***********|********   |           |
 6.31-09     11 1.10+01   1.042 ************|***********|***********|***********|***********|***********|***        |
 1.00-08     32 2.02+01   1.306 ************|***********|***********|***********|***********|***********|*******    |
 1.58-08     53 2.11+01   1.325 ************|***********|***********|***********|***********|***********|*******    |
 2.51-08    142 3.57+01   1.553 ************|***********|***********|***********|***********|***********|***********|
 3.98-08    376 5.97+01   1.776 ************|***********|***********|***********|***********|***********|***********|************
 6.31-08   1092 1.09+02   2.039 ************|***********|***********|***********|***********|***********|***********|************|***
 1.00-07   2671 1.69+02   2.227 ************|***********|***********|***********|***********|***********|***********|************|*****
 1.58-07   6228 2.48+02   2.395 ************|***********|***********|***********|***********|***********|***********|************|*******
 2.51-07  15093 3.80+02   2.580 ************|***********|***********|***********|***********|***********|***********|************|***********
 3.98-07  25652 4.07+02   2.610 ************|***********|***********|***********|***********|***********|***********|************|***********
 6.31-07  47142 4.72+02   2.674 ************|***********|***********|***********|***********|***********|***********|************|***********
 1.00-06  65498 4.14+02   2.617 mmmmmmmmmmmm|mmmmmmmmmmmm|mmmmmmmmmmmm|mmmmmmmmmmmm|mmmmmmmmmmmm|mmmmmmmmmmmm|mmmmmmmmmmmm|mmmmmmmmmmm
 1.58-06  45293 1.81+02   2.257 ************|***********|***********|***********|***********|***********|***********|************|******
 2.51-06  11013 2.77+01   1.443 ************|***********|***********|***********|***********|***********|***********|********    |
 3.98-06   1064 1.69+00   0.228 ************|***********|***********|***********|***********|*****      |   s       |
 6.31-06     22 2.20-02  -1.657 ************|***********|***********|*******    |           |          s|           |
 1.00-05      1 6.32-04  -3.199 ************|***********|           |           |           |      s    |           |
 1.58-05      0 0.00+00   0.000             |           |           |           |         s |           |           |
 2.51-05      1 2.52-04  -3.599 ************|*******    |           |           |          s|           |           |
 3.98-05      2 3.18-04  -3.498 ************|********   |           |           |     s     |           |           |
 6.31-05      2 2.00-04  -3.698 ************|******     |           |         s |           |           |           |
 1.00-04      0 0.00+00   0.000             |           |           |        s  |           |           |           |
 1.58-04      1 3.99-05  -4.399 **********  |           |           |      s    |           |           |           |
 2.51-04      0 0.00+00   0.000             |           |          s|           |           |           |           |
 3.98-04      0 0.00+00   0.000             |           |        s  |           |           |           |           |
 6.31-04      3 3.01-05  -4.522 ********    |           |      s    |           |           |           |           |
 1.00-03      5 3.16-05  -4.500 *********   |           |   s       |           |           |           |           |
 1.58-03      2 7.98-06  -5.098 *           |          s|           |           |           |           |           |
  total  221406 5.16-04         d-----------d-----------d-----------d-----------d-----------d-----------d-----------d-----------

1tally       22        nps =   428693066
```

```
+                                    2-meter Dose (mrem/hr)                                  $ 2-m detector
          tally type 2    particle flux averaged over a surface.
          tally for  photons

          this tally is modified by a dose function.

          areas
               surface:      80
              segment
                1       1.00000E+00
                2       8.07023E+03
                3       1.00000E+00
             whole      1.00000E+00

 surface  80
 segment:          888
                1.42578E-10 0.0182

 surface  80
 segment:         -888        777
                6.90806E-16 0.0099

 surface  80
 segment:         -888       -777
                1.30121E-10 0.0136

 surface  80
 segment:   whole surface
                2.78274E-10 0.0114


 ============================================================================================================================

          results of 10 statistical checks for the estimated answer for the tally fluctuation chart (tfc) bin of tally       22

 tfc bin     --mean--      ---------relative error---------      ----variance of the variance----      --figure of merit--     -pdf-
 behavior    behavior      value   decrease   decrease rate      value   decrease   decrease rate       value     behavior     slope

 desired      random       <0.10      yes      1/sqrt(nps)       <0.10      yes        1/nps           constant    random      >3.00
 observed     random        0.01      yes          yes            0.27      yes         yes            constant    random       1.90
 passed?        yes          yes      yes          yes              no      yes         yes               yes        yes          no

 ============================================================================================================================


 warning.  the tally in the tally fluctuation chart bin did not pass  2 of the 10 statistical checks.

1analysis of the results in the tally fluctuation chart bin (tfc) for tally       22 with nps=   428693066 print table 160


 normed average tally per history  = 2.78274E-10          unnormed average tally per history  = 2.78274E-10
 estimated tally relative error    = 0.0114               estimated variance of the variance  = 0.2703
 relative error from zero tallies  = 0.0021               relative error from nonzero scores  = 0.0112

 number of nonzero history tallies =      221258          efficiency for the nonzero tallies  = 0.0005
 history number of largest  tally  =   107272928          largest  unnormalized history tally = 8.23565E-04
 (largest  tally)/(average tally)  = 2.95955E+06          (largest  tally)/(avg nonzero tally)= 1.52749E+03
```

```
 (confidence interval shift)/mean  = 0.0028              shifted confidence interval center  = 2.79063E-10


 if the largest  history score sampled so far were to occur on the next history, the tfc bin quantities would change as follows:

      estimated quantities          value at nps          value at nps+1          value(nps+1)/value(nps)-1.

      mean                           2.78274E-10           2.80195E-10                0.006904
      relative error                 1.13907E-02           1.32282E-02                0.161311
      variance of the variance       2.70334E-01           2.16766E-01               -0.198152
      shifted center                 2.79063E-10           2.79109E-10                0.000165
      figure of merit                3.21128E+01           2.38112E+01               -0.258513

 the estimated inverse power slope of the 200 largest  tallies starting at 2.34575E-06 is 1.9019
 the history score probability density function appears to have an unsampled region at the largest  history scores:
 please examine. see print table 161.

 fom = (histories/minute)*(f(x) signal-to-noise ratio)**2 = (1.786E+06)*( 4.240E-03)**2 = (1.786E+06)*(1.798E-05) = 3.211E+01

1unnormed tally density for tally       22          nonzero tally mean(m) = 5.392E-07   nps =   428693066  print table 161

 abscissa              ordinate   log plot of tally probability density function in tally fluctuation chart bin(d=decade,slope= 1.9)
  tally  number num den log den:d-----------d-----------d-----------d-----------d-----------d-----------d-----------d-----------
1.58-09     35 2.50+02   2.399 ************|***********|***********|***********|***********|***********|***********|*****
2.00-09     56 3.18+02   2.503 ************|***********|***********|***********|***********|***********|***********|******
2.51-09     74 3.34+02   2.524 ************|***********|***********|***********|***********|***********|***********|******
3.16-09     87 3.12+02   2.494 ************|***********|***********|***********|***********|***********|***********|******
3.98-09    177 5.04+02   2.703 ************|***********|***********|***********|***********|***********|***********|*********
5.01-09    248 5.61+02   2.749 ************|***********|***********|***********|***********|***********|***********|*********
6.31-09    274 4.93+02   2.692 ************|***********|***********|***********|***********|***********|***********|*********
7.94-09    435 6.21+02   2.793 ************|***********|***********|***********|***********|***********|***********|**********
1.00-08    559 6.34+02   2.802 ************|***********|***********|***********|***********|***********|***********|**********
1.26-08    665 5.99+02   2.778 ************|***********|***********|***********|***********|***********|***********|*********
1.58-08    708 5.07+02   2.705 ************|***********|***********|***********|***********|***********|***********|*********
2.00-08    750 4.26+02   2.630 ************|***********|***********|***********|***********|***********|***********|********
2.51-08    768 3.47+02   2.540 ************|***********|***********|***********|***********|***********|***********|*******
3.16-08    808 2.90+02   2.462 ************|***********|***********|***********|***********|***********|***********|******
3.98-08    913 2.60+02   2.415 ************|***********|***********|***********|***********|***********|***********|******
5.01-08   1132 2.56+02   2.409 ************|***********|***********|***********|***********|***********|***********|******
6.31-08   1621 2.91+02   2.464 ************|***********|***********|***********|***********|***********|***********|******
7.94-08   2248 3.21+02   2.506 ************|***********|***********|***********|***********|***********|***********|*******
1.00-07   3229 3.66+02   2.564 ************|***********|***********|***********|***********|***********|***********|********
1.26-07   5023 4.53+02   2.656 ************|***********|***********|***********|***********|***********|***********|*********
1.58-07   8673 6.21+02   2.793 ************|***********|***********|***********|***********|***********|***********|**********
2.00-07  12050 6.85+02   2.836 ************|***********|***********|***********|***********|***********|***********|**********
2.51-07  10987 4.96+02   2.696 ************|***********|***********|***********|***********|***********|***********|*********
3.16-07  17230 6.18+02   2.791 ************|***********|***********|***********|***********|***********|***********|**********
3.98-07  23628 6.73+02   2.828 ************|***********|***********|***********|***********|***********|***********|**********
5.01-07  26566 6.01+02   2.779 ************|***********|***********|***********|***********|***********|***********|**********
6.31-07  29846 5.36+02   2.730 mmmmmmmmmmmm|mmmmmmmmmmmm|mmmmmmmmmmmm|mmmmmmmmmmmm|mmmmmmmmmmmm|mmmmmmmmmmmm|mmmmmmmmmm
7.94-07  28985 4.14+02   2.617 ************|***********|***********|***********|***********|***********|***********|********
1.00-06  22317 2.53+02   2.403 ************|***********|***********|***********|***********|***********|***********|*****
1.26-06  12825 1.16+02   2.063 ************|***********|***********|***********|***********|***********|***********|*
1.58-06   5714 4.09+01   1.612 ************|***********|***********|***********|***********|***********|********   |
2.00-06   1985 1.13+01   1.052 ************|***********|***********|***********|***********|***********|*          |
2.51-06    524 2.37+00   0.374 ************|***********|***********|***********|***********|*****      |  s        |
3.16-06     98 3.51-01  -0.454 ************|***********|***********|***********|*******    |           |s          |
3.98-06      9 2.56-02  -1.591 ************|***********|***********|******     |           |        s  |           |
```

```
 5.01-06      1 2.26-03  -2.645 ***********|**********|*****      |           |           |       s   |           |
 6.31-06      0 0.00+00   0.000             |          |           |           |           |     s     |           |
 7.94-06      0 0.00+00   0.000             |          |           |           |           |   s       |           |
 1.00-05      0 0.00+00   0.000             |          |           |           |           |s          |           |
 1.26-05      0 0.00+00   0.000             |          |           |           |         s |           |           |
 1.58-05      2 1.43-03  -2.844 ***********|**********|***        |           |       s   |           |           |
 2.00-05      0 0.00+00   0.000             |          |           |           |     s     |           |           |
 2.51-05      1 4.52-04  -3.345 ***********|********  |           |           |   s       |           |           |
 3.16-05      0 0.00+00   0.000             |          |           |           | s         |           |           |
 3.98-05      2 5.70-04  -3.244 ***********|********** |           |           s           |           |           |
 5.01-05      0 0.00+00   0.000             |          |           |         s |           |           |           |
 6.31-05      0 0.00+00   0.000             |          |           |       s   |           |           |           |
 7.94-05      0 0.00+00   0.000             |          |           |     s     |           |           |           |
 1.00-04      0 0.00+00   0.000             |          |           |   s       |           |           |           |
 1.26-04      1 9.01-05  -4.045 ***********|          |           |s          |           |           |           |
 1.58-04      0 0.00+00   0.000             |          |         s |           |           |           |           |
 2.00-04      0 0.00+00   0.000             |          |       s   |           |           |           |           |
 2.51-04      0 0.00+00   0.000             |          |     s     |           |           |           |           |
 3.16-04      0 0.00+00   0.000             |          |   s       |           |           |           |           |
 3.98-04      1 2.85-05  -4.545 ******      |          |s          |           |           |           |           |
 5.01-04      0 0.00+00   0.000             |        s |           |           |           |           |           |
 6.31-04      1 1.80-05  -4.745 ****        |      s   |           |           |           |           |           |
 7.94-04      1 1.43-05  -4.845 **          |    s     |           |           |           |           |           |
 1.00-03      1 1.13-05  -4.945 *           |  s       |           |           |           |           |           |
  total  221258 5.16-04         d----------d----------d-----------d-----------d-----------d-----------d-----------d-----------
```

1status of the statistical checks used to form confidence intervals for the mean for each tally bin

tally result of statistical checks for the tfc bin (the first check not passed is listed) and error magnitude check for all bins

2 missed 2 of 10 tfc bin checks: the variance of the variance exceeds the recommended value of 0.1
passed all bin error check: 4 tally bins all have relative errors less than 0.10 with no zero bins

22 missed 2 of 10 tfc bin checks: the variance of the variance exceeds the recommended value of 0.1
passed all bin error check: 4 tally bins all have relative errors less than 0.10 with no zero bins

the 10 statistical checks are only for the tally fluctuation chart bin and do not apply to other tally bins.

warning. 2 of the 2 tally fluctuation chart bins did not pass all 10 statistical checks.

1tally fluctuation charts

	tally 2				tally 22			
nps	mean	error	vov	slope	fom	mean	error	vov	slope	fom
32768000	4.1333E-10	0.0502	0.9392	3.0	22	2.8896E-10	0.0667	0.9644	3.1	12
65536000	4.3351E-10	0.0468	0.2655	2.2	12	2.8667E-10	0.0390	0.5904	2.7	18
98304000	4.2130E-10	0.0322	0.2614	2.2	18	2.8230E-10	0.0266	0.5754	2.7	26
131072000	4.2077E-10	0.0289	0.2147	2.0	16	2.8551E-10	0.0296	0.4171	2.3	16
163840000	4.1746E-10	0.0235	0.2083	2.0	20	2.8407E-10	0.0240	0.4038	2.2	19
196608000	4.1303E-10	0.0198	0.2062	2.0	23	2.8167E-10	0.0202	0.3995	2.2	22
229376000	4.1586E-10	0.0218	0.2306	1.9	16	2.8008E-10	0.0175	0.3953	2.2	25
262144000	4.1252E-10	0.0192	0.2290	1.9	18	2.7855E-10	0.0154	0.3905	2.2	29
294912000	4.1715E-10	0.0203	0.1566	1.8	15	2.7787E-10	0.0138	0.3864	2.2	32
327680000	4.1548E-10	0.0184	0.1559	1.7	16	2.7771E-10	0.0125	0.3821	2.1	35
360448000	4.1533E-10	0.0172	0.1415	1.7	17	2.7722E-10	0.0114	0.3780	2.1	38
393216000	4.1396E-10	0.0159	0.1409	1.7	18	2.7700E-10	0.0105	0.3734	2.0	41
425984000	4.1425E-10	0.0153	0.1249	1.7	18	2.7833E-10	0.0115	0.2705	1.9	32

```
   428693066   4.1411E-10 0.0152 0.1249  1.6      18   2.7827E-10 0.0114 0.2703  1.9      32
 ************************************************************************************************************************

 dump no.    5 on file runtpe     nps =   428693066     coll =     4836140021     ctm =      240.00   nrn =
 61414201720
 tally data written to file mctal

        23 warning messages so far.


 run terminated when it had used  240  minutes of computer time.

 computer time =  240.02 minutes

 mcnp     version 5     09282010                     03/01/14 21:49:36                     probid =  03/01/14 17:49:22
```

5.7.2.2.2 HAC 60Co Gamma Source – 9hg001.io

```
          Thread Name & Version = MCNP5, 1.60

            _ _   _  _   _      _
           | | |  (_  |  |_)    _)
                        |

  +-------------------------------------------------------------------+
  | Copyright 2010. Los Alamos National Security, LLC.  All rights    |
  | reserved.                                                         |
  |   This material was produced under U.S. Government contract       |
  | DE-AC52-06NA25396 for Los Alamos National Laboratory, which is    |
  | operated by Los Alamos National Security, LLC, for the U.S.       |
  | Department of Los Energy. The Government is granted for itself and |
  | others acting on its behalf a paid-up, nonexclusive, irrevocable  |
  | worldwide license in this material to reproduce, prepare derivative |
  | works, and perform publicly and display publicly. Beginning five  |
  | (5) years after 2010, subject to additional five-year worldwide   |
  | renewals, the Government is granted for itself and others acting on |
  | its behalf a paid-up, nonexclusive, irrevocable worldwide license |
  | in this material to reproduce, prepare derivative works, distribute |
  | copies to the public, perform publicly and display publicly, and to |
  | permit others to do so. NEITHER THE UNITED STATES NOR THE UNITED  |
  | STATES DEPARTMENT OF ENERGY, NOR LOS ALAMOS NATIONAL SECURITY, LLC, |
  | NOR ANY OF THEIR EMPLOYEES, MAKES ANY WARRANTY, EXPRESS OR IMPLIED, |
  | OR ASSUMES ANY LEGAL LIABILITY OR RESPONSIBILITY FOR THE ACCURACY, |
  | COMPLETENESS, OR USEFULNESS OF ANY INFORMATION, APPARATUS, PRODUCT, |
  | OR PROCESS DISCLOSED, OR REPRESENTS THAT ITS USE WOULD NOT INFRINGE |
  | PRIVATELY OWNED RIGHTS.                                           |
  +-------------------------------------------------------------------+

1mcnp     version 5     ld=09282010                     02/27/14 16:47:17
 ************************************************************************                     probid =  02/27/14 16:47:17
 inp=9hg001.i

         1-       title RH-TRU 72-B NS15 HAC Gamma Concentrated 1 g/cc Co60
         2-       C
         3-       C Cell Cards
         4-       C
```

```
 5-       10  1 -1        10  -11  -16                imp:p=1    $ Source #1
 6-       11  1 -1        12  -13  -17                imp:p=1    $ Source #2
 7-       20  0           20  -21  -26
 8-                     (-10:  11:  16)               imp:p=1    $ Drum #1 cavity
 9-       21  0           22  -23  -27
10-                     (-12:  13:  17)               imp:p=1    $ Drum #2 cavity
11-       30  0           31  -35  -33
12-                      #10  #20                     imp:p=1    $ NS15 cavity
13-       31  5 -0.94000  30  -31  -32                imp:p=1    $ NS15 botcap
14-       32  5 -0.94000  31  -35   33  -32           imp:p=1    $ NS15 body
15-       33  5 -0.94000  35  -34  -32                imp:p=1    $ NS15 topcap
16-       40  0           41  -45  -43
17-                     (-30:  32:  34) #11  #21      imp:p=1    $ RLC cavity
18-       41  3 -7.85260  40  -41  -42                imp:p=1    $ RLC base
19-       42  3 -7.85260  41  -46   43  -42           imp:p=1    $ RLC shell
20-       43  3 -7.85260  45  -44  -43                imp:p=1    $ RLC lid
21-       50  0           51  -53  -55
22-                     (-40:  42:  46)
23-                    :( 44  -46  -43)               imp:p=1    $ IV cavity
24-       51  2 -8.01280  50  -51  -52                imp:p=1    $ IV base
25-       52  2 -8.01280  51  -55   53  -52           imp:p=2    $ IV shell
26-       53  2 -8.01280  55  -54  -52                imp:p=1    $ IV lid
27-       60  0           61  -63  -65
28-                     (-50:  52:  54)               imp:p=2    $ OC cavity
29-       61  2 -8.01280  60  -61  -69                imp:p=1    $ OC base
30-       62  2 -8.01280  61  -66   65  -64           imp:p=5    $ OC ishell
31-       63  4 -11.3500  61  -66   64  -76  71       imp:p=3E1  $ OC lead in
32-       64  4 -11.3500  61  -66   76  -68  71       imp:p=3E2  $ OC lead out
33-       65  2 -8.01280  61  -66   68  -77  71       imp:p=3E3  $ OC oshell in
34-       66  2 -8.01280  61  -66   77  -67  71       imp:p=6E3  $ OC oshell out
35-       67  0           61  -66   67  -70  71       imp:p=1E5  $ OC airgap
36-       68  2 -8.01280  61  -66   70  -69  71       imp:p=2E5  $ OC tshell
37-       69  2 -8.01280  66  -63   65  -69           imp:p=1    $ OC flange
38-       70  2 -8.01280  63  -62  -69                imp:p=1    $ OC lid
39-       71  4 -11.3500  64  -78  -71                imp:p=3E1  $ OC lead punct in
40-       72  4 -11.3500  78  -73  -71                imp:p=3E2  $ OC lead punct out
41-       73  2 -8.01280  73  -79  -71                imp:p=3E3  $ OC oshell punct in
42-       74  2 -8.01280  79  -72  -71                imp:p=6E3  $ OC oshell punct out
43-       75  0           74  -69  -71                imp:p=1E5  $ OC airgap punct
44-       76  2 -8.01280  75  -74  -71                imp:p=2E5  $ OC tshell punct
45-       777 0           69  -80   60  -62           imp:p=2E5  $ Outside to tally
46-       888 0         -999
47-                     (-60:  80:  62)               imp:p=1E1  $ Outside pkg
48-       999 0           999                         imp:p=0    $ Outside world
49-
50-       C
51-       C Geometry Cards
52-       C
53-       10  pz 163.513                                        $ Source #1 bottom
54-       11  pz 164.783                                        $ Source #1 top
55-       12  pz 163.513                                        $ Source #2 bottom
56-       13  pz 164.783                                        $ Source #2 top
57-       16  c/z 29.873 0 0.635                                 $ Source #1 radius
58-       17  c/z 38.885 0 0.635                                 $ Source #2 radius
59-       C
60-       20  pz 163.511                                        $ Drum #1 bottom
61-       21  pz 164.784                                        $ Drum #1 top
62-       22  pz 163.511                                        $ Drum #2 bottom
```

```
 63-       23  pz 164.784                          $ Drum #2 top
 64-       26  c/z 29.873 0 0.636                  $ Drum #1 radius
 65-       27  c/z 38.885 0 0.636                  $ Drum #2 radius
 66-       C
 67-       30  pz 21.908                          $ NS15 botcap (outside)
 68-       31  pz 34.608                          $ NS15 botcap (inside)
 69-       32  c/z 7.748 0 30.48                  $ NS15 body (outside)
 70-       33  c/z 7.748 0 22.763                 $ NS15 body (inside)
 71-       34  pz 306.388                         $ NS15 topcap (outside)
 72-       35  pz 293.688                         $ NS15 topcap (inside)
 73-       C
 74-       40  pz 19.368                          $ RLC base (outside)
 75-       41  pz 20.638                          $ RLC base (inside)
 76-       42  c/z 7.139 0 33.02                  $ RLC shell (outside)
 77-       43  c/z 7.139 0 32.385                 $ RLC shell (inside)
 78-       44  pz 309.563                         $ RLC lid (outside)
 79-       45  pz 307.658                         $ RLC lid (inside)
 80-       46  pz 325.438                         $ RLC top (outside)
 81-       C
 82-       50  pz 14.288                          $ IV base (outside)
 83-       51  pz 18.098                          $ IV base (inside)
 84-       52  c/z 0.474 0 40.64                  $ IV shell (outside)
 85-       53  c/z 0.474 0 39.688                 $ IV shell (inside)
 86-       54  pz 343.218                         $ IV top (outside)
 87-       55  pz 326.708                         $ IV top (inside)
 88-       C
 89-       60  pz 0                               $ OC bottom (outside)
 90-       61  pz 12.7                            $ OC bottom (inside)
 91-       62  pz 360.045                         $ OC top (outside)
 92-       63  pz 344.805                         $ OC top (inside)
 93-       64  cz 43.656                          $ OC ishell (outside)
 94-       65  cz 41.116                          $ OC ishell (inside)
 95-       66  pz 320.675                         $ OC lead (upper)
 96-       67  cz 52.229                          $ OC oshell (outside)
 97-       68  cz 48.419                          $ OC oshell (inside)
 98-       69  cz 52.838                          $ OC therm (outside)
 99-       70  cz 52.495                          $ OC therm (inside)
100-       71  c/x 0 164.148 10.033               $ OC puncture radius
101-       72  cz 50.563                          $ OC oshell punct (out)
102-       73  cz 46.753                          $ OC oshell punct (in)
103-       74  cz 50.905                          $ OC therm punct (out)
104-       75  cz 50.563                          $ OC therm punct (in)
105-       76  cz 46.038                          $ OC lead (mid)
106-       77  cz 50.324                          $ OC oshell (mid)
107-       78  cz 45.204                          $ OC lead punct (mid)
108-       79  cz 48.658                          $ OC oshell punct (mid)
109-       C
110-       80  cz 150.905                         $ 1-meter from OC therm
111-       C
112-       777 c/x 0 164.148 2.54                 $ Tally cylinder
113-       888 px 0                               $ Tally truncation
114-       999 sz 164.148 277.905                 $ Outside world
115-
116-       C
117-       C Physics Cards
118-       C
119-       mode p
120-       C
```

```
C Source Cards
C
C Cylindrical Sources
sdef pos=d1 erg=d2 par=2 axs=0 0 1 rad=d3 ext=d4
sc1 Co60
C Source Position and Fraction
si1 L 29.873 0 164.148
      38.885 0 164.148
sp1   98 2
C Source Energy (MeV) and Intensity (%)
si2 L 3.469300E-01 8.262800E-01 1.173237E+00 1.332501E+00
     2.158770E+00 2.505000E+00
sp2 7.600000E-03 7.600000E-03 9.997360E+01 9.998560E+01
     1.110000E-03 2.000000E-06
C Source Radius
si3 0 0.635
sp3 -21 1
C Source Extent
si4 -0.635 0.635
sp4 -21 0
C
C Tally Cards
C
f2:p 69
fc2 Surface Dose (mrem/hr)                              $ Surface detector
fs2 -888 -777 t
sd2 1.0 20.268 1.0 1.0                                  $ Surface tally area
f22:p 80
fc22 1-meter Dose (mrem/hr)                             $ 1-m detector
fs22 -888 -777 t
sd22 1.0 20.268 1.0 1.0                                 $ Surface tally area
C
C ANSI/ANS-6.1.1-1977 Gamma Flux to Dose Factors (mrem/hr)
de0 1.0e-02 3.0e-02 5.0e-02 7.0e-02 1.0e-01             $ Energy (Mev)
     1.5e-01 2.0e-01 2.5e-01 3.0e-01 3.5e-01
     4.0e-01 4.5e-01 5.0e-01 5.5e-01 6.0e-01
     6.5e-01 7.0e-01 8.0e-01 1.00 1.40
     1.80 2.20 2.60 2.80 3.25
     3.75 4.25 4.75 5.00 5.25
     5.75 6.25 6.75 7.50 9.00
     11.00 13.00 15.0000
df0 3.96e-03 5.82e-04 2.90e-04 2.58e-04 2.83e-04        $ Conversion (mrem/hr)
     3.79e-04 5.01e-04 6.31e-04 7.59e-04 8.78e-04
     9.85e-04 1.08e-03 1.17e-03 1.27e-03 1.36e-03
     1.44e-03 1.52e-03 1.68e-03 1.98e-03 2.51e-03
     2.99e-03 3.42e-03 3.82e-03 4.01e-03 4.41e-03
     4.83e-03 5.23e-03 5.60e-03 5.80e-03 6.01e-03
     6.37e-03 6.74e-03 7.11e-03 7.66e-03 8.77e-03
     1.03e-02 1.18e-02 1.33e-02
C
C Material Cards
C
m1   40000 -1.00                                       $ Zirconium
m2   14000 -0.01                                       $ Stainless Steel
     24000 -0.19
     25000 -0.02
     26000 -0.68
     28000 -0.10
```

```
      179-       m3   26000 -1.00                                    $ Carbon Steel (iron)
      180-       m4   82000 -1.00                                    $ Lead
      181-       m5   1000   2                                       $ EHMW Polyethylene
      182-            6000   1
      183-       C
      184-       C Runtime and Print Cards
      185-       C
      186-       prdmp j j 1 2
      187-       ctme 480

 surface       10   and surface       12   are the same.       12   will be deleted.

 surface       11   and surface       13   are the same.       13   will be deleted.

 surface       20   and surface       22   are the same.       22   will be deleted.

 surface       21   and surface       23   are the same.       23   will be deleted.

 surface       72   and surface       75   are the same.       75   will be deleted.

  comment.           5 surfaces were deleted for being the same as others.

  warning.    1 materials had unnormalized fractions. print table 40.

  warning.  sum of segment sizes differs from total in   2 cases.
1cells                                                                    print table 60

                          atom        gram                                      photon
             cell     mat    density     density     volume       mass           pieces importance

        1       10        1  6.60141E-03 1.00000E+00 1.60880E+00 1.60880E+00           1  1.0000E+00
        2       11        1  6.60141E-03 1.00000E+00 1.60880E+00 1.60880E+00           1  1.0000E+00
        3       20        0  0.00000E+00 0.00000E+00 8.88335E-03 0.00000E+00           1  1.0000E+00
        4       21        0  0.00000E+00 0.00000E+00 8.88335E-03 0.00000E+00           1  1.0000E+00
        5       30        0  0.00000E+00 0.00000E+00 0.00000E+00 0.00000E+00           0  1.0000E+00
        6       31        5  1.21068E-01 9.40000E-01 3.70667E+04 3.48427E+04           1  1.0000E+00
        7       32        5  1.21068E-01 9.40000E-01 3.34422E+05 3.14357E+05           1  1.0000E+00
        8       33        5  1.21068E-01 9.40000E-01 3.70667E+04 3.48427E+04           1  1.0000E+00
        9       40        0  0.00000E+00 0.00000E+00 0.00000E+00 0.00000E+00           0  1.0000E+00
       10       41        3  8.46757E-02 7.85260E+00 4.35019E+03 3.41603E+04           1  1.0000E+00
       11       42        3  8.46757E-02 7.85260E+00 3.97694E+04 3.12294E+05           1  1.0000E+00
       12       43        3  8.46757E-02 7.85260E+00 6.27672E+03 4.92886E+04           1  1.0000E+00
       13       50        0  0.00000E+00 0.00000E+00 0.00000E+00 0.00000E+00           0  1.0000E+00
       14       51        2  8.80825E-02 8.01280E+00 1.97689E+04 1.58404E+05           1  1.0000E+00
       15       52        2  8.80825E-02 8.01280E+00 7.41419E+04 5.94084E+05           1  2.0000E+00
       16       53        2  8.80825E-02 8.01280E+00 8.56652E+04 6.86418E+05           1  1.0000E+00
       17       60        0  0.00000E+00 0.00000E+00 0.00000E+00 0.00000E+00           0  2.0000E+00
       18       61        2  8.80825E-02 8.01280E+00 1.11390E+05 8.92546E+05           1  1.0000E+00
       19       62        2  8.80825E-02 8.01280E+00 2.08330E+05 1.66931E+06           1  5.0000E+00
       20       63        4  3.29849E-02 1.13500E+01 0.00000E+00 0.00000E+00           0  3.0000E+01
       21       64        4  3.29849E-02 1.13500E+01 0.00000E+00 0.00000E+00           0  3.0000E+02
       22       65        2  8.80825E-02 8.01280E+00 0.00000E+00 0.00000E+00           0  3.0000E+03
       23       66        2  8.80825E-02 8.01280E+00 0.00000E+00 0.00000E+00           0  6.0000E+03
       24       67        0  0.00000E+00 0.00000E+00 0.00000E+00 0.00000E+00           0  1.0000E+05
       25       68        2  8.80825E-02 8.01280E+00 0.00000E+00 0.00000E+00           0  2.0000E+05
       26       69        2  8.80825E-02 8.01280E+00 8.34880E+04 6.68973E+05           1  1.0000E+00
       27       70        2  8.80825E-02 8.01280E+00 1.33668E+05 1.07106E+06           1  1.0000E+00
       28       71        4  3.29849E-02 1.13500E+01 0.00000E+00 0.00000E+00           0  3.0000E+01
```

```
       29       72        4  3.29849E-02 1.13500E+01 0.00000E+00 0.00000E+00          0  3.0000E+02
       30       73        2  8.80825E-02 8.01280E+00 0.00000E+00 0.00000E+00          0  3.0000E+03
       31       74        2  8.80825E-02 8.01280E+00 0.00000E+00 0.00000E+00          0  6.0000E+03
       32       75        0  0.00000E+00 0.00000E+00 0.00000E+00 0.00000E+00          0  1.0000E+05
       33       76        2  8.80825E-02 8.01280E+00 0.00000E+00 0.00000E+00          0  2.0000E+05
       34      777        0  0.00000E+00 0.00000E+00 2.26002E+07 0.00000E+00          1  2.0000E+05
       35      888        0  0.00000E+00 0.00000E+00 6.41456E+07 0.00000E+00          1  1.0000E+01
       36      999        0  0.00000E+00 0.00000E+00 0.00000E+00 0.00000E+00          0  0.0000E+00

 total                                              8.79212E+07 6.52057E+06

    minimum source weight = 1.0000E+00    maximum source weight = 1.0000E+00

 ************************************************
 * Random Number Generator  =                  1 *
 * Random Number Seed       =       19073486328125 *
 * Random Number Multiplier =       19073486328125 *
 * Random Number Adder      =                  0 *
 * Random Number Bits Used  =                 48 *
 * Random Number Stride     =             152917 *
 ************************************************


        2 warning messages so far.
1cross-section tables                                                                print table 100

     table    length

                        tables from file mcplib04

   1000.04p    1898  ENDF/B-VI Release 8 Photoatomic Data for 1-H                    mat 100      02/07/03
   6000.04p    3152  ENDF/B-VI Release 8 Photoatomic Data for 6-C                    mat 600      02/07/03
  14000.04p    4792  ENDF/B-VI Release 8 Photoatomic Data for 14-SI                  mat1400      02/07/03
  24000.04p    5682  ENDF/B-VI Release 8 Photoatomic Data for 24-CR                  mat2400      02/07/03
  25000.04p    5598  ENDF/B-VI Release 8 Photoatomic Data for 25-MN                  mat2500      02/07/03
  26000.04p    5718  ENDF/B-VI Release 8 Photoatomic Data for 26-FE                  mat2600      02/07/03
  28000.04p    5826  ENDF/B-VI Release 8 Photoatomic Data for 28-NI                  mat2800      02/07/03
  40000.04p    7703  ENDF/B-VI Release 8 Photoatomic Data for 40-ZR                  mat4000      02/07/03
  82000.04p   10010  ENDF/B-VI Release 8 Photoatomic Data for 82-PB                  mat8200      02/07/03

  total       50379

 maximum photon energy set to  100.0 mev (maximum electron energy)

                        tables from file el03

   1000.03e    2329                                                                                6/6/98
   6000.03e    2333                                                                                6/6/98
  14000.03e    2339                                                                                6/6/98
  24000.03e    2345                                                                                6/6/98
  25000.03e    2345                                                                                6/6/98
  26000.03e    2345                                                                                6/6/98
  28000.03e    2347                                                                                6/6/98
  40000.03e    2353                                                                                6/6/98
  82000.03e    2373                                                                                6/6/98

  warning.  material        1 has been set to a conductor.
```

```
 warning.  material        2 has been set to a conductor.

 warning.  material        3 has been set to a conductor.

 warning.  material        4 has been set to a conductor.

 ************************************************************************************************************************

 dump no.    1 on file runtpe     nps =           0     coll =             0     ctm =        0.00   nrn =
    0

        6 warning messages so far.

 ************************************************************************************************************************

 dump no.    2 on file runtpe     nps =     1613395     coll =      581686503     ctm =       60.02   nrn =
 8414740954

 ************************************************************************************************************************

 dump no.    3 on file runtpe     nps =     3223086     coll =     1166470585     ctm =      120.02   nrn =
 16878160785

 ************************************************************************************************************************

 dump no.    4 on file runtpe     nps =     4839116     coll =     1751733725     ctm =      180.03   nrn =
 25346914132

 ************************************************************************************************************************

 dump no.    5 on file runtpe     nps =     6457600     coll =     2337093453     ctm =      240.05   nrn =
 33817145589

 ************************************************************************************************************************

 dump no.    6 on file runtpe     nps =     8073792     coll =     2920251963     ctm =      300.06   nrn =
 42254160653

 ************************************************************************************************************************

 dump no.    7 on file runtpe     nps =     9690432     coll =     3504058119     ctm =      360.06   nrn =
 50700714784

 ************************************************************************************************************************

 dump no.    8 on file runtpe     nps =    11310592     coll =     4089000527     ctm =      420.07   nrn =
 59164915705
1problem summary

      run terminated when it had used  480  minutes of computer time.
+                                                                                    02/28/14 00:47:33
      title RH-TRU 72-B NS15 HAC Gamma Concentrated 1 g/cc Co60                probid =  02/27/14 16:47:17
0
 photon creation     tracks      weight        energy           photon loss         tracks      weight        energy
                                 (per source particle)                                        (per source particle)

 source            12930438    1.0000E+00    1.2529E+00         escape          4758299126    1.8795E-03    1.4302E-03
                                                                 energy cutoff             0    0.            1.0321E-04
```

weight window	0	0.	0.
cell importance	6080862487	1.7777E-01	6.9747E-02
weight cutoff	0	0.	0.
e or t importance	0	0.	0.
dxtran	0	0.	0.
forced collisions	0	0.	0.
exp. transform	0	0.	0.
from neutrons	0	0.	0.
bremsstrahlung	385251249	4.2463E-01	1.3649E-02
p-annihilation	1840080	2.7073E-03	1.3835E-03
photonuclear	0	0.	0.
electron x-rays	0	0.	0.
1st fluorescence	374876182	5.1098E-01	1.4567E-02
2nd fluorescence	33448095	4.3011E-02	4.8413E-04
total	6889208531	2.1591E+00	1.3527E+00

time cutoff	0	0.	0.
weight window	0	0.	0.
cell importance	719336654	1.7784E-01	6.9764E-02
weight cutoff	0	0.	0.
e or t importance	0	0.	0.
dxtran	0	0.	0.
forced collisions	0	0.	0.
exp. transform	0	0.	0.
compton scatter	0	0.	1.0612E+00
capture	1410652711	1.9780E+00	2.1837E-01
pair production	920040	1.3537E-03	1.7672E-03
photonuclear abs	0	0.	0.
total	6889208531	2.1591E+00	1.3527E+00

number of photons banked	821499167
photon tracks per source particle	5.3279E+02
photon collisions per source particle	3.6143E+02
total photon collisions	4673477297

average time of (shakes)	
escape	9.2990E-01
capture	1.7004E-01
capture or escape	1.7076E-01
any termination	1.6724E-01

cutoffs	
tco	1.0000E+33
eco	1.0000E-03
wc1	-5.0000E-01
wc2	-2.5000E-01

computer time so far in this run	480.02 minutes
computer time in mcrun	480.01 minutes
source particles per minute	2.6938E+04
random numbers generated	67621418865

maximum number ever in bank	15
bank overflows to backup file	0

most random numbers used was 483347 in history 8960875

warning. random number stride 152917 exceeded 14719 times.

range of sampled source weights = 1.0000E+00 to 1.0000E+00

warning. importance function may be poor. see print table 120.

1photon activity in each cell print table 126

	cell	tracks entering	population	collisions	collisions * weight (per history)	number weighted energy	flux weighted energy	average track weight (relative)	average track mfp (cm)
1	10	12700692	12795970	493877	3.8195E-02	1.2325E+00	1.2325E+00	1.0000E+00	1.9215E+01
2	11	290550	290180	16735	1.2942E-03	1.1613E+00	1.1613E+00	1.0000E+00	1.8260E+01
3	20	12738263	12685294	0	0.0000E+00	1.2312E+00	1.2312E+00	1.0000E+00	0.0000E+00
4	21	320640	287562	0	0.0000E+00	1.1287E+00	1.1287E+00	1.0000E+00	0.0000E+00
5	30	17819382	13008539	0	0.0000E+00	7.7501E-01	7.7501E-01	1.0000E+00	0.0000E+00
6	31	287006	255216	642717	4.9706E-02	4.5404E-01	4.5404E-01	1.0000E+00	9.4539E+00
7	32	19538748	13432000	32541035	2.5166E+00	6.6103E-01	6.6103E-01	1.0000E+00	1.1354E+01
8	33	286684	255165	642374	4.9679E-02	4.5426E-01	4.5426E-01	1.0000E+00	9.4536E+00
9	40	16976022	13195272	0	0.0000E+00	5.9370E-01	5.9370E-01	1.0000E+00	0.0000E+00
10	41	171919	163177	266609	2.0619E-02	6.0909E-01	6.0909E-01	1.0000E+00	1.4900E+00
11	42	16011413	14211007	16630995	1.2862E+00	6.5946E-01	6.5946E-01	1.0000E+00	1.5469E+00
12	43	163218	165517	329899	2.5513E-02	6.2227E-01	6.2227E-01	1.0000E+00	1.5175E+00
13	50	13393845	11375035	0	0.0000E+00	6.4778E-01	6.4778E-01	8.0912E-01	0.0000E+00
14	51	114472	127824	411127	3.1795E-02	5.9500E-01	5.9500E-01	1.0000E+00	1.4674E+00
15	52	22185384	22062607	31223849	1.2074E+00	6.4577E-01	6.4577E-01	1.0000E+00	1.5231E+00
16	53	72356	90060	381580	2.9510E-02	5.8781E-01	5.8781E-01	1.0000E+00	1.4598E+00
17	60	19711861	16841021	0	0.0000E+00	6.1967E-01	6.1967E-01	7.6154E-01	0.0000E+00
18	61	31777	38594	165441	1.2795E-02	5.5403E-01	5.5403E-01	1.0000E+00	1.4167E+00
19	62	34748029	39617127	104411802	1.6150E+00	6.1615E-01	6.1615E-01	1.0000E+00	1.4962E+00

```
        20       63    64097617    124328752    239036060    6.1621E-01   8.4922E-01   8.4922E-01   1.0000E+00   1.0110E+00
        21       64    73434975    157338715    298313364    7.6902E-02   9.1713E-01   9.1713E-01   1.0000E+00   1.1036E+00
        22       65   160201677    174495675    349983657    9.0222E-03   6.8248E-01   6.8248E-01   1.0000E+00   1.6055E+00
        23       66   198114781    219219901    451304727    5.8171E-03   6.0986E-01   6.0986E-01   1.0000E+00   1.5051E+00
        24       67   391812185    378577312            0    0.0000E+00   6.2202E-01   6.2202E-01   3.0290E+00   0.0000E+00
        25       68  3490463733   3576484006   1527599792    5.9070E-04   6.4028E-01   6.4028E-01   1.0000E+00   1.5658E+00
        26       69        8158         9338        36006    2.7846E-03   4.9636E-01   4.9636E-01   1.0000E+00   1.3317E+00
        27       70         250          294         1214    9.3887E-05   4.8964E-01   4.8964E-01   1.0000E+00   1.3367E+00
        28       71    14327728     25356812     43151984    1.1124E-01   8.6970E-01   8.6970E-01   1.0000E+00   1.0358E+00
        29       72    35326905     65352384    107043362    2.7595E-02   9.2801E-01   9.2801E-01   1.0000E+00   1.1152E+00
        30       73   124957967    136009635    239804859    6.1819E-03   7.1049E-01   7.1049E-01   1.0000E+00   1.6430E+00
        31       74   141317159    154559709    287563371    3.7065E-03   6.2802E-01   6.2802E-01   1.0000E+00   1.5283E+00
        32       75  1959340935   1955320726            0    0.0000E+00   6.9312E-01   6.9312E-01   5.2356E-01   0.0000E+00
        33       76  2272829636   2327179871    941480861    3.6406E-04   6.4897E-01   6.4897E-01   1.0000E+00   1.5735E+00
        34      777  4758298824   4758298824            0    0.0000E+00   7.3469E-01   7.3469E-01   1.0104E+00   0.0000E+00
        35      888  4758299126   4758299126            0    0.0000E+00   7.7046E-01   7.7046E-01   5.1096E-05   0.0000E+00

            total   18630393917  18981728247   4673477297    7.7448E+00

1tally        2        nps =    12930438
+                              Surface Dose (mrem/hr)                                $ Surface detector
            tally type 2    particle flux averaged over a surface.
            tally for  photons

            this tally is modified by a dose function.

            areas
                 surface:      69
                segment
                  1       1.00000E+00
                  2       2.02680E+01
                  3       1.00000E+00
                whole      1.00000E+00

 surface  69
 segment:          -888
                1.25458E-06 0.0015

 surface  69
 segment:           888       -777
                4.59639E-09 0.0047

 surface  69
 segment:           888        777
                2.32291E-06 0.0012

 surface  69
 segment:   whole surface
                3.67065E-06 0.0009


 ============================================================================================================================

            results of 10 statistical checks for the estimated answer for the tally fluctuation chart (tfc) bin of tally        2

 tfc bin     --mean--      ---------relative error---------      ----variance of the variance----      --figure of merit--     -pdf-
 behavior    behavior      value   decrease   decrease rate      value   decrease   decrease rate       value     behavior     slope
```

```
 desired      random       <0.10      yes      1/sqrt(nps)       <0.10      yes        1/nps          constant    random      >3.00
 observed     random        0.00      yes          yes            0.00      yes         yes           constant    random       2.11
 passed?        yes          yes      yes          yes             yes      yes         yes              yes        yes          no

 ================================================================================================================================

 warning.  the tally in the tally fluctuation chart bin did not pass  1 of the 10 statistical checks.

1analysis of the results in the tally fluctuation chart bin (tfc) for tally        2 with nps=    12930438 print table 160

 normed average tally per history  = 3.67065E-06          unnormed average tally per history  = 3.67065E-06
 estimated tally relative error    = 0.0009               estimated variance of the variance  = 0.0001
 relative error from zero tallies  = 0.0005               relative error from nonzero scores  = 0.0008

 number of nonzero history tallies =     2735089          efficiency for the nonzero tallies  = 0.2115
 history number of largest  tally  =    10921416          largest  unnormalized history tally = 2.77763E-03
 (largest  tally)/(average tally)  = 7.56714E+02          (largest  tally)/(avg nonzero tally)= 1.60063E+02

 (confidence interval shift)/mean  = 0.0000               shifted confidence interval center  = 3.67065E-06

 if the largest  history score sampled so far were to occur on the next history, the tfc bin quantities would change as follows:

      estimated quantities           value at nps           value at nps+1          value(nps+1)/value(nps)-1.

      mean                            3.67065E-06            3.67086E-06                  0.000058
      relative error                  9.46159E-04            9.47907E-04                  0.001847
      variance of the variance        5.65449E-05            7.05634E-05                  0.247917
      shifted center                  3.67065E-06            3.67066E-06                  0.000000
      figure of merit                 2.32713E+03            2.31856E+03                 -0.003684

 the estimated inverse power slope of the 198 largest  tallies starting at 2.37604E-04 is 2.1060
 the large score tail of the empirical history score probability density function appears to have no unsampled regions.

 fom = (histories/minute)*(f(x) signal-to-noise ratio)**2 = (2.694E+04)*( 2.939E-01)**2 = (2.694E+04)*(8.639E-02) = 2.327E+03

1unnormed tally density for tally       2          nonzero tally mean(m) = 1.735E-05   nps =    12930438  print table 161

 abscissa              ordinate   log plot of tally probability density function in tally fluctuation chart bin(d=decade,slope= 2.1)
  tally  number num den log den:d----------d----------d----------d----------d----------d----------d----------d----------
 2.00-09     15 1.58+03   3.197 ***********|***********|***********|***********|***********|***********|**********  |
 3.16-09     28 1.86+03   3.268 ***********|***********|***********|***********|***********|***********|***********|
 5.01-09     53 2.22+03   3.346 ***********|***********|***********|***********|***********|***********|***********|
 7.94-09     75 1.98+03   3.296 ***********|***********|***********|***********|***********|***********|***********|
 1.26-08    107 1.78+03   3.251 ***********|***********|***********|***********|***********|***********|***********|
 2.00-08    171 1.80+03   3.254 ***********|***********|***********|***********|***********|***********|***********|
 3.16-08    371 2.46+03   3.391 ***********|***********|***********|***********|***********|***********|***********|
 5.01-08    793 3.32+03   3.521 ***********|***********|***********|***********|***********|***********|***********|*
 7.94-08   2023 5.34+03   3.727 ***********|***********|***********|***********|***********|***********|***********|****
 1.26-07   4320 7.19+03   3.857 ***********|***********|***********|***********|***********|***********|***********|*****
 2.00-07   9220 9.68+03   3.986 ***********|***********|***********|***********|***********|***********|***********|*******
 3.16-07  15755 1.04+04   4.019 ***********|***********|***********|***********|***********|***********|***********|*******
 5.01-07  28955 1.21+04   4.083 ***********|***********|***********|***********|***********|***********|***********|********
 7.94-07  55415 1.46+04   4.165 ***********|***********|***********|***********|***********|***********|***********|*********
 1.26-06  99240 1.65+04   4.218 ***********|***********|***********|***********|***********|***********|***********|**********
 2.00-06 155125 1.63+04   4.212 ***********|***********|***********|***********|***********|***********|***********|**********
```

```
 3.16-06 209821 1.39+04   4.143 ************|************|************|************|************|************|************|*********
 5.01-06 273418 1.14+04   4.058 ************|************|************|************|************|************|************|*********
 7.94-06 343325 9.06+03   3.957 ************|************|************|************|************|************|************|*******
 1.26-05 389680 6.49+03   3.812 ************|************|************|************|************|************|************|*****
 2.00-05 389244 4.09+03   3.612 mmmmmmmmmmmm|mmmmmmmmmmmm|mmmmmmmmmmmm|mmmmmmmmmmmm|mmmmmmmmmmmm|mmmmmmmmmmmm|mmmmmmmmmmmm|mm
 3.16-05 329885 2.19+03   3.340 ************|************|************|************|************|************|************|
 5.01-05 228240 9.54+02   2.980 ************|************|************|************|************|************|*******     |
 7.94-05 128130 3.38+02   2.529 ************|************|************|************|************|************|*           |
 1.26-04  56246 9.36+01   1.971 ************|************|************|************|************|*******     |           |
 2.00-04  14389 1.51+01   1.179 ************|************|************|************|***********  |            |           |
 3.16-04   1023 6.78-01  -0.169 ************|************|************|*****       |  s         |            |           |
 5.01-04      8 3.35-03  -2.476 ************|*           |            |          s |            |            |           |
 7.94-04      2 5.28-04  -3.278 ****        |            |            |     s      |            |            |           |
 1.26-03      3 4.99-04  -3.302 ***         |            |            s|            |            |            |           |
 2.00-03      4 4.20-04  -3.377 **          |            |       s    |            |            |            |           |
 3.16-03      5 3.31-04  -3.480 *           |            | s          |            |            |            |           |
  total 2735089 2.12-01         d-----------d------------d------------d-----------d------------d------------d-----------d----------

1tally       22        nps =    12930438
+                                  1-meter Dose (mrem/hr)                                $ 1-m detector
          tally type 2    particle flux averaged over a surface.
          tally for  photons

          this tally is modified by a dose function.

          areas
               surface:      80
              segment
                1       1.00000E+00
                2       2.02680E+01
                3       1.00000E+00
               whole      1.00000E+00

 surface  80
 segment:          -888
                1.07350E-06 0.0014

 surface  80
 segment:           888       -777
                1.12475E-10 0.0174

 surface  80
 segment:           888        777
                2.03617E-06 0.0013

 surface  80
 segment:   whole surface
                3.11195E-06 0.0010


 ============================================================================================================================================

          results of 10 statistical checks for the estimated answer for the tally fluctuation chart (tfc) bin of tally       22

 tfc bin     --mean--      ---------relative error---------      ----variance of the variance----      --figure of merit--     -pdf-
 behavior    behavior      value   decrease   decrease rate      value   decrease   decrease rate       value     behavior     slope

 desired      random       <0.10      yes      1/sqrt(nps)       <0.10      yes        1/nps           constant    random      >3.00
```

```
 observed     random        0.00      yes          yes            0.00      yes         yes            constant    random       3.12
 passed?        yes          yes      yes          yes             yes      yes         yes               yes        yes         yes

 ================================================================================================================================


 this tally meets the statistical criteria used to form confidence intervals: check the tally fluctuation chart to verify.
 the results in other bins associated with this tally may not meet these statistical criteria.

 ----- estimated confidence intervals:  -----

 estimated asymmetric confidence interval(1,2,3 sigma): 3.1089E-06 to 3.1150E-06; 3.1059E-06 to 3.1180E-06; 3.1029E-06 to 3.1210E-06
 estimated  symmetric confidence interval(1,2,3 sigma): 3.1089E-06 to 3.1150E-06; 3.1059E-06 to 3.1180E-06; 3.1029E-06 to 3.1210E-06

1analysis of the results in the tally fluctuation chart bin (tfc) for tally       22 with nps=    12930438 print table 160


 normed average tally per history  = 3.11195E-06          unnormed average tally per history  = 3.11195E-06
 estimated tally relative error    = 0.0010               estimated variance of the variance  = 0.0000
 relative error from zero tallies  = 0.0005               relative error from nonzero scores  = 0.0008

 number of nonzero history tallies =     2735044          efficiency for the nonzero tallies  = 0.2115
 history number of largest  tally  =     4877242          largest  unnormalized history tally = 1.45738E-03
 (largest  tally)/(average tally)  = 4.68318E+02          (largest  tally)/(avg nonzero tally)= 9.90586E+01

 (confidence interval shift)/mean  = 0.0000               shifted confidence interval center  = 3.11195E-06


 if the largest  history score sampled so far were to occur on the next history, the tfc bin quantities would change as follows:

      estimated quantities           value at nps           value at nps+1          value(nps+1)/value(nps)-1.

      mean                            3.11195E-06            3.11206E-06                  0.000036
      relative error                  9.70085E-04            9.70723E-04                  0.000658
      variance of the variance        9.18696E-06            1.10824E-05                  0.206318
      shifted center                  3.11195E-06            3.11195E-06                  0.000000
      figure of merit                 2.21376E+03            2.21085E+03                 -0.001314

 the estimated inverse power slope of the 198 largest  tallies starting at 2.15148E-04 is 3.1221
 the history score probability density function appears to have an unsampled region at the largest  history scores:
 please examine. see print table 161.

 fom = (histories/minute)*(f(x) signal-to-noise ratio)**2 = (2.694E+04)*( 2.867E-01)**2 = (2.694E+04)*(8.218E-02) = 2.214E+03

1status of the statistical checks used to form confidence intervals for the mean for each tally bin


 tally   result of statistical checks for the tfc bin (the first check not passed is listed) and error magnitude check for all bins

        2   missed  1 of 10 tfc bin checks: the slope of decrease of largest tallies is less than the minimum acceptable value of 3.0
          passed all bin error check:     4 tally bins all have relative errors less than 0.10 with no zero bins

       22   passed the 10 statistical checks for the tally fluctuation chart bin result
          passed all bin error check:     4 tally bins all have relative errors less than 0.10 with no zero bins


 the 10 statistical checks are only for the tally fluctuation chart bin and do not apply to other tally bins.
```

```
 warning.       1 of the     2 tally fluctuation chart bins did not pass all 10 statistical checks.
1tally fluctuation charts

                          tally        2                          tally       22
         nps      mean     error   vov  slope    fom      mean     error   vov  slope    fom
     1024000   3.6606E-06 0.0034 0.0021  4.0    2259   3.1016E-06 0.0034 0.0001 10.0    2214
     2048000   3.6702E-06 0.0024 0.0006  3.2    2309   3.1111E-06 0.0024 0.0000  8.5    2222
     3072000   3.6780E-06 0.0019 0.0003  3.3    2326   3.1182E-06 0.0020 0.0000  5.6    2218
     4096000   3.6773E-06 0.0017 0.0002  3.1    2337   3.1178E-06 0.0017 0.0000  4.9    2218
     5120000   3.6761E-06 0.0015 0.0002  2.6    2321   3.1166E-06 0.0015 0.0000  4.0    2211
     6144000   3.6744E-06 0.0014 0.0001  2.5    2315   3.1150E-06 0.0014 0.0000  4.1    2211
     7168000   3.6747E-06 0.0013 0.0001  2.4    2319   3.1155E-06 0.0013 0.0000  3.4    2207
     8192000   3.6735E-06 0.0012 0.0001  2.3    2323   3.1145E-06 0.0012 0.0000  3.3    2207
     9216000   3.6713E-06 0.0011 0.0001  2.3    2328   3.1127E-06 0.0011 0.0000  3.2    2209
    10240000   3.6708E-06 0.0011 0.0001  2.4    2333   3.1123E-06 0.0011 0.0000  3.3    2211
    11264000   3.6718E-06 0.0010 0.0001  2.2    2326   3.1129E-06 0.0010 0.0000  3.2    2213
    12288000   3.6708E-06 0.0010 0.0001  2.1    2323   3.1120E-06 0.0010 0.0000  3.1    2212
    12930438   3.6707E-06 0.0009 0.0001  2.1    2327   3.1119E-06 0.0010 0.0000  3.1    2214

 ************************************************************************************************************************

 dump no.    9 on file runtpe     nps =    12930438     coll =     4673477297     ctm =      480.01   nrn =
 67621418865
 tally data written to file mctal

        10 warning messages so far.


 run terminated when it had used  480  minutes of computer time.

 computer time =  480.02 minutes

 mcnp     version 5     09282010                     02/28/14 00:47:33                     probid =  02/27/14 16:47:17
```

5.7.2.3 RH-TRU 72-B – NS30 Neutron Shielded Canister

5.7.2.3.1 NCT Concentrated 60Co Gamma Source – 8ng001.io

```
          Thread Name & Version = MCNP5, 1.60

            _  _     _  _  _      _
           |_||_|  (_  |_||  |_)  |_)
                          |

  +-------------------------------------------------------------------+
  | Copyright 2010. Los Alamos National Security, LLC.  All rights    |
  | reserved.                                                         |
  |   This material was produced under U.S. Government contract       |
  | DE-AC52-06NA25396 for Los Alamos National Laboratory, which is    |
  | operated by Los Alamos National Security, LLC, for the U.S.       |
  | Department of Los Energy. The Government is granted for itself and|
  | others acting on its behalf a paid-up, nonexclusive, irrevocable  |
  | worldwide license in this material to reproduce, prepare derivative|
  | works, and perform publicly and display publicly. Beginning five  |
  | (5) years after 2010, subject to additional five-year worldwide   |
```

| renewals, the Government is granted for itself and others acting on |
| its behalf a paid-up, nonexclusive, irrevocable worldwide license |
| in this material to reproduce, prepare derivative works, distribute |
| copies to the public, perform publicly and display publicly, and to |
| permit others to do so. NEITHER THE UNITED STATES NOR THE UNITED |
| STATES DEPARTMENT OF ENERGY, NOR LOS ALAMOS NATIONAL SECURITY, LLC, |
| NOR ANY OF THEIR EMPLOYEES, MAKES ANY WARRANTY, EXPRESS OR IMPLIED, |
| OR ASSUMES ANY LEGAL LIABILITY OR RESPONSIBILITY FOR THE ACCURACY, |
| COMPLETENESS, OR USEFULNESS OF ANY INFORMATION, APPARATUS, PRODUCT, |
| OR PROCESS DISCLOSED, OR REPRESENTS THAT ITS USE WOULD NOT INFRINGE |
| PRIVATELY OWNED RIGHTS. |

```
1mcnp     version 5     ld=09282010                    02/28/14 04:47:39
 ***********************************************************************                probid =  02/28/14 04:47:39
 inp=8ng001.i

         1-       title RH-TRU 72-B NS30 NCT Gamma Concentrated 1 g/cc Co60
         2-       C
         3-       C Cell Cards
         4-       C
         5-       10  1 -1        10  -11  -16                imp:p=1    $ Source #1
         6-       11  1 -1        12  -13  -17                imp:p=1    $ Source #2
         7-       12  1 -1        14  -15  -18                imp:p=1    $ Source #3
         8-       20  0           20  -21  -26
         9-                     (-10:  11:  16)               imp:p=1    $ Drum #1 cavity
        10-       21  0           22  -23  -27
        11-                     (-12:  13:  17)               imp:p=1    $ Drum #2 cavity
        12-       22  0           24  -25  -28
        13-                     (-14:  15:  18)               imp:p=1    $ Drum #3 cavity
        14-       30  0           31  -35  -33
        15-                      #10  #11  #12
        16-                      #20  #21  #22                imp:p=1    $ NS30 cavity
        17-       31  5 -0.94000  30  -31  -32                imp:p=1    $ NS30 botcap
        18-       32  5 -0.94000  31  -35   33  -32           imp:p=1    $ NS30 body
        19-       33  5 -0.94000  35  -34  -32                imp:p=1    $ NS30 topcap
        20-       40  0           41  -45  -43
        21-                     (-30:  32:  34)               imp:p=1    $ RLC cavity
        22-       41  3 -7.85260  40  -41  -42                imp:p=1    $ RLC base
        23-       42  3 -7.85260  41  -46   43  -42           imp:p=1    $ RLC shell
        24-       43  3 -7.85260  45  -44  -43                imp:p=1    $ RLC lid
        25-       50  0           51  -53  -55
        26-                     (-40:  42:  46)
        27-                    :( 44  -46  -43)               imp:p=1    $ IV cavity
        28-       51  2 -8.01280  50  -51  -52                imp:p=1    $ IV base
        29-       52  2 -8.01280  51  -55   53  -52           imp:p=2    $ IV shell
        30-       53  2 -8.01280  55  -54  -52                imp:p=1    $ IV lid
        31-       60  0           61  -63  -65
        32-                     (-50:  52:  54)               imp:p=2    $ OC cavity
        33-       61  2 -8.01280  60  -61  -69                imp:p=1    $ OC base
        34-       62  2 -8.01280  61  -66   65  -64           imp:p=5    $ OC ishell
        35-       63  4 -11.3500  61  -66   64  -76  71       imp:p=3E1  $ OC lead in
        36-       64  4 -11.3500  61  -66   76  -68  71       imp:p=3E2  $ OC lead out
        37-       65  2 -8.01280  61  -66   68  -77  71       imp:p=3E3  $ OC oshell in
        38-       66  2 -8.01280  61  -66   77  -67  71       imp:p=6E3  $ OC oshell out
        39-       67  0           61  -66   67  -70  71       imp:p=1E5  $ OC airgap
        40-       68  2 -8.01280  61  -66   70  -69  71       imp:p=2E5  $ OC tshell
        41-       69  2 -8.01280  66  -63   65  -69           imp:p=1    $ OC flange
```

```
      42-       70  2 -8.01280  63  -62  -69                imp:p=1    $ OC lid
      43-       71  4 -11.3500  64  -78  -71                imp:p=3E1  $ OC lead punct in
      44-       72  4 -11.3500  78  -73  -71                imp:p=3E2  $ OC lead punct out
      45-       73  2 -8.01280  73  -79  -71                imp:p=3E3  $ OC oshell punct in
      46-       74  2 -8.01280  79  -72  -71                imp:p=6E3  $ OC oshell punct out
      47-       75  0           72  -75  -71                imp:p=1E5  $ OC airgap punct
      48-       76  2 -8.01280  75  -74  -71                imp:p=2E5  $ OC tshell punct
      49-       777 0           69  -80   60  -62           imp:p=2E5  $ Outside to tally
      50-       888 0          -999
      51-                     (-60:  80:  62)               imp:p=1E1  $ Outside pkg
      52-       999 0           999                          imp:p=0    $ Outside world
      53-
      54-       C
      55-       C Geometry Cards
      56-       C
      57-       10  pz 88.9                                              $ Source #1 bottom
      58-       11  pz 91.44                                             $ Source #1 top
      59-       12  pz 162.878                                           $ Source #2 bottom
      60-       13  pz 165.418                                           $ Source #2 top
      61-       14  pz 236.855                                           $ Source #3 bottom
      62-       15  pz 239.395                                           $ Source #3 top
      63-       16  c/z 0 0 1.27                                        $ Source #1 radius
warning.  this surface has been replaced by a surface of type cz
      64-       17  c/z 0 0 1.27                                        $ Source #2 radius
warning.  this surface has been replaced by a surface of type cz
      65-       18  c/z 0 0 1.27                                        $ Source #3 radius
      66-       C
warning.  this surface has been replaced by a surface of type cz
      67-       20  pz 53.34                                            $ Drum #1 bottom
      68-       21  pz 127                                              $ Drum #1 top
      69-       22  pz 127.318                                          $ Drum #2 bottom
      70-       23  pz 200.978                                          $ Drum #2 top
      71-       24  pz 201.295                                          $ Drum #3 bottom
      72-       25  pz 274.955                                          $ Drum #3 top
      73-       26  c/z 0 0 24.765                                      $ Drum #1 radius
warning.  this surface has been replaced by a surface of type cz
      74-       27  c/z 0 0 24.765                                      $ Drum #2 radius
warning.  this surface has been replaced by a surface of type cz
      75-       28  c/z 0 0 24.765                                      $ Drum #3 radius
      76-       C
warning.  this surface has been replaced by a surface of type cz
      77-       30  pz 21.908                                           $ NS30 botcap (outside)
      78-       31  pz 34.608                                           $ NS30 botcap (inside)
      79-       32  c/z 0 0 30.48                                       $ NS30 body (outside)
warning.  this surface has been replaced by a surface of type cz
      80-       33  c/z 0 0 26.787                                      $ NS30 body (inside)
warning.  this surface has been replaced by a surface of type cz
      81-       34  pz 306.388                                          $ NS30 topcap (outside)
      82-       35  pz 293.688                                          $ NS30 topcap (inside)
      83-       C
      84-       40  pz 19.368                                           $ RLC base (outside)
      85-       41  pz 20.638                                           $ RLC base (inside)
      86-       42  c/z 0 0 33.02                                       $ RLC shell (outside)
warning.  this surface has been replaced by a surface of type cz
      87-       43  c/z 0 0 32.385                                      $ RLC shell (inside)
warning.  this surface has been replaced by a surface of type cz
      88-       44  pz 309.563                                          $ RLC lid (outside)
      89-       45  pz 307.658                                          $ RLC lid (inside)
```

```
      90-       46  pz 325.438                                          $ RLC top (outside)
      91-       C
      92-       50  pz 14.288                                           $ IV base (outside)
      93-       51  pz 18.098                                           $ IV base (inside)
      94-       52  c/z 0 0 40.64                                       $ IV shell (outside)
 warning.  this surface has been replaced by a surface of type cz
      95-       53  c/z 0 0 39.688                                      $ IV shell (inside)
 warning.  this surface has been replaced by a surface of type cz
      96-       54  pz 343.218                                          $ IV top (outside)
      97-       55  pz 326.708                                          $ IV top (inside)
      98-       C
      99-       60  pz 0                                                $ OC bottom (outside)
     100-       61  pz 12.7                                             $ OC bottom (inside)
     101-       62  pz 360.045                                          $ OC top (outside)
     102-       63  pz 344.805                                          $ OC top (inside)
     103-       64  cz 43.656                                           $ OC ishell (outside)
     104-       65  cz 41.116                                           $ OC ishell (inside)
     105-       66  pz 320.675                                          $ OC lead (upper)
     106-       67  cz 52.229                                           $ OC oshell (outside)
     107-       68  cz 48.419                                           $ OC oshell (inside)
     108-       69  cz 52.838                                           $ OC therm (outside)
     109-       70  cz 52.495                                           $ OC therm (inside)
     110-       71  c/x 0 164.148 10.033                                $ OC puncture radius
     111-       72  cz 52.229                                           $ OC oshell punct (out)
     112-       73  cz 48.419                                           $ OC oshell punct (in)
     113-       74  cz 52.838                                           $ OC therm punct (out)
     114-       75  cz 52.495                                           $ OC therm punct (in)
     115-       76  cz 46.038                                           $ OC lead (mid)
     116-       77  cz 50.324                                           $ OC oshell (mid)
     117-       78  cz 46.038                                           $ OC lead punct (mid)
     118-       79  cz 50.324                                           $ OC oshell punct (mid)
     119-       C
     120-       80  cz 252.838                                          $ 2-meter from OC therm
     121-       C
     122-       777 pz 161.608                                          $ Ring tally (lower)
     123-       888 pz 166.688                                          $ Ring tally (upper)
     124-       999 sz 164.148 379.838                                  $ Outside world
     125-
     126-       C
     127-       C Physics Cards
     128-       C
     129-       mode p
     130-       C
     131-       C Source Cards
     132-       C
     133-       C Cylindrical Sources
     134-       sdef pos=d1 erg=d2 par=2 axs=0 0 1 rad=d3 ext=d4
     135-       sc1 Co60
     136-       C Source Position and Fraction
     137-       si1 L 0 0 90.17
     138-             0 0 164.148
     139-             0 0 238.125
     140-       sp1   1 1 1
     141-       C Source Energy (MeV) and Intensity (%)
     142-       si2 L 3.469300E-01 8.262800E-01 1.173237E+00 1.332501E+00
     143-            2.158770E+00 2.505000E+00
     144-       sp2 7.600000E-03 7.600000E-03 9.997360E+01 9.998560E+01
     145-            1.110000E-03 2.000000E-06
```

```
      146-       C Source Radius
      147-       si3 0 1.27
      148-       sp3 -21 1
      149-       C Source Extent
      150-       si4 -1.27 1.27
      151-       sp4 -21 0
      152-       C
      153-       C Tally Cards
      154-       C
      155-       f2:p 69
      156-       fc2 Surface Dose (mrem/hr)                              $ Surface detector
      157-       fs2 888 777 t
      158-       sd2 1.0 1686.525 1.0 1.0                                $ Surface tally area
      159-       f22:p 80
      160-       fc22 2-meter Dose (mrem/hr)                             $ 2-m detector
      161-       fs22 888 777 t
      162-       sd22 1.0 8070.229 1.0 1.0                               $ Surface tally area
      163-       C
      164-       C ANSI/ANS-6.1.1-1977 Gamma Flux to Dose Factors (mrem/hr)
      165-       de0 1.0e-02 3.0e-02 5.0e-02 7.0e-02 1.0e-01             $ Energy (Mev)
      166-            1.5e-01 2.0e-01 2.5e-01 3.0e-01 3.5e-01
      167-            4.0e-01 4.5e-01 5.0e-01 5.5e-01 6.0e-01
      168-            6.5e-01 7.0e-01 8.0e-01 1.00 1.40
      169-            1.80 2.20 2.60 2.80 3.25
      170-            3.75 4.25 4.75 5.00 5.25
      171-            5.75 6.25 6.75 7.50 9.00
      172-            11.00 13.00 15.0000
      173-       df0 3.96e-03 5.82e-04 2.90e-04 2.58e-04 2.83e-04        $ Conversion (mrem/hr)
      174-            3.79e-04 5.01e-04 6.31e-04 7.59e-04 8.78e-04
      175-            9.85e-04 1.08e-03 1.17e-03 1.27e-03 1.36e-03
      176-            1.44e-03 1.52e-03 1.68e-03 1.98e-03 2.51e-03
      177-            2.99e-03 3.42e-03 3.82e-03 4.01e-03 4.41e-03
      178-            4.83e-03 5.23e-03 5.60e-03 5.80e-03 6.01e-03
      179-            6.37e-03 6.74e-03 7.11e-03 7.66e-03 8.77e-03
      180-            1.03e-02 1.18e-02 1.33e-02
      181-       C
      182-       C Material Cards
      183-       C
      184-       m1   40000 -1.00                                         $ Zirconium
      185-       m2   14000 -0.01                                         $ Stainless Steel
      186-            24000 -0.19
      187-            25000 -0.02
      188-            26000 -0.68
      189-            28000 -0.10
      190-       m3   26000 -1.00                                         $ Carbon Steel (iron)
      191-       m4   82000 -1.00                                         $ Lead
      192-       m5   1000   2                                           $ EHMW Polyethylene
      193-            6000   1
      194-       C
      195-       C Runtime and Print Cards
      196-       C
      197-       prdmp j j 1 2
      198-       ctme 120

surface       16   and surface       17   are the same.       17   will be deleted.

surface       16   and surface       18   are the same.       18   will be deleted.
```

```
 surface       26   and surface       27   are the same.       27   will be deleted.

 surface       26   and surface       28   are the same.       28   will be deleted.

 surface       67   and surface       72   are the same.       72   will be deleted.

 surface       68   and surface       73   are the same.       73   will be deleted.

 surface       69   and surface       74   are the same.       74   will be deleted.

 surface       70   and surface       75   are the same.       75   will be deleted.

 surface       76   and surface       78   are the same.       78   will be deleted.

 surface       77   and surface       79   are the same.       79   will be deleted.

  comment.          10 surfaces were deleted for being the same as others.

  warning.    1 materials had unnormalized fractions. print table 40.

  warning.  sum of segment sizes differs from total in   2 cases.
1cells                                                                          print table 60
```

	cell	mat	atom density	gram density	volume	mass	pieces	photon importance
1	10	1	6.60141E-03	1.00000E+00	1.28704E+01	1.28704E+01	1	1.0000E+00
2	11	1	6.60141E-03	1.00000E+00	1.28704E+01	1.28704E+01	1	1.0000E+00
3	12	1	6.60141E-03	1.00000E+00	1.28704E+01	1.28704E+01	1	1.0000E+00
4	20	0	0.00000E+00	0.00000E+00	1.41912E+05	0.00000E+00	1	1.0000E+00
5	21	0	0.00000E+00	0.00000E+00	1.41912E+05	0.00000E+00	1	1.0000E+00
6	22	0	0.00000E+00	0.00000E+00	1.41912E+05	0.00000E+00	1	1.0000E+00
7	30	0	0.00000E+00	0.00000E+00	1.58251E+05	0.00000E+00	1	1.0000E+00
8	31	5	1.21068E-01	9.40000E-01	3.70667E+04	3.48427E+04	1	1.0000E+00
9	32	5	1.21068E-01	9.40000E-01	1.72134E+05	1.61806E+05	1	1.0000E+00
10	33	5	1.21068E-01	9.40000E-01	3.70667E+04	3.48427E+04	1	1.0000E+00
11	40	0	0.00000E+00	0.00000E+00	1.15399E+05	0.00000E+00	1	1.0000E+00
12	41	3	8.46757E-02	7.85260E+00	4.35019E+03	3.41603E+04	1	1.0000E+00
13	42	3	8.46757E-02	7.85260E+00	3.97694E+04	3.12294E+05	1	1.0000E+00
14	43	3	8.46757E-02	7.85260E+00	6.27672E+03	4.92886E+04	1	1.0000E+00
15	50	0	0.00000E+00	0.00000E+00	5.31049E+05	0.00000E+00	1	1.0000E+00
16	51	2	8.80825E-02	8.01280E+00	1.97689E+04	1.58404E+05	1	1.0000E+00
17	52	2	8.80825E-02	8.01280E+00	7.41419E+04	5.94084E+05	1	2.0000E+00
18	53	2	8.80825E-02	8.01280E+00	8.56652E+04	6.86418E+05	1	1.0000E+00
19	60	0	0.00000E+00	0.00000E+00	5.70765E+04	0.00000E+00	1	2.0000E+00
20	61	2	8.80825E-02	8.01280E+00	1.11390E+05	8.92546E+05	1	1.0000E+00
21	62	2	8.80825E-02	8.01280E+00	2.08330E+05	1.66931E+06	1	5.0000E+00
22	63	4	3.29849E-02	1.13500E+01	0.00000E+00	0.00000E+00	0	3.0000E+01
23	64	4	3.29849E-02	1.13500E+01	0.00000E+00	0.00000E+00	0	3.0000E+02
24	65	2	8.80825E-02	8.01280E+00	0.00000E+00	0.00000E+00	0	3.0000E+03
25	66	2	8.80825E-02	8.01280E+00	0.00000E+00	0.00000E+00	0	6.0000E+03
26	67	0	0.00000E+00	0.00000E+00	0.00000E+00	0.00000E+00	0	1.0000E+05
27	68	2	8.80825E-02	8.01280E+00	0.00000E+00	0.00000E+00	0	2.0000E+05
28	69	2	8.80825E-02	8.01280E+00	8.34880E+04	6.68973E+05	1	1.0000E+00
29	70	2	8.80825E-02	8.01280E+00	1.33668E+05	1.07106E+06	1	1.0000E+00
30	71	4	3.29849E-02	1.13500E+01	0.00000E+00	0.00000E+00	0	3.0000E+01
31	72	4	3.29849E-02	1.13500E+01	0.00000E+00	0.00000E+00	0	3.0000E+02
32	73	2	8.80825E-02	8.01280E+00	0.00000E+00	0.00000E+00	0	3.0000E+03

```
       33       74        2  8.80825E-02 8.01280E+00 0.00000E+00 0.00000E+00          0  6.0000E+03
       34       75        0  0.00000E+00 0.00000E+00 0.00000E+00 0.00000E+00          0  1.0000E+05
       35       76        2  8.80825E-02 8.01280E+00 0.00000E+00 0.00000E+00          0  2.0000E+05
       36      777        0  0.00000E+00 0.00000E+00 6.91509E+07 0.00000E+00          1  2.0000E+05
       37      888        0  0.00000E+00 0.00000E+00 1.57245E+08 0.00000E+00          1  1.0000E+01
       38      999        0  0.00000E+00 0.00000E+00 0.00000E+00 0.00000E+00          0  0.0000E+00

 total                                              2.28696E+08 6.36806E+06

    minimum source weight = 1.0000E+00    maximum source weight = 1.0000E+00

 ************************************************
 * Random Number Generator  =                  1 *
 * Random Number Seed       =       19073486328125 *
 * Random Number Multiplier =       19073486328125 *
 * Random Number Adder      =                  0 *
 * Random Number Bits Used  =                 48 *
 * Random Number Stride     =             152917 *
 ************************************************


        14 warning messages so far.
1cross-section tables                                                                print table 100

     table    length

                         tables from file mcplib04

   1000.04p    1898  ENDF/B-VI Release 8 Photoatomic Data for 1-H                    mat 100      02/07/03
   6000.04p    3152  ENDF/B-VI Release 8 Photoatomic Data for 6-C                    mat 600      02/07/03
  14000.04p    4792  ENDF/B-VI Release 8 Photoatomic Data for 14-SI                  mat1400      02/07/03
  24000.04p    5682  ENDF/B-VI Release 8 Photoatomic Data for 24-CR                  mat2400      02/07/03
  25000.04p    5598  ENDF/B-VI Release 8 Photoatomic Data for 25-MN                  mat2500      02/07/03
  26000.04p    5718  ENDF/B-VI Release 8 Photoatomic Data for 26-FE                  mat2600      02/07/03
  28000.04p    5826  ENDF/B-VI Release 8 Photoatomic Data for 28-NI                  mat2800      02/07/03
  40000.04p    7703  ENDF/B-VI Release 8 Photoatomic Data for 40-ZR                  mat4000      02/07/03
  82000.04p   10010  ENDF/B-VI Release 8 Photoatomic Data for 82-PB                  mat8200      02/07/03

  total       50379

 maximum photon energy set to  100.0 mev (maximum electron energy)

                         tables from file el03

   1000.03e    2329                                                                                6/6/98
   6000.03e    2333                                                                                6/6/98
  14000.03e    2339                                                                                6/6/98
  24000.03e    2345                                                                                6/6/98
  25000.03e    2345                                                                                6/6/98
  26000.03e    2345                                                                                6/6/98
  28000.03e    2347                                                                                6/6/98
  40000.03e    2353                                                                                6/6/98
  82000.03e    2373                                                                                6/6/98

  warning.  material        1 has been set to a conductor.

  warning.  material        2 has been set to a conductor.
```

```
  warning.  material        3 has been set to a conductor.

  warning.  material        4 has been set to a conductor.

 ************************************************************************************************************************

 dump no.    1 on file runtpe     nps =           0     coll =              0     ctm =        0.00   nrn =
    0

       18 warning messages so far.

 ************************************************************************************************************************

 dump no.    2 on file runtpe     nps =     1030864     coll =      579658311     ctm =       60.00   nrn =
 8350620522
1problem summary

      run terminated when it had used  120  minutes of computer time.
+                                                                                    02/28/14 06:47:41
      title RH-TRU 72-B NS30 NCT Gamma Concentrated 1 g/cc Co60                probid =  02/28/14 04:47:39
0
 photon creation     tracks      weight        energy            photon loss         tracks      weight        energy
                                 (per source particle)                                         (per source particle)

 source              2060012    1.0000E+00    1.2528E+00         escape          1290538247    3.2105E-03    2.5086E-03
                                                                 energy cutoff             0    0.            1.3907E-04
                                                                 time cutoff               0    0.            0.
 weight window             0    0.            0.                 weight window             0    0.            0.
 cell importance 1553877704    2.0588E-01    9.0842E-02         cell importance   115537196    2.0540E-01    9.0655E-02
 weight cutoff             0    0.            0.                 weight cutoff             0    0.            0.
 e or t importance         0    0.            0.                 e or t importance         0    0.            0.
 dxtran                    0    0.            0.                 dxtran                    0    0.            0.
 forced collisions         0    0.            0.                 forced collisions         0    0.            0.
 exp. transform            0    0.            0.                 exp. transform            0    0.            0.
 from neutrons             0    0.            0.                 compton scatter           0    0.            1.0135E+00
 bremsstrahlung    101081427    5.8716E-01    2.0072E-02         capture           353548688    2.2698E+00    2.7792E-01
 p-annihilation       532328    4.1684E-03    2.1301E-03         pair production      266164    2.0842E-03    2.7218E-03
 photonuclear              0    0.            0.                 photonuclear abs          0    0.            0.
 electron x-rays           0    0.            0.
 1st fluorescence   93768369    6.1888E-01    2.0884E-02
 2nd fluorescence    8570455    6.4399E-02    7.2467E-04
     total        1759890295    2.4805E+00    1.3874E+00             total        1759890295    2.4805E+00    1.3874E+00

   number of photons banked                209501352        average time of (shakes)              cutoffs
   photon tracks per source particle      8.5431E+02          escape            1.2863E+00          tco   1.0000E+33
   photon collisions per source particle  5.6267E+02          capture           1.6951E-01          eco   1.0000E-03
   total photon collisions                1159106632          capture or escape 1.7109E-01          wc1  -5.0000E-01
                                                              any termination   1.6993E-01          wc2  -2.5000E-01

 computer time so far in this run   120.01 minutes            maximum number ever in bank        14
 computer time in mcrun             120.00 minutes            bank overflows to backup file       0
 source particles per minute            1.7167E+04
 random numbers generated              16698739020            most random numbers used was      415416 in history     1964437

  warning.   random number stride   152917 exceeded       28 times.

 range of sampled source weights = 1.0000E+00 to 1.0000E+00
```

```
  warning.  importance function may be poor.  see print table 120.
1photon   activity in each cell                                                print table 126
```

cell	tracks entering	population	collisions	collisions * weight (per history)	number weighted energy	flux weighted energy	average track weight (relative)	average track mfp (cm)
1 10	688232	701409	55202	2.6797E-02	1.2190E+00	1.2190E+00	1.0000E+00	1.9061E+01
2 11	686549	699662	55112	2.6753E-02	1.2189E+00	1.2189E+00	1.0000E+00	1.9060E+01
3 12	686321	699298	54658	2.6533E-02	1.2191E+00	1.2191E+00	1.0000E+00	1.9063E+01
4 20	904458	796088	0	0.0000E+00	1.0202E+00	1.0202E+00	1.0000E+00	0.0000E+00
5 21	975148	858960	0	0.0000E+00	1.0049E+00	1.0049E+00	1.0000E+00	0.0000E+00
6 22	903542	794800	0	0.0000E+00	1.0195E+00	1.0195E+00	1.0000E+00	0.0000E+00
7 30	3255796	2110070	0	0.0000E+00	7.8133E-01	7.8133E-01	1.0000E+00	0.0000E+00
8 31	91462	82915	173891	8.4413E-02	5.4084E-01	5.4084E-01	1.0000E+00	1.0302E+01
9 32	2700247	2076698	1594060	7.7381E-01	7.5916E-01	7.5916E-01	1.0000E+00	1.2261E+01
10 33	91578	83001	175469	8.5179E-02	5.4089E-01	5.4089E-01	1.0000E+00	1.0299E+01
11 40	2710992	2132958	0	0.0000E+00	7.3761E-01	7.3761E-01	1.0000E+00	0.0000E+00
12 41	54238	51745	82608	4.0101E-02	6.3726E-01	6.3726E-01	1.0000E+00	1.5307E+00
13 42	2549946	2284576	2241672	1.0882E+00	7.5847E-01	7.5847E-01	1.0000E+00	1.6934E+00
14 43	51301	52311	103912	5.0442E-02	6.4239E-01	6.4239E-01	1.0000E+00	1.5450E+00
15 50	2462650	2101785	0	0.0000E+00	7.4440E-01	7.4440E-01	8.1582E-01	0.0000E+00
16 51	41854	47114	148832	7.2248E-02	6.1898E-01	6.1898E-01	1.0000E+00	1.4988E+00
17 52	4142081	4100052	5255888	1.2757E+00	7.0696E-01	7.0696E-01	1.0000E+00	1.6047E+00
18 53	22982	28339	118260	5.7407E-02	5.8210E-01	5.8210E-01	1.0000E+00	1.4512E+00
19 60	3912161	3367615	0	0.0000E+00	6.8536E-01	6.8536E-01	7.6820E-01	0.0000E+00
20 61	11767	14359	61987	3.0091E-02	5.6389E-01	5.6389E-01	1.0000E+00	1.4305E+00
21 62	7046008	8106687	20291656	1.9701E+00	6.6621E-01	6.6621E-01	1.0000E+00	1.5646E+00
22 63	17945902	35855962	67910255	1.0989E+00	8.9264E-01	8.9264E-01	1.0000E+00	1.0660E+00
23 64	27639037	59382172	111159225	1.7987E-01	9.3910E-01	9.3910E-01	1.0000E+00	1.1296E+00
24 65	65346304	71386316	140714095	2.2769E-02	7.0085E-01	7.0085E-01	1.0000E+00	1.6278E+00
25 66	80656846	89578410	183099364	1.4814E-02	6.2678E-01	6.2678E-01	1.0000E+00	1.5264E+00
26 67	145411239	141167964	0	0.0000E+00	6.4008E-01	6.4008E-01	3.1396E+00	0.0000E+00
27 68	1442363024	1478294493	611615812	1.4845E-03	6.5943E-01	6.5943E-01	1.0000E+00	1.5901E+00
28 69	4234	5084	19497	9.4645E-03	5.6244E-01	5.6244E-01	1.0000E+00	1.4238E+00
29 70	69	77	286	1.3883E-04	4.4574E-01	4.4574E-01	1.0000E+00	1.2521E+00
30 71	241487	469783	859701	1.3911E-02	9.0204E-01	9.0204E-01	1.0000E+00	1.0780E+00
31 72	395666	818030	1480731	2.3960E-03	9.4339E-01	9.4339E-01	1.0000E+00	1.1350E+00
32 73	970500	1041878	1860279	3.0101E-04	7.0481E-01	7.0481E-01	1.0000E+00	1.6322E+00
33 74	1160260	1262341	2345994	1.8980E-04	6.3108E-01	6.3108E-01	1.0000E+00	1.5318E+00
34 75	1892190	1841702	0	0.0000E+00	6.4594E-01	6.4594E-01	3.2058E+00	0.0000E+00
35 76	18856998	19305184	7628186	1.8515E-05	6.6429E-01	6.6429E-01	1.0000E+00	1.5965E+00
36 777	1290538108	1290538108	0	0.0000E+00	7.7330E-01	7.7330E-01	1.0021E+00	0.0000E+00
37 888	1290538247	1290538247	0	0.0000E+00	7.7481E-01	7.7481E-01	5.2384E-05	0.0000E+00
total	4417949424	4512676193	1159106632	6.9519E+00				

```
1tally        2        nps =     2060012
+                                Surface Dose (mrem/hr)                          $ Surface detector
          tally type 2    particle flux averaged over a surface.
          tally for  photons

          this tally is modified by a dose function.

          areas
               surface:      69
              segment
                1       1.00000E+00
```

```
               2       1.68653E+03
               3       1.00000E+00
           whole       1.00000E+00

 surface  69
 segment:          888
               3.07928E-06 0.0024

 surface  69
 segment:         -888        777
               1.27016E-10 0.0077

 surface  69
 segment:         -888       -777
               3.09018E-06 0.0027

 surface  69
 segment:   whole surface
               6.38368E-06 0.0017
```

tfc bin behavior	--mean-- behavior	relative error value	relative error decrease	relative error decrease rate	variance of the variance value	variance of the variance decrease	variance of the variance decrease rate	--figure of merit-- value	--figure of merit-- behavior	-pdf- slope
desired	random	<0.10	yes	1/sqrt(nps)	<0.10	yes	1/nps	constant	random	>3.00
observed	random	0.00	yes	yes	0.02	yes	yes	constant	random	1.74
passed?	yes	yes	yes	yes	yes	yes	yes	yes	yes	no

results of 10 statistical checks for the estimated answer for the tally fluctuation chart (tfc) bin of tally 2

warning. the tally in the tally fluctuation chart bin did not pass 1 of the 10 statistical checks.

```
1analysis of the results in the tally fluctuation chart bin (tfc) for tally        2 with nps=     2060012 print table 160


 normed average tally per history  = 6.38368E-06         unnormed average tally per history  = 6.38368E-06
 estimated tally relative error    = 0.0017              estimated variance of the variance  = 0.0189
 relative error from zero tallies  = 0.0009              relative error from nonzero scores  = 0.0014

 number of nonzero history tallies =      726031         efficiency for the nonzero tallies  = 0.3524
 history number of largest  tally  =      346743         largest  unnormalized history tally = 8.13343E-03
 (largest  tally)/(average tally)  = 1.27410E+03         (largest  tally)/(avg nonzero tally)= 4.49043E+02

 (confidence interval shift)/mean  = 0.0001              shifted confidence interval center  = 6.38402E-06


 if the largest  history score sampled so far were to occur on the next history, the tfc bin quantities would change as follows:

      estimated quantities          value at nps           value at nps+1          value(nps+1)/value(nps)-1.

      mean                           6.38368E-06            6.38762E-06                   0.000618
      relative error                 1.70351E-03            1.81103E-03                   0.063115
      variance of the variance       1.89255E-02            2.83058E-02                   0.495643
```

```
      shifted center                6.38402E-06          6.38421E-06                0.000030
      figure of merit               2.87162E+03          2.54078E+03               -0.115211

 the estimated inverse power slope of the 200 largest  tallies starting at 1.29170E-04 is 1.7417
 the history score probability density function appears to have an unsampled region at the largest  history scores:
 please examine. see print table 161.

 fom = (histories/minute)*(f(x) signal-to-noise ratio)**2 = (1.717E+04)*( 4.090E-01)**2 = (1.717E+04)*(1.673E-01) = 2.872E+03

1unnormed tally density for tally       2          nonzero tally mean(m) = 1.811E-05   nps =     2060012  print table 161

 abscissa             ordinate   log plot of tally probability density function in tally fluctuation chart bin(d=decade,slope= 1.7)
  tally  number num den log den:d----------d----------d----------d----------d----------d----------d----------d----------d---
 2.51-09      2 1.05+03   3.020 **********|**********|**********|**********|**********|**********|**********|          |
 3.98-09      2 6.61+02   2.820 **********|**********|**********|**********|**********|**********|*********  |          |
 6.31-09      4 8.34+02   2.921 **********|**********|**********|**********|**********|**********|**********|          |
 1.00-08      9 1.18+03   3.073 **********|**********|**********|**********|**********|**********|**********|          |
 1.58-08      8 6.64+02   2.822 **********|**********|**********|**********|**********|**********|*********  |          |
 2.51-08     45 2.36+03   3.372 **********|**********|**********|**********|**********|**********|**********|****      |
 3.98-08     79 2.61+03   3.417 **********|**********|**********|**********|**********|**********|**********|****      |
 6.31-08    241 5.02+03   3.701 **********|**********|**********|**********|**********|**********|**********|********  |
 1.00-07    546 7.18+03   3.856 **********|**********|**********|**********|**********|**********|**********|********* |
 1.58-07   1078 8.95+03   3.952 **********|**********|**********|**********|**********|**********|**********|**********|
 2.51-07   2095 1.10+04   4.040 **********|**********|**********|**********|**********|**********|**********|**********|
 3.98-07   3794 1.25+04   4.098 **********|**********|**********|**********|**********|**********|**********|**********|
 6.31-07   7333 1.53+04   4.184 **********|**********|**********|**********|**********|**********|**********|**********|*
 1.00-06  14063 1.85+04   4.267 **********|**********|**********|**********|**********|**********|**********|**********|**
 1.58-06  24768 2.06+04   4.313 **********|**********|**********|**********|**********|**********|**********|**********|***
 2.51-06  37154 1.95+04   4.289 **********|**********|**********|**********|**********|**********|**********|**********|***
 3.98-06  50556 1.67+04   4.223 **********|**********|**********|**********|**********|**********|**********|**********|**
 6.31-06  69343 1.45+04   4.160 **********|**********|**********|**********|**********|**********|**********|**********|*
 1.00-05  92715 1.22+04   4.086 **********|**********|**********|**********|**********|**********|**********|**********|
 1.58-05 114319 9.49+03   3.977 **********|**********|**********|**********|**********|**********|**********|**********|
 2.51-05 123173 6.45+03   3.810 mmmmmmmmmmm|mmmmmmmmmmm|mmmmmmmmmmm|mmmmmmmmmmm|mmmmmmmmmmm|mmmmmmmmmmm|mmmmmmmmmm|mmmmmmmmm |
 3.98-05 105007 3.47+03   3.540 **********|**********|**********|**********|**********|**********|**********|******    |
 6.31-05  60108 1.25+03   3.098 **********|**********|**********|**********|**********|**********|**********|          |
 1.00-04  17954 2.36+02   2.373 **********|**********|**********|**********|**********|**********|****      |          |
 1.58-04   1602 1.33+01   1.124 **********|**********|**********|**********|**********|*         s|          |          |
 2.51-04     11 5.76-02  -1.240 **********|**********|*********  |          |          |       s  |          |          |
 3.98-04      0 0.00+00   0.000            |          |           |          |        s |          |          |          |
 6.31-04      1 2.08-03  -2.681 **********|***       |           |          |       s  |          |          |          |
 1.00-03      4 5.26-03  -2.279 **********|********  |           |          |    s     |          |          |          |
 1.58-03      9 7.47-03  -2.127 **********|********** |           |          | s        |          |          |          |
 2.51-03      4 2.09-03  -2.679 **********|****      |           |        s |          |          |          |          |
 3.98-03      3 9.91-04  -3.004 **********|          |           |     s    |          |          |          |          |
 6.31-03      0 0.00+00   0.000            |          |           | s        |          |          |          |          |
 1.00-02      1 1.32-04  -3.881 *          |          |         s |          |          |          |          |          |
  total  726031 3.52-01         d----------d----------d----------d----------d----------d----------d----------d----------d---

1tally       22        nps =     2060012
+                              2-meter Dose (mrem/hr)                                $ 2-m detector
           tally type 2    particle flux averaged over a surface.
           tally for  photons

           this tally is modified by a dose function.

           areas
                surface:      80
```

```
               segment
                 1       1.00000E+00
                 2       8.07023E+03
                 3       1.00000E+00
               whole     1.00000E+00

 surface  80
 segment:          888
                2.28930E-06 0.0020

 surface  80
 segment:         -888        777
                1.06242E-11 0.0047

 surface  80
 segment:         -888       -777
                2.09669E-06 0.0019

 surface  80
 segment:   whole surface
                4.47173E-06 0.0016

 ================================================================================================================================

          results of 10 statistical checks for the estimated answer for the tally fluctuation chart (tfc) bin of tally       22

 tfc bin     --mean--      ---------relative error---------      ----variance of the variance----      --figure of merit--     -pdf-
 behavior    behavior      value   decrease   decrease rate      value   decrease   decrease rate       value     behavior     slope

 desired      random       <0.10      yes      1/sqrt(nps)       <0.10      yes        1/nps           constant    random      >3.00
 observed     random        0.00      yes          yes            0.00      yes         yes            constant    random       2.24
 passed?        yes          yes      yes          yes              yes      yes         yes               yes        yes          no

 ================================================================================================================================

 warning.  the tally in the tally fluctuation chart bin did not pass  1 of the 10 statistical checks.

1analysis of the results in the tally fluctuation chart bin (tfc) for tally       22 with nps=     2060012 print table 160

 normed average tally per history  = 4.47173E-06          unnormed average tally per history  = 4.47173E-06
 estimated tally relative error    = 0.0016               estimated variance of the variance  = 0.0003
 relative error from zero tallies  = 0.0009               relative error from nonzero scores  = 0.0013

 number of nonzero history tallies =      725972          efficiency for the nonzero tallies  = 0.3524
 history number of largest  tally  =      925862          largest  unnormalized history tally = 1.33093E-03
 (largest  tally)/(average tally)  = 2.97632E+02          (largest  tally)/(avg nonzero tally)= 1.04889E+02

 (confidence interval shift)/mean  = 0.0000               shifted confidence interval center  = 4.47175E-06

 if the largest  history score sampled so far were to occur on the next history, the tfc bin quantities would change as follows:

      estimated quantities           value at nps           value at nps+1           value(nps+1)/value(nps)-1.

      mean                            4.47173E-06             4.47238E-06                    0.000144
```

```
      relative error               1.59299E-03          1.59925E-03                0.003932
      variance of the variance     2.79344E-04          3.40512E-04                0.218969
      shifted center               4.47175E-06          4.47176E-06                0.000001
      figure of merit              3.28393E+03          3.25825E+03               -0.007818

 the estimated inverse power slope of the 198 largest  tallies starting at 1.00352E-04 is 2.2441
 the history score probability density function appears to have an unsampled region at the largest  history scores:
 please examine. see print table 161.

 fom = (histories/minute)*(f(x) signal-to-noise ratio)**2 = (1.717E+04)*( 4.374E-01)**2 = (1.717E+04)*(1.913E-01) = 3.284E+03

1unnormed tally density for tally       22          nonzero tally mean(m) = 1.269E-05   nps =     2060012  print table 161

 abscissa              ordinate   log plot of tally probability density function in tally fluctuation chart bin(d=decade,slope= 2.2)
  tally  number num den log den:d-----------d-------------d------------d-------------d------------d------------d-------------d------
2.00-09     38 2.51+04   4.399 ************|*************|************|*************|************|************|*************|****
3.16-09     39 1.62+04   4.210 ************|*************|************|*************|************|************|*************|*
5.01-09     88 2.31+04   4.364 ************|*************|************|*************|************|************|*************|***
7.94-09    218 3.61+04   4.558 ************|*************|************|*************|************|************|*************|******
1.26-08    342 3.57+04   4.553 ************|*************|************|*************|************|************|*************|******
2.00-08    486 3.20+04   4.506 ************|*************|************|*************|************|************|*************|*****
3.16-08    592 2.46+04   4.391 ************|*************|************|*************|************|************|*************|****
5.01-08    790 2.07+04   4.317 ************|*************|************|*************|************|************|*************|***
7.94-08   1342 2.22+04   4.347 ************|*************|************|*************|************|************|*************|***
1.26-07   2291 2.39+04   4.379 ************|*************|************|*************|************|************|*************|***
2.00-07   4566 3.01+04   4.479 ************|*************|************|*************|************|************|*************|*****
3.16-07   7975 3.32+04   4.521 ************|*************|************|*************|************|************|*************|*****
5.01-07  13630 3.58+04   4.554 ************|*************|************|*************|************|************|*************|******
7.94-07  22346 3.70+04   4.568 ************|*************|************|*************|************|************|*************|******
1.26-06  33770 3.53+04   4.548 ************|*************|************|*************|************|************|*************|******
2.00-06  45586 3.01+04   4.478 ************|*************|************|*************|************|************|*************|*****
3.16-06  58890 2.45+04   4.389 ************|*************|************|*************|************|************|*************|****
5.01-06  73343 1.92+04   4.284 ************|*************|************|*************|************|************|*************|**
7.94-06  89886 1.49+04   4.173 ************|*************|************|*************|************|************|*************|*
1.26-05 103794 1.08+04   4.035 ************|*************|************|*************|************|************|*************|
2.00-05 107863 7.11+03   3.852 mmmmmmmmmmmm|mmmmmmmmmmmmm|mmmmmmmmmmmm|mmmmmmmmmmmmm|mmmmmmmmmmmm|mmmmmmmmmmmm|mmmmmmmmm   |
3.16-05  90391 3.76+03   3.575 ************|*************|************|*************|************|************|*******    |
5.01-05  51152 1.34+03   3.128 ************|*************|************|*************|************|************|*          |
7.94-05  15209 2.52+02   2.401 ************|*************|************|*************|************|****        |           |
1.26-04   1325 1.38+01   1.141 ************|*************|************|*************|            s |            |           |
2.00-04     11 7.25-02  -1.140 ************|************ |            |             |    s         |            |           |
3.16-04      0 0.00+00   0.000 |            |            |             |         s|              |            |           |
5.01-04      0 0.00+00   0.000 |            |            |          s  |          |              |            |           |
7.94-04      1 1.66-03  -2.781 **           |            |          s  |          |              |            |           |
1.26-03      7 7.31-03  -2.136 **********   |            |       s     |          |              |            |           |
1.58-03      1 1.49-03  -2.827 *            |            |  s          |          |              |            |           |
 total  725972 3.52-01         d-----------d-------------d------------d-------------d------------d------------d-------------d------

1status of the statistical checks used to form confidence intervals for the mean for each tally bin


 tally   result of statistical checks for the tfc bin (the first check not passed is listed) and error magnitude check for all bins

       2   missed  1 of 10 tfc bin checks: the slope of decrease of largest tallies is less than the minimum acceptable value of 3.0
         passed all bin error check:     4 tally bins all have relative errors less than 0.10 with no zero bins

      22   missed  1 of 10 tfc bin checks: the slope of decrease of largest tallies is less than the minimum acceptable value of 3.0
         passed all bin error check:     4 tally bins all have relative errors less than 0.10 with no zero bins
```

```
 the 10 statistical checks are only for the tally fluctuation chart bin and do not apply to other tally bins.

 warning.       2 of the     2 tally fluctuation chart bins did not pass all 10 statistical checks.
1tally fluctuation charts

                          tally        2                          tally       22
         nps      mean     error   vov  slope    fom      mean     error   vov  slope    fom
      128000   6.3118E-06 0.0061 0.0045  5.6    3641   4.4333E-06 0.0065 0.0081  5.8    3170
      256000   6.3524E-06 0.0044 0.0038  3.0    3440   4.4570E-06 0.0046 0.0035  3.4    3118
      384000   6.3773E-06 0.0049 0.2125  2.4    1874   4.4607E-06 0.0038 0.0027  3.0    3121
      512000   6.3781E-06 0.0040 0.1568  2.5    2143   4.4629E-06 0.0032 0.0016  3.0    3194
      640000   6.3851E-06 0.0035 0.1091  2.2    2198   4.4675E-06 0.0029 0.0013  2.8    3191
      768000   6.3884E-06 0.0031 0.0878  2.1    2366   4.4713E-06 0.0026 0.0009  2.6    3230
      896000   6.3855E-06 0.0028 0.0667  2.0    2389   4.4663E-06 0.0024 0.0007  2.7    3261
     1024000   6.3845E-06 0.0026 0.0557  1.9    2493   4.4678E-06 0.0023 0.0008  2.4    3231
     1152000   6.3847E-06 0.0024 0.0472  1.9    2579   4.4694E-06 0.0022 0.0007  2.3    3220
     1280000   6.3793E-06 0.0022 0.0410  1.9    2667   4.4653E-06 0.0020 0.0006  2.4    3242
     1408000   6.3856E-06 0.0021 0.0339  1.8    2641   4.4682E-06 0.0019 0.0006  2.3    3236
     1536000   6.3845E-06 0.0020 0.0298  1.8    2700   4.4686E-06 0.0019 0.0005  2.3    3251
     1664000   6.3833E-06 0.0019 0.0265  1.8    2754   4.4689E-06 0.0018 0.0004  2.3    3251
     1792000   6.3829E-06 0.0018 0.0237  1.7    2805   4.4686E-06 0.0017 0.0004  2.3    3262
     1920000   6.3819E-06 0.0018 0.0210  1.7    2822   4.4687E-06 0.0017 0.0003  2.2    3273
     2048000   6.3830E-06 0.0017 0.0191  1.7    2867   4.4711E-06 0.0016 0.0003  2.2    3283
     2060012   6.3837E-06 0.0017 0.0189  1.7    2872   4.4717E-06 0.0016 0.0003  2.2    3284

 ************************************************************************************************************************

 dump no.    3 on file runtpe     nps =     2060012     coll =     1159106632     ctm =      120.00   nrn =
16698739020
 tally data written to file mctal

        23 warning messages so far.


 run terminated when it had used  120  minutes of computer time.

 computer time =  120.01 minutes

 mcnp     version 5     09282010                    02/28/14 06:47:41                    probid =  02/28/14 04:47:39
```

5.7.2.3.2 HAC 252Cf Neutron Source – 8hn001.io

```
          Thread Name & Version = MCNP5, 1.60

            _ _   _  _   _    _
           |_|_|  (_  |_|  |_)  _)
                        |

  +-------------------------------------------------------------------+
  | Copyright 2010. Los Alamos National Security, LLC.  All rights    |
  | reserved.                                                         |
  |   This material was produced under U.S. Government contract       |
  | DE-AC52-06NA25396 for Los Alamos National Laboratory, which is    |
  | operated by Los Alamos National Security, LLC, for the U.S.       |
  | Department of Los Energy. The Government is granted for itself and |
```

```
  | others acting on its behalf a paid-up, nonexclusive, irrevocable    |
  | worldwide license in this material to reproduce, prepare derivative |
  | works, and perform publicly and display publicly. Beginning five    |
  | (5) years after 2010, subject to additional five-year worldwide     |
  | renewals, the Government is granted for itself and others acting on |
  | its behalf a paid-up, nonexclusive, irrevocable worldwide license   |
  | in this material to reproduce, prepare derivative works, distribute |
  | copies to the public, perform publicly and display publicly, and to |
  | permit others to do so. NEITHER THE UNITED STATES NOR THE UNITED    |
  | STATES DEPARTMENT OF ENERGY, NOR LOS ALAMOS NATIONAL SECURITY, LLC, |
  | NOR ANY OF THEIR EMPLOYEES, MAKES ANY WARRANTY, EXPRESS OR IMPLIED, |
  | OR ASSUMES ANY LEGAL LIABILITY OR RESPONSIBILITY FOR THE ACCURACY,  |
  | COMPLETENESS, OR USEFULNESS OF ANY INFORMATION, APPARATUS, PRODUCT, |
  | OR PROCESS DISCLOSED, OR REPRESENTS THAT ITS USE WOULD NOT INFRINGE |
  | PRIVATELY OWNED RIGHTS.                                            |
  +--------------------------------------------------------------------+
```


```
1mcnp     version 5     ld=09282010                    02/27/14 22:47:23
 ***********************************************************************                probid =  02/27/14 22:47:23
 inp=8hn001.i

         1-       title RH-TRU 72-B NS30 HAC Neutron Concentrated 1 g/cc Cf252
         2-       C
         3-       C Cell Cards
         4-       C
         5-       10  1 -1        10  -11  -16                imp:n=1    $ Source #1
         6-       11  1 -1        12  -13  -17                imp:n=1    $ Source #2
         7-       20  0           20  -21  -26
         8-                     (-10:  11:  16)               imp:n=1    $ Drum #1 cavity
         9-       21  0           22  -23  -27
        10-                     (-12:  13:  17)               imp:n=1    $ Drum #2 cavity
        11-       30  0           31  -35  -33
        12-                      #10  #20                     imp:n=1    $ NS30 cavity
        13-       31  5 -0.94000  30  -31  -32                imp:n=1    $ NS30 botcap
        14-       32  5 -0.94000  31  -35   33  -32           imp:n=1    $ NS30 body
        15-       33  5 -0.94000  35  -34  -32                imp:n=1    $ NS30 topcap
        16-       40  0           41  -45  -43
        17-                     (-30:  32:  34) #11  #21       imp:n=1    $ RLC cavity
        18-       41  3 -7.85260  40  -41  -42                imp:n=1    $ RLC base
        19-       42  3 -7.85260  41  -46   43  -42           imp:n=1    $ RLC shell
        20-       43  3 -7.85260  45  -44  -43                imp:n=1    $ RLC lid
        21-       50  0           51  -53  -55
        22-                     (-40:  42:  46)
        23-                    :( 44  -46  -43)               imp:n=1    $ IV cavity
        24-       51  2 -8.01280  50  -51  -52                imp:n=1    $ IV base
        25-       52  2 -8.01280  51  -55   53  -52           imp:n=1    $ IV shell
        26-       53  2 -8.01280  55  -54  -52                imp:n=1    $ IV lid
        27-       60  0           61  -63  -65
        28-                     (-50:  52:  54)               imp:n=1    $ OC cavity
        29-       61  2 -8.01280  60  -61  -69                imp:n=1    $ OC base
        30-       62  2 -8.01280  61  -66   65  -64           imp:n=1    $ OC ishell
        31-       63  4 -11.3500  61  -66   64  -76  71       imp:n=1    $ OC lead in
        32-       64  4 -11.3500  61  -66   76  -68  71       imp:n=1    $ OC lead out
        33-       65  2 -8.01280  61  -66   68  -77  71       imp:n=1    $ OC oshell in
        34-       66  2 -8.01280  61  -66   77  -67  71       imp:n=1    $ OC oshell out
        35-       67  0           61  -66   67  -70  71       imp:n=1    $ OC airgap
        36-       68  2 -8.01280  61  -66   70  -69  71       imp:n=1    $ OC tshell
        37-       69  2 -8.01280  66  -63   65  -69           imp:n=1    $ OC flange
```

```
38-       70  2 -8.01280  63  -62  -69                imp:n=1    $ OC lid
39-       71  4 -11.3500  64  -78  -71                imp:n=1    $ OC lead punct in
40-       72  4 -11.3500  78  -73  -71                imp:n=1    $ OC lead punct out
41-       73  2 -8.01280  73  -79  -71                imp:n=1    $ OC oshell punct in
42-       74  2 -8.01280  79  -72  -71                imp:n=1    $ OC oshell punct out
43-       75  0           74  -69  -71                imp:n=1    $ OC airgap punct
44-       76  2 -8.01280  75  -74  -71                imp:n=1    $ OC tshell punct
45-       777 0           69  -80   60  -62           imp:n=1    $ Outside to tally
46-       888 0         -999
47-                     (-60:  80:  62)               imp:n=1    $ Outside pkg
48-       999 0           999                         imp:n=0    $ Outside world
49-
50-       C
51-       C Geometry Cards
52-       C
53-       10  pz 163.513                                        $ Source #1 bottom
54-       11  pz 164.783                                        $ Source #1 top
55-       12  pz 163.513                                        $ Source #2 bottom
56-       13  pz 164.783                                        $ Source #2 top
57-       16  c/z 34.638 0 0.635                                $ Source #1 radius
58-       17  c/z 38.885 0 0.635                                $ Source #2 radius
59-       C
60-       20  pz 163.511                                        $ Drum #1 bottom
61-       21  pz 164.784                                        $ Drum #1 top
62-       22  pz 163.511                                        $ Drum #2 bottom
63-       23  pz 164.784                                        $ Drum #2 top
64-       26  c/z 34.638 0 0.636                                $ Drum #1 radius
65-       27  c/z 38.885 0 0.636                                $ Drum #2 radius
66-       C
67-       30  pz 21.908                                         $ NS30 botcap (outside)
68-       31  pz 34.608                                         $ NS30 botcap (inside)
69-       32  c/z 7.748 0 30.48                                 $ NS30 body (outside)
70-       33  c/z 7.748 0 27.529                                $ NS30 body (inside)
71-       34  pz 306.388                                        $ NS30 topcap (outside)
72-       35  pz 293.688                                        $ NS30 topcap (inside)
73-       C
74-       40  pz 19.368                                         $ RLC base (outside)
75-       41  pz 20.638                                         $ RLC base (inside)
76-       42  c/z 7.139 0 33.02                                 $ RLC shell (outside)
77-       43  c/z 7.139 0 32.385                                $ RLC shell (inside)
78-       44  pz 309.563                                        $ RLC lid (outside)
79-       45  pz 307.658                                        $ RLC lid (inside)
80-       46  pz 325.438                                        $ RLC top (outside)
81-       C
82-       50  pz 14.288                                         $ IV base (outside)
83-       51  pz 18.098                                         $ IV base (inside)
84-       52  c/z 0.474 0 40.64                                 $ IV shell (outside)
85-       53  c/z 0.474 0 39.688                                $ IV shell (inside)
86-       54  pz 343.218                                        $ IV top (outside)
87-       55  pz 326.708                                        $ IV top (inside)
88-       C
89-       60  pz 0                                              $ OC bottom (outside)
90-       61  pz 12.7                                           $ OC bottom (inside)
91-       62  pz 360.045                                        $ OC top (outside)
92-       63  pz 344.805                                        $ OC top (inside)
93-       64  cz 43.656                                         $ OC ishell (outside)
94-       65  cz 41.116                                         $ OC ishell (inside)
95-       66  pz 320.675                                        $ OC lead (upper)
```

```
 96-       67  cz 52.229                                        $ OC oshell (outside)
 97-       68  cz 48.419                                        $ OC oshell (inside)
 98-       69  cz 52.838                                        $ OC therm (outside)
 99-       70  cz 52.495                                        $ OC therm (inside)
100-       71  c/x 0 164.148 10.033                             $ OC puncture radius
101-       72  cz 50.563                                        $ OC oshell punct (out)
102-       73  cz 46.753                                        $ OC oshell punct (in)
103-       74  cz 50.905                                        $ OC therm punct (out)
104-       75  cz 50.563                                        $ OC therm punct (in)
105-       76  cz 46.038                                        $ OC lead (mid)
106-       77  cz 50.324                                        $ OC oshell (mid)
107-       78  cz 45.204                                        $ OC lead punct (mid)
108-       79  cz 48.658                                        $ OC oshell punct (mid)
109-       C
110-       80  cz 150.905                                       $ 1-meter from OC therm
111-       C
112-       777 c/x 0 164.148 2.54                               $ Tally cylinder
113-       888 px 0                                             $ Tally truncation
114-       999 sz 164.148 277.905                               $ Outside world
115-
116-       C
117-       C Physics Cards
118-       C
119-       mode n
120-       C
121-       C Source Cards
122-       C
123-       C Cylindrical Sources
124-       sdef pos=d1 erg=d2 par=1 axs=0 0 1 rad=d3 ext=d4
125-       sc1 Cf252
126-       C Source Position and Fraction
127-       si1 L 34.638 0 164.148
128-             38.885 0 164.148
129-       sp1   98 2
130-       C Source Energy (MeV) and Fraction
131-       si2 0.1 0.5 1.0 2.0 3.0
132-            4.0 6.0 8.0 10.0 15.0
133-       sp2 0.00E+00 1.80E+11 2.71E+11 5.36E+11 4.10E+11
134-            2.73E+11 2.66E+11 8.53E+10 2.44E+10 8.36E+09
135-       C Source Radius
136-       si3 0 0.635
137-       sp3 -21 1
138-       C Source Extent
139-       si4 -0.635 0.635
140-       sp4 -21 0
141-       C
142-       C Tally Cards
143-       C
144-       f2:n 69
145-       fc2 Surface Dose (mrem/hr)                           $ Surface detector
146-       fs2 -888 -777 t
147-       sd2 1.0 20.268 1.0 1.0                               $ Surface tally area
148-       f22:n 80
149-       fc22 1-meter Dose (mrem/hr)                          $ 1-m detector
150-       fs22 -888 -777 t
151-       sd22 1.0 20.268 1.0 1.0                              $ Surface tally area
152-       C
153-       C ANSI/ANS-6.1.1-1977 Neutron Flux to Dose Factors (mrem/hr)
```

```
154-       de0  2.5e-08 1.0e-07 1.0e-06 1.0e-05 1.0e-04            $ Energy (Mev)
155-            1.0e-03 1.0e-02 1.0e-01 5.0e-01 1.0
156-            2.5 5.0 7.0 10.0 14.0 20.0
157-       df0  3.67e-03 3.67e-03 4.46e-03 4.54e-03 4.18e-03       $ Conversion (mrem/hr)
158-            3.76e-03 3.56e-03 2.17e-02 9.26e-02 1.32e-01
159-            1.25e-01 1.56e-01 1.47e-01 1.47e-01 2.08e-01 2.27e-01
160-       C
161-       C Material Cards
162-       C
163-       m1   40000.60c -1.00                                    $ Zirconium
164-       m2   14000.60c -0.01                                    $ Stainless Steel
165-            24052.60c -0.19
166-            25055.60c -0.02
167-            26057.60c -0.68
168-            28058.60c -0.10
169-       m3   26057.60c -1.00                                    $ Carbon Steel (iron)
170-       m4   82000.50c -1.00                                    $ Lead
171-       m5   1001.60c   2                                       $ EHMW Polyethylene
172-            6000.60c   1
173-       mt5  poly.60t
174-       C
175-       C Runtime and Print Cards
176-       C
177-       prdmp j j 1 2
178-       ctme 360

 surface       10   and surface       12   are the same.       12   will be deleted.

 surface       11   and surface       13   are the same.       13   will be deleted.

 surface       20   and surface       22   are the same.       22   will be deleted.

 surface       21   and surface       23   are the same.       23   will be deleted.

 surface       72   and surface       75   are the same.       75   will be deleted.

  comment.           5 surfaces were deleted for being the same as others.

  warning.    1 materials had unnormalized fractions. print table 40.

  warning.  sum of segment sizes differs from total in   2 cases.
1cells                                                                    print table 60

                          atom        gram                                    neutron
             cell     mat    density     density     volume       mass          pieces importance

        1       10        1  6.60141E-03 1.00000E+00 1.60880E+00 1.60880E+00          1  1.0000E+00
        2       11        1  6.60141E-03 1.00000E+00 1.60880E+00 1.60880E+00          1  1.0000E+00
        3       20        0  0.00000E+00 0.00000E+00 8.88335E-03 0.00000E+00          1  1.0000E+00
        4       21        0  0.00000E+00 0.00000E+00 8.88335E-03 0.00000E+00          1  1.0000E+00
        5       30        0  0.00000E+00 0.00000E+00 0.00000E+00 0.00000E+00          0  1.0000E+00
        6       31       5s 1.21070E-01 9.40000E-01 3.70667E+04 3.48427E+04          1  1.0000E+00
        7       32       5s 1.21070E-01 9.40000E-01 1.39331E+05 1.30971E+05          1  1.0000E+00
        8       33       5s 1.21070E-01 9.40000E-01 3.70667E+04 3.48427E+04          1  1.0000E+00
        9       40        0  0.00000E+00 0.00000E+00 0.00000E+00 0.00000E+00          0  1.0000E+00
       10       41        3  8.30568E-02 7.85260E+00 4.35019E+03 3.41603E+04          1  1.0000E+00
       11       42        3  8.30568E-02 7.85260E+00 3.97694E+04 3.12294E+05          1  1.0000E+00
       12       43        3  8.30568E-02 7.85260E+00 6.27672E+03 4.92886E+04          1  1.0000E+00
```

```
       13       50        0  0.00000E+00 0.00000E+00 0.00000E+00 0.00000E+00          0  1.0000E+00
       14       51        2  8.70856E-02 8.01280E+00 1.97689E+04 1.58404E+05          1  1.0000E+00
       15       52        2  8.70856E-02 8.01280E+00 7.41419E+04 5.94084E+05          1  1.0000E+00
       16       53        2  8.70856E-02 8.01280E+00 8.56652E+04 6.86418E+05          1  1.0000E+00
       17       60        0  0.00000E+00 0.00000E+00 0.00000E+00 0.00000E+00          0  1.0000E+00
       18       61        2  8.70856E-02 8.01280E+00 1.11390E+05 8.92546E+05          1  1.0000E+00
       19       62        2  8.70856E-02 8.01280E+00 2.08330E+05 1.66931E+06          1  1.0000E+00
       20       63        4  3.29849E-02 1.13500E+01 0.00000E+00 0.00000E+00          0  1.0000E+00
       21       64        4  3.29849E-02 1.13500E+01 0.00000E+00 0.00000E+00          0  1.0000E+00
       22       65        2  8.70856E-02 8.01280E+00 0.00000E+00 0.00000E+00          0  1.0000E+00
       23       66        2  8.70856E-02 8.01280E+00 0.00000E+00 0.00000E+00          0  1.0000E+00
       24       67        0  0.00000E+00 0.00000E+00 0.00000E+00 0.00000E+00          0  1.0000E+00
       25       68        2  8.70856E-02 8.01280E+00 0.00000E+00 0.00000E+00          0  1.0000E+00
       26       69        2  8.70856E-02 8.01280E+00 8.34880E+04 6.68973E+05          1  1.0000E+00
       27       70        2  8.70856E-02 8.01280E+00 1.33668E+05 1.07106E+06          1  1.0000E+00
       28       71        4  3.29849E-02 1.13500E+01 0.00000E+00 0.00000E+00          0  1.0000E+00
       29       72        4  3.29849E-02 1.13500E+01 0.00000E+00 0.00000E+00          0  1.0000E+00
       30       73        2  8.70856E-02 8.01280E+00 0.00000E+00 0.00000E+00          0  1.0000E+00
       31       74        2  8.70856E-02 8.01280E+00 0.00000E+00 0.00000E+00          0  1.0000E+00
       32       75        0  0.00000E+00 0.00000E+00 0.00000E+00 0.00000E+00          0  1.0000E+00
       33       76        2  8.70856E-02 8.01280E+00 0.00000E+00 0.00000E+00          0  1.0000E+00
       34      777        0  0.00000E+00 0.00000E+00 2.26002E+07 0.00000E+00          1  1.0000E+00
       35      888        0  0.00000E+00 0.00000E+00 6.41456E+07 0.00000E+00          1  1.0000E+00
       36      999        0  0.00000E+00 0.00000E+00 0.00000E+00 0.00000E+00          0  0.0000E+00

 total                                              8.77261E+07 6.33719E+06

    minimum source weight = 1.0000E+00    maximum source weight = 1.0000E+00

 ************************************************
 * Random Number Generator  =                  1 *
 * Random Number Seed       =       19073486328125 *
 * Random Number Multiplier =       19073486328125 *
 * Random Number Adder      =                  0 *
 * Random Number Bits Used  =                 48 *
 * Random Number Stride     =             152917 *
 ************************************************


        2 warning messages so far.
1cross-section tables                                                                print table 100

     table    length

                        tables from file endf60

   1001.60c    1782  1-h-1 from endf-vi.1                                          mat 125      11/25/93
   6000.60c   17879  6-c-nat from endf-vi.1                                       mat 600      11/25/93
  14000.60c   51392  14-si-nat from endf/b-vi                                     mat1400      11/25/93
  24052.60c   66325  24-cr-52 from endf/b-vi.1                                    mat2431      11/25/93
  25055.60c   84549  25-mn-55 from endf/b-vi                                      mat2525      11/25/93
  26057.60c   72092  endf/b-vi.1 fe57a                                           mat2634      11/25/93
  28058.60c   83305  28-ni-58 from endf/b-vi.1                                    mat2825      11/25/93
  40000.60c   45269  40-zr-nat from endf-vi.1                                     mat4000      11/27/93

                        tables from file rmccs

  82000.50c   28695  njoy                                                      ( 1382)     03/10/82
```

```
                        tables from file sab2002

   poly.60t   69775  1-h-1 in polyethylene at 293.6k from endf-vi.5 njoy99.0                1001     0     0  09/14/99

  total      521063

 ********************************************************************************************************************************

 dump no.    1 on file runtpe     nps =           0     coll =              0     ctm =        0.00   nrn =
    0

        2 warning messages so far.

 ********************************************************************************************************************************

 dump no.    2 on file runtpe     nps =    21870946     coll =     2447373198     ctm =       60.01   nrn =
 21647644894

 ********************************************************************************************************************************

 dump no.    3 on file runtpe     nps =    43741892     coll =     4894674664     ctm =      120.02   nrn =
 43294396573

 ********************************************************************************************************************************

 dump no.    4 on file runtpe     nps =    65633216     coll =     7343470105     ctm =      180.03   nrn =
 64953659814

 ********************************************************************************************************************************

 dump no.    5 on file runtpe     nps =    87515996     coll =     9791597310     ctm =      240.04   nrn =
 86608364548

 ********************************************************************************************************************************

 dump no.    6 on file runtpe     nps =   109394252     coll =    12240722678     ctm =      300.05   nrn =
 108269211273
1problem summary

      run terminated when it had used  360  minutes of computer time.
+                                                                                    02/28/14 04:47:34
      title RH-TRU 72-B NS30 HAC Neutron Concentrated 1 g/cc Cf252                probid =  02/27/14 22:47:23
0
 neutron creation    tracks      weight        energy           neutron loss        tracks      weight        energy
                                 (per source particle)                                        (per source particle)

 source           131248204    1.0000E+00    2.5771E+00         escape            50855010    3.5027E-01    2.5994E-01
                                                                 energy cutoff            0    0.            0.
                                                                 time cutoff              0    0.            0.
 weight window            0    0.            0.                 weight window            0    0.            0.
 cell importance          0    0.            0.                 cell importance          0    0.            0.
 weight cutoff            0    1.2156E-01    4.2180E-07         weight cutoff     80653778    1.2158E-01    4.3056E-07
 e or t importance        0    0.            0.                 e or t importance        0    0.            0.
 dxtran                   0    0.            0.                 dxtran                   0    0.            0.
 forced collisions        0    0.            0.                 forced collisions        0    0.            0.
 exp. transform           0    0.            0.                 exp. transform           0    0.            0.
 upscattering             0    0.            2.8409E-07         downscattering           0    0.            2.2675E+00
```

photonuclear	0	0.	0.	capture	0	6.5158E-01	3.2877E-02
(n,xn)	521055	3.7500E-03	4.4824E-03	loss to (n,xn)	260471	1.8746E-03	2.1253E-02
prompt fission	0	0.	0.	loss to fission	0	0.	0.
delayed fission	0	0.	0.				
total	131769259	1.1253E+00	2.5816E+00	total	131769259	1.1253E+00	2.5816E+00

number of neutrons banked	260584	average time of (shakes)	cutoffs
neutron tracks per source particle	1.0040E+00	escape 3.2471E+03	tco 1.0000E+33
neutron collisions per source particle	1.1191E+02	capture 4.6684E+04	eco 0.0000E+00
total neutron collisions	14687509560	capture or escape 3.1498E+04	wc1 -5.0000E-01
net multiplication	1.0019E+00 0.0000	any termination 3.7959E+04	wc2 -2.5000E-01

computer time so far in this run	360.04 minutes	maximum number ever in bank	2
computer time in mcrun	360.01 minutes	bank overflows to backup file	0
source particles per minute	3.6457E+05		
random numbers generated	129910265577	most random numbers used was	18822 in history 115776655

range of sampled source weights = 1.0000E+00 to 1.0000E+00

1neutron activity in each cell print table 126

cell	tracks entering	population	collisions	collisions * weight (per history)	number weighted energy	flux weighted energy	average track weight (relative)	average track mfp (cm)
1 10	129720985	128659480	2439336	1.8573E-02	1.8135E-01	2.5454E+00	9.9943E-01	3.0946E+01
2 11	4389890	4244111	115583	8.6114E-04	6.8390E-03	1.9330E+00	9.7952E-01	2.8456E+01
3 20	130823920	128659598	0	0.0000E+00	1.2409E-01	2.5352E+00	9.9916E-01	0.0000E+00
4 21	6163268	4250120	0	0.0000E+00	5.3922E-03	1.8054E+00	9.7557E-01	0.0000E+00
5 30	486910014	130216635	0	0.0000E+00	1.6619E-04	6.7119E-01	7.4116E-01	0.0000E+00
6 31	15701773	10118366	1026493850	4.0082E+00	3.6906E-05	2.1782E-01	5.6564E-01	5.9515E-01
7 32	572346591	129289006	10659539536	5.1917E+01	1.5757E-04	5.9867E-01	7.5010E-01	1.1259E+00
8 33	15650934	10134173	1024091757	3.9957E+00	3.6779E-05	2.1748E-01	5.6506E-01	5.9445E-01
9 40	348786852	124645201	0	0.0000E+00	4.5444E-04	6.7215E-01	8.1940E-01	0.0000E+00
10 41	1524234	785982	1143894	6.6277E-03	4.2484E-04	5.7107E-01	7.5890E-01	4.5586E+00
11 42	343106074	124005881	148472453	9.4031E-01	5.5613E-04	6.9390E-01	8.2738E-01	4.3897E+00
12 43	1418218	833732	1512432	8.8048E-03	4.6461E-04	5.6294E-01	7.5956E-01	4.6347E+00
13 50	344647054	120386653	0	0.0000E+00	4.8624E-04	5.7831E-01	8.0761E-01	0.0000E+00
14 51	2329326	1278556	6512086	3.8986E-02	9.8612E-04	5.1746E-01	8.0773E-01	2.9780E+00
15 52	343822193	119831912	286735808	1.7538E+00	7.0762E-04	6.5053E-01	8.3224E-01	2.9390E+00
16 53	1710280	928955	16227613	9.7418E-02	2.1128E-03	3.4993E-01	7.9440E-01	2.9541E+00
17 60	316608597	110621818	0	0.0000E+00	6.9994E-04	5.6471E-01	8.1989E-01	0.0000E+00
18 61	1214700	732389	11874805	7.5160E-02	3.9000E-03	4.0877E-01	8.4001E-01	3.1286E+00
19 62	288770197	110261536	602878458	3.7714E+00	1.0752E-03	6.1250E-01	8.4795E-01	3.0532E+00
20 63	192596343	75144643	271222157	1.6908E+00	1.1601E-03	5.3209E-01	8.4870E-01	3.8460E+00
21 64	157623920	67031676	218988055	1.3794E+00	1.3922E-03	5.2356E-01	8.5695E-01	3.9015E+00
22 65	118343844	60475774	189567109	1.2320E+00	2.1319E-03	5.2489E-01	8.7032E-01	3.1447E+00
23 66	74289659	52052723	110377065	7.2647E-01	3.2181E-03	5.5952E-01	8.8328E-01	3.3297E+00
24 67	52211802	45258317	0	0.0000E+00	4.1322E-03	6.1724E-01	8.9278E-01	0.0000E+00
25 68	48507294	45381520	11156603	7.4062E-02	4.3948E-03	6.3821E-01	8.9545E-01	3.5589E+00
26 69	972627	506314	6847445	4.1870E-02	3.3383E-03	3.1397E-01	8.0745E-01	3.0028E+00
27 70	431616	188034	5760360	3.2856E-02	5.3156E-03	1.6668E-01	7.4248E-01	2.8427E+00
28 71	33189715	19469291	23797347	1.6296E-01	3.1910E-03	8.3601E-01	9.2147E-01	4.1505E+00
29 72	26746543	15955957	19052977	1.3049E-01	3.4412E-03	7.9736E-01	9.2145E-01	4.1686E+00
30 73	20396759	13200427	25949396	1.7940E-01	4.5971E-03	7.6157E-01	9.2270E-01	3.3072E+00
31 74	12665343	9760797	15173802	1.0532E-01	6.4595E-03	7.7004E-01	9.2688E-01	3.4470E+00
32 75	7153538	6947781	0	0.0000E+00	8.8368E-03	8.7133E-01	9.3455E-01	0.0000E+00
33 76	7450565	6981767	1579633	1.1017E-02	8.4253E-03	8.4031E-01	9.3301E-01	3.6275E+00
34 777	50543107	50543107	0	0.0000E+00	5.1323E-03	7.2826E-01	9.0442E-01	0.0000E+00

```
       35      888    50855010     50855010            0    0.0000E+00   5.0904E-03   7.4551E-01   9.0423E-01   0.0000E+00

           total    4209622785   1779637242  14687509560    7.2400E+01

1tally        2        nps =   131248204
+                                Surface Dose (mrem/hr)                                $ Surface detector
           tally type 2    particle flux averaged over a surface.
           tally for  neutrons

           this tally is modified by a dose function.

           areas
                surface:      69
               segment
                  1       1.00000E+00
                  2       2.02680E+01
                  3       1.00000E+00
              whole       1.00000E+00

 surface  69
 segment:          -888
                1.44781E-02 0.0004

 surface  69
 segment:           888       -777
                1.65087E-05 0.0021

 surface  69
 segment:           888        777
                2.34934E-02 0.0003

 surface  69
 segment:   whole surface
                3.83061E-02 0.0002


 ================================================================================================================================

           results of 10 statistical checks for the estimated answer for the tally fluctuation chart (tfc) bin of tally        2

 tfc bin     --mean--      ---------relative error---------      ----variance of the variance----      --figure of merit--     -pdf-
 behavior    behavior      value   decrease   decrease rate      value   decrease   decrease rate       value     behavior     slope

 desired      random       <0.10      yes      1/sqrt(nps)       <0.10      yes        1/nps           constant    random      >3.00
 observed     random        0.00      yes          yes            0.00      yes         yes            constant    random       3.36
 passed?        yes          yes      yes          yes              yes      yes         yes               yes        yes         yes

 ================================================================================================================================


 this tally meets the statistical criteria used to form confidence intervals: check the tally fluctuation chart to verify.
 the results in other bins associated with this tally may not meet these statistical criteria.

 ----- estimated confidence intervals:  -----

 estimated asymmetric confidence interval(1,2,3 sigma): 3.8298E-02 to 3.8315E-02; 3.8289E-02 to 3.8323E-02; 3.8281E-02 to 3.8332E-02
 estimated  symmetric confidence interval(1,2,3 sigma): 3.8298E-02 to 3.8315E-02; 3.8289E-02 to 3.8323E-02; 3.8281E-02 to 3.8332E-02
```

```
1analysis of the results in the tally fluctuation chart bin (tfc) for tally        2 with nps=   131248204 print table 160


 normed average tally per history  = 3.83061E-02          unnormed average tally per history  = 3.83061E-02
 estimated tally relative error    = 0.0002              estimated variance of the variance  = 0.0000
 relative error from zero tallies  = 0.0001              relative error from nonzero scores  = 0.0002

 number of nonzero history tallies =    50446342         efficiency for the nonzero tallies  = 0.3844
 history number of largest  tally  =    70936096         largest  unnormalized history tally = 4.21736E+00
 (largest  tally)/(average tally)  = 1.10096E+02         (largest  tally)/(avg nonzero tally)= 4.23165E+01

 (confidence interval shift)/mean  = 0.0000              shifted confidence interval center  = 3.83061E-02


 if the largest  history score sampled so far were to occur on the next history, the tfc bin quantities would change as follows:

      estimated quantities           value at nps           value at nps+1           value(nps+1)/value(nps)-1.

      mean                            3.83061E-02            3.83061E-02                    0.000001
      relative error                  2.20951E-04            2.20952E-04                    0.000006
      variance of the variance        1.38382E-06            1.38398E-06                    0.000116
      shifted center                  3.83061E-02            3.83061E-02                    0.000000
      figure of merit                 5.68984E+04            5.68977E+04                   -0.000012

 the estimated inverse power slope of the 196 largest  tallies starting at 3.04204E+00 is 3.3611
 the empirical history score probability density function appears to be increasing at the largest  history scores:
 please examine. see print table 161.
 the large score tail of the empirical history score probability density function appears to have no unsampled regions.

 fom = (histories/minute)*(f(x) signal-to-noise ratio)**2 = (3.646E+05)*( 3.951E-01)**2 = (3.646E+05)*(1.561E-01) = 5.690E+04

1tally       22        nps =   131248204
+                                1-meter Dose (mrem/hr)                                $ 1-m detector
           tally type 2    particle flux averaged over a surface.
           tally for  neutrons

           this tally is modified by a dose function.

           areas
                surface:      80
               segment
                  1       1.00000E+00
                  2       2.02680E+01
                  3       1.00000E+00
               whole      1.00000E+00

 surface  80
 segment:          -888
                 9.47201E-03 0.0003

 surface  80
 segment:           888       -777
                 3.37000E-07 0.0112

 surface  80
 segment:           888        777
                 1.62597E-02 0.0002
```

```
 surface  80
 segment:   whole surface
                2.57385E-02 0.0002


 ================================================================================================================================

          results of 10 statistical checks for the estimated answer for the tally fluctuation chart (tfc) bin of tally       22

 tfc bin     --mean--      ---------relative error---------      ----variance of the variance----      --figure of merit--     -pdf-
 behavior    behavior      value   decrease   decrease rate      value   decrease   decrease rate       value     behavior     slope

 desired      random       <0.10      yes      1/sqrt(nps)       <0.10      yes        1/nps           constant    random      >3.00
 observed     random        0.00      yes          yes            0.00      yes         yes            constant    random      10.00
 passed?        yes          yes      yes          yes             yes      yes         yes               yes        yes         yes

 ================================================================================================================================


 this tally meets the statistical criteria used to form confidence intervals: check the tally fluctuation chart to verify.
 the results in other bins associated with this tally may not meet these statistical criteria.

 ----- estimated confidence intervals:  -----

 estimated asymmetric confidence interval(1,2,3 sigma): 2.5734E-02 to 2.5743E-02; 2.5730E-02 to 2.5747E-02; 2.5725E-02 to 2.5752E-02
 estimated  symmetric confidence interval(1,2,3 sigma): 2.5734E-02 to 2.5743E-02; 2.5730E-02 to 2.5747E-02; 2.5725E-02 to 2.5752E-02

1analysis of the results in the tally fluctuation chart bin (tfc) for tally       22 with nps=   131248204 print table 160


 normed average tally per history  = 2.57385E-02          unnormed average tally per history  = 2.57385E-02
 estimated tally relative error    = 0.0002               estimated variance of the variance  = 0.0000
 relative error from zero tallies  = 0.0001               relative error from nonzero scores  = 0.0001

 number of nonzero history tallies =    47256810          efficiency for the nonzero tallies  = 0.3601
 history number of largest  tally  =    79240332          largest  unnormalized history tally = 5.33428E-01
 (largest  tally)/(average tally)  = 2.07249E+01          (largest  tally)/(avg nonzero tally)= 7.46214E+00

 (confidence interval shift)/mean  = 0.0000               shifted confidence interval center  = 2.57385E-02


 if the largest  history score sampled so far were to occur on the next history, the tfc bin quantities would change as follows:

      estimated quantities           value at nps           value at nps+1           value(nps+1)/value(nps)-1.

      mean                            2.57385E-02            2.57385E-02                    0.000000
      relative error                  1.73713E-04            1.73713E-04                    0.000000
      variance of the variance        3.33168E-08            3.33173E-08                    0.000015
      shifted center                  2.57385E-02            2.57385E-02                    0.000000
      figure of merit                 9.20506E+04            9.20505E+04                    0.000000

 the estimated slope of the 198 largest  tallies starting at  4.05841E-01 appears to be decreasing at least exponentially.
 the large score tail of the empirical history score probability density function appears to have no unsampled regions.

 fom = (histories/minute)*(f(x) signal-to-noise ratio)**2 = (3.646E+05)*( 5.025E-01)**2 = (3.646E+05)*(2.525E-01) = 9.205E+04

1status of the statistical checks used to form confidence intervals for the mean for each tally bin
```

```
 tally   result of statistical checks for the tfc bin (the first check not passed is listed) and error magnitude check for all bins

        2   passed the 10 statistical checks for the tally fluctuation chart bin result
          passed all bin error check:     4 tally bins all have relative errors less than 0.10 with no zero bins

       22   passed the 10 statistical checks for the tally fluctuation chart bin result
          passed all bin error check:     4 tally bins all have relative errors less than 0.10 with no zero bins


 the 10 statistical checks are only for the tally fluctuation chart bin and do not apply to other tally bins.

1tally fluctuation charts

                          tally        2                          tally       22
         nps      mean     error   vov  slope    fom      mean     error   vov  slope    fom
      8192000   3.8291E-02 0.0009 0.0000 10.0   57136   2.5741E-02 0.0007 0.0000 10.0   92015
     16384000   3.8282E-02 0.0006 0.0000 10.0   57079   2.5737E-02 0.0005 0.0000 10.0   92007
     24576000   3.8276E-02 0.0005 0.0000 10.0   57075   2.5734E-02 0.0004 0.0000 10.0   92000
     32768000   3.8284E-02 0.0004 0.0000 10.0   57060   2.5738E-02 0.0003 0.0000 10.0   91999
     40960000   3.8287E-02 0.0004 0.0000 10.0   57037   2.5736E-02 0.0003 0.0000 10.0   92004
     49152000   3.8290E-02 0.0004 0.0000 10.0   57006   2.5738E-02 0.0003 0.0000 10.0   92015
     57344000   3.8291E-02 0.0003 0.0000 10.0   57054   2.5740E-02 0.0003 0.0000 10.0   92035
     65536000   3.8296E-02 0.0003 0.0000 10.0   57017   2.5740E-02 0.0002 0.0000 10.0   92049
     73728000   3.8297E-02 0.0003 0.0000  9.0   57019   2.5739E-02 0.0002 0.0000 10.0   92049
     81920000   3.8299E-02 0.0003 0.0000  6.0   56986   2.5738E-02 0.0002 0.0000 10.0   92050
     90112000   3.8300E-02 0.0003 0.0000  4.2   56948   2.5738E-02 0.0002 0.0000 10.0   92053
     98304000   3.8299E-02 0.0003 0.0000  4.2   56936   2.5738E-02 0.0002 0.0000 10.0   92055
    106496000   3.8301E-02 0.0002 0.0000  3.8   56920   2.5739E-02 0.0002 0.0000 10.0   92055
    114688000   3.8303E-02 0.0002 0.0000  3.6   56932   2.5740E-02 0.0002 0.0000 10.0   92064
    122880000   3.8304E-02 0.0002 0.0000  3.4   56912   2.5739E-02 0.0002 0.0000 10.0   92058
    131072000   3.8307E-02 0.0002 0.0000  3.4   56897   2.5739E-02 0.0002 0.0000 10.0   92052
    131248204   3.8306E-02 0.0002 0.0000  3.4   56898   2.5739E-02 0.0002 0.0000 10.0   92051

 ************************************************************************************************************************

 dump no.    7 on file runtpe     nps =   131248204     coll =    14687509560     ctm =      360.01   nrn =
 129910265577
 tally data written to file mctal

        2 warning messages so far.


 run terminated when it had used  360  minutes of computer time.

 computer time =  360.04 minutes

 mcnp     version 5     09282010                    02/28/14 04:47:39                    probid =  02/27/14 22:47:23
```

6.0 CRITICALITY EVALUATION

The following analyses demonstrate that the RH-TRU 72-B package complies with the requirements of 10 CFR §71.55[1]and §71.59. The analyses presented herein show that the criticality requirements are satisfied when limiting the RH-TRU 72-B package as follows for the payloads described in the *Remote-Handling Transuranic Waste Authorization Methods for Payload Control* (RH-TRAMPAC)[2]. These limits are summarized in Table 6.1-1.

- Case A – General Payload: maximum mass limit of 315 fissile gram equivalent (FGE) of ^{239}Pu, of manually compacted waste (i.e., not machine compacted) with less than or equal to 1% of special reflectors by weight. In addition, with 5 grams ^{240}Pu the waste is limited to 325 FGE ^{239}Pu, with 15 grams ^{240}Pu the waste is limited to 350 FGE ^{239}Pu, and with 25 grams ^{240}Pu the waste is limited to 370 FGE ^{239}Pu. These additional limits also require manually compacted waste (i.e., not machine compacted) with less than or equal to 1% of special reflectors by weight.
- Case B – Special Reflector Payload: maximum mass limit of 100 FGE ^{239}Pu, of manually compacted waste (i.e., not machine compacted) with greater than 1% of special reflectors by weight where the fissile material is not chemically or mechanically bound to the special reflector material, and maximum of 305 FGE of ^{239}Pu, where the fissile material is chemically or mechanically bound to the special reflector material.
- Case C – Machine-Compacted Payload: maximum mass limit of 245 FGE ^{239}Pu, of machine-compacted waste with less than or equal to 1% of special reflectors by weight.
- Case D – Low Enriched Uranium (LEU) Homogeneous Payload: maximum enrichment limit of 0.96 wt% ^{235}U fissile equivalent mass (^{235}U FEM), of manually compacted (i.e., not machine compacted) waste with distributed fissile isotope(s) in the non-fissile ^{238}U exhibiting particle/lump size characteristic dimensions (i.e., diameter or thickness) that are all less than 0.1 cm (0.039 inches) and/or greater than 6 cm (2.36 inches) with no restriction on special reflector materials.
- Case E – Low Enriched Uranium (LEU) Heterogeneous Payload: maximum enrichment limit of 0.84 wt% ^{235}U FEM, of manually compacted (i.e., not machine compacted) waste with distributed fissile isotopes in the non-fissile ^{238}U up to a total contents net weight of 3,100 pounds with no restriction on special reflector materials.

Based on an unlimited array of undamaged or damaged RH-TRU 72-B packages, the CSI, per 10 CFR §71.59[1], is 0.0.

[1] Title 10, Code of Federal Regulations, Part 71 (10 CFR 71), *Packaging and Transportation of Radioactive Material*, 01-01-14 Edition.

[2] U.S. Department of Energy (DOE), *Remote-Handled Transuranic Waste Authorized Methods for Payload Control* (RH-TRAMPAC), U.S. Department of Energy, Carlsbad Field Office, Carlsbad, New Mexico.

An evaluation of the applicability of the criticality evaluations contained in this chapter to the neutron shielded canister is provided in Appendix 5.1 of the *RH-TRU Payload Appendices*[1]. The following evaluations are generally presented for payload canisters without supplemental neutron shielding components.

6.1 Discussion of Results

A comprehensive description of the RH-TRU 72-B packaging is provided in Section 1.2, *Package Description*, and in the packaging drawings in Appendix 1.3.1, *Packaging General Arrangement Drawings*. For the contents of the RH-TRU 72-B package specified in Section 6.2, *Package Contents*, the outer diameter of the package is required to maintain criticality safety for any number of RH-TRU 72-B packages for both normal conditions of transport (NCT) and hypothetical accident conditions (HAC). The stainless steel shells (inner vessel (IV) shell and outer cask (OC) outer shell) and the lead filled cavity between these shells provide better reflection than water such that the package would be further subcritical without it.

The primary criterion for ensuring that a package (or package array) is safely subcritical is:

$$k_s = k_{eff} + 2\sigma < USL$$

where the quantity k_s is the neutron multiplication factor computed for a given configuration plus twice the uncertainty, σ, in the computed result.

This quantity is computed and reported in order to permit a direct comparison of results against the upper subcritical limit (USL) determined in Section 6.5, *Critical Benchmark Experiments*. The USL is determined on the basis of a benchmark analysis and incorporates the combined effects of code computational bias, the uncertainty in the bias based on both experimental and computational uncertainties, and an administrative margin. Further discussion regarding the USL is provided in Chapter 4, *Determination of Bias and Subcritical Limits*, of NUREG/CR-6361[2].

The fissile mass limits are summarized in Table 6.1-1, and the results of the criticality calculations are summarized in Table 6.1-2. All k_s values are less than the respective USLs of:

- 0.9382 for Pu systems in Cases A through C;
- 0.9257 for the LEU systems in Case D;
- 0.9327 for 0.84 wt% LEU systems in Case E with up to 1% special reflectors; and
- USL(EALF) = 0.9336-6.9580E-03*EALF for LEU systems in Case E with unlimited special reflectors where EALF is the Energy of Average Lethargy of Fission (in eV).

For all cases, the modeled conditions are considered to be extremely conservative and provide an upper limit on k_s. Therefore, the requirements of 10 CFR §71.55 are satisfied when the contents of a single RH-TRU 72-B package is limited in accordance with the limits presented in Table 6.1-1. The application of these limits is described the RH-TRAMPAC[2].

[1] U.S. Department of Energy (DOE), *RH-TRU Payload Appendices*, U.S. Department of Energy, Carlsbad Field Office, Carlsbad, New Mexico.

[2] J. J. Lichtenwalter, S. M. Bowman, M. D. DeHart, and C. M. Hopper, *Criticality Benchmark Guide for Light-Water Reactor Fuel in Transportation and Storage Packages*, NUREG/CR-6361, ORNL/TM-13211, March 1997.

Infinite arrays of both damaged and undamaged RH-TRU 72-B packages, as defined in Section 6.3.4, *Array Models*, are also safely subcritical. The post-accident geometry model for the damaged RH-TRU 72-B package conservatively bounds the damage postulated from HAC analyses documented in Section 2.7, *Hypothetical Accident Conditions*. The model conservatively assumes that the impact limiters are deformed to one-half their initial dimensions.

Calculations performed for Case A of the RH-TRU 72-B package single unit and infinite array of single units of damaged packages indicate that the maximum reactivity of the package arrays are essentially the same as that of the HAC single-unit cases[3] to within the calculated uncertainty of the Monte Carlo analysis (typically about 0.0010). This occurs because:

- The packages are large in comparison with the optimum moderated geometric size of the postulated worst case sphere which results in two effects. First, when full reflection is applied to the optimally moderated spheres, the reflectors tend to isolate the units. Second, since the package is large compared to the spheres, the solid angle to adjacent spheres is small. Both of these effects reduce the interaction between units.
- The package design results in essentially equivalent physical conditions for the NCT and HAC with respect to the inner vessel (IV) region. Consequently, the NCT and HAC single-unit models were identical. In the HAC infinite case, the size of the units under HAC is not significantly reduced by compression of the impact limiters. Consequently the distance between units remains great enough for unit isolation.

In Case D and Case E, using the postulated representation of the LEU payload, interaction at very low interspersed moderation levels was demonstrated. This is primarily caused by the much larger size of the fissile geometry allowed in the package. This increased size both reduced the solid angle to adjacent spheres (and therefore increased the potential for interaction) and reduced the isolating effects of a reflector. Consequently, in Case D, the difference between the NCT and HAC single unit and the HAC infinite unit cases differs by 0.5 percent, increasing from 0.9150 to 0.9200 for the poly/water reflected system and 0.9180 to 0.9224 for the special reflector reflected system.

For an infinite array of damaged RH-TRU 72-B packages, the maximum calculated k_s values for each case occurred for optimal internal moderation and maximum reflection within the IV and in between the packages. All limits were developed to maintain k_s below the respective USL. The highest k_s from all cases was 0.9370 occurring for Case A in evaluating the 315 FGE unrestricted limit and the 370 FGE limit with 25 g ^{240}Pu present in the waste matrix. These both occurred for infinite arrays of packages at optimal moderation and full reflection. All specific calculations are detailed in Section 6.4.3, *Criticality Results*. These evaluations provide conservative representations of the postulated materials, geometries, and interaction effects from full to decreased volume fractions of interspersed moderation in infinite arrays of units. Therefore, the requirements in 10 CFR §71.59[1] are satisfied for the arrays of RH-TRU 72-B packages under the fissile limitations indicated in Table 6.1-1.

[3] Note that the NCT and HAC single-unit models were identical since the package contents are optimally located for the NCT model, the damage to the package during the HAC results in no significant structural damage (the impact limiters were conservatively not modeled in the single unit case), and flooding with water is already bounded by the optimum moderator/reflector assumptions of 25% polyethylene/74% water/1% beryllium.

Table 6.1-1 – Fissile Material Limit per RH-TRU 72-B Package

Fissile Content Special Conditions	Fissile Material Limit per RH-TRU 72-B Package①				
	Case A	Case B	Case C	Case D	Case E
None②	315 ^{239}Pu FGE	100 ^{239}Pu FGE	245 ^{239}Pu FGE	0.96 wt% ^{235}U FEM	0.84 wt% ^{235}U FEM
>5 g ^{240}Pu	325 ^{239}Pu FGE	—	—	—	—
>15 g ^{240}Pu	350 ^{239}Pu FGE	—	—	—	—
>25 g ^{240}Pu	370 ^{239}Pu FGE	—	—	—	—
Fissile material bound to special reflector	—	305 ^{239}Pu FGE	—	—	—

Notes:

① Other physical contents limits apply based on each Case A through E. For example, Case A is limited to manually compacted waste (not machine compacted) with up to 1 wt% beryllium. For complete summary of applicability for each case see Section 6.4.3.4, *Applicable Criticality Limits for RH-TRU Waste*.

② These limits apply to the payload regardless of the ^{240}Pu content or the distribution of the ^{239}Pu.

Table 6.1-2 – Summary of Criticality Analysis Results

	Case A	Case B	Case C	Case D	Case E
Normal Conditions of Transport (NCT)					
Number of undamaged packages calculated to be subcritical	∞	∞	∞	∞	∞
Single Unit Maximum k_s	Bound by HAC Single Unit k_s	Bound by HAC Infinite Array k_s		Bound by HAC Single Unit k_s	Bound by HAC Single Unit k_s
Infinite Array Maximum k_s	Bound by HAC Infinite Array k_s				
Hypothetical Accident Conditions (HAC)					
Number of damaged packages calculated to be subcritical	∞	∞	∞	∞	∞
Single Unit Maximum k_s (0 g ^{240}Pu)	0.9370	Bound by HAC Infinite Array k_s		0.9180	0.9295
Infinite Array Maximum k_s (0 g ^{240}Pu)	0.9361	0.9086	0.9372	0.9224	0.9316
Infinite Array Maximum k_s (with ^{240}Pu)	0.9370	—	—	—	—
Infinite Array Maximum k_s (with fissile material bound to special reflector)	—	0.9340	—	—	—
Upper Subcritical Limit (USL)	0.9382			0.9257	0.9323

This page intentionally left blank.

6.2 Package Contents

The payload cavity of an RH-TRU 72-B package can accommodate one payload canister, containing one of five authorized payload types: a General Payload (Case A), a Special Reflected Payload (Case B), a Machine-Compacted Payload (Case C), and a Low Enriched Uranium (LEU) Payload (Cases D and E). The different FGE limits apply depending on the contents of the shipment as discussed in the subsections below.

The quantities of all fissile isotopes other than ^{239}Pu present in the RH-TRU waste matrix may be converted to a FGE using the conversion factors outlined in the *Remote-Handling Transuranic Waste Authorization Methods for Payload Control* (RH-TRAMPAC)[1]. For modeling purposes, the package is assumed to contain ^{239}Pu at the FGE limit. The fissile composition of the RH-TRU waste matrix will typically be as follows:

Nuclide	Weight-Percent
Pu-238	Trace
Pu-239	93.0
Pu-240	5.8
Pu-241	0.4
Pu-242	Trace
Am-241	Trace
All other fissile isotopes	0.7

Additionally, when other fissile isotopes are present in the LEU Payload, the quantities of other contaminating fissile isotopes may be accounted for in the % ^{235}U FEM calculations using the conversion factors also outlined in the RH-TRAMPAC[1].

6.2.1 Applicability of Case A Limits – General Payload

The Case A, General Payload, limits are applicable to canisters of RH-TRU waste material where the ^{239}Pu fissile nuclides (or FGEs of other fissile nuclides), in any form or distribution, with or without ^{240}Pu, are contained in manually compacted (i.e., not machine compacted) wastes and the waste contains less than or equal to 1% of special reflectors by weight. No credit is taken for parasitic neutron absorption of the waste materials and other authorized payload components consisting of the canister, dunnage, and any packing materials, except to the extent that the fissile, moderator, and special reflector elements absorb neutrons. The contents of the RH-TRU 72-B package is conservatively modeled with an optimally moderated sphere of ^{239}Pu and a mixture of 25% polyethylene and 75% water (by volume). The size of the sphere is determined by the specific H/^{239}Pu number density ratio, and this parameter is varied in order to determine the most reactive configuration (i.e., an optimally moderated sphere for a given ^{239}Pu

[1] U.S. Department of Energy (DOE), *Remote-Handled Transuranic Waste Authorized Methods for Payload Control* (RH-TRAMPAC), U.S. Department of Energy, Carlsbad Field Office, Carlsbad, New Mexico.

mass). The RH-TRU waste material and other authorized payload components may contain plastic materials such as anti-contamination clothing, plastic bags, and other plastic refuse that are manually compacted only.

The utilization of polyethylene as the bounding hydrogenous moderating material is justified by the SAIC-1322-001[2] study which concludes that polyethylene is the most reactive moderator that could credibly moderate the transuranic waste in a pure form. A 25% volumetric packing fraction for polyethylene is used as a conservative value which is based on physical testing that bounds the packing fraction of polyethylene in manually compacted TRU waste of 13.36%[3]. Higher packing fractions of up to 100% polyethylene resulting from machine compacted waste are evaluated under the Case C limits presented in Section 6.2.3, *Applicability of Case C Limits – Machine-Compacted Payload*.

This evaluation also addresses the addition of special reflectors in the waste matrix. Materials that can credibly provide better than 25% polyethylene/75% water equivalent reflection are termed "special reflectors" and are not authorized for shipment under the General Payload case in quantities that exceed 1% by weight except in those specific configurations discussed below. Based on the studies of reflector material documented in SAIC-1322-001[2], Be, BeO, C, D_2O, MgO, and depleted uranium (less than 0.72 wt% and greater than or equal to 0.3 wt% ^{235}U) are the only materials considered special reflectors because they provide reflection equivalent to 2 ft thickness of 25% polyethylene and 75% water mixture under the following conditions:

- Less than 5/8-inch thick at 100% of theoretical density4 in the form of large solids;
- Less than 11/16-inch thick at 70% of theoretical density in the form of tightly-packed particulate solids;
- Less than 20% packing fraction at 24 inches thick in the form of randomly dispersed particulate solids.

The utilization of 1% by volume beryllium in the modeled waste matrix bounds the presence of up to 1 wt% quantities of special reflectors that are randomly dispersed in the payload containers for the purposes of the calculations. This substitution of 1% by volume for 1 wt% is valid based on the large volume of the IV, the maximum allowed payload canister weight allowed in the package, and the low densities of the most reactive payload configurations using the poly/water mixtures. SAIC-1322-001[2] found that beryllium is the bounding special reflector as it provides the best reflection of the system and results in the highest k_s.

Limits for these special reflectors in excess of 1 wt% are addressed in Section 6.2.2, *Applicability of Case B Limits – Special Reflector Payload* for Pu payloads and in Section 6.2.4, *Applicability of Case D Limits – LEU Homogeneous Payload*, and Section 6.2.5, *Applicability of Case E Limits – LEU Heterogeneous Payload*, for LEU payloads.

[2] Neeley, G. W., D. L. Newell, S. L. Larson, and R. J. Green, *Reactivity Effects of Moderator and Reflector Materials on a Finite Plutonium System*, SAIC-1322-001, Revision 1, Science Applications International Corporation, Oak Ridge, Tennessee, May 2004.

[3] WP-8-PT.09, *Test Plan to Determine the TRU Waste Polyethylene Packing Fraction*, Washington TRU Solutions, LLC., Revision 0, June 2003.

[4] The theoretical densities used in the study (refer Footnote 2) are 1.85 g/cc for Be, 2.69 g/cc for BeO, 2.1 g/cc for C, 1.1054 g/cc for D_2O, 3.22 g/cc for MgO, and 19.05 g/cc for depleted U.

6.2.2 Applicability of Case B Limits – Special Reflector Payload

The Case B, Special Reflector Payload, limit is applicable for contents containing greater than 1% by weight quantities of special reflector materials provided the contents are manually compacted (i.e., not machine compacted). These requirements drive the assumptions regarding the appropriately bounding moderator and reflector materials that are utilized in the analysis to bound the presence of all materials that are authorized for shipment under the Case B FGE limit of 100 g ^{239}Pu. However, if the special reflector materials can be shown to be in thicknesses and/or packing fractions that are less than 25% polyethylene/ 75% water equivalent parameters given in Table 6.2-1, then Case A, General Payload limits can be used. Note that equivalent thicknesses for Be and BeO are not given as, for thin reflectors of these materials, 100% packing fraction does not result in the highest reactivity and the equivalent thickness increases inversely with the packing fraction; thus, only a packing fraction comparison can be used for Be and BeO. The contents model assumptions are provided in Section 6.3.1.2, *Case B, Special Reflector Payload, Contents Model*. A summary discussion of special reflectors is provided in Section 6.4.3.3, *Special Reflectors in RH-TRU Waste*.

The utilization of polyethylene as a bounding hydrogenous moderating material at a 25% packing fraction is consistent with the justification provided in Section 6.2.1, *Applicability of Case A Limits – General Payload*. However, the fissile sphere is moderated with varying volume fractions of beryllium as beryllium was also found in SAIC-1322-001[2] to increase reactivity when significant quantities are included in the moderator. The use of a 100% dense thick Be reflector in the model bounds the presence of other special reflector materials.

To obtain a second less restrictive limit, the fissile isotope is assumed to be chemically or mechanically bound to the special reflector material and the remainder of the waste is assumed to be hydrogenous reflector material consisting of a 25% polyethylene/74% water/1% beryllium mixture. Having the fissile isotope chemically or mechanically bound to the special reflector material allows the higher 305 FGE limit since the material is not available as a reflector (above 1 wt% that represents contamination in the remaining waste matrix) and is not as effective as a moderator. This limit allows for packaging of larger quantities of special reflector material where the fissile isotope is chemically or mechanically bound to the reflector material as a higher concentration contaminant. The use of a variable volume fraction Be moderator in the model bounds the presence of other special reflector materials.

6.2.3 Applicability of Case C Limits – Machine-Compacted Payload

The Case C, Machine-Compacted Payload, limit is applicable provided the contents are machine compacted and contain less than or equal to 1% by weight quantities of special reflector materials. These requirements drive the assumptions regarding the appropriately bounding moderator and reflector materials that are utilized in the analyses to bound the presence of all materials that are authorized for shipment under the Case C 245 FGE limit. The contents model assumptions are provided in Section 6.3.1.3, *Case C, Machine-Compacted Payload, Contents Model*.

The utilization of polyethylene as a bounding hydrogenous moderating material at 100% packing fraction is consistent with the machine compacted polyethylene waste that can be compacted at some facilities under extremely high pressures. Additionally, SAIC-1322-001[2] concluded no material, that could credibly moderate a fissile sphere in a pure form, resulted in a higher

reactivity than the 100% polyethylene moderated system. Thus, compared to Case A, the packing fraction of the moderator is the dominant factor that results in an increase in reactivity and a subsequent lowering of the FGE limit in this Case C. The only inorganic material that increased reactivity when added to the fissile mixture was beryllium, thus up to 1wt% beryllium is modeled in the moderator. The effect of more than 1% by weight quantities of beryllium in the moderator is studied separately under Case B as beryllium is also the leading special moderator. The use of 99% polyethylene and 1% beryllium (by volume) in the reflector region is an appropriately bounding reflector material as it is consistent with the moderator assumption and accounts for the less than or equal to 1% by weight quantities of special reflector materials allowed in the package under the Case C limitations.

6.2.4 Applicability of Case D Limits – LEU Homogeneous Payload

The LEU contents are restricted to material that is primarily uranium (in terms of the heavy metal component) and waste matrix material distributed within a canister in such a manner that the maximum enrichment of the uranium does not exceed 0.96% ^{235}U FEM in any location of the waste material, and there are no variations in the fissile concentration that exceed 0.96% ^{235}U FEM in any location. The Case D homogeneous limits apply to a mixture with particle/lump size characteristic dimensions (i.e., diameter or thickness) that are all less than 0.1 cm (0.039 inches) and/or greater than 6 cm (2.36 inches). For waste mixtures of unlimited particle/lump size characteristic dimensions, see Section 6.2.5, *Applicability of Case E Limits – LEU Heterogeneous Payload*.

Based on subcritical limits published in ANSI/ANS-8.1,[5] the subcritical enrichment limit for uranium oxides mixed homogeneously with water with no limitations on mass or concentration is 0.96 wt% ^{235}U. Uranium nitrates show a higher subcritical limit. The uranium oxide case bounds the low enriched uranium payloads approved in this evaluation. ANSI/ANS-8.12[6] establishes subcritical concentration limits for plutonium-uranium oxide mixtures. A homogenous mixture of plutonium oxide mixed with natural enrichment uranium oxide is assigned a subcritical concentration limit of 0.13 wt% Pu in the mixture of (Pu + U) of unlimited mass. However, these general limits are not equivalent and offer limited application in determining the wt% ^{235}U FEM for any other fissile isotopes that may exist in low concentrations in the waste matrix primarily made or contaminated with ^{238}U. Evaluation of the limit is needed because these standards do not address the higher hydrogen content of the polyethylene/water moderator (the standards are based water reflected aqueous systems only), the special reflector materials allowed in the waste matrix, and the thick steel and lead walls of the package that provide for a higher amount of neutron backscatter. Conversion factors are outlined in the RH-TRAMPAC[1] for calculating the contribution of other fissile isotopes to the % ^{235}U FEM.

A parameter study was performed to determine the maximum k_s under varying 25% polyethylene and 75% water moderator mixtures with the uranium oxide assuming a homogeneous media. Additionally, the presence of special reflector material in the waste matrix was evaluated. The same combinations of special reflector conditions as evaluated in Case B were evaluated for the

[5] ANSI/ANS-8.1 1998, *Nuclear Criticality Safety in Operations with Fissionable Materials Outside Reactors*, American Nuclear Society (ANS), La Grange Park, Illinois.

[6] ANSI/ANS-8.12 1987, *Nuclear Criticality Control and Safety of Plutonium-Uranium Fuel Mixtures Outside Reactors*, American Nuclear Society (ANS), La Grange Park, Illinois.

LEU payload and found to be acceptable with the enrichment limit. The maximum k_s found during these parametric evaluations identified the most reactive waste matrix. The NCT and HAC criticality calculations were then made for the optimum mixtures within the package.

6.2.5 Applicability of Case E Limits – LEU Heterogeneous Payload

The LEU contents are restricted to material that is primarily uranium (in terms of the heavy metal component) and waste matrix material distributed within a canister in such a manner that the maximum enrichment of the uranium does not exceed 0.84% ^{235}U FEM in any location of the waste material, and there are no variations in the fissile concentration that exceed 0.84% ^{235}U FEM in any location. The Case E heterogeneous limits apply to a mixture with particle/lump size characteristic dimensions (i.e., diameter or thickness) of any size up to a total contents net weight of 3,100 pounds. Conversion factors are outlined in the RH-TRAMPAC[1] for calculating the contribution of other fissile isotopes to the % ^{235}U FEM.

A parameter study was performed to determine the maximum k_s for varying uranium rod or sphere sizes in a square-pitched array moderated with 25% polyethylene/ 74% water / 1% beryllium mixture. At 0.96 wt% ^{235}U FEM, some uranium sphere/cylinder sizes (between 0.1 and 6 cm) exceeded the USL and the Case D results. These sizes were further evaluated at a lower enrichment and total contents net weight. Additionally, the presence of special reflector material in the waste matrix was evaluated. The same combinations of special reflector conditions as evaluated in Case D were evaluated for the LEU heterogeneous payload and found to be acceptable with the 0.84 wt% ^{235}U enrichment limit. The maximum k_s found during these parametric evaluations identified the most reactive waste matrix. The NCT and HAC criticality calculations were then made for the optimum mixtures within the package.

Table 6.2-1 – Special Reflector Material Parameters that Achieve the Reactivity of a 25%/75% Polyethylene/Water Mixture Reflector

Special Reflector Material	Equivalent Thickness at 100% of Theoretical Density (inches)	Equivalent Thickness at 70% of Theoretical Density (inches)	Equivalent Packing Fraction at 24-inch Thickness (%)
Be	N/A	N/A	7
BeO	N/A	N/A	7
C	0.18	0.25	9
D_2O	0.24	0.27	14
MgO	0.26	0.33	15
U(Natural)	0.08	0.10	1
U(0.6% ^{235}U)	0.14	0.18	1
U(0.5% ^{235}U)	0.18	0.28	2
U(0.4% ^{235}U)	0.33	0.51	3
U(0.3% ^{235}U)	0.56	0.73	5

6.3 Model Specifications

6.3.1 Contents Models

Criticality calculations for the RH-TRU 72-B package are performed using the three-dimensional Monte Carlo computer code KENO-V.a[1] by using the CSAS25[2] driver utility module. Calculations for Cases A through D used the SCALE v4.4a software package[3], whereas Case E calculations used the SCALE 5.1 software package.[4,5,6] Descriptions of the calculational models are given in Section 6.3.1, *Contents Models*, for all cases. A summary of materials and atom densities that are used in the evaluation of the RH-TRU 72-B package is given in Section 6.3.2, *Package Model*.

The limiting mass of fissile material that may be transported in a single RH-TRU 72-B package is shown to provide adequate subcritical margin based on the detailed KENO-V.a analysis. These calculations are performed for an optimally moderated single-unit model and an infinite array model of the RH-TRU 72-B package under both normal conditions of transport (NCT) and hypothetical accident conditions (HAC) for each of the four cases presented.

In all cases, the computational model consists of a contents model and a packaging model. The contents models conservatively represent the package contents, including all authorized payload components and the waste matrix as allowed by each of the cases evaluated. The packaging model represents the remaining structural materials comprising the RH-TRU 72-B packaging. The amount of moderating and reflecting material assumed present in the computational model is varied to maximize reactivity for the single unit and infinite array unit models of the NCT and HAC cases.

6.3.1.1 Case A, General Payload, Contents Model

The Case A, General Payload, contents model is represented as an optimally moderated homogeneous sphere of fissile material with a moderating material consisting of one of the following mixtures: 25% polyethylene and 75% water, or 25% polyethylene, 74% water, and 1% beryllium (each by volume). The remainder of the waste matrix is represented by one or the

---

[1] Petrie, L. M., and N. F. Landers, *KENO-V.a: An Improved Monte Carlo Criticality Program with Supergrouping*, ORNL/NUREG/CSD-2/V2/R6, Volume 2, Section F11, March 2000.

[2] Landers, N. F., and L. M. Petrie, *CSAS: Control Module for Enhanced Criticality Safety Analysis Sequences*, NUREG/CR-0200, ORNL/NUREG/CSD-2/V2/R6, Volume 1, Section C4, March 2000.

[3] Oak Ridge National Laboratory (ORNL), *SCALE 4.4a: Modular Code System for Performing Standardized Computer Analyses for Licensing Evaluation for Workstations and Personal Computers*, NUREG/CR-0200, ORNL/NUREG/CSD-2/R6, March 2000.

[4] Petrie, L. M., *et al.*, *KENO-V.a: An Improved Monte Carlo Criticality Program*, ORNL/TM-2005/39, SCALE Version 5.1, Volume II, Book 2, Section F11, November 2006.

[5] Goluoglu, S., *et al.*, *CSAS: Control Module for Enhanced Criticality Safety Analysis Sequences*, ORNL/TM-2005/39, SCALE Version 5.1, Volume I, Book 1, Section C4, November 2006.

[6] Oak Ridge National Laboratory (ORNL), *SCALE 5.1: Modular Code System for Performing Standardized Computer Analyses for Licensing Evaluation for Workstations and Personal Computers*, ORNL/TM-2005/39, SCALE Version 5.1, November 1, 2006.

other of the moderator mixtures only. This representation of the waste matrix conservatively locates the entire fissile isotope mass in one location and provides optimum moderation and reflection using the worst case expected materials allowed in the waste matrix, namely, the hydrogenous polyethylene and water and the trace amounts of special reflector, beryllium. Both mixtures are evaluated to determine which is optimal as a moderated mixture. Based on the expected payload weight, volume of the payload container, the densities of the most reactive systems modeled, and on the density of Be at 1.85 g/cc, modeling the 1% beryllium by volume bounds the limit of 1% by weight.

Since the canister within the package is not credited with containing the waste in any specific configuration, various locations for the Pu sphere are evaluated to determine the effects on package neutron multiplication factor. The sphere is evaluated centered in the container, as shown in Figure 6.3-2, located centered against the thickest end (to evaluate the thick steel reflector conditions at the container top closure) as shown in Figure 6.3-3, and located in the "corner," that is, against the thickest end and displaced radially to the outside of the package, as shown in Figure 6.3-4. Because the payload configuration and IV is unaffected by the HAC conditions, the NCT and HAC contents models are equivalent and the location of the sphere resulting in the maximum neutron multiplication factor is used throughout the remaining evaluations, as applicable.

6.3.1.2 Case B, Special Reflector Payload, Contents Model

The Case B, Special Reflector Payload, contents model also consists of a fissile sphere. The composition of the sphere is modified with the addition of greater amounts of Be and, due to the more efficient Be reflector conditions, the fissile material is reduced to a lower limit of 100 FGE. The first condition assumes that the Pu sphere is optimally moderated with the same mixture as evaluated in Case A, namely, a mixture of 25% polyethylene, 74% water, and 1% beryllium. Since unlimited beryllium is allowed under the limitations of Case B, a beryllium reflector fills the remainder of the IV space. This case evaluates the effect of a pure Be reflector with an optimally moderated Pu sphere. Since the beryllium is a better reflector than steel, the Pu sphere is moved back to the center of the package for this evaluation (scoping calculations showed this to be the most reactive location for the sphere). In order to evaluate voids in the reflector, the volume fraction of beryllium reflector in the IV region is also varied from 100% down to 1%. The second conditions assume that a higher percentage of beryllium is also in the moderator and a solid beryllium reflector exists around the sphere. In order to evaluate this condition, beryllium is added to the sphere and displaces the poly/water mixture raising the volume percent of the beryllium in the moderator from 1% to 80% to evaluate the trend. Between these two evaluations, the waste matrix is evaluated with beryllium at greater than 1% as special reflector of an optimally moderated sphere, with and without significant special reflector in the moderator, thus conservatively evaluating the case where the fissile isotope is not necessarily bound chemically or mechanically to the special reflector material.

A third configuration of the contents is also modeled that assumes that all of the fissile isotope is bound to special reflector material (this also conservatively leaves allowance for 1% by volume special reflector material to be distributed throughout the waste matrix). This contents model evaluates varying volume percents of beryllium displacing the 25% polyethylene/75% water mixture in the moderator with 305 FGE in the sphere. The reflector in the model remains a 25% polyethylene, 74% water, and 1% beryllium (each by volume) mixture that accounts for some

special reflector contamination in the remainder of the waste matrix. This contents model is designed to provide a higher fissile loading limit where the waste matrix is known to consist of larger quantities of special reflector materials with higher fissile concentrations chemically or mechanically bound to the special reflector (such as alloys, molds, and crucibles) and where the remainder of the waste matrix is at most contaminated with special reflector (such as, personnel protective equipment, trash, inert packaging material). In this model, the location of the sphere was again found to be most reactive in the "corner" of the IV where neutrons were more effectively backscattered into the hydrogenous reflector region.

6.3.1.3 Case C, Machine-Compacted Payload, Contents Model

The fissile sphere composition in the Case C contents model is moderated with 100% polyethylene and the IV region is filled with a reflector consisting of 99% polyethylene and 1% beryllium (by volume). The 1% beryllium (by volume) accounts for the increased neutron moderation that is caused by less than or equal to 1 wt% special reflector material that is allowed in the Machine-Compacted Payload package. The volume fraction of the 99% polyethylene/1% beryllium reflector in the IV region is varied to assure that voids in the waste matrix are less reactive than the fully compacted conditions.

6.3.1.4 Case D, LEU Homogeneous Payload, Contents Model

Since 0.96 wt% ^{235}U FEM fissile concentrations are so low, the most reactive system from a neutron multiplication factor standpoint grows very large. ANSI/ANS-8.1[7] lists 0.96 wt% ^{235}U as a subcritical enrichment limit for uranium oxides mixed homogenously with water. Consequently, this enrichment should be subcritical for infinite systems.[8] For this waste matrix, uranium oxide at 0.96 wt% ^{235}U is mixed homogenously throughout the IV with varying amounts of 25% polyethylene/ 74% water/ 1% beryllium moderator mixture to represent the worst case waste matrix. The only physical limit placed on the system is that the total mass of the uranium/moderator mixture in the IV does not exceed the contents weight limit of 6,900 pounds. Any voids are filled with the lighter 25% polyethylene/ 74% water/ 1% beryllium reflector mixture used in Case A. The package is filled from the top to the bottom with the U/ 25% polyethylene/ 74% water/ 1% beryllium mixture and followed with the 25% polyethylene/ 74% water/ 1% beryllium reflector mixture to completely fill the container. To evaluate the special reflector materials, the reflector region in the IV was replaced with Be and the percentage of Be in the moderator was increased to evaluate the trend in added special reflector in the moderator. Three different fissile region/reflector region configurations using the Be reflector are evaluated. These are shown in Figure 6.3-6 (these changes in location were evaluated due to results in evaluating Case B). In all cases the additional reflector material is conservatively included in excess of the payload weight limit. A range of H/^{235}U ratios are evaluated to determine the optimum moderated configuration. As before, since the contents models for the NCT and HAC physical conditions are identical, only the HAC conditions are evaluated to represent both.

[7] ANSI/ANS-8.1-1998, *Nuclear Criticality Safety in Operations with Fissionable Materials Outside Reactors*, American Nuclear Society (ANS), La Grange Park, Illinois.

[8] Note that the ANSI/ANS-8.1 is applicable to aqueous, water reflected systems. The system modeled in Case D and throughout this evaluation contains some special reflector material and is reflected by significant thicknesses of steel. The presence of both of these materials invalidates the use of the ANSI/ANS-8.1 limits.

6.3.1.5 Case E, LEU Heterogeneous Payload, Contents Model

For this waste matrix, uranium metal at 0.84 wt% ^{235}U is arrayed both in cylindrical arrays of cylinders (rods) and cylindrical arrays of spheres. Square pitched arrays were used as representative of credible waste configurations. Based on the results of Case D studies, the arrays were located in the top of the IV with varying amounts of 25% polyethylene/ 74% water/ 1% beryllium moderator mixture to represent the worst case waste matrix (scoping calculations with arrays located in the center, radially, validated this behavior). The only physical limit placed on the system is that the total mass of the uranium/moderator mixture in the IV does not exceed a contents net weight limit of 3,100 pounds. Any voids are filled with the 25% polyethylene/ 74% water/ 1% beryllium reflector mixture which was not included in the 3,100-pound limit. The U lattice moderated by the 25% polyethylene/ 74% water/ 1% beryllium mixture was placed at the top of the IV and the remainder of the volume was filled with the 25% polyethylene/ 74% water/ 1% beryllium reflector mixture to completely fill the container. The spacing between array units (rods or spheres of uranium) was varied and equivalent H/^{235}U ratios were calculated for comparison to homogenous studies. The arrays were generally filled to the edge of the IV radially and were adjusted in the axial direction to account for the loading restriction on total net weight of the contents. Configurations for the cylindrical arrays of cylinders and spheres are shown in Figure 6.3-7 and Figure 6.3-8, respectively.

To evaluate the special reflector materials, the reflector region of the IV was replaced with Be in increments of 1 cm and up in the axial direction until the Be filled the reflector region. The axial Be and the uranium weight totaled the 3,100-pound limit in these models. The Be also filled the void outside of the array in the radial direction which was ignored in the weight calculation. Cylindrical arrays at the top of the IVand at the center of the IV were tested and cylindrical arrays at the center were found to be more reactive. Additionally, models were evaluated with the percentage of Be in the poly/water/Be mixture increased to evaluate the trend in added special reflector in the moderator/reflector. Configurations using the Be reflector are shown in Figure 6.3-9. The configurations for the variable Be in the moderator/reflector region were similar. In these cases the uranium mass is reduced by the weight of the Be and polyethylene (in the moderator region around the uranium only) such that the overall payload net weight remains at or above the loading limit of 3,100 pounds. The water is ignored in the net weight calculation as it may leak in under HAC conditions after loading. When arrays of spherical units are modeled, excess uranium mass is conservatively included to reduce the modeling complexity as only whole spherical units are used to fill the array of spheres. A range of lattice pitches are evaluated to determine the optimum configuration. As before, since the contents models for the NCT and HAC physical conditions are identical, only the HAC conditions are evaluated to represent both.

6.3.2 Package Model

A comprehensive description of the RH-TRU 72-B packaging is provided in Section 1.2, *Package Description*, and in the packaging drawings in Appendix 1.3.1, *Packaging General Arrangement Drawings*. The packaging includes an inner vessel (IV), an outer cask (OC), and impact limiters. The impact limiters cover each end of the OC and are steel shells filled with polyurethane foam. The OC includes a steel shell structure that encloses and supports lead shielding, and surrounds the independent steel IV. The nested IV and OC each provide independent leak-tight containment under NCT.

The packaging is robust due to the heavy wall design needed to provide gamma shielding. For modeling simplicity, miscellaneous hardware (such as the trunnions) is neglected for both NCT and HAC models. The impact limiters are neglected for all of the single package models of Cases A through E. The impact limiters are assumed to provide one half their respective thicknesses in all directions for infinite array Cases A through E. The modeled impact limiters are assumed to only provide spacing, and are treated in the same manner as the other regions outside of the package. These assumptions conservatively:

- Allow for greater reflection in the single package cases by allowing the water reflector outside the package to be closer fitting;
- Account for array HAC damage to the impact limiters due to crush damage during impact;
- Reduce spacing between packages in infinite array calculations to conservatively increase interaction between packages; and
- Allow greater external interspersed moderation in the infinite array cases by filling the region normally occupied by the impact limiter with interspersed moderator (low density water).

Since the IV and OC sustain little damage during HAC (except for localized puncture damage of the OC) and minor variations in the package dimensions have little effect on the neutron multiplication calculations (due to the large size of the packages), nominal packaging dimensions are used for both NCT and HAC models. The waste canister within the package is not explicitly modeled and no credit is taken for materials or shape of this container. A generalized sphere or cylinder of the optimally moderated fissile isotope, with an optimized reflector filling the remainder of the package IV void is used to represent the containerized waste matrix. The sphere or cylinder is evaluated in various locations in the IV to determine the most reactive conditions under NCT and HAC.

The package model represents the IV and OC structural materials as follows. The model consists of nested, right circular cylindrical shells of Type 304 stainless steel (SS304) and lead shielding (Pb). The inner diameter of the IV cavity is modeled with an inner diameter of 31.25 inches (79.375 cm), and an inside length of 121.5 inches (308.61 cm). The IV wall and the inner shell of the OC are represented as a single region of SS304 with a thickness of 1.626 inches (3.493 cm). The lead shield inside the OC inner and outer walls is modeled as 1.875 inches (4.763 cm) thick. Outside of the lead shield, the thermal shield and the OC outer shell are represented as a single SS304 region of 1.625 inches (4.127 cm). All gaps between components are neglected. This representation of the package therefore results in a model that has an outer diameter that is slightly less than the actual outer diameter of the vessel. With respect to the length of the vessel, the end caps are modeled as solid SS304 with a thickness of 13 inches (33.02 cm) on the closure end and 6.5 inches (16.51 cm) on the vessel bottom. This results in an overall package length of 141 inches without the impact limiters. The impact limiters, when used in the models as described above, are modeled in dimension only (with interspersed moderator filling the void) and extend the overall diameter of the package by 16 inches (40.64 cm) and the overall length by 23 inches (58.42 cm).

The RH-TRU 72-B package model for the damaged and undamaged unit is depicted in Figure 6.3-1.

6.3.3 Single Package Models

Compliance with the requirements of 10 CFR §71.55[9] is demonstrated by analyzing optimally moderated damaged and undamaged, single-unit RH-TRU 72-B packages.

The NCT and HAC single-unit model consists of the contents models described in Section 6.3.1, *Contents Models*, combined with the packaging model described in Section 6.3.2, *Package Model*, for each of the four cases evaluated. In all cases, the package with its contents is surrounded with a 12 inch (30.5 cm) thick, close-fitting full density water reflector. This representation of the single unit conservatively replaces the impact limiter volume with full density water which tends to be a better reflector than foam when positioned closer to the fissile region. Representations of the KENO-V.a[1] models are shown in Figure 6.3-2 through Figure 6.3-6 with the contents in the various modeled locations. Since the NCT and HAC configurations are not different under these assumptions, both are represented by the same model. Single-unit calculations are performed with the fissile contents in various locations to determine optimum neutron multiplication of the system.

6.3.4 Array Models

Calculations are performed for infinite arrays of damaged and undamaged RH-TRU 72-B packages in a close packed, square-pitch configuration. Triangular-pitched array configurations are not considered because the size of the package is sufficiently large compared to the size of the most reactive contents configuration that the triangular-pitched configuration is not significant as indicated by the square-pitched array analyses showing that the interaction effects are of minor consequence as compared to the single unit fully reflected cases. The package includes the impact limiters reduced to half-thickness to simulate the damage under HAC conditions. This reduced spacing conservatively bounds the NCT configuration and only the HAC configurations are calculated. A specularly reflective boundary condition is applied to all six faces of the unit cell defining the array configuration in order to represent an infinite array of RH-TRU 72-B packages. The contents sphere or cylinder is modeled in various locations within the package to achieve maximum interaction between packages. Additionally, interspersed moderation between RH-TRU 72-B packages is evaluated using various volume fractions up to full density water to evaluate the maximum interaction achievable between units. The contents configuration modeled are described in Section 6.3.1, *Contents Models*.

6.3.5 Package Regional Densities

A summary of all material densities and compositions used in the KENO-V.a[1] models for the RH-TRU 72-B package is given in the following tables as indicated by the case study. Specifically, Case A, General Payload, regional densities are recorded in Table 6.3-1 and Table 6.3-2; Case B, Special Reflector Payload, in Table 6.3-3; Case C, Machine-Compacted Payload, in Table 6.3-4; and Case D, LEU Homogeneous Payload, in Table 6.3-5 and Table 6.3-6; and Case E, LEU Heterogeneous Payload, in Table 6.3-7 through Table 6.3-9. The parameters are

[9] Title 10, Code of Federal Regulations, Part 71 (10 CFR 71), *Packaging and Transportation of Radioactive Material*, 01-01-14 Edition.

computed based on the SCALE Standard Composition Library[10] provided values of density as follows: plutonium density of 19.84 g/cc, uranium density of 19.05 g/cc, beryllium density of 1.850 g/cc, polyethylene density of 0.9230 g/cc, water density of 0.9982 g/cc, SS304 density of 7.94 g/cc, and lead density of 11.344 g/cc. The materials used to represent the RH-TRU package are Type 304 stainless steel (SS304) and lead (Pb) as given in Table 6.3-10. The SCALE Standard Composition Library identifier "BEBOUND", nuclide identifier 4309, was used to model the beryllium reflector. The cross-section of BEBOUND is based on a beryllium metal whereas the cross-section for standard material BE is based on a free gas representation. BEBOUND is also used to model beryllium in the benchmark cases discussed in Section 6.5, *Critical Benchmark Experiments*.

For Cases A through E with data shown in Table 6.3-1 through Table 6.3-9, the fissile material composition is determined by defining the mass of fissile material (in this case the Pu limit for the specific case or the uranium enrichment) and then inputting the desired H/X ratio to be evaluated. Using these two input parameters the material composition for the arbitrary mixture used to represent the moderated fissile region is calculated. To use an arbitrary mixture in SCALE the percentages by weight of each constituent must be specified. In our modeling, the fissile material and the moderator are treated in a volume additive manner. The moderator is a combination of volume percentages of the indicated combinations of water, polyethylene and beryllium. The process is described for the Pu sphere as follows.

Since the system is evaluated for optimum H/Pu ratio, the desired Pu mass and the H/Pu ratio are used to calculate the mass of hydrogen in the sphere as follows:

$$\mathrm{mH} = \frac{\mathrm{H/Pu} \times \mathrm{mPu} \times \mathrm{MwH}}{\mathrm{MwPu}}$$

where mH is mass of hydrogen, H/Pu is the hydrogen to plutonium ratio desired, mPu is mass of plutonium, MwH is atomic weight of hydrogen, and MwPu is atomic weight of plutonium.

Once the mass of hydrogen is known for the composition the mass of polyethylene can be shown to equal:

$$\mathrm{mCH_2} = \frac{\mathrm{mH}}{2\mathrm{MwH} \times \left(\frac{\mathrm{Vol\%H_2O}}{\mathrm{Vol\%CH_2}} \times \frac{\rho\mathrm{H_2O}}{\rho\mathrm{CH_2} \times \mathrm{MwH_2O}} + \frac{1}{\mathrm{MwCH_2}} \right)}$$

where mCH_2 is the mass of polyethylene, $Vol\%H_2O$ and $Vol\%CH_2$ are the volume percentages of water and polyethylene, respectively, ρH_2O and ρCH_2 are the densities of water and polyethylene, respectively, and MwH_2O and $MwCH_2$ are the molecular weights of water and polyethylene, respectively.

Once the mass of polyethylene is known the mass of O, C, and Be can be shown to equal:

$$\mathrm{mO} = \mathrm{mCH_2} \times \frac{\mathrm{Vol\%H_2O}}{\mathrm{Vol\%CH_2}} \times \frac{\rho\mathrm{H_2O}}{\rho\mathrm{CH_2}} \times \frac{\mathrm{MwO}}{\mathrm{MwH_2O}}$$

[10] L. M. Petrie, P. B. Fox and K. Lucius, *Standard Composition Library*, ORNL/NUREG/CSD-2/V3/R6, Volume 3, Section M8, March 2000.

$$mC = \frac{mCH_2}{MwCH_2} \times MwC$$

$$mBe = \frac{Vol\%Be}{Vol\%CH_2} \times mCH_2 \times \frac{\rho Be}{\rho CH_2}$$

where mO, mC, and mBe are the masses of oxygen, carbon, and beryllium, respectively, Vol%C and Vol%Be are the volume percentage of carbon and beryllium, respectively, ρBe is the density of beryllium, and MwO is the atomic weight of oxygen.

Using the masses and densities of Pu and CH_2 in a volume additive manner, the volume of the moderated Pu sphere can be shown to equal:

$$V_s = \frac{mPu}{\rho Pu} + \frac{mCH_2}{\rho CH_2} \times \left(1 + \frac{Vol\%H_2O}{Vol\%CH_2} + \frac{Vol\%Be}{Vol\%CH_2}\right)$$

In the cases with the additional ^{240}Pu (Case A, General Payload, evaluations), the volume of the sphere is increased as follows and all other calculations remain the same:

$$V_s = \frac{m^{240}Pu + m^{239}Pu}{\rho Pu} + \frac{mCH_2}{\rho CH_2} \times \left(1 + \frac{Vol\%H_2O}{Vol\%CH_2} + \frac{Vol\%Be}{Vol\%CH_2}\right).$$

In the Case D and E evaluations, the same approach was used except ^{235}U was substituted for ^{239}Pu, ^{238}U was substituted for ^{240}Pu, and the values of uranium densities and atomic weights were appropriately substituted for those of Pu in the above equations and the ratio of ^{235}U to ^{238}U was related using the enrichment value applicable to each case. For the heterogeneous arrays, the volumes of uranium metal and moderator mixture calculated using this method was then used to set the pitch of the array using the ratio of the respective volumes. This provided an approximate array spacing that could be compared loosely to a homogeneously moderated system. Although other approaches are equivalent, this method maintained the evaluations of the Pu and U systems consistent by using a volume additive method between the fissile isotope and the moderator constituents.

Once all of the elemental masses and volume of the mixture are known, total mass of the mixture, the weight percentages for each constituent, and the solution densities are calculated in the usual manner. These weight percentages and solution density values are used in the arbitrary material definition of the Pu sphere composition in the KENO-V.a[1] input file. From these values the number densities are calculated in the usual manner to obtain the number densities reported in Table 6.3-1 through Table 6.3-6. These number densities were compared to those calculated by SCALE as a check of the input. Results agree to within 3 significant digits with differences attributed to round off errors in the various calculations. Material composition data for Case E studies used the volume additive method and volume percents calculated above directly.

Material compositions for the reflector mixtures filling the IV around the fissile contents are given in Table 6.3-11 for Cases A through E.

Table 6.3-1 – Fissile Contents Model Properties for 315 g Pu Spheres (Case A)①

H/Pu Ratio	Pu Concentration (g Pu/L)	Sphere Radius (cm)	Solution Density (g/cc)	Number Densities (atoms/b-cm)				
				^{239}Pu	H	O	C	Be
25% Polyethylene/75% Water Moderator								
700	39.56	12.3872	1.0170	9.9673E-05	6.9772E-02	2.4990E-02	9.8955E-03	
800	34.63	12.9499	1.0123	8.7236E-05	6.9788E-02	2.4996E-02	9.8979E-03	
900	30.79	13.4676	1.0087	7.7561E-05	6.9806E-02	2.5002E-02	9.9003E-03	N/A
1,000	27.71	13.9483	1.0057	6.9810E-05	6.9811E-02	2.5004E-02	9.9011E-03	
1,100	25.20	14.3979	1.0034	6.3478E-05	6.9826E-02	2.5010E-02	9.9033E-03	
25% Polyethylene/74% Water/1% Beryllium Moderator								
700	39.19	12.4268	1.0252	9.8730E-05	6.9110E-02	2.4659E-02	9.8962E-03	1.2338E-03
800	34.30	12.9914	1.0205	8.6405E-05	6.9124E-02	2.4664E-02	9.8982E-03	1.2341E-03
900	30.49	13.5107	1.0169	7.6821E-05	6.9138E-02	2.4669E-02	9.9002E-03	1.2344E-03
1,000	27.45	13.9929	1.0140	6.9148E-05	6.9148E-02	2.4672E-02	9.9017E-03	1.2345E-03
1,100	24.96	14.4440	1.0116	6.2867E-05	6.9155E-02	2.4675E-02	9.9026E-03	1.2346E-03
1,200	22.88	14.8685	1.0097	5.7639E-05	6.9167E-02	2.4679E-02	9.9044E-03	1.2349E-03
1,300	21.12	15.2701	1.0080	5.3210E-05	6.9172E-02	2.4681E-02	9.9050E-03	1.2350E-03

Notes:

① Number densities in this table are calculated from the raw input data as a check to SCALE. SCALE duplicated these densities to the third significant digit. The differences are attributed to round-off errors.

Table 6.3-2 – Fissile Contents Model Properties for Various Pu Spheres with Pu-240 Added as Indicated (Case A)①

H/Pu Ratio	Pu Concentration (g Pu/L)	Sphere Radius (cm)	Solution Density (g/cc)	Number Densities (atoms/b-cm)					
				^{240}Pu	^{239}Pu	H	O	C	Be
5g ^{240}Pu/325 g ^{235}Pu/25% Polyethylene/74% Water/1% Beryllium Moderator									
700	39.77	12.5595	1.0251	1.5122E-06	9.8661E-05	6.9063E-02	2.4642E-02	9.8895E-03	1.2330E-03
800	34.81	13.1297	1.0205	1.3236E-06	8.6361E-05	6.9088E-02	2.4651E-02	9.8931E-03	1.2335E-03
900	30.95	13.6543	1.0169	1.1761E-06	7.6785E-05	6.9106E-02	2.4657E-02	9.8957E-03	1.2338E-03
1,000	27.86	14.1414	1.0140	1.0583E-06	6.9120E-05	6.9120E-02	2.4662E-02	9.8976E-03	1.2340E-03
1,100	25.33	14.5971	1.0116	9.6187E-07	6.2845E-05	6.9128E-02	2.4665E-02	9.8989E-03	1.2342E-03
15g ^{240}Pu/350 g ^{235}Pu/25% Polyethylene/74% Water/1% Beryllium Moderator									
700	40.80	12.8782	1.0251	4.2074E-06	9.8558E-05	6.8990E-02	2.4616E-02	9.8791E-03	1.2317E-03
800	35.71	13.4623	1.0205	3.6816E-06	8.6282E-05	6.9024E-02	2.4628E-02	9.8840E-03	1.2323E-03
900	31.76	13.9997	1.0169	3.2732E-06	7.6721E-05	6.9049E-02	2.4637E-02	9.8875E-03	1.2328E-03
1,000	28.59	14.4988	1.0140	2.9484E-06	6.9068E-05	6.9068E-02	2.4644E-02	9.8902E-03	1.2331E-03
1,100	26.00	14.9656	1.0116	2.6800E-06	6.2801E-05	6.9082E-02	2.4649E-02	9.8922E-03	1.2334E-03
25g ^{240}Pu/370 g ^{235}Pu/25% Polyethylene/74% Water/1% Beryllium Moderator									
700	41.72	13.1232	1.0251	6.6249E-06	9.8465E-05	6.8925E-02	2.4593E-02	9.8698E-03	1.2306E-03
800	36.53	13.7179	1.0205	5.8015E-06	8.6210E-05	6.8967E-02	2.4608E-02	9.8758E-03	1.2313E-03
900	32.49	14.2650	1.0169	5.1585E-06	7.6665E-05	6.8998E-02	2.4619E-02	9.8802E-03	1.2319E-03
1,000	29.25	14.7732	1.0140	4.6452E-06	6.9022E-05	6.9022E-02	2.4627E-02	9.8836E-03	1.2323E-03
1,100	26.60	15.2485	1.0116	4.2231E-06	6.2763E-05	6.9040E-02	2.4634E-02	9.8861E-03	1.2326E-03

Notes:

① Number densities in this table are calculated from the raw input data as a check to SCALE. SCALE duplicated these densities to the third significant digit. The differences are attributed to round-off errors.

Table 6.3-3 – Fissile Contents Model Properties for 100 g Pu Spheres (Case B)

H/Pu Ratio	Pu Concentration (g Pu/L)	Sphere Radius (cm)	Solution Density (g/cc)	Number Densities (atoms/b-cm)				
				^{239}Pu	H	O	C	Be
25% Polyethylene/74% Water/1% Beryllium Moderator								
600	45.70	8.0536	1.0313	1.1514E-04	6.9082E-02	2.4649E-02	9.8921E-03	1.2333E-03
700	39.19	8.4773	1.0252	9.8730E-05	6.9110E-02	2.4659E-02	9.8962E-03	1.2338E-03
800	34.30	8.8624	1.0205	8.6405E-05	6.9124E-02	2.4664E-02	9.8982E-03	1.2341E-03
900	30.49	9.2167	1.0169	7.6821E-05	6.9138E-02	2.4669E-02	9.9002E-03	1.2344E-03
1,000	27.45	9.5456	1.0140	6.9148E-05	6.9148E-02	2.4672E-02	9.9017E-03	1.2345E-03
1,100	24.96	9.8533	1.0116	6.2867E-05	6.9155E-02	2.4675E-02	9.9026E-03	1.2346E-03
24.5% Polyethylene/73.5% Water/2% Beryllium Moderator								
600	45.22	8.0820	1.0398	1.1393E-04	6.8360E-02	2.4485E-02	9.6953E-03	2.4670E-03
700	38.77	8.5072	1.0336	9.7683E-05	6.8377E-02	2.4491E-02	9.6977E-03	2.4676E-03
800	33.94	8.8937	1.0290	8.5492E-05	6.8394E-02	2.4497E-02	9.7001E-03	2.4682E-03
900	30.17	9.2493	1.0255	7.6014E-05	6.8412E-02	2.4503E-02	9.7026E-03	2.4688E-03
1,000	27.16	9.5794	1.0226	6.8420E-05	6.8419E-02	2.4506E-02	9.7037E-03	2.4691E-03
1,100	24.69	9.8882	1.0203	6.2210E-05	6.8431E-02	2.4510E-02	9.7054E-03	2.4695E-03
24% Polyethylene/72% Water/4% Beryllium Moderator								
600	44.30	8.1376	1.0563	1.1161E-04	6.6968E-02	2.3986E-02	9.4979E-03	4.9342E-03
700	37.98	8.5658	1.0503	9.5699E-05	6.6989E-02	2.3994E-02	9.5009E-03	4.9357E-03
800	33.24	8.9550	1.0458	8.3757E-05	6.7005E-02	2.3999E-02	9.5031E-03	4.9369E-03
900	29.56	9.3130	1.0423	7.4465E-05	6.7017E-02	2.4004E-02	9.5049E-03	4.9378E-03
1,000	26.60	9.6454	1.0395	6.7026E-05	6.7027E-02	2.4007E-02	9.5063E-03	4.9386E-03
1,100	24.19	9.9563	1.0372	6.0941E-05	6.7035E-02	2.4010E-02	9.5074E-03	4.9391E-03
23.5% Polyethylene/70.5% Water/6% Beryllium Moderator								
600	43.38	8.1948	1.0728	1.0929E-04	6.5576E-02	2.3487E-02	9.3004E-03	7.4016E-03
700	37.19	8.6260	1.0669	9.3707E-05	6.5594E-02	2.3494E-02	9.3030E-03	7.4036E-03
800	32.55	9.0179	1.0625	8.2011E-05	6.5610E-02	2.3500E-02	9.3052E-03	7.4054E-03
900	28.94	9.3784	1.0591	7.2914E-05	6.5623E-02	2.3504E-02	9.3071E-03	7.4069E-03
1,000	26.05	9.7132	1.0563	6.5629E-05	6.5629E-02	2.3506E-02	9.3080E-03	7.4076E-03
1,100	23.69	10.0263	1.0541	5.9672E-05	6.5639E-02	2.3510E-02	9.3094E-03	7.4087E-03
23% Polyethylene/69% Water/8% Beryllium Moderator								
600	42.46	8.2536	1.0893	1.0697E-04	6.4183E-02	2.2989E-02	9.1030E-03	9.8692E-03
700	36.40	8.6880	1.0835	9.1712E-05	6.4199E-02	2.2994E-02	9.1052E-03	9.8716E-03
800	31.86	9.0827	1.0792	8.0269E-05	6.4214E-02	2.3000E-02	9.1073E-03	9.8739E-03
900	28.33	9.4458	1.0759	7.1366E-05	6.4228E-02	2.3005E-02	9.1093E-03	9.8761E-03
1,000	25.50	9.7830	1.0732	6.4235E-05	6.4236E-02	2.3008E-02	9.1104E-03	9.8773E-03
1,100	23.18	10.0984	1.0710	5.8402E-05	6.4244E-02	2.3010E-02	9.1114E-03	9.8785E-03

H/Pu Ratio	Pu Concentration (g Pu/L)	Sphere Radius (cm)	Solution Density (g/cc)	Number Densities (atoms/b-cm)				
				^{239}Pu	H	O	C	Be
22.5% Polyethylene/67.5% Water/10% Beryllium Moderator								
600	41.54	8.3142	1.1058	1.0465E-04	6.2791E-02	2.2490E-02	8.9055E-03	1.2337E-02
700	35.61	8.7517	1.1002	8.9727E-05	6.2810E-02	2.2497E-02	8.9081E-03	1.2341E-02
800	31.17	9.1494	1.0960	7.8531E-05	6.2825E-02	2.2502E-02	8.9102E-03	1.2344E-02
900	27.71	9.5152	1.0927	6.9815E-05	6.2834E-02	2.2505E-02	8.9115E-03	1.2346E-02
1,000	24.94	9.8548	1.0901	6.2844E-05	6.2844E-02	2.2509E-02	8.9130E-03	1.2347E-02
1,100	22.68	10.1726	1.0879	5.7134E-05	6.2848E-02	2.2510E-02	8.9135E-03	1.2348E-02
20% Polyethylene/60% Water/20% Beryllium Moderator								
600	36.93	8.6465	1.1883	9.3041E-05	5.5825E-02	1.9995E-02	7.9175E-03	2.4679E-02
700	31.66	9.1015	1.1833	7.9769E-05	5.5838E-02	2.0000E-02	7.9194E-03	2.4685E-02
800	27.71	9.5152	1.1796	6.9813E-05	5.5850E-02	2.0004E-02	7.9211E-03	2.4690E-02
900	24.64	9.8957	1.1767	6.2064E-05	5.5859E-02	2.0007E-02	7.9223E-03	2.4694E-02
1,000	22.18	10.2490	1.1744	5.5866E-05	5.5867E-02	2.0010E-02	7.9234E-03	2.4697E-02
1,100	20.16	10.5794	1.1725	5.0792E-05	5.5872E-02	2.0012E-02	7.9242E-03	2.4700E-02
15% Polyethylene/45% Water/40% Beryllium Moderator								
600	27.71	9.5152	1.3535	6.9814E-05	4.1889E-02	1.5003E-02	5.9409E-03	4.9381E-02
700	23.76	10.0162	1.3498	5.9854E-05	4.1896E-02	1.5006E-02	5.9421E-03	4.9391E-02
800	20.79	10.4716	1.3470	5.2379E-05	4.1902E-02	1.5008E-02	5.9428E-03	4.9397E-02
900	18.48	10.8905	1.3449	4.6564E-05	4.1908E-02	1.5010E-02	5.9438E-03	4.9405E-02
1,000	16.64	11.2794	1.3432	4.1914E-05	4.1913E-02	1.5012E-02	5.9444E-03	4.9410E-02
1,100	15.12	11.6432	1.3418	3.8108E-05	4.1917E-02	1.5013E-02	5.9449E-03	4.9414E-02
10% Polyethylene/30% Water/60% Beryllium Moderator								
600	18.48	10.8905	1.5188	4.6563E-05	2.7937E-02	1.0007E-02	3.9624E-03	7.4104E-02
700	15.84	11.4642	1.5164	3.9918E-05	2.7942E-02	1.0008E-02	3.9629E-03	7.4116E-02
800	13.87	11.9856	1.5146	3.4933E-05	2.7945E-02	1.0009E-02	3.9634E-03	7.4125E-02
900	12.33	12.4652	1.5132	3.1054E-05	2.7948E-02	1.0010E-02	3.9638E-03	7.4132E-02
1,000	11.09	12.9105	1.5120	2.7948E-05	2.7949E-02	1.0011E-02	3.9639E-03	7.4133E-02
1,100	10.09	13.3270	1.5111	2.5411E-05	2.7951E-02	1.0011E-02	3.9642E-03	7.4138E-02
5% Polyethylene/15% Water/80% Beryllium Moderator								
600	9.25	13.7190	1.6843	2.3291E-05	1.3976E-02	5.0056E-03	1.9821E-03	9.8852E-02
700	7.93	14.4420	1.6831	1.9967E-05	1.3976E-02	5.0060E-03	1.9823E-03	9.8859E-02
800	6.94	15.0991	1.6822	1.7473E-05	1.3978E-02	5.0063E-03	1.9824E-03	9.8864E-02
900	6.16	15.7035	1.6815	1.5530E-05	1.3978E-02	5.0065E-03	1.9824E-03	9.8868E-02
1,000	5.55	16.2647	1.6810	1.3980E-05	1.3979E-02	5.0068E-03	1.9826E-03	9.8875E-02
1,100	5.04	16.7896	1.6805	1.2710E-05	1.3979E-02	5.0069E-03	1.9826E-03	9.8875E-02

Table 6.3-4 – Fissile Contents Model Properties for 245 g Pu Spheres (Case C)

H/Pu Ratio	Pu Concentration (g Pu/L)	Sphere Radius (cm)	Solution Density (g/cc)	Number Densities (atoms/b-cm)			
				^{239}Pu	H	C	Be
100% Polyethylene Moderator							
700	44.88	10.9231	0.9658	1.1306E-04	7.9145E-02	3.9572E-02	
800	39.28	11.4192	0.9605	9.8963E-05	7.9170E-02	3.9585E-02	
900	34.92	11.8756	0.9563	8.7983E-05	7.9184E-02	3.9592E-02	N/A
1,000	31.44	12.2994	0.9530	7.9199E-05	7.9199E-02	3.9600E-02	
1,100	28.58	12.6958	0.9503	7.2012E-05	7.9213E-02	3.9606E-02	
99% Polyethylene/1% Beryllium Moderator							
700	44.43	10.9597	1.8939	1.1193E-04	7.8353E-02	3.9177E-02	1.2334E-03
800	38.89	11.4575	1.9048	9.7967E-05	7.8374E-02	3.9187E-02	1.2338E-03
900	34.57	11.9154	1.9133	8.7102E-05	7.8392E-02	3.9196E-02	1.2341E-03
1,000	31.12	12.3406	1.9202	7.8405E-05	7.8404E-02	3.9202E-02	1.2343E-03
1,100	28.30	12.7383	1.9259	7.1285E-05	7.8415E-02	3.9207E-02	1.2345E-03

Table 6.3-5 – Fissile Contents Model Properties for 0.96 wt% U-235 FEM (Case D)

H/^{235}U Ratio	^{235}U Concentration (g ^{235}U/L)	Fissile Cylinder Height (cm)	Mixture Density (g/cc)	Number Densities (atoms/b-cm)					
				^{238}U	^{235}U	H	O	C	Be
25% Polyethylene/74% Water/1% Beryllium Moderator (Cases in Table 6.4-10 through Table 6.4-13)									
300	60.35	91.2100	6.9487	1.5752E-02	1.5464E-04	4.6393E-02	1.6553E-02	6.6432E-03	8.2839E-04
400	49.34	108.1520	5.8605	1.2877E-02	1.2641E-04	5.0566E-02	1.8042E-02	7.2407E-03	9.0270E-04
500	41.72	124.0774	5.1083	1.0889E-02	1.0690E-04	5.3448E-02	1.9071E-02	7.6534E-03	9.5410E-04
600	36.14	139.0790	4.5573	9.4327E-03	9.2599E-05	5.5560E-02	1.9824E-02	7.9559E-03	9.9189E-04
700	31.88	153.2384	4.1362	8.3199E-03	8.1680E-05	5.7175E-02	2.0400E-02	8.1871E-03	1.0207E-03
800	28.51	166.6162	3.8041	7.4422E-03	7.3065E-05	5.8450E-02	2.0855E-02	8.3696E-03	1.0435E-03
900	25.79	179.2845	3.5353	6.7319E-03	6.6090E-05	5.9479E-02	2.1222E-02	8.5170E-03	1.0619E-03
1,000	23.55	191.2971	3.3133	6.1453E-03	6.0327E-05	6.0328E-02	2.1525E-02	8.6387E-03	1.0772E-03

Table 6.3-6 – Fissile Contents Model Properties for 0.96 wt% U-235 FEM (Case D with Variable Beryllium Moderator and H/U-235=500)

Vol% Be①	^{235}U Concentration (g ^{235}U/L)	Fissile Cylinder Height (cm)	Mixture Density (g/cc)	Number Densities (atoms/b-cm)					
				^{238}U	^{235}U	H	O	C	Be
Variable Beryllium in Moderator (Cases in Table 6.4-14)									
1	41.72	124.0774	5.1083	1.0889E-02	1.0690E-04	5.3448E-02	1.9071E-02	7.6534E-03	9.5410E-04
2	41.38	124.7318	5.0815	1.0800E-02	1.0602E-04	5.3010E-02	1.8987E-02	7.5184E-03	1.9131E-03
4	40.72	126.0013	5.0303	1.0629E-02	1.0434E-04	5.2172E-02	1.8686E-02	7.3992E-03	3.8438E-03
6	40.06	127.3124	4.9785	1.0456E-02	1.0264E-04	5.1323E-02	1.8382E-02	7.2788E-03	5.7927E-03
8	39.39	128.6614	4.9263	1.0281E-02	1.0093E-04	5.0466E-02	1.8075E-02	7.1573E-03	7.7599E-03
10	38.72	130.0526	4.8736	1.0105E-02	9.9201E-05	4.9600E-02	1.7766E-02	7.0347E-03	9.7455E-03
20	35.24	137.7161	4.6024	9.1986E-03	9.0308E-05	4.5151E-02	1.6172E-02	6.4037E-03	1.9961E-02
40	27.77	157.7149	4.0188	7.2482E-03	7.1154E-05	3.5578E-02	1.2743E-02	5.0459E-03	4.1942E-02
60	19.50	187.9168	3.3729	5.0897E-03	4.9961E-05	2.4982E-02	8.9482E-03	3.5433E-03	6.6265E-02
80	10.30	238.7916	2.6543	2.6881E-03	2.6388E-05	1.3195E-02	4.7260E-03	1.8714E-03	9.3329E-02
85	7.83	257.4534	2.4619	2.0449E-03	2.0072E-05	1.0038E-02	3.5952E-03	1.4236E-03	1.0058E-01

Notes:

① Volume-% beryllium in the moderator.

Table 6.3-7 – Fissile Contents Model Properties Cylindrical Arrays of Cylinders (Rods) for 0.84 wt% U-235 FEM (Case E)

Case	Effective $H/^{235}U$	Diameter of Rod, $2r$ (cm)	Pitch, p (cm)	$n_{centerarray}$	n_{edge}	Number of Rods, n	Height of Rods, h, (cm)
CT.1	180	10	12.7435	16	0	16	58.86189
CT.2	197	10	13.0526	16	0	16	58.86189
CT.3	226	10	13.5522	16	0	16	58.86189
CT.4	283	10	14.4998	9	4	13	72.44540
CT.5	397	10	16.2298	9	0	9	104.6434
CT.6	626	10	19.2284	4	0	4	235.4475
CT.7	180	5	6.3717	64	32	96	39.24126
CT.8	197	5	6.5263	64	24	88	42.80864
CT.9	226	5	6.7761	64	24	88	42.80864
CT.10	283	5	7.2499	49	20	69	54.59653
CT.11	397	5	8.1149	36	16	52	72.44540
CT.12	626	5	9.6142	25	12	37	101.8152
CT.13	283	2.5	3.6249	225	108	333	45.25118
CT.14	397	2.5	4.0574	169	92	261	57.73426
CT.15	512	2.5	4.4481	144	64	208	72.44540
CT.16	626	2.5	4.8071	121	56	177	85.13357
CT.17	740	2.5	5.1411	100	56	156	96.59386
CT.18	854	2.5	5.4547	100	40	140	107.6332
CT.19	283	1.25	1.8125	900	496	1396	43.17663
CT.20	397	1.25	2.0287	729	388	1117	53.96112
CT.21	512	1.25	2.2241	625	308	933	64.60297
CT.22	626	1.25	2.4036	529	268	797	75.62681
CT.23	740	1.25	2.5706	441	232	673	89.56103
CT.24	854	1.25	2.7273	400	208	608	99.13581
CT.25	283	0.625	0.9062	3721	1944	5665	42.55927
CT.26	397	0.625	1.0144	3025	1496	4521	53.32853
CT.27	512	0.625	1.112	2500	1264	3764	64.05374
CT.28	626	0.625	1.2018	2116	1120	3236	74.50503
CT.29	740	0.625	1.2853	1849	964	2813	85.70860
CT.30	854	0.625	1.3637	1681	832	2513	95.94042

Table 6.3-8 – Fissile Contents Model Properties Cylindrical Arrays of Spheres for 0.84 wt% U-235 FEM (Case E)

Case	Effective H/^{235}U	Diameter of Sphere, *2r* (cm)	Pitch, *p* (cm)	*n*, Target Number of Spheres	$n_{centerarray}$	n_{edge}	n_z ①	Height of Array, *h*, (cm)
ST.1	269	10	11.0720	141	25	4	5	55.36
ST.2	369	10	11.8581	141	16	8	6	71.15
ST.3	469	10	12.5519	141	16	0	9	112.97
ST.4	569	10	13.1764	141	16	0	9	118.59
ST.5	669	10	13.7468	141	16	0	9	123.72
ST.6	769	10	14.2734	141	9	4	11	157.01
ST.7	269	5	5.5360	1130	100	32	9	49.82
ST.8	369	5	5.9291	1130	81	28	11	65.22
ST.9	469	5	6.2760	1130	64	32	12	75.31
ST.10	569	5	6.5882	1130	64	24	13	85.65
ST.11	669	5	6.8734	1130	64	16	15	103.1
ST.12	769	5	7.1367	1130	49	20	17	121.32
ST.13	269	2.5	2.7680	9041	400	200	16	44.29
ST.14	369	2.5	2.9645	9041	324	184	18	53.36
ST.15	469	2.5	3.1380	9041	289	148	21	65.9
ST.16	569	2.5	3.2941	9041	289	124	22	72.47
ST.17	669	2.5	3.4367	9041	256	120	25	85.92
ST.18	769	2.5	3.5683	9041	225	124	26	92.78
ST.19	269	1.25	1.3840	72329	1600	840	30	41.52
ST.20	369	1.25	1.4823	72329	1369	752	35	51.88
ST.21	469	1.25	1.5690	72329	1225	652	39	61.19
ST.22	569	1.25	1.6471	72329	1156	544	43	70.83
ST.23	669	1.25	1.7184	72329	1024	544	47	80.76
ST.24	769	1.25	1.7842	72329	961	504	50	89.21
ST.25	269	0.625	0.6920	578635	6561	3228	60	41.52
ST.26	369	0.625	0.7411	578635	5625	2916	68	50.39
ST.27	469	0.625	0.7845	578635	5041	2576	76	59.62
ST.28	569	0.625	0.8235	578635	4624	2280	84	69.17
ST.29	669	0.625	0.8592	578635	4225	2156	91	78.19
ST.30	769	0.625	0.8921	578635	3844	2024	99	88.32

Notes:

① For the spherical arrays, n_z, is rounded up to the whole integer. Array units were removed from the top and bottom of the very outside arrays near the wall to reduce the mass of the overall heterogeneous spherical unit array to close to the net mass of uranium allowed. Some case have a conservative excess of mass in extra units to simplify the KENO V.a geometry input data.

Table 6.3-9 – Fissile Contents Model Properties Special Reflector Studies Yielding Adjusted Height at 0.84 wt% U-235 FEM (Case E)

For Cases of Cylindrical Arrays Centered with Be Reflector around the Central Array			
Case	**Core Case**	**Be Reflector (cm)**	**Adjusted Uranium Array Height (cm)**
CCR.19.1	CT.19	1	37.38
CCR.19.2	CT.19	2	45.35
CCR.19.3	CT.19	4	52.78
CCR.19.4	CT.19	8	59.99
CCR.19.5	CT.19	16	68.04
CCR.19.6	CT.19	32	73.80
CCR.20.1	CT.20	1	36.89
CCR.20.2	CT.20	2	44.75
CCR.20.3	CT.20	4	52.08
CCR.20.4	CT.20	8	59.20
CCR.20.5	CT.20	16	67.14
CCR.20.6	CT.20	32	72.83
CCR.21.1	CT.21	1	35.91
CCR.21.2	CT.21	2	43.56
CCR.21.3	CT.21	4	50.70
CCR.21.4	CT.21	8	57.62
CCR.21.5	CT.21	16	65.35
CCR.21.6	CT.21	32	70.88
CCR.22.1	CT.22	1	33.94
CCR.22.2	CT.22	2	41.17
CCR.22.3	CT.22	4	47.92
CCR.22.4	CT.22	8	54.47
CCR.22.5	CT.22	16	61.77
CCR.22.6	CT.22	32	67.00
CCR.23.1	CT.23	1	30.00
CCR.23.2	CT.23	2	36.39
CCR.23.3	CT.23	4	42.36
CCR.23.4	CT.23	8	48.15
CCR.23.5	CT.23	16	54.60
CCR.23.6	CT.23	32	59.23
CCR.24.1	CT.24	1	22.13
CCR.24.2	CT.24	2	26.84
CCR.24.3	CT.24	4	31.24
CCR.24.4	CT.24	8	35.51

For Cases of Cylindrical Arrays Centered with Be Reflector around the Central Array			
Case	**Core Case**	**Be Reflector (cm)**	**Adjusted Uranium Array Height (cm)**
CCR.24.5	CT.24	16	40.27
CCR.24.6	CT.24	32	43.68

For Cylindrical Arrays Located at the Top (CTVR) and the Center (CCVR) of the IV where the Be in the Moderator/Reflector Region is Varied						
Case Nos.		**Core Case**	**Vol % H2O**	**Vol% CH2**	**Vol % Be**	**Height of Rods (cm)**
CTVR.19.a	CCVR.19.a	CT.19	0.74	0.25	0.01	42.2
CTVR.19.b	CCVR.19.b	CT.19	0.70	0.25	0.05	42.0
CTVR.19.c	CCVR.19.c	CT.19	0.65	0.25	0.10	41.7
CTVR.19.d	CCVR.19.d	CT.19	0.55	0.25	0.20	41.0
CTVR.19.e	CCVR.19.e	CT.19	0.25	0.25	0.50	39.2
CTVR.19.f	CCVR.19.f	CT.19	0.00	0.25	0.75	37.8
CTVR.20.a	CCVR.20.a	CT.20	0.74	0.25	0.01	52.3
CTVR.20.b	CCVR.20.b	CT.20	0.70	0.25	0.05	51.9
CTVR.20.c	CCVR.20.c	CT.20	0.65	0.25	0.10	51.3
CTVR.20.d	CCVR.20.d	CT.20	0.55	0.25	0.20	50.2
CTVR.20.e	CCVR.20.e	CT.20	0.25	0.25	0.50	47.2
CTVR.20.f	CCVR.20.f	CT.20	0.00	0.25	0.75	45.0
CTVR.21.a	CCVR.21.a	CT.21	0.74	0.25	0.01	62.1
CTVR.21.b	CCVR.21.b	CT.21	0.70	0.25	0.05	61.4
CTVR.21.c	CCVR.21.c	CT.21	0.65	0.25	0.10	60.6
CTVR.21.d	CCVR.21.d	CT.21	0.55	0.25	0.20	59.0
CTVR.21.e	CCVR.21.e	CT.21	0.25	0.25	0.50	54.6
CTVR.21.f	CCVR.21.f	CT.21	0.00	0.25	0.75	51.4
CTVR.22.a	CCVR.22.a	CT.22	0.74	0.25	0.01	72.1
CTVR.22.b	CCVR.22.b	CT.22	0.70	0.25	0.05	71.2
CTVR.22.c	CCVR.22.c	CT.22	0.65	0.25	0.10	70.0
CTVR.22.d	CCVR.22.d	CT.22	0.55	0.25	0.20	67.7
CTVR.22.e	CCVR.22.e	CT.22	0.25	0.25	0.50	61.7
CTVR.22.f	CCVR.22.f	CT.22	0.00	0.25	0.75	57.5
CTVR.23.a	CCVR.23.a	CT.23	0.74	0.25	0.01	84.7
CTVR.23.b	CCVR.23.b	CT.23	0.70	0.25	0.05	83.4
CTVR.23.c	CCVR.23.c	CT.23	0.65	0.25	0.10	81.7
CTVR.23.d	CCVR.23.d	CT.23	0.55	0.25	0.2	78.7
CTVR.23.e	CCVR.23.e	CT.23	0.25	0.25	0.5	70.7
CTVR.23.f	CCVR.23.f	CT.23	0.00	0.25	0.75	65.3

For Cylindrical Arrays Located at the Top (CTVR) and the Center (CCVR) of the IV where the Be in the Moderator/Reflector Region is Varied						
Case Nos.		Core Case	Vol % H2O	Vol% CH2	Vol % Be	Height of Rods (cm)
CTVR.24.a	CCVR.24.a	CT.24	0.74	0.25	0.01	93.0
CTVR.24.b	CCVR.24.b	CT.24	0.70	0.25	0.05	91.3
CTVR.24.c	CCVR.24.c	CT.24	0.65	0.25	0.10	89.3
CTVR.24.d	CCVR.24.d	CT.24	0.55	0.25	0.20	85.5
CTVR.24.e	CCVR.24.e	CT.24	0.25	0.25	0.50	75.8
CTVR.24.f	CCVR.24.f	CT.24	0.00	0.25	0.75	69.3

Table 6.3-10 – Structural Model Properties for the RH-TRU 72-B Package (All Cases)

Nuclide	SCALE Nuclide Identifier	Percentage of Composition	Number Density (atoms/b-cm)
Type 304 Stainless Steel for RH-TRU 72-B Package Walls and End Caps			
C	6012	0.080 wt%	3.1877E-04
Si	14000	1.000 wt%	1.7025E-03
P	15031	0.045 wt%	6.9468E-05
Cr	24304	19.000 wt%	1.7473E-02
Mn	25055	2.000 wt%	1.7407E-03
Fe	26304	68.375 wt%	5.8545E-02
Ni	28304	9.500 wt%	7.7402E-03
Lead for RH- TRU 72-B Package Shielding			
Pb	82000	100 wt%	3.2969E-02

Table 6.3-11 – Reflector Model Properties for the RH-TRU 72-B Package by Case

Nuclide	SCALE Nuclide Identifier	Number Density (atoms/b-cm)
25% Polyethylene/75% Water IV Reflector used in Case A		
H	1001	6.99063E-02
C	6012	9.91472E-03
O	8016	2.50384E-02
25% Polyethylene/74% Water/1% Beryllium IV Reflector used in Cases A, D and E		
H	1001	6.92387E-02
Bebound	4309	1.23621E-03
C	6012	9.91472E-03
O	8016	2.47046E-02
100% Beryllium IV Reflector used in Case B①		
Bebound	4309	1.23621E-01
99% Polyethylene/1% Beryllium IV Reflector used in Case C		
H	1001	7.85246E-02
Bebound	4309	1.23621E-03
C	6012	3.92623E-02

Notes:

① For the variable density reflector cases of Section 6.4.3.2.2, *Case B, Special Reflector Payload, Infinite Array Results*, this quantity is reduced by the indicated volume fraction multiplier, as shown in Table 6.4-6.

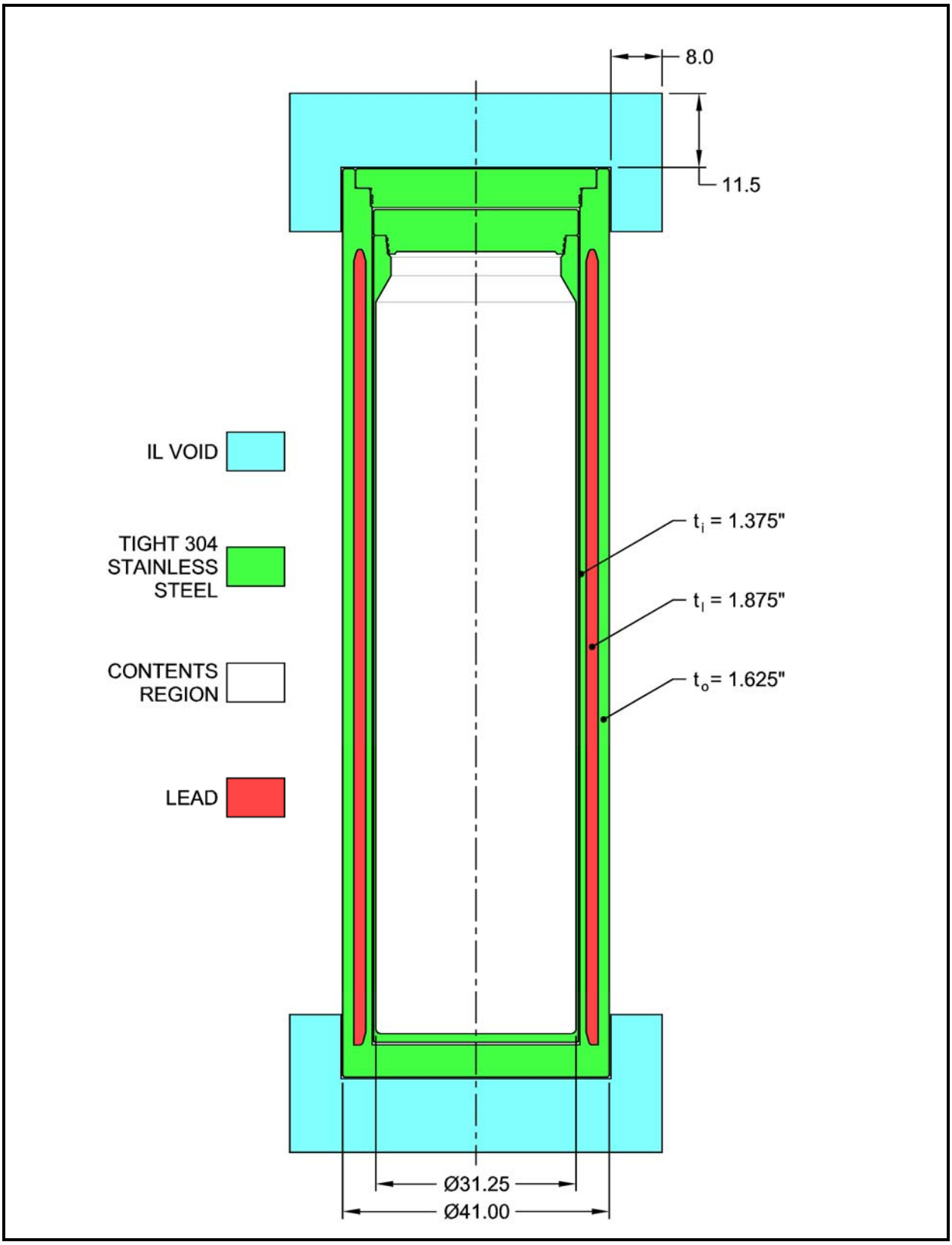

Figure 6.3-1 – Simplified Drawing of RH-TRU 72-B Package

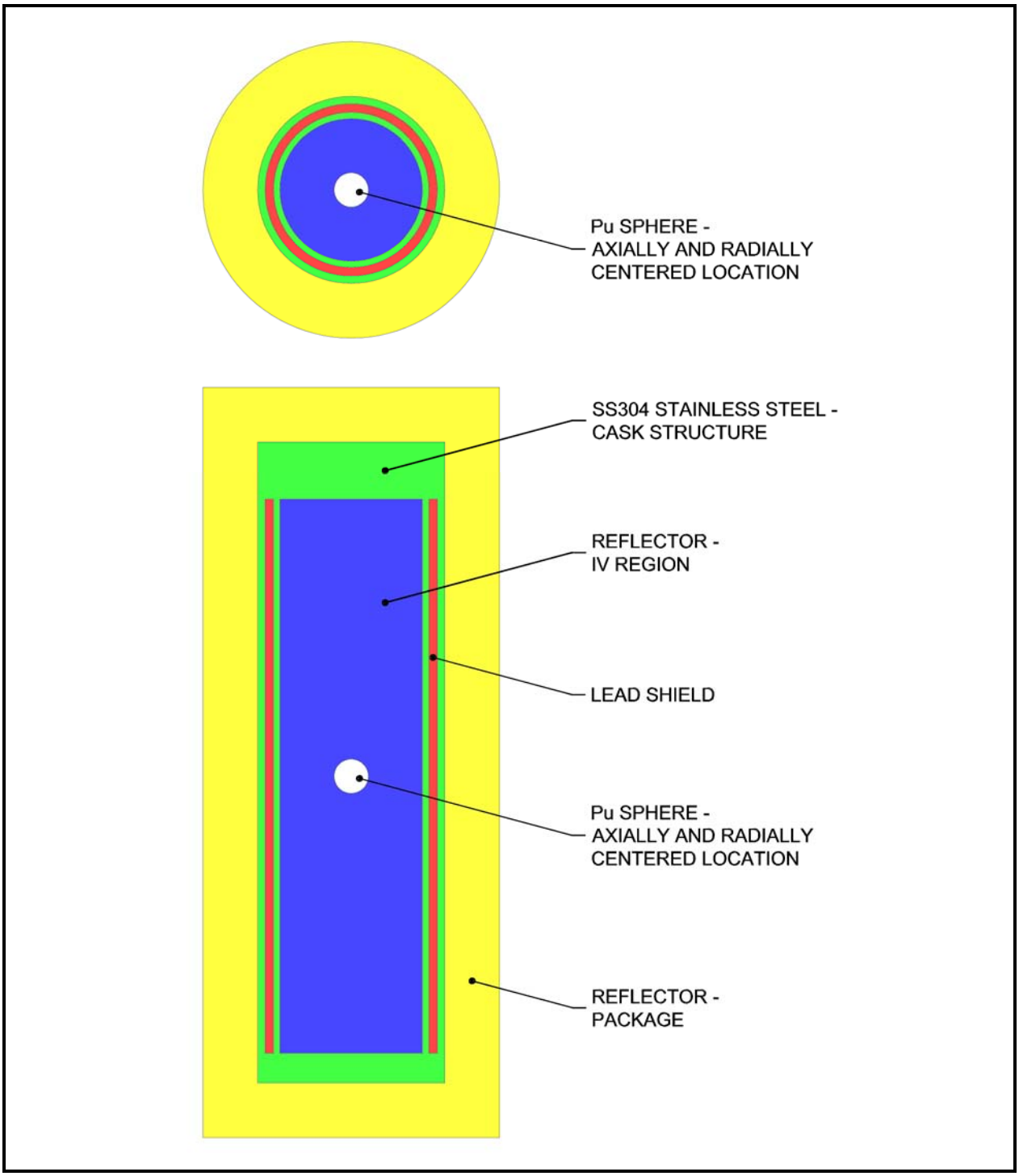

Figure 6.3-2 – KENO-V.a NCT and HAC Single Unit, Case A through C, Sphere Centered Model Representation (Top and Side Views)[11]

[11] Infinite unit depiction is the same with the exception of the outside cylindrical reflector. The infinite unit is modeled with a cuboid shaped outer region that extends a distance of one half the thickness of the impact limiters from all sides of the package and reflected on all sides with a mirror boundary to model an infinite array of packages (see Figure 6.3-5).

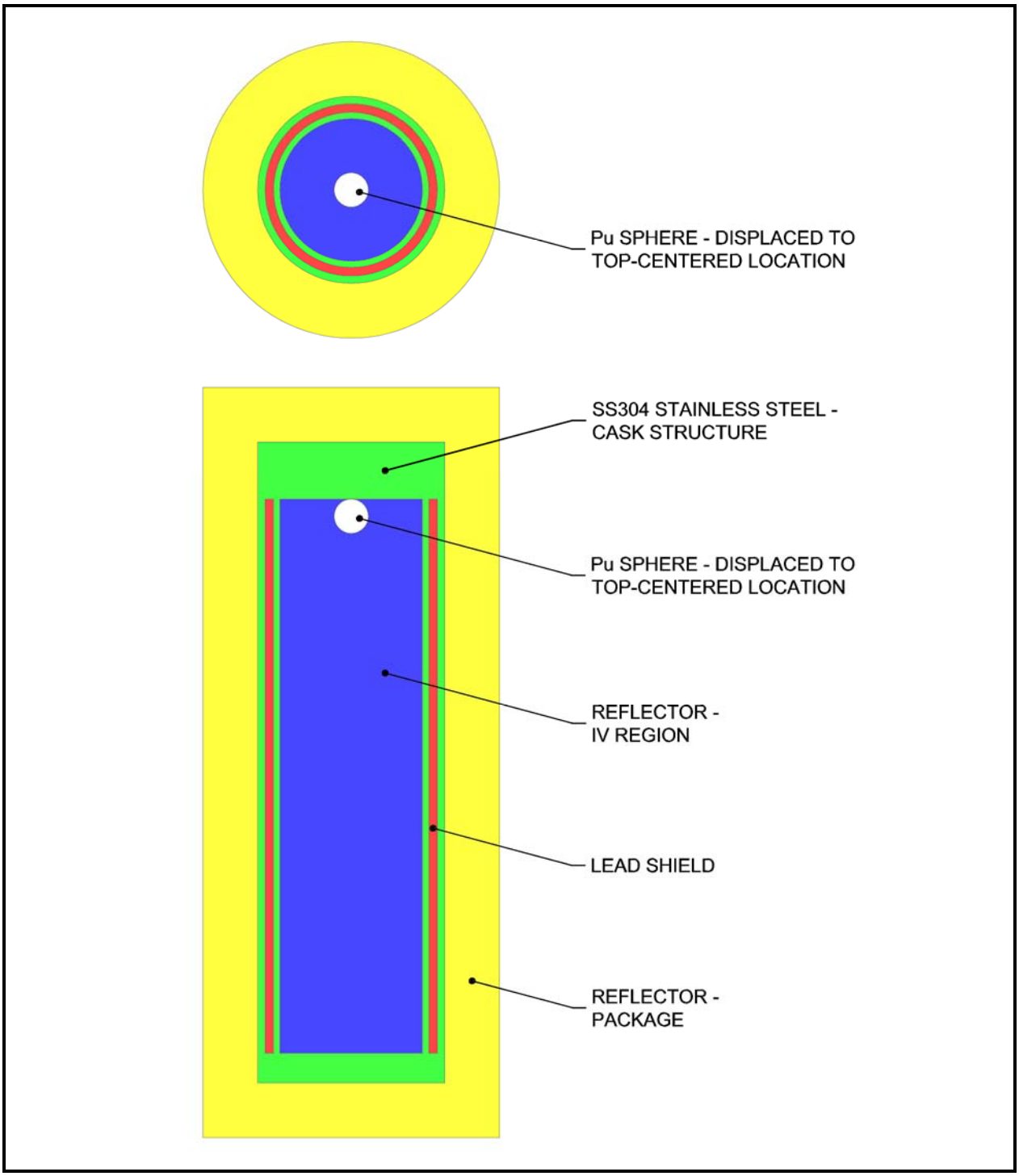

Figure 6.3-3 - KENO-V.a NCT and HAC Single Unit, Case A through C, Sphere Centered Top Model Representation (Top and Side Views)[11]

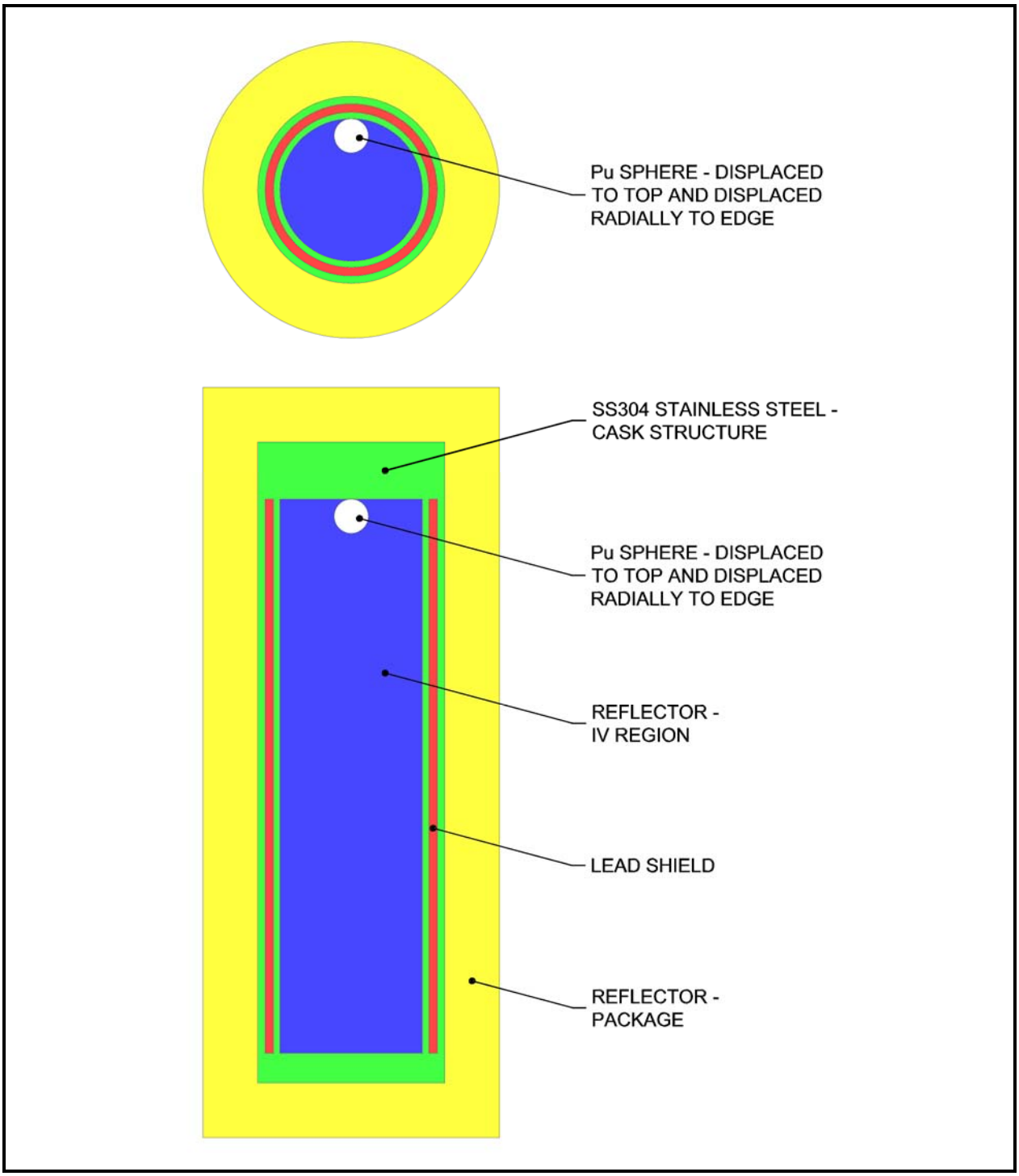

Figure 6.3-4 – KENO-V.a NCT and HAC Single Unit, Case A through C, Sphere Centered Top and Displaced Radially, Model Representation (Top and Side Views)[11]

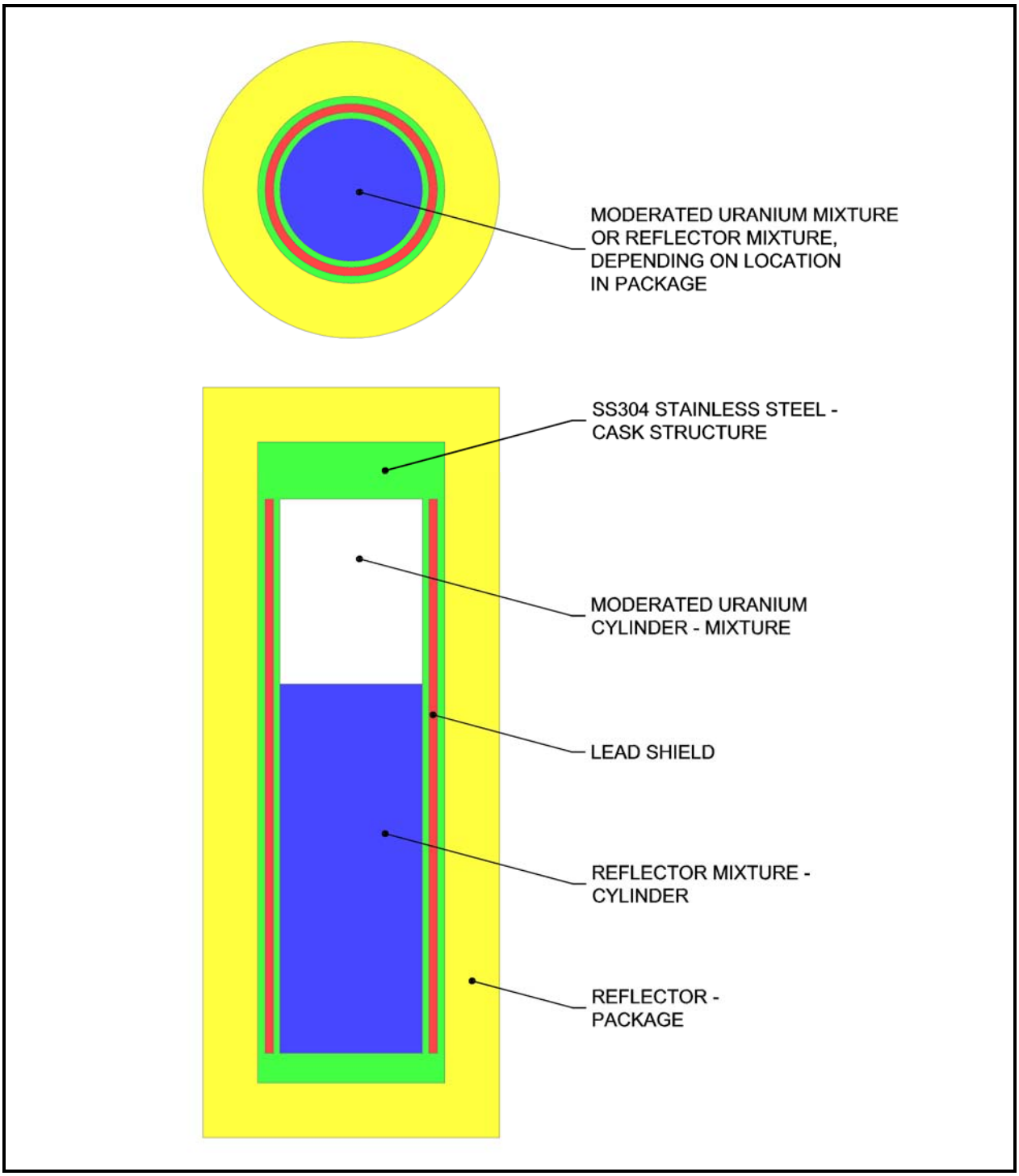

Figure 6.3-5 – KENO-V.a NCT and HAC Infinite Unit, Case D, Cylindrical Fissile Region Model Representation (Top and Side Views)[12]

[12] Both the NCT and HAC models of the single case unit were bounded by this infinite case model based on evaluation of the package during the Case A studies.

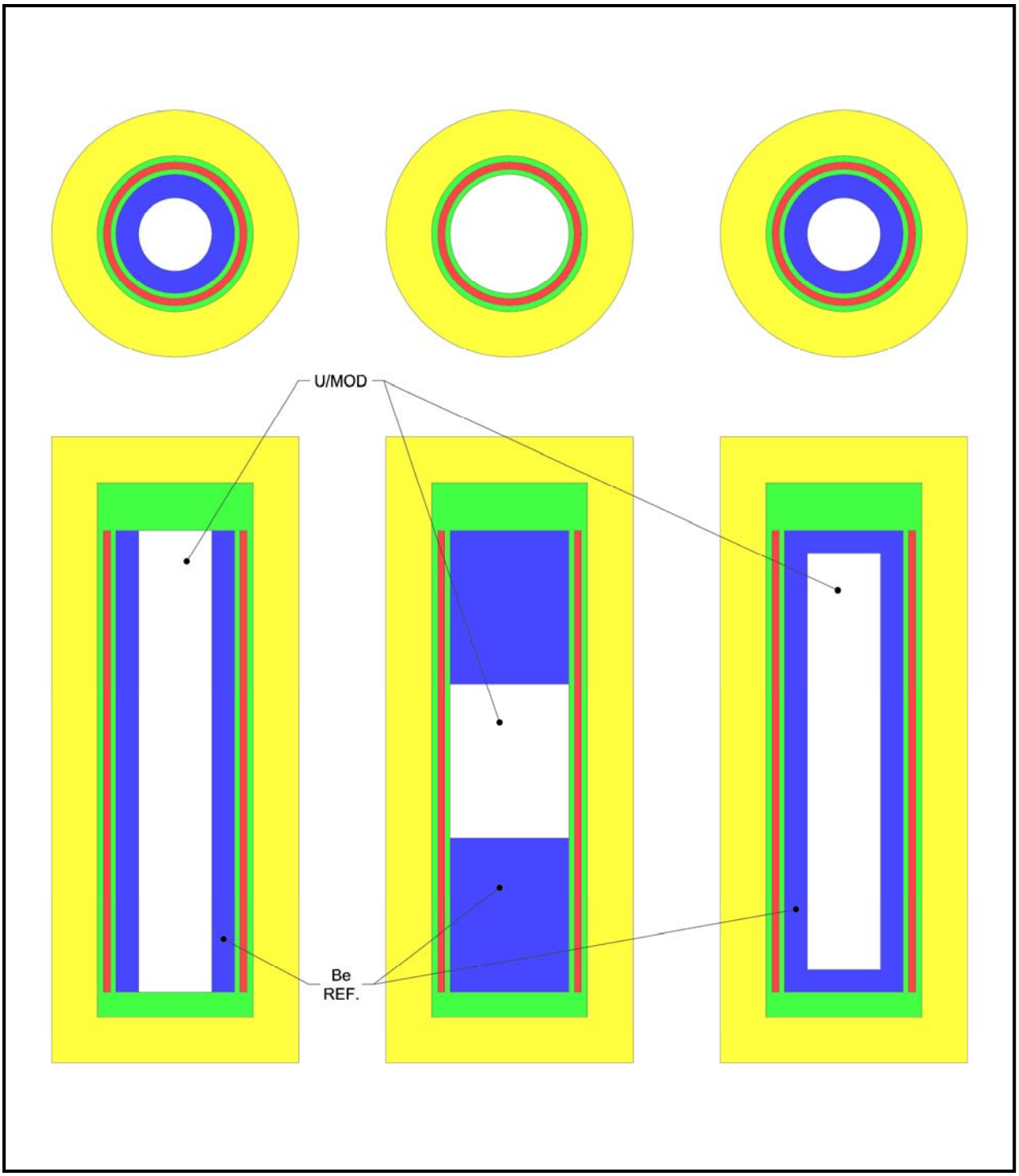

Figure 6.3-6 – KENO-V.a NCT and HAC Single-Unit, Case D, Cylindrical Fissile Region Models with Various Be Reflector Regions (Long, Skinny; Short, Squat; and Encapsulated Location Models both Top and Side Views)

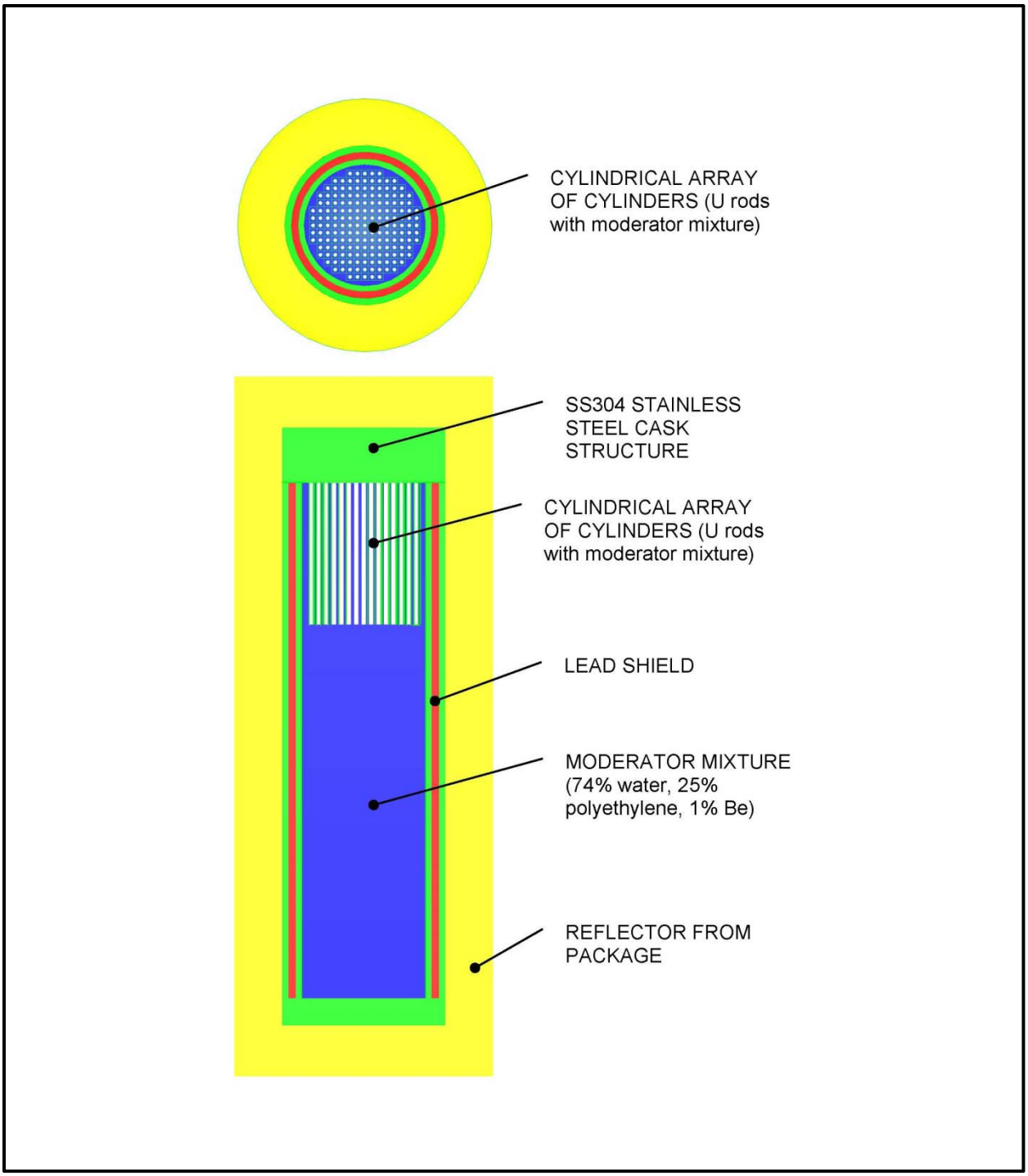

Figure 6.3-7 – KENO-V.A (SCALE 5.1) NCT and HAC Single-Unit, Case E, Cylindrical Array of Cylinders at the Top of the IV

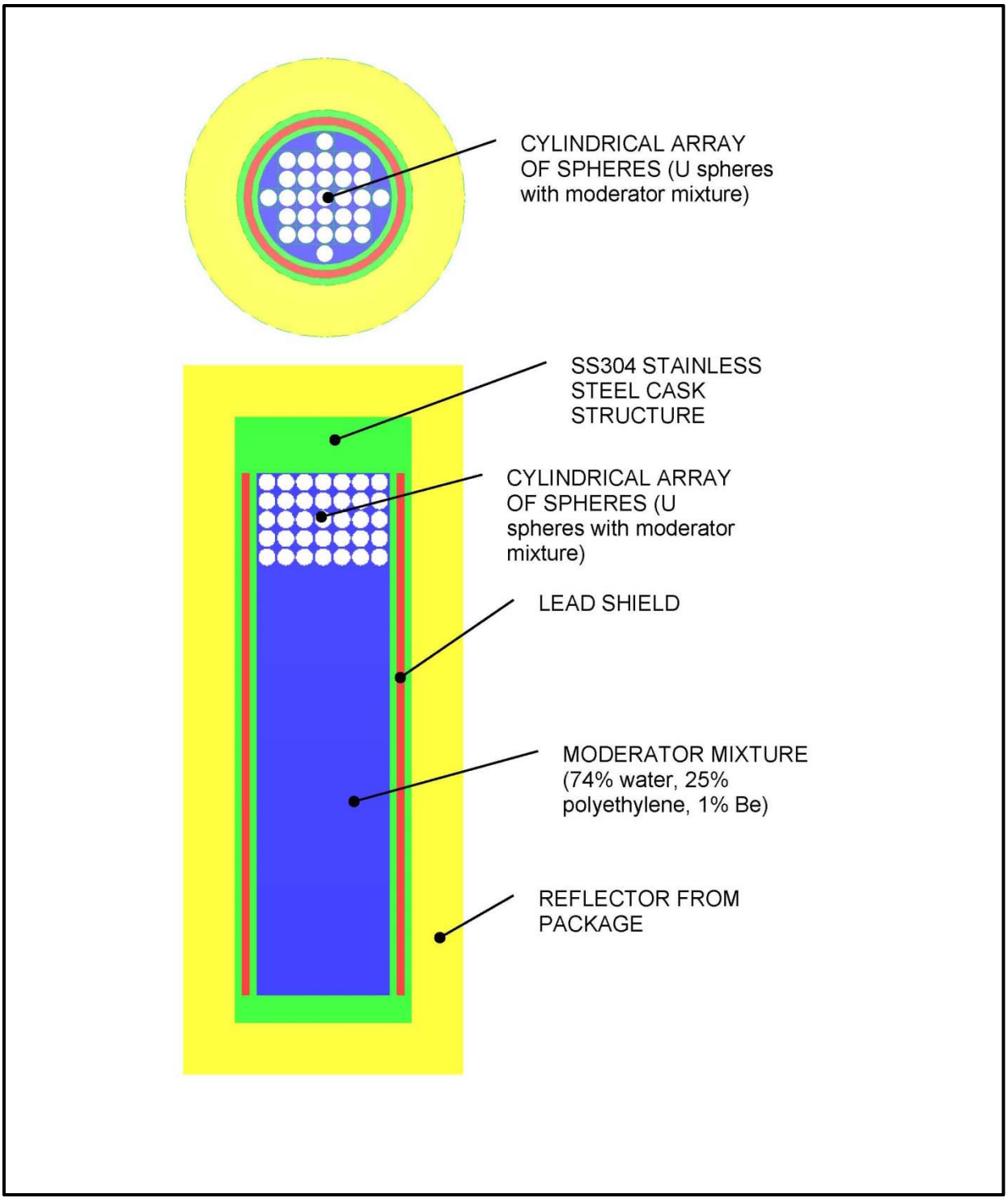

Figure 6.3-8 – KENO-V.A (SCALE 5.1) NCT and HAC Single-Unit, Case E, Cylindrical Array of Spheres at the Top of the IV

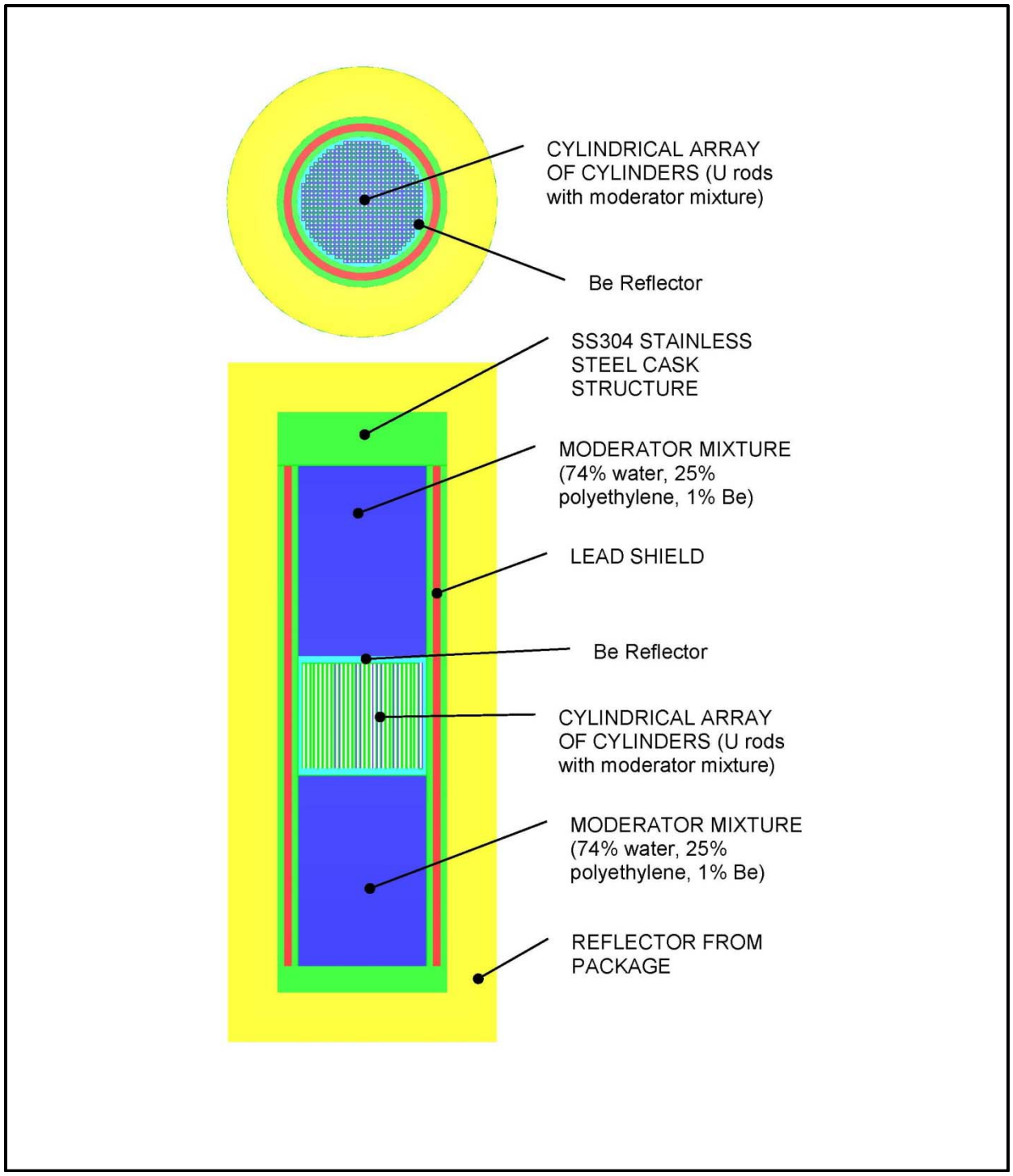

Figure 6.3-9 – KENO-V.A (SCALE 5.1) NCT and HAC Single-Unit, Case E, Cylindrical Array of Cylinders at the Center of the IV with Be Reflector (Cylindrical Array of Spheres is similar)

This page intentionally left blank.

6.4 Criticality Calculations

A description of the criticality calculations performed for the RH-TRU 72-B package is presented in this section. The calculational methodology is discussed in Section 6.4.1, *Calculational or Experimental Method*. The optimization of the payload model is discussed in Section 6.4.2, *Fuel Loading or Other Contents Loading Assumptions*. The results of all calculations are presented in Section 6.4.3, *Criticality Results*.

The intent of the analysis is to demonstrate that the RH-TRU 72-B package is safely subcritical under normal conditions of transport (NCT) and hypothetical accident conditions (HAC) provided the loading limits for each package payload are observed.

6.4.1 Calculational or Experimental Method

Calculations for the RH-TRU 72-B package are performed using the three-dimensional Monte Carlo transport theory code, KENO-V.a[1]. The CSAS25 utility[2] is used as a driver for the KENO code. In this role, CSAS25 determines nuclide number densities, performs resonance processing, and automatically prepares the necessary input for the KENO code based on a simplified input description. Calculations for cases A through D used the SCALE-PC v4.4a software package[3] whereas Case E calculations used the SCALE 5.1 software package[4] on a Linux workstation. The 238 energy-group (238GROUPNDF5), cross-section library based on ENDF/B-V cross-section data[5] is used as the nuclear data library for the KENO-V.a code.

The KENO code has been used extensively in the criticality safety industry for several years. KENO-V.a is an extension of earlier versions of the KENO code and includes many versatile geometry capabilities and screen plots to facilitate geometry verification. The KENO-V.a code and the associated 238GROUPNDF5 cross-section data set are validated for proper operation on the respective platform by performing criticality analyses of a number of relevant benchmark criticality experiments. A description of these benchmark calculations, along with justification for the computed bias in the code and library for the relevant region of applicability, is provided in Section 6.5, *Critical Benchmark Experiments*.

[1] L. M. Petrie and N. F. Landers, *KENO-V.a: An Improved Monte Carlo Criticality Program with Supergrouping*, ORNL/NUREG/CSD-2/V2/R6, Volume 2, Section F11, March 2000.

[2] N. F. Landers and L. M. Petrie, *CSAS: Control Module for Enhanced Criticality Safety Analysis Sequences*, ORNL/NUREG/CSD-2/V1/R6, Volume 1, Section C4, March 2000.

[3] N. F. Landers and L. M. Petrie, *CSAS: Control Module for Enhanced Criticality Safety Analysis Sequences*, ORNL/NUREG/CSD-2/V1/R6, Volume 1, Section C4, March 2000.

[4] Oak Ridge National Laboratory (ORNL), *SCALE 5.1: Modular Code System for Performing Standardized Computer Analyses for Licensing Evaluation for Workstations and Personal Computers*, ORNL/TM-2005/39, SCALE Version 5.1, November 1, 2006.

[5] W. C. Jordan and S. M. Bowman, *Scale Cross-Section Libraries*, ORNL/NUREG/CSD-2/V3/R6, Volume 3, Section M4, March 2000.

6.4.2 Fuel Loading or Other Contents Loading Assumptions

The allowable fuel loading for a single RH-TRU 72-B package is based on the FGE package fissile loading limit established by this analysis for each of the contents and package Cases A through C and based on the FEM enrichment loading limit established for Cases D and E. The limits for each case are chosen to demonstrate that the RH-TRU 72-B package is safely subcritical under NCT and HAC. Calculations are based on the following conservative general assumptions, additional conservative assumptions already addressed in Section 6.3.1, *Contents Models*, and Section 6.3.2, *Package Model*, and upon the specific assumptions discussed during each evaluation in Section 6.4.3.1, *Criticality Results for Single RH-TRU 72-B Package*, and Section 6.4.3.2, *Criticality Results for Infinite Arrays of RH-TRU 72-B Packages*.

(1) ^{239}Pu is present at the FGE limit assigned to the payload type. Special FGE limits with 0 g, 5 g, 15 g, and 25 g ^{240}Pu are calculated for Case A only.

(2) All Pu is assumed to be optimally moderated and reflected with the optimal degree of moderation determined in each case for the applicable moderator (by adjusting the H/Pu ratio and/or by adjusting the Be percentage in the fissile sphere, as applicable). Studies indicate that the presence of voids in the optimal spherical contents model significantly reduces k_{eff} (demonstrated by evaluating a reduced density reflector in the IV region). The presence of less than or equal to 1% by weight beryllium in the moderator was also shown to have a small effect on k_{eff}, and larger quantities are evaluated as a special case (See Case B).

(3) The reflector material is tight fitting around the fissile geometry and assumed to fill the IV at up to 100% of theoretical density of the applicable reflector. In Case B, using a beryllium reflector, results show that the presence of voids in the reflector reduces k_{eff} (again, as demonstrated by evaluating a reduced density reflector in the IV region). Additionally, Case B evaluates special reflector material at greater than 1 wt% that is chemically bound to the fissile material.

(4) The fissile material is represented in a spherical geometry for the Pu systems or a cylinder for the larger LEU systems where a sphere does not fit within the IV. Other geometries allow for higher neutron leakage such that calculations performed for other geometries result in a reduction in k_{eff} for single units and for infinite units with the large spacing provided by the packaging.

(5) All structural materials comprising the authorized payload contents, including the canister, dunnage, and packing material, are conservatively neglected. The waste matrix outside the sphere or cylinder is represented by a polyethylene/water/beryllium mixture.

The same conservative assumptions that are used to analyze the single-unit RH-TRU 72-B package are used for the infinite array calculations. However, the presence of a variable density interspersed moderator between units in the infinite array cases is evaluated in addition to a full density water interspersed moderator to better evaluate the interaction between units.

6.4.3 Criticality Results

The results of the calculations for the RH-TRU 72-B package criticality evaluation are divided into two sections. Results for the single RH-TRU 72-B package are presented in Section 6.4.3.1,

Criticality Results for Single RH-TRU 72-B Package, and results for infinite arrays of RH-TRU 72-B packages are presented in Section 6.4.3.2, *Criticality Results for Infinite Arrays of RH-TRU 72-B Packages*. Reported neutron multiplication factors represent the computed k_{eff} values plus twice the standard deviation, σ, for the result calculated, as follows:

$$k_s = k_{eff} + 2\sigma < USL$$

This quantity is then compared with the upper subcritical limit (USL) in order to demonstrate an adequate margin of subcriticality. Generally, the Monte Carlo calculations reported here are performed with sufficient histories to bring the computed relative standard deviation in the result to approximately 0.1% and until other indicators in the output file indicate the source term has converged. Typical KENO parameters required to obtain this level of uncertainty are 1000 generations of 1000 histories per generation, with the information from the initial 50 generations skipped, as a minimum, when performing the statistic evaluation of the generations. More generations may have been run when convergence was not indicated using these basic parameters.

6.4.3.1 Criticality Results for Single RH-TRU 72-B Package

With the models described in Section 6.3.3, *Single Package Models*, subcriticality of the RH-TRU 72-B package under both NCT and HAC is demonstrated for each of the cases discussed in Section 6.4.3.1.1, *Case A, General Payload, Single Unit Results*, through Section 6.4.3.1.5, *Case E, LEU Heterogeneous Payload, Single Unit Results,* below.

6.4.3.1.1 Case A, General Payload, Single Unit Results

The initial evaluation of the General Payload case was designed to evaluate the optimum combinations of moderator composition, reflector composition, and fissile sphere location for the NCT case. Since this approach optimizes the neutron multiplication factor of the package contents and since the HAC configuration, as modeled, is identical to the NCT configuration, results from this evaluation will be used on subsequent evaluations of single and infinite unit NCT and HAC analyses. Initial scoping calculations showed a limit of 315 FGE was necessary to demonstrate subcriticality with the most reactive configuration in Case A and was used throughout the Case A single unit and infinite array evaluations without ^{240}Pu.

First, the single unit model was evaluated with a sphere located in the center of the RH-TRU 72-B at various H/Pu ratios using a moderator with 25% polyethylene/75% water and a moderator with 25% polyethylene/74% water/1% beryllium by volume. The remainder of the IV was filled with a reflector consisting of 25% polyethylene/75% water or 25% polyethylene/74% water/1% beryllium by volume. Three of the four possible combinations of moderator/reflector conditions were evaluated for comparison with the sphere centered in the package. The results of these three baseline evaluations are shown in Table 6.4-1. This initial evaluation demonstrates that the addition of Be into the moderator (the Pu sphere) and the reflector (the IV region) results in a slightly higher k_s than the system moderated and reflected with the 25% polyethylene/75% water, although all of the results are statistically equivalent. The 25% polyethylene/74% water/1% Be mixture was used in the moderator and reflector as the standard to more accurately reflect the 1% allowable beryllium throughout the waste matrix under the General Payload limits.

To evaluate whether the thick SS304 walls would provide better reflection than the 25% polyethylene/74% water/1% beryllium by volume alone, the sphere was moved to the top center of the container near the 13 inch thick SS304 top closure and into the top, radially displaced corner locations of the cylinder. The results of the evaluation of these two alternate locations are shown in Table 6.4-1 for comparison. The most reactive location is in the top, radially displaced corner. This indicates that the thick steel and lead reflector provided by the top and sides of the vessel is more significant than the poly/water mixture.

To evaluate the effects of a reduced density reflector (for example, to represent voids in the waste matrix), the case with an H/Pu of 900 was evaluated with various volume fractions of the 25% polyethylene/74% water portion of the reflector while leaving the approved 1% beryllium by volume throughout the reflector region (this conservatively captures the presence of the beryllium, up to the allowable limit, for this case while reducing the other postulated reflecting effects of the waste matrix represented by the water/polyethylene mixture). The results of the evaluation are shown in Table 6.4-2. The results indicate that the full density reflector optimizes the single unit neutron multiplication factor. This evaluation demonstrates that any voids reduce the k_s of the package and are allowable.

Based on the above evaluation, the maximum k_s appears under the conditions that result from a Pu sphere optimally moderated with the mixture of 25% polyethylene/74% water /1% beryllium at an H/Pu of 800 – 900. The location of the sphere is at the top of the container near the thick steel closure lids and radially displaced to the outside edge. This combination of steel reflector back scattering neutrons in the direction of the fissile sphere provides a slight increase in k_s over the sphere centered in the package location. This configuration will be used in each of the following evaluations where scoping calculations confirm the maximum reactivity conditions are satisfied.

6.4.3.1.2 Case B, Special Reflector Payload, Single Unit Results

Based on the evaluations of Section 6.4.3.1.1, *Case A, General Payload, Single Unit Results*, and Section 6.4.3.2.1, *Case A, General Payload, Infinite Array Results*, the maximum reactivity of a single unit RH-TRU 72-B package under NCT and HAC conditions is statistically equivalent to that of an infinite array of HAC packages under maximum reflection conditions. Additionally, the due to the large size of the package and the small size of the most reactive fissile sphere, the fully reflected single package and the infinite array of packages with full interspersed moderation are physically identical with the exception of a small amount of water reflection at the contact points. Thus, the analysis given in Section 6.4.3.2.2, *Case B, Special Reflector Payload, Infinite Array Results* is used to evaluate the Case B single-unit analysis.

6.4.3.1.3 Case C, Machine-Compacted Payload, Single Unit Results

Based on the evaluations of Section 6.4.3.1.1, *Case A, General Payload, Single Unit Results*, and Section 6.4.3.2.1, *Case A, General Payload, Infinite Array Results*, the maximum reactivity of a single unit RH-TRU 72-B package under NCT and HAC conditions is statistically equivalent to that of an infinite array of HAC packages under maximum reflection conditions. Additionally, the due to the large size of the package and the small size of the most reactive fissile sphere, the fully reflected single package and the infinite array of packages with full interspersed moderation are physically identical with the exception of a small amount of water reflection at the contact

points. Thus the analysis given in Section 6.4.3.2.3, *Case C, Machine-Compacted Payload, Infinite Array Results*, is used to evaluate the Case C single-unit analysis.

6.4.3.1.4 Case D, LEU Homogeneous Payload, Single Unit Results

Due to the change in the form of control from a mass controlled system to an enrichment controlled system and due to the low enrichment level desired for this limiting package, the size of the optimum fissile mass could conceivably fill the RH-TRU 72-B package volume. Unlike the spherical geometries evaluated in the previous cases, the spheres of optimally moderated LEU would exceed the size of the package and a cylindrical geometry was selected to attain the maximum reactivity of a single unit RH-TRU 72-B package under NCT and HAC conditions. To place a realistic limit on the quantity of fissile material available, the package loading limit of 6,900 pounds was chosen as a bounding amount of waste material to model. 0.96 wt% ^{235}U moderated at optimum H/^{235}U using a 25% polyethylene, 74% water, and 1% beryllium mixture was modeled as filling the container nearest the thick steel reflector at the top and extending through the IV until 6,900 pounds of waste material was placed into the package. The remainder of the void was filled with the same 25% polyethylene, 74% water, and 1% beryllium mixture. The single unit model was then evaluated to identify the optimum H/^{235}U. The results of the evaluation are reported in Table 6.4-10. The optimum H/^{235}U appears near 500 as expected with large, well moderated, uranium systems.

To evaluate the effects of unlimited special reflectors in the container (other than LEU), the single unit case was modified to evaluate three variations of a single unit fissile material region with a Be reflector: a long, skinny cylinder with radially distributed Be; a short, squat cylinder with axially distributed Be (similar to the cases above but moved away from the steel end caps); and a cylinder encapsulated in a Be reflector. In these three single unit cases, the moderated region remained as a 0.96 wt% ^{235}U matrix moderated with a 25% polyethylene, 74% water, and 1% beryllium mixture to various H/^{235}U ratios and the reflector region in the IV was replaced with Be. The outside of the package continued to be modeled with a full density water reflector. Results of these three evaluations as reported in Table 6.4-12. All configurations are subcritical and the most reactive is the short squat cylinder with Be on either side.

Since no new or worse configuration conditions appear under HAC, this single-unit analysis bounds both NCT and HAC and all single case results are less than the USL of 0.9257 for the LEU systems with beryllium.

6.4.3.1.5 Case E, LEU Heterogeneous Payload, Single Unit Results

Cylindrical arrays of both heterogeneously distributed cylinders and spheres were evaluated in the IV to attain the maximum reactivity of a single unit RH-TRU 72-B package under NCT and HAC conditions. Cylindrical arrays located at the top of IV were found to be more reactive when using limited special reflector materials in the moderator region. To provide a reasonable working enrichment limit a net weight limit of 3,100 pounds was placed on the contents of the package. 0.84 wt% ^{235}U, moderated at optimum H/^{235}U using a 25% polyethylene, 74% water, and 1% beryllium mixture, was modeled in cylindrical arrays of cylinders (rods) or spheres located in the top the container. The height of these arrays were extended until 3,100 pounds of uranium was placed into the array and the all voids within the IV were filled with 25% polyethylene, 74% water, and 1% beryllium mixture (without regard to weight). The single unit

model was then evaluated to identify the optimum pitch. The more reactive array of cylinders evaluated are reported in Table 6.4-15. The maximum k_s occurs at an effective H/^{235}U ratios of around 500 (as expected for the arrays of smaller elements) and at lower effective H/^{235}U ratios for the larger elements. The parametric study performed is better viewed as a study to determine the optimum pitch. For lumps less than 0.1 cm (0.039 inches) or greater than 6 cm (2.36 inches), the reactivities are well bounded by the homogenous condition evaluation of Case D. Figure 6.4-1 depicts results of initial Case E models of cylindrical arrays of spheres (cylindrical arrays of cylinders show similar behavior) where the peak reactivities at optimum array pitch are plotted for various diameters of spheres. Case DSIN is shown representing diameters of 0 cm. This plot shows that the heterogeneously distributed arrays of uranium at 0.96 wt% ^{235}U FEM are conservatively subcritical for diameters of 0.1 cm, or less and 6 cm, or greater. The Case D homogenous limits can be applied to waste with characteristic lump diameters of 0.1 cm, and smaller, and to systems with lumps of 6 cm and larger. The Case E evaluation provides new enrichment limits within this range of characteristic lump diameters.

To evaluate the effects of more than 1 wt% special reflectors in the container (other than LEU), the single unit case was modified to evaluate two conditions. First, a successively thicker solid Be reflector around the most reactive cylindrical array of cylinders at various pitches near the optimum limited special reflector case were evaluated from 1 cm thick to 32 cm thick. Payload net weight was conserved at 3,100 pounds of uranium and Be so that uranium was removed as more Be was added in the reflector around the cylindrical array. Second, the Be concentration in both the moderator and reflector regions was increased from 1% by volume to 75% by volume to establish the trend. In this case, uranium was removed as the Be and polyethylene content in the moderator region around the array elements increased to maintain the maximum payload weight constant. Cylindrical arrays were evaluated at the top and in the center of the IV. Cylindrical arrays located in the center of the IV were more reactive. Results of these two evaluations are reported in Table 6.4-17 for the solid special reflector studies and Table 6.4-19 for the interspersed special reflector studies. All configurations are subcritical and the most reactive being the variable moderator special reflector cases.

Since no new or worse configuration conditions appear under HAC, this single-unit analysis bounds both NCT and HAC and all single case results are less than the USL of USL= 0.9336-6.9580E-03*EALF for the LEU systems with beryllium.

6.4.3.1.6 Conclusions for Single Unit Calculations

Based on optimum moderation of the fissile contents and maximum reflection conditions modeled by filling the IV with full density materials, as approved for each case, and surrounding the package by an additional 30.5 cm of water, all Case A single unit results are less than the USL. Based on Case A infinite array results, the infinite arrays of units for Case B and C will also bound the results of the single-unit cases. All subsequent cases were evaluated with the infinite array cases bounding the single-unit cases for the Case A, B, and C studies. All infinite arrays cases were found subcritical as discussed and summarized in Section 6.4.3.2, *Criticality Results for Infinite Arrays of RH-TRU 72-B Packages*. The single unit Case D evaluation also found that for a single-unit, optimally moderated low enriched uranium waste stream in the RH-TRU 72-B package remained subcritical under NCT and HAC with no restrictions on special reflectors. The single unit Case E evaluation for an LEU Heterogeneous Payload found that for a single unit, optimally moderated low enriched uranium waste stream that is heterogeneously

distributed (lumps between 0.1 cm (0.039 inches) and 6 cm (2.39 inches) in diameter) that the RH-TRU 72-B package, loaded to 3,100 pounds total contents net weight, remained subcritical under NCT and HAC at 0.84 wt% ^{235}U FEM with no restrictions on special reflectors. Thus, a single RH-TRU 72-B package will remain subcritical under both NCT and HAC conditions and under the prescribed limits for each case A through E above.

6.4.3.2 Criticality Results for Infinite Arrays of RH-TRU 72-B Packages

The infinite array model studies the interaction between the fissile contents in adjacent RH-TRU 72-B packages. The models described in Section 6.3, *Model Specifications*, provide the basis of the KENO-V.a calculations. The only difference in the NCT and HAC models is that the thickness of the impact limiter changes. OC wall puncturing was ignored as a physical impact to the neutronics model of the package. Since the HAC model provided a closer spacing between units due to the reduced impact limiter dimensions, the HAC model was used to bound the NCT model. The infinite array calculation assumes the presence of interspersed moderation between the packages of the array. This moderation was modeled with various volume fraction of water in the array interstitial space to determine the most reactive conditions.

6.4.3.2.1 Case A, General Payload, Infinite Array Results

As in the single unit analysis for Case A, the contents are assumed to be in an optimal geometry with optimal moderation resulting from the plausible packaging materials including polyethylene wastes and the in leakage of water into the IV. The maximum polyethylene density for the manually compacted waste allowed in the General Payload is assumed to be 25% by volume with 74% water and 1% beryllium filling the remaining void in the IV. The fissile material is assumed to mix homogenously with the same mixture of 25% polyethylene/74% water/1% Be (by volume).

In the infinite-unit Case A evaluation, the RH-TRU 72-B package modeled in an infinite square-pitched array with spacing provided by the half-thickness impact limiters (as described in Section 6.3.2, *Package Model*), is used to represent the HAC infinite-unit configuration which bounds the NCT infinite-unit configuration. The package with its contents is evaluated with full interspersed moderation in the IV region and with full water density interspersed moderation in between units. Additionally, these same regions are modeled with voids. These two evaluations demonstrate the two extreme conditions of interspersed moderation between the spheres contained within the package. For this evaluation, the spheres were located in the most reactive configuration next to the top and radially displaced to the side of the container. This configuration conservatively models the thick steel reflector that does not change during NCT or HAC conditions. Results for these two analyses are shown in Table 6.4-3. These results indicate that the maximum reactivity of the package is achieved under full density reflection conditions. With the IV and exterior regions of the package modeled as a void, the interaction of the packages is presumably maximized, but probably due to the size of the units the infinite array reactivity is less than the fully reflected unit reactivity.

Table 6.4-4 shows the results of evaluating the most reactive moderated fissile spheres from Table 6.4-3 (H/Pu = 900 and 1200 cases) through the range of interspersed moderation in both the IV Region and between the RH-TRU 72-B packages. This range of interspersed moderation between fissile units should reveal significant trends in interaction with increased moderation.

The results in Table 6.4-4 demonstrate a smooth rise in k_s as the density of interspersed moderation increases from low to full density values. This result suggests poor coupling between the fissile material in adjacent packages and indicates that the interaction with adjacent units is minimal.

Based on the results of the evaluation of the unrestricted loading limit of 315 g ^{239}Pu, the alternate limits that include specific measured quantities of ^{240}Pu in addition to the ^{239}Pu are evaluated to demonstrate that the most reactive reflector conditions above (namely, a reflector of 25% polyethylene/74% water/1% Be (by volume) in the IV region and full density water in between packages) is also subcritical for over a range of interstitially moderated fissile spheres with the various combinations of ^{240}Pu and ^{239}Pu. These alternate limits allow more ^{239}Pu contamination in the waste matrix where the ^{240}Pu is present in known quantities. The k_s for each of these evaluations are shown in Table 6.4-5. Maximum k_s for all three cases stays centered at an H/^{239}Pu of 900, and all are less than the USL of 0.9382.

Note that due to the large size of the package and the small size of the most reactive fissile sphere, each package in the infinite array is essentially a fully reflected single package. Consequently, although the fully reflected infinite array results are slightly lower, the results are statistically equivalent (within one standard deviation) to the fully reflected single-unit results and the infinite arrays can be used to evaluate the single-unit cases in Case B and Case C evaluations. All Case A results are less than the USL of 0.9382.

6.4.3.2.2 Case B, Special Reflector Payload, Infinite Array Results

In the infinite-unit Case B analysis evaluated, the RH-TRU 72-B package modeled in an infinite square-pitched array with spacing provided by the half-thickness impact limiters (as described in Section 6.3.2, *Package Model*) is used to represent the HAC infinite-unit configuration which bounds the NCT infinite unit-configuration just like the Case A study. Two special conditions are evaluated. The first evaluation examines the special reflector material and the Pu in an unbounded state. As such, the special reflector is allowed in unlimited amounts in the waste stream (that is, greater than 1 wt% Be) and with no restriction as to location and proximity to the fissile material. The package was evaluated with the higher percentages of Be in two regions.

First, the Be was added to the reflector region in the IV to determine the effects of high amounts of Be as a reflector around the optimally moderated Pu sphere. This demonstrated the effects of Be as a reflector. Scoping calculations resulted in lowering the mass limit for this Case to 100 FGE to account of the higher reactivity of the system using a special reflector such as Be. The Be reflector was found to be more effective than the steel in the top and sides of the package. Consequently, based on these scoping calculations, the Pu sphere was moved back to the center of the package where the Be reflector could have maximal impact. The package with its contents is evaluated first with variable density Be moderation/reflection in the IV region ranging from 1% to 100% Be (by volume). In all cases, the interspersed moderation outside of the packages was modeled with full density water to obtain optimum reactivity as indicated in evaluation of the Case A results. Results of these calculations are shown in Table 6.4-6. Following this initial evaluation the additional Be was added to the Pu mixture to evaluate the impact of the Be tightly bound to the Pu and having a Be reflector. This model used the full density Be moderator/reflector conditions in the IV and full water density interspersed moderation outside the package. Results of these calculations are also shown in Table 6.4-7. The trends indicate the full density Be in the moderator/reflector region of

the IV provide maximum system reactivity and the system is subcritical at this FGE limit for both full density and voided loadings. The evaluation of bound Pu/Be in the Be reflected package indicates that adding Be to the sphere in a manner that displaces the hydrogenous moderator, lowers the system reactivity also resulting in a subcritical package for all concentrations of Be throughout the package as a special reflector.

The results for the second evaluation are shown in Table 6.4-8 using the higher mass content of 305 FGE as obtained during scoping calculations. This evaluation assumes a special condition that the fissile material and the special reflector material are chemically or mechanically bound. The Pu and Be (utilized as the most reactive special reflector) are mixed, also with poly and water in such a manner as to evaluate optimum moderation by varying the weight percent of the Be in the moderator and leaving the contribution of the poly-to-water at a ratio of about 25% poly to 75% water. Since all of the fissile material is chemically or mechanically bound to the special reflector material in the moderator region and the special reflector material is not as effective as a poly/water moderator, the spheres were evaluated with a higher mass content of 305 FGE and still remained subcritical. The remaining reflection region inside the package was filled with the same 25% by volume with 74% water and 1% beryllium to represent the non-special reflector portion of the waste matrix and still account for some contamination with beryllium in this region. All results from both evaluations are less than the USL of 0.9382.

6.4.3.2.3 Case C, Machine-Compacted Payload, Infinite Array Results

In the infinite-unit Case C analysis evaluated, the RH-TRU 72-B package, modeled in an infinite square-pitched array with spacing provided by the half-thickness impact limiters (as described in Section 6.3.2, *Package Model*), is used to represent the HAC infinite-unit configuration which bounds the NCT infinite unit-configuration just like the Case A study. The spherical contents of 100% polyethylene moderated ^{239}Pu is evaluated with a reflector consisting of 99% polyethylene and 1% beryllium to represent the contents of machine compacted waste. Scoping calculations identified that the full density poly was indeed a better moderator that the poly/water combinations assumed in the Case A studies and that it was necessary to reduce the mass limit for this payload from 315 FGE to 245 FGE to maintain the evaluated cases below the USL. Scoping calculations also confirmed that the maximum reactivity of the package continued to be obtained using the Pu sphere displaced radially at the top of the package as it had shown in the Case A studies. Results for the sphere centered and top centered locations are not reported. Following this evaluation, the moderator was modified to add the 1% beryllium resulting in a 99% polyethylene/1% beryllium (by volume) mixture in both the moderator and reflector region. In all cases, the interspersed moderation outside of the packages was modeled with full density water to obtain optimum reactivity as indicated in evaluation of the Case A results. Results from both of these evaluations using a range of H/Pu values are shown in Table 6.4-9. Optimum conditions are centered on an H/Pu of 900 as in the other poly/water moderated cases and the 1% beryllium in the moderator resulted in a slight increase in reactivity as previously found in the Case A studies. Since the Case A studies identified that the full density reflector was more effective than a reduced density reflector and since the full density polyethylene reflector has similar characteristics, these cases were not reevaluated. Also, since the infinite arrays evaluated in Case A studies were optimum using full density water between packages and the full density polyethylene in the Case C contents model is a more effective reflector, Case C was only evaluated with full density water between packages. All results are less than the USL of 0.9382.

6.4.3.2.4 Case D, LEU Homogeneous Payload, Infinite Array Results

In the infinite-unit Case D analysis evaluated, the RH-TRU 72-B package modeled in an infinite square-pitched array with spacing provided by the half-thickness impact limiters (as described in Section 6.3.2, *Package Model*), is used to represent the HAC infinite-unit configuration which bounds the NCT infinite unit-configuration just like the previous case studies. Using the low enriched uranium limit, the optimally moderated volume is very large with respect to the container. Consequently, the contents are modeled as filling the cylinder at one end as described in Section 6.3.1.4, *Case D, LEU Homogeneous Payload, Contents* Model. The $H/^{235}U$ was varied to identify the optimal moderation of the infinite package. Results for the model using full water density between units are reported in Table 6.4-11. As with the single unit case evaluated in Section 6.4.3.1.4, *Case D, LEU Homogeneous Payload, Single Unit* Results, the optimum moderation condition occurs at an $H/^{235}U$ of 500. Since physical geometry of this model differs significantly from that evaluated in Section 6.4.3.2.1, *Case A, General Payload, Infinite Array Results*, the model was also evaluated with varying interspersed moderation between packages at the optimum interstitial moderation value of $H/^{235}U = 500$. These results are also reported in Table 6.4-11. Unlike the Pu cases evaluated above, the packages show significantly more interaction at the lower interspersed moderation values with a slight peaking at a volume fraction of 0.1% full density water between packages. As with the previous cases, the results of the evaluation bound both the NCT and HAC.

In evaluating the effects of special reflectors, the most reactive location model (the short, squat cylinder model determined most reactive in the Single Unit evaluations) was used to evaluate the infinite unit Be reflected case (see Figure 6.3-6 center model). The package was initially evaluated using the same fissile material mixture as above at varying $H/^{235}U$ ratios. The results are reported in Table 6.4-13. In this case the addition of Be special reflector material does increase k_s slightly over the poly/water/Be reflected case above. The most reactive case at an $H/^{235}U$ of 400 was run varying the interspersed moderation between units in the infinite array. These results are also reported in Table 6.4-13. As was seen from the poly/water/Be reflected cases above, there is a slight increase in k_s at an interspersed moderation value of 0.1 vol% water. Finally, the uranium moderator region of the infinite model is evaluated for the addition of Be in quantities greater than 1 wt% Be. Table 6.4-14 shows the results of the evaluation over a range of Be volume percent additions to the fissile region. The moderator mixture was maintained such that the water to polyethylene ratio remained at 75% to 25% and the $H/^{235}U$ remained at 500 (near optimum to show the trend). The trend shows that the addition of special reflector material to the moderator causes a smooth reduction in the k_s as moderator concentration increases. This evaluation was conducted in such a manner that the $H/^{235}U$ was maintained constant (without hydrogen moderation the overall k_s is much lower).

All results are less than the USL of 0.9257 and the results are consistent with the ANSI/ANS-8.1[6] standard that states the subcritical limit of 0.96 wt% ^{235}U for aqueous moderated and reflected low enriched uranium systems.

[6] ANSI/ANS-8.1-1998, *Nuclear Criticality Safety in Operations with Fissionable Materials Outside Reactors*, American Nuclear Society (ANS), La Grange Park, Illinois.

6.4.3.2.5 Case E, LEU Heterogeneous Payload, Infinite Array Results

In the infinite-unit Case E analysis evaluated, the RH-TRU 72-B package modeled in an infinite square-pitched array with spacing provided by the half-thickness impact limiters (as described in Section 6.3.2, *Package Model*), is used to represent the HAC infinite-unit configuration which bounds the NCT infinite unit-configuration just like the previous case studies. Using the low enriched uranium limit of 0.84 wt% ^{235}U FEM, the most reactive cylindrical arrays of rods and spheres identified in the single unit cases were evaluated in the infinite array configurations over a range of H/^{235}U ratios (and hence, pitches). The results for the models using full water density between packages are reported in Table 6.4-16. The reactivity of these arrays of rods and spheres were fairly flat across large ranges of spacing and the optimum reactivity shifted slightly over the single unit cases reported in Section 6.4.3.1.5, *Case E, LEU Heterogeneous Payload, Single Unit Results*. The most reactive of these models were also evaluated with varying interspersed moderation between packages to evaluate differing degrees of post-accident conditions around the packages. These results are also reported in Table 6.4-16. Like the Case D, homogeneous payload cases evaluated above, the packages show very slightly more interaction at the lower interspersed water densities between packages. As with the previous cases, the results of the evaluation bound both the NCT and HAC.

In evaluating the effects of special reflectors, models of cylindrical arrays of spheres were used in two types of evaluations with the enrichment at 0.84 wt% ^{235}U. Unlike the Case D studies on homogenous material, the special reflector additions were the limiting cases for the uranium enrichment. For the first models, solid Be special reflector was modeled filling the void between the cylindrical array and in various thicknesses of 1, 2, 4, 8, 16, and 32 cm on top and bottom of the array. The remainder of the package contents on either side of the array, radially, remained filled with the 25% polyethylene/74% water/1% Be (by volume) mixture. The most reactive normal array of 1.25 cm spheres from Section 6.4.3.1.5 was evaluated over a range of pitches to address the optimum moderation of the array. Arrays against the top and centered in the IV were evaluated and cylindrical arrays of cylinders located in the center were most reactive. The payload net weight was maintained constant by removing uranium to account for the higher density Be as more Be was added. The most reactive single unit series of cases occurred at a pitch of 2.0287 cm. These cases were run in the infinite array to evaluate the HAC conditions. The results are reported in Table 6.4-18. The infinite array results were within calculational error of the single unit results. The most reactive case of the infinite array cases was run by varying the interspersed moderation between units in the infinite array. These results are also reported in Table 6.4-18. As was seen from the Case E, polyethylene/water/Be reflected cases above, there is a slight increase in k_s at an lower interspersed water densities.

For the second series of models, the uranium moderator region of the infinite model is evaluated for the addition of Be into the moderator in quantities greater than 1 wt% Be. Be was increased from 1% to 75% in increments. The single unit model identified during the single unit evaluations with the most reactive conditions was evaluted in an infinite array. Table 6.4-20 shows the results of the evaluation over a range of Be volume percent additions to the fissile region. The moderator mixture was maintained such that the water was removed as Be was added and the polyethelene remained at 25%. The most reactive case of the infinite array cases was run by varying the interspersed moderation between units in the infinite array. These results are also reported in Table 6.4-20. The infinite arrays were statisically similar to the single unit arrays.

All results are less than the USL as a function of EALF.

6.4.3.2.6 Conclusions for Infinite Array Calculations

The calculations reported in this section are performed with conservative representations of arrays of undamaged and damaged RH-TRU 72-B packages. The HAC model used bounds the NCT model by using a smaller spacing of one half the impact limiter radius and end thickness. In addition, the results indicated that the reactivity effects of array interaction are less than those of close, full reflection of the package contents. Hence, maximum reactivity results for arrays of RH-TRU 72-B packages under NCT are essentially the same as under HAC at optimum moderation and reflection conditions. Therefore, infinite arrays of RH-TRU 72-B packages are safely subcritical under both NCT and HAC, and the requirements of 10 CFR §71.59[7] are satisfied. Furthermore, a CSI of zero (0.0) is justified.

6.4.3.3 Special Reflectors in RH-TRU Waste

As described previously, the only "special reflectors" credibly applicable to RH-TRU waste criticality analysis are: beryllium (Be), beryllium oxide (BeO), carbon (C), deuterium (D_2O), magnesium oxide (MgO), and depleted uranium (≥0.3 wt% ^{235}U and <0.72 wt% ^{235}U) when present in quantities greater than 1 wt%. Each special reflector with regard to its possible presence in RH-TRU waste is discussed below:

Beryllium and Beryllium Oxide – Be, and/or BeO, may be present in RH-TRU waste in quantities greater than 1 wt% by weight. The limits for payload containers are found in Table 6.1-1 under Case B. As described in Section 6.2.1, *Applicability of Case A Limits – General Payload*, beryllium is the limiting special reflector for RH-TRU waste. Limits for both bound and unbound Be have been evaluated for the Special Reflector Payload in Case B.

Carbon – Carbon is present as a constituent in the RH-TRU waste as discussed below:

(1) Carbon may be present as graphite molds, solids, or crucibles. In these forms the carbon will be chemically and irreversibly bound to the plutonium or other fissile material and cannot separate and may be handled using limits for Special Reflector Payloads with Pu bound to the special reflector;

(2) Carbon may be present in filter media as spent or activated carbon (for example, in activated charcoal filters). The plutonium or other fissile material would then be attached to the carbon media, would not be easily separated, and may be handled using limits for Special Reflector Payloads with Pu bound to the special reflector.

(3) Carbon may also be present in alloys, which are by definition chemically and/or mechanically bound, and may be handled using limits for Special Reflector Payloads with Pu bound to the special reflector.

Deuterium – The presence of liquid waste in the payload containers, except for residual amounts, is prohibited. As specified by the *Remote-Handling Transuranic Waste Authorization Methods for*

[7] Title 10, Code of Federal Regulations, Part 71 (10 CFR 71), *Packaging and Transportation of Radioactive Material*, 01-01-14 Edition.

Payload Control (RH-TRAMPAC)[8], the total volume of residual liquid in a payload container shall be less than 1 percent (volume) of the payload container. This limitation on the authorized contents is such that the D_2O will not be present in greater than 1 wt%, and the waste may be handled using limits for the General Payload with less than or equal to 1 wt% special reflector.

Magnesium Oxide – Magnesium oxide crucibles used in high temperature-controlled applications, such as reduction processes, may be present in solid inorganic waste forms such as glass, metal, and pyrochemical salts. If present, MgO will be bound to the fissile material and would not be easily separated. MgO used for neutralization in solidified material cannot be separated out as it is chemically reacted in the waste generation process. There is no identified mechanism that could cause the magnesium oxide in RH-TRU waste to be reconfigured as a reflector. This waste may be handled using limits for Special Reflector Payloads with Pu bound to the special reflector

Depleted Uranium (≥0.3 wt% ^{235}U and < 0.72 wt% ^{235}U) – Depleted uranium may be present in RH-TRU waste, but it will be chemically and/or mechanically bound to the plutonium or physically inseparable because the densities of U and Pu are similar. Separation by mechanical means or by leaching is extremely difficult and is considered highly unlikely in the RH-TRU waste after packaging. Depleted uranium in the RH-TRU waste will, therefore, not be separated from the fissile material and/or reconfigured as a reflector.

6.4.3.4 Applicable Criticality Limits for RH-TRU Waste

Case A covers manually compacted (not machine compacted) waste contaminated with up to 1 wt% special reflectors and extends the payload limit from 315 g ^{239}Pu FGE with no ^{240}Pu or unknown ^{240}Pu to 325, 350, and 370 g ^{239}Pu FGE with 5 g ^{240}Pu, 15 g ^{240}Pu, and 25 g ^{240}Pu, respectively. Case B covers manually compacted (not machine compacted) waste containing greater than 1 wt% special reflectors and extends the payload limit from 100 g ^{239}Pu FGE to 305 g ^{239}Pu FGE when the fissile material is known to be chemically or mechanically bound to the special reflector/moderator. Case C covers machine compacted waste contaminated with up to 1 wt% special reflectors and limits the fissile isotope to 245 g ^{239}Pu FGE. Case D covers manually compacted (not machine compacted) waste, with particle/lump size characteristic dimensions all less than 0.039 inches and/or greater than 2.36 inches, containing special reflectors and low enriched uranium contaminated with other distributed fissile isotopes. The Case D evaluation limits the enrichment of the fissile isotopes to 0.96 wt% ^{235}U FEM, with no restriction on special reflector materials. The Case E evaluation covers the same waste form as Case D without the particle/lump size restriction and further limits the enrichment of the fissile isotopes to 0.84 wt% ^{235}U FEM with a total contents net weight limit of 3,100 pounds.

In conclusion, the specific payload limits are summarized in Table 6.4-21.

[8] U.S. Department of Energy (DOE), *Remote-Handled Transuranic Waste Authorized Methods for Payload Control* (RH-TRAMPAC), U.S. Department of Energy, Carlsbad Field Office, Carlsbad, New Mexico.

Table 6.4-1 – Single-Unit, NCT and HAC, Case A, Sphere Centered, 315 FGE, k_s vs. H/Pu Ratio with Different Moderator/Reflector Combinations[9]

Case	H/Pu	Moderator/Reflector Conditions	k_{eff}	σ	k_s	AEG
Sphere Centered in Package						
NPWPW	700	Moderator and Reflector = 25% Poly/75% Water	0.9166	0.0009	0.9184	216.5
	800		0.9206	0.0009	0.9224	217.1
	900		0.9230	0.0009	**0.9248**	217.5
	1,000		0.9221	0.0009	0.9239	217.8
	1,100		0.9174	0.0009	0.9192	218.1
NPWPWB	700	Moderator = 25% Poly/75% Water, and Reflector = 25% Poly/74% Water/1% Beryllium	0.9173	0.0011	0.9195	216.6
	800		0.9230	0.0009	0.9248	217.1
	900		0.9244	0.0009	**0.9262**	217.5
	1,000		0.9228	0.0010	0.9248	217.8
	1,100		0.9203	0.0010	0.9223	218.1
NPWBPWB	700	Moderator and Reflector = 25% Poly/74% Water/1% Beryllium	0.9187	0.0010	0.9207	216.6
	800		0.9238	0.0010	0.9258	217.1
	900		0.9246	0.0009	**0.9264**	217.5
	1,000		0.9243	0.0009	0.9261	217.8
	1,100		0.9212	0.0010	0.9232	218.1
Sphere Centered at Top of Package						
NPWBPWBTOP	700	Moderator and Reflector = 25% Poly/74% Water/1% Beryllium	0.9246	0.0009	0.9264	216.5
	800		0.9293	0.0009	**0.9311**	217.0
	900		0.9285	0.0009	0.9303	217.4
	1,000		0.9280	0.0009	0.9298	217.8
	1,100		0.9252	0.0009	0.9270	218.1
Sphere at Top and Radially Displaced to Side of Package						
NPWBPWBTOP SIDE	700	Moderator and Reflector = 25% Poly/74% Water/1% Beryllium	0.9298	0.0010	0.9318	216.4
	800		0.9352	0.0009	**0.9370**	217.0
	900		0.9340	0.0009	0.9358	217.4
	1,000		0.9327	0.0009	0.9345	217.7
	1,100		0.9311	0.0010	0.9331	218.0

[9] All of the largest k_ss are highlighted within 1σ of each other.

Table 6.4-2 – Single-Unit, NCT and HAC, Case A, Sphere Top and Radially Displaced, 315 FGE, H/Pu at 900, k_s vs. Variable Interspersed Moderation Volume Fraction in the IV

Case	H/Pu	Moderator/Reflector Conditions	VF	k_{eff}	σ	k_s	AEG
NPWBPWBTOP SIDEIM	900	Moderator (Sphere) = 25% Poly/74% Water/1% Beryllium Reflector (IV Region) = 25% Poly/74% Water at Volume Fraction (VF) Given Maintaining the 1% Beryllium in the Mixture Constant	0.01	0.8256	0.0010	0.8276	216.4
			0.05	0.8351	0.0010	0.8371	216.5
			0.1	0.8481	0.0009	0.8499	216.6
			0.2	0.8673	0.0010	0.8693	216.8
			0.3	0.8855	0.0011	0.8877	217.0
			0.4	0.8975	0.0010	0.8995	217.1
			0.5	0.9058	0.0009	0.9076	217.2
			0.6	0.9154	0.0009	0.9172	217.2
			0.7	0.9204	0.0009	0.9222	217.3
			0.8	0.9242	0.0010	0.9262	217.3
			0.9	0.9307	0.0008	0.9323	217.3
			1	0.9340	0.0009	**0.9358**	217.4

Table 6.4-3 – Infinite-Unit, NCT and HAC, Case A, Sphere Top and Radially Displaced, 315 FGE, k_s vs. H/Pu Ratio with Different Moderator/Interspersed Moderator Combinations

Case	H/Pu	Moderator/Reflector Conditions	k_{eff}	σ	k_s	AEG
IFULL①	700	Moderator and Reflector = 25% Poly/74% Water/ 1% Beryllium Interspersed Moderator Between Units = Full Density Water	0.9299	0.0010	0.9319	216.4
	800		0.9333	0.0010	0.9353	217.0
	900		0.9341	0.0010	**0.9361**	217.4
	1,000		0.9330	0.0008	0.9346	217.7
	1,100		0.9282	0.0009	0.9300	218.0
IVOID	700	Moderator (Sphere) = 25% Poly/74% Water/ 1% Beryllium Reflector (IV Region) and Interspersed Moderator Between Units = Void	0.8150	0.0010	0.8170	215.1
	800		0.8288	0.0010	0.8308	215.8
	900		0.8400	0.0011	0.8422	216.4
	1,000		0.8441	0.0009	0.8459	216.8
	1,100		0.8484	0.0009	0.8502	217.2
	1,200		0.8488	0.0009	**0.8506**	217.5
	1,300		0.8473	0.0009	0.8491	217.8

Notes:

① Set run with random number seed different than the default to correct an unusual trend in this data set (one value significantly higher than expected). The value from this original run (physically the same input file) using the default random number seed is shown in H/Pu=900 entry of Table 6.4-4.

Table 6.4-4 – Infinite-Unit, NCT and HAC, Case A, Sphere Top and Radially Displaced, 315 FGE, k_s vs. Variable Interspersed Moderator at H/Pu Ratios of Interest

Case	H/Pu	Moderator/Reflector Conditions	VF	k_{eff}	σ	k_s	AEG
I900IM①	900	Moderator (Sphere) = 25% Poly/ 74% Water/ 1% Beryllium Interspersed Moderator (IV Region) = 25% Poly/ 74% Water/ 1% Beryllium at Given VF Interspersed Moderator (Between Units) = Water at Given VF	0.01	0.8273	0.0009	0.8291	216.4
			0.05	0.8315	0.0010	0.8335	216.5
			0.1	0.8426	0.0010	0.8446	216.6
			0.2	0.8675	0.0009	0.8693	216.8
			0.3	0.8834	0.0010	0.8854	217.0
			0.4	0.8944	0.0010	0.8964	217.1
			0.5	0.9055	0.0010	0.9075	217.2
			0.6	0.9157	0.0009	0.9175	217.2
			0.7	0.9223	0.0009	0.9241	217.3
			0.8	0.9261	0.0009	0.9279	217.3
			0.9	0.9299	0.0009	0.9317	217.3
			1	0.9339	0.0009	**0.9357**	217.4
I1200IM	1,200	Moderator (Sphere) = 25% Poly/ 74% Water/ 1% Beryllium Interspersed Moderator (IV Region) = 25% Poly/ 74% Water/ 1% Beryllium at Given VF Interspersed Moderator (Between Units) = Water at Given VF	0.01	0.8385	0.0009	0.8403	217.5
			0.05	0.8405	0.0009	0.8423	217.6
			0.1	0.8504	0.0009	0.8522	217.7
			0.2	0.8686	0.0010	0.8706	217.9
			0.3	0.8823	0.0009	0.8841	218.0
			0.4	0.8944	0.0009	0.8962	218.0
			0.5	0.9011	0.0009	0.9029	218.1
			0.6	0.9080	0.0009	0.9098	218.1
			0.7	0.9131	0.0009	0.9149	218.2
			0.8	0.9161	0.0009	0.9179	218.2
			0.9	0.9207	0.0009	0.9225	218.2
			1	0.9224	0.0009	**0.9242**	218.2

Notes:

① The case with VF = 1 does not agree with the value in Table 6.4-3. See Table 6.4-3 note explaining the random number seed difference in the runs. This data run is designed to show the k_s trend vs. reduced interspersed moderation values only.

Table 6.4-5 – Infinite-Unit, NCT and HAC, Case A, Sphere Top and Radially Displaced, k_s vs. H/Pu Ratio for Limiting Pu-240/Pu-239 Combinations with Optimum Moderator/Reflector

Case	^{240}Pu (g)	^{239}Pu (g)	H/^{239}Pu	Moderator/Reflector Conditions	k_{eff}	σ	k_s	AEG
I05Pu240	5	325	700	Moderator and Reflector = 25% Poly/ 74% Water/ 1% Beryllium Interspersed Moderator Between Units = Full Density Water	0.9253	0.0009	0.9271	216.4
			800		0.9314	0.0009	0.9332	216.9
			900		0.9327	0.0009	**0.9345**	217.3
			1,000		0.9321	0.0009	0.9339	217.7
			1,100		0.9276	0.0008	0.9292	218.0
I15Pu240	15	350	700		0.9277	0.0011	0.9299	216.3
			800		0.9320	0.0009	0.9338	216.8
			900		0.9345	0.0009	**0.9363**	217.3
			1,000		0.9329	0.0010	0.9349	217.6
			1,100		0.9295	0.0008	0.9311	217.9
I25Pu240	25	370	700		0.9272	0.0010	0.9292	216.2
			800		0.9346	0.0010	0.9366	216.8
			900		0.9352	0.0009	**0.9370**	217.2
			1,000		0.9346	0.0009	0.9364	217.6
			1,100		0.9337	0.0010	0.9357	217.9

Table 6.4-6 – Infinite-Unit, NCT and HAC, Case B, Sphere Centered, 100 FGE, k_s vs. H/Pu Ratio with Different Reflector Conditions

Case	Volume % Beryllium in Reflector	H/Pu	k_{eff}	σ	k_s	AEG
IBEREF100	1	600	0.8975	0.0009	0.8993	215.8
		700	0.9035	0.0009	0.9053	216.5
		800	0.9063	0.0009	**0.9081**	217.0
		900	0.9047	0.0009	0.9065	217.4
		1,000	0.9025	0.0008	0.9041	217.7
		1,100	0.8974	0.0007	0.8988	218.0
IBEREFIM100	0.01	900	0.4468	0.0008	0.4484	215.5
	0.05	900	0.4633	0.0009	0.4651	215.5
	0.1	900	0.4907	0.0008	0.4923	215.6
	0.2	900	0.5491	0.0008	0.5507	215.9
	0.3	900	0.6041	0.0009	0.6059	216.2
	0.4	900	0.6618	0.0008	0.6634	216.5
	0.5	900	0.7115	0.0009	0.7133	216.7
	0.6	900	0.7616	0.0010	0.7636	216.9
	0.7	900	0.8048	0.0008	0.8064	217.0
	0.8	900	0.8408	0.0009	0.8426	217.2
	0.9	900	0.8757	0.0008	0.8773	217.3
	1	900	0.9047	0.0009	**0.9065**	217.4

Table 6.4-7 – Infinite-Unit, NCT and HAC, Case B, Sphere Centered, 100 FGE, k_s vs. H/Pu Ratio with Different Moderator Conditions in 100% Be Reflector

Case	Moderator Mixture	H/Pu	k_{eff}	σ	k_s	AEG
I01TO18BEMOD100	25% Poly/ 74% Water/ 1% Beryllium	600	0.8975	0.0009	0.8993	215.8
		700	0.9035	0.0009	0.9053	216.5
		800	0.9063	0.0009	**0.9081**	217.0
		900	0.9047	0.0009	0.9065	217.4
		1,000	0.9025	0.0008	0.9041	217.7
		1,100	0.8974	0.0007	0.8988	218.0
	24.5% Poly/ 73.5% Water/ 2% Beryllium	600	0.8963	0.0009	0.8981	215.8
		700	0.9026	0.0009	0.9044	216.5
		800	0.9066	0.0009	**0.9084**	217.0
		900	0.9038	0.0009	0.9056	217.4
		1,000	0.9024	0.0009	0.9042	217.7
		1,100	0.8954	0.0009	0.8972	218.0
	24% Poly/ 72% Water/ 4% Beryllium	600	0.8971	0.0010	0.8991	215.8
		700	0.9046	0.0009	0.9064	216.5
		800	0.9058	0.0009	**0.9076**	217.0
		900	0.9044	0.0008	0.9060	217.4
		1,000	0.9007	0.0008	0.9023	217.7
		1,100	0.8981	0.0008	0.8997	218.0
I19TO36BEMOD100	23.5% Poly/ 70.5% Water/ 6% Beryllium	600	0.8977	0.0009	0.8995	215.9
		700	0.9044	0.0008	0.9060	216.5
		800	0.9066	0.0010	**0.9086**	217.0
		900	0.9043	0.0008	0.9059	217.4
		1,000	0.9009	0.0008	0.9025	217.7
		1,100	0.8962	0.0008	0.8978	218.0
	23% Poly/ 69% Water/ 8% Beryllium	600	0.8941	0.0009	0.8959	215.9
		700	0.9046	0.0009	**0.9064**	216.5
		800	0.9043	0.0009	0.9061	217.0
		900	0.9024	0.0009	0.9042	217.4
		1,000	0.9001	0.0009	0.9019	217.8
		1,100	0.8950	0.0008	0.8966	218.0

Case	Moderator Mixture	H/Pu	k_{eff}	σ	k_s	AEG
I19TO36BEMOD100	22.5% Poly/ 67.5% Water/ 10% Beryllium	600	0.8957	0.0009	0.8975	215.9
		700	0.9023	0.0010	0.9043	216.5
		800	0.9060	0.0010	**0.9080**	217.0
		900	0.9025	0.0009	0.9043	217.4
		1,000	0.9002	0.0008	0.9018	217.8
		1,100	0.8955	0.0008	0.8971	218.0
I37TO54BEMOD100	20% Poly/ 60% Water/ 20% Beryllium	600	0.8943	0.0010	0.8963	216.0
		700	0.8997	0.0009	0.9015	216.6
		800	0.9023	0.0010	**0.9043**	217.1
		900	0.9002	0.0009	0.9020	217.5
		1,000	0.8963	0.0008	0.8979	217.8
		1,100	0.8900	0.0008	0.8916	218.1
	15% Poly/ 45% Water/ 40% Beryllium	600	0.8870	0.0009	0.8888	216.3
		700	0.8900	0.0009	0.8918	216.8
		800	0.8915	0.0009	**0.8933**	217.3
		900	0.8899	0.0009	0.8917	217.7
		1,000	0.8860	0.0009	0.8878	218.0
		1,100	0.8793	0.0008	0.8809	218.2
	10% Poly/ 30% Water/ 60% Beryllium	600	0.8706	0.0009	0.8724	216.7
		700	0.8738	0.0009	**0.8756**	217.2
		800	0.8723	0.0008	0.8739	217.6
		900	0.8709	0.0009	0.8727	218.0
		1,000	0.8647	0.0008	0.8663	218.2
		1,100	0.8565	0.0009	0.8583	218.5
I55TO60BEMOD100	5% Poly/ 15% Water/ 80% Beryllium	600	0.8408	0.0010	**0.8428**	217.5
		700	0.8371	0.0009	0.8389	217.9
		800	0.8319	0.0008	0.8335	218.2
		900	0.8227	0.0008	0.8243	218.5
		1,000	0.8152	0.0008	0.8168	218.8
		1,100	0.8043	0.0007	0.8057	218.9

Table 6.4-8 – Infinite-Unit, NCT and HAC, Case B, Sphere Centered, 305 FGE, k_s vs. H/Pu Ratio with the Indicated Moderator Conditions

Case	Moderator Mixture	H/Pu	k_{eff}	σ	k_s	AEG
I01TO12BE	25% Poly/ 74% Water/ 1% Beryllium	600	0.9108	0.0010	0.9128	215.8
		700	0.9229	0.0010	0.9249	216.4
		800	0.9268	0.0009	**0.9286**	216.9
		900	0.9268	0.0009	**0.9286**	217.4
		1,000	0.9266	0.0010	**0.9286**	217.7
		1,100	0.9211	0.0008	0.9227	218.0
	24.5% Poly/ 73.5% Water/ 2% Beryllium	600	0.9137	0.0010	0.9157	215.8
		700	0.9227	0.0011	0.9249	216.4
		800	0.9268	0.0010	**0.9288**	217.0
		900	0.9270	0.0009	**0.9288**	217.4
		1,000	0.9257	0.0010	0.9277	217.7
		1,100	0.9223	0.0010	0.9243	218.0
I13TO24BE	24% Poly/ 72% Water/ 4% Beryllium	600	0.9141	0.0009	0.9159	215.8
		700	0.9221	0.0009	0.9239	216.4
		800	0.9265	0.0009	0.9283	217.0
		900	0.9275	0.0010	**0.9295**	217.4
		1,000	0.9272	0.0009	0.9290	217.7
		1,100	0.9228	0.0009	0.9246	218.0
	23.5% Poly/ 70.5% Water/ 6% Beryllium	600	0.9135	0.0010	0.9155	215.8
		700	0.9227	0.0010	0.9247	216.5
		800	0.9279	0.0010	0.9299	217.0
		900	0.9281	0.0010	**0.9301**	217.4
		1,000	0.9270	0.0010	0.9290	217.7
		1,100	0.9241	0.0009	0.9259	218.0
I25TO36BE	23% Poly/ 69% Water/ 8% Beryllium	600	0.9137	0.0010	0.9157	215.8
		700	0.9233	0.0009	0.9251	216.5
		800	0.9271	0.0009	0.9289	217.0
		900	0.9294	0.0009	**0.9312**	217.4
		1,000	0.9268	0.0009	0.9286	217.7
		1,100	0.9247	0.0008	0.9263	218.0
	22.5% Poly/ 67.5% Water/ 10% Beryllium	600	0.9145	0.0010	0.9165	215.8
		700	0.9241	0.0010	0.9261	216.5
		800	0.9267	0.0010	0.9287	217.0
		900	0.9290	0.0009	0.9308	217.4
		1,000	0.9294	0.0009	**0.9312**	217.8
		1,100	0.9242	0.0009	0.9260	218.0

Case	Moderator Mixture	H/Pu	k_{eff}	σ	k_s	AEG
I37TO48BE	20% Poly/ 60% Water/ 20% Beryllium	600	0.9172	0.0009	0.9190	215.9
		700	0.9272	0.0011	0.9294	216.6
		800	0.9287	0.0010	0.9307	217.1
		900	0.9316	0.0010	**0.9336**	217.5
		1,000	0.9298	0.0010	0.9318	217.8
		1,100	0.9276	0.0010	0.9296	218.1
	15% Poly/ 45% Water/ 40% Beryllium	600	0.9143	0.0009	0.9161	216.2
		700	0.9241	0.0009	0.9259	216.8
		800	0.9289	0.0011	0.9311	217.3
		900	0.9320	0.0010	**0.9340**	217.7
		1,000	0.9291	0.0009	0.9309	218.0
		1,100	0.9256	0.0009	0.9274	218.2
I49TO60BE	10% Poly/ 30% Water/ 60% Beryllium	600	0.9096	0.0010	0.9116	216.6
		700	0.9192	0.0009	0.9210	217.1
		800	0.9239	0.0010	**0.9259**	217.6
		900	0.9234	0.0009	0.9252	217.9
		1,000	0.9193	0.0010	0.9213	218.2
		1,100	0.9170	0.0009	0.9188	218.5
	5% Poly/ 15% Water/ 80% Beryllium	600	0.8954	0.0010	0.8974	217.3
		700	0.9000	0.0010	0.9020	217.8
		800	0.9032	0.0009	**0.9050**	218.2
		900	0.8988	0.0010	0.9008	218.5
		1,000	0.8937	0.0010	0.8957	218.7
		1,100	0.8859	0.0008	0.8875	219.0
I61TO66BE	1.25% Poly/ 3.75% Water/ 95% Beryllium	600	0.8492	0.0009	**0.8510**	219.2
		700	0.8348	0.0008	0.8364	219.5
		800	0.8174	0.0008	0.8190	219.8
		900	0.7990	0.0009	0.8008	219.9
		1,000	0.7786	0.0008	0.7802	220.1
		1,100	0.7597	0.0007	0.7611	220.2

Table 6.4-9 – Infinite Unit, NCT and HAC, Case C, Sphere Top Side, 245 FGE, k_s vs. H/Pu Ratio with Different Moderator/Reflector Combinations

Case	H/Pu	Moderator/Reflector Conditions	k_{eff}	σ	k_s	AEG
ITOPSIDE245	700	Moderator = 100% Poly Reflector = 99% Poly/ 1% Beryllium	0.9307	0.0009	0.9325	216.5
	800		0.9332	0.0010	0.9352	217.0
	900		0.9343	0.0009	**0.9361**	217.4
	1,000		0.9328	0.0009	0.9346	217.7
	1,100		0.9296	0.0009	0.9314	218.0
ITOPSIDEBEMOD245	700	Moderator and Reflector = 99% Poly/ 1% beryllium	0.9287	0.0011	0.9309	216.5
	800		0.9338	0.0010	0.9358	217.0
	900		0.9350	0.0011	**0.9372**	217.4
	1,000		0.9332	0.0009	0.9350	217.7
	1,100		0.9301	0.0009	0.9319	218.0

Table 6.4-10 – Single-Unit, NCT and HAC, Case D, Cylindrical Fissile Region, 0.96 wt% U-235 FEM, k_s vs. H/U-235 Ratio

Case	H/^{235}U	k_{eff}	σ	k_s	AEG
DSIN	300	0.8981	0.0006	0.8993	190.6
	400	0.9111	0.0007	0.9125	197.0
	500	0.9136	0.0007	**0.9150**	201.1
	600	0.9087	0.0006	0.9099	203.9
	700	0.8990	0.0006	0.9002	206.0
	800	0.8852	0.0006	0.8864	207.6
	900	0.8727	0.0006	0.8739	208.8
	1000	0.8580	0.0005	0.8590	209.9

Table 6.4-11 – Infinite-Unit, NCT and HAC, Case D, Cylindrical Fissile Region, 0.96 wt% U-235, k_s vs. H/U-235 Ratio and Variable Density Interspersed Moderation Conditions

Case	Interspersed Moderation Condition	$H/^{235}U$	k_{eff}	σ	k_s	AEG
DINF	1	300	0.8987	0.0007	0.9001	190.6
		400	0.9124	0.0007	0.9138	197.0
		500	0.9144	0.0006	**0.9156**	201.1
		600	0.9070	0.0005	0.9080	203.9
		700	0.8986	0.0006	0.8998	206.0
		800	0.8843	0.0006	0.8855	207.6
		900	0.8721	0.0005	0.8731	208.8
		1000	0.8576	0.0007	0.8590	209.9
DINFIM	0.00001	500	0.9183	0.0007	0.9197	201.2
	0.001	500	0.9188	0.0006	**0.9200**	201.2
	0.01	500	0.9168	0.0005	0.9178	201.1
	0.05	500	0.9156	0.0006	0.9168	201.1
	0.1	500	0.9138	0.0007	0.9152	201.0
	0.2	500	0.9140	0.0006	0.9152	201.0
	0.4	500	0.9132	0.0006	0.9144	201.1
	0.6	500	0.9125	0.0005	0.9135	201.0
	0.8	500	0.9139	0.0006	0.9151	201.0
	1	500	0.9144	0.0006	0.9156	201.1

Table 6.4-12 – Single-Unit, NCT and HAC, Case D, Be Reflected, Cylindrical Fissile Region, 0.96 wt% U-235 FEM, k_s vs. H/U-235 Ratio

Case	IV Region Reflector Condition	$H/^{235}U$	k_{eff}	σ	k_s	AEG
Long Cylinder with Be Reflector Radially Distributed						
LEUBEREFLSIN0	Reflector = 25% poly/ 74% water/ 1% beryllium	300	0.8912	0.0007	0.8926	193.5
		400	0.9033	0.0006	0.9045	198.8
		500	0.9052	0.0005	**0.9062**	202.4
		600	0.8999	0.0006	0.9011	204.9
		700	0.8889	0.0005	0.8899	206.7
		800	0.8770	0.0006	0.8782	208.2
		900	0.8654	0.0005	0.8664	209.4
		1,000	0.8513	0.0006	0.8525	210.3
Short Squat Cylinder with Be Reflector Axially Distributed on Ends						
LEUBEREFLSIN1	Reflector = 25% poly/ 74% water/ 1% beryllium	300	0.9037	0.0006	0.9049	191.1
		400	0.9167	0.0006	0.9179	197.3
		500	0.9168	0.0006	**0.9180**	201.2
		600	0.9088	0.0006	0.9100	204.0
		700	0.9005	0.0006	0.9017	206.1
		800	0.8875	0.0006	0.8887	207.7
		900	0.8740	0.0005	0.8750	208.9
		1,000	0.8590	0.0005	0.8600	210.0
Cylinder with Be Reflector Encapsulating Cylinder						
LEUBEREFLSIN2	Reflector = 25% poly/ 74% water/ 1% beryllium	300	0.8950	0.0006	0.8962	193.2
		400	0.9075	0.0005	0.9085	198.8
		500	0.9080	0.0006	**0.9092**	202.4
		600	0.9020	0.0006	0.9032	204.9
		700	0.8907	0.0007	0.8921	206.7
		800	0.8809	0.0006	0.8821	208.2
		900	0.8678	0.0006	0.8690	209.3
		1,000	0.8527	0.0005	0.8537	210.2

Table 6.4-13 – Infinite-Unit, NCT and HAC, Case D, Be Reflected, Short, Squat, Cylindrical Fissile Region, 0.96 wt% U-235 FEM, k_s vs. H/U-235 Ratio and Variable Interspersed Moderation Between Packages

Case	Interspersed Moderation Condition (vol fraction H_2O)	$H/^{235}U$	k_{eff}	σ	k_s	AEG
Infinite Unit Package Array with Full Density Interspersed Moderation						
LEUBEREFLINF1	1	300	0.9067	0.0007	0.9081	191.1
		400	0.9175	0.0006	**0.9187**	197.3
		500	0.9168	0.0007	0.9182	201.2
		600	0.9111	0.0006	0.9123	204.0
		700	0.8998	0.0006	0.9010	206.1
		800	0.8880	0.0005	0.8890	207.7
		900	0.8733	0.0006	0.8745	208.9
		1,000	0.8585	0.0006	0.8597	210.0
Infinite Unit Package Array at H/X=400 with Variable Density Interspersed Moderation						
LEUBEREFLINF1IM	0.00001	400	0.9228	0.0006	0.9240	197.4
	0.001	400	0.9214	0.0005	**0.9224**	197.4
	0.01	400	0.9206	0.0006	0.9218	197.4
	0.05	400	0.9177	0.0006	0.9189	197.3
	0.1	400	0.9179	0.0007	0.9193	197.3
	0.2	400	0.9165	0.0006	0.9177	197.3
	0.4	400	0.916	0.0006	0.9172	197.3
	0.6	400	0.916	0.0006	0.9172	197.3
	0.8	400	0.9169	0.0006	0.9181	197.3
	1	400	0.9175	0.0006	0.9187	197.3

Table 6.4-14 – Infinite-Unit, NCT and HAC, Case D, Be Reflected, Short, Squat, Cylindrical Fissile Region, 0.96 wt% U-235 FEM, Moderated to H/U-235=500, k_s vs. Be in Moderator

Case	Be in Moderator (Vol% Be)	k_{eff}	σ	k_s	AEG
LEUBEMODREFLINF1	1	0.9168	0.0007	**0.9182**	201.2
	2	0.9166	0.0006	0.9178	201.3
	4	0.916	0.0007	0.9174	201.5
	6	0.9153	0.0007	0.9167	201.7
	8	0.9144	0.0005	0.9154	201.8
	10	0.9151	0.0006	0.9163	202.0
	20	0.9101	0.0007	0.9115	202.9
	40	0.8978	0.0007	0.8992	205.0
	60	0.8705	0.0007	0.8719	207.8
	80	0.8111	0.0006	0.8123	212.0
	85	0.7814	0.0006	0.7826	213.5

Table 6.4-15 – Single-Unit, NCT and HAC, Case E, Cylindrical Array Fissile Region, 0.84 wt% ^{235}U FEM, k_s vs. H/^{235}U Ratio (and Array Pitch) for Arrays of Cylinders and Spheres (most reactive element diameter of 1.25 cm)

Case	H/^{235}U	Pitch	k_{eff}	σ	k_s
CT.19-24	283	1.8125	0.8947	0.0007	0.8960
	397	2.0287	0.9201	0.0005	**0.9212**
	512	2.2241	0.9192	0.0006	0.9203
	626	2.4036	0.9060	0.0007	0.9073
	740	2.5706	0.8833	0.0006	0.8845
	854	2.7273	0.8592	0.0005	0.8603
ST.19-24	269	1.384	0.8753	0.0007	0.8767
	369	1.4823	0.9103	0.0007	0.9116
	469	1.569	0.9205	0.0006	**0.9218**
	569	1.6471	0.9195	0.0007	0.9209
	669	1.7184	0.9112	0.0005	0.9123
	769	1.7842	0.8981	0.0005	0.8991

Table 6.4-16 – Infinite-Unit, NCT and HAC, Case E, Cylindrical Fissile Region, 0.84 wt% ^{235}U, k_s vs. H/^{235}U Ratio and Variable Density Interspersed Moderation Conditions

Case	Interspersed Moderation Condition	H/^{235}U	k_{eff}	σ	k_s
CT.19i-24i	1	283	0.8937	0.0006	0.8949
		397	0.9190	0.0006	0.9203
		512	0.9199	0.0006	**0.9210**
		626	0.9042	0.0006	0.9053
		740	0.8832	0.0006	0.8843
		854	0.8588	0.0006	0.8600
CT.21iim1-10	0.00001	512	0.9217	0.0006	0.9228
	0.0001	512	0.9218	0.0005	**0.9229**
	0.001	512	0.9216	0.0005	0.9226
	0.05	512	0.9202	0.0006	0.9213
	0.1	512	0.9184	0.0007	0.9199
	0.2	512	0.9192	0.0006	0.9204
	0.4	512	0.9184	0.0006	0.9195
	0.6	512	0.9190	0.0006	0.9203
	0.8	512	0.9192	0.0006	0.9204
	1.0	512	0.9199	0.0006	0.9210
ST.19i-24i	1	269	0.8743	0.0006	0.8756
		369	0.9096	0.0006	0.9109
		469	0.9218	0.0007	**0.9231**
		569	0.9197	0.0006	0.9209
		669	0.9104	0.0005	0.9114
		769	0.8983	0.0006	0.8995

Case	Interspersed Moderation Condition	$H/^{235}U$	k_{eff}	σ	k_s
ST.21iim1-10	0.00001	469	0.9242	0.0006	**0.9254**
	0.0001	469	0.9229	0.0006	0.9241
	0.001	469	0.9240	0.0006	0.9253
	0.05	469	0.9222	0.0006	0.9234
	0.1	469	0.9223	0.0006	0.9234
	0.2	469	0.9214	0.0006	0.9226
	0.4	469	0.9205	0.0006	0.9217
	0.6	469	0.9203	0.0006	0.9214
	0.8	469	0.9212	0.0006	0.9224
	1.0	469	0.9218	0.0007	0.9231

Table 6.4-17 – Single-Unit, NCT and HAC, Case E, Cylindrical Array Fissile Region, 0.84 wt% ^{235}U FEM with Unlimited Special Reflector at 1, 2, 4, 8, 16, and 32 30 cm, k_s vs. Array Pitch for Arrays of Cylinders (most reactive element diameter of 1.25 cm)

Case	Pitch (cm)	Be Reflector Thickness (cm)	k_{eff}	σ	k_s	EALF (eV)	USL (EALF)
CCR.19	1.8125	1	0.8824	0.0006	0.8836	0.6292	0.9292
	1.8125	2	0.8861	0.0006	0.8873	0.6263	0.9292
	1.8125	4	0.8918	0.0006	0.8929	0.6139	0.9293
	1.8125	8	0.8996	0.0007	0.9010	0.5932	0.9295
	1.8125	16	0.9032	0.0006	0.9044	0.5570	0.9297
	1.8125	32	0.8885	0.0006	0.8897	0.5140	0.9300
CCR.20	2.0287	1	0.9077	0.0005	0.9088	0.3566	0.9311
	2.0287	2	0.9105	0.0005	0.9116	0.3556	0.9311
	2.0287	4	0.9153	0.0006	0.9165	0.3507	0.9312
	2.0287	8	0.9196	0.0006	0.9208	0.3437	0.9312
	2.0287	16	0.9205	0.0005	0.9216	0.3313	0.9313
	2.0287	32	0.9061	0.0006	0.9073	0.3161	0.9314
CCR.21	2.2241	1	0.9076	0.0005	0.9086	0.2575	0.9318
	2.2241	2	0.9093	0.0006	0.9105	0.2562	0.9318
	2.2241	4	0.9122	0.0006	0.9133	0.2539	0.9318
	2.2241	8	0.9147	0.0006	0.9159	0.2503	0.9319
	2.2241	16	0.9139	0.0006	0.9150	0.2447	0.9319
	2.2241	32	0.8996	0.0005	0.9006	0.2375	0.9319
CCR.22	2.4036	1	0.8955	0.0007	0.8968	0.2097	0.9321
	2.4036	2	0.8957	0.0006	0.8969	0.2102	0.9321
	2.4036	4	0.8973	0.0006	0.8984	0.2087	0.9321
	2.4036	8	0.8986	0.0006	0.8998	0.2051	0.9322
	2.4036	16	0.8980	0.0005	0.8990	0.2019	0.9322
	2.4036	32	0.8837	0.0005	0.8847	0.1979	0.9322

Case	Pitch (cm)	Be Reflector Thickness (cm)	k_{eff}	σ	k_s	EALF (eV)	USL (EALF)
CCR.23	2.5706	1	0.8751	0.0006	0.8763	0.1808	0.9323
	2.5706	2	0.8767	0.0005	0.8778	0.1813	0.9323
	2.5706	4	0.8772	0.0007	0.8786	0.1799	0.9323
	2.5706	8	0.8782	0.0005	0.8793	0.1796	0.9324
	2.5706	16	0.8764	0.0005	0.8775	0.1765	0.9324
	2.5706	32	0.8642	0.0005	0.8652	0.1743	0.9324
CCR.24	2.7273	1	0.8519	0.0005	0.8529	0.1644	0.9325
	2.7273	2	0.8514	0.0006	0.8525	0.1639	0.9325
	2.7273	4	0.8535	0.0005	0.8545	0.1645	0.9325
	2.7273	8	0.8534	0.0006	0.8545	0.1626	0.9325
	2.7273	16	0.8524	0.0005	0.8534	0.1613	0.9325
	2.7273	32	0.8394	0.0005	0.8405	0.1600	0.9325

Table 6.4-18 – Infinite-Unit, NCT and HAC, Case E, Cylindrical Fissile Region, 0.84 wt% ^{235}U, k_s vs. H/^{235}U Ratio with Unlimited Special Reflector at 30 cm for Arrays of Spheres (most reactive element diameter of 1.25 cm)

Case	Interspersed Moderation Condition	k_{eff}	σ	k_s	EALF	USL (EALF)
CCR.20i1-6	1	0.9079	0.0006	0.9091	0.3578	0.9311
		0.9098	0.0006	0.9109	0.3563	0.9311
		0.9150	0.0008	0.9165	0.3537	0.9311
		0.9186	0.0006	0.9198	0.3436	0.9312
		0.9212	0.0006	**0.9224**	0.3317	0.9313
		0.9053	0.0006	0.9065	0.3172	0.9314
CCR.20i.5im1-10	0.00001	0.9218	0.0006	0.9230	0.3302	0.9313
	0.0001	0.9229	0.0007	**0.9243**	0.3296	0.9313
	0.001	0.9225	0.0006	0.9237	0.3283	0.9313
	0.05	0.9208	0.0005	0.9218	0.3303	0.9313
	0.1	0.9201	0.0006	0.9213	0.3319	0.9313
	0.2	0.9217	0.0006	0.9229	0.3323	0.9313
	0.4	0.9209	0.0006	0.9221	0.3324	0.9313
	0.6	0.9212	0.0006	0.9224	0.3323	0.9313
	0.8	0.9204	0.0006	0.9217	0.3333	0.9313
	1.0	0.9212	0.0006	0.9224	0.3317	0.9313

Table 6.4-19 – Single-Unit, NCT and HAC, Case E, Cylindrical Array Fissile Region, 0.84 wt% ^{235}U FEM with Unlimited Special Reflector Interspersed in the Moderator/Reflector Regions, k_s vs. Be Concentration at Various Array Pitches for Arrays of Spheres (most reactive element diameter of 1.25 cm)

Case E	Pitch (cm)	Be (Vol %)	k_{eff}	σ	k_s	EALF	USL (EALF)
Array Located at Top of IV							
CTVR.19.a-f	1.8125	1	0.8917	0.0006	0.8930	0.6402	0.9291
		5	0.8875	0.0006	0.8886	0.6648	0.9290
		10	0.8831	0.0006	0.8844	0.6972	0.9287
		20	0.8730	0.0008	0.8745	0.7940	0.9281
		50	0.8064	0.0006	0.8076	1.4286	0.9237
		75	0.6953	0.0007	0.6967	3.8548	0.9068
CTVR.20.a-f	2.0287	1	0.9174	0.0006	0.9187	0.3585	0.9311
		5	0.9162	0.0006	0.9175	0.3687	0.9310
		10	0.9162	0.0006	0.9175	0.3803	0.9310
		20	0.9121	0.0006	0.9133	0.4134	0.9307
		50	0.8693	0.0006	0.8704	0.6228	0.9293
		75	0.7708	0.0008	0.7723	1.3487	0.9242
CTVR.21.a-f	2.2241	1	0.9165	0.0006	0.9178	0.2573	0.9318
		5	0.9179	0.0007	0.9192	0.2608	0.9318
		10	0.9204	0.0006	0.9216	0.2678	0.9317
		20	0.9236	0.0006	0.9248	0.2816	0.9316
		50	0.9042	0.0006	0.9055	0.3811	0.9309
		75	0.8226	0.0006	0.8238	0.6938	0.9288
CTVR.22.a-f	2.4036	1	0.9023	0.0007	0.9036	0.2079	0.9322
		5	0.9062	0.0006	0.9073	0.2104	0.9321
		10	0.9118	0.0006	0.9130	0.2142	0.9321
		20	0.9204	0.0006	0.9216	0.2220	0.9321
		50	0.9213	0.0007	0.9227	0.2771	0.9317
		75	0.8594	0.0007	0.8607	0.4467	0.9305

Case E	Pitch (cm)	Be (Vol %)	k_{eff}	σ	k_s	EALF	USL (EALF)
CTVR.23.a-f	2.5706	1	0.8811	0.0006	0.8823	0.1801	0.9323
		5	0.8875	0.0006	0.8886	0.1822	0.9323
		10	0.8950	0.0006	0.8962	0.1823	0.9323
		20	0.9086	0.0005	0.9097	0.1877	0.9323
		50	0.9266	0.0006	**0.9278**	0.2209	0.9321
		75	0.8870	0.0008	0.8885	0.3232	0.9314
CTVR.24.a-f	2.7273	1	0.8571	0.0005	0.8581	0.1632	0.9325
		5	0.8650	0.0006	0.8661	0.1639	0.9325
		10	0.8749	0.0005	0.8759	0.1641	0.9325
		20	0.8915	0.0005	0.8925	0.1669	0.9324
		50	0.9245	0.0007	0.9259	0.1883	0.9323
		75	0.9018	0.0007	0.9032	0.2587	0.9318
Array Located at Center of IV							
CCVR.19.a-f	1.8125	1	0.8888	0.0007	0.8902	0.6155	0.9293
		5	0.8862	0.0006	0.8874	0.6440	0.9291
		10	0.8812	0.0007	0.8825	0.6707	0.9289
		20	0.8698	0.0007	0.8711	0.7509	0.9284
		50	0.8124	0.0007	0.8138	1.2811	0.9247
		75	0.7148	0.0006	0.7160	3.0575	0.9123
CCVR.20.a-f	2.0287	1	0.9149	0.0007	0.9163	0.3537	0.9311
		5	0.9142	0.0007	0.9155	0.3615	0.9311
		10	0.9128	0.0006	0.9141	0.3723	0.9310
		20	0.9108	0.0006	0.9120	0.4016	0.9308
		50	0.8723	0.0007	0.8736	0.5899	0.9295
		75	0.7826	0.0006	0.7838	1.1873	0.9253
CCVR.21.a-f	2.2241	1	0.9148	0.0006	0.9160	0.2549	0.9318
		5	0.9180	0.0007	0.9194	0.2592	0.9318
		10	0.9197	0.0006	0.9209	0.2644	0.9318
		20	0.9227	0.0006	0.9239	0.2798	0.9317
		50	0.9060	0.0006	0.9073	0.3671	0.9310
		75	0.8313	0.0006	0.8324	0.6436	0.9291

Case E	Pitch (cm)	Be (Vol %)	k_{eff}	σ	k_s	EALF	USL (EALF)
CCVR.22.a-f	2.4036	1	0.9010	0.0006	0.9022	0.2073	0.9322
		5	0.9067	0.0005	0.9078	0.2090	0.9321
		10	0.9103	0.0007	0.9116	0.2112	0.9321
		20	0.9204	0.0006	0.9216	0.2202	0.9321
		50	0.9216	0.0007	0.9230	0.2708	0.9317
		75	0.8655	0.0007	0.8668	0.4219	0.9307
CCVR.23.a-f	2.5706	1	0.8812	0.0006	0.8823	0.1801	0.9323
		5	0.8864	0.0006	0.8876	0.1806	0.9323
		10	0.8937	0.0005	0.8947	0.1818	0.9323
		20	0.9095	0.0006	0.9107	0.1862	0.9323
		50	0.9286	0.0006	0.9299	0.2161	0.9321
		75	0.8913	0.0006	0.8925	0.3114	0.9314
CCVR.24.a-f	2.7273	1	0.8564	0.0005	0.8574	0.1633	0.9325
		5	0.8654	0.0006	0.8665	0.1635	0.9325
		10	0.8738	0.0006	0.8749	0.1635	0.9325
		20	0.8915	0.0006	0.8926	0.1664	0.9324
		50	0.9280	0.0008	**0.9295**	0.1859	0.9323
		75	0.9069	0.0007	0.9083	0.2519	0.9318

Table 6.4-20 – Infinite-Unit, NCT and HAC, Case E, Cylindrical Fissile Region, 0.84 wt% ^{235}U, k_s vs. H/^{235}U Ratio with Unlimited Special Reflector Interspersed in the Moderator/Reflector Regions, k_s vs. Be Volume % at 1.25 cm Array Pitch for Arrays of Cylinders (most reactive element diameter of 1.25 cm)

Case	Interspersed Moderation Condition	Be in Moderator/ Reflector (Vol %)	k_{eff}	σ	k_s	EALF	USL (EALF)
CCVR.24i.a-f	1	1	0.8560	0.0005	0.8571	0.1631	0.9325
		5	0.8648	0.0006	0.8659	0.1632	0.9325
		10	0.8728	0.0005	0.8739	0.1641	0.9325
		20	0.8911	0.0007	0.8925	0.1653	0.9324
		50	0.9269	0.0006	**0.9282**	0.1858	0.9323
		75	0.9069	0.0007	0.9083	0.2516	0.9318
CCVR.24i.eim1-10	0.00001	50	0.9296	0.0006	0.9308	0.1847	0.9323
	0.0001		0.9304	0.0006	**0.9316**	0.1842	0.9323
	0.001		0.9293	0.0007	0.9307	0.1857	0.9323
	0.05		0.9272	0.0007	0.9285	0.1860	0.9323
	0.1		0.9278	0.0006	0.9289	0.1861	0.9323
	0.2		0.9265	0.0006	0.9277	0.1860	0.9323
	0.4		0.9283	0.0006	0.9295	0.1847	0.9323
	0.6		0.9269	0.0006	0.9280	0.1863	0.9323
	0.8		0.9278	0.0006	0.9291	0.1857	0.9323
	1.0		0.9269	0.0006	0.9282	0.1858	0.9323

Table 6.4-21 – Fissile Payload Limits

Payload Name	Physical Form and Other Contents Restrictions	Fissile Isotope Special Conditions	Fissile Limit per Package (g ^{239}Pu FGE)	Applicable Analysis Case
General Payload	Not Machine Compacted with ≤1% by weight Be	None	315	A
		≥5 g ^{240}Pu	325	A
		≥15 g ^{240}Pu	350	A
		≥25 g ^{240}Pu	370	A
Special Reflector Payload	Not Machine Compacted with >1% by weight Be	Fissile material not bound to Special Reflector	100	B
		Fissile material bound to Special Reflector	305	B
Machine-Compacted Payload	≤1% by weight Be	None	245	C

Payload Name	Physical Form and Other Contents Restrictions	Fissile Isotope Special Conditions	Fissile Limit per Package (wt% ^{235}U FEM)	Applicable Analysis Case
Low Enriched Uranium (LEU) Homogeneous Payload	Not Machine Compacted with particle/lump size characteristic dimensions all less than 0.039 inches and/or greater than 2.36 inches	Primarily uranium (in terms of the heavy metal component) with waste matrix distributed to not exceed enrichment limit	0.96	D
LEU Heterogeneous Payload	Not Machine Compacted up to 3,100 pounds net contents weight	Primarily uranium (in terms of the heavy metal component) with waste matrix distributed to not exceed enrichment limit	0.84	E

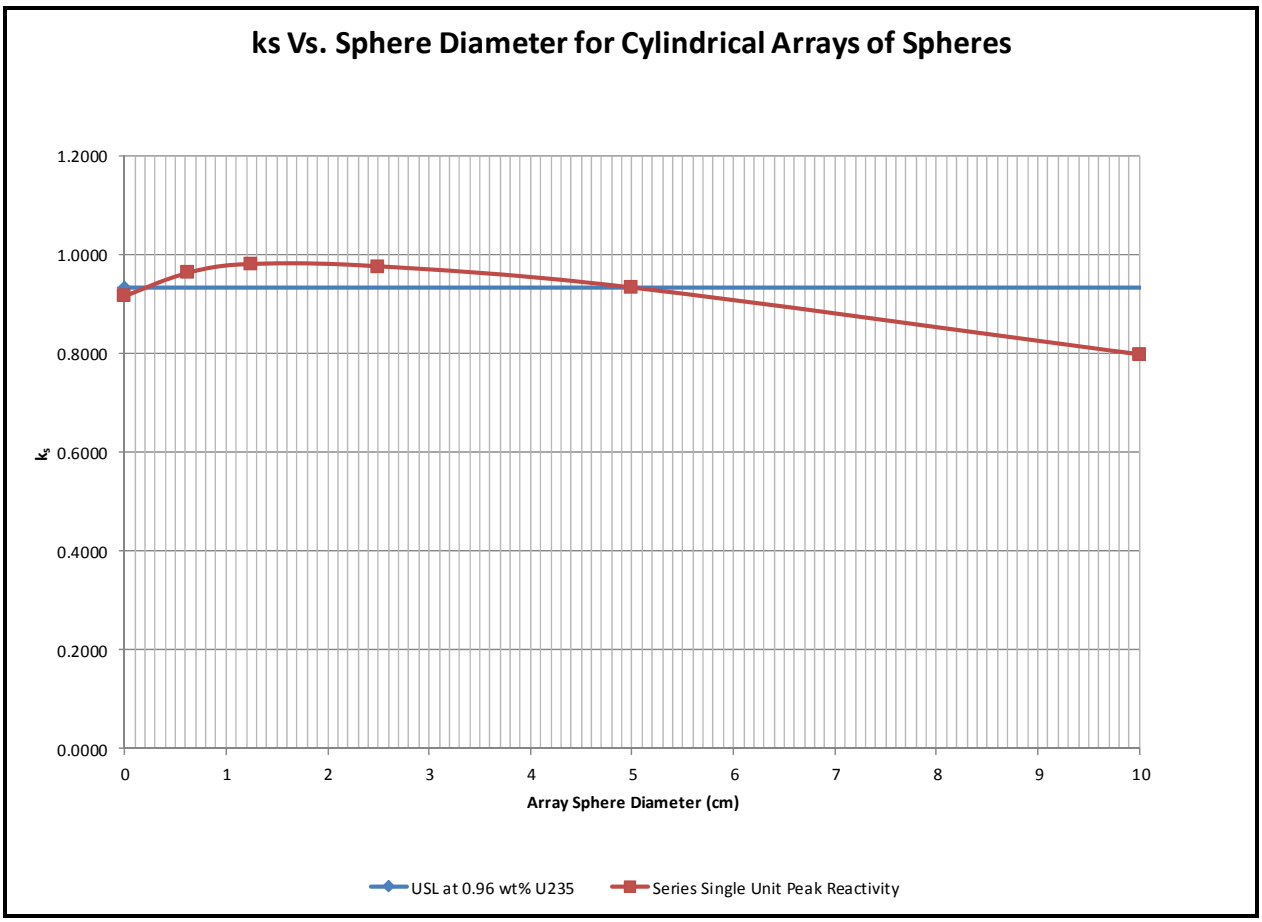

Figure 6.4-1 – Plot of Peak Reactivities of Cylindrical Arrays of Spheres at Optimum Pitch and at 0.96 wt% ^{235}U Vs. Sphere Diameter

6.5 Critical Benchmark Experiments

The KENO-V.a Monte Carlo criticality code[1] has been used extensively in criticality evaluations. The 238 energy-group, ENDF-B/V cross-section library[2] employed here has been selected based on its relatively fine neutron energy group structure. This section justifies the validity of this computation tool and data library combination for application to the RH-TRU 72-B package criticality analysis.

The ORNL USLSTATS code, described in Appendix C, *User's Manual for USLSTATS V1.0*, of NUREG/CR-6361[3], is used to establish an upper subcriticality limit, USL, for the analysis. Computed neutron multiplication factors, k_{eff}, for the RH-TRU 72-B package are deemed to be adequately subcritical if the computed value of k_{eff} plus two standard deviations is below the USL as follows:

$$k_s = k_{eff} + 2\sigma < USL$$

The USL includes the combined effects of code bias, uncertainty in the benchmark experiments, uncertainty in the computational evaluation of the benchmark experiments, and an administrative margin of subcriticality. The USL is determined using the confidence band with administrative margin technique (USLSTATS Method 1).

The result of the statistical analysis of the Pu fissile isotope benchmark experiments is a USL of 0.9382. Due to the significant positive bias exhibited by the code and library for the benchmark experiments, the USL is constant with respect to the various parameters selected for the benchmark analysis.

The result of the statistical analysis of the LEU benchmark experiments is a USL of 0.9257.

6.5.1 Benchmark Experiments and Applicability

6.5.1.1 PU Benchmarks

A total of 196 benchmark experiments of water-reflected solutions of plutonium nitrate are evaluated using the KENO-V.a[1] Monte Carlo criticality code with the SCALE-PC v4.4a[4], 238 energy-group, ENDF-B/V cross-section library. The benchmark cases are evaluated with respect to three independent parameters: 1) the H/Pu ratio, 2) the average fission energy group (AEG), and 3) the ratio of ^{240}Pu to total Pu.

---

[1] L. M. Petrie and N. F. Landers, *KENO-V.a: An Improved Monte Carlo Criticality Program with Supergrouping*, ORNL/NUREG/CSD-2/V2/R6, Volume 2, Section F11, March 2000.

[2] W. C. Jordan and S. M. Bowman, *Scale Cross-Section Librarie*s, ORNL/NUREG/CSD-2/V3/R6, Volume 3, Section M4, March 2000.

[3] J. J. Lichtenwalter, S. M. Bowman, M. D. DeHart, C. M. Hopper, *Criticality Benchmark Guide for Light-Water-Reactor Fuel in Transportation and Storage Packages*, NUREG/CR-6361, ORNL/TM-13211, March 1997.

[4] Oak Ridge National Laboratory (ORNL), SCALE 4.4a: *Modular Code System for Performing Standardized Computer Analysis for Licensing Evaluation for Workstations and Personal Computers*, ORNL/NUREG/CSD-2/R6, March 2000.

Detailed descriptions of the benchmark experiments are obtained from the OECD Nuclear Energy Agency's *International Handbook of Evaluated Criticality Safety Benchmark Experiments*[5]. The critical experiments selected for this analysis are presented in Table 6.5-1. Experiments with beryllium and Pu as the fissile component are not available. The only experiments with beryllium in the thermal energy range identified from the OECD Handbook contained ^{233}U as the fissile isotope. Thus, 31 benchmarks with ^{233}U and beryllium in the thermal energy range and 15 benchmarks with ^{233}U and no beryllium also in the thermal energy range were evaluated. With respect to validation of polyethylene, CH_2, in the models, some of the ^{233}U benchmarks contained polyethylene and some of the plutonium experiments contained Plexiglas, which also contains carbon. All criticality models of the RH-TRU 72-B package fall within the range of applicability of the benchmark experiments for the H/Pu ratio and AEG trending parameters as follows:

Range of Applicability for Trending Parameters
$45 \leq$ H/Pu Ratio $\leq 2{,}730$
$173 \leq$ AEG ≤ 220
$4.95 \times 10^{-3} \leq {}^{240}Pu/Pu\ Ratio \leq 2.32 \times 10^{-1}$

The intent of using the $^{240}Pu/Pu$ ratio is to demonstrate the validity of an extension of the range of applicability of this parameter to the RH-TRU 72-B package criticality models. The Case A models include a $^{240}Pu/Pu$ Ratio of up to 6.6×10^{-2}, which is within the range of applicability. Only thermal benchmark experiments are analyzed. Criticality analysis of the RH-TRU 72-B package and package arrays demonstrate that neutron multiplication factors are insignificant when the package contents are unmoderated.

6.5.1.2 LEU Benchmarks

For the Case D calculations, a total of 82 benchmark experiments of various low enriched uranium experiments ranging from uranium solutions to moderated uranium oxide rod arrays with reflectors ranging from water to polythene (similar in properties to polyethylene with respect to C and H constituents) are evaluated using the KENO-V.a[1] Monte Carlo criticality code with the SCALE-PC v4.4a[4] , 238 energy-group, ENDF-B/V cross-section library[2]. The benchmark case results are evaluated with respect to three parameters: 1) the H/X ratio, 2) the average fission energy group (AEG), and 3) the enrichment of ^{235}U.

Detailed descriptions of the benchmark experiments are obtained from the OECD Nuclear Energy Agency's *International Handbook of Evaluated Criticality Safety Benchmark Experiments*[5]. The critical experiments selected for this analysis are presented in Table 6.5-4. With respect to validation of polyethylene, CH_2, in the models, some of the ^{235}U benchmarks contained polythene (a polymer of the gas ethene -C_2H_4) which also contains carbon and similar C to H ratios as polyethylene. All criticality models of the RH-TRU 72-B package fall within

[5] OECD Nuclear Energy Agency, *International Handbook of Evaluated Criticality Safety Benchmark Experiment*s, NEA/NSC/DOC(95)03, September 2002.

the range of applicability of the benchmark experiments for the H/Pu ratio and AEG trending parameters as follows:

Range of Applicability for Trending Parameters
$300 \leq H/^{235}U \leq 1438$
$168.7 \leq AEG \leq 220$
$2.6 \leq {}^{235}U \text{ enrichment} \leq 10.1$

The enrichments at which the package contents are analyzed fall outside of the range of applicability of the benchmark cases. The USL method 1 provides a means of projecting the USL to areas outside the range and this was used to develop a USL for the 0.96 wt% ^{235}U enrichment for comparison only. Since this low enrichment is expected to always be subcritical in aqueous, water-reflected systems according to ANSI/ANS-8.1[6], and since these systems did indeed evaluate to k_s values in the 0.8 to 0.9 region, the calculations are accepted to fall within the range of applicability and the USL, for the purpose of this analysis, is extended to the lower enrichment of 0.96 wt% ^{235}U. The Be analysis described in Section 6.5.1.1, *PU Benchmarks*, also applies here.

For the Case E calculations with limited special reflectors, the 82 benchmark cases discussed above were revised to run under SCALE 5.1 and were evaluated with the KENO-V.a[1] code with the SCALE Version 5.1[7], 238 group, ENDF-B/V cross-section library[8]. The benchmark case results are evaluated with respect to two parameters: the H/X ratio and the enrichment of ^{235}U as measured independent variables that the cases have in common. The USL method 1 results were evaluated, extending the enrichments outside the range of applicable benchmark cases using the USL method 1 results. The USL based on enrichment was found to be more limiting than the USL based on H/X ratio and was used for all LEU cases with limited special reflectors.

For the Case E calculations with unlimited special reflectors, Pu Benchmark cases were evaluated with the 82 LEU benchmark cases using a calculated independent parameter of Energy of Average Lethargy of Fission (EALF). The EALF factor provides a better representation of the fission energy profile of the system that the Average Energy Group Causing Fission (AEG) used in earlier work. No other measured independent variables are common to the combined group of LEU and Pu Benchmark Cases.

6.5.2 Details of Benchmark Calculations

A total of 196 experimental benchmarks with Pu in the thermal energy range were evaluated with the KENO-V.a[1] code with the SCALE-PC v4.4a[4], 238 group, ENDF-B/V cross-section library[2]. Detailed descriptions of these experiments are found in the OECD Handbook. A

[6] ANSI/ANS-8.1-1998, *Nuclear Criticality Safety in Operations with Fissionable Materials Outside Reactors*, American Nuclear Society (ANS), La Grange Park, Illinois.

[7] Oak Ridge National Laboratory (ORNL), *SCALE 5.1: Modular Code System for Performing Standardized Computer Analyses for Licensing Evaluation for Workstations and Personal Computers*, ORNL/TM-2005/39, SCALE Version 5.1, November 1, 2006.

[8] Bowman, S.M, *et al.*, *Scale Cross-Section Librarie*s, ORNL/TM-2005/39, Volume III, Section M4, November 2006.

summary of the experiment titles is provided in Table 6.5-1. The benchmark results were evaluated using the USLSTATS program as discussed in the next section.

A total of 82 experimental benchmarks with LEU in the thermal energy range were evaluated with the KENO-V.a[1] code with the SCALE-PC v4.4a[4], 238 group, ENDF-B/V cross-section library[2]. Detailed descriptions of these experiments are found in the OECD Handbook. A summary of the LEU benchmark experiment titles selected for this study is provided in Table 6.5-4. The benchmark results were evaluated using the USLSTATS program (Version 1.4, April 23, 2003), as discussed in the next section. The evaluated results for each benchmark case are shown in Table 6.5-5.

A total of 82 experimental benchmarks with LEU in the thermal energy range were evaluated with the KENO-V.a[4] code with the SCALE Version 5.1[7], 238 group, ENDF-B/V cross-section library[8]. Detailed descriptions of these experiments are found in the OECD Handbook. A summary of the LEU benchmark experiment titles selected for this study is provided in Table 6.5-4. The benchmark results were evaluated using the USLSTATS program (Version 1.4, April 23, 2003), as discussed in the next section. The evaluated results for each benchmark case are shown in Table 6.5-6.

To evaluate LEU and special reflector systems containing Beryllium, 31 experimental benchmark cases from U233-SOL-THERM-015 were added to the 82 LEU benchmark cases. These are the same cases described in Table 6.5-1. All were evaluated with the KENO-V.a code with the SCALE Version 5.1, 238 group, ENDF-B/V cross-section library. The evaluated results for each benchmark case are shown in Table 6.5-6.

6.5.3 Results of Benchmark Calculations

6.5.3.1 PU Benchmarks

Table 6.5-2 summarizes the trending parameter values, computed k_{eff} values, and uncertainties for each case. The uncertainty value, σ_c, assigned to each case is a combination of the benchmark uncertainty for each experiment, σ_{exp}, and the Monte Carlo uncertainty associated with the particular computational evaluation of the case, σ_{comp}, or:

$$\sigma_c = \sqrt{\sigma_{exp}^2 + \sigma_{comp}^2}$$

These values were input into the USLSTATS program in addition to the following parameters:

- P, proportion of population falling above lower tolerance level = 0.995
- $1-\gamma$, confidence on fit = 0.95
- α , confidence on proportion P = 0.95
- x_{min}, minimum value of AEG for which USL correlation are computed = N/A, minimum of supplied data used by code
- x_{max}, maximum value of AEG for which USL correlation are computed = N/A, maximum of supplied data used by code
- σ_{eff}, estimate in average standard deviation of all input values of k_{eff} = -1.0, use supplied values
- Δk_m, administrative margin used to ensure subcriticality = 0.05.

This data is followed by triplets of trending parameter value, computed k_{eff}, and uncertainty for each case. The USL Method 1 result was chosen which performs a confidence band analysis on the data for the trending parameter.

Three trending parameters are identified for determination of the bias. First, the AEG is used in order to characterize any code bias with respect to neutron spectral effects. The USL is calculated vs. AEG separately for the Pu experiments, ^{233}U experiments with beryllium and ^{233}U experiments without beryllium in addition to the combined results of the Pu and ^{233}U with beryllium experiments. Because the ^{233}U fissile isotope introduces a component that is not relative to the calculations performed for the RH-TRU 72-B and may have a distinct bias of its own, comparison of the USL for the ^{233}U experiments with beryllium to the USL for those without beryllium allows the effect of the beryllium reflector to be separated from the effect of the ^{233}U isotope. Next, the H/Pu ratio of each experimental case containing Pu is used in order to characterize the material and geometric properties of each sphere. Finally, since all the Pu experiments include ^{240}Pu to some extent and the RH-TRU 72-B models contain varying amount of ^{240}Pu, a trending analysis of the results of the Pu experiments with respect to $^{240}Pu/Pu$ ratio is performed. The ^{233}U results are not considered in the trending with respect to H/Pu as the optimum H/Pu range will be significantly different for a ^{233}U system vs. a Pu system. For obvious reasons, the ^{233}U results are also not considered in the trending with respect to the $^{240}Pu/Pu$ ratio.

The USLs calculated using USLSTATS Method 1 for the benchmark combinations discussed above are tabulated in Table 6.5-3. The USL calculated based on the combined results of the ^{233}U with beryllium and Pu experiments of 0.9382 is chosen as the USL for this analysis. This USL value is ~0.001 below that of the Pu experiments alone. The ^{233}U benchmarks without Be result in a lower USL (0.0032) than calculated from the ^{233}U benchmark results without beryllium. This difference is greater than the benchmark uncertainty of each benchmark case (~0.001). Both of the ^{233}U USL values are lower than the Pu experiment USL values indicating that the ^{233}U isotope in the experiments has a more significant effect on the USL than the beryllium. Thus, the USL based on the combined results of the ^{233}U with beryllium and Pu experiments chosen adequately accounts for any bias attributable to beryllium. In addition, the USLs calculated for the Pu experiments using either H/X or the $^{240}Pu/Pu$ ratio as the trending parameter do not differ significantly from the Pu USL vs. AEG and are bounded by the chosen USL value of 0.9382. USLSTATS calculated constant USL values with respect to H/Pu and $^{240}Pu/Pu$ ratio indicating no appreciable trend with respect to these parameters.

6.5.3.2 LEU and LEU with Be Benchmarks

Table 6.5-5 summarizes the computed k_{eff} values, trending parameter values, and uncertainties for each case. The uncertainty value, σ_c, assigned to each case is a combination of the benchmark uncertainty for each experiment, σ_{exp}, and the Monte Carlo uncertainty associated with the particular computational evaluation of the case, σ_{comp}, or:

$$\sigma_c = \sqrt{\sigma_{exp}^2 + \sigma_{comp}^2}$$

These values were input into the USLSTATS program in addition to the following parameters:

- P, proportion of population falling above lower tolerance level = 0.995

- $1-\gamma$, confidence on fit = 0.95
- α , confidence on proportion P = 0.95
- x_{min}, minimum value of AEG for which USL correlation are computed = N/A, minimum of supplied data used by code
- x_{max}, maximum value of AEG for which USL correlation are computed = N/A, maximum of supplied data used by code
- σ_{eff}, estimate in average standard deviation of all input values of k_{eff} = -1.0, use supplied values
- Δk_m, administrative margin used to ensure subcriticality = 0.05.

This data is followed by triplets of trending parameter value, computed k_{eff}, and uncertainty for each case. The USL Method 1 result was chosen which performs a confidence band analysis on the data for the trending parameter.

For the USL evaluation for the SCALE 4.4a code, three trending parameters are identified for determination of the bias. The data is trended against AEG, H/X, and ^{235}U enrichment to determine bias resulting from all of these parameters. The output values of USLSTATS, USL Method 1 are shown in Table 6.5-6 for comparison. Each value is calculated using the USL Method 1 for the region of interest as indicated by the footnotes. For the region of interest in this evaluation, the enrichment value of 0.96 wt% ^{235}U falls outside of the range of applicability of the benchmark experiments. However, since this value of enrichment is expected to always result in subcritical configurations for the region of interest in this analysis, the USL has been conservatively projected to the 0.96 wt% for comparison with the other USL results. As indicated in Table 6.5-6 the USL based on AEG is the most limiting and the value of 0.9257 will be used in this analysis as the USL for ^{235}U systems.

For the USL evaluation for the SCALE 5.1, two trending parameters are identified for determination of the bias for LEU systems. The data is trended against $H/^{235}U$ and ^{235}U enrichment to determine bias against the two major measured independent parameters. The USLSTATS results for trending against $H/^{235}U$ was $0.9329 + 8.9149E\text{-}6 \times H/^{235}U$ for $H/^{235}U < 1027.1$. This was higher than the USL result for ^{235}U enrichment of 0.9327 for 0.84 wt% ^{235}U and was not used. The output values of USLSTATS, USL Method 1 are shown in Table 6.5-7 for comparison. Each value is calculated using the USL Method 1 for the region of interest as indicated by the footnotes. For the region of interest in this evaluation, the enrichment value of LEU falls outside of the range of applicability of the benchmark experiments. However, since this value of enrichment is expected to always result in subcritical configurations for the region of interest in this analysis, the USL has been conservatively projected to the respective LEU enrichments for comparison with the other USL results. For the LEU and Be Benchmark case analysis EALF was used as an independent parameter since the cases lack any other similarity. USLSTATS , USL Method 1 for this set of benchmarks yielded an USL(EALF) = $0.9336 - 6.9580E\text{-}03 \times EALF$. As indicated in Table 6.5-6, the USL as a function of EALF will be used for Special Reflector Cases.

Table 6.5-1 – ^{239}Pu Benchmark Experiment Description

Series①	Title
PU-SOL-THERM-001	Water-reflected 11.5 inch diameter spheres of plutonium nitrate solutions
PU-SOL-THERM-002	Water-reflected 12 inch diameter spheres of plutonium nitrate solutions
PU-SOL-THERM-003	Water-reflected 13 inch diameter spheres of plutonium nitrate solutions
PU-SOL-THERM-004	Water-reflected 14 inch diameter spheres of plutonium nitrate solutions 0.54% to 3.43% Pu-240
PU-SOL-THERM-005	Water-reflected 14 inch diameter spheres of plutonium nitrate solutions 4.05% and 4.40% Pu-240
PU-SOL-THERM-006	Water-reflected 15 inch diameter spheres of plutonium nitrate solutions
PU-SOL-THERM-007	Water-reflected 11.5 inch diameter spheres partly filled with plutonium nitrate solutions
PU-SOL-THERM-009	Unreflected 48 inch-diameter sphere of plutonium nitrate solution
PU-SOL-THERM-010	Water-reflected 9-, 10-, 11-, and 12 inch-diameter cylinders of plutonium nitrate solutions
PU-SOL-THERM-011	Bare 16- and 18 inch-diameter spheres of plutonium nitrate solutions
PU-SOL-THERM-014	Interacting cylinders of 300-mm diameter with plutonium nitrate solution (115.1gPu/l) in air
PU-SOL-THERM-015	Interacting cylinders of 300-mm diameter with plutonium nitrate solution (152.5gPu/l) in air
PU-SOL-THERM-016	Interacting cylinders of 300-mm and 256-mm diameters with plutonium nitrate solution (152.5 and 115.1gPu/l) and nitric acid (2N) in air
PU-SOL-THERM-017	Interacting cylinders of 256-mm and 300-mm diameters with plutonium nitrate solution (115.1gPu/l) in air
PU-SOL-THERM-020	Water-reflected and water-cadmium reflected 14-inch diameter spheres of plutonium nitrate solutions
PU-SOL-THERM-021	Water-reflected and bare 15.2-inch-diameter spheres of plutonium nitrate solutions
PU-SOL-THERM-024	Slabs of plutonium nitrate solutions reflected by 1-inch-thick Plexiglas
U233-SOL-THERM-001	Unreflected spheres of 233U nitrate solutions
U233-SOL-THERM-003	Paraffin-reflected 5-, 5.4-, 6-, 6.6-, 7.5- 8-, 8.5-, 9- and 12-inch-diameter cylinders of 233U uranyl fluoride solutions
U233-SOL-THERM-015	Uranyl-fluoride (233U) solutions in spherical stainless steel vessels with reflectors of Be, CH2, and Be-CH2 composites

Notes:

① These benchmarks are found under the experimental series noted in the first column in the following reference: OECD Nuclear Energy Agency, *International Handbook of Evaluated Criticality Safety Benchmark Experiment*s, NEA/NSC/DOC(95)03, September 2002.

Table 6.5-2 – ^{239}Pu Benchmark Case Parameters and Computed Results

Case Name①	k_{eff}	σ_{comp}	AEG	H/X②	^{240}Pu/ Pu Ratio	Benchmark Uncertainty σ_{exp}③
PUST001_CASE_1	1.0080	0.0010	212.494	352.9	0.04650	0.0050
PUST001_CASE_2	1.0100	0.0010	209.961	258.1	0.04650	0.0050
PUST001_CASE_3	1.0133	0.0010	207.777	204.1	0.04650	0.0050
PUST001_CASE_4	1.0073	0.0010	206.439	181	0.04650	0.0050
PUST001_CASE_5	1.0111	0.0011	205.757	171.2	0.04650	0.0050
PUST001_CASE_6	1.0089	0.0010	195.766	86.7	0.04650	0.0050
PUST002_CASE_1	1.0074	0.0010	214.693	508	0.03110	0.0047
PUST002_CASE_2	1.0088	0.0011	214.457	489.2	0.03110	0.0047
PUST002_CASE_3	1.0074	0.0010	213.798	437.3	0.03110	0.0047
PUST002_CASE_4	1.0103	0.0010	213.343	407.5	0.03110	0.0047
PUST002_CASE_5	1.0125	0.0011	212.898	380.6	0.03110	0.0047
PUST002_CASE_6	1.0099	0.0010	211.974	333.5	0.03110	0.0047
PUST002_CASE_7	1.0101	0.0010	211.146	299.3	0.03110	0.0047
PUST003_CASE_1	1.0089	0.0010	216.630	774.1	0.01750	0.0047
PUST003_CASE_2	1.0076	0.0011	216.438	742.7	0.01750	0.0047
PUST003_CASE_3	1.0103	0.0010	216.055	677.2	0.03110	0.0047
PUST003_CASE_4	1.0094	0.0010	215.948	660.5	0.03110	0.0047
PUST003_CASE_5	1.0097	0.0010	215.535	607.2	0.03110	0.0047
PUST003_CASE_6	1.0099	0.0011	214.960	545.3	0.03110	0.0047
PUST003_CASE_7	1.0121	0.0009	216.482	714.8	0.03110	0.0047
PUST003_CASE_8	1.0091	0.0011	216.321	692.1	0.03110	0.0047
PUST004_CASE_1	1.0080	0.0010	217.470	981.7	0.00538	0.0047
PUST004_CASE_2	1.0032	0.0009	217.408	898.6	0.04180	0.0047
PUST004_CASE_3	1.0059	0.0008	217.241	864	0.04500	0.0047
PUST004_CASE_4	1.0033	0.0009	217.034	842	0.03260	0.0047
PUST004_CASE_5	1.0043	0.0010	217.257	780.2	0.03630	0.0047
PUST004_CASE_6	1.0074	0.0009	217.195	668	0.00495	0.0047
PUST004_CASE_7	1.0104	0.0010	217.030	573.3	0.00495	0.0047
PUST004_CASE_8	1.0040	0.0009	216.917	865	0.00504	0.0047
PUST004_CASE_9	1.0041	0.0009	216.580	872.2	0.01530	0.0047
PUST004_CASE_10	1.0078	0.0009	215.881	971.6	0.02510	0.0047

Case Name[1]	k_{eff}	σ_{comp}	AEG	H/X[2]	^{240}Pu/ Pu Ratio	Benchmark Uncertainty σ_{exp}[3]
PUST004_CASE_11	1.0041	0.0010	215.106	929.6	0.02330	0.0047
PUST004_CASE_12	1.0094	0.0009	217.031	884.1	0.03160	0.0047
PUST004_CASE_13	1.0042	0.0009	217.074	925.5	0.03350	0.0047
PUST005_CASE_1	1.0072	0.0010	217.069	866.4	0.04030	0.0047
PUST005_CASE_2	1.0084	0.0009	216.909	832.7	0.04030	0.0047
PUST005_CASE_3	1.0092	0.0009	216.749	800.7	0.04030	0.0047
PUST005_CASE_4	1.0091	0.0010	216.360	734.4	0.04030	0.0047
PUST005_CASE_5	1.0102	0.0010	215.906	666.1	0.04030	0.0047
PUST005_CASE_6	1.0112	0.0010	215.451	607.9	0.04030	0.0047
PUST005_CASE_7	1.0099	0.0010	215.004	557.2	0.04030	0.0047
PUST005_CASE_8	1.0024	0.0010	216.903	830.6	0.04030	0.0047
PUST005_CASE_9	1.0078	0.0010	216.687	788.9	0.04030	0.0047
PUST006_CASE_1	1.0059	0.0008	217.615	1028.2	0.03110	0.0035
PUST006_CASE_2	1.0079	0.0009	217.459	986.2	0.03110	0.0035
PUST006_CASE_3	1.0072	0.0010	217.147	910.9	0.03110	0.0035
PUST007_CASE_2	1.0090	0.0011	198.911	102.6	0.04570	0.0047
PUST007_CASE_3	1.0024	0.0010	199.553	110.11	0.04570	0.0047
PUST007_CASE_5	1.0099	0.0010	209.885	253.3	0.04570	0.0047
PUST007_CASE_6	1.0054	0.0011	209.689	247.3	0.04570	0.0047
PUST007_CASE_7	1.0072	0.0010	209.816	250.5	0.04570	0.0047
PUST007_CASE_8	1.0007	0.0012	209.577	246.5	0.04570	0.0047
PUST007_CASE_9	0.9996	0.0011	209.628	246.5	0.04570	0.0047
PUST007_CASE_10	1.0009	0.0011	210.426	275.5	0.04570	0.0047
PUST009_CASE_1	1.0202	0.0007	219.730	2579.3	0.02510	0.0033
PUST009_CASE_2	1.0242	0.0005	219.819	2706.5	0.02510	0.0033
PUST009_CASE_3	1.0232	0.0006	219.830	2729.8	0.02510	0.0033
PUST010_CASE_1.11	1.0158	0.0011	219.830	471.3	0.02840	0.0048
PUST010_CASE_1.12	1.0125	0.0009	214.122	527.7	0.02890	0.0048
PUST010_CASE_1.9	1.0183	0.0012	214.895	259.3	0.02840	0.0048
PUST010_CASE_2.11	1.0124	0.0011	210.075	542.3	0.02840	0.0048
PUST010_CASE_2.12	1.0136	0.0010	214.882	600.5	0.02890	0.0048
PUST010_CASE_2.9	1.0140	0.0011	215.514	346.8	0.02840	0.0048

Case Name[1]	k_{eff}	σ_{comp}	AEG	H/X[2]	^{240}Pu/ Pu Ratio	Benchmark Uncertainty σ_{exp}[3]
PUST010_CASE_3.11	1.0128	0.0011	212.361	542.3	0.02840	0.0048
PUST010_CASE_3.12	1.0208	0.0009	215.036	707	0.02890	0.0048
PUST010_CASE_3.9	1.0120	0.0010	216.250	470.4	0.02840	0.0048
PUST010_CASE_4.11	1.0055	0.0011	214.300	588.7	0.02840	0.0048
PUST010_CASE_4.12	1.0142	0.0009	215.366	825.1	0.02890	0.0048
PUST010_CASE_5.11	1.0068	0.0010	216.852	646.5	0.02840	0.0048
PUST010_CASE_6.11	1.0176	0.0012	215.739	402.3	0.02890	0.0048
PUST010_CASE_7.11	1.0065	0.0010	213.340	519.8	0.02890	0.0048
PUST011_CASE_1.16	1.0135	0.0010	214.790	733	0.04150	0.0052
PUST011_CASE_1.18	1.0001	0.0009	215.818	1157.3	0.04180	0.0052
PUST011_CASE_2.16	1.0196	0.0010	217.686	705.5	0.04150	0.0052
PUST011_CASE_2.18	1.0065	0.0011	215.633	1103.2	0.04180	0.0052
PUST011_CASE_3.16	1.0213	0.0010	217.509	662.8	0.04150	0.0052
PUST011_CASE_3.18	1.0027	0.0010	215.281	1109.8	0.04180	0.0052
PUST011_CASE_4.16	1.0139	0.0011	217.525	653.4	0.04150	0.0052
PUST011_CASE_4.18	0.9991	0.0011	215.196	1053.7	0.04180	0.0052
PUST011_CASE_5.16	1.0113	0.0010	217.313	550.7	0.04150	0.0052
PUST011_CASE_5.18	1.0099	0.0010	214.156	995.4	0.04180	0.0052
PUST011_CASE_6.18	1.0068	0.0010	217.071	870.4	0.04180	0.0052
PUST011_CASE_7.18	1.0050	0.0010	216.471	1056.4	0.04180	0.0052
PUST014_CASE_1	1.0068	0.0012	205.455	210.2	0.04230	0.0032
PUST014_CASE_3	1.0065	0.0010	205.477	210.2	0.04230	0.0032
PUST014_CASE_4	1.0079	0.0011	205.504	210.2	0.04230	0.0032
PUST014_CASE_5	1.0065	0.0011	205.510	210.2	0.04230	0.0032
PUST014_CASE_6	1.0073	0.0013	205.516	210.2	0.04230	0.0032
PUST014_CASE_7	1.0082	0.0012	205.434	210.2	0.04230	0.0043
PUST014_CASE_8	1.0051	0.0012	205.462	210.2	0.04230	0.0032
PUST014_CASE_9	1.0068	0.0012	205.477	210.2	0.04230	0.0032
PUST014_CASE_10	1.0060	0.0011	205.499	210.2	0.04230	0.0032
PUST014_CASE_11	1.0046	0.0010	205.526	210.2	0.04230	0.0032
PUST014_CASE_12	1.0076	0.0010	205.522	210.2	0.04230	0.0032
PUST014_CASE_13	1.0080	0.0011	205.420	210.2	0.04230	0.0043

Case Name[1]	k_{eff}	σ_{comp}	AEG	H/X[2]	^{240}Pu/ Pu Ratio	Benchmark Uncertainty σ_{exp}[3]
PUST014_CASE_14	1.0062	0.0011	205.458	210.2	0.04230	0.0043
PUST014_CASE_15	1.0067	0.0011	205.507	210.2	0.04230	0.0043
PUST014_CASE_16	1.0057	0.0011	205.512	210.2	0.04230	0.0043
PUST014_CASE_17	1.0033	0.0011	205.506	210.2	0.04230	0.0043
PUST014_CASE_18	1.0070	0.0011	205.430	210.2	0.04230	0.0043
PUST014_CASE_19	1.0045	0.0011	205.469	210.2	0.04230	0.0043
PUST014_CASE_20	1.0061	0.0011	205.487	210.2	0.04230	0.0043
PUST014_CASE_21	1.0066	0.0012	205.514	210.2	0.04230	0.0043
PUST014_CASE_22	1.0060	0.0012	205.527	210.2	0.04230	0.0043
PUST014_CASE_23	1.0048	0.0012	205.530	210.2	0.04230	0.0043
PUST014_CASE_24	1.0080	0.0012	205.393	210.2	0.04230	0.0043
PUST014_CASE_25	1.0042	0.0011	205.445	210.2	0.04230	0.0043
PUST014_CASE_26	1.0066	0.0011	205.490	210.2	0.04230	0.0043
PUST014_CASE_27	1.0044	0.0011	205.504	210.2	0.04230	0.0043
PUST014_CASE_28	1.0052	0.0011	205.534	210.2	0.04230	0.0043
PUST014_CASE_29	1.0050	0.0011	205.525	210.2	0.04230	0.0043
PUST014_CASE_30	1.0060	0.0010	205.416	210.2	0.04230	0.0043
PUST014_CASE_31	1.0046	0.0011	205.444	210.2	0.04230	0.0043
PUST014_CASE_33	1.0021	0.0011	205.446	210.2	0.04230	0.0043
PUST014_CASE_34	1.0045	0.0011	205.480	210.2	0.04230	0.0043
PUST015_CASE_1	1.0065	0.0010	201.243	155.3	0.04230	0.0038
PUST015_CASE_2	1.0069	0.0011	201.272	155.3	0.04230	0.0038
PUST015_CASE_3	1.0060	0.0011	201.289	155.3	0.04230	0.0038
PUST015_CASE_4	1.0056	0.0012	201.324	155.3	0.04230	0.0038
PUST015_CASE_5	1.0072	0.0011	201.311	155.3	0.04230	0.0038
PUST015_CASE_6	1.0078	0.0012	201.327	155.3	0.04230	0.0038
PUST015_CASE_7	1.0078	0.0011	201.209	155.3	0.04230	0.0047
PUST015_CASE_8	1.0056	0.0011	201.255	155.3	0.04230	0.0047
PUST015_CASE_9	1.0062	0.0012	201.292	155.3	0.04230	0.0047
PUST015_CASE_10	1.0060	0.0011	201.333	155.3	0.04230	0.0047
PUST015_CASE_11	1.0012	0.0010	201.196	155.3	0.04230	0.0047
PUST015_CASE_12	1.0053	0.0011	201.280	155.3	0.04230	0.0047

Case Name[1]	k_{eff}	σ_{comp}	AEG	H/X[2]	^{240}Pu/ Pu Ratio	Benchmark Uncertainty σ_{exp}[3]
PUST015_CASE_13	1.0084	0.0010	201.307	155.3	0.04230	0.0047
PUST015_CASE_14	1.0065	0.0012	201.335	155.3	0.04230	0.0047
PUST015_CASE_15	1.0082	0.0013	201.196	155.3	0.04230	0.0047
PUST015_CASE_16	1.0064	0.0010	201.222	155.3	0.04230	0.0047
PUST015_CASE_17	1.0067	0.0010	201.299	155.3	0.04230	0.0047
PUST016_CASE_1	1.0077	0.0011	201.225	155.3	0.04230	0.0043
PUST016_CASE_2	1.0048	0.0011	201.265	155.3	0.04230	0.0043
PUST016_CASE_3	1.0072	0.0011	201.295	155.3	0.04230	0.0043
PUST016_CASE_4	1.0075	0.0011	201.318	155.3	0.04230	0.0043
PUST016_CASE_5	1.0054	0.0012	205.463	210.2	0.04230	0.0038
PUST016_CASE_6	1.0047	0.0011	205.476	210.2	0.04230	0.0038
PUST016_CASE_7	1.0093	0.0013	205.511	210.2	0.04230	0.0038
PUST016_CASE_8	1.0072	0.0011	205.508	210.2	0.04230	0.0038
PUST016_CASE_9	1.0070	0.0012	205.607	210.2	0.04230	0.0033
PUST016_CASE_10	1.0065	0.0012	205.556	210.2	0.04230	0.0033
PUST016_CASE_11	1.0063	0.0011	205.516	210.2	0.04230	0.0033
PUST017_CASE_1	1.0076	0.0011	205.535	210.2	0.04230	0.0038
PUST017_CASE_2	1.0050	0.0011	205.488	210.2	0.04230	0.0038
PUST017_CASE_3	1.0041	0.0011	205.492	210.2	0.04230	0.0038
PUST017_CASE_4	1.0054	0.0012	205.482	210.2	0.04230	0.0038
PUST017_CASE_5	1.0066	0.0012	205.488	210.2	0.04230	0.0038
PUST017_CASE_6	1.0056	0.0011	205.479	210.2	0.04230	0.0038
PUST017_CASE_7	1.0069	0.0011	205.485	210.2	0.04230	0.0038
PUST017_CASE_8	1.0051	0.0011	205.497	210.2	0.04230	0.0038
PUST017_CASE_9	1.0071	0.0012	205.525	210.2	0.04230	0.0038
PUST017_CASE_10	1.0060	0.0011	205.500	210.2	0.04230	0.0038
PUST017_CASE_11	1.0050	0.0011	205.531	210.2	0.04230	0.0038
PUST017_CASE_12	1.0057	0.0011	205.509	210.2	0.04230	0.0038
PUST017_CASE_13	1.0047	0.0011	205.490	210.2	0.04230	0.0038
PUST017_CASE_14	1.0049	0.0013	205.487	210.2	0.04230	0.0038
PUST017_CASE_15	1.0072	0.0012	205.533	210.2	0.04230	0.0038
PUST017_CASE_16	1.0075	0.0010	205.522	210.2	0.04230	0.0038

Case Name[1]	k_{eff}	σ_{comp}	AEG	H/X[2]	^{240}Pu/ Pu Ratio	Benchmark Uncertainty σ_{exp}[3]
PUST017_CASE_17	1.0068	0.0012	205.519	210.2	0.04230	0.0038
PUST017_CASE_18	1.0056	0.0010	205.487	210.2	0.04230	0.0038
PUST020_CASE_1	1.0075	0.0010	215.482	596.5	0.04570	0.0059
PUST020_CASE_2	1.0117	0.0010	215.622	615.6	0.04570	0.0059
PUST020_CASE_3	1.0049	0.0009	216.499	743.8	0.04570	0.0059
PUST020_CASE_5	1.0074	0.0010	213.992	462.9	0.04570	0.0059
PUST020_CASE_6	1.0078	0.0009	213.637	450.5	0.04570	0.0059
PUST020_CASE_7	1.0022	0.0009	216.277	722.9	0.04570	0.0059
PUST020_CASE_8	1.0066	0.0011	210.650	341.1	0.04570	0.0059
PUST020_CASE_9	1.0004	0.0010	214.048	543.2	0.04570	0.0059
PUST021_CASE_7	1.0109	0.0011	215.405	662	0.04570	0.0032
PUST021_CASE_8	1.0044	0.0010	197.712	125	0.04570	0.0065
PUST021_CASE_9	1.0117	0.0010	215.136	634	0.04570	0.0032
PUST021_CASE_10	1.0123	0.0008	218.033	1107	0.04570	0.0025
PUST024_CASE_1	1.0018	0.0010	191.676	87.5	0.18400	0.0062
PUST024_CASE_2	0.9999	0.0009	191.828	87.5	0.18400	0.0062
PUST024_CASE_3	1.0002	0.0011	191.933	87.5	0.18400	0.0062
PUST024_CASE_4	1.0020	0.0010	192.026	87.5	0.18400	0.0062
PUST024_CASE_5	0.9986	0.0011	192.017	87.5	0.18400	0.0062
PUST024_CASE_6	0.9988	0.0009	173.477	44.9	0.18400	0.0077
PUST024_CASE_7	1.0072	0.0010	201.097	143.9	0.18400	0.0053
PUST024_CASE_8	1.0073	0.0010	201.200	143.9	0.18400	0.0053
PUST024_CASE_9	1.0068	0.0010	201.253	143.9	0.18400	0.0053
PUST024_CASE_10	1.0090	0.0010	201.353	143.9	0.18400	0.0053
PUST024_CASE_11	1.0065	0.0011	201.418	143.9	0.18400	0.0053
PUST024_CASE_12	1.0069	0.0010	201.452	143.9	0.18400	0.0053
PUST024_CASE_13	1.0066	0.0010	201.493	143.9	0.18400	0.0053
PUST024_CASE_14	1.0019	0.0011	197.708	115.8	0.23200	0.0053
PUST024_CASE_15	1.0033	0.0012	197.781	115.8	0.23200	0.0053
PUST024_CASE_16	1.0017	0.0009	197.845	115.8	0.23200	0.0053
PUST024_CASE_17	1.0026	0.0010	197.990	115.8	0.23200	0.0053
PUST024_CASE_18	1.0085	0.0010	212.039	367.3	0.18400	0.0051

Case Name[1]	k_{eff}	σ_{comp}	AEG	H/X[2]	^{240}Pu/ Pu Ratio	Benchmark Uncertainty σ_{exp}[3]
PUST024_CASE_19	1.0079	0.0009	212.057	367.3	0.18400	0.0051
PUST024_CASE_20	1.0100	0.0010	212.074	367.3	0.18400	0.0051
PUST024_CASE_21	1.0075	0.0010	212.106	367.3	0.18400	0.0051
PUST024_CASE_22	1.0054	0.0010	212.142	367.3	0.18400	0.0051
PUST024_CASE_23	1.0068	0.0011	212.166	367.3	0.18400	0.0051
233ST001CASE_1	0.9975	0.0008	218.415	1531.5	N/A	0.0031
233ST001CASE_2	0.9959	0.0008	218.224	1471.7	N/A	0.0033
233ST001CASE_3	0.9955	0.0007	218.055	1420.1	N/A	0.0033
233ST001CASE_4	0.9970	0.0007	217.875	1369.7	N/A	0.0033
233ST001CASE_5	0.9956	0.0008	217.697	1325.4	N/A	0.0033
233ST003CASE_40	1.0029	0.0011	192.780	74.1	N/A	0.0087
233ST003CASE_41	1.0164	0.0011	191.195	74.1	N/A	0.0151
233ST003CASE_42	1.0002	0.0013	191.824	74.1	N/A	0.0087
233ST003CASE_45	1.0040	0.0013	180.246	45.9	N/A	0.0126
233ST003CASE_55	1.0102	0.0011	176.271	39.4	N/A	0.0122
233ST003CASE_57	1.0196	0.0012	204.026	154	N/A	0.0087
233ST003CASE_58	1.0119	0.0012	209.393	250	N/A	0.0087
233ST003CASE_61	1.0056	0.0011	211.723	329	N/A	0.0087
233ST003CASE_62	1.0079	0.0012	213.031	396	N/A	0.0087
233ST003CASE_65	1.0039	0.0010	216.519	775	N/A	0.0087
233ST015_CASE_1	0.9928	0.0012	175.241	51.58	N/A	0.0075
233ST015_CASE_2	0.9869	0.0013	173.581	51.58	N/A	0.0070
233ST015_CASE_3	0.9863	0.0012	181.133	51.58	N/A	0.0068
233ST015_CASE_4	0.9863	0.0012	181.133	51.58	N/A	0.0041
233ST015_CASE_5	0.9844	0.0012	172.140	51.58	N/A	0.0055
233ST015_CASE_6	0.9750	0.0012	171.626	51.58	N/A	0.0099
233ST015_CASE_7	0.9807	0.0012	179.879	51.58	N/A	0.0070
233ST015_CASE_8	0.9719	0.0012	171.311	51.58	N/A	0.0067
233ST015_CASE_9	0.9664	0.0013	171.019	51.58	N/A	0.0050
233ST015_CASE_10	0.9841	0.0012	174.951	51.58	N/A	0.0051
233ST015_CASE_11	0.9937	0.0012	181.620	64.23	N/A	0.0075
233ST015_CASE_12	0.9942	0.0012	180.243	64.23	N/A	0.0069

Case Name①	k_{eff}	σ_{comp}	AEG	H/X②	^{240}Pu/ Pu Ratio	Benchmark Uncertainty σ_{exp}③
233ST015_CASE_13	0.9924	0.0011	179.562	64.23	N/A	0.0069
233ST015_CASE_14	0.9930	0.0011	187.157	64.23	N/A	0.0036
233ST015_CASE_15	0.9881	0.0012	178.911	64.23	N/A	0.0060
233ST015_CASE_16	0.9877	0.0013	178.599	64.23	N/A	0.0043
233ST015_CASE_17	0.9924	0.0012	186.084	64.23	N/A	0.0029
233ST015_CASE_18	0.9727	0.0014	178.045	64.23	N/A	0.0056
233ST015_CASE_19	0.9728	0.0012	177.964	64.23	N/A	0.0052
233ST015_CASE_20	0.9969	0.0011	193.458	102.54	N/A	0.0079
233ST015_CASE_21	0.9992	0.0012	192.290	102.54	N/A	0.0070
233ST015_CASE_22	0.9966	0.0011	191.669	102.54	N/A	0.0062
233ST015_CASE_23	0.9949	0.0011	191.140	102.54	N/A	0.0055
233ST015_CASE_24	0.9901	0.0013	190.850	102.54	N/A	0.0051
233ST015_CASE_25	0.9917	0.0012	196.919	102.54	N/A	0.0023
233ST015_CASE_26	0.9964	0.0011	204.143	199.4	N/A	0.0066
233ST015_CASE_27	0.9982	0.0011	203.709	199.4	N/A	0.0063
233ST015_CASE_28	0.9948	0.0010	203.459	199.4	N/A	0.0058
233ST015_CASE_29	0.9928	0.0012	203.220	199.4	N/A	0.0051
233ST015_CASE_30	0.9940	0.0011	203.118	199.4	N/A	0.0048
233ST015_CASE_31	0.9946	0.0012	203.041	199.4	N/A	0.0055

Notes:

① All cases were run with 1,000 neutrons per generation for 1,000 generations, with the initial 50 generations skipped.

② X refers to Pu or ^{233}U as applicable for the benchmark cases.

③ The *International Handbook of Evaluated Criticality Safety Benchmark Experiment*s provides a benchmark uncertainty for each case approved for a benchmark. This uncertainty is based on evaluation of the effects of various errors and model simplifications on the calculated k_{eff} of the individual experiment.

Table 6.5-3 – Calculation of Pu-239 USL with Be

Benchmark Set	Number of Cases	USL vs. AEG	USL vs. H/X	USL vs. ^{240}Pu/Pu
^{233}U without Be	15	0.9270	N/A	N/A
^{233}U with Be	31	0.9302 (204.14)①	N/A	N/A
Pu	196	0.9395	0.9393	0.9395
Pu + ^{233}U with Be	227	**0.9382**②	N/A	N/A

Notes:

① This value is calculated at an AEG of 204.14. USL increases with AEG such that this is conservative for the AEG of the calculations (~217).

② Range of applicability is 195.928 < AEG < 219.83.

Table 6.5-4 – Low Enriched U-235 Benchmark Experiment Description

Series①	Title
LEU-SOL-THERM-003	Full and Truncated Bare Spheres of 10% Enriched Uranyl Nitrate Water Solutions
LEU-SOL-THERM-004	STACY: Water-Reflected 10% Enriched Uranyl Nitrate Solution in a 60-cm Diameter Cylindrical Tank
LEU-COMP-THERM-006	Critical Arrays of Low Enriched UO_2 Fuel Rods with Water-to-Fuel Volume Ratios Ranging from 1.5 to 3.0
LEU-COMP-THERM-010	Critical Arrays of Water-Moderated U(4.31)O_2 Fuel Rods Reflected by Two Lead, Uranium, or Steel Walls
LEU-COMP-THERM-049	Maracas Program: Polythene Reflected Critical Configurations with Low Enriched and Low Moderated Uranium Dioxide Powder U(5)O_2

Notes:

① These benchmarks are found under the experimental series noted in the first column in the following reference: OECD Nuclear Energy Agency, *International Handbook of Evaluated Criticality Safety Benchmark Experiment*s, NEA/NSC/DOC(95)03, September 2002.

Table 6.5-5 – Low Enriched U-235 Benchmark Case Parameters, Computed Results and Reported Experimental Benchmark Uncertainty

Case Name	k_{eff}	σ_{comp}	AEG	H/X[1]	Enrichment (wt% ^{235}U)	Benchmark Uncertainty σ_{exp}[2]
LST03C1M238.OUT	1.0007	0.0019	218.0	770	10.07	0.0039
LST03C2M238.OUT	1.0000	0.0016	218.5	878	10.07	0.0042
LST03C3M238.OUT	1.0009	0.0018	218.6	897	10.07	0.0042
LST03C4M238.OUT	0.9955	0.0015	218.7	913	10.07	0.0042
LST03C5M238.OUT	0.9971	0.0014	219.5	1173	10.07	0.0048
LST03C6M238.OUT	0.9995	0.0015	219.6	1213	10.07	0.0049
LST03C7M238.OUT	0.9984	0.0013	219.6	1240	10.07	0.0049
LST03C8M238.OUT	1.0018	0.0012	220.0	1412	10.07	0.0052
LST03C9M238.OUT	0.9994	0.0011	220.0	1438	10.07	0.0052
STACYC01M238.OUT	1.0052	0.0020	217.8	719	9.97	0.0008
STACYC29M238.OUT	1.0059	0.0019	218.1	771	9.97	0.0009
STACYC33M238.OUT	0.9993	0.0015	218.4	842	9.97	0.0009
STACYC34M238.OUT	1.0033	0.0018	218.7	896	9.97	0.0010
STACYC46M238.OUT	1.0038	0.0017	218.8	942	9.97	0.0010
STACYC51M238.OUT	1.0007	0.0015	219.0	983	9.97	0.0011
STACYC54M238.OUT	1.0021	0.0013	219.1	1018	9.97	0.0011
LCT006.OUT - case1	0.9920	0.0008	198.0	167	2.596	0.0020
LCT006.OUT – case 2	0.9927	0.0009	197.8	167	2.596	0.0020
LCT006.OUT – case 3	0.9927	0.0009	197.3	167	2.596	0.0020
LCT006.OUT – case 4	0.9933	0.0008	201.2	203	2.596	0.0020
LCT006.OUT – case 5	0.9934	0.0008	200.9	203	2.596	0.0020
LCT006.OUT – case 6	0.9948	0.0010	200.6	203	2.596	0.0020
LCT006.OUT – case 7	0.9939	0.0009	200.2	203	2.596	0.0020
LCT006.OUT – case 8	0.9927	0.0007	199.9	203	2.596	0.0020
LCT006.OUT – case 9	0.9942	0.0009	204.9	276	2.596	0.0020
LCT006.OUT – case 10	0.9956	0.0009	204.5	276	2.596	0.0020
LCT006.OUT – case 11	0.9938	0.0008	204.2	276	2.596	0.0020
LCT006.OUT – case 12	0.9955	0.0010	204.0	276	2.596	0.0020
LCT006.OUT – case 13	0.9954	0.0008	203.6	276	2.596	0.0020

Case Name	k_{eff}	σ_{comp}	AEG	H/X[1]	Enrichment (wt% ^{235}U)	Benchmark Uncertainty σ_{exp}[2]
LCT006.OUT – case 14	0.9942	0.0009	206.9	333	2.596	0.0020
LCT006.OUT – case 15	0.9952	0.0009	206.6	333	2.596	0.0020
LCT006.OUT – case 16	0.9957	0.0009	206.4	333	2.596	0.0020
LCT006.OUT – case 17	0.9956	0.0008	206.1	333	2.596	0.0020
LCT006.OUT – case 18	0.9942	0.0008	205.8	333	2.596	0.0020
LEUCT010-01.OUT	1.0068	0.0009	206.8	N/A	4.31	0.0021
LEUCT010-02.OUT	1.0056	0.0008	207.2	N/A	4.31	0.0021
LEUCT010-03.OUT	1.0054	0.0009	207.4	N/A	4.31	0.0021
LEUCT010-04.OUT	0.9931	0.0009	207.7	N/A	4.31	0.0021
LEUCT010-05.OUT	0.9948	0.0008	193.5	N/A	4.31	0.0021
LEUCT010-06.OUT	0.9956	0.0008	197.3	N/A	4.31	0.0021
LEUCT010-07.OUT	0.9976	0.0009	200.1	N/A	4.31	0.0021
LEUCT010-08.OUT	0.9915	0.0009	201.5	N/A	4.31	0.0021
LEUCT010-09.OUT	0.9999	0.0010	206.5	N/A	4.31	0.0021
LEUCT010-10.OUT	1.0006	0.0009	206.9	N/A	4.31	0.0021
LEUCT010-11.OUT	0.9995	0.0008	207.2	N/A	4.31	0.0021
LEUCT010-12.OUT	0.9977	0.0009	207.5	N/A	4.31	0.0021
LEUCT010-13.OUT	0.9903	0.0009	207.7	N/A	4.31	0.0021
LEUCT010-14.OUT	0.9963	0.0010	194.9	N/A	4.31	0.0028
LEUCT010-15.OUT	0.9948	0.0009	195.4	N/A	4.31	0.0028
LEUCT010-16.OUT	0.9960	0.0008	195.8	N/A	4.31	0.0028
LEUCT010-17.OUT	0.9965	0.0009	196.1	N/A	4.31	0.0028
LEUCT010-18.OUT	0.9948	0.0009	196.3	N/A	4.31	0.0028
LEUCT010-19.OUT	0.9955	0.0008	196.7	N/A	4.31	0.0028
LEUCT010-20.OUT	0.9987	0.0009	195.4	N/A	4.31	0.0028
LEUCT010-21.OUT	0.9977	0.0009	195.8	N/A	4.31	0.0028
LEUCT010-22.OUT	0.9964	0.0008	196.4	N/A	4.31	0.0028
LEUCT010-23.OUT	0.9956	0.0009	196.7	N/A	4.31	0.0028
LEUCT010-24.OUT	0.9898	0.0010	186.6	N/A	4.31	0.0028
LEUCT010-25.OUT	0.9930	0.0009	187.7	N/A	4.31	0.0028
LEUCT010-26.OUT	0.9942	0.0009	188.6	N/A	4.31	0.0028
LEUCT010-27.OUT	0.9943	0.0010	189.5	N/A	4.31	0.0028

Case Name	k_{eff}	σ_{comp}	AEG	H/X①	Enrichment (wt% ^{235}U)	Benchmark Uncertainty σ_{exp}②
LEUCT010-28.OUT	0.9956	0.0010	190.4	N/A	4.31	0.0028
LEUCT010-29.OUT	0.9942	0.0011	191.1	N/A	4.31	0.0028
LEUCT010-30.OUT	0.9920	0.0010	192.8	N/A	4.31	0.0028
LEUCT049-01.OUT	0.9907	0.0009	169.7	40	5	0.0034
LEUCT049-02.OUT	0.9923	0.0008	169.7	40	5	0.0034
LEUCT049-03.OUT	0.9899	0.0009	168.9	40	5	0.0034
LEUCT049-04.OUT	0.9940	0.0008	168.7	40	5	0.0034
LEUCT049-05.OUT	0.9904	0.0008	177.2	50	5	0.0042
LEUCT049-06.OUT	0.9904	0.0009	177.1	50	5	0.0042
LEUCT049-07.OUT	0.9899	0.0009	177.6	50	5	0.0042
LEUCT049-08.OUT	0.9909	0.0008	176.6	50	5	0.0042
LEUCT049-09.OUT	0.9895	0.0009	182.8	60	5	0.0037
LEUCT049-10.OUT	0.9920	0.0009	182.7	60	5	0.0037
LEUCT049-11.OUT	0.9904	0.0009	182.8	60	5	0.0037
LEUCT049-12.OUT	0.9911	0.0009	182.0	60	5	0.0037
LEUCT049-13.OUT	0.9910	0.0009	174.5	N/A	5	0.0037
LEUCT049-14.OUT	0.9905	0.0011	174.5	N/A	5	0.0037
LEUCT049-15.OUT	0.9931	0.0009	174.4	N/A	5	0.0037
LEUCT049-16.OUT	0.9909	0.0010	177.6	N/A	5	0.0037
LEUCT049-17.OUT	0.9907	0.0008	176.7	N/A	5	0.0037
LEUCT049-18.OUT	0.9934	0.0008	178.8	N/A	5	0.0030

Notes:

① X refers to ^{235}U for the benchmark cases in this study. Where sufficient data was available, the effective H/^{235}U was calculated for the heterogeneous system of closely spaced uranium oxide rods and water moderator.

② The *International Handbook of Evaluated Criticality Safety Benchmark Experiment*s provides an benchmark uncertainty for each case approved for a benchmark. This uncertainty is based on evaluation of the effects of various errors and model simplifications on the calculated k_{eff} of the individual experiment.

Table 6.5-6 – SCALE 5.1 LEU and Be Benchmark Case Parameters, Computed Results and Reported Experimental Benchmark Uncertainty

Case Name	k_{eff}	σ_{comp}	EALF	H/X[1]	Enrichment (wt% ^{235}U)	Benchmark Uncertainty σ_{exp}[2]
LST03C1M238.OUT	0.9957	0.0020	0.04055	770	10.07	0.0039
LST03C2M238.OUT	0.9971	0.0017	0.03869	878	10.07	0.0042
LST03C3M238.OUT	1.0001	0.0016	0.03835	897	10.07	0.0042
LST03C4M238.OUT	0.9922	0.0015	0.03823	913	10.07	0.0042
LST03C5M238.OUT	0.9974	0.0017	0.03552	1173	10.07	0.0048
LST03C6M238.OUT	0.9985	0.0012	0.03522	1213	10.07	0.0049
LST03C7M238.OUT	0.9975	0.0014	0.03502	1240	10.07	0.0049
LST03C8M238.OUT	1.0031	0.0013	0.03401	1412	10.07	0.0052
LST03C9M238.OUT	0.9993	0.0017	0.03385	1438	10.07	0.0052
STACYC01M238.OUT	1.0009	0.0021	0.04128	719	9.97	0.0008
STACYC29M238.OUT	1.0023	0.0020	0.04029	771	9.97	0.0009
STACYC33M238.OUT	1.0032	0.0020	0.03905	842	9.97	0.0009
STACYC34M238.OUT	1.0050	0.0015	0.03831	896	9.97	0.0010
STACYC46M238.OUT	1.0029	0.0013	0.03771	942	9.97	0.0010
STACYC51M238.OUT	1.0004	0.0014	0.03725	983	9.97	0.0011
STACYC54M238.OUT	1.0058	0.0014	0.03686	1018	9.97	0.0011
LCT006.OUT - case1	0.9908	0.0009	0.24723	167	2.596	0.0020
LCT006.OUT – case 2	0.9930	0.0009	0.25508	167	2.596	0.0020
LCT006.OUT – case 3	0.9913	0.0009	0.26221	167	2.596	0.0020
LCT006.OUT – case 4	0.9928	0.0009	0.18901	203	2.596	0.0020
LCT006.OUT – case 5	0.9929	0.0008	0.19543	203	2.596	0.0020
LCT006.OUT – case 6	0.9932	0.0009	0.20050	203	2.596	0.0020
LCT006.OUT – case 7	0.9926	0.0008	0.20707	203	2.596	0.0020
LCT006.OUT – case 8	0.9931	0.0008	0.21238	203	2.596	0.0020
LCT006.OUT – case 9	0.9933	0.0009	0.14044	276	2.596	0.0020
LCT006.OUT – case 10	0.9941	0.0008	0.14430	276	2.596	0.0020
LCT006.OUT – case 11	0.9945	0.0008	0.14716	276	2.596	0.0020
LCT006.OUT – case 12	0.9948	0.0008	0.15134	276	2.596	0.0020
LCT006.OUT – case 13	0.9924	0.0008	0.15455	276	2.596	0.0020

Case Name	k_{eff}	σ_{comp}	EALF	H/X[1]	Enrichment (wt% ^{235}U)	Benchmark Uncertainty σ_{exp}[2]
LCT006.OUT – case 14	0.9960	0.0009	0.11829	333	2.596	0.0020
LCT006.OUT – case 15	0.9963	0.0010	0.12061	333	2.596	0.0020
LCT006.OUT – case 16	0.9941	0.0009	0.12316	333	2.596	0.0020
LCT006.OUT – case 17	0.9960	0.0008	0.12662	333	2.596	0.0020
LCT006.OUT – case 18	0.9960	0.0009	0.12896	333	2.596	0.0020
LEUCT010-01.OUT	1.0066	0.0009	0.12068	N/A	4.31	0.0021
LEUCT010-02.OUT	1.0055	0.0008	0.11786	N/A	4.31	0.0021
LEUCT010-03.OUT	1.0054	0.0009	0.11547	N/A	4.31	0.0021
LEUCT010-04.OUT	0.9917	0.0009	0.11293	N/A	4.31	0.0021
LEUCT010-05.OUT	0.9953	0.0009	0.38765	N/A	4.31	0.0021
LEUCT010-06.OUT	0.9941	0.0008	0.28067	N/A	4.31	0.0021
LEUCT010-07.OUT	0.9993	0.0009	0.21706	N/A	4.31	0.0021
LEUCT010-08.OUT	0.9930	0.0011	0.19248	N/A	4.31	0.0021
LEUCT010-09.OUT	1.0010	0.0009	0.12476	N/A	4.31	0.0021
LEUCT010-10.OUT	0.9998	0.0008	0.12108	N/A	4.31	0.0021
LEUCT010-11.OUT	0.9993	0.0008	0.11794	N/A	4.31	0.0021
LEUCT010-12.OUT	0.9964	0.0008	0.11497	N/A	4.31	0.0021
LEUCT010-13.OUT	0.9937	0.0009	0.11271	N/A	4.31	0.0021
LEUCT010-14.OUT	0.9960	0.0009	0.32197	N/A	4.31	0.0028
LEUCT010-15.OUT	0.9972	0.0008	0.30959	N/A	4.31	0.0028
LEUCT010-16.OUT	0.9969	0.0009	0.29875	N/A	4.31	0.0028
LEUCT010-17.OUT	0.9959	0.0008	0.29203	N/A	4.31	0.0028
LEUCT010-18.OUT	0.9945	0.0008	0.28809	N/A	4.31	0.0028
LEUCT010-19.OUT	0.9946	0.0009	0.28052	N/A	4.31	0.0028
LEUCT010-20.OUT	0.9976	0.0008	0.30861	N/A	4.31	0.0028
LEUCT010-21.OUT	0.9968	0.0010	0.29763	N/A	4.31	0.0028
LEUCT010-22.OUT	0.9959	0.0008	0.28616	N/A	4.31	0.0028
LEUCT010-23.OUT	0.9948	0.0008	0.27870	N/A	4.31	0.0028
LEUCT010-24.OUT	0.9912	0.0009	0.65498	N/A	4.31	0.0028
LEUCT010-25.OUT	0.9938	0.0009	0.60105	N/A	4.31	0.0028
LEUCT010-26.OUT	0.9950	0.0009	0.55522	N/A	4.31	0.0028
LEUCT010-27.OUT	0.9937	0.0009	0.52011	N/A	4.31	0.0028

Case Name	k_{eff}	σ_{comp}	EALF	H/X[1]	Enrichment (wt% ^{235}U)	Benchmark Uncertainty σ_{exp}[2]
LEUCT010-28.OUT	0.9949	0.0009	0.48467	N/A	4.31	0.0028
LEUCT010-29.OUT	0.9955	0.0010	0.45678	N/A	4.31	0.0028
LEUCT010-30.OUT	0.9915	0.0009	0.39141	N/A	4.31	0.0028
LEUCT049-01.OUT	0.9923	0.0017	2.20344	40	5	0.0034
LEUCT049-02.OUT	0.9912	0.0017	2.15652	40	5	0.0034
LEUCT049-03.OUT	0.9908	0.0023	2.35193	40	5	0.0034
LEUCT049-04.OUT	0.9942	0.0017	2.36537	40	5	0.0034
LEUCT049-05.OUT	0.9890	0.0019	1.23542	50	5	0.0042
LEUCT049-06.OUT	0.9932	0.0018	1.23437	50	5	0.0042
LEUCT049-07.OUT	0.9879	0.0018	1.19230	50	5	0.0042
LEUCT049-08.OUT	0.9889	0.0019	1.30111	50	5	0.0042
LEUCT049-09.OUT	0.9872	0.0021	0.79437	60	5	0.0037
LEUCT049-10.OUT	0.9894	0.0020	0.79853	60	5	0.0037
LEUCT049-11.OUT	0.9888	0.0022	0.79367	60	5	0.0037
LEUCT049-12.OUT	0.9895	0.0018	0.83723	60	5	0.0037
LEUCT049-13.OUT	0.9861	0.0020	1.53864	N/A	5	0.0037
LEUCT049-14.OUT	0.9912	0.0022	1.54278	N/A	5	0.0037
LEUCT049-15.OUT	0.9921	0.0017	1.53244	N/A	5	0.0037
LEUCT049-16.OUT	0.9892	0.0019	1.18053	N/A	5	0.0037
LEUCT049-17.OUT	0.9905	0.0017	1.28257	N/A	5	0.0037
LEUCT049-18.OUT	0.9932	0.0017	1.09806	N/A	5	0.0030
233ST015_CASE_1	0.9893	0.0011	1.04878	51.58	N/A	0.0075
233ST015_CASE_2	0.9847	0.0011	1.17889	51.58	N/A	0.0070
233ST015_CASE_3	0.9841	0.0011	0.68737	51.58	N/A	0.0068
233ST015_CASE_4	0.9841	0.0011	0.68737	51.58	N/A	0.0041
233ST015_CASE_5	0.9843	0.0011	1.30566	51.58	N/A	0.0055
233ST015_CASE_6	0.9750	0.0011	1.35444	51.58	N/A	0.0099
233ST015_CASE_7	0.9806	0.0011	0.75641	51.58	N/A	0.0070
233ST015_CASE_8	0.9701	0.0011	1.39326	51.58	N/A	0.0067
233ST015_CASE_9	0.9627	0.0015	1.43335	51.58	N/A	0.0050
233ST015_CASE_10	0.9844	0.0012	1.07786	51.58	N/A	0.0051
233ST015_CASE_11	0.9940	0.0012	0.65825	64.23	N/A	0.0075

Case Name	k_{eff}	σ_{comp}	EALF	H/X①	Enrichment (wt% ^{235}U)	Benchmark Uncertainty σ_{exp}②
233ST015_CASE_12	0.9922	0.0013	0.72719	64.23	N/A	0.0069
233ST015_CASE_13	0.9906	0.0010	0.76494	64.23	N/A	0.0069
233ST015_CASE_14	0.9943	0.0011	0.44144	64.23	N/A	0.0036
233ST015_CASE_15	0.9862	0.0013	0.80544	64.23	N/A	0.0060
233ST015_CASE_16	0.9852	0.0011	0.82739	64.23	N/A	0.0043
233ST015_CASE_17	0.9921	0.0011	0.47975	64.23	N/A	0.0029
233ST015_CASE_18	0.9715	0.0012	0.85718	64.23	N/A	0.0056
233ST015_CASE_19	0.9716	0.0012	0.86943	64.23	N/A	0.0052
233ST015_CASE_20	0.9930	0.0011	0.27692	102.54	N/A	0.0079
233ST015_CASE_21	0.9937	0.0012	0.30231	102.54	N/A	0.0070
233ST015_CASE_22	0.9936	0.0011	0.31679	102.54	N/A	0.0062
233ST015_CASE_23	0.9927	0.0011	0.32845	102.54	N/A	0.0055
233ST015_CASE_24	0.9864	0.0012	0.33649	102.54	N/A	0.0051
233ST015_CASE_25	0.9909	0.0011	0.21415	102.54	N/A	0.0023
233ST015_CASE_26	0.9895	0.0010	0.12274	199.4	N/A	0.0066
233ST015_CASE_27	0.9944	0.0012	0.12684	199.4	N/A	0.0063
233ST015_CASE_28	0.9931	0.0010	0.12904	199.4	N/A	0.0058
233ST015_CASE_29	0.9915	0.0012	0.13098	199.4	N/A	0.0051
233ST015_CASE_30	0.9907	0.0011	0.13223	199.4	N/A	0.0048
233ST015_CASE_31	0.9882	0.0011	0.13343	199.4	N/A	0.0055

Notes:

① X refers to ^{235}U for the benchmark cases in this study. Where sufficient data was available, the effective H/^{235}U was calculated for the heterogeneous system of closely spaced uranium oxide rods and water moderator.

② The *International Handbook of Evaluated Criticality Safety Benchmark Experiment*s provides an benchmark uncertainty for each case approved for a benchmark. This uncertainty is based on evaluation of the effects of various errors and model simplifications on the calculated k_{eff} of the individual experiment.

Table 6.5-7 – Calculation of Low Enriched U-235 USL

SCALE 4.4a Benchmark Set	Number of Cases	USL vs. AEG	USL vs. H/X	USL vs. ^{235}U Enrichment
^{235}U	82 (46)①	0.9339②	0.9393③	0.9353④
^{235}U + ^{233}U w/ Be	113	**0.9257**⑤	N/A	N/A
SCALE 5.1 Benchmark Set	**Number of Cases**	**USL vs. EALF**	**USL vs. H/X**	**USL vs. ^{235}U Enrichment**
^{235}U	82 (46)①	N/A	Not Used⑥	0.9327
^{235}U + ^{233}U w/ Be	113	0.9336 – 6.9580E-03 × EALF	N/A	N/A

Notes:

① Calculated H/^{235}U values were provided for only 46 of the cases. The remaining cases consisted of heterogeneous solid fuel rod arrays.

② USL increases with AEG. Calculated benchmark AEGs ranged from 168.7 to 220.0. Range of applicability for this USL is 168.7 ≤ AEG ≤ 220 based on the USL at AEG = 168.7.

③ USL increases with H/^{235}U. Benchmark H/^{235}Us ranged from 40 to 1438. Range of applicability for this USL is 300 ≤ H/^{235}U ≤ 1438 based on the USL at H/^{235}U = 300.

④ USL increases with ^{235}U Enrichment. Benchmark enrichments ranged from 2.6 to 10.1 wt% ^{235}U. There are no benchmark experiments that extend enrichment to 0.96 wt% ^{235}U and based on ANSI/ANS, at and below this enrichment any aqueous, water-reflected systems are always subcritical. Consequently, evaluations of systems at 0.96 wt% ^{235}U will technically, by definition, fall outside the range of applicability of the USL. This USL is based on projections of the USL provided by USLSTATS method 1 equation to an enrichment of 0.96 wt% ^{235}U (which is conservatively lower than the value at 2.6 wt% ^{235}U). Range of applicability for this USL is 0.96 ≤ ^{235}U enrichment ≤ 10.1 based on the projected USL at ^{235}U enrichment of 0.96 wt% ^{235}U.

⑤ USL increases with AEG. Calculated benchmark AEGs ranged from 168.7 to 220.0. Range of applicability for this USL is 168.7 ≤ AEG ≤ 220 based on the USL at AEG = 168.7.

⑥ The USL for the SCALE 5.1 Validation using H/^{235}U yielded a USL that was higher than that for the enrichment in this region and was not used.

6.6 Appendices

6.6.1 *KENO-V.a Input Files for the Criticality Analyses*

This page intentionally left blank.

6.6.1 KENO-V.a Input Files for the Criticality Analyses

The following is a listing of the most reactive Case A, B, C, D, and E criticality analysis input decks.

6.6.1.1 Case A – NPWBPWBTOPSIDE

```
#CSAS25   PARM=SIZE=2000000
Case A, 6.4-1,25%P/74%W/1%Be/315gPU-TOP-SID;25%P/74%W/1%Be-REFL;H/Pu=700
238GROUPNDF5
INFHOMMEDIUM
ARBMPUHP 1.0252 5 0 0 1 1001  11.2795  4309  1.801
6012  19.234  8016  63.8629  94239  3.8226 1 1.0 293 END
BEBOUND   2  DEN=1.8500                          0.01  293 END
H2O           2 DEN=0.9982                          0.74  293 END
POLY(H2O) 2 DEN=0.9230                          0.25  293 END
SS304         4                                       1.0 293 END
H2O       5 DEN=0.9982                          1.0 293 END
PB      6                                             1.0  293 END
END COMPOSITION
Case A, 6.4-1,25%P/74%W/1%Be/315gPU-TOP-SID;25%P/74%W/1%Be-REFL;H/Pu=700
READ PARAMETERS  GEN=1000  NPG=1000  NSK=50  TBA=5 END PARAMETERS
READ GEOMETRY
UNIT 1
COM='PU SPHERE'
SPHERE    1  1     12.4268  ORIGIN  0 0 0
GLOBAL UNIT 10
COM='RU-TRU 72-B PACKAGE W/ PU SPHERE'
CYLINDER  2  1    39.6875   2P154.31
HOLE 1    0.0  27.26   141.88
CYLINDER  4  1    43.18   2P154.31
CYLINDER  6  1    47.9425   2P154.31
CYLINDER  4  1    52.07   2P154.31
CYLINDER  4  1    52.07   187.33    -170.82
CYLINDER  5  1    82.57   217.83    -201.32
END GEOMETRY
END DATA
END
#CSAS25   PARM=SIZE=2000000
Case A, 6.4-1,25%P/74%W/1%Be/315gPU-TOP-SID;25%P/74%W/1%Be-REFL;H/Pu=800
238GROUPNDF5
INFHOMMEDIUM
ARBMPUHP 1.0205 5 0 0 1 1001  11.3336  4309  1.8097
6012  19.3264  8016  64.1695  94239  3.3608 1 1.0 293 END
BEBOUND   2  DEN=1.8500                          0.01  293 END
H2O           2 DEN=0.9982                          0.74  293 END
POLY(H2O) 2 DEN=0.9230                          0.25  293 END
SS304         4                                       1.0 293 END
H2O       5 DEN=0.9982                          1.0 293 END
PB      6                                             1.0  293 END
END COMPOSITION
Case A, 6.4-1,25%P/74%W/1%Be/315gPU-TOP-SID;25%P/74%W/1%Be-REFL;H/Pu=800
READ PARAMETERS  GEN=1000  NPG=1000  NSK=50  TBA=5 END PARAMETERS
READ GEOMETRY
UNIT 1
COM='PU SPHERE'
SPHERE    1  1     12.9914  ORIGIN  0 0 0
GLOBAL UNIT 10
COM='RU-TRU 72-B PACKAGE W/ PU SPHERE'
CYLINDER  2  1    39.6875   2P154.31
HOLE 1    0.0  26.69   141.31
CYLINDER  4  1    43.18   2P154.31
CYLINDER  6  1    47.9425   2P154.31
CYLINDER  4  1    52.07   2P154.31
CYLINDER  4  1    52.07   187.33    -170.82
CYLINDER  5  1    82.57   217.83    -201.32
END GEOMETRY
END DATA
END
#CSAS25   PARM=SIZE=2000000
Case A, 6.4-1,25%P/74%W/1%Be/315gPU-TOP-SID;25%P/74%W/1%Be-REFL;H/Pu=900
238GROUPNDF5
INFHOMMEDIUM
ARBMPUHP 1.0169 5 0 0 1 1001  11.3761  4309  1.8165
```

```
6012  19.3988  8016  64.41  94239  2.9986 1 1.0 293 END
BEBOUND   2  DEN=1.8500                          0.01  293 END
H2O            2 DEN=0.9982                          0.74  293 END
POLY(H2O) 2 DEN=0.9230                          0.25  293 END
SS304          4                                      1.0 293 END
H2O       5 DEN=0.9982                          1.0 293 END
PB      6                                             1.0  293 END
END COMPOSITION
Case A, 6.4-1,25%P/74%W/1%Be/315gPU-TOP-SID;25%P/74%W/1%Be-REFL;H/Pu=900
READ PARAMETERS  GEN=1000  NPG=1000  NSK=50  TBA=5 END PARAMETERS
READ GEOMETRY
UNIT 1
COM='PU SPHERE'
SPHERE    1  1     13.5107  ORIGIN  0 0 0
GLOBAL UNIT 10
COM='RU-TRU 72-B PACKAGE W/ PU SPHERE'
CYLINDER  2  1    39.6875   2P154.31
HOLE 1    0.0  26.17   140.79
CYLINDER  4  1    43.18   2P154.31
CYLINDER  6  1    47.9425   2P154.31
CYLINDER  4  1    52.07   2P154.31
CYLINDER  4  1    52.07   187.33    -170.82
CYLINDER  5  1    82.57   217.83    -201.32
END GEOMETRY
END DATA
END
#CSAS25   PARM=SIZE=2000000
Case A, 6.4-1,25%P/74%W/1%Be/315gPU-TOP-SID;25%P/74%W/1%Be-REFL;H/Pu=1000
238GROUPNDF5
INFHOMMEDIUM
ARBMPUHP 1.014 5 0 0 1 1001  11.4103  4309  1.8219
6012  19.4572  8016  64.6037  94239  2.7068 1 1.0 293 END
BEBOUND   2  DEN=1.8500                          0.01  293 END
H2O            2 DEN=0.9982                          0.74  293 END
POLY(H2O) 2 DEN=0.9230                          0.25  293 END
SS304          4                                      1.0 293 END
H2O       5 DEN=0.9982                          1.0 293 END
PB      6                                             1.0  293 END
END COMPOSITION
Case A, 6.4-1,25%P/74%W/1%Be/315gPU-TOP-SID;25%P/74%W/1%Be-REFL;H/Pu=1000
READ PARAMETERS  GEN=1000  NPG=1000  NSK=50  TBA=5 END PARAMETERS
READ GEOMETRY
UNIT 1
COM='PU SPHERE'
SPHERE    1  1     13.9929  ORIGIN  0 0 0
GLOBAL UNIT 10
COM='RU-TRU 72-B PACKAGE W/ PU SPHERE'
CYLINDER  2  1    39.6875   2P154.31
HOLE 1    0.0  25.69   140.31
CYLINDER  4  1    43.18   2P154.31
CYLINDER  6  1    47.9425   2P154.31
CYLINDER  4  1    52.07   2P154.31
CYLINDER  4  1    52.07   187.33    -170.82
CYLINDER  5  1    82.57   217.83    -201.32
END GEOMETRY
END DATA
END
#CSAS25   PARM=SIZE=2000000
Case A, 6.4-1,25%P/74%W/1%Be/315gPU-TOP-SID;25%P/74%W/1%Be-REFL;H/Pu=1100
238GROUPNDF5
INFHOMMEDIUM
ARBMPUHP 1.0116 5 0 0 1 1001  11.4385  4309  1.8264
6012  19.5052  8016  64.7631  94239  2.4668 1 1.0 293 END
BEBOUND   2  DEN=1.8500                          0.01  293 END
H2O            2 DEN=0.9982                          0.74  293 END
POLY(H2O) 2 DEN=0.9230                          0.25  293 END
SS304          4                                      1.0 293 END
H2O       5 DEN=0.9982                          1.0 293 END
PB      6                                             1.0  293 END
END COMPOSITION
Case A, 6.4-1,25%P/74%W/1%Be/315gPU-TOP-SID;25%P/74%W/1%Be-REFL;H/Pu=1100
READ PARAMETERS  GEN=1000  NPG=1000  NSK=50  TBA=5 END PARAMETERS
READ GEOMETRY
UNIT 1
COM='PU SPHERE'
SPHERE    1  1     14.444  ORIGIN  0 0 0
GLOBAL UNIT 10
COM='RU-TRU 72-B PACKAGE W/ PU SPHERE'
CYLINDER  2  1    39.6875   2P154.31
HOLE 1    0.0  25.24   139.86
CYLINDER  4  1    43.18   2P154.31
```

```
CYLINDER  6  1    47.9425   2P154.31
CYLINDER  4  1    52.07   2P154.31
CYLINDER  4  1    52.07   187.33    -170.82
CYLINDER  5  1    82.57   217.83    -201.32
END GEOMETRY
END DATA
END
```

6.6.1.2 Case B – I37TO48BE

```
#CSAS25   PARM=SIZE=2000000
Case A, 6.4-6,20%P/60%W/20%Be/305gPU-TOP-SID;25%P/74%W/1%Be-REFL;H/Pu=600
238GROUPNDF5
INFHOMMEDIUM
ARBMPUHP 1.1883 5 0 0 1 1001  7.8606  4309  31.0788
6012  13.2761  8016  44.6765  94239  3.1079 1 1.0 293 END
BEBOUND   2  DEN=1.8500                          0.01  293 END
H2O            2 DEN=0.9982                        0.74  293 END
POLY(H2O) 2 DEN=0.9230                          0.25  293 END
SS304        4                                        1.0 293 END
H2O       5 DEN=0.9982                          1  293 END
PB      6                                             1.0  293 END
END COMPOSITION
Case A, 6.4-6,20%P/60%W/20%Be/305gPU-TOP-SID;25%P/74%W/1%Be-REFL;H/Pu=600
READ PARAMETERS  GEN=1000  NPG=1000  NSK=50  TBA=5 END PARAMETERS
READ GEOMETRY
UNIT 1
COM='PU SPHERE'
SPHERE    1  1     12.5392  ORIGIN  0 0 0
GLOBAL UNIT 10
COM='RU-TRU 72-B PACKAGE W/ PU SPHERE'
CYLINDER  2  1    39.6875   2P154.31
HOLE 1    0.0  27.14   141.77
CYLINDER  4  1    43.18   2P154.31
CYLINDER  6  1    47.9425   2P154.31
CYLINDER  4  1    52.07   2P154.31
CYLINDER  4  1    52.07   187.33    -170.82
CUBOID  5  1    4P72.39   216.54    -200.03
END GEOMETRY
READ BOUNDS
ALL=MIRROR
END BOUNDS
END DATA
END
#CSAS25   PARM=SIZE=2000000
Case A, 6.4-6,20%P/60%W/20%Be/305gPU-TOP-SID;25%P/74%W/1%Be-REFL;H/Pu=700
238GROUPNDF5
INFHOMMEDIUM
ARBMPUHP 1.1833 5 0 0 1 1001  7.8957  4309  31.2174
6012  13.3353  8016  44.8757  94239  2.6758 1 1.0 293 END
BEBOUND   2  DEN=1.8500                          0.01  293 END
H2O            2 DEN=0.9982                        0.74  293 END
POLY(H2O) 2 DEN=0.9230                          0.25  293 END
SS304        4                                        1.0 293 END
H2O       5 DEN=0.9982                          1  293 END
PB      6                                             1.0  293 END
END COMPOSITION
Case A, 6.4-6,20%P/60%W/20%Be/305gPU-TOP-SID;25%P/74%W/1%Be-REFL;H/Pu=700
READ PARAMETERS  GEN=1000  NPG=1000  NSK=50  TBA=5 END PARAMETERS
READ GEOMETRY
UNIT 1
COM='PU SPHERE'
SPHERE    1  1     13.1992  ORIGIN  0 0 0
GLOBAL UNIT 10
COM='RU-TRU 72-B PACKAGE W/ PU SPHERE'
CYLINDER  2  1    39.6875   2P154.31
HOLE 1    0.0  26.48   141.11
CYLINDER  4  1    43.18   2P154.31
CYLINDER  6  1    47.9425   2P154.31
CYLINDER  4  1    52.07   2P154.31
CYLINDER  4  1    52.07   187.33    -170.82
CUBOID  5  1    4P72.39   216.54    -200.03
END GEOMETRY
READ BOUNDS
ALL=MIRROR
END BOUNDS
END DATA
END
#CSAS25   PARM=SIZE=2000000
```

```
Case A, 6.4-6,20%P/60%W/20%Be/305gPU-TOP-SID;25%P/74%W/1%Be-REFL;H/Pu=800
238GROUPNDF5
INFHOMMEDIUM
ARBMPUHP 1.1796 5 0 0 1 1001  7.9222  4309  31.3222
6012  13.3801  8016  45.0263  94239  2.3492 1 1.0 293 END
BEBOUND   2  DEN=1.8500                          0.01  293 END
H2O            2 DEN=0.9982                        0.74  293 END
POLY(H2O) 2 DEN=0.9230                           0.25  293 END
SS304          4                                       1.0 293 END
H2O       5 DEN=0.9982                           1  293 END
PB      6                                              1.0  293 END
END COMPOSITION
Case A, 6.4-6,20%P/60%W/20%Be/305gPU-TOP-SID;25%P/74%W/1%Be-REFL;H/Pu=800
READ PARAMETERS  GEN=1000  NPG=1000  NSK=50  TBA=5 END PARAMETERS
READ GEOMETRY
UNIT 1
COM='PU SPHERE'
SPHERE    1  1     13.7991  ORIGIN  0 0 0
GLOBAL UNIT 10
COM='RU-TRU 72-B PACKAGE W/ PU SPHERE'
CYLINDER  2  1    39.6875   2P154.31
HOLE 1    0.0  25.88   140.51
CYLINDER  4  1    43.18   2P154.31
CYLINDER  6  1    47.9425   2P154.31
CYLINDER  4  1    52.07   2P154.31
CYLINDER  4  1    52.07   187.33    -170.82
CUBOID  5  1    4P72.39   216.54    -200.03
END GEOMETRY
READ BOUNDS
ALL=MIRROR
END BOUNDS
END DATA
END
#CSAS25   PARM=SIZE=2000000
Case A, 6.4-6,20%P/60%W/20%Be/305gPU-TOP-SID;25%P/74%W/1%Be-REFL;H/Pu=900
238GROUPNDF5
INFHOMMEDIUM
ARBMPUHP 1.1767 5 0 0 1 1001  7.9429  4309  31.4042
6012  13.4151  8016  45.1442  94239  2.0936 1 1.0 293 END
BEBOUND   2  DEN=1.8500                          0.01  293 END
H2O            2 DEN=0.9982                        0.74  293 END
POLY(H2O) 2 DEN=0.9230                           0.25  293 END
SS304          4                                       1.0 293 END
H2O       5 DEN=0.9982                           1  293 END
PB      6                                              1.0  293 END
END COMPOSITION
Case A, 6.4-6,20%P/60%W/20%Be/305gPU-TOP-SID;25%P/74%W/1%Be-REFL;H/Pu=900
READ PARAMETERS  GEN=1000  NPG=1000  NSK=50  TBA=5 END PARAMETERS
READ GEOMETRY
UNIT 1
COM='PU SPHERE'
SPHERE    1  1     14.3509  ORIGIN  0 0 0
GLOBAL UNIT 10
COM='RU-TRU 72-B PACKAGE W/ PU SPHERE'
CYLINDER  2  1    39.6875   2P154.31
HOLE 1    0.0  25.33   139.95
CYLINDER  4  1    43.18   2P154.31
CYLINDER  6  1    47.9425   2P154.31
CYLINDER  4  1    52.07   2P154.31
CYLINDER  4  1    52.07   187.33    -170.82
CUBOID  5  1    4P72.39   216.54    -200.03
END GEOMETRY
READ BOUNDS
ALL=MIRROR
END BOUNDS
END DATA
END
#CSAS25   PARM=SIZE=2000000
Case A, 6.4-6,20%P/60%W/20%Be/305gPU-TOP-SID;25%P/74%W/1%Be-REFL;H/Pu=1000
238GROUPNDF5
INFHOMMEDIUM
ARBMPUHP 1.1744 5 0 0 1 1001  7.9596  4309  31.4701
6012  13.4432  8016  45.2389  94239  1.8882 1 1.0 293 END
BEBOUND   2  DEN=1.8500                          0.01  293 END
H2O            2 DEN=0.9982                        0.74  293 END
POLY(H2O) 2 DEN=0.9230                           0.25  293 END
SS304          4                                       1.0 293 END
H2O       5 DEN=0.9982                           1  293 END
PB      6                                              1.0  293 END
END COMPOSITION
Case A, 6.4-6,20%P/60%W/20%Be/305gPU-TOP-SID;25%P/74%W/1%Be-REFL;H/Pu=1000
```

```
READ PARAMETERS  GEN=1000  NPG=1000  NSK=50  TBA=5 END PARAMETERS
READ GEOMETRY
UNIT 1
COM='PU SPHERE'
SPHERE    1  1     14.8632  ORIGIN  0 0 0
GLOBAL UNIT 10
COM='RU-TRU 72-B PACKAGE W/ PU SPHERE'
CYLINDER  2  1    39.6875   2P154.31
HOLE 1    0.0  24.82   139.44
CYLINDER  4  1    43.18   2P154.31
CYLINDER  6  1    47.9425   2P154.31
CYLINDER  4  1    52.07   2P154.31
CYLINDER  4  1    52.07   187.33    -170.82
CUBOID  5  1    4P72.39   216.54    -200.03
END GEOMETRY
READ BOUNDS
ALL=MIRROR
END BOUNDS
END DATA
END
#CSAS25   PARM=SIZE=2000000
Case A, 6.4-6,20%P/60%W/20%Be/305gPU-TOP-SID;25%P/74%W/1%Be-REFL;H/Pu=1100
238GROUPNDF5
INFHOMMEDIUM
ARBMPUHP 1.1725 5 0 0 1 1001  7.9733  4309  31.5242
6012  13.4664  8016  45.3167  94239  1.7195 1 1.0 293 END
BEBOUND   2  DEN=1.8500                          0.01  293 END
H2O            2 DEN=0.9982                        0.74  293 END
POLY(H2O) 2 DEN=0.9230                           0.25  293 END
SS304          4                                       1.0 293 END
H2O       5 DEN=0.9982                           1  293 END
PB      6                                              1.0  293 END
END COMPOSITION
Case A, 6.4-6,20%P/60%W/20%Be/305gPU-TOP-SID;25%P/74%W/1%Be-REFL;H/Pu=1100
READ PARAMETERS  GEN=1000  NPG=1000  NSK=50  TBA=5 END PARAMETERS
READ GEOMETRY
UNIT 1
COM='PU SPHERE'
SPHERE    1  1     15.3425  ORIGIN  0 0 0
GLOBAL UNIT 10
COM='RU-TRU 72-B PACKAGE W/ PU SPHERE'
CYLINDER  2  1    39.6875   2P154.31
HOLE 1    0.0  24.34   138.96
CYLINDER  4  1    43.18   2P154.31
CYLINDER  6  1    47.9425   2P154.31
CYLINDER  4  1    52.07   2P154.31
CYLINDER  4  1    52.07   187.33    -170.82
CUBOID  5  1    4P72.39   216.54    -200.03
END GEOMETRY
READ BOUNDS
ALL=MIRROR
END BOUNDS
END DATA
END
#CSAS25   PARM=SIZE=2000000
Case A, 6.4-6,15%P/45%W/40%Be/305gPU-TOP-SID;25%P/74%W/1%Be-REFL;H/Pu=600
238GROUPNDF5
INFHOMMEDIUM
ARBMPUHP 1.3535 5 0 0 1 1001  5.1784  4309  54.5968
6012  8.7459  8016  29.4315  94239  2.0474 1 1.0 293 END
BEBOUND   2  DEN=1.8500                          0.01  293 END
H2O            2 DEN=0.9982                        0.74  293 END
POLY(H2O) 2 DEN=0.9230                           0.25  293 END
SS304          4                                       1.0 293 END
H2O       5 DEN=0.9982                           1  293 END
PB      6                                              1.0  293 END
END COMPOSITION
Case A, 6.4-6,15%P/45%W/40%Be/305gPU-TOP-SID;25%P/74%W/1%Be-REFL;H/Pu=600
READ PARAMETERS  GEN=1000  NPG=1000  NSK=50  TBA=5 END PARAMETERS
READ GEOMETRY
UNIT 1
COM='PU SPHERE'
SPHERE    1  1     13.7991  ORIGIN  0 0 0
GLOBAL UNIT 10
COM='RU-TRU 72-B PACKAGE W/ PU SPHERE'
CYLINDER  2  1    39.6875   2P154.31
HOLE 1    0.0  25.88   140.51
CYLINDER  4  1    43.18   2P154.31
CYLINDER  6  1    47.9425   2P154.31
CYLINDER  4  1    52.07   2P154.31
CYLINDER  4  1    52.07   187.33    -170.82
```

```
CUBOID  5  1    4P72.39   216.54    -200.03
END GEOMETRY
READ BOUNDS
ALL=MIRROR
END BOUNDS
END DATA
END
#CSAS25   PARM=SIZE=2000000
Case A, 6.4-6,15%P/45%W/40%Be/305gPU-TOP-SID;25%P/74%W/1%Be-REFL;H/Pu=700
238GROUPNDF5
INFHOMMEDIUM
ARBMPUHP 1.3498 5 0 0 1 1001  5.1935  4309  54.757
6012  8.7716  8016  29.5179  94239  1.7601 1 1.0 293 END
BEBOUND   2  DEN=1.8500                          0.01  293 END
H2O            2 DEN=0.9982                         0.74  293 END
POLY(H2O) 2 DEN=0.9230                           0.25  293 END
SS304        4                                          1.0 293 END
H2O       5 DEN=0.9982                           1  293 END
PB      6                                              1.0  293 END
END COMPOSITION
Case A, 6.4-6,15%P/45%W/40%Be/305gPU-TOP-SID;25%P/74%W/1%Be-REFL;H/Pu=700
READ PARAMETERS  GEN=1000  NPG=1000  NSK=50  TBA=5 END PARAMETERS
READ GEOMETRY
UNIT 1
COM='PU SPHERE'
SPHERE    1  1     14.5257  ORIGIN  0 0 0
GLOBAL UNIT 10
COM='RU-TRU 72-B PACKAGE W/ PU SPHERE'
CYLINDER  2  1    39.6875   2P154.31
HOLE 1    0.0  25.16   139.78
CYLINDER  4  1    43.18   2P154.31
CYLINDER  6  1    47.9425   2P154.31
CYLINDER  4  1    52.07   2P154.31
CYLINDER  4  1    52.07   187.33    -170.82
CUBOID  5  1    4P72.39   216.54    -200.03
END GEOMETRY
READ BOUNDS
ALL=MIRROR
END BOUNDS
END DATA
END
#CSAS25   PARM=SIZE=2000000
Case A, 6.4-6,15%P/45%W/40%Be/305gPU-TOP-SID;25%P/74%W/1%Be-REFL;H/Pu=800
238GROUPNDF5
INFHOMMEDIUM
ARBMPUHP 1.347 5 0 0 1 1001  5.205  4309  54.8777
6012  8.7909  8016  29.5829  94239  1.5435 1 1.0 293 END
BEBOUND   2  DEN=1.8500                          0.01  293 END
H2O            2 DEN=0.9982                         0.74  293 END
POLY(H2O) 2 DEN=0.9230                           0.25  293 END
SS304        4                                          1.0 293 END
H2O       5 DEN=0.9982                           1  293 END
PB      6                                              1.0  293 END
END COMPOSITION
Case A, 6.4-6,15%P/45%W/40%Be/305gPU-TOP-SID;25%P/74%W/1%Be-REFL;H/Pu=800
READ PARAMETERS  GEN=1000  NPG=1000  NSK=50  TBA=5 END PARAMETERS
READ GEOMETRY
UNIT 1
COM='PU SPHERE'
SPHERE    1  1     15.1861  ORIGIN  0 0 0
GLOBAL UNIT 10
COM='RU-TRU 72-B PACKAGE W/ PU SPHERE'
CYLINDER  2  1    39.6875   2P154.31
HOLE 1    0.0  24.5   139.12
CYLINDER  4  1    43.18   2P154.31
CYLINDER  6  1    47.9425   2P154.31
CYLINDER  4  1    52.07   2P154.31
CYLINDER  4  1    52.07   187.33    -170.82
CUBOID  5  1    4P72.39   216.54    -200.03
END GEOMETRY
READ BOUNDS
ALL=MIRROR
END BOUNDS
END DATA
END
#CSAS25   PARM=SIZE=2000000
Case A, 6.4-6,15%P/45%W/40%Be/305gPU-TOP-SID;25%P/74%W/1%Be-REFL;H/Pu=900
238GROUPNDF5
INFHOMMEDIUM
ARBMPUHP 1.3449 5 0 0 1 1001  5.2139  4309  54.972
6012  8.806  8016  29.6338  94239  1.3743 1 1.0 293 END
```

```
BEBOUND   2  DEN=1.8500                              0.01  293 END
H2O            2 DEN=0.9982                             0.74  293 END
POLY(H2O) 2 DEN=0.9230                              0.25  293 END
SS304        4                                             1.0 293 END
H2O       5 DEN=0.9982                              1  293 END
PB      6                                                  1.0  293 END
END COMPOSITION
Case A, 6.4-6,15%P/45%W/40%Be/305gPU-TOP-SID;25%P/74%W/1%Be-REFL;H/Pu=900
READ PARAMETERS  GEN=1000  NPG=1000  NSK=50  TBA=5 END PARAMETERS
READ GEOMETRY
UNIT 1
COM='PU SPHERE'
SPHERE    1  1     15.7936  ORIGIN  0 0 0
GLOBAL UNIT 10
COM='RU-TRU 72-B PACKAGE W/ PU SPHERE'
CYLINDER  2  1    39.6875   2P154.31
HOLE 1    0.0  23.89   138.51
CYLINDER  4  1    43.18   2P154.31
CYLINDER  6  1    47.9425   2P154.31
CYLINDER  4  1    52.07   2P154.31
CYLINDER  4  1    52.07   187.33    -170.82
CUBOID  5  1    4P72.39   216.54    -200.03
END GEOMETRY
READ BOUNDS
ALL=MIRROR
END BOUNDS
END DATA
END
#CSAS25   PARM=SIZE=2000000
Case A, 6.4-6,15%P/45%W/40%Be/305gPU-TOP-SID;25%P/74%W/1%Be-REFL;H/Pu=1000
238GROUPNDF5
INFHOMMEDIUM
ARBMPUHP 1.3432 5 0 0 1 1001  5.2211  4309  55.0476
6012  8.8181  8016  29.6745  94239  1.2386 1 1.0 293 END
BEBOUND   2  DEN=1.8500                              0.01  293 END
H2O            2 DEN=0.9982                             0.74  293 END
POLY(H2O) 2 DEN=0.9230                              0.25  293 END
SS304        4                                             1.0 293 END
H2O       5 DEN=0.9982                              1  293 END
PB      6                                                  1.0  293 END
END COMPOSITION
Case A, 6.4-6,15%P/45%W/40%Be/305gPU-TOP-SID;25%P/74%W/1%Be-REFL;H/Pu=1000
READ PARAMETERS  GEN=1000  NPG=1000  NSK=50  TBA=5 END PARAMETERS
READ GEOMETRY
UNIT 1
COM='PU SPHERE'
SPHERE    1  1     16.3576  ORIGIN  0 0 0
GLOBAL UNIT 10
COM='RU-TRU 72-B PACKAGE W/ PU SPHERE'
CYLINDER  2  1    39.6875   2P154.31
HOLE 1    0.0  23.32   137.95
CYLINDER  4  1    43.18   2P154.31
CYLINDER  6  1    47.9425   2P154.31
CYLINDER  4  1    52.07   2P154.31
CYLINDER  4  1    52.07   187.33    -170.82
CUBOID  5  1    4P72.39   216.54    -200.03
END GEOMETRY
READ BOUNDS
ALL=MIRROR
END BOUNDS
END DATA
END
#CSAS25   PARM=SIZE=2000000
Case A, 6.4-6,15%P/45%W/40%Be/305gPU-TOP-SID;25%P/74%W/1%Be-REFL;H/Pu=1100
238GROUPNDF5
INFHOMMEDIUM
ARBMPUHP 1.3418 5 0 0 1 1001  5.227  4309  55.1097
6012  8.8281  8016  29.708  94239  1.1273 1 1.0 293 END
BEBOUND   2  DEN=1.8500                              0.01  293 END
H2O            2 DEN=0.9982                             0.74  293 END
POLY(H2O) 2 DEN=0.9230                              0.25  293 END
SS304        4                                             1.0 293 END
H2O       5 DEN=0.9982                              1  293 END
PB      6                                                  1.0  293 END
END COMPOSITION
Case A, 6.4-6,15%P/45%W/40%Be/305gPU-TOP-SID;25%P/74%W/1%Be-REFL;H/Pu=1100
READ PARAMETERS  GEN=1000  NPG=1000  NSK=50  TBA=5 END PARAMETERS
READ GEOMETRY
UNIT 1
COM='PU SPHERE'
SPHERE    1  1     16.8852  ORIGIN  0 0 0
```

```
GLOBAL UNIT 10
COM='RU-TRU 72-B PACKAGE W/ PU SPHERE'
CYLINDER  2  1    39.6875   2P154.31
HOLE 1    0.0  22.8   137.42
CYLINDER  4  1    43.18   2P154.31
CYLINDER  6  1    47.9425   2P154.31
CYLINDER  4  1    52.07   2P154.31
CYLINDER  4  1    52.07   187.33    -170.82
CUBOID  5  1    4P72.39   216.54    -200.03
END GEOMETRY
READ BOUNDS
ALL=MIRROR
END BOUNDS
END DATA
END
```

6.6.1.3 Case C – ITOPSIDEBEMOD245

```
#CSAS25   PARM=SIZE=2000000
Case C, 6.4-9,99%P/0%W/1%Be/245gPU-TOP-SID;99%P/0%W/1%Be-REFL;H/Pu=700
238GROUPNDF5
INFHOMMEDIUM
ARBMPUHP 0.9746 5 0 0 1 1001  13.4519  4309  1.8939
6012  80.0954  8016  0  94239  4.5588 1 1.0 293 END
BEBOUND   2  DEN=1.8500                          0.01  293 END

POLY(H2O) 2 DEN=0.9230                          0.99  293 END
SS304       4                                             1.0 293 END
H2O       5 DEN=0.9982                          1.0 293 END
PB      6                                               1.0  293 END
END COMPOSITION
Case C, 6.4-9,99%P/0%W/1%Be/245gPU-TOP-SID;99%P/0%W/1%Be-REFL;H/Pu=700
READ PARAMETERS  GEN=1000  NPG=1000  NSK=50  TBA=5 END PARAMETERS
READ GEOMETRY
UNIT 1
COM='PU SPHERE'
SPHERE    1  1     10.9597  ORIGIN  0 0 0
GLOBAL UNIT 10
COM='RU-TRU 72-B PACKAGE W/ PU SPHERE'
CYLINDER  2  1    39.6875   2P154.31
HOLE 1    0.0  28.72   143.35
CYLINDER  4  1    43.18   2P154.31
CYLINDER  6  1    47.9425   2P154.31
CYLINDER  4  1    52.07   2P154.31
CYLINDER  4  1    52.07   187.33    -170.82
CUBOID  5  1    4P72.39   216.54    -200.03
END GEOMETRY
READ BOUNDS
ALL=MIRROR
END BOUNDS
END DATA
END
#CSAS25   PARM=SIZE=2000000
Case C, 6.4-9,99%P/0%W/1%Be/245gPU-TOP-SID;99%P/0%W/1%Be-REFL;H/Pu=800
238GROUPNDF5
INFHOMMEDIUM
ARBMPUHP 0.9693 5 0 0 1 1001  13.529  4309  1.9048
6012  80.5544  8016  0  94239  4.0118 1 1.0 293 END
BEBOUND   2  DEN=1.8500                          0.01  293 END

POLY(H2O) 2 DEN=0.9230                          0.99  293 END
SS304       4                                             1.0 293 END
H2O       5 DEN=0.9982                          1.0 293 END
PB      6                                               1.0  293 END
END COMPOSITION
Case C, 6.4-9,99%P/0%W/1%Be/245gPU-TOP-SID;99%P/0%W/1%Be-REFL;H/Pu=800
READ PARAMETERS  GEN=1000  NPG=1000  NSK=50  TBA=5 END PARAMETERS
READ GEOMETRY
UNIT 1
COM='PU SPHERE'
SPHERE    1  1     11.4575  ORIGIN  0 0 0
GLOBAL UNIT 10
COM='RU-TRU 72-B PACKAGE W/ PU SPHERE'
CYLINDER  2  1    39.6875   2P154.31
HOLE 1    0.0  28.23   142.85
CYLINDER  4  1    43.18   2P154.31
CYLINDER  6  1    47.9425   2P154.31
CYLINDER  4  1    52.07   2P154.31
CYLINDER  4  1    52.07   187.33    -170.82
```

```
CUBOID  5  1    4P72.39   216.54    -200.03
END GEOMETRY
READ BOUNDS
ALL=MIRROR
END BOUNDS
END DATA
END
#CSAS25   PARM=SIZE=2000000
Case C, 6.4-9,99%P/0%W/1%Be/245gPU-TOP-SID;99%P/0%W/1%Be-REFL;H/Pu=900
238GROUPNDF5
INFHOMMEDIUM
ARBMPUHP 0.9652 5 0 0 1 1001  13.5896  4309  1.9133
6012  80.9151  8016  0  94239  3.582 1 1.0 293 END
BEBOUND   2  DEN=1.8500                          0.01  293 END

POLY(H2O) 2 DEN=0.9230                          0.99  293 END
SS304       4                                             1.0 293 END
H2O       5 DEN=0.9982                          1.0 293 END
PB      6                                               1.0  293 END
END COMPOSITION
Case C, 6.4-9,99%P/0%W/1%Be/245gPU-TOP-SID;99%P/0%W/1%Be-REFL;H/Pu=900
READ PARAMETERS  GEN=1000  NPG=1000  NSK=50  TBA=5 END PARAMETERS
READ GEOMETRY
UNIT 1
COM='PU SPHERE'
SPHERE    1  1     11.9154  ORIGIN  0 0 0
GLOBAL UNIT 10
COM='RU-TRU 72-B PACKAGE W/ PU SPHERE'
CYLINDER  2  1    39.6875   2P154.31
HOLE 1    0.0  27.77   142.39
CYLINDER  4  1    43.18   2P154.31
CYLINDER  6  1    47.9425   2P154.31
CYLINDER  4  1    52.07   2P154.31
CYLINDER  4  1    52.07   187.33    -170.82
CUBOID  5  1    4P72.39   216.54    -200.03
END GEOMETRY
READ BOUNDS
ALL=MIRROR
END BOUNDS
END DATA
END
#CSAS25   PARM=SIZE=2000000
Case C, 6.4-9,99%P/0%W/1%Be/245gPU-TOP-SID;99%P/0%W/1%Be-REFL;H/Pu=1000
238GROUPNDF5
INFHOMMEDIUM
ARBMPUHP 0.9619 5 0 0 1 1001  13.6384  4309  1.9202
6012  81.206  8016  0  94239  3.2354 1 1.0 293 END
BEBOUND   2  DEN=1.8500                          0.01  293 END

POLY(H2O) 2 DEN=0.9230                          0.99  293 END
SS304       4                                             1.0 293 END
H2O       5 DEN=0.9982                          1.0 293 END
PB      6                                               1.0  293 END
END COMPOSITION
Case C, 6.4-9,99%P/0%W/1%Be/245gPU-TOP-SID;99%P/0%W/1%Be-REFL;H/Pu=1000
READ PARAMETERS  GEN=1000  NPG=1000  NSK=50  TBA=5 END PARAMETERS
READ GEOMETRY
UNIT 1
COM='PU SPHERE'
SPHERE    1  1     12.3406  ORIGIN  0 0 0
GLOBAL UNIT 10
COM='RU-TRU 72-B PACKAGE W/ PU SPHERE'
CYLINDER  2  1    39.6875   2P154.31
HOLE 1    0.0  27.34   141.96
CYLINDER  4  1    43.18   2P154.31
CYLINDER  6  1    47.9425   2P154.31
CYLINDER  4  1    52.07   2P154.31
CYLINDER  4  1    52.07   187.33    -170.82
CUBOID  5  1    4P72.39   216.54    -200.03
END GEOMETRY
READ BOUNDS
ALL=MIRROR
END BOUNDS
END DATA
END
#CSAS25   PARM=SIZE=2000000
Case C, 6.4-9,99%P/0%W/1%Be/245gPU-TOP-SID;99%P/0%W/1%Be-REFL;H/Pu=1100
238GROUPNDF5
INFHOMMEDIUM
ARBMPUHP 0.9592 5 0 0 1 1001  13.6787  4309  1.9259
6012  81.4455  8016  0  94239  2.9499 1 1.0 293 END
```

```
BEBOUND   2  DEN=1.8500                              0.01  293 END

POLY(H2O) 2 DEN=0.9230                              0.99  293 END
SS304       4                                                 1.0 293 END
H2O       5 DEN=0.9982                              1.0 293 END
PB      6                                                     1.0  293 END
END COMPOSITION
Case C, 6.4-9,99%P/0%W/1%Be/245gPU-TOP-SID;99%P/0%W/1%Be-REFL;H/Pu=1100
READ PARAMETERS  GEN=1000  NPG=1000  NSK=50  TBA=5 END PARAMETERS
READ GEOMETRY
UNIT 1
COM='PU SPHERE'
SPHERE    1  1     12.7383  ORIGIN  0 0 0
GLOBAL UNIT 10
COM='RU-TRU 72-B PACKAGE W/ PU SPHERE'
CYLINDER  2  1    39.6875   2P154.31
HOLE 1    0.0  26.94   141.57
CYLINDER  4  1    43.18   2P154.31
CYLINDER  6  1    47.9425   2P154.31
CYLINDER  4  1    52.07   2P154.31
CYLINDER  4  1    52.07   187.33    -170.82
CUBOID  5  1    4P72.39   216.54    -200.03
END GEOMETRY
READ BOUNDS
ALL=MIRROR
END BOUNDS
END DATA
END
```

6.6.1.4 Case D – LEUBEREFLINF1IM

```
#CSAS25   PARM=SIZE=2000000
Case D, Inf Unit, 6.4-13,25%P/74%W/1%Be/0%P/0%W/100%Be-REFL;IM=0.00001;H/235U=400
238GROUPNDF5
INFHOMMEDIUM
ARBMPUHP 5.8605 6 0 0 1 1001  1.4437  4309  0.2305
6012  2.4618  8016  8.1738  92238  86.8484  92235  0.8418 1 1.0 293 END
BEBOUND   2  DEN=1.8500                              1  293 END


SS304       4                                                 1.0 293 END
H2O       5 DEN=0.9982                           0.00001  293 END
PB      6                                                     1.0  293 END
END COMPOSITION
Case D, Inf Unit, 6.4-13,25%P/74%W/1%Be/0%P/0%W/100%Be-REFL;IM=0.00001;H/235U=400
READ PARAMETERS  GEN=1000  NPG=1000  NSK=50  TBA=5 END PARAMETERS
READ GEOMETRY
GLOBAL UNIT 10
COM='RU-TRU 72-B PACKAGE FILLED TO 6900 LBS FROM END'
CYLINDER  1  1    39.6875   2p54.076
CYLINDER  2  1    39.6875   2p154.31
CYLINDER  4  1    43.18   2P154.31
CYLINDER  6  1    47.9425   2P154.31
CYLINDER  4  1    52.07   2P154.31
CYLINDER  4  1    52.07   187.33    -170.82
CUBOID  5  1   4p72.39   216.54    -200.03
END GEOMETRY
READ BOUNDS
ALL=MIRROR
END BOUNDS
END DATA
END
#CSAS25   PARM=SIZE=2000000
Case D, Inf Unit, 6.4-13,25%P/74%W/1%Be/0%P/0%W/100%Be-REFL;IM=0.001;H/235U=400
238GROUPNDF5
INFHOMMEDIUM
ARBMPUHP 5.8605 6 0 0 1 1001  1.4437  4309  0.2305
6012  2.4618  8016  8.1738  92238  86.8484  92235  0.8418 1 1.0 293 END
BEBOUND   2  DEN=1.8500                              1  293 END


SS304       4                                                 1.0 293 END
H2O       5 DEN=0.9982                           0.001  293 END
PB      6                                                     1.0  293 END
END COMPOSITION
Case D, Inf Unit, 6.4-13,25%P/74%W/1%Be/0%P/0%W/100%Be-REFL;IM=0.001;H/235U=400
READ PARAMETERS  GEN=1000  NPG=1000  NSK=50  TBA=5 END PARAMETERS
READ GEOMETRY
GLOBAL UNIT 10
```

```
COM='RU-TRU 72-B PACKAGE FILLED TO 6900 LBS FROM END'
CYLINDER  1  1    39.6875   2p54.076
CYLINDER  2  1    39.6875   2p154.31
CYLINDER  4  1    43.18   2P154.31
CYLINDER  6  1    47.9425   2P154.31
CYLINDER  4  1    52.07   2P154.31
CYLINDER  4  1    52.07   187.33    -170.82
CUBOID  5  1   4p72.39   216.54    -200.03
END GEOMETRY
READ BOUNDS
ALL=MIRROR
END BOUNDS
END DATA
END
#CSAS25   PARM=SIZE=2000000
Case D, Inf Unit, 6.4-13,25%P/74%W/1%Be/0%P/0%W/100%Be-REFL;IM=0.01;H/235U=400
238GROUPNDF5
INFHOMMEDIUM
ARBMPUHP 5.8605 6 0 0 1 1001  1.4437  4309  0.2305
6012  2.4618  8016  8.1738  92238  86.8484  92235  0.8418 1 1.0 293 END
BEBOUND   2  DEN=1.8500                            1  293 END


SS304        4                                                 1.0 293 END
H2O       5 DEN=0.9982                         0.01  293 END
PB      6                                                  1.0  293 END
END COMPOSITION
Case D, Inf Unit, 6.4-13,25%P/74%W/1%Be/0%P/0%W/100%Be-REFL;IM=0.01;H/235U=400
READ PARAMETERS  GEN=1000  NPG=1000  NSK=50  TBA=5 END PARAMETERS
READ GEOMETRY
GLOBAL UNIT 10
COM='RU-TRU 72-B PACKAGE FILLED TO 6900 LBS FROM END'
CYLINDER  1  1    39.6875   2p54.076
CYLINDER  2  1    39.6875   2p154.31
CYLINDER  4  1    43.18   2P154.31
CYLINDER  6  1    47.9425   2P154.31
CYLINDER  4  1    52.07   2P154.31
CYLINDER  4  1    52.07   187.33    -170.82
CUBOID  5  1   4p72.39   216.54    -200.03
END GEOMETRY
READ BOUNDS
ALL=MIRROR
END BOUNDS
END DATA
END
#CSAS25   PARM=SIZE=2000000
Case D, Inf Unit, 6.4-13,25%P/74%W/1%Be/0%P/0%W/100%Be-REFL;IM=0.05;H/235U=400
238GROUPNDF5
INFHOMMEDIUM
ARBMPUHP 5.8605 6 0 0 1 1001  1.4437  4309  0.2305
6012  2.4618  8016  8.1738  92238  86.8484  92235  0.8418 1 1.0 293 END
BEBOUND   2  DEN=1.8500                            1  293 END


SS304        4                                                 1.0 293 END
H2O       5 DEN=0.9982                         0.05  293 END
PB      6                                                  1.0  293 END
END COMPOSITION
Case D, Inf Unit, 6.4-13,25%P/74%W/1%Be/0%P/0%W/100%Be-REFL;IM=0.05;H/235U=400
READ PARAMETERS  GEN=1000  NPG=1000  NSK=50  TBA=5 END PARAMETERS
READ GEOMETRY
GLOBAL UNIT 10
COM='RU-TRU 72-B PACKAGE FILLED TO 6900 LBS FROM END'
CYLINDER  1  1    39.6875   2p54.076
CYLINDER  2  1    39.6875   2p154.31
CYLINDER  4  1    43.18   2P154.31
CYLINDER  6  1    47.9425   2P154.31
CYLINDER  4  1    52.07   2P154.31
CYLINDER  4  1    52.07   187.33    -170.82
CUBOID  5  1   4p72.39   216.54    -200.03
END GEOMETRY
READ BOUNDS
ALL=MIRROR
END BOUNDS
END DATA
END
#CSAS25   PARM=SIZE=2000000
Case D, Inf Unit, 6.4-13,25%P/74%W/1%Be/0%P/0%W/100%Be-REFL;IM=0.1;H/235U=400
238GROUPNDF5
INFHOMMEDIUM
ARBMPUHP 5.8605 6 0 0 1 1001  1.4437  4309  0.2305
```

```
6012  2.4618  8016  8.1738  92238  86.8484  92235  0.8418 1 1.0 293 END
BEBOUND   2  DEN=1.8500                            1  293 END


SS304        4                                                 1.0 293 END
H2O       5 DEN=0.9982                          0.1  293 END
PB      6                                                     1.0  293 END
END COMPOSITION
Case D, Inf Unit, 6.4-13,25%P/74%W/1%Be/0%P/0%W/100%Be-REFL;IM=0.1;H/235U=400
READ PARAMETERS  GEN=1000  NPG=1000  NSK=50  TBA=5 END PARAMETERS
READ GEOMETRY
GLOBAL UNIT 10
COM='RU-TRU 72-B PACKAGE FILLED TO 6900 LBS FROM END'
CYLINDER  1  1    39.6875   2p54.076
CYLINDER  2  1    39.6875   2p154.31
CYLINDER  4  1    43.18   2P154.31
CYLINDER  6  1    47.9425   2P154.31
CYLINDER  4  1    52.07   2P154.31
CYLINDER  4  1    52.07   187.33    -170.82
CUBOID  5  1   4p72.39   216.54    -200.03
END GEOMETRY
READ BOUNDS
ALL=MIRROR
END BOUNDS
END DATA
END
#CSAS25   PARM=SIZE=2000000
Case D, Inf Unit, 6.4-13,25%P/74%W/1%Be/0%P/0%W/100%Be-REFL;IM=0.2;H/235U=400
238GROUPNDF5
INFHOMMEDIUM
ARBMPUHP 5.8605 6 0 0 1 1001  1.4437  4309  0.2305
6012  2.4618  8016  8.1738  92238  86.8484  92235  0.8418 1 1.0 293 END
BEBOUND   2  DEN=1.8500                            1  293 END


SS304        4                                                 1.0 293 END
H2O       5 DEN=0.9982                          0.2  293 END
PB      6                                                     1.0  293 END
END COMPOSITION
Case D, Inf Unit, 6.4-13,25%P/74%W/1%Be/0%P/0%W/100%Be-REFL;IM=0.2;H/235U=400
READ PARAMETERS  GEN=1000  NPG=1000  NSK=50  TBA=5 END PARAMETERS
READ GEOMETRY
GLOBAL UNIT 10
COM='RU-TRU 72-B PACKAGE FILLED TO 6900 LBS FROM END'
CYLINDER  1  1    39.6875   2p54.076
CYLINDER  2  1    39.6875   2p154.31
CYLINDER  4  1    43.18   2P154.31
CYLINDER  6  1    47.9425   2P154.31
CYLINDER  4  1    52.07   2P154.31
CYLINDER  4  1    52.07   187.33    -170.82
CUBOID  5  1   4p72.39   216.54    -200.03
END GEOMETRY
READ BOUNDS
ALL=MIRROR
END BOUNDS
END DATA
END
#CSAS25   PARM=SIZE=2000000
Case D, Inf Unit, 6.4-13,25%P/74%W/1%Be/0%P/0%W/100%Be-REFL;IM=0.4;H/235U=400
238GROUPNDF5
INFHOMMEDIUM
ARBMPUHP 5.8605 6 0 0 1 1001  1.4437  4309  0.2305
6012  2.4618  8016  8.1738  92238  86.8484  92235  0.8418 1 1.0 293 END
BEBOUND   2  DEN=1.8500                            1  293 END


SS304        4                                                 1.0 293 END
H2O       5 DEN=0.9982                          0.4  293 END
PB      6                                                     1.0  293 END
END COMPOSITION
Case D, Inf Unit, 6.4-13,25%P/74%W/1%Be/0%P/0%W/100%Be-REFL;IM=0.4;H/235U=400
READ PARAMETERS  GEN=1000  NPG=1000  NSK=50  TBA=5 END PARAMETERS
READ GEOMETRY
GLOBAL UNIT 10
COM='RU-TRU 72-B PACKAGE FILLED TO 6900 LBS FROM END'
CYLINDER  1  1    39.6875   2p54.076
CYLINDER  2  1    39.6875   2p154.31
CYLINDER  4  1    43.18   2P154.31
CYLINDER  6  1    47.9425   2P154.31
CYLINDER  4  1    52.07   2P154.31
CYLINDER  4  1    52.07   187.33    -170.82
```

```
CUBOID  5  1   4p72.39   216.54    -200.03
END GEOMETRY
READ BOUNDS
ALL=MIRROR
END BOUNDS
END DATA
END
#CSAS25   PARM=SIZE=2000000
Case D, Inf Unit, 6.4-13,25%P/74%W/1%Be/0%P/0%W/100%Be-REFL;IM=0.6;H/235U=400
238GROUPNDF5
INFHOMMEDIUM
ARBMPUHP 5.8605 6 0 0 1 1001  1.4437  4309  0.2305
6012  2.4618  8016  8.1738  92238  86.8484  92235  0.8418 1 1.0 293 END
BEBOUND   2  DEN=1.8500                          1  293 END


SS304        4                                                 1.0 293 END
H2O       5 DEN=0.9982                        0.6  293 END
PB      6                                                 1.0  293 END
END COMPOSITION
Case D, Inf Unit, 6.4-13,25%P/74%W/1%Be/0%P/0%W/100%Be-REFL;IM=0.6;H/235U=400
READ PARAMETERS  GEN=1000  NPG=1000  NSK=50  TBA=5 END PARAMETERS
READ GEOMETRY
GLOBAL UNIT 10
COM='RU-TRU 72-B PACKAGE FILLED TO 6900 LBS FROM END'
CYLINDER  1  1    39.6875   2p54.076
CYLINDER  2  1    39.6875   2p154.31
CYLINDER  4  1    43.18   2P154.31
CYLINDER  6  1    47.9425   2P154.31
CYLINDER  4  1    52.07   2P154.31
CYLINDER  4  1    52.07   187.33    -170.82
CUBOID  5  1   4p72.39   216.54    -200.03
END GEOMETRY
READ BOUNDS
ALL=MIRROR
END BOUNDS
END DATA
END
#CSAS25   PARM=SIZE=2000000
Case D, Inf Unit, 6.4-13,25%P/74%W/1%Be/0%P/0%W/100%Be-REFL;IM=0.8;H/235U=400
238GROUPNDF5
INFHOMMEDIUM
ARBMPUHP 5.8605 6 0 0 1 1001  1.4437  4309  0.2305
6012  2.4618  8016  8.1738  92238  86.8484  92235  0.8418 1 1.0 293 END
BEBOUND   2  DEN=1.8500                          1  293 END


SS304        4                                                 1.0 293 END
H2O       5 DEN=0.9982                        0.8  293 END
PB      6                                                 1.0  293 END
END COMPOSITION
Case D, Inf Unit, 6.4-13,25%P/74%W/1%Be/0%P/0%W/100%Be-REFL;IM=0.8;H/235U=400
READ PARAMETERS  GEN=1000  NPG=1000  NSK=50  TBA=5 END PARAMETERS
READ GEOMETRY
GLOBAL UNIT 10
COM='RU-TRU 72-B PACKAGE FILLED TO 6900 LBS FROM END'
CYLINDER  1  1    39.6875   2p54.076
CYLINDER  2  1    39.6875   2p154.31
CYLINDER  4  1    43.18   2P154.31
CYLINDER  6  1    47.9425   2P154.31
CYLINDER  4  1    52.07   2P154.31
CYLINDER  4  1    52.07   187.33    -170.82
CUBOID  5  1   4p72.39   216.54    -200.03
END GEOMETRY
READ BOUNDS
ALL=MIRROR
END BOUNDS
END DATA
END
#CSAS25   PARM=SIZE=2000000
Case D, Inf Unit, 6.4-13,25%P/74%W/1%Be/0%P/0%W/100%Be-REFL;IM=1;H/235U=400
238GROUPNDF5
INFHOMMEDIUM
ARBMPUHP 5.8605 6 0 0 1 1001  1.4437  4309  0.2305
6012  2.4618  8016  8.1738  92238  86.8484  92235  0.8418 1 1.0 293 END
BEBOUND   2  DEN=1.8500                          1  293 END


SS304        4                                                 1.0 293 END
H2O       5 DEN=0.9982                         1  293 END
PB      6                                                 1.0  293 END
```

```
END COMPOSITION
Case D, Inf Unit, 6.4-13,25%P/74%W/1%Be/0%P/0%W/100%Be-REFL;IM=1;H/235U=400
READ PARAMETERS  GEN=1000  NPG=1000  NSK=50  TBA=5 END PARAMETERS
READ GEOMETRY
GLOBAL UNIT 10
COM='RU-TRU 72-B PACKAGE FILLED TO 6900 LBS FROM END'
CYLINDER  1  1    39.6875   2p54.076
CYLINDER  2  1    39.6875   2p154.31
CYLINDER  4  1    43.18   2P154.31
CYLINDER  6  1    47.9425   2P154.31
CYLINDER  4  1    52.07   2P154.31
CYLINDER  4  1    52.07   187.33    -170.82
CUBOID  5  1   4p72.39   216.54    -200.03
END GEOMETRY
READ BOUNDS
ALL=MIRROR
END BOUNDS
END DATA
END
```

6.6.1.5 Case E – CCVR.24i.eimx (Example)

```
#CSAS25      PARM=NITAWL
CASE E.CCVR.24i.eim1,Inf.Unit, Cyl.Arr.Center,d=1.25cm,Pitch=2.7273cm,,0.84wt%
238GROUPNDF5
READ COMP
U     1     DEN=19.05    1.0   293    92235   0.84   92238    99.16  END
BEBOUND     2     DEN=1.85       0.5     293   END
H2O               2    DEN=0.9982       0.25     293   END
POLY(H2O)  2    DEN=0.923       0.25     293   END
SS304          4                          1.0   293  END
H2O    5   DEN=0.9982   0.00001   293  END
PB      6                              1.0   293   END
END COMP
READ CELLDATA
LATTICECELL  SQUAREPITCH  PITCH=2.7273    2   FUELR=0.625  1  END
END CELLDATA
READ PARAM   GEN=1100  NPG=1000  NSK=100  TBA=5  END PARAM
READ GEOM
UNIT 1
CYLINDER      1      1     0.625         2p37.9233
CUBOID                2      1   4P1.36365    2p37.9233
UNIT 2
ARRAY     1    3*0.0
UNIT 3
ARRAY     2    3*0.0
UNIT 4
ARRAY     3    3*0.0
UNIT 5
ARRAY     4    3*0.0
UNIT 6
ARRAY     5    3*0.0
UNIT 7
ARRAY     6    3*0.0
UNIT 8
ARRAY     7    3*0.0
UNIT 9
ARRAY     8    3*0.0
UNIT 10
ARRAY     9    3*0.0
GLOBAL UNIT 14
CYLINDER   2   1     39.6875    2P154.31
HOLE     2       -27.273  -27.273  -37.9232
HOLE     3       -30.000305   -24.5457  -37.9232
HOLE     3       27.273005   -24.5457  -37.9232
HOLE     4       -24.5457   27.273005  -37.9232
HOLE     4       -24.5457   -30.000305  -37.9232
HOLE     5       -32.72761   -21.8184  -37.9232
HOLE     5       30.00031   -21.8184  -37.9232
HOLE     6       -21.8184   30.00031  -37.9232
HOLE     6       -21.8184   -32.72761  -37.9232
HOLE     7       -35.454915   -16.3638  -37.9232
HOLE     7       32.727615   -16.3638  -37.9232
HOLE     8       -16.3638   32.727615  -37.9232
HOLE     8       -16.3638   -35.454915  -37.9232
HOLE     9       -38.18222   -8.1819  -37.9232
HOLE     9       35.45492   -8.1819  -37.9232
HOLE     10       -8.1819   35.45492  -37.9232
```

```
HOLE     10       -8.1819   -38.18222  -37.9232
CYLINDER   4   1     43.18        2p154.31
CYLINDER   6   1     47.9425   2p154.31
CYLINDER   4   1     52.07       2p154.31
CYLINDER   4   1     52.07       187.33     -170.82
CYLINDER   5   1    72.39     216.54    -200.03
CUBOID     5   1    4P72.39   216.54    -200.03
END GEOM
READ ARRAY
ARA=1      NUX=20          NUY=20         NUZ=1    FILL  F1   END FILL
ARA=2      NUX=1          NUY=18         NUZ=1    FILL  F1   END FILL
ARA=3      NUX=18          NUY=1         NUZ=1    FILL  F1   END FILL
ARA=4      NUX=1          NUY=16         NUZ=1    FILL  F1   END FILL
ARA=5      NUX=16          NUY=1         NUZ=1    FILL  F1   END FILL
ARA=6      NUX=1          NUY=12         NUZ=1    FILL  F1   END FILL
ARA=7      NUX=12          NUY=1         NUZ=1    FILL  F1   END FILL
ARA=8      NUX=1          NUY=6         NUZ=1    FILL  F1   END FILL
ARA=9      NUX=6          NUY=1         NUZ=1   FILL  F1   END FILL
END ARRAY
READ BOUNDS
ALL=MIRROR
END BOUNDS
END DATA
END
```

This page intentionally left blank.

7.0 OPERATING PROCEDURES

7.1 Procedures for Loading the Package

Loading the RH-TRU 72-B package for transport involves: 1) prior loading and measuring the payload canisters, 2) dry-loading the prepared payload canister into the RH-TRU 72-B package, 3) leakage rate testing the RH-TRU 72-B package outer cask (OC) and, optionally, the inner vessel (IV) seals, and (4) securing the external impact limiters to the RH-TRU 72-B package. All leakage rate testing procedures implemented for the pre-shipment leak tests identified within this section shall be developed and approved by personnel certified through the American Society for Nondestructive Testing (ASNT) as a Level III in the method of Leak Testing.

7.1.1 Loading the Payload Canister

The RH-TRU payload canister shall be prepared in accordance with the *Remote-Handled Transuranic Waste Authorized Methods for Payload Control* (RH-TRAMPAC)[1].

7.1.2 Loading the RH-TRU 72-B Package

This section delineates the procedures for loading the payload canister into the RH-TRU 72-B package. The package may be transported on either of two trailers, the Center-Pivot Trailer (CPT) or the Lift-Off Trailer (LOT). Because of differences in tie-down and loading/unloading method, the following procedures note where the differences exist and provide specific directions for each trailer.

The loading operation shall only be performed in a dry (no precipitation) environment. In the event of sudden precipitation during outdoor loading operations, precautions, such as covering the OC and IV cavities, shall be implemented to prevent water from entering the cavities. If precipitation enters the cavities, the free-standing water shall be removed. For the IV cavity, the payload canister shall be removed from the IV, and the IV cavity shall be dried using a vacuum system or absorbent materials attached to the end of a rod to remove the free-standing water. For the OC cavity, the payload canister shall be removed from the IV, the IV shall be removed from the OC, and the OC cavity shall be dried using a vacuum system or absorbent materials attached to the end of a rod to remove the free-standing water.

Only the lid shall be lifted by the pintle socket. If the IV is to be lifted, either empty or loaded, it shall be lifted using a handling fixture that interfaces with the holes on the lid, as indicated on the drawings in Appendix 1.3.1, *Packaging General Arrangement Drawings*. The approximate weight of the loaded IV is 12,023 pounds.

For all venting, loading, and unloading operations, ensure that appropriate controls are in place to control spread of contamination and protect against excessive personnel radiation exposure.

[1] U.S. Department of Energy (DOE), *Remote-Handled Transuranic Waste Authorized Methods for Payload Control* (RH-TRAMPAC), U.S. Department of Energy, Carlsbad Field Office, Carlsbad, New Mexico.

The only special tools, other than standard socket sets for bolts and the lifting equipment for the package, are the leakage rate test tool and standard leakage rate test equipment, including the optional rate-of-rise leakage rate test equipment.

While disassembling the packaging in preparation for loading, the shipping facility personnel shall check the condition of the packaging components for acceptability. Damaged or defective components shall be replaced or suitably repaired before loading and reassembling the package for shipment.

Prior to loading, packaging surfaces shall be radiologically surveyed and checked for contamination, and the results of the checks shall be recorded.

If the OC lid has been removed, proceed directly to Paragraph 7.1.2.4. If both the OC and IV lids have been removed, proceed directly to Paragraph 7.1.2.7. Hereafter, reference to each RH-TRU 72-B package component may be found in Appendix 1.3.1, *Packaging General Arrangement Drawings*.

7.1.2.1 If possible, locate the RH-TRU 72-B package under a temporary structure or in a building where it will not be exposed to precipitation and remove the impact limiters.

CPT: Disconnect the fixed tie-down links, rotate the package to a vertical orientation about the package center-pivot trunnions, and secure. Alternatively, if desired, lift the package off the trailer and place in a vertical holding fixture, supported by the center-pivot trunnions.

LOT: Disconnect the main tie-down trunnion caps (may additionally include lower trunnion caps) and attach a lift yoke to the upper trunnions. Upend the package, rotating about the lower trunnions. Remove remaining tie-down caps, as necessary. Lift the package off the trailer and place in a vertical holding fixture, supported by the center-pivot trunnions.

7.1.2.2 Unscrew the OC lid gas sampling port closure bolt. As an option, install appropriate fittings into the OC lid gas sampling port to unscrew the gas sampling port closure bolt. The appropriate fittings will include a specially-designed tool that will allow manipulation of the gas sampling port closure bolt in predetermined increments. This tool will be referred to as a "test port tool".

7.1.2.3 Remove the eighteen (18), 1¼-7UNC bolts from the OC lid. If not already in place, optionally install the OC lid to body alignment pins. Remove the lid and store in a protected area to preclude damage to the lid sealing surface.

7.1.2.4 If an optional OC sealing area protection device is to be used, install over the sealing area on the OC.

7.1.2.5 Unscrew the IV lid gas sampling port closure bolt. As an option, install a test port tool into the IV lid gas sampling port and rotate the knurled handle to unscrew the gas sampling port closure bolt.

7.1.2.6 Remove the eight (8), 7/8-9UNC bolts from the IV lid. If not already in place, optionally install the IV lid to body alignment pins. Remove the lid and store in a protected area to preclude damage to the lid sealing surface.

7.1.2.7 If an optional IV sealing area/protection device is to be used, install over the sealing area on the IV. If an optional guide funnel or package loading collar is to be used, install over the package.

7.1.2.8 Transfer the payload canister into the IV. (If a horizontal transfer is planned, the package must be moved to the transfer fixture and downended prior to transfer.)

7.1.2.9 If necessary, upend the package prior to installing lids. If utilized in Paragraph 7.1.2.7, remove the optionally installed guide funnel and/or package loading collar, and remove the IV sealing area protection device from the IV. If not installed in Paragraph 7.1.2.6, install the IV lid to body alignment pins.

7.1.2.10 Optionally clean and visually inspect the three O-ring seals on the IV lid in accordance with Section 8.2.3.4.1, *Sealing Area Routine Inspection and Repair*. Clean and visually inspect both O-ring seals on the OC lid, also in accordance with Section 8.2.3.4.1, *Sealing Area Routine Inspection and Repair*. Sparingly apply new vacuum grease to the seals. Replace the O-ring seals if the inspection reveals any condition that may affect the sealing capability of the elastomer seal. This may be done anytime prior to installation as long as the cleanliness is verified just prior to installation. Inspect and clean as necessary the seals on the test and gas sample ports.

7.1.2.11 Optionally clean and visually inspect the sealing area on the IV body in accordance with Section 8.2.3.4.1, *Sealing Area Routine Inspection and Repair*.

7.1.2.12 Install the IV lid, tightening in a star pattern the eight (8), 7/8-9UNC bolts to 100 – 200 lb-ft torque.

7.1.2.13 If utilized in Paragraph 7.1.2.7, remove the guide funnel or package loading collar from the package. Optionally remove the IV lid to body alignment pins.

7.1.2.14 Install the gas sampling port closure bolt and tighten to approximately 15 – 20 lb-ft torque.

7.1.2.15 Optionally perform a *Preshipment Leakage Rate Test* per Appendix 7.4.1, *Preshipment Leakage Rate Test*, or *Maintenance Leakage Rate Test* per Section 8.2.2, *Maintenance/Periodic Leakage Rate Tests*, on each IV containment sealing component (i.e., the lid seal, using the seal test port, the gas sampling port plug seal, and the helium backfill port plug seal).

(Maintenance leakage rate testing per Section 8.2.2, *Maintenance/Periodic Leakage Rate Tests*, is required if any containment O-ring seals are replaced.)

7.1.2.16 If utilized in Paragraph 7.1.2.4, remove the OC sealing area protection device from the OC. If not installed in Paragraph 7.1.2.3, install the OC lid to body alignment pins.

7.1.2.17 Clean and visually inspect the sealing area on the OC body in accordance with Section 8.2.3.4.1, *Sealing Area Routine Inspection and Repair*.

7.1.2.18 Install the OC lid, tightening in a star pattern the eighteen (18), 1¼-7UNC bolts to 600 – 700 lb-ft torque. Optionally remove the OC lid to body alignment pins.

7.1.2.19 If not previously done so in Paragraph 7.1.2.2, install a test port tool into the OC lid gas sampling port.

7.1.2.20 Utilizing the test port tool, install the gas sampling port closure bolt (tighten to approximately 15 – 20 lb-ft torque).

7.1.2.21 Perform a *Preshipment Leakage Rate Test* per Appendix 7.4.1, *Preshipment Leakage Rate Test*, or *Maintenance Leakage Rate Test* per Section 8.2.2, *Maintenance/Periodic Leakage Rate Tests*, on each OC containment sealing component (i.e., the lid seal, using the seal test port, and the gas sampling port plug seal).

7.1.2.22 Monitor the radiation level to ensure the package meets the requirements of 10 CFR §71.47[2] and 49 CFR §173.441[3] in accordance with Section 3.2 of the RH-TRAMPAC[1]. Survey the package surface and ensure that non-fixed contamination levels meet the requirements of 49 CFR §173.443.

7.1.2.23 CPT: If previously removed, return the RH-TRU 72-B package to the trailer. Return the RH-TRU 72-B package to a horizontal orientation by rotating it about the center-pivot trunnions.

7.1.2.24 LOT: Return the RH-TRU 72-B package to the trailer and downend it to a horizontal orientation by rotating it about its lower tie-down trunnions. (Lower tie-down trunnion caps may be secured prior to downending the package.)

7.1.2.25 Secure the package to the trailer using the fixed tie-down links (CPT) or trunnion caps (LOT).

7.1.2.26 Install the impact limiters and secure each via the six (6), 1¼-7UNC impact limiter attachment bolts. Tighten the bolts to 600 – 700 lb-ft torque.

7.1.2.27 Install a bolt, flat washer, and nut into each of the two impact limiter lifting lugs on each impact limiter to preclude their use as tie-down devices.

7.1.2.28 Install the tamper-indicating device.

7.1.2.29 Complete all necessary shipping papers in accordance with Subpart C of 49 CFR 172[4].

7.1.2.30 Package marking shall be in accordance with Subpart D, labeling shall be in accordance with Subpart E, and placarding shall be in accordance with Subpart F of 49 CFR 172[4].

[2] Title 10, Code of Federal Regulations, Part 71 (10 CFR 71), *Packaging and Transportation of Radioactive Material*, 01-01-14 Edition.

[3] Title 49, Code of Federal Regulations, Part 173 (49 CFR 173), *Shippers—General Requirements for Shipments and Packagings*, U.S. Department of Transportation, Washington, D.C., Current Version.

[4] Title 49, Code of Federal Regulations, Part 172 (49 CFR 172), *Hazardous Materials Table, Special Provisions, Hazardous Materials Communications, Emergency Response Information, and Training Requirements*, U.S. Department of Transportation, Washington, D.C., Current Version.

7.2 Procedures for Unloading the Package

In general, procedures for unloading the RH-TRU 72-B package are the reverse of Section 7.1.2, *Loading the RH-TRU 72-B Package*.

Upon receipt of the package, the receiving facility personnel shall check and record the condition of the tamper-indicating device. If the device shows damage, but there is no indication that the packaging containment was breached, the incident should be dispositioned under the requirements of 10 CFR 71[1]. If there are indications that packaging containment has been compromised (this would involve removal of the upper impact limiter, at a minimum), the incident should be treated as a substantial hazard to public safety, and dealt with under the requirements of 10 CFR §71.95.

Upon receipt of the package and removal of the impact limiters, rotate the package to a vertical orientation and secure, if the Center-Pivot Trailer (CPT) is used. The package may be unloaded while still on the CPT or, if desired, remove the trunnion restraints and lift the package off the trailer. If the Lift-Off Trailer (LOT) is used, upend the package, rotating about the lower trunnions, and lift the package off the trailer. After removal from either trailer, place the package into a vertical holding fixture, supported by the center-pivot trunnions. Prior to removing either the OC or IV lids, a test port tool shall be installed in the respective gas sampling port and the containment vessel gas shall be vented. After each vessel has been vented, the respective lid may be removed. Store the lids in a manner such that potential damage to the lids is minimized.

After unloading the package, the receiving facility personnel shall check the internal surfaces for contamination and record the findings. The shipping labeling shall be removed.

[1] Title 10, Code of Federal Regulations, Part 71 (10 CFR 71), *Packaging and Transportation of Radioactive Material*, 01-01-14 Edition.

This page intentionally left blank.

7.3 Preparation of an Empty Package for Transport

Previously used and empty (i.e., without contents but fully assembled with the 1¼-7UNC OC lid closure and impact limiter attachment bolts optionally installed with 100 – 200 lb-ft torque) RH-TRU 72-B packages shall be handled per the requirements of 49 CFR §173.428[1]. Among other stipulations, the referenced regulation requires: 1) verification that the radiation on the external surface of the package does not exceed 0.5 millirem per hour, and 2) affixing an "EMPTY" label to the package. Leakage rate testing of the seals is not required for shipping an empty package meeting the requirements of 49 CFR §173.428.

7.3.1 Shipment of the Package as LSA Material

If the contents and the internal contamination of the package meet the definition of *Low Specific Activity* (LSA) material per 49 CFR §173.403[1], the RH-TRU 72-B package shall be handled per the requirements of 49 CFR §173.427 and shipped in accordance with the following.

7.3.1.1 With the package disassembled, verify that the contents, including internal contamination, meet the requirements of 49 CFR 173.403[1].

7.3.1.2 Close the inner vessel (IV) and outer cask (OC) in accordance with Paragraphs 7.1.2.9 through 7.1.2.13, Paragraphs 7.1.2.16 through 7.1.2.18, and Paragraphs 7.1.2.22 through 7.1.2.28 of Section 7.1.2, *Loading the RH-TRU 72-B Package*. Ensure all seal test ports, gas sampling ports, and helium backfill ports are properly sealed and covered.

7.3.1.3 If shipped in accordance with Section 7.3.1, *Shipment of the Package as LSA Material*, the package must be labeled as an LSA material shipment.

[1] Title 49, Code of Federal Regulations, Part 173 (49 CFR 173), *Shippers—General Requirements for Shipments and Packagings*, U.S. Department of Transportation, Washington, D.C., Current Version.

This page intentionally left blank.

7.4 Appendices

7.4.1 *Preshipment Leakage Rate Test*

This page intentionally left blank.

7.4.1 Preshipment Leakage Rate Test

After the RH-TRU 72-B package is assembled and prior to shipment, leakage rate testing shall be performed to confirm proper assembly of the package following the guidelines of Section 7.6, *Preshipment Leakage Rate Test*, and Appendix A.5.2, *Gas Pressure Rise*, of ANSI N14.5[1].

7.4.1.1 Gas Pressure Rise Leakage Rate Test Acceptance Criteria

In order to demonstrate containment integrity in preparation for shipment, no leakage shall be detected when tested to a sensitivity of 1×10^{-3} reference cubic centimeters per second (scc/s) air, or less, per Section 7.6, *Preshipment Leakage Rate Test*, of ANSI N14.5.

7.4.1.2 Determining the Test Volume and Test Time

1. Assemble a leakage rate test apparatus that consists of, at a minimum, the components illustrated in Figure 7.4-1, using a calibrated volume with a range of 100 – 500 cubic centimeters, and a calibrated pressure transducer with a minimum sensitivity of 100 millitorr. Connect the test apparatus to the test volume (i.e., the outer cask (OC) seal test port or gas sampling port, or the inner vessel (IV) seal test port, gas sampling port, or helium backfill port, as appropriate).
2. Set the indicated sensitivity on the digital readout of the calibrated pressure transducer, ΔP, to, at a minimum, the resolution (i.e., sensitivity) of the calibrated pressure transducer (e.g, $\Delta P = 0.1$, 0.01, or 0.001 torr for a pressure transducer with a 1 millitorr sensitivity).
3. Open all valves (i.e., the vent valve, calibration valve, and vacuum pump isolation valve), and record ambient atmospheric pressure, P_{atm}.
4. Isolate the calibrated volume by closing the vent and calibration valves.
5. Evacuate the test volume to a pressure greater than 10% below the ambient atmospheric pressure.
6. Isolate the vacuum pump from the test volume by closing the vacuum pump isolation valve. Allow the test volume pressure to stabilize and record the test volume pressure, P_{test}.
7. Open the calibration valve and, after allowing the system to stabilize, record the total volume pressure, P_{total}.
8. Knowing the calibrated volume, V_c, calculate and record the test volume, V_t, using the following equation:

$$V_t = V_c \left(\frac{P_{atm} - P_{total}}{P_{total} - P_{test}} \right)$$

[1] ANSI N14.5-2014, *American National Standard for Radioactive Materials – Leakage Tests on Packages for Shipment,* American National Standards Institute, Inc. (ANSI).

9. Knowing the indicated sensitivity on the digital readout of the calibrated pressure transducer, ΔP (torr), the test volume, V_t (cubic centimeters), atmospheric pressure, P_{atm} (torr), test pressure, P_{test} (torr), and leakage rate test sensitivity, 1×10^{-3} scc/s, calculate and record the test time, t (seconds), using the following equation:

$$t = \left(\frac{V_t \Delta P}{1 \times 10^{-3} \text{ scc/s}} \right) \left(\frac{P_{atm}}{P_{atm}^2 - P_{test}^2} \right)$$

7.4.1.3 Performing the Gas Pressure Rise Leakage Rate Test

1. Isolate the calibrated volume by closing the calibration valve.

2. Open the vacuum pump isolation valve and evacuate the test volume to a pressure less than the test volume pressure, P_{test}, determined in step 6 of Section 7.4.1.2, *Determining the Test Volume and Test Time*.

3. Isolate the vacuum pump from the test volume by closing the vacuum pump isolation valve. Allow the test volume pressure to stabilize and record the beginning test temperature, T_1, and test pressure, P_1. After a period of time equal to "t" seconds, determined in step 9 of Section 7.4.1.2, *Determining the Test Volume and Test Time*, record the ending test temperature, T_2, and test pressure, P_2. To be acceptable, there shall be no difference between the final and initial temperatures and pressures such that the requirements of Section 7.4.1.1, *Gas Pressure Rise Leakage Rate Test Acceptance Criteria*, are met.

4. If, after repeated attempts, the O-ring seal fails to pass the leakage rate test, replace the damaged seal and/or repair the damaged sealing surfaces per Section 8.2.3.4.1, *Sealing Area Routine Inspection and Repair*. Perform verification leakage rate test per the applicable procedure delineated in Section 8.2.2, *Maintenance/Periodic Leakage Rate Tests*.

7.4.1.4 Optional Preshipment Leakage Rate Test

As an option to Section 7.4.1.3, *Performing the Gas Pressure Rise Leakage Rate Test*, Section 8.2.2, *Maintenance/Periodic Leakage Rate Tests*, may be performed in its entirety or on individual containment seals that have not otherwise been shown to pass the *Gas Pressure Rise Leakage Rate Test*.

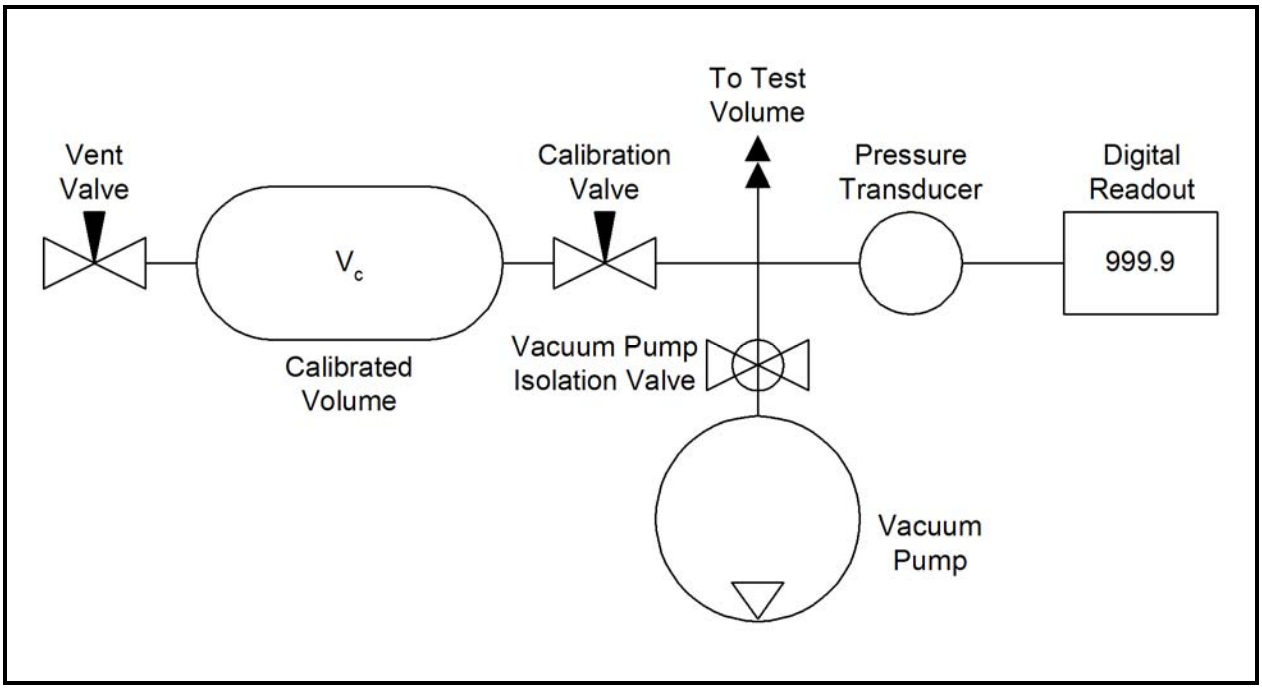

Figure 7.4-1 – Pressure Rise Leakage Rate Test Schematic

This page intentionally left blank.

8.0 ACCEPTANCE TESTS AND MAINTENANCE PROGRAM

This section describes the acceptance test and the maintenance program that shall be used on the RH-TRU 72-B package in compliance with Subpart G of 10 CFR 71[1].

8.1 Acceptance Tests

This section discusses the tests to be performed prior to first use of the RH-TRU 72-B package.

8.1.1 Visual Inspection

All RH-TRU 72-B packaging materials of construction and welds shall be examined in accordance with requirements delineated on the drawings in Appendix 1.3.1, *Packaging General Arrangement Drawings*, per the requirements of 10 CFR 71.85(a)[1].

Each package shall be visually inspected to ensure that it is conspicuously and durably marked with its model number, serial number, gross weight, and packaging identification number, per the requirements of 10 CFR 71.85(c)[1].

8.1.2 Structural and Pressure Tests

8.1.2.1 Lifting Device Load Testing

The maximum working load for any pair of lifting/tie-down trunnions is 45,000 pounds, or 22,500 pounds per trunnion. Each pair of the lifting/tie-down trunnions shall be load tested to a minimum of 150% of their maximum working load, or 67,500 pounds.

The maximum working load of the two center-pivot trunnions is 45,000 pounds, or 22,500 pounds per trunnion. The pair of center-pivot trunnions shall be load tested to a minimum of 150% of their maximum working load, or 67,500 pounds.

The maximum working load for the inner vessel (IV) lift pintle socket is 4,000 pounds (1,390 pounds for the lid weight, plus 2,610 pounds for residual vacuum and lid separation force due to O-ring seal resistance). The IV lid lift pintle socket shall be load tested to 150% of the maximum working load, or 6,000 pounds.

The maximum working load for the outer cask (OC) lid lift pintle socket is 4,000 pounds (1,670 pounds for the lid weight, plus 2,330 pounds for residual vacuum and lid separation force due to O-ring seal resistance). The OC lid lift pintle socket shall be load tested to 150% of the maximum working load, or 6,000 pounds.

All accessible welds and adjacent base material (minimum 1/2-inch on each side of the weld) directly related to the load testing of the lifting devices shall be visually inspected for plastic deformation or cracking, and liquid penetrant inspected per ASME Boiler and Pressure Vessel

[1] Title 10, Code of Federal Regulations, Part 71 (10 CFR 71), *Packaging and Transportation of Radioactive Material*, 01-01-14 Edition.

Code, Section V[2], Article 6, and ASME Boiler and Pressure Vessel Code, Section III[3], Division 1, Subsection NB, Article NB-5000, as delineated on the drawings in Appendix 1.3.1, *Packaging General Arrangement Drawings*. Indications of cracking or distortion shall be recorded on a nonconformance report and dispositioned prior to final acceptance in accordance with the cognizant quality assurance program.

8.1.2.2 Inner Vessel and Outer Cask Pressure Testing

Per the requirements of 10 CFR §71.85(b) [1], the IV and OC shall be pressure tested to 150% of the maximum normal operating pressure (MNOP) to verify structural integrity. The MNOP of the IV and OC is equal to the 150 psig design pressure. Thus, each containment vessel shall be tested to 150 × 1.5 = 225 psig.

Following containment vessel pressure testing, all accessible welds and adjacent base material (minimum 1/2-inch on each side of the weld) directly related to the pressure testing of the containment vessels shall be visually inspected for plastic deformation or cracking, and liquid penetrant inspected per ASME Boiler and Pressure Vessel Code, Section V[2], Article 6, and ASME Boiler and Pressure Vessel Code, Section III[3], Division 1, Subsection NB, Article NB-5000. Indications of cracking or distortion shall be recorded on a nonconformance report and dispositioned prior to final acceptance in accordance with the cognizant quality assurance program.

8.1.3 Fabrication Leakage Rate Tests

Fabrication Leakage Rate Testing shall conform to the requirements of Section 7.3 of ANSI N14.5[4]. All leakage rate testing procedures implemented for the fabrication leak tests identified within this section shall be developed and approved by personnel certified through the American Society for Nondestructive Testing (ASNT) as a Level III in the method of Leak Testing.

The *Fabrication Leakage Rate Test* shall be performed after the structural and/or pressure test(s) delineated in Section 8.1.2, *Structural and Pressure Tests*, above, to verify package configuration and performance to design criteria.

To begin the test, the IV is assumed separate from the OC, and the lids of each are removed. The *Fabrication Leakage Rate Test* is separated into seven (7) tests, four (4) for the IV and three (3) for the OC. The seven (7) separate tests are: 1) IV structure integrity, 2) IV lid seal integrity, 3) IV gas sampling port closure bolt seal integrity, 4) IV backfill port seal integrity, 5) OC structure integrity, 6) OC lid seal integrity, and 7) OC gas sampling port closure bolt seal integrity.

8.1.3.0.1 Obtain a helium mass spectrometer leak detector capable of detecting a leak of 5×10^{-8} standard cubic centimeters per second (scc/s), air, or better (1.3×10^{-7} scc/s, helium).

---

[2] American Society of Mechanical Engineers (ASME) Boiler and Pressure Vessel Code, Section V, *Nondestructive Examination*, 1986 Edition.

[3] American Society of Mechanical Engineers (ASME) Boiler and Pressure Vessel Code, Section III, *Rules for Construction of Nuclear Power Plant Components*, 1986 Edition.

[4] ANSI N14.5-2014, *American National Standard for Radioactive Materials – Leakage Tests on Packages for Shipment,* American National Standards Institute, Inc. (ANSI).

8.1.3.0.2 Calibrate the leak detector to a minimum sensitivity of 5×10^{-8} scc/s, air (1.3×10^{-7} scc/s, helium) following the guidelines of Section 8.4, *Sensitivity*, and Annex A.5.3.4, *Test Method and Considerations*, of ANSI N14.5 for establishing the system response (dwell time) using a calibrated standard leak.

8.1.3.1 Testing the IV Structure Integrity

The *Fabrication Leakage Rate Test* of the IV structure shall be performed per Section A.5.4, *Evacuated Envelope – Gas Detector*, or Section A.5.3, *Gas Filled Envelope – Gas Detector*, of ANSI N14.5[4]. For testing the IV structure integrity using the *Evacuated Envelope Method*, go to Section 8.1.3.1.1, *Testing the IV Structure Integrity – Evacuated Envelope Method*, and for testing the IV structure integrity using the *Gas Filled Envelope Method*, go to Section 8.1.3.1.2, *Testing the IV Structure Integrity – Gas Filled Envelope Method*.

8.1.3.1.1 Testing the IV Structure Integrity – Evacuated Envelope Method

8.1.3.1.1.1 The IV shall be assembled with all three main O-ring seals installed in the IV lid. Assembly is as shown on the drawing in Appendix 1.3.1, *Packaging General Arrangement Drawings*.

8.1.3.1.1.2 Install the assembled IV into a functional OC body.

8.1.3.1.1.3 Install a test port tool into the IV gas sampling port.

8.1.3.1.1.4 Fully retract the IV gas sampling port closure bolt by rotating the cap on the test port tool to the fully open position.

8.1.3.1.1.5 Connect a vacuum pump to the IV gas sampling port.

8.1.3.1.1.6 Evacuate the IV cavity through the gas sampling port to 90% vacuum or better (≤10% ambient atmospheric pressure) at an ambient temperature of 40 ºF, or greater. Isolate the vacuum pump from the system.

8.1.3.1.1.7 Provide a helium atmosphere in the cavity of the IV by backfilling with helium gas to a pressure slightly greater than atmospheric pressure (+1 psi, -0 psi) and close the valve to isolate the source of helium gas from the system. Correction for tracer gas concentration shall be performed.

8.1.3.1.1.8 Install the IV gas sampling port closure bolt using the test port tool and tighten to 15 – 20 lb-ft torque.

8.1.3.1.1.9 Remove the IV test port tool.

8.1.3.1.1.10 Remove the OC gas sampling port closure bolt and install the OC lid.

8.1.3.1.1.11 Evacuate air from the OC/IV annulus through the OC gas sampling port until the vacuum is sufficient to operate the helium mass spectrometer leak detector.

8.1.3.1.1.12 Perform the leakage rate test to the requirements of Section 8.1.3.8, *Fabrication Leakage Rate Test Acceptance Criteria*. If after repeated attempts, the IV structure fails to pass the leakage rate test, isolate the leak path and, prior to repairing the leak path and repeating the IV structure leakage rate test, record the results of the

test and any recommended actions for disposition in accordance with the requirements of the cognizant quality assurance program.

8.1.3.1.2 Testing the IV Structure Integrity – Gas Filled Envelope Method

8.1.3.1.2.1 The IV shall be assembled with all three main O-ring seals installed in the lid. Assembly is as shown on the drawing in Appendix 1.3.1, *Packaging General Arrangement Drawings*.

8.1.3.1.2.2 Remove the IV gas sampling port closure bolt and install the helium mass spectrometer to the IV gas sampling port.

8.1.3.1.2.3 Surround the assembled IV with an envelope.

8.1.3.1.2.4 Evacuate the IV cavity through the IV gas sampling port until the vacuum is sufficient to operate the helium mass spectrometer leak detector.

8.1.3.1.2.5 Provide a helium environment at a pressure slightly above one atmosphere around the exterior of the IV, taking care to purge all other gases from any pockets or cavities adjacent to the vessel.

8.1.3.1.2.6 Determine the leakage rate of the system. Per Section A.3.6, *Tracer Gas Partial Pressure*, of ANSI N14.5[4], the measured leakage rate shall conservatively be multiplied by a factor of two to account for the less than 100% concentration of the helium in the envelope surrounding the IV.

8.1.3.1.2.7 Perform the leakage rate test to the requirements of Section 8.1.3.8, *Fabrication Leakage Rate Test Acceptance Criteria*. If after repeated attempts, the IV structure fails to pass the leakage rate test, isolate the leak path and, prior to repairing the leak path and repeating the IV structure leakage rate test, record the results of the test and any recommended actions for disposition in accordance with the requirements of the cognizant quality assurance program.

8.1.3.2 Testing the IV Lid Seal Integrity

8.1.3.2.1 The *Fabrication Leakage Rate Test* of the IV lid middle seal shall be performed per Section A.5.4, *Evacuated Envelope – Gas Detector*, of ANSI N14.5[4].

8.1.3.2.2 The IV shall be assembled with all three main O-ring seals installed in the IV lid. Assembly is as shown on the drawing in Appendix 1.3.1, *Packaging General Arrangement Drawings*.

8.1.3.2.3 Attach a vacuum pump and a source of helium gas, in parallel, to the backfill port. Fittings will include a specially-designed tool that will maintain a leak-tight interface between the backfill port and the helium supply/vacuum pump, while allowing manipulation of the backfill port closure bolt. This tool will be referred to as a "test port tool." Install valves on each of the lines to allow independent isolation of the vacuum pump and the source of helium gas to the backfill port. Close the valve to the source of helium gas, and open the valve to the vacuum pump. Figure 8.1-1 provides a schematic of this configuration.

8.1.3.2.4 Utilizing the test port tool, rotate the backfill port closure bolt fully open.

8.1.3.2.5 Evacuate the system to 90% vacuum or better (≤10% ambient atmospheric pressure). Isolate the vacuum pump from the system.

8.1.3.2.6 Provide a helium atmosphere inside the evacuated cavity by backfilling with helium gas to a pressure slightly greater than atmospheric pressure (+1 psi, -0 psi) and close the valve to isolate the source of helium gas from the system. Correction for tracer gas concentration shall be performed.

8.1.3.2.7 Utilizing the test port tool, rotate the backfill port closure bolt closed and tighten to 15 – 20 lb-ft torque.

8.1.3.2.8 Remove the helium-contaminated test port tool from the backfill port.

8.1.3.2.9 Install a clean (helium-free) test port tool into the seal test port.

8.1.3.2.10 Attach a leak detector to the test port tool.

8.1.3.2.11 Utilizing the test port tool, rotate the seal test port closure bolt fully open.

8.1.3.2.12 Evacuate the cavity above the lid containment seal until the vacuum is sufficient to operate the leak detector.

8.1.3.2.13 Determine the leakage rate of the system using the leak detector.

8.1.3.2.14 Perform the leakage rate test to the requirements of Section 8.1.3.8, *Fabrication Leakage Rate Test Acceptance Criteria*. If after repeated attempts, the IV lid containment seal fails to pass the leakage rate test, isolate the leak path and, prior to repairing the leak path and repeating the IV lid containment seal leakage rate test, record the results of the test and any recommended actions for disposition in accordance with the requirements of the cognizant quality assurance program.

8.1.3.3 Testing the IV Gas Sampling Port Closure Bolt Seal Integrity

8.1.3.3.1 The *Fabrication Leakage Rate Test* of the IV gas sampling port closure bolt containment seal shall be performed per Section A.5.4, *Evacuated Envelope – Gas Detector*, of ANSI N14.5[4].

8.1.3.3.2 The IV shall be assembled with all three main O-ring seals installed in the IV lid. Assembly is as shown on the drawing in Appendix 1.3.1, *Packaging General Arrangement Drawings*.

8.1.3.3.3 Verify the presence of a helium atmosphere below the gas sampling port closure bolt containment seal, as provided for in Paragraphs 8.1.3.2.3 through 8.1.3.2.8.

8.1.3.3.4 Tighten the IV gas sampling port closure bolt to 15 – 20 lb-ft torque.

8.1.3.3.5 Install a test port tool into the gas sampling port.

8.1.3.3.6 Attach a leak detector to the test port tool.

8.1.3.3.7 Evacuate the cavity above the gas sampling port closure bolt containment seal until the vacuum is sufficient to operate the leak detector.

8.1.3.3.8 Determine the leakage rate of the system using the leak detector.

8.1.3.3.9 Perform the leakage rate test to the requirements of Section 8.1.3.8, *Fabrication Leakage Rate Test Acceptance Criteria*. If after repeated attempts, the IV gas sampling port closure bolt containment seal fails to pass the leakage rate test, isolate the leak path and, prior to repairing the leak path and repeating the IV gas sampling port closure bolt containment seal leakage rate test, record the results of the test and any recommended actions for disposition in accordance with the requirements of the cognizant quality assurance program.

8.1.3.4 Testing the IV Backfill Port Closure Bolt Seal Integrity

8.1.3.4.1 The *Fabrication Leakage Rate Test* of the IV backfill port closure bolt containment seal shall be performed per Section A.5.4, *Evacuated Envelope – Gas Detector*, of ANSI N14.5[4].

8.1.3.4.2 The IV shall be assembled with all three main O-ring seals installed in the IV lid. Assembly is as shown on the drawing in Appendix 1.3.1, *Packaging General Arrangement Drawings*.

8.1.3.4.3 Verify the presence of a helium atmosphere below the backfill port closure bolt containment seal, as provided for in Paragraphs 8.1.3.2.3 through 8.1.3.2.8.

8.1.3.4.4 Install a clean (helium-free) test port tool into the backfill port. Attach a leak detector to the test port tool.

8.1.3.4.5 Evacuate the cavity above the backfill port closure bolt until the vacuum is sufficient to operate the leak detector.

8.1.3.4.6 Determine the leakage rate of the system using the leak detector.

8.1.3.4.7 Perform the leakage rate test to the requirements of Section 8.1.3.8, *Fabrication Leakage Rate Test Acceptance Criteria*. If after repeated attempts, the IV backfill port closure bolt containment seal fails to pass the leakage rate test, isolate the leak path and, prior to repairing the leak path and repeating the IV backfill port closure bolt containment seal leakage rate test, record the results of the test and any recommended actions for disposition in accordance with the requirements of the cognizant quality assurance program.

8.1.3.5 Testing the OC Structure Integrity

8.1.3.5.1 The *Fabrication Leakage Rate Test* of the OC structure shall be performed per Section A.5.3, *Gas Filled Envelope – Gas Detector*, of ANSI N14.5[4]. During fabrication, the OC containment shell shall be leakage rate tested prior to lead installation. Special lids and IV mock ups may be used for this component test. To test the OC structure in its entirety, the following steps shall be used.

8.1.3.5.2 As an option, remove the OC lid and install a functional or mock-up IV within the OC cavity for volume reduction.

8.1.3.5.3 Assemble the OC with both main O-ring seals installed in the OC lid. Assembly is as shown on the drawing in Appendix 1.3.1, *Packaging General Arrangement Drawings*.

8.1.3.5.4 Remove the OC gas sampling port closure bolt and install the helium mass spectrometer leak detector to the OC gas sampling port.

8.1.3.5.5 Surround the assembled OC with an envelope.

8.1.3.5.6 Evacuate the OC internal cavity annulus through the OC gas sampling port until the vacuum is sufficient to operate the helium mass spectrometer leak detector.

8.1.3.5.7 Provide helium at a pressure slightly above one atmosphere about the exterior of the OC, taking care to purge all other gases from any pockets or cavities adjacent to the vessel.

8.1.3.5.8 Determine the leakage rate of the system using the leak detector. Per Section A.3.6, *Tracer Gas Partial Pressure*, of ANSI N14.5[4], the measured leakage rate shall conservatively be multiplied by a factor of two to account for the less than 100% concentration of the helium in the envelope surrounding the OC.

8.1.3.5.9 Perform the leakage rate test to the requirements of Section 8.1.3.8, *Fabrication Leakage Rate Test Acceptance Criteria*. If after repeated attempts, the OC structure fails to pass the leakage rate test, isolate the leak path and, prior to repairing the leak path and repeating the OC structure leakage rate test, record the results for disposition in accordance with the requirements of the cognizant quality assurance program.

8.1.3.6 Testing the OC Lid Seal Integrity

8.1.3.6.1 The Fabrication Leakage Rate Test of the OC lid seal shall be performed per Section A.5.4, *Evacuated Envelope – Gas Detector*, of ANSI N14.5[4].

8.1.3.6.2 The OC shall be assembled with both main O-ring seals installed in the OC lid. Assembly is as shown on the drawing in Appendix 1.3.1, *Packaging General Arrangement Drawings*.

8.1.3.6.3 Install a test port tool into the OC gas sampling port.

8.1.3.6.4 Utilizing the test port tool, rotate the OC gas sampling port closure bolt fully open.

8.1.3.6.5 Attach a vacuum pump and a source of helium gas, in parallel, to the test port tool. Install valves on each of the lines to allow independent isolation of the vacuum pump and the source of helium gas to the test port tool. Close the valve to the source of helium gas, and open the valve to the vacuum pump. Figure 8.1-2 provides a schematic of this configuration.

8.1.3.6.6 Evacuate the system through the gas sampling port to 90% vacuum or better (≤10% ambient atmospheric pressure). Isolate the vacuum pump from the system.

8.1.3.6.7 Backfill with helium gas to a pressure slightly greater than atmospheric pressure (+1 psi, -0 psi) and close the valve to isolate the source of helium gas from the system. Correction for tracer gas concentration shall be performed.

8.1.3.6.8 Utilizing the test port tool, rotate the gas sampling port closure bolt closed, and tighten to 15 – 20 lb-ft torque.

8.1.3.6.9 Remove the helium-contaminated test port tool from the gas sampling port.

8.1.3.6.10 Install a clean (helium-free) test port tool into the seal test port.

8.1.3.6.11 Attach the leak detector to the test port tool.

8.1.3.6.12 Utilizing the test port tool, rotate the seal test port closure bolt fully open.

8.1.3.6.13 Evacuate the system through the test port tool until the vacuum is sufficient to operate the leak detector.

8.1.3.6.14 Determine the leakage rate of the system using the leak detector.

8.1.3.6.15 Perform the leakage rate test to the requirements of Section 8.1.3.8, *Fabrication Leakage Rate Test Acceptance Criteria*. If after repeated attempts, the OC lid containment seal fails to pass the leakage rate test, isolate the leak path and, prior to repairing the leak path and repeating the OC lid containment seal leakage rate test, record the results for disposition in accordance with the requirements of the cognizant quality assurance program.

8.1.3.7 Testing the OC Gas Sampling Port Closure Bolt Seal Integrity

8.1.3.7.1 The *Fabrication Leakage Rate Test* of the OC gas sampling port closure bolt containment seal shall be performed per Section A.5.4, *Evacuated Envelope – Gas Detector*, of ANSI N14.5[4].

8.1.3.7.2 The OC shall be assembled with both main O-ring seals installed in the OC lid. Assembly is as shown on the drawing in Appendix 1.3.1, *Packaging General Arrangement Drawings*.

8.1.3.7.3 Verify the presence of a helium atmosphere below the gas sampling port closure bolt containment seal, as provided for in Paragraphs 8.1.3.6.3 through 8.1.3.6.9.

8.1.3.7.4 Install a clean (helium-free) test port tool into the gas sampling port. Attach a leak detector to the test port tool.

8.1.3.7.5 Evacuate the cavity above the gas sampling port closure bolt until the vacuum is sufficient to operate the leak detector.

8.1.3.7.6 Determine the leakage rate of the system using the leak detector.

8.1.3.7.7 Perform the leakage rate test to the requirements of Section 8.1.3.8, *Fabrication Leakage Rate Test Acceptance Criteria*. If after repeated attempts, the OC gas sampling port closure bolt containment seal fails to pass the leakage rate test, isolate the leak path and, prior to repairing the leak path and repeating the OC gas sampling port closure bolt containment seal leakage rate test, record the results for disposition in accordance with the requirements of the cognizant quality assurance program.

8.1.3.8 Fabrication Leakage Rate Test Acceptance Criteria

8.1.3.8.1 To be acceptable, per Section 6.3.2, *Minimum Reference Air Leakage Rate*, of ANSI N14.5[4], each vessel test and each containment seal test shall demonstrate a leakage rate of 1×10^{-7} scc/s, air, (leaktight) (2.6×10^{-7} helium), or less.

8.1.3.8.2 In order to demonstrate that the package is leaktight, per Section 8.4, *Sensitivity*, of ANSI N14.5[4], the sensitivity of the leakage rate test procedure shall be 5×10^{-8} scc/s, air (1.3×10^{-7} helium), or less.

8.1.3.8.3 Indications of non-conformance with the above stated standards shall be recorded for disposition prior to repair and final acceptance in accordance with the requirements of the cognizant quality assurance program.

8.1.4 Component Tests

8.1.4.1 Polyurethane Foam

This section establishes the requirements and acceptance criteria for installation, inspection, and testing of rigid, closed cell, polyurethane foam utilized within the RH-TRU 72-B packaging.

8.1.4.1.1 Introduction and General Requirements

The polyurethane foam used within the RH-TRU 72-B packaging is comprised of a specific "formulation" of foam constituents that, when properly apportioned, mixed, and reacted, produce a polyurethane foam material with physical characteristics consistent with the requirements given in this section. In practice, the chemical constituents are batched into multiple parts (e.g., parts A and B) for later mixing in accordance with a formulation. Therefore, a foam "batch" is considered to be a specific grouping and apportionment of chemical constituents into separate and controlled vats or bins for each foam formulation part. Portions from each batch part are combined in accordance with the foam formulation requirements to produce the liquid foam material for pouring into a component. Thus, a foam "pour" is defined as apportioning and mixing the batch parts into a desired quantity for subsequent installation (pouring).

The following sections describe the general requirements for chemical composition, constituent storage, foamed component preparation, foam material installation, and foam pour and test data records.

8.1.4.1.1.1 Polyurethane Foam Chemical Composition

The foam supplier shall certify that the chemical composition of the polyurethane foam is as delineated below, with the chemical component weight percents falling within the specified ranges. In addition, the foam supplier shall certify that the finished (cured) polyurethane foam does not contain halogen-type flame retardants or trichloromonofluoromethane (Freon 11).

Carbon	50% – 70%	Phosphorus	0% – 2%
Oxygen	14% – 34%	Silicon	< 1%
Nitrogen	4% – 12%	Chlorine	< 1%
Hydrogen	4% – 10%	Other	< 1%

8.1.4.1.1.2 Polyurethane Foam Constituent Storage

The foam supplier shall certify that the polyurethane foam constituents have been properly stored prior to use, and that the polyurethane foam constituents have been used within their shelf life.

8.1.4.1.1.3 Foamed Component Preparation

Prior to polyurethane foam installation, the foam supplier shall verify that an anti-bond agent, such as Johnson's Wax, has been applied to all of the component shell interior surfaces. In addition, due to the internal pressures generated during the foam pouring/curing process, the foam supplier shall visually verify that adequate bracing/shoring of the component shells is provided to maintain the dimensional configuration throughout the foam pouring/curing process.

8.1.4.1.1.4 Polyurethane Foam Installation

The direction of foam rise shall be vertically aligned with the shell component axis.

The surrounding walls of the component shell where the liquid foam material is to be installed shall be between 55 ºF and 95 ºF prior to foam installation. Measure and record the component shell temperature to an accuracy of ±2 ºF prior to foam installation.

In the case of multiple pours into a single foamed component, the cured level of each pour shall be measured and recorded to an accuracy of ±1 inch.

Measure and record the weight of liquid foam material installed during each pour to an accuracy of ±10 pounds.

All test samples shall be poured into disposable containers at the same time as the actual pour it represents, clearly marking the test sample container with the pour date and a unique pour identification number. All test samples shall be cut from a larger block to obtain freshly cut faces. Prior to physical testing, each test sample shall be cleaned of superfluous foam dust.

8.1.4.1.1.5 Polyurethane Foam Pour and Test Data Records

A production pour and testing record shall be compiled by the foam supplier during the foam pouring operation and subsequent physical testing. Upon completion of production and testing, the foam supplier shall issue certification referencing the production record data and test data pertaining to each foamed component. At a minimum, relevant pour and test data shall include:

- formulation, batch, and pour numbers, with foam material traceability, and pour date,
- foamed component description, part number, and serial number,
- instrumentation description, serial number, and calibration due date,
- pour and test data (e.g., date, temperature, dimensional, and/or weight measurements, thermal conductivity, compressive stress, etc., as applicable), and
- technician and Quality Assurance/Quality Control (QA/QC) sign-off.

8.1.4.1.2 Physical Characteristics

The following subsections define the required physical characteristics of the polyurethane foam material used for the RH-TRU 72-B packaging design.

Testing for the various polyurethane foam physical characteristics is based on a "formulation", "batch", or "pour", as appropriate, as defined in Section 8.1.4.1.1, *Introduction and General Requirements*. The physical characteristics determined for a specific foam formulation are relatively insensitive to small variations in chemical constituents and/or environmental

conditions, and therefore include physical testing for thermal conductivity, specific heat, and leachable chlorides. Similarly, the physical characteristics determined for a batch are only slightly sensitive to small changes in formulation and/or environmental conditions during batch mixing, and therefore include physical testing for flame retardancy and intumescence. Finally, the physical characteristics determined for a pour are also only slightly sensitive to small changes in formulation and slightly more sensitive to variations in environmental conditions during pour mixing, and therefore include physical testing for density and compressive stress.

8.1.4.1.2.1 Physical Characteristics Determined for a Foam Formulation

1. Foam material physical characteristics for the following parameters shall be determined once for a particular foam formulation. If multiple components are to be foamed utilizing a specific foam formulation, then additional physical testing, as defined below, need not be performed.

8.1.4.1.2.1.1 Thermal Conductivity

1. The thermal conductivity test shall be performed using a heat flow meter (HFM) apparatus. The HFM establishes steady state unidirectional heat flux through a test specimen between two parallel plates at constant but different temperatures. By measurement of the plate temperatures and plate separation, Fourier's law of heat conduction is used by the HFM to automatically calculate thermal conductivity. Description of a typical HFM is provided in ASTM C518[5]. The HFM shall be calibrated against a traceable reference specimen per the HFM manufacturer's operating instructions.

2. Three (3) test samples shall be taken from the sample pour. Each test sample shall be of sufficient size to enable testing per the HFM manufacturer's operating instructions.

3. Measure and record the necessary test sample parameters as input data to the HFM per the HFM manufacturer's operating instructions.

4. Perform thermal conductivity testing and record the measured thermal conductivity for each test sample following the HFM manufacturer's operating instructions.

5. Determine and record the average thermal conductivity of the three test samples. The numerically averaged thermal conductivity of the three test samples shall be 0.019 Btu/hr-ft-ºF ±20% (i.e., within the range of 0.016 to 0.022 Btu/hr-ft-ºF).

8.1.4.1.2.1.2 Specific Heat

1. The specific heat test shall be performed using a differential scanning calorimeter (DSC) apparatus. The DSC establishes a constant heating rate and measures the differential heat flow into both a test specimen and a reference specimen. Description of a typical DSC is

[5] ASTM C518-04, *Standard Test Method for Steady-State Heat Flux Measurements and Thermal Transmission Properties by Means of the Heat Flux Meter Apparatus*, American Society for Testing and Materials, Philadelphia, PA, Volume 04.06, 2004.

provided in ASTM E1269[6]. The DSC shall be calibrated against a traceable reference specimen per the DSC manufacturer's operating instructions.

2. Three (3) test samples shall be taken from the sample pour. Each test sample shall be of sufficient size to enable testing per the DSC manufacturer's operating instructions.
3. Measure and record the necessary test sample parameters as input data to the DSC per the DSC manufacturer's operating instructions.
4. Perform specific heat testing and record the measured specific heat for each test sample following the DSC manufacturer's operating instructions.
5. Determine and record the average specific heat of the three test specimens. The numerically averaged specific heat at 77 °F of the three test samples shall be 0.30 Btu/lb-ºF ±20% (i.e., within the range of 0.24 to 0.36 Btu/lb-ºF).

8.1.4.1.2.1.3 Leachable Chlorides

1. The leachable chlorides test shall be performed using an ion chromatograph (IC) apparatus. The IC measures inorganic anions of interest (i.e., chlorides) in water. Description of a typical IC is provided in EPA Method 300.0[7]. The IC shall be calibrated against a traceable reference specimen per the IC manufacturer's operating instructions.
2. One (1) test sample shall be taken from the sample pour. The test sample shall be a cube with dimensions of 2.00 ±0.03 inches.
3. Place the test sample in a room (ambient) temperature environment (i.e., 65 ºF to 85 ºF) for sufficient time to thermally stabilize the test sample. Measure and record the room temperature to an accuracy of ±2 ºF.
4. Measure and record the thickness, width, and length of each test sample to an accuracy of ±0.001 inches.
5. Obtain a minimum of 550 ml of distilled or de-ionized water for testing. The test water shall be from a single source to ensure consistent anionic properties for testing control.
6. Obtain a 400 ml, or larger, contaminant free container that is capable of being sealed. Fill the container with 262 ±3 ml of test water. Fully immerse the test sample inside the container for a duration of 72 ±3 hours. If necessary, use an inert standoff to ensure the test sample is completely immersed for the full test duration. Seal the container prior to the 72 hour duration.
7. Obtain a second, identical container to use as a "control". Fill the control container with 262 ±3 ml of the same test water. Seal the control container for a 72 ±3 hour duration.
8. At the end of the test period, measure and record the leachable chlorides in the test water per the IC manufacturer's operating instructions. The leachable chlorides in the test water shall not exceed one part per million (1 ppm).

---

[6] ASTM E1269-05, *Standard Test Method for Determining Specific Heat Capacity by Differential Scanning Calorimetry*, American Society for Testing and Materials, Philadelphia, PA, Volume 14.02, 2005.

[7] EPA Method 300.0, *Determination of Inorganic Anions in Water by Ion Chromatography*, U.S. Environmental Protection Agency.

9. Should leachable chlorides in the test water exceed 1 ppm, measure and record the leachable chlorides in the test water from the "control" container. The difference in leachable chlorides from the test water and "control" water sample shall not exceed 1 ppm.

8.1.4.1.2.2 Physical Characteristics Determined for a Foam Batch

Foam material physical characteristics for the following parameters shall be determined once for a particular foam batch based on the batch definition from Section 8.1.4.1.1, *Introduction and General Requirements*. If a single or multiple components are to be poured utilizing multiple pours from a single foam batch, then additional physical testing, as defined below, need not be performed for each foam pour.

8.1.4.1.2.2.1 Flame Retardancy

1. Three (3) test samples shall be taken from a pour from each foam batch. Each test sample shall be a rectangular prism with nominal dimensions of 0.5 inches thick, 3.0 inches wide, and a minimum length of 6.0 inches. In addition, individual sample lengths must not be less than the total burn length observed for the sample when tested.

2. Place the test samples in a room (ambient) temperature environment (i.e., 65ºF to 85ºF) for sufficient time to thermally stabilize the test samples. Measure and record the room temperature to an accuracy of ±2ºF.

3. Measure and record the length of each test sample to an accuracy of ±0.1 inches.

4. Install a Ø3/8 inches (10 mm), or larger, Bunsen or Tirrill burner inside an enclosure of sufficient size to perform flame retardancy testing. Adjust the burner flame height to 1½ ±1/8 inches. Verify that the burner flame temperature is 1,550 ºF, minimum.

5. Support the test sample with the long axis oriented vertically within the enclosure such that the test sample's bottom edge will be 3/4 ±1/16 inches above the top edge of the burner.

6. Move the burner flame under the test sample for an elapsed time of 60 ±2 seconds. As illustrated, align the burner flame with the front edge of the test sample thickness and the center of the test sample width.

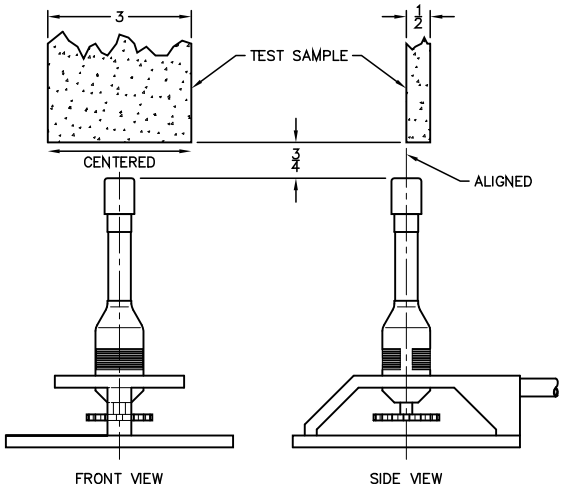

7. Immediately after removal of the test sample from the burner flame, measure and record the following data:

- **a.** Measure and record, to the nearest second, the elapsed time until flames from the test sample extinguish.
- **b.** Measure and record, to the nearest second, the elapsed time from the occurrence of drips, if any, until drips from the test sample extinguish.
- **c.** Measure and record, to the nearest 0.1 inches, the burn length following cessation of all visible burning and smoking.

8. Flame retardancy testing acceptance is based on the following criteria:

a. The numerically averaged flame extinguishment time of the three test samples shall not exceed fifteen (15) seconds.

b. The numerically averaged flame extinguishment time of drips from the three test samples shall not exceed three (3) seconds.

c. The numerically averaged burn length of the three test samples shall not exceed six (6) inches.

8.1.4.1.2.2.2 Intumescence

1. Three (3) test samples shall be taken from a pour from each foam batch. Each test sample shall be a cube with nominal dimensions of 2.0 inches.

2. Place the test samples in a room (ambient) temperature environment (i.e., 65 ºF to 85 ºF) for sufficient time to thermally stabilize the test samples. Measure and record the room temperature to an accuracy of ±2 ºF.

3. Preheat a furnace to 1,475 ºF ±18 ºF.

4. Identify two opposite faces on each test sample as the thickness direction. The thickness dimension shall be in the parallel-to-rise direction. Measure and record the initial thickness (t_i) of each test sample to an accuracy of ±0.01 inches.

5. Mount a test sample onto a fire resistant fiberboard, with one face of the thickness direction contacting to the board. As illustrated above, the test samples may be mounted by installing onto a 12 to 16 gauge wire (Ø0.105 to Ø0.063 inches, respectively) of sufficient length, oriented perpendicular to the fiberboard face. The test samples may be pre-drilled with an undersized hole to allow installation onto the wire.

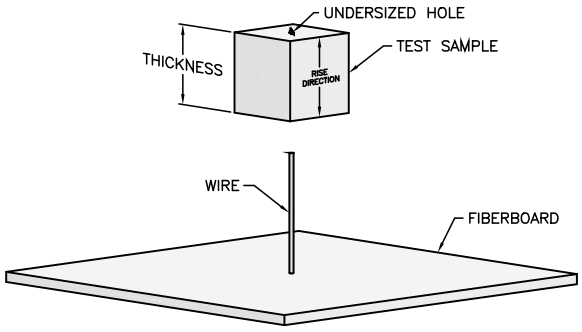

6. Locate the test sample/fiberboard assembly over the opening of the pre-heated furnace for a 90 ±3 second duration. After removal of the test sample/fiberboard assembly from the furnace, gently extinguish any remaining flames and allow the test sample to cool.

7. Measure and record the final thickness (t_f) of the test sample to an accuracy of ±0.1 inches.

8. For each sample tested, determine and record the intumescence, I, as a percentage of the original sample length as follows:

$$I = \frac{t_f - t_i}{t_i} \times 100$$

9. Determine and record the average intumescence of the three test samples. The numerically averaged intumescence of the three test samples shall be a minimum of 50%.

8.1.4.1.2.3 Physical Characteristics Determined for a Foam Pour

Foam material physical characteristics for the following parameters shall be determined for each foam pour based on the pour definition from Section 8.1.4.1.1, *Introduction and General Requirements*

8.1.4.1.2.3.1 Density

1. Three (3) test samples shall be taken from the foam pour. Each test sample shall be a rectangular prism with nominal dimensions of 1.0 inch thick (T) × 2.0 inches wide (W) × 2.0 inches long (L).
2. Place the test samples in a room (ambient) temperature environment (i.e., 65 ºF to 85 ºF) for sufficient time to thermally stabilize the test samples. Measure and record the room temperature to an accuracy of ±2 ºF.
3. Measure and record the weight of each test sample to an accuracy of ±0.01 grams.
4. Measure and record the thickness, width, and length of each test sample to an accuracy of ±0.001 inches.
5. Determine and record the room temperature density of each test sample utilizing the following formula:

$$\rho_{foam}\,(lb/ft^3) = \frac{Weight\,(g)}{453.6\,g/lb} \times \frac{1{,}728\,in^3/ft^3}{T\,(in) \times W\,(in) \times L\,(in)}$$

6. Determine and record the average density of the three test samples. The numerically averaged density of the three test samples shall nominally be 11.5 lb/ft^3 ±15% (i.e., within the range of 9.8 to 13.2 lb/ft^3).

8.1.4.1.2.3.2 Parallel-to-Rise Compressive Stress

1. Three (3) test samples shall be taken from the foam pour. Each test sample shall be a rectangular prism with nominal dimensions of 1.0 inch thick (T) × 2.0 inches wide (W) × 2.0 inches long (L). The thickness dimension shall be the parallel-to-rise direction.
2. Place the test samples in a room (ambient) temperature environment (i.e., 65 ºF to 85 ºF) for sufficient time to thermally stabilize the test samples. Measure and record the room temperature to an accuracy of ±2 ºF.
3. Measure and record the thickness, width, and length of each test sample to an accuracy of ±0.001 inches.

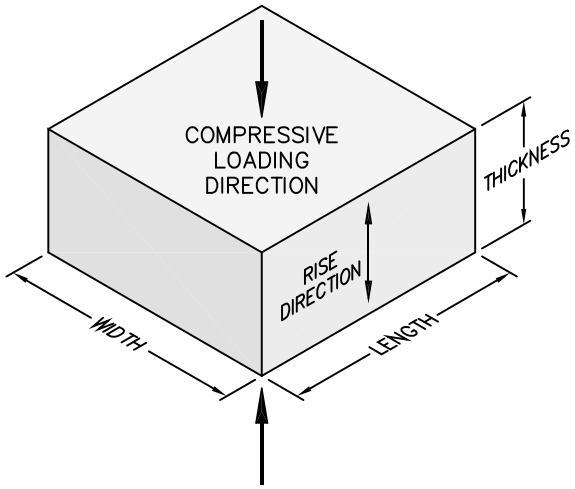

4. Compute and record the surface area of each test sample by multiplying the width by the length (i.e., W × L).

5. Place a test sample in a Universal Testing Machine. Lower the machine's crosshead until it touches the test sample. Set the machine's parameters for the thickness of the test sample.
6. Apply a compressive load to each test sample at a rate of 0.10 ±0.05 inches/minute until a strain of 70%, or greater, is achieved. For each test sample, plot the compressive stress versus strain and record the compressive stress at strains of 10%, 40%, and 70%.
7. Determine and record the average parallel-to-rise compressive stress of the three test samples from each pour. As delineated in Table 8.1-1, the average parallel-to-rise compressive stress for each pour shall be the nominal compressive stress ±15% at strains of 10%, 40%, and 70%.
8. Determine and record the average parallel-to-rise compressive stress of all test samples from each foamed component. As delineated in Table 8.1-1, the average parallel-to-rise compressive stress for a foamed component shall be the nominal compressive stress ±10% at strains of 10%, 40%, and 70%.

8.1.4.1.2.3.3 Perpendicular-to-Rise Compressive Stress

1. Three (3) test samples shall be taken from the foam pour. Each test sample shall be a rectangular prism with nominal dimensions of 1.0 inch thick (T) × 2.0 inches wide (W) × 2.0 inches long (L). The thickness dimension shall be the perpendicular-to-rise direction.
2. Place the test samples in a room (ambient) temperature environment (i.e., 65 ºF to 85 ºF) for sufficient time to thermally stabilize the test samples. Measure and record the room temperature to an accuracy of ±2 ºF.
3. Measure and record the thickness, width, and length of each test sample to an accuracy of ±0.001 inches.

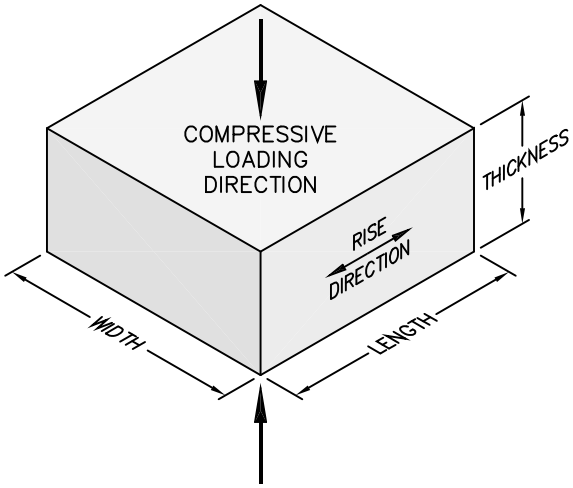

4. Compute and record the surface area of each test sample by multiplying the width by the length (i.e., W × L).
5. Place a test sample in a Universal Testing Machine. Lower the machine's crosshead until it touches the test sample. Set the machine's parameters for the thickness of the test sample.
6. Apply a compressive load to each test sample at a rate of 0.10 ±0.05 inches/minute until a strain of 70%, or greater, is achieved. For each test sample, plot the compressive stress versus strain and record the compressive stress at strains of 10%, 40%, and 70%.
7. Determine and record the average perpendicular-to-rise compressive stress of the three test samples from each pour. As delineated in Table 8.1-1, the average perpendicular-to-rise compressive stress for each pour shall be the nominal compressive stress ±15% at strains of 10%, 40%, and 70%.

8. Determine and record the average perpendicular-to-rise compressive stress of all test samples from each foamed component. As delineated in Table 8.1-1, the average perpendicular-to-rise compressive stress for a foamed component shall be the nominal compressive stress ±10% at strains of 10%, 40%, and 70%.

8.1.5 Tests for Shielding Integrity

Poured lead shielding integrity shall be confirmed via gamma scanning. There are two gamma scan techniques utilized. The main difference is in the method utilized to determine acceptance criteria. Both gamma scan techniques are exactly the same in all other respects and are conducted as follows.

An Eberline E120 probe, or equivalent, is used to scan the OC surface while an iridium-192 or cobalt-60 source of sufficient strength is present at the center of the OC cavity. The source is first placed on the bottom of the package cavity while the outer surface is scanned around its circumference, parallel to the source. The source is then moved up a predetermined distance and the circumference scanned again. This sequence is repeated until the entire package surface is scanned.

The OC outer surface is gridded and a chart is made to reflect the gridded surface. Dose rates are recorded from each grid square by scanning every point in the grid and recording the maximum dose rates in the corresponding grid on the chart. This data then serves as the raw gamma scan results. All dose rates are in milliroentgens per hour (mR/hr).

The dose rates are evaluated by comparing them to predetermined dose rate values for nominal (as designed) lead thickness and nominal less 10% lead thickness. The two different methods utilized to determine acceptance criteria are discussed below.

The first method, the *Laboratory Calibration Method*, utilizes test blocks of the package wall made up of lead and steel sheets. The test blocks simulate nominal, or as designed, and nominal less 10% lead thicknesses. The source is placed behind the nominal test block assembly at a distance equal to the inside radius of the package. The probe is then placed on the outside of the test block assembly and dose readings are recorded. This test sequence is repeated on the nominal less 10% test block assembly. The resultant dose values are then utilized as acceptance criteria for the actual gamma scan. Additionally, the expected dose rate values for nominal and reduced thickness shielding are calculated utilizing attenuation values for steel, lead, and air as correlation verification.

The second method, the *Field Calibration Method*, utilizes a specially fabricated test lid which incorporates a holder for various lead and steel sheet thicknesses. This fixture is installed onto the package to be scanned, with the test lid set up to simulate the nominal lead thickness. The source is placed below the test lid, inside the package, at a distance equal to the inside radius of the package. A dose reading is then recorded. The lead sheet thickness in the test lid holder is then adjusted to establish the nominal less 10% lead thickness configuration. Again, the source is placed below the test lid at a distance equal to the inside radius of the package and a dose reading is recorded. Additional dose readings are taken in 1/8-inch lead thickness increments between and beyond the two base readings until four-to-eight dose readings are obtained. The resultant data is then plotted on a chart for dose values versus lead thickness. The value for

nominal less 10% lead thickness is utilized as the maximum acceptable dose value for the inspected package.

Indications of non-conformance with the above stated standards shall be recorded for disposition prior to repair and final acceptance in accordance with the requirements of the cognizant quality assurance program.

8.1.6 Thermal Acceptance Tests

Material properties established in Section 3.2, *Summary of Thermal Properties of Materials*, are consistently conservative for the analyses performed. As such, with the exception of the polyurethane foam (addressed in Section 8.1.4.1, *Polyurethane Foam*), acceptance tests for material thermal properties are not performed.

8.1.7 Lead Installation Tests

Testing during the lead installation process involves pre- and post-pour diameter and straightness measurements of the OC inner shell and close monitoring of the package temperatures during the preheat, lead pour, and cooldown processes. A more detailed description of the lead installation and testing is presented in Appendix 8.3.1, *Lead Installation Procedure*.

Table 8.1-1 – Compressive Stress Ranges at Room Temperature (psi)

	Parallel-to-Rise at Strain, $\varepsilon_{//}$			Perpendicular-to-Rise at Strain, $\varepsilon_{\perp}$		
Sample Range	**ε = 10%**	**ε = 40%**	**ε = 70%**	**ε = 10%**	**ε = 40%**	**ε = 70%**
Nominal –15%	320	382	1,132	296	371	1,185
Nominal –10%	338	404	1,199	313	392	1,255
Nominal	376	449	1,332	348	436	1,394
Nominal +10%	414	494	1,465	383	480	1,533
Nominal +15%	432	516	1,532	400	501	1,603

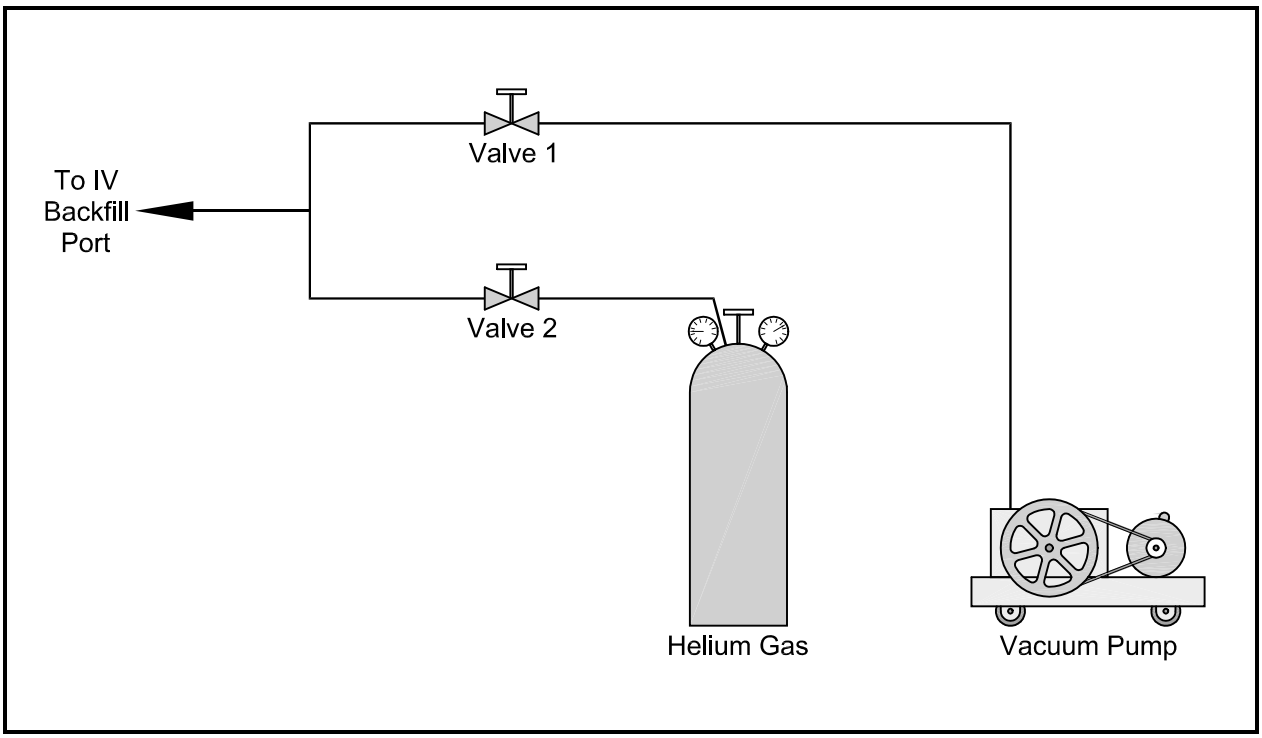

Figure 8.1-1 – Testing the IV Lid Seal Integrity

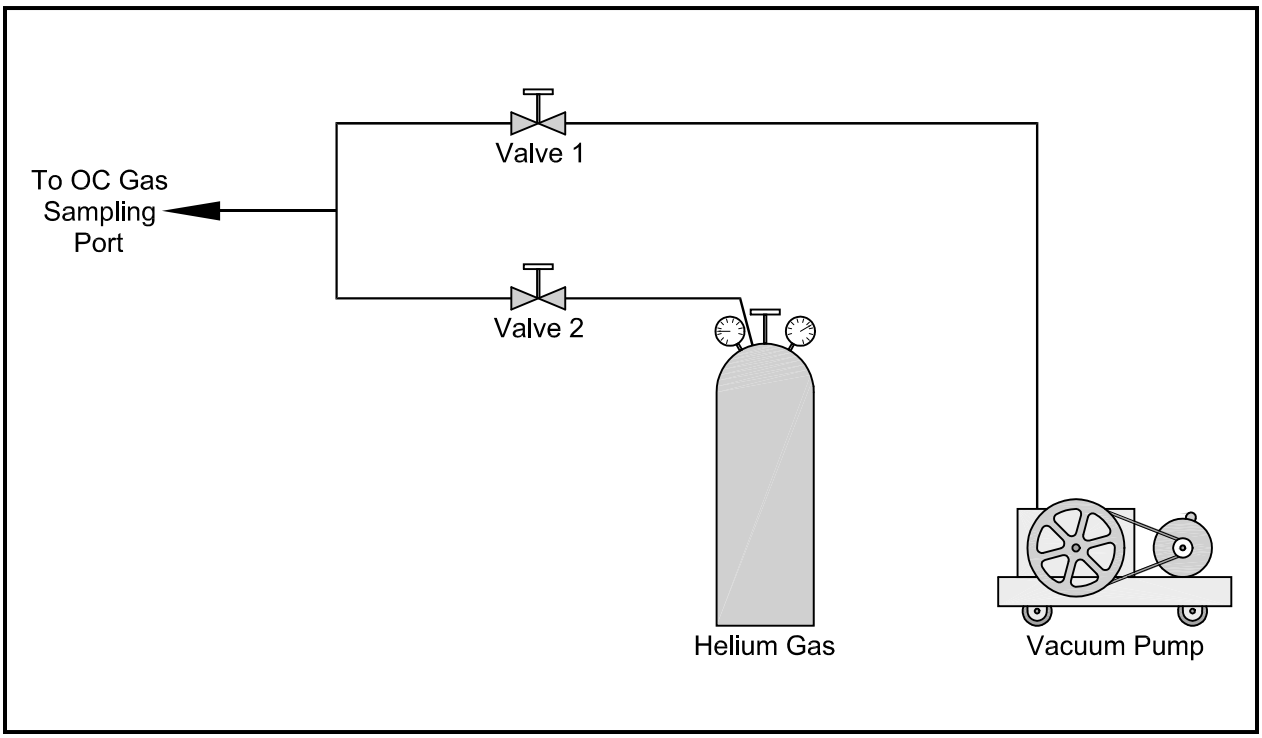

Figure 8.1-2 – Testing the OC Lid Seal Integrity

This page intentionally left blank.

8.2 Maintenance Program

This section describes the maintenance program used to ensure continued performance of the RH-TRU 72-B package.

The criteria for repair of the packaging are dictated by the design, as detailed in the drawings in Appendix 1.3.1, *Packaging General Arrangement Drawings*. When the packaging is not in compliance with the design configuration, it must be removed from service. Repairs will involve returning the packaging to a compliant configuration. Repair verification procedures will be equivalent to fabrication verification procedures.

Packaging repairs fall into two categories, minor and major. Minor repairs are those that can be readily accomplished and require no special tools, supplies, equipment, or highly skilled personnel. Minor repairs would include replacement of damaged consumables, polishing out scratches on the seal surfaces, and so forth. Such repairs can be undertaken by users that have the necessary equipment and qualified personnel.

Major repairs consist of all repairs requiring welding or machining to correct a deficiency that affects the performance integrity of the packaging or its components. Major repairs and major component replacements are the responsibility of the packaging licensee, and will be performed at a facility designated and approved by the licensee.

8.2.1 Structural and Pressure Tests

8.2.1.1 Structural Tests

Other than the stress corrosion tests specified in Section 8.2.1.3, *Inner Vessel Interior Surface Inspection*, and the lifting device load tests required for first use (see Section 8.1.2.1, *Lifting Device Load Testing*), no structural tests are necessary to ensure continuous performance of the package.

8.2.1.2 Containment Vessel Pressure Testing

Other than the acceptance tests required for first use (see Section 8.1.2.2, *Inner Vessel and Outer Cask Pressure Testing*), no pressure tests are necessary to ensure continued performance of the package.

8.2.1.3 Inner Vessel Interior Surface Inspection

Prior to first use and annually thereafter, inspections shall be performed on the accessible interior surfaces of the inner vessel (IV) for evidence of chemically induced stress corrosion. This shall consist of a visual inspection for indication of IV interior surface corrosion. Should evidence of corrosion exist, a liquid penetrant inspection of the entire IV interior surface including accessible lid, end forging, shell, base, and associated weld surfaces shall be performed per ASME Boiler and Pressure Vessel Code, Section V[1], Article 6, and ASME Boiler and Pressure Vessel Code,

[1] American Society of Mechanical Engineers (ASME) Boiler and Pressure Vessel Code, Section V, *Nondestructive Examination*, 1986 Edition.

Section III[2], Division 1, Subsection NB, Article NB-5000. Indications of cracking or distortion shall be recorded on a nonconformance report and dispositioned prior to corrective actions in accordance with the cognizant quality assurance program.

Once the packaging is put into service, at a maximum interval of five (5) years, inspections shall be performed on the accessible interior surfaces of the IV for evidence of chemically induced stress corrosion. This shall consist of a liquid penetrant inspection of the entire IV interior surface including accessible lid, end forging, shell, base, and associated weld surfaces per ASME Boiler and Pressure Vessel Code, Section V[1], Article 6, and ASME Boiler and Pressure Vessel Code, Section III[2], Division 1, Subsection NB, Article NB-5000. Indications of cracking or distortion shall be recorded on a nonconformance report and dispositioned prior to corrective actions in accordance with the cognizant quality assurance program.

8.2.2 Maintenance/Periodic Leakage Rate Tests

Maintenance/Periodic Leakage Rate Testing shall conform to the requirements of Section 7.4, *Maintenance Leakage Rate Test*, of ANSI N14.5[3]. All leakage rate testing procedures implemented for the maintenance/periodic leak tests identified within this section shall be developed and approved by personnel certified through the American Society for Nondestructive Testing (ASNT) as a Level III in the method of Leak Testing.

Appropriate sections of the *Maintenance/Periodic Leakage Rate Test* shall be performed during routine maintenance to verify package configuration and performance to design criteria. *Maintenance/Periodic Leakage Rate Tests* of the lid O-ring seals and port closure bolt seals are to be performed upon replacement, but seals need not necessarily be replaced at the same time (i.e., seals are to be replaced annually or when damaged). Sections of the *Maintenance/Periodic Leakage Rate Test* can be performed in lieu of corresponding *Preshipment Leakage Rate Tests* and shall be performed upon component failure, repair, or replacement during the *Preshipment Leakage Rate Test* (see Appendix 7.4.1, *Preshipment Leakage Rate Test*).

To begin the test, it is assumed the IV and OC lids are removed. The *Maintenance Leakage Rate Test* is separated into five (5) tests, three (3) for the IV and two (2) for the outer cask (OC). The five (5) separate tests are: 1) IV lid seal integrity, 2) IV gas sampling port closure bolt seal integrity, 3) IV backfill port closure bolt seal integrity, 4) OC lid seal integrity, and 5) OC gas sampling port closure bolt seal integrity.

8.2.2.0.1 Obtain a helium mass spectrometer leak detector capable of detecting a leak of 5×10^{-8} standard cubic centimeters per second (scc/s), air, or better (1.3×10^{-7} scc/s, helium).

8.2.2.0.2 Calibrate the leak detector to a minimum sensitivity of 5×10^{-8} scc/s, air (1.3×10^{-7} scc/s, helium) following the guidelines of Section 8.4, *Sensitivity*, and Annex A.5.3.4, *Test Method and Considerations*, of ANSI N14.5 for establishing the system response (dwell time) using a calibrated standard leak.

[2] American Society of Mechanical Engineers (ASME) Boiler and Pressure Vessel Code, Section III, *Rules for Construction of Nuclear Power Plant Components*, 1986 Edition.

[3] ANSI N14.5-2014, *American National Standard for Radioactive Materials – Leakage Tests on Packages for Shipment,* American National Standards Institute, Inc. (ANSI).

8.2.2.1 Testing the IV Lid Seal Integrity

8.2.2.1.1 Clean and visually inspect the three IV lid O-ring seals. Sparingly apply new vacuum grease to the seals. Install the O-ring seals into the O-ring grooves.

8.2.2.1.2 Clean and visually inspect the sealing area on the IV body. Install the IV lid, tightening the eight (8) 7/8-9UNC bolts to 100 – 200 lb-ft torque.

8.2.2.1.3 Tighten the gas sampling port closure bolt to 15 – 20 lb-ft torque.

8.2.2.1.4 Install a test port tool into the backfill port.

8.2.2.1.5 Attach a vacuum pump and a source of helium gas, in parallel, to the test port tool. Install valves on each of the lines to allow independent isolation of the vacuum pump and the source of helium gas to the test port tool. Close the valve to the source of helium gas, and open the valve to the vacuum pump.

8.2.2.1.6 Utilizing the test port tool, rotate the backfill port closure bolt fully open.

8.2.2.1.7 Evacuate the system through the test port tool to 90% vacuum or better (≤10% ambient atmospheric pressure). Isolate the vacuum pump from the system.

8.2.2.1.8 Backfill the evacuated cavity with helium gas to a pressure slightly greater than atmospheric pressure (+1 psi, -0 psi), and close the valve to isolate the source of helium gas from the system. Correction for tracer gas concentration shall be performed.

8.2.2.1.9 Utilizing the test port tool, rotate the backfill port closure bolt closed and tighten to 15 – 20 lb-ft torque.

8.2.2.1.10 Remove the helium-contaminated test port tool from the backfill port.

8.2.2.1.11 Install a clean (helium-free) test port tool into the seal test port.

8.2.2.1.12 Attach a leak detector to the test port tool.

8.2.2.1.13 Utilizing the test port tool, rotate the seal test port closure bolt fully open.

8.2.2.1.14 Evacuate the cavity above the IV lid containment seal until the vacuum is sufficient to operate the leak detector.

8.2.2.1.15 Determine the leakage rate of the system using the leak detector.

8.2.2.1.16 If the leakage rate of the system exceeds the level indicated in Section 8.2.2.6, *Maintenance/Periodic Leakage Rate Test Acceptance Criteria*, release the vacuum, remove the IV lid and inspect the seals for cuts, tears, or abrasion, and the sealing areas for cleanliness and surface condition. If necessary, replace the defective seal(s) and/or repair the sealing areas. Repeat Paragraphs 8.2.2.1.1 through 8.2.2.1.15. If, after repeated testing, it has been determined that the lid containment seal cannot be made to pass the requirements of Section 8.2.2.6, *Maintenance/Periodic Leakage Rate Test Acceptance Criteria*, utilize appropriate methods to locate/isolate the leak path. Repair the leak path and repeat Paragraphs 8.2.2.1.1 through 8.2.2.1.15 to verify integrity of the IV lid containment seal.

8.2.2.1.17 After successfully completing Paragraphs 8.2.2.1.1 through 8.2.2.1.16, rotate the seal test port closure bolt closed, tighten to 15 – 20 lb-ft torque, and remove the leak detector/test port tool.

8.2.2.2 Testing the IV Gas Sampling Port Closure Bolt Seal Integrity

8.2.2.2.1 Verify the presence of a helium atmosphere below the gas sampling port closure bolt containment seal, as provided for in Paragraphs 8.2.2.1.3 through 8.2.2.1.10.

8.2.2.2.2 Install a test port tool into the gas sampling port.

8.2.2.2.3 Attach a leak detector to the test port tool.

8.2.2.2.4 Evacuate the cavity above the gas sampling port closure bolt containment seal until the vacuum is sufficient to operate the leak detector.

8.2.2.2.5 Determine the leakage rate of the system using the leak detector.

8.2.2.2.6 If the leakage rate of the system exceeds the level indicated in Section 8.2.2.6, *Maintenance/Periodic Leakage Rate Test Acceptance Criteria*, release the vacuum, remove the gas sampling port closure bolt and inspect the seal for cuts, tears, or abrasion, and the sealing areas for cleanliness and surface condition. If necessary, replace the defective components and/or repair the sealing areas. Repeat Paragraphs 8.2.2.2.1 through 8.2.2.2.5. If, after repeated testing, it has been determined that the gas sampling port closure bolt containment seal cannot be made to pass the requirements of Section 8.2.2.6, *Maintenance/Periodic Leakage Rate Test Acceptance Criteria*, utilize appropriate methods to locate/isolate the leak path. Repair the leak path and repeat Paragraphs 8.2.2.2.1 through 8.2.2.2.5 to verify integrity of the gas sampling port closure bolt containment seal.

8.2.2.2.7 After successfully completing Paragraphs 8.2.2.2.1 through 8.2.2.2.6, remove the leak detector/test port tool.

8.2.2.3 Testing the IV Backfill Port Closure Bolt Seal Integrity

8.2.2.3.1 Verify the presence of a helium atmosphere below the backfill port closure bolt containment seal, as provided for in Paragraphs 8.2.2.1.3 through 8.2.2.1.10.

8.2.2.3.2 Install a clean (helium-free) test port tool into the backfill port. Attach a leak detector to the test port tool.

8.2.2.3.3 Evacuate the cavity above the backfill port closure bolt until the vacuum is sufficient to operate the leak detector.

8.2.2.3.4 Determine the leakage rate of the system using the leak detector.

8.2.2.3.5 If the leakage rate of the system exceeds the level indicated in Section 8.2.2.6, *Maintenance/Periodic Leakage Rate Test Acceptance Criteria*, release the vacuum, remove the backfill port closure bolt and inspect the seal for cuts, tears, or abrasion, and the sealing areas for cleanliness and surface condition. If necessary, replace the defective components and/or repair the sealing areas. Repeat Paragraphs 8.2.2.3.1 through 8.2.2.3.4. If, after repeated testing, it has been determined that the backfill port closure bolt containment seal cannot be made to pass the requirements of Section

8.2.2.6, *Maintenance/Periodic Leakage Rate Test Acceptance Criteria*, utilize appropriate methods to locate/isolate the leak path. Repair the leak path and repeat Paragraphs 8.2.2.3.1 through 8.2.2.3.4 to verify integrity of the backfill port closure bolt seal.

8.2.2.3.6 After successfully completing Paragraphs 8.2.2.3.1 through 8.2.2.3.5, remove the leak detector/test port tool.

8.2.2.4 Testing the OC Lid Seal Integrity

8.2.2.4.1 Clean and visually inspect both OC O-ring lid seals. Sparingly apply new vacuum grease to the seals. Install the O-ring seals into the O-ring grooves.

8.2.2.4.2 Clean and visually inspect the sealing area on the OC body. Install the OC lid, tightening the eighteen (18), 1¼-7UNC bolts to 600 – 700 lb-ft torque.

8.2.2.4.3 Install a test port tool into the gas sampling port.

8.2.2.4.4 Utilizing the test port tool, rotate the OC gas sampling port closure bolt fully open.

8.2.2.4.5 Attach a vacuum pump and a source of helium gas, in parallel, to the test port tool. Install valves on each of the lines to allow independent isolation of the vacuum pump and the source of helium gas to the test port tool. Close the valve to the source of helium gas, and open the valve to the vacuum pump.

8.2.2.4.6 Evacuate the system through the test port tool to 90% vacuum or better (≤10% ambient atmospheric pressure). Isolate the vacuum pump from the system.

8.2.2.4.7 Backfill with helium gas to a pressure slightly greater than atmospheric pressure (+1 psi, -0 psi) and close the valve to isolate the source of helium gas from the system. Correction for tracer gas concentration shall be performed.

8.2.2.4.8 Utilizing the test port tool, rotate the OC gas sampling closure bolt closed and tighten to 15 – 20 lb-ft torque.

8.2.2.4.9 Remove the helium-contaminated test port tool from the gas sampling port.

8.2.2.4.10 Install a clean (helium-free) test port tool into the seal test port.

8.2.2.4.11 Attach the leak detector to the test port tool.

8.2.2.4.12 Utilizing the test port tool, rotate the seal test port closure bolt fully open.

8.2.2.4.13 Evacuate the system through the test port tool until the vacuum is sufficient to operate the leak detector.

8.2.2.4.14 Determine the leakage rate of the system using the leak detector.

8.2.2.4.15 If the leakage rate of the system exceeds the level indicated in Section 8.2.2.6, *Maintenance/Periodic Leakage Rate Test Acceptance Criteria*, release the vacuum, remove the OC lid and inspect the closure seals for cuts, tears, or abrasion, and the sealing areas for cleanliness and surface condition. If necessary, replace the defective seal(s) and/or repair the sealing areas. Repeat Paragraphs 8.2.2.4.1 through 8.2.2.4.14. If, after repeated testing, it has been determined that the lid containment seal cannot be made to pass the requirements of Section 8.2.2.6,

Maintenance/Periodic Leakage Rate Test Acceptance Criteria, utilize appropriate methods to locate/isolate the leak path. Repair the leak path and repeat Paragraphs 8.2.2.4.1 through 8.2.2.4.14 to verify integrity of the OC lid containment seal.

8.2.2.4.16 After successfully completing Paragraphs 8.2.2.4.1 through 8.2.2.4.15, rotate the seal test port closure bolt closed, tighten to 15 – 20 lb-ft torque, and remove the leak detector/test port tool.

8.2.2.5 Testing the OC Gas Sampling Port Closure Bolt Seal Integrity

8.2.2.5.1 Verify the presence of a helium atmosphere below the gas sampling port closure bolt containment seal, as provided for in Paragraphs 8.2.2.4.4 through 8.2.2.4.9.

8.2.2.5.2 Install a clean (helium-free) test port tool into the gas sampling port. Attach a leak detector to the test port tool.

8.2.2.5.3 Evacuate the cavity above the gas sampling port closure bolt until the vacuum is sufficient to operate the leak detector.

8.2.2.5.4 Determine the leakage rate of the system using the leak detector.

8.2.2.5.5 If the leakage rate of the system exceeds the level indicated in Section 8.2.2.6, *Maintenance/Periodic Leakage Rate Test Acceptance Criteria*, release the vacuum, remove the gas sampling port closure bolt and inspect the seal for cuts, tears, or abrasion, and the sealing areas for cleanliness and surface condition. If necessary, replace the defective components and/or repair the sealing areas. Repeat Paragraphs 8.2.2.5.1 through 8.2.2.5.4. If, after repeated testing, it has been determined that the gas sampling port closure bolt containment seal cannot be made to pass the requirements of Section 8.2.2.6, *Maintenance/Periodic Leakage Rate Test Acceptance Criteria*, utilize appropriate methods to locate/isolate the leak path. Repair the leak path and repeat Paragraphs 8.2.2.5.1 through 8.2.2.5.4 to verify integrity of the gas sampling port closure bolt seal.

8.2.2.5.6 After successfully completing Paragraphs 8.2.2.5.1 through 8.2.2.5.5, remove the leak detector/test port tool.

8.2.2.6 Maintenance/Periodic Leakage Rate Test Acceptance Criteria

8.2.2.6.1 To be acceptable, per Section 6.3.2, *Minimum Reference Air Leakage Rate*, of ANSI N14.5[3], each vessel test and each containment seal test shall demonstrate a leakage rate of 1×10^{-7} scc/s, air, (leaktight) (2.6×10^{-7} helium), or less.

8.2.2.6.2 In order to demonstrate that the package is leaktight, per Section 8.4, *Sensitivity*, of ANSI N14.5[3], the sensitivity of the leakage rate test procedure shall be 5×10^{-8} scc/s, air (1.3×10^{-7} helium), or less.

8.2.2.6.3 Indications of non-conformance with the above stated standards shall be recorded for disposition prior to repair and final acceptance in accordance with the requirements of the cognizant quality assurance program.

8.2.3 Subsystems Maintenance

8.2.3.1 Fasteners

All threaded components shall be inspected annually and prior to each use for deformed or stripped threads. Any damaged components shall be replaced prior to further use. In the event that an OC closure bolt, an IV closure bolt, or an impact limiter attachment bolt were to fail during installation, all corresponding bolts currently in use on that particular packaging shall be replaced prior to continued use of the packaging.

8.2.3.2 Impact Limiters

A sound industrial maintenance program should be followed to assure the integrity of the impact limiters. Such a program should include procedures for periodic inspection, cleaning, replacement of damaged consumables (attachment bolts, pipe plugs, lifting lug hinges), and the associated record-keeping and quality assurance controls. Inspections should include surveys of the impact limiter exterior for dents, cuts and/or punctures, indications of loss of weld integrity, and general cleanliness of the outer shell. If any damage is detected which might prevent the impact limiter from performing its design functions, the impact limiter must be removed from service until a detailed evaluation is made and remediation approach can be determined. Remediation of such damage must be carried out in a manner which will return the impact limiter to its original design condition.

Specifically, the impact limiter attachment bolts shall be inspected annually and after each use for damaged or stripped threads. The plastic pipe plugs at the ends of the impact limiters shall be inspected for damage after each use and replaced prior to further use if damage is present. The pipe plugs shall be removed on an annual basis and the foam shall be visually inspected. Inspections of the foam will be for determination of deviations from the design requirements of the foam which might prevent the impact limiter from performing its design functions. Such discrepancies would include discontinuities in the foam, such as cracks or voids, or indications of egress of moisture. If any such discrepancies are detected, and the potential exists that they are widespread (i.e., are not limited to the visible portion of the foam), the impact limiter must be removed from service until a detailed evaluation is made and a remediation approach can be determined. Remediation of such damage must be carried out in a manner which will return the impact limiter to its original design condition. Minor problems, such as ingress of moisture, should be corrected as appropriate, either by the user or the packaging licensee. Loss of integrity of the polyurethane foam (unless it can be conclusively demonstrated to be highly localized) is not considered a repairable condition.

8.2.3.3 Trunnions

The trunnions shall be inspected annually and before each use for excessive wear, galling, or distortion. Trunnions exhibiting such damage shall be corrected prior to further use.

8.2.3.4 Sealing Areas and Grooves

8.2.3.4.1 Sealing Area Routine Inspection and Repair

Before each use, OC and IV sealing surfaces and the visible portion of the O-ring seals and grooves shall be visually inspected for damage that could impair the sealing capabilities of the

RH-TRU 72-B packaging. Furthermore, at the time of O-ring seal replacement, visually inspect the O-ring seal grooves for damage that could impair the sealing capabilities of the RH-TRU 72-B packaging. Damage shall be corrected prior to further use (e.g., using 400 – 600 grit emery cloth to polish the sealing surfaces) to the surface finish specified in Section 8.2.3.4.2, *Annual Sealing Area Inspection*.

Upon completion of sealing area and/or groove repairs, perform a sealing area inspection per Section 8.2.3.4.2, *Annual Sealing Area Inspection*, and leakage rate test per the applicable subsection of the *Maintenance Leakage Rate Test* per Section 8.2.2, *Maintenance/Periodic Leakage Rate Tests*.

8.2.3.4.2 Annual Sealing Area Inspection

In order to maintain an effective seal at the OC and IV lid-to-body joint, an annual inspection of the OC and IV body O-ring sealing area surface finishes shall be performed. The surface finish in the containment sealing areas shall be maintained at a maximum 125 RMS micro-inches finish. The following surfaces shall be measured annually:

(1) Bottom surface of each O-ring seal groove, and

(2) Surface of the OC and IV body containment O-ring sealing areas.

If the surface condition of the above sealing areas is determined to exceed 125 RMS micro-inches, repair the sealing area(s) per the requirements of Section 8.2.3.4.1, *Sealing Area Routine Inspection and Repair*.

8.2.4 Valves, Rupture Discs, and Gaskets

This section describes the inspection and replacement schedule for these components.

8.2.4.1 Valves

No valves are used on the RH-TRU 72-B packaging.

8.2.4.2 Rupture Discs

No rupture discs are used on the RH-TRU 72-B packaging.

8.2.4.3 Gaskets

All O-ring seals and gaskets shall be replaced annually or when damaged, per the size and material specifications delineated on the drawings in Appendix 1.3.1, *Packaging General Arrangement Drawings*. Following seal replacement, the seal(s) shall be leakage rate tested to the requirements of Section 8.2.2, *Maintenance/Periodic Leakage Rate Tests*.

8.2.5 Shielding

Other than the tests required prior to first use, no shielding tests are necessary to ensure continued performance of the RH-TRU 72-B packaging.

8.2.6 Thermal

No thermal inspections or tests are necessary to ensure continued performance of the RH-TRU 72-B packaging.

8.2.7 Criticality Control Materials

No materials designed specifically for criticality control are employed in the RH-TRU 72-B packaging. As such, no tests of criticality control materials are necessary to ensure continued performance.

This page intentionally left blank.

8.3 Appendices

8.3.1 *Lead Installation Procedure*

This page intentionally left blank.

8.3.1 Lead Installation Procedure

The following delineates the procedure for installation of poured lead into the RH-TRU 72-B packaging outer cask (OC). The procedure presents pre-pour, lead pour, gamma scan inspection of the lead shielding, and post-pour requirements. Note that the OC thermal shield is attached after lead pour and cooldown.

8.3.1.1 Interior cavities and surfaces of the OC shells which are to be in contact with the lead shielding shall be swabbed with solvent, wiped down, sandblasted, or otherwise cleansed of loose mill scale, weld slag, and all carbonaceous materials prior to lead pour.

8.3.1.2 All OC inner and outer surfaces shall be supported or braced, as necessary, to prevent distortion during the lead-pouring and cooldown operations.

8.3.1.3 The lead-pouring operation is performed with the packaging inverted (i.e., the OC base plate is up, lid-end is down).

Fill pipes shall be provided through the OC outer shell, adjacent to the lid-end forging, sized as required to allow for rapid and even lead fill.

Standpipes shall be provided through the OC outer shell, adjacent to the base plate, sized as required to allow for easy access of lead during the cooldown operation.

Vent risers shall be provided through the OC base plate to allow for escape of air and impurities.

8.3.1.4 The OC shall be instrumented with thermocouple wires at eight (8) locations on the inside and outside to monitor temperature differentials between the two shells. A total of sixteen (16) thermocouples shall be required. Internal and/or external bracing may be temporarily removed to facilitate thermocouple installation.

The thermocouples shall be mounted opposite each other on the inside and outside shells to assure proper temperature differential measurements. The thermocouple sets shall be mounted at equal intervals over the full length of the OC. The sets shall also be located around the shell circumference so that all areas of the OC are instrumented.

In addition, a calibrated strip recorder with the thermocouples capable of measuring temperatures to 1,000 ºF and plotting time/temperature data every 60 seconds shall be utilized.

Adequate precautions must be taken to assure that the thermocouples are protected from impact or flame impingement during the preheat, lead pour, and cooldown phases.

8.3.1.5 All OC components (i.e., outer shell, inner shell, lid-end forging, and bottom-end closure) shall be uniformly preheated to a temperature of 600 ºF to 700 ºF over the entire surface prior to lead pouring. Preheating shall be done in a suitable enclosure to assure uniform preheating. During preheat, the maximum temperature change for any thermocouple shall not exceed 100 ºF in any thirty (30) minute period.

8.3.1.6 The temperature of the lead at the time of lead pour shall range from 750 ºF to 850 ºF.

8.3.1.7 The rate of lead flow shall be controlled to fill the OC as rapidly and evenly as possible. The lead shall enter the cavity in such a way as to minimize impingement on the OC shells.

8.3.1.8 Heat sources shall be controlled during the cooldown period so that the OC is cooled to ensure that only one solidifying front exists in the lead.

During cooldown, the maximum temperature change for any thermocouple shall not exceed 100 ºF in any thirty (30) minute period, and the maximum difference in temperatures between any pair of thermocouples mounted directly opposite each other (one on the OD and the corresponding one on the ID) shall not exceed 300 ºF at any instant in time.

8.3.1.9 Molten lead at a minimum temperature of 750 ºF shall be added to the standpipes, as necessary, at a rate consistent with normal shrinkage.

8.3.1.10 After all the thermocouples indicate a temperature less than 100 ºF, the thermocouples and any internal and/or external bracing shall be removed and the OC gamma scanned in accordance with the tests delineated in Section 8.1.5, *Tests for Shielding Integrity*.

8.3.1.11 Upon a successful gamma scan, inspection measurements taken after lead pour must meet the requirements specified on the drawings in Appendix 1.3.1, *Packaging General Arrangement Drawings*. (NOTE: Specifically, the tolerance requirements of ASME Boiler and Pressure Vessel Code, Division 1, Section III[1], Subsection NE, Article NE-4220, as defined in drawing Flag Note 27, shall be met.)

8.3.1.12 Remove all fill pipes, vent pipes, and standpipes, clean the holes thoroughly of all lead, and install plugs of identical material as the base material.

[1] American Society of Mechanical Engineers (ASME) Boiler and Pressure Vessel Code, Section III, *Rules for Construction of Nuclear Power Plant Components*, 1986 Edition.

9.0 QUALITY ASSURANCE

This section describes quality assurance (QA) requirements and methods of compliance applicable to the RH-TRU 72-B package.

9.1 Introduction

The RH-TRU 72-B package is designed and shall be built for the U.S. Department of Energy (DOE) and must be approved by the U.S. Nuclear Regulatory Commission (NRC) for the shipment of radioactive material in accordance with the applicable provisions of the U.S. Department of Transportation, described in Subpart I of 49 CFR Part 173[1]. Procurement, design, fabrication, assembly, testing, maintenance, repair, modification, and use of the RH-TRU 72-B package are all done under QA programs that meet all applicable NRC and DOE QA requirements. QA requirements for payloads to be transported in the RH-TRU 72-B package are discussed in the *Remote-Handled Transuranic Waste Authorized Methods for Payload Control* (RH-TRAMPAC)[2].

[1] Title 49, Code of Federal Regulations, Part 173 (49 CFR 173), *Shippers–General Requirements for Shipments and Packagings*, Current Version.

[2] U.S. Department of Energy (DOE), *Remote-Handled Transuranic Waste Authorized Methods for Payload Control* (RH-TRAMPAC), U.S. Department of Energy, Carlsbad Field Office, Carlsbad, New Mexico.

This page intentionally left blank.

9.2 Quality Assurance Requirements

9.2.1 U.S. Nuclear Regulatory Commission

The QA requirements for packaging established by the NRC are described in Subpart H of 10 CFR 71[1]. Subpart H is an 18 criteria QA program based on ANSI/ASME NQA-1[2]. Guidance for QA programs for packaging is provided in NRC Regulatory Guide 7.10[3].

9.2.2 U.S. Department of Energy

The QA requirements of DOE for the use of NRC certified packaging are described in Chapter 4 of DOE Order 460.1C[4]. According to Chapter 4.a.(2)(a)1, the DOE and its contractors may use NRC certified Type B packaging only under the conditions specified in the certificate of compliance.

9.2.3 Transportation to/from WIPP

Public Law 102-579, enacted by the 102nd Congress, reads as follows:

SEC. 16. TRANSPORTATION.

(a) SHIPPING CONTAINERS.— No transuranic waste may be transported by or for the Secretary [of Energy] to or from WIPP, except in packages—

(1) the design of which has been certified by the Nuclear Regulatory Commission; and

(2) that have been determined by the Nuclear Regulatory Commission to satisfy its quality assurance requirements.

The determination under paragraph (2) shall not be subject to rulemaking or judicial review.

[1] Title 10, Code of Federal Regulations, Part 71 (10 CFR 71), *Packaging and Transportation of Radioactive Material*, 01-01-14 Edition.

[2] ANSI/ASME NQA-1, *Quality Assurance Requirements of Nuclear Power Plants*, American National Standards Institute.

[3] U.S. Nuclear Regulatory Commission, Regulatory Guide 7.10, *Establishing Quality Assurance Programs for Packaging Used in the Transport of Radioactive Material,* Revision 2, March 2005.

[4] U.S. Department of Energy Order 460.1C, *Packaging and Transportation Safety,* May 2010.

This page intentionally left blank.

9.3 Quality Assurance Program

9.3.1 NRC Regulatory Guide 7.10

Guidance for QA programs applicable to design, fabrication, assembly, testing, maintenance, repair, modification, and use of packaging used in transport of radioactive material is covered in NRC Regulatory Guide 7.10[1].

9.3.2 Design

The RH-TRU 72-B package was designed under a QA program approved by the NRC for packaging design. Requests for modification or changes to the design will be submitted to the NRC for approval prior to modification of the RH-TRU 72-B packaging. Any future design changes shall be made under an appropriate QA program that has been verified to satisfy 10 CFR 71, Subpart H[2].

9.3.3 Procurement, Fabrication, Assembly, Testing, and Modificaton

Procurement, fabrication, assembly, testing, and modification of each RH-TRU 72-B packaging are performed under a QA program verified to satisfy 10 CFR 71, Subpart H[2] and approved for these activities.

9.3.4 Use

The RH-TRU 72-B package will be used primarily by the DOE for shipments of authorized contents to the WIPP site. However, it may also be used between DOE sites other than WIPP (inter-site) and for DOE on-site shipments within site boundaries (intra-site). The DOE is registered with the NRC as a user of the RH-TRU 72-B package under the general license provisions of 49 CFR §173.471[3]. The RH-TRU 72-B packaging may also be used for non-DOE shipments as authorized by the NRC.

9.3.4.1 DOE Shipments: To/From WIPP

Use of the RH-TRU 72-B packaging for shipments to/from the WIPP site shall be made under a QA program that meets the QA requirements of the NRC. The appropriate DOE Field Office(s) shall evaluate and approve the QA programs of the DOE contractors that make shipments to/from WIPP in the RH-TRU 72-B package. DOE or the DOE managing and operating contractor for the WIPP shall perform surveillances of the RH-TRU 72-B package users' QA programs to ensure that the package is used in accordance with the requirements of the certificate of compliance.

---

[1] U.S. Nuclear Regulatory Commission, Regulatory Guide 7.10, *Establishing Quality Assurance Programs for Packaging Used in the Transport of Radioactive Material,* Revision 2, March 2005.

[2] Title 10, Code of Federal Regulations, Part 71 (10 CFR 71), *Packaging and Transportation of Radioactive Material*, 01-01-14 Edition.

[3] Title 49, Code of Federal Regulations, Part 173 (49 CFR 173), *Shippers—General Requirements for Shipments and Packagings*, U.S. Department of Transportation, Washington, D.C., Current Version.

9.3.4.2 Other DOE Shipments: Non-WIPP

The appropriate DOE Field Office(s) shall evaluate and approve the shipper's and receiver's QA programs for equivalency to the NRC's QA program requirements in Subpart H of 10 CFR 71[2]. For example, a contractor working under an 18 criteria QA program per ANSI/ASME NQA-1[4] could be deemed acceptable if the portion of the program applicable to packaging is found compliant with 10 CFR 71, Subpart H[2]. DOE or the DOE managing and operating contractor for the WIPP shall perform surveillances of the RH-TRU 72-B package users' QA programs to ensure that the package is used in accordance with the requirements of the certificate of compliance.

9.3.4.3 Non-DOE Users of RH-TRU 72-B package

Non-DOE users of the RH-TRU 72-B package shall have QA programs verified to satisfy 10 CFR 71, Subpart H[2].

9.3.5 Maintenance and Repair

Minor maintenance, such as changing seals or fasteners, may be performed under the user's QA program. Major maintenance, such as cutting or welding a containment boundary, shall be performed under an appropriate QA program that has been verified to satisfy 10 CFR 71, Subpart H[2].

[4] ANSI/ASME NQA-1, *Quality Assurance Requirements of Nuclear Power Plants*, American National Standards Institute.